

Advances in **Green and Sustainable Chemistry**

---



# Heterogeneous Catalysis in Sustainable Synthesis



Béla Török, Christian Schäfer, Anne Kokel

# Heterogeneous Catalysis in Sustainable Synthesis

---

Advances in Green and Sustainable  
Chemistry

# Heterogeneous Catalysis in Sustainable Synthesis

---

Béla Török

Christian Schäfer

Anne Kokel



ELSEVIER

Elsevier

Radarweg 29, PO Box 211, 1000 AE Amsterdam, Netherlands  
The Boulevard, Langford Lane, Kidlington, Oxford OX5 1GB, United Kingdom  
50 Hampshire Street, 5th Floor, Cambridge, MA 02139, United States

Copyright © 2022 Elsevier Inc. All rights reserved.

No part of this publication may be reproduced or transmitted in any form or by any means, electronic or mechanical, including photocopying, recording, or any information storage and retrieval system, without permission in writing from the publisher. Details on how to seek permission, further information about the Publisher's permissions policies and our arrangements with organizations such as the Copyright Clearance Center and the Copyright Licensing Agency, can be found at our website: [www.elsevier.com/permissions](http://www.elsevier.com/permissions).

This book and the individual contributions contained in it are protected under copyright by the Publisher (other than as may be noted herein).

### Notices

Knowledge and best practice in this field are constantly changing. As new research and experience broaden our understanding, changes in research methods, professional practices, or medical treatment may become necessary.

Practitioners and researchers must always rely on their own experience and knowledge in evaluating and using any information, methods, compounds, or experiments described herein. In using such information or methods they should be mindful of their own safety and the safety of others, including parties for whom they have a professional responsibility.

To the fullest extent of the law, neither the Publisher nor the authors, contributors, or editors, assume any liability for any injury and/or damage to persons or property as a matter of products liability, negligence or otherwise, or from any use or operation of any methods, products, instructions, or ideas contained in the material herein.

### Library of Congress Cataloging-in-Publication Data

A catalog record for this book is available from the Library of Congress

### British Library Cataloguing-in-Publication Data

A catalogue record for this book is available from the British Library

ISBN: 978-0-12-817825-6

For information on all Elsevier publications  
visit our website at <https://www.elsevier.com/books-and-journals>

*Publisher:* Susan Dennis  
*Acquisitions Editor:* Kathryn Eryilmaz  
*Editorial Project Manager:* Emily Thomson  
*Production Project Manager:* Sruthi Satheesh  
*Cover Designer:* Alan Studholme

Typeset by STRAIVE, India



# Contents

|   |     |
|---|-----|
| Preface   | xii |
| <b>1. Heterogeneous catalysis for organic synthesis: Historical background and fundamentals</b>                   |     |
| 1.1 Introduction and historical background  | 1   |
| 1.2 Catalysis   | 3   |
| 1.2.1 Fundamentals and basic definitions  | 3   |
| 1.2.2 Heterogeneous catalysis   | 9   |
| 1.3 Conclusions and outlook   | 15  |
| References  | 15  |
| <b>2. Solid catalysts for environmentally benign synthesis</b>  |     |
| 2.1 Introduction  | 23  |
| 2.2 Metal catalysts   | 23  |
| 2.2.1 Unsupported metals  | 28  |
| 2.2.2 Supported metal catalyst  | 30  |
| 2.2.3 Heterogenized metal complexes and organocatalysts   | 37  |
| 2.2.4 Metal nanoparticle-based catalysts  | 38  |
| 2.3 Nonmetallic catalysts   | 39  |
| 2.3.1 Metal oxides  | 41  |
| 2.3.2 Heteropoly acids  | 44  |
| 2.3.3 Clays   | 45  |
| 2.3.4 Zeolites  | 48  |
| 2.3.5 Ion exchange resins   | 51  |
| 2.3.6 Metal-organic frameworks  | 53  |
| 2.3.7 Other nonmetallic catalytic materials   | 55  |
| 2.4 Conclusions and outlook   | 57  |
| References  | 58  |
| <b>3. Application of heterogeneous catalysis in the development of environmentally benign synthetic processes</b> |     |
| References  | 82  |

### 3.1 Hydrogenation

|         |   |     |
|---------|---|-----|
| 3.1.1   | Introduction  | 85  |
| 3.1.2   | Carbon-carbon multiple bond hydrogenations: Alkenes, alkynes, dienes  | 86  |
| 3.1.3   | Hydrogenation of aromatic and heteroaromatic compounds  | 96  |
| 3.1.4   | Reduction of carbonyl compounds by heterogeneous catalytic hydrogenation: Aldehydes, ketones, and carboxylic acid derivatives | 103 |
| 3.1.5   | Hydrogenation of nitrogen-containing groups: N=O, N=N, C=N, and C≡N groups  | 108 |
| 3.1.5.1 | Hydrogenation of the nitro group  | 108 |
| 3.1.5.2 | Hydrogenation of nitriles   | 112 |
| 3.1.5.3 | Hydrogenation of imines   | 114 |
| 3.1.5.4 | Hydrogenation of azides   | 117 |
| 3.1.6   | Chemo- and regioselective hydrogenation of compounds with multiple hydrogenation sensitive groups                             | 118 |
| 3.1.6.1 | Selective C=C bond hydrogenation of $\alpha,\beta$ -unsaturated carbonyl compounds  | 118 |
| 3.1.6.2 | Selective C=O reduction of $\alpha,\beta$ -unsaturated carbonyl compounds   | 119 |
| 3.1.6.3 | Complete hydrogenation of multiple functional groups using the same catalytic system  | 123 |
| 3.1.7   | Heterogeneous catalytic hydrogenations by nonconventional activation methods  | 123 |
| 3.1.7.1 | Microwave-assisted hydrogenations   | 123 |
| 3.1.7.2 | Ultrasound-assisted hydrogenations  | 126 |
| 3.1.8   | Conclusions and outlook   | 130 |
|         | References  | 130 |

### 3.2 Heterogeneous catalytic hydrogenolysis of organic compounds

|         |   |     |
|---------|---|-----|
| 3.2.1   | Introduction  | 157 |
| 3.2.2   | C–C bonds   | 158 |
| 3.2.3   | C–O bonds   | 167 |
| 3.2.4   | C–N bonds   | 177 |
| 3.2.5   | C-halogen bonds—Dehalogenation                                      | 186 |
| 3.2.6   | N–N and N–O bonds   | 190 |
| 3.2.7   | C–S bonds   | 195 |
| 3.2.8   | Hydrogenolysis of C-other elements (Si, metals) bonds               | 198 |
| 3.2.9   | Hydrogenolysis of biomass-related compounds                         | 199 |
| 3.2.9.1 | Hydrogenolysis of biomass-derived oxygen-containing heterocycles    | 199 |
| 3.2.9.2 | Hydrogenolysis of biomass-derived other oxygen-containing compounds | 199 |
| 3.2.10  | Conclusions and outlook   | 201 |
|         | References  | 204 |

### 3.3 Heterogeneous catalytic oxidations

|         |  |     |
|---------|--|-----|
| 3.3.1   | Introduction   | 227 |
| 3.3.2   | Epoxidation reactions                                  | 228 |
| 3.3.3   | Dihydroxylation reactions                              | 235 |
| 3.3.3.1 | Dihydroxylations with osmium                           | 235 |
| 3.3.3.2 | Dihydroxylations with metals other than osmium         | 240 |
| 3.3.4   | Wacker-type oxidation reactions                        | 241 |
| 3.3.5   | Oxidative cleavage of hydrocarbons                     | 243 |
| 3.3.5.1 | Cleavage to generate aldehydes and ketones             | 244 |
| 3.3.5.2 | Cleavage to generate carboxylic acids and esters       | 248 |
| 3.3.5.3 | Other oxidative cleavage reactions                     | 250 |
| 3.3.6   | Oxidation of C–O and C–N bonds                         | 251 |
| 3.3.6.1 | Oxidation of C–O bonds                                 | 251 |
| 3.3.6.2 | Oxidation of C–N bonds                                 | 260 |
| 3.3.7   | Dehydrogenation and aromatization of C–C and C–X bonds | 263 |
| 3.3.8   | Conclusions and outlook                                | 269 |
|         | References   | 269 |

### 3.4 Metathesis by heterogeneous catalysts

|       |   |     |
|-------|---|-----|
| 3.4.1 | Introduction                                  | 279 |
| 3.4.2 | Cross-metathesis                              | 280 |
| 3.4.3 | Ring-closing metathesis                       | 288 |
| 3.4.4 | Ring-opening metathesis                       | 301 |
| 3.4.5 | Alkyne metathesis                             | 302 |
| 3.4.6 | Heterogeneous catalytic asymmetric metathesis | 303 |
| 3.4.7 | Metathesis applied to bioderived alkenes      | 305 |
| 3.4.8 | Conclusions and outlook                       | 309 |
|       | References                                    | 310 |

### 3.5 Friedel-Crafts and related reactions catalyzed by solid acids

|         |   |     |
|---------|---|-----|
| 3.5.1   | Introduction  | 317 |
| 3.5.2   | Alkylation, hydroxyalkylation                             | 318 |
| 3.5.2.1 | Alkylations with hydrocarbons                             | 318 |
| 3.5.2.2 | Alkylations with alcohols, ethers, aldehydes, and ketones | 326 |
| 3.5.2.3 | Alkylations with alkyl halides                            | 338 |
| 3.5.2.4 | Hydroxyalkylations  | 341 |
| 3.5.2.5 | Intramolecular transalkylations—Rearrangements            | 343 |
| 3.5.3   | Acylation   | 344 |
| 3.5.3.1 | Acylations with carboxylic acids                          | 345 |
| 3.5.3.2 | Acylations with activated carboxylic acid derivatives     | 348 |
| 3.5.3.3 | Intramolecular transacylations—Rearrangements             | 355 |
| 3.5.4   | Friedel-Crafts cycliacylations                            | 356 |
| 3.5.5   | Halogenation  | 357 |

|   |     |
|---|-----|
| 3.5.6 Nitration   | 360 |
| 3.5.7 Sulfonation   | 364 |
| 3.5.8 Conclusions and outlook   | 365 |
| References  | 365 |
| <b>3.6 Cross-coupling reactions for environmentally benign synthesis</b>            |     |
| 3.6.1 Introduction  | 379 |
| 3.6.2 The Heck coupling   | 380 |
| 3.6.2.1 Heck reactions using a heterogeneous catalyst in solution                   | 380 |
| 3.6.2.2 Solvent-free Heck reactions   | 389 |
| 3.6.2.3 Heck reactions without palladium  | 392 |
| 3.6.3 The Suzuki coupling   | 393 |
| 3.6.3.1 Palladium-catalyzed heterogeneous Suzuki coupling reactions                 | 393 |
| 3.6.3.2 Palladium-free heterogeneous catalytic Suzuki coupling reactions            | 405 |
| 3.6.4 The Hiyama coupling   | 407 |
| 3.6.5 The Negishi coupling  | 411 |
| 3.6.6 The Kumada coupling   | 414 |
| 3.6.7 The Sonogashira coupling  | 415 |
| 3.6.8 The Tsuji-Trost allylation  | 424 |
| 3.6.9 Coupling reactions not involving a C–C bond formation                         | 426 |
| 3.6.9.1 C–N bond-forming reactions  | 426 |
| 3.6.9.2 C–O bond-forming reactions  | 429 |
| 3.6.9.3 C–S bond-forming reactions  | 430 |
| 3.6.10 Conclusions and outlook  | 431 |
| References  | 432 |
| <b>3.7 Multicomponent reactions</b>   |     |
| 3.7.1 Introduction  | 443 |
| 3.7.2 Carbonyl-based multicomponent reactions                                       | 444 |
| 3.7.2.1 Formation of 6-membered rings with multicomponent reactions                 | 444 |
| 3.7.2.2 Formation of 5-membered rings with multicomponent reactions                 | 453 |
| 3.7.2.3 Formation of aliphatic bonds  | 459 |
| 3.7.3 Isocyanide-based reactions  | 464 |
| 3.7.3.1 Isocyanide-based MCRs for the preparation of 5-membered rings               | 466 |
| 3.7.3.2 Isocyanide-based MCRs for the preparation of 5- and 6-membered heterocycles | 469 |
| 3.7.3.3 Aliphatic bond formation  | 475 |
| 3.7.4 Conclusions and outlook   | 479 |
| References  | 480 |

### 3.8 Ring transformations by heterogeneous catalysis

|         |                                       |     |
|---------|---------------------------------------|-----|
| 3.8.1   | Introduction                          | 491 |
| 3.8.2   | Cyclization                           | 492 |
| 3.8.2.1 | Intermolecular cyclization reactions  | 492 |
| 3.8.2.2 | Intramolecular cyclization reactions  | 508 |
| 3.8.3   | Ring opening reactions                | 517 |
| 3.8.3.1 | Ring opening of small heterocycles    | 517 |
| 3.8.3.2 | Ring opening polymerization           | 525 |
| 3.8.3.3 | Other types of ring opening reactions | 529 |
| 3.8.4   | Conclusions and outlook               | 530 |
|         | References                            | 530 |

### 3.9 Heterogeneous catalytic rearrangements and other transformations

|         |   |     |
|---------|---|-----|
| 3.9.1   | Rearrangements                                | 543 |
| 3.9.1.1 | Beckmann rearrangement                        | 543 |
| 3.9.1.2 | Fries rearrangement                           | 548 |
| 3.9.1.3 | Epoxide rearrangements                        | 549 |
| 3.9.1.4 | Ferrier rearrangement                         | 551 |
| 3.9.1.5 | Johnson-Claisen rearrangement                 | 552 |
| 3.9.1.6 | The <i>ortho</i> -Claisen-rearrangement       | 552 |
| 3.9.1.7 | Benzylimine-benzaldimine rearrangement        | 553 |
| 3.9.1.8 | Pinacol rearrangement                         | 554 |
| 3.9.1.9 | Baeyer-Villiger oxidation                     | 554 |
| 3.9.2   | Aldol and related reactions                   | 556 |
| 3.9.2.1 | The aldol reaction                            | 556 |
| 3.9.2.2 | Mukaiyama reaction                            | 558 |
| 3.9.3   | Condensations                                 | 558 |
| 3.9.3.1 | Schiff-base formation                         | 558 |
| 3.9.3.2 | Knoevenagel condensation                      | 563 |
| 3.9.3.3 | Pechmann condensation                         | 566 |
| 3.9.3.4 | Aldol condensation                            | 568 |
| 3.9.4   | Hydrolysis                                    | 573 |
| 3.9.4.1 | Hydrolysis of cellulose                       | 573 |
| 3.9.5   | Introduction and removal of protecting groups | 574 |
| 3.9.6   | Hydroformylations                             | 577 |
| 3.9.7   | Conclusions and outlook                       | 580 |
|         | References                                    | 580 |

### 3.10 Asymmetric synthesis by solid catalysts

|          |                     |     |
|----------|---------------------|-----|
| 3.10.1   | Introduction        | 593 |
| 3.10.2   | Oxidation reactions | 594 |
| 3.10.2.1 | Epoxidation         | 594 |
| 3.10.2.2 | Dihydroxylation     | 596 |
| 3.10.2.3 | Other oxidations    | 598 |

x Contents

|  |         |
|--|---------|
| <b>3.10.3 Hydrogenation</b>                              | 599     |
| 3.10.3.1 Reduction of carbonyl compounds                 | 600     |
| 3.10.3.2 Reduction of C=C double bonds                   | 614     |
| <b>3.10.4 Aldol-reaction and related chemistry</b>       | 618     |
| 3.10.4.1 Aldol reactions                                 | 619     |
| 3.10.4.2 Michael additions                               | 624     |
| 3.10.4.3 Henry reactions                                 | 629     |
| <b>3.10.5 Multicomponent and various other reactions</b> | 630     |
| 3.10.5.1 Multicomponent reactions                        | 630     |
| 3.10.5.2 Cascade and tandem reactions                    | 632     |
| 3.10.5.3 Other reactions                                 | 634     |
| <b>3.10.6 Conclusions and outlook</b>                    | 640     |
| <b>References</b>  | 640     |
| <br>Index  | <br>655 |

## Preface

The commencement of the idea and concept of this book has been on my mind (BT) for quite some time. As a graduate student, I worked in the overlapping area of organic chemistry and heterogeneous catalysts, and one of the most comprehensive books that surveyed this research field was Augustine's *Heterogeneous Catalysis for the Synthetic Chemist*. Although it has been an invaluable resource for a generation of scientists, this book has been published a quarter of century ago (in 1996) and a new edition never came. Since then, extensive developments occurred in heterogeneous catalysis including its broadening applications in synthetic and industrial chemistry. With this book, we intended to follow the footsteps of Professor Augustine and provide a useful resource for those who work in organic synthesis and use heterogeneous catalytic methods, and also those who are synthetic chemists but new to the application of solid catalysts in their work. The book is intended for a broad audience including researchers working in industry and academia. It is aimed to deliver a synthesis-oriented heterogeneous catalytic text that also takes the principles of Green Chemistry into account. Although heterogeneous catalysis began its contribution to the development of environmentally benign synthetic processes well over a century ago, the formulation of the conscious Green Chemistry principles did not occur until the mid-1990s. Thus, interestingly, the time period our work surveys (1996–2021) witnessed the intertwinement of heterogeneous catalysis and Green Chemistry. The main goal of the work was to show an as broad as possible snapshot of synthetic heterogeneous catalysis in the review period and consider the surveyed protocols keeping in mind the contemporary aspects of Green Chemistry. The book includes three distinct parts: the first part describes the historical aspects of heterogeneous catalysis and its becoming a vital part of green synthesis developments. It also covers the basic definitions of catalysis, especially those that are focused not only on catalysis but also its heterogeneous applications. The next part gives an overview of solid catalysts, including metal catalysts and nonmetallic alternatives, such as metal oxides, synthetic, and natural aluminosilicates, polymer-based solid acids and bases, and several emerging types of catalytic materials, such as nanoparticles, metal-organic frameworks, or covalent-organic frameworks. The centerpiece of the most extensive part of the book is heterogeneous catalysis in practical synthesis. This third part describes the relevant examples of the most common processes where heterogeneous catalysis is applied: hydrogenation, hydrogenolysis, oxidation,

metathesis, cross-coupling reactions, Friedel-Crafts, and multicomponent reactions just to name a few, all of them are common in organic synthesis. These subchapters are in-depth reviews on these topics. However, we must admit that the material available in the literature is overwhelming, thus we focused on providing a broad picture with representative examples, rather than attempting to write comprehensive chapters on these individual methods. Each would fill a separate book on its own. We hope that the book will serve as a primary resource for those who are new to heterogeneous catalytic synthesis and those who intend to branch out and discover other topics that are related to their own research fields.

Finally, we thank our colleagues, editors at Elsevier, for contributing to this unique endeavor: Anneka Hess who helped us through the proposal phase of the book and Sruthi Satheesh, who handled the galley proofs. Although, we had several editorial project managers throughout the project, we are particularly grateful to Emily Thomson, our final Editorial Project Manager for her help in ushering the work to completion.

Béla Török  
Christian Schäfer  
Anne Kokel

## Chapter 1

# Heterogeneous catalysis for organic synthesis: Historical background and fundamentals

### 1.1. Introduction and historical background

The phenomenon of catalysis itself has been around in the form of fermentation (i.e., bio-catalysis) for thousands of years. The earliest written report on a catalytic reaction was published in 1552 by Cordus, who carried out the dehydration of alcohol to ether.<sup>1</sup> The roots of modern catalysis originate from over two hundred years ago when Elizabeth Fulhame described the concept of catalysis in her 1794 essay regarding her experiments on oxidation-reduction, suggesting that a small amount of water was required for the reaction to occur.<sup>2,3</sup> There were several others who later observed and reported catalytic reactions, such as Parmentier, Kirchhoff, or Döbereiner, who focused on the hydrolysis of starch, and also described the decomposition of potassium chlorate catalyzed by manganese dioxide.<sup>4-6</sup> There have been many more who contributed to the developments. One of the most important ones was when the term catalysis was coined by the Swedish chemist, Berzelius, in 1835.<sup>7</sup> The significant breakthrough that gave a major push to the development of heterogeneous catalysis occurred at the end of the 19th century when Paul Sabatier carried out his experiments regarding catalytic hydrogenation on Ni/kieselguhr.<sup>8</sup> This discovery, with his other contributions, earned Sabatier the Nobel Prize in Chemistry in 1912.<sup>9</sup> In addition to developing catalytic hydrogenation, which became a new field of organic synthesis, he also made several fundamental observations, such as that the particle size of Pt significantly changed its activity/reaction rates, that became a common knowledge in heterogeneous catalysis. By the early 1900 similar observations were made regarding other metals or, in general, other catalytic substances.<sup>10</sup> Sabatier's experiments with metal catalysts, especially with Ni, generated considerable interest in the field and shortly new applications, such as the development of the Raney Ni catalyst, revolutionized metal catalysis.<sup>11-13</sup>

Just like Sabatier was the pioneer of heterogeneous metal catalysis, Vladimir Ipatieff earned the same distinction for his studies using nonmetal or solid acid catalysts ( $\gamma$ -alumina) in the early 1900s.<sup>14</sup> The two scientists worked in parallel

## 2 Heterogeneous catalysis in sustainable synthesis

and spearheaded the development of the two main directions of heterogeneous catalysis independently. Among Ipatieff's many contributions, he studied the dehydration of alcohols to alkenes (e.g., ethanol to ethylene), butadiene synthesis, development of catalysts for hydrogenation, the discovery of oligomerization, paraffin alkylation, and acid-catalyzed aromatic alkylation. To be successful he had to develop a special technique using high pressure in steel autoclaves, a major tool that he introduced to heterogeneous catalysis. Unlike Sabatier, Ipatieff's focus was more on commercial applications. As a milestone in his achievements he has developed the process that produced high octane (about 100 octane number) gasoline that was used by the British Air Force during WWII and aided them to succeed in the aerial battle over Great Britain.<sup>15, 16</sup> Following Ipatieff's introduction of  $\gamma$ -alumina as a catalyst, the field underwent an explosion-like development, new acidic solids were developed and applied as heterogeneous acid catalysts.

The earlier mentioned practical developments also initiated extensive research at the mechanistic side of catalysis, particularly in finding explanations for the observed phenomena. Early efforts by Duclaux, Moissan, or Ostwald<sup>17</sup> were followed by other researchers, many of whom focused on heterogeneous catalysis and the surface phenomena occurring on catalysts. Starting with the measurement of solid surfaces, such as the Brunauer-Emmett-Teller (BET) surface area,<sup>18</sup> several explanations were reported to elucidate surface phenomena, including the Langmuir-Hinshelwood,<sup>19, 20</sup> Eley-Rideal,<sup>21</sup> or Horiuti-Polanyi mechanisms.<sup>22</sup> Later, in the 1960s, these investigations led to the development of a new field, commonly referred to as surface science,<sup>23</sup> pioneered by Ertl<sup>24</sup> and Somorjai.<sup>25</sup> Since then, heterogeneous catalysis research became a widespread field within the overlapping areas of chemistry, chemical engineering, and surface science. Contemporary developments added material science to this company, as many new materials, such as carbon nanostructures (nanotubes, graphene, graphene oxide, etc.), metal-organic frameworks, covalent organic frameworks, synthetic zeolites, or clays, that hold significant promise in catalyst development have been prepared. The history and development of catalysis, including heterogeneous catalysis, has attracted the attention of many educators, science historians, and active researchers as well, and have been extensively reviewed.<sup>26-31</sup> The reader is advised to consult with these accounts for more details.

Catalytic processes are major contributors to the green chemistry movement, including sustainable synthesis, renewable fuel production, or environmental protection, e.g., automotive applications. Catalytic processes can replace the use of nonrenewable, low atom economy reagents, significantly decreasing the environmental impact of the production of pharmaceuticals or fine chemicals. Catalysis also contributes to the fulfillment of several principles of green chemistry and green engineering.<sup>32, 33</sup>

Based on the importance of these methods, they have been frequently reviewed. There are many seminal books<sup>34-40</sup> and major accounts<sup>41-43</sup> that time

to time provided extensive background regarding these processes. One of these books, Augustine's *Heterogeneous Catalysis for the Synthetic Chemist*,<sup>44</sup> was focused on the application side of heterogeneous catalysis, with particular attention to processes that are related to organic synthesis. Although it is an excellent summary of the progress until its publication in 1996 it has been published 25 years ago and several processes, such as metathesis or cross-coupling reactions, are not covered in it. Our goal in this book was to give an up-to-date description about heterogeneous catalytic processes used for the synthesis of fine chemicals and pharmaceuticals, and provide representative illustrations of the contemporary advances made in the application of these methods in environmentally benign and sustainable synthesis.

The following parts of this chapter describe the fundamentals of catalysis with several terms and definitions that are necessary to understand the forthcoming chapters.

## 1.2. Catalysis

Catalysis, whether in its homogeneous or heterogeneous form, has been a major contributor to green chemistry in general, and to sustainable synthesis in particular. Catalytic processes make the traditional nonrenewable, low atom economy, wasteful protocols obsolete and provide green alternatives to often century-old protocols. The use of catalysis supports the fulfillment of the generic Green Chemistry principles in more than one way; it contributes to several points as listed here with the condensed descriptions: 1 (prevent waste), 2 (maximize atom economy), 5 (limit auxiliary substances), 6 (energy efficiency), 8 (reduce derivatives), 9 (catalysis), and 12 (safer chemistry) from the twelve points of Green Chemistry.<sup>32,33</sup> In addition to Green Chemistry principles, heterogeneous catalysis contributes to the improvement of the engineering aspects of chemical processes as well, according to similar principles of Green Engineering. For example, principles 2 (waste prevention), 3 (design for separation), 4 (maximize efficiency), 8 (minimize excess), and 10 (integrate material and energy flows) are all improved by the application of heterogeneous catalysis.<sup>45</sup> In order to provide a clear introduction for those who are unfamiliar with the terms of catalysis, particularly those of heterogeneous catalysis, in the following subchapters we describe the basic definitions and fundamentals of this field.

### 1.2.1 Fundamentals and basic definitions

#### 1.2.1.1 Catalyst and catalytic cycle

A *catalyst* is a compound or material that enables a chemical process to occur, without being changed by the end of the process. It must be a natural or synthetic substance; light, heat, or other forms of energy (e.g., microwave irradiation, ultrasounds, etc.), cannot be considered catalysts. After the first reaction is completed, the catalyst returns to the beginning of the process and initiates

#### 4 Heterogeneous catalysis in sustainable synthesis

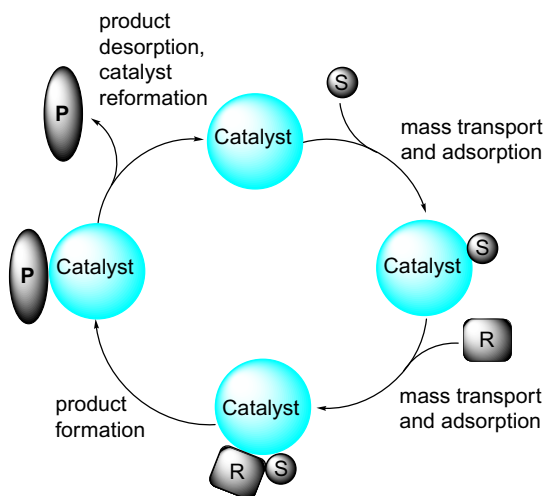


FIG. 1 A generic scheme of a catalytic cycle with the elementary steps.

a new reaction. These reactions are called *catalytic cycles* (Fig. 1). It must be noted, however, that this is the ideal picture. Many catalysts eventually undergo an irreversible change due to unintended and undesirable phenomena. These could be due to the reaction conditions, heat, active component leaching out of a reactor, and many others.

The major role of a catalyst is to alter the original noncatalytic reaction pathway into a series of lower energy demanding processes, called *elementary steps*. While doing this, by changing the reaction mechanism, the catalyst often increases the rate of the reactions as well. The elementary steps and their combination to a catalytic cycle are illustrated in Fig. 1.

Catalysts come in many different forms, some are single atoms<sup>46,47</sup> or small compounds such as acids or bases,<sup>48</sup> some are larger such as metal complexes<sup>49,50</sup> or even supramolecular assemblies including enzymes or metal-organic frameworks,<sup>51–53</sup> others are elements in different forms.<sup>54</sup> Catalytic materials are commonly distinguished based on their solubility, whether they are soluble in the reaction medium (*homogeneous catalysis*) or they are largely insoluble solids (*heterogeneous catalysts*). In this book we will focus on the application of heterogeneous catalysis, thus the emphasis in this chapter will be on the solid catalytic materials.

##### 1.2.1.2 Activation energy

In the course of a chemical reaction, chemical bonds are cleaved and new bonds made. As all chemical bonds possess an energy content to keep the atoms together, that energy needs to be provided to cleave a bond and initiate a reaction. The energy that is required to initiate a reaction is called the *activation energy*

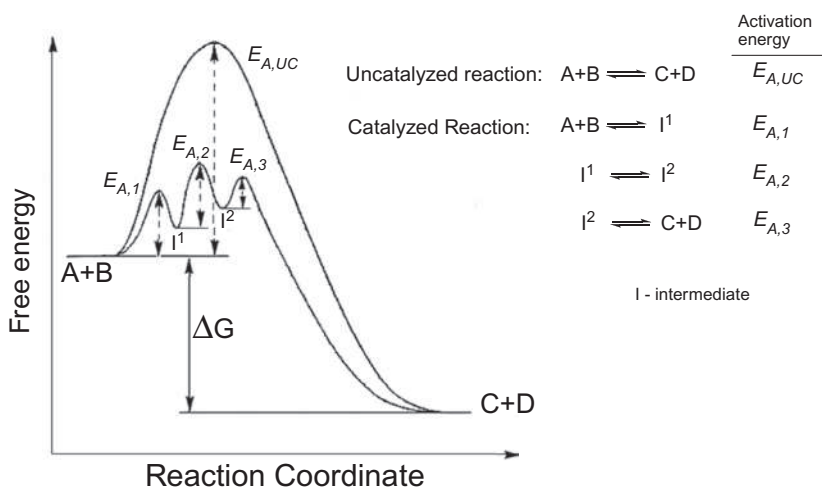


**FIG. 2** Illustration of the energy profile of a hypothetical catalytic and noncatalytic reaction.

(*EA*). Typically, the activation energy of a noncatalytic reaction is significantly higher than that of a catalytic reaction. The catalyst alters the reaction mechanism to separate elementary steps that require significantly lower activation energy as illustrated in Fig. 2.

In addition to explaining the major role a catalyst plays in a chemical process, Fig. 2 also points out that the application of a catalyst does not modify the basic thermodynamic features of the process. The overall energy of the substrates and the final products will not be altered by the presence of a catalyst, thus catalysis is a kinetic phenomenon. Typical catalysts increase the rate by three orders of magnitude; biocatalysts, however, are able to produce  $10^{20}$  times rate increase. The kinetic nature of the catalytic action also means that if a process is an equilibrium reaction the use of a catalyst allows to achieve the equilibrium faster, but the equilibrium constant remains the same.

### 1.2.1.3 Other definitions

In addition to the earlier mentioned basic definitions, there are several other important terms that describe the efficiency and selectivity of catalysts.

*Reaction rate.* The reaction rate in the case of catalytic reactions is often described by the *turnover frequency* (TOF). When a catalyst is contributing to a reaction it is released after one catalytic cycle and returns to initiate another one. When the number of catalytic cycles are normalized for one catalytic unit, such as an active site or an active metal complex, the number of cycles run is called *turnover number* (number of reactions/active center). When the number of turnovers is also normalized for a time unit (TON/time = TOF) one can characterize the rate of the reaction.

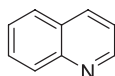
## 6 Heterogeneous catalysis in sustainable synthesis

*Lifetime.* As mentioned already, ideally the catalyst should remain unaltered after a catalytic cycle; however, in real-life experiments catalytic substances undergo changes that include deactivation. Some of the changes are chemical (reduction, oxidation, functionalization, etc.) while others are physical (particle size increase or decrease); nonetheless, they will result in undesirable changes in activity and/or selectivity. The factor of how long a catalyst can function without major changes in its performance is the catalyst's *lifetime*. This is often expressed by the turnover number (TON) up to the point when the performance starts declining.

*Catalyst poisons.* The specific features of a catalyst can be fundamentally and negatively altered by certain changes the catalyst undergoes during a reaction. When these changes are caused by chemical agents then we talk about catalyst poisoning and the agent is a catalyst poison. These compounds not only bind very strongly, often irreversibly, to the catalyst, but they also bind to the active center that will become partially or completely inactive. The strong adsorption means that a minute amount of these compounds can alter the activity significantly, which highlights the need for high purity starting materials and solvents. For example, organosulfur compounds deactivate most noble metal catalysts, thus all sulfur-containing impurities must be removed from the starting material. This is a common problem not only in heterogeneous catalytic synthesis but also in the automotive industry as well, as most reactants and fuels of petrochemical origin could contain sulfur. Catalyst poisoning can be accidental, natural, or intentional. In the first case, the poison enters the catalytic system accidentally, for example from the atmosphere or via a contaminated solvent and shuts it down. This is often the case with sulfur- or nitrogen-containing compounds. In the second case, the catalyst poison is gradually deposited or building up on the surface of the catalyst throughout the reaction, such as the formation of surface carbonaceous deposits, that is typical for solid catalysts, for example supported metals or zeolites.<sup>55</sup> The third case is when the catalyst is intentionally and partially poisoned as a part of the design process, in order to modify its activity and/or selectivity. By the selective poisoning of a catalyst, its activity and selectivity can be fine-tuned and undesirable side or successive reactions can be blocked, and in parallel, the yield of the target product can be improved. A typical example is the Lindlar catalyst (Pd/CaCO<sub>3</sub> is partially poisoned with Pb(OAc)<sub>2</sub> and quinoline) that can selectively hydrogenate alkynes to alkenes (Fig. 3).<sup>56</sup>

### Lindlar catalyst

5% Pd/CaCO<sub>3</sub>  
+  
Pd(OAc)<sub>2</sub> and



quinoline

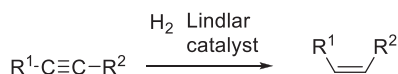


FIG. 3 The Lindlar catalyst and its use for the partial hydrogenation of alkynes to alkenes.

*Chemical promoters.* Additives can also play the opposite role and significantly improve the activity and/or selectivity of an otherwise imperfect catalytic material. These additives are called promoters. *Chemical promoters* enhance the activity and selectivity of catalysts by altering the electron density/distribution on the surface of the catalyst. The typical example of chemical promoters is molybdenum that is used in improving the catalyst of ammonia synthesis. In this process the main catalyst is iron and a small amount of molybdenum is used as a chemical promoter.<sup>57</sup> Another example is the methanol synthesis from syngas where the most common catalyst is Cu-ZnO that is made better by chromium oxide (Cr<sub>2</sub>O<sub>3</sub>) as a promoter.<sup>58</sup> Other materials are used as *structural promoters* as they improve formulation, general mechanical properties, and stability of catalysts.<sup>59</sup> Structural promoters can prevent *sintering* (the formation of large particles that would decrease the active surface of the catalyst) and maintain the particle size of the catalysts.<sup>60</sup>

*Catalyst reuse, regeneration, and recycling.* Although catalyst deactivation, whether by poisoning or other physical changes, is an undesirable phenomenon, it is part of the laboratory and industrial practice. Due to the often expensive nature of catalysts, the process chemistry protocols for batch systems commonly attempt to reuse the catalyst after one batch is completed.<sup>61</sup> Sometimes catalysts can be reused in several cycles without meaningful drop in their performance; however, in many other cases, significant deactivation is observed even after one run. When that occurs, the potential regeneration of the catalyst is investigated. Reactivation is commonly carried out by periodical physical (heat, surface cleaning by ultrasounds, etc.) or chemical (oxidation, reduction, etc.) treatment to restore the original activity.<sup>62</sup> However, despite all efforts, at some point catalysts reach the end of their lifetime. Due to the often expensive rare metals used as catalysts the so-called spent catalysts are also recycled, which, in this context, means that the spent catalysts are collected and returned to industrial recycling facilities, where using a variety of methods the noble metals can be separated from the support material and recycled back to their bulk metal form, which then can reenter the catalyst production pipeline. The catalyst end-of-lifetime recycling is particularly desirable, it is economic, and also environmentally conscious, as it spares the waste deposition facilities/landfills and ultimately the water supply (through ground water) from the toxic heavy metal contamination.<sup>63, 64</sup> These processes are extended beyond the catalysts used in the chemical industry to automotive catalysts as well. This is a particularly important issue due to the large volume of automotive exhaust catalysts used.<sup>65</sup>

*Selectivity.* Describes the catalyst's ability to carry out a chemical process to produce the major expected product in high excess compared to all other by-products. Selectivity is a general term that includes several specific subcategories (Fig. 4). An earlier book by Davis and Suib provided a detailed discussion of this issue, here we only discuss the most common terms.<sup>66</sup>

Having a substrate that includes more than one functional group the compound could undergo parallel and or subsequent reactions. *Chemoselectivity*

8 Heterogeneous catalysis in sustainable synthesis

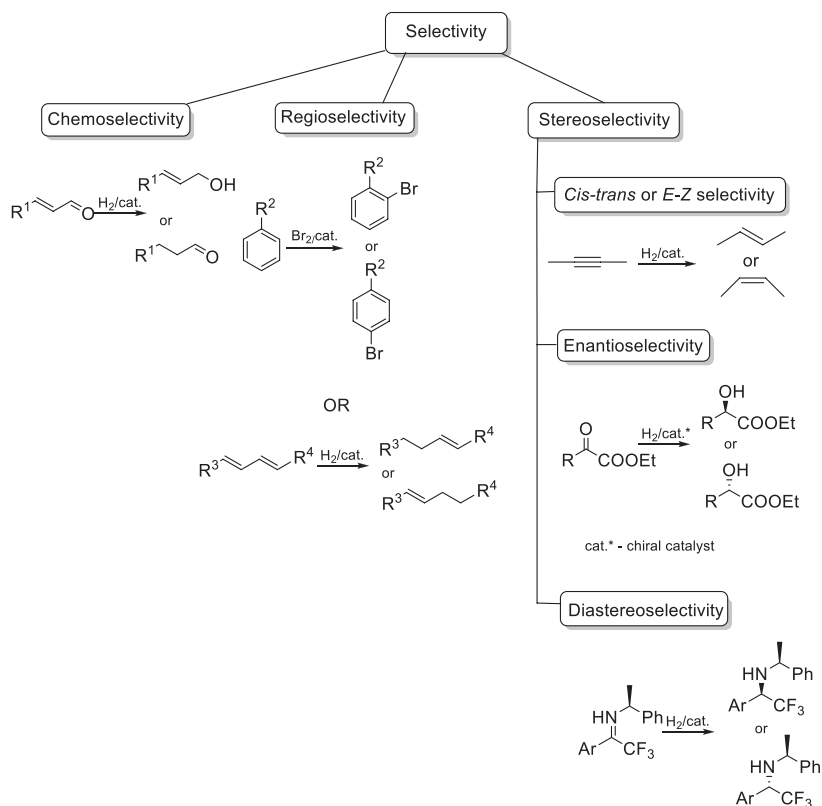


FIG. 4 Representative examples for different forms of selectivity.

describes how well the catalyst can facilitate the exclusive transformation of only one functional group while all others remain untouched. When the outcome of the reaction results in the formation of at least two different constitutional isomers we talk about *regioselectivity*. There are different examples for this subcategory. For example, in a typical catalytic bromination of substituted benzene derivatives with activating substituents, the *ortho*- (or 2-) and *para*- (or 4-) brominated products can form. In another example, the reaction could occur on the same functional groups in a compound, e.g., the hydrogenation of either of the C=C double bonds in dienes in different positions. In the case of asymmetric catalysis the reaction produces chiral compounds; *enantioselectivity* will describe the ratio of the two enantiomers with descriptive factors such as enantiomeric excess (ee) or enantiomeric ratio (er). If a reaction is carried out on a prochiral functional group in a starting material that already possesses a chiral center, the products are called diastereomers and their ratio is described by the *diastereoselectivity*. Although some catalysts exhibit high activity and selectivity at the same time, high activity catalysts often do not discriminate between

different functional groups or the location of the same functional group, hence they will exhibit low selectivity. Along the same line, low activity catalysts can often distinguish between reacting groups based on minor differences and will show high selectivity. Thus activity and selectivity are generally in an inverse relationship.

*Type of catalysis.* Catalytic processes are characterized based on the phase of the catalyst in the reaction medium, mostly on their solubility in the solvents. Traditionally, they are placed into three main groups, which are *homogeneous*, *heterogeneous*, and *phase transfer* catalysts. The distinction between homogeneous and heterogeneous catalysis is obvious; if the catalyst is soluble, then homogeneous, if not, heterogeneous is the case. Phase transfer catalysis is somewhere in between and is neither of the earlier two; the catalyst's function is to ensure mass transport through the phase boundary of the two solvents in the system.

*Catalysts.* Catalytic materials include a broad range of materials from simple mineral acids, and soluble metal complexes, bulk or supported metals, metal oxides, natural or synthetic aluminosilicates to highly organized synthetic materials such as metal-organic frameworks or biocatalysts. Here, we will not discuss catalysts further as Chapter 2 is dedicated to the description of catalysts, with exclusive highlight on heterogeneous catalysts, given the focus of this book.

### 1.2.2 Heterogeneous catalysis

By definition, in a heterogeneous catalytic process, the catalyst and the reaction mixture are present in different phases. The most common example, especially for laboratory applications, is when the catalyst is solid and the reaction mixture is in a solvent (solid/liquid (S/L) reactions). Although these systems are popular in industrial applications as well, the solid/gas (S/G) reactions are perhaps even more prevalent in industry, especially in large-scale operations such as those in the petrochemical industry (e.g., isomerization, cracking) or the oxidation of sulfur to SO<sub>3</sub> during the production of sulfuric acid. There are special applications, both at laboratory and industrial scales, when all three phases, solid-liquid and gas (S/L/G), are involved in a reaction. Examples include the widely used hydrogenation or hydroformylation reactions.

Heterogeneous catalytic processes possess several advantages. One of the most commonly mentioned benefit is that the catalysts are solid and can easily be separated from the reaction medium, whether it is a liquid or gas. This aids in the removal of the catalyst from the product and facilitates easy recovery and reactivation if needed, promoting catalyst recycling and thus could decrease the environmental impact and improve the sustainability of a process. Solid catalysts are commonly not moisture or oxygen sensitive, and thus have longer shelf life and stability than the sensitive metal complexes.

However, heterogeneous catalysts also have their own drawbacks. While in homogeneous catalysis every dissolved catalytic species is considered an

active center, regarding solid catalysts, a considerable part of the material is buried under the surface where the reactions occur. This phenomenon decreases the number of available active centers, which decreases the activity (per unit weight). Another common issue is the mass-transport limitation, which refers to the necessity of the substrates and reacting partners to be transferred to the surface of the catalyst for the reaction to occur. This phenomenon is particularly of concern when three-phase systems, such as hydrogenations, are applied. Another serious issue is the use of special preparation techniques, particularly for industrial catalysts. Although every step of a catalyst's preparation has its own importance, the process is often considered an art form. Since the preparation conditions have strong influence on the characteristics and thus the performance of the catalyst, minor alterations in the synthetic process could result in notable changes in performance.

### 1.2.2.1 Catalytic surfaces

As in heterogeneous catalysis all reactions occur on the surface of the catalyst, whether it is the outer surface or the internal surface of porous materials; the surfaces possess a role of primary importance in this field. The chemical and physical nature of the surface will essentially determine the mechanism of surface interactions and ultimately lead to the product formation. Studying reactant-surface interactions is an important field that attracted significant attention over the past several decades even before the establishment of surface science as a specific area of research.

### 1.2.2.2 Physical and chemical adsorption

Independently of the catalyst itself, the interaction of the catalyst's surface with the substrate(s) is of utmost importance in heterogeneous catalysis. A substrate must interact with the surface to initiate any transformation. *Adsorption* is the process through which the catalysts form a surface complex with the substrate(s), which is the first step of every heterogeneous catalytic process. Once the surface reaction is complete, the product undergoes *desorption*.<sup>67</sup> In an effective process, the adsorption capability of the substrate is much greater than that of the product, thus ensuring that once the reaction is complete the substrate can replace the product on the catalyst's surface. Any compound that is to participate in such a process must be able to adsorb on the surface. The process of adsorption can occur by *physisorption* when simple, and usually weak physical bonds develop between the surface and the compound. Such weak interactions occur between, e.g., nonpolar compound and surfaces, such as the nitrogen adsorption on surfaces that enable the determination of the physical surface area of a catalyst, commonly known as the BET surface (vide supra).<sup>18</sup> Different and much stronger interaction drives *chemisorption*, when the substrate-surface interaction is due to chemical forces, such as acid-base, nucleophilic-electrophilic interactions that are commonly based on the electronic processes. For example,

many hydrogenation processes begin with the adsorption of a C=X double bond where the electron-rich double bonds make contact with the partially electron deficient metal surface. While the adsorption of the substrate(s) must occur through an interaction of considerable strength, it must remain a reversible process. If the adsorption is irreversible then the compounds would stay on the catalyst's surface for indefinite time, blocking the sites from further substrate molecules, thus deactivating the catalysts. Essentially, irreversible adsorption is a characteristic of catalyst poisons.

### 1.2.2.3 *The active site of solid catalysts*

The concept of the active sites of catalysts was put forth by Taylor in the 1920s.<sup>68</sup> Essentially the active site is a group of atoms that catalyzes a reaction. Taylor suggested that these active sites are in a relatively small number compared to the number of the atoms in the bulk of the catalysts.<sup>69</sup> Modern surface science measurements confirmed Taylor's original hypothesis, namely that a catalyst is a largely inactive surface with comparatively few active spots.<sup>70</sup> It is also known that these active sites come in many different shapes, such as single or multiatom sites, surface clusters, kinks, terraces, steps, and most of these come with additional defects when commonly one or more atoms are vacant.<sup>71</sup> The active sites should have appropriate adsorptive capability and substrate adsorption would follow the Sabatier principle; the substrate needs to be able to adsorb and desorb as the product from the active site. In addition to the adsorption strength, later it has been suggested that active sites can catalyze *structure-sensitive* (otherwise called demanding) and *structure-insensitive* (facile) reactions.<sup>72</sup> Structure-sensitive reactions are dependent on the geometry and/or crystallographic orientation of the active site, while structure-insensitive reactions occur independently of the shape/form of the active site. This initiated broad-ranging studies in heterogeneous metal catalysis when different metal single crystals and atomically precise nanoclusters are applied to mimic different active sites.<sup>73–75</sup> Later, mechanistic investigations for reactions carried out on supported metal catalysts used single crystal studies for comparative analyses.

The active site has a somewhat different nature in solid acid-base catalysts, such as metal oxides, zeolites, or clays. Instead of focusing on special geometric formations on the surface of the metal, here the active site is commonly identified as a Brønsted or Lewis acid or base site.<sup>76–79</sup>

### 1.2.2.4 *Anchoring effects*

There are a broad range of examples when one component of a commonly bifunctional catalyst serves as a specific anchoring moiety for the substrate and through that interaction ensures that the other component of the catalyst can execute the actual reaction. The anchoring can occur through a variety of interactions, such as acid-base, hydrogen bonding, or simple van der Waals forces.

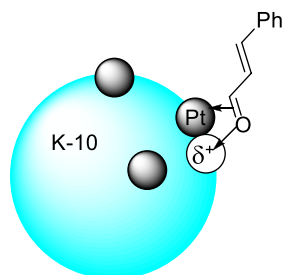


**FIG. 5** Anchoring effect of the Lewis acid centers of K-10 montmorillonite that ensures the chemoselective adsorption of the carbonyl group of cinnamaldehyde and the selective formation of cinnamyl alcohol (>99% selectivity) in the hydrogenation.

One of the most common examples is the chemoselective hydrogenation of  $\alpha,\beta$ -unsaturated carbonyl compounds, which is a process of practical importance in the fragrance industry.<sup>80</sup> The hydrogenation of these substrates on generic metal catalysts commonly occurs on the C=C bond before the C=O bond would undergo reduction. Using a special support with reasonably strong Lewis acid centers would selectively anchor the more electron-rich carbonyl group and ensure that the hydrogenation of this group would proceed selectively (up to 99%) leaving the C=C bond intact (Fig. 5).<sup>81</sup>

#### 1.2.2.5 Experimental variables

As mentioned before, heterogeneous catalytic transformations occur in a liquid or gaseous reaction mixture while the catalyst is a solid material. In most processes of synthetic importance, the reaction medium is a liquid, thus here we focus on liquid-phase reactions. Therefore the role of the *solvents* in these reactions is of utmost relevance. The solvent could possess several roles in a heterogeneous catalytic reaction. Its primary role is to dissolve the substrate and ensure that the substrate can be transported to the surface of the catalyst where the reaction would occur. If the reaction is a three-phase system (e.g., hydrogenation with a solid catalyst/liquid solvent/gaseous hydrogen) then the solvent should be able to dissolve the gas as well, although with proper agitation the metal particles can adsorb the hydrogen at the liquid/gas phase border as well. The solvent does not have to dissolve the substrate completely, a reasonable solubility can guarantee an efficient process. However, it is expected that the product is soluble in the solvent, otherwise the product will remain on the surface of the catalyst after a complete cycle and will block the active centers. In addition to dissolving the substrate(s), the solvent could have other important contributions to the success of a catalytic reaction. For example, it can act as an agent that modifies one of the reaction participants. For example, in the Pt-catalyzed cinchona alkaloid-modified heterogeneous catalytic hydrogenations of  $\alpha$ -ketoesters, acetic acid was found to be the best solvent. The broadly accepted explanation is that the acid protonates the basic quinuclidine nitrogen

of the alkaloid and enables it to form a complex with the carbonyl group of the ketoester.<sup>82</sup> The solvent itself can also serve to trap an intermediate or a product to inhibit successive reactions that may decrease the yield or selectivity. Although these examples indicate that the solvent may participate in the reaction, it should not strongly adsorb on the catalyst's surface, otherwise, due to its large excess it could block the adsorption of the substrate(s).

The application of nontraditional activation methods, particularly microwave-assisted organic synthesis, enabled the preparation of a broad variety of compounds under *solvent-free* conditions. The specific microwave absorbing ability of the support K-10 montmorillonite and similar catalysts ensured effective internal heating of the system and a simple protocol provided several N-heterocyclic compounds, such as pyrroles,<sup>83–85</sup> quinolines,<sup>86,87</sup> pyrazoles,<sup>88–90</sup>  $\beta$ -carboline,<sup>91, 92</sup> benzodiazepines,<sup>93, 94</sup> and multicyclic products<sup>95</sup> in high yields, and in short (few minutes) reaction times.

The physical and chemical *properties of the catalyst* are also important experimental variables. The support (if supported catalyst), the particle size, and the pore volume/size/diameter are all vital in the design of a successful protocol. The catalysts are discussed in detail later in the book, and the reader is referred to [Chapter 2](#) regarding more information.

Many catalytic reactions are carried out in a system that includes at least one gas. In these reactions the *pressure* of the system often plays a crucial role in determining reaction rates, yields, and selectivities.<sup>96</sup> Many of these reactions are carried out under high-pressure conditions, while others work better in low-pressure environment. The role of the pressure is often determined by a competition regarding adsorption on the catalyst's surface. For example, in many hydrogenation reactions the substrate has an equal or lower adsorption capability than the reactant hydrogen; in such cases too high hydrogen pressure would sweep the reactant off the surface and the effect of the pressure on the conversion/yield is described by a maximum curve (Langmuir-Hinshelwood mechanism).<sup>97</sup> The effect of the pressure is also dependent on the type of reaction that occurs. Hydrogenation reactions prefer higher pressures, while dehydrogenation (or reactions that result in the loss of a gaseous product) rather proceed well at lower pressures. As a special case, some reactions are carried out in solvents that are gases at room temperature (e.g., ethane or CO<sub>2</sub>), but would turn to *supercritical fluids* under certain conditions. In these reactions an appropriate pressure and temperature should be applied to maintain the supercritical state of the medium. Heterogeneous catalysis in supercritical fluids attracted significant attention and have been extensively reviewed,<sup>98–100</sup> including applications regarding biobased technologies, such as biodiesel production.<sup>101</sup>

Nearly every chemical reaction, heterogeneous catalytic ones included, requires *activation* at some level. The activation energy for a reaction is commonly provided by increasing the *temperature*, which has a profound effect on the rate of reactions, heterogeneous catalytic ones included. The traditional convective heating is often ineffective and slow, and due to the uneven heating profile the

temperature gradient within a system could result in undesirable side reactions. A recent book provides an overview on nontraditional activation methods, including microwave and ultrasound irradiation; photo-, electro-, and mechanochemistry; and high hydrostatic pressure.<sup>102</sup> In addition, several reviews also summarize specific areas of this field related to heterogeneous catalysis, such as microwave-assisted organic synthesis,<sup>42, 103, 104</sup> sonochemistry,<sup>105–107</sup> photochemistry,<sup>108–110</sup> electrochemistry,<sup>111–113</sup> mechanochemistry,<sup>114–116</sup> and high hydrostatic pressure.<sup>117–119</sup> Although the efficacy of these methods has been broadly illustrated, one must not forget that not all of them work through generating internal heating and thus elevated temperatures. Ultrasounds, photo and electrochemistry, and high hydrostatic pressure initiate reactions by different mechanisms. The earlier referenced book and reviews provide detailed description of the mode of action of these activation methods.

### 1.2.2.6 Catalytic reactors

Heterogeneous catalytic reactions are generally carried out in two different reactor systems: batch reactors and flow reactors.<sup>120</sup> Depending on the actual process both systems possess their own benefits as well as disadvantages.

*Batch reactors* are highly popular in laboratory-level syntheses, and certain industrial processes, such as many catalytic hydrogenations, are carried out in a batch reactor.<sup>121</sup> These reactors are finite volume systems that can be operated in an open or closed format. Depending on their use the reactors are made of a variety of materials, such as glass (mostly laboratory applications), stainless steel, with or without a Teflon liner, or monel (for high acidity reaction mixtures) just to name a few. When the reactor is applied in a closed format, the user may have the opportunity to operate under pressurized conditions, in which case the pressure can vary from 1 bar to several hundred bars.<sup>122, 123</sup> Most of the pressurized systems are applied for reactions when at least one component is a gas, such as hydrogenation or hydroformylation. Low-pressure (e.g., atmospheric) systems can be connected to a gas burette, and the user would be able to measure the consumed gaseous reactant, e.g., hydrogen, and thus these systems are quite useful for mechanistic and kinetic studies. These systems can also be applied in the reverse process; when a reaction releases a gas as product, the gas burette can measure the produced gas amount. High-pressure reactors are connected to gas tanks that supply the gases.

In all batch reactors *agitation* is a crucial issue. Many heterogeneous catalytic applications qualify as three-phase systems, with the catalyst being solid in a solvent with an additional gas. Only effective agitation can ensure that the mass transport limitations are properly addressed. Laboratory size systems can efficiently work with an internal magnetic spin bar, and an external magnetic stirrer, that can also serve as an external heating unit. The larger pilot plant or industrial units are stirred with external motor-operated turbines of various designs.<sup>44</sup>

Major advantages include the relatively simple design and handling; however, the separation and the potential recycling of the catalyst may present challenges. In addition, the potentially uneven heat profile of the reactor may cause overheating at the heating elements (usually the wall) and could result in undesired by-product formation.

The *flow reactors* represent the other major type.<sup>121</sup> Many catalytic reactions can be carried out in a continuous process by the application of flow reactors. Although the chemical industry used flow systems for a long time, especially for large-scale processes, now, laboratory-scale flow chemistry became highly popular.<sup>124</sup> In general, a flow reactor is based on a pump or set of pumps that will move the reactant mixture through a fixed or fluid bed reactor that is designed to block the catalyst's way out so it stays in place and at the end the product mixture is amassed in a collector. Flow systems can operate in several ways using liquid or gaseous mobile phase. In special applications (e.g., hydrogenation) the substrate is carried by a liquid mobile phase and the reactant hydrogen is added via a special valve system, thus even three-phase reactions can be applied. Several older and current designs are described in the literature.<sup>125, 126</sup>

Flow systems have several major advantages. One of the most important ones is that these reactors allow continuous production of chemicals.<sup>127</sup> In addition, the well-defined catalytic bed makes catalyst recycling and recovery relatively simple. For the modern laboratory-scale flow reactors the catalyst is supplied in the form of cartridges that can be easily replaced and moved to regeneration. The main disadvantage is that the potentially short residence time the reactants spend in the reactor may result in lower than expected conversion.

### 1.3. Conclusions and outlook

This introductory chapter summarized the brief history of catalysis and also described the most important characteristics of catalytic reactions, primarily focusing on heterogeneous catalysis, which is the main focus of this book. Many different terms and phenomena have been described with the goal of providing a short introduction to nonexperts into the realm of heterogeneous catalysis and make the terminology used in the upcoming chapters clear.

### References

1. Cordus, V. *Le Guidon des Apotiquaires: C'est à dire, la Vraye Forme et Maniere de Composer les Médicamens*; L. Cloquemin, E. Michel: Lyons, **1575**.
2. Ogilvie, M. B. *Women in Science: Antiquity Through the Nineteenth Century*, 4th print. ed.; MIT Press: Cambridge, MA, 1986; pp. 28–31.
3. Jarvis, C. Elizabeth Fulhame, a Forgotten Chemistry Pioneer. *Phys. Today* **2020**, 1945-0699.
4. Parmentier, A. A. *Expériences et Réflexions Relatives à l'Analyse du Blé et des Farines*; Paris, 1781.
5. Kirchoff, S. K. Die Verfertigung des Zuckers aus Buchweizen- und andere Mehlarthen. *Bull. Neusten. Wiss. Naturwiss.* **1811**, 10, 88–89.

16 Heterogeneous catalysis in sustainable synthesis

6. Döbereiner, J. W. Versuche Über die Gährung. *Schweiger J.* **1816**, 20, 213–214.
7. Berzelius, J. J. *Sur un Force Jusqu'ici Peu Remarquée qui est Probablement Active Dans la Formation des Composés Organiques, Section on Vegetable Chemistry*; Jahres-Bericht, 14, 1835; p. 237.
8. Sabatier, P. *La Catalyse en Chimie Organique Catalysis in Organic Chemistry (translated by Reidl, E. E.)*; Van Norstrand: Princeton, NJ, 1913; p. 923.
9. <https://www.nobelprize.org/prizes/chemistry/1912/sabatier/biographical/> (Accessed 30 October 2020).
10. Bertrand, G. Paul Sabatier and Catalysis. *Bull. Soc. Chim.* **1955**, 473–475.
11. Raney, M. *Catalytic Nickel*; US patent 1,563,587, 1925.
12. Raney, M. *Finely Divided Nickel*; US patent 1,628,190, 1927.
13. Raney, M. Hydrogenation: Catalysts from Alloys. Ni catalysts. *Ind. Eng. Chem.* **1940**, 32, 1199–1203.
14. Ipatiew, W. Zur Frage Über die Zersetzung des Äthylalkohols in Gegenwart verschiedener Katalysatoren. *J. Prakt. Chem.* **1903**, 67, 420–425.
15. Ipatieff, V. N. Aviation Gasoline by Polymerization and Alkylation of Cracking Gases. *Chem. Eng. News* **1942**, 20, 1367–1368.
16. Nicholas, C. P. Dehydration, Dienes, High Octane, and High Pressures: Contributions from Vladimir Nikolaevich Ipatieff, a Father of Catalysis. *ACS Catal.* **2018**, 8, 8531–8539.
17. Wisniak, J. The History of Catalysis. From the Beginning to Nobel Prizes. *Educ. Quím.* **2010**, 21, 60–69.
18. Brunauer, S.; Emmett, P. H.; Teller, E. Adsorption of Gases in Multimolecular Layers. *J. Am. Chem. Soc.* **1938**, 60, 309–319.
19. Langmuir, I. The Adsorption of Gases on Plane Surfaces of Glass, Mica and Platinum. *J. Am. Chem. Soc.* **1918**, 40, 1361–1403.
20. Hinshelwood, C. N. *Kinetics of Chemical Change in Gaseous Systems*, 3rd ed.; Clarendon Press: Oxford, 1933.
21. Eley, D. D.; Rideal, E. K. Parahydrogen Conversion on Tungsten. *Nature* **1940**, 146, 401.
22. Horiuti, J.; Polanyi, M. A Catalysed Reaction of Hydrogen With Water. *Nature* **1933**, 132, 819.
23. Duke, C. B. The Birth and Evolution of Surface Science: Child of the Union of Science and Technology. *Proc. Nat. Acad. Sci. U. S. A.* **2003**, 100, 3858–3864.
24. Ertl, G.; Rau, P. Chemisorption und katalytische Reaktion von Sauerstoff und Kohlenmonoxid an einer Palladium (110)-Oberfläche. *Surf. Sci.* **1969**, 15, 443–465.
25. Hagstrom, S.; Lyon, H. B.; Somorjai, G. A. Surface Structures on the Clean Platinum (100) Surface. *Phys. Rev. Lett.* **1965**, 15, 491–493.
26. Robertson, A. J. B. The Early History of Catalysis. *Platin. Met. Rev.* **1975**, 19, 64–69.
27. Lindström, B.; Pettersson, L. J. A Brief History of Catalysis. *CATTECH* **2003**, 7, 130–138.
28. Moulijn, J. A.; van Leeuwen, P. W. N. M.; van Santen, R. A., Eds. Catalysis: An Integrated Approach to Homogeneous, Heterogeneous and Industrial Catalysis. In *History of Catalysis*; Stud. Surf. Sci. Catal., Vol. 79; 1993; pp. 3–21.
29. van Santen, R. A. Catalysis in Perspective: Historic Review. In *Catalysis: From Principles to Applications*; Beller, M., Renken, A., van Santen, R. A., Eds.; 1st ed.; Wiley-VCH: Weinheim, 2012.
30. Prins, R. Eley-Rideal, the Other Mechanism. *Top. Catal.* **2018**, 61, 714–721.
31. Piumetti, M. A Brief History of the Science of Catalysis-I: From the Early Concepts to Single-site Heterogeneous Catalysts. *Chim. Oggi* **2014**, 32, 22–27.

32. Anastas, P. T.; Warner, J. C. *Green Chemistry: Theory and Applications*, Oxford University Press: Oxford, 1998.
33. Török, B.; Dransfield, T., Eds. *Green Chemistry: An Inclusive Approach*; Elsevier: Cambridge, Oxford, 2018.
34. Smith, G. V.; Notheisz, F. *Heterogeneous Catalysis in Organic Chemistry*, Academic Press: San Diego, CA, 1999.
35. Horvath, I., Ed. *Encyclopedia of Catalysis*; Wiley: New York, 2003.
36. Rylander, P. N. *Catalytic Hydrogenation over Platinum Metals*, Academic Press: New York, London, 1967.
37. Bartók, M., Ed. *Stereochemistry of Heterogeneous Metal Catalysis*; Wiley: Chichester, 1985.
38. Ertl, G.; Knözinger, H.; Weitkamp, J., Eds. *Handbook of Heterogeneous Catalysis*; Wiley-VCH: New York-Weinheim, 2008.
39. Olah, G. A., Ed. *Friedel-Crafts and Related Reactions*; Wiley: New York, 1964.
40. Rothenberg, G. *Catalysis: Concepts and Green Applications*, 2nd ed.; Wiley-VCH: Weinheim, 2017.
41. Kokel, A.; Schäfer, C.; Török, B. Organic Synthesis Using Environmentally Benign Acid Catalysis. *Curr. Org. Synth.* **2019**, *16*, 615–649.
42. Kokel, A.; Schäfer, C.; Török, B. Application of Microwave-assisted Heterogeneous Catalysis in Sustainable Synthesis Design. *Green Chem.* **2017**, *19*, 3729–3751.
43. Ilamanova, M.; Mastuygin, M.; Schäfer, C.; Kokel, A.; Török, B. Heterogeneous Metal Catalysis for the Environmentally Benign Synthesis of Medicinally Important Scaffolds, Intermediates and Building Blocks. *Curr. Org. Chem.* **2021**. <https://doi.org/10.2174/1385272825666210519095808> (in press).
44. Augustine, R. L. *Heterogeneous Catalysis for the Synthetic Chemist*, Marcel Dekker: New York, 1996.
45. Coish, P.; McGovern, E.; Zimmerman, J. B.; Anastas, P. T. The Value-Adding Connections Between the Management of Ecoinnovation and the Principles of Green Chemistry and Green Engineering. In *Green Chemistry: An inclusive Approach*; Török, B., Dransfield, T., Eds.; Elsevier: Cambridge, Oxford, **2018**; pp. 981–998 (chapter 3.28).
46. Wang, A.; Li, J.; Zhang, T. Heterogeneous Single-Atom Catalysis. *Nat. Rev. Chem.* **2018**, *2*, 65–81.
47. Mitchell, S.; Pérez-Ramírez, J. Single Atom Catalysis: A Decade of Stunning Progress and the Promise for a Bright Future. *Nat. Commun.* **2020**, *11*, 4302.
48. Mitchinson, A.; Finkelstein, J. Small-Molecule Catalysis. *Nature* **2008**, *455*, 303. and articles in this issue.
49. Takaya, J. Catalysis Using Transition Metal Complexes Featuring Main Group Metal and Metalloid Compounds as Supporting Ligands. *Chem. Sci.* **2021**, *12*, 1964–1981.
50. Shao, Z.; Zhang, H. Combining Transition Metal Catalysis and Organocatalysis: A Broad New Concept for Catalysis. *Chem. Soc. Rev.* **2009**, *38*, 2745–2755.
51. Meeuwissen, J.; Reek, J. N. H. Supramolecular Catalysis Beyond Enzyme Mimics. *Nat. Chem.* **2010**, *2*, 615–621.
52. Brown, C. J.; Toste, F. D.; Bergman, R. G.; Raymond, K. N. Supramolecular Catalysis in Metal–Ligand Cluster Hosts. *Chem. Rev.* **2015**, *115*, 3012–3035.
53. Pascanu, V.; González Miera, G.; Inge, A. K.; Martín-Matute, B. Metal–Organic Frameworks as Catalysts for Organic Synthesis: A Critical Perspective. *J. Am. Chem. Soc.* **2019**, *141*, 7223–7234.
54. Ponc, V.; Bond, G. C. *Catalysis by Metals and Alloys*, *Stud. Surf. Sci. Catal.*, Vol. 95; Elsevier: Amsterdam, 1995.

18 Heterogeneous catalysis in sustainable synthesis

55. Török, B.; Molnár, Á.; Pálincó, I.; Bartók, M. Surface Carbonaceous Deposits as Activity and Selectivity Influencing Species in the Ring-Opening Reactions of Propylcyclobutane Catalyzed by Pt/SiO<sub>2</sub>. *J. Catal.* **1994**, *145*, 295–299.
56. Lindlar, H. Ein neuer Katalysator für selektive Hydrierungen. *Helv. Chim. Acta* **1952**, *35*, 446–450.
57. Humphreys, J.; Lan, R.; Tao, S. Development and Recent Progress on Ammonia Synthesis Catalysts for Haber–Bosch Process. *Adv. Energy Sust. Res.* **2021**, *2*, 2000043.
58. Sheldon, D. Methanol Production—A Technical History. A Review of the Last 100 Years of the Industrial History of Methanol Production and a Look Into the Future of the Industry. *Johnson Matthey Technol. Rev.* **2017**, *61*, 172–182.
59. Xie, J.; Torres Galvis, H. M.; Koeken, A. C. J.; Kirilin, A.; Dugulan, A. I.; Ruitenbeek, M.; de Jong, K. P. Size and Promoter Effects on Stability of Carbon-Nanofiber-Supported Iron-Based Fischer–Tropsch Catalysts. *ACS Catal.* **2016**, *6*, 4017–4024.
60. Goodman, E. D.; Schwalbe, J. A.; Cargnello, M. Mechanistic Understanding and the Rational Design of Sinter-Resistant Heterogeneous Catalysts. *ACS Catal.* **2017**, *7*, 7156–7173.
61. Molnár, Á.; Papp, A. Catalyst Recycling—A Survey of Recent Progress and Current Status. *Coord. Chem. Rev.* **2017**, *349*, 1–65.
62. Argyle, M. D.; Bartholomew, C. H. Heterogeneous Catalyst Deactivation and Regeneration: A Review. *Catalysts* **2015**, *5*, 145–269.
63. Marafi, M.; Stanislaus, A. Studies on Recycling and Utilization of Spent Catalysts: Preparation of Active Hydrodemetallization Catalyst Compositions From Spent Residue Hydroprocessing Catalysts. *Appl. Catal. B Environ.* **2007**, *71*, 199–206.
64. Chauhan, G.; Pant, K. K.; Nigam, K. D. P. Metal Recovery from Hydroprocessing Spent Catalyst: A Green Chemical Engineering Approach. *Ind. Eng. Chem. Res.* **2013**, *52*, 16724–16736.
65. Zhang, L.; Song, Q.; Liu, Y.; Xu, Z. An Integrated Capture of Copper Scrap and Electrodeposition Process to Enrich and Prepare Pure Palladium for Recycling of Spent Catalyst From Automobile. *Waste Manag.* **2020**, *108*, 172–182.
66. Davis, M. E.; Suib, S. L. *Selectivity in Catalysis*, American Chemical Society: Washington, DC, 1993.
67. Lombardo, S. J.; Bell, A. T. A Review of Theoretical Models of Adsorption, Diffusion, Desorption, and Reaction of Gases on Metal Surfaces. *Surf. Sci. Rep.* **1991**, *13*, 3–72.
68. Taylor, H. S. A Theory of the Catalytic Surface. *Proc. R. Soc. Lond. A* **1925**, *108*, 105–111.
69. Greeley, J. P. Active Site of an Industrial Catalyst. *Science* **2012**, *336*, 810–811.
70. Kondrat, S. A.; van Bokhoven, J. A. A Perspective on Counting Catalytic Active Sites and Rates of Reaction Using X-Ray Spectroscopy. *Top. Catal.* **2019**, *62*, 1218–1227.
71. Nørskov, J. K.; Bligaard, T.; Hvolbaek, B.; Abild-Pedersen, F.; Chorkendorff, I.; Christensen, C. The Nature of the Active Site in Heterogeneous Metal Catalysis. *Chem. Soc. Rev.* **2008**, *37*, 2163–2171.
72. Boudart, M. Catalysis by Supported Metals. *Adv. Catal.* **1969**, *20*, 153–167.
73. Védrine, J. C. Revisiting Active Sites in Heterogeneous Catalysis: Their Structure and Their Dynamic Behaviour. *Appl. Catal. A: Gen.* **2014**, *474*, 40–50.
74. Zaera, F.; Somorjai, G. A. Hydrogenation of Ethylene Over Platinum (111) Single-Crystal Surfaces. *J. Am. Chem. Soc.* **1984**, *106*, 2288–2293.
75. Jin, R.; Li, G.; Sharma, S.; Li, Y.; Du, X. Toward Active-Site Tailoring in Heterogeneous Catalysis by Atomically Precise Metal Nanoclusters with Crystallographic Structures. *Chem. Rev.* **2021**, *121*, 567–648.

76. Ward, J. W. The Nature of Active Sites on Zeolites: I. The Decationated Y Zeolite. *J. Catal.* **1967**, *9*, 225–236.
77. Occelli, M. L.; Lester, J. E. Nature of Active Sites and Coking Reactions in a Pillared Clay Mineral. *Ind. Eng. Chem. Prod. Res. Dev.* **1985**, *24*, 27–32.
78. Idriss, H.; Barteau, M. A. Active Sites on Oxides: From Single Crystals to Catalysts. *Adv. Catal.* **2000**, *45*, 261–331.
79. Gao, M.; Li, H.; Liu, W.; Xu, Z.; Peng, S.; Yang, M.; Ye, M.; Liu, Z. Imaging Spatiotemporal Evolution of Molecules and Active Sites in Zeolite Catalyst During Methanol-to-Olefins Reaction. *Nat. Commun.* **2020**, *11*, 3641.
80. Kraft, P.; Swift, K. A. D., Eds. *Perspectives in Flavor and Fragrance Research*; Wiley-Verlag Helv. Chim. Acta: Zurich, 2005.
81. Szöllösi, G.; Török, B.; Baranyi, L.; Bartók, M. Chemoselective Hydrogenation of Cinnamaldehyde to Cinnamyl Alcohol over Pt/K-10 Catalyst. *J. Catal.* **1998**, *179*, 619–623.
82. Török, B.; Balázsik, K.; Felföldi, K.; Bartók, M. Effect of Medium and Coacid Acidity on the Cinchona-Modified Pt-Catalyzed Enantioselective Hydrogenations. *Stud. Surf. Sci. Catal.* **2000**, *130*, 3381–3386.
83. Abid, M.; Spaeth, A.; Török, B. Solvent-Free Solid Acid Catalyzed Electrophilic Annulations: A New Green Approach for the Synthesis of Substituted Five-Membered N-Heterocycles. *Adv. Synth. Catal.* **2006**, *348*, 2191–2196.
84. Abid, M.; Teixeira, L.; Török, B. Triflic Acid Controlled Successive Annulation of Aromatic Sulfonamides: An Efficient One-pot Synthesis of N-Sulfonyl Pyrroles, Indoles and Carbazoles. *Tetrahedron Lett.* **2007**, *48*, 4047–4050.
85. Abid, M.; DePaolis, O.; Török, B. A Novel One-Pot Synthesis of N-Acylindoles from Primary Aromatic Amides. *Synlett* **2008**, 410–413.
86. Kulkarni, A.; Török, B. Microwave-Assisted Multicomponent Domino Cyclization-Aromatization: An Efficient Approach for the Synthesis of Substituted Quinolines. *Green Chem.* **2010**, *12*, 875–878.
87. De Paolis, O.; Teixeira, L.; Török, B. Synthesis of Quinolines by a Solid Acid-Catalyzed Microwave-assisted Domino Cyclization-aromatization Approach. *Tetrahedron Lett.* **2009**, *50*, 2939–2942.
88. Borkin, D. A.; Puscau, M.; Carlson, A.; Wheeler, A. K.; Török, B.; Dembinski, R. Synthesis of Diversely 1,3,5-Substituted Pyrazoles via 5-Exo-dig Cyclization. *Org. Biomol. Chem.* **2012**, *10*, 4505–4508.
89. Rudnitskaya, A.; Borkin, D. A.; Huynh, K.; Török, B.; Stieglitz, K. Rational Design, Synthesis and Potency of N-Substituted-Indoles, Pyrroles and Triaryl-Pyrazoles as Potential Fructose 1,6-Bisphosphatase Inhibitors. *ChemMedChem* **2010**, *5*, 384–389.
90. Landge, S. M.; Török, B. Synthesis of 1,3,5-Triphenylpyrazole by a Heterogeneous Catalytic Domino Reaction. In *Experiments in Green and Sustainable Chemistry*; Roesky, H. W., Kennepohl, D., Eds.; Wiley-VCH: New York-Weinheim, **2009**; pp. 45–49.
91. Cho, H.; Török, F.; Török, B. Energy Efficiency of Heterogeneous Catalytic Microwave-assisted Organic Reactions. *Green Chem.* **2014**, *16*, 3623–3634.
92. Kulkarni, A.; Abid, M.; Török, B.; Huang, X. A Direct Synthesis of  $\beta$ -Carbolines via a Three-step One-pot Domino Approach With Bifunctional Pd/C/K-10 Catalyst. *Tetrahedron Lett.* **2009**, *50*, 1791–1794.
93. Young, J.; Schäfer, C.; Solan, A.; Baldrice, A.; Belcher, M.; Nişancı, B.; Wheeler, K. A.; Trivedi, E.; Török, B.; Dembinski, R. Regio- and Stereoselective Hydroamination of Alk-3-ynones With *o*-Phenylenediamines. Synthesis of Diversely Substituted 3H-1,5-Benzodiazepines Via 3-Amino-2-Alkenones. *RSC Adv.* **2016**, *6*, 107081–107093.

20 Heterogeneous catalysis in sustainable synthesis

94. Landge, S. M.; Török, B. Synthesis of Condensed Benzo[*N,N*]-Heterocycles by Microwave-Assisted Solid Acid Catalysis. *Catal. Lett.* **2008**, *122*, 338–343.
95. Borkin, D. A.; Morzhina, E.; Datta, S.; Rudnitskaya, A.; Sood, A.; Török, M.; Török, B. Heteropoly Acid-Catalyzed Microwave-Assisted Three-Component Aza-Diels-Alder Cyclizations: Diastereoselective Synthesis of Potential Drug Candidates for Alzheimer's Disease. *Org. Biomol. Chem.* **2011**, *9*, 1394–1401.
96. Österlund, L. Pressure Gaps in Heterogeneous Catalysis. In *Heterogeneous Catalysts: Advanced Design, Characterization and Applications, I*; Teoh, W. Y., Urakawa, A., Ng, Y. H., Sit, P., Eds.; Wiley-VCH: Weinheim, 2021.
97. Török, B.; Pálincó, I.; Molnár, Á.; Bartók, M. Hydrogen Pressure Dependence of the Ring-Opening Reactions of Propyl-cyclobutane over Pt/SiO<sub>2</sub> Catalyst at Different Temperatures. *J. Catal.* **1993**, *143*, 111–121.
98. Baiker, A. Supercritical Fluids in Heterogeneous Catalysis. *Chem. Rev.* **1999**, *99*, 453–474.
99. Wandeler, R.; Baiker, A. Supercritical Fluids: Opportunities in Heterogeneous Catalysis. *CATTECH* **2000**, *4*, 128–143.
100. Kruse, A.; Vogel, H. Heterogeneous Catalysis in Supercritical Media: 1. Carbon Dioxide. *Chem. Eng. Technol.* **2008**, *31*, 23–32.
101. Lee, J.-S.; Saka, S. Biodiesel Production by Heterogeneous Catalysts and Supercritical Technologies. *Bioresour. Technol.* **2010**, *101*, 7191–7200.
102. Török, B.; Schäfer, C., Eds. *Non-traditional Activation Methods in Green and Sustainable Applications: Microwaves, Ultrasounds, Photo, Electro and Mechanochemistry and High Hydrostatic Pressure*; Elsevier: Cambridge, Oxford, 2021.
103. Daştan, A.; Kulkarni, A.; Török, B. Environmentally Benign Synthesis of Heterocyclic Compounds by Combined Microwave-Assisted Heterogeneous Catalytic Approaches. *Green Chem.* **2012**, *14*, 17–37.
104. Horikoshi, S.; Serpone, N., Eds. *Microwaves in Catalysis: Methodology and Applications*; Wiley-VCH: Weinheim, 2016.
105. Mason, T. J.; Lorimer, J. P. *Applied Sonochemistry—The Uses of Power Ultrasound in Chemistry and Processing*, Wiley-VCH: Weinheim, 2002.
106. Török, B.; Balázsik, K.; Felföldi, K.; Bartók, M. Asymmetric Reactions in Sonochemistry. *Ultrason. Sonochem.* **2001**, *8*, 191–200.
107. Cintas, P. Ultrasound and Green Chemistry—Further Comments. *Ultrason. Sonochem.* **2016**, *28*, 257–258.
108. Evans, R. C.; Douglas, P.; Burrows, H. D., Eds. *Applied Photochemistry*; Springer: Dodrecht, 2013.
109. Kisch, H. Semiconductor Photocatalysis for Chemoselective Radical Coupling Reactions. *Acc. Chem. Res.* **2017**, *50*, 1002–1010.
110. Corrigan, N.; Shanmugam, S.; Xu, J.; Boyer, C. Photocatalysis in Organic and Polymer Synthesis. *Chem. Soc. Rev.* **2016**, *4*, 6165–6212.
111. Horn, E. J.; Rosen, B. R.; Baran, P. S. Synthetic Organic Electrochemistry: An Enabling and Innately Sustainable Method. *ACS Cent. Sci.* **2016**, *2*, 302–308.
112. Yan, M.; Kawamata, Y.; Baran, P. Synthetic Organic Electrochemical Methods Since 2000: On the Verge of a Renaissance. *Chem. Rev.* **2017**, *117*, 13230–13319.
113. Frontana-Uribe, B. A.; Little, R. D.; Ibanez, J. G.; Palma, A.; Vasquez-Medrano, R. Organic Electrosynthesis: A Promising Green Methodology in Organic Chemistry. *Green Chem.* **2010**, *12*, 2099–2119.
114. Margetić, D.; Štrukil, V. *Mechanochemical Organic Synthesis*, Elsevier, 2016.
115. James, S. L.; Friščić, T. Mechanochemistry. *Chem. Soc. Rev.* **2013**, *42*, 7494–7496.

116. Friščić, T.; Mottillo, C.; Titi, H. M. Mechanochemistry for Synthesis. *Angew. Chem. Int. Ed.* **2020**, *59*, 1018–1029.
117. Holzapfel, W.; Isaacs, N. *High Pressure Techniques in Chemistry and Physics. A Practical Approach*, Oxford University Press, 1997; p. 400.
118. Tomin, A.; Lazarev, A.; Bere, M. P.; Redjeb, H.; Török, B. Selective Reduction of Ketones Using Water as a Hydrogen Source Under High Hydrostatic Pressure. *Org. Biomol. Chem.* **2012**, *10*, 7321–7326.
119. Chataigner, I.; Maddaluno, J. High-Pressure Synthesis: An Eco-friendly Chemistry. In *Activation Methods: Sonochemistry and High Pressure*; Goddard, J.-P., Malacria, M., Ollivier, C., Eds.; 1st ed.; ISTE Ltd and John Wiley & Sons, Inc, 2019.
120. <https://www.essentialchemicalindustry.org/processes/chemical-reactors.html> (Accessed 21 June 2021).
121. Foutcha, G. L.; Johannes, A. H. *Reactors in Process Engineering. Encyclopedia of Physical Science and Technology*, 3rd ed.; Academic Press, 2003; pp. 23–43.
122. <https://www.berghof-instruments.com/en/application/selective-hydrogenation-of-polyunsaturated-hydrocarbons/> (Accessed 21 June 2021).
123. <https://www.parrinst.com/products/non-stirred-pressure-vessels/materials-of-construction/> (Accessed 21 June 2021).
124. Noël, T.; Cao, Y.; Laudadio, G. The Fundamentals Behind the Use of Flow Reactors in Electrochemistry. *Acc. Chem. Res.* **2019**, *52* (10), 2858–2869.
125. Bianchi, P.; Williams, J. D.; Kappe, C. O. Oscillatory Flow Reactors for Synthetic Chemistry Applications. *J. Flow Chem.* **2020**, *10*, 475–490.
126. He, Y.; Kim, K.-J.; Chang, C. Segmented Microfluidic Flow Reactors for Nanomaterial Synthesis. *Nanomaterials* **2020**, *10*, 1421.
127. Wiles, C.; Watts, P. Continuous Flow Reactors: A Perspective. *Green Chem.* **2012**, *14*, 38–54.



## Chapter 2

# Solid catalysts for environmentally benign synthesis

### 2.1. Introduction

By the definition of heterogeneous catalysis, the catalyst has to be in a different phase than the reactants. Since most reactions occur either in the gas or the liquid phase, this practically means that the catalysts must be solid materials. Solid catalysts played an important role in the implementation of major recommendations of Green Chemistry<sup>1</sup> for the sustainable production of pharmaceuticals and fine chemicals by replacing the outdated procedures and catalysts with more contemporary environmentally benign alternatives.<sup>2, 3</sup> The application possibilities include synthesis design,<sup>4</sup> biomass conversion,<sup>5, 6</sup> water and supercritical CO<sub>2</sub>-based synthesis,<sup>7, 8</sup> biocatalysis,<sup>9, 10</sup> and the development of new green metrics.<sup>11</sup> The continued development of heterogeneous catalysis involves the preparation and application of solid catalysts.<sup>12</sup> As mentioned in Chapter 1, solid catalysts are favored in large-scale, continuous flow-based industrial processes.<sup>13–16</sup> Since the beginning of the field of heterogeneous catalysis more than a century ago, the development of new solid catalysts and their application for the synthesis of large-scale chemicals, fine chemicals, and pharmaceuticals have always been a leading area of research.<sup>17–21</sup> Solid catalysts are commonly placed into two major categories: metal catalysts where the metal usually occurs in a zero valence (elemental) form and nonmetallic catalysts that either do not possess any metal component or the metal is in an oxidized form such as metal oxides, salts, or complex metal compounds and minerals (zeolites, clays, etc.). The classification of solid catalysts is summarized in **Fig. 1**.

The design and preparation of catalysts have a long history and accordingly, extensive literature covers this field. Several periodic or stand-alone monographs describe the progress in this area.<sup>22–25</sup>

### 2.2. Metal catalysts

Although the name metal catalyst may suggest a broader implication, when discussing these catalysts one commonly refers to transition metals. These metals

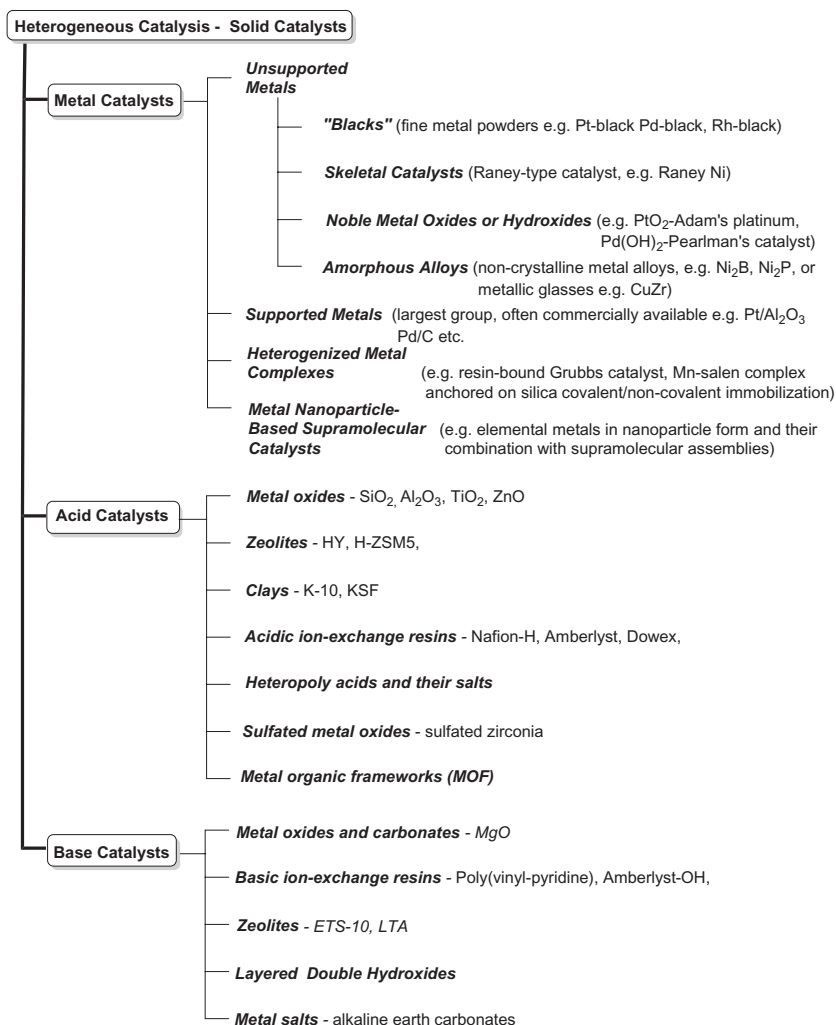
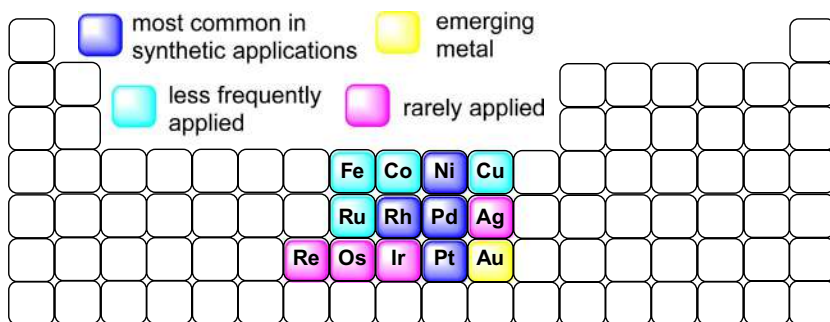


FIG. 1 A schematic classification of solid catalyst with few representative examples.

play a significant role in nearly all forms of catalysis.<sup>26, 27</sup> Although the term metal catalyst usually implies to the elemental form of metals, the ionic forms of transition metals are also considered, as these salts (e.g., PdCl<sub>2</sub> for coupling reactions), oxides (PtO<sub>2</sub>), or hydroxides (Pd(OH)<sub>2</sub>) are often reduced to the zero valence form in situ. Organometallic complexes of transition metals are also dominant catalysts. In addition to being the catalyst of choice for homogeneous catalysis, their surface-bound, heterogenized forms are well-known solid catalysts. While being excellent catalysts, all of the transition metals, or otherwise called heavy metal catalysts, have one significant drawback—they possess quite



**FIG. 2** The periodic table of elements highlighting the metals that are most commonly used in heterogeneous catalytic processes.

significant toxicity.<sup>28, 29</sup> Although the toxicity is independent of whether the catalyst is a soluble complex or a solid, the insignificant solubility of the solid forms ensures low level of leaching to the solution. In contrast, metal complexes are dissolved in the reaction medium and to remove them completely from the solution is often challenging, thus raising the issue of toxic metal contamination in the product or spent solvents. The thematic classification of metal catalysts is depicted in Fig. 1.

Among the metals in the periodic table a relatively small group is considered catalytically active in heterogeneous catalysis, although many more are active in their metal complex forms in homogeneous catalysis. The periodic table (Fig. 2) highlights the metals most commonly used in heterogeneous catalytic processes.

As shown in Fig. 2, Ni, Pd, Pt, and Rh are the most often used transition metals in synthetic processes. Among these metals *nickel* is the most inexpensive, thus it is quite frequently used in laboratory and industrial processes.<sup>30</sup> In fact, Ni was the first metal that was used in heterogeneous catalytic hydrogenation by Sabatier in the late 1800s.<sup>31</sup> It is commonly used as a supported Ni catalyst, e.g., Ni/kieselguhr, for the hydrogenation of unsaturated fats or other hydrocarbon transformations.<sup>32, 33</sup> The most frequently applied form of nickel, however, is the well-known skeletal metal catalyst, Raney Ni.<sup>34</sup> Raney Ni can be prepared ahead of a reaction and is commercially available, or it can be prepared in situ from NiAl alloy.<sup>35</sup> Essentially, Raney Ni is capable of hydrogenating all hydrogenation-sensitive functional groups, although for example aromatic hydrogenation occurs under rather harsh conditions.<sup>36</sup>

*Palladium* is another member of the most frequently used group of metals. Although more expensive than Ni, its properties are extremely versatile and Pd catalysts are used in a myriad of transformations from hydrogenation,<sup>37, 38</sup> to oxidations,<sup>39–41</sup> or carbon-carbon coupling reactions.<sup>42, 43</sup> Although it is the most common hydrogenation catalyst, its use has a somewhat limited scope. The lower reactivity, however, is coupled with higher selectivity in several reactions.<sup>44, 45</sup>

*Platinum* and *rhodium* are probably the most powerful hydrogenation catalysts.<sup>46, 47</sup> They can hydrogenate nearly all functional groups, with the exception of carboxylic acid derivatives. Under mild conditions, they can act as an oxidative dehydrogenation catalyst, e.g., in aromatization reactions.<sup>27, 48</sup> In addition, they are frequently applied in multiple other transformations, such as oxidation, dehydrogenation, hydrogenolysis, or hydroformylation.<sup>49, 50</sup>

*Ruthenium* and *iridium* are comparatively less often used metals that still belong to the earlier mentioned group. They are extremely powerful catalysts but due to their low natural abundance and high cost, the applications are mostly focused on homogeneous catalysis, such as Ru complexes for enantioselective hydrogenation<sup>51</sup> or alkene metathesis,<sup>52</sup> and Ir complexes for C-H activation<sup>53</sup> or catalytic hydrogenation.<sup>54</sup> These metals are also applied in environmental exhaust systems, e.g., those of automotive engines.<sup>55–57</sup>

The second major group of metals includes several, nonnoble metal catalysts that were not frequently used earlier; however, multiple factors such as cost, availability, abundance, and a favorable toxicology profile (moderate to low toxicity) (e.g., Fe, Co, Cu) initiated more extensive exploration of the catalytic properties these metals possess. Several application opportunities were reported over the past two decades, such as hydrogenation (Fe, Co),<sup>58–60</sup> dehydrogenation (Co),<sup>61</sup> hydroformylation (Fe, Co),<sup>62</sup> cyclopropanation/aziridination (Cu, Co),<sup>63, 64</sup> Mukaiyama aldol reactions (Cu),<sup>65</sup> Fischer-Tropsch (Co),<sup>66</sup> and the list of successful transformations is continuously expanding.<sup>67, 68</sup>

Among the emerging metals gold stands out. Long thought of being largely inert, the discovery that it can catalyze a host of reactions<sup>69, 70</sup> attracted significant attention to this metal.<sup>71</sup> Due to its unique characteristics it became the catalyst of choice for many transformations in both major branches of catalysis. In addition to its ability to carry out established processes, gold catalysts became part of the development of new processes that do not occur or are highly challenging with other traditional metal catalysts, even at the industrial level.<sup>72</sup> In addition to its unique and beneficial catalytic features, such as room temperature applications, one of gold's most beneficial property is its low toxicity, especially in comparison with other transition metals,<sup>29, 73</sup> that could make it the catalyst of the future for green and sustainable chemistry applications.<sup>74</sup> Gold catalysts were prepared in several forms, such as supported nanoparticles.<sup>75</sup> After nearly three decades of research, gold has been established as a catalyst of choice for many transformations, including hydrogenation of C–C, C–O, or N=O bonds; oxidation of different functional groups; hydration; hydrohalogenation; hydroamination; hydrothiolation; condensation; additions in homogeneous and heterogeneous applications alike.<sup>76–78</sup> Due to the importance of this metal, its applications were subject of frequent reviews.<sup>79–82</sup>

The previously discussed metals and their available catalysts with common applications are summarized in [Table 1](#).

**TABLE 1** Catalytic metals that are commonly used in heterogeneous catalysis and their commercially available forms and application possibilities.

| Metal     | Commercially available forms   | Applications   |
|-----------|--|--|
| Platinum  | Pt wire, sponge or granules, salts and complexes, Pt black and powder, Pt/SiO <sub>2</sub> , Pt/Al <sub>2</sub> O <sub>3</sub> , Pt/C, PtO <sub>2</sub> , Pt/polyethylenimine/SiO <sub>2</sub> , Pt/graphite | Hydrogenation, oxidation, dehydrogenation, hydrogenolysis, automobile exhaust catalyst, hydrosilylation, fuel cells, isomerization, cyclization  |
| Rhodium   | Rh wire, salts and complexes, Rh/SiO <sub>2</sub> , Rh/Al <sub>2</sub> O <sub>3</sub> , Rh/C, Rh black and powder, Rh <sub>3</sub> O <sub>2</sub>  | Hydrogenation, oxidation, hydroformylation, carbonylation, automobile exhaust catalyst, fuel cells   |
| Palladium | Pd/SiO <sub>2</sub> , Pd/Al <sub>2</sub> O <sub>3</sub> , Pd(OH) <sub>2</sub> , PdCl <sub>2</sub> , Pd/BaCO <sub>3</sub> , Pd/SrCO <sub>3</sub> , Pd/CaCO <sub>3</sub> , Pd/C, Pd/black                      | Hydrogenation, oxidation, dehydrogenation, hydrogenolysis, MeOH synthesis, automobile exhaust catalyst   |
| Nickel    | Ni wire, gauze, sponge, granules, salts and complexes, Ni/SiO <sub>2</sub> , Ni/SiO <sub>2</sub> -Al <sub>2</sub> O <sub>3</sub> , Raney Ni, Ni powder, NiAl alloy, NiB, NiO, Ni <sub>2</sub> Si             | Hydrogenation, hydrogenolysis, carbonylative cycloaddition, coupling reactions of C=X bonds, C-H functionalization, C-C bond functionalization, cross-coupling reactions, CO <sub>2</sub> fixation |
| Iridium   | Mostly in complex and salt form, Ir black, IrO <sub>2</sub> , Ir wire, Ir/C  | Hydrogenation, oxidation, hydroformylation, C-H bond functionalization, 1,3-dipolar cycloaddition  |
| Ruthenium | Ru black and powders, salts and complexes, RuO <sub>2</sub> , Ru/C, Ru/Al <sub>2</sub> O <sub>3</sub>  | Hydrogenation, oxidation, hydrogenolysis, NH <sub>3</sub> synthesis, hydroformylation  |
| Copper    | Cu wire, gauze, sponge, granules, salts and complexes, Cu powder, CuO, Cu/Al <sub>2</sub> O <sub>3</sub> , Cu/SiO <sub>2</sub> , Cr <sub>2</sub> CuO <sub>4</sub>  | Cyclopropanation, aziridination, Mukaiyama aldol reaction, some cross-coupling reaction, multicomponent reactions, click reactions, C-H activation, cyclopropanation                               |
| Iron      | Fe wire, granules, powder, oxides, salts, complexes, Fe <sub>2</sub> O <sub>3</sub> , Fe <sub>3</sub> O <sub>4</sub>   | Hydrogenation, hydroformylation, ring opening, cross-coupling, electrophilic substitutions, magnetic oxides serve as base for magnetic catalysts   |

*Continued*

**TABLE 1** Catalytic metals that are commonly used in heterogeneous catalysis and their commercially available forms and application possibilities—cont'd

| Metal  | Commercially available forms  | Applications  |
|--------|---|---|
| Cobalt | Co powder, sponge, salts, CoO <sub>3</sub> , Co mixed (II/III) oxide      | Hydrogenation, dehydrogenation, cyclopropanation, aziridination, hydroformylation, Fischer-Tropsch reaction                       |
| Gold   | Au powder, wire, sponge, salts, complexes, Au <sub>2</sub> O <sub>3</sub> | Hydrogenation, dehydrogenation, oxidation, hydration, hydrohalogenation, hydroamination, hydrothiolation, condensation, additions |

Many samples are available in a variety of metal concentrations and preparation protocols.

### 2.2.1 Unsupported metals

The first large group of metal catalysts is the neat or unsupported metals. These catalysts are composed of pure metal (or metals if alloys), thus, with few exceptions, they are not considered economic from a financial as well as from an environmental point of view. Often their particle size is relatively large, therefore the surface available for reactions is limited, resulting in a large amount of unutilized metal. Skeletal metals are one notable group with high surface area; however, most of these materials are pyrophoric and need to be dealt with caution, for example, they need to be stored under water. The major groups of unsupported metals include massive metals, such as wires, ribbons, sponges, or single crystals with well-defined surface<sup>83</sup>; neat metal powders or *blacks*<sup>84</sup>; skeletal metals, e.g., Raney-type catalysts<sup>85</sup>; in situ reduced oxides (e.g., PtO<sub>2</sub>)<sup>86</sup>; and amorphous metal alloys<sup>87</sup> (e.g., NiB or CuZr).

#### 2.2.1.1 Bulk or massive metals

The term massive metals stands for large metal formations that range from large particle single crystals,<sup>88, 89</sup> metal wires, foams<sup>90</sup> to metal mesh.<sup>91</sup> Most of these formulations are commonly used in large-scale industrial processes.<sup>92</sup> In contrast, single crystals prepared of catalytically active metals are quite useful in studying surface science and mechanisms of heterogeneous catalytic reactions.<sup>93</sup>

#### 2.2.1.2 Metal “blacks”

As described before, metal blacks are neat elemental metals mostly in a powder form with varying particle sizes prepared by the direct reduction of metal salts. Although they are very effective and are commonly used, they are expensive due

to the relatively high amount of metal used and the high cost of these, especially the noble metals.<sup>84</sup> Their large particle size and accordingly low active surface area mean that a large amount of the metal is not available to the reactants.<sup>94</sup>

### 2.2.1.3 Skeletal metals

Skeletal metals are an evolved form of the metal blacks. Despite the fact that they are neat metals, they possess an extremely large surface area. They are usually prepared from bimetallic metal alloys by selectively removing one of the metal components. The most common group of skeletal metals is the Raney-type catalysts that are prepared from commercially available metal-Al alloys (e.g., NiAl, CoAl, etc.).<sup>34–36</sup> One of the primary use of these metal-Al alloys is to prepare skeletal metal catalysts,<sup>85</sup> thus their preparation is of high practical importance. Usually a dilute base dissolves the aluminum component leaving the other metal behind in a skeletal, sponge-like structure of high surface area. Due to the large clean metal surface these materials are very active and pyrophoric and must be stored under water.<sup>85</sup> Murray Raney developed the first method to prepare skeletal metal catalysts from a 50%–50% nickel-silicon alloy in 1924.<sup>34</sup> The obtained material, named after him as the Raney Ni catalyst, was an extremely active hydrogenation catalyst. In 1927 Raney applied a 50%–50% Ni-Al alloy in a similar protocol and obtained an even more reactive hydrogenation catalyst than that from the Ni-Si alloy.<sup>95</sup> Since this discovery, the Ni-Al alloy, or in general metal-Al alloys, have been used for the preparation of Raney-type catalysts. The alloy is made by mixing nickel to molten aluminum and after proper mixing the alloy is cooled down, a process called quenching. As in many catalyst preparations, often promoter metal additives are used to enhance catalytic features of the Raney Ni catalyst. The extra metals are added to improve the selectivity of the final catalyst toward the hydrogenation of the target functional group. The most common promoters for the preparation of Raney Ni are Cr,<sup>96</sup> Mo,<sup>97</sup> Zn,<sup>98</sup> Fe,<sup>99</sup> Cu, and Co.<sup>100</sup> Some of these metals are also made into metal-Al alloys (e.g., Co-Al, Cu-Al) that are also commercially available and are used to prepare the corresponding Raney Co or Raney Cu. The earlier reports are summarized in the literature.<sup>22</sup> Recent applications include the hydrogenolysis of C–X and C–O bonds or the racemization of amines or the hydrogenative dehydroxylation of glycerol (Raney Co),<sup>101–103</sup> methanol synthesis, hydrogenative dehydroxylation of glycerol to propylene glycol, or the catalytic gasification of biomass (Raney Cu).<sup>104–106</sup>

### 2.2.1.4 Noble metal oxides and hydroxides

Although limited in actual examples, the few commercially available metal oxide or hydroxide-based catalysts,<sup>107</sup> e.g., the Adams' platinum (PtO<sub>2</sub>), are relatively popular as they are shelf-stable and thus easy to turn to. These catalysts are very effective and commonly used, however, expensive given the relatively high amount of metal used and the high cost of these metals. In fact, the metal

oxide catalysts are usually undergoing a prereduction step in the presence of hydrogen gas and eventually will be used as metal blacks. In contemporary applications they are particularly popular in hydrogenation of pyridines,<sup>108</sup> or organofluorine compounds,<sup>109</sup> as well as in the hydrogenolysis of the cyclopropane ring.<sup>110</sup>

Another typical example is the Pearlman's catalyst, Pd(OH)<sub>2</sub>. In principle it works the same way as the Adams' platinum; however, due to the change of metal, some of the reactions are specific to this catalyst. For example, the Pearlman's catalyst has been applied for Fukuyama, Sonogashira, and Suzuki couplings<sup>111</sup>; hydrogenation of complex molecules<sup>112</sup>; diastereoselective hydrogenations<sup>113</sup>; hydrogenolysis of the cyclopropane ring<sup>114</sup>; and it is a typical debenzoylation catalyst for protected alcohols and amines as well.<sup>115, 116</sup>

### 2.2.1.5 Amorphous metal alloys

Amorphous metal alloys are prepared as simple powders and metallic glasses. The powders are obtained by the reduction of metal salts by the appropriate reducing agents, and the metallic glasses are prepared by metallurgy.<sup>87, 117</sup> The first group includes, for example NiB or NiP, that are commonly obtained by the reduction of the appropriate metal salts often chlorides, in the presence of boron or phosphorus compounds, respectively. The most common reducing agents are NaBH<sub>4</sub> for the boron alloys and NaH<sub>2</sub>PO<sub>2</sub> for the phosphorus alloys. Another way to prepare these alloys is via electrodeposition.<sup>118</sup> The metallic glasses are prepared from their melt by extremely rapid cooling, commonly at the temperature of liquid nitrogen. Due to the nearly immediate solidification the material cannot develop a crystal structure and remains amorphous.<sup>119, 120</sup> The application of amorphous metal alloys in synthetic chemistry has an extensive history; however, a large majority of these applications are related to heterogeneous catalysis.<sup>87, 121, 122</sup> They are applied in oxidations,<sup>123</sup> hydrogenations,<sup>117, 124–126</sup> or water oxidation.<sup>127, 128</sup> In addition to synthetic applications, amorphous alloys are also commonly applied for the preparation of skeletal metal catalysts (*vide supra*).<sup>129</sup> Recent reviews summarize the contemporary applications.<sup>130–132</sup>

### 2.2.2 Supported metal catalyst

The catalytic activity of Ni has been known since 1897 when Paul Sabatier hydrogenated alkenes over nickel catalysts when the nickel was dispersed on the surface of silica support,<sup>31</sup> thus supported metals are the earliest examples of heterogeneous metal catalysis.

The concept of supported metal catalysts is relatively simple; small particles of the active metal component are dispersed on the surface of a support material that is commonly inert (e.g., C, Al<sub>2</sub>O<sub>3</sub>, or polystyrene); however, it also could contribute to the catalytic reaction (zeolites, clays, etc. that will promote bifunctional catalysis),<sup>133–136</sup> or in the form of a self-supported catalyst.<sup>137</sup> The preparation of supported metals achieves two benefits: efficacy and economics.

Namely, a much larger portion of the metal will be accessible due to the small particle size, which means less metal has to be used.<sup>138</sup> Supported metal catalysts are usually prepared from commercially available metal salts via reduction in the presence of the support. The preparation of supported metal catalysts is often called an art: the experimental conditions applied during their preparation will determine the performance of catalysts, including activity and selectivity. The most common experimental variables that one considers during the preparation of a catalyst are the reduction method, pH, and temperature. Obviously the applied support has an utmost importance as well. In many cases when the catalyst undergoes postsynthesis treatments, such as heat treatment, further reduction with H<sub>2</sub> gas at high temperatures and the likes, they all modify the original catalyst and fine-tune its properties. All these specific options make the catalyst preparation a time-consuming and work-intensive process that often becomes a patented trade secret and is a frequent target for reviews.<sup>135, 136, 139, 140</sup> The description of major techniques that are applied for catalyst preparation is beyond the scope of this work; however, the topic is described in detail in several sources.<sup>22, 141, 142</sup>

### 2.2.2.1 Catalyst supports

While there are several important variables during the preparation of supported metal catalysts, probably the most important one is the material of the support itself.<sup>143</sup> Depending on the catalytic application, the support can be inert or it can possess acidic, basic, or special electronic (insulator, conductor, etc.) properties.<sup>133, 134</sup> The field is extremely broad and is dynamically growing. Thus it is impossible to provide an exhaustive account of catalyst supports. In addition, the upcoming chapters include over two thousand references presented by application areas that are all related to the use of supported catalysts. In this subchapter, our goal is to rather give a short summary that highlights the well-known supports and major directions in the development of new ones with a few representative examples. The most common catalyst supports and their major characteristics are summarized in [Table 2](#).

#### SiO<sub>2</sub>

Silica-supported metal catalysts are the oldest heterogeneous catalysts dating back to Sabatier's pioneering works on catalytic hydrogenations.<sup>31, 144</sup> These materials are based on various forms of silicon dioxide that can be prepared by a multitude of methods, e.g., from SiCl<sub>4</sub> by flame hydrolysis (nonporous silica), sodium metasilicate via acidic treatment (porous silica), or tetraethyl orthosilicate by hydrolysis (mesoporous silica). In several cases the preparation of the silica occurs in the presence of an active catalyst, and at the end of the process silica nanocomposite materials are obtained.<sup>145–148</sup> In other examples, the silica surface is applied for modifications and active catalysts are covalently bound to it.<sup>149</sup> The most common forms include Aerosil, Cab-O-Sil, Suprasil, Borsil, Eurosil, kieselguhr, just to name a few of those samples that are all

**TABLE 2** The most common solid support materials that are used for the preparation of supported metal catalysts and their major physical and chemical properties.

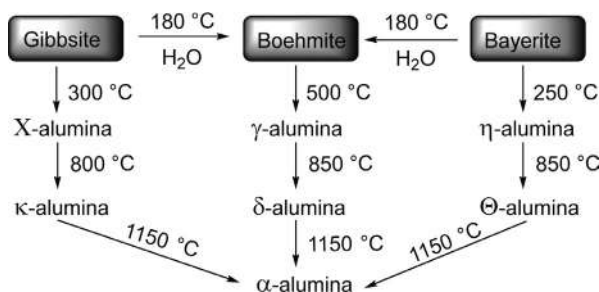
| Support                         | Composition/material  | Supported metal catalysts   |
|---------------------------------|---|---|
| Silica                          | SiO <sub>2</sub> , kieselguhr, mesoporous silicas (e.g., MCM-41, SBA-15, etc.)              | Nearly all catalytically active metals  |
| Alumina                         | Al <sub>2</sub> O <sub>3</sub> including a wide variety of samples                          | Nearly all catalytically active metals  |
| Other metal oxides              | TiO <sub>2</sub> , CeO <sub>2</sub>   | Nearly all catalytically active metals  |
| Alkaline earth metal carbonates | CaCO <sub>3</sub> , BaCO <sub>3</sub> , SrCO <sub>3</sub>                                   | Pd/CaCO <sub>3</sub> , Pd/BaCO <sub>3</sub> , Pd/SrCO <sub>3</sub>  |
| Carbon-based materials          | Activated carbon (AC), graphite, graphene, graphene oxide, fullerenes, and carbon nanotubes | Nearly all catalytically active metals  |
| Polymeric materials             | Poly(styrene) (PS), poly(vinyl)pyridine (PVP), polydopamine (PDA), aminomethylated PS       | Many catalytically active metals, some are commercially available   |
| Clays                           | K-10, KSF, bentonite, montmorillonites  | Some metals, usually tailored catalyst  |
| Zeolites                        | A wide variety of zeolites, e.g., Y, beta, ZSM  | Some metals, usually tailored catalyst  |
| Biomass-based supports          | Chitosan, biomass ashes, metal-carbonates, various carbon materials                         | A variety of metals, tailored catalysts, when a metal bioaccumulating plant is used it will determine the metal |
| Magnetic supports               | Fe <sub>2</sub> O <sub>3</sub> , Fe <sub>3</sub> O <sub>4</sub>                             | Applicable for all metals, generally tailored catalysts   |

commercially available. Another advantage of silica is that it is essentially inert to all chemicals except HF. Its chemical inertness, coupled with its practically insoluble nature and negligible vapor pressure, ensures low toxicity on contact (e.g., some forms make it into toothpaste). However, if inhaled, it can cause a host of serious issues in the respiratory tract including cancer. Its toxicity is also dependent on the size of the particles; nanosized silica particles can enter the cells via endocytosis and cause damage.<sup>150</sup>

Silica support materials are used in many different forms. A recent review provides an extensive account regarding the types and characteristics of silica supports in heterogeneous catalysis.<sup>151</sup> *Amorphous silica* is a commonly used catalyst support due to its thermal stability as well as tunable porosity and surface area.<sup>152, 153</sup> *Mesoporous silica* materials became increasingly popular since the 1990s.<sup>154</sup> The MCM series (MCM-41 being the most popular) or the SBA series (SBA-15 is the most commonly used) were used as supports for many metals in nearly every application possibilities.<sup>155</sup> They are particularly sought after due to the variable pore size (1.5–30 nm) and high surface area (800–1000 m<sup>2</sup>/g).<sup>151</sup> These materials are viable catalysts on their own<sup>156</sup> and will be discussed later under nonmetallic catalysts.

### Al<sub>2</sub>O<sub>3</sub>

Aluminum oxide, or, as commonly referred to, alumina, is a collective name for a large group of materials that has been used in heterogeneous catalysis for over a century.<sup>157</sup> The members of the group are structurally different, sometimes even in their chemical composition. The simplest form, Al(OH)<sub>3</sub>, exists in many forms, the two most common ones are Gibbsite and Bayerite. Different levels of dehydration of the basic forms result in the formation of various other materials, such as Boehmite, γ, κ, α, δ, τ, ε aluminas just to name a few variants, many of them are interconvertible to each other, although in a one-way process (Scheme 1). These materials possess a broad range of properties, including amphoteric nature, variable surface area (low to 400 m<sup>2</sup>/g), pore volume (0.1–1.5 cm<sup>3</sup>/g), or pore size (2 nm to 170 μm).<sup>158–160</sup> Due to its versatility, alumina has been the support of choice for a large number of supported metal catalysts. Simply, the large variety allows the preparation of a specifically tailored support for individual applications.



**SCHEME 1** Interconversion of various alumina samples

Alumina-supported metal catalysts enjoy considerable popularity in heterogeneous catalysis ranging from hydrogenation, oxidation to coupling reactions, or automotive applications.<sup>161</sup> In fact, nearly every metal is produced in an alumina-supported form. In addition to the beneficial physical features and

highly variable synthetic pathways, alumina possesses low chemical toxicity, which is a considerable advantage in green and sustainable applications, although exposure to its dust and nanoparticles could cause harm.<sup>162</sup>

*Clays* and *zeolites* are natural and synthetic aluminosilicates that have been frequently used in catalytic applications as solid acid catalysts and also as catalyst supports.<sup>163–168</sup> Despite being support materials for the preparation of metal catalysts, the majority of their applications are in acid-catalyzed reactions in a neat form without a metal component. Thus they are mentioned here; however, their detailed description including structural and catalytic properties will be provided in the solid acid catalyst subchapter.

### Other metal oxides and metal carbonates

In addition to silica and alumina, there are several other metal oxide- or metal carbonate-based supports that are applied for their task-specific properties. Several of them are used as promoters. *Titania* ( $\text{TiO}_2$ ) is commonly used in two of its crystalline forms, rutile and anatase. It is prepared either by the solvothermal or hydrothermal hydrolysis of Ti salts, sol-gel method, or the flame hydrolysis of  $\text{TiCl}_4$ ; the crystalline form of the product depends on the experimental conditions used.<sup>169</sup> Recent reviews focus on the preparation of  $\text{TiO}_2$  in its nanoparticle form.<sup>170</sup> What makes titania a special catalyst/catalyst support is that unlike silica or alumina that are insulators, it is a semiconductor and also that the surface  $\text{Ti}^{4+}$  ions can be reduced to  $\text{Ti}^{3+}$  by hydrogen spillover, which makes it able to participate in strong metal-support interactions (SMSI). The most common application of  $\text{TiO}_2$  catalysts is in photocatalytic reactions<sup>171, 172</sup>; however, they are also applied as promoters.<sup>173, 174</sup> There are several other oxides, such as *ceria* ( $\text{CeO}_2$ ), or  $\text{RuO}_2$ , that are also used in a host of applications ranging from photo- and electrocatalysis to water-gas shift reaction.<sup>175–178</sup>

Some *other metal oxides* (e.g.,  $\text{MgO}$ ) and *alkaline earth metal carbonates* ( $\text{Ca}$ -,  $\text{Sr}$ -,  $\text{BaCO}_3$ ) are generating interest mainly due to their significant basic properties. The basic support, when applied, commonly contributes to the outcome of the reaction, thus most of these catalysts are considered bifunctional metal-base catalysts. The scope of the applications is broad from  $\text{CO}_2$  activation,<sup>179</sup> hydrogenation,<sup>180, 181</sup> oxidation,<sup>182, 183</sup> to methane activation.<sup>184</sup> Likely, the Lindlar catalyst (5%  $\text{Pd/CaCO}_3$ ,  $\text{PbO}$  and quinoline) is the most well-known example of this group. This catalyst is best known for its ability to hydrogenate alkynes to alkenes, in a stereoselective manner<sup>185, 186</sup>; however, recent applications extend the scope of this catalyst to the hydrogenation of vegetable oils<sup>187</sup> or azides.<sup>188</sup>

### Magnetic catalyst supports

With the emergence of the green chemistry principles, the recovery and reuse of catalysts, particularly metal catalysts, became an increasingly important task. Applying magnetic materials as catalyst supports appears to be the ultimate solution to this issue. With the use of magnetic catalysts, a simple external magnet

can separate the catalyst from the reaction mixture without the use of tedious filtration or centrifugation.<sup>189, 190</sup> The early catalysts with magnetic character were somewhat accidental and were based on the intrinsic magnetic character of the catalysts themselves, such as Fe, Ni, Co, or certain oxides of iron.<sup>191</sup> Since then, the field considerably extended and magnetic support materials were designed and prepared to carry the active component, be it a neat metal, metal complex, organocatalyst, or an enzyme.<sup>192</sup> Due to the extensive interest in these magnetically recoverable materials a number of reviews summarize the developments.<sup>193–195</sup> Magnetic supports can be prepared in two major ways, either using uncoated<sup>196</sup> or coated magnetic particles (Fig. 3).<sup>197, 198</sup> The major sources of magnetic supports are either elemental magnetic materials such as Fe, Co, and Ni (mostly in the form of nanoparticles), or some of their oxides, Fe<sub>3</sub>O<sub>4</sub>,  $\gamma$ -Fe<sub>2</sub>O<sub>3</sub>, or MFe<sub>2</sub>O<sub>4</sub> (M=Co, Mn). The most common application is the use of coated magnetic nanoparticles. The often used coatings are made of silica, carbon, polymers, metal oxides and hydroxides, or metals (core shell coating).

### Carbon-based supports

Carbon is a well-known catalyst support material that originally made its way to catalytic chemistry due to its extensive surface area and strong adsorption capability. There are several benefits in using carbon as a catalyst support: it is largely inert and resistant to many chemicals such as acids and bases; it is noncorrosive, stable even at high temperatures, hydrophobic, and nontoxic.<sup>199</sup> In many instances, *activated carbon* (AC) is commonly synthesized from biological sources, thus it can be considered a renewable material.<sup>200</sup> The sources are quite broad from date or cherry stones, coconut shells, corn cob, or lignin just to list a few.<sup>201–203</sup> Activated carbon serves as a support for most catalytically active metals as well as catalytically active metal complexes due to its high surface area and inert characteristic. Accordingly, the catalytic applications are very broad, as reviewed.<sup>199</sup>

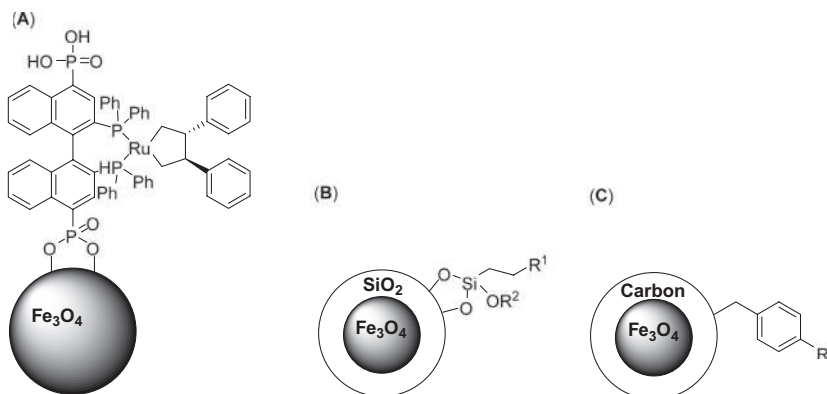


**FIG. 3** Functionalization of magnetic particles in their noncoated (A), silica-coated (B), and carbon-coated (C) forms.

*Graphite* is the most stable form of carbon and as such it has been applied in catalysis either in its neat form or as a support for metal catalysts. The deposited metals show a broad range, from platinum metals to Ni, Fe, or amorphous NiB alloys and consequently the catalytic applications are also wide ranging including hydrogenation, Fischer-Tropsch synthesis, or Baeyer-Villiger oxidation.<sup>204–206</sup>

In addition to the previously discussed traditional carbon-based supports, several relatively new carbon nanomaterials attracted significant attention in catalysis. A group of these materials, such as *graphene* and its modified forms (*graphene oxide* (GO), *reduced graphene oxide* (rGO)), is quickly gaining interest in the preparation of supported metal catalysts and their applications.<sup>207</sup> Graphene has exceptional properties, such as great intrinsic carrier mobility at room temperature, with a perfect atomic lattice and excellent mechanical, thermal, electrical, and optical properties. Numerous metals have been deposited on graphene support and applied in a variety of transformations, including hydrogenation, CO oxidation, aerobic oxidation of alcohols, or fuel cell applications.<sup>208–211</sup>

*Carbon nanotubes* (CNTs) are another group of the more recent forms of carbon.<sup>212, 213</sup> They possess unique properties, such as high mechanical strengths and high thermal stability, which make them a good alternative to conventional catalyst supports.<sup>214, 215</sup> Pd is one of the most commonly applied metal to be deposited on the surface of CNTs due to its ability to catalyze a multitude of reactions, from hydrogenations to C-C coupling reactions.<sup>216–220</sup> In addition to the nanotubes, *carbon nanofibers* (CNF) are also frequently applied in catalysis.<sup>221–223</sup>

## Polymeric materials

There are a large number of reports in which polymeric materials are applied as a catalyst support. In early studies polymers were applied to stabilize metal colloids. Later, synthetic polymers have been applied in the preparation of immobilized metal complexes (*vide infra*).<sup>224</sup> The preparation of these catalysts usually goes through two major pathways. In the first, preformed polymer particles are used and the metal is deposited on the surface of the polymers commonly by reduction of metal salts. The second pathway involves the introduction of the metal during the polymerization process. In this case the metal will be embedded into the polymer.

With the development of highly selective methods for the synthesis of well-defined, submicrometer size polymer beads, the applications were extended to the preparation of supported metal catalysts as well.<sup>225</sup> *Poly(styrene)* and its cross-linked derivatives (with divinyl benzene) are likely the most common support materials; however, *poly(vinylpyridine)* is also often applied. They are applied for several processes, such as hydrogenation,<sup>226, 227</sup> metal-catalyzed couplings,<sup>225</sup> and the polymerization of lactones.<sup>228</sup> There are several polymer supports, such as *poly(vinylpyridine)* (PVP), *aminomethylated polystyrene* (AMPS), or *Amberlyst-OH* (AOH), that possess reasonable basic properties and thus are applied in potentially bifunctional catalysis, where the basic supports

fulfill an important role in the selective adsorption of acidic reactants or chiral modifiers, similarly to the alkaline metal carbonate-supported catalysts.<sup>37</sup>

*Polydopamine* (PDA) is a nature-inspired highly basic, functional polymeric material. PDA is a green, environmentally benign synthetic polymer that is produced from renewable starting materials. As a strong base it has been used as an organocatalyst on its own and has also been utilized as a support for metal nanoparticles.<sup>229, 230</sup>

In recent applications, polymers have been applied as support materials for nanoparticles.<sup>231</sup> In order to extend the scope of these catalysts, renewable biopolymers such as alginate or chitosan have been also applied as support materials.<sup>232–235</sup>

### Biomass-based materials

The preparation of renewable catalytic materials, including supports for metal deposition, is another of the emerging areas. These materials are prepared from various renewable biological sources. Based on the source and the preparation method there are several classes of these materials. *Biomass ashes* form after the combustion of various forms of biomass and include mostly compounds of basic properties (CaO, K<sub>2</sub>O, MgO, carbonates, etc.). Similar basic materials are obtained from waste shells (e.g., egg or shellfish shells) and bone materials. *Activated carbon* materials are mostly produced from high carbon materials, such as wood or coconut shells. *Chitosan* is an abundant, biodegradable, and renewable material with reasonable thermal and chemical stability. It is a carbohydrate heteropolymer similar to cellulose having hydroxy, amino, and acetyl-amino groups on its surface and produced on a large scale from crustacean shells (waste from the food industry). Chitosan is applied as a neat catalyst,<sup>236, 237</sup> as well as support material for metals.<sup>238</sup>

Several recent accounts provide in-depth information regarding these materials.<sup>239–241</sup>

### Self-supported catalysts

Although they are not directly support materials, the development of these catalysts has been inspired by the immobilization of chiral complexes on surfaces. These catalysts are based on polymeric materials, usually applying chiral monomers, that are combined with metals. The embedded metal is responsible for the catalytic activity, and the chiral matrix provides the environment for enantioselection. These catalysts have attracted growing attention and are widely used in organic transformations, such as cyclopropanation, oxidation, amination, and addition reactions.<sup>242</sup>

#### 2.2.3 Heterogenized metal complexes and organocatalysts

In order to combine the advantages of the high performing metal complexes of homogeneous catalysis and the more robust, stable, and higher stability solid catalysts, several techniques were developed for the immobilization of metal complexes on mostly inert, solid surfaces.<sup>243, 244</sup>

When a metal complex that was used as a homogeneous catalyst is immobilized on a solid support the same effective catalyst could be applied in heterogeneous catalysis. This change offers several benefits, as compared to the original homogeneous alternatives, that are related to the solid nature of the catalyst such as ease of separation, applicability in flow systems, stability, and the likes. One must not forget, however, that, on average, heterogenized metal complexes are usually less active or selective than the parent complexes in the solution phase.<sup>245</sup> There are several methods to anchor metal complexes to surfaces by covalent, ionic, or noncovalent interactions. A host of support materials were used, from functional polymers, or graphene to mesoporous silicas, such as SBA-15, including chiral complexes.<sup>246–251</sup>

In contrast to the previously highlighted potential benefits, it appears that the pharmaceutical and fine chemical industries, at least up to now, did not embrace the idea of heterogenized metal complexes. Despite the extensive efforts that have been made in the past nearly three decades, researchers are still yet to develop a catalyst based on immobilized metal complexes that would surpass the parent homogeneous metal complex, in terms of turnover number and turnover frequency. In addition, the preparation of such catalysts is often tedious and expensive, sometimes even the support material needed to be developed separately, and the addition of the large amount of support eventually leads to more waste. In short, thus far the concept, while appeared promising, could not make the potential benefits real.<sup>252</sup>

Similar approaches exist for the immobilization of organocatalysts as well, using polymers and porous materials as supports.<sup>224, 253–255</sup>

#### 2.2.4 Metal nanoparticle-based catalysts

Metal species with size below the  $\mu\text{m}$  range (single atoms, nanoclusters, and nanoparticles) are considered in this category. Based on their extremely small size, these materials often exhibit unusual catalytic behavior in various heterogeneous catalytic transformations. It is well known in the literature that several catalyst characteristics, such as particle size, metal-support interaction, mass transport limitations, and others, significantly influence the individual, inherent elemental characteristics of metals.<sup>256, 257</sup> As nanoparticles are often unstable on their own, stabilizers such as organic polymers or supramolecular assemblies are applied.<sup>258</sup> The most commonly applied stabilizers are polymers,<sup>259, 260</sup> starch,<sup>261</sup> organic ligands,<sup>262</sup> ionic liquids,<sup>263</sup> the surface fluorination of supported nanoparticles (e.g., on  $\text{TiO}_2$  support),<sup>264</sup> or special heating methods.<sup>265</sup>

A group of carbohydrates, cyclodextrins, also provides stabilization of metal nanoparticles, and in addition, they open up a possibility to combine the efficacy of nanoparticle catalysis with the versatility of supramolecular host-guest chemistry.<sup>266</sup> When a properly modified cyclodextrin derivative (host) is immobilized on the surface of the metal nanoparticle it opens up opportunities for biphasic reactions. Essentially the cyclodextrin acts as an immobilized phase

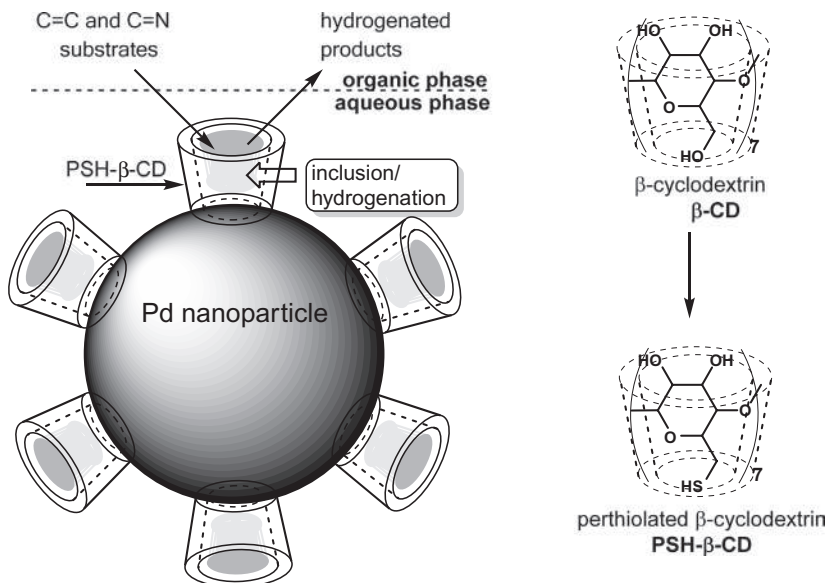


**FIG. 4** Catalytic inverse phase transfer/hydrogenation of hydrophobic C=C and C=N group-containing compounds in aqueous medium using  $\beta$ -cyclodextrin-stabilized Pd nanoparticles.

transfer catalyst, thus allowing the reactions to be carried out in water. This proof-of-concept model was demonstrated by Liu's group in biphasic hydrogenation reactions (Fig. 4). The nonpolar cavity of the cyclodextrin component can attract and host small hydrophobic organic compounds in aqueous solvent, and the metal nanoparticles could catalyze the reaction, in this case the hydrogenation of a broad variety of C=C and C=N bonds. The reaction provided the hydrogenated products in excellent yields.

Nanoparticle-based catalysts, whether supported or stabilized samples, are widely used in catalytic applications. They are applied in oxidations, hydrogenations, oil refining, environmental applications, catalytic reforming, or photocatalysis, just to name a few.<sup>257, 267</sup>

### 2.3. Nonmetallic catalysts

In addition to metal-based catalysts, there is a large and diverse group of materials that are commonly used as catalysts, often on industrial scale. In an effort to replace harmful and corrosive mineral acids and bases, solid acids/bases have become the catalysts of choice in organic synthesis. The same way heterogeneous metal catalysis began with Sabatier's hydrogenation studies,<sup>31</sup> the catalysis by nonmetal catalysts (aluminum oxide) was initiated by Vladimir Ipatieff in the early 1900s.<sup>268</sup> Ipatieff's discoveries led to early industrial applications and he is widely credited with the development of the process that allowed the

preparation of high octane (~100 octane number) gasoline that was used in RAF aircrafts during WWII and allowed them to win the aerial battle over Great Britain.<sup>269, 270</sup> After the early start with  $\gamma$ -alumina, several new solid acid catalysts have been developed and applied. Solid acid catalysis has become a definite choice in industrial as well as laboratory applications. The traditional solid Brønsted, Lewis, and mixed acids such as metal oxides and natural aluminosilicates have been in use for over 50 years. Somewhat later, new materials have been introduced into the realm of solid acid catalysis, such as polymeric ion exchange resins (e.g., Nafion-H, Amberlyst, Dovex, Deloxane, etc.); heteropoly acids and their derivatives (e.g.,  $H_4[SiMo_{12}O_{40}]$  or  $H_{0.5}Cs_{2.5}[PW_{12}O_{40}]$ ); immobilized metal halides (e.g.,  $ZnCl_2$ ,  $AlCl_3$  etc.) or triflates; sulfated metal oxides (e.g., sulfated zirconia) or natural and semisynthetic clays (e.g., montmorillonite K-10, KSF, and their metal-doped derivatives such as ClayFen, ClayCop, etc.) and zeolites (e.g., HY, H-ZSM-5, and other modified or synthetic zeolites) among many others. The other major nonmetal catalyst group is the solid bases. The traditional solid bases are well known for many decades, and some were mentioned above as catalyst supports for metals as they are frequently applied in bifunctional heterogeneous catalysis. These materials include magnesium oxide, alumina, or alkaline earth carbonates. Later, other materials such as basic polymers (e.g., poly(vinylpyridine)) or basic, ion-exchanged clays, hydrotalcites or zeolites have been introduced to this group. In the following subchapters these materials will be discussed by the most common groups. Due to the limited scope of this chapter we will focus on giving a broad overview discussing general features of these catalytic materials instead of going into specific details regarding their structure or mode of action. Nonetheless, the literature regarding these catalysts is abundant and the reader is encouraged to consult with specialized accounts for more detailed information.<sup>271–284</sup>

Solid acid catalysts have become the catalyst of choice and are extensively applied in the synthesis of fine chemicals as well as in the pharmaceutical industry.<sup>285–289</sup> In addition to their physical advantages such as practical utility, durability, easy separation, their chemical properties are also beneficial to facilitate their use in green synthesis. They are potentially recyclable, their cost is mostly low, and most of all, they exhibit high tolerance against water.<sup>290</sup> Many of these materials possess additional interesting properties, one of these is being an excellent microwave absorber. This feature enables them to serve not only as a catalyst but also as an internal heating medium. Through this characteristic, many of these materials can promote solvent-free reactions which is an additional green benefit in applications.<sup>291–294</sup>

In addition to solid acid catalysts, solid bases are also important and can replace the very corrosive soluble bases such as NaOH or KOH. They are also much less sensitive to the carbon dioxide content of air that reacts with the earlier mentioned base solutions. Therefore solid base-catalyzed reactions and the catalysts themselves also attracted extensive attention as indicated by the substantial number of reviews regarding this topic.<sup>284, 295–300</sup>

### 2.3.1 Metal oxides

The first extended group of solid acids is that of metal oxides.<sup>301–303</sup> Although their surface acid strength is somewhat modest, they are broadly available and relatively inexpensive and constitute a versatile group of acid catalysts for organic synthesis.<sup>304</sup> The most well-known members are common silica or acidic alumina catalysts that have been discussed before. The surface acidity of metal oxides can be adjusted with a sulfuric acid treatment, which results in the formation of a special group commonly called sulfated metal oxides.<sup>305, 306</sup> The sulfuric acid treatment appears to improve the Lewis acid character of the oxides and at the same time results in stronger acidity. Some of these materials, particularly sulfated zirconia, are popular solid Lewis acid catalysts in a wide variety of synthetic transformations.<sup>307–311</sup>

Metal oxides are one of the oldest types of catalysts; see Ipatieff's early works that established these materials as catalysts.<sup>268–270</sup> Their broad applications and popularity were aided in part by the fact that many of these oxides are naturally occurring and cost effective; they became prominent in the mid-1950s after their catalytic potential was revealed.<sup>312</sup> They constitute a class of inorganic materials that typically exist in crystalline solid form containing metal cations and oxide anions. They exhibit specific surface defects and environments that are largely responsible for the widely varied properties attributed to them. In particular, the presence of  $O^{2-}$  anions, typical of metal oxides, is observed at the surface because their size is superior to that of metal cations. The existing unsaturations are usually counterbalanced by a reaction with water generating hydroxyl groups, further conferring acid/base properties. Nonstoichiometric features can also give rise to vacancies (e.g., cation deficiency) contributing to interesting redox and electronic behavior. Accordingly, these catalysts have numerous applications in the laboratory as well as at the industrial level, in particular, they are widely employed for acid/base, oxidation, and selective industrial catalytic processes.<sup>312, 313</sup>

The metal oxides term covers a wide range of catalysts including one-, two-, or three-dimensional simple oxides such as silica, alumina, layered clays, zeolites, titania, zirconia, zinc oxide and copper oxide, porous and mesoporous metal oxides, and complex or mixed oxides such as polyoxometalates (POMs) of Keggin or Dawson type (the conjugate bases of heteropolyacids), phosphates (e.g., silica phosphoric acid, VPO), multicomponent mixed oxides (e.g., molybdates, antimonates, tungstates), hexaaluminates, perovskites, etc.<sup>314</sup>

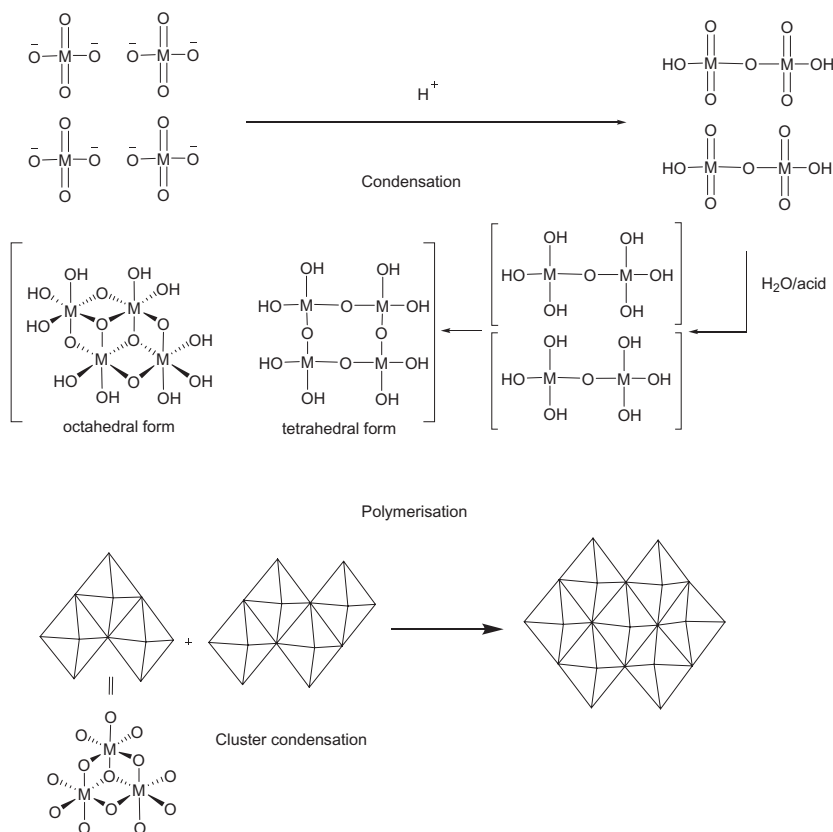
Simple oxides having the formula  $MxOy$  usually possess structures based on cubic or hexagonal packing of oxygen atoms with the octahedral or tetrahedral sites (or both) occupied by the same metal ions, whereas mixed oxides have two nonequivalent metal sites similar to the spinel structure with the general formula  $AB_2O_4$ .<sup>315, 316</sup> Simple and mixed oxide catalysts and some typical industrial applications are presented in Table 3. It should be noted that heteropoly acids, zeolites, MOFs, and clays are not included because they will be detailed in the following separate sections.

**TABLE 3** Simple and mixed metal oxide catalysts and their major applications.

| Metal oxide                                      | Typical applications   | Ref. |
|--|--|------|
| TiO <sub>2</sub>                                 | Major component of denitrification catalysts and photocatalysts  | 314  |
| Fe <sub>2</sub> O <sub>3</sub>                   | Fischer-Tropsch reactions  | 314  |
| Cu-Cr oxides                                     | Hydrogenations   | 314  |
| AlPO <sub>4</sub>                                | Acid-catalyzed reactions, polymerization   | 314  |
| Sn-SB oxides                                     | Selective oxidation  | 314  |
| FeO or mixed oxides Zn, Cu, Cr                   | Water-gas shift reaction   | 314  |
| Fe <sub>2</sub> O <sub>3</sub> /SiO <sub>2</sub> | H <sub>2</sub> S oxidation to SO <sub>2</sub> and H <sub>2</sub> SO <sub>4</sub>                           | 314  |
| Fe <sub>3</sub> O <sub>4</sub>                   | Friedel-Crafts acylation   | 317  |
| CuO, Cu <sub>2</sub> O                           | CO and NO oxidation  | 318  |
| ZnO, Cr <sub>2</sub> O <sub>3</sub> , CuO        | Ethylene + HCl + O <sub>2</sub> to dichloromethane<br>Aromatic carboxylic acids hydrogenation to aldehydes | 312  |
| Zirconia   | Aromatic carboxylic acids hydrogenation to aldehydes   | 312  |

Concerning the synthesis of metal oxides, it is crucial to control parameters such as the morphology, the porosity, and the surface area in addition to the thermal, chemical, and mechanical stability as these properties will determine the activity and robustness of the catalyst. The synthetic routes to prepare simple oxides and mixed oxides are different. For simple oxides, common approaches include aqueous-phase precipitation, sol-gel methods, and solvothermal synthesis. They all rely on the reaction of water or an organic solvent with inorganic precursors.<sup>140, 312</sup> Notably, the sol-gel method is a process during which the raw materials are dispersed in solution and undergo condensation-polymerization steps after formation of an active monomer as illustrated in [Scheme 2](#).<sup>319</sup> For the solvothermal method, the medium can be anything from water to organic solvents, and the synthesis occurs in a closed vessel with controlled temperature and pressure. Thus it allows a precise control over the size distribution, the shape, and the porosity.

Parallel methods employing a surfactant as a template were developed to maximize the specific surface area.<sup>320</sup> Often, the obtained materials are further activated by thermal treatment to eliminate colloidal template and inorganic anions.



**SCHEME 2** Schematic representation of the sol-gel condensation—polymerization method (M=metal).

For mixed oxides, the most common approach is to coprecipitate two metal salts by mixing them in a solution and initiating the precipitation by carefully selecting the appropriate base at a given pH. The resulting precipitate is then calcined under specific atmosphere.<sup>312</sup>

While the properties of synthetic metal oxides can easily be tuned by adjusting experimental parameters such as the pressure, the temperature, or the precursors, various techniques exist to further improve the catalytic properties of metal oxides.<sup>321</sup> Notably, their features can be enhanced by the addition of other chemicals, a process called doping. Doped metal oxides have other cations substituting the host cation and these exchanges disrupt the original structure and will modify the catalytic properties.<sup>322</sup> Another common way to improve the acidity and catalytic performance of several metal oxides is to prepare anion-modified metal oxides. Although there are several such catalysts, the most successful and commonly applied is sulfated zirconia, first reported in the 1960s.<sup>310</sup>

Supported metal oxide catalysts, consisting of an active form of metal oxide dispersed on a high surface area oxide support, provide another solution to enhance the catalytic activity.<sup>323, 324</sup> In particular, the metal oxide and its support can achieve a synergetic activation of substrates and increase the thermal and electron conductivity among other properties.

### 2.3.2 Heteropoly acids

Heteropoly acids (HPAs) are fundamentally different from other nonmetallic catalysts; they are made of hydrogen, oxygen, heteroatoms, and metals. HPAs can be characterized as clusters of transition metal oxides that develop various structures. They have a unique property, that makes them generally soluble both in water and a variety of organic solvents.<sup>325, 326</sup> One of the common methods that turn HPAs to insoluble solids, thus true heterogeneous catalysts, is to prepare their salts using large cations such as cesium.<sup>327–329</sup> These materials possess negligible solubility in either hydrophilic or hydrophobic media, presenting a strong potential for the recycling of these catalysts, in most cases, without significant loss in activity.<sup>330</sup> After an HPA salt-catalyzed reaction, the catalyst can easily be separated from the reaction mixture by filtration, centrifugation, or evaporation, and then washed with proper solvent, dried, and reused for another consecutive cycle.<sup>331</sup> In addition, HPAs are generally regarded as safe and green; they exhibit minimal toxicity and they are mildly noncorrosive.

HPAs are often categorized according to the structure of the heteropolyanion forming the fundamental unit called the primary structure. The connection of these heteropoly anions by hydrogen bonding generates the secondary structure as shown in Fig. 5.<sup>332, 333</sup>

HPA salts possess unique superacidic and multielectronic properties, hence they have the ability to operate as strong acids and multielectron oxidants. In fact, their acid strength is substantially stronger than that of  $\text{H}_3\text{PO}_4$  and usual inorganic acids such as  $\text{HCl}$ ,  $\text{H}_2\text{SO}_4$ , and  $\text{HNO}_3$ .<sup>330</sup> Consequently, HPA salts are highly active catalysts employed for a range of organic transformations going from redox to acid/base reactions.<sup>334–336</sup> These materials have successfully

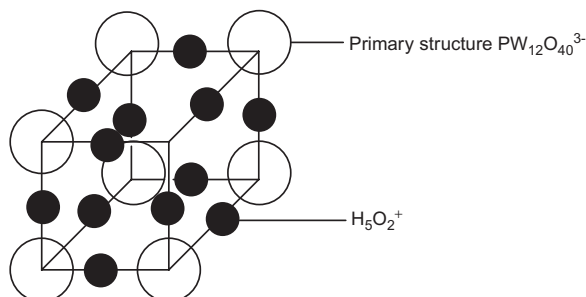


FIG. 5 Secondary structure of Keggin HPAs.

catalyzed alcohol dehydration, alkylation, esterification, hydrolysis, polymerization, and oxidation among other reactions.<sup>337, 338</sup> Generally, the mechanism involved in HPA-catalyzed reactions starts with protonation of the reagents followed by the conversion of the ionic intermediates to the corresponding products. The yields and reaction rates are often related to the number and the strength of surface active sites. The most common HPA types with their applications are summarized in Table 4.

The conventional preparation of HPA salts involves mixing the cationic and anionic species in solution; the precipitate, being too small to filter can be isolated by solvent evaporation.<sup>345</sup> Some salts require further calcination to become compositionally uniform.

Because some HPAs suffer from a rather low surface area,<sup>341</sup> the inclusion or entrapping of the HPAs into an inorganic or organosilica matrix is commonly performed.<sup>346, 347</sup> In this case, HPAs can be used in their original form, not as salts, because the heterogeneity is provided by the solid support. Such supported HPAs are prepared by impregnation of the salt onto silica (interactions occur between Si-OH and HPA molecules) or other inert supporting material, followed by drying and calcination.<sup>345</sup> Mesoporous silica and mesoporous silica molecular sieves are ideal supports for HPAs as their pores are large enough to host them and they do not cause decomposition.<sup>348</sup> Supported HPAs have demonstrated high catalytic activities and selectivities in comparison to the parent HPAs for organic transformations such as Friedel-Crafts reactions, dehydration, aldol condensation, and oxidation reactions, as well as acetalization, Beckmann rearrangement, and syntheses of heterocyclic compounds.<sup>348</sup> There are examples for immobilizing HPAs onto the surface of magnetic supports for even easier separation.<sup>349</sup>

### 2.3.3 Clays

Clay catalysts, along with zeolites, are aluminosilicates and probably one of the most often applied solid acid catalysts primarily in the laboratory practice. Although the early efforts focused on natural materials, their structure and catalytic properties inspired extensive efforts on the modification of natural clays to semisynthetic and modified derivatives.<sup>17, 271, 273, 276</sup>

Structurally, clays are aluminosilicates constituted of multiple layers of polyhedrons such as tetrahedral silicon oxides and octahedral hydrous alumina.<sup>350</sup> Each aluminosilicate layer generally consists of one (1:1 type) or two (2:1 type) silicon oxide tetrahedral sheets bonded to one aluminum or magnesium oxide octahedral sheet by electrostatic and hydrogen-bonding forces in a sandwich fashion.<sup>351</sup> Clays can be classified into two categories: the negatively charged clays that welcome balancing cations in their interlayer space (e.g., smectite, vermiculite, mica) and the positively charged clays possessing counterbalancing anions instead (e.g., chloride).<sup>17</sup> While the first class is most commonly prepared from natural sources of clays, the second class is often synthetic because

**TABLE 4** The four most common HPA types, their general formula and typical examples of organic transformations they catalyze.

| HPA type    | Formula                                | Representative example of catalyzed transformation |   | Ref.                |
|-------------|--|--|---|---------------------|
| Anderson    | $H_xA_y[BD_6O_{24}] \cdot zH_2O$       | $(NH_4)_4[ZnMo_6O_{18}(OH)_6]$                     | Oxidation of halides to aldehydes or ketones  | <a href="#">339</a> |
|             |  | $(NH_4)_4[CuMo_6O_{18}(C_5H_9O_3)_2]$              | Addition of $CO_2$ to epoxides to form cyclic carbonate                                       | <a href="#">340</a> |
| Keggin      | $H_xA_y[BD_{12}O_{40}] \cdot zH_2O$    | $H_3PMo_{12}O_{40}$                                | Oxidation of sulfides to sulfoxides   | <a href="#">341</a> |
|             |  | $H_3PW_{12}O_{40}$                                 | Friedel-Crafts alkylation of indoles  | <a href="#">342</a> |
| Preyssler   | $H_xA_y[B_5D_{30}O_{110}] \cdot zH_2O$ | $H_{14}[NaP_5W_{30}O_{110}]$                       | Synthesis of hydroxytriarylmethane from 2-sulfobenzoic anhydride and phenols                  | <a href="#">342</a> |
|             |  | $H_{14}[NaP_5W_{29}MoO_{110}]$                     | Esterification of cinnamic acids with phenols and imidoalcohols                               | <a href="#">343</a> |
| Well-Dawson | $H_xA_y[B_2D_{18}O_{62}] \cdot zH_2O$  | $H_6P_2W_{18}O_{62}$                               | Three-component synthesis of 2-amino-chromene derivatives                                     | <a href="#">342</a> |
|             |  | $H_6P_2W_{18}O_{62}$                               | Synthesis of quinoxaline via condensation of 1,2-dicarbonyl compounds with o-phenylenediamine | <a href="#">344</a> |

A=Li, Na, K, Rb, Cs, Mg, Ca, Al,  $NH_4$ , an ammonium salt, or a phosphonium salt; B=P, Si, As, or Ge; D=Ti, V, Cr, Mn, Fe, Co, Ni, Cu, Zn, Ga, Zr, Nb, Mo, Tc, Rh, Cd, In, Sn, Ta, W, Re, and Tl.

they are less frequent in nature. Notably, the cationic smectite clays are derived from the minerals talc and pyrophyllite possessing neutral interlayer that are rendered negatively charged by isomorphous substitution of a metal ion by another of different valence (e.g., Si(IV) by M(III), Mg(II) by M(I), or Al(III) by M(II)).<sup>352</sup> Consequently, the negative charge is compensated by cations. The general structure of common clays is represented in Fig. 6.

Clays have demonstrated remarkable catalytic activity because they have the ability to act as a microreactor capable of initiating reactions on account of their porous structure within which molecules can interact in specific ways and on account of their inherent properties such as adsorption-, swelling-, and ion-exchange capacities.<sup>165, 166, 353</sup> Depending on the type of clay and its properties, various transformations can be catalyzed.<sup>354, 355</sup> Notably, the widespread cationic clay montmorillonite, member of the smectite group,<sup>356</sup> exhibits an excellent adsorption capacity in addition to a high surface area and interesting acidic properties which altogether contribute to its success as catalyst in various reactions, including Friedel-Crafts alkylation, oxidative deprotection, nucleophilic additions, and many others.<sup>357-359</sup> On the other hand, the negatively charged clays exhibit anion adsorption, anion diffusion, and exchange properties together with surface basicity which open up other applications possibilities, also including the catalysis of organic transformations.<sup>356</sup>

Clays can be used directly in their natural form or after undergoing chemical or thermal treatments or a combination of the two in order to remove impurities

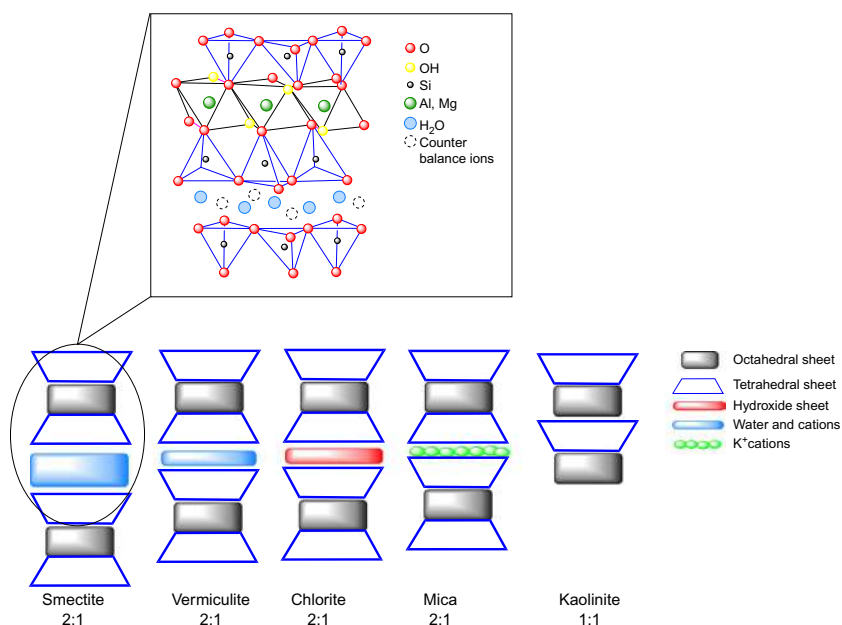


FIG. 6 Schematic representation of the generic structure of common clays.

and enhance specific properties.<sup>360</sup> In particular, the acidic properties of clays can easily be enhanced by an acidic activation method during which a mineral acid solution is applied such as phosphoric acid, sulfuric acid, or nitric acid.<sup>361</sup> The resulting materials exhibit improved acidity and increased number of active sites and surface area. Montmorillonites K-10 and KSF, both acid-treated montmorillonites, are the most widely used acidic clays in the field of clay-catalyzed organic chemistry.<sup>362</sup> Concerning thermal treatments, they have the ability to modify the concentration of hydroxyl groups directly related to the clay acidity.<sup>363</sup> Interestingly, the total surface Brønsted acidity increases with heating until a certain temperature (around 120°C), due to enhanced dissociation of the interlayer water molecules, after which the Brønsted acidity decreases due to the complete removal of the water. In parallel, the amount of Lewis acid sites increases with increasing temperature due to the dehydration and dehydroxylation process (Fig. 7).<sup>365</sup> Pillared clays constitute another modification to improve the properties of the clay by making the active sites more accessible. Modification of natural clay minerals by pillaring involves the exchange of existing cations with robust inorganic molecules forming oxides strongly bound to layers of the minerals. The method allows for opening of the clay layers, producing high resistance and thermal stability, increased porosity, and surface area among other benefits.<sup>366</sup>

### 2.3.4 Zeolites

Heterogeneous catalysis by zeolites is one of the most active areas of catalysis research; zeolite-based catalysts certainly dominate industrial applications in the nonmetallic catalyst segment. They are widely used in a large number of protocols from industrial processes to automotive applications, and thus are frequently the topic of reviews.<sup>367–371</sup>

Similarly to clays, zeolites are also aluminosilicates; however, in contrast to the layered structure of clays, zeolites exhibit a well-defined channel and cage-based framework,<sup>372–375</sup> or less commonly a lamellar structure.<sup>376</sup> Most zeolites are composed of aluminosilicate sheets although the layers can be a combination of both silicates and aluminosilicates.<sup>376</sup> They are built from interconnected tetrahedra made of oxygen, silicon, and aluminum, which correspond to the primary building units (Fig. 8). These units then undergo assembly to form secondary building units, themselves serving as higher level

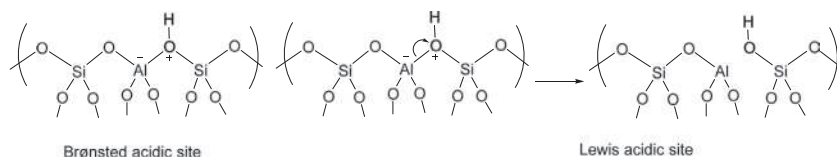
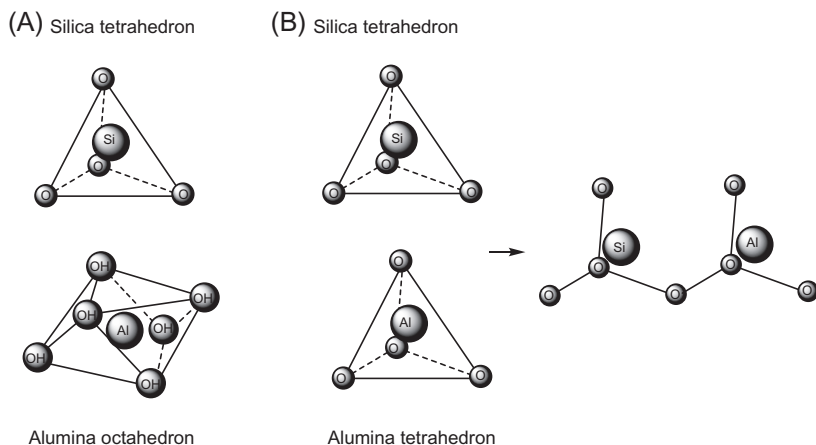


FIG. 7 Schematic representation of a possible structure of Brønsted and Lewis active sites for an aluminosilicate material.<sup>364</sup>



**FIG. 8** Common building blocks for clays (A) and zeolites (B).

building blocks for the composite building units (such as the sodalite cage) further combining to constitute the final structure of the zeolite. As a result, the arrangement of atoms creates a network of one, two, or three channels of molecular dimensions.<sup>377, 378</sup>

Zeolites possess great ion exchange capability, high surface area, an interconnected channel network in addition to high adsorption ability, a combination of these generates interesting behavior for different applications, mainly catalysis, separation or adsorption applications. These beneficial features highly depend on the type of zeolite and their individual characteristics.<sup>379</sup> For instance, the number of charges (extra framework cations and framework Si/Al ratio) has an influence on the hydrophilicity of the zeolites which are therefore more or less selective adsorbents for polar or nonpolar molecules. The morphology of the channel network, on the other hand, can favor catalyst-substrate interactions and confinement effects. Similarly, the number of redox or acidic active sites of the zeolite has an impact on the activation of reactants in catalytic reactions.<sup>380</sup> As mentioned before, the three-dimensional structure and the chemical composition, notably the ratio of silica to alumina, vary in each zeolite type, the general formula being  $M_x/mAl_xSi_{1-x}O_2$ . Given the multiple combinations of structure and composition, several hundreds of natural and synthetic zeolites exist.<sup>381</sup> Commercially available zeolites include Silicalite-1 and ZSM-5 (MFI), Linde Types X and Y (Al-rich and Si-rich FAU), Linde Type A (LTA), ferrierite (FER), beta zeolites (BEA), the mordenite family (MOR), and the Linde Type L family (LTL) among others.<sup>382</sup> Their respective Si/Al ratio, their origin as well as common applications for each are presented in Table 5. Despite the many existing zeolitic materials, the development of new synthetic methods for their preparation is an ongoing process.<sup>384-387</sup>

Examples of structure of zeolites are presented in Fig. 9.

**TABLE 5** Commercially available common zeolites, their properties and applications.<sup>383</sup>

| Zeolite type      | Origin                | Ratio Si/Al | Common applications  |
|-------------------|-----------------------|-------------|--|
| MFI: Mobil Five   | Synthetic             | > 10        | Catalysts in petroleum field and for fine chemical synthesis |
| FAU: Faujasite    | Synthetic mostly      | 1–4         | Catalysts  |
| LTA: Linde Type A | Synthetic             | 1           | Ion exchange   |
| FER: Ferrierite   | Natural and synthetic | 5           | Catalysts, separating agents                                 |
| BEA: Beta         | Synthetic             | > 5         | Catalysts, adsorption agents                                 |
| MOR: Mordenite    | Natural or synthetic  | 5           | Catalysts, separating agents                                 |
| LTL: Linde Type L | Synthetic             | 1–6         | Catalysts in petroleum chemistry, adsorption agents          |

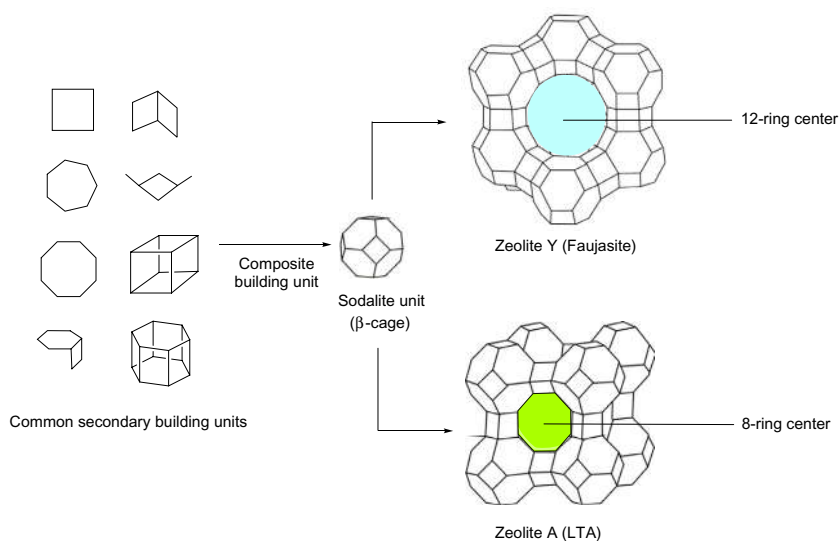


**FIG. 9** Examples of basic zeolite structures constructed from the so-called sodalite unit.

Synthetic zeolites are usually prepared under hydrothermal conditions involving a process that can be described as multiphase (liquid phase and amorphous/crystalline solid phase) reaction-crystallization. The reaction usually occurs at temperatures above 100°C in alkaline medium with amorphous reactant precursors containing silica, alumina, and a cationic source.<sup>388</sup> An alternative synthetic pathway, performed at neutral pH, is based on fluoride-containing compositions such as mineralizing media, usually providing reduced nucleation rates giving rise to larger crystals.<sup>389</sup>

A notable limitation of zeolites lies in the slow mass transport of reagents in the micropores and even more so when bulky molecules are involved in the catalytic reaction.<sup>380</sup> Synthetic and postsynthetic strategies such as supramolecular self-assembly and in situ synthesis using organic template molecules have been designed to improve the control of the mesoporous structure of the zeolite, thus significantly enhancing mass transport.<sup>390</sup> It should also be stressed that, although zeolites are strong acids at high temperatures, their acidity is moderate at the common temperature range of most organic syntheses. Here again, significant efforts were undertaken to prepare zeolites with enhanced catalytic activity. Their tunable structure can easily be taken advantage of by exchanging the cations or introducing specific active sites by functionalization with organic moieties, thus modulating the existing electronic features.<sup>391</sup> These advances in the development of novel synthetic routes have largely contributed to the broadening of the scope of zeolitic catalysis.<sup>392</sup>

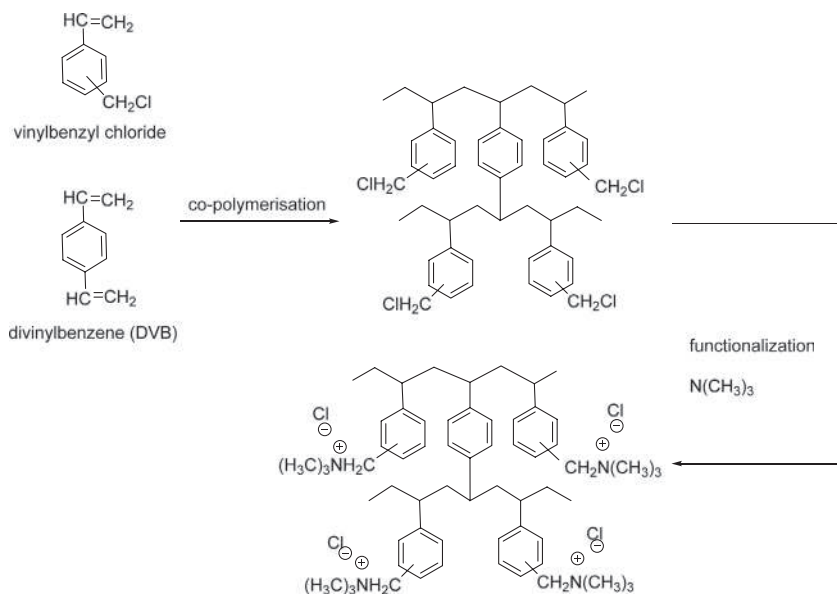
### 2.3.5 Ion exchange resins

*Ion exchange resins* are versatile materials possessing a modifiable framework based on cross-linked copolymers bearing functional groups that can participate in ion exchange.<sup>393</sup> Resins can be either cationic or anionic with different intensities of acid or base exchange abilities depending on the nature of the functional group. Accordingly, they can therefore be classified into four main groups: (1) cationic resins with strong acid exchange ability, and (2) with weak acid exchange ability; (3) anionic resins with strong base exchange ability and (4) with weak base exchange ability. Although the common functional group for the first category is the sulfonic acid group, the second category of resins usually bears carboxylic acid groups with much weaker acidity. Regarding anionic resins, strong and weak base exchange properties are often provided by quaternary ammonium groups and ammonium groups, respectively.<sup>393</sup> Another discriminating factor between resins is the degree of cross-linking, which controls the porosity. Typically, high cross-linking percentage results in macroporous structures whereas low cross-linked resins display a microporous gel structure, with resulting higher moisture content and loading capability.<sup>393</sup>

Depending upon their pore size, chemical structure, and formulation, ion exchange resins are useful in a number of transformations.<sup>145, 394, 395</sup> In general, industrial applications of cationic exchange resins as solid acid catalysts include the

dehydration of alcohols to olefins or ethers, the alkylation of phenols to alkyl phenols, olefin hydration to form alcohols, ester hydrolysis, and other reactions.<sup>396</sup> More specifically, the sulfonic acid-based functionalized cationic resins Amberlyst and Nafion are commonly employed in numerous catalytic processes.<sup>397</sup> While the Amberlyst type is based on a polystyrene-sulfonic acid motif, Nafion possesses sulfonic acid entities attached to a perfluorinated backbone that enhances its acidity to the superacidic level due to the high electron withdrawing character of fluorine. Amberlysts are able to catalyze transesterifications, Michael addition, Prins cyclization, Friedel-Crafts alkylations, protection of carbonyls, deprotection of acetals, cleavage of epoxides, crossed aldol condensations, and synthesis of quinolines, among others.<sup>395</sup> Nafion-H has been a commonly applied solid acid catalyst for a broad variety of synthetic reactions, such as oxidation, protection, and deprotection of alcohols and carbonyl containing compounds, Friedel-Crafts alkylations and acylations, as well as rearrangements.<sup>398</sup> Both ion exchange resin types offer the possibility to catalyze the aforementioned reactions under environmentally friendly conditions and unless the reaction temperature is too high, they appear recyclable with or without regeneration.<sup>393, 399-402</sup>

The synthesis of ion exchange resins entails a two-step process: a polymerization step involving two distinct polymer precursors followed by a functionalization step introducing an anion or a cation to produce an acid or a base exchange site on the resin, respectively. These sites can be exchanged with other metal ions to alter the basic properties.<sup>403</sup> Scheme 3 illustrates an example of the



**SCHEME 3** Schematic polymerization/functionalization for the preparation of an anionic exchange resin.

preparation of an anionic exchange resin from chloromethyl styrene copolymerized with divinylbenzene.<sup>404</sup>

It should be mentioned that the BET surface area of common ion exchange resins including Nafion-H is rather low ( $\sim 9 \text{ m}^2/\text{g}$ ) and they often suffer from poor porosity. To address these issues and fully take advantage of the strong acidity of Nafion-H, small Nafion-H particles can be trapped in a porous silica network significantly enhancing both the BET surface and the number of available active centers.<sup>405–407</sup>

### 2.3.6 Metal-organic frameworks

*Metal-organic frameworks* (MOF) are crystalline and porous compounds that are composed of organic linkers and inorganic metal ions.<sup>408</sup> Unlike zeolites that have a restricted number of structures, the hybrid nature of MOFs allows a broad array of ligand/metal cluster combinations yielding practically infinite structural possibilities with tunable properties. Indeed, a major advantage of MOFs is that their pore size, shape, and chemical composition can be precisely controlled by the appropriate selection of the starting materials.

MOFs generally exhibit high porosity and internal surface area that are largely responsible for the broad application possibilities, including gas storage media, adsorbents, and catalysts.<sup>409, 410</sup> It should be noted, however, that MOFs as catalysts are relatively limited in terms of thermal and chemical stability, excluding them from reactions performed above  $300^\circ\text{C}$  as it is the case for oil-refining or petrochemical processes. Nonetheless, they hold a great potential for catalytic applications in the synthesis of fine chemicals carried out at lower temperatures.<sup>411</sup> These materials usually are robust catalysts minimally prone to deactivation. In addition, the possibility to synthesize MOFs incorporating dual metal/acid sites with high density is of great interest. These materials are commonly applied in acid,<sup>412</sup> base,<sup>413</sup> and redox<sup>414</sup> even solid/gas phase<sup>415</sup> catalysis. The incorporation of chiral linkers extends the potential applications of MOFs to asymmetric catalysis. Therefore MOFs not only have the ability to enhance the reaction rate but also to control the selectivity of a given organic reaction.<sup>411, 416</sup>

There are an extensive number of protocols for the synthesis of MOFs. The most common method is the self-assembly approach, which includes the mixing of two solutions, one contains the organic and the other the inorganic components, respectively. The process is often carried out under solvothermal conditions producing a crystalline framework.<sup>417</sup> Metal-carboxylate clusters are common secondary building blocks acting as nodes in the MOF architecture. The metal cluster links together with the carboxylates, such as terephthalic acid, to form a periodic network of the building blocks (Fig. 10).

Although the presence of the organic component makes it possible to introduce any number of chemical moieties, the functionalization of MOFs is somewhat limited by the solvothermal synthetic methods, causing solubility or

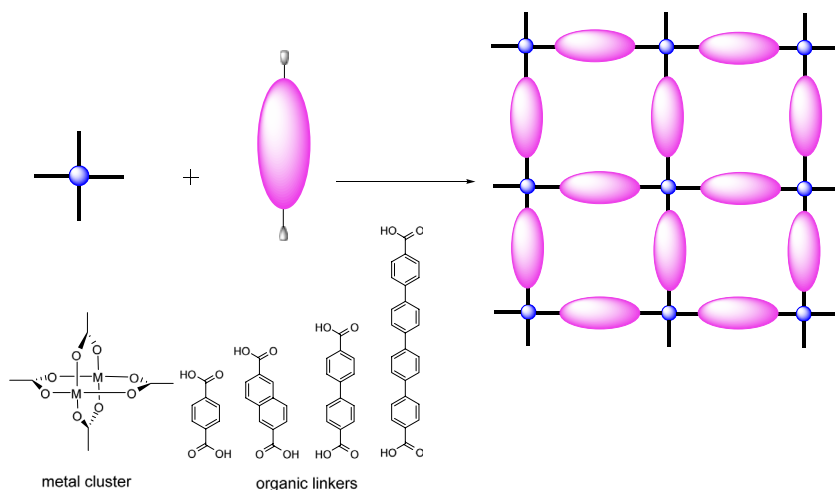


**FIG. 10** A schematic assembly of a metal-organic framework with examples of metal cluster/organic linkers.<sup>418</sup>

thermal instability issues for the ligands.<sup>419</sup> Therefore, in addition to developing protocols to build MOF structures from their individual building blocks, the postsynthetic functionalization of existing MOFs also attracted significant attention. It allows the introduction of new physical properties or chemical behaviors and therefore broadens the application scope of MOFs as catalysts. Fig. 11 illustrates two different approaches to encapsulate Brønsted acids within the

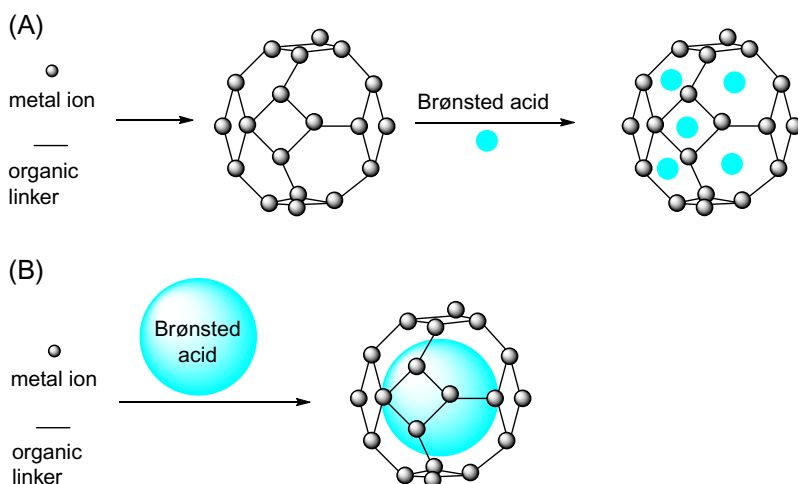


**FIG. 11** Schematic illustration of encapsulation of Brønsted acids within MOFs: (A) two-step method and (B) one-step method.

framework of MOFs: in the first the acid is added to the preformed MOF (two steps), in the second the acid is present during the MOF synthesis and the MOF grows around the encapsulated acid (one step).<sup>412</sup>

## 2.3.7 Other nonmetallic catalytic materials

### 2.3.7.1 Molecular sieves, pillared layer solids, and other mesoporous solids

Structurally similar to clays and zeolite molecular sieves, the synthesis and catalytic applications of pillared layered solids and ordered mesoporous materials have also attracted extensive interest.<sup>420</sup>

Mesoporous inorganic solids possess pore diameters of 20–500 Å which discriminate them from microporous materials with a crystalline framework. The particular advantage of these mesoporous molecular sieves therefore lies in the size of the pores that make them suitable catalysts for the transformations of large molecules. The synthesis of such mesostructures is traditionally performed in the presence of surfactant micelles as directing agents to allow a precise control of the pores and tailored dimensions of the obtained channels (Fig. 12).<sup>421</sup> The first mesoporous molecular sieves referred to as the “M41S family” were developed in the 1980s by a Mobil group and continues to be widely used; it is now commonly identified as MCM-41.<sup>422</sup>

Another highly popular mesoporous material is the commercially available Santa Barbara Amorphous-15 (SBA-15).<sup>423</sup> SBA-15 has been widely applied in heterogeneous catalysis due to its versatile properties, such as the comparatively thicker walls and the excellent thermal and mechanical stability.<sup>424</sup> It is used as acid-doped material<sup>425</sup> or as a support for metal catalysts.<sup>426</sup>

Pillaring is an interesting approach transforming a layered crystalline inorganic material into a thermally stable material with hierarchical porosity while retaining the initial layered structure. Therefore a pillaring agent is a compound that can be intercalated between two adjacent layers inducing an additional level of pores between the layers.<sup>427</sup> The resulting material possesses tailored pore size and volume, controlled accessibility to the active sites in addition to a high surface area.<sup>428</sup> These materials are usually described as 3D pillared layers, 2D pillared bilayers, interpenetrated and interdigitated layers. In addition, they are also used in conjunction with metal-organic frameworks.<sup>429</sup> A representative example of a pillared layer material and its possible applications is pillared

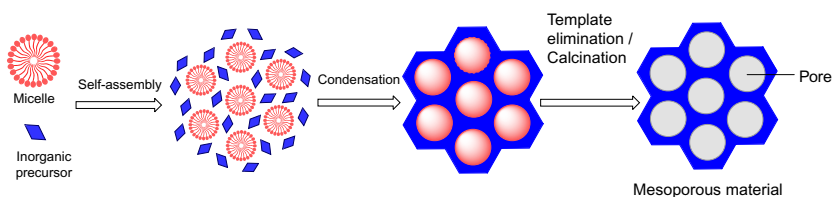


FIG. 12 Synthesis of mesoporous materials via surfactant templating.

layered perovskite oxides (HLaNb<sub>2</sub>O<sub>7</sub> with SiO<sub>2</sub>, or TiO<sub>2</sub> in the interlayer) that demonstrated excellent activity for the dehydration of alcohols.<sup>428</sup> Pillared clays (PILCs) are also commonly used as catalysts, especially in acid-catalyzed reactions but also in the synthesis of fine chemicals which includes hydroxylation, esterification, epoxidation, alkylation, hydrogenation, aromatization, and reduction of nitroso compounds.<sup>354, 428, 430</sup> In general, it is observed that the pillared clays exhibit better performance than that of the parent clays.

### 2.3.7.2 Composites and related materials

Composite materials are also frequently applied as solid acid catalysts. The major groups that belong to this category are (i) carbon-, (ii) ionic liquid-, and (iii) carbon silica composite-based solid acids.

The first group includes *carbon composites* that are commonly sulfonated, which results in highly acidic and effective solid Brønsted acid catalysts.<sup>431</sup> These materials are similar to oxidized graphite with its layered structure and carboxylic acid groups. However, the sulfonation used in this case will result in a high density of sulfonic acid groups, which ensures much stronger acidity. Depending on the preparation method, the density of the sulfonic acid groups in these materials is five times higher than that of Nafion-H, although the acid strength will not be as high. These catalysts are synthesized from renewable materials, such as natural carbohydrates, e.g., starch, cellulose etc., by partial carbonization and a subsequent sulfonation.<sup>432</sup> The applications are broad, from typical acid catalysis to Suzuki coupling and oxidation with metal-doped derivatives.<sup>433</sup> Special examples include the application of carbon nanotubes as the carbon material,<sup>434</sup> or metal/carbon composites to broaden their use to metal catalysis as well.<sup>435</sup>

The next group includes *ionic liquid-based composites*. Traditionally, these materials are prepared by immobilizing ionic liquids on solid surfaces, e.g., sulfonated silica.<sup>436–438</sup> Additional examples are ionic liquid coated sulfonated carbon-silica composites that are versatile solid acid catalysts for aqueous phase organic synthesis.<sup>439</sup> More recent examples include the preparation and application of IL-polymer composites.<sup>440</sup>

The last group, the *sulfonated carbon-silica composites*, has also been frequently applied as catalytic materials<sup>441, 442</sup> in numerous acid-catalyzed reactions, such as Hantzsch cyclization,<sup>443</sup> multicomponent synthesis of heterocycles,<sup>444</sup> Michael addition of indoles to  $\alpha,\beta$ -unsaturated ketones,<sup>445</sup> chemoselective protection of aldehydes, and C, N, O-acylations.<sup>446</sup> Overall, the preparation of nanocomposite materials often results in novel catalyst with potential synergistic effect of the individual components.<sup>447</sup>

A new emerging class of solid acids is the so-called *nanoacids* that are the nanomaterial form of traditional polymer-supported acid catalysts, essentially polymer-based nanoparticles functionalized with sulfonic acid groups.<sup>448</sup> These materials are prepared by traditional polymerization methods, such as emulsion polymerization, using reactive surfactants. The structural foundation of the

material is formed by the polymerization of the mixture of styrene and divinylbenzene to achieve appropriate level of cross-linking under specific conditions. Octylbenzene sulfonic acid was used as the surfactant, to ensure the deposition of the benzenesulfonate moiety on the surface of the particles. The obtained catalyst exhibited high activity and selectivity promoting the synthesis of urethane from isocyanate and alcohol. Nanoacids possess an obvious theoretical potential to show greater catalytic activity than traditional polystyrene-based sulfonic acids (e.g., Amberlyst-15) due to their larger surface area. However, this potential is yet to be achieved and extensively documented in practical, acid-catalyzed organic synthesis; the few examples that are available in the literature are promising, but more data are needed.<sup>448</sup> It is worth noting that the term nanoacid has already been coined for heteropolyoxometalate-based materials that possess strong acidic properties and prepared as nanoparticles.<sup>449</sup>

Finally, an emerging new area of acid catalysts is the application of carbon-based catalysts commonly referred to as *carbocatalysis*. Many of these catalysts are derived from some form of biomass, thus these catalysts represent a step toward sustainability in heterogeneous acid catalysis.<sup>218,450</sup> The elemental composition of these catalysts is mainly, though often functionalized, carbon that acts similar to organocatalysts, however, not as individual compounds, rather as a carbonaceous material. These materials are well known; they are mostly unwelcome catalyst poisons or modifiers in metal catalysis.<sup>451</sup> When the carbonaceous material forms under controlled conditions the particle size is often in the few nanometers range and the obtained material can catalyze reactions such as oxidation, reduction, or acid-base reactions. Other forms of carbon, such as graphene, are also frequently used in carbocatalysis.<sup>452</sup>

## 2.4. Conclusions and outlook

Catalysts from metal-based to nonmetallic materials have been reviewed in this chapter. While the relevant available literature is extensive, topics presented in subchapters could fill entire books, it was our intention to provide a broad overview and describe a scope as broad as possible. Although the traditional fields, such as metal-catalytic hydrogenations, or coupling reactions still apply well-known catalysts, in the past few decades a large number of new materials have been introduced to the preparation of heterogeneous catalysts. In some cases they serve as actual catalysts, in some others as a support material. These new materials include metal-organic frameworks (MOFs), new synthetic zeolites, or graphene-based samples. In addition to new materials, the introduction of nanoparticles to heterogeneous catalysis has been of major importance in this field. Nanoparticles appear to significantly contribute to the synthesis of highly active catalysts, metal or otherwise. It is safe to expect that these two trends will continue in the next decade or so, by new synthetic materials being introduced, and unambiguously we will also see a dynamically growing number of catalytic applications of nanoparticles. At the same time, some concepts that

were encouraging but have not fulfilled their promise (e.g., immobilized metal complexes or organocatalysts) will likely see a decline in activities. All in all, the demand for environmentally benign, stable, and nontoxic catalysts is continuously growing, which will ensure that the development of solid catalysts will remain a thriving and active field in the future.

## References

1. Anastas, P. T.; Warner, J. C. *Green Chemistry: Theory and Practice*, Oxford University Press: Oxford, 1998.
2. Török, B.; Dransfield, T., Eds. *Green Chemistry: An Inclusive Approach*; Elsevier: Oxford, Cambridge, MA, 2018.
3. Li, C.-J., Ed. *Handbook of Green Chemistry-Green Processes, Vol. 7. Green Synthesis*; Wiley-VCH, Weinheim, 2012.
4. Sheldon, R. A. Fundamentals of Green Chemistry: Efficiency in Reaction Design. *Chem. Soc. Rev.* **2012**, *41*, 1437–1451.
5. Gallezot, P. Conversion of Biomass to Selected Chemical Products. *Chem. Soc. Rev.* **2012**, *41*, 1538–1558.
6. Kokel, A.; Török, B. Sustainable Production of Fine Chemicals and Materials Using Non-Toxic Renewable Sources. *Toxicol. Sci.* **2018**, *161*, 214–224.
7. Simon, M.-O.; Li, C.-J. Green Chemistry Oriented Organic Synthesis in Water. *Chem. Soc. Rev.* **2012**, *41*, 1415–1427.
8. Han, X.; Poliakov, M. Continuous Reactions in Supercritical Carbon Dioxide: Problems, Solutions and Possible Ways Forward. *Chem. Soc. Rev.* **2012**, *41*, 1428–1436.
9. Clouthierzab, C. M.; Pelletier, J. N. Expanding the Organic Toolbox: a Guide to Integrating Biocatalysis in Synthesis. *Chem. Soc. Rev.* **2012**, *41*, 1585–1605.
10. Himmelberger, J. A.; Cole, K. E.; Dowling, D. P. Biocatalysis: Nature's Chemical Toolbox. In *Green Chemistry: An Inclusive Approach*; Török, B., Dransfield, T., Eds.; Elsevier: Oxford, 2018; pp. 471–512 (chapter 3.14).
11. Jiménez-González, C.; Constable, D. J. C.; Ponder, C. S. Evaluating the “Greenness” of Chemical Processes and Products in the Pharmaceutical Industry—A Green Metrics Primer. *Chem. Soc. Rev.* **2012**, *41*, 1485–1498.
12. Sheldon, R. A.; Arends, I.; Hanefeld, U. *Green Chemistry and Catalysis*, 2nd ed.; Wiley-VCH: Weinheim, 2014.
13. Somorjai, G. A.; Li, Y. *Introduction to Surface Chemistry and Catalysis*, 2nd ed.; Wiley: New York, 2010.
14. Thomas, J. M.; Thomas, W. J. *Principles and Practice of Heterogeneous Catalysis*, Wiley-VCH: New York, Weinheim, 1996.
15. Horvath, I., Ed. *Encyclopedia of Catalysis*; Wiley: New York, 2003.
16. Ertl, G., Ed. *Handbook of Heterogeneous Catalysis*; 2nd ed.; Wiley-VCH: Weinheim-New York, 2008.
17. Dasgupta, S.; Török, B. Application of Clay Catalysts in Organic Synthesis. A Review. *Org. Prep. Proced. Int.* **2008**, *40*, 1–65.
18. Dasgupta, S.; Török, B. Environmentally Benign Contemporary Friedel-Crafts Chemistry by Solid Acids. *Curr. Org. Synth.* **2008**, *5*, 321–342.
19. Martins, M. A. P.; Frizzo, C. P.; Moreira, D. N.; Dayse, N.; Buriol, L.; Machado, P. Solvent-Free Heterocyclic Synthesis. *Chem. Rev.* **2009**, *109*, 4140–4182.

20. Climent, M. J.; Corma, A.; Iborra, S. Heterogeneous Catalysts for the One-Pot Synthesis of Chemicals and Fine Chemicals. *Chem. Rev.* **2011**, *111*, 1072–1133.
21. Corma, A.; Navas, J.; Sabater, M. J. Advances in One-Pot Synthesis Through Borrowing Hydrogen Catalysis. *Chem. Rev.* **2018**, *118*, 1410–1459.
22. Augustine, R. L. *Heterogeneous Catalysis for the Synthetic Chemist*, Marcel Dekker: New York, Basel, Hong Kong, 1996.
23. Ertl, G.; Knözinger, H.; Weitkamp, J., Eds. *Preparation of Solid Catalysts*; Wiley-VCH Verlag GmbH, 1999.
24. Regalbutto, J., Ed. *Catalyst Preparation: Science and Engineering*; 2nd ed.; CRC Press: Boca Raton, FL, 2016.
25. de Jong, K. P., Ed. *Synthesis of Solid Catalysts*; Wiley-VCH Verlag, 2009.
26. Kokel, A.; Schäfer, C. Application of Green Chemistry in Homogeneous Catalysis. In *Green Chemistry: An Inclusive Approach*; Török, B., Dransfield, T., Eds.; Elsevier: Oxford, 2018; pp. 375–414 (chapter 3.11).
27. Pálinkó, I. Heterogeneous Catalysis: A Fundamental Pillar of Sustainable Synthesis. In *Green Chemistry: An inclusive Approach*; Török, B., Dransfield, T., Eds.; Elsevier: Oxford, Cambridge, MA, **2018**; pp. 416–447 (chapter 12).
28. Anastas, N. D.; Maertens, A. Integrating the Principles of Toxicology into a Chemistry Curriculum. In *Green Chemistry: An inclusive Approach*; Török, B., Dransfield, T., Eds.; Elsevier: Oxford, Cambridge, MA, **2018**; pp. 91–108 (chapter 2.3).
29. Hodgson, E., Ed. *A Textbook of Modern Toxicology*; Wiley: Hoboken, NJ, 2010.
30. Ogoshi, S., Ed. *Nickel Catalysis in Organic Synthesis: Methods and Reactions*; Wiley-VCH: Weinheim, 2020.
31. Sabatier, P. *La Catalyse en Chimie Organique, Catalysis in Organic Chemistry*, Van Nostrand: Princeton, NJ, 1913; p. 923. Translated by Reidl, E.E.
32. Balakos, M. W.; Hernandez, E. E. Catalyst Characteristics and Performance in Edible Oil Hydrogenation. *Catal. Today* **1997**, *35*, 415–425.
33. Török, B.; Bartók, M. Ring-Opening Hydrogenation Reactions of Monoalkyl-Substituted Cyclobutanes over Ni/SiO<sub>2</sub> Catalyst. *J. Catal.* **1995**, *151*, 315–322.
34. Raney, M. *Catalytic Nickel*; US patent 1,563,587, 1925.
35. Cho, H.; Schäfer, C.; Török, B. Hydrogenations and Deuterium Labeling with Aluminum-Based Metal Alloys under Aqueous Conditions. *Curr. Org. Synth.* **2016**, *13*, 255–277.
36. Rayhan, U.; Kowser, Z.; Nurul Islam, M.; Redshaw, C.; Yamato, T. A Review on the Recent Advances in the Reductions of Carbon–Carbon/Oxygen Multiple Bonds Including Aromatic Rings Using Raney Ni–Al Alloy or Al Powder in the Presence of Noble Metal Catalysts in Water. *Top. Catal.* **2018**, *61*, 560–574.
37. Schäfer, C.; Mhadgut, S. C.; Kugyela, N.; Török, M.; Török, B. Proline Induced Enantioselective Heterogeneous Catalytic Hydrogenation of Isophorone on Basic Polymer Supported Pd Catalysts. *Cat. Sci. Technol.* **2015**, *5*, 716–723.
38. Kuwahara, Y.; Hiroto, K.; Yamashita, H. Pd Nanoparticles and Aminopolymers Confined in Hollow Silica Spheres as Efficient and Reusable Heterogeneous Catalysts for Semihydrogenation of Alkynes. *ACS Catal.* **2019**, *9*, 1993–2006.
39. De Paolis, O.; Baffoe, J.; Landge, S. M.; Török, B. Multicomponent Domino Cyclization-Oxidative Aromatization on a Bifunctional Pd/C/K-10 Catalyst: An Environmentally Benign Approach toward the Synthesis of Pyridines. *Synthesis* **2008**, 3423–3428.
40. Kulkarni, A.; Abid, M.; Török, B.; Huang, X. A Direct Synthesis of  $\beta$ -Carbolines Via a Three-Step One-Pot Domino Approach with Bifunctional Pd/C/K-10 Catalyst. *Tetrahedron Lett.* **2009**, *50*, 1791–1794.

60 Heterogeneous catalysis in sustainable synthesis

41. Gao, X.; Zhou, J.; Peng, X. Efficient Palladium(0) Supported on Reduced Graphene Oxide for Selective Oxidation of Olefins Using Graphene Oxide as a 'Solid Weak Acid'. *Catal. Commun.* **2019**, *122*, 73–78.
42. Yin, L.; Liebscher, J. Carbon-Carbon Coupling Reactions Catalyzed by Heterogeneous Palladium Catalysts. *Chem. Rev.* **2007**, *107*, 133–173.
43. Molnár, Á. Efficient, Selective, and Recyclable Palladium Catalysts in Carbon-Carbon Coupling Reactions. *Chem. Rev.* **2011**, *111*, 2251–2320.
44. Dasgupta, S.; Morzhina, E.; Schäfer, C.; Mhadgut, S. C.; Prakash, G. K. S.; Török, B. Synthesis of Chiral Trifluoromethyl Benzylamines by Heterogeneous Catalytic Reductive Amination. *Top. Catal.* **2016**, *59*, 1207–1213.
45. Schäfer, C.; Ellstrom, C. J.; Cho, H.; Török, B. Pd/C-Al-Water Facilitated Selective Reduction of a Broad Variety of Functional Groups. *Green Chem.* **2017**, *19*, 1230–1234.
46. Rylander, P. N. *Catalytic Hydrogenation over Platinum Metals*, Academic Press: New York, London, 1967.
47. Blaser, H. U.; Malan, C.; Pugin, B.; Spindler, F.; Steiner, H.; Studer, M. Selective Hydrogenation for Fine Chemicals: Recent Trends and New Developments. *Adv. Synth. Catal.* **2003**, *345*, 103–151.
48. Kulkarni, A.; Török, B. Heterogeneous Catalytic Hydrogenation as an Environmentally Benign Tool for Organic Synthesis. *Curr. Org. Synth.* **2011**, *8*, 187–207.
49. Acres, G. J. K. Platinum Group Metal Catalysis at the End of this Century. *Platin. Met. Rev.* **1984**, *28*, 150–157.
50. Franke, R.; Selent, D.; Börner, A. Applied Hydroformylation. *Chem. Rev.* **2012**, *112*, 5675–5732.
51. Noyori, R. Asymmetric Catalysis: Science and Opportunities (Nobel Lecture). *Angew. Chem. Int. Ed.* **2002**, *41*, 2008–2022.
52. Grubbs, R. Olefin-Metathesis Catalysts for the Preparation of Molecules and Materials (Nobel Lecture). *Angew. Chem. Int. Ed.* **2006**, *45*, 3760–3765.
53. Choi, J.; Wang, D. Y.; Kundu, S.; Choliy, Y.; Emge, T. J.; Krogh-Jespersen, K.; Goldman, A. S. Net Oxidative Addition of C(sp<sup>3</sup>)-F Bonds to Iridium Via Initial C-H Bond Activation. *Science* **2011**, *332*, 1545–1548.
54. Roseblade, S. J.; Pfaltz, A. Iridium-Catalyzed Asymmetric Hydrogenation of Olefins. *Acc. Chem. Res.* **2007**, *40*, 1402–1411.
55. Heck, R. M.; Farrauto, R. J. Automobile exhaust catalysts. *Applied Catal. A: Gen.* **2001**, *221*, 443–457.
56. Herreros, J. M.; Gill, S. S.; Lefort, I.; Tsolakis, A.; Millington, P.; Moss, E. Enhancing the Low Temperature Oxidation Performance over a Pt and a Pt–Pd Diesel Oxidation Catalyst. *Appl. Catal. B Environ.* **2014**, *147*, 835–841.
57. Wiebenga, M. H.; Kim, C. H.; Schmiege, S. J.; Oh, S. H.; Brown, D. B.; Kim, D. H.; Lee, J.-H.; Peden, C. H. F. Deactivation Mechanisms of Pt/Pd-Based Diesel Oxidation Catalysts. *Catal. Today* **2012**, *184*, 197–204.
58. Formenti, D.; Ferretti, F.; Korbinian Scharnagl, F.; Beller, M. Reduction of Nitro Compounds Using 3d-Non-Noble Metal Catalysts. *Chem. Rev.* **2019**, *119*, 2611–2680.
59. Korstanje, T. J.; van der Vlugt, J. I.; Elsevier, C. J.; de Bruin, B. Hydrogenation of Carboxylic Acids with a Homogeneous Cobalt Catalyst. *Science* **2015**, *350*, 298–302.
60. Westerhaus, F. A.; Jagadeesh, R. V.; Wienhöfer, G.; Pohl, M.-M.; Radnik, J.; Surkus, A.-E.; Rabeah, J.; Junge, K.; Junge, H.; Nielsen, M.; Brückner, A.; Beller, M. Heterogenized Cobalt Oxide Catalysts for Nitroarene Reduction by Pyrolysis of Molecularly Defined Complexes. *Nat. Chem.* **2013**, *5*, 537–543.

61. Lin, T.-P.; Peters, J. C. Boryl-Mediated Reversible H<sub>2</sub> Activation at Cobalt: Catalytic Hydrogenation, Dehydrogenation, and Transfer Hydrogenation. *J. Am. Chem. Soc.* **2013**, *135*, 15310–15313.
62. Srivastava, A. K.; Ali, M.; Siangwata, S.; Satrawala, N.; Smith, G. S.; Joshi, R. K. Multitasking FeOCN Composite as an Economic, Heterogeneous Catalyst for 1-Octene Hydroformylation and Hydration Reactions. *Asian J. Org. Chem.* **2020**, *9*, 377–384.
63. Aldea, L.; Fraile, J. M.; Garcia-Marin, H.; Garcia, J. I.; Herrerias, C. I.; Mayoral, J. A.; Perez, I. Study of the Recycling Possibilities for Azabis(Oxazoline)-Cobalt Complexes as Catalysts for Enantioselective Conjugate Reduction. *Green Chem.* **2010**, *12*, 435–440.
64. Fraile, J. M.; Garcia, J. I.; Mayoral, J. A.; Roldan, M. Simple and Efficient Heterogeneous Copper Catalysts for Enantioselective C-H Carbene Insertion. *Org. Lett.* **2007**, *9*, 731–733.
65. Fraile, J. M.; Perez, I.; Mayoral, J. A. Comparison of Immobilized Box and azaBox-Cu(II) Complexes as Catalysts for Enantioselective Mukaiyama Aldol Reactions. *J. Catal.* **2007**, *252*, 303–311.
66. Saib, A. M.; Moodley, D. J.; Ciobic, I. M.; Hauman, M. M.; Sigwebela, B. H.; Weststrate, C. J.; Niemantsverdriet, J. W.; van de Loosdrecht, J. Fundamental Understanding of Deactivation and Regeneration of Cobalt Fischer–Tropsch Synthesis Catalysts. *Catal. Today* **2010**, *154*, 271–282.
67. Bauer, I.; Knölker, H.-J. Iron Catalysis in Organic Synthesis. *Chem. Rev.* **2015**, *115* (9), 3170–3387.
68. Anilkumar, G.; Saranya, S., Eds. *Copper Catalysis in Organic Synthesis*; Wiley-VCH: Weinheim, 2020.
69. Hutchings, G. J. Vapor Phase Hydrochlorination of Acetylene: Correlation of Catalytic Activity of Supported Metal Chloride Catalysts. *J. Catal.* **1985**, *96*, 292–295.
70. Haruta, M.; Hiroshi, S. *Japanese Patent 60238148*; 1985.
71. Bond, G. C.; Louis, C.; Thompson, D. T. *Catalysis by Gold*, Imperial College Press: London, 2006.
72. Corti, C. W.; Holliday, R. C.; Thompson, D. T. Progress towards the Commercial Application of Gold Catalysts. *Top. Catal.* **2007**, *44*, 331–343.
73. Klaassen, C. D., Ed. *Casarett and Doull's Toxicology: The Basic Science of Poisons*; McGraw-Hill: New York, 2008.
74. Hutchings, G. J. A Golden Future for Green Chemistry. *Catal. Today* **2007**, *122*, 196–200.
75. Stratakis, M.; Garcia, H. Catalysis by Supported Gold Nanoparticles: beyond Aerobic Oxidative Processes. *Chem. Rev.* **2012**, *112*, 4469–4506.
76. Bowker, M.; Nuhu, A.; Soares, J. High Activity Supported Gold Catalysts by Incipient Wetness Impregnation. *Catal. Today* **2007**, *122*, 245–247.
77. Moreau, F.; Bond, G. C. Influence of the Surface Area of the Support on the Activity of Gold Catalysts for CO Oxidation. *Catal. Today* **2007**, *122*, 215–221.
78. Thielecke, N.; Vorlop, K.-D.; Prübe, U. Long-Term Stability of an Au/Al<sub>2</sub>O<sub>3</sub> Catalyst Prepared by Incipient Wetness in Continuous-Flow Glucose Oxidation. *Catal. Today* **2007**, *122*, 266–269.
79. Arcadi, A. Alternative Synthetic Methods through New Developments in Catalysis by Gold. *Chem. Rev.* **2008**, *108*, 3266–3325.
80. Hashmi, A. S. K. Gold-Catalyzed Organic Reactions. *Chem. Rev.* **2007**, *107*, 3180–3211.
81. Corma, A.; Leyva-Pérez, A.; Sabater, M. J. Gold-Catalyzed Carbon-Heteroatom Bond-Forming Reactions. *Chem. Rev.* **2011**, *111*, 1657–1712.
82. Li, Z.; Brouwer, C.; He, C. Gold-Catalyzed Organic Transformations. *Chem. Rev.* **2008**, *108*, 3239–3265.

62 Heterogeneous catalysis in sustainable synthesis

83. Somorjai, G. A.; Aliaga, C. Molecular Studies of Model Surfaces of Metals from Single Crystals to Nanoparticles under Catalytic Reaction Conditions. Evolution from Prenatal and Postmortem Studies of Catalysts. *Langmuir* **2010**, *26*, 16190–16203.
84. Ishiyama, J.; Senda, Y.; Imaizumi, S. Catalytic Hydrogenation of Methylbicyclo[3.3.1]Non-6-en-3-One. Anomalous High Selectivities on Pd and Co Black Catalysts. *Chem. Lett.* **1983**, 1243–1244.
85. Smith, A. J.; Trimm, D. L. The Preparation of Skeletal Catalysts. *Annu. Rev. Mat. Res.* **2005**, *35*, 127–142.
86. Tuley, W. F.; Adams, R. The Reduction of Cinnamic Aldehyde to Cinnamyl Alcohol in the Presence of Platinum-Oxideplatinum Black and Promoters. *J. Am. Chem. Soc.* **1925**, *47*, 3061–3068.
87. Molnár, Á.; Smith, G. V.; Bartók, M. New Catalytic Materials from Amorphous Metal Alloys. *Adv. Catal.* **1989**, *36*, 329–383.
88. Bent, B. E. Mimicking Aspects of Heterogeneous Catalysis: Generating, Isolating, and Reacting Proposed Surface Intermediates on Single Crystals in Vacuum. *Chem. Rev.* **1996**, *96*, 1361–1390.
89. Somorjai, G. A.; Park, J. Y. Evolution of the Surface Science of Catalysis from Single Crystals to Metal Nanoparticles under Pressure. *J. Chem. Phys.* **2008**, *128*, 182504.
90. Kolaczkowski, S. T.; Awdry, S.; Smith, T.; Thomas, D.; Torkuhl, L.; Kolvenbach, R. Potential for Metal Foams to Act as Structured Catalyst Supports Infixed-Bed Reactors. *Catal. Today* **2016**, *273*, 221–233.
91. Porsina, A. V.; Kulikova, A. V.; Rogozhnikova, V. N.; Serkova, A. N.; Salanova, A. N.; Shefer, K. I. Structured Reactors on a Metal Mesh Catalyst for Various Applications. *Catal. Today* **2016**, *273*, 213–220.
92. Chiusoli, G. P.; Maitlis, P. M. *Metal-Catalysis in Industrial Organic Processes*, The Royal Society of Chemistry: Cambridge, UK, 2007.
93. Musselwhite, N.; Somorjai, G. A. Investigations of Structure Sensitivity in Heterogeneous Catalysis: From Single Crystals to Monodisperse Nanoparticles. *Top. Catal.* **2013**, *56*, 1277–1283.
94. Rodriguez, N. M.; Anderson, P. E.; Wootsch, A.; Wild, U.; Schlögl, R.; Paál, Z. XPS, EM, and Catalytic Studies of the Accumulation of Carbon on Pt Black. *J. Catal.* **2001**, *197*, 365–377.
95. Raney, M. *Finely Divided Nickel*; US patent 1,628,190, 1927.
96. Paul, R. The Activation of Raney Ni by the Addition of Metals Other than the Precious Metals. *Bull. Soc. Chim. Fr.* **1946**, *13*, 208–211.
97. Montgomery, S. R. Functional Group Activity of Promoted Raney Ni Catalysts. In *Catalysis of Organic Reactions*; Moser, W. R., Ed.; New York: Dekker, 1981; pp. 383–409.
98. Mardsen, W. L.; Wainwright, M. S.; Friedrich, J. B. Zinc Promoted Raney Copper Catalysts for Methanol Synthesis. *Ind. Eng. Chem. Prod. Res. Dev.* **1980**, *19*, 551–556.
99. Raney, M. *Catalytic Material Suitable for Use in Hydrogenation of Oils, etc*; US Patent 1,915,473, 1933.
100. Orchard, J. P.; Tomsett, A. D.; Wainwright, M. S.; Young, D. J. Preparation and Properties of Raney Nickel-Cobalt Catalyst. *J. Catal.* **1983**, *84*, 189–199.
101. Banwell, M. G.; Jones, M. T.; Reekie, T. A.; Schwartz, B. D.; Tan, S. H.; White, L. V. RANEY® Cobalt—An Underutilised Reagent for the Selective Cleavage of C–X and N–O Bonds. *Org. Biomol. Chem.* **2014**, *12*, 7433–7444.
102. Parvulescu, A. N.; Jacobs, P. A.; De Vos, D. E. Heterogeneous Raney Nickel and Cobalt Catalysts for Racemization and Dynamic Kinetic Resolution of Amines. *Adv. Synth. Catal.* **2008**, *350*, 113–121.

103. Korolev, Y. A.; Greish, A. A.; Kozlova, L. M.; Kopyshv, M. V.; Litvin, E. F.; Kustov, L. M. Glycerol Dehydroxylation in Hydrogen on a Raney Cobalt Catalyst. *Catal. Ind.* **2010**, *2*, 287–289.
104. Heßelmann, C.; Wolf, T.; Galgon, F.; Körner, C.; Albert, J.; Wasserscheid, P. Additively Manufactured RANEY®-Type Copper Catalyst for Methanol Synthesis. *Cat. Sci. Technol.* **2020**, *10*, 164–168.
105. Tanielyan, S. K.; Marin, N.; Alvez, G.; Bhagat, R.; Miryala, B.; Augustine, R. L.; Schmidt, S. R. An Efficient, Selective Process for the Conversion of Glycerol to Propylene Glycol Using Fixed Bed Raney Copper Catalysts. *Org. Process Res. Dev.* **2014**, *18*, 1419–1426.
106. Azadi, P.; Syed, K. M.; Farnood, R. Catalytic Gasification of Biomass Model Compound in near-Critical Water. *Applied Catal. A: Gen.* **2009**, *358*, 65–72.
107. Caga, I. T.; Winterbottom, J. M. Behavior of Mixed Metal Adams Oxide Catalysts in the Liquid-Phase Hydrogenation of 1-Octyne. 1. Platinum-Palladium Oxides. *J. Catal.* **1979**, *57*, 494–503.
108. Piras, L.; Genesio, E.; Ghiron, C.; Taddei, M. Microwave-Assisted Hydrogenation of Pyridines. *Synlett* **2008**, 1125–1128.
109. Carcenac, Y.; Tordeux, M.; Wakselman, C.; Diter, P. Convenient Synthesis of Fluorinated Alkanes and Cycloalkanes by Hydrogenation of Perfluoroalkylalkenes under Ultrasound Irradiation. *J. Fluor. Chem.* **2005**, *126*, 1347–1355.
110. Irie, O.; Yokokawa, F.; Ehara, T.; Iwasaki, A.; Iwaki, Y.; Hitomi, Y.; Konishi, K.; Kishida, M.; Toyao, A.; Masuya, K.; Gunji, H.; Sakaki, J.; Iwasaki, G.; Hirao, H.; Kanazawa, T.; Tanabe, K.; Kosaka, T.; Hart, T. W.; Hallett, A. 4-Amino-2-Cyanopyrimidines: Novel Scaffold for Nonpeptidic Cathepsin S Inhibitors. *Bioorg. Med. Chem. Lett.* **2008**, *18*, 4642–4646.
111. Mori, Y.; Seki, M. Pd(OH)<sub>2</sub>/C (Pearlman's Catalyst): A Highly Active Catalyst for Fukuyama, Sonogashira, and Suzuki Coupling Reactions. *J. Org. Chem.* **2003**, *68*, 1571–1574.
112. Kikuchi, H.; Yamamoto, K.; Horoiwa, S.; Hirai, S.; Kasahara, R.; Hariguchi, R.; Matsumoto, M.; Oshima, Y. Exploration of a New Type of Antimalarial Compounds Based on Febri-fugine. *J. Med. Chem.* **2006**, *49*, 4698–4706.
113. Sebek, M.; Holz, J.; Börner, A.; Jähnisch, K. Highly Distereoselective Hydrogenation of Furan-2-Carboxylic Acid Derivatives on Heterogeneous Catalysts. *Synlett* **2009**, 461–465.
114. Carreira, E. M.; Ledford, B. E. Enantioselective Synthesis of the C(1)-C(6') Subunit of Zarga-zoic Acid C. *J. Braz. Chem. Soc.* **1998**, *9*, 405–408.
115. Håkansson, A. E.; Palmelund, A.; Holm, H.; Madsen, R. Synthesis of 7-Deoxypancratistatin from Carbohydrates by the Use of Olefin Metathesis. *Chem. A Eur. J.* **2006**, *12*, 3243–3253.
116. Davies, S. G.; Figuccia, A. L. A.; Fletcher, A. I.; Roberts, P. M.; Thomson, J. E. Asymmetric Syntheses of (–)-ADMJ and (+)-ADANJ: 2-Deoxy-2-amino Analogues of (–)-1-Deoxymannojirimycin and (+)-1-Deoxyallonojirimycin. *J. Org. Chem.* **2016**, *81*, 6481–6495.
117. Török, B.; Molnár, Á.; Borszék, K.; Tóth-Kádár, E.; Bakonyi, I. Selective Catalytic Hydrogenation of Bifunctional Compounds over Amorphous Nickel Alloys. *Stud. Surf. Sci. Catal.* **1993**, *78*, 176–184.
118. Lin, C. S.; Lee, C. Y.; Chen, F. J.; Chien, C. T.; Lin, P. L.; Chung, W. C. Electrodeposition of Nickel-Phosphorus Alloy from Sulfamate Baths with Improved Current Efficiency. *J. Electrochem. Soc.* **2006**, *153*, C387–C392.
119. Greer, A. L. Metallic Glasses. *Science* **1995**, *267*, 1947–1953.
120. Baiker, A.; Molnár, Á. Metallic Glasses. In *Handbook of Heterogeneous Catalysis*; Ertl, G., Ed.; 2nd ed.; 3; Wiley-VCH: Weinheim, **2008**; pp. 1285–1298.
121. Baiker, A. Metallic Glasses in Heterogeneous Catalysis. *Faraday Discuss. Chem. Soc.* **1989**, *87*, 239–251.

64 Heterogeneous catalysis in sustainable synthesis

122. Pisarek, M.; Janik-Czachor, M.; Gebert, A.; Molnár, Á.; Kedzierzawski, P.; Rác, B. Effect of Cathodic Hydrogen Charging on Catalytic Activity of Cu-Hf Amorphous Alloys. *Applied Catal. A: Gen.* **2004**, *267*, 1–8.
123. Kesavan, V.; Dhar, D.; Koltypin, Y.; Perkas, N.; Palchik, O.; Gedanken, A.; Chandrasekaran, S. Nanostructured Amorphous Metals, Alloys, and Metal Oxides as New Catalysts for Oxidation. *Pure Appl. Chem.* **2001**, *73*, 85–91.
124. Zong, B. Amorphous Ni Alloy Hydrogenation Catalyst and Magnetically Stabilized Bed Reaction Technology. *Catal. Surv. Asia* **2007**, *11*, 87–94.
125. Zhao, J. J.; Malgras, V.; Na, J.; Liang, R.; Cai, Y.; Kang, Y.; Mohsen, A.; Al Shehrie, A.; Alzahranie, K. A.; Gamaan, Y.; Toru, A.; Zhang, D.; Hexin, B.; Yamauchi, Y. Magnetically Induced Synthesis of Mesoporous Amorphous CoB Nanochains for Efficient Selective Hydrogenation of Cinnamaldehyde to Cinnamyl Alcohol. *Chem. Eng. J.* **2020**, *398*, 125564.
126. Varga, M.; Molnár, Á.; Mohai, M.; Bertóti, I.; Janik-Czachor, M.; Szummer, A. Selective Hydrogenation of Pentyne over PdZr and PdCuZr Prepared from Amorphous Precursors. *Applied Catal. A: Gen.* **2002**, *234*, 167–178.
127. Smith, R. D. L.; Prévot, M. S.; Fagan, R. D.; Trudel, S.; Berlinguette, C. P. Water Oxidation Catalysis: Electrocatalytic Response to Metal Stoichiometry in Amorphous Metal Oxide Films Containing Iron, Cobalt, and Nickel. *J. Am. Chem. Soc.* **2013**, *135*, 11580–11586.
128. Cai, W.; Chen, R.; Yang, H.; Tao, H. B.; Wang, H.-Y.; Gao, J.; Liu, W.; Liu, S.; Hung, S. F.; Liu, B. Amorphous Versus Crystalline in Water Oxidation Catalysis: A Case Study of NiFe Alloy. *Nano Lett.* **2020**, *20*, 4278–4285.
129. Salinas-Torres, D.; Nozaki, D.; Navlani-García, M.; Kuwahara, Y.; Mori, K.; Yamashita, H. Recent Applications of Amorphous Alloys to Design Skeletal Catalysts. *Bull. Chem. Soc. Jpn.* **2020**, *93*, 438–454.
130. Alexander, A.-M.; Hargreaves, J. S. J. Alternative Catalytic Materials: Carbides, Nitrides, Phosphides and Amorphous Boron Alloys. *Chem. Soc. Rev.* **2010**, *39*, 4388–4401.
131. Molnár, Á. Catalytic Applications of Amorphous Alloys: Expectations, Achievements, and Disappointments. *Appl. Surf. Sci.* **2011**, *257*, 8151–8164.
132. Pei, Y.; Zhou, G.; Luan, N.; Zong, B.; Qiao, M.; Tao, F. Synthesis and Catalysis of Chemically Reduced Metal–Metalloid Amorphous Alloys. *Chem. Soc. Rev.* **2012**, *41*, 8140–8162.
133. Corma, A. Preparation and Catalytic Properties of New Mesoporous Materials. *Top. Catal.* **1997**, *4*, 249–260.
134. Davis, R. J. New Perspectives on Basic Zeolites as Catalysts and Catalyst Supports. *J. Catal.* **2003**, *216*, 396–405.
135. de Jong, K. P. Synthesis of Supported Catalysts. *Curr. Opin. Solid State Mater. Sci.* **1999**, *4*, 55–62.
136. White, R. J.; Luque, R.; Budarin, V. L.; Clark, J. H.; Macquarrie, D. J. Supported Metal Nanoparticles on Porous Materials. Methods and applications. *Chem. Soc. Rev.* **2009**, *38*, 481–494.
137. Wang, Z.; Chen, G.; Ding, K. Self-Supported Catalysts. *Chem. Rev.* **2009**, *109*, 322–359.
138. Bond, G. C. *Metal-Catalyzed Reactions of Hydrocarbons*, Springer: New York, 2005.
139. Meille, V. Review on Methods to Deposit Catalysts on Structured Surfaces. *Applied Catal. A: Gen.* **2006**, *315*, 1–17.
140. Munnik, P.; de Jongh, P. E.; de Jong, K. P. Recent Developments in the Synthesis of Supported Catalysts. *Chem. Rev.* **2015**, *115*, 6687–6718.
141. Rothenberg, G. *Catalysis: Concepts and Green Applications*, Wiley-VCH: Weinheim, 2008.
142. Mehrabadi, B. A. T.; Eskandari, S.; Khan, U.; White, R. D.; Regalbuto, J. R. A Review of Preparation Methods for Supported Metal Catalysts. *Adv. Catal.* **2017**, *61*, 1–35.

143. Coq, B.; Figueras, F. Structure–Activity Relationships in Catalysis by Metals: some Aspects of Particle Size, Bimetallic and Supports Effects. *Coord. Chem. Rev.* **1998**, *178–180*, 1753–1783.
144. Soled, S. Silica-Supported Catalysts Get a New Breath of Life. *Science* **2015**, *350*, 1171–1172.
145. Molnár, Á. Nafion-Silica Nanocomposites: a New Generation of Water-Tolerant Solid Acids of High Efficiency. *Curr. Org. Chem.* **2008**, *12*, 159–181.
146. Zou, H.; Wu, S.; Shen, J. Polymer/Silica Nanocomposites: Preparation, Characterization, Properties, and Applications. *Chem. Rev.* **2008**, *108*, 3893–3957.
147. Molnár, Á. Nafion-Silica Nanocomposites: A New Generation of Water-Tolerant Solid Acids of High Efficiency—an Update. *Curr. Org. Chem.* **2011**, *15*, 3928–3960.
148. Wang, H.; Pan, X.; Wang, X.; Wang, W.; Huang, Z.; Gu, K.; Liu, S.; Zhang, F.; Shen, H.; Yuan, Q.; Ma, J.; Yuan, W.; Liu, H. Degradable Carbon–Silica Nanocomposite with Immuno-adjutant Property for Dual-Modality Photothermal/Photodynamic Therapy. *ACS Nano* **2020**, *14*, 2847–2859.
149. Molnár, Á.; Rác, B. Organic Transformations over Silica Materials Modified by Covalently Bonded Surface Functional Groups. *Curr. Org. Chem.* **2006**, *10*, 1697–1726.
150. Kim, I.-Y.; Joachim, E.; Choi, H.; Kim, K. Toxicity of Silica Nanoparticles Depends on Size, Dose, and Cell Type. *Nanomed. Nanotechnol. Biol. Med.* **2015**, *11*, 1407–1416.
151. Shinde, P. S.; Suryawanshi, P. S.; Patil, K. K.; Belekar, V. M.; Sankpal, S. A.; Delekar, S. D.; Jadhav, S. A. A Brief Overview of Recent Progress in Porous Silica as Catalyst Supports. *J. Compos. Sci.* **2021**, *5*, 75.
152. Ewing, C. S.; Vesper, G.; McCarthy, J. J.; Lambrecht, D. S.; Johnson, J. K. Predicting Catalyst-Support Interactions between Metal Nanoparticles and Amorphous Silica Supports. *Surf. Sci.* **2016**, *652*, 278–285.
153. An, N.; Zhang, W.; Yuan, X.; Pan, B.; Liu, G.; Jia, M.; Yan, W.; Zhang, W. Catalytic Oxidation of Formaldehyde over Different Silica Supported Platinum Catalysts. *Chem. Eng. J.* **2013**, *215–216*, 1–6.
154. Da'na, E. Adsorption of Heavy Metals on Functionalized-Mesoporous Silica: A Review. *Microporous Mesoporous Mater.* **2017**, *247*, 145–157.
155. Davidson, M.; Ji, Y.; Leong, G. J.; Kovach, N. C.; Trewyn, B. G.; Richards, R. M. Hybrid Mesoporous Silica/Noble-Metal Nanoparticle Materials—Synthesis and Catalytic Applications. *ACS Appl. Nano Mater.* **2018**, *1*, 4386–4400.
156. Liang, J.; Liang, Z.; Zou, R.; Zhao, Y. Heterogeneous Catalysis in Zeolites, Mesoporous Silica, and Metal–Organic Frameworks. *Adv. Mater.* **2017**, *29*, 1701139.
157. Trueba, M.; Trasatti, S. P.  $\gamma$ -Alumina as a Support for Catalysts: A Review of Fundamental Aspects. *Eur. J. Inorg. Chem.* **2005**, *2005*, 3393–3403.
158. Russell, A. S.; Cochran, C. N. Alumina Surface Area Measurements. *Ind. Eng. Chem.* **1950**, *42*, 1332–1335.
159. Hong, T.-L.; Liu, H.-T.; Yeh, C.-T.; Chen, S. H.; Sheu, F.-C.; Leu, L.-J.; Wang, C. I. Electron Microscopic Studies on Pore Structure of Alumina. *Applied Catal. A: Gen.* **1997**, *158*, 257–271.
160. Xu, J.; Ibrahim, A.-R.; Hu, X.; Hong, Y.; Su, Y.; Wang, H.; Li, J. Preparation of Large Pore Volume  $\gamma$ -Alumina and its Performance as Catalyst Support in Phenol Hydroxylation. *Microporous Mesoporous Mater.* **2016**, *231*, 1–8.
161. Ilamanova, M.; Mastuyugin, M.; Schäfer, C.; Kokel, A.; Török, B. Heterogeneous Metal Catalysis for the Environmentally Benign Synthesis of Medicinally Important Scaffolds, Intermediates and Building Blocks. *Curr. Org. Chem.* **2021**, *25*. <https://doi.org/10.2174/1385272825666210519095808> (in press).

162. Krewski, D.; Yokel, R. A.; Nieboer, E.; Borchelt, D.; Cohen, J.; Harry, J.; Kacew, S.; Lindsay, J.; Mahfouz, A. M.; Rondeau, V. Human Health Risk Assessment for Aluminium, Aluminium Oxide, and Aluminium Hydroxyde. *J. Toxicol. Environ. Health B Crit. Rev.* **2007**, *10* (Suppl 1), 1–269.
163. Balázsik, K.; Török, B.; Szakonyi, G.; Bartók, M. Enantioselective Hydrogenations over K-10 Montmorillonite-Supported Noble Metal Catalysts with Anchored Modifier. *Applied Catal. A: Gen.* **1999**, *182*, 53–63.
164. Török, B.; Bartók, M.; Dékány, I. The Structure of Chiral Phenylethyl-Ammonium Montmorillonites in Ethanol-Toluene Mixtures. *Colloid Polym. Sci.* **1999**, *277*, 340–346.
165. Török, B.; Szöllösi, G.; Rózsa-Tarjáni, M.; Bartók, M. Preparation, Characterization and Application of Chirally Modified K-10 Montmorillonite Ion-Exchanged with Chiral Ammonium Salts. *Mol. Cryst. Liq. Cryst.* **1998**, *311*, 289–294.
166. Török, B.; Balázsik, K.; Dékány, I.; Bartók, M. Preparation and Characterization of New Chirally Modified Laponites. *Mol. Cryst. Liq. Cryst.* **2000**, *341*, 339–344.
167. Szöllösi, G.; Kun, I.; Török, B.; Bartók, M. Chemoselective Hydrogenation of C=O Group in Unsaturated Aldehydes over Clay-Supported Platinum Catalysts. *Stud. Surf. Sci. Catal.* **1999**, *125*, 539–546.
168. Török, B.; Balázsik, K.; Kun, I.; Szöllösi, G.; Szakonyi, G.; Bartók, M. Clay-Supported Noble Metal Catalysts in Enantioselective Hydrogenations. *Stud. Surf. Sci. Catal.* **1999**, *125*, 515–522.
169. Oi, L. E.; Choo, M.-Y.; Lee, H. V.; Ong, H. C.; Hamida, S. B. A.; Juan, J. C. Recent Advances of Titanium Dioxide (TiO<sub>2</sub>) for Green Organic Synthesis. *RSC Adv.* **2016**, *6*, 108741–108754.
170. Chen, X.; Mao, S. S. Titanium Dioxide Nanomaterials: Synthesis, Properties, Modifications, and Applications. *Chem. Rev.* **2007**, *107*, 2891–2959.
171. Ismail, A. A.; Bahnemann, D. F. Mesoporous Titania Photocatalysts: Preparation, Characterization and Reaction Mechanisms. *J. Mater. Chem.* **2011**, *21*, 11686–11707.
172. Lan, Y.; Lu, Y.; Ren, Z. Mini Review on Photocatalysis of Titanium Dioxide Nanoparticles and their Solar Applications. *Nano Energy* **2013**, *2*, 1031–1045.
173. Lázaro, M. J.; Echegoyen, Y.; Alegre, C.; Moliner, S. R.; Palacios, J. M. TiO<sub>2</sub> as Textural Promoter on High Loaded Ni Catalysts for Methane Decomposition. *Int. J. Hydrogen Energy* **2008**, *33*, 3320–3329.
174. Zhang, L.; Zhang, Y.; Chen, S. Effect of Promoter SiO<sub>2</sub>, TiO<sub>2</sub> or SiO<sub>2</sub>-TiO<sub>2</sub> on the Performance of CuO-ZnO-Al<sub>2</sub>O<sub>3</sub> Catalyst for Methanol Synthesis from CO<sub>2</sub> Hydrogenation. *Applied Catal. A: Gen.* **2012**, *415–416*, 118–123.
175. Montini, T.; Melchionna, M.; Monai, M.; Fornasiero, P. Fundamentals and Catalytic Applications of CeO<sub>2</sub>-Based Materials. *Chem. Rev.* **2016**, *116*, 5987–6041.
176. Wang, J.; Xiao, X.; Liu, Y.; Pan, K.; Pang, H.; Wei, S. The Application of CeO<sub>2</sub>-Based Materials in Electrocatalysis. *J. Mater. Chem. A* **2019**, *7*, 17675–17702.
177. Majumdar, D.; Maiyalagan, T.; Jiang, Z. Recent Progress in Ruthenium Oxide-Based Composites for Supercapacitor Applications. *ChemElectroChem* **2019**, *6*, 4343–4372.
178. Iqbal, M. N.; Abdel-Magied, A. F.; Abdelhamid, H. N.; Olsén, P.; Shatskiy, A.; Zou, X.; Åkermar, B.; Kärkäs, M. D.; Johnston, E. V. Mesoporous Ruthenium Oxide: A Heterogeneous Catalyst for Water Oxidation. *ACS Sustain. Chem. Eng.* **2017**, *5*, 9651–9656.
179. Aziz, M. A. A.; Jalil, A. A.; Wongsakulphasatch, S.; Vo, D. V. N. Understanding the Role of Surface Basic Sites of Catalysts in CO<sub>2</sub> Activation in Dry Reforming of Methane: A Short Review. *Cat. Sci. Technol.* **2020**, *10*, 35–45.
180. Mhadgut, S. C.; Török, M.; Esquibel, J.; Török, B. Highly Asymmetric Heterogeneous Catalytic Hydrogenation of Isophorone on Proline Modified Base-Supported Palladium Catalysts. *J. Catal.* **2006**, *238*, 441–448.

181. Mhadgut, S. C.; Török, M.; Dasgupta, S.; Török, B. Nature of Proline-Induced Enantiodifferentiation in Asymmetric Pd Catalyzed Hydrogenations: Is the Catalyst Really Indifferent? *Catal. Lett.* **2008**, *123*, 156–163.
182. Shi, S.; Chen, C.; Wang, M.; Ma, J.; Gao, J.; Xu, J. Mesoporous Strong Base Supported Cobalt Oxide as a Catalyst for the Oxidation of Ethylbenzene. *Cat. Sci. Technol.* **2014**, *4*, 3606–3610.
183. Yang, J.; Guan, Y.; Verhoeven, T.; van Santen, R.; Li, C.; Hensen, E. J. M. Basic Metal Carbonate Supported Gold Nanoparticles: Enhanced Performance in Aerobic Alcohol Oxidation. *Green Chem.* **2009**, *11*, 322–325.
184. Omata, K.; Nukui, N.; Hottai, T.; Showa, Y.; Yamada, M. Strontium Carbonate Supported Cobalt Catalyst for Dry Reforming of Methane under Pressure. *Catal. Commun.* **2004**, *5*, 755–758.
185. Ghosh, A. K.; Krishnan, K. Chemoselective Catalytic Hydrogenation of Alkenes by Lindlar Catalyst. *Tetrahedron Lett.* **1998**, *39*, 947–948.
186. García-Mota, M.; Gómez-Díaz, J.; Novell-Leruth, G.; Vargas-Fuentes, C.; Bellarosa, L.; Bridier, B.; Pérez-Ramírez, J.; López, N. A Density Functional Theory Study of the ‘Mythic’ Lindlar Hydrogenation Catalyst. *Theor. Chem. Acc.* **2011**, *128*, 663–673.
187. Laverdura, U. P.; Rossi, L.; Ferella, F.; Courson, C.; Zarli, A.; Alhajjoussef, R.; Gallucci, K. Selective Catalytic Hydrogenation of Vegetable Oils on Lindlar Catalyst. *ACS Omega* **2020**, *5*, 22901–22913.
188. Reddy, P. G.; Pratap, T. V.; Kumar, G. D. K.; Mohanty, S. K.; Baskaran, S. The Lindlar Catalyst Revitalized: A Highly Chemoselective Method for the Direct Conversion of Azides to N-(Tert-Butoxycarbonyl)Amines. *Eur. J. Org. Chem.* **2002**, 3740–3743.
189. Guéniñ, E. Nanomagnetic-Supported Catalysts. In *Novel Magnetic Nanostructures Unique Properties and Applications Advanced Nanomaterials*; Terrasson, V., Domracheva, N., Caporali, M., Rentschler, E., Eds.; 2018; pp. 333–371 (chapter 10).
190. Rossi, L. M.; Costa, N. J. S.; Silva, F. P.; Wojcieszak, R. Magnetic Nanomaterials in Catalysis: Advanced Catalysts for Magnetic Separation and beyond. *Green Chem.* **2014**, *16*, 2906–2933.
191. Yoo, J. S. Metal Recovery and Rejuvenation of Metal-Loaded Spent Catalysts. *Catal. Today* **1998**, *44*, 27–46.
192. Tsang, S. C.; Caps, V.; Paraskevas, I.; Chadwick, D.; Thompsett, D. Magnetically Separable, Carbon-Supported Nanocatalysts for the Manufacture of Fine Chemicals. *Angew. Chem. Int. Ed.* **2004**, *43*, 5649.
193. Shylesh, S.; Schünemann, V.; Thiel, W. R. Magnetically Separable Nanocatalysts: Bridges between Homogeneous and Heterogeneous Catalysis. *Angew. Chem. Int. Ed.* **2010**, *49*, 3428–3459.
194. Polshettiwar, V.; Luque, R.; Fihri, A.; Zhu, H.; Bouhrara, M.; Basset, J.-M. Magnetically Recoverable Nanocatalysts. *Chem. Rev.* **2011**, *111*, 3036–3075.
195. Baig, R. B. N.; Varma, R. S. Magnetically Retrievable Catalysts for Organic Synthesis. *Chem. Commun.* **2013**, *49*, 752–770.
196. Hu, A.; Liu, S.; Lin, W. Immobilization of Chiral Catalysts on Magnetite Nanoparticles for Highly Enantioselective Asymmetric Hydrogenation of Aromatic Ketones. *RSC Adv.* **2012**, *2*, 2576–2580.
197. Song, C. E.; Lee, S.-G. Supported Chiral Catalysts on Inorganic Materials. *Chem. Rev.* **2002**, *102*, 3495–3524.
198. Diaz, U.; Brunel, D.; Corma, A. Catalysis Using Multifunctional Organosiliceous Hybrid Materials. *Chem. Soc. Rev.* **2013**, *42*, 4083–4097.

68 Heterogeneous catalysis in sustainable synthesis

199. Pérez-Mayoral, E.; Calvino-Casilda, V.; Soriano, E. Metal-Supported Carbon-Based Materials: Opportunities and Challenges in the Synthesis of Valuable Products. *Cat. Sci. Technol.* **2016**, *6*, 1265–1291.
200. Ao, W.; Fu, J.; Mao, X.; Kang, Q.; Ran, C.; Liu, Y.; Zhang, H.; Gao, Z.; Li, J.; Liu, G.; Dai, J. Microwave Assisted Preparation of Activated Carbon from Biomass: A Review. *Renew. Sust. Energ. Rev.* **2018**, *92*, 958–979.
201. Heidarinejad, Z.; Dehghani, M. H.; Heidari, M.; Javedan, G.; Ali, I.; Sillanpää, M. Methods for Preparation and Activation of Activated Carbon: A Review. *Environ. Chem. Lett.* **2020**, *18*, 393–415.
202. Feng, P.; Li, J.; Wang, H.; Xu, Z. Biomass-Based Activated Carbon and Activators: Preparation of Activated Carbon from Corn cob by Chemical Activation with Biomass Pyrolysis Liquids. *ACS Omega* **2020**, *5*, 24064–24072.
203. Hayashia, J.; Kazehaya, A.; Muroyama, K.; Watkinson, P. Preparation of Activated Carbon from Lignin by Chemical Activation. *Carbon* **2000**, *38*, 1873–1878.
204. Li, W.; Han, C.; Liu, W.; Zhang, M.; Tao, K. Expanded Graphite Applied in the Catalytic Process as a Catalyst Support. *Catal. Today* **2007**, *125*, 278–281.
205. Li, C.; Sayak, I.; Chisato, F.; Fujimoto, K. Development of High Performance Graphite-Supported Iron Catalyst for Fischer–Tropsch Synthesis. *Applied Catal. A: Gen.* **2016**, *509*, 123–129.
206. Li, Y.-F.; Guo, M. Q.; Yin, S. F.; Chen, L.; Zhou, Y.-B.; Qiu, R. H.; Au, C.-T. Graphite as a Highly Efficient and Stable Catalyst for the Production of Lactones. *Carbon* **2013**, *55*, 269–275.
207. Julkapli, N. M.; Bagheri, S. Graphene Supported Heterogeneous Catalysts: An Overview. *Int. J. Hydrogen Energy* **2015**, *40*, 948–979.
208. Nişancı, B.; Ganjehyan, K.; Metin, Ö.; Dastan, A.; Török, B. Graphene-Supported NiPd Alloy Nanoparticles: A Novel and Highly Efficient Heterogeneous Catalyst System for the Reductive Amination of Aldehydes. *J. Mol. Catal. A* **2015**, *409*, 191–197.
209. Li, Y.; Yu, Y.; Wang, J.-G.; Song, J.; Li, Q.; Dong, M.; Liu, C.-J. CO Oxidation over Graphene Supported Palladium Catalyst. *Appl. Catal. B Environ.* **2012**, *125*, 189–196.
210. Wu, G.; Wang, X.; Guan, N.; Li, L. Palladium on Graphene as Efficient Catalyst for Solvent-Free Aerobic Oxidation of Aromatic Alcohols: Role of Graphene Support. *Appl. Catal. B Environ.* **2013**, *136–137*, 177–185.
211. Shaari, N.; Kamarudin, S. K. Graphene in Electrocatalyst and Proton Conduction Membrane in Fuel Cell Applications: An Overview. *Renew. Sust. Energ. Rev.* **2017**, *69*, 862–870.
212. Iijima, S. Helical Microtubules of Graphitic Carbon. *Nature* **1991**, *354*, 56–58.
213. Iijima, S. Carbon Nanotubes: Past, Present, and Future. *Phys. B Condens. Matter* **2002**, *323*, 1–5.
214. Yan, Y.; Miao, J.; Yang, Z.; Xiao, F.-X.; Yang, H. B.; Liu, B.; Yang, Y. Carbon Nanotube Catalysts: Recent Advances in Synthesis, Characterization and Applications. *Chem. Soc. Rev.* **2015**, *44*, 3295–3346.
215. Esteves, L. M.; Oliveira, H. A.; Passos, F. B. Carbon Nanotubes as Catalyst Support in Chemical Vapor Deposition Reaction: A Review. *J. Ind. Eng. Chem.* **2018**, *65*, 1–12.
216. Oosthuizen, R. S.; Nyamori, V. O. Carbon Nanotubes as Supports for Palladium and Bimetallic Catalysts for Use in Hydrogenation Reactions. *Platin. Met. Rev.* **2011**, *55*, 154–169.
217. Serp, P.; Machado, B. *Nanostructured Carbon Materials for Catalysis*, RSC: Cambridge, 2015.
218. Schaez, A.; Zeltner, M.; Stark, W. J. Carbon Modifications and Surfaces for Catalytic Organic Transformations. *ACS Catal.* **2012**, *2*, 1267–1284.
219. Haag, D. R.; Kung, H. H. Metal Free Graphene Based Catalysts: A Review. *Top. Catal.* **2014**, *57*, 762–773.

220. Su, D. S.; Perathoner, S.; Centi, G. Nanocarbons for the Development of Advanced Catalysts. *Chem. Rev.* **2013**, *113*, 5782–5816.
221. Bezemer, G. L.; Bitter, J. H.; Kuipers, H. P. C. E.; Oosterbeek, H.; Holewijn, J. E.; Xu, X.; Kapteijn, F.; van Dillen, A. J.; de Jong, K. P. Cobalt Particle Size Effects in the Fischer-Tropsch Reaction Studied with Carbon Nanofiber Supported Catalysts. *J. Am. Chem. Soc.* **2006**, *128*, 3956–3964.
222. Din, I. U.; Shaharun, M. S.; Naeem, A.; Alotaibi, M. A.; Alharthi, A. I.; Bakht, M. A.; Nasir, Q. Carbon Nanofibers as Potential Materials for Catalysts Support, A Mini-Review on Recent Advances and Future Perspective. *Ceram. Int.* **2020**, *46*, 18446–18452.
223. Chinthaginjala, J. K.; Seshan, K.; Lefferts, L. Preparation and Application of Carbon-Nanofiber Based Microstructured Materials as Catalyst Supports. *Ind. Eng. Chem. Res.* **2007**, *46*, 3968–3978.
224. Benaglia, M.; Puglisi, A.; Cozzi, F. Polymer-Supported Organic Catalysts. *Chem. Rev.* **2003**, *103*, 3401–3429.
225. Pathak, S.; Greci, M. T.; Kwong, R. C.; Mercado, K.; Prakash, G. K. S.; Olah, G. A.; Thompson, M. E. Synthesis and Applications of Palladium-Coated Poly(Vinylpyridine) Nanospheres. *Chem. Mater.* **2000**, *12*, 1985–1989.
226. Bykov, A.; Matveeva, V.; Sulman, M.; Valetskiy, P.; Tkachenko, O.; Kustov, L.; Bronstein, L.; Sulman, E. Enantioselective Catalytic Hydrogenation of Activated Ketones Using Polymer-Containing Nanocomposites. *Catal Today* **2009**, *140*, 64–69.
227. Török, B.; Kulkarni, A.; DeSousa, R.; Satuluri, K.; Török, M.; Prakash, G. K. S. Synthesis and Application of Polystyrene Nanospheres Supported Platinum Catalysts in Enantioselective Hydrogenations. *Catal. Lett.* **2011**, *141*, 1435–1441.
228. Howard, I. C.; Hammond, C.; Buchard, A. Polymer-Supported Metal Catalysts for the Heterogeneous Polymerisation of Lactones. *Polym. Chem.* **2019**, *10*, 5894–5904.
229. Kunfi, A.; London, G. Polydopamine: An Emerging Material in the Catalysis of Organic Transformations. *Synthesis* **2019**, *51*, 2829–2838.
230. Molnár, Á. Polydopamine—Its Prolific Use as Catalyst and Support Material. *ChemCatChem* **2020**, *12*, 2649–2689.
231. Sarkar, S.; Guibal, E.; Quignard, F.; SenGupta, A. K. Polymer-Supported Metals and Metal Oxide Nanoparticles: Synthesis, Characterization, and Applications. *J. Nanopart. Res.* **2012**, *14*, 715.
232. Krajangpan, S.; Bermudez, J. J. E.; Bezbaruah, A. N.; Chisholm, B. J.; Khan, E. Nitrate Removal by Entrapped Zero-Valent Iron Nanoparticles in Calcium Alginate. *Water Sci. Technol.* **2008**, *58*, 2215–2222.
233. Ma, H. L.; Xu, Y. F.; Qi, X. R.; Maitani, Y.; Nagai, T. Superparamagnetic Iron Oxide Nanoparticles Stabilized by Alginate: Pharmacokinetics, Tissue Distribution, and Applications in Detecting Liver Cancers. *Int. J. Pharm.* **2008**, *354*, 217–226.
234. Guibal, E. Heterogeneous Catalysis on Chitosan-Based Materials: A Review. *Prog. Polym. Sci.* **2005**, *30*, 71–109.
235. Guibal, E.; Vincent, T. Chitosan-Supported Palladium Catalyst. IV. Influence of Temperature on Nitrophenol Degradation and Thermodynamic Parameters. *J. Environ. Manage.* **2004**, *71*, 15–23.
236. Rani, D.; Singla, P.; Agarwal, J. ‘Chitosan in Water’ as an Eco-Friendly and Efficient Catalytic System for Knoevenagel Condensation Reaction. *Carbohydr. Polym.* **2018**, *202*, 355–364.
237. Motahharifar, N.; Nasrollahzadeh, M.; Taheri-Kafrani, A.; Varma, R. S.; Shokouhimehr, M. Magnetic Chitosan-Copper Nanocomposite: A Plant Assembled Catalyst for the Synthesis of Amino- and N-Sulfonyl Tetrazoles in Eco-Friendly Media. *Carbohydr. Polym.* **2020**, *232*, 115819.

70 Heterogeneous catalysis in sustainable synthesis

238. Sadjadi, S.; Heravi, M. M.; Kazemi, S. S. Ionic Liquid Decorated Chitosan Hybridized with Clay: A Novel Support for Immobilizing Pd Nanoparticles. *Carbohydr. Polym.* **2018**, *200*, 183–190.
239. Chakraborty, R.; Chatterjee, S.; Mukhopadhyay, P.; Barman, S. Progresses in Waste Biomass Derived Catalyst for Production of Biodiesel and Bioethanol: A Review. *Procedia Environ. Sci.* **2016**, *35*, 546–554.
240. Abdullah, S. H. Y. S.; Hanapia, N. H. M.; Azida, A.; Umar, R.; Juahir, H.; Khatoon, H.; Endut, A. A Review of Biomass-Derived Heterogeneous Catalyst for a Sustainable Biodiesel Production. *Renew. Sustain. Energy Rev.* **2017**, *70*, 1040–1051.
241. Molnár, Á. The Use of Chitosan-Based Metal Catalysts in Organic Transformations. *Coord. Chem. Rev.* **2019**, *388*, 126–171.
242. Bellemin-Laponnaz, S.; Achard, T.; Bissessar, D.; Geiger, Y.; Maise-François, A. Synthesis and Application of Dynamic Self-Supported Enantioselective Catalysts. *Coord. Chem. Rev.* **2017**, *332*, 38–47.
243. de Vos, D. E.; Vankelecom, I. F. J.; Jacobs, P. A., Eds. *Chiral Catalyst Immobilization and Recycling*; Wiley-VCH: Weinheim, 2000.
244. Kirschning, A., Ed. *Top. Curr. Chem.*, Vol. 242; *Immobilized Catalysts: Solid Phases, Immobilization and Applications*; Springer-Verlag Berlin Heidelberg, 2004.
245. Leadbeater, N. E.; Marco, M. Preparation of Polymer-Supported Ligands and Metal Complexes for Use in Catalysis. *Chem. Rev.* **2002**, *102*, 3217–3274.
246. Pomogailo, A. D. *Polymer-Supported Platinum Metals Catalysis: Catalysis by Polymer-Immobilized Metal Complexes*, Gordon and Breach Science Publishers: The Netherlands, 1998.
247. Sabater, S.; Mata, J. A.; Peris, E. Catalyst Enhancement and Recyclability by Immobilization of Metal Complexes onto Graphene Surface by Noncovalent Interactions. *ACS Catal.* **2014**, *4*, 2038–2047.
248. Fraile, J. M.; García, J. I.; Herrerías, C. I.; Mayoral, J. A.; Piresa, E. Enantioselective Catalysis with Chiral Complexes Immobilized on Nanostructured Supports. *Chem. Soc. Rev.* **2009**, *38*, 695–706.
249. Nakazawa, J.; Smith, B. J.; Stack, T. D. P. Discrete Complexes Immobilized onto Click-SBA-15 Silica: Controllable Loadings and the Impact of Surface Coverage on Catalysis. *J. Am. Chem. Soc.* **2012**, *134*, 2750–2759.
250. Haga, M.; Kobayashi, K.; Terada, K. Fabrication and Functions of Surface Nanomaterials Based on Multilayered or Nanoarrayed Assembly of Metal Complexes. *Coord. Chem. Rev.* **2007**, *251*, 2688–2701.
251. Conley, M. P.; Copéret, C.; Thieuleux, C. Mesostructured Hybrid Organic–Silica Materials: Ideal Supports for Well-Defined Heterogeneous Organometallic Catalysts. *ACS Catal.* **2014**, *4*, 1458–1469.
252. Hübner, S.; de Vries, J. G.; Farina, V. Why Does Industry Not Use Immobilized Transition Metal Complexes as Catalysts? *Adv. Synth. Catal.* **2016**, *358*, 3–25.
253. Bartók, M. Advances in Immobilized Organocatalysts for the Heterogeneous Asymmetric Direct Aldol Reactions. *Catal. Rev. Sci. Eng.* **2015**, *57*, 192–255.
254. Zhang, L.; Luo, S.; Cheng, J.-P. Non-covalent Immobilization of Asymmetric Organocatalysts. *Cat. Sci. Technol.* **2011**, *1*, 507–516.
255. de Oliveira, P. H. R.; da Santos, B. M. S.; Leão, R. A. A.; Miranda, L. S. M.; San Gil, R. A. S.; de Souza, R. O. M. A.; Finelli, F. G. From Immobilization to Catalyst Use: A Complete Continuous-Flow Approach Towards the Use of Immobilized Organocatalysts. *Chem-CatChem* **2019**, *11*, 5553–5561.

256. Török, B.; Balázsik, K.; Török, M.; Felföldi, K.; Bartók, M. Enantiodifferentiation in Cinchona-Modified Platinum-Catalyzed Sonochemical Hydrogenations. *Catal. Lett.* **2002**, *81*, 55–62.
257. Liu, L.; Corma, A. Metal Catalysts for Heterogeneous Catalysis: From Single Atoms to Nanoclusters and Nanoparticles. *Chem. Rev.* **2018**, *118*, 4981–5079.
258. Cao, A.; Lu, R.; Vesper, G. Stabilizing Metal Nanoparticles for Heterogeneous Catalysis. *Phys. Chem. Chem. Phys.* **2010**, *12*, 13499–13510.
259. Alexandridis, P.; Tsianou, M. Block Copolymer-Directed Metal Nanoparticle Morphogenesis and Organization. *Eur. Polym. J.* **2011**, *47*, 569–583.
260. Wang, Y.; Quinsaat, J. E. Q.; Ono, T.; Maeki, M.; Tokeshi, M.; Isono, T.; Tajima, K.; Satoh, T.; Sato, S.; Miura, Y.; Yamamoto, T. Enhanced Dispersion Stability of Gold Nanoparticles by the Physisorption of Cyclic Poly(Ethylene Glycol). *Nat. Commun.* **2020**, *11*, 6089.
261. Raveendran, P.; Fu, J.; Wallen, S. L. Completely “Green” Synthesis and Stabilization of Metal Nanoparticles. *J. Am. Chem. Soc.* **2003**, *125*, 13940–13941.
262. Nath, A.; Jana, S.; Pradhan, M.; Pal, T. Ligand-Stabilized Metal Nanoparticles in Organic Solvent. *J. Colloid Interface Sci.* **2010**, *341*, 333–352.
263. Manojkumar, K.; Sivaramakrishna, A.; Vijayakrishna, K. A Short Review on Stable Metal Nanoparticles Using Ionic Liquids, Supported Ionic Liquids, and Poly(Ionic Liquids). *J. Nanopart. Res.* **2016**, *18*, 103.
264. Ji, W.; Wang, X.; Tang, M.; Yang, L.; Rui, Z.; Tong, Y.; Lin, J. Y. S. Strategy for Stabilizing Noble Metal Nanoparticles without Sacrificing Active Sites. *Chem. Commun.* **2019**, *55*, 6846–6849.
265. Huang, Z.; Yao, Y.; Pang, Z.; Yuan, Y.; Li, T.; He, K.; Hu, X.; Cheng, J.; Yao, W.; Liu, Y.; Nie, A.; Sharifi-Asl, S.; Cheng, M.; Song, B.; Amine, K.; Lu, J.; Li, T.; Hu, L.; Shahbazian-Yassar, R. Direct Observation of the Formation and Stabilization of Metallic Nanoparticles on Carbon Supports. *Nat. Commun.* **2020**, *11*, 6373.
266. Mhadgut, S. C.; Palaniappan, K.; Thimmaiah, M.; Hackney, S. A.; Török, B.; Liu, J. A Metal Nanoparticle-Based Supramolecular Approach for Aqueous Biphasic Reactions. *Chem. Commun.* **2005**, 3207–3209.
267. Ndolomingo, M. J.; Bingwa, N.; Meijboom, R. Review of Supported Metal Nanoparticles: Synthesis Methodologies, Advantages and Application as Catalysts. *J. Mater. Sci.* **2020**, *55*, 6195–6241.
268. Ipatiew, W. Zur Frage Über die Zersetzung des Äthylalkohols in Gegenwart verschiedener Katalysatoren. *J. Prakt. Chem.* **1903**, *67*, 420–425.
269. Ipatieff, V. N. Aviation Gasoline by Polymerization and Alkylation of Cracking Gases. *Chem. Eng. News* **1942**, *20*, 1367–1368.
270. Nicholas, C.; Dehydration, P. Dienes, High Octane, and High Pressures: Contributions from Vladimir Nikolaevich Ipatieff, A Father of Catalysis. *ACS Catal.* **2018**, *8*, 8531–8539.
271. Theng, B. K. G. *The Chemistry of Clay-Organic Reactions*, Halsted Press-a Wiley division: New York, 1974.
272. Hattori, H.; Ono, Y. *Solid Acid Catalysis: From Fundamentals to Applications*, Taylor and Francis-CRC Press: Boca Raton, FL, 2015.
273. Benesi, H. A.; Winquest, B. H. C. Surface Acidity of Solid Catalysts. *Adv. Catal.* **1979**, *27*, 97–182.
274. Prakash, G. K. S.; Olah, G. A. In *Acid-Base Catalysis*; Tanabe, K., Hattori, H., Yamaguchi, T., Tanaka, T., Eds.; Kodansha: Tokyo, 1989; p. 59.
275. Török, B.; Molnár, Á. Electrophilic Transformations Induced by Heteropoly Acids: Applications and Structural Studies. *Compt. Rend. Acad. Sci. Paris, Ser. II C* **1998**, 381–396.

72 Heterogeneous catalysis in sustainable synthesis

276. Balogh, M.; Laszlo, P. *Organic Chemistry Using Clays*, Springer-Verlag: Berlin, Heidelberg, 1993.
277. Gates, B. C. Catalysis by Solid Acids. In *Encyclopedia of Catalysis*; Horvath, I. T., Ed.; Vol. 2; Wiley: New York, **2003**; pp. 104–142.
278. Cejka, J.; Corma, A.; Zones, S., Eds. *Zeolites and Catalysis: Synthesis, Reactions and Applications*; Wiley-VCH: Weinheim, **2010**.
279. Dai, P.-S. E. Zeolite Catalysis for a Better Environment. *Catal. Today* **1995**, *26*, 3–11.
280. Baba, T.; Kato, A.; Takahashi, H.; Toriyama, F.; Handa, H.; Ono, Y.; Sugisawa, H. Metathesis of Silylalkynes and Cross-Metathesis of Silylalkyne and 1-Alkyne over Solid-Base Catalysts. *J. Catal.* **1998**, *176*, 488–494.
281. Béres, A.; Pálinkó, I.; Kiricsi, I.; Nagy, J. B.; Kiyozumi, Y.; Mizukami, F. Layered Double Hydroxides and their Pillared Derivatives—Materials for Solid Base Catalysis; Synthesis and Characterization. *Applied Catal. A: Gen.* **1999**, *182*, 237–247.
282. Lopez-Pestana, J. M.; Avila-Rey, M. J.; Martin-Aranda, R. M. Ultrasound-Promoted N-Alkylation of Imidazole. Catalysis by Solid-Base, Alkali-Metal Doped Carbons. *Green Chem.* **2002**, *4*, 628–630.
283. Figueras, F. Base Catalysis in the Synthesis of Fine Chemicals. *Top. Catal.* **2004**, *29*, 189–196.
284. Figueras, F.; Kantam, M. L.; Choudary, B. M. Solid Base Catalysts in Organic Synthesis. *Curr. Org. Chem.* **2006**, *10*, 1627–1637.
285. Clark, J. H. Solid Acids for Green Chemistry. *Acc. Chem. Res.* **2002**, *35*, 791–797.
286. Gupta, P.; Mahajan, A. Green Chemistry Approaches as Sustainable Alternatives to Conventional Strategies in the Pharmaceutical Industry. *RSC Adv.* **2015**, *5*, 26686–26705.
287. Gupta, P.; Paul, S. Solid Acids: Green Alternatives for Acid Catalysis. *Catal. Today* **2014**, *236*, 153–170.
288. Corma, A.; García, H. Lewis Acids: from Conventional Homogeneous to Green Homogeneous and Heterogeneous Catalysis. *Chem. Rev.* **2003**, *103*, 4307–4365.
289. Kokel, A.; Schäfer, C.; Török, B. Organic Synthesis Using Environmentally Benign Acid Catalysis. *Curr. Org. Synth.* **2019**, *16*, 615–649.
290. Okuhara, T. Water-Tolerant Solid Acid Catalysts. *Chem. Rev.* **2002**, *102*, 3641–3666.
291. Bag, S.; Dasgupta, S.; Török, B. Microwave-Assisted Heterogeneous Catalysis: An Environmentally Benign Tool for Contemporary Organic Synthesis. *Curr. Org. Synth.* **2011**, *8*, 237–261.
292. Kokel, A.; Schäfer, C.; Török, B. Application of Microwave-Assisted Heterogeneous Catalysis in Sustainable Synthesis Design. *Green Chem.* **2017**, *19*, 3729–3751.
293. Cho, H.; Schäfer, C.; Török, B. Microwave-assisted Solid Acid Catalysis. In *Microwaves in Catalysis—Fundamental Research and Scale-up Technology*; Horikoshi, S., Serpone, N., Eds.; Wiley, 2015; pp. 193–213 (chapter 10).
294. Daştan, A.; Kulkarni, A.; Török, B. Environmentally Benign Synthesis of Heterocyclic Compounds by Combined Microwave-Assisted Heterogeneous Catalytic Approaches. *Green Chem.* **2012**, *14*, 17–37.
295. Hattori, H. Heterogeneous Basic Catalysis. *Chem. Rev.* **1995**, *95*, 537–558.
296. Ono, Y.; Baba, T. Selective Reactions over Solid Base Catalysts. *Catal. Today* **1997**, *38*, 321–337.
297. Hattori, H. Solid Base Catalysts: Generation of Basic Sites and Application to Organic Synthesis. *Applied Catal. A: Gen.* **2001**, *222*, 247–259.
298. Ono, Y. Solid Base Catalysts for the Synthesis of Fine Chemicals. *J. Catal.* **2003**, *216*, 406–415.
299. Hattori, H. Solid Base Catalysts: Fundamentals and their Applications in Organic Reactions. *Applied Catal. A: Gen.* **2015**, *504*, 103–109.

300. Jambhulkar, D. K.; Ugwekar, R. P.; Bhanvase, B. A.; Barai, D. P. A Review on Solid Base Heterogeneous Catalysts: Preparation, Characterization and Applications. *Chem. Eng. Commun.* **2020**,. <https://doi.org/10.1080/00986445.2020.1864623>.
301. Wachs, I. E.; Briand, L. E.; Jehng, J.-M. Molecular Structure and Reactivity of the Group V Metal Oxides. *Catal. Today* **2000**, *57*, 323–330.
302. Ushikubo, T. Recent Topics of Research and Development of Catalysis by Niobium and Tantalum Oxides. *Catal. Today* **2000**, *57*, 331–338.
303. Hutchings, G. J.; Bartley, J. K.; Rhodes, C.; Taylor, S. H.; Wells, R. P. K.; Willock, D. J. In *Metal Oxides*, in *Encyclopedia of Catalysis*; Horvath, I. T., Ed.; Vol. 4; Wiley: New York, 2003; pp. 602–694.
304. Gawande, M. B.; Pandey, R. K.; Jayaram, R. V. Role of Mixed Metal Oxides in Catalysis Science—Versatile Applications in Organic Synthesis. *Cat. Sci. Technol.* **2012**, *2*, 1113–1125.
305. Venkatesh, K. R.; Hu, J.; Dogan, C.; Tierney, J. W.; Wender, I. Sulfated Metal Oxides and Related Solid Acids: Comparison of Protonic Acid Strengths. *Energy Fuel* **1995**, *9*, 888–893.
306. Brown, A. S. C.; Hargreaves, J. S. J. Sulfated Metal Oxide Catalysts. Superactivity through Superacidity? *Green Chem.* **1999**, *1*, 17–20.
307. Yang, H.; Lu, R.; Zhao, J.; Yang, X.; Shen, L.; Wang, Z. Sulfated Binary Oxide Solid Superacids. *Mater. Chem. Phys.* **2003**, *80*, 68–72.
308. Reddy, B. M.; Sreekanth, P. M.; Lakshmanan, P. Sulfated Zirconia as an Efficient Catalyst for Organic Synthesis and Transformation Reactions. *J. Mol. Catal. A Chem.* **2005**, *237*, 93–100.
309. Arata, K. Organic Syntheses Catalyzed by Superacidic Metal Oxides: Sulfated Zirconia and Related Compounds. *Green Chem.* **2009**, *11*, 1719–1728.
310. Reddy, B. M.; Patil, M. K. Organic Syntheses and Transformations Catalyzed by Sulfated Zirconia. *Chem. Rev.* **2009**, *109*, 2185–2208.
311. Yan, G. X.; Wang, A.; Wachs, I. E.; Baltrusaitis, J. Critical Review on the Active Site Structure of Sulfated Zirconia Catalysts and Prospects in Fuel Production. *Applied Catal. A: Gen.* **2019**, *572*, 210–225.
312. Vadrine, J. C. Heterogeneous Catalysis on Metal Oxides. *Catalysts* **2017**, *7*, 341.
313. Thakuria, H.; Borah, B. M.; Das, G. Macroporous Metal Oxides as an Efficient Heterogeneous Catalyst for Various Organic Transformations—A Comparative Study. *J. Mol. Catal. A-Chem.* **2007**, *274*, 1–10.
314. Vadrine, J. C. Metal Oxides in Heterogeneous Oxidation Catalysis: State of the Art and Challenges for a More Sustainable World. *ChemSusChem* **2019**, *12*, 577–588.
315. Yuan, C.; Wu, H. B.; Xie, Y.; Lou, X. W. Mixed Transition-Metal Oxides: Design, Synthesis, and Energy-Related Applications. *Angew. Chem. Int. Ed.* **2014**, *53*, 1488–1504.
316. Vozniuk, O.; Tabanelli, T.; Tanchoux, N.; Millet, J. M.; Albonetti, S.; Di Renzo, F.; Cavani, F. Mixed-Oxide Catalysts with Spinel Structure for the Valorization of Biomass: The Chemical-Loop Reforming of Bioethanol. *Catalysts* **2018**, *8*, 332.
317. Ghorpade, S. P.; Darshane, V. S.; Dixit, S. G. Liquid-Phase Friedel-Crafts Alkylation Using  $\text{CuCr}_2\text{-xFe}_x\text{O}_4$  Spinel Catalysts. *Appl. Catal., A* **1998**, *166*, 135–142.
318. Zhang, Q.; Wang, H.; Jia, X.; Liu, B.; Yang, Y. One-Dimensional Metal Oxide Nanostructures for Heterogeneous Catalysis. *Nanoscale* **2013**, *5*, 7175–7183.
319. Breedon, M.; Spizzirri, P.; Taylor, M.; du Plessis, J.; McCulloch, D.; Zhu, J.; Yu, L.; Hu, Z.; Rix, C.; Wlodarski, W.; Kalantar-zadeh, K. Synthesis of Nanostructured Tungsten Oxide Thin Films: A Simple, Controllable, Inexpensive, Aqueous Sol-Gel Method. *Cryst. Growth Des.* **2010**, *10*, 430–439.
320. Fu, Z.; Zhang, G.; Tang, Z.; Zhang, H. Preparation and Application of Ordered Mesoporous Metal Oxide Catalytic Materials. *Catal. Surv. Asia* **2020**, *24*, 38–58.

74 Heterogeneous catalysis in sustainable synthesis

321. Voon, C. H.; Foo, K. L.; Lim, B. Y.; Gopinath, S. C. B.; Al-Douri, Y. Synthesis and Preparation of Metal Oxide Powders. In *Metal Oxide Powder Technologies Fundamentals, Processing Methods and Applications Metal Oxides*; 2020; pp. 31–65 (chapter 3).
322. McFarland, E. W.; Metiu, H. Catalysis by Doped Oxides. *Chem. Rev.* **2013**, *113*, 4391–4427.
323. Morris, S. M.; Fulvio, P. F.; Jaroniec, M. Ordered Mesoporous Alumina-Supported Metal Oxides. *J. Am. Chem. Soc.* **2008**, *130*, 15210–15216.
324. Biswas, S.; Pal, A.; Pal, T. Supported Metal and Metal Oxide Particles with Proximity Effect for Catalysis. *RSC Adv.* **2020**, *10*, 35449–35472.
325. Misono, M. Heteropoly Acids. In *Encyclopedia of Catalysis*; Horvath, I. T., Ed.; Vol. 3; Wiley: New York, **2003**; pp. 433–447.
326. Kozhevnikov, I. V. Friedel–Crafts Acylation and Related Reactions Catalysed by Heteropoly Acids. *Appl. Catal. A-Gen.* **2003**, *256*, 3–18.
327. Okuhara, T.; Watanabe, H.; Nishimura, T.; Inumaru, K.; Misono, M. Microstructure of Cesium Hydrogen Salts of 12-Tungstophosphoric Acid Relevant to Novel Acid Catalysis. *Chem. Mater.* **2000**, *12*, 2230–2238.
328. Gromov, N. V.; Medvedeva, T. B.; Rodikova, Y. A.; Babushkin, D. E.; Panchenko, V. N.; Timofeeva, M. N.; Zhizhina, E. G.; Tarana, O. P.; Parmon, V. N. One-Pot Synthesis of Formic Acid Via Hydrolysis–Oxidation of Potato Starch in the Presence of Cesium Salts of Heteropoly Acid Catalysts. *RSC Adv.* **2020**, *10*, 28856–28864.
329. Li, X.; Zhang, Y. Oxidative Dehydration of Glycerol to Acrylic Acid over Vanadium-Substituted Cesium Salts of Keggin-Type Heteropolyacids. *ACS Catal.* **2016**, *6*, 2785–2791.
330. Kozhevnikov, I. V. *Catalysis by Polyoxometalates*, Wiley: Chichester, 2002.
331. Jeong, B. H.; Han, J. S.; Ko, S. W.; Lee, J. H.; Lee, B. J. Deactivation and Reuse of Cesium-Containing Heteropolyacid for the Isomerization of THDCPD. *J. Ind. Eng. Chem.* **2007**, *13*, 310–313.
332. Pope, M. *Heteropoly and Isopoly Oxometalates*, Springer-Verlag: Berlin Heidelberg, 1983.
333. Gumerova, N. I.; Rempel, A. Synthesis, Structures and Applications of Electron-Rich Polyoxometalates. *Nat. Rev. Chem.* **2018**, *2*, 0112.
334. Misono, M. Unique Acid Catalysis of Heteropoly Compounds (Heteropolyoxometalates) in the Solid State. *Chem. Commun.* **2001**, 1141–1152.
335. Timofeeva, M. N. Acid Catalysis by Heteropoly Acids. *Applied Catal. A: Gen.* **2003**, *256*, 19–35.
336. Contreras Coronel, N.; da Silva, M. J. Lacunar Keggin Heteropolyacid Salts: Soluble, Solid and Solid-Supported Catalysts. *J. Clust. Sci.* **2018**, *29*, 195–205.
337. Heravi, M. M.; Sadjadi, S.; Oskooie, H. A.; Shoar, R. H.; Bamoharram, F. F. Heteropolyacids as Heterogeneous and Recyclable Catalysts for the Synthesis of Benzimidazoles. *Catal. Commun.* **2008**, *9*, 504–507.
338. Micek-Ilnicka, A. The Role of Water in the Catalysis on Solid Heteropolyacids. *J. Mol. Catal. A-Chem.* **2009**, *308*, 1–14.
339. Zheyu, W.; Yalin, C.; Yu, H.; Sheng, H. Wei Yongge Application of Anderson Type Heteropoly Acids as Catalysts in Organic Synthesis. *Acta Chim. Sin.* **2020**, *78*, 725–732.
340. Yu, W.; Zhang, Y.; Han, Y.; Li, B.; Shao, S.; Zhang, L.; Xie, H.; Yan, J. Microwave-Assisted Synthesis of Tris-Anderson Polyoxometalates for Facile CO<sub>2</sub> Cycloaddition. *Inorg. Chem.* **2021**, *60*, 3980–3987.
341. Sathicq, A. G.; Romanelli, G. P.; Palermo, V.; Vazquez, P. G.; Thomas, H. J. Heterocyclic Amine Salts of Keggin Heteropolyacids Used as Catalyst for the Selective Oxidation of Sulfides to Sulfoxides. *Tetrahedron Lett.* **2008**, *49*, 1441–1444.
342. Heravi, M. M.; Fard, M. V.; Faghihi, Z. Heteropoly Acids-Catalyzed Organic Reactions in Water: Doubly Green Reactions. *Green Chem. Lett. Rev.* **2013**, *6*, 282–300.

343. Ruiz, D. M.; Romanelli, G. P.; Vazquez, P. G.; Autino, J. C. Preyssler Catalyst: An Efficient Catalyst for Esterification of Cinnamic Acids with Phenols and Imidoalcohols. *Appl. Catal. A Gen.* **2010**, *374*, 110–119.
344. Heravi, M. M.; Bakhtiari, K.; Bamoharram, F. F.; Tehrani, M. H. Wells-Dawson Type Heteropolyacid Catalyzed Synthesis of Quinoxaline Derivatives at Room Temperature. *Monat. Chem.* **2007**, *138*, 465–467.
345. Soled, S.; Miseo, S.; McVicker, G.; Gates, W.; Gutierrez, A.; Paes, J. Preparation of Bulk and Supported Heteropolyacid Salts. *Catal. Today* **1997**, *36*, 441–450.
346. Molnár, Á.; Keresszegi, C.; Török, B. Heteropoly Acids Immobilized into a Silica Matrix: Characterization and Catalytic Applications. *Appl. Catal. A Gen.* **1999**, *189*, 217–224.
347. Okada, T.; Miyamoto, K.; Sakai, T.; Mishima, S. Encapsulation of a Polyoxometalate into an Organosilica Microcapsule for Highly Active Solid Acid Catalysis. *ACS Catal.* **2014**, *4*, 73–78.
348. Ren, Y.; Yue, B.; Gu, M.; He, H. Progress of the Application of Mesoporous Silica-Supported Heteropolyacids in Heterogeneous Catalysis and Preparation of Nanostructured Metal Oxides. *Materials* **2010**, *3*, 764–785.
349. Javid, A.; Khojastehnezhad, A.; Pombeiro, A. J. L. Preparation, Characterization, and Application of Preyssler Heteropoly Acid Immobilized on Magnetic Nanoparticles as a Green and Recoverable Catalyst for the Synthesis of Imidazoles. *Russ. J. Gen. Chem.* **2017**, *87*, 3000–3005.
350. Vaccari, A. Clays and Catalysis: a Promising Future. *Appl. Clay Sci.* **1999**, *14*, 161–198.
351. Zhou, C. H. An Overview on Strategies towards Clay-Based Designer Catalysts for Green and Sustainable Catalysis. *Appl. Clay. Sci.* **2011**, *53*, 87–96.
352. Rajamathi, M.; Thomas, G.; Kamath, P. The Many Ways of Making Anionic Clays. *Proc. Indian Acad. Sci. Chem. Sci.* **2001**, *113*, 671–680.
353. Török, B.; Bartók, M.; Dékány, I. The Structure of Chiral Phenylethylammonium Montmorillonites in Ethanol-Toluene Mixtures. *Colloid Polym. Sci.* **1999**, *277*, 340–346.
354. Nikalje, M. D.; Phukan, P.; Sudalai, A. Recent Advances in Clay-Catalyzed Organic Transformations. *Org. Prep. Proced. Int.* **2000**, *32*, 1–40.
355. Varma, R. S. Clay and Clay-Supported Reagents in Organic Synthesis. *Tetrahedron* **2002**, *58*, 1235–1255.
356. Nagendrappa, G. Organic Synthesis Using Clay and Clay-Supported Catalysts. *Appl. Clay. Sci.* **2011**, *53*, 106–138.
357. Akiyama, T.; Matsuda, K.; Fuchibe, K. Montmorillonite K10 Catalyzed Nucleophilic Addition Reaction to Aldimines in Water. *Synthesis-Stuttgart* **2005**, 2606–2608.
358. Ghadirri, M.; Chrzanowski, W.; Rohanzadeh, R. Biomedical Applications of Cationic Clay Minerals. *RSC Adv.* **2015**, *5*, 29467–29481.
359. Baghernejad, B. Montmorillonite K-10: As a Useful Catalyst in Organic Preparations. *Lett. Org. Chem.* **2010**, *7*, 255–268.
360. Bastida, J.; Lores, M.; De La Torre, J.; Pardo, P.; Buendia, Y. Microstructural Modification of Clay Minerals in Blal Clays from Teruel by Thermal Treatment. *Bol. SECV* **2006**, *45*, 38–45.
361. Cseri, T.; Békássy, S.; Figueras, F.; Cseke, E.; de Menorval, L.-C.; Dutartre, R. Characterization of Clay-Based K Catalysts and their Application in Friedel-Crafts Alkylation of Aromatics. *Applied Catal. A: Gen.* **1995**, *132*, 141–155.
362. Kumar, B. S.; Dhakshinamoorthy, A.; Pitchumani, K. K10 Montmorillonite Clays as Environmentally Benign Catalysts for Organic Reactions. *Cat. Sci. Technol.* **2014**, *4*, 2378–2396.
363. Varga, M.; Török, B.; Molnár, Á. Thermal Stability of Heteropoly Acids and Characterization of the Water Content in the Keggin Structure. *J. Thermal Anal.* **1998**, *53*, 207–215.

76 Heterogeneous catalysis in sustainable synthesis

364. White, J. L.; Truitt, M. J. Heterogeneous Catalysis in Solid Acids. *Prog. Nucl. Magn. Reson. Spectrosc.* **2007**, *51*, 139–154.
365. Liu, D.; Yuan, P.; Liu, H.; Cai, J.; Qin, Z.; Tan, D.; Zhou, Q.; He, H.; Zhu, J. Influence of Heating on the Solid Acidity of Montmorillonite: a Combined Study by DRIFT and Hammett Indicators. *Appl. Clay. Sci.* **2011**, *52*, 358–363.
366. Baloyi, J.; Ntho, T.; Moma, J. Synthesis and Application of Pillared Clay Heterogeneous Catalysts for Wastewater Treatment: A Review. *RSC Adv.* **2018**, *8*, 5197–5211.
367. Li, Y.; Li, L.; Yu, J. Applications of Zeolites in Sustainable Chemistry. *Chem* **2017**, *3*, 928–949.
368. Dusselier, M.; Davis, M. E. Small-Pore Zeolites: Synthesis and Catalysis. *Chem. Rev.* **2018**, *118*, 5265–5329.
369. Bukhtiyarova, M. V.; Echevsky, G. V. Modern Research in the Field of Zeolites and Zeolite-like Materials: A Review of the Works of the Borekov Institute of Catalysis, Siberian Branch, Russian Academy of Sciences. *Petrol. Chem.* **2019**, *59*, 802–821.
370. Beale, A. M.; Gao, F.; Lezcano-Gonzalez, I.; Peden, C. H. F.; Szanyi, J. Recent Advances in Automotive Catalysis for NO Emission Control by Small-Pore Microporous Materials. *Chem. Soc. Rev.* **2015**, *44*, 7371–7405.
371. Vogt, E. T. C.; Weckhuysen, B. M. Fluid Catalytic Cracking: Recent Developments on the Grand Old Lady of Zeolite Catalysis. *Chem. Soc. Rev.* **2015**, *44*, 7342–7370.
372. Nagy, J. B.; Bodart, P.; Hannus, I.; Kiricsi, P. *Synthesis, Characterization, and Use of Zeolitic Microporous Materials*; DecaGen Ltd: Szeged, 1998.
373. Janssens, B.; Catry, P.; Claessens, R.; Baron, G.; Jacobs, P. A. In *Progress in Zeolite and Microporous Materials, Studies in Surface Science and Catalysis*; Chon, H., Ihm, S.-K., Uh, Y. S., Eds.; Vol. 105; Elsevier: Amsterdam, 1997; p. 1211.
374. Csicsery, S. M.; Kiricsi, I. Shape-Selective Catalysis. In *Encyclopedia of Catalysis*; Horvath, I. T., Ed.; Vol. 6; Wiley: New York, 2003; pp. 307–338.
375. Van Speybroeck, V.; Hemelsoet, K.; Joos, L.; Waroquier, M.; Bell, R. G.; Catlow, C. R. A. Advances in Theory and their Application within the Field of Zeolite Chemistry. *Chem. Soc. Rev.* **2015**, *44*, 7044–7111.
376. Tsapatsis, M.; Fan, W. A New, Yet Familiar, Lamellar Zeolite. *ChemCatChem* **2010**, *2*, 246–248.
377. Wei, Y.; Parmentier, T. E.; de Jong, K. P.; Zečević, J. Tailoring and Visualizing the Pore Architecture of Hierarchical Zeolites. *Chem. Soc. Rev.* **2015**, *44*, 7234–7261.
378. Mintova, S.; Jaber, M.; Valtchev, V. Nanosized Microporous Crystals: Emerging Applications. *Chem. Soc. Rev.* **2015**, *44*, 7207–7233.
379. Busca, G. Acidity and Basicity of Zeolites: A Fundamental Approach. *Microporous Mesoporous Mater.* **2017**, *254*, 3–16.
380. Corma, A. State of the Art and Future Challenges of Zeolites as Catalysts. *J. Catal.* **2003**, *216*, 298–312.
381. Baerlocher, C.; McCusker, L. B.; Olson, D. H. *Atlas of Zeolite Framework Types*, 6th ed.; Elsevier: Cambridge, MA, Oxford, 2007.
382. Sherman, J. Synthetic Zeolites and Other Microporous Oxide Molecular Sieves. *Proc. Natl. Acad. Sci. U. S. A.* **1999**, *96*, 3471–3478.
383. Bouizi, Y. *Micro-composites formés d'une couche continue de zéolithe recouvrant un coeur de zéolithe—Etude des processus de formation* (Doctoral thesis); Université de Haute-Alsace: France, 2006, Retrieved from [https://tel.archives-ouvertes.fr/tel-00011719/file/These\\_Bouizi\\_Younes.pdf](https://tel.archives-ouvertes.fr/tel-00011719/file/These_Bouizi_Younes.pdf).
384. Eliášová, P.; Opanasenko, M.; Wheatley, P. S.; Shamzhy, M.; Mazur, M.; Nachtigall, P.; Roth, W. J.; Morris, R. E.; Čejka, J. The ADOR Mechanism for the Synthesis of New Zeolites. *Chem. Soc. Rev.* **2015**, *44*, 7177–7206.

385. Dapsens, P. Y.; Mondelli, C.; Pérez-Ramírez, J. Design of Lewis-Acid Centres in Zeolitic Matrices for the Conversion of Renewables. *Chem. Soc. Rev.* **2015**, *44*, 7025–7043.
386. Li, J.; Corma, A.; Yu, J. Synthesis of New Zeolite Structures. *Chem. Soc. Rev.* **2015**, *44*, 7112–7127.
387. Shi, J.; Wang, Y.; Yang, W.; Tang, Y.; Xie, Z. Recent Advances of Pore System Construction in Zeolite-Catalyzed Chemical Industry Processes. *Chem. Soc. Rev.* **2015**, *44*, 8877–8903.
388. Cundy, C.; Cox, P. The Hydrothermal Synthesis of Zeolites: Precursors, Intermediates and Reaction Mechanism. *Microporous Mesoporous Mater.* **2005**, *82*, 1–78.
389. Louis, B.; Kiwi-Minsker, L. Synthesis of ZSM-5 Zeolite in Fluoride Media: an Innovative Approach to Tailor both Crystal Size and Acidity. *Microporous Mesoporous Mater.* **2004**, *74*, 171–178.
390. Qiyu, L. Fan Wei Recent Advances in the Synthesis of Mesoporous Zeolites by Post-Synthetic Method, Supramolecular Self-Assembly and Mesopore Generation Agent. *Chem. J. Chin. Univ.* **2021**, *42*, 60–73.
391. Cejka, J.; Millini, R.; Opanasenko, M.; Serrano, D. P.; Roth, W. J. Advances and Challenges in Zeolite Synthesis and Catalysis. *Catal. Today* **2020**, *345*, 2–13.
392. Cundy, C. S.; Cox, P. A. The Hydrothermal Synthesis of Zeolites: History and Development from the Earliest Days to the Present Time. *Chem. Rev.* **2003**, *103*, 663–701.
393. Barbaro, P.; Liguori, F. Ion Exchange Resins: Catalyst Recovery and Recycle. *Chem. Rev.* **2009**, *109*, 515–529.
394. Olah, G. A.; Iyer, P. S.; Prakash, G. K. S. Perfluorinated Resinsulphonic Acid (Nafion-H) Catalysis in Synthesis. *Synthesis* **1986**, 513–531.
395. Pal, R.; Sarkar, T.; Khasnobis, S. Amberlyst-15 in organic synthesis. *ARKIVOC* **2012**, *i*, 570–609.
396. Harmer, M.; Sun, Q. Solid Acid Catalysis Using Ion-Exchange Resins. *Appl. Catal. A Gen.* **2001**, *221*, 45–62.
397. Xu, Y.; Gu, W.; Gin, D. Heterogeneous Catalysis Using a Nanostructured Solid Acid Resin Based on Lyotropic Liquid Crystals. *J. Am. Chem. Soc.* **2004**, *126*, 1616–1617.
398. Kidwai, M.; Chauhan, R.; Bhatnagar, S. Nafion-H (R): A Versatile Catalyst for Organic Synthesis. *Curr. Org. Chem.* **2015**, *19*, 72–98.
399. Lingaiah, B. P. V.; Ezekiel, G.; Yakaiah, T.; Reddy, G. V.; Rao, P. S. Nafion-H: An Efficient and Recyclable Heterogeneous Catalyst for the One-Pot Synthesis of 2,3-Disubstituted 4-(3H)-Quinazolinones under Solvent-Free Microwave Irradiation Conditions. *Synlett* **2006**, 2507–2509.
400. Yakaiah, T.; Lingaiah, B. P. V.; Reddy, G. V.; Narsaiah, B.; Rao, P. S. Perfluorinated Resin-Sulfonic Acid (Nafion-H): An Efficient, Environment Friendly and Recyclable Heterogeneous Catalyst for the One-Pot Multicomponent Synthesis of  $\beta$ -Acetamido Ketones. *ARKIVOC* **2007**, *xiii*, 227–234.
401. Prakash, G. K. S.; Munoz, S. B.; Papp, A.; Masood, K.; Bychinskaya, I.; Mathew, T.; Olah, G. A. Nafion-Ru: A Sustainable Catalyst for Selective Hydration of Nitriles to Amides. *Asian J. Org. Chem.* **2012**, *1*, 146–149.
402. Prakash, G. K. S.; Glington, K. E.; Panja, C.; Gurung, L.; Battamack, P. T.; Török, B.; Mathew, T.; Olah, G. A. Thermocontrolled Benzylimine–Benzaldimine Rearrangement over Nafion-H Catalysts for Efficient Entry into  $\alpha$ -Trifluoromethylbenzylamines. *Tetrahedron Lett.* **2012**, *53*, 607–611.
403. Prakash, G. K. S.; Bychinskaya, I.; Marinez, E. R.; Mathew, T.; Olah, G. A. Nafion-Fe: A New Efficient “Green” Lewis Acid Catalyst for the Ketonic Strecker Reaction. *Catal. Lett.* **2013**, *143*, 303–312.

78 Heterogeneous catalysis in sustainable synthesis

404. Ezzeldin, H. A.; Apblett, A.; Foutch, G. L. Synthesis and Properties of Anion Exchangers Derived from Chloromethyl Styrene Codivinylbenzene and their Use in Water Treatment. *Int. J. Polym. Sci.* **2010**, *2010*, 684051.
405. Harmer, M. A.; Farneth, W. E.; Sun, Q. High Surface Area Nafion Resin/Silica Nanocomposites: A New Class of Solid Acid Catalyst. *J. Am. Chem. Soc.* **1996**, *118*, 7708–7715.
406. Török, B.; Kiricsi, I.; Molnár, Á.; Olah, G. A. Acidity and Catalytic Activity of Nafion-H/Silica Nanocomposite Catalyst and a Comparison with Silica-Supported Perfluorinated Acids. *J. Catal.* **2000**, *193*, 132–138.
407. Rác, B.; Mulas, G.; Csongrádi, A.; Lóki, K.; Molnár, Á. SiO<sub>2</sub>-Supported Dodecatungstophosphoric Acid and Nafion-H Prepared by Ball-Milling for Catalytic Application. *Applied Catal. A: Gen.* **2005**, *282*, 255–265.
408. Zhou, H.; Kitagawa, S. Metal–Organic Frameworks (MOFs). *Chem. Soc. Rev.* **2014**, *43*, 5415–5418.
409. Li, H.; Eddaoudi, M.; O’Keeffe, M.; Yaghi, O. M. Design and Synthesis of an Exceptionally Stable and Highly Porous Metal–Organic Framework. *Nature* **1999**, *402*, 276–279.
410. Eddaoudi, M.; Kim, J.; Rosi, N.; Vodak, D.; Wachter, J.; O’Keeffe, M.; Yaghi, O. M. Systematic Design of Pore Size and Functionality in Isoreticular MOFs and their Application in Methane Storage. *Science* **2002**, *295*, 469–472.
411. Corma, A.; García, H.; Llabrés i Xamena, F. X. Engineering Metal Organic Frameworks for Heterogeneous Catalysis. *Chem. Rev.* **2010**, *110*, 4606–4655.
412. Jiang, J.; Yaghi, O. M. Brønsted Acidity in Metal–Organic Frameworks. *Chem. Rev.* **2015**, *115*, 6966–6997.
413. Zhu, L.; Liu, X.-Q.; Jiang, H.-L.; Sun, L.-B. Metal–Organic Frameworks for Heterogeneous Basic Catalysis. *Chem. Rev.* **2017**, *117*, 8129–8176.
414. Ruano, D.; Diaz-García, M.; Alfayate, A.; Sanchez-Sanchez, M. Nanocrystalline M-MOF-74 as Heterogeneous Catalysts in the Oxidation of Cyclohexene: Correlation of the Activity and Redox Potential. *ChemCatChem* **2015**, *7*, 674–681.
415. Wang, C.; An, B.; Lin, W. Metal–Organic Frameworks in Solid–Gas Phase Catalysis. *ACS Catal.* **2019**, *9*, 130–146.
416. Yoon, M.; Srirambalaji, R.; Kim, K. Homochiral Metal–Organic Frameworks for Asymmetric Heterogeneous Catalysis. *Chem. Rev.* **2012**, *112*, 1196–1231.
417. Liang, W.; D’Alessandro, D. M. Microwave-Assisted Solvothermal Synthesis of Zirconium Oxide Based Metal–Organic Frameworks. *Chem. Commun.* **2013**, *49*, 3706–3708.
418. Liu, J.; Lukose, B.; Shekha, O.; Arslan, H. K.; Weidler, P.; Gliemann, H.; Braese, S.; Grosjean, S.; Godt, A.; Feng, X.; Muellen, K.; Magdau, I.; Heine, T.; Woell, C. A Novel Series of Isoreticular Metal Organic Frameworks: Realizing Metastable Structures by Liquid Phase Epitaxy. *Sci. Rep.* **2012**, *2*, 921–936.
419. Cohen, S. M. Postsynthetic Methods for the Functionalization of Metal Organic Frameworks. *Chem. Rev.* **2012**, *112*, 970–1000.
420. Corma, A. From Microporous to Mesoporous Molecular Sieve Materials and their Use in Catalysis. *Chem. Rev.* **1997**, *97*, 2373–2419.
421. Bagshaw, S.; Prouzet, E.; Pinnavaia, T. Templating of Mesoporous Molecular-Sieves by Nonionic Polyethylene Oxide Surfactants. *Science* **1995**, *269*, 1242–1244.
422. Kresge, C. T.; Roth, W. J. The Discovery of Mesoporous Molecular Sieves from the Twenty Year Perspective. *Chem. Soc. Rev.* **2013**, *42*, 3663–3670.
423. Kruk, M.; Jaroniec, M.; Ko, C. H.; Ryoo, R. Characterization of the Porous Structure of SBA-15. *Chem. Mater.* **2000**, *12*, 1961–1968.
424. Verma, P.; Kuwahara, Y.; Mori, K.; Raja, R.; Yamashita, H. Functionalized Mesoporous SBA-15 Silica: Recent Trends and Catalytic Applications. *Nanoscale* **2020**, *12*, 11333–11363.

425. Margolese, D.; Melero, J. A.; Christiansen, S. C.; Chmelka, B. F.; Stucky, G. D. Direct Syntheses of Ordered SBA-15 Mesoporous Silica Containing Sulfonic Acid Groups. *Chem. Mater.* **2000**, *12*, 2448–2459.
426. Yin, Y.; Yang, Z.-F.; Wen, Z.-H.; Yuan, A.-H.; Liu, X.-Q.; Zhang, Z.-Z.; Zhou, H. Modification of as Synthesized SBA-15 with Pt Nanoparticles: Nanoconfinement Effects Give a Boost for Hydrogen Storage at Room Temperature. *Sci. Rep.* **2017**, *7*, 4509.
427. Schoonheydt, R.; Pinnavaia, T.; Lagaly, G.; Gangas, N. Pillared Clays and Pillared Layered Solids - (Technical Report). *Pure Appl. Chem.* **1999**, *71*, 2367–2371.
428. Centi, G.; Perathoner, S. Catalysis by Layered Materials: A Review. *Microporous Mesoporous Mater.* **2008**, *107*, 3–15.
429. Luo, X.-L.; Yin, Z.; Zeng, M.-H.; Kurmoo, M. The Construction, Structures, and Functions of Pillared Layer Metal–Organic Frameworks. *Inorg. Chem. Front.* **2016**, *3*, 1208–1226.
430. Tomlinson, A. A. G. Characterization of Pillared Layered Structures. *J. Porous. Mater.* **1998**, *5*, 259–274.
431. Hara, M.; Yoshida, T.; Takagaki, A.; Takata, T.; Kondo, J. N.; Domen, K.; Hayashi, S. A. A Carbon Material as a Strong Protonic Acid. *Angew. Chem. Int. Ed.* **2004**, *43*, 2955–2958.
432. Suganuma, S.; Nakajima, K.; Kitano, M.; Yamaguchi, D.; Kato, H.; Hayashi, S.; Hara, M. Synthesis and Acid Catalysis of Cellulose Derived Carbon-Based Solid Acid. *Solid State Sci.* **2010**, *12*, 1029–1034.
433. Jamwal, N.; Sodhi, R. K.; Gupta, P.; Paul, S. Nano Pd(0) Supported on Cellulose: A Highly Efficient and Recyclable Heterogeneous Catalyst for the Suzuki Coupling and Aerobic Oxidation of Benzyl Alcohols under Liquid Phase Catalysis. *Int. J. Biol. Macromol.* **2011**, *49*, 930–935.
434. Wolf, P.; Logemann, M.; Schörner, M.; Keller, L.; Haumann, M.; Wessling, M. Multi-Walled Carbon Nanotube-Based Composite Materials as Catalyst Support for Water–Gas Shift and Hydroformylation Reactions. *RSC Adv.* **2019**, *9*, 27732–27742.
435. Cao, Y.; Mao, S.; Li, M.; Chen, Y.; Wang, Y. Metal/Porous Carbon Composites for Heterogeneous Catalysis: Old Catalysts with Improved Performance Promoted by N-Doping. *ACS Catal.* **2017**, *7*, 8090–8112.
436. Chrobok, A.; Baj, S.; Pudło, W.; Jarzebski, A. Supported Hydrogensulfate Ionic Liquid Catalysis in Baeyer–Villiger Reaction. *Appl. Catal. A Gen.* **2009**, *366*, 22–28.
437. Sugimura, R.; Qiao, K.; Tomida, D.; Yokoyama, C. Immobilization of Acidic Ionic Liquids by Copolymerization with Styrene and their Catalytic Use for Acetal Formation. *Catal. Commun.* **2007**, *8*, 770–772.
438. Amarasekara, A. S.; Owereh, O. S. Synthesis of a Sulfonic Acid Functionalized Acidic Ionic Liquid Modified Silica Catalyst and Applications in the Hydrolysis of Cellulose. *Catal. Commun.* **2010**, *11*, 1072–1075.
439. Gupta, P.; Kour, M.; Paul, S.; Clark, J. H. Ionic Liquid Coated Sulfonated Carbon/Silica Composites: Novel Heterogeneous Catalysts for Organic Syntheses in Water. *RSC Adv.* **2014**, *4*, 7461–7470.
440. Correia, D. M.; Fernandes, L. C.; Martins, P. M.; García-Astrain, C.; Costa, C. M.; Reguera, J.; Lanceros-Méndez, S. Ionic Liquid–Polymer Composites: A New Platform for Multifunctional Applications. *Adv. Funct. Mater.* **2020**, *30*, 1909736.
441. Nakajima, K.; Okamura, M.; Kondo, J. N.; Domen, K.; Tatsumi, T.; Hayashi, S.; Hara, M. Amorphous Carbon Bearing Sulfonic Acid Groups in Mesoporous Silica as a Selective Catalyst. *Chem. Mater.* **2009**, *21*, 186–193.
442. De Vyver, S. V.; Peng, L.; Geboers, J.; Schepers, H.; de Clippel, F.; Gommès, C. J.; Goderis, B.; Jacobs, P. A.; Sels, B. F. Sulfonated Silica/Carbon Nanocomposites as Novel Catalysts for Hydrolysis of Cellulose to Glucose. *Green Chem.* **2010**, *12*, 1560–1563.

80 Heterogeneous catalysis in sustainable synthesis

443. Gupta, P.; Paul, S. Sulfonated Carbon/Silica Composites: Highly Efficient Heterogeneous Catalysts for the One-Pot Synthesis of Hantzsch 1,4-Dihydropyridines, 2,4,5-Trisubstituted Imidazoles and 2-Arylbenzimidazoles. *Curr. Catal.* **2014**, *3*, 53–64.
444. Gupta, P.; Kumar, V.; Paul, S. Silica Functionalized Sulfonic Acid Catalyzed One-Pot Synthesis of 4,5,8a-Triarylhexahydroimidazo[4,5-d]pyrimidine-2,7(1H,3H)-Diones under Liquid Phase Catalysis. *J. Braz. Chem. Soc.* **2010**, *21*, 349–354.
445. Gupta, P.; Paul, S. Sulfonated Carbon/Silica Composite Functionalized Lewis Acids for One-Pot Synthesis of 1,2,4,5-Tetrasubstituted Imidazoles, 3,4-Dihydropyrimidin-2(1H)-Ones and for Michael Addition of Indole to  $\alpha,\beta$ -Unsaturated Ketones. *J. Mol. Catal. A Chem.* **2012**, *352*, 75–80.
446. Gupta, P.; Paul, S. Amorphous Carbon-Silica Composites Bearing Sulfonic Acid as Solid Acid Catalysts for the Chemoselective Protection of Aldehydes as 1,1-Diacetates and for *N*-, *O*- and *S*-Acylation. *Green Chem.* **2011**, *13*, 2365–2372.
447. Shi, J. On the Synergetic Catalytic Effect in Heterogeneous Nanocomposite Catalysts. *Chem. Rev.* **2013**, *113*, 2139–2181.
448. Chen, Z.; Zhong, W.; Tang, D.; Zhang, G. Preparation of Organic Nanoacid Catalyst for Urethane Formation. *Chin. J. Chem. Phys.* **2017**, *30*, 339–342.
449. Liu, T.; Imber, B.; Diemann, E.; Liu, G.; Cokleski, K.; Li, H.; Chen, Z.; Müller, A. Deprotonations and Charges of Well-Defined  $\{Mo_7Fe_{30}\}$  Nanoacids Simply Stepwise Tuned by pH Allow Control/Variation of Related Self-Assembly Processes. *J. Am. Chem. Soc.* **2006**, *128*, 15914–15920.
450. Titirici, M.-M.; Antonietti, M. Chemistry and Materials Options of Sustainable Carbon Materials Made by Hydrothermal Carbonization. *Chem. Soc. Rev.* **2010**, *39*, 103–116.
451. Török, B.; Molnár, Á.; Pálkó, I.; Bartók, M. Surface Carbonaceous Deposits as Activity and Selectivity Influencing Species in the Ring-Opening Reactions of Propylcyclobutane Catalyzed by Pt/SiO<sub>2</sub>. *J. Catal.* **1994**, *145*, 295–299.
452. Navalon, S.; Dhakshinamoorthy, A.; Alvaro, M.; Garcia, H. Carbocatalysis by Graphene-Based Materials. *Chem. Rev.* **2014**, *114*, 6179–6212.

## Chapter 3

# Application of heterogeneous catalysis in the development of environmentally benign synthetic processes

The earlier chapters covered the discussion of the historical background of heterogeneous catalysis, its fundamentals, and the classification of solid catalysts including their preparation and characterization. The entirety of this chapter will detail the application of these principles and catalysts in practical synthetic processes. Here, we provide a short introduction to the upcoming subchapters that will discuss the individual contributors to heterogeneous catalytic synthesis.

Based on the importance of heterogeneous catalytic methods, they have been frequently reviewed. There are many seminal books<sup>1-9</sup> and major accounts<sup>10, 11</sup> that time to time provided extensive background regarding these processes. One of these books, Augustine's *Heterogeneous Catalysis for the Synthetic Chemist*,<sup>12</sup> was focused on the application side of heterogeneous catalysis, with particular attention to processes that are related to organic synthesis. Although it is an excellent summary of the progress until its publication in 1996 it has been published 25 years ago and several processes, such as metathesis or cross-coupling reactions, are not covered in it. Our goal with the following subchapters was to give detailed accounts on the individual processes that provide representative illustrations of the current advances made in those fields. In addition to providing the state of the art in the respective fields, the major focus of our attention will be on environmentally benign and sustainable applications. Keeping the major principles of green chemistry and engineering<sup>13-15</sup> in mind, we will select examples that fulfill several principles; or even if not completely green, the processes will be a step forward as compared to more traditional protocols, from the point of view of environmental responsibility.

Here we only list the mainstream processes that are the major contributors to efforts that aim to improve the pharmaceutical and chemical industries to better meet the current environmental and safety requirements. In that respect, extensive separate subchapters will follow on hydrogenation, hydrogenolysis, oxidation, metathesis, Friedel-Crafts and related reactions, cross-coupling reactions, multicomponent reactions, ring transformation, rearrangements, and finally asymmetric reactions. In each case the focus will be on synthetic applications;

however, other aspects such as potential environmental uses (e.g. dehalogenation or dehydrosulfurization, etc.) will also be discussed.

A large part of recent efforts in green and sustainable chemistry focuses on the conversion of biomass to valuable chemicals, such as pharmaceuticals and fine chemical building blocks, commonly called as biovalorization, that is more important today than ever.<sup>16</sup> The continued reliance on the currently used mineral oil-based feedstock is not sustainable due to the limited supply available. Additionally, the use of fossil fuels negatively affects the carbon balance of the planet thus significantly contributing to global warming. As a result, phasing out these materials in the chemical industry and replacing them with sustainable resources are of utmost importance.<sup>17–19</sup> Despite its unique nature, biovalorization still applies the common transformations, such as hydrogenolysis or acid-catalyzed cleavage, etc. as discussed before. Thus, instead of devoting a separate chapter to heterogeneous catalytic biovalorization itself, the relevant information will be included in the other methodology-based chapters discussing the contribution of the individual methods to biovalorization right at the source, where the technical details are provided.

## References

1. Smith, G. V.; Notheisz, F. *Heterogeneous Catalysis in Organic Chemistry*; Academic Press: San Diego, CA, 1999.
2. Horvath, I., Ed. *Encyclopedia of Catalysis*; Wiley: New York, 2003.
3. Rylander, P. N. *Catalytic Hydrogenation over Platinum Metals*; Academic Press: New York, London, 1967.
4. Bartók, M., Ed. *Stereochemistry of Heterogeneous Metal Catalysis*; Wiley: Chichester, 1985.
5. Ertl, G.; Knözinger, H.; Weitkamp, J., Eds. *Handbook of Heterogeneous Catalysis*; 2nd ed.; Wiley-VCH: New York, Weinheim, 2008.
6. Olah, G. A., Ed. *Friedel-Crafts and Related Reactions*; Wiley: New York, 1964.
7. Sheldon, R. A.; Arends, I.; Hanefeld, U. *Green Chemistry and Catalysis*, 2nd ed.; Wiley-VCH: Weinheim, 2014.
8. Somorjai, G. A.; Li, Y. *Introduction to Surface Chemistry and Catalysis*, 2nd ed.; Wiley: New York, 2010.
9. Thomas, J. M.; Thomas, W. J. *Principles and Practice of Heterogeneous Catalysis*; Wiley-VCH: New York, Weinheim, 1996.
10. Kokel, A.; Schäfer, C.; Török, B. Organic Synthesis Using Environmentally Benign Acid Catalysis. *Curr. Org. Synth.* **2019**, *16*, 615–649.
11. Kokel, A.; Schäfer, C.; Török, B. Application of Microwave-Assisted Heterogeneous Catalysis in Sustainable Synthesis Design. *Green Chem.* **2017**, *19*, 3729–3751.
12. Augustine, R. L. *Heterogeneous Catalysis for the Synthetic Chemist*; Marcel Dekker: New York, 1996.
13. Anastas, P. T.; Warner, J. C. *Green Chemistry: Theory and Applications*; Oxford University Press: Oxford, 1998.
14. Török, B.; Dransfield, T., Eds. *Green Chemistry: An Inclusive Approach*; Elsevier: Cambridge, Oxford, 2018.
15. Li, C.-J., Ed. *Handbook of Green Chemistry-Green Processes, Vol. 7. Green Synthesis*; Wiley-VCH: Weinheim, 2012.

16. Rathinam, N. K.; Sani, R. K. *Biovalorisation of Wastes to Renewable Chemicals and Biofuels*; Elsevier: Amsterdam, Oxford, Cambridge, MA, 2020.
17. Kokel, A.; Török, B. Sustainable Production of Fine Chemicals and Materials Using Non-Toxic Renewable Sources. *Toxicol. Sci.* **2018**, *161*, 214–224.
18. Besson, M.; Gallezot, P.; Pinel, C. Conversion of Biomass into Chemicals over Metal Catalysts. *Chem. Rev.* **2014**, *114*, 1827–1870.
19. Zakzeski, J.; Bruijninx, P. C. A.; Jongerius, A. L.; Weckhuysen, B. M. The Catalytic Valorization of Lignin for the Production of Renewable Chemicals. *Chem. Rev.* **2010**, *110*, 3552–3599.



## Chapter 3.1

# Hydrogenation

### 3.1.1 Introduction

Reduction is a fundamental transformation in organic synthesis.<sup>1-3</sup> Heterogeneous catalytic hydrogenation<sup>4-10</sup> is one of the most established methods in synthetic chemistry providing essential protocols for the reduction of many substrates. Although developed nearly a century before the formal establishment of the Green Chemistry movement,<sup>11</sup> catalytic hydrogenation is one of the main contributors to the development of environmentally benign processes. Due to growing concerns regarding environmental conservation and occupational safety, the traditional methods applying stoichiometric reagents are being phased out and replaced by more contemporary catalytic methods. Interestingly, catalytic hydrogenations on solid metal catalysts have most of the attributes that one expects from a green technology, such as the 100% atom economy, commonly recyclable catalysts, no waste generation, and, in most cases, the use of green solvents, such as alcohols.<sup>12</sup> Additionally, as a catalytic method it is favored over reagent-based reductions in sustainable applications. Based on the above, heterogeneous catalytic hydrogenation is perhaps the most often used heterogeneous catalytic process in organic synthesis at the laboratory as well as the industrial scale.<sup>13, 14</sup> In addition to the clear advantages that these catalysts possess in terms of green applications, they are robust, convenient to handle, less sensitive to moisture than their homogeneous counterparts, and can be applied in catalytic beds that are major parts of automated flow reactor designs.<sup>15</sup> Hydrogenation catalysts are available in several different forms; however, all of them are based on transition metals. The traditional hydrogenation catalysts focus on platinum group metals and nickel, although more economic and often greener metals such as copper or iron are also applied, especially on the industrial scale. Due to their practical importance in the pharmaceutical, fine chemicals, and petrochemicals industries, the design, preparation, and characterization of metal catalysts are subject of extensive interest. Their development and surface chemistry also attracted unparalleled attention.<sup>16-30</sup> The general characterization of metal catalysts is described in Chapter 2.

However, despite the earlier listed benefits, heterogeneous catalytic hydrogenation also has several significant drawbacks that somewhat overshadow the advantages. One of the main issues is the use of the explosive and flammable gas that hydrogen is. Handling such a gas at high pressures certainly mounts

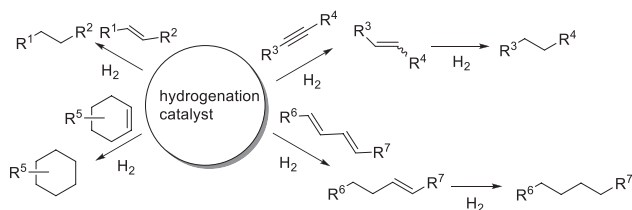
challenges; however, over the past century the chemical industry dealt with these problems sufficiently and hydrogenation plants are one of the safest ones in the industry. Another issue that is yet to be overcome is the generation of the reactant hydrogen. At present, hydrogen is produced via steam reforming that occurs at very high temperatures (700–1000°C) requiring significant energy investment. In addition to the high energy demand, the energy is provided by the partial combustion of methane, which produces a large amount of carbon dioxide, one of the most well-known greenhouse gases.<sup>31</sup> Thus the overall environmental impact of catalytic hydrogenation, homogeneous or heterogeneous, cannot be overlooked. Despite the present blemishes on the green label of hydrogenation, when enough energy will be provided by green sources, such as solar, wind, or hydroelectric, at a reasonable cost, the same hydrogen can be obtained by water electrolysis making the process significantly greener.

Heterogeneous catalytic hydrogenation is one of the oldest methods developed for organic synthesis. The first such data were published in 1897 by Paul Sabatier. He developed solid nickel catalysts and applied them in the hydrogenation of alkenes, which eventually won him the Nobel Prize in Chemistry in 1912,<sup>32</sup> and also established heterogeneous catalysis and its application in hydrogenation as a new field of organic synthesis.<sup>33</sup> A few decades later, Murray Raney developed the Raney Ni catalyst<sup>34–37</sup> to add new dimensions to hydrogenations via the application of this skeletal catalysts.<sup>38</sup> Due to its nearly endless application possibilities, hydrogenation attracted extensive attention. Rylander's seminal monograph on the topic is probably the most comprehensive early account in this field.<sup>39</sup> Several other books followed Rylander's work and new developments have been reviewed periodically in extensive books.<sup>40, 41</sup> In addition to books, the several subtopics of hydrogenation have been the target of a large number of reviews and major accounts in nearly every catalysis journal.<sup>42–48</sup> Due to the practical importance of hydrogenation it has always received significant attention. Accordingly, the available literature is more than sizeable, including surface phenomena, catalyst development, and certainly applications of industrial and/or synthetic relevance. An earlier book by Augustine<sup>5</sup> gave an excellent and detailed description of the state of the art of this field up to 1996, thus we will focus on new developments that occurred in the application field after 1996, and refer the reader searching for earlier information to that source. In the following pages these applications will be discussed based on the functional groups. Due to the extensive number of publications, our goal is to provide a representative survey of the available applications and not an exhaustive account of the topic.

### 3.1.2 Carbon-carbon multiple bond hydrogenations: Alkenes, alkynes, dienes

Hydrogenation of carbon-carbon double (C=C) and triple bonds (C≡C) (Scheme 1) was attempted first during the development of hydrogenation as a

method. The hydrogenation of these substrates is particularly important in the petrochemical, pharmaceutical, and fine chemical industries. Significant expansion occurred in the hydrogenation of C–C multiple bonds since Sabatier’s early publications<sup>33</sup> in the development of effective and commercially available catalysts and their applications.<sup>4–6, 39</sup> Heterogeneous catalytic hydrogenations are now carried out using a broad variety of catalysts (e.g. bulk metals, supported metal catalysts, or immobilized metal complexes) and conditions. As C–C multiple bonds are often only a part of a larger compound with other potentially reduction sensitive groups, much effort was focused on the development of chemo, regio-, and even enantioselective applications. A number of examples summarizing C=C double bond hydrogenations are listed in Table 1.



**SCHEME 1** Catalytic hydrogenation of C=C double and C≡C triple bonds.

Table 1 presents the broad use of the process; the applications range from simple starting materials such as alkenes to C–C multiple bond-containing natural products such as fatty acids or steroids, even mixtures of natural products (e.g., soybean oil). Although the most commonly applied catalytic metal is Pd, a wide variety of transition metals (Rh, Pt, Ru, Ni, Cu, Co) were used in various applications, although metal-free examples, while a rarity, have also been reported. In addition to the active metal itself, the catalyst formulation also includes a range of forms, such as regular supported metals, nanoparticles, polymer-included particles, bimetallic alloys. Novel materials, such as graphene or graphitic carbon nitride, have also been utilized as a support material for metals, for example, in the hydrogenation of styrene-butadiene rubber on Pd/g-C<sub>3</sub>N<sub>4</sub> catalyst.<sup>98</sup> The source of hydrogen in the examples listed in Table 1 is, to an overwhelming extent, hydrogen gas under various pressures. Nevertheless, other sources such as metallic Al that in situ generates H<sub>2</sub> from water or hydrogen donors, e.g., hydrazine, isopropanol, Hantzsch esters, or NaBH<sub>4</sub> are also commonly applied in transfer hydrogenations. Ensured by the high sensitivity of C–C multiple bond toward hydrogenation, the reactions occur at relatively modest temperatures and such high reactivity offers opportunities for carrying out chemoselective hydrogenation of C=C or C≡C bond in the presence of other, hydrogenation sensitive but less active functional groups.

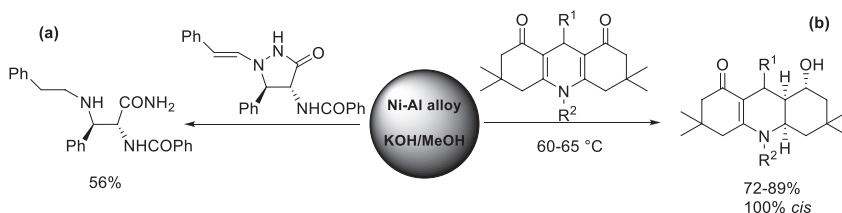
**TABLE 1** Heterogeneous catalytic hydrogenation of alkenes and cycloalkenes to their corresponding saturated products.

| Entry | Substrate  | Catalyst   | Hydrogen source                                  | Conditions  | Comments   | Ref.  |
|-------|--|--|--|---|--|-------|
| 1     | Straight chain and cyclic alkenes, styrene, stilbene | Pt@hmc, Pd-PEI, Pd/FFMPA, Pd, Pt, Ni/metal phosphonates, Pt/Al <sub>2</sub> O <sub>3</sub> , Pd/C WO <sub>2.72</sub> , Crabtree's cat in MIL-101 (MOF), Cu <sub>7</sub> Pt <sub>3</sub> -rGO, IrH(O-SBA-15)(POCOP), resin supported Rh NPs, Pd-AmP-MCF, Cu NPs/diamond, Pd/SBA15, Ir-nanosponge, Rh-complex/SiO <sub>2</sub> or porous organic polymer | 0.2–10 bar H <sub>2</sub><br>Al-H <sub>2</sub> O | Batch reactor, 60–80°C<br>RT, 25 h                                  | Yields and selectivities: up to 99%, recyclable catalysts, magnetically recoverable catalyst | 49–65 |
| 2     | Allyl alcohol, unsaturated alcohols                  | Pd-PAMAM-SBA-15, Pd-DEN, Pd(0)-polystyrene coated SiO <sub>2</sub> , Pd/PEI  | H <sub>2</sub> (2.0–3.0 MPa)                     | Suspension in MeOH/H <sub>2</sub> O, RT<br>scCO <sub>2</sub> , 40°C | Excellent TOFs, recyclable catalyst, rate dependent on Pd particle size                      | 66–69 |
| 3     | Bicyclo[2.2.2]octenes                                | Rh/TPPTS/LDH   | H <sub>2</sub> (20–40 bar)                       | Varied temps  | Recyclable catalyst, no metal leaching   | 70    |
| 4     | Sorbic acid  | [Cp*Ru(sorbic acid)]CF <sub>3</sub> SO <sub>3</sub> on SiO <sub>2</sub>  | H <sub>2</sub> (20 bar)                          | MTBE, 50°C  | Selective to <i>cis</i> -3-hexenoic acid   | 71    |

|    |  |  |   |   |   |              |
|----|--|--|---|---|---|--------------|
| 5  | Substituted alkenes  | Pd nanoparticles,<br>Pd-PEG2000, Pd/PS· Ni-K10<br>10% Pd/C with 0.01 eq. Ph <sub>2</sub> S;<br>Pd(II)-schiff base complex<br>PSDVB<br>Ni NPs, 10 wt% Pd/C, MTS-<br>BT-Ru, Pd/CR11 and CR20 | H <sub>2</sub> (1–10 atm)<br>NH <sub>2</sub> NH <sub>2</sub><br><i>i</i> PrOH<br>Hantzsch esters<br>NaBH <sub>4</sub> | H <sub>2</sub> O, THF, MeOH,<br>EtOH, <i>i</i> PrOH,<br>[BMMIM][PF <sub>6</sub> ],<br>RT-70°C | Tolerates other functional<br>groups (NO <sub>2</sub> , CN, Bn, and<br>Cl), recyclable catalyst,<br>selective hydrogenation-<br>no deprotection, or<br>full hydrogenation and<br>deprotection | 72–84        |
| 6  | Styrene, stilbene  | [Rh]@Ag, Pd/C, Pd@SiO <sub>2</sub><br>NACs, SiNA-Pd, Pd/BN,<br>Ru-g-C <sub>3</sub> N <sub>4</sub> , Cu/MOF, Pd/MOF   | H <sub>2</sub> (14 bar)<br>Al/H <sub>2</sub> O<br>NH <sub>2</sub> -NH <sub>2</sub>                                    | 1,2-diCl-ethane, 80°C,<br>24 h<br>RT-50°C, 10–24 h  | Nonleachable catalyst,<br>aqueous medium  | 54,<br>85–92 |
| 7  | Linoleic acid  | 5 wt% Pd/C   | H <sub>2</sub> (0.5–20 bar)   | <i>n</i> -Decane, 40–100°C  | Kinetic studies   | 93           |
| 8  | Oxosteroids  | Rh/TPPMS   | H <sub>2</sub> (20 bar)   | Toluene   | Selective for $\alpha$ -diastereomer,<br>recyclable catalyst  | 94           |
| 9  | Open-chain and<br>cyclic alkenes,<br>diphenylethylenes,<br>other derivatives<br>(OH, C=O, NH,<br>etc.) | Defect-laden h-BN (dh-BN)<br>Cu-Co bimetallic catalyst   | H <sub>2</sub> (1 atm)  | RT-240°C, MeOH, RT,<br>10–20 min  | Metal-free hydrogenation,<br>ball milling<br>(mechanochemical<br>activation)<br>Yields: 66%–97%   | 95, 96       |
| 10 | Soybean oil  | Bio-Pd-NPs   | H <sub>2</sub> (2 bar)  | <i>i</i> PrOH, 50–125°C, 3 h  | Recyclable catalyst   | 97           |

[Rh]@Ag-Rh(II) complex entrapped in a Ag matrix; AmP-MCF-amino functionalized mesocellular foam; MOF, metal-organic framework; MTS-BT-Ru-Ru complexes immobilized on tannin grafted micelle templated silica; NAC-nanoassembled microcapsules; PAA-polyacrylic acid; PEI-poly(ethylenimine); Pd/FFMPA-palladium nanoparticles on thiol-modified magnetic particles; Pd/PS-Pd nanoparticles in polystyrene; Pd-DEN-Pd nanoparticles encapsulated in dendrimers; Pd-PAMAM-SBA-15-Pd nanoparticles supported on polyamidoamine organic-inorganic hybrid dendrimers; Pd-PEI-Pd nanoparticles stabilized by alkylated polyethylenimine; PEG-polyethylene glycol; POCOP-1,3-bis((di-*tert*-butylphosphino)oxy)benzene; PSDVB-poly(styrene-divinylbenzene) copolymer with 6.5% crosslinking; Pt@hmc, Pt nanoparticles encapsulated in a hollow porous carbon shell; Rh/TPPMS-Rh(II) complex immobilized on amberlite linked to (3-sulfonatophenyl)(diphenyl)phosphine monosodium salt; Rh/TPPTS/LDH-Rh on trisodium salt of 3,3',3''-phosphanetriyl benzenesulfonic acid complexed with double-layered hydroxides; SBA-15-mesoporous silica; SiNA-Pd-silicon nanowire-Pd hybrid; BN-boron nitride; rGO-reduced graphene oxide.

Although [Table 1](#) summarizes the hydrogenation of the most common substrates, often with the goal of a catalyst development, there are several applications with more complicated substrates. For example, the hydrogenation of the unsaturated side chain of pyrazolidinones resulted in the saturation of the C=C bond as well as the hydrogenative ring opening of the pyrazole ring via the cleavage of the N–N bond ([Scheme 2a](#)).<sup>99</sup> The reaction occurred with retention of chirality on the two chiral carbons and was achieved by the in situ generated H<sub>2</sub> by the reaction of Al with H<sub>2</sub>O, while the also in situ formed Raney Ni catalyzed the process. The oxovinyl moiety of decahydroacridinediones can also be selectively hydrogenated with Ni–Al alloy in 1 M KOH/MeOH ([Scheme 2b](#)).<sup>100</sup> The products were obtained in good yields and exclusive *cis* selectivity. Although the reaction is not sensitive to the R groups and a variety of H, alkyl, aryl N-aryl groups can be applied, the R group appeared to be of utmost importance; when it was a carbocyclic aromatic system, the reaction did not proceed.

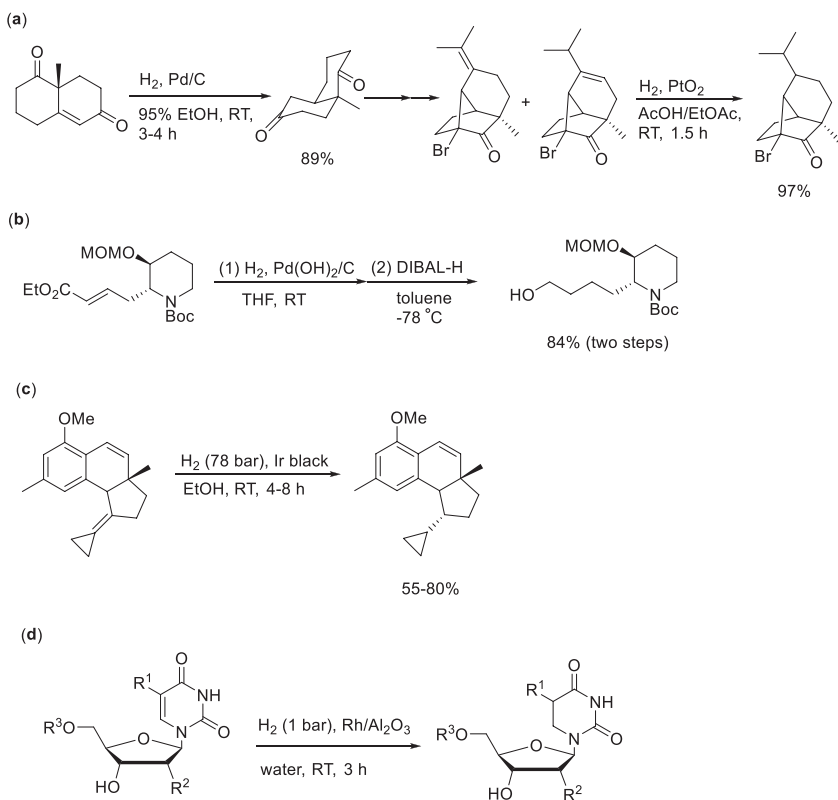


**SCHEME 2** Hydrogenation of pyrazolidinones and decahydroacridinediones over in situ-generated Raney Ni catalyst.

It is worth noting that the development of metal-free solid hydrogenation catalysts is also in progress. A metal-free heterogeneous catalytic hydrogenation of diethyl benzylidenemalonate has been accomplished by Willms et al. via the development of a semisolid frustrated Lewis pair (FLP). The catalyst was based on a solid polyamine organic framework and molecular tris(pentafluorophenyl) borane (BCF) that formed a semiimmobilized FLP in situ in the catalytic hydrogenation.<sup>101</sup>

Heterogeneous catalytic hydrogenation is often used as a tool to achieve the total synthesis of complex molecules, such as natural products. The total synthesis of the racemic sesquiterpenoid sativene was achieved by the application of two catalytic hydrogenation steps in the sequence of reactions, in both cases the C=C bond was hydrogenated to the saturated products ([Scheme 3a](#)).<sup>102</sup> A similar Pd(OH)<sub>2</sub>/C-catalyzed hydrogenation process was applied during the total synthesis of a new antimalarial compound based on febrifugine ([Scheme 3b](#)).<sup>103</sup> An interesting case of selective alkene hydrogenation was described by Taber and Tian. During the total synthesis of (–)-hamigeran B, an Ir black catalyst was applied to selectively hydrogenate a C=C bond connecting two rings, while the cyclohexene or cyclopropyl moieties remained intact under the

reaction conditions (Scheme 3c).<sup>104</sup> The synthesis of dihydronucleosides has been achieved by the catalytic hydrogenation of the corresponding nucleosides, nucleotide phosphates, and pyrimidine nucleotides. The 5,6-dihydrouridyl sugars and uridyl and thymidinyl nucleosides were obtained in high yields. Although cytidyl pyrimidines underwent hydrogenation, however, in addition to the reduction, a deamination reaction of the cytosine ring also occurred simultaneously (Scheme 3d).<sup>105</sup>



**SCHEME 3** Heterogeneous catalytic hydrogenation of C=C bonds during the total synthesis of sativene (a), and a febrifugine derivative (b), (–)-hamigeran B (c), and 5,6-dihydronucleosides (d).

Similar hydrogenations aiming for the full saturation of alkynes and dienes are also common. Representative examples are summarized in Table 2.

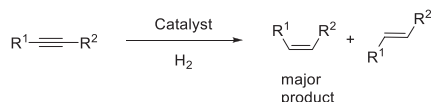
As presented in Table 2, a variety of metals and supports can be selected to complete this task. As the goal was to fully hydrogenate the C–C multiple bonds, these systems usually follow tendencies described under Table 1, in terms of experimental conditions and catalysts applied. The full hydrogenation, even in the case of more than one C–C multiple bonds cause negligible complications.

**TABLE 2** Heterogeneous catalytic hydrogenation of alkynes and dienes to their corresponding saturated products.

| Entry | Substrate scope                                   | Catalyst  | Hydrogen source   | Conditions   | Comments  | Ref.                        |
|-------|---|---|---|--|---|-----------------------------|
| 1     | Substituted alkynes                               | 10 wt% Pd/C with 0.01 eq. Ph <sub>2</sub> S, Pd/PS, Ni-K10 Pd/C, Pd/BN, Pd/CR11 and CR20, Pd NP/ nanoporous C | H <sub>2</sub> (1–5 bar)<br>NH <sub>2</sub> -NH <sub>2</sub><br>NaBH <sub>4</sub> | MeOH, THF, EtOH, <i>i</i> PrOH, RT-70°C                  | Selective hydrogenation— with and without deprotection, recyclable catalyst | 75, 77, 78, 82, 84, 88, 106 |
| 2     | Optically active conjugated dienes                | Raney Ni  | H <sub>2</sub> (1 bar)  | MeOH, EtOAc, hexane, RT                                  | 98% Pure stereoisomer after saturation                                      | 107                         |
| 3     | Diphenylacetylene                                 | [Rh]@Ag<br>1 wt% Pd/Al <sub>2</sub> O <sub>3</sub>  | H <sub>2</sub> (5–14 bar)   | 1,2-diCl-ethane, 80°C, 24 h                              | Nonleachable catalyst   | 85, 108                     |
| 4     | 2,4-Dimethyl-1,3-penta-diene                      | Pd(0)-cross linked polystyrene coated SiO <sub>2</sub>  | H <sub>2</sub> (20 bar)   | Supercritical CO <sub>2</sub> (scCO <sub>2</sub> ), 40°C | Selective to 2,4-dimethyl-2-pentene   | 68                          |
| 5     | 1,3-Butadiene                                     | Pd/Al <sub>2</sub> O <sub>3</sub>   | H <sub>2</sub> (1 bar)  | 50°C fixed-bed flow reactor                              | Performance improved with 80% θ- and 20% α-Al <sub>2</sub> O <sub>3</sub>   | 109                         |
| 6     | Substituted open-chain and cyclic dienes, alkynes | Cu-Co bimetallic catalyst   | H <sub>2</sub> (1 bar)  | MeOH, RT, 10–20 min                                      | Yields: 66%–97%   | 96                          |

BN, boron nitride; NP, nanoparticle; PS, polystyrene; [Rh]@Ag-Rh(II) complex entrapped in a Ag matrix.

The above discussed reactions (Tables 1 and 2) focused on the hydrogenation of alkenes and alkynes to fully saturated alkanes. However, the appropriate selection of the catalyst and reaction conditions allows the partial hydrogenation of alkynes (Scheme 4) to alkenes both in the laboratory and industrial setting.



**SCHEME 4** Partial hydrogenation of alkynes to alkenes.

The control of chemo- and stereoselectivity, however, requires fine tuning of the catalytic systems. Yields of the alkenes are affected by secondary transformations such as (*E*)-(*Z*) isomerization, shift of double bond and mostly, potential overreduction to alkanes. Earlier reports indicate that the (*E*)-(*Z*) selectivities could be controlled by the amount of added H<sub>2</sub>, essentially by adjusting the hydrogen pressure, although the partial hydrogenation of nonterminal alkynes yields the (*Z*)-product predominantly.<sup>110</sup> Despite the significant achievements in this field, the design of new catalysts is still in progress to improve reproducibility, chemo- and stereoselectivity, and recyclability of the catalyst. The data summarizing advances in the partial hydrogenation of alkynes is summarized in Table 3.

As Table 3 indicates, the heterogeneous catalytic hydrogenation of C≡C triple bond favors the formation of (*Z*)-alkenes as products, as expected based on the typical reaction mechanism that involves the *syn* addition of hydrogen. In the past decades, this reaction was typically carried out using the Lindlar catalyst. New advances focus on the design and preparation of greener catalysts including supported metals and nanoparticles. There are several examples, when the hydrogenation is highly chemoselective, for instance, using the Pd/boron nitride catalyst (Table 3, entry 7) the alkyne could be hydrogenated in high yields and selectivity in the presence of several functional (N<sub>3</sub>, NO<sub>2</sub>, C=O, etc.) or protecting groups (e.g., Cbz, benzyl).<sup>88</sup> Although most applications fulfill the criteria for being a green process, in certain cases dichloromethane was used as a solvent, which certainly should be avoided as much as possible.

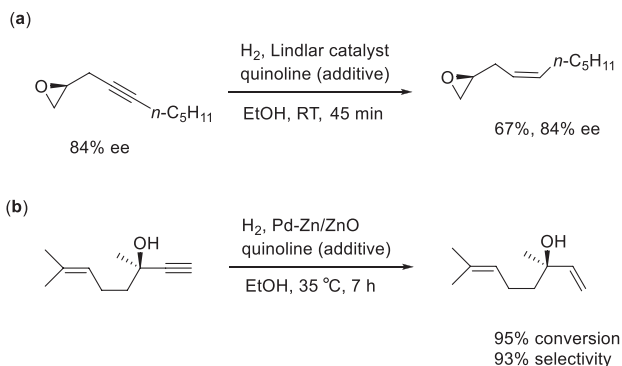
The earlier processes have often been applied during total synthesis procedures as tools to achieve the preparation of complex molecules. The Lindlar catalyst-driven partial hydrogenation of a C≡C bond to a *cis*-alkene has been carried out during the enantioconvergent asymmetric total synthesis of the antibiotic (*R*)-fridamycin E (Scheme 5a).<sup>129</sup> Although the yield was modest (67%) the enantioselectivity of the epoxide was retained at the same level it was before the reaction, and the protocol did not result in the ring opening of the epoxide either. A similar hydrogenation was accomplished for the synthesis of linalool from dehydrolinalool (Scheme 5b).<sup>130</sup>

**TABLE 3** Heterogeneous catalytic partial hydrogenation of alkynes to alkenes.

| Entry | Substrate  | Catalyst  | Hydrogen source   | Conditions  | Comments   | Ref.    |
|-------|--|---|---|---|--|---------|
| 1     | Various internal and terminal alkynes, and alkynyl ethers and alcohols | Pt-Pd, Ni NPs<br>Au@N-doped carbon/<br>TiO <sub>2</sub><br>PdCu <sub>4</sub> /SiO <sub>2</sub> , Pd-NPs,<br>Au > 99Ag1NPore | H <sub>2</sub> (1–6 atm), <i>i</i> PrOH<br>(transfer hydrogenation) | THF, MeCN,<br>EtOH or IPA,<br>4,4'-di- <i>tert</i> -butyl-<br>biphenyl as an<br>electron carrier,<br>30–100°C,<br>RT-20 h | Predominantly<br>( <i>Z</i> )-isomer, no<br>metal leaching<br>In situ formation<br>Ni(0) nanoparticles             | 111–116 |
| 2     | Propargylic sulfones   | Zn powder   | Zn-NH <sub>4</sub> Cl   | Sat. aq.-THF, RT  | Selectively<br><i>Z</i> -allylsulfones,<br>alkene and<br>benzyloxy groups<br>not affected                          | 117     |
| 3     | Acetylene  | Ni-Zn alloys on MgAl <sub>2</sub> O <sub>4</sub> ,<br>Pd <sub>4</sub> S, Ni/MCM-41<br>intermetallic Pd alloys               | H <sub>2</sub> (flow)   | 100–300°C<br>300 mL/min<br>C <sub>2</sub> H <sub>2</sub> + H <sub>2</sub> in<br>N <sub>2</sub> , RT                       | Selectivity<br>increases with<br>amount of Zn,<br>high selectivity for<br>the alkene even at<br>elevated pressures | 118–121 |
| 4     | Phenylacetylene  | Ru (II)-phosphine/<br>mesoporous silica   | H <sub>2</sub> (1 atm)  | IPA, H <sub>2</sub> (1 atm),<br>40°C  | Catalyst can be<br>reused with no<br>loss of activity/<br>selectivity  | 122     |

|   |  |   |  |   |  |   |
|---|--|---|--|---|--|---|
| 5 | Acetylene, phenylacetylene             | Au/Al <sub>2</sub> O <sub>3</sub> , Au-Ni/Al <sub>2</sub> O <sub>3</sub>                    | H <sub>2</sub> (flow)                    | Reactant passed through a fixed-bed reactor (00 – 300 h <sup>-1</sup> ) | Selectivity increased with decrease in Au particle size            | <a href="#">123</a>                       |
| 6 | 3-Butyn-2-ol and 2-methyl-3-butyn-2-ol | Pd/Fe <sub>3</sub> O <sub>4</sub><br>Pd-Zn-nanoalloys,<br>Pd/Al <sub>2</sub> O <sub>3</sub> | H <sub>2</sub> (4–6 bar)                 | Cyclohexane, 50–75°C  | 93%–100% selectivity for the alkene at 99% conversion              | <a href="#">124–126</a>                   |
| 7 | Substituted aryl/alkyl alkynes         | Pd/boron nitride  | H <sub>2</sub> (1 bar)                   | MeOH/pyridine. RT, 1–4 h  | 81%–99% yield, high selectivity, other functional groups tolerated | <a href="#">88</a>                        |
| 8 | Terminal alkynes                       | SGR/PANI/Ni<br>Colloid template PdAu<br>NPs   | H <sub>2</sub> (100 psi) and flow system | CH <sub>2</sub> Cl <sub>2</sub> , RT, 24 h                              | Yields: 74%–83% for alkene, 97% selectivity                        | <a href="#">127</a> , <a href="#">128</a> |

Au > 99Ag1NPore-unsupported nanoporous gold; NP, nanoparticle; PI-Pd incarnated in a phosphinated styrene-based polymer; SGR/PANI/Ni-Ni nanoparticles on polyaniline/graphene oxide composite.

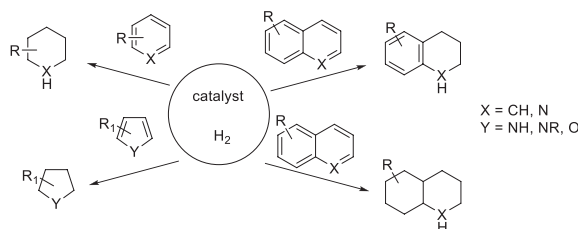


**SCHEME 5** Partial hydrogenation of the  $\text{C}\equiv\text{C}$  bond during the enantioconvergent asymmetric total synthesis of the antibiotic (*R*)-fridamycin E (A) and linalool (B).

Efforts have been made to accomplish the partial hydrogenation of dienes as well. The partial saturation of 1,3-butadiene has been achieved by using a non-noble metal intermetallic solid,  $\gamma\text{-Al}_4\text{Cu}_9(110)$ . The gas phase hydrogenation was carried out under relatively mild conditions, 2–20 bar hydrogen, at 110–180°C, with 100% selectivity to butenes.<sup>131</sup>  $\text{PtZn}/\text{SiO}_2$  catalyst can lead to nearly identical selectivity for butenes.<sup>132</sup> Similarly, silica-supported Rh-based ordered alloys ( $M = \text{Bi}, \text{Cu}, \text{Fe}, \text{Ga}, \text{In}, \text{Pb}, \text{Sn}, \text{and Zn}$ ) were found to be effective catalysts for selective hydrogenation of *trans*-1,4-hexadiene to *trans*-2-hexene.<sup>133</sup>

### 3.1.3 Hydrogenation of aromatic and heteroaromatic compounds

Saturated and partially saturated carbocyclic or heterocyclic scaffolds are important building blocks in pharmaceutical and fine chemical industries, often serve as solvents, even can fulfill the role of a catalyst. Given their otherwise often tedious synthesis, the hydrogenation of aromatic and heteroaromatic compounds is considered a convenient and environmentally friendly approach for their preparation (Scheme 6). In most cases heterogeneous catalytic hydrogenation provides the dearomatized products in good yields. However, the stability of the aromatic system is high and it is difficult to disrupt it, once it occurred the hydrogenation commonly yields the fully saturated rings. Table 4 summarizes the results achieved in the hydrogenation of carbocyclic compounds.



**SCHEME 6** Hydrogenation of aromatic compounds.

**TABLE 4** Heterogeneous catalytic hydrogenation of carbocyclic aromatic compounds.

| Entry | Substrate                                     | Catalyst   | Hydrogen source                                   | Conditions  | Comments  | Ref.     |
|-------|---|--|---|---|---|----------|
| 1     | Benzene                                       | Ru NPs <sup>a</sup> /montmorillonite by ionic liquid<br>Ru NPs in carbon<br>Ru NPs/C   | H <sub>2</sub> (8 MPa)                            | 100–110°C,<br>0.8–2.5 h   | Stable catalyst, yields up to 100%  | 134–136  |
| 2     | Substituted benzenes                          | Ru NPs stabilized by cyclodextrins Rh complex-Pd NPs/SiO <sub>2</sub> )<br>10 wt% Rh/C<br>Pd/Carbon nanofibers, Pd/C   | H <sub>2</sub> (1–30 bar)                         | 20–85°C,<br><i>n</i> -pentane, H <sub>2</sub> O,<br><i>i</i> PrOH, 2–24 h | Excellent conversions, aqueous medium, mild conditions, <i>cis</i> -selectivity up to 98%, recyclable catalysts | 137–142  |
| 3     | Substituted benzenes, naphthalene, anthracene | tetrahedral Rh NPs/charcoal Fe <sub>2</sub> (MoO <sub>4</sub> ) <sub>3</sub>   | H <sub>2</sub> (1 atm)<br>HCOOH                   | MeOH, H <sub>2</sub> O, RT  | conversions up to 100%  | 143, 144 |
| 4     | Aromatic carboxylic acids                     | Pd/carbon nanofiber  | H <sub>2</sub> (15 bar)                           | H <sub>2</sub> O, 24 h, 85°C  | No protecting group required for COOH   | 145      |
| 5     | Substituted phenols                           | Ru/Al <sub>2</sub> O <sub>3</sub><br>10% Pd/C<br>5% Rh/C-nanofiber<br>Pd/hydrophilic C<br>5 wt% Pd/C-AlCl <sub>3</sub><br>In situ Raney Ni,<br>NiCo/SiO <sub>2</sub> -TiO <sub>2</sub> | H <sub>2</sub> (10–40 bar)<br>Al-H <sub>2</sub> O | THF, scCO <sub>2</sub> (140 bar)<br>40–140°C,<br>0.5–20 h                 | Major product: <i>cis</i> -isomer, up to 100 conversion, >95% selectivity                                       | 146–152  |

*Continued*

**TABLE 4** Heterogeneous catalytic hydrogenation of carbocyclic aromatic compounds— cont'd

| Entry | Substrate                                   | Catalyst  | Hydrogen source                                  | Conditions                      | Comments  | Ref.     |
|-------|---|---|--|---------------------------------|---|----------|
| 6     | <i>t</i> Bu-benzene, benzoic acid, biphenyl | Rh NPs/C shell  | H <sub>2</sub> (0.5 MPa)                         | H <sub>2</sub> O, 2–14 h, 80°C  | Excellent conversions   | 153      |
| 7     | Binaphthyls                                 | Ru NPs/carbon nanofibers<br>PtO <sub>2</sub><br>Pd/C<br>In situ prepared Raney Ni | H <sub>2</sub> (1–50 atm)<br>Al-H <sub>2</sub> O | EtOH, AcOH,<br>3–48 h, RT-100°C | No racemization, high yields, partial hydrogenation to optically pure tetra and octahydro-1,1'-binaphthyls, multigram synthesis | 154–158  |
| 8     | Biphenyl                                    | Raney Ni prepared from Ni-Al alloy<br>in situ prepared Raney Ni                   | H <sub>2</sub> (10 bar)<br>Al-H <sub>2</sub> O   | THF, 4 h,<br>70–90°C            | Up to 100% conversion and 99.4% selectivity to cyclohexylbenzene  | 159, 160 |

NP, nanoparticles.

The examples outlined in Table 4 describe relatively simple carbocyclic aromatic compounds, including benzene and naphthalene derivatives. Several of these examples serve as test reactions during the development of new catalysts. More complex structures with typically primary interest in synthesis have also been studied. However, due to the high stability of the aromatic rings, to achieve these hydrogenations selectively in the presence of other functional group often cause complications. Accordingly, these applications use metals that are known to be powerful hydrogenation catalysts, such as Pt, Rh, Ru, although there are examples with Pd or Ni as the catalytic metal. Highly active nanoparticle-based catalysts dominate these examples, although the traditional supported catalysts or cyclodextrin stabilized samples are also listed. The source of hydrogen is usually hydrogen gas under various pressures. Other sources such as water-Al combination for in situ generation of H<sub>2</sub> or hydrogen donors, e.g. formic acid have also been used. Provided the high stabilization energy of the aromatic electron structure, in addition to the use of powerful metals, usually these hydrogenations require higher activation energy, namely elevated reaction temperatures. Although certain conditions allow the use of ambient temperatures, mostly these reactions occur at 50–150°C temperatures. Accordingly, when aromatic compounds possess side chains with C=C or C≡C bonds the complete hydrogenation of the compound will occur.

Aromatic heterocycles such as pyrroles, pyridines, indoles, quinolones, and their substituted derivatives are important building blocks for the synthesis of a large number of natural products and compounds that possess biological activity.<sup>161–163</sup> Due to their synthetic importance the transformations, such as partial or complete hydrogenation, of these rings are of exceptional interest in the pharmaceutical and fine chemical industries. At the same time, the hydrogenation of heterocycles present significant challenges, due to many factors, such as their low activity and catalyst poison character (e.g., pyridine, quinolines, etc.) or their high sensitivity and tendency for polymerization (indoles or pyrroles). Accordingly, there is an extensive number of reports available regarding these compounds, many of them are synthetically highly relevant. The most representative examples are collected in Table 5.

As Table 5 indicates, the individual properties of the heterocyclic compounds will determine the reaction conditions. The traditional hydrogenation catalysts, whether in the supported, nanoparticle, polymer, or ionic liquid stabilized form, are still applicable for these hydrogenations; however, the temperature and hydrogen pressure are widely varied depending on the ring system and the heteroatom. Most reactions effectively occur at 60–80°C; however, some compounds undergo hydrogenation at ambient temperature, some others require 150°C to react. In addition to the common solvents, several of these reactions apply acetic acid as a solvent, which not only acts as a typical solvent, but via acid-base interaction it also can improve the solubility of, especially N-containing, heterocycles.

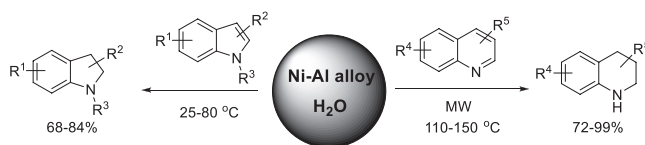
**TABLE 5** Heterogeneous catalytic hydrogenation of aromatic heterocycles.

| Entry | Substrate                                  | Catalyst  | Hydrogen source                             | Conditions  | Comments   | Ref.     |
|-------|--|---|---|---|--|----------|
| 1     | Pyridines and 2-pentylfuran                | 10 wt% Rh/C   | H <sub>2</sub> (5 atm)                      | H <sub>2</sub> O, 80°C                            | Broad substrate scope, mild and neutral conditions   | 141      |
| 2     | Substituted pyrroles                       | Rh/Al <sub>2</sub> O <sub>3</sub><br>Pt NPs/mesoporous SiO <sub>2</sub> | H <sub>2</sub> (10 atm);<br>400 Torr (flow) | EtOH or MeOH,<br>RT-140°C                         | Excellent <i>de</i> (up to 4 new stereocenters) hydrogenation followed by ring opening to butyl amine                | 164, 165 |
| 3     | Pyridinol                                  | Rh NPs/porous carbon shell  | H <sub>2</sub> (5 bar)                      | H <sub>2</sub> O, 2–14 h,<br>80°C                 | Excellent conversions, aqueous medium  | 153      |
| 4     | Substituted furfurals                      | PtSn, Co@N-doped graphene shell catalyst                                | H <sub>2</sub> (10 bar)                     | <i>i</i> PrOH, 100°C                              | 98% Selectivity to furfuryl alcohol, cat. Deactivation (25%) upon reuse; dimethyl furane, 100% conv. 95% selectivity | 166, 167 |
| 5     | Chiral furan-2-carboxylic acid derivatives | Pd(OH) <sub>2</sub> /C  | H <sub>2</sub> (30 bar)                     | AcOH- <i>i</i> PrOH,<br>25°C                      | <i>de</i> up to 95% upon addition of additive  | 168      |
| 6     | 4-Pyridine-carboxamides                    | 10 wt% Pd/C   | H <sub>2</sub> (1 atm)                      | ClCH <sub>2</sub> CHCl <sub>2</sub> ,<br>MeOH, RT | up to 99% yields   | 169      |

|    |                       |  |   |                               |   |   |
|----|-----------------------|--|---|-------------------------------|---|---|
| 7  | Cinchonidine          | Pt NPs stabilized by polyacrylic acid<br>Pt/Al <sub>2</sub> O <sub>3</sub> | H <sub>2</sub> (2–10 bar)                         | Toluene or AcOH,<br>25°C      | Selective hydrogenation to hexahydro-cinchonidine               | <a href="#">170</a> , <a href="#">171</a> |
| 8  | Substituted pyridines | Pd/C, Pt/C, Rh/C,<br>Pd(OH) <sub>2</sub> /C<br>In situ prepared Raney Ni   | H <sub>2</sub> (30–90 bar)<br>Al-H <sub>2</sub> O | flow reactor,<br>AcOH 60–80°C | excellent conversions,<br>easy scale-up                         | <a href="#">172</a> , <a href="#">173</a> |
| 9  | Heteroaromatics       | 10 wt% Rh/C  | H <sub>2</sub> (5 atm)                            | <i>i</i> PrOH, 60°C           | 100% Selectivity and<br>>95% conversion,<br>recyclable catalyst | <a href="#">141</a>                       |
| 10 | Bipyridines           | In situ prepared Raney Ni  | Al-H <sub>2</sub> O                               | Water, KOH<br>solution        | Piperidinyipyridines<br>3-N ring favored                        | <a href="#">174</a>                       |
| 11 | Benzofurans           | Ru@SILP-LA   | H <sub>2</sub> (10 bar)                           | Decalin, 150 °C               | Dihydrobenzofurans  | <a href="#">175</a>                       |

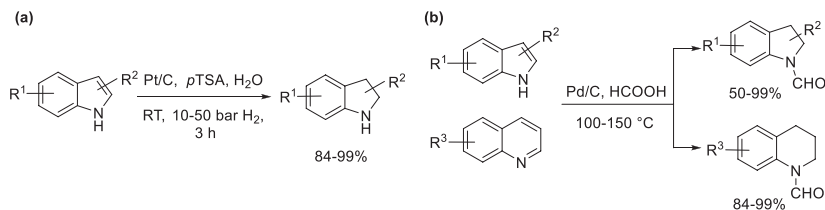
NP, nanoparticles; Ru@SILP-LA, ruthenium nanoparticles immobilized on a Lewis acid-functionalized supported ionic liquid phase.

The heterogeneous catalytic hydrogenation of pyrroles, indoles, or quinolines is often not selective due to overhydrogenation or other side reactions. The reduction of unprotected indoles and quinolines to indolines and tetrahydroquinolines could be achieved by applying Ni-Al alloy in water as a hydrogen source (Scheme 7) with good to excellent yields.<sup>176</sup> To occur efficiently, the alloy required a short ultrasonic pretreatment to remove the blocking Al<sub>2</sub>O<sub>3</sub> layer from the Al surface.<sup>177, 178</sup> A similar hydrogenation of the N-containing ring was achieved on Ni-based bimetallic catalysts in the presence of formic acid as a hydrogen source. Under hydrogen-free conditions ring opening and hydrodenitrogenation were found to be the preferred pathway.<sup>179</sup>



**SCHEME 7** Hydrogenation of indoles and quinolines with Ni-Al alloy in water.

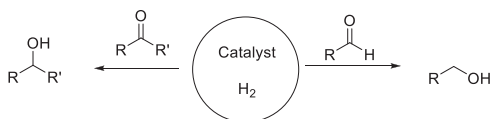
Indoles were also selectively hydrogenated on their N-containing ring in water by the aid of *p*-toluenesulfonic acid using a commercially available Pt/C catalyst.<sup>180</sup> The reaction was based on the partial protonation of the heterocyclic ring that destabilized the aromatic structure making the ring susceptible for hydrogenation even under the mild conditions (Scheme 8a). The products were isolated by nearly quantitative yields. A similar process was applied for the transfer hydrogenation of unprotected indoles and quinolines using Pd/C catalyst and formic acid.<sup>181</sup> Formic acid had a dual role, it served as a hydrogen donor as well as an acid to disrupt the aromaticity of the heterocycles making them more reactive in the reaction. After the hydrogenation of the heteroatom-containing ring, the N underwent formylation as well (Scheme 8b).



**SCHEME 8** Pt/C and Pd/C-catalyzed hydrogenation of unprotected indoles using *p*-toluenesulfonic acid as modifier (A) and formic acid as modifier and hydrogen donor (B).

### 3.1.4 Reduction of carbonyl compounds by heterogeneous catalytic hydrogenation: Aldehydes, ketones, and carboxylic acid derivatives

The hydrogenation of the C=O bond is one of the most commonly applied functional group transformations in organic synthesis (Scheme 9). The most common catalysts for this purpose are Pt, Ru, and Rh. Although Pd is broadly applied for C–C double and triple bond reductions, it does not appear to be a practical catalyst here. A more economical alternative is using Ni catalysts that are also often employed for the hydrogenation of aldehydes and ketones, albeit these reactions require somewhat harsher conditions than those catalyzed by noble metals.



**SCHEME 9** Hydrogenation of aldehydes and ketones to primary and secondary alcohols.

Table 6 presents representative examples for the reduction of carbonyl compounds focusing on nonasymmetric applications.

As presented in Table 6 in addition to the above-mentioned typical C=O hydrogenation catalysts, efforts have been made to apply the generally less active Pd catalysts mostly doped with another metal, such as gold. Supported Au itself appears to be active for the reduction of aldehydes even at ambient temperatures. Other catalysts of interest include metal complexes immobilized on various supports, often mesoporous silicates. Although some of the reactions were carried out at room temperature, the reaction temperatures are generally in the 80–90°C range; in rare cases it is as high as 400°C. The hydrogen source of the reactions is H<sub>2</sub> gas; however, several reactions use alternative sources, e.g., water–Al system, or hydrogen donors (*i*PrOH, formate derivatives, etc.) via transfer hydrogenation.

Although the data in Table 6 are mostly related to the carbonyl to hydroxyl reduction, several studies attempted to selectively achieve the C=O to CH<sub>2</sub> transformation. Essentially these hydrogenations function as the environmentally benign versions of the Clemmensen or Wolff-Kishner/Huang-Minlon reductions.<sup>200–202</sup> The hydrogen and Raney Ni catalysts that formed in situ from Ni–Al alloy and water hydrogenated benzaldehyde primarily to toluene although the ratio of benzyl alcohol and/or the desired toluene was dependent on the reaction time used (Scheme 10a).<sup>203</sup> Longer reaction times favored the formation of toluene in good yield. The process could be extended to a much broader scope, including substituted benzaldehydes and acetophenones. The same group

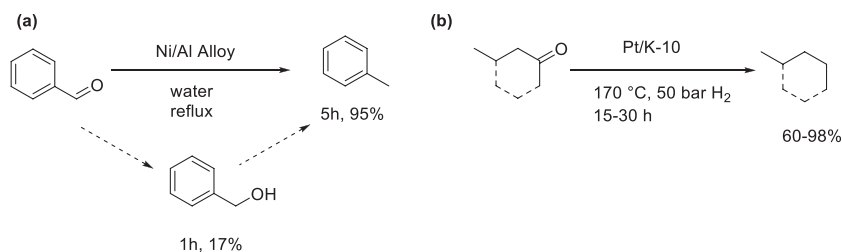
**TABLE 6** Heterogeneous catalytic hydrogenation of aldehydes and ketones.

| Entry | Substrate                                    | Catalyst   | Hydrogen source   | Conditions   | Comments   | Ref.             |
|-------|--|--|---|--|--|------------------|
| 1     | Substituted acetophenones                    | Pd/ZnO/ZnAl <sub>2</sub> O <sub>4</sub><br>Ni-Al alloy<br>Pd/C<br>Pt/CeO <sub>2</sub> -MO <sub>x</sub> (M = Si, Ti, Al, Zr)  | H <sub>2</sub> (9 bar)<br>Al/H <sub>2</sub> O<br>H <sub>2</sub> (5% in N <sub>2</sub> , flow) | <i>n</i> -Hexane, H <sub>2</sub> O, 25–400°C   | Moderate to high selectivity, mild heating required, high hydrostatic pressure, vapor phase reaction                           | 182–184          |
| 2     | Substituted benzaldehyde                     | Pd-Au/C<br>Pt/FDU-14<br>Co/ $\gamma$ -Al <sub>2</sub> O <sub>3</sub> -SiO <sub>2</sub><br>Pd/C   | H <sub>2</sub> (1–40 atm)   | EtOH, H <sub>2</sub> O, 20–130°C, batch and flow systems, electrocatalytic reduction | S poisoning, activity improved by Au addition, no activity/selectivity loss after 9 cycles; conversion 98%, selectivity: 95%   | 185–188          |
| 3     | Aromatic and aliphatic aldehydes and ketones | Ru-Sn-B/SiO <sub>2</sub><br>[Ru(salen)(NO)] encapsulated in mesoporous SBA-16<br>Ni NPs<br>In situ Raney Ni, Cu <sub>7</sub> Pt <sub>3</sub> -rGO, Au > 99Ag1NPore | H <sub>2</sub> (1–20 atm)<br><i>i</i> PrOH<br>Al-H <sub>2</sub> O                             | THF, <i>i</i> PrOH, H <sub>2</sub> O, RT-100°C; 0.5–1 h                              | Sn addition improved activity<br>Activity close to homogeneous systems<br>Conversion; selectivity >99%<br>Recyclable catalysts | 57, 116, 189–192 |
| 4     | Substituted diketones                        | Ru(Phen) <sub>2</sub> Cl-NH-MCM-41   | H <sub>2</sub> (20 bar)   | H <sub>2</sub> O, <i>t</i> -BuOK, 120°C  | Selectivity of ketol $\geq$ 95%  | 193              |

|   |                              |                                      |  |   |   |   |
|---|------------------------------|--------------------------------------|--|---|---|---|
| 5 | Substituted ketones          | Pd/urea-MCF<br>Silica-SMAP-Rh        | HCOOH/TEA<br>(1:1)                     | EtOAc, hexane 25°C                              | High yields, recyclable catalyst                              | <a href="#">194</a> , <a href="#">195</a> |
| 6 | 5-Ethoxy-methyl-<br>furfural | Ir/Cr-Al <sub>2</sub> O <sub>3</sub> | H <sub>2</sub> (25 N mL/<br>min, flow) | 400 μmL/min feed<br>(1 wt% substrate)           | Up to 99% selectivity toward<br>alcohol                       | <a href="#">196</a>                       |
| 7 | Substituted aldehydes        | Au/meso-CeO <sub>2</sub>             | HCOOK<br>(5 eq.)                       | H <sub>2</sub> O, 25°C                          | Tolerates alkenes, halogens,<br>ketones                       | <a href="#">197</a>                       |
| 8 | Me-levulinate                | Zr-based mesoporous<br>materials     | H <sub>2</sub> (30 bar)                | 200°C, flow system                              | Conversion: 15%–89%, selectivity<br>(valerolactone): 76%–100% | <a href="#">198</a>                       |
| 9 | Butanal                      | Shvo's catalyst on SiO <sub>2</sub>  | H <sub>2</sub> (flow<br>system, 1 bar) | Flow rate at 100 cm <sup>3</sup> /<br>min, 90°C | Mechanistic study   | <a href="#">199</a>                       |

Au > 99Ag1NPore-unsupported nanoporous gold; Pd/urea-MCF-Pd nanoparticles supported on siliceous mesocellular foam; rGO, graphene oxide; Ru(Phen)<sub>2</sub>Cl-NH-MCM-41-Ru(Phen)<sub>2</sub>Cl<sub>2</sub> [Phen = phenanthroline] anchored in organo-functionalized MCM-4; Silica-SMAP-Rh, silica immobilized caged, compact, trialkylphosphine Rh.

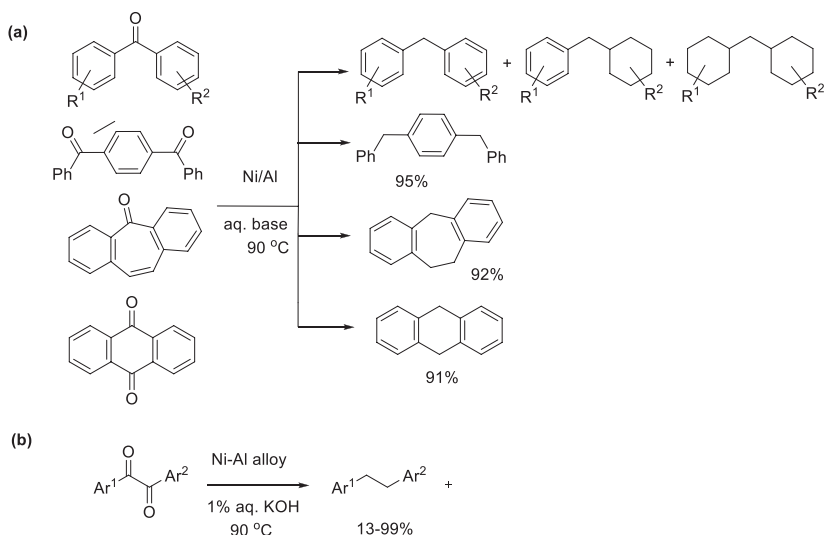
extended these applications to microwave-assisted catalysis that appeared to be more selective and higher yielding than the conventional process.<sup>204</sup> A similar application used a bifunctional, K-10 montmorillonite-supported Pt catalyst in a multistep sequence.<sup>205</sup> First, the platinum reduced the carbonyl compound to the corresponding alcohol, which underwent an acid (K-10)-catalyzed dehydration to produce an alkene intermediate. Then, the alkene immediately underwent a platinum-catalyzed C=C bond hydrogenation. The alkanes were obtained in good to excellent yields (Scheme 10b).



**SCHEME 10** Selective C=O to CH<sub>2</sub> hydrogenation of benzaldehyde and acetophenones with Ni-Al alloy in water (a) and of various aliphatic ketones on Pt/K-10 catalyst (b).

The earlier Ni-Al process was extended to the C=O to CH<sub>2</sub> transition of benzophenones, cyclic and open included, using the alloy in a dilute alkaline solution. In addition to the expected diphenylmethanes, benzylcyclohexanes and the fully hydrogenated dicyclohexylmethanes also formed (Scheme 11a).<sup>206</sup> Cyclic substrates, such as anthraquinone, benzoylnaphthalenes, benzoylanthracene, dibenzosuberone, and dibenzosuberone can also be hydrogenated to the corresponding hydrocarbons in good to excellent yields. The same catalytic system was also applied for the C=O to CH<sub>2</sub> reduction of alkylbenzils and alkoxybenzils to yield the corresponding 1,2-diarylethanes at 90°C (Scheme 11b).<sup>207</sup> When 4,4'-dinitrobenzil was used as a substrate, the NO<sub>2</sub> groups also underwent hydrogenation to NH<sub>2</sub> yielding 1,2-bis(4-aminophenyl)-ethane. The method was greatly time dependent and the aromatic rings also underwent hydrogenation if enough time was allowed.

While the reduction of aldehydes and ketones by hydrogenation is a relatively straightforward reaction, the catalytic hydrogenation of carboxylic acids and esters is a notoriously difficult task. Other than accomplishing this transformation by using complex hydrides these reductions by hydrogenation still pose significant challenges, in terms of conversion and selectivity. One of the rare examples is the hydrogenation of methyl formate over a Co/MgO heterogeneous catalyst mainly to chain-lengthened hydrocarbons. The reaction provided time-dependent product spectra, ranging from methanol, olefins, to C<sub>2</sub> + hydrocarbons.<sup>208</sup> The catalytic hydrogenation of oleic acid on Rh-Sn-B/γ-Al<sub>2</sub>O<sub>3</sub>



**SCHEME 11** C=O to CH<sub>2</sub> reduction of acetophenone and cyclic arylketones (A) and alkylbenzyls (B).

catalysts yielded oleyl alcohol with high selectivity with the appropriate selection of the Rh/Sn ratio (1%/4%). In contrast, at low Sn content, the catalyst favored complete deoxygenation and the formation of the fully hydrogenated octadecane.<sup>209</sup> The hydrogenation of succinic acid, a biorenewable feedstock, can be achieved by a hydrogenation on a RePd/C catalyst at 140–200°C under 95–175 bar hydrogen pressure. Although the hydrogenation occurred with high conversion values it provided a product mixture containing several value-added chemicals such as 1,4-butanediol,  $\gamma$ -butyrolactone, and tetrahydrofuran.<sup>210</sup> In a related study,  $\gamma$ -valerolactone was produced from biomass-derived levulinic acid esters on support-free mesoporous Ni catalyst.<sup>211</sup> Similarly, the hydrogenative transformation of sugars, such as glucose to furan-based chemicals also attracted attention.<sup>212, 213</sup>

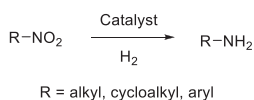
The reduction of CO<sub>2</sub> is also a highly important and active research area. Due to the increasing CO<sub>2</sub> levels in the atmosphere, in addition to the natural sequestration there are extensive efforts to develop chemical means to mitigate the CO<sub>2</sub> level. Although the catalytic reduction of CO<sub>2</sub> (and CO as well) is dominated by homogeneous catalytic approaches, there are several heterogeneous catalytic protocols that appear to be successful at the laboratory level.<sup>214–233</sup>

In addition to the earlier applications there is significant interest in the enantioselective C=O hydrogenation of  $\alpha$ -ketoesters,<sup>234–243</sup>  $\beta$ -ketoesters,<sup>244–247</sup> and other activated carbonyl compounds.<sup>248–253</sup> However, as a special chapter is devoted to enantioselective heterogeneous catalysis, these applications will be discussed in Chapter 3.10.

### 3.1.5 Hydrogenation of nitro-containing groups: N=O, N=N, C=N, and C≡N groups

#### 3.1.5.1 Hydrogenation of the nitro group

Amines and their derivatives are key building blocks and intermediates in a multitude of industries, such as the dye, pharmaceutical, fine chemicals, or materials industries. Aromatic amines are commonly produced via the nitration of aromatic compounds and the subsequent reduction of the nitro group (Scheme 12).



**SCHEME 12** Hydrogenation of the nitro group to amino functionality.

The nitro to amino reduction can be achieved by a plethora of methods<sup>254, 255</sup>; however, the heterogeneous catalytic hydrogenation of the NO<sub>2</sub> group to NH<sub>2</sub> is the environmentally most benign protocol as most of the other methods apply stoichiometric reagents and produce significant amount of waste. In contrast, catalytic hydrogenation has a nearly 100% atom economy, and the only by-product is water. A large number and variety of catalytic systems are available for this transformation; however, the selective reduction of the nitro group still represents a challenge when other reducible functionalities (e.g., C=C, C≡C, halogen, C=O, etc.) are present. First, the recent advances in the hydrogenation of nitrobenzenes to anilines are summarized in Table 7.

Due to the relatively easy and straightforward access to aromatic nitro compounds via electrophilic nitrations, the reduction of these compounds is a major pathway to obtain aromatic amines. In addition, aniline derivatives play a major role in many industries as a frequent building block. The selection of metals for the NO<sub>2</sub> to NH<sub>2</sub> reduction is quite broad; many transition metals are capable to catalyze this process. Most notably, the traditional hydrogenation catalysts, such as Pd, Pt, Rh, Ru, Ir, and Ni, represent the core group of the applicable metals; however, several new applications are focused on metals (Au, Ag, Co) that are less commonly used in hydrogenations. Similarly to the earlier applications, a widespread use of nanoparticles can be found. In most applications the metal is used in a supported format using a broad variety of support materials from traditional ones such as SiO<sub>2</sub>, Al<sub>2</sub>O<sub>3</sub>, or C but also newly developed, often emerging materials, e.g., graphene, carbon nitrides, mixed oxides, or nanofibers. The reaction conditions are also widely different and dependent on the metal. Low to high pressure hydrogen gas is often replaced by transfer hydrogenation conditions using isopropanol or hydrazine as a hydrogen source. The temperature also ranges from ambient temperature to 160°C. New trends include the generation of specialty catalysts by using advanced materials, such as graphene oxide,

**TABLE 7** Heterogeneous catalytic hydrogenation of nitrobenzenes to the corresponding anilines.

| Entry | Substrate                 | Catalyst  | Hydrogen Source   | Conditions   | Comments  | Ref.  |
|-------|---------------------------|---|---|--|---|---|
| 1     | Substituted nitrobenzenes | Au/TiO <sub>2</sub> , Au/Fe <sub>2</sub> O <sub>3</sub><br>Pt/CNT <sup>a</sup> , and Mn, Fe, Co, Ni, Cu modified samples, $\gamma$ -Fe <sub>2</sub> O <sub>3</sub> <sup>b</sup> , Pt/TiO <sub>2</sub> , Ni/TiO <sub>2</sub> , Ru/TiO <sub>2</sub> , Au/TiO <sub>2</sub> , Pt/C nanofibers <sup>b</sup> , Pd NPs <sup>b,c</sup> , Ni/C nanofibers, Au/Pt NPs, Ni/ $\gamma$ -Al <sub>2</sub> O <sub>3</sub><br>Pt/polysiloxane gel, Ag/Al <sub>2</sub> O <sub>3</sub> , in situ formed Raney Ni, WO <sub>2.72</sub> , Pd@SiO <sub>2</sub> NACs, SiNA-Pd, Cu <sub>7</sub> Pt <sub>3</sub> -rGO, ImmFe-IL, Ru-g-C <sub>3</sub> N <sub>4</sub> , Co <sub>3</sub> O <sub>4</sub> @Al <sub>2</sub> O <sub>3</sub> /SiO <sub>2</sub> , UiO-66-NH <sub>2</sub> @COP@Pd, N-doped-CNTs, Pd@Co/C-SiO <sub>2</sub> -NH <sub>2</sub> , Cu-SN/nanoplates, Pd/alginate-poly(ethyleneimine), Pd@P(QPTVP) | H <sub>2</sub><br>(3–40 bar)<br><i>i</i> PrOH<br>NH <sub>2</sub> -NH <sub>2</sub><br>Al-H <sub>2</sub> O/<br>NH <sub>4</sub> Cl,<br>NaBH <sub>4</sub> | EtOH, EtOH/<br>H <sub>2</sub> O, scCO <sub>2</sub><br>(12 MPa),<br>EtOAc, THF,<br>0.35–20 h,<br>RT-160°C<br>or flow<br>systems | Selective reduction of NO <sub>2</sub> in presence of C=C, C=O, C≡N, CONH <sub>2</sub> groups, excellent yields and selectivities (> 95%) | <a href="#">55</a> , <a href="#">57</a> ,<br><a href="#">86</a> , <a href="#">87</a> ,<br><a href="#">89</a> ,<br><a href="#">256–274</a> |
| 2     | 1,3-Dinitrobenzene        | Ni/K <sub>2</sub> O-La <sub>2</sub> O <sub>3</sub> -SiO <sub>2</sub>  | H <sub>2</sub> (30 bar)   | EtOH, 100°C  | Conversions/selectivity (up to 99.9%) to phenylenediamine, some cat. deactivation   | <a href="#">275</a>   |

*Continued*

**TABLE 7** Heterogeneous catalytic hydrogenation of nitrobenzenes to the corresponding anilines—cont'd

| Entry | Substrate           | Catalyst  | Hydrogen Source   | Conditions   | Comments   | Ref.                                      |
|-------|---------------------|---|---|--|--|---|
| 3     | Nitrobenzylamines   | 10 wt% Pd/C<br>In situ formed Raney Ni  | H <sub>2</sub> (1 atm)<br>Al-H <sub>2</sub> O/<br>formic acid | MeOH, aq.<br>HCl, RT,<br>13–88 min                                       | Highly chemoselective<br>(up to 99%) reduction,<br>no debenylation<br>Diformamide products | <a href="#">276</a> , <a href="#">277</a> |
| 4     | Chloronitrobenzenes | Ni/C nanofiber<br>Pt/ $\gamma$ -ZrP<br>Pt NPs/acidic attapulgite<br>Ru-V/MgF <sub>2</sub><br>Pd/ $\gamma$ -Fe <sub>2</sub> O <sub>3</sub> <sup>b</sup><br>Ni/TiO <sub>2</sub> | H <sub>2</sub><br>(1–40 bar)                                  | MeOH,<br>EtOH, scCO <sub>2</sub><br>(10 MPa),<br>10–300 min,<br>30–140°C | Conversion (up to<br>99%), selectivity (up to<br>95%), liquid and gas<br>phase reactions   | <a href="#">278–283</a>                   |

<sup>a</sup> Carbon nanotubes.

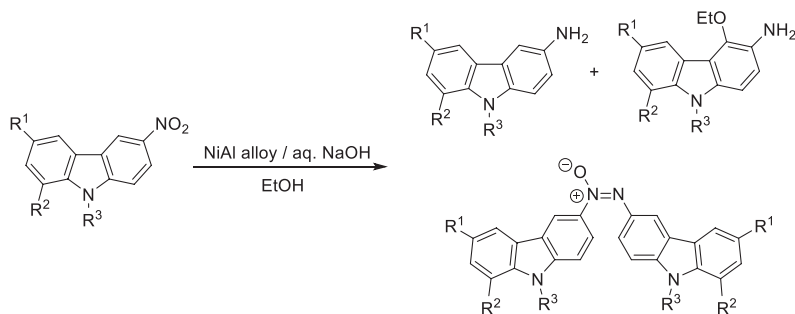
<sup>b</sup> Recyclable catalyst.

<sup>c</sup> Nanoparticles.

CNT, carbon nanotubes; ImmFe-IL, immobilized Iron-containing ionic liquids; NAC, nanoassembled microcapsules; P(QPTVP), phosphine-functionalized porous ionic polymer; SiNA-Pd, silicon nanowire-Pd.

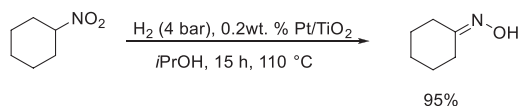
grafted with chitosan and Ag nanoparticles, that was tested in the hydrogenation of nitrobenzene to aniline.<sup>284</sup>

Larger aromatic nitro compounds have also been target of catalytic hydrogenation. The synthesis of 2-semidines has been achieved via the reductive dimerization of 3-nitrocarbazoles using Ni-Al alloy under slightly basic conditions.<sup>285</sup> The data showed that the direct NO<sub>2</sub> to NH<sub>2</sub> hydrogenation resulted in the minor product 3-aminocarbazoles (Scheme 13). The major product of this reaction was the azoxycarbazole (no yields provided), although using methanol as a solvent and Zn as reducing agent improved the 3-aminocarbazole selectivity.



**SCHEME 13** Hydrogenation of nitrocarbazoles on in situ formed Raney Ni catalyst.

While the hydrogenation of aromatic nitro compounds dominates the applications due to the relatively easy synthesis of these molecules, the hydrogenation of aliphatic derivatives also attracted significant interest to produce aliphatic amines. Serna et al. described the selective catalytic hydrogenation of nitro-cyclohexane to cyclohexanone oxime on decorated Pt nanoparticles on titania support. The catalyst had a low (0.2 wt%) platinum loading making it both environmentally better as well as more economic. The reactions occurred under moderately harsh conditions; low hydrogen pressure, but relatively high temperature and provided the cyclohexanone oxime in high yield (95%) and selectivities (Scheme 14).<sup>286</sup>

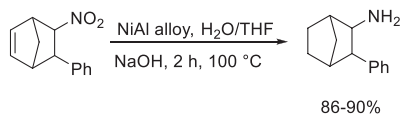


**SCHEME 14** Selective hydrogenation of nitro-cyclohexane to cyclohexanone oxime.

The hydrogenation of a bridged phenyl-nitro-cyclohexene using Ni-Al alloy in basic (dilute NaOH) water/THF mixture led to the perhydrogenated amine precursor for the synthesis of *N*-(3-phenylbicyclo[2.2.1]-yl)-*N*-ethylamine

112 Heterogeneous catalysis in sustainable synthesis

hydrochloride<sup>287</sup> also known as fencamfamine, a known stimulant and appetite suppressant. The method is a typical application of the dissolving aluminum method; the Al-water reaction provides the necessary hydrogen, while the dealuminated alloy becomes a highly active Raney Ni catalyst to facilitate the actual hydrogenation reaction. As common, the reaction leads to the perhydrogenated product (Scheme 15).



**SCHEME 15** Hydrogenation of a bridged nitro-phenylcyclohexene to the corresponding cyclohexyl amine.

### 3.1.5.2 Hydrogenation of nitriles

Similarly to the earlier examples, the hydrogenation of nitriles is the environmentally most benign method of choice to prepare aliphatic primary amines (Scheme 16).<sup>288</sup>



**SCHEME 16** Hydrogenation of nitriles to primary amines.

Given that the replacement of many leaving groups, such as halogens, tosylate, etc. with  $\text{CN}^-$  can be conveniently carried out by  $\text{S}_{\text{N}}2$  substitutions, this method has a broad versatility. Consequently, the substitution of these entities with  $\text{CN}^-$  and subsequent hydrogenation of the nitrile open up access to a nearly unlimited variety of aliphatic amines. The reduction occurs step by step, gradually progressing via a  $\text{C}=\text{N}$  double bond to a single bond. However, the reaction conditions must be designed carefully, as the slow reaction and the reasonable presence of the intermediate may initiate reactions with the final product primary amine resulting in undesirable by-products, including secondary or tertiary amines. Thus designing a chemoselective protocol for the hydrogenation of nitriles is still a challenge. The most common examples are listed in Table 8.

Unlike many of the earlier applications, for the hydrogenation of nitriles the use of Ni-based catalysts is favored, as the most common metal in these reactions. Co also appears to be a frequently applied metal, despite its overall limited use in hydrogenation of other functional groups. Another nonnoble metal, copper is also common in these hydrogenations, although often in the form of Co or Cr-doped forms. The traditional hydrogenation metals, such as Ru, Rh, Ir, Pt, or Pd are also represented, although with lower frequency than normal. Reactions carried out with hydrogen gas often require elevated pressures, although several other examples, e.g. using water-Al system for hydrogen

**TABLE 8** Heterogeneous catalytic reduction of nitriles to primary amines and other products.

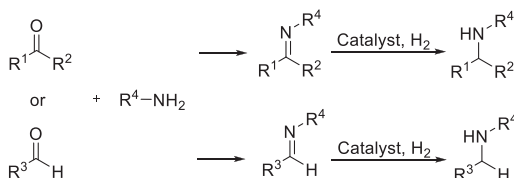
| Entry | Substrate               | Catalyst  | Hydrogen source                       | Conditions   | Comments  | Ref.                     |
|-------|-------------------------|---|---------------------------------------|--|---|--------------------------|
| 1     | Butyronitrile           | Ni-Cr promoted Raney Co or LiOH modified Raney Co   | H <sub>2</sub> (15–45 bar)            | Octane, 45–60 min, 100°C                           | LiOH modified Raney Co showed highest selectivity toward butylamine             | <a href="#">289</a>      |
| 2     | Propionitriles          | Ru/C, Cu/γ-Al <sub>2</sub> O <sub>3</sub>   | H <sub>2</sub> (100 bar)              | Organic solvent + ionic liquid, 100°C; flow system | Biphasic solvent system enhanced selectivity toward propylamine and derivatives | <a href="#">290, 291</a> |
| 3     | Benzonitriles           | Ru NPs, Ni NPs, Ni@mSiO <sub>2</sub> @LDO and LDH, Co-MOFs, Co(OAc) <sub>2</sub> /Al <sub>2</sub> O <sub>3</sub> , Cu/MgO, Pd NPs, Pd/SiC with NiO nanodots, Ir-Pd/Al <sub>2</sub> O <sub>3</sub> | H <sub>2</sub> (5–40 bar)             | 2–72 h, 85–110°C, water                            | Exclusive reduction of CN (no ring hydrogenation), up to 100% yield             | <a href="#">292–301</a>  |
| 4     | Biphenyl-4-carbonitrile | In situ formed Raney Ni   | Al-H <sub>2</sub> O                   | 1% aq. KOH   | Methylbiphenyl by-product (9%)  | <a href="#">160</a>      |
| 5     | Various nitriles        | In situ formed Raney Ni, CuFe <sub>2</sub> O <sub>4</sub>   | Al-aq. formic acid, NaBH <sub>4</sub> | RT–100°C   | Major product: aldehydes, amines  | <a href="#">302, 303</a> |
| 6     | Aliphatic nitriles      | Co(OAc) <sub>2</sub> /Al <sub>2</sub> O <sub>3</sub>  | H <sub>2</sub> (5–45 bar)             | 2–24 h, 85–130°C                                   | Primary amine products, 84%–99% yield   | <a href="#">296</a>      |
| 7     | Acetonitrile            | Pt on Al <sub>2</sub> O <sub>3</sub> , MgO, SiO <sub>2</sub> , CeO <sub>2</sub>   | H <sub>2</sub> (flow)                 | Flow system, 60°C                                  | Catalyst characterization, mechanistic studies                                  | <a href="#">304, 305</a> |

LDH, layered double hydroxide; LDO, layered double oxide; MOF, metal-organic framework; NPs, nanoparticles.

generation or typical transfer hydrogenations are also common. In addition to high hydrogen pressures, the temperatures applied in these reactions are also relatively high, commonly 85–130°C.

### 3.1.5.3 Hydrogenation of imines

As the preparation of imines from carbonyl compounds and primary amines is a common and rather readily occurring transformation, the hydrogenation of the product imines is a frequently applied method for the synthesis of secondary amines (Scheme 17). When the two steps are conducted without the isolation of the imine, the process is called reductive amination, which is a frequent protocol. Similarly to the earlier discussed nitrile reduction, this process may also yield undesirable by-products, such as tertiary amines.



**SCHEME 17** Generic pathways for the reductive amination of ketones and aldehydes.

The actual task is the hydrogenation of the C=N double bond. In contrast to the reduction of the C≡N triple bond of nitriles, this process occurs under much milder conditions. Some representative data for the hydrogenation of simple imines are tabulated in Table 9.

The comparison of the data in Tables 8 and 9 clearly supports the earlier observations. The most popular imine hydrogenation catalysts are based on Ni and Pd. Other metals (Pt, Rh, etc.) can also be applied; however, the more moderate activity of Ni and Pd ensures high chemoselectivity in imine hydrogenations, e.g., no aromatic ring saturation would occur. In addition, most of the reactions readily take place at moderate temperatures, commonly at room temperature. Similarly to temperature, the hydrogen pressures, when hydrogen gas is used as an H-source, are also moderate in these hydrogenations, often ranging from 1 bar to no higher than 20 bar. Overall, the C=N double hydrogenation is a fairly straightforward process that applies mild experimental conditions. Some of the applications in Table 9 belong to a specific type of the C=N hydrogenation, the so-called reductive amination, that is also a commonly used process in synthetic applications. The heterogeneous catalytic reductive amination of a broad variety of carbonyl compounds with aqueous ammonium hydroxide and various primary amines readily yielded primary (when NH<sub>3</sub> was used) and secondary amines. The process was catalyzed by an in situ formed Raney Ni catalyst that was obtained from Ni-Al alloy, while the hydrogen was generated by the dissolution of Al in water (Scheme 18).<sup>313</sup> The reaction occurred in

**TABLE 9** Catalytic hydrogenation of imines to their corresponding secondary amines.

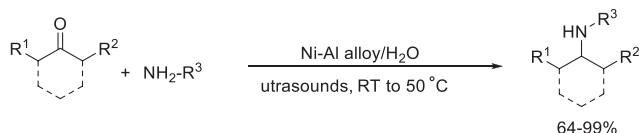
| Entry | Substrate                             | Catalyst  | Hydrogen Source  | Conditions   | Comments   | Ref.                     |
|-------|---------------------------------------|---|--|--|--|--------------------------|
| 1     | Substituted ketimines                 | Raney Ni, Pd/C, Pt/C                                | H <sub>2</sub> (120 psi)                                       | In situ generated imine, solvent, RT   | Reductive amination, high <i>de</i>  | <a href="#">306, 307</a> |
| 2     | Substituted aldimines                 | Pd/C<br>10 wt% Pd/C<br>Ni NPs <sup>a</sup>          | HCOONH <sub>4</sub><br>H <sub>2</sub> (1 atm)<br><i>i</i> PrOH | In situ generated imine<br><i>i</i> PrOH, MeOH, CHCl <sub>3</sub> , RT,<br>10–60 min | Reductive amination<br>(anilines or nitrobenzenes, yields up to 99%)       | <a href="#">308–310</a>  |
| 3     | Substituted benzylidene-anilines      | Polymer supported Pd-imidazole complex <sup>b</sup> | H <sub>2</sub> (0.8 bar)                                       | EtOH, H <sub>2</sub> , 30°C  | Cat. recycled up to 6 times without loss of activity, no leaching of metal | <a href="#">311</a>      |
| 4     | Benzylidene anilines and benzylamines | β-CD/Pd <sup>c</sup>                                | H <sub>2</sub> (20 bar)  | Aqueous solution, RT, 1 h  | Excellent yields   | <a href="#">312</a>      |

<sup>a</sup> Nanoparticles.

<sup>b</sup> Recyclable catalyst.

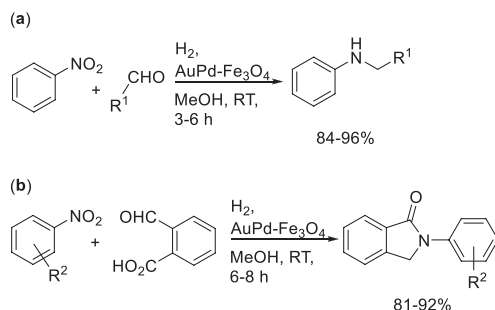
<sup>c</sup> β-cyclodextrin stabilized Pd nanoparticles.

two steps, the first step being the formation of the Schiff base, and the second was the hydrogenation of the imine intermediate. A similar reductive amination of benzylamines with aromatic and aliphatic amines was successfully carried out on graphene-supported NiPd alloy nanoparticles under mild condition. The product benzylidenebenzylamines were obtained in moderate to excellent yields (64%–99%).<sup>314</sup>



**SCHEME 18** Reductive amination of carbonyl compounds with  $\text{NH}_3$  and primary amines on an in situ formed Raney Ni catalyst.

The cascade nitro reduction-reductive amination have been successfully developed by Cho et al. using  $\text{AuPd/Fe}_3\text{O}_4$  nanoparticles.<sup>315</sup> Although it was a one-pot system containing the substituted nitrobenzenes with substituted benzaldehydes, the first step was the reduction of the  $\text{NO}_2$  group to  $\text{NH}_2$ , which underwent an immediate Schiff base formation with the aldehyde, and finally the imine was hydrogenated to secondary amine (Scheme 19a). Further application of the catalytic system led to the formation of heterocyclic products (Scheme 19b) via the  $\text{NO}_2$  to C-N-Ar reduction and subsequent ring closure of the intermediate, successfully combining four steps in a one-pot reaction.

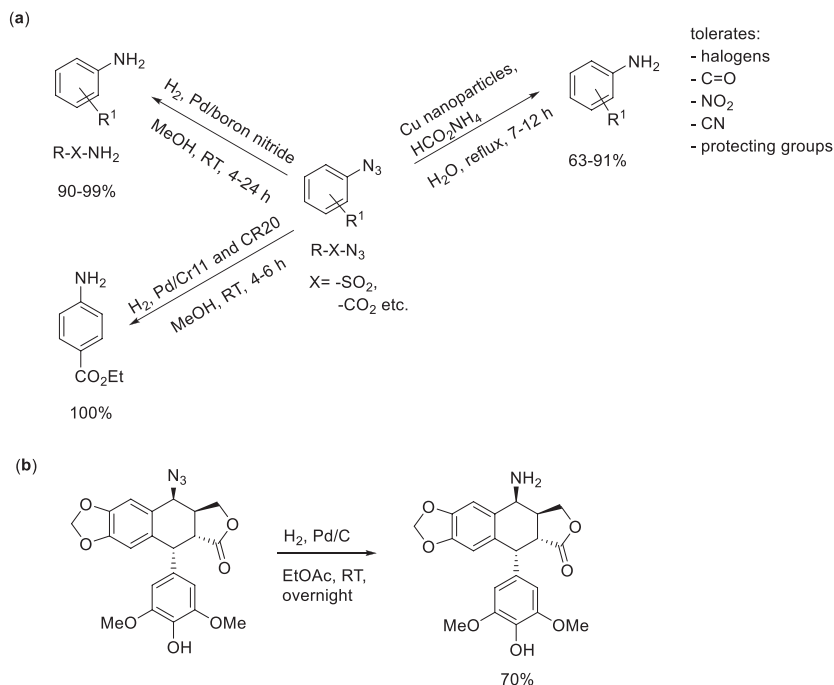


**SCHEME 19** One-pot cascade nitro reduction-reductive aminations by  $\text{AuPd-Fe}_3\text{O}_4$  catalyst.

In addition to the earlier applications there is significant interest in the di- and enantioselective hydrogenation of imines and enamines.<sup>316, 317</sup> However, as a special chapter is devoted to enantioselective heterogeneous catalysis, these applications will be discussed in detail in Chapter 3.10.

### 3.1.5.4 Hydrogenation of azides

Alkyl and aryl azides are important synthons for the preparation of a broad range of compounds from heterocycles to amines. The reduction of the azide group readily provides primary amines that also have widespread applicability in the synthesis of bioactive compounds, materials, or fine chemicals. Ahammed et al. applied copper nanoparticles for the transfer hydrogenation of aryl azides using ammonium formate as the hydrogen source in water (Scheme 20a). The reaction occurred under relatively mild conditions providing the products in moderate to good yields. Most importantly copper as a hydrogenation catalyst shows remarkable selectivity toward the reduction of the azides and several reduction sensitive groups, such as halogens, carbonyl, nitro, protecting groups (allyl, benzyl), or nitrile, are tolerated.<sup>318</sup> A similar, highly selective approach was described by using Pd/boron nitride<sup>88</sup> or resin-supported Pd (Pd/CR11 and CR20) catalysts<sup>84</sup> (Scheme 20a). The reduction of the azide group is also a convenient way to introduce an amino function to more complex compounds as it was achieved during the synthesis of epipodophyllotoxin-*N*-mustard hybrid compounds for complex formation with topoisomerase II and DNA (Scheme 15b).<sup>319, 320</sup>



**SCHEME 20** Heterogeneous catalytic hydrogenation of azides on various catalysts.

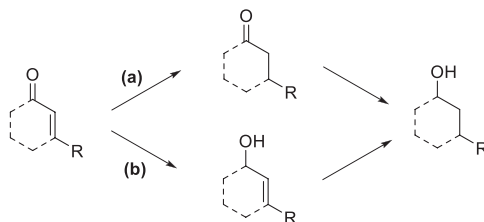
The examples show that the hydrogenation of the  $N_3$  group to  $NH_2$  readily occurs on Pd and Cu catalysts, both are known for their efficacy in the hydrogenation of highly sensitive groups, such as  $C=C$ , etc., and in the same time a moderate hydrogenation power for the reduction of more resistant functional groups, e.g. aromatic rings or nitriles. Accordingly, the reaction conditions for the hydrogenation of the azido group using these two metals appear to be mild, often involving ambient temperature reactions and low hydrogen pressures.

### 3.1.6 Chemo- and regioselective hydrogenation of compounds with multiple hydrogenation sensitive groups

The earlier subchapters described the hydrogenation of a broad variety of functional groups; however, in an overwhelming majority, the examples were related to the hydrogenation of isolated groups; there was no other functional group in the compounds that also could undergo hydrogenation. Although often even the hydrogenation of such isolated groups can cause difficulty, the real challenge is when two or more hydrogenation sensitive groups are in one compound. In such cases, there are two possibilities: (i) to carry out an uncontrolled hydrogenation that will saturate/reduce all possible functional groups and (ii) to aim for a chemo- (two or more different groups) or regioselective (two or more of the same functional groups, e.g., two  $C=C$  double bonds or two carbonyl groups, etc.) hydrogenation. In the following subchapter efforts on such chemo- and regioselective hydrogenations will be summarized. One of the primary examples is the hydrogenation of unsaturated carbonyl compounds.

#### 3.1.6.1 Selective $C=C$ bond hydrogenation of $\alpha,\beta$ -unsaturated carbonyl compounds

The selective hydrogenation of unsaturated carbonyl compounds is difficult; however, to selectively achieve these transformations with the conjugated  $\alpha,\beta$ -unsaturated carbonyl compounds is an even more challenging task. There are two different pathways that could lead to the fully hydrogenated saturated alcohol as depicted in [Scheme 21](#). The hydrogenation of the  $C=C$  double bond



**SCHEME 21** Potential pathways in the hydrogenation of  $\alpha,\beta$ -unsaturated compounds yielding saturated alcohols.

often occurs first under common conditions (pathway (a)); however, subsequent hydrogenation of the unsaturated alcohol intermediate (pathway (b)) also yields the same product.

Although the selective hydrogenation of these compounds to their corresponding saturated carbonyl product (pathway (a) in [Scheme 21](#)) is highly desirable from an industrial point of view,<sup>321</sup> one must not overlook that this is the less challenging task. The hydrogenation of the C=C bond commonly occurs under very mild conditions and especially when a catalyst of reduced strength is used, the appropriate selection of hydrogen pressure and/or reaction temperature solves the problem. Thus the C=C bond hydrogenation of  $\alpha,\beta$ -unsaturated compounds is a successful process in the case of most substrates as demonstrated in [Table 10](#).

As presented in [Table 10](#), Pd catalysts dominate these hydrogenations, similarly to the overwhelming majority of applications in C=C bond hydrogenations. Essentially, as for alkene hydrogenations, the reaction conditions are also mild, serving two purposes: one to ensure to meet green synthesis requirements and two, to avoid the reduction of the carbonyl group.

In addition to the earlier applications there is significant interest in the enantioselective C=C hydrogenation of  $\alpha,\beta$ -unsaturated compounds, including unsaturated ketones<sup>341–345</sup> and carboxylic acids.<sup>346–351</sup> However, as a special chapter is devoted to enantioselective heterogeneous catalysis, these applications will be discussed in Chapter 3.10.

### 3.1.6.2 Selective C=O reduction of $\alpha,\beta$ -unsaturated carbonyl compounds

The chemoselective hydrogenation of the C=O group in  $\alpha,\beta$ -unsaturated carbonyl compounds results in unsaturated alcohols ([Scheme 21](#)). Unsaturated alcohols are valuable products and building blocks in the pharmaceutical and fine chemicals industries, and important fragrance additives in the food and perfume industry. As described before, the selective reduction of the C=O group in the presence of a C=C bond is challenging, thus the synthesis of unsaturated alcohols via catalytic hydrogenation of unsaturated carbonyl compounds had attracted significant interest. Despite the technical difficulties, however, several methods that produce nearly 100% chemoselectivity have been reported as tabulated in [Table 11](#).

As the data in [Table 11](#) show the application of platinum catalysts dominates this research field, although other metals such as Ru, Fe, or Au have also been applied. Commonly, the solution lies in the preparation of a special catalyst that enhances the surface adsorption of the C=O vs the C=C bond. Au- and Pt-based catalysts are the most efficient for this selective transformation. Other metals such as Fe, Zn, and Ag have also been studied.

**TABLE 10** Selective C=C bond hydrogenation of  $\alpha,\beta$ -unsaturated compounds to their corresponding saturated carbonyl derivative.

| Entry | Substrate                                 | Catalyst  | Hydrogen source                                  | Conditions   | Comments  | Ref.            |
|-------|---|---|--|--|---|-----------------|
| 1     | Cinnamaldehyde                            | Pd NPs <sup>a</sup> immobilized on ionic liquids<br>$\beta$ -CD/Pd <sup>b</sup><br>Ni <sub>12</sub> P <sub>5</sub> /SiO <sub>2</sub><br>and Ni <sub>2</sub> P/SiO <sub>2</sub><br>Pt-Ni/CNT <sup>c</sup><br>in situ formed Raney Ni | H <sub>2</sub> (5–20 MPa)<br>Al-H <sub>2</sub> O | <i>m</i> -Xylene,<br>cyclohexane,<br>EtOH, water RT-<br>120°C      | 90%–100% Yield, catalyst recycled 9 times with no loss of activity or leaching, increased selectivity in presence of NaOAc, KBH <sub>4</sub> <sup>b</sup> | 312,<br>322–326 |
| 2     | Cinnamaldehyde, ethyl and vinyl cinnamate | 10 wt% Pd/C   | H <sub>2</sub> (1 atm)                           | Ionic liquid   | 100% yield, recyclable catalyst   | 327             |
| 3     | Substituted 2-cyclohex-en-1-ones          | Pt/MCM <sup>d</sup><br>$\beta$ -CD/Pd <sup>b</sup>  | H <sub>2</sub> (2 MPa),<br>10 min, 40°C          | scCO <sub>2</sub> (7–<br>14 MPa), water,<br>10 min-2 h,<br>RT-40°C | Yield >95%  | 312, 328        |
| 4     | Isophorone                                | $\beta$ -CD/Pd <sup>b</sup><br>Pd/Al <sub>2</sub> O <sub>3</sub><br>Pd/BaCO <sub>3</sub><br>Raney Ni  | H <sub>2</sub> (20 bar)                          | Aqueous solution,<br>MeOH, proline<br>modifier, RT, 2 h            | 100% Yield  | 312,<br>329–337 |

|   |  |  |                             |                   |   |     |
|---|--|--|-----------------------------|-------------------|---|-----|
| 5 | $\alpha$ -N-acetyl-amino-cinnamic acid | In situ formed Raney Ni                    | Al-H <sub>2</sub> O         | Aqueous solution  | 90% yield, 100% chemoselectivity for N-acetyl-phenylalanine | 338 |
| 6 | Mesityl-oxide, 3-Me-1-pentyne-3-ol     | Pd/ZSM-5 <sup>e</sup> , Pd/silicalite chip | H <sub>2</sub> (1.5–20 bar) | Gas phase, flow   | Conversions: 40%–100%                                       | 339 |
| 7 | Cinnamic acid                          | Pd/C                                       | H <sub>2</sub> (10 mbar)    | EtOH, 8 min, 25°C | Kinetic comparison of commercial Pd/C catalysts             | 340 |

<sup>a</sup> NP, nanoparticles.

<sup>b</sup> Cyclodextrin stabilized Pd nanoparticles, KBH<sub>4</sub> was used as reducing agent while preparing the catalyst.

<sup>c</sup> Carbon nanotubes.

<sup>d</sup> A mesoporous silica material.

<sup>e</sup> A synthetic zeolite.

**TABLE 11** Chemoselective C=O hydrogenation of  $\alpha,\beta$ -unsaturated carbonyl compounds to produce  $\alpha,\beta$ -unsaturated alcohols.

| Entry | Substrate   | Catalyst  | Hydrogen source            | Conditions   | Comments  | Ref.     |
|-------|---|---|----------------------------|--|---|----------|
| 1     | Cinnamaldehyde                                    | Pt/CNT <sup>a</sup><br>Pt-CTA-MM or Pt-CTA-Hec <sup>b</sup><br>Pt/RHC <sup>c</sup><br>Pt/Cr-ZnO<br>Fe and Zn promoted Pt/C<br>Ru-mesoporous carbon, modified ZrO <sub>2</sub><br>Pt/K-10<br>Pt/SiO <sub>2</sub> | H <sub>2</sub> (0.5–7 MPa) | <i>i</i> PrOH, EtOH, scCO <sub>2</sub> , cyclohexane, 50–110°C | Nanotubes of 3 nm diameter showed best selectivity, T dependence of selectivity, 3 phase system, bifunctional Pt/K-10 (clay) catalyst, ultrasonic enhancement | 352–364  |
| 2     | Crotonaldehyde                                    | Ru-Ti/SiO <sub>2</sub><br>Au/CeO <sub>2</sub><br>Br-promoted PtZn   | H <sub>2</sub> (1 MPa),    | 60–80°C, vapor phase system, flow system-200°C                 | Ti or CH <sub>3</sub> Br in H <sub>2</sub> increased the selectivity  | 365–367  |
| 3     | $\alpha,\beta$ -unsaturated aldehydes and ketones | Au <sup>0</sup> , Ag <sup>0</sup> and polymer stabilized Au <sup>0</sup> -Ag <sup>0</sup> nanocolloids, Au <sub><i>n</i></sub> (SR) <sub><i>m</i></sub> <sup>d</sup>  | H <sub>2</sub> (0.1–4 MPa) | 0–60°C   | High selectivities for allylic alcohols, long reaction times, Au <sub>25</sub> (SR) <sub>18</sub> showed 100% selectivity                                     | 368, 369 |

<sup>a</sup> Pt nanoparticles deposited on carbon nanotubes.

<sup>b</sup> MM, montmorillonite; Hec, hectorite.

<sup>c</sup> Pt supported on rice husk-based porous carbon.

<sup>d</sup> Thiolate stabilized Au nanoparticles.

### 3.1.6.3 Complete hydrogenation of multiple functional groups using the same catalytic system

The earlier discussed hydrogenations focused on the selective (chemo or regio) hydrogenation of various substrates. Hence, the goal was always to develop a catalytic system with the combination of the actual catalyst and experimental conditions that would focus on one, and only one functional group. In addition to these efforts, investigations are also underway to establish catalytic systems that reduce different functional groups such as carbonyls, alkenes, alkynes, nitro groups, azides, etc. that are present in the same compound in one reaction. These hydrogenation reactions will result in the complete hydrogenation of each group in the target compounds. Representative examples of this area are described in [Table 12](#).

The data indicate a greater variety in the catalytic metals than as it was in the chemoselective hydrogenations; most noble metals are represented with the addition of Ni. However, the major developments occurred in the testing of different catalyst supports from zeolites or mesoporous silica to carbon nanofibers. Several examples focused on the potential recyclability of the catalysts and experimented with magnetic supports that can be easily separated from the reaction mixtures. In most examples hydrogen gas was used as a hydrogen source; however, alcohols have also been applied for the same purpose in transfer hydrogenations. The use of glycerol is particularly notable, as this material is a multimillion ton by-product of the biodiesel production and as such it is a sustainable hydrogen source. The conditions are widely varied based on the substrates and the targeted hydrogenation-sensitive functional group.

## 3.1.7 Heterogeneous catalytic hydrogenations by nonconventional activation methods

The emergence of the nontraditional activation methods appears to strengthen the green and sustainable chemistry movement; these methods are frequently applied in synthesis development and environmental applications.<sup>381</sup> Heterogeneous catalysis, including catalytic hydrogenation, is no different; several methods have been applied with success in this field. Here, the focus will be on the application of microwave irradiation and ultrasound-aided heterogeneous catalytic hydrogenations as these methods are now considered mainstream activation methods in chemical reactions.

### 3.1.7.1 Microwave-assisted hydrogenations

Since the 1980s Microwave-Assisted Organic Synthesis (MAOS) became one of the most dynamically developing fields that particularly aided the growth of organic synthesis.<sup>382–390</sup> However, due to the common arcing phenomenon, especially in flammable organic solvents, metals and microwave irradiation were

**TABLE 12** Hydrogenation of multiple functional groups present in a compound using the same catalytic system.

| Entry | Substrates/functional group                         | Catalyst   | Hydrogen source                               | Conditions                 | Comments   | Ref.    |
|-------|---|--|---|----------------------------|--|---------|
| 1     | Citronellal   | Ni/Zr-Beta, Zr-beta/Ni-MCM-41 <sup>a</sup>                           | H <sub>2</sub> (2 MPa)                        | 80°C, tBuOH, 7–22 h        | One-pot conversion to menthol, high <i>de</i> (up to 94%)                                  | 370     |
| 2     | Alkenes, alkynes, NO <sub>2</sub> , carbonyl        | Polymer caged Pt catalyst  | H <sub>2</sub> (1 bar)                        | RT, THF, 1 h               | Excellent yields, broad scope  | 371     |
| 3     | Alkenes, NO <sub>2</sub> , N <sub>3</sub>           | 10 wt% Pd/C with Ph <sub>2</sub> S                                   | H <sub>2</sub> (1 bar)                        | RT, MeOH, 24 h             | Extremely unreactive toward hydrogenolysis, nitrile reduction, recyclable catalyst         | 372     |
| 4     | Alkenes, NO <sub>2</sub> , N <sub>3</sub> , alkynes | Pd/NH <sub>2</sub> -ferrite nanoparticles<br>In situ formed Raney Ni | H <sub>2</sub> (1 bar)<br>Al-H <sub>2</sub> O | RT, EtOH, EtOAc, 15–35 min | Magnetically recovered catalyst, excellent yields (75%–99%)                                | 54, 373 |
| 5     | Alkenes, alkynes, carbonyl                          | Ni/NH <sub>2</sub> -ferrite nanoparticles                            | H <sub>2</sub> (100 psi)                      | RT, MeOH, 24 h             | Unreactive toward NO <sub>2</sub> , magnetically recovered catalyst, and leach proof       | 374     |
| 6     | Alkenes, alkynes, N <sub>3</sub>                    | 0.5% Pd/MS <sup>b</sup> (3 Å)  | H <sub>2</sub> (1 bar)                        | RT, MeOH, 24 h             | Unreactive toward NO <sub>2</sub> , halogens, benzyl groups, up to 100% yields, recyclable | 375     |

|    |  |   |                             |                                  |  |     |
|----|--|---|-----------------------------|----------------------------------|--|-----|
| 7  | Benzene and $\alpha,\beta$ -unsaturated amino acids                  | Rh nanoparticles in ionic liquids                                       | H <sub>2</sub> (40–100 bar) | 40–120°C, <i>i</i> PrOH, 0.5–2 h | Rh nanoparticles stabilized in simple ammonium halide salts  | 376 |
| 8  | Alkenes, aromatics, ketones  | Pt(0)/Fe <sub>3</sub> O <sub>4</sub> @SiO <sub>2</sub> -NH <sub>2</sub> | H <sub>2</sub> (6 bar)      | 75°C, neat, 0.27–4 h             | Magnetically recoverable and reusable catalyst, high activity, mild conditions                                     | 377 |
| 9  | Benzenes, stilbene, phenols, pyridines and furans                    | Rh supported on carbon nanofibers                                       | H <sub>2</sub> (1–10 bar)   | RT, hexane, 12–24 h              | Efficient arene hydrogenation, mild conditions without leaching of Rh, highly tolerant toward epoxide substitution | 378 |
| 10 | Cyclohexene, nitrobenzene, styrene                                   | 5 wt% Pd/C, Raney Ni  | glycerol                    | 70°C, glycerol, 1–24 h           | Glycerol as a hydrogen source, moderate yield for nitrobenzene   | 379 |
| 11 | Acetophenone, benzaldehyde, cyclohexanone, nitrobenzene, and styrene | Pd/Al <sub>2</sub> O <sub>3</sub>                                       | MeOH, other alcohols        | 20°C, aq. alcohol, flow system   | Reaction under aqueous conditions  | 380 |

<sup>a</sup> A mesoporous silica material.

<sup>b</sup> MS, molecular sieve.

considered incompatible for some time.<sup>391, 392</sup> Further studies, however, pointed out that arcing was strongly size dependent, and using catalysts with reasonably small metal particles make these materials safe to use. Since most commercially available supported metal catalysts inherently fulfill this requirement with their mostly nm size metal particles, metal-catalyzed organic synthesis can be safely carried out by microwave activation. Pioneering works on microwave-assisted hydrogenations, focusing mainly on transfer hydrogenations, were established in the early 2000s. These examples used readily available hydrogen donor agents such as formate, isopropyl alcohol, or cyclohexene. However, these reactions used (super)stoichiometric hydrogen donor agents and produce significant amount of waste, thus they do not conform to the principles of sustainable chemistry. Later, molecular hydrogen, the traditional hydrogen source of catalytic hydrogenations, became the hydrogen source of choice.<sup>393</sup> The development of special pressurized attachments to the regular microwave reactors significantly improved the interest in microwave-assisted heterogeneous catalytic hydrogenations.<sup>394</sup> Since it is a relatively new field within MAOS the available processes that are tabulated in Table 13 are somewhat limited.

The data listed in Table 13 shows a broad scope for these reactions. The applications range from simple C=C double bond hydrogenations to chemo- and regioselective reactions and reductive aminations. With few exemptions (neat metals, e.g., PtO<sub>2</sub> or Raney Ni), the catalysts are supported metals that possess the appropriate metal particle size that can be safely used in microwave-assisted applications. Given the need for activation, the reactions are usually carried out at elevated but still moderate temperatures in very short reaction times. The application of microwaves often results in not only faster reactions but also higher yields and selectivities as compared to the regularly heated examples.

### 3.1.7.2 Ultrasound-assisted hydrogenations

The sonochemical heterogeneous catalysis was introduced several decades ago and now it is an established research field.<sup>178, 405–408</sup> Sonocatalysis is broadly applicable, and its use in heterogeneous hydrogenations also attracted significant interest.<sup>409, 410</sup> Applications are explored in three related areas such as catalyst preparation,<sup>411</sup> the sonochemical modification of commercial catalysts, most commonly by chiral auxiliaries, and reactions carried out under ultrasonic irradiation. When it concerns heterogeneous catalytic hydrogenations, sonochemistry nearly always enhanced catalytic performance, whether this improvement was related to reaction rates or selectivity. Representative applications are tabulated in Table 14.

Similarly to the microwave-assisted applications, ultrasonic irradiation is also applied in heterogeneous catalytic hydrogenations for a broad variety of functional groups such as nitro, alkenes, or carbonyl, covering  $\alpha$ -ketoesters to natural products. Accordingly, the applied metal catalysts are widely varied both by the metal and the type of the catalyst (e.g., supported or bulk metal), the

**TABLE 13** Microwave-assisted heterogeneous catalytic hydrogenations.

| Entry | Substrate   | Catalyst   | Hydrogen source            | Conditions                                | Comments  | Ref. |
|-------|---|--|----------------------------|---|---|------|
| 1     | $\alpha,\beta$ -Unsaturated carbonyl compounds            | PdCl <sub>2</sub> /SiO <sub>2</sub>                            | HCOOH                      | MeOH, H <sub>2</sub> O, 22–55 min         | 100% Selectivity for C=C, broad scope, yields up to 96%, aq. medium | 395  |
| 2     | Acetophenone and propiophenone                            | In situ formed Raney Ni  | Al-H <sub>2</sub> O        | H <sub>2</sub> O/D <sub>2</sub> O, 10 min | Quantitative yields, C=O to CH <sub>2</sub> conversion              | 204  |
| 3     | Aliphatic primary amines                                  | Pt/C   | Al-H <sub>2</sub> O        | Water                                     | Coupling of amines to imines and their hydrogenation                | 396  |
| 4     | Mono-, dinitro-arenes                                     | Pd/C   | Methylcyclohexene          | Alcohols                                  | Reduction to anilines   | 397  |
| 6     | Cinnamic acid esters                                      | 10% Pd/carbon nanotubes  | HCOONH <sub>4</sub>        | EtOH, 5 min                               | Selective reduction of C=C double bond                              | 398  |
| 7     | Cinnamic acids, stilbene                                  | 10 wt% Pd/C  | 1,4-Cyclohexadiene         | EtOAc, 5 min, 100°C                       | Yields up to 99%  | 399  |
| 8     | Substituted pyridines                                     | PtO <sub>2</sub>   | H <sub>2</sub> (120 psi)   | AcOH, 80°C, 20–60 min                     | Compatible with acid-labile groups                                  | 400  |
| 9     | ( <i>E,E</i> )-1,4-diphe-nyl-1,3-butadiene, cholesterol   | 10 wt% Pd/C  | H <sub>2</sub> (4 bar)     | EtOAc, 5 min, 80°C                        | Dependent upon agitation  | 401  |
| 10    | Various aromatic ketones                                  | Pt-Al-SBA-15   | <i>i</i> PrOH              | NaOH, 15 min                              | TOFs of 5000–40,000 h <sup>-1</sup>                                 | 402  |
| 11    | Terminal alkynes, aromatic ketones and aromatic aldehydes | Ru nanoparticles supported on NiFe <sub>2</sub> O <sub>4</sub> |                            | Differ according to the substrate         | Cat. magnetically recoverable, and recyclable                       | 403  |
| 12    | Various substituted nitroaromatics                        | Pd/C or Pt/C   | 1,4-Cyclohexadiene (6 eq.) | MeOH, 5 min, 120°C                        | Broad scope, tolerates labile functional groups like halo, CN       | 404  |

SBA, Santa Barbara amorphous material, a form of mesoporous silica.

**TABLE 14** Application of sonochemical activation in heterogeneous catalytic hydrogenations.

| Entry | Substrate  | Catalyst                          | Hydrogen source            | Conditions  | Comments  | Ref.  |
|-------|--|-----------------------------------|----------------------------|---|---|---|
| 1     | $\alpha$ -Ketoesters   | Pt/Al <sub>2</sub> O <sub>3</sub> | H <sub>2</sub> (1–100 atm) | AcOH, cinchona alkaloids  | Excellent ee values, ee enhancement upon sonication, ultrasonic bath  | <a href="#">178</a> , <a href="#">234–239</a> , <a href="#">250</a> , <a href="#">251</a> , <a href="#">346</a> , <a href="#">361</a> , <a href="#">412–416</a> |
| 2     | 3-Buten-1-ol   | Pd black                          | H <sub>2</sub> (6.8 bar)   | RT, 1-pentanol  | Probe type reactor, isomerization to <i>cis</i> - and <i>trans</i> -2-buten-1-ol favored over hydrogenation, 700-fold selectivity increase upon use of 1-pentanol | <a href="#">364</a> , <a href="#">417</a> , <a href="#">418</a>   |
| 4     | Cinnamaldehyde   | Pd black, Raney Ni Co-B alloy     | H <sub>2</sub> (8.5 atm)   | <i>i</i> PrOH, water, RT  | Benzenepropanol via benzen-propanal, cinnamyl alcohol   | <a href="#">364</a> , <a href="#">419</a>   |
| 5     | 2-Buten-1-ol, <i>cis</i> -2-penten-1-ol ( <i>cis/trans</i> ) | Pd black                          | H <sub>2</sub> (80 psi)    | H <sub>2</sub> O, 1-propanol, RT  | 1-Propanol is added to enhance cavitation   | <a href="#">420</a>   |
| 6     | Ketopantolactone, 1,1,1-trifluoro-2,4-pentandione            | Pt/Al <sub>2</sub> O <sub>3</sub> | H <sub>2</sub> (10 bar)    | RT (3 <i>R</i> )-dihydro-4,4-dimethyl-3-[[[(1 <i>R</i> )-1-(1-naphthyl)ethyl]amino]-2(3 <i>H</i> )-furanone | Excellent ee's (93%, ketopantolactone) and 100% chemoselectivity of the activated C=O of the diketone   | <a href="#">421</a>   |

|    |  |   |                                |   |   |     |
|----|--|---|--------------------------------|---|---|-----|
| 7  | D-fructose                                   | Cu/SiO <sub>2</sub> ,<br>Cu/ZnO/<br>Al <sub>2</sub> O <sub>3</sub> , Raney<br>Ni              | H <sub>2</sub> (10–<br>50 bar) | Water, 24–54 min,<br>70–110°C,<br>0–130 W/cm <sup>2</sup> | D-mannitol is the major product, significant<br>rate enhancement  | 422 |
| 8  | Trifluoromethyl-<br>alkenes,<br>cycloalkanes | PtO <sub>2</sub>  | H <sub>2</sub> (1 bar)         | Et <sub>2</sub> O, RT                                     | Increased yields  | 423 |
| 9  | 1-Phenyl-1,2-<br>propanedione                | Pt/Al <sub>2</sub> O <sub>3</sub> ,<br>Pt/SiO <sub>2</sub> , Pt/SF<br>(silica fiber),<br>Pt/C | H <sub>2</sub> (1 bar)         | Cat. substrate,<br>cinchonidine<br>ultrasounds            | Significant increase in ee on Pt/SF catalyst up<br>to 60% ee  | 252 |
| 10 | 3-Buten-2-ol and<br>1,4-pentadien-3-ol       | Pd black  | H <sub>2</sub> (6.8 bar)       | RT, 20 kHz<br>ultrasound                                  | Probe reactor, competing isomerization and<br>hydrogenation   | 424 |
| 11 | Alkenes                                      | Raney Ni  | D <sub>2</sub> (7 atm)         | H <sub>2</sub> O (50 mL), RT                              | Probe reactor, competing isomerization and<br>hydrogenation   | 425 |
| 12 | Dehydrocholic<br>acid                        | Raney Ni  | H <sub>2</sub> (1 bar)         | Water as solvent,<br>30°C, 20 h                           | High intensity ultrasounds, high regio- and<br>stereoselectivity, product: 7,12-diketo-<br>lithocholic acid | 426 |
| 14 | Methyl<br>acetoacetate                       | Raney Ni  | H <sub>2</sub> (0.6 MPa)       | Tartaric acid, NaBr,<br>MeOH, 60°C, 1 h                   | Excellent ee's  | 427 |
| 15 | 4-Chloronitro-<br>benzene                    | Ni-B alloy  | H <sub>2</sub> (1 MPa)         | EtOH, 80°C,<br>1.5–6.5 h                                  | Cat. prepared under sonication  | 428 |
| 16 | Nitrobenzene                                 | Pd/<br>maghemite  | H <sub>2</sub> (10 bar)        | No extra solvent  | Selective formation of anilines   | 429 |
| 17 | Maltose                                      | Ru-B<br>amorphous<br>alloy  | H <sub>2</sub> (3 MPa)         | Water, 100°C, 3 h   | Catalyst prepared under 60 W ultrasonic<br>activation, activity increases 10-fold                           | 430 |

sonochemical treatment appears to uniformly activate these reactions. Although the detailed description of the underlying principles is beyond the scope of this chapter, ultimately there are two major sources for the enhanced catalytic performances: (i) the so-called surface cleaning effect that ensures the removal of impurities, such as oxides, from the surface of the metals thus providing pristine metal surfaces and (ii) the particle size decreasing effect of the ultrasounds that is caused by the breaking up of larger particles upon cavitation. With the decreasing particle size the metal surface available for the hydrogenations increases, thus resulting in higher reaction rates.

### 3.1.8 Conclusions and outlook

Advances, reported in the 1996–2021 period, in the applications of heterogeneous catalytic hydrogenations have been reviewed in this chapter. Heterogeneous catalytic hydrogenation is one of the major contributors to the sustainable synthetic endeavor and remains an important method in synthetic and industrial applications alike. The recent developments target new areas and also extend traditional ones. Among the traditional areas catalyst design and preparation remain the focus, bridging out to materials science by using various functional polymers as catalyst supports, by applying metal-organic framework based catalysts in hydrogenations or employing magnetically separable supports to enhance catalyst recovery and recycling. Based on the significant advancements made in the past two decades and the number of applications published in industrial and synthetic chemistry, it is apparent that heterogeneous catalytic hydrogenation will remain an important tool for environmentally benign and sustainable chemistry and will be a major driving force in sustainable synthesis development.

## References

1. Hudlicky, M. *Reductions in Organic Chemistry*; Ellis-Horwood and Wiley: Chichester, 1984; pp. 13–35 (chapters 2–4).
2. Mackie, R. M.; Smith, D. M.; Aitken, R. A. *Guidebook to Organic Synthesis*, 3rd ed.; Pearson, 1999 (chapter 8).
3. Smith, M. B.; March, J. *March's Advanced Organic Chemistry*, 6th ed.; Wiley: Hoboken, NJ, 2007.
4. Nishimura, S. *Handbook of Heterogeneous Catalytic Hydrogenation for Organic Synthesis*; Wiley: New York, 2001.
5. Augustine, R. L. *Heterogeneous Catalysis for the Synthetic Chemist*; Marcel Dekker: New York, 1996.
6. Bartók, M.; Molnár, Á. Heterogeneous Catalytic Hydrogenation. In *Chemistry of Functional Groups*; Patai, S., Ed.; Wiley: Chichester, 1997; p. 843. Suppl. A3. (chapter 16).
7. Smith, G. V.; Notheisz, F. *Heterogeneous Catalysis in Organic Chemistry*; Academic Press: San Diego, CA, 1999.
8. Consiglio, G. In *Encyclopedia of Catalysis*; Horváth, I. T., Ed.; Vol. 1; Wiley: New York, 2003; p. 407.

- Klabunovski, E.; Smith, G. V.; Zsigmond, Á. *Heterogeneous Enantioselective Hydrogenations—Theory and Practice, Catalysis by Metal Complexes*, Vol. 31; Springer: Dordrecht, 2006.
- Zhang, L.; Zhou, M.; Wang, A.; Zhang, T. Selective Hydrogenation Over Supported Metal Catalysts: From Nanoparticles to Single Atoms. *Chem. Rev.* **2020**, *120*, 683–733.
- Anastas, P. T.; Warner, J. C. *Green Chemistry: Theory and Practice*; Oxford University Press: Oxford, 1998.
- Török, B.; Dransfield, T. *Green Chemistry: An Inclusive Approach*; Elsevier: Oxford, Cambridge, 2018.
- Horvath, I., Ed. *Encyclopedia of Catalysis*; Wiley: New York, 2003.
- Tungler, A.; Szabados, E. Overcoming Problems at Elaboration and Scale-up of Liquid-Phase Pd/C Mediated Catalytic Hydrogenations in Pharmaceutical Production. *Org. Process Res. Dev.* **2016**, *20*, 1246–1251.
- Beck, J. S.; Haag, W. O.; Buonomo, F.; Sanfilippo, D.; Trifirò, F.; Arnold, H.; Döbert, F.; Gaube, J. Organic Reactions: Sections 4.1–4.4. In *Handbook of Heterogeneous Catalysis*; Ertl, G., Knözinger, H., Weitkamp, J., Eds.; Wiley-VCH: New York, Weinheim, 2008; pp. 2123–2231 (chapter 4).
- Zaera, F. The Surface Chemistry of Metal-Based Hydrogenation Catalysis. *ACS Catal.* **2017**, *7*, 4947–4967.
- García-Melchor, M.; Bellarosa, L.; López, N. Unique Reaction Path in Heterogeneous Catalysis: The Concerted Semi-Hydrogenation of Propyne to Propene on CeO<sub>2</sub>. *ACS Catal.* **2014**, *4*, 4015–4020.
- Conley, M. P.; Copéret, C.; Thieuleux, C. Messtructured Hybrid Organic – Silica Materials: Ideal Supports for Well-Defined Heterogeneous Organometallic Catalysts. *ACS Catal.* **2014**, *4*, 1458–1469.
- Jung, U.; Elsen, A.; Li, Y.; Smith, J. G.; Small, M. W.; Stach, E. A.; Frenkel, A. I.; Nuzzo, R. G. Comparative in Operando Studies in Heterogeneous Catalysis: Atomic and Electronic Structural Features in the Hydrogenation of Ethylene Over Supported Pd and Pt Catalysts. *ACS Catal.* **2015**, *5*, 1539–1551.
- Wang, C.; An, B.; Lin, W. Metal – Organic Frameworks in Solid – Gas Phase Catalysis. *ACS Catal.* **2019**, *9*, 130–146.
- Yabe, Y.; Sawama, Y.; Monguchi, Y.; Sajiki, H. New Aspect of Chemoselective Hydrogenation Utilizing Heterogeneous Palladium Catalysts Supported by Nitrogen- and Oxygen-Containing Macromolecules. *Cat. Sci. Technol.* **2014**, *4*, 260–271.
- Venezia, A. M.; La Parola, V.; Liotta, L. F. Structural and Surface Properties of Heterogeneous Catalysts: Nature of the Oxide Carrier and Supported Particle Size Effects. *Catal. Today* **2017**, *285*, 114–124.
- Salnikov, O. G.; Burueva, D. B.; Gerasimov, E. Y.; Bukhtiyarov, A. V.; Khudorozhkov, A. K.; Prosvirin, I. P.; Kovtunova, L. M.; Barskiy, D. A.; Bukhtiyarov, V. I.; Kovtunov, K. V.; Koptuyug, I. V. The Effect of Oxidative and Reductive Treatments of Titania-Supported metal Catalysts on the Pairwise Hydrogen Addition to Unsaturated Hydrocarbons. *Catal. Today* **2017**, *283*, 82–88.
- Copéret, C.; Comas-Vives, A.; Conley, M. P.; Estes, D. P.; Fedorov, A.; Mougél, V.; Nagae, H.; Núñez-Zarur, F.; Zhizhko, P. A. Surface Organometallic and Coordination Chemistry Toward Single-Site Heterogeneous Catalysts: Strategies, Methods, Structures, and Activities. *Chem. Rev.* **2016**, *116*, 323–421.
- Chen, Z.; Chen, J.; Li, Y. Metal–Organic-Framework-Based Catalysts for Hydrogenation Reactions. *Chin. J. Catal.* **2017**, *38*, 1108–1126.

132 Heterogeneous catalysis in sustainable synthesis

26. Saha, D.; Maity, T.; Koner, S. Metal–Organic Frameworks Based on Alkaline Earth Metals—Hydrothermal Synthesis, X-ray Structures, Gas Adsorption, and Heterogeneously Catalyzed Hydrogenation Reactions. *Eur. J. Inorg. Chem.* **2015**, *2015*, 1053–1064.
27. Kent, P. D.; Mondloch, J. E.; Finke, R. G. A Four-Step Mechanism for the Formation of Supported-Nanoparticle Heterogeneous Catalysts in Contact With Solution: The Conversion of Ir(1,5-COD)Cl/ $\gamma$ -Al<sub>2</sub>O<sub>3</sub> to Ir(0)~170/ $\gamma$ -Al<sub>2</sub>O<sub>3</sub>. *J. Am. Chem. Soc.* **2014**, *136*, 1930–1941.
28. Pei, Q.; He, T.; Yu, Y.; Jing, Z.; Guo, J.; Liu, L.; Xiong, Z.; Chen, P. Liberating Active Metals From Reducible Oxide Encapsulation for Superior Hydrogenation Catalysis. *ACS Appl. Mater. Interfaces* **2020**, *12*, 7071–7080.
29. Wang, X.; Liu, N.; Xu, R.; Chen, B.; Dai, C.; Wu, B.; Yu, G. Insights Into the Shape Effect of H<sub>2</sub> Self-Selective Ni Catalysts for Efficient Acetone Hydrogenation. *Appl. Surf. Sci.* **2021**, *536*, 147844.
30. Saleh, T. A.; Al-Hammadi, S. A. A Novel Catalyst of Nickel-Loaded Graphene Decorated on Molybdenum-Alumina for the HDS of Liquid Fuels. *Chem. Eng. J.* **2021**, *406*, 125167.
31. Press, R. J.; Santhanam, K. S. V.; Miri, M. J.; Bailey, A. V.; Takacs, G. A. *Introduction to Hydrogen Technology*; Wiley: Hoboken, NJ, 2009; pp. 195–210 (chapter 4.1).
32. <https://www.nobelprize.org/prizes/chemistry/1912/sabatier/biographical/> (accessed 30 October 2020).
33. Sabatier, P. *La Catalyse en Chimie Organique (Catalysis in Organic Chemistry (translated by Reidl, E. E.))*; Van Norstrand: Princeton, NJ, 1913; p. 923.
34. Raney, M. *Catalytic Nickel*; US patent 1,563,587, 1925.
35. Raney, M. *Finely Divided Nickel*; US patent 1,628,190, 1927.
36. Raney, M. Hydrogenation: Catalysts From Alloys. Ni Catalysts. *Ind. Eng. Chem.* **1940**, *32*, 1199–1203.
37. Adkins, H.; Bilica, H. R. The Preparation of Raney Nickel Catalysts and Their Use Under Conditions Comparable With Those for Platinum and Palladium Catalysts. *J. Am. Chem. Soc.* **1948**, *70*, 6095–6098.
38. Smith, A. J.; Trimm, D. L. The Preparation of Skeletal Catalysts. *Annu. Rev. Mat. Res.* **2005**, *35*, 127–142.
39. Rylander, P. N. *Catalytic Hydrogenation Over Platinum Metals*; Academic Press: New York, London, 1967.
40. Bartók, M., Ed. *Stereochemistry of Heterogeneous Metal Catalysis*; Wiley: Chichester, 1985.
41. Augustine, R. L. *Catalytic Hydrogenation. Techniques and Applications in Organic Synthesis*; Dekker: New York, 1965.
42. Molnár, Á.; Sárkány, A.; Varga, M. Hydrogenation of Carbon–Carbon Multiple Bonds: Chemo-, Regio- and Stereo-Selectivity. *J. Mol. Catal. A: Chem.* **2001**, *173*, 185–221.
43. Kacer, P.; Cerveny, L. Structure Effects in Hydrogenation Reactions on Noble Metal Catalysts. *Appl. Catal. A Gen.* **2002**, *229*, 193–216.
44. Blaser, H. U.; Malan, C.; Pugin, B.; Spindler, F.; Steiner, H.; Studer, M. Selective Hydrogenation for Fine Chemicals: Recent Trends and New Developments. *Adv. Synth. Catal.* **2003**, *345*, 103–151.
45. Tungler, A.; Sipos, E.; Háda, V. Heterogeneous Catalytic Asymmetric Hydrogenation of the C=C bond. *Curr. Org. Chem.* **2006**, *10*, 1569–1583.
46. Mallat, T.; Orglmeister, E.; Baiker, A. Asymmetric Catalysis at Chiral Metal Surfaces. *Chem. Rev.* **2007**, *107*, 4863–4890.
47. Studer, M.; Blaser, H.-U. Cinchona-Modified Platinum Catalysts: From Ligand Acceleration to Technical Processes. *Acc. Chem. Res.* **2007**, *40*, 1348–1356.

48. Mitsudome, T.; Kaneda, K. Gold Nanoparticle Catalysts for Selective Hydrogenations. *Green Chem.* **2013**, *15*, 2636–2654.
49. Ikeda, S.; Ishino, S.; Harada, T.; Okamoto, N.; Sakata, T.; Mori, H.; Kuwabata, S.; Torimoto, T.; Matsumura, M. Ligand-Free Platinum Nanoparticles Encapsulated in a Hollow Porous Carbon Shell as a Highly Active Heterogeneous Hydrogenation Catalyst. *Angew. Chem. Int. Ed.* **2006**, *45*, 7063–7066.
50. Vasylyev, M. V.; Maayan, G.; Hovav, Y.; Haimov, A.; Neumann, R. Palladium Nanoparticles Stabilized by Alkylated Polyethyleneimine as Aqueous Biphasic Catalysts for the Chemoselective Stereocontrolled Hydrogenation of Alkenes. *Org. Lett.* **2006**, *8*, 5445–5448.
51. Rossi, L. M.; Vono, L. L. R.; Silva, F. P.; Kiyohara, P. K.; Duarte, E. L.; Matos, J. R. A Magnetically Recoverable Scavenger for Palladium Based on Thiol-Modified Magnetite Nanoparticles. *Appl. Catal., A* **2007**, *330*, 139–144.
52. Álvaro, V.; Johnstone, R. A. W. High Surface Area Pd, Pt and Ni Ion-Exchanged Zr, Ti and Sn(IV) Phosphates and Their Application to Selective Heterogeneous Catalytic Hydrogenation of Alkenes. *J. Mol. Catal. A: Chem.* **2008**, *280*, 131–141.
53. Khodadadi-Moghaddam, M.; Habibi-Yangjeh, A.; Reza Gholami, M. Solvent Effects on the Reaction Rate and Selectivity of Synchronous Heterogeneous Hydrogenation of Cyclohexene and Acetone in Ionic Liquid/Alcohols Mixtures. *J. Mol. Catal. A: Chem.* **2009**, *306*, 11–16.
54. Schäfer, C.; Ellstrom, C. J.; Cho, H.; Török, B. Pd/C–Al–Water Facilitated Selective Reduction of a Broad Variety of Functional Groups. *Green Chem.* **2017**, *19*, 1230–1234.
55. Song, J.; Huang, Z.-F.; Pan, L.; Zou, J.-J.; Zhang, X.; Wang, L. Oxygen-Deficient Tungsten Oxide as Versatile and Efficient Hydrogenation Catalyst. *ACS Catal.* **2015**, *5*, 6594–6599.
56. Grigoropoulos, A.; McKay, A. I.; Katsoulidis, A. P.; Davies, R. P.; Haynes, A.; Brammer, L.; Xiao, J.; Weller, A. S.; Rosseinsky, M. J. Encapsulation of Crabtree's Catalyst in Sulfonated MIL-101(Cr): Enhancement of Stability and Selectivity Between Competing Reaction Pathways by the MOF Chemical Microenvironment. *Angew. Chem. Int. Ed.* **2018**, *57*, 4532–4537.
57. Ganjehyan, K.; Nişancı, B.; Sevim, M.; Daştan, A.; Metin, Ö. Monodisperse CuPt Alloy Nanoparticles Assembled on Reduced Graphene Oxide as Catalysts in the Transfer Hydrogenation of Various Functional Organic Groups. *Appl. Organomet. Chem.* **2019**, *33*, e4863.
58. Rimoldi, M.; Fodor, D.; van Bokhoven, J.; Mezzetti, A. Catalytic Hydrogenation of Liquid Alkenes With a Silica-Grafted Hydride Pincer Iridium(III) Complex: Support for a Heterogeneous Mechanism. *Cat. Sci. Technol.* **2015**, *5*, 4575–4586.
59. Moreno-Marrodan, C.; Liguori, F.; Mercadé, E.; Godard, C.; Claver, C.; Barbaro, P. A Mild Route to Solid-Supported Rhodium Nanoparticle Catalysts and Their Application to the Selective Hydrogenation Reaction of Substituted Arenes. *Cat. Sci. Technol.* **2015**, *5*, 3762–3772.
60. Verho, O.; Nagendiran, A.; Johnston, E. V.; Tai, C.; Bäckvall, J. E. Nanopalladium on Amino-Functionalized Mesocellular Foam: An Efficient Catalyst for Suzuki Reactions and Transfer Hydrogenations. *ChemCatChem* **2013**, *5*, 612–618.
61. Dhakshinamoorthy, A.; Navalon, S.; Sempere, D.; Alvaro, M.; Garcia, H. Reduction of Alkenes Catalyzed by Copper Nanoparticles Supported on Diamond Nanoparticles. *Chem. Commun.* **2013**, *49*, 2359–2361.
62. Bhuyan, D.; Saikia, L. Scavenging Pd<sup>2+</sup> on Amine-Functionalized SBA-15: A Facile Synthesis of Leach-Free Pd<sup>0</sup> Nanocatalyst for Base-Free Chemoselective Transfer Hydrogenation of Olefins. *ChemistrySelect* **2017**, *2*, 6350–6358.

134 Heterogeneous catalysis in sustainable synthesis

63. Ghosh, S.; Jagirdar, B. R. Synthesis of Mesoporous Iridium Nanosponge: A Highly Active, Thermally Stable and Efficient Olefin Hydrogenation Catalyst. *Dalton Trans.* **2017**, *46*, 11431–11439.
64. Pederzolli, F. R. S.; Wolke, S. I.; da Rosa, R. G. Recyclable Rhodium-Cp0-Heterogenized Catalysts for Hydrogenation of Olefins. *J. Catal.* **2018**, *360*, 201–212.
65. Campos, C. H.; Belmar, J. B.; Jeria, S. E.; Urbano, B. F.; Torres, C. C.; Alderete, J. B. Rhodium(I) Diphenylphosphine Complexes Supported on Porous Organic Polymers as Efficient and Recyclable Catalysts for Alkene Hydrogenation. *RSC Adv.* **2017**, *7*, 3398–3407.
66. Jiang, Y.; Gao, Q. Heterogeneous Hydrogenation Catalyses over Recyclable Pd(0) Nanoparticle Catalysts Stabilized by PAMAM-SBA-15 Organic-Inorganic Hybrid Composites. *J. Am. Chem. Soc.* **2006**, *128*, 716–717.
67. Wilson, O. M.; Knecht, M. R.; Garcia-Martinez, J. C.; Crooks, R. M. Effect of Pd Nanoparticle Size on the Catalytic Hydrogenation of Allyl Alcohol. *J. Am. Chem. Soc.* **2006**, *128*, 4510–4511.
68. Wu, T.; Jiang, T.; Hu, B.; Han, B.; He, J.; Zhou, X. Cross-Linked Polymer Coated Pd Nanocatalysts on SiO<sub>2</sub> Support: Very Selective and Stable Catalysts for Hydrogenation in Supercritical CO<sub>2</sub>. *Green Chem.* **2009**, *11*, 798–803.
69. Bhattacharjee, S.; Dotzauer, D. M.; Bruening, M. L. Selectivity as a Function of Nanoparticle Size in the Catalytic Hydrogenation of Unsaturated Alcohols. *J. Am. Chem. Soc.* **2009**, *131*, 3601–3610.
70. Iosif, F.; Parvulescu, V. I.; Pérez-Bernal, M. E.; Ruano-Casero, R. J.; Rives, V.; Kranjc, K.; Polanc, S.; Kočevár, M.; Genin, E.; Genêt, J. P.; Michelet, V. Heterogeneous Hydrogenation of Bicyclo[2.2.2]Octenes on Rh/TPPTS/LDH Catalysts. *J. Mol. Catal. A: Chem.* **2007**, *276*, 34–40.
71. Leitmannová, E.; Červený, L. Immobilization of [Cp\*Ru(Sorbic Acid)]CF<sub>3</sub>SO<sub>3</sub> Catalyst: Application for Sorbic Acid Hydrogenation and Comparison With Homogeneous and Two-Phase Catalysis. *J. Mol. Catal. A: Chem.* **2007**, *261*, 242–245.
72. Callis, N.; Thiery, E.; Le Bras, J.; Muzart, J. Palladium Nanoparticles-Catalyzed Chemoselective Hydrogenations, a Recyclable System in Water. *Tetrahedron Lett.* **2007**, *48*, 8128–8131.
73. Ma, X.; Jiang, T.; Han, B.; Zhang, J.; Miao, S.; Ding, K.; An, G.; Xie, Y.; Zhou, Y.; Zhu, A. Palladium Nanoparticles in Polyethylene Glycols: Efficient and Recyclable Catalyst System for Hydrogenation of Olefins. *Catal. Commun.* **2008**, *9*, 70–74.
74. Mukherjee, D. Potential Application of Palladium Nanoparticles as Selective Recyclable Hydrogenation Catalysts. *J. Nanopart. Res.* **2008**, *10*, 429–436.
75. Min Park, C.; Serk Kwon, M.; Park, J. Palladium Nanoparticles in Polymers: Catalyst for Alkene Hydrogenation, Carbon–Carbon Cross-Coupling Reactions, and Aerobic Alcohol Oxidation. *Synthesis* **2006**, *2006*, 3790–3794.
76. Hu, Y.; Yang, H.; Zhang, Y.; Hou, Z.; Wang, X.; Qiao, Y.; Li, H.; Feng, B.; Huang, Q. The Functionalized Ionic Liquid-Stabilized Palladium Nanoparticles Catalyzed Selective Hydrogenation in Ionic Liquid. *Catal. Commun.* **2009**, *10*, 1903–1907.
77. Dhakshinamoorthy, A.; Pitchumani, K. Clay Entrapped Nickel Nanoparticles as Efficient and Recyclable Catalysts for Hydrogenation of Olefins. *Tetrahedron Lett.* **2008**, *49*, 1818–1823.
78. Mori, A.; Miyakawa, Y.; Ohashi, E.; Haga, T.; Maegawa, T.; Sajiki, H. Pd/C-Catalyzed Chemoselective Hydrogenation in the Presence of Diphenylsulfide. *Org. Lett.* **2006**, *8*, 3279–3281.

79. Alexander, S.; Udayakumar, V.; Gayathri, V. Hydrogenation of Olefins by Polymer-Bound Palladium(II) Schiff Base Catalyst. *J. Mol. Catal. A: Chem.* **2009**, *314*, 21–27.
80. Alonso, F.; Riente, P.; Yus, M. Transfer Hydrogenation of Olefins Catalysed by Nickel Nanoparticles. *Tetrahedron* **2009**, *65*, 10637–10643.
81. Liu, Q.; Li, J.; Shen, X.; Xing, R.; Yang, J.; Liu, Z.; Zhou, B. Hydrogenation of Olefins Using Hantzsch Ester Catalyzed by Palladium on Carbon. *Tetrahedron Lett.* **2009**, *50*, 1026–1028.
82. Tran, A. T.; Huynh, V. A.; Friz, E. M.; Whitney, S. K.; Cordes, D. B. A General Method for the Rapid Reduction of Alkenes and Alkynes Using Sodium Borohydride, Acetic Acid, and Palladium. *Tetrahedron Lett.* **2007**, *50*, 1817–1819.
83. Huang, X.; Wu, H.; Liao, X.; Shi, B. Liquid Phase Hydrogenation of Olefins Using Heterogenized Ruthenium Complexes as High Active and Reusable Catalyst. *Catal. Commun.* **2010**, *11*, 487–492.
84. Monguchi, Y.; Ichikawa, T.; Nozaki, K.; Kihara, K.; Yamada, Y.; Miyake, Y.; Sawama, Y.; Sajiki, H. Development of Chelate Resin-Supported Palladium Catalysts for Chemoselective Hydrogenation. *Tetrahedron* **2015**, *71*, 6499–6505.
85. Yosef, I.; Abu-Reziq, R.; Avnir, D. Entrapment of an Organometallic Complex Within a Metal: A Concept for Heterogeneous Catalysis. *J. Am. Chem. Soc.* **2008**, *130*, 11880–11882.
86. Kumar, B. S.; Amali, A. J.; Pitchumani, K. Mesoporous Microcapsules Through D-Glucose Promoted Hydrothermal Self-Assembly of Colloidal Silica: Reusable Catalytic Containers for Palladium Catalyzed Hydrogenation Reactions. *ACS Sustain. Chem. Eng.* **2017**, *5*, 667–674.
87. Yamada, Y. M. A.; Yuyama, Y.; Sato, T.; Fujikawa, S.; Uozumi, Y. A Palladium-Nanoparticle and Silicon-Nanowire-Array Hybrid: A Platform for Catalytic Heterogeneous Reactions. *Angew. Chem. Int. Ed.* **2014**, *53*, 127–131.
88. Yabe, Y.; Sawama, Y.; Yamada, T.; Nagata, S.; Monguchi, Y.; Sajiki, H. Easily-Controlled Chemoselective Hydrogenation by Using Palladium on Boron Nitride. *ChemCatChem* **2013**, *5*, 2360–2366.
89. Sharma, P.; Sasson, Y. Highly Active Ru-g-C<sub>3</sub>N<sub>4</sub> Photocatalyst for Visible Light Assisted Selective Hydrogen Transfer Reaction Using Hydrazine at Room Temperature. *Catal. Commun.* **2017**, *102*, 48–52.
90. Wang, J.-C.; Hu, Y.-H.; Chen, G. J.; Dong, Y.-B. Cu(II)/Cu(0)@UiO-66-NH<sub>2</sub>: Base Metal@MOFs as Heterogeneous Catalysts for Olefin Oxidation and Reduction. *Chem. Commun.* **2016**, *52*, 13116–13119.
91. Gong, L.-H.; Cai, Y.-Y.; Li, X.-H.; Zhang, Y.-N.; Su, J.; Chen, J.-S. Room-Temperature Transfer Hydrogenation and Fast Separation of Unsaturated Compounds Over Heterogeneous Catalysts in an Aqueous Solution of Formic Acid. *Green Chem.* **2014**, *16*, 3746–3751.
92. Gole, B.; Sanyal, U.; Banerjee, R.; Mukherjee, P. R. High Loading of Pd Nanoparticles by Interior Functionalization of MOFs for Heterogeneous Catalysis. *Inorg. Chem.* **2016**, *55*, 2345–2354.
93. Bernas, A.; Myllyoja, J.; Salmi, T.; Murzin, D. Y. Kinetics of Linoleic Acid Hydrogenation on Pd/C Catalyst. *Appl. Catal., A* **2009**, *353*, 166–180.
94. Nunes, R. M. D.; Fernandes, T. F.; Carvalho, G. A.; dos Santos, E. N.; José, M.; Moreno, S. M.; Piedade, A. P.; Pereira, M. M. Recyclable Immobilized Rhodium Catalysts in the Diastereoselective Hydrogenation of Unsaturated Steroids. *J. Mol. Catal. A: Chem.* **2009**, *307*, 115–120.
95. Nash, D. J.; Restrepo, D. T.; Parra, N. S.; Giesler, K. E.; Penabade, R. A.; Aminpour, M.; Le, D.; Li, Z.; Farha, O. K.; Harper, J. K.; Rahman, T. S.; Blair, R. G. Heterogeneous Metal-Free Hydrogenation Over Defect-Laden Hexagonal Boron Nitride. *ACS Omega* **2016**, *1*, 1343–1354.

136 Heterogeneous catalysis in sustainable synthesis

96. Ficker, M.; Svenningsen, S. W.; Larribeau, T.; Christensen, J. B. Inexpensive and Rapid Hydrogenation Catalyst From  $\text{CuSO}_4/\text{CoCl}_2$ —Chemoselective Reduction of Alkenes and Alkynes in the Presence of Benzyl Protecting Groups. *Tetrahedron Lett.* **2018**, *59*, 1125–1129.
97. Zhu, J.; Wood, J.; Deplanche, K.; Mikheenko, I.; Macaskie, L. E. Selective Hydrogenation Using Palladium Bioinorganic Catalyst. *Appl. Catal. B: Environ.* **2016**, *199*, 108–122.
98. Guo, J.; Yang, J.; Zhuang, J.; Suna, H.; Zhang, H.; Yue, Y.; Zhu, H.; Bao, X.; Yuan, P. Selectively Catalytic Hydrogenation of Styrene-Butadiene Rubber Over Pd/g- $\text{C}_3\text{N}_4$  Catalyst. *Appl. Catal. A: Gen.* **2020**, *589*, 117312.
99. Zupancic, S.; Svete, J.; Stanovnik, B. Reductive Ring Cleavage of 1-Alkyl-4-Benzoylamino-5-Phenyl-3-Pyrazolidinones With Raney-Nickel Alloy. Synthesis of N-Benzoyl-3-Alkylamino-3-Phenylalanine Amides From *rel*-(4*R*,5*R*)-4-Benzoylamino-5-Phenyl-3-Pyrazolidinone. *J. Heterocyclic Chem.* **1999**, *36*, 607–610.
100. Nikolaeva, T. G.; Shchekotikhin, Y. M. Stereodirected Catalytic Synthesis of Perhydroacridines and Their Isologs From Decahydroacridine-1,8-Diones. *Chem. Heterocycl. Compd.* **2004**, *40*, 582–593.
101. Willms, A.; Schumacher, H.; Tabassum, T.; Qi, L.; Scott, S. L.; Hausoul, P. J. C.; Rose, M. Solid Molecular Frustrated Lewis Pairs in a Polyamine Organic Framework for the Catalytic Metal-Free Hydrogenation of Alkenes. *ChemCatChem* **2018**, *10*, 1835–1843.
102. Karimi, S. A Formal Total Synthesis of Racemic Sesquiterpenoid Sativene. *J. Nat. Prod.* **2001**, *64*, 406–410.
103. Kikuchi, H.; Yamamoto, K.; Horoiwa, S.; Hirai, S.; Kasahara, R.; Hariguchi, R.; Matsumoto, M.; Oshima, Y. Exploration of a New Type of Antimalarial Compounds Based on Febri-fugine. *J. Med. Chem.* **2006**, *49*, 4698–4706.
104. Taber, D. F.; Tian, W. Synthesis of (-)-Hamigeran B. *J. Org. Chem.* **2008**, *73*, 7560–7564.
105. Price, N. P. J.; Jackson, M. A.; Vermillion, K. E.; Blackburn, J. A.; Hartman, T. M. Rhodium-Catalyzed Reductive Modification of Pyrimidine Nucleosides, Nucleotide Phosphates, and Sugar Nucleotides. *Carbohydr. Res.* **2020**, *488*, 107893.
106. Modak, A.; Bhaumik, A. Surface-Exposed Pd Nanoparticles Supported Over Nanoporous Carbonhollow Tubes as an Efficient Heterogeneous Catalyst for the C C Bondformation and Hydrogenation Reactions. *J. Mol. Catal. A: Chem.* **2016**, *425*, 147–156.
107. Sugimura, T.; Im, C. Y.; Sato, Y.; Okuyama, T. Stereoselective Hydrogenation of Conjugate Diene Directed by Hydroxy Group and Asymmetric Synthesis of Deoxypolypropionate Units. *Tetrahedron* **2007**, *63*, 4027.
108. Markov, P. V.; Mashkovsky, I. S.; Bragina, G. O.; Warna, J.; Bukhtiyarov, V. I.; Stakheev, A. Y.; Murzin, D. Y. Experimental and Theoretical Analysis of Particle Size Effect in Liquid-Phase Hydrogenation of Diphenylacetylene. *Chem. Eng. J.* **2021**, *404*, 126409.
109. Pattamakomsan, K.; Suriye, K.; Dokjampa, S.; Mongkolsiri, N.; Praserttham, P.; Panpranot, J. Effect of Mixed  $\text{Al}_2\text{O}_3$  Structure Between  $\theta$ - and  $\alpha$ - $\text{Al}_2\text{O}_3$  on the Properties of Pd/ $\text{Al}_2\text{O}_3$  in the Selective Hydrogenation of 1,3-Butadiene. *Catal. Commun.* **2010**, *11*, 311–316.
110. Sharma, G. V. M.; Choudary, B. M.; Sarma, M. R.; Rao, K. K. Stereoselective Hydrogenation of Alkynes, Enynes and Dienes by Interlamellar Montmorillonite-Diphenylphosphinepalladium(II) Complex. *J. Org. Chem.* **1989**, *54*, 2998–3000.
111. Nishio, R.; Sugiura, M.; Kobayashi, S. Semi-Hydrogenation of Alkynes Using Phosphinated Polymer Incarcerated (PI) Palladium Catalysts. *Org. Biomol. Chem.* **2006**, *4*, 992–995.
112. Alonso, F.; Osante, I.; Yus, M. Highly Selective Hydrogenation of Multiple Carbon–Carbon Bonds Promoted by Nickel(0) Nanoparticles. *Tetrahedron* **2007**, *63*, 93–102.

113. Fiorio, J. L.; Gonçalves, R. V.; Teixeira-Neto, E.; Ortuño, M. A.; López, N.; Rossi, L. M. Accessing Frustrated Lewis Pair Chemistry Through Robust Gold@N-Doped Carbon for Selective Hydrogenation of Alkynes. *ACS Catal.* **2018**, *8*, 3516–3524.
114. da Silva, F. P.; Fiorio, J. L.; Gonçalves, R. V.; Teixeira-Neto, E.; Rossi, L. M. Synergic Effect of Copper and Palladium for Selective Hydrogenation of Alkynes. *Ind. Eng. Chem. Res.* **2018**, *57*, 16209–16216.
115. Uberman, P. M.; Costa, N. J. S.; Philippot, K.; Carmona, R. C.; Dos Santos, A. A.; Rossi, L. M. A Recoverable Pd Nanocatalyst for Selective Semi-Hydrogenation of Alkynes: Hydrogenation of Benzyl-Propargylamines as a Challenging Model. *Green Chem.* **2014**, *16*, 4566–4574.
116. Takale, B. S.; Feng, X.; Lu, Y.; Bao, M.; Jin, T.; Minato, T.; Yamamoto, Y. Unsupported Nanoporous Gold Catalyst for Chemoselective Hydrogenation Reactions Under Low Pressure: Effect of Residual Silver on the Reaction. *J. Am. Chem. Soc.* **2016**, *138*, 10356–10364.
117. Sheldrake, H. M.; Wallace, T. W. Reduction of Propargylic Sulfones to (Z)-Allylic Sulfones Using Zinc and Ammonium Chloride. *Tetrahedron Lett.* **2007**, *48*, 4407–4411.
118. Studt, F.; Abild-Pedersen, F.; Bligaard, T.; Sørensen, R. Z.; Christensen, C. H.; Nørskov, J. K. Identification of Non-Precious Metal Alloy Catalysts for Selective Hydrogenation of Acetylene. *Science* **2008**, *320*, 1320–1322.
119. McCue, A. J.; Guerrero-Ruiz, A.; Ramirez-Barria, C.; Rodríguez-Ramos, I.; Anderson, J. A. Selective Hydrogenation of Mixed Alkyne/Alkene Streams at Elevated Pressure Over a Palladium Sulfide Catalyst. *J. Catal.* **2017**, *355*, 40–52.
120. Zhou, S.; Kang, L.; Xu, Z.; Zhu, M. Catalytic Performance and Deactivation of Ni/MCM-41 Catalyst in the Hydrogenation of Pure Acetylene to Ethylene. *RSC Adv.* **2020**, *10*, 1937–1945.
121. Wang, Y.; Zheng, W.; Wang, B.; Ling, L.; Zhang, R. The Effects of Doping Metal Type and Ratio on the Catalytic Performance of C<sub>2</sub>H<sub>2</sub> Semi-Hydrogenation Over the Intermetallic Compound-Containing Pd Catalysts. *Chem. Eng. Sci.* **2021**, *229*, 116131.
122. Duraczynska, D.; Serwicka, E. M.; Drelinkiewicz, A.; Olejniczak, Z. Ruthenium (II) Phosphine/Mesoporous Silica Catalysts: The impact of Active Phase Loading and Active Site Density on Catalytic Activity in Hydrogenation of Phenylacetylene. *Appl. Catal., A Gen.* **2009**, *371*, 166–172.
123. Nikolaev, S. A.; Smirnov, V. V. Synergistic and Size Effects in Selective Hydrogenation of Alkynes on Gold. Nanocomposites. *Catal. Today* **2009**, *147S*, S336–S341.
124. da Silva, F. P.; Rossi, L. M. Palladium on Magnetite: Magnetically Recoverable Catalyst for Selective Hydrogenation of Acetylenic to Olefinic Compounds. *Tetrahedron* **2014**, *70*, 3314–3318.
125. Okhlopko, L. B.; Cherepanova, S. V.; Prosvirin, I. P.; Kerzhentsev, M. A.; Ismagilov, Z. R. Semihydrogenation of 2-Methyl-3-butyn-2-ol on Pd-Zn Nanoalloys: Effect of Composition and Heterogenization. *Appl. Catal. A Gen.* **2018**, *549*, 245–253.
126. Navarro-Fuentes, F.; Keane, M.; Ni, X.-W. The Effects of Modes of Hydrogen Input and Reactor Configuration on Reaction Rate and H<sub>2</sub> Efficiency in the Catalytic Hydrogenation of Alkynol to Alkenol. *Can. J. Chem. Eng.* **2020**, *98*, 308–315.
127. Panwar, V.; Kumar, A.; Singh, R.; Gupta, P.; Ray, S. S.; Jain, S. L. Nickel-Decorated Graphene Oxide/Polyaniline Hybrid: A Robust and Highly Efficient Heterogeneous Catalyst for Hydrogenation of Terminal Alkynes. *Ind. Eng. Chem. Res.* **2015**, *54*, 11493–11499.
128. Luneau, M.; Shirman, T.; Foucher, A. C.; Duanmu, K.; Verbart, D. M. A.; Sautet, P.; Stach, E. A.; Aizenberg, J.; Madix, R. J.; Friend, C. M. Achieving High Selectivity for Alkyne Hydrogenation at High Conversions With Compositionally Optimized PdAu Nanoparticle Catalysts in Raspberry Colloid-Templated SiO<sub>2</sub>. *ACS Catal.* **2020**, *10*, 441–450.

**138** Heterogeneous catalysis in sustainable synthesis

129. Ueberbacher, B. J.; Osprian, I.; Mayer, S. F.; Faber, K. A. Chemoenzymatic, Enantioconvergent, Asymmetric Total Synthesis of (*R*)-Fridamycin E. *Eur. J. Org. Chem.* **2005**, 2005, 1266–1270.
130. Shen, L.; Mao, S.; Li, J.; Li, M.; Chen, P.; Li, H.; Chen, Z.; Wang, Y. PdZn Intermetallic on a CN@ZnO Hybrid as an Efficient Catalyst for the Semihydrogenation of Alkynols. *J. Catal.* **2017**, 350, 13–20.
131. Piccolo, L.; Kibis, L.; De Weerd, M.-C.; Gaudry, E.; Ledieu, J.; Fournée, V. Intermetallic Compounds as Potential Alternatives to Noble Metals in Heterogeneous Catalysis: The Partial Hydrogenation of Butadiene on g-Al<sub>3</sub>Cu<sub>9</sub>(110). *ChemCatChem* **2017**, 9, 2292–2296.
132. Camacho-Bunquin, J.; Ferrandon, M.; Sohn, H.; Yang, D.; Liu, C.; Ignacio-de Leon, P. E.; Perras, F. A.; Pruski, M.; Stair, P. C.; Delferro, M. Chemoselective Hydrogenation With Supported Organoplatinum(IV) Catalyst on Zn(II)-Modified Silica. *J. Am. Chem. Soc.* **2018**, 140, 3940–3951.
133. Miyazaki, M.; Furukawa, S.; Komatsu, T. Regio- and Chemoselective Hydrogenation of Dienes to Monoenes Governed by a Well-Structured Bimetallic Surface. *J. Am. Chem. Soc.* **2017**, 139, 18231–18239.
134. Miao, S.; Liu, Z.; Han, B.; Huang, J.; Sun, Z.; Zhang, J.; Jiang, T. Ru Nanoparticles Immobilized on Montmorillonite by Ionic Liquids: A Highly Efficient Heterogeneous Catalyst for the Hydrogenation of Benzene. *Angew. Chem. Int. Ed.* **2006**, 45, 266–269.
135. Su, F.; Yin Lee, F.; Lv, L.; Liu, J.; Ning Tian, X.; Song Zhao, X. Sandwiched Ruthenium/Carbon Nanostructures for Highly Active Heterogeneous Hydrogenation. *Adv. Funct. Mater.* **2007**, 17, 1926–1931.
136. Su, F.; Lv, L.; Yin Lee, F.; Liu, T.; Cooper, A. I.; Song Zhao, X. Thermally Reduced Ruthenium Nanoparticles as a Highly Active Heterogeneous Catalyst for Hydrogenation of Monoaromatics. *J. Am. Chem. Soc.* **2007**, 129, 14213–14223.
137. Nowicki, A.; Zhang, Y.; Léger, B.; Rolland, J.; Bricout, H.; Monflier, E.; Roucoux, A. Supramolecular Shuttle and Protective Agent: A Multiple Role of Methylated Cyclodextrins in the Chemoselective Hydrogenation of Benzene Derivatives With Ruthenium Nanoparticles. *Chem. Commun.* **2006**, 296–298.
138. Barbaro, P.; Bianchini, C.; Dal Santo, V.; Meli, A.; Moneti, S.; Psaro, R.; Scaffidi, A.; Sordelli, L.; Vizza, F. Hydrogenation of Arenes Over Silica-Supported Catalysts That Combine a Grafted Rhodium Complex and Palladium Nanoparticles: Evidence for Substrate Activation on Rh Single-Site-Pd Metal Moieties. *J. Am. Chem. Soc.* **2006**, 128, 7065–7076.
139. Maegawa, T.; Akashi, A.; Sajiki, H. A Mild and Facile Method for Complete Hydrogenation of Aromatic Nuclei in Water. *Synlett* **2006**, 1440–1442.
140. Denicourt-Nowicki, A.; Roucoux, A.; Wyrwalski, F.; Kania, N.; Monflier, E.; Ponchel, A. Carbon-Supported Ruthenium Nanoparticles Stabilized by Methylated Cyclodextrins: A New Family of Heterogeneous Catalysts for the Gas-Phase Hydrogenation of Arenes. *Chem. A Eur. J.* **2008**, 14, 8090–8093.
141. Maegawa, T.; Akashi, A.; Yaguchi, K.; Iwasaki, Y.; Shigetsura, M.; Monguchi, Y.; Sajiki, H. Efficient and Practical Arene Hydrogenation by Heterogeneous Catalysts Under Mild Conditions. *Chem. A Eur. J.* **2009**, 15, 6953–6963.
142. Anderson, J.; Athawale, A.; Imrie, F.; McKenna, F.; McCue, A.; Molyneux, D.; Power, K.; Shand, M.; Wells, R. P. K. Aqueous Phase Hydrogenation of Substituted Phenyls Over Carbon Nanofibre and Activated Carbon Supported Pd. *J. Catal.* **2010**, 270, 9–15.
143. Park, K.; Jang, K.; Jin Kim, H.; Uk Son, S. Near-Monodisperse Tetrahedral Rhodium Nanoparticles on Charcoal: The Shape-Dependent Catalytic Hydrogenation of Arenes. *Angew. Chem. Int. Ed.* **2007**, 46, 1152–1155.

144. Cheng, Y.; Fan, H.; Wu, S.; Wang, Q.; Guo, J.; Gao, L.; Zong, B.; Han, B. Enhancing the Selectivity of the Hydrogenation of Naphthalene to Tetralin by High Temperature Water. *Green Chem.* **2009**, *11*, 1061–1065.
145. Anderson, J. A.; McKenna, F.; Linares-Solano, A.; Wells, R. P. K. Use of Water as a Solvent in Directing Hydrogenation Reactions of Aromatic Acids Over Pd/carbon Nanofibre Catalysts. *Catal. Lett.* **2007**, *119*, 16–20.
146. Solladié-Cavallo, A.; Baram, A.; Choucair, E.; Norouzi-Arasi, H.; Schmitt, M.; Garin, F. Heterogeneous Hydrogenation of Substituted Phenols Over Al<sub>2</sub>O<sub>3</sub> Supported Ruthenium. *J. Mol. Catal. A: Chem.* **2007**, *273*, 92–98.
147. Xin, J.; Lu, L.; Wang, Y.; Peng, X. Regioselective Hydrogenation of *p*-Phenylphenol to *p*-Cyclohexylphenol Over Pd/C Catalyst in THF Solvent. *Catal. Commun.* **2008**, *9*, 2345–2348.
148. Wang, H.; Zhao, F.; Fujita, S.; Arai, M. Hydrogenation of Phenol in scCO<sub>2</sub> Over Carbon Nanofiber Supported Rh Catalyst. *Catal. Commun.* **2008**, *9*, 362–368.
149. Makowski, P.; Demir Cakan, R.; Antonietti, M.; Goettmann, F.; Titirici, M. Selective Partial Hydrogenation of Hydroxy Aromatic Derivatives With Palladium Nanoparticles Supported on Hydrophilic Carbon. *Chem. Commun.* **2008**, 999–1001.
150. Liu, H.; Jiang, T.; Han, B.; Liang, S.; Zhou, Y. Selective Phenol Hydrogenation to Cyclohexanone Over a Dual Supported Pd–Lewis Acid Catalyst. *Science* **2009**, *326*, 1250–1252.
151. Tan, S.; Liu, G.; Gao, X.; Thiemann, T. Raney Ni–Al Alloy-Mediated Reduction of Alkylated Phenols in Water. *J. Chem. Res.* **2009**, *2009*, 5–7.
152. Li, Y.; Liu, J.; He, J.; Wang, L.; Lei, J. Silica/Titania Composite-Supported NiCo Catalysts With Combined Catalytic Effects for Phenol Hydrogenation Under Fast and Mild Conditions. *Appl. Catal. A Gen.* **2020**, *591*, 117409.
153. Harada, T.; Ikeda, S.; Hau Ng, Y.; Sakata, T.; Mori, H.; Torimoto, T.; Matsumura, M. Rhodium Nanoparticle Encapsulated in a Porous Carbon Shell as an Active Heterogeneous Catalyst for Aromatic Hydrogenation. *Adv. Funct. Mater.* **2008**, *18*, 2190–2196.
154. Takasaki, M.; Motoyama, Y.; Yoon, S.; Mochida, I.; Nagashima, H. Highly Efficient Synthesis of Optically Pure 5,5',6,6',7,7',8,8'-Octahydro-1,1'-Bi-2-Naphthol and -Naphthylamine Derivatives by Partial Hydrogenation of 1,1'-Binaphthyls With Carbon Nanofiber Supported Ruthenium Nanoparticles. *J. Org. Chem.* **2008**, *72*, 10291–10293.
155. Heumann, L.; Keck, G. A New Method for the Synthesis of H<sub>4</sub>-BINOL. *J. Org. Chem.* **2008**, *73*, 4725–4727.
156. Li, X.; Ding, Q.; Ge, J.; Xie, J.; Xu, D. A Convenient Synthesis of (*S*)-H<sub>4</sub>-BINOL and Its Derivatives Via Hydrogenation of Monoesters of BINOL. *J. Org. Chem.* **2009**, *74*, 1785–1787.
157. Guo, H.; Ding, K. Reduction of 1,1'-Binaphthyls to Octahydro-1,1'-Binaphthyl Derivatives With Raney Ni–Al Alloy in Aqueous Solution. *Tetrahedron Lett.* **2000**, *41*, 10061–10064.
158. Shen, X.; Guo, H.; Ding, K. The Synthesis of a Novel Non-C<sub>2</sub> Symmetric H<sub>4</sub>-BINOL Ligand and its Application to Titanium-Catalyzed Enantioselective Addition of Diethylzinc to Aldehydes. *Tetrahedron* **2000**, *11*, 4321–4327.
159. Lu, L.; Rong, Z.; Du, W.; Ma, S.; Hu, S. Selective Hydrogenation of Single Benzene Ring in Biphenyl Catalyzed by Skeletal Ni. *ChemCatChem* **2009**, *1*, 369–371.
160. Tsukinoki, T.; Kanda, T.; Liu, G.; Tsuzuki, H.; Tashiro, M. Organic Reaction in Water. Part 3: A Facile Method for Reduction of Aromatic Rings Using A Raney Ni–Al Alloy in Dilute Aqueous Alkaline Solution Under Mild Conditions. *Tetrahedron Lett.* **2000**, *41*, 5865–5868.
161. Török, B.; Abid, M.; London, G.; Esquibel, J.; Török, M.; Mhadgut, S. C.; Yan, P.; Prakash, G. K. S. Highly Enantioselective Organocatalytic Hydroxyalkylation of Indoles With Ethyl Trifluoropyruvate. *Angew. Chem. Int. Ed.* **2005**, *44*, 3086–3089.

140 Heterogeneous catalysis in sustainable synthesis

162. Török, M.; Abid, M.; Mhadgut, S. C.; Török, B. Organofluorine Inhibitors of Amyloid Fibrillogenesis. *Biochemistry* **2006**, *45*, 5377–5383.
163. Török, B.; Sood, A.; Bag, S.; Kulkarni, A.; Borkin, D.; Lawler, E.; Dasgupta, S.; Landge, S. M.; Abid, M.; Zhou, W.; Foster, M.; LeVine, H., III; Török, M. Structure–Activity Relationships of Organofluorine Inhibitors of  $\beta$ -Amyloid Self-Assembly. *ChemMedChem* **2012**, *7*, 910–919.
164. Jiang, C.; Frontier, A. J. Stereoselective Synthesis of Pyrrolidine Derivatives *Via* Reduction of Substituted Pyrroles. *Org. Lett.* **2007**, *9*, 4939–4942.
165. Kuhn, J.; Huang, W.; Tsung, C.; Zhang, Y.; Somorjai, G. A. Structure Sensitivity of Carbon-Nitrogen Ring Opening: Impact of Platinum Particle Size From Below 1 to 5 nm Upon Pyrrole Hydrogenation Product Selectivity Over Monodisperse Platinum Nanoparticles Loaded Onto Mesoporous Silica. *J. Am. Chem. Soc.* **2008**, *130*, 14026–14027.
166. Merlo, A.; Vetere, V.; Ruggera, J.; Casella, M. Bimetallic PtSn Catalyst for the Selective Hydrogenation of Furfural to Furfuryl Alcohol in Liquid-Phase. *Catal. Commun.* **2009**, *10*, 1665–1669.
167. Wang, J.; Wei, Q.; Ma, Q.; Guo, Z.; Qina, F.; Ismagilov, Z. R.; Shen, W. Constructing Co@N-Doped Graphene Shell Catalyst Via Mott-Schottky Effect for Selective Hydrogenation of 5-Hydroxymethylfurfural. *Appl. Catal. Environ.* **2020**, *263*, 118339.
168. Sebek, M.; Holz, J.; Börner, A.; Jähnisch, K. Highly Distereoselective Hydrogenation of Furan-2-Carboxylic Acid Derivatives on Heterogeneous Catalysts. *Synlett* **2009**, *2009*, 461–465.
169. Cheng, C.; Xu, J.; Zhu, R.; Xing, L.; Wang, X.; Hu, Y. A Highly Efficient Pd–C Catalytic Hydrogenation of Pyridine Nucleus Under Mild Conditions. *Tetrahedron* **2009**, *65*, 8538–8541.
170. Schmidt, E.; Kleist, W.; Krumeich, F.; Mallat, T.; Baiker, A. Platinum Nanoparticles: The Crucial Role of Crystal Face and Colloid Stabilizer in the Diastereoselective Hydrogenation of Cinchonidine. *Chem. A Eur. J.* **2010**, *16*, 2181–2192.
171. Török, B.; Balázsik, K.; Török, M.; Felföldi, K.; Bartók, M. Heterogeneous Asymmetric Reactions 20. Effect of Ultrasonic Variables on the Enantiodifferentiation of Cinchona-Modified Platinum-Catalyzed Sonochemical Hydrogenations. *Catal. Lett.* **2002**, *81*, 55–62.
172. Irfan, M.; Petricci, E.; Glasnov, T.; Taddei, M.; Kappe, C. O. Continuous Flow Hydrogenation of Functionalized Pyridines. *Eur. J. Org. Chem.* **2009**, *2009*, 1327–1334.
173. Lunn, G.; Sansone, E. B. Facile Reduction of Pyridines With Nickel-Aluminum Alloy. *J. Org. Chem.* **1986**, *51*, 513–517.
174. Lunn, G. Preparation of Piperidinylpyridines Via Selective Reduction of Bipyridines With Nickel-Aluminum Alloy. *J. Org. Chem.* **1992**, *57*, 6317–6320.
175. El Sayed, S.; Bordet, A.; Weidenthaler, C.; Hetaba, W.; Luska, K. L.; Leitner, W. Selective Hydrogenation of Benzofurans Using Ruthenium Nanoparticles in Lewis Acid-Modified Ruthenium-Supported Ionic Liquid Phases. *ACS Catal.* **2020**, *10*, 2124–2130.
176. Cho, H.; Török, F.; Török, B. Selective Reduction of Condensed N-Heterocycles Using Water as a Solvent and a Hydrogen Source. *Org. Biomol. Chem.* **2013**, *11*, 1209–1215.
177. Luche, J. L. *Synthetic Organic Sonochemistry*; Plenum Press: New York, 1998.
178. Török, B.; Balázsik, K.; Felföldi, K.; Bartók, M. Asymmetric Reactions in Sonochemistry. *Ultrason. Sonochem.* **2001**, *8*, 191–200.
179. Guo, Y.; He, H.; Liu, X.; Chen, Z.; Rioux, R. M.; Janik, M. J.; Savage, P. E. Ring-Opening and Hydrodenitrogenation of Indole Under Hydrothermal Conditions Over Ni, Pt, Ru, and Ni-Ru Bimetallic Catalysts. *Chem. Eng. J.* **2021**, *406*, 126853.

180. Kulkarni, A.; Zhou, W.; Török, B. Heterogeneous Catalytic Hydrogenation of Unprotected In-Doles in Water: A Green Solution to a Long-Standing Challenge. *Org. Lett.* **2011**, *13*, 5124–5127.
181. Kulkarni, A.; Gianatassio, R.; Török, B. Pd/C Catalyzed Reductive Formylation of Indoles and Quinolines Using Formic Acid. *Synthesis* **2011**, *2011*, 1227–1237.
182. Lenarda, M.; Casagrande, M.; Moretti, E.; Storaro, L.; Frattini, R.; Polizzi, S. Selective Catalytic Low Pressure Hydrogenation of Acetophenone on Pd/ZnO/ZnAl<sub>2</sub>O<sub>4</sub>. *Catal. Lett.* **2007**, *114*, 79–84.
183. Tomin, A.; Lazarev, A.; Bere, M. P.; Redjeb, H.; Török, B. Selective Reduction of Ketones Using Water as a Hydrogen Source Under High Hydrostatic Pressure. *Org. Biomol. Chem.* **2012**, *10*, 7321–7326.
184. Reddy, B. M.; Rao, K. N.; Reddy, G. K. Controlled Hydrogenation of Acetophenone Over Pt/CeO<sub>2</sub>-MO<sub>x</sub> (M = Si, Ti, Al, and Zr) Catalysts. *Catal. Lett.* **2009**, *131*, 328–336.
185. Menegazzo, F.; Canton, P.; Pinna, F.; Pernicone, N. Bimetallic Pd–Au Catalysts for Benzaldehyde Hydrogenation: Effects of Preparation and of Sulfur Poisoning. *Catal. Commun.* **2008**, *9*, 2353–2356.
186. Li, X.; Shen, Y.; Song, L.; Wang, H.; Wu, H.; Liu, Y.; Wu, P. Efficient Hydrogenation of Benzaldehydes Over Mesopolymer-Entrapped Pt Nanoparticles in Water. *Chem. Asian J.* **2009**, *4*, 699–706.
187. Kong, X.; Chen, L. Chemoselective Hydrogenation of Aromatic Aldehydes Over SiO<sub>2</sub> Modified Co/γ-Al<sub>2</sub>O<sub>3</sub>. *Appl. Catal. A. Gen.* **2014**, *476*, 34–38.
188. Singh, N.; Sanyal, U.; Ruehl, G.; Stoerzinger, K. A.; Gutiérrez, O. Y.; Camaioni, D. M.; Fulton, J. L.; Lercher, J. A.; Campbell, C. T. Aqueous Phase Catalytic and Electrocatalytic Hydrogenation of Phenol and Benzaldehyde Over Platinum Group Metals. *J. Catal.* **2020**, *382*, 372–384.
189. Ji, H.; Huang, Y.; Pei, L.; Yao, X. Supported RuB Amorphous Alloy Mediated 1 atm Hydrogenation of Carbonyl Compounds Under Ambient Temperature. *Catal. Commun.* **2008**, *9*, 27–34.
190. Bordoloi, A.; Amrute, A. P.; Halligudi, S. B. [Ru(salen)(NO)] complex encapsulated in mesoporous SBA-16 as catalyst for hydrogenation of ketones. *Catal. Commun.* **2008**, *10*, 45–48.
191. Alonso, F.; Riente, P.; Yus, M. Hydrogen-Transfer Reduction of Carbonyl Compounds Catalysed by Nickel Nanoparticles. *Tetrahedron Lett.* **2008**, *49*, 1939–1942.
192. Suceveanu, M.; Raicopol, M.; Enache, R.; Finaru, A.; Rosca, S. I. Selective Reductions of the Carbonyl Compounds and Aryl Halides With Ni-Al Alloy in Aqueous Alkali Medium. *Lett. Org. Chem.* **2011**, *8*, 690–695.
193. Deshmukh, A. A.; Kinage, A. K.; Kumar, R. Highly Chemoselective Catalytic System for Hydrogenation of Diketones to Ketols: An Environmentally Benevolent System. *Catal. Lett.* **2008**, *120*, 257–260.
194. Erathodiyil, N.; Ooi, S.; Seayad, A. M.; Han, Y.; Lee, S. S.; Ying, J. Y. Palladium Nanoclusters Supported on Propylurea-Modified Siliceous Mesocellular Foam for Coupling and Hydrogenation Reactions. *Chem. A Eur. J.* **2008**, *14*, 3118–3125.
195. Kawamorita, S.; Hamasaka, G.; Ohmiya, H.; Hara, K.; Fukuoka, A.; Sawamura, M. Hydrogenation of Hindered Ketones Catalyzed by a Silica-Supported Compact Phosphine-Rh System. *Org. Lett.* **2008**, *10*, 4697–4700.
196. Ras, E.; Maisuls, S.; Haesackers, P.; Gruter, G.; Rothenberg, G. Selective Hydrogenation of 5-Ethoxymethylfurfural Over Alumina-Supported Heterogeneous Catalysts. *Adv. Synth. Catal.* **2009**, *351*, 3175–3185.

142 Heterogeneous catalysis in sustainable synthesis

197. He, L.; Ni, J.; Wang, L.; Yu, F.; Cao, Y.; He, H.; Fan, K. Aqueous Room-Temperature Gold-Catalyzed Chemoselective Transfer Hydrogenation of Aldehydes. *Chem. A Eur. J.* **2009**, *15*, 11833–11836.
198. Lázaro, N.; Franco, A.; Ouyang, W.; Balu, A. M.; Romero, A. A.; Luque, R.; Pineda, A. Continuous-Flow Hydrogenation of Methyl Levulinate Promoted by Zr-Based Mesoporous Materials. *Catalysts* **2019**, *9*, 142.
199. Hanna, D. G.; Shylesh, S.; Parada, P. A.; Bell, A. T. Hydrogenation of Butanal Over Silica-Supported Shvo's Catalyst and its Use for the Gas-Phase Conversion of Propene to Butanol Via Tandem Hydroformylation and Hydrogenation. *J. Catal.* **2014**, *311*, 52–58.
200. Martin, E. L. The Clemmensen Reduction. *Org. React.* **1942**, *1*, 155–209.
201. Todd, D. The Wolff-Kishner Reduction. *Org. React.* **1948**, *4*, 378–422.
202. Hutchins, R. O. Reduction of C=X to CH<sub>2</sub> by Wolff-Kishner and Other Hydrazone Methods. In *Comprehensive Org. Synth*; Trost, B. M., Fleming, I., Eds.; 8; Pergamon: Oxford, 1991; p. 327.
203. Ishimoto, K.; Mitoma, Y.; Nagashima, A.; Tashiro, H.; Prakash, G. K. S.; Olah, G. A.; Tashiro, M. Reduction of Carbonyl Groups to the Corresponding Methylenes With Ni–Al Alloy in Water. *Chem. Commun.* **2003**, 514–515.
204. Miyazawa, A.; Tashiro, M.; Prakash, G. K. S.; Olah, G. A. Microwave-Assisted Reduction of Acetophenones Using Ni–Al Alloy in Water. *Bull. Chem. Soc. Jpn.* **2006**, *79*, 791–792.
205. Török, B.; London, G.; Bartók, M. Reduction of Carbonyl Compounds to Hydrocarbons by Catalytic Hydrogenation: A Novel One-Pot Method Using Pt/K-10 Montmorillonite Catalyst. *Synlett* **2000**, 631–632.
206. Liu, G.; Zhao, H.; Zhu, J.; He, H.; Yang, H.; Thiemann, T.; Tashiro, H.; Tashiro, M. New Method for the Reduction of Benzophenones With Raney Ni–Al Alloy in Water. *Synth. Commun.* **2008**, *38*, 1651–1661.
207. Liu, G.; Zhao, H.; Dai, L.; Thiemann, T.; Tashiro, H.; Tashiro, M. Raney Ni–Al Alloy-Mediated Reduction of Benzils in Water. *J. Chem. Res.* **2009**, 579–581.
208. Iablokov, V.; Kruse, N. Discovery of a Fischer-Tropsch Hybrid Reaction: Hydrogenation of Methylformate to Long-Chain Hydrocarbons With Anderson-Schulz-Flory Chain Length Distribution. *ChemCatChem* **2019**, *11*, 1200–1204.
209. Fonseca Benítez, C. A.; Mazzieri, V.; Sánchez, M. A.; Benitez, V. M.; Pieck, C. L. Selective Hydrogenation of Oleic Acid to Fatty Alcohols on Rh-Sn-B/Al<sub>2</sub>O<sub>3</sub> Catalysts. Influence of Sn Content. *Appl. Catal. A. Gen.* **2019**, *584*, 117149.
210. Heisig, C.; Dienenhoven, J.; Jensen, C.; Gehrke, H.; Turek, T. Selective Hydrogenation of Biomass-Derived Succinic Acid: Reaction Network and Kinetics. *Chem. Eng. Technol.* **2020**, *43*, 1–10.
211. Chen, H.; Xu, Q.; Zhang, D.; Liu, W.; Liu, X.; Yin, D. Highly Efficient Synthesis of  $\gamma$ -Valerolactone by Catalytic Conversion of Biomass-Derived Levulinate Esters Over Support-Free Mesoporous Ni. *Renew. Energy* **2021**, *163*, 1023–1032.
212. Zuo, M.; Jia, W.; Feng, Y.; Zeng, X.; Tang, X.; Sun, Y.; Lin, L. Effective Selectivity Conversion of Glucose to Furan Chemicals in the Aqueous Deep Eutectic Solvent. *Renew. Energy* **2021**, *164*, 23–33.
213. Aho, A.; Engblom, S.; Eranen, K.; Russo, V.; Maki-Arvela, P.; Kumar, N.; Warna, J.; Salmi, T.; Murzin, D. Y. Glucose Transformations Over a Mechanical Mixture of ZnO and Ru/C Catalysts: Product Distribution, Thermodynamics and Kinetics. *Chem. Eng. J.* **2021**, *405*, 126945.
214. Dokania, A.; Ramirez, A.; Bavykina, A.; Gascon, J. Heterogeneous Catalysis for the Valorization of CO<sub>2</sub>: Role of Bifunctional Processes in the Production of Chemicals. *ACS Energy Lett.* **2019**, *4*, 167–176.

215. Álvarez, A.; Bansode, A.; Urakawa, A.; Bavykina, A. V.; Wezendonk, T. A.; Makkee, M.; Gascon, J.; Kapteijn, F. Challenges in the Greener Production of Formates/Formic Acid, Methanol, and DME by Heterogeneously Catalyzed CO<sub>2</sub> Hydrogenation Processes. *Chem. Rev.* **2017**, *117*, 9804–9838.
216. Dinh, C.-T.; Burdyny, T.; Kibria, M. G.; Seifitokaldani, A.; Gabardo, C. M.; García de Arquer, F. P.; Kiani, A.; Edwards, J. P.; De Luna, P.; Bushuyev, O. S.; Zou, C.; Quintero-Bermudez, R.; Pang, Y.; Sinton, D.; Sargent, E. H. CO<sub>2</sub> Electroreduction to Ethylene Via Hydroxide-Mediated Copper Catalysis at an Abrupt Interface. *Science* **2018**, *360*, 783–787.
217. Yang, H.; Zhang, C.; Gao, P.; Wang, H.; Li, X.; Zhong, L.; Wei, W.; Sun, Y. A Review of the Catalytic Hydrogenation of Carbon Dioxide Into Value-Added Hydrocarbons. *Cat. Sci. Technol.* **2017**, *7*, 4580–4598.
218. Li, W.; Wang, H.; Jiang, X.; Zhu, J.; Liu, Z.; Guo, X.; Song, C. A Short Review of Recent Advances in CO<sub>2</sub> Hydrogenation to Hydrocarbons Over Heterogeneous Catalysts. *RSC Adv.* **2018**, *8*, 7651–7669.
219. Ni, Y.; Chen, Z.; Fu, Y.; Liu, Y.; Zhu, W.; Liu, Z. Selective Conversion of CO<sub>2</sub> and H<sub>2</sub> Into Aromatics. *Nat. Commun.* **2018**, *9*, 3457.
220. Shadravan, V.; Bukas, V. J.; Gunasooriya, G. T. K. K.; Waleson, J.; Drewery, M.; Karibika, J.; Jones, J.; Kennedy, E.; Adesina, A.; Nørskov, J. K.; Stockenhuber, M. Effect of Manganese on the Selective Catalytic Hydrogenation of COX in the Presence of Light Hydrocarbons Over Ni/Al<sub>2</sub>O<sub>3</sub>: An Experimental and Computational Study. *ACS Catal.* **2020**, *10*, 1535–1547.
221. Bahmanpour, A. M.; Héroguel, F.; Kılıç, M.; Baranowski, C. J.; Schouwink, P.; Röthlisberger, U.; Luterbacher, J. S.; Kröcher, O. Essential Role of Oxygen Vacancies of Cu-Al and Co-Al Spinel Oxides in Their Catalytic Activity for the Reverse Water Gas Shift Reaction. *Appl. Catal. Environ.* **2020**, *266*, 118669.
222. Hui, Y.; Ullah, N.; Zhang, L.; Li, Z. CO<sub>2</sub> Methanation Over Nickel-Based Catalysts Prepared by Citric Acid Complexation Method. *Appl. Organomet. Chem.* **2020**, *34*, e5268.
223. Ahmad, W.; Chan, F. L.; Chaffee, A. L.; Wang, H.; Hoadley, A.; Tanksale, A. Dimethoxymethane Production via Catalytic Hydrogenation of Carbon Monoxide in Methanol Media. *ACS Sustain. Chem. Eng.* **2020**, *8*, 2081–2092.
224. Bonura, G.; Khassin, A. A.; Yurieva, T. M.; Cannilla, C.; Frusteri, F.; Frusteri, L. Structure Control on Kinetics of Copper Reduction in Zr-Containing Mixed Oxides During Catalytic Hydrogenation of Carbon Oxides to Methanol. *Catal. Today* **2020**, *342*, 39–45.
225. Podrojkova, N.; Sans, V.; Oriňak, A.; Oriňakova, R. Recent Developments in the Modelling of Heterogeneous Catalysts for CO<sub>2</sub> Conversion to Chemicals. *ChemCatChem* **2020**, *12*, 1802–1825.
226. Cimino, S.; Boccia, F.; Lisi, L. Effect of Alkali Promoters (Li, Na, K) on the Performance of Ru/Al<sub>2</sub>O<sub>3</sub> Catalysts for CO<sub>2</sub> Capture and Hydrogenation to Methane. *J. CO<sub>2</sub> Util.* **2020**, *37*, 195–203.
227. Jiang, H.; Lin, J.; Wu, X.; Wang, W.; Chen, Y.; Zhang, M. Efficient Hydrogenation of CO<sub>2</sub> to Methanol Over Pd/In<sub>2</sub>O<sub>3</sub>/SBA-15 Catalysts. *J. CO<sub>2</sub> Util.* **2020**, *36*, 33–39.
228. Tshuma, P.; Makhubela, B. C. E.; Öhrström, L.; Bourne, S. A.; Chatterjee, N.; Beas, I. N.; Darkwa, J.; Mehlana, G. Cyclometalation of Lanthanum(III) Based MOF for Catalytic Hydrogenation of Carbon Dioxide to Formate. *RSC Adv.* **2020**, *10*, 3593–3605.
229. Siakavelas, G. I.; Charisiou, N. D.; AlKhoori, S.; AlKhoori, A. A.; Sebastian, V.; Hinder, S. J.; Baker, M. A.; Yentekakis, I. V.; Polychronopoulou, K.; Goula, M. A. Highly Selective and Stable Nickel Catalysts Supported on Ceria Promoted With Sm<sub>2</sub>O<sub>3</sub>, Pr<sub>2</sub>O<sub>3</sub> and MgO for the CO<sub>2</sub> Methanation. *Appl. Catal. B. Environ.* **2021**, *282*, 119562.

**144** Heterogeneous catalysis in sustainable synthesis

230. Zhua, M.; Tian, P.; Cao, X.; Chen, J.; Pu, T.; Shi, B.; Xu, J.; Moon, J.; Wu, Z.; Han, Y.-F. Vacancy Engineering of the Nickel-Based Catalysts for Enhanced CO<sub>2</sub> Methanation. *Appl. Catal. B. Environ.* **2021**, *282*, 119561.
231. Lonis, F.; Tola, V.; Cau, G. Assessment of Integrated Energy Systems for the Production and Use of Renewable Methanol by Water Electrolysis and CO<sub>2</sub> Hydrogenation. *Fuel* **2021**, *285*, 119160.
232. Chaipraditgul, N.; Numpilai, T.; Kui Cheng, C.; Siri-Nguan, N.; Sornchamni, T.; Wattanakit, C.; Limtrakul, J.; Witoon, T. Tuning Interaction of Surface-Adsorbed Species Over Fe/K-Al<sub>2</sub>O<sub>3</sub> Modified With Transition Metals (Cu, Mn, V, Zn or Co) on Light Olefins Production From CO<sub>2</sub> Hydrogenation. *Fuel* **2021**, *283*, 119248.
233. Yang, Q.; Skrypnik, A.; Matvienko, A.; Lund, H.; Holena, M.; Kondratenko, E. V. Revealing Property-Performance Relationships for Efficient CO<sub>2</sub> Hydrogenation to Higher Hydrocarbons Over Fe-Based Catalysts: Statistical Analysis of Literature Data and its Experimental Validation. *Appl. Catal. B. Environ.* **2021**, *282*, 119554.
234. Török, B.; Felföldi, K.; Szakonyi, G.; Balázsik, K.; Bartók, M. Enantiodifferentiation in Asymmetric Sonochemical Hydrogenations. *Catal. Lett.* **1998**, *52*, 81–84.
235. Bartók, M.; Felföldi, K.; Török, B.; Bartók, T. A New Cinchona-Modified Platinum Catalyst for the Enantioselective Hydrogenation of Pyruvate: The Structure of the 1:1 Alkaloid-Reactant Complex. *Chem. Commun.* **1998**, 2605–2606.
236. Török, B.; Felföldi, K.; Balázsik, K.; Bartók, M. New Synthesis of a Useful C<sub>3</sub> Chiral Building Block by Heterogeneous Method: Enantioselective Hydrogenation of Methylglyoxal 1,1-Dimethyl Acetal Over Cinchona Modified Pt/Al<sub>2</sub>O<sub>3</sub> Catalysts. *Chem. Commun.* **1999**, 1725–1726.
237. Török, B.; Balázsik, K.; Felföldi, K.; Bartók, M. Effect of Medium and Coacid Acidity on the Cinchona-Modified Pt-Catalyzed Enantioselective Hydrogenations. *Stud. Surf. Sci. Catal.* **2000**, *130*, 3381–3386.
238. Balázsik, K.; Szöri, K.; Felföldi, K.; Török, B.; Bartók, M. Asymmetric Synthesis of Alkyl 5-Oxo-Tetrahydrofuran-2-Carboxylates by Enantioselective Hydrogenation of Dialkyl 2-Oxoglutarates Over Cinchona Modified Pt/Al<sub>2</sub>O<sub>3</sub> Catalysts. *Chem. Commun.* **2000**, 555–556.
239. Bartók, M.; Török, B.; Balázsik, K.; Bartók, T. Enantioselective Hydrogenation of Ethyl Pyruvate Over Cinchonine and  $\alpha$ -Isocinchonine Modified Platinum Catalysts. *Catal. Lett.* **2001**, *73*, 127–131.
240. Blaser, H. U.; Jalett, H. P.; Garland, M.; Studer, M.; Thies, H.; Wirth-Tijani, A. Kinetic Studies of the Enantioselective Hydrogenation of Ethyl Pyruvate Catalyzed by a Cinchona Modified Pt/Al<sub>2</sub>O<sub>3</sub> Catalyst. *J. Catal.* **1998**, *173*, 282–294.
241. Solladié-Cavallo, A.; Marsol, C.; Azyat, K.; Roje, M.; Welch, C.; Chilenski, J.; Taillisson, P.; D'Orchymont, H. Enantiopure (9-Anthryl)(2-Piperidyl)- and (9-Anthryl)(2-Pyridyl)Methanols—Their Use as Chiral Modifiers for Heterogeneous Hydrogenation of Keto Esters Over Pt/Al<sub>2</sub>O<sub>3</sub>. *Eur. J. Org. Chem.* **2007**, 826–830.
242. Schmidt, E.; Vargas, A.; Mallat, T.; Baiker, A. Shape-Selective Enantioselective Hydrogenation on Pt Nanoparticles. *J. Am. Chem. Soc.* **2009**, *131*, 12358–12367.
243. Hoxha, F.; van Vegten, N.; Urakawa, A.; Krumeich, F.; Mallat, T.; Baiker, A. Remarkable Particle Size Effect in Rh-Catalyzed Enantioselective Hydrogenations. *J. Catal.* **2009**, *261*, 224–231.
244. Tai, A.; Kikukawa, T.; Sugimura, T.; Inoue, Y.; Abe, S.; Osawa, T. Harada, An Improved Asymmetrically-Modified Nickel Catalyst Prepared From Ultrasonicated Raney Nickel. *Bull. Chem. Soc. Jpn.* **1994**, *67*, 2473–2477.

245. Sugimura, T.; Osawa, T.; Nakagawa, S.; Harada, T.; Tai, A. Stereochemical Studies of the Enantio-Differentiating Hydrogenation of Various Prochiral Ketones Over Tartaric Acid-Modified Nickel Catalyst. *Stud. Surf. Sci. Catal.* **1996**, *101*, 231–240.
246. Nakagawa, S.; Sugimura, T.; Tai, A. Almost Perfect Enantio-Differentiating Hydrogenation of Methyl 3-Cyclopropyl-3-Oxopropanoate Over Tartaric Acid Modified Raney Nickel Catalyst. *Chem. Lett.* **1997**, *26*, 859–860.
247. Nakagawa, S.; Sugimura, T.; Tai, A. A Substrate Specific Chiral Modifier Activation on Enantio-Differentiating Hydrogenation Over Tartaric Acid-Modified Raney Nickel. *Chem. Lett.* **1998**, *27*, 1257–1258.
248. Jiang, H.; Yang, C.; Li, C.; Fu, H.; Chen, H.; Li, R.; Li, X. Heterogeneous Enantioselective Hydrogenation of Aromatic Ketones Catalyzed by Cinchona- and Phosphine-Modified Iridium Catalysts. *Angew. Chem. Int. Ed.* **2008**, *47*, 9240–9244.
249. Bykov, A.; Matveeva, V.; Sulman, M.; Valetskiy, P.; Tkachenko, O.; Kustov, L.; Bronstein, L.; Sulman, E. Enantioselective Catalytic Hydrogenation of Activated Ketones Using Polymer-Containing Nanocomposites. *Catal. Today* **2009**, *140*, 64–69.
250. Török, B.; Balázsik, K.; Szöllösi, G.; Felföldi, K.; Bartók, M. Ultrasonics in Asymmetric Syntheses. Sonochemical Enantioselective Hydrogenation of Prochiral C=O Groups Over Platinum Catalysts. *Chirality* **1999**, *11*, 470–474.
251. Balázsik, K.; Török, B.; Felföldi, K.; Bartók, M. Sonochemical Enantioselective Hydrogenation of Trifluoromethyl Ketones Over Platinum Catalysts. *Ultrason. Sonochem.* **1999**, *5*, 149–155.
252. Toukoniitty, B.; Toukoniitty, E.; Maeki-Arvela, P.; Mikkola, J.-P.; Salmi, T.; Murzin, D. Y.; Kooyman, P. J. Effect of Ultrasound on Enantioselective Hydrogenation of 1-Phenyl-1,2-Propanedione: Comparison of Catalyst Activation, Solvents and Supports. *Ultrason. Sonochem.* **2006**, *13*, 68–75.
253. Zhan, E.; Chen, C.; Li, Y.; Shen, W. Heterogeneous Asymmetric Hydrogenation Over Chiral Molecule-Modified Metal Particles. *Cat. Sci. Technol.* **2015**, *5*, 650–659.
254. Tafesh, A. M.; Weiguny, J. A Review of the Selective Catalytic Reduction of Aromatic Nitro Compounds Into Aromatic Amines, Isocyanates, Carbamates, and Ureas Using CO. *Chem. Rev.* **1996**, *96*, 2035–2052.
255. Song, J.; Huang, Z.-F.; Pan, L.; Li, K.; Zhang, X.; Wang, L.; Zou, J.-J. Review on Selective Hydrogenation of Nitroarene by Catalytic, Photocatalytic and Electrocatalytic Reactions. *Appl. Catal. B. Environ.* **2018**, *227*, 386–408.
256. Corma, A.; Serna, P. Chemoselective Hydrogenation of Nitro Compounds With Supported Gold Catalysts. *Science* **2006**, *313*, 332–334.
257. Xiang Han, X.; Chen, Q.; Xian Zhou, R. Study on the Hydrogenation of *p*-Chloronitrobenzene Over Carbon Nanotubes Supported Platinum Catalysts Modified by Mn, Fe, Co, Ni and Cu. *J. Mol. Catal. A: Chem.* **2007**, *277*, 210–214.
258. Sonavane, S.; Gawande, M.; Deshpande, S.; Venkataraman, A.; Jayaram, R. Chemoselective Transfer Hydrogenation Reactions Over Nanosized  $\gamma$ -Fe<sub>2</sub>O<sub>3</sub> Catalyst Prepared by Novel Combustion Route. *Catal. Commun.* **2007**, *8*, 1803–1806.
259. Corma, A.; Serna, P.; Concepción, P.; Juan Calvino, J. Transforming Nonselective Into Chemoselective Metal Catalysts for the Hydrogenation of Substituted Nitroaromatics. *J. Am. Chem. Soc.* **2008**, *130*, 8748–8753.
260. Wu, H.; Zhuo, L.; He, Q.; Liao, X.; Shi, B. Heterogeneous Hydrogenation of Nitrobenzenes Over Recyclable Pd(0) Nanoparticle Catalysts Stabilized by Polyphenol-Grafted Collagen Fibers. *Appl. Catal., A Gen.* **2009**, *366*, 44–56.

146 Heterogeneous catalysis in sustainable synthesis

261. Nieto-Márquez, A.; Gil, S.; Romero, A.; Valverde, J.; Gómez-Quero, S.; Keane, M. Gas Phase Hydrogenation of Nitrobenzene Over Acid Treated Structured and Amorphous Carbon Supported Ni Catalysts. *Appl. Catal., A Gen.* **2009**, *363*, 188–198.
262. Zhang, W.; Li, L.; Du, Y.; Wang, X.; Yang, P. Gold/Platinum Bimetallic Core/Shell Nanoparticles Stabilized by a Fréchet-Type Dendrimer: Preparation and Catalytic Hydrogenations of Phenylaldehydes and Nitrobenzenes. *Catal. Lett.* **2009**, *127*, 429–436.
263. Meng, X.; Cheng, H.; Akiyama, Y.; Hao, Y.; Qiao, W.; Yu, Y.; Zhao, F.; Fujita, S.; Arai, M. Selective Hydrogenation of Nitrobenzene to Aniline in Dense Phase Carbon Dioxide Over Ni/ $\gamma$ -Al<sub>2</sub>O<sub>3</sub>: Significance of Molecular Interactions. *J. Catal.* **2009**, *264*, 1–10.
264. Motoyama, Y.; Kamo, K.; Nagashima, H. Catalysis in Polysiloxane Gels: Platinum-Catalyzed Hydrosilylation of Polymethylhydrosiloxane Leading to Reusable Catalysts for Reduction of Nitroarenes. *Org. Lett.* **2009**, *11*, 1345–1348.
265. Shimizu, K.; Miyamoto, Y.; Satsuma, A. Size- and Support-Dependent Silver Cluster Catalysis for Chemoselective Hydrogenation of Nitroaromatics. *J. Catal.* **2010**, *270*, 86–94.
266. Bhaumik, K.; Akamanchi, K. G. Nitroarene Reduction Using Raney Nickel Alloy With Ammonium Chloride in Water. *Can. J. Chem.* **2003**, *81*, 197–198.
267. Patil, N. M.; Sasaki, T.; Bhanage, B. M. Immobilized Iron Metal-Containing Ionic Liquid-Catalyzed Chemoselective Transfer Hydrogenation of Nitroarenes Into Anilines. *ACS Sustain. Chem. Eng.* **2016**, *4*, 429–436.
268. Reddy, P. L.; Tripathi, M.; Arundhathi, R.; Rawat, D. S. Chemoselective Hydrazine-Mediated Transfer Hydrogenation of Nitroarenes by Co<sub>3</sub>O<sub>4</sub> Nanoparticles Immobilized on an Al/Si-mixed Oxide Support. *Chem. Asian J.* **2017**, *12*, 785–791.
269. Zhu, Y.; Wang, W. D.; Sun, X.; Fan, M.; Hu, X.; Dong, Z. Palladium Nanoclusters Confined in MOF@COP as a Novel Nanoreactor for Catalytic Hydrogenation. *ACS Appl. Mater. Interfaces* **2020**, *12*, 7285–7294.
270. Xiong, W.; Wang, Z.; He, S.; Hao, F.; Yang, Y.; Lv, Y.; Zhang, W.; Liu, P.; Luo, H. Nitrogen-Doped Carbon Nanotubes as a Highly Active Metal-Free Catalyst for Nitrobenzene Hydrogenation. *Appl. Catal. Environ.* **2020**, *260*, 118105.
271. Purohit, G.; Rawat, D. S.; Reiser, O. Palladium Nanocatalysts Encapsulated on Porous Silica @Magnetic Carbon-Coated Cobalt Nanoparticles for Sustainable Hydrogenation of Nitroarenes, Alkenes and Alkynes. *ChemCatChem* **2020**, *12*, 569–575.
272. Li, Z.; He, M.; Wen, Y.; Zhang, X.; Hu, M.; Li, R.; Liu, J.; Chu, J.; Ma, Z.; Xing, X.; Yu, C.; Wei, Z.; Li, Y. Highly Monodisperse Cu–Sn Alloy Nanoplates for Efficient Nitrophenol Reduction Reaction Via Promotion Effect of Tin. *Inorg. Chem.* **2020**, *59*, 1522–1531.
273. Wang, S.; Mo, Y.; Vincent, T.; Roux, J.-C.; Rodríguez-Castellón, E.; Faur, C.; Guibal, E. Palladium Nanoparticles Supported on Aminefunctionalized Alginate Foams for Hydrogenation of 3-Nitrophenol. *J. Mater. Sci.* **2020**, *55*, 2032–2051.
274. Lei, Y.; Chen, Z.; Lan, G.; Wang, R.; Zhou, X.-Y. Pd nanoparticles Stabilized With Phosphinefunctionalized Porous Ionic Polymer for Efficient Catalytic Hydrogenation of Nitroarenes in Water. *New J. Chem.* **2020**, *44*, 3681–3689.
275. Zhao, L.; Chen, J.; Zhang, J. Deactivation of Ni/K<sub>2</sub>O-La<sub>2</sub>O<sub>3</sub>-SiO<sub>2</sub> Catalyst in Hydrogenation of *m*-Dinitrobenzene to *m*-Phenylenediamine. *J. Mol. Catal. A: Chem.* **2006**, *246*, 140–145.
276. Cheng, C.; Wang, X.; Xing, L.; Liu, B.; Zhu, R.; Hu, Y. An Efficient and Practical Method for Highly Chemoselective Hydrogenation of Nitrobenzylamines to Aminobenzylamine Hydrochlorides. *Adv. Synth. Catal.* **2007**, *349*, 1775–1780.
277. Hanack, M.; Kamenzin, S.; Kamenzin, C.; Subramanian, L. Synthesis and Properties of Axially Disubstituted Monomeric and Oligomeric Phthalocyaninato Ruthenium(II) Compounds. *Synth. Met.* **2000**, *110*, 93–103.

278. Wang, C.; Qiu, J.; Liang, C.; Xing, L.; Yang, X. Carbon Nanofiber Supported Ni Catalysts for the Hydrogenation of Chloronitrobenzenes. *Catal. Commun.* **2008**, *9*, 1749–1753.
279. Wang, F.; Liu, J.; Xu, X. Layered Material  $\gamma$ -ZrP Supported Platinum Catalyst for Liquid-Phase Reaction: A Highly Active and Selective Catalyst for Hydrogenation of the Nitro Group in Para-Chloronitrobenzene. *Chem. Commun.* **2008**, 2040–2042.
280. Ma, H.; Sun, K.; Li, Y.; Xu, X. Ultra-Chemosselective Hydrogenation of Chloronitrobenzenes to Chloroanilines Over HCl-Acidified Attapulgite-Supported Platinum Catalyst With High Activity. *Catal. Commun.* **2009**, *10*, 1363–1366.
281. Pietrowski, M.; Wojciechowska, M. An Efficient Ruthenium-Vanadium Catalyst for Selective Hydrogenation of *ortho*-Chloronitrobenzene. *Catal. Today* **2009**, *142*, 211–214.
282. Liu, H.; Liang, M.; Xiao, C.; Zheng, N.; Feng, X.; Liu, Y.; Xie, J.; Wang, Y. An Excellent Pd-Based Nanocomposite Catalyst for the Selective Hydrogenation of *para*-Chloronitrobenzene. *J. Mol. Catal. A: Chem.* **2009**, *308*, 79–86.
283. Meng, X.; Cheng, H.; Fujita, S.; Hao, Y.; Shang, Y.; Yu, Y.; Cai, S.; Zhao, F.; Arai, M. Selective Hydrogenation of Chloronitrobenzene to Chloroaniline in Supercritical Carbon Dioxide Over Ni/TiO<sub>2</sub>: Significance of Molecular Interactions. *J. Catal.* **2010**, *269*, 131–139.
284. Quadrado, R. F. N.; Fajardo, A. R. Hydrogen Generation and Hydrogenation Reactions Efficiently Mediated by a Thin Film of Reduced Graphene Oxide-Grafted With Carboxymethyl Chitosan and Ag Nanoparticles. *J. Colloid Interface Sci.* **2021**, *583*, 626–641.
285. Fanghänel, E.; Chtcheglov, D. Alkaliinduzierte Bildung von *ortho*-Semidinen aus 3-Nitro- und 3-Azo-carbazolen—Synthese von 8,16-Dialkyldiindolo[3,2-a,d]phenazinen. *J. Prakt. Chem.* **1996**, *338*, 731–737.
286. Serna, P.; Lopez-Haro, M.; Calvino, J.; Corma, A. Selective Hydrogenation of Nitrocyclohexane to Cyclohexanone Oxime With H<sub>2</sub> on Decorated Pt Nanoparticles. *J. Catal.* **2009**, *263*, 328–334.
287. Novakov, I.; Orlinson, B.; Brunilin, R.; Navrotskii, M.; Eremiichuk, A.; Dumler, S.; Gordeva, E. An Improved Synthesis of N-(3-phenylbicyclo[2.2.1]-yl)-N-Ethylamine Hydrochloride (Fencamfamine). *Pharm. Chem. J.* **2011**, *45*, 419–422.
288. Lévy, K.; Hegedűs, L. Recent Achievements in the Hydrogenation of Nitriles Catalyzed by Transitional Metals. *Curr. Org. Chem.* **2019**, *23*, 1881–1900.
289. Chojecki, A.; Veprek-Heijman, M.; Müller, T.; Schäringer, P.; Veprek, S.; Lercher, J. Tailoring Raney-Catalysts for the Selective Hydrogenation of Butyronitrile to *n*-Butylamine. *J. Catal.* **2007**, *245*, 237–248.
290. Obert, K.; Roth, D.; Ehrig, M.; Schönweiz, A.; Assenbaum, D.; Lange, H.; Wasserscheid, P. Selectivity Enhancement in the Catalytic Hydrogenation of Propionitrile Using Ionic Liquid Multiphase Reaction Systems. *Appl. Catal., A Gen.* **2009**, *356*, 43–51.
291. Lin, C.; Li, J.; Guo, H.; Wu, X.; Wang, B.; Yan, X. Controllable Synthesis of bis[3-(Dimethylamino)propyl]amine Over Cr and Co Double-Doped Cu/ $\gamma$ -Al<sub>2</sub>O<sub>3</sub>. *Cat. Com.* **2018**, *111*, 64–69.
292. Prechtel, M.; Scholten, J.; Dupont, J. Tuning the Selectivity of Ruthenium Nanoscale Catalysts With Functionalised Ionic Liquids: Hydrogenation of Nitriles. *J. Mol. Catal. A: Chem.* **2009**, *313*, 74–78.
293. Rodríguez, A. A.; Garduño, J. A.; García, J. J. Nickel(II) and Nickel(0) Complexes as Precursors of Nickel Nanoparticles for the Catalytic Hydrogenation of Benzonitrile. *New J. Chem.* **2020**, *44*, 1082–1089.
294. Cao, Y.; Niu, L.; Wen, X.; Feng, W.; Huo, L.; Bai, G. Novel Layered Double Hydroxide/Oxide-Coated Nickel-Based Core-Shell Nanocomposites for Benzonitrile Selective Hydrogenation: An Interesting Water Switch. *J. Catal.* **2016**, *339*, 9–13.

148 Heterogeneous catalysis in sustainable synthesis

295. Ji, P.; Manna, K.; Lin, Z.; Feng, X.; Urban, A.; Song, Y.; Lin, W. Single-Site cobalt Catalysts at New  $Zr_{12}(\mu_3-O)_8(\mu_3-OH)_8(\mu_2-OH)_6$  Metal-Organic Frameworknodes for Highly Active Hydrogenation of Nitroarenes, Nitriles, and Isocyanides. *J. Am. Chem. Soc.* **2017**, *139*, 7004–7011.
296. Chen, F.; Topf, C.; Radnik, J.; Kreyenschulte, C.; Lund, H.; Schneider, M.; Surkus, A.-E.; He, L.; Junge, K.; Beller, M. Stable and Inert Cobalt Catalysts for Highly Selective and Practical Hydrogenation of  $C\equiv N$  and  $C=O$  Bonds. *J. Am. Chem. Soc.* **2016**, *138*, 8781–8788.
297. Murugesan, K.; Senthamarai, T.; Sohail, M.; Alshammari, A. S.; Pohl, M.-M.; Beller, M.; Jagadeesh, R. V. Cobalt-Based Nanoparticles Prepared From MOF Carbon Templates as Efficient Hydrogenation Catalysts. *Chem. Sci.* **2018**, *9*, 8553–8560.
298. Marella, R. K.; Koppadi, K. S.; Jyothi, Y.; Rama Rao, K. S.; Burri, D. R. Selective Gas-Phase Hydrogenation of Benzonitrile Into Benzylamine Over Cu-MgO Catalysts Without Using Any Additives. *New J. Chem.* **2013**, *37*, 3229–3235.
299. Liu, Y.; He, S.; Quan, Z.; Cai, H.; Zhao, Y.; Wang, B. Mild Palladium Catalysed Highly Efficient Hydrogenation of  $C\equiv N$ ,  $C-NO_2$ , and  $C=O$  Bonds Using  $H_2$  of 1 atm in  $H_2O$ . *Green Chem.* **2019**, *21*, 830–838.
300. Jiao, Z.-F.; Zhao, J.-X.; Guo, X.-N.; Tong, X.-L.; Zhang, B.; Jin, G.-Q.; Qin, Y.; Guo, X.-Y. Turning the Product Selectivity of Nitrile Hydrogenation From Primary to Secondary Amines by Precise Modification of Pd/SiC Catalysts Using NiO Nanodots. *Cat. Sci. Technol.* **2019**, *9*, 2266–2272.
301. López-De Jesús, Y. M.; Johnson, C. E.; Monnier, J. R.; Williams, C. T. Selective Hydrogenation of Benzonitrile by Alumina-Supported Ir-Pd Catalysts. *Top. Catal.* **2010**, *53*, 1132–1137.
302. Staskun, B.; van Es, T. The Reduction of Nitriles to Aldehydes: Applications of Raney Nickel/Sodium Hypophosphite Monohydrate, of RANEY Nickel/Formic Acid, or of Raney(Ni/Al)Alloy/Formic Acid, Respectively. *S. Afr. J. Chem.* **2008**, *61*, 144–156.
303. Zeynizadeh, B.; Aminzadeh, F. M.; Mousavi, H. Green and Convenient Protocols for the Efficient Reduction of Nitriles and Nitro Compounds to Corresponding Amines With  $NaBH_4$  in Water Catalyzed by Magnetically Retrievable  $CuFe_2O_4$  Nanoparticles. *Res. Chem. Intermed.* **2019**, *45*, 3329–3357.
304. Saad, F.; Comparot, J. D.; Brahmi, R.; Bensitel, M.; Pirault-Roy, L. Influence of Acid-Base Properties of the Support on the Catalytic Performances of Pt Based Catalysts in a Gas-Phase Hydrogenation of Acetonitrile. *Appl. Catal. A. Gen.* **2017**, *544*, 1–9.
305. Aguirre, A.; Collins, S. E. Insight Into the Mechanism of Acetonitrile Hydrogenation in Liquid Phase on  $Pt/Al_2O_3$  by ATR-FTIR. *Catal. Today* **2019**, *336*, 22–32.
306. Nugent, T.; Ghosh, A.; Wakchaure, V.; Mohanty, R. Asymmetric Reductive Amination: Convenient Access to Enantioenriched Alkyl-Alkyl or Aryl-Alkyl Substituted  $\alpha$ -Chiral Primary Amines. *Adv. Synth. Catal.* **2006**, *348*, 1289–1299.
307. Nugent, T.; El-Shazly, M.; Wakchaure, V. Ytterbium Acetate Promoted Asymmetric Reductive Amination: Significantly Enhanced Stereoselectivity. *J. Org. Chem.* **2008**, *73*, 1297–1305.
308. Byun, E.; Hong, B.; De Castro, K.; Lim, M.; Rhee, H. One-Pot Reductive Mono-*N*-alkylation of Aniline and Nitroarene Derivatives Using Aldehydes. *J. Org. Chem.* **2007**, *72*, 9815–9817.
309. Xing, L.; Cheng, C.; Zhu, R.; Zhang, B.; Wang, X.; Hu, Y. Self-Modulated Highly Chemoselective Direct-Reductive-Amination (DRA) of Benzaldehydes Straight Forward to *N*-Monosubstituted Benzylamine Hydrochlorides. *Tetrahedron* **2008**, *64*, 11783–11788.
310. Alonso, F.; Riente, P.; Yus, M. Hydrogen-Transfer Reductive Amination Aldehydes Catalyzed by Nickel Nanoparticles. *Synlett* **2008**, 1289–1292.

311. Udayakumar, V.; Alexander, S.; Gayathri, V.; Shivakumaraiah, P. K. R.; Viswanathan, B. Polymer-Supported Palladium-Imidazole Complex Catalyst for Hydrogenation of Substituted Benzylideneanilines. *J. Mol. Catal. A: Chem.* **2010**, *317*, 111–117.
312. Mhadgut, S. C.; Palaniappan, K.; Thimmaiah, M.; Hackney, S. A.; Török, B.; Liu, J. A Metal Nanoparticle-Based Supramolecular Approach for Aqueous Biphasic Reactions. *Chem. Commun.* **2005**, 3207–3209.
313. Schäfer, C.; Nişancı, B.; Bere, M. P.; Daştan, A.; Török, B. Heterogeneous Catalytic Reductive Amination of Carbonyl Compounds With Ni-Al Alloy in Water as Solvent and Hydrogen Source. *Synthesis* **2016**, *48*, 3127–3133.
314. Nisancı, B.; Ganjehyan, K.; Metin, Ö.; Dastan, A.; Török, B. Graphene-Supported NiPd Alloy Nanoparticles: A Novel and Highly Efficient Heterogeneous Catalyst System for the Reductive Amination of Aldehydes. *J. Mol. Catal. A: Chem.* **2015**, *409*, 191–197.
315. Cho, A.; Byun, S.; Kim, B. M. AuPd-Fe<sub>3</sub>O<sub>4</sub> Nanoparticle Catalysts for Highly Selective, One-Pot Cascade Nitro-Reduction and Reductive Amination. *Adv. Synth. Catal.* **2018**, *360*, 1253–1261.
316. Török, B.; Prakash, G. K. S. Synthesis of Chiral Trifluoromethylated Amines by Palladium-Catalyzed Diastereoselective Hydrogenation-Hydrogenolysis Approach. *Adv. Synth. Catal.* **2003**, *345*, 165–168.
317. Dasgupta, S.; Morzhina, E.; Schäfer, C.; Mhadgut, S. C.; Prakash, G. K. S.; Török, B. Synthesis of Chiral Trifluoromethyl Benzylamines by Heterogeneous Catalytic Reductive Amination. *Top. Catal.* **2016**, *59*, 1207–1213.
318. Ahammed, S.; Saha, A.; Ranu, B. C. Hydrogenation of Azides Over Copper Nanoparticle Surface Using Ammonium Formate in Water. *J. Org. Chem.* **2011**, *76*, 7235–7239.
319. Yadav, A. A.; Wu, X.; Patel, D.; Yalowich, J. C.; Hasinoff, B. B. Structure-Based Design, Synthesis and Biological Testing of Etoposide Analog Epipodophyllotoxin–N-Mustard Hybrid Compounds Designed to Covalently Bind to Topoisomerase II and DNA. *Bioorg. Med. Chem.* **2014**, *22*, 5935–5949.
320. Zhou, X. M.; Wang, Z. Q.; Chang, J. Y.; Chen, H. X.; Cheng, Y. C.; Lee, K. H. Antitumor Agents. 120. New 4-Substituted Benzylamine and Benzyl Ether Derivatives of 4'-O-Demethylepipodophyllotoxin as Potent Inhibitors of Human DNA Topoisomerase II. *J. Med. Chem.* **1991**, *34*, 3346–3350.
321. Chambers, A.; Jackson, S. D.; Stirling, D.; Webb, G. Selective Hydrogenation of Cinnamaldehyde Over Supported Copper Catalysts. *J. Catal.* **1997**, *168*, 301–314.
322. Kume, Y.; Qiao, K.; Tomida, D.; Yokoyama, C. Selective Hydrogenation of Cinnamaldehyde Catalyzed by Palladium Nanoparticles Immobilized on Ionic Liquids Modified-Silica Gel. *Catal. Commun.* **2008**, *9*, 369–375.
323. Wang, H.; Shu, Y.; Zheng, M.; Zhang, T. Selective Hydrogenation of Cinnamaldehyde to Hydrocinnamaldehyde Over SiO<sub>2</sub> Supported Nickel Phosphide Catalysts. *Catal. Lett.* **2008**, *124*, 219–225.
324. Li, Y.; Ge, C.; Zhao, J.; Zhou, R. Influence of Preparation Modes on Pt–Ni/CNTs Catalysts Used in the Selective Hydrogenation of Cinnamaldehyde to Hydrocinnamaldehyde. *Catal. Lett.* **2008**, *126*, 280–285.
325. Simion, A.-M.; Arimura, T.; Simion, C. Reaction of Cinnamaldehyde and Derivatives With Raney Ni-Al alloy and Al Powder in Water. Reduction or Oxido-Reduction? *C. R. Chim.* **2013**, *16*, 476–481.
326. Simion, A.; Arimura, T.; Simion, C. Reaction of Cinnamaldehyde and Derivatives With Raney Ni–Al Alloy and Al Powder in Water. Reduction or Oxido-Reduction? *Tetrahedron Lett.* **2013**, *53*, 476–481.

150 Heterogeneous catalysis in sustainable synthesis

327. Morrissey, S.; Beadham, I.; Gathergood, N. Selective Hydrogenation of *trans*-Cinnamaldehyde and Hydrogenolysis-Free Hydrogenation of Benzyl Cinnamate in Imidazolium ILs. *Green Chem.* **2009**, *11*, 466–474.
328. Chatterjee, M.; Yokoyama, T.; Kawanami, H.; Sato, M.; Suzuki, T. An Exceptionally Rapid and Selective Hydrogenation of 2-Cyclohexen-1-One in Supercritical Carbon Dioxide. *Chem. Commun.* **2009**, 701–703.
329. Mhadgut, S. C.; Bucsi, I.; Török, M.; Török, B. Sonochemical Asymmetric Hydrogenation of Isophorone on Proline Modified Pd/Al<sub>2</sub>O<sub>3</sub> Catalysts. *Chem. Commun.* **2004**, 984–985.
330. Mhadgut, S. C.; Török, M.; Esquibel, J.; Török, B. Highly Asymmetric Heterogeneous Catalytic Hydrogenation of Isophorone on Proline Modified Base-Supported Palladium Catalysts. *J. Catal.* **2006**, *238*, 441–448.
331. McIntosh, A. I.; Watson, D. J.; Burton, J. W.; Lambert, R. M. Heterogeneously Catalyzed Asymmetric CdC Hydrogenation: Origin of Enantioselectivity in the Proline-Directed Pd/Isophorone System. *J. Am. Chem. Soc.* **2006**, *128*, 7329–7334.
332. McIntosh, A. I.; Watson, D. J.; Lambert, R. M. Mechanistic Insights Into the Proline-Directed Enantioselective Heterogeneous Hydrogenation of Isophorone. *Langmuir* **2007**, *23*, 6113–6118.
333. Zhan, E.; Li, S.; Xu, Y.; Shen, W. Heterogeneous Enantioselective Hydrogenation of Isophorone Over Proline Modified Pd Catalysts. *Catal. Commun.* **2007**, *8*, 1239–1243.
334. Li, S.; Zhan, E.; Li, Y.; Xu, Y.; Shen, W. Enantioselective Hydrogenation of Isophorone and Kinetic Resolution of 3,3,5-Trimethylcyclohexanone Over Pd Catalysts in the Presence of (*S*)-Proline. *Catal. Today* **2008**, *131*, 347–352.
335. Mhadgut, S. C.; Török, M.; Dasgupta, S.; Török, B. Nature of Proline-Induced Enantiodifferentiation in Asymmetric Pd Catalyzed Hydrogenations: Is the Catalyst Really Indifferent? *Catal. Lett.* **2008**, *123*, 156–163.
336. Fodor, M.; Tungler, A.; Vida, L. Asymmetric Hydrogenation of Isophorone in the Presence of (*S*)-Proline: Revival of a 20 Years Old Reaction. *Catal. Today* **2009**, *140*, 58–63.
337. Pisarek, M.; Łukaszewski, M.; Winiarek, P.; Kedzierzawski, P.; Janik-Czachor, M. Influence of Cr Addition to Raney Ni Catalyst on Hydrogenation of Isophorone. *Catal. Commun.* **2008**, *10*, 213–216.
338. Boeriu, C.; Oana, D. Synthesis and Optical Resolution of N-Acetyl-D,L-Phenylalanine. *Rev. Roum. Biochim.* **1992**, *29*, 89–95.
339. Trutera, L. A.; Ordonsky, V.; Schouten, J. C.; Nijhuis, T. A. The Application of Palladium and Zeolite Incorporated Chip-Based Microreactors. *Appl. Catal. A. Gen.* **2016**, *515*, 72–82.
340. Mousavi, S.; Nazari, B.; Keshavarz, M. H.; Bordbar, A.-K. A Simple Method for Safe Determination of the Activity of Palladium on Activated Carbon Catalysts in the Hydrogenation of Cinnamic Acid to Hydrocinnamic Acid. *Ind. Eng. Chem. Res.* **2020**, *59*, 1862–1874.
341. Szabados, E.; Györfly, N.; Tungler, A.; Balla, J.; Konczol, L. Asymmetric Hydrogenation of Prochiral and Kinetic Resolution of Chiral Cyclohexanone Derivatives With Pd Catalysts. *React. Kinet. Mech. Catal.* **2014**, *111*, 107–114.
342. Györfly, N.; Tungler, A. Effect of Basic and Acidic Additives on the (*S*)-Proline and Pd Mediated Kinetic Resolution of 3,5,5-Trimethyl Cyclohexanone and Asymmetric Hydrogenation of Isophorone. *J. Mol. Catal. A: Chem.* **2011**, *336*, 72–77.
343. Schäfer, C.; Mhadgut, S. C.; Kugyela, N.; Török, M.; Török, B. Proline-Induced Enantioselective Heterogeneous Catalytic Hydrogenation of Isophorone on Basic Polymer-Supported Pd Catalysts. *Cat. Sci. Technol.* **2015**, *5*, 716–723.

344. Beaumont, S. K.; Kyriakou, G.; Watson, D. J.; Vaughan, O. P. H.; Papageorgiou, A. H.; Lambert, R. M. Influence of Adsorption Geometry in the Heterogeneous Enantioselective Catalytic Hydrogenation of a Prototypical Enone. *J. Phys. Chem. C* **2010**, *114*, 15075–15077.
345. Watson, D. J.; Jesudason, R. J. B.; Beaumont, S. K.; Kyriakou, G.; Burton, J. W.; Lambert, R. M. Heterogeneously Catalyzed Asymmetric Hydrogenation of C=C Bonds Directed by Surface-Tethered Chiral Modifiers. *J. Am. Chem. Soc.* **2009**, *131*, 14584–14589.
346. Kun, I.; Török, B.; Felföldi, K.; Bartók, M. Heterogeneous Asymmetric Reactions Part 17. Asymmetric Hydrogenation of 2-Methyl-2-Pentenoic Acid Over Cinchona Modified Pd/Al<sub>2</sub>O<sub>3</sub> Catalysts. *Appl. Catal. A. Gen.* **2000**, *203*, 71–79.
347. Szöllösi, G.; Szabó, E.; Bartók, M. Enantioselective Hydrogenation of N-Acetyldehydroamino Acids Over Supported Palladium Catalysts. *Adv. Synth. Catal.* **2007**, *349*, 405–410.
348. Szöllösi, G.; Hermán, B.; Felföldi, K.; Fülöp, F.; Bartók, M. Up to 96% Enantioselectivities in the Hydrogenation of Fluorine Substituted (*E*)-2,3-Diphenylpropenoic Acids Over Cinchonidine-Modified Palladium Catalyst. *Adv. Synth. Catal.* **2008**, *350*, 2804–2814.
349. Impalá, D.; Franceschini, S.; Piccolo, O.; Vaccari, A. Pd-based Sol–Gel Catalysts for the Enantioselective Hydrogenation of (*E*)-2-Methyl-2-Butenoic Acid. *Catal. Lett.* **2008**, *125*, 243–249.
350. Kubota, T.; Kubota, H.; Kubota, T.; Moriyasu, E.; Uchida, T.; Nitta, Y.; Sugimura, T.; Okamoto, Y. Enantioselective Hydrogenation of (*E*)- $\alpha$ -Phenylcinnamic Acid Over Cinchonidine-Modified Pd Catalysts Supported on TiO<sub>2</sub> and CeO<sub>2</sub>. *Catal. Lett.* **2009**, *129*, 387–393.
351. Hermán, B.; Szöllösi, G.; Felföldi, K.; Fülöp, F.; Bartók, M. Enantioselective Hydrogenation of Propenoic Acids Bearing Heteroaromatic Substituents Over Cinchonidine Modified Pd/Alumina. *Catal. Commun.* **2009**, *10*, 1107–1110.
352. Ma, H.; Wang, L.; Chen, L.; Dong, C.; Yu, W.; Huang, T.; Qian, Y. Pt Nanoparticles Deposited Over Carbon Nanotubes for Selective Hydrogenation of Cinnamaldehyde. *Catal. Commun.* **2007**, *8*, 452–456.
353. Manikandan, D.; Divakar, D.; Sivakumar, T. Utilization of Clay Minerals for Developing Pt Nanoparticles and Their Catalytic Activity in the Selective Hydrogenation of Cinnamaldehyde. *Catal. Commun.* **2007**, *8*, 1781–1786.
354. Xi, C.; Wang, H.; Liu, R.; Cai, S.; Zhao, F. Hydrogenation of Cinnamaldehyde Over Pt/RHCs in Supercritical Carbon Dioxide—Influence of Support Pretreatment and Phase Behavior. *Catal. Commun.* **2008**, *9*, 140–145.
355. Ramos-Fernández, E. V.; Ferreira, A. F. P.; Sepúlveda-Escribano, A.; Kapteijn, F.; Rodríguez-Reinoso, F. Enhancing the Catalytic Performance of Pt/ZnO in the Selective Hydrogenation of Cinnamaldehyde by Cr Addition to the Support. *J. Catal.* **2008**, *258*, 52–60.
356. Mahata, N.; Gonçalves, F.; Pereira, M. F. R.; Figueiredo, J. Selective Hydrogenation of Cinnamaldehyde to Cinnamyl Alcohol Over Mesoporous Carbon Supported Fe and Zn Promoted Pt Catalyst. *Appl. Catal., A Gen.* **2008**, *339*, 159–168.
357. Gao, P.; Wang, A.; Wang, X.; Zhang, T. Synthesis and Catalytic Performance of Highly Ordered Ru-Containing Mesoporous Carbons for Hydrogenation of Cinnamaldehyde. *Catal. Lett.* **2008**, *125*, 289.
358. Urbano, F. J.; Aramendía, M. A.; Marinas, A.; Marinas, J. M. An Insight Into the Meerwein–Ponndorf–Verley Reduction of  $\alpha,\beta$ -Unsaturated Carbonyl Compounds: Tuning the Acid–Base Properties of Modified Zirconia Catalysts. *J. Catal.* **2009**, *268*, 79–88.
359. Szöllösi, G.; Török, B.; Baranyi, L.; Bartók, M. Chemoselective Hydrogenation of Cinnamaldehyde to Cinnamyl Alcohol Over Pt/K-10 Catalyst. *J. Catal.* **1998**, *179*, 619–623.

152 Heterogeneous catalysis in sustainable synthesis

360. Szöllösi, G.; Török, B.; Szakonyi, G.; Kun, I.; Bartók, M. Ultrasonic Irradiation as Activity and Selectivity Improving Factor in the Hydrogenation of Cinnamaldehyde over Pt/SiO<sub>2</sub> Catalysts. *Appl. Catal., A Gen.* **1998**, *172*, 225–232.
361. Török, B.; Balázsik, K.; Szöllösi, G.; Felföldi, K.; Kun, I.; Bartók, M. Ultrasonics in Heterogeneous Metal Catalysis. Sonochemical Chemo- and Enantioselective Hydrogenations Over Supported Platinum Catalysts. *Ultrason. Sonochem.* **1999**, *6*, 97–103.
362. Szöllösi, G.; Kun, I.; Török, B.; Bartók, M. Chemoselective Hydrogenation of C=O Group in Unsaturated Aldehydes Over Clay-Supported Platinum Catalysts. *Stud. Surf. Sci. Catal.* **1999**, *125*, 539–546.
363. Szöllösi, G.; Kun, I.; Török, B.; Bartók, M. Ultrasonics in Chemoselective Heterogeneous Metal Catalytic Processes. Sonochemical Hydrogenation of  $\alpha,\beta$ -Unsaturated Carbonyl Compounds Over Platinum Catalysts. *Ultrason. Sonochem.* **2000**, *7*, 173–176.
364. Disselkamp, R. S.; Hart, T. R.; Williams, A. M.; White, J. F.; Peden, C. H. F. Ultrasound-Assisted Hydrogenation of Cinnamaldehyde. *Ultrason. Sonochem.* **2005**, *12*, 319–324.
365. Ruiz-Martínez, J.; Fukui, Y.; Komatsu, T.; Sepúlveda-Escribano, A. Ru–Ti Intermetallic Catalysts for the Selective Hydrogenation of Crotonaldehyde. *J. Catal.* **2008**, *260*, 150–156.
366. Campo, B.; Santori, G.; Petit, C.; Volpe, M. Liquid Phase Hydrogenation of Crotonaldehyde Over Au/CeO<sub>2</sub> Catalysts. *Appl. Catal., A Gen.* **2009**, *359*, 79–83.
367. Galloway, E.; Armbruster, M.; Kovnir, K.; Tikhov, M. S.; Lambert, R. M. Bromine-Promoted PtZn is Very Effective for the Chemoselective Hydrogenation of Crotonaldehyde. *J. Catal.* **2009**, *261*, 60–65.
368. Mertens, P.; Vandezande, P.; Ye, X.; Poelman, H.; Vankelecom, I.; De Vos, D. Recyclable Au<sub>0</sub>, Ag<sub>0</sub> and Au<sub>0</sub>–Ag<sub>0</sub> Nanocolloids for the Chemoselective Hydrogenation of  $\alpha,\beta$ -Unsaturated Aldehydes and Ketones to Allylic Alcohols. *Appl. Catal., A Gen.* **2009**, *355*, 176–183.
369. Zhu, Y.; Qian, H.; Drake, B. A.; Jin, R. Atomically Precise Au<sub>25</sub>(SR)<sub>18</sub> Nanoparticles as Catalysts for the Selective Hydrogenation of  $\alpha,\beta$ -Unsaturated Ketones and Aldehydes. *Angew. Chem. Int. Ed.* **2010**, *49*, 1295–1298.
370. Nie, Y.; Chuah, G.; Jaenicke, S. Domino-Cyclisation and Hydrogenation of Citronellal to Menthol Over Bifunctional Ni/Zr-Beta and Zr-Beta/Ni-MCM-41 Catalysts. *Chem. Commun.* **2006**, 790–792.
371. Miyazaki, Y.; Hagio, H.; Kobayashi, S. Practical Access to the Polymer Incarcerated Platinum (PI Pt) Catalyst and its Application to Hydrogenation. *Org. Biomol. Chem.* **2006**, *4*, 2529–2531.
372. Mori, A.; Mizusaki, T.; Miyakawa, Y.; Ohashi, E.; Haga, T.; Maegawa, T.; Monguchi, Y.; Sajiki, H. Chemoselective Hydrogenation Method Catalyzed by Pd/C Using Diphenylsulfide as a Reasonable Catalyst Poison. *Tetrahedron* **2006**, *62*, 11925–11932.
373. Guin, D.; Baruwati, B.; Manorama, S. Pd on Amine-Terminated Ferrite Nanoparticles: A Complete Magnetically Recoverable Facile Catalyst for Hydrogenation Reactions. *Org. Lett.* **2007**, *9*, 1419–1421.
374. Polshettiwar, V.; Baruwati, B.; Varma, R. Nanoparticle-Supported and Magnetically Recoverable Nickel Catalyst: A Robust and Economic Hydrogenation and Transfer Hydrogenation Protocol. *Green Chem.* **2009**, *11*, 127–131.
375. Maegawa, T.; Takahashi, T.; Yoshimura, M.; Suzuka, H.; Monguchi, Y.; Sajiki, H. Development of Molecular Sieves-Supported Palladium Catalyst and Chemoselective Hydrogenation of Unsaturated Bonds in the Presence of Nitro Groups. *Adv. Synth. Catal.* **2009**, *351*, 2091–2095.

376. Cimpeanu, V.; Kočevár, M.; Parvulescu, V.; Leitner, W. Preparation of Rhodium Nanoparticles in Carbon Dioxide Induced Ionic Liquids and Their Application to Selective Hydrogenation. *Angew. Chem. Int. Ed.* **2009**, *48*, 1085–1088.
377. Jacinto, M.; Landers, R.; Rossi, L. Preparation of Supported Pt(0) Nanoparticles as Efficient Recyclable Catalysts for Hydrogenation of Alkenes and Ketones. *Catal. Commun.* **2009**, *10*, 1971–1974.
378. Motoyama, Y.; Takasaki, M.; Yoon, S.; Mochida, I.; Nagashima, H. Rhodium Nanoparticles Supported on Carbon Nanofibers as an Arene Hydrogenation Catalyst Highly Tolerant to a Coexisting Epoxido Group. *Org. Lett.* **2009**, *11*, 5042–5045.
379. Wolfson, A.; Dlugy, C.; Shotland, Y.; Tavor, D. Glycerol as Solvent and Hydrogen Donor in Transfer Hydrogenation–Dehydrogenation Reactions. *Tetrahedron Lett.* **2009**, *50*, 5951–5953.
380. Xiang, Y.; Li, X.; Lu, C.; Ma, L.; Zhang, Q. Water-Improved Heterogeneous Transfer Hydrogenation Using Methanol as Hydrogen Donor Over Pd-Based Catalyst. *Appl. Catal., A Gen.* **2010**, *375*, 289–294.
381. Török, B.; Schäfer, C., Eds. *Non-traditional Activation Methods in Green and Sustainable Applications: Microwaves, Ultrasounds, Photo, Electro and Mechanochemistry and High Hydrostatic Pressure*; Elsevier: Cambridge, MA/Oxford, 2021.
382. Kappe, C. O. Controlled Microwave Heating in Modern Organic Synthesis. *Angew. Chem. Int. Ed.* **2004**, *43*, 6250–6284.
383. Roberts, B. A.; Strauss, C. R. Toward Rapid, “Green”, Predictable Microwave-Assisted Synthesis. *Acc. Chem. Res.* **2005**, *38*, 653–661.
384. Loupy, A. *Microwaves in Organic Synthesis*, 2nd ed.; Wiley-VCH: Weinheim, New York, 2006.
385. Tierney, J. P.; Lidstrom, P. *Microwave Assisted Organic Synthesis*; Blackwell: Oxford, 2005.
386. Dallinger, D.; Kappe, C. O. Microwave-Assisted Synthesis in Water as Solvent. *Chem. Rev.* **2007**, *107*, 2563–2591.
387. Daştan, A.; Kulkarni, A.; Török, B. Environmentally Benign Synthesis of Heterocyclic Compounds by Combined Microwave-Assisted Heterogeneous Catalytic Approaches. *Green Chem.* **2012**, *14*, 17–37.
388. Horikoshi, S.; Serpone, N., Eds. *Microwaves in Catalysis—Fundamental Research and Scale-up Technology*; Wiley: Hoboken, NJ, 2015.
389. Kokel, A.; Schäfer, C.; Török, B. Application of Microwave-Assisted Heterogeneous Catalysis in Sustainable Synthesis Design. *Green Chem.* **2017**, *19*, 3729–3751.
390. Kokel, A.; Schäfer, C.; Török, B. Microwave-Assisted Reactions in Green Chemistry. In *Encyclopedia of Sustainable Science and Technology*; Meyers, R. A., Ed.; Springer-Nature, 2018. [https://doi.org/10.1007/978-1-4939-2493-6\\_1008-1](https://doi.org/10.1007/978-1-4939-2493-6_1008-1).
391. Whittaker, A. G.; Mingos, D. M. P. Arcing and Other and Other Microwave Characteristics of Metal Powders in Liquid Systems. *J. Chem. Soc. Dalton Trans.* **2000**, 1521–1526.
392. Dressen, M. H. C. L.; van de Kruijs, B. H. P.; Meuldijk, J.; Vekemans, J. A. J. M.; Hulshof, L. A. Vanishing Microwave Effects: Influence of Heterogeneity. *Org. Process Res. Dev.* **2007**, *11*, 865.
393. Heller, E.; Lautenschläger, W.; Holzgrabe, U. Microwave-Enhanced Hydrogenations at Medium Pressure Using a Newly Constructed Reactor. *Tetrahedron Lett.* **2005**, *46*, 1247–1249.
394. Vanier, G. S. Simple and Efficient Microwave-Assisted Hydrogenation Reactions at Moderate Temperature and Pressure. *Synlett* **2007**, 131–135.

154 Heterogeneous catalysis in sustainable synthesis

395. Sharma, A.; Kumar, V.; Sinha, A. A Chemoselective Hydrogenation of the Olefinic Bond of  $\alpha,\beta$ -Unsaturated Carbonyl Compounds in Aqueous Medium Under Microwave Irradiation. *Adv. Synth. Catal.* **2006**, *348*, 354–360.
396. Miyazawa, A.; Saitou, K.; Tanaka, K.; Gädda, T. M.; Tashiro, M.; Prakash, G. K. S.; Olah, G. A. Reaction of Primary Amines With Pt/C catalyst in Water Under Microwave Irradiation: A Convenient Synthesis of Secondary Amines From Primary Amines. *Tetrahedron Lett.* **2006**, *47*, 1437–1439.
397. Chapman, N.; Conway, B.; O'Grady, F.; Wall, M. D. A Convenient Method to Aniline Compounds Using Microwave-Assisted Transfer Hydrogenation. *Synlett* **2006**, 1043–1046.
398. Olivier, J.; Camerel, F.; Ziesel, R.; Retailleau, P.; Amadou, J.; Pham-Huu, C. Microwave-Promoted Hydrogenation and Alkynylation Reactions With Palladium-Loaded Multi-Walled Carbon Nanotubes. *New J. Chem.* **2008**, *32*, 920–924.
399. Quinn, J.; Razzano, D.; Golden, K.; Gregg, B. 1,4-Cyclohexadiene With Pd/C as a Rapid, Safe Transfer Hydrogenation System with Microwave Heating. *Tetrahedron Lett.* **2008**, *49*, 6137–6140.
400. Piras, L.; Genesio, E.; Ghiron, C.; Taddei, M. Microwave-Assisted Hydrogenation of Pyridines. *Synlett* **2008**, 1125–1128.
401. Irfan, M.; Fuchs, M.; Glasnov, T. N.; Kappe, C. O. Microwave-Assisted Cross-Coupling and Hydrogenation Chemistry by Using Heterogeneous Transition-Metal Catalysts: An Evaluation of the Role of Selective Catalyst Heating. *Chem. A Eur. J.* **2009**, *15*, 11608–11618.
402. Gracia, M.; Campelo, J.; Losada, E.; Luque, R.; Marinas, J.; Romero, A. Microwave-Assisted Versatile Hydrogenation of Carbonyl Compounds Using Supported Metal Nanoparticles. *Org. Biomol. Chem.* **2009**, *7*, 4821–4824.
403. Baruwati, B.; Polshettiwar, V.; Varma, R. Magnetically Recoverable Supported Ruthenium Catalyst for Hydrogenation of Alkynes and Transfer Hydrogenation of Carbonyl Compounds. *Tetrahedron Lett.* **2009**, *50*, 1215–1218.
404. Quinn, J. F.; Bryant, C. E.; Golden, K. C.; Gregg, B. T. Rapid Reduction of Heteroaromatic Nitro Groups Using Catalytic Transfer Hydrogenation With Microwave Heating. *Tetrahedron Lett.* **2010**, *51*, 786–789.
405. Mason, T. J.; Lorimer, J. P. *Sonochemistry*; Ellis Horwood: Chichester, 1988.
406. Suslick, K. S. *Ultrasounds. Its Chemical, Physical, and Biological Effects*; VCH: New York, Weinheim, 1998.
407. Suslick, K. S.; Skrabalak, S. E. In *Sonocatalysis in Handbook of Heterogeneous Catalysis*; Ertl, G., Ed.; Vol. 4; Wiley-VCH, **2008**; p. 2007.
408. Ellstrom, C. J.; Török, B. Application of Sonochemical Activation in Green Synthesis. In *Green Chemistry: An Inclusive Approach*; Török, B., Dransfield, T., Eds.; Elsevier, **2018**; pp. 673–693 (chapter 3.19).
409. Barge, A.; Tagliapietra, S.; Tei, L.; Cintas, P.; Cravotto, G. Pd-Catalyzed Reactions Promoted by Ultrasound and/or Microwave Irradiation. *Curr. Org. Chem.* **2008**, *12*, 1588–1612.
410. Toukoniitty, B.; Mikkola, J.-P.; Murzin, D. Y.; Salmi, T. Utilization of Electromagnetic and Acoustic Irradiation in Enhancing Heterogeneous Catalytic Reactions. *Trends Chem. Eng.* **2008**, *11*, 1–22.
411. Atobe, M.; Okamoto, M.; Fuchigami, T.; Park, J. E. Selective Hydrogenation by Polymer-Encapsulated Platinum Nanoparticles Prepared by an Easy Single-Step Sonochemical Synthesis. *Ultrason. Sonochem.* **2009**, *17*, 26–29.
412. Török, B.; Felföldi, K.; Szakonyi, G.; Bartók, M. Sonochemical Enantioselective Hydrogenation of Ethyl Pyruvate over Platinum Catalysts. *Ultrason. Sonochem.* **1997**, *4*, 301–304.

413. Török, B.; Felföldi, K.; Szakonyi, G.; Molnár, Á.; Bartók, M. Ultrasonics in Chiral Metal Catalysis. Effect of Presonation on the Asymmetric Hydrogenation of Ethyl Pyruvate over Platinum Catalysts. In *Catalysis of Organic Reactions*; Herkes, F., Ed.; Marcel Dekker: New York, 1998; pp. 129–137.
414. Török, B.; Balázsik, K.; Török, M.; Szöllösi, G.; Bartók, M.; Studer, M.; Neto, S. Asymmetric Sonochemical Reactions. Enantioselective Hydrogenation of  $\alpha$ -Ketoesters over Platinum Catalysts. In *Proceeding of 2nd Conference on Applications of Power Ultrasound in Chemical and Physical Processing*; Wilhelm, A. M., Delmas, H., Eds.; ENSIGC, **1999**; p. 13.
415. Szóri, K.; Török, B.; Felföldi, K.; Bartók, M. Enantioselective Hydrogenation of  $\alpha$ -Ketoesters over a Pt/Al<sub>2</sub>O<sub>3</sub> Catalyst. Effect of Steric Constraints on the Enantioselection. In *Catalysis of Organic Reactions*; Ford, M., Ed.; Marcel Dekker: New York, 2000; p. 489 (chapter 44).
416. Török, B.; Balázsik, K.; Török, M.; Szöllösi, G.; Bartók, M. Asymmetric Sonochemical Hydrogenation of  $\alpha$ -Ketoesters Over Cinchona-Modified Platinum Catalysts. *Ultrason. Sonochem.* **2000**, *7*, 151–155.
417. Disselkamp, R. S.; Judd, K. M.; Hart, T. R.; Peden, C. H. F.; Posakony, G. J.; Bond, L. J. A Comparison Between Conventional and Ultrasound-Mediated Heterogeneous Catalysis: Hydrogenation of 3-Buten-1-ol Aqueous Solutions. *J. Catal.* **2004**, *221*, 347–353.
418. Disselkamp, R. S.; Chin, Y. H.; Peden, C. H. F. The Effect of Cavitating Ultrasound on the Heterogeneous Aqueous Hydrogenation of 3-Buten-2-ol on Pd-Black. *J. Catal.* **2004**, *227*, 552–555.
419. Li, H.; Li, H.; Zhang, J.; Dai, W. Q. Ultrasound-Assisted Preparation of a Highly Active and Selective Co-B Amorphous Alloy Catalyst in Uniform Spherical Nanoparticles. *J. Catal.* **2007**, *246*, 301–307.
420. Disselkamp, R. S.; Denslow, K. M.; Hart, T. R.; White, J. F.; Peden, C. H. F. The Effect of Cavitating Ultrasound on the Aqueous Phase Hydrogenation of cis-2-Buten-1-ol and cis-2-Penten-1-ol on Pd-Black. *Appl. Catal., A Gen.* **2005**, *288*, 62–66.
421. Diezi, S.; Hess, M.; Orglmeister, E.; Mallat, T.; Baiker, A. An Efficient Synthetic Chiral Modifier for Platinum. *Catal. Lett.* **2005**, *102*, 121–125.
422. Toukoniitty, B.; Kuusisto, J.; Mikkola, J. P.; Salmi, T.; Murzin, D. Y. Effect of Ultrasound on Catalytic Hydrogenation of D-Fructose to D-Mannitol. *Ind. Eng. Chem. Res.* **2005**, *44*, 9370–9375.
423. Carcenac, Y.; Tordeux, M.; Wakselman, C.; Diter, P. Convenient Synthesis of Fluorinated Alkanes and Cycloalkanes by Hydrogenation of Perfluoroalkylalkenes Under Ultrasound Irradiation. *J. Fluor. Chem.* **2005**, *126*, 1347–1355.
424. Disselkamp, R. S.; Peden, C. H. F. The Effect of Ultrasound on the Isomerization Versus Reduction Reaction Pathways in the Hydrogenation of 3-Buten-2-ol and 1,4-Pentadien-3-ol on Pd-Black. *Chem. Ind.* **2005**, *104*, 303–312.
425. Disselkamp, R. S.; Denslow, K. M.; Hart, T. R.; Peden, C. H. F. Non-Equilibrium Effects in the Hydrogenation-Mediated Isomerization Mechanism of Olefins During Cavitating Ultrasound Processing. *Catal. Commun.* **2006**, *7*, 348–350.
426. Cravotto, G.; Binello, A.; Boffa, L.; Rosati, O.; Boccalini, M.; Chimichi, S. Regio- and Stereoselective Reductions of Dehydrocholic Acid. *Steroids* **2006**, *71*, 469–475.
427. Chen, H.; Li, R.; Wang, H.; Liu, J.; Wang, F.; Ma, J. Highly Efficient Enantioselective Hydrogenation of Methyl Acetoacetate Over Chirally Modified Raney Nickel Catalytic System. *J. Mol. Catal. A: Chem.* **2007**, *269*, 125–132.
428. Li, H.; Zhang, J.; Li, H. Ultrasound-Assisted Preparation of a Novel Ni-B Amorphous Catalyst in Uniform Nanoparticles for *p*-Chloronitrobenzene Hydrogenation. *Catal. Commun.* **2007**, *8*, 2212–2216.

**156** Heterogeneous catalysis in sustainable synthesis

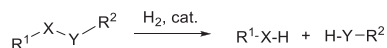
429. Mizukoshi, Y.; Sato, K.; Konno, T. J.; Masahashi, N.; Tanabe, S. Magnetically Retrievable Palladium/Maghemite Nanocomposite Catalysts Prepared by Sonochemical Reduction Method. *Chem. Lett.* **2008**, *37*, 922–923.
430. Li, H.; Wang, Y.; Zhao, Q.; Li, H. Ultrasound-Assisted Synthesis of Monodisperse Ru-B Amorphous Alloys With Enhanced Catalytic Activity in Maltose Hydrogenation. *Res. Chem. Intermed.* **2009**, *35*, 779–790.

## Chapter 3.2

# Heterogeneous catalytic hydrogenolysis of organic compounds

### 3.2.1. Introduction

A reaction is defined as hydrogenolysis when an X-Y  $\sigma$ -bond is broken by the introduction of a hydrogen molecule and X-H and Y-H bonds form (Scheme 1).<sup>1</sup> In open-chain compounds two products are obtained, while the hydrogenolysis of cyclic compounds yields one product. As a general rule the bond polarization plays an important role; a more polarized bond breaks more readily than nonpolarized counterparts.



**SCHEME 1** Generic reaction scheme of a hydrogenolysis reaction.

Hydrogenolysis reactions are commonly classified by the bonds that break and accept the two hydrogen atoms. In this chapter the hydrogenolysis of all common C-C and C-heteroatom bonds is discussed focusing on C-C, C-O, C-N, C-halogen, C-Si, C-S bonds; however, the hydrogenolysis of heteroatom-heteroatom bonds, such as N-O, N-N, or Si-O bonds will also be reviewed. Hydrogenolysis can be carried out under homogeneous as well as heterogeneous conditions that are largely similar to the conditions of hydrogenation.<sup>2-7</sup> Thus the best catalysts are the typical hydrogenation catalysts, namely transition metals as described earlier, although other materials, such as silica supported Zr-hydrides,<sup>8,9</sup> LaCoO<sub>3</sub>,<sup>10</sup> Cu<sub>x</sub>Mo<sub>6</sub>S<sub>8- $\delta$</sub> ,<sup>11</sup> CuZn bimetallic catalysts,<sup>12</sup> Fe-containing nanocatalysts<sup>13</sup> or single atom catalysis<sup>14,15</sup> have also been studied. Due to the activity, stability, applicability, and potential recyclability of supported metals that conform to the green chemistry requirements<sup>16,17</sup> these are the most frequently applied catalysts for hydrogenolysis reactions. The most commonly applied metals for hydrogenolysis reactions are Pt, Pd, Rh, Ni.<sup>3,5</sup> In addition to the traditional catalytic hydrogenolysis methods, microwave-assisted methods have also been extensively explored.<sup>18-20</sup> Although an overwhelming majority of studies focus on experimental approaches, theoretical density functional theory studies also investigate the impact of the metal of the catalysts and heteroatoms on the hydrogenolysis reactions.<sup>21</sup>

As a new addition to the traditional fields of hydrogenolysis, the emergence of green chemistry resulted in the development and applications of new catalysts that are used for the hydrogenolysis of biomass-related chemicals, such as glycerol or tetrahydrofurfuryl alcohol.<sup>22</sup> Thus a separate subchapter will be devoted to these reactions.

### 3.2.2. C–C bonds

The hydrogenative cleavage of C–C bond in alkanes is quite challenging due to the low polarity and hence high stability of these compounds. The aliphatic, open-chain compounds are the most unlikely to undergo C–C bond hydrogenolysis in a controlled manner to form a product selectively. While these reactions are carried out in the chemical industry regularly, the processes yield product mixtures, often from competing reactions.<sup>23</sup> In contrast to open-chain alkanes, cycloalkanes undergo hydrogenolysis more readily due to their ring strain. However, the size of the ring significantly affects the required reaction conditions. The transition metal catalyzed ring opening of cycloalkanes was studied extensively due to their importance in theoretical and industrial catalytic hydrocarbon chemistry.<sup>24</sup> Cyclopropane, metallacyclobutane and cyclopentane-like adsorbed species are well-established intermediates in the skeletal isomerization of saturated hydrocarbons. This research area enjoyed considerable attention in the 1970–80s period and was extensively reviewed.<sup>25–28</sup> As a general rule, higher the ring strain, the less harsh temperatures are required. Thus the ring opening of cyclopropanes occurs at the lowest temperatures without any side reactions and the highly stable cyclohexanes react very sluggishly even at high temperatures. Substituted cycloalkanes can form various cleavage products depending on their structures and the bond hydrogenolyzed. Representative examples of cycloalkane hydrogenolysis are summarized in [Table 1](#).

The hydrogenative ring opening of the earlier cyclic hydrocarbons usually occurs in the sterically less hindered **a** position ([Table 1](#)). The only exceptions are propylcyclopropane and propylcyclobutane ([Table 1](#), entries 2, 3). In these cases the sterically hindered **b** direction dominates. Based on several studies on a variety of metal catalysts (Pt, Pd, Rh, and Ni) it was confirmed that the effect is not metal dependent, the acidity of the support was also excluded as a potential source of this unexpected selectivity. It has been proposed that the long alkyl chain also undergoes adsorption on the surface of the catalyst and anchors the molecule in an orientation where the sterically more hindered C–C bond is closer to the metal surface, hence the cleavage occurs predominantly at the bond that is adjacent to the side chain. Interestingly, the shorter ethyl and methyl cycloalkanes do not show this behavior. While the ring opening of cycloalkanes is not a large-scale synthetic reaction, the ring-opening hydrogenolysis of cyclopentane, methylcyclopentane, and cyclohexane is one of the most frequently used test reactions to evaluate the activity and selectivity of tailored catalysts ([Table 1](#), entries 4, 5, 9).

**TABLE 1** Hydrogenolysis of substituted cycloalkanes on metal catalysts.



| Entry | Substrate                                | Catalyst  | Conditions  | Comments   | Ref.   |
|-------|--|---|---|--|--------|
| 1     | Alkylcyclopropanes and butanes           | Cu/SiO <sub>2</sub> , Pt/SiO <sub>2</sub> , Pd/SiO <sub>2</sub> , Rh/SiO <sub>2</sub> , Ni/SiO <sub>2</sub> | 50–170°C, 20–80 kPa H <sub>2</sub>                    | Cyclopropane ring opening occurs at lower T and hydrogen pressure, selectivities are similar for both groups   | 29–33  |
| 2     | Propylcyclopropan, propylcyclobutane     | Pt/SiO <sub>2</sub> , Pd/SiO <sub>2</sub> , Rh/SiO <sub>2</sub>   | 100–400°C, 3.3–80 kPa H <sub>2</sub>                  | At lower temperatures the unexpected <b>b</b> product dominates, at higher temperatures and low hydrogen pressures ring enlargement and aromatization occurs | 34–40  |
| 3     | Monoalkylcyclobutanes                    | Pt/SiO <sub>2</sub> , Pd/SiO <sub>2</sub> , Rh/SiO <sub>2</sub> , Ni/SiO <sub>2</sub>                       | 200–400°C, 3.3–60 kPa H <sub>2</sub>                  | With short side chains (Me, Et) the sterically less hindered <b>a</b> cleavage dominates, with propyl pathway <b>b</b> is the major cleavage route           | 41–44  |
| 4     | Methylcyclobutane and methylcyclopentane | Pt/SiO <sub>2</sub> , Pd/SiO <sub>2</sub>   | 200–400°C, 3.3–73 kPa H <sub>2</sub>                  | Kinetic measurement, statistical <b>a/b</b> selectivity, H-D exchange studied by surface FT-IR   | 45     |
| 5     | Methylcyclohexane                        | Ir/Al <sub>2</sub> O <sub>3</sub>   | 250°C, 0.63 MPa H <sub>2</sub> /D <sub>2</sub>        | Mechanistic, H-D exchange, isotope effect, cleavage at <i>a</i> and <i>b</i> dominates   | 46     |
| 6     | Tetracyclopropylmethane                  | PtO <sub>2</sub>  | H <sub>2</sub> , PtO <sub>2</sub> , AcOH, 20°C, 4.5 h | Ring opening of all cyclopropyl rings to tetra- <i>i</i> Pr-methane, quantitative yield  | 47, 48 |

*Continued*

**TABLE 1** Hydrogenolysis of substituted cycloalkanes on metal catalysts—cont'd

| Entry | Substrate                                  | Catalyst  | Conditions  | Comments   | Ref.   |
|-------|--|---|---|--|--------|
| 7     | Perspirocyclopropanated bicyclopropylidene | (a) Pd/BaSO <sub>4</sub> ;<br>(b) PtO <sub>2</sub>  | (a) H <sub>2</sub> , hexane/<br>MeOH, 20°C,<br>2 h;<br>(b) H <sub>2</sub> , hexane/<br>AcOH, 20°C,<br>2.5 h | Selective ring opening of specific cyclopropane units, yields: 23%–82% | 49     |
| 8     | Tetracyclopropyl adamantane                | PtO <sub>2</sub>  | H <sub>2</sub> , hexane/AcOH,<br>20°C, 2 h  | Ring opening to tetraisopropyl adamantane, 100% yield                  | 50     |
| 9     | Cyclopentane, Methylcyclopentane           | Rh-Sn-B/Al <sub>2</sub> O <sub>3</sub><br>Pt-Ir/TiO <sub>2</sub> , Rh-Sn/<br>Al <sub>2</sub> O <sub>3</sub> , Pt-Rh | H <sub>2</sub> (up to 1 atm),<br>100–300°C, flow  | Used for catalyst characterization                                     | 51–55  |
| 10    | Decalin                                    | Pt-Ir/TiO <sub>2</sub>  | H <sub>2</sub> (3 MPa), 325°C,<br>6 h   | Ring opening is the main reaction, dehydrogenation, etc. also occur    | 53     |
| 11    | <i>n</i> -Heptane                          | Pt/γ-Al <sub>2</sub> O <sub>3</sub> -Cl<br>Pt-Sn-Ce/Al <sub>2</sub> O <sub>3</sub>                                  | H <sub>2</sub> (0.4–10 bar),<br>up to 500°C, flow<br>system   | Alkenes, aromatics, cracking products, conversion up to 70%            | 56, 57 |

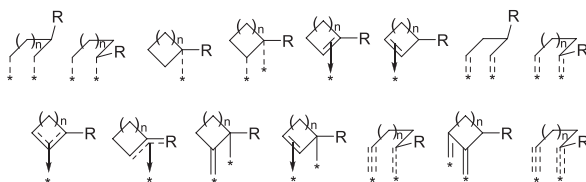
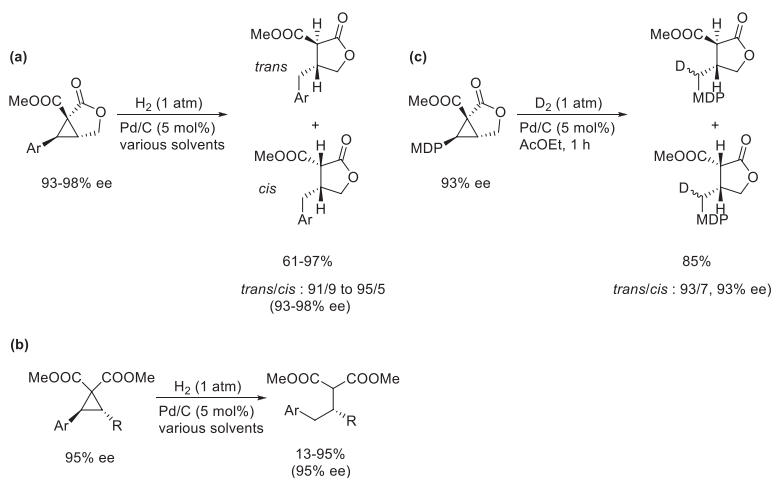


**FIG. 1** Proposed surface intermediates for the hydrogenative ring opening of methylcyclobutane ( $n=1$ ) and methylcyclopentane ( $n=2$ ).

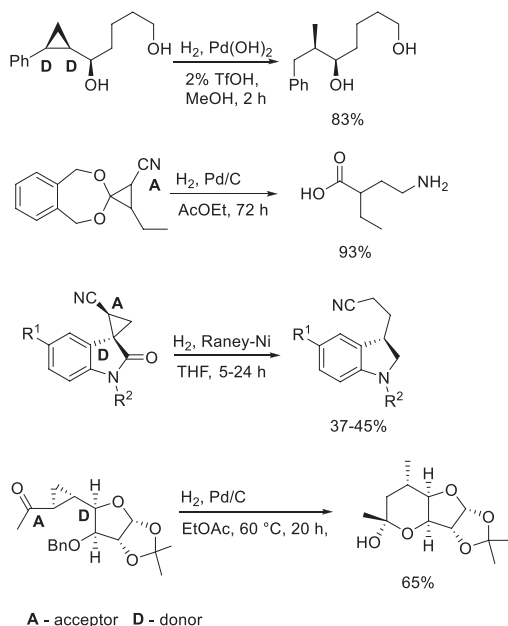
The mechanism of these hydrogenolysis reactions occurs via various surface-bound intermediates, whether it purely involves metal-carbon anchoring or takes place with the participation metal-support interfaces.<sup>58</sup> The most common types of intermediates of alkylcycloalkane ring-opening hydrogenolysis are illustrated in Fig. 1.

The hydrogenolysis of cyclopropane derivatives was broadly applied in synthetic chemistry as well.<sup>3, 5, 59</sup> The heterogeneous catalytic hydrogenolysis of enantioenriched cyclopropanes on Pd/C catalyst under mild conditions readily yielded *trans*- $\alpha$ -alkoxycarbonyl- $\beta$ -benzyl- $\gamma$ -lactones or  $\beta$ -substituted  $\gamma$ -aryl- $\alpha,\alpha$ -diesters in excellent yields and with high enantiomeric excess (Scheme 2a and b).<sup>60</sup> The reaction can be applied for the synthesis of chiral natural products, such as yatein. When the ring opening was carried out with deuterium gas, the corresponding monodeuterated products were obtained (Scheme 2c). The deuteration only occurred at the benzylic position; there was only a trace amount of D found in the  $\alpha$ -position. Although the mechanism is unclear at this point, the authors explained the presence of H in that position by exchange occurring with the H<sub>2</sub>O content of the Pd/C catalyst or the solvent itself.



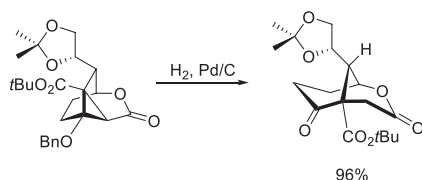
**SCHEME 2** Heterogeneous catalytic hydrogenolysis of bicyclic cyclopropyl lactones (A) and tetrasubstituted cyclopropanes (B) as well as deuteration (C) on Pd/C catalyst.

Similar applications of Pd and Raney-Ni catalysts have also been described for the ring opening of enantiomeric cyclopropanes (Scheme 3).<sup>61–64</sup>



**SCHEME 3** Hydrogenolysis of cyclopropanes with donor (D) and acceptor (A) groups on Raney-Ni and Pd catalysts.

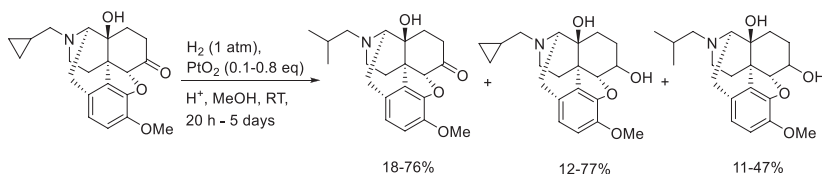
The synthesis of highly functionalized enantiopure oxatricyclo[3.3.1.0<sup>4,6</sup>]nonanes has been achieved by the selective hydrogenative ring opening of an activated cyclopropane containing precursor by Pd/C-catalyzed hydrogenolysis (Scheme 4).<sup>65</sup> Although the hydrogenolysis is essentially a debenzoylation reaction, the highly strained system opens up during the reaction to provide the products.



**SCHEME 4** Hydrogenolysis of the cyclopropane ring in a multiring system with Pd/C catalyst.

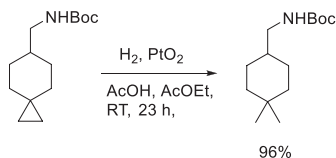
The PtO<sub>2</sub>-catalyzed hydrogenolysis of cyclopropyl-methylamine moiety attached to multiring systems resulted in the formation of the corresponding isobutyl amine derivative with good to modest selectivity, depending on the

reaction time and the amount of the catalyst used (Scheme 5).<sup>66</sup> The ring opening occurred under mild conditions, e.g., at room temperature. The scope of the reaction included N-, O-, and C-cyclopropylalkyl derivatives. Even nonactivated cyclopropane rings underwent cleavage; however, cyclobutyl derivatives were resistant to the ring opening.



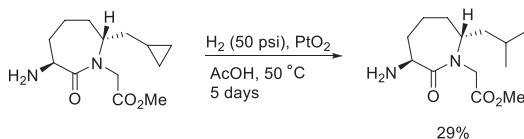
**SCHEME 5** Hydrogenolysis of the cyclopropyl ring of naltrexone methyl ether to an isopropyl group catalyzed by  $\text{PtO}_2$  in the presence of various acids.

The heterogeneous catalytic ring opening of the cyclopropane unit of a Boc protected spiro[2.5]oct-6-ylmethylamine was applied during the synthesis of 4-amino-2-cyanopyrimidines (Scheme 6),<sup>67</sup> that is a novel scaffold for non-peptidic cathepsin S inhibitors. The reaction occurred with nearly quantitative yield (96%).



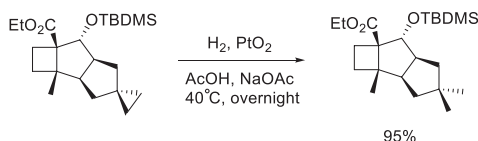
**SCHEME 6** Hydrogenative ring opening of the cyclopropane ring during the synthesis of non-peptidic cathepsin S inhibitors.

The selective ring opening of the cyclopropyl group in (3*S*)-*trans*-3-aminohexahydro-7-(cyclopropyl-methyl)-2-oxo-1*H*-azepine-1-acetic acid methyl ester to the corresponding 7-(2-methylpropyl) product was achieved, though with low yield (29%) using  $\text{PtO}_2$  on carbon catalyst in acidic solutions (Scheme 7).<sup>68</sup> This step was a part of the synthesis of dual metalloprotease inhibitors.



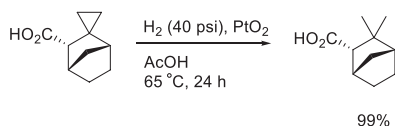
**SCHEME 7** Hydrogenolysis of the cyclopropyl ring of a dual metalloprotease inhibitor intermediate.

The ring opening of the cyclopropyl group is one of the last steps during the synthesis of (+)-sulcatine G. The reaction uses the traditional  $\text{PtO}_2$  catalyst under acidic conditions (Scheme 8).<sup>69</sup> The C–C bond hydrogenolysis occurs under mild conditions with nearly quantitative yield (95%) though in a relatively long reaction (overnight).



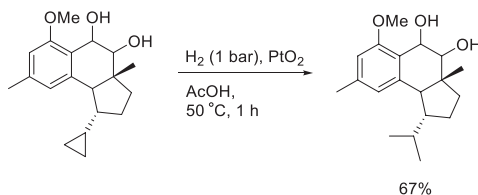
**SCHEME 8** Hydrogenolysis of the cyclopropyl ring during the synthesis of (+)-sulcatine G.

During the asymmetric total synthesis of spirocyclopropane and *gem*-dimethyl norbornyl carboxylic acids, one of the last steps of the synthesis involved the ring opening of the cyclopropane unit by  $\text{PtO}_2$ -catalyzed hydrogenolysis (Scheme 9).<sup>70</sup> The reaction occurred under mild experimental conditions with quantitative yield (99%).



**SCHEME 9** Preparation of *gem*-dimethyl norbornyl carboxylic acid from the corresponding spirocyclopropyl precursor by  $\text{PtO}_2$ -catalyzed hydrogenolysis.

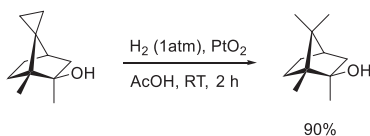
A nearly identical approach was used by Taber and Tian during the synthesis of (–)-hamigeran B, a natural compound with significant antiviral activities against herpes and polio. The cyclopropyl ring was introduced by the Petasis reagent, and the product later was subjected to a  $\text{PtO}_2$ -catalyzed hydrogenolysis that yielded the corresponding isopropyl product under mild conditions, however, with only moderate (67%) yield (Scheme 10).<sup>71</sup>



**SCHEME 10**  $\text{PtO}_2$ -catalyzed hydrogenolysis of an intermediate during the synthesis of (–)-hamigeran B.

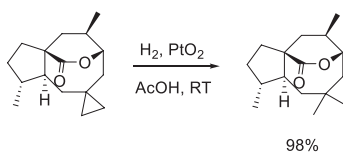
The earlier method was successfully extended for the synthesis of camphor derivatives from an unusual starting material, 7-spirocyclopropyl camphor derivative.

The Adam's catalyst appeared to effectively catalyze the hydrogenolysis of the cyclopropane ring (90%) under mild conditions (Scheme 11).<sup>72</sup>



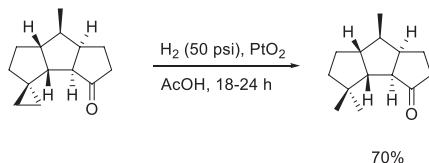
**SCHEME 11** Hydrogenolysis of a spirocyclopropyl compound to the corresponding camphor derivative.

Harmata and Rashatasakhon also applied the same concept, namely the hydrogenative ring opening of a spirocyclopropylcyclooctane for the synthesis of the expected *gem*-dimethyl product (Scheme 12).<sup>73</sup> This step was applied during the synthesis of a cyclooctanoid sesquiterpen, (–)-dactylol.



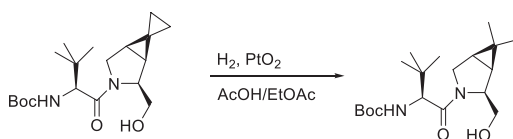
**SCHEME 12** Hydrogenative ring opening of a spirocyclopropylcyclooctane during the synthesis of (–)-dactylol.

In a similar manner, the synthesis of novel triquinane sesquiterpenes was accomplished. The process involved a step when the C3-ring hydrogenolysis of a spirocyclopropyl cyclopentane system was carried out using PtO<sub>2</sub> catalyst under mild condition, albeit with moderate yield (70%) only (Scheme 13).<sup>74</sup>



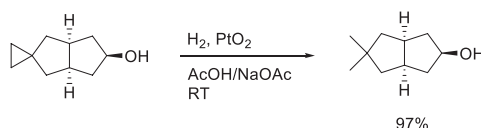
**SCHEME 13** PtO<sub>2</sub>-catalyzed hydrogenative C3-ring opening of a spirocyclopropyl-cyclopentane.

The selective hydrogenolysis of one of two cyclopropyl rings in a fused/spirocyclopropyl-cyclopropane unit containing dipeptide was successfully completed by Hendrata et al. with the aim of developing novel antiviral peptides. The traditional PtO<sub>2</sub> catalysis achieved the goal under mild experimental conditions (Scheme 14).<sup>75</sup>



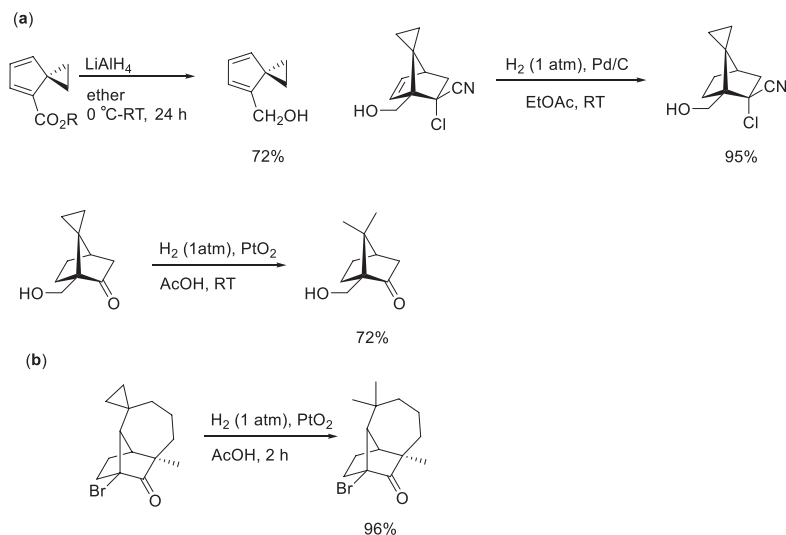
**SCHEME 14** Selective heterogeneous catalytic ring opening of a spirocyclopropyl-cyclopropane to the corresponding 1,1-dimethyl-cyclopropane derivative.

The ring-opening hydrogenolysis of the cyclopropyl ring in a spirocyclopropyl-cyclopentanol was carried out by Harrowven et al. to produce a key intermediate for the synthesis of ( $\pm$ )-desoxyhypnophilin, a natural product with significant antimicrobial activity. The traditional PtO<sub>2</sub> catalysis was used under mild, acidic conditions (Scheme 15).<sup>76</sup>



**SCHEME 15** Ring-opening hydrogenolysis of the cyclopropane ring during the total synthesis of ( $\pm$ )-desoxyhypnophilin.

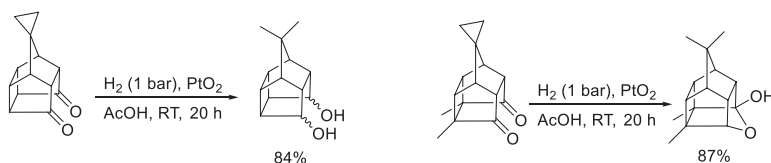
The cyclopropyl group shows interesting stability features. During the development of a novel synthesis for the bornane skeleton, several different conditions were applied for various reduction steps, including a LiAlH<sub>4</sub> reduction and two heterogeneous catalytic protocols involving Pd/C and PtO<sub>2</sub> as catalysts. While the cyclopropane ring showed excellent resistance toward the hydride reduction or the Pd/C-catalyzed hydrogenation, it readily underwent a hydrogenative ring opening in the presence of PtO<sub>2</sub> in acidic medium. In addition, the carbonyl group in the compound also remained intact after the hydrogenation (Scheme 16a).<sup>77</sup>



**SCHEME 16** Reactivity of the cyclopropyl ring under various experimental conditions.

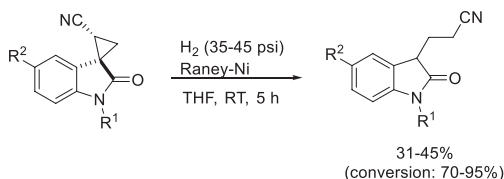
Similar conditions were applied for the ring opening of the cyclopropyl unit during the total synthesis of a sesquiterpenoid, longifolene (Scheme 16b).<sup>78</sup>

A similar approach has been applied for the synthesis of *gem*-dimethyl containing cage systems. The Adam's catalyst was used under standard conditions to cleave the cyclopropyl ring. At the same time, the two carbonyl groups that were present in the compounds also underwent a reduction to form a diol (Scheme 17).<sup>79</sup> Interestingly, when the dimethyl substituted starting material was used, the diol formed a cyclic acetal.



**SCHEME 17** Parallel ring opening of the cyclopropane unit and the hydrogenation of the carbonyl groups in cage systems.

The selective hydrogenolysis of the cyclopropyl group in diastereomeric nitrile substituted spirocyclopropyloxindoles on Raney Ni catalyst under mild conditions (RT, 35–45 psi H<sub>2</sub>) has been achieved (Scheme 18).<sup>64</sup> The original stereochemistry appeared to determine the chemoselectivity of the ring opening. The *syn* diastereomer provided the corresponding 3-propylacetamide products, as evidenced by X-ray crystallography. Theoretical (DFT) calculations were also carried out and revealed that the chemo- and regioselectivity were determined by the bond length asymmetry of the cyclopropane moiety.



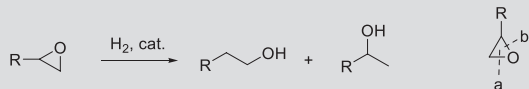
**SCHEME 18** Raney Ni-catalyzed hydrogenolysis of spiro[cyclopropyl-1,3'-oxindoles].

### 3.2.3. C–O bonds

The hydrogenolysis of the C–O bond is more common in synthetic processes than that of the C–C bond. However, breaking the C–O bond is still notoriously difficult, unless the alkyl group contains features that facilitate the bond cleavage (e.g., benzyl, *tert*-butyl) or the C–O bond is otherwise activated.<sup>3,5</sup>

Hydrogenolysis of cyclic ethers is an important process as the product alcohols are in high demand. Two commercially available cyclic ethers, such as methyl- and phenyloxirane (also called propylene- and styrene oxides), are typical test substrates to evaluate the performance of catalysts. Representative examples of cyclic ether hydrogenolysis are summarized in Table 2.

**TABLE 2** Hydrogenolysis of common oxiranes.



| Entry | Substrate   | Catalyst  | Conditions   | Comments   | Ref.   |
|-------|---|---|--|--|--------|
| 1     | Methyl-oxirane  | Pd/SiO <sub>2</sub> , Rh/SiO <sub>2</sub> , Au, Au/C, Pt/SiO <sub>2</sub> , Euro-Pt-1 | 100–400°C, 3.3–80 kPa  | Various type of C support  | 80–85  |
| 2     | Cyclohexane-oxide   | Cu/SiO <sub>2</sub> , Pd/SiO <sub>2</sub> , Rh/SiO <sub>2</sub>                       | H <sub>2</sub> (0–100 kPa), 130°C, deuteration as well   | Single C–O scission via isomerization and hydrogenation; double C–O cleavage (deoxygenation) was also found          | 86, 87 |
| 3     | <i>cis</i> -, <i>trans</i> -2,3-dimethyl oxiranes                                 | Cu/SiO <sub>2</sub>   | H <sub>2</sub> (0–101 kPa), 80–130°C   | Deoxygenation and isomerization competing  | 88     |
| 4     | Stilbene oxide, substituted styrene oxides, cyclohexene oxide, and alkyl-oxiranes | Pt nanoparticles on TiO <sub>2</sub>  | <i>hν</i> ( $\lambda > 300$ nm), 30°C, 6 h, alcohols ( <i>i</i> PrOH, EtOH) as solvents and hydrogen transfer agents | Styrene oxides: route <b>b</b> , alkyl oxiranes: route <b>a</b> dominates, yield: 72%–99%, some deoxygenation occurs | 89     |
| 5     | Terminal epoxides (aryl, benzyl, alkyl)   | Pd/C, doped with Lewis acids (Co-, Ni-salts)  | H <sub>2</sub> (1 atm), MeOH, RT, 1–12 h   | Route <b>a</b> dominates, yield: 15%–99%   | 90     |
| 6     | Phenyl-, benzyl oxiranes  | Pd nanoparticles  | H <sub>2</sub> (1 atm), MeOH, RT, 15–20 h  | Route <b>b</b> dominates, yield: 51%–98%   | 91     |
| 7     | 1-Methyl-2-phenyl oxirane   | Pd/C  | H <sub>2</sub> (1 atm), MeOH, RT, 3 h  | 1-Hydroxy-2-methoxy product, 80%–95%, syn/anti/60:40   | 92     |
| 8     | Variety of substituted aryl epoxides  | Pd <sup>0</sup> EnCat<br>Pd/iron oxide  | HCOOH (4 equiv), Et <sub>3</sub> N (4 equiv), EtOAc, 23 °C, 0.5–24 h   | Yield 82%–99%, 10 times recycled without activity drop; magnetically separable catalyst, yields: 85%–99%             | 93, 94 |
| 9     | A variety of sugar bound epoxides   | 10% Pd/C  | H <sub>2</sub> (1 bar), MeOH, RT, 24–48 h  | Yield: 71%–89%, de: 26%–70%  | 95     |

The data in [Table 2](#) indicate that the most common catalytic metals for the hydrogenolysis of the epoxide ring are the noble metals (Pt, Pd, Rh) on various supports. Copper and gold were also applied in these reactions either in their supported metal or nanoparticle forms. Due to the small size and considerable ring strain of epoxides, the reactions commonly occur under mild conditions with varied selectivities; depending on the catalyst both routes **a** and **b** ([Table 2](#)) can dominate. In addition, deoxygenation and isomerization are the most common side reactions. In fact, when the catalyst support is somewhat acidic it can shift the selectivity of the ring opening to the primary alcohol product. The most common application of the earlier applied simple oxiranes is to use them as test compounds in the characterization of metal catalysts, most commonly tailored samples and potentially compare them to the performance of well-known commercially available reference catalysts.

Similarly to oxiranes other ethers and simple alcohols can also undergo hydrogenolysis. In these cases the applied catalysts show a greater variation, including Ru, Pd, Pt, Re, Ni in different forms, such as supported catalysts, bimetallic nanoparticles, oxide doped metals, or a single crystal applied as an electrode for electrochemical hydrogenolysis. Although the reaction conditions strongly depend on the metal and the alkyl groups, generally the hydrogenolysis of these compounds requires harsher conditions than that of the oxiranes. The most common, representative applications are tabulated in [Table 3](#).

As a notable application of the Rh-MO<sub>x</sub>/SiO<sub>2</sub> (M=Mo or Re) catalysts, these materials are able to carry out the hydrogenolysis of esters, that is a particularly difficult process to achieve.<sup>105</sup>

Despite the numerous applications listed in [Tables 2 and 3](#) the most common application of C–O hydrogenolysis is the hydrogenative cleavage of the benzyl group, which is one of the most frequently used protecting groups in synthetic organic chemistry. Several typical hydrogenative *O*-debenzylation processes are presented in [Table 4](#).

As [Table 4](#) presents, the most common metal applied for the debenylation of various alcohols is Pd in agreement with earlier literature; other metals such as Rh or Ni are rarely applied.<sup>3–6</sup> The typical protocol involves the use of low pressure, mostly 1 bar, hydrogen gas at moderate temperatures that ranges from RT to 70–80°C, affording generally high (>75%), often quantitative yields.

Similarly to the hydrogenative cleavage of benzylated alcohols ([Table 4](#)), although not as commonly used, the deprotection of Cbz or Alloc derivatized alcohols also plays an occasional role in synthetic chemistry.<sup>117, 121</sup>

In addition to the importance of C–O hydrogenolysis in deprotection reactions, there are several relevant synthetic procedures, including multistep synthesis where these reactions are of practical importance. Examples include the hydrogenative ring opening of epoxides and other cyclic ethers. Adams et al. successfully applied the ring opening of a cyclohexene oxide derivative during the synthesis of an akkuammiline alkaloid, (+)-scholarisine. The reaction was carried out applying an alumina-supported Rh catalyst under mild conditions,

**TABLE 3** Hydrogenolysis of simple ethers and alcohols.

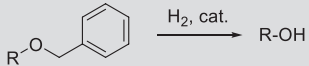
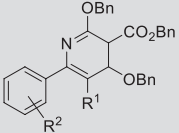
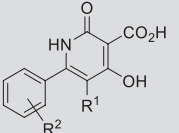
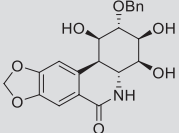
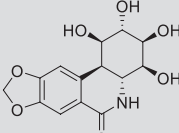
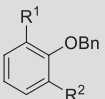
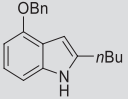
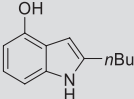
| $\text{R}^1\text{---O---R}^2 \xrightarrow{\text{H}_2, \text{cat.}} \text{R}^1\text{---OH, R}^2\text{---H, R}^1\text{---H, R}^2\text{---OH etc.}$ |                                   |  |  |  |         |
|--|-----------------------------------|--|--|--|---------|
| Entry  | Substrate                         | Catalyst   | Conditions   | Comments   | Ref.    |
| 1  | Biphenyl ether                    | RuPd <sub>5</sub> /NH <sub>2</sub> -SiO <sub>2</sub><br>Pd-Pt NPs <sup>a</sup> | 110°C, 10 bar H <sub>2</sub> , aq.<br>medium<br>95°C, 1 bar H <sub>2</sub> , aq.<br>medium         | Multiple products, product<br>distribution is dependent<br>on reaction time<br>100% conversion   | 96, 97  |
| 2  | Phenolic β-O-4 model<br>compounds | Ru/C<br>ReO <sub>x</sub> /C  | 160°C, 20 bar H <sub>2</sub> , MeOH<br>medium, 3 h<br>200°C, 3 MPa H <sub>2</sub> , hexane,<br>5 h | C2 and C3 phenols as<br>products (23% yield and<br>44% C2 phenol selectivity)<br>up to 98% yield | 98, 99  |
| 3  | Lignin models<br>methylphenols    | Ru/C<br>Co-MoS <sub>2-x</sub>  | 80–140°C, 10–40 bar H <sub>2</sub> ,<br>0.5–4 h, AcOH  | Alkylcyclohexanol<br>products with up to 96%<br>conversion and nearly<br>100% selectivity        | 100–102 |
| 4  | Isoeugenol                        | Ni/SBA <sup>b</sup> -15  | 300°C, 3 MPa H <sub>2</sub> ,<br>dodecane  | Multiple product,<br>deoxygenation occurs to a<br>large extent                                   | 103     |
| 5  | Eugenol                           | supported Cu,<br>Ni, Pd, Pt, Rh,<br>and Ru catalyst                            | 275°C, 5 MPa H <sub>2</sub> ,<br>hexadecane (solvent)  | Multiple hydrogenation<br>and deoxygenation<br>products  | 104     |

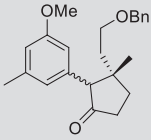
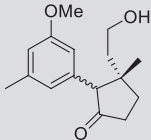
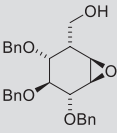
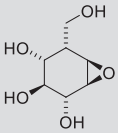
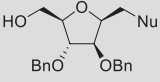
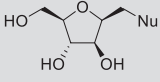
|    |   |   |   |   |          |
|----|---|---|---|---|----------|
| 6  | Ethers (and polyols)  | Rh-MO <sub>x</sub> /SiO <sub>2</sub><br>(M= Mo or Re) | 120°C, 8.0 MPa H <sub>2</sub> , 2–4 h                       | Alcohols and deoxygenated products  | 105      |
| 7  | Methyl benzyl alcohol   | Pt single crystal electrode                           | Electrochemical hydrogenolysis                              | Pt(100) surface is specifically active for the hydrogenolysis             | 106      |
| 8  | Phenyl benzyl ether   | Ni/γ-Al <sub>2</sub> O <sub>3</sub>                   | H <sub>2</sub> (225–400 bar), 20–250°C                      | MAS NMR mechanistic study   | 107      |
| 9  | Dibenzofuran  | Co/MoO <sub>3</sub><br>Co-Ni/MoO <sub>3</sub>         | 360°C, 0.1 MPa H <sub>2</sub> , flow reactor                | Up to nearly quantitative yield for biphenyl                              | 108, 109 |
| 10 | Variety of open and cyclic ethers, and secondary/ tertiary alcohols | MOF-OTf-PdCl <sub>2</sub>                             | 20 bar H <sub>2</sub> , 1,2-dichloroethane, 100–200°C, 24 h | 61%–99% yield for deoxygenated hydrocarbons, aromatic rings remain stable | 110      |
| 11 | Alkyl aryl ethers   | Skeletal Ni   | Electrocatalytic process                                    | Yields up to 90%, various hydrocarbon and hydroxy products                | 111      |

<sup>a</sup> NPs, nanoparticles.

<sup>b</sup> SBA, Santa Barbara amorphous silica; MOF, metal-organic framework.

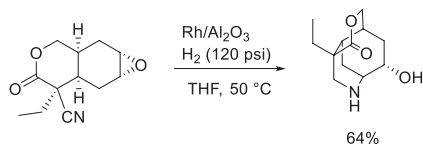
**TABLE 4** Representative examples for the hydrogenolysis of benzyl ethers (*R*-OBn).

|  |   |   |   |  |      |
|--|---|---|---|--|------|
| Entry  | Substrate   | Product   | Catalysts and conditions  | Comments   | Ref. |
| 1  |  |  | H <sub>2</sub> , 10% Pd/C, MeOH, RT   | In the preparation of DNA synthesis targeting antibacterial agents         | 112  |
| 2  |  |  | H <sub>2</sub> (1 bar), Pd(OH) <sub>2</sub> /C, EtOAc                         | During the synthesis of 7-deoxypancratistatin from carbohydrates           | 113  |
| 3  |  |  | H <sub>2</sub> (10 bar), various Rh and Ni NPs <sup>a</sup> , 25–60°C, 1–40 h | up to 100% conversion, up to 88% selectivity to C–O cleavage               | 114  |
| 4  |  |  | H <sub>2</sub> (1 bar), Pd/C, MeOH, RT  | 61% Yield, during the synthesis of phospholipase A <sub>2</sub> inhibitors | 115  |

|    |   |   |  |   |     |
|----|---|---|--|---|-----|
| 5  | A broad variety of benzyl ethers  | Debenzylated alkyl-, aryl-OH  | 15% Pd/C and 15% Pd(OH) <sub>2</sub> /C, 70°C, 6–48 h  | 70%–95% yield, aryl and alkyl ethers including chiral alkyl chains (with retention)               | 116 |
| 6  |  |  | H <sub>2</sub> (1 bar), Pd/C, THF/H <sub>2</sub> O, RT   | during the synthesis of (–)-Hamigeran B, hydrogenolysis yield: 98%                                | 71  |
| 7  | Benzyl protected alcohols and phenols   | Alcohols, phenols   | H <sub>2</sub> O-Al (H <sub>2</sub> source) Ni/Al, or Pd/C, 25–70°C, 24 h  | Nearly quantitative debenzylation (92%–100%)  | 117 |
| 8  |  |  | H <sub>2</sub> , Pd/C + Pd(OH) <sub>2</sub> (1:1), EtOH, RT, 40 h  | Yield: 61%–88%, a step during the synthesis of chiral 1,2-epoxy-3- or 1-hydroxypropylphosphonates | 118 |
| 9  |  |  | H <sub>2</sub> (1 bar), 5% Pd/C, MeOH, RT, 72 h  | 98% Yield, epoxide remains stable   | 119 |
| 10 |  |  | (a) H <sub>2</sub> (1 bar), Pd black, AcOH, RT, 15 h<br>(b) Pd/C 10%, HCO <sub>2</sub> NH <sub>4</sub> , MeOH, reflux, 5 h | Yield: 70%–94%  | 120 |

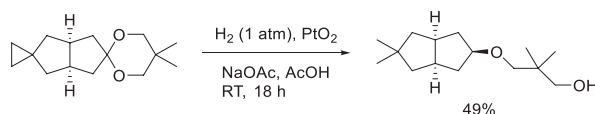
<sup>a</sup> NP, nanoparticle; Bn, benzyl; Nu, nucleophile, Ms, mesyl group.

although providing only moderate yield (64%) (Scheme 19).<sup>122</sup> It must be noted, however, that although formally the epoxide ring opens up during the reaction, it is the result of the hydrogenation of the nitrile to primary amino group that is immediately followed by the in situ epoxide ring opening generating the final product.



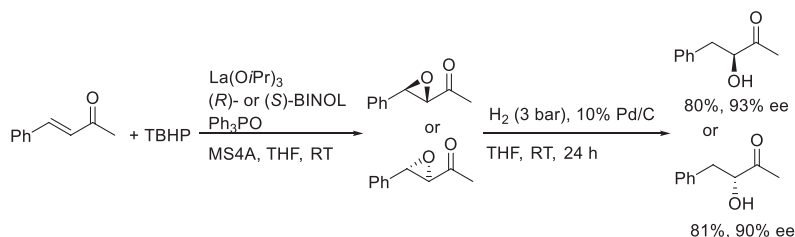
**SCHEME 19** Rh-catalyzed heterogeneous catalytic hydrogenolysis of a cyclohexene epoxide during the synthesis of (+)-scholarisine.

The partial C–O hydrogenolysis of the 1,3-dioxane ring occurs simultaneously with the C–C hydrogenolysis of the spirocyclopropyl unit during a step in the total synthesis of ( $\pm$ )-desoxyhyphnophilin. The typical C–C hydrogenolysis conditions (PtO<sub>2</sub>, NaOAc, AcOH) produced moderate yield (49%) for the product (Scheme 20).<sup>76</sup>



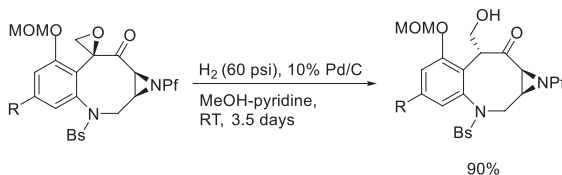
**SCHEME 20** Parallel ring opening of the cyclopropane unit and the partial hydrogenolysis of the dioxane ring during the total synthesis of ( $\pm$ )-desoxyhyphnophilin.

The enantioselective synthesis of 3-hydroxy-4-phenylbutan-2-one has been achieved by an asymmetric epoxidation of an enone that was followed by the ring opening of the epoxide on a Pd/C catalyst (Scheme 21).<sup>123</sup> The epoxide hydrogenolysis was carried out under mild conditions (5 bar H<sub>2</sub> pressure at room temperature) and provided good yield (80%) with high (90%) enantiomeric excess.



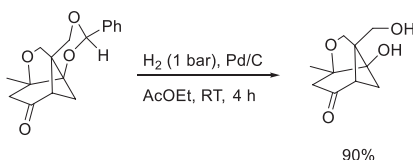
**SCHEME 21** Enantioselective synthesis of 3-hydroxy-4-phenylbutan-2-one via Pd/C-catalyzed ring opening of the intermediate epoxide.

A similar Pd/C-catalyzed methodology was applied during the synthesis of FK973, an intermediate to an antitumor antibiotic (+)-FR900482. The reaction was carried out in methanol using pyridine as an additive to modulate the activity of the catalysts resulting in the selective hydrogenolysis of the epoxide while leaving the carbonyl group and the aziridine ring intact (Scheme 22).<sup>124</sup>



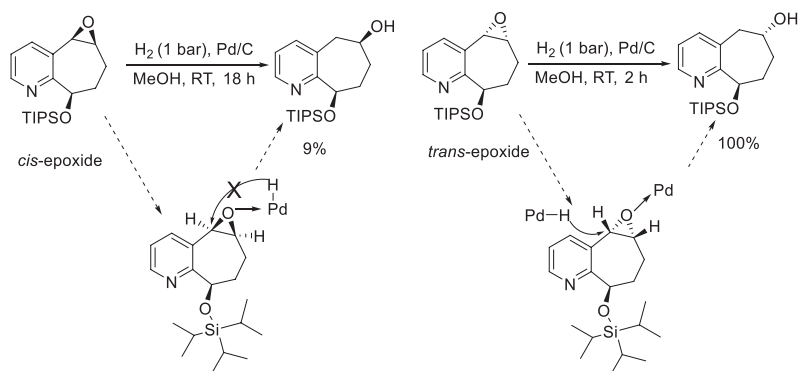
**SCHEME 22** Hydrogenolysis of the epoxide ring during the synthesis of an antitumor antibiotics (+)-FR900482.

The removal of the protecting group from a benzaldehyde derivatized diol via a Pd/C-catalyzed double debenzoylation was carried out in good yield by Martín-Rodríguez et al. during the synthesis of (+)-paeonisuffrone (Scheme 23). The spectroscopic properties of the product of the catalytic hydrogenolysis were found to be in agreement with those of the natural enantiomer.<sup>125</sup>



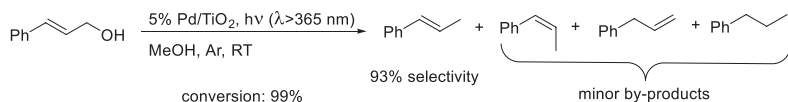
**SCHEME 23** Pd/C-catalyzed double hydrogenative debenzoylation of a protected diol during the synthesis of (+)-paeonisuffrone.

The enantioselective hydrogenolysis of chiral epoxides has been achieved as a key step during the asymmetric synthesis of the major metabolite of a calcitonin gene-related peptide receptor antagonist (Scheme 24).<sup>126</sup> As an additional challenge, the mechanism of epoxide hydrogenolysis was also studied. Drastically different hydrogenolysis rates were observed for the two diastereomeric epoxides. It appeared that the relative positions of the triisopropyl (TIPS) groups compared to the epoxide ring inhibited the hydrogenolysis in the case of the *cis*-epoxide due to its closeness to the palladium surface.



**SCHEME 24** Reactivity difference of *cis*- vs *trans*-epoxides in ring-opening hydrogenolysis.

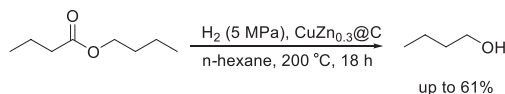
The hydrogenolysis or deoxygenation of the C–O bond in alcohols, primary and secondary alike, carboxylic acids, or furan derivatives is a common side reaction during the hydrogenation of these compounds, such as ethyl-anthraquinone,<sup>127, 128</sup> benzaldehyde,<sup>129, 130</sup> ketones,<sup>131–133</sup> furans,<sup>134–136</sup> diols and polyols,<sup>137, 138</sup> phenol,<sup>139, 140</sup> anisole,<sup>10, 141–144</sup> cresols,<sup>145–150</sup> guaiacol,<sup>151–153</sup> vanillin (either one step or via benzaldehyde),<sup>154</sup> methyl laureate<sup>155, 156</sup> and other esters,<sup>157</sup> or propionic acid.<sup>158</sup> Although the majority of the deoxygenation protocols produce simple hydrocarbons, often the hydrogenative deoxygenation can be carried out selectively and thus it could be of synthetic importance. Takeda et al. reported the Pd/TiO<sub>2</sub>-catalyzed hydrogenolysis of the C–O bond in allyl alcohols by a photocatalytic transfer hydrogenation method (Scheme 25).<sup>159</sup> By the application of this protocol the short synthesis of (*R*)-(-)-carvone was achieved from (*S*)-(+)-lavandulol. This environmentally benign method showed excellent tolerance toward C–C multiple bonds and allowed the synthesis to be carried out without the application of the undesirable protection/deprotection protocols.



**SCHEME 25** Photocatalytic transfer hydrogenolysis of allylic alcohols on a Pd/TiO<sub>2</sub> catalyst.

Although the hydrogenation of esters is a notoriously difficult process, it has been reported by Yao et al. that core-shell CuZn<sub>x</sub>@C materials synthesized via pyrolysis of a Zn(NO<sub>3</sub>)<sub>2</sub>-loaded metal-organic framework (MOF) was able to reduce butyl butyrate to butanol through the hydrogenolysis of one of the C–O bonds (Scheme 26). The Cu/Zn ratio played a significant role in the activity of the catalyst: CuZn<sub>0.3</sub> showing superior performance versus higher or lower ratios. In follow-up investigations, the catalyst appeared to produce similar

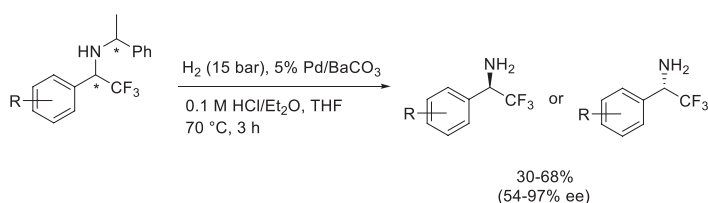
yields in the hydrogenation/hydrogenolysis of methyl caprylate (74% conversion, 82% selectivity) and methyl laurate (81% conversion, 77% selectivity) in 72 h long reactions.<sup>160</sup> In contrast, a Ni-based catalyst will reduce the esters to hydrocarbon via a deoxygenation.<sup>161</sup>



**SCHEME 26** Hydrogenation/hydrogenolysis of butyl butyrate over  $\text{CuZn}_{0.3}@\text{C}$  catalyst.

### 3.2.4. C–N bonds

The deprotection of functionalized amines, namely the hydrogenative cleavage of the N-bound protecting group, is the most common application of C–N bond hydrogenolysis. Among these, the removal of the *N*-benzyl moiety is the leading application due to its practicality and easy adaptability. This synthetic step can be applied as a simple deprotection of amino acids and other benzyl-protected amines.<sup>162</sup> As an extension of these applications to asymmetric synthesis, chiral methyl benzyl amines (Chiraselect reagents) are used as a chiral information source and added via Schiff-base formation. The following diastereoselective hydrogenation generates a new chiral center and in the final step, the methylbenzyl group is removed by catalytic hydrogenolysis resulting in the formation of chiral amines. This concept was applied in the synthesis of chiral 2,2,2-trifluoro-1-phenylethylamines (Scheme 27).<sup>163</sup> As a first step, the K-10 montmorillonite-catalyzed microwave-assisted condensation readily yielded the Schiff bases.<sup>164</sup> After an extensive examination of several catalysts, Pd/BaCO<sub>3</sub> was found to provide the best performance in the diastereoselective hydrogenation of the C=N bond. The same catalyst was able to initiate the hydrogenolysis of the C–N bond and remove the benzyl group and produce the (*R*)- and (*S*)-1,1,1-trifluoromethylbenzylamines, respectively, in 90%–93% ee and 50%–55% yield.<sup>163</sup> In a follow-up study, the same group extended the scope of the protocol to aryl-substituted derivatives, obtaining the products in 30%–68% yield with 54%–97% ee.<sup>165</sup>

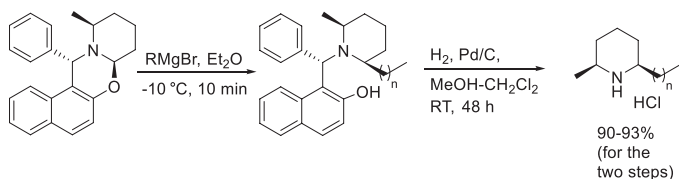


**SCHEME 27** Hydrogenolysis of the benzyl group of  $\alpha,\alpha,\alpha$ -trifluoromethyl benzyl-methylbenzylamines on 5% Pd/BaCO<sub>3</sub> catalyst in THF using 0.1 M HCl/Et<sub>2</sub>O.

Due to the expansion of the practical applications of green synthesis, there are extensive efforts to make the hydrogenative deprotection processes more effective and environmentally friendly. Several studies attempted to develop new improved protocols for the removal of protecting groups from the amino function. For instance, Choi et al. applied ionic liquids during a Pd/C-mediated debenzoylation process. The mild and efficient debenzoylation of *N*-benzyl- and *N,N*-dibenzylamino derivatives using 1-*n*-butyl-3-methylimidazolium (bmim) salts as cosolvents to MeOH was developed. In addition, the recycling of the Pd/C catalyst was also achieved.<sup>166</sup> In a similar process, Li et al. experimented with a mixture of Pd/C and Pd(OH)<sub>2</sub>/C catalysts that provided better yields than the two catalysts separately.<sup>116</sup>

Various multistep and total synthesis approaches involve the earlier concept: applying the benzyl group for the protection of a sensitive amino group and later the removal of the benzyl group, commonly by heterogeneous catalytic hydrogenolysis. Several applications are summarized in Table 5.

Often the C–N benzyl cleavage is applied with other than simple benzyl protecting group. Wang et al. developed the total syntheses of enantiopure alkaloid natural products (2*S*,6*R*)-dihydropinidine (as hydrochloride) and (2*S*,6*R*)-isosolenopsins (as hydrochlorides) in four steps. They used (*S*)-Betti base as a chiral auxiliary and a novel Pd/C-catalyzed *N*-debenzylation provided a route to the intermediate amine hydrochloride (Scheme 28).<sup>192</sup> Depending on the alkyl chain introduced by the Grignard reaction (first step) several complexes were hydrogenolyzed with nearly quantitative yields (94%–98%). The same group extended this protocol to the total syntheses of natural quinolizidine-,<sup>193</sup> and indolizidine-alkaloids.<sup>194</sup>

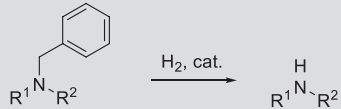


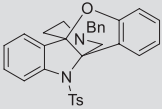
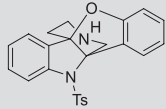
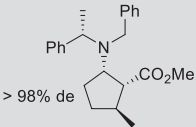
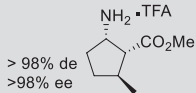
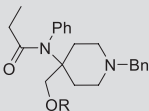
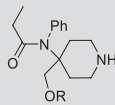
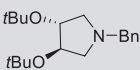
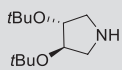
**SCHEME 28** Hydrogenolysis of a Betti base-tartaric acid complex on Pd/C catalyst.

The hydrogenolysis of other N-protecting groups was also widely applied in synthetic applications. The *N*-carbobenzyloxy group (*N*-Cbz) is routinely hydrogenolyzed by several supported Pd catalysts. Although the reaction is a simple debenzoylation and the cleavage occurs on the O–Bn bond the product carbamic acid decomposes, thus one formally removes the Cbz group from the amine therefore we include these deprotections under C–N hydrogenolysis. Recent hydrogenative deprotection of the Cbz group is tabulated in Table 6.

In addition to earlier processes, the hydrogenolysis of aromatic heterocycles also gained attention. Guo et al. reported the hydrogenolysis of indole over Ni, Pt, Ru, and Ni-Ru bimetallic catalysts under hydrothermal conditions.

**TABLE 5** Debenzylation of amines by the hydrogenolysis of the *N*-benzyl group.

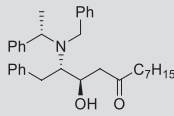
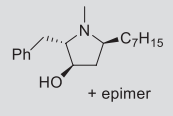
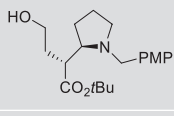
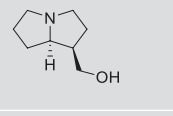
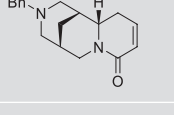
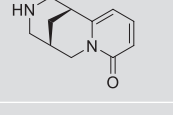
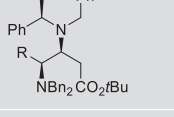
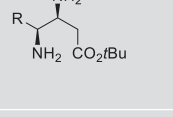
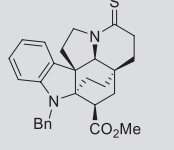
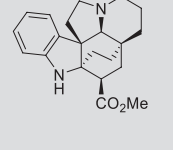
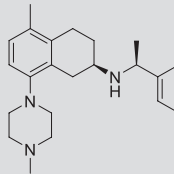
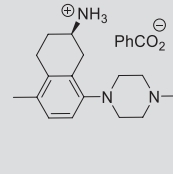


| Entry | Substrate   | Product   | Catalysts and conditions  | Comments   | Ref. |
|-------|---|---|---|--|------|
| 1     |  |  | H <sub>2</sub> , 10% Pd/C, MeOH, RT   | Applied for the synthesis of (±)-phalarine, yield 54%  | 167  |
| 2     |  |  | H <sub>2</sub> (1 bar), Pd(OH) <sub>2</sub> /C, MeOH/AcOH (40:1), RT, 2 h, then TFA/CH <sub>2</sub> Cl <sub>2</sub> (1:1) | Parallel kinetic resolution of both enantiomers for the asymmetric synthesis of 5-methyl-cispentacin enantiomers                                 | 168  |
| 3     |  |  | H <sub>2</sub> (50 psi), 10% Pd(OH) <sub>2</sub> /C, MeOH, RT   | During the preparation of [ <sup>2</sup> H <sub>3</sub> ]-sufentanil and metabolites, deprotection of several <i>N</i> -Bn-piperidines (85%–93%) | 169  |
| 4     |  |  | H <sub>2</sub> , Pd/C, 10 eq. AcOH, MeOH, RT, 3 h   | In synthesis of (–)-7 <i>S</i> -OH lentiginosine, deprotection yield 87%   | 170  |

Continued

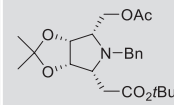
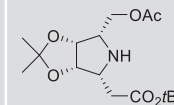
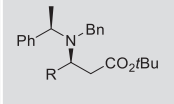
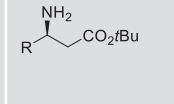
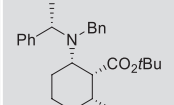
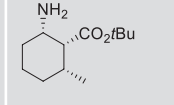
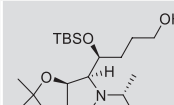
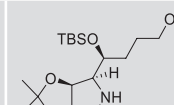
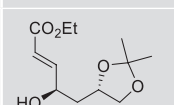
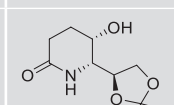
**TABLE 5** Debenzylation of amines by the hydrogenolysis of the *N*-benzyl group—cont'd

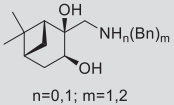
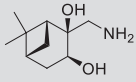
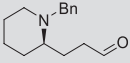
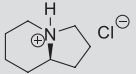
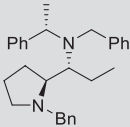
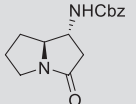
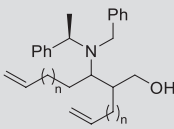
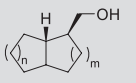
| Entry | Substrate | Product | Catalysts and conditions  | Comments   | Ref. |
|-------|-----------|---------|---|--|------|
| 5     |           |         | H <sub>2</sub> , 10% Pd/C, MeOH, RT, 4 days; then NEt <sub>3</sub> (cat. 12 h)        | Synthesis of alkaloid (S)-3-hydroxypiperidin-2-one; debenzylation and then cyclization (85%)                   | 171  |
| 6     |           |         | H <sub>2</sub> , 10% Pd(OH) <sub>2</sub> /C, MeOH, RT                                 | New type of antimalarial compounds based on febrifugine  | 172  |
| 7     |           |         | NH <sub>4</sub> HCO <sub>2</sub> , Pd(OH) <sub>2</sub> /C, MeOH                       | Total synthesis of (+)-scholarisine A  | 122  |
| 8     |           |         | H <sub>2</sub> (1 atm), 10% Pd/C, ClCH <sub>2</sub> CH <sub>2</sub> Cl, MeOH, RT, 1 h | 18 Examples, 96%–99% yield   | 173  |
| 9     |           |         | H <sub>2</sub> (1 atm), 10% Pd(OH) <sub>2</sub> /C, MeOH, RT, 12 h                    | Asymmetric syntheses of imino and amino sugars, quantitative yield with retention of configuration             | 174  |
| 10    |           |         | H <sub>2</sub> (5 atm), Pd(OH) <sub>2</sub> /C, MeOH, RT, 48 h                        | synthesis of (–)- and (+)-1-deoxymannojirimycin analogs, yield: 87%, both <i>O</i> and <i>N</i> -debenzylation | 175  |

|    |  |   |   |   |     |
|----|--|---|---|---|-----|
| 11 |   | <br>+ epimer | (1) H <sub>2</sub> , Pd(OH) <sub>2</sub> /C, MeOH, RT, 16 h;<br>(2) HCHO, H <sub>2</sub> , Pd/C, RT, 10 min | Asymmetric syntheses of (+)-preussin B and its derivatives  | 176 |
| 12 |   |              | H <sub>2</sub> , Pd(OH) <sub>2</sub> /C, MeOH, RT, 6 days   | Syntheses of pyrrolidines, indolizidines, and quinolizidines via two tandem ring-closure/ <i>N</i> -debenzylation processes, yield: 48% | 177 |
| 13 |   |              | Cyclohexene/toluene (1:2), Pd/C, 100°C, 12 h  | Synthesis of (±)-cytisine, cyclohexene as H-transfer agent, yield: 76%  | 178 |
| 14 |   |              | H <sub>2</sub> (5 atm), Pd(OH) <sub>2</sub> /C, MeOH, HCl, RT, 48 h   | Asymmetric synthesis of 4-aminopyrrolidin-2-ones  | 179 |
| 15 |   |              | H <sub>2</sub> , Raney-Ni, EtOH, RT, 3 h  | Synthesis of kopsinine, 95% yield with desulfurization  | 180 |
| 16 |  |             | H <sub>2</sub> , Pd/C, H <sub>2</sub> O/AcOH  | Synthesis of a novel 5-HT1B receptor antagonist, yield: 88%, ee: 98%  | 181 |

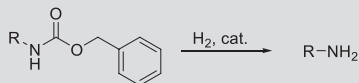
Continued

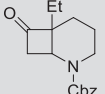
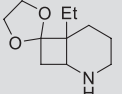
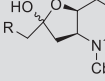
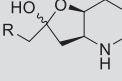
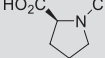
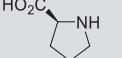
**TABLE 5** Debenzylation of amines by the hydrogenolysis of the *N*-benzyl group—cont'd

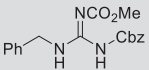
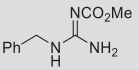
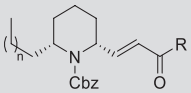
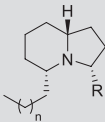
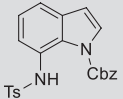
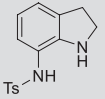
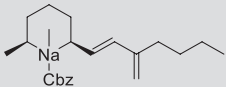
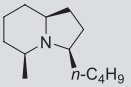
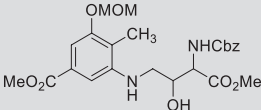
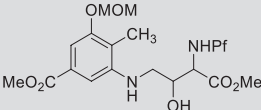
| Entry | Substrate   | Product   | Catalysts and conditions   | Comments   | Ref.        |
|-------|---|---|--|--|-------------|
| 17    |  |  | H <sub>2</sub> (1 atm), Pd(OH) <sub>2</sub> /C,<br>MeOH, RT, 15 h                        | Asymmetric synthesis of polyhydroxylated pyrrolidines, yield: 99%  | 182         |
| 18    |  |  | (i) H <sub>2</sub> (5 atm), Pd/C,<br>MeOH;<br>(ii) H <sub>2</sub> (5 atm), Pd/C,<br>AcOH | Asymmetric synthesis of α- and β-amino acids, yields 58%–97%   | 183,<br>184 |
| 19    |  |  | H <sub>2</sub> (1 atm), Pd(OH) <sub>2</sub> /C,<br>MeOH, RT, 24 h                        | Kinetic resolution for the asymmetric synthesis of 6-methyl-cis-hexacin enantiomers, yield: 97%            | 185         |
| 20    |  |  | H <sub>2</sub> (1 atm), 10%<br>Pd(OH) <sub>2</sub> /C, MeOH, RT,<br>6 h                  | Stereoselective synthesis of (–)-8-epi-swainsonine, yield: 88%   | 186         |
| 21    |  |  | HCO <sub>2</sub> NH <sub>4</sub> , 10% Pd/C,<br>MeOH, 60°C                               | synthesis of <i>cis</i> 3-hydroxy-pipecolic acids; debenzylated product undergoes ring closure, yield: 90% | 187         |

|    |  |   |   |  |     |
|----|--|---|---|--|-----|
| 22 |  <p><math>n=0,1; m=1,2</math></p> |                                  | <p><math>H_2</math> (1 atm), 10% Pd/C,<br/>MeOH, RT</p>   | <p>During the synthesis of monoterpene-based<br/>chiral aminodiols, yield: 95%</p>   | 188 |
| 23 |                                   |                                  | <p><math>H_2</math> (1 atm), Pd(OH)<sub>2</sub>/C<br/>(20% wt), MeOH, RT,<br/>24–48h then HCl</p>   | <p>Debenzylation and ring closure in one step,<br/>yield: 94%</p>  | 189 |
| 24 |                                   |                                  | <p>(a) <math>H_2</math> (5 atm), Pd(OH)<sub>2</sub>/C,<br/>HCl/MeOH, RT, 48 h;<br/>(b) HCl, 90°C, 18 h;<br/>(c) <math>K_2CO_3</math> toluene, reflux,<br/>18 h, then CbzCl, THF,<br/>RT, 16 h</p> | <p>during the asymmetric synthesis of<br/>(–)-(1<i>R</i>,7<i>aS</i>)-absouline yields: 34%–53%</p>   | 190 |
| 25 |                                   |  <p><math>n, m = 1, 2</math></p> | <p><math>H_2</math> (1 bar), Pd(OH)<sub>2</sub>/C,<br/>MeOH/ AcOH (25:1),<br/>35°C, 24 h</p>  | <p>During the asymmetric syntheses of<br/>(+)-trachelanthamidine, (+)-tashiromine, and<br/>(+)-epilupinine isolated in 8%–14% combined<br/>yield</p> | 191 |

**TABLE 6** Hydrogenative deprotection of *N*-carbobenzyloxy (Cbz) group.



| Entry | Substrate   | Product   | Catalysts and conditions   | Comments  | Ref. |
|-------|---|---|--|---|------|
| 1     |  |  | (i) ethylene glycol, TsOH/<br>H <sub>2</sub> O, benzene reflux,<br>12 h<br>(ii) H <sub>2</sub> , Pd/C, RT, 3 h | Protection of carbonyl before<br>reduction, quantitative, in the total<br>synthesis of (±)-aspido-spermidines | 195  |
| 2     |  |  | H <sub>2</sub> (1 atm), Pd(OH) <sub>2</sub> /C,<br>MeOH, RT  | A new antimalarial compounds based<br>on Febrifugine, 65%–80% yield   | 172  |
| 3     |  |  | H <sub>2</sub> (3.5 atm), 1% Pd/C,<br>EtOAc, 80–100°C, MW,<br>5 min  | 99% Yield, microwave-assisted<br>hydrogenolysis   | 196  |
| 4     | Cbz-protected amines  | R-NH <sub>2</sub>   | 20 wt% Pd/C, 10 eq.<br>Et <sub>3</sub> SiH, MeOH, RT,<br>10–50 min   | Transfer hydrogenolysis   | 197  |
| 5     | Cbz-protected secondary<br>amines   | R-NH-R  | H <sub>2</sub> (1 atm), 0.05 mol%<br>Pd(OAc) <sub>2</sub> /C, EtOAc, RT,<br>12 h                               | In situ preparation of Pd/C from<br>Pd(OAc) <sub>2</sub>  | 198  |

|    |   |   |  |   |          |
|----|---|---|--|---|----------|
| 6  |  |  | H <sub>2</sub> (1 atm), 5 mol% Pd/C, THF/MeOH (1:1), RT, 1 h               | Selective deprotection: from <i>N,N'</i> -diprotected guanidines to <i>N</i> -mono-protected guanidines | 199      |
| 7  |  |  | H <sub>2</sub> (55 psi), 10% Pd/C, RT, 12 h                                | Synthesis of indolizidine alkaloids; yield: 83–92   | 194      |
| 8  | N-Cbz-protected peptides  | Cbz-free peptides   | H <sub>2</sub> (1 atm-2.7 MPa), 10 mol% Pd/C, MeOH, tBuOH, RT-65°C, 1–12 h | Deprotecting peptides during multistep synthesis  | 200, 201 |
| 9  |  |  | H <sub>2</sub> (1 atm), Pd/C, MeOH, RT, 6 h                                | 95% Yield   | 202      |
| 10 |  |  | H <sub>2</sub> (1 atm), Pd(OH) <sub>2</sub> /C, MeOH, RT, 18 h             | During the synthesis of (+)-monomorine I, yield: 67%  | 203      |
| 11 |  |  | H <sub>2</sub> (1 bar), Pd/C, MeOH, RT                                     | During the synthesis of an antitumor antibiotic (+)-FR900482; 82% yield                                 | 124      |

The reaction provided a broad array of products, including ethylcyclohexane, ethylbenzene, 2-ethylaniline, *o*-toluidine, toluene, and methylcyclohexane. Although the catalyst showed high activity, the lack of selectivity in the product formation provides little synthetic potential; the process is rather considered to be a hydrodenitrogenation process of environmental importance.<sup>204</sup> Due to the ever stricter vehicle and power plant emission controls this area generates growing attention.<sup>205</sup>

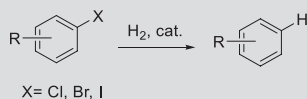
### 3.2.5. C-halogen bonds—Dehalogenation

The hydrogenative removal of halogens from organic compounds is of high importance from both synthetic and environmental point of view. In synthesis, halogens often serve in a placeholder role and drive the regio/stereochemistry of a synthetic process, and are only removed at the end of a process, similar to the protection/deprotection concept. In environmental applications hydrogenolysis is used to remove the halogen.<sup>206</sup> Several halogen-containing compounds belong to the group of volatile organic compound (VOCs) contaminants and via the water circle they commonly accumulate in groundwater.<sup>207</sup> In addition, these compounds often possess enhanced toxicity and slow biodegradability, thus extending their half-life in the environment.<sup>208, 209</sup> Therefore the dehalogenation of organic compounds is of high interest. Iodine is the most easily cleavable halogen, the reactivity of the C–Br and C–Cl bonds is lower and quite similar to each other, and the C–F bond is the most stable; hence F is the most difficult to remove halogen. The most active hydrogenation catalysts serve well for the hydrogenolysis of the C-halogen bonds as well; thus the commonly applied catalysts are Pd, Pt, Ni, in multiple forms such as supported or skeletal metal catalysts (see Chapter 2). Due to their particular importance from environmental point of view, the dehydrohalogenation processes are frequently reviewed.<sup>210, 211</sup>

The first large group of compounds that are prime targets for dehydrohalogenation is the aryl-halides, whether with a functional group (e.g., halogenated phenols) or without it. The hydrogenolysis could aim the simple replacement of the halogen with hydrogen or deuterium for synthetic purposes or simply to carry out environmental remediation. In general, the dehydrohalogenation of simple aromatic and aliphatic halogenated hydrocarbons is carried out for environmental purposes with the main goal of remediation; more complex compounds are also subjected to these investigations for synthetic purposes. The hydrogenolysis of the most common aromatic contaminants is summarized in Table 7.

As mentioned before, one of the major driving forces of studying hydrodehalogenation reactions is the environmentally harmful nature of organohalogen compounds, particularly those that are light and can rise to the stratosphere. It is due to their ability to form radicals there that decompose Earth's protective ozone layer. Therefore much attention was devoted to the hydrodehalogenation of alkylhalogenides, focusing mainly on methane derivatives (Table 8).<sup>235</sup>

**TABLE 7** Hydrogenolysis of simple arylhalides.



| Entry | Substrate                     | Catalyst   | Conditions   | Comments  | Ref.                                      |
|-------|-------------------------------|--|--|---|---|
| 1     | Chlorobenzene                 | Ni-NP <sup>3</sup> /TiO <sub>2</sub> ,<br>MgO/Ni-SBA-16                        | Neat or EtOH, 1–15 bar H <sub>2</sub> ,<br>100–300°C   | Recyclable catalyst, up to 85% removal<br>of chlorine                                     | <a href="#">212</a> , <a href="#">213</a> |
| 2     | Poly-chlorinated<br>aromatics | Raney Ni, Pd<br>catalysts  | H-source- <i>i</i> Pr-OH, 150–200°C  | KOH additive, aqueous medium,<br>surfactants  | <a href="#">214</a> , <a href="#">215</a> |
| 3     | Chlorophenols                 | Raney Ni<br>Ni-Al alloy  | 1 bar H <sub>2</sub> , 30–40°C, H <sub>2</sub> O as H <sub>2</sub><br>source, basic solution | Aqueous medium, nearly quantitative<br>yield  | <a href="#">216–218</a>                   |
| 4     | Aryl halides                  | Pd <sub>3</sub> PM2<br>Pd(OAc) <sub>2</sub>                                    | H <sub>2</sub> , HCOOK, <i>i</i> PrOH, DMSO,<br>80°C   | Even C–F bond reacts, selective<br>hydrodeiodination in the presence of<br>other halogens | <a href="#">219</a> , <a href="#">220</a> |
| 5     | Arylbenzal-<br>dehydes        | Pd/C   | H-source:Al-H <sub>2</sub> O   | F-derivative is stable  | <a href="#">221</a>                       |
| 6     | Chlorinated<br>N-heterocycles | SiO <sub>2</sub> sol-gel<br>entrapped Pd-<br>[Rh( <i>cod</i> )Cl] <sub>2</sub> | 27.6 bar H <sub>2</sub> , 80–140°C   | Ring hydrogenation also occurs  | <a href="#">222</a>                       |
| 7     | Chlorinated<br>biphenyls      | Ni-Al alloy  | H <sub>2</sub> O as H <sub>2</sub> source, basic solution                                    | Biphenyls and cyclohexyl-benzenes form,<br>selectivity depends on base                    | <a href="#">223</a> , <a href="#">224</a> |

*Continued*

**TABLE 7** Hydrogenolysis of simple arylhalides—cont'd

| Entry | Substrate                            | Catalyst    | Conditions  | Comments   | Ref.                |
|-------|--------------------------------------|-------------|---|--|---------------------|
| 8     | Polychlorinated arenes               | Ni-Al alloy | H <sub>2</sub> O as H <sub>2</sub> source, basic solution               | Complete dechlorination, no overhydrogenation (95%–100% yield) | <a href="#">225</a> |
| 9     | Chloro- and bromophenols             | Ni-Al alloy | H <sub>2</sub> O as H <sub>2</sub> source, Ba(OH) <sub>2</sub> solution | Dehalogenated cyclohexanols are the major products (30%–91%)   | <a href="#">226</a> |
| 10    | 2,4,6-Tri-Br-phenol                  | Ni-Al alloy | H <sub>2</sub> O as H <sub>2</sub> source, NaOH solution                | Quantitative debromination, no overhydrogenation               | <a href="#">227</a> |
| 11    | Halogenated polyphenols              | Ni-Al alloy | H <sub>2</sub> O as H <sub>2</sub> source, KOH solution                 | Overhydrogenated cyclohexane products (52%–94% yield)          | <a href="#">228</a> |
| 12    | 2,4-Di-Cl-phenol, 2- and 4-Cl-phenol | Pd NP       | Flow system, film reactor, water  | Over 90% reduction of the chlorinated substrates to phenol     | <a href="#">229</a> |

<sup>a</sup> NP, nanoparticles.

**TABLE 8** Examples for the environmental dehydrohalogenation of alkyl halides.

| alkylhalogenides $\xrightarrow{\text{H}_2, \text{cat.}}$ alkanes |                                 |   |   |   |   |
|--|---------------------------------|---|---|---|---|
| Entry  | Substrate                       | Catalyst  | Conditions  | Comments  | Ref.                                      |
| 1  | Trichloro-ethylene              | Pd/SOMS   | H <sub>2</sub> /N <sub>2</sub> stream, 100–200°C                              | Water addition improved conversion  | <a href="#">230</a>                       |
| 2  | CCl <sub>2</sub> F <sub>2</sub> | Pd/Al <sub>2</sub> O <sub>3</sub> , Pd/Nb <sub>2</sub> O <sub>5</sub> -Al <sub>2</sub> O <sub>3</sub> | Excess H <sub>2</sub> , flow system, 250°C                                    | Both dechlorination and defluorination                                    | <a href="#">231</a>                       |
| 3  | CHClF <sub>2</sub>              | Ni/SiO <sub>2</sub> -Al <sub>2</sub> O <sub>3</sub> , Pd/γ-Al <sub>2</sub> O <sub>3</sub> , Pd/C      | Flow system, H <sub>2</sub> (up to 100 bar), up to 400°C                      | Supercritical phase assistance, complete dehalogenation to methane        | <a href="#">232</a>                       |
| 4  | Chloro-methanes                 | Pt-Pd/sulfated zirconia   | Flow system, N <sub>2</sub> stream, H <sub>2</sub> /reactant added, 150–200°C | Conversions up to 90%, with up to 90% CH <sub>4</sub> selectivity         | <a href="#">233</a>                       |
| 5  | F-, Cl-, Br- and I-pentanes     | Nb, Mo, Ta, and W halide clusters with Re chloride cluster  | Flow system, H-stream, 300°C  | Major products are pentenes, even C–F bond undergoes hydrogenolysis on Re | <a href="#">234</a>                       |
| 6  | Halogenated aliphatic compounds | Ni-Al alloy   | H <sub>2</sub> O as H <sub>2</sub> source, KOH solution                       | All halogens removed, hydrocarbon products                                | <a href="#">206</a> , <a href="#">225</a> |

SOMS, swellable organically modified silica.

As shown, most applications use the traditional hydrogenation/hydrogenolysis catalysts (Pt, Pd, Ni, etc.). Due to the relatively high stability of the C-halogen bonds, the applications are only successful at relatively high temperatures (100°C and mostly above). In addition, since the processes are mostly designed for industrial-scale hydrodehalogenation, the reactor of choice is commonly the flow system that allows for continuous operation.

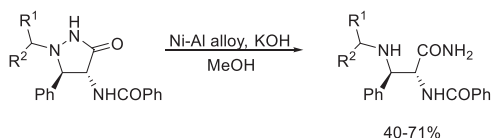
In addition to environmental applications, the hydrogenative replacement of halogens has also been frequently applied in organic synthesis. Representative examples are tabulated in Table 9.

As presented in Table 9, in addition to the typical metal-catalyzed hydrogenation with gaseous hydrogen, the dehalogenation of organic compounds can also be carried out by Ni-Al alloy, or in general, using Al as a hydrogen source in aqueous medium.<sup>246</sup> Although this system is effective in removing halogens the synthetic importance of early applications is limited due to selectivity issues that is likely caused by the use of strong base that made the system essentially uncontrollable. More recent applications (e.g., Table 9, entry 8) do not use base and apply Pd/C as catalyst and result in high yields and selectivities. Despite the synthetic benefits, the majority of applications consider dehydrohalogenation from an environmental chemistry perspective.<sup>247</sup>

### 3.2.6. N–N and N–O bonds

The hydrogenolysis of N–N bonds includes the hydrogenative cleavage of N–N single bonds (common heterocycles), N=N double bonds (e.g., azo compounds), and N≡N triple bonds (e.g., diazonium salts) and azides.

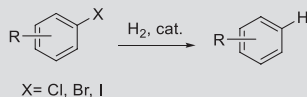
The ring-opening hydrogenolysis of the N–N single bond of pyrazolidinones was achieved by applying Ni-Al alloy in methanolic 1 M potassium hydroxide under mild conditions. The protocol resulted in moderate to good yields (Scheme 29).<sup>248</sup>



**SCHEME 29** Ring-opening hydrogenolysis of the N–N bond of pyrazolidinones.

The same alloy was applied for the hydrogenolysis of N–N bonds in nitrosoamines. The reaction, which was part of the synthesis of deuterated azamacrocycles (Scheme 30), yielded the corresponding secondary amines.<sup>249</sup> The Ni-Al alloy was applied in a basic solution and readily removed the nitroso groups, under mild conditions, in a process that is greener than the currently known alternatives. The hydrogenolysis was carried out in D<sub>2</sub>O, in order to avoid the

**TABLE 9** Hydrodehalogenation of various halogenated aromatics with a variety of substituents.



| Entry | Substrate  | Catalyst    | Conditions  | Comments   | Ref.     |
|-------|--|-------------|---|--|----------|
| 1     | Halogenated azo-compounds, benzophenones, acetophenones, benzaldehydes, etc. | Pd/MCM41    | NH <sub>4</sub> HCO <sub>2</sub> , 70°C   | Dehalogenated and hydrogenated products, recyclable catalyst                     | 236      |
| 2     | Tetrahalohydro-chinones, resorcinol and catechols                            | Ni-Al alloy | H <sub>2</sub> O as H <sub>2</sub> source, NaOH solution, with different concentration                                    | Quantitative dehalogenation, however, overhydrogenation could result in mixtures | 237, 238 |
| 3     | Tetra-Br- and tetra-Cl-bisphenols  | Ni-Al alloy | H <sub>2</sub> O as H <sub>2</sub> source, NaOH or Na <sub>2</sub> CO <sub>3</sub> solution, with different concentration | Selective, complete dehalogenation, 82%–100% yield                               | 239, 240 |
| 4     | Poly-Br-diphenyl ethers  | Ni-Al alloy | H <sub>2</sub> O as H <sub>2</sub> source, NaOH or Na <sub>2</sub> CO <sub>3</sub> solution, with different concentration | Selective, complete dehalogenation, 90%–100% yield                               | 239      |

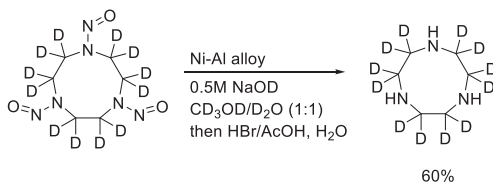
*Continued*

**TABLE 9** Hydrodehalogenation of various halogenated aromatics with a variety of substituents—cont'd

| Entry | Substrate   | Catalyst                       | Conditions   | Comments  | Ref.     |
|-------|---|--------------------------------|--|---|----------|
| 5     | Halogenated anilines  | Ni-Al alloy                    | H <sub>2</sub> O as H <sub>2</sub> source, NaOH solution, with different concentration             | All halogens (even F) can be removed, no overhydrogenation                        | 241, 242 |
| 6     | <i>m</i> -CF <sub>3</sub> -aniline  | Ni-Al alloy                    | H <sub>2</sub> O as H <sub>2</sub> source, KOH solution, with different concentration, RT          | All fluorine removed, no overhydrogenation  | 206      |
| 7     | Halogenated (Cl, Br) benzoic acids, acetamides, benzamides                      | Several supported Pd catalysts | Flow system, in situ generated D <sub>2</sub> gas (100 bar), 100°C, propylene carbonate as solvent | Br, Cl applicable I, F do not react properly, yields: 94%–96%, D content: 95%–98% | 243      |
| 8     | Halogenated aromatics: anilines, phenols, thiophenols, indoles, pyridines, etc. | Pd/C                           | Al and D <sub>2</sub> O as D <sub>2</sub> source, 25–50°C, 12–48 h                                 | Yields: 80%–100%, broad scope   | 244      |
| 9     | Halophenols   | Pd/CeO <sub>2</sub> SACs       | H <sub>2</sub> /N <sub>2</sub> mixture (1:1) at 1 bar, RT  | Nearly 90% elimination of the halogen over a 140 min period                       | 245      |

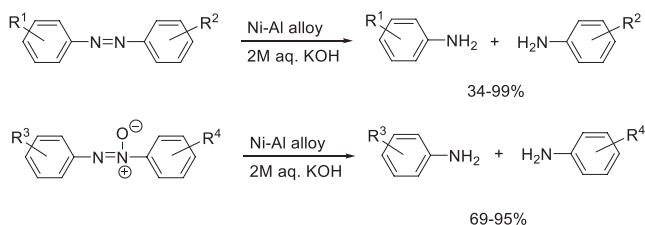
NP, nanoparticles; SACs, single atom catalysts.

D–H exchange on the C–D bonds that could be initiated by the in situ formed Raney Ni catalyst. After the reaction, the N–D groups were exchanged to N–H by treatment with HBr/AcOH in H<sub>2</sub>O.



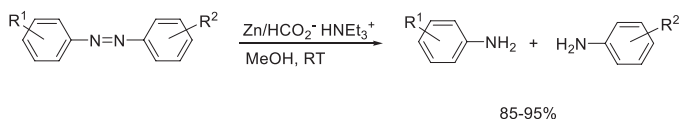
**SCHEME 30** Hydrogenolysis of the nitroso group in a deuterated aza-macrocyclic.

The hydrogenolysis of azo compounds is the most common example of the hydrogenative cleavage of N=N double bond.<sup>250</sup> During a study on waste detoxification, the hydrogenolysis of aromatic azo and azoxy compounds with Ni–Al alloy was observed in basic solution (Scheme 31).<sup>251</sup> The reaction was carried out at room temperature and the corresponding aniline derivatives were obtained in moderate to good yields.



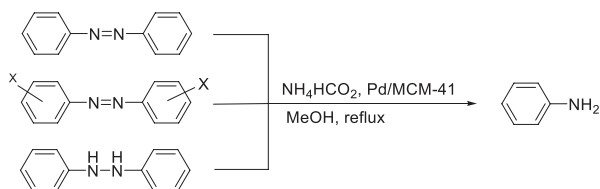
**SCHEME 31** Hydrogenolysis of the N=N double bond in azo and azoxy compounds by Ni–Al alloy in water.

The hydrogenative cleavage of the N=N bond of azo-compounds to the corresponding anilines was achieved by the application of triethyl ammonium formate catalyzed by zinc powder (Scheme 32).<sup>252</sup> The reaction appeared to be effective even at room temperature providing high yields in short times. The reductive system tolerated several hydrogenolysis sensitive groups such as methoxy, hydroxy, carboxylic acid, ether linkage, etc., and no dehalogenation was detected either. According to the proposed mechanism, the Zn acts as a catalyst and not a consumable reagent. This work is essentially a somewhat upgraded version of an earlier study by the same group.<sup>253</sup>



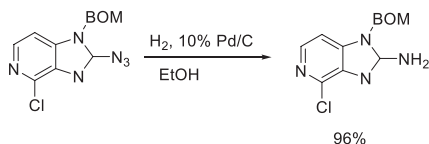
**SCHEME 32** Cleavage of the N=N bond of azo compounds by a Zn-catalyzed transfer hydrogenolysis.

A similar hydrogenolysis of azo-compounds was carried out by Selvan et al. using an MCM-41-supported Pd catalyst (Scheme 33).<sup>236</sup> The newly described catalyst has also been used for the hydrogenation of a variety of functional groups. In addition to the good performance, the catalytic activity was found to be unaffected after three consecutive reactions and thus the catalyst appears to be recyclable.



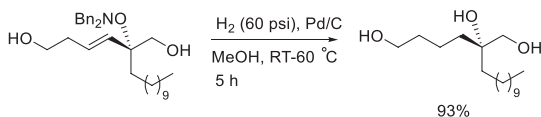
**SCHEME 33** Hydrogenolysis of azo, halogenated azo-compounds, and diarylhydrazines by Pd/MCM-41 catalysts using ammonium formate as hydrogen transfer agent.

The reduction and subsequent cleavage of the N–N bond in azides was an integral part of a total synthetic procedure developed for the synthesis of age-ladine A (Scheme 34).<sup>254</sup> The reaction took place under mild conditions, producing nearly quantitative yields (96%). The conditions were selective for the reduction and cleavage of the azido group; neither the protecting group, nor the chlorine present in the compound was affected.



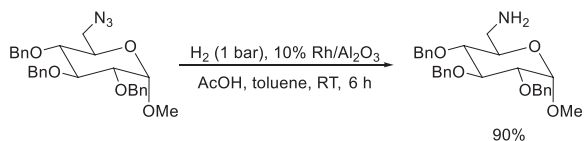
**SCHEME 34** Hydrogenolysis of the azido group to amino on Pd/C under hydrogen atmosphere.

As a part of the enantiospecific total synthesis of (+)-tanikolide, the hydrogenolysis of 2-((dibenzylamino)oxy)-2-undecylhex-3-ene-1,6-diol was carried out successfully, providing a rare example of N–O bond hydrogenolysis (Scheme 35).<sup>255</sup>



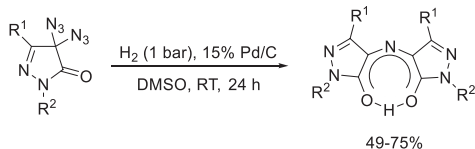
**SCHEME 35** Deprotection of a dibenzylamino protected alcohol via Pd/C-catalyzed hydrogenolysis of the N–O bond.

The chemoselective hydrogenation of azides yields primary amines via the hydrogenolysis of the azido group. This transformation has been carried out using a commercially available Rh/Al<sub>2</sub>O<sub>3</sub> catalyst in combination with mild conditions resulting in high selectivities. For example, the conditions tolerated benzyl or Cbz groups (Scheme 36). This strategy has been verified using a broad range of carbohydrate derivatives carrying a variety of protecting groups.<sup>256</sup>



**SCHEME 36** Synthesis of benzyl-protected carbohydrate amines by the hydrogenolysis of azido-sugars.

The hydrogenolysis of the azido group in diazido pyrazolonones and the subsequent reaction readily provided rubazonic acid. Among the several reducing agents/processes assessed for this protocol the heterogeneous catalytic hydrogenolysis on Pd/C catalyst provided the highest yield (Scheme 37). The reaction also appeared to work with several substituted derivatives, including methyl to phenyl for R<sup>1</sup> or phenyl, *p*-tolyl to *tert*butyl for R<sup>2</sup>.<sup>257</sup>



**SCHEME 37** Synthesis of rubazonic acid by the hydrogenolysis of the azido group in diazido pyrazolonones.

### 3.2.7. C–S bonds

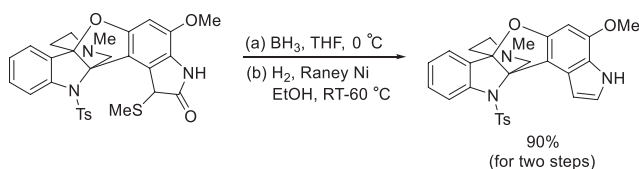
The hydrogenolysis of the C–S bond, commonly referred to as hydrodesulfurization, is one of the most important processes in the petrochemical industry. As the sulfur-containing compounds in any fuel will turn to sulfur oxides in engines essentially contributing to acid rain (and of course engine corrosion), limiting the sulfur content in fuel was made an environmental priority.<sup>258–261</sup> Due to its importance, the topic has been frequently reviewed.<sup>262–266</sup> In order to produce better, more effective, and selective catalysts, significant efforts have been devoted to the development of new catalysts on both the experimental<sup>267–270</sup> and theoretical level.<sup>271, 272</sup> A list of representative examples is tabulated in Table 10.

**TABLE 10** Representative examples for the hydrodesulfurization of organosulfur compounds.

| Entry | Substrate                                      | Catalyst   | Conditions   | Comments  | Ref.                    |
|-------|--|--|--|---|-------------------------|
| 1     | 4,6-Dimethyl-dibenzothio-<br>phene (4,6-DMDBT) | Ga-doped Ni <sub>2</sub> P<br>Ni-W/Al <sub>2</sub> O <sub>3</sub><br>Ni-Mo/ $\gamma$ -Al <sub>2</sub> O <sub>3</sub> | 3.0 MPa H <sub>2</sub> , 613–523 K,<br>1–6 h         | Major product: 3,3-dimet-<br>hylbiphenyl (3,3-DMBP),<br>the pore structure of the alumina had<br>a significant effect | <a href="#">273–275</a> |
| 2     | Dibenzothio-phene (DBT)                        | Mo <sub>2</sub> C/carbon acidic<br>zeolite cluster, TiO <sub>2</sub><br>AlMoGNi                                      | 4.1–5.3 MPa, 300–350°C,<br>flow system               | Yield: 65%–98% biphenyl, catalyst<br>deactivation due to MoS <sub>2</sub> formation;<br>DFT calculations, flow system | <a href="#">276–279</a> |
| 3     | Benzothiophene                                 | zeolites   | H <sub>2</sub> (2–20 bar), 340–400°C,<br>flow system | S-Zorb process  | <a href="#">280</a>     |
| 4     | Thiophene                                      | MoS/ $\gamma$ -Al <sub>2</sub> O <sub>3</sub> , Pt/TiO <sub>2</sub>  | H <sub>2</sub> (1 bar), 200–600°C,<br>flow system    | Product:1–3-butadiene, mechanistic<br>study   | <a href="#">281</a>     |
| 5     | 2-Phenylcyclohexanethiol                       | Ni <sub>2</sub> P, MoP, WP   | 4.0 MPa H <sub>2</sub> , 240°C, flow<br>system       | Conversion up to 50%, various<br>desulfurized hydrocarbon products  | <a href="#">282</a>     |

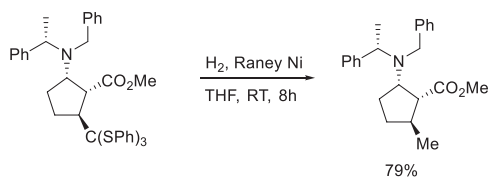
AlMoGNi, Ni doped graphene decorated on molybdenum-alumina.

In addition to the environmental aspects, sulfur removal from organic compounds is also of synthetic importance. However, the presence and properties of sulfur atoms represent a significant problem when the traditional hydrogenation catalysts are involved. Pd, Pt, or Rh catalysts commonly undergo deactivation due to sulfur poisoning.<sup>283</sup> Accordingly, the examples in Table 10 mostly apply metals that, with the exception of Ni, are not considered to be traditional hydrogenation/hydrogenolysis catalysts. In synthetic applications, the most commonly applied catalyst for C–S bond hydrogenolysis is Raney Ni that has a broadly established resistance to sulfur. For instance, Raney Ni was selected as the catalysts for the hydrogenolysis of a methylthioxy group during the synthesis of (±)-phalarine (Scheme 38).<sup>167</sup>



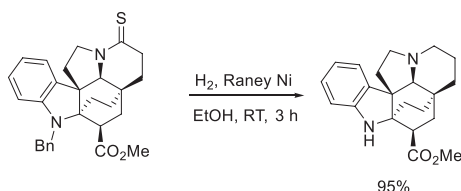
**SCHEME 38** Hydrogenolysis of the methylthioxy group as a step in the total synthesis of (±)-phalarine.

A similar Raney Ni-catalyzed C–S bond hydrogenolysis was applied during the kinetic resolution of methyl (*R,S*)-5-tris(phenylthio)methylcyclopent-1-ene-carboxylate to achieve the asymmetric synthesis of (1*R*,2*S*,5*S*)- and (1*S*,2*R*,5*R*)-5-methyl-cispentacin (Scheme 39).<sup>168</sup> Interestingly, the Raney Ni hydrogenolysis did not remove the benzyl groups from the tertiary N of the compound.



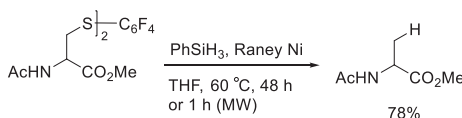
**SCHEME 39** Raney Ni-catalyzed hydrogenative desulfurization of a cispentacin precursor.

The hydrogenative desulfurization of organic compounds is commonly carried out by Ni-based catalysts: Raney Ni or supported Ni catalysts. The hydrogenolysis of the C=S bond and its transformation to a CH<sub>2</sub> is a well-known alternative for the Clemmensen or Kishner-Wolff reactions for sulfur compounds. The reaction occurs without problems under mild conditions and yields the desulfurized product in nearly quantitative yields (Scheme 40).<sup>180</sup>



**SCHEME 40** Hydrogenolysis (and debenzylation of the N-Bn) of the thio-carbonyl group by Raney Ni under mild conditions.

Perfluoroarene tags play an important role in several processes, for example in protein chemistry. As a form of labeling, the safe and effective removal of the tags is also of primary importance. The microwave-assisted removal of perfluoroarene tags from cysteine-perfluoroaryl thioethers has been successfully achieved by the application of metal-catalyzed transfer hydrogenolysis. Several metal catalysts, such as Ni<sub>2</sub>B, Pd/C, or Raney Ni, were tested in the reaction, Raney-Ni exhibiting the best performance.<sup>284</sup> Phenylsilane was used as hydrogen donor, and the reaction provided moderate to good yields depending on the conditions used. The microwave-accelerated reaction resulted in the highest yield (Scheme 41).



**SCHEME 41** Raney Ni-catalyzed hydrogenolysis of cysteine-perfluoroaryl thioethers.

### 3.2.8. Hydrogenolysis of C-other elements (Si, metals) bonds

There is relatively limited information on the hydrogenolysis of organometallic compounds, due to the inherent sensitivity of the carbon-metal bonds. Among the few examples, the controlled hydrogenolysis of C–Sn organometallic compounds on Rh/SiO<sub>2</sub> was described by Taoufik et al.<sup>285</sup> The hydrogenolysis of the Sn–C bonds was observed without any C–C bond cleavage, which led to the formation of grafted organometallic fragments.

Although the dehydrogenation of alkylsilanes to form oligo- and polysilanes is a frequently studied process, the available reports on the reverse process, namely the hydrogenolysis of Si–Si bond are scarce. The highly selective hydrogenolysis of oligo- and polysilanes to silanes with molecular hydrogen and low-valent Ni-hydrides occurred under mild conditions and appears to be a green alternative to the earlier low selectivity and harsh processes.<sup>286</sup>

### 3.2.9. Hydrogenolysis of biomass-related compounds

As a rapidly emerging topic, the preparation of fine chemicals or general starting materials from biomass attracted significant attention. Considering the finite nature of the petroleum reserves these investigations may prove to be the future basis of the chemical industry.<sup>287</sup> Although many different types of catalysts are involved, heterogeneous catalytic hydrogenolysis-based protocols play an important role in this field. The major directions include the conversion of biomass to furan derivatives,<sup>288</sup> and glycerol to other compounds, such as propanols, or propanediols and lignin depolymerization mainly to aromatic chemicals.<sup>289</sup>

#### 3.2.9.1 Hydrogenolysis of biomass-derived oxygen-containing heterocycles

Biomass is a rich source of oxygen-containing heterocyclic compounds, such as furans.<sup>290</sup> The hydrogenolysis of these compounds is carried out with the ultimate goal to generate fine chemicals and building blocks from these sustainable resources.<sup>291</sup>

The ring-opening hydrogenolysis of biomass-derived heterocyclic compounds, mostly furan derivatives, to diols has been studied by Jenness et al. using Ir catalyst.<sup>292</sup> The results provided significant mechanistic insights that could help the further catalyst development for the effective transformations of biomass-derived oxygenates to value-added products. The experimental data have been supplemented by density functional theory calculations. There are several other similar applications that focus on the same principal class of compounds that originate from biomass. Representative examples are tabulated in Table 11.

As the data indicate, this is a relatively new area, thus the search for the best class of catalysts (metals, etc.) is still ongoing. Unlike in several other instances where one of the metals dominate (e.g., PtO<sub>2</sub> for C–C, or Raney Ni for C–S bond hydrogenolysis), Table 11 includes nearly all metals that have been listed for other hydrogenolysis applications, from the noble metals, to nickel or copper with a broad variety of supports. Often the support appears to contribute to the cleavage reactions via their acidic properties (e.g., zeolites, silica, and other metal oxides).

#### 3.2.9.2 Hydrogenolysis of biomass-derived other oxygen-containing compounds

Several biomass sourced compounds are manufactured in extremely large amounts as a by-product of multimillion ton processes. Glycerol is one of the prime examples. This compound forms as a by-product during biodiesel

**TABLE 11** Hydrogenolysis of biomass-derived oxygen-containing heterocycles.

| Entry | Substrate | Catalyst   | Products   | Conditions/comments   | Ref.     |
|-------|-----------|--|--|---|----------|
| 1     |           | Pd/C + 0.3 M HI  | Adipic acid  | Acidic solution, 50–500 psi, 115°C  | 293      |
| 2     |           | Rh/OMS-2, Cu/CuFe <sub>2</sub> O <sub>4</sub> @MOF, ZSM5-encapsulated Pt NPs                                       | 1,2-Pentanediol, a variety of deoxygenated and ring-opening products | 100% Conversion, 87% selectivity at 160°C, 30 atm H <sub>2</sub> , 8 h, effect of temperature, hydrogen pressure, MOF, etc. | 294–296  |
| 3     |           | Ru, Pt, Pd, Ni, Co, Cu-based catalysts, Ir/SiO <sub>2</sub> , Ru-hydro-talcite or ZrO <sub>2</sub> , NiCu, Ni/ZSM5 |  | 1–50 bar H <sub>2</sub> , MeOH, formic acid as hydrogen source, nearly quantitative yields                                  | 297–313  |
| 4     |           | Cu-Mg <sub>3</sub> AlO <sub>4.5</sub><br>Pt/CeO <sub>2</sub><br>Cu-LaCoO <sub>3</sub> , Cu-Mg-Al                   | 1,2- and 1,5-pentane-diols   | Bifunctional catalysis, 60%–100% yield, 55% combined selectivity, RT, 6 MPa H <sub>2</sub> , 8 h, 100–180°C                 | 314–317  |
| 5     |           | Cu/ZrO <sub>2</sub>  | 1,4-Pentanediol, or 2-methyltetrahydro-furan                         | Yield/selectivity up to 97%/99%, 200°C, 6 MPa H <sub>2</sub> , 6 h  | 318      |
| 6     |           | Rh-MoO <sub>3</sub> /SiO <sub>2</sub><br>ReO <sub>3</sub> -promoted Rh/C   | 1,5-Pentanediol<br>$\alpha,\omega$ -diols                            | Conversion/selectivity up to 51%/98%, 120°C, 34–60 bar H <sub>2</sub>   | 319, 320 |
| 5     |           | Cu-electrode   | Methylfuran  | Electrocatalytic conversion, –0.55 to –0.75V, water   | 321      |

MOF, metal-organic framework; NP, nanoparticle; OMS, octahedral molecular sieve.

production. Several examples show that in fact, glycerol can be transformed to several other products, including propanol or propanediol. Several other aliphatic compounds such as cellulose, sorbitol, or lignin derivatives have also been considered as an abundant and sustainable resource for the preparation of chemicals through hydrogenolysis approaches. The data are tabulated in [Table 12](#).

The information presented in [Table 12](#) is somewhat similar to that in [Table 11](#). A wide variety of catalysts were applied due to the relatively unexplored nature of these reactions. The other reason is the need for the presence of an acid catalyst. Many catalysts listed in [Table 12](#), are bifunctional, containing a metal part that facilitates hydrogenolysis, and the acid part that could initiate dehydration, cracking, and other typically acid-catalyzed reactions.<sup>359</sup> Although in some cases the product is a hydrocarbon (or mixture of hydrocarbons), often the deoxygenation of the starting natural products is only partial, e.g., glycerol, a triol, can produce diols, or simple alcohols, depending on the conditions applied.

The deoxygenation of other small organic compounds was already discussed under the hydrogenolysis of the C–O bond. The catalytic deoxygenation of biomass-related compound is also a desirable process, for the synthesis of biofuels.<sup>360</sup> For example during the production of pyrolysis- or bio-oils, the second generation of sustainable liquid fuels obtained from biomass, mostly lignins,<sup>361–365</sup> and for the production of biodiesel from waste fat.<sup>366</sup>

### 3.2.10. Conclusions and outlook

Advances made in the 1996–2021 period in the field of heterogeneous catalytic hydrogenolysis have been reviewed. Hydrogenolysis is one of the most important and commonly applied procedures in heterogeneous catalysis and appears to continue attracting significant attention and remains a major method in industrial processes as well as in organic synthesis. The main focus of the progress is the development of new catalysts that could improve activity and selectivity of the reactions, and the application of well-established protocols on new substrates. The earlier chapter provides an up-to-date overview of this field, including the hydrogenolysis of the C–C, C–O, C–N, C-halogen, and several other bonds. Due to the available large number of publications, in many cases we have refrained from providing an exhaustive list of papers and rather focused on to mention representative examples for these transformations. Based on the extensive number of reports published in the past two decades, significant advancements were made since 1996; particularly the pace of the new developments increased unambiguously. All signs point toward the forecast that hydrogenolysis will remain an important tool in green and sustainable synthesis and environmental chemistry.

**TABLE 12** Hydrogenolysis of biomass-derived oxygen-containing aliphatic compounds.

| Entry | Substrate | Catalyst   | Products                          | Conditions/comments  | Ref.    |
|-------|-----------|--|-----------------------------------|--|---------|
| 1     | Lactate   | SiO <sub>2</sub> supported Fe, Co, Ni, Ru, Pd  | 1,2-Propanediol                   | Vapor phase hydrogenolysis, 90% conversion, 98% selectivity at 160°C, 2.5 MPa H <sub>2</sub>                               | 322     |
| 2     | Glycerol  | Cu/ZrO <sub>2</sub> , Cu/ZnO<br>Cu/CeO <sub>2</sub> , Cu/MgO<br>Pt on zeolites, Al <sub>2</sub> O <sub>3</sub><br>Pd/CuCr <sub>2</sub> O <sub>4</sub> , Cu/MgO, Cu-Mg/<br>SiO <sub>2</sub> , Cu-SBA15/SiO <sub>2</sub><br>Ni/Al-Fe | 1,2-Propanediol                   | Aq. phase, 84%–95% selectivity at 175–240°C, 25–60 bar H <sub>2</sub> ; with Ni/Al-Fe no external hydrogen is needed       | 323–330 |
| 3     | Glycerol  | Pt/WO <sub>x</sub> /Al <sub>2</sub> O <sub>3</sub><br>Pt on various supports, Pt/H-WO <sub>3</sub>   | 1,3-Propanediol                   | Bifunctional catalysis, up to 100% conversion, 35%–38.5% yield, 200°C, 90 bar H <sub>2</sub> , 4 h and flow system as well | 331–334 |
| 4     | Glycerol  | Pt-H <sub>4</sub> SiW <sub>12</sub> O <sub>40</sub> /ZrO <sub>2</sub>  | 1- and 2-propanol                 | 94% Yield, 200°C, 5.0 MPa  | 335     |
| 5     | Glycerol  | Amorphous Zr-phosphate doped supported Ru  | 1-Propanol                        | Conversion/selectivity up to 100%/96%, 315°C, 2 MPa H <sub>2</sub> , flow system   | 336     |
| 6     | Glycerol  | Cu, Pd, Rh on ZnO, C, Al <sub>2</sub> O <sub>3</sub>   | 1,2-, and 1,3-propanediol         | H <sub>2</sub> O, sulfolane, dioxane as solvents, up to 100% selectivity, 180°C, 80 bar H <sub>2</sub> , 168 h             | 337     |
| 7     | Xylitol   | Cu/SiO <sub>2</sub><br>NiCu/SiO <sub>2</sub><br>Ru/C<br>CuNi/ZrO <sub>2</sub>  | Ethylene glycol, propylene glycol | With or without base cocatalysis, 0–10 MPa H <sub>2</sub> , 160–240°C, 100% conversion, up to 60% combined selectivity     | 338–343 |

|    |                                       |  |                                     |  |   |
|----|---------------------------------------|--|-------------------------------------|--|---|
| 8  | Vicinal diols                         | PdFe bimetallic nanoparticles  | C-C cleavage products (MeOH, etc.)  | 95% Conversion, 250, 50 bar H <sub>2</sub> , 24 h  | <a href="#">344</a>                       |
| 9  | Sorbitol                              | Ni-MgO, PtPd/C   | Glycols, glycerol, hydroxyacids     | 68% Conversion, 81% combined selectivity, 200°C, 4 MPa H <sub>2</sub> , 4.5 h  | <a href="#">345</a> , <a href="#">346</a> |
| 10 | Biomass based polyols                 | Ru/C   | C2-C6 polyols                       | Neutral and acidic conditions, 100–150°C, 6 MPa H <sub>2</sub> , 16 h  | <a href="#">347</a>                       |
| 11 | Cellulose                             | Fe <sub>3</sub> O <sub>4</sub> @SiO <sub>2</sub> /Ru-WO <sub>x</sub> | 1,2-Propyleneglycol                 | Water, 200°C, 5 MPa H <sub>2</sub> , 2 h   | <a href="#">348</a>                       |
| 12 | 1,4-Anhydroerythritol                 | Pt-WO <sub>x</sub> /SiO <sub>2</sub>                                 | 1,3-Butanediol, 1,2,3-butanetriol   | Water, 140°C, 8 MPa H <sub>2</sub> , 24 h  | <a href="#">349</a>                       |
| 13 | Lignin and lignin-derived aryl ethers | Pd/C and CrCl <sub>3</sub><br>Ni/N-C<br>Ni-Cu/C<br>Ru/C              | Hydrocarbons, alkyl phenols,        | Hydrodeoxygenation, MeOH, RT-280°C, 4 MPa H <sub>2</sub> , 5 h, yield up to 20%, conversion up to 100%; in EtOH/iPrOH no external H <sub>2</sub> is needed | <a href="#">350–354</a>                   |
| 14 | Bio-polyols and sugars                | Cu/TiO <sub>2</sub>  | MeOH, syngas (CO + H <sub>2</sub> ) | Photoreforming, 365 nm LED light source, yields up to 50%  | <a href="#">355</a>                       |
| 15 | Cellobiose                            | Ru/N-doped C   | Sorbitol                            | Water, 120–160°C, 30 bar H <sub>2</sub> , 2 h  | <a href="#">356</a>                       |
| 16 | Guaiacol and biocrude oil             | Ru/BEA, Ru/ZSM-5, Ru/Al <sub>2</sub> O <sub>3</sub>                  | Cyclohexane, 2-methoxycyclohexanol  | Neat, 230–250°C, 4 MPa H <sub>2</sub> , 2 h  | <a href="#">357</a>                       |
| 17 | Cellulose                             | Ni/SiO <sub>2</sub>  | 1,6-Hexanediol                      | Prehydrolyzed aq. mixture of cellulose, 80°C, 68 atm H <sub>2</sub> , flow system  | <a href="#">358</a>                       |

## References

1. Smith, M. B.; March, J. *March's Advanced Organic Chemistry*, 6th ed.; Wiley: Hoboken, NJ, 2007.
2. Nishimura, S. *Handbook of Heterogeneous Catalytic Hydrogenation for Organic Synthesis*; Wiley: New York, 2001.
3. Augustine, R. L. *Heterogeneous Catalysis for the Synthetic Chemist*; Marcel Dekker: New York, 1996.
4. Bartók, M.; Molnár, Á. Heterogeneous Catalytic Hydrogenation. In *Chemistry of Functional Groups*; Patai, S., Ed.; Suppl. A3; Wiley: Chichester, 1997; p. 843 (chapter 16).
5. Smith, G. V.; Notheisz, F. *Heterogeneous Catalysis in Organic Chemistry*; Academic Press: San Diego, CA, 1999.
6. Rylander, P. N. *Catalytic Hydrogenation over Platinum Metals*; Academic Press: New York, London, 1967.
7. Bartók, M., Ed. *Stereochemistry of Heterogeneous Metal Catalysis*; Wiley: Chichester, 1985.
8. Corker, J.; Lefebvre, F.; Lecuyer, C.; Dufaud, V.; Quignard, F.; Choplin, A.; Evans, J.; Basset, J.-M. Catalytic Cleavage of the C-H and C-C Bonds of Alkanes by Surface Organometallic Chemistry: An EXAFS and IR Characterization of a Zr-H Catalyst. *Science* **1996**, *271*, 966–969.
9. Besedin, D. V.; Ustynyuk, L. Y.; Ustynyuk, Y. A.; Lunin, V. V. A Theoretical DFT Study of the Mechanism of C–C Bond Hydrogenolysis in Alkanes on Silica-Supported Zirconium Hydrides. *Mendeleev Commun.* **2002**, *12*, 173–175.
10. Shetty, M.; Zanchet, D.; Green, W. H.; Román-Leshkov, Y. Cooperative Co<sup>0</sup>/Co<sup>II</sup> Sites Stabilized by a Perovskite Matrix Enable Selective C-O and C-C Bond Hydrogenolysis of Oxygenated Arenes. *ChemSusChem* **2019**, *12*, 2171–2175.
11. Kamiguchi, S.; Arai, K.; Okumura, K.; Iida, H.; Nagashima, S.; Chihara, T. Solid-State Molybdenum Sulfide Clusters with an Octahedral Metal Framework as Hydrogenation, Dehydrogenation, and Hydrogenolysis Catalysts Similar to the Platinum Group Metals. *Appl. Catal. A Gen.* **2015**, *505*, 417–421.
12. Pospelova, V.; Aubrecht, J.; Pacultová, K.; Lhotka, M.; Kikhtyanin, O.; Kubička, D. Does the Structure of CuZn Hydroxycarbonate Precursors Affect the Intrinsic Hydrogenolysis Activity of CuZn Catalysts? *Cat. Sci. Technol.* **2020**, *10*, 3303–3314.
13. Shesterkina, A. A.; Kustov, L. M.; Strelkova, A. A.; Kazansky, V. B. Heterogeneous Iron-Containing Nanocatalysts—Promising Systems for Selective Hydrogenation and Hydrogenolysis. *Cat. Sci. Technol.* **2020**, *10*, 3160–3174.
14. Zhou, M.; Yang, M.; Yang, X.; Zhao, X.; Sun, L.; Deng, W.; Wang, A.; Li, J.; Zhang, T. on the Mechanism of H<sub>2</sub> Activation over Single-Atom Catalyst: An Understanding of Pt<sub>1</sub>/WO<sub>x</sub> in the Hydrogenolysis Reaction. *Chin. J. Catal.* **2020**, *41*, 524–532.
15. Pagliaro, M. *Single-Atom Catalysis: A Forthcoming Revolution in Chemistry*; Elsevier: St. Louis, MO, 2019.
16. Anastas, P. T.; Warner, J. C. *Green Chemistry: Theory and Practice*; Oxford University Press: Oxford, 1998.
17. Török, B.; Dransfield, T. *Green Chemistry: An Inclusive Approach*; Elsevier: Oxford, Cambridge, 2018.
18. Petricci, E.; Cini, E.; Taddei, M. Metal Catalysis with Microwaves in Organic Synthesis: a Personal Account. *Eur. J. Org. Chem.* **2020**, *29*, 4435–4446.
19. Kokel, A.; Schäfer, C.; Török, B. Application of Microwave-Assisted Heterogeneous Catalysis in Sustainable Synthesis Design. *Green Chem.* **2017**, *19*, 3729–3751.

20. Török, B.; Schäfer, C., Eds. *Non-traditional Activation Methods in Green and Sustainable Applications: Microwaves, Ultrasounds, Photo, Electro and Mechanochemistry and High Hydrostatic Pressure*; Elsevier: Cambridge, Oxford, 2021.
21. Almithn, A. S.; Hibbitts, D. D. Impact of Metal and Heteroatom Identities in the Hydrogenolysis of C–X Bonds (X = C, N, O, S, and Cl). *ACS Catal.* **2020**, *10*, 5086–5100.
22. Nakagawa, Y.; Tomishige, K. Catalyst Development for the Hydrogenolysis of Biomass-Derived Chemicals to Value-Added Ones. *Catal. Surv. Jpn.* **2011**, *15*, 111–116.
23. Wang, G.; Zhang, S.; Zhu, X.; Li, C.; Shan, H. Dehydrogenation Versus Hydrogenolysis in the Reaction of Light Alkanes Over Ni-Based Catalysts. *J. Ind. Eng. Chem.* **2020**, *86*, 1–12.
24. Olah, G. A.; Molnár, Á.; Prakash, G. K. S. *Hydrocarbon Chemistry*, 3rd ed.; Wiley: Hoboken, NJ, 2017.
25. Anderson, J. R.; Boudart, M., Eds., Vols. 1–11; *Catalysis: Science and Technology*; Springer-Verlag Berlin: Heidelberg, 1996.
26. Gault, F. G. Mechanisms of Skeletal Isomerization of Hydrocarbons on Metals. *Adv. Catal.* **1981**, *30*, 1–95.
27. Bond, G. C.; Webb, G.; Paál, Z.; Tétényi, P. Reactions of Hydrocarbons on Metallic Catalysts. In *Specialist Periodical Reports on Catalysis*; Vol. 5; The Royal Society of Chemistry: London, 1982; pp. 80–126.
28. Paál, Z. XPS of Carbon on Pt-Black and EUROPT-1. Is Methylcyclopentane Ring Opening a ‘Coke Sensitive’ Reaction? *J. Mol. Catal.* **1994**, *94*, 225–232.
29. Pálínkó, I.; Notheisz, F.; Bartók, M. The Role of Carbonaceous Overlayer in the Competitive Hydrogenation of Cyclopropanes and Olefins. *Catal. Lett.* **1988**, *1*, 127–131.
30. Pálínkó, I.; Molnár, Á.; Kiss, J. T.; Bartók, M. Activity, Selectivity and Stereochemical Features in the Copper-Catalyzed Hydrogenative Ring Opening of Alkylsubstituted Cyclopropanes; Nature of Active Sites. *J. Catal.* **1990**, *121*, 396–407.
31. Pálínkó, I.; Notheisz, F.; Bartók, M. Ni-Catalyzed Ring-Opening Reactions of Alkyl-Substituted Cyclopropanes; Role of Unreduced Ni Species. *J. Mol. Catal.* **1991**, *68*, 237–241.
32. Pálínkó, I.; Notheisz, F.; Kiss, J. T.; Bartók, M. Hydrogenative Ring-Opening Reactions of Alkyl-Substituted Cyclopropanes over Pt/SiO<sub>2</sub> Catalyst. *J. Mol. Catal.* **1992**, *77*, 313–319.
33. Fási, A.; Kiss, J. T.; Török, B.; Pálínkó, I. The Selectivity and Activity Determining Roles of Carbonaceous Species and Metal-Metal Oxide Interface in Metal-Catalyzed Hydrogenation and Isomerization Reactions. *Appl. Catal. A Gen.* **2000**, *200*, 189–200.
34. Török, B.; Molnár, Á.; Bartók, M. Hydrogenative Ring Opening of Propylcyclopropane over Silica-Supported Pt and Pd Catalysts. *Catal. Lett.* **1995**, *33*, 331–339.
35. Török, B.; Pálínkó, I.; Molnár, Á.; Bartók, M. Hydrogen Pressure Dependence of the Ring-Opening Reactions of Propyl-Cyclobutane over Pt/SiO<sub>2</sub> Catalyst at Different Temperatures. *J. Catal.* **1993**, *143*, 111–121.
36. Bartók, M.; Török, B.; Molnár, Á.; Apjok, J. Substituent Effect in the Hydrogenative Ring-Opening of Cyclobutanes on Pt/SiO<sub>2</sub>. *React. Kinet. Catal. Lett.* **1993**, *49*, 111–118.
37. Török, B.; Molnár, Á.; Pálínkó, I.; Bartók, M. Surface Carbonaceous Deposits as Activity and Selectivity Influencing Species in the Ring-Opening Reactions of Propylcyclobutane Catalyzed by Pt/SiO<sub>2</sub>. *J. Catal.* **1994**, *145*, 295–299.
38. Török, B.; Pálínkó, I.; Bartók, M. Hydrogen Pressure Dependence of the Ring-Opening Reactions of Propylcyclobutane over Pd/SiO<sub>2</sub> Catalyst. *Catal. Lett.* **1995**, *31*, 421–429.
39. Pálínkó, I.; Török, B. Multiple Steady-State in the Hydrogenative Ring Opening of Propylcyclobutane over Rh/SiO<sub>2</sub>. *Catal. Lett.* **1997**, *45*, 193–195.
40. Török, B.; Pálínkó, I.; Molnár, Á.; Bartók, M. Ring Enlargement and Aromatization of Propylcyclobutane Over Silica-Supported Pt, Pd and Rh in Hydrogen Atmosphere. *J. Mol. Catal.* **1994**, *91*, 61–69.

41. Török, B.; Bartók, M. Hydrogenative Transformations of Methylcyclobutane over Silica-Supported Pt, Pd, Rh and Ni Catalysts at Different Temperatures. *Catal. Lett.* **1994**, *27*, 281–287.
42. Török, B.; Bartók, M. Ring-Opening Hydrogenation Reactions of Monoalkyl-Substituted Cyclobutanes over Ni/SiO<sub>2</sub> Catalyst. *J. Catal.* **1995**, *151*, 315–322.
43. Török, B.; Pálincó, I.; Molnár, Á.; Bartók, M. Hydrogen Pressure Dependence in the Ring-Opening Reactions of Substituted Cyclobutanes over Rh/SiO<sub>2</sub> Catalyst at Various Temperatures. *J. Catal.* **1996**, *159*, 500–503.
44. Török, B.; Török, M.; Bartók, M. Temperature and Hydrogen Pressure Dependence in the Ring Opening of Methylcyclobutane over Pt/SiO<sub>2</sub> Catalyst. *Catal. Lett.* **1995**, *33*, 321–330.
45. Török, B.; Kiss, J. T.; Bartók, M. Hydrogen Pressure Dependence in the Hydrogenative Ring Opening of Methylcyclobutane and Methylcyclopentane over Silica-Supported Pt and Pd Catalysts. *Catal. Lett.* **1997**, *46*, 169–179.
46. Shi, H.; Gutiérrez, O. Y.; Zheng, A.; Haller, G. L.; Lercher, J. A. Mechanistic Pathways for Methylcyclohexane Hydrogenolysis over Supported Ir Catalysts. *J. Phys. Chem. C* **2014**, *118*, 20948–20958.
47. Kozhushkov, S. I.; Kostikov, R. R.; Molchanov, A. P.; Boese, R.; Benet-Buchholz, J.; Schreiner, P. R.; Rinderspacher, C.; Ghiviriga, I.; de Meijere, A. Tetracyclopropylmethane: A Unique Hydrocarbon With S<sub>4</sub> Symmetry. *Angew. Chem. Int. Ed.* **2001**, *40*, 180–183.
48. Anderson, J. E.; de Meijere, A.; Kozhushkov, S. I.; Lunazzi, L.; Mazzanti, A. Conformational Dynamics of Tetraisopropylmethane and of Tetracyclopropylmethane. *J. Am. Chem. Soc.* **2002**, *124*, 6706–6713.
49. de Meijere, A.; von Seebach, M.; Zöllner, S.; Kozhushkov, S. I.; Belov, V. N.; Boese, R.; Haumann, T.; Benet-Buchholz, J.; Yufit, D. S.; Howard, J. A. K. Spirocyclopropanated Bicyclopropylidenes: Straightforward Preparation, Physical Properties, and Chemical Transformations. *Chem. Eur. J.* **2001**, *7*, 4021–4034.
50. Kozhushkov, S. I.; Yufit, D. S.; Boese, R.; Bläser, D.; Schreiner, P. R.; de Meijere, A. Conformational Studies on Oligosubstituted Adamantane Derivatives—Structural Features of Tetravinyl-, Tetracyclopropyl-, and Tetraisopropyladamantane. *Eur. J. Org. Chem.* **2005**, 1409–1415.
51. Fonseca Benítez, C. A.; Mazzieri, V. A.; Sánchez, M. A.; Benitez, V. M.; Pieck, C. L. Selective Hydrogenation of Oleic Acid to Fatty Alcohols on Rh-Sn-B/Al<sub>2</sub>O<sub>3</sub> Catalysts. Influence of Sn Content. *Appl. Catal. A Gen.* **2019**, *584*, 1171492.
52. Maina, S. C. P.; Ballarini, A. D.; Vilella, J. I.; de Miguel, S. R. Study of the Performance and Stability in the Dry Reforming of Methane of Doped Alumina Supported Iridium Catalysts. *Catal. Today* **2020**, *344*, 129–142.
53. Vicerich, M. A.; Sánchez, M. A.; Benitez, V. M.; Pieck, C. L. Pretreatment Temperature Influence on the Selective Ring Opening of Decalin on Pt–Ir/TiO<sub>2</sub> Catalysts. *Catal. Lett.* **2017**, *147*, 758–764.
54. Chamam, M.; Lázár, K.; Pirault-Roy, L.; Boghian, I.; Paál, Z.; Wootsch, A. Characterization and Catalytic Properties of Rh–Sn/Al<sub>2</sub>O<sub>3</sub> Catalyst Prepared by Organometallic Grafting. *Appl. Catal. A Gen.* **2007**, *332*, 27–36.
55. Paál, Z.; Györfy, N.; Wootsch, A.; Tóth, L.; Bakos, I.; Szabó, S.; Wild, U.; Schlögl, R. Preparation, Physical Characterization and Catalytic Properties of Unsupported Pt–Rh Catalyst. *J. Catal.* **2007**, *250*, 254–263.
56. Said-Aizpuru, O.; Batista, A. T. F.; Bouchy, C.; Petrazzuoli, V.; Allain, F.; Diehl, F.; Farusseng, D.; Morfin, F.; Joly, J.-F.; Dandeu, A. Non Monotonous Product Distribution Dependence on Pt/γ-Al<sub>2</sub>O<sub>3</sub>-Cl Catalysts Formulation in *n*-Heptane Reforming. *ChemCatChem* **2020**, *12*, 2262–2270.

57. Lin, C.; Pan, H.; Yang, Z.; Han, X.; Tian, P.; Li, P.; Xiao, Z.; Xu, J.; Han, Y.-F. Effects of Cerium Doping on Pt–Sn/Al<sub>2</sub>O<sub>3</sub> Catalysts for n-Heptane Reforming. *Ind. Eng. Chem. Res.* **2020**, *59*, 6424–6434.
58. Hibbitts, D. D.; Flaherty, D. W.; Iglesia, E. Role of Branching on the Rate and Mechanism of C–C Cleavage in Alkanes on Metal Surfaces. *ACS Catal.* **2016**, *6*, 469–482.
59. Danishefsky, S.; Singh, R. K. Highly Activated Cyclopropane for Homoconjugate Reactions. *J. Am. Chem. Soc.* **1975**, *97*, 3239–3241.
60. Sone, Y.; Kimura, Y.; Ota, R.; Mochizuki, T.; Ito, J.; Nishii, Y. Catalytic Hydrogenolysis of Enantioenriched Donor–Acceptor Cyclopropanes Using H<sub>2</sub> and Palladium on Charcoal. *Eur. J. Org. Chem.* **2017**, 2842–2847.
61. Carreira, E. M.; Ledford, B. E. Enantioselective Synthesis of the C(1)–C(6′) Subunit of Zargaonic Acid C. *J. Braz. Chem. Soc.* **1998**, *9*, 405–408.
62. Royer, F.; Felpin, F.-X.; Doris, E. Synthesis of  $\gamma$ -Amino Acids by Rearrangement of  $\alpha$ -Cyanocyclopropanone Hydrates: Application to the Regioselective Labeling of Amino Acids. *J. Org. Chem.* **2001**, *66*, 6487–6489.
63. Mohapatra, D. K.; Chaudhuri, S. R.; Sahoo, G.; Gurjar, K. Stereoselective Synthesis of the Polyketide Chain of Nagahamide A. *Tetrahedron Asymmetry* **2006**, *17*, 2609–2616.
64. Gonzalez-Juarez, D. E.; Garcia-Vazquez, J. B.; Zunga-Garcia, V.; Trujillo-Serrato, J. J.; Suarez-Castillo, O. R.; Joseph-Nathan, P.; Morales-Rios, M. S. Stereochemistry Modulates the Catalytic Hydrogenolysis of Nitrile-Substituted Cyclopropanes. *Tetrahedron* **2012**, *68*, 7187–7195.
65. Braun, N. A.; Spitzner, D. Highly Functionalized Enantiopure Oxatricyclo[3.3.1.0<sup>4,6</sup>]Nonanes; Selective Opening of an Activated Cyclopropane Ring. *Tetrahedron Lett.* **1996**, *37*, 9187–9188.
66. Fujii, H.; Okada, K.; Ishihara, M.; Hanamura, S.; Osa, Y.; Nemoto, T.; Nagase, H. Hydrogenolysis of the Cyclopropyl Group into an Isopropyl Group in the Presence of a Platinum Catalyst and Hydrobromic Acid. *Tetrahedron* **2009**, *65*, 10623–10630.
67. Irie, O.; Yokokawa, F.; Ehara, T.; Iwasaki, A.; Iwaki, Y.; Hitomi, Y.; Konishi, K.; Kishida, M.; Toyao, A.; Masuya, K.; Gunji, H.; Sakaki, J.; Iwasaki, G.; Hirao, H.; Kanazawa, T.; Tanabe, K.; Kosaka, T.; Hart, T. W.; Hallett, A. 4-Amino-2-Cyanopyrimidines: Novel Scaffold for Nonpeptidic Cathepsin S Inhibitors. *Bioorg. Med. Chem. Lett.* **2008**, *18*, 4642–4646.
68. Robl, J. A.; Cimarusti, M. P.; Simpkins, L. M.; Brown, B.; Ryono, D. E.; Bird, J. E.; Asaad, M. M.; Schaeffer, T. R.; Trippodo, N. C. Dual Metalloprotease Inhibitors. 6. Incorporation of Bicyclic and Substituted Monocyclic Azepinones as Dipeptide Surrogates in Angiotensin-Converting Enzyme/Neutral Endopeptidase Inhibitors. *J. Med. Chem.* **1996**, *39*, 494–502.
69. Taber, D. F.; Frankowski, K. J. Synthesis of (+)-Sulcatine G. *J. Org. Chem.* **2005**, *70*, 6417–6421.
70. Kuethe, J. T.; Zhao, D.; Humphrey, G. R.; Journet, M.; McKeown, A. E. Asymmetric Diels–Alder Reactions of Chiral Cyclopropylidene Imide Dienophiles: Preparation of *gem*-Dimethyl- and Spirocyclopropane Norbornyl Carboxylic Acids. *J. Org. Chem.* **2006**, *71*, 2192–2195.
71. Taber, D. F.; Tian, W. Synthesis of (–)-Hamigeran B. *J. Org. Chem.* **2008**, *73*, 7560–7564.
72. Li, W.-D. Z.; Yang, Y.-R. Unusual Cyclopropanation of 9-Bromocamphor Derivatives: A Novel Formal C(1)–C(7) Bond Cleavage of Camphor. *Org. Lett.* **2005**, *7*, 3107–3110.
73. Harmata, M.; Rashatasakhon, P. Intramolecular 4+3 Cycloadditions. Aspects of Stereocontrol in the Synthesis of Cyclooctanoids. A Synthesis of (+)-Dactylol. *Org. Lett.* **2000**, *2*, 2913–2915.
74. Mehta, G.; Krishna Murthy, A. S.; Umarye, J. D. Total Synthesis of the Putative Structure of the Novel Triquinane Natural Product Isocapnellenone. *Tetrahedron Lett.* **2002**, *43*, 8301–8305.

75. Hendrata, S.; Bennett, F.; Huang, Y.; Sannigrahi, M.; Pinto, P. A.; Chan, T.-M.; Evans, C. A.; Osterman, R.; Buevicha, A.; McPhail, A. T. Syntheses of Dipeptides Containing (1*R*,5*S*)-6,6-Dimethyl-3-Azabicyclo[3.1.0]Hexane-2(*S*)-Carboxylic Acid (4), (1*R*,5*S*)-Spiro[3-Azabicyclo[3.1.0]Hexane-6,10-Cyclopropane]-2(*S*)-Carboxylic Acid (5) and (1*S*,5*R*)-6,6-Dimethyl-3-Azabicyclo[3.1.0]Hexane-2(*S*)-Carboxylic Acid (6). *Tetrahedron Lett.* **2006**, *47*, 6469–6472.
76. Harrowven, D. C.; Lucas, M. C.; Howes, P. D. The First Total Synthesis of ( $\pm$ )-Desoxyhynophilin. *Tetrahedron* **2001**, *57*, 9157–9162.
77. Föhlisch, B.; Bakr, D. A.; Fischer, P. A Novel Bornane Synthesis by an Old Idea. *J. Org. Chem.* **2002**, *67*, 3682–3686.
78. Karimi, S.; Tavares, P. An Efficient Formal Synthesis of the Sesquiterpenoid Longifolene. *J. Nat. Prod.* **2003**, *66*, 520–523.
79. Kotha, S.; Cheekatla, S. R. Design, Synthesis, and Rearrangement Studies of Gem-Dimethyl Containing Cage Systems. *Tetrahedron* **2020**, *76*, 130898.
80. Pálínkó, I.; Ocskó, J. Hydrogen Pressure Dependence in the Ring Opening of Methyloxirane over Silica-Supported Pd and Rh Catalysts; Effect of High Temperature on Ring-Opening Routes. *J. Mol. Catal.* **1996**, *104*, 261–265.
81. Pálínkó, I. Activity and Regioselectivity in the Ring-Opening Reaction of Methyloxirane at Metal-Metal Oxide Interfaces. *J. Mol. Catal. A Chem.* **1999**, *140*, 195–198.
82. Fási, A.; Pálínkó, I.; Hernadi, K.; Kiricsi, I. Ring-Opening Reactions of Propylene Oxide (Methyloxirane) over Gold Catalysts. *Catal. Lett.* **2002**, *81*, 237–240.
83. Fási, A.; Hernadi, K.; Pálínkó, I.; Galbács, G.; Kiricsi, I. The Activity of Au Supported on Various Types of Carbon in the Ring Transformation Reactions of Methyloxirane. *React. Kinet. Catal. Lett.* **2006**, *87*, 343–348.
84. Notheisz, F.; Fási, A.; Bartók, M.; Ostgard, D. J.; Smith, G. V. Regioselective Ring-Opening of Oxiranes on Pd/SiO<sub>2</sub> Catalysts. *Chem. Ind.* **1996**, *68*, 397–403.
85. Notheisz, F.; Zsigmond, Á.; Ostgard, D.; Bartók, M.; Smith, G. V. Structure Sensitive Hydrogen Effect during Pt/SiO<sub>2</sub> Catalyzed Hydrogenolysis of Methyloxirane: Absence of Effect with EuroPt-1. *Catal. Lett.* **1994**, *26*, 315–324.
86. Fási, A.; Pálínkó, I. Transformation of Cyclohexene Oxide over Silica-Supported Cu, Pd and Rh Catalysts in H<sub>2</sub>/D<sub>2</sub> Atmosphere. *J. Catal.* **1999**, *181*, 28–36.
87. Fási, A.; Pálínkó, I. Changes in the Hydrogenative Ring Opening Mechanism of Cyclohexene Oxide over Cu/SiO<sub>2</sub> Resulting From the Addition of Cyclohexene, a Major Product. *Catal. Lett.* **1999**, *58*, 103–106.
88. Fási, A.; Notheisz, F.; Bartók, M. Transformation of *cis*- and *trans*-2,3-Dimethyloxiranes on a Cu/SiO<sub>2</sub> Catalyst. *J. Catal.* **1997**, *169*, 114–119.
89. Hirakawa, H.; Shiraiishi, Y.; Sakamoto, H.; Ichikawa, S.; Tanaka, S.; Hirai, T. Photocatalytic Hydrogenolysis of Epoxides Using Alcohols as Reducing Agents on TiO<sub>2</sub> Loaded with Pt Nanoparticles. *Chem. Commun.* **2015**, *51*, 2294–2297.
90. Shen, X.; Tang, C.-J.; Wu, Y.-K. Remarkably Accelerated Regioselective Hydrogenolysis of Terminal Epoxides in the Presence of CoCl<sub>2</sub> or NiSO<sub>4</sub>. *Chin. J. Chem.* **2003**, *21*, 972–974.
91. Thiery, E.; Le Bras, J.; Muzart, J. Palladium Nanoparticles-Catalyzed Regio- and Chemoselective Hydrogenolysis of Benzylic Epoxides in Water. *Green Chem.* **2007**, *9*, 326–327.
92. Thiery, E.; Chevrin, C.; Le Bras, J.; Harakat, D.; Muzart, J. Mechanistic Insights into the Palladium<sup>II</sup>-Catalyzed Hydroxyalkoxylation of 2-Allylphenols. *J. Org. Chem.* **2007**, *72*, 1859–1862.
93. Ley, S. V.; Mitchell, C.; Pears, D.; Ramarao, C.; Yu, J.-Q.; Zhou, W. Recyclable Polyurea-Microencapsulated Recyclable Polyurea-Microencapsulated Pd(0) Nanoparticles: An Efficient Catalyst for Hydrogenolysis of Epoxides. *Org. Lett.* **2003**, *5*, 4665–4668.

94. Kwon, M. S.; Park, I. S.; Jang, J. S.; Lee, J. S.; Park, J. Magnetically Separable Pd Catalyst for Highly Selective Epoxide Hydrogenolysis under Mild Conditions. *Org. Lett.* **2007**, *9*, 3417–3419.
95. Vega-Pérez, J. M.; Vega, M.; Blanco, E.; Iglesias-Guerra, F. Stereoselective Epoxidation of Alkenylidene Acetals Derived From Carbohydrates with D-Allo, D-Altro, D-Galacto, D-Gluco and D-Xylo Configurations. *Tetrahedron Asymmetry* **2007**, *18*, 1850–1867.
96. Guo, M.; Peng, J.; Yang, Q.; Li, C. Highly Active and Selective RuPd Bimetallic NPs for the Cleavage of the Diphenyl Ether C–O Bond. *ACS Catal.* **2018**, *8*, 11174–11183.
97. van Muyden, A. P.; Siankevich, S.; Yan, N.; Dyson, P. J. Discovery of a Highly Active Catalyst for Hydrogenolysis of C–O Bonds Via Systematic, Multi-Metallic Catalyst Screening. *ChemCatChem* **2019**, *11*, 2743–2752.
98. Li, H.; Song, G. Ru-Catalyzed Hydrogenolysis of Lignin: Base-Dependent Tunability of Monomeric Phenols and Mechanistic Study. *ACS Catal.* **2019**, *9*, 4054–4064.
99. Zhang, B.; Qi, Z.; Li, X.; Ji, J.; Luo, W.; Li, C.; Wang, A.; Zhang, T. ReO<sub>x</sub>/AC-Catalyzed Cleavage of C–O Bonds in Lignin Model Compounds and Alkaline Lignins. *ACS Sustain. Chem. Eng.* **2019**, *7*, 208–215.
100. Charles, E. J. J.; Vriamont, C. E. J. J.; Chen, T.; Romain, C.; Corbett, P.; Manageracharath, P.; Peet, J.; Conifer, C. M.; Hallett, J. P.; Britovsek, G. J. P. From Lignin to Chemicals: Hydrogenation of Lignin Models and Mechanistic Insights into Hydrodeoxygenation Via Low-Temperature C–O Bond Cleavage. *ACS Catal.* **2019**, *9*, 2345–2354.
101. Hossain, M. A.; Phung, T. K.; Rahamana, M. S.; Tulaphol, S.; Jasinski, J. B.; Sathitsuksanoh, N. Catalytic Cleavage of the β-O-4 Aryl Ether Bonds of Lignin Model Compounds by Ru/C Catalyst. *Appl. Catal. A Gen.* **2019**, *582*, 117100.
102. Wu, K.; Wang, W.; Guo, H.; Yang, Y.; Huang, Y.; Li, W.; Li, C. Engineering Co Nanoparticles Supported on Defect MoS<sub>2-x</sub> for Mild Deoxygenation of Lignin-Derived Phenols to Arenes. *ACS Energy Lett.* **2020**, *5*, 1330–1336.
103. Tieuli, S.; Mäki-Arvela, P.; Peurla, M.; Eränen, K.; Wärnå, J.; Cruciani, G.; Menegazzo, F.; Murzin, D. Y.; Signoretto, M. Hydrodeoxygenation of Isoeugenol Over Ni-SBA-15: Kinetics and Modelling. *Appl. Catal. A Gen.* **2019**, *580*, 1–10.
104. Bjelić, A.; Grilc, M.; Likozar, B. Bifunctional Metallic-Acidic Mechanisms of Hydrodeoxygenation of Eugenol as Lignin Model Compound Over Supported Cu, Ni, Pd, Pt, Rh and Ru Catalyst Materials. *Chem. Eng. J.* **2020**, *394*, 124914.
105. Koso, S.; Watanabe, H.; Okumura, K.; Nakagawa, Y.; Tomishige, K. Comparative Study of Rh–MoO<sub>x</sub> and Rh–ReO<sub>x</sub> Supported on SiO<sub>2</sub> for the Hydrogenolysis of Ethers and Polyols. *Appl. Catal. B Environ.* **2012**, *111–112*, 27–37.
106. Bondue, C. J.; Koper, M. T. M. Electrochemical Reduction of the Carbonyl Functional Group: The Importance of Adsorption Geometry, Molecular Structure, and Electrode Surface Structure. *J. Am. Chem. Soc.* **2019**, *141*, 12071–12078.
107. Walter, E. D.; Qi, L.; Chamas, A.; Mehta, H. S.; Sears, J. A.; Scott, S. L.; Hoyt, D. W. Operando MAS NMR Reaction Studies at High Temperatures and Pressures. *J. Phys. Chem. C* **2018**, *122*, 8209–8215.
108. Zhang, J.; Li, C.; Guan, W.; Chen, X.; Chen, X.; Tsang, C.-W.; Liang, C. Deactivation and Regeneration Study of a Co-Promoted MoO<sub>3</sub> Catalyst in Hydrogenolysis of Dibenzofuran. *Ind. Eng. Chem. Res.* **2020**, *59*, 4313–4321.
109. Zhang, J.; Li, C.; Guan, W.; Chen, X.; Chen, X.; Tsang, C.-W.; Liang, C. Promotional Effect of Co and Ni on MoO<sub>3</sub> Catalysts for Hydrogenolysis of Dibenzofuran to Biphenyl under Atmospheric Hydrogen Pressure. *J. Catal.* **2020**, *383*, 311–321.

**210** Heterogeneous catalysis in sustainable synthesis

110. Song, Y.; Feng, X.; Chen, J. S.; Brzezinski, C.; Xu, Z.; Lin, W. Multistep Engineering of Synergistic Catalysts in a Metal–Organic Framework for Tandem C–O Bond Cleavage. *J. Am. Chem. Soc.* **2020**, *142*, 4872–4882.
111. Zhou, Y.; Klinger, G. E.; Hegg, E. L.; Saffron, C. M.; Jackson, J. E. Multiple Mechanisms Mapped in Aryl Alkyl Ether Cleavage Via Aqueous Electrocatalytic Hydrogenation Over Skeletal Nickel. *J. Am. Chem. Soc.* **2020**, *142*, 4037–4050.
112. Arnold, M. A.; Gerasyuto, A. I.; Wang, J.; Du, W.; Kim Gorske, Y. J.; Arasu, T.; Baird, J.; Almstead, N. J.; Narasimhan, J.; Peddi, S.; Ginzburg, O.; Lue, S. W.; Hedrick, J.; Sheedy, J.; Lagaud, G.; Branstrom, A. A.; Weetall, M.; Vara Prasad, J. V. N.; Karp, G. M. 4-Hydroxy-2-Pyridones: Discovery and Evaluation of a Novel Class of Antibacterial Agents Targeting DNA Synthesis. *Bioorg. Med. Chem. Lett.* **2017**, *27*, 5014–5021.
113. Håkansson, A. E.; Palmelund, A.; Holm, H.; Madsen, R. Synthesis of 7-Deoxypancratistatin from Carbohydrates by the Use of Olefin Metathesis. *Chem. Eur. J.* **2006**, *12*, 3243–3253.
114. Zhang, J.; Ibrahim, M.; Collière, V.; Asakura, H.; Tanaka, T.; Teramura, K.; Philippot, K.; Yan, Y. Rh Nanoparticles With NiO<sub>x</sub> Surface Decoration for Selective Hydrogenolysis of CO Bond Over Arene Hydrogenation. *J. Mol. Catal. A Chem.* **2016**, *422*, 188–197.
115. Sanz, R.; Castroviejo, M. P.; Guilarte, V.; Pérez, A.; Fananás, F. J. Regioselective Synthesis of 4- and 7-Alkoxyindoles from 2,3-Dihalophenols: Application to the Preparation of Indole Inhibitors of Phospholipase A2. *J. Org. Chem.* **2007**, *72*, 5113–5118.
116. Li, Y.; Manickam, G.; Ghoshal, A.; Subramaniam, P. More Efficient Palladium Catalyst for Hydrogenolysis of Benzyl Groups. *Synth. Commun.* **2006**, *36*, 925–928.
117. Kokel, A.; Schäfer, C.; Zorigt, N.; Cho, H.; Grau, S.; Török, B. Efficient Green Deprotection of Benzyl, Benzylloxycarbonyl and Allyloxycarbonyl-Protected Amines, Alcohols and Amino Acids. *Appl. Catal. B Environ.* **2021**, submitted.
118. Wróblewski, A. E.; Bąk-Sypień, I. I. Studies Towards the Synthesis of (1*R*,2*S*)- and (1*S*,2*S*)-1,2-Epoxy-3-Hydroxypropylphosphonates and (1*S*,2*S*)- and (1*R*,2*S*)-2,3-Epoxy-1-Hydroxypropylphosphonates. *Tetrahedron Asymmetry* **2007**, *18*, 2218–2226.
119. Serrano, P.; Egado-Gabás, M.; Llebaria, A.; Delgado, A. An Unexpected Access to 5-Epi-Cyclophellitol, a New Cyclitol Member. *Tetrahedron Asymmetry* **2007**, *18*, 1971–1974. corrigendum: *Tetrahedron: Asymmetry* 2009, *20*, 1093.
120. Rigolet, S.; McCort, I.; Le Merrer, Y. Efficient Access to ATP Mimics, Potential FGF Receptor Tyrosine Kinase Inhibitors. *Tetrahedron Lett.* **2002**, *43*, 8129–8132.
121. Iwaki, T.; Nomura, T.; Narukawa, Y.; Uotani, K. A Simple Method for Deprotection of the N- and O-Carbobenzyoxy Groups and N-Methylation of the Desosamine Sugar Moiety of Ketolides. Application to the Synthesis of Ketolide Analogues With Various 9-Iminoether Moieties and Their Antibacterial Activities. *J. Antibiotics* **2005**, *58*, 679–685.
122. Adams, G. L.; Carroll, P. J.; Smith, A. B., III. Access to the Akummliline Family of Alkaloids: Total Synthesis of (+)-S-Cholarisine A. *J. Am. Chem. Soc.* **2013**, *135*, 519–528.
123. Liang, S.; Sun, B.-G.; Tian, H.-Y.; Wang, Y.-L.; Sun, Y.-M. A Highly Enantioselective Synthesis of the Odorant, 3-Hydroxy-4-Phenylbutan-2-One. *J. Chem. Res.* **2013**, 105–106.
124. Paleo, M. R.; Aurrecoechea, N.; Jung, K.-Y.; Rapoport, H. Formal Enantiospecific Synthesis of (+)-FR900482. *J. Org. Chem.* **2003**, *68*, 130–138.
125. Martín-Rodríguez, M.; Galán-Fernández, R.; Marcos-Escribano, A.; Bermejo, F. A. Ti(III)-Promoted Radical Cyclization of Epoxy Enones. Total Synthesis of (+)-Paeonisuffrone. *J. Org. Chem.* **2009**, *74*, 1798–1801.
126. Luo, G.; Chen, L.; Conway, C. M.; Kostich, W.; Johnson, B. M.; Ng, A.; Macor, J. E.; Dubowchik, G. E. Asymmetric Synthesis of the Major Metabolite of a Calcitonin Gene-Related Peptide Receptor Antagonist and Mechanism of Epoxide Hydrogenolysis. *J. Org. Chem.* **2017**, *82*, 3710–3720.

127. Drelinkiewicz, A.; Laitinen, R.; Kangas, R.; Pursiainen, J. 2-Ethylanthraquinone Hydrogenation on Pd/Al<sub>2</sub>O<sub>3</sub>. The Effect of Water and NaOH on the Degradation Process. *Appl. Catal. A Gen.* **2005**, *284*, 59–67.
128. Li, X.; Su, H.; Li, D.; Chen, H.; Yang, X.; Wang, S. Highly Dispersed Pd/AIPO-5 Catalyst for Catalytic Hydrogenation of 2-Ethylanthraquinone. *Appl. Catal. A Gen.* **2016**, *528*, 168–174.
129. Procházková, D.; Zámotný, P.; Bejblova, M.; Červený, L.; Čejka, J. Hydrodeoxygenation of Aldehydes Catalyzed by Supported Palladium Catalysts. *Appl. Catal. A Gen.* **2007**, *332*, 56–64.
130. Liu, S.; Fan, X.; Yan, X.; Du, X.; Chen, L. Catalytic Reduction of Benzaldehyde to Toluene Over Ni/ $\gamma$ -Al<sub>2</sub>O<sub>3</sub> in the Presence of Aniline and H<sub>2</sub>. *Appl. Catal. A Gen.* **2011**, *400*, 99–103.
131. Török, B.; London, G.; Bartók, M. Reduction of Carbonyl Compounds to Hydrocarbons by Catalytic Hydrogenation: A Novel One-Pot Method Using Pt/K-10 Montmorillonite Catalyst. *Synlett* **2000**, 631–632.
132. Mokhov, V. M.; Popov, Y. V.; Nebykov, D. N. Colloid and Nanodimensional Catalysts in Organic Synthesis: VI.1 Hydrogenation and Hydrogenolysis of Carbonyl Compounds. *Russ. J. Gen. Chem.* **2014**, *84*, 1656–1661.
133. Li, H.; Gao, Z.; Lei, L.; Liu, H.; Han, J.; Hong, F.; Luo, N.; Wang, F. Photocatalytic Transfer Hydrogenolysis of Aromatic Ketones Using Alcohols. *Green Chem.* **2020**, *22*, 3802–3808.
134. Zhang, J.; Matsubara, K.; Yun, G.-N.; Zheng, H.; Takagaki, A.; Kikuchi, R.; Oyama, S. T. Comparison of Phosphide Catalysts Prepared by Temperature-Programmed Reduction and Liquid-Phase Methods in the Hydrodeoxygenation of 2-Methylfuran. *Appl. Catal. A Gen.* **2017**, *548*, 39–46.
135. Dickinson, J. G.; Poberezny, J. T.; Savage, P. E. Deoxygenation of Benzofuran in Supercritical Water Over a Platinum Catalyst. *Appl. Catal. B Environ.* **2012**, *123–124*, 357–366.
136. Yang, J.; Li, S.; Zhang, L.; Liu, X.; Wang, J.; Pan, X.; Li, N.; Wang, A.; Cong, Y.; Wang, X.; Zhang, T. Hydrodeoxygenation of Furans Over Pd-FeO<sub>x</sub>/SiO<sub>2</sub> catalyst Under Atmospheric Pressure. *Appl. Catal. B Environ.* **2017**, *201*, 266–277.
137. Jun, J.-W.; Suh, Y.-W.; Suh, D. J.; Lee, Y.-K. Strong metal-support interaction effect of Pt/Nb<sub>2</sub>O<sub>5</sub> catalysts on aqueous phase hydrodeoxygenation of 1,6-hexanediol. *Catal. Today* **2018**, *302*, 108–114.
138. Said, A.; Da Silva Perez, D.; Perret, N.; Pinel, C.; Besson, M. Selective C-O Hydrogenolysis of Erythritol over Supported Rh-ReO<sub>x</sub> Catalysts in the Aqueous Phase. *ChemCatChem* **2017**, *9*, 2768–2783.
139. Resende, K. A.; Teles, C.; Jacobs, G.; Davis, B. H.; Cronauer, D. C.; Kropf, A. J.; Marshall, C. L.; Hori, C. E.; Noronha, F. B. Hydrodeoxygenation of Phenol Over Zirconia Supported Pd Bimetallic Catalysts. The Effect of Second Metal on Catalyst Performance. *Appl. Catal. B Environ.* **2018**, *232*, 213–231.
140. Barrios, A. M.; Telesa, C. A.; de Souza, P. M.; Rabelo-Neto, R. C.; Jacobs, G.; Davis, B. H.; Borges, L. E. P.; Noronha, F. B. Hydrodeoxygenation of Phenol over Niobia Supported Pd Catalyst. *Catal. Today* **2018**, *302*, 115–124.
141. Yang, Y.; Ochoa-Hernández, C.; de la Peña O’Shea, V. A.; Pizarro, P.; Coronado, J. M.; Ser-rano, D. P. Effect of Metal-Support Interaction on the Selective Hydrodeoxygenation of Anisole to Aromatics Over Ni-Based Catalysts. *Appl. Catal. B Environ.* **2014**, *145*, 91–100.
142. Zheng, Y.; Zhao, N.; Chen, J. Enhanced Direct Deoxygenation of Anisole to Benzene on SiO<sub>2</sub>-Supported Ni-Ga Alloy and Intermetallic Compound. *Appl. Catal. B Environ.* **2019**, *250*, 280–291.
143. Hewer, T. L. R.; Souza, A. G. F.; Roseno, K. T. C.; Bonfim, P. F. M. R.; Alves, R. M. B.; Schmal, M. Influence of Acid Sites on the Hydrodeoxygenation of Anisole With Metal Supported on SBA-15 and SAPO-11. *Renew. Energy* **2018**, *119*, 615–624.

144. Saidi, M.; Baharan, S. N. R. Kinetic Modeling and Experimental Investigation of Hydro-Catalytic Upgrading of Anisole as a Model Compound of Bio-Oils Derived from Fast Pyrolysis of Lignin Over Co/ $\gamma$ -Al<sub>2</sub>O<sub>3</sub>. *ChemistrySelect* **2020**, *5*, 2379–2387.
145. Gonçalves, V. O. O.; de Souza, P. M.; Cabioch, T.; da Silva, V. T.; Noronha, F. B.; Richard, F. Hydrodeoxygenation of m-Cresol over Nickel and Nickel Phosphide Based Catalysts. Influence of the Nature of the Active Phase and the Support. *Appl. Catal. B Environ.* **2017**, *219*, 619–628.
146. Gonçalves, V. O. O.; de Souza, P. M.; da Silva, V. T.; Noronha, F. B.; Richard, F. Kinetics of the Hydrodeoxygenation of Cresol Isomers over Ni<sub>2</sub>P/SiO<sub>2</sub>: Proposals of Nature of Deoxygenation Active Sites Based on An Experimental Study. *Appl. Catal. B Environ.* **2017**, *205*, 357–367.
147. Gonçalves, V. O. O.; de Souza, P. M.; Cabioch, T.; da Silva, V. T.; Noronha, F. B.; Richard, F. Effect of P/Ni Ratio on the Performance of Nickel Phosphide Phases Supported on Zirconia for the Hydrodeoxygenation of m-Cresol. *Catal. Commun.* **2019**, *119*, 33–38.
148. Wu, X.; Sun, Q.; Wang, H.; Han, J.; Ge, Q.; Zhu, X. Effect of Acid-Metal Balance of Bifunctional Pt/Beta Catalysts on Vapor Phase Hydrodeoxygenation of m-Cresol. *Catal. Today* **2020**, *355*, 43–50.
149. Liu, X.; An, W.; Turner, H.; Resasco, D. E. Hydrodeoxygenation of m-Cresol over Bimetallic NiFe Alloys: Kinetics and Thermodynamics Insight into Reaction Mechanism. *J. Catal.* **2018**, *359*, 272–286.
150. Dickinson, J. G.; Savage, P. E. Stability and Activity of Pt and Ni Catalysts for Hydrodeoxygenation in Supercritical Water. *J. Mol. Catal. A Chem.* **2014**, *388–389*, 56–65.
151. Fang, H.; Roldan, A.; Tian, C.; Zheng, Y.; Duan, X.; Chen, K.; Ye, L.; Leoni, S.; Yuan, Y. Structural Tuning and Catalysis of Tungsten Carbides for the Regioselective Cleavage of C-O Bonds. *J. Catal.* **2019**, *369*, 283–295.
152. Zhou, H.; Wang, H.; Sadow, A. D.; Slowing, I. I. Toward Hydrogen Economy: Selective Guaiacol Hydrogenolysis Under Ambient Hydrogen Pressure. *Appl. Catal. B Environ.* **2020**, *270*, 118890.
153. Wijaya, J. P.; Grossmann-Neuhausler, T.; Putra, R. D. D.; Smith, K. J.; Kim, C. S.; Gyenge, E. L. Electrocatalytic Hydrogenation of Guaiacol in Diverse Electrolytes Using a Stirred Slurry Reactor. *ChemSusChem* **2020**, *13*, 629–639.
154. Zhao, T.-J.; Zhang, J.-J.; Wang, H.-H.; Su, J.; Li, X.-H.; Chen, J.-S. Biomimetic Design of a 3D Transition Metal/Carbon Dyad for the One-Step Hydrodeoxygenation of Vanillin. *ChemSusChem* **2020**, *13*, 1900–1905.
155. Chen, J.; Shi, H.; Li, L.; Li, K. Deoxygenation of Methyl Laurate as a Model Compound to Hydrocarbons on Transition Metal Phosphide Catalysts. *Appl. Catal. B Environ.* **2014**, *144*, 870–884.
156. Pan, Z.; Wang, R.; Chen, J. Deoxygenation of Methyl Laurate as a Model Compound on Ni-Zn Alloy and Intermetallic Compound Catalysts: Geometric and Electronic Effects of Oxophilic Zn. *Appl. Catal. B Environ.* **2018**, *224*, 88–100.
157. Kukushkin, R. G.; Bulavchenko, O. A.; Kaichev, V. V.; Yakovlev, V. A. Influence of Mo on Catalytic Activity of Ni-Based Catalysts Inhydrodeoxygenation of Esters. *Appl. Catal. B Environ.* **2015**, *163*, 531–538.
158. Lugo-José, Y. K.; Monnier, J. R.; Williams, C. T. Gas-Phase, Catalytic Hydrodeoxygenation of Propanoic Acid, Over Supported Group VIII Noble Metals: Metal and Support Effects. *Appl. Catal. A Gen.* **2014**, *469*, 410–418.
159. Takada, Y.; Caner, J.; Kaliyamoorthy, S.; Naka, H.; Saito, S. Photocatalytic Transfer Hydrogenolysis of Allylic Alcohols on Pd/TiO<sub>2</sub>: A Shortcut to (S)-(+)-Lavandulol. *Chem. Eur. J.* **2017**, *23*, 18025–18032.

160. Yao, Y.; Wu, X.; Gutiérrez, O. Y.; Ji, J.; Jin, P.; Wang, S.; Xu, J.; Zhao, Y.; Wang, S.; Ma, X.; Lercher, J. A. Roles of Cu<sup>+</sup> and Cu<sup>0</sup> Sites in Liquid-Phase Hydrogenation of Esters on Core Shell CuZn@C Catalysts. *Appl. Catal. B Environ.* **2020**, *267*, 118698.
161. Cook, A.; Prakash, S.; Zheng, Y.-L.; Newman, S. G. Exhaustive Reduction of Esters Enabled by Nickel Catalysis. *J. Am. Chem. Soc.* **2020**, *142*, 8109–8115.
162. Srinivasa, G. R.; Narendra Babu, S. N.; Lakshmi, C.; Channe Gowda, D. Conventional and Microwave Assisted Hydrogenolysis Using Zinc and Ammonium Formate. *Synth. Commun.* **2004**, *34*, 1831–1837.
163. Török, B.; Prakash, G. K. S. Synthesis of Chiral Trifluoromethylated Amines by Palladium-Catalyzed Diastereoselective Hydrogenation-Hydrogenolysis Approach. *Adv. Synth. Catal.* **2003**, *345*, 165–168.
164. Abid, M.; Savolainen, M.; Landge, S.; Hu, J.; Prakash, G. K. S.; Olah, G. A.; Török, B. Synthesis of Trifluoromethyl-Imines by Solid Acid/Superacid Catalyzed Microwave Assisted Approach. *J. Fluor. Chem.* **2007**, *128*, 587–594.
165. Dasgupta, S.; Morzhina, E.; Schäfer, C.; Mhadgut, S. C.; Prakash, G. K. S.; Török, B. Synthesis of Chiral Trifluoromethyl Benzylamines by Heterogeneous Catalytic Reductive Amination. *Top. Catal.* **2016**, *59*, 1207–1213.
166. Choi, J. K.; Jeon, B. S.; Cho, J. H.; Kim, B. M. Use of an Ionic Liquid as a Co-Solvent for Recyclable Pd/C-Mediated *N*-Debenzylation. *Bull. Kor. Chem. Soc.* **2010**, *31*, 735–738.
167. Trzupke, J. D.; Li, C.; Chan, C.; Crowley, B. M.; Heimann, A. C.; Danishefsky, S. J. Lessons From the Total Synthesis of (±)-Phalarine: Insights into the Mechanism of the Pictet–Spengler Reaction. *Pure Appl. Chem.* **2010**, *82*, 1735–1748.
168. Abraham, A.; Davies, S. G.; Docherty, A. J.; Ling, K. B.; Roberts, P. M.; Russell, A. J.; Thomson, J. E.; Toms, S. M. Parallel Kinetic Resolution of Methyl (*R,S*)-5-Tris(Phenylthio) Methylcyclopent-1-Ene-Carboxylate for the Asymmetric Synthesis of (1*R*,2*S*,5*S*)- and (1*S*,2*R*,5*R*)-5-Methyl-Cispentacin. *Tetrahedron Asymmetry* **2008**, *19*, 1356–1362.
169. Srimurugan, S.; Murugan, K.; Chen, C. A Facile Method for Preparation of [<sup>2</sup>H<sub>3</sub>]-Sufentanil and its Metabolites. *Chem. Pharm. Bull.* **2009**, *57*, 1421–1424.
170. Cordero, F. M.; Bonanno, P.; Khairnar, B. B.; Cardona, F.; Brandi, A.; Macchi, B.; Minutolo, A.; Grelli, S.; Mastino, A. (–)-(1*R*,2*R*,7*S*,8*aR*)-1,2,7-Trihydroxyindolizidine ((–)-7*S*-OH Lentiginosine): Synthesis and Proapoptotic Activity. *ChemPlusChem* **2012**, *77*, 224–233.
171. Huang, P.-Q.; Chen, G.; Zheng, X. A New Synthesis of Alkaloid (*S*)-3-Hydroxypiperidin-2-One and its *O*-TBS Protected Derivative. *J. Heterocyclic Chem.* **2007**, *44*, 499–501.
172. Kikuchi, H.; Yamamoto, K.; Horoiwa, S.; Hirai, S.; Kasahara, R.; Hariguchi, N.; Matsumoto, M.; Oshima, Y. Exploration of a New Type of Antimalarial Compounds Based on Febri-fugine. *J. Med. Chem.* **2006**, *49*, 4698–4706.
173. Cheng, C.; Sun, J.; Xing, L.; Xu, J.; Wang, X.; Hu, Y. Highly Chemoselective Pd-C Catalytic Hydrodechlorination Leading to the Highly Efficient *N*-Debenzylation of Benzylamines. *J. Org. Chem.* **2009**, *74*, 5671–5674.
174. Davies, S. G.; Foster, E. M.; Lee, J. A.; Roberts, P. M.; Thomson, J. E. Stereospecific Cyclization Strategies for α,ε-Dihydroxy-β-amino Esters: Asymmetric Syntheses of Imino and Amino Sugars. *J. Org. Chem.* **2014**, *79*, 9686–9698.
175. Davies, S. G.; Figuccia, A. L. A.; Fletcher, A. I.; Roberts, P. M.; Thomson, J. E. Asymmetric Syntheses of (–)-ADMJ and (+)-ADANJ: 2-Deoxy-2-Amino Analogues of (–)-1-Deoxymannojirimycin and (+)-1-Deoxyallonojirimycin. *J. Org. Chem.* **2016**, *81*, 6481–6495.
176. Buchman, M.; Csatayová, K.; Davies, S. G.; Fletcher, A. I.; Houlby, I. T. T.; Roberts, P. M.; Rowe, S. M.; Thomson, J. E. Asymmetric Syntheses of (+)-Preussin B, the C(2)-Epimer of (–)-Preussin B, and 3-Deoxy-(+)-Preussin B. *J. Org. Chem.* **2016**, *81*, 4907–4922.

177. Davies, S. G.; Fletcher, A. I.; Foster, E. M.; Houlsby, I. T. T.; Roberts, P. M.; Schofield, T. M.; Thomson, J. E. The Asymmetric Syntheses of Pyrrolizidines, Indolizidines and Quinolizidines Via Two Sequential Tandem Ring-Closure/N-Debenzylation Processes. *Org. Biomol. Chem.* **2014**, *12*, 9223–9235.
178. Stead, D.; O'Brien, P.; Sanderson, A. J. Concise Synthesis of ( $\pm$ )-Cytisine Via Lithiation of N-Boc-Bispidine. *Org. Lett.* **2005**, *7*, 4459–4462.
179. Davies, S. G.; Lee, J. A.; Roberts, P. M.; Thomson, J. E.; Yin, J. Parallel Kinetic Resolution of Acyclic  $\gamma$ -Amino- $\alpha,\beta$ -unsaturated Esters: Application to the Asymmetric Synthesis of 4-Aminopyrrolidin-2-ones. *Org. Lett.* **2012**, *14*, 218–221.
180. Xie, J.; Wolfe, A. L.; Boger, D. L. Total Synthesis of Kopsinine. *Org. Lett.* **2013**, *15*, 868–870.
181. Federsel, H.-J.; Hedberg, M.; Qvarnström, F. R.; Tian, W. Optimization and Scale-Up of a Pd-Catalyzed Aromatic C-N Bond Formation: A Key Step in the Synthesis of a Novel 5-HT1B Receptor Antagonist. *Org. Process. Res. Dev.* **2008**, *12*, 512–521.
182. Davies, S. G.; Nicholson, R. L.; Price, P. D.; Roberts, P. M.; Russell, A. J.; Savory, A. D.; Smith, A. D.; Thomson, J. E. Iodine-Mediated Ring-Closing Iodoamination With Concomitant N-Debenzylation for the Asymmetric Synthesis of Polyhydroxylated Pyrrolidines. *Tetrahedron Asymmetry* **2009**, *20*, 758–772.
183. Davies, S. G.; Garrido, N. M.; Kruchinin, D.; Ichihara, O.; Kotchie, L. J.; Price, P. D.; Price Mortimer, A. J.; Russell, A. J.; Smith, A. D. Homochiral Lithium Amides for the Asymmetric Synthesis of  $\beta$ -Amino Acids. *Tetrahedron Asymmetry* **2006**, *17*, 1793–1811.
184. Davies, S. G.; Fletcher, A. M.; Hanby, A. R.; Roberts, P. M.; Thomson, J. E. Asymmetric Syntheses of the N-Terminal  $\alpha$ -Hydroxy- $\beta$ -Amino Acid Components of Microginins 612, 646 and 680. *Tetrahedron Asymmetry* **2017**, *28*, 1756–1764.
185. Davies, S. G.; Durbin, M. J.; Hartman, S. J. S.; Matsuno, A.; Roberts, P. M.; Russell, A. J.; Smith, A. D.; Thomson, J. E.; Toms, S. M. Parallel Kinetic Resolution of Tert-Butyl (*RS*)-6-Alkyl-Cyclohex-1-Ene-Carboxylates for the Asymmetric Synthesis of 6-Alkyl-Substituted Cishexacin Derivatives. *Tetrahedron Asymmetry* **2008**, *19*, 2870–2881.
186. Lee, B. K.; Choi, H. G.; Roh, E. J.; Lee, W. K.; Sim, T. Stereoselective Synthesis of (–)-8-Epi-Swainsonine Starting With a Chiral Aziridine. *Tetrahedron Lett.* **2013**, *54*, 553–556.
187. Chavan, S. P.; Khairnar, L. B.; Chavan, P. N.; Dumare, N. B.; Kalbhor, D. B.; Gonnade, R. J. Chiron Approach to Formal Synthesis of both Antipodes of *cis* 3-Hydroxypipercolic Acid. *Tetrahedron Lett.* **2014**, *55*, 6423–6426.
188. Szakonyi, Z.; Hetényi, A.; Fülöp, F. Synthesis and Application of Monoterpene-Based Chiral Aminodiols. *Tetrahedron* **2008**, *64*, 1034–1039.
189. Davies, S. G.; Fletcher, A. M.; Hughes, D. G.; Lee, J. A.; Price, P. D.; Roberts, P. M.; Russell, A. J.; Smith, A. D.; Thomson, J. E.; Williams, O. M. H. Asymmetric Synthesis of Piperidines and Octahydroindolizines Using a One-Pot Ring-Closure/N-Debenzylation Procedure. *Tetrahedron* **2011**, *67*, 9975–9992.
190. Davies, S. G.; Fletcher, A. I.; Lebé, C.; Roberts, P. M.; Thomson, J. E.; Yin, J. Asymmetric Synthesis of (–)-(1*R*,7*aS*)-Absoulone. *Tetrahedron* **2013**, *69*, 1369–1377.
191. Brambilla, M.; Davies, S. G.; Fletcher, A. I.; Roberts, P. M.; Thomson, J. E.; Zimmer, D. Pyrrolizidines, Indolizidines and Quinolizidines Via a Double Reductive Cyclisation Protocol: Concise Asymmetric Syntheses of (+)-Trachelanthamidine, (+)-Tashiromine and (+)-Epilupinine. *Tetrahedron* **2016**, *72*, 7417–7429.
192. Wang, X.; Dong, Y.; Sun, J.; Xu, X.; Li, R.; Hu, Y. Nonracemic Betti Base as a New Chiral Auxiliary: Application to Total Syntheses of Enantiopure (2*S*,6*R*)-Dihydropinidine and (2*S*,6*R*)-Isosolenopsins. *J. Org. Chem.* **2005**, *70*, 1897–1900.

193. Cheng, G.; Wang, X.; Su, D.; Liu, H.; Liu, F.; Hu, Y. Preparation of Enantiopure Substituted Piperidines Containing 2-Alkene or 2-Alkyne Chains: Application to Total Syntheses of Natural Quinolizidine-Alkaloids. *J. Org. Chem.* **2010**, *75*, 1911–1916.
194. Liu, H.; Su, D.; Cheng, G.; Xu, J.; Wang, X.; Hu, Y. Enantiopure 2,6-Disubstituted Piperidines Bearing One Alkene- or Alkyne-Containing Substituent: Preparation and Application to Total Syntheses of Indolizidine-Alkaloids. *Org. Biomol. Chem.* **2010**, *8*, 1899–1904.
195. Kawano, M.; Kiuchi, T.; Negishi, S.; Tanaka, H.; Hoshikawa, T.; Matsuo, J.; Ishibashi, H. Regioselective Inter- and Intramolecular Formal [4+2] Cycloaddition of Cyclobutanones with Indoles and Total Synthesis of ( $\pm$ )-Aspidospermidine. *Angew. Chem. Int. Ed.* **2013**, *52*, 906–910.
196. Vanier, G. S. Simple and Efficient Microwave-Assisted Hydrogenation Reactions at Moderate Temperature and Pressure. *Synlett* **2007**, 131–135.
197. Mandal, P. K.; McMurray, J. S. Pd–C-Induced Catalytic Transfer Hydrogenation With Triethylsilane. *J. Org. Chem.* **2007**, *72*, 6599–6601.
198. Felpin, F.-X.; Fouquet, E. A Useful, Reliable and Safer Protocol for Hydrogenation and the Hydrogenolysis of *O*-Benzyl Groups: The In Situ Preparation of an Active Pd/C Catalyst With Well-Defined Properties. *Chem. Eur. J.* **2010**, *16*, 12440–12445.
199. Maki, T.; Tsuritani, T.; Yasukata, T. A Mild Method for the Synthesis of Carbamate-Protected Guanidines Using the Burgess Reagent. *Org. Lett.* **2014**, *16*, 1868–1871.
200. Ozores, H. L.; Amorfn, M.; Granja, J. R. Self-Assembling Molecular Capsules Based on  $\alpha,\gamma$ -Cyclic Peptides. *J. Am. Chem. Soc.* **2017**, *139*, 776–784.
201. Landeros, J. M.; Suchy, L.; Ávila-Ortiz, C. J.; Maulide, N.; Juaristi, E. Dendrimeric  $\alpha,\beta$ -Dipeptidic Conjugates as Organocatalysts in the Asymmetric Michael Addition Reaction of Isobutyraldehyde to *N*-Phenylmaleimides. *Monatsh. Chem.* **2019**, *150*, 777–788.
202. Shin, K.; Chang, S. Iridium(III)-Catalyzed Direct C-7 Amination of Indolines With Organic Azides. *J. Org. Chem.* **2014**, *79*, 12197–12204.
203. Asai, M.; Takemoto, Y.; Deguchi, A.; Hattori, Y.; Makabe, H. An Asymmetric Synthesis of (+)-Monomorine I. *Tetrahedron Asymmetry* **2017**, *28*, 1582–1586.
204. Guo, Y.; He, H.; Liu, X.; Chen, Z.; Rioux, R. M.; Janik, M. J.; Savage, P. E. Ring-Opening and Hydrodenitrogenation of Indole Under Hydrothermal Conditions Over Ni, Pt, Ru, and Ni–Ru Bimetallic Catalysts. *Chem. Eng. J.* **2021**, *406*, 126853.
205. Liu, X.; Ding, S.; Wei, Q.; Zhou, Y.; Zhang, P.; Xu, Z. DFT Insights in to the Hydrodenitrogenation Behavior Differences Between Indole and Quinoline. *Fuel* **2021**, *285*, 119039.
206. Lunn, G.; Sansone, E. B. Validated Methods for Degrading Hazardous Chemicals: Some Halogenated Compounds. *Am. Ind. Hyg. Assoc. J.* **1991**, *52*, 252–257.
207. Moran, M. J.; Zogorski, J. S.; Squillace, P. J. Chlorinated Solvents in Groundwater of the United States. *Environ. Sci. Technol.* **2006**, *41*, 74–81.
208. Hodgson, E., Ed. *A Textbook of Modern Toxicology*; 4th ed.; Wiley: Hoboken, NJ, 2010.
209. U.S. E.P.A. *Toxicological Review of Trichloroethylene in Support of Summary Information on the Integrated Risk Information System (Iris)*; U.S. Environmental Protection Agency: Washington, DC, 2011.
210. Urbano, F. J.; Marinas, J. M. Hydrogenolysis of Organohalogen Compounds Over Palladium Supported Catalysts. *J. Mol. Catal. A Chem.* **2001**, *173*, 329–345.
211. Alonso, F.; Beletskaya, I. P.; Yus, M. Metal-Mediated Reductive Hydrodehalogenation of Organic Halides. *Chem. Rev.* **2002**, *102*, 4009–4092.
212. Xu, Y.; Ma, J.; Xu, Y.; Li, H.; Li, H.; Li, P.; Zhou, X. Nickel Nanoparticles Embedded in the Framework of Mesoporous TiO<sub>2</sub>: Efficient and Highly Stable Catalysts for Hydrodechlorination of Chlorobenzene. *Appl. Catal. A Gen.* **2012**, *413–414*, 350–357.

216 Heterogeneous catalysis in sustainable synthesis

213. Hussain, A. A.; Nazir, S.; Irshad, R.; Tahir, K.; Raza, M.; Khan, Z. U. H.; Khan, A. U. Synthesis of Functionalized Mesoporous Ni-SBA-16 Decorated With MgO Nanoparticles for Cr (VI) Adsorption and an Effective Catalyst for Hydrodechlorination of Chlorobenzene. *Mater. Res. Bull.* **2021**, *133*, 111059.
214. Zinovyev, S.; Shelepchikov, A.; Tundo, P. Design of New Systems for Transfer Hydrogenolysis of Polychlorinated Aromatics with 2-Propanol Using a Raney Nickel Catalyst. *Appl. Catal. B Environ.* **2007**, *72*, 289–298.
215. Kopinke, F. D.; Angeles-Wedler, D.; Fritsch, D.; Mackenzie, K. Pd-Catalyzed Hydrodechlorination of Chlorinated Aromatics in Contaminated Waters—Effects of Surfactants, Organic Matter and Catalyst Protection by Silicone Coating. *Appl. Catal. B Environ.* **2010**, *96*, 323–328.
216. Ma, X.; Liu, Y.; Li, X.; Xu, J.; Gu, G.; Xia, C. Water: The Most Effective Solvent for Liquid-Phasehydrodechlorination of Chlorophenols Over Raney Ni Catalyst. *Appl. Catal. B Environ.* **2015**, *165*, 351–359.
217. Mukumoto, M.; Mashimo, T.; Tsuzuki, H.; Tsukinoki, T.; Uezu, N.; Mataka, S.; Tashiro, M.; Kakinami, T. Synthesis of [2H11]Cyclohexanol by Reduction of Pentachlorophenol Using Raney Nickel-Aluminum Alloy in a BaO-D<sub>2</sub>O Solution Under Sonication. *J. Chem. Res.* **1995**, 412–413.
218. Yang, B.; Zhang, F.; Deng, S.; Yu, G.; Zhang, H.; Xiao, J.; Shi, L.; Shen, J. A Facile Method for the Highly Efficient Hydrodechlorination of 2-Chlorophenol Using Al-Ni Alloy in the Presence of Fluorine Ion. *Chem. Eng. J.* **2012**, *209*, 79–85.
219. Aramendí, M. A.; Borau, V.; García, I. M.; Jiménez, C.; Marinas, A.; Marinas, J. M.; Urbano, F. J. Hydrogenolysis of Aryl Halides by Hydrogen Gas and Hydrogen Transfer Over Palladium-Supported Catalysts. *C. R. Acad. Sci., Ser. IIc: Chim.* **2000**, *3*, 465–470.
220. Pyo, A.; Kim, S.; Kumar, M. R.; Byeun, A.; Eom, M. S.; Han, M. S.; Lee, S. Palladium-Catalyzed Hydrodehalogenation of Aryl Halides Using Paraformaldehyde as the Hydride Source: High-Throughput Screening by Paper-Based Colorimetric Iodide Sensor. *Tetrahedron Lett.* **2013**, *54*, 5207–5210.
221. Schäfer, C.; Ellstrom, C. J.; Cho, H.; Török, B. Pd/C-Al-Water Facilitated Selective Reduction of a Broad Variety of Functional Groups. *Green Chem.* **2017**, *19*, 1230–1234.
222. Omari-Qadry, K.; Hamza, K.; Sasson, Y.; Blum, J. Liquid Phase Hydrodechlorination of Some Chlorinated Aromatic Nitrogen-Containing Heterocyclics. *J. Mol. Catal. A Chem.* **2009**, *308*, 182–185.
223. Liu, G.-B.; Tashiro, M.; Thiemann, T. A Facile Method for the Dechlorination of Mono- and Dichlorobiphenyls Using Raney Ni-Al Alloy in Dilute Aqueous Solutions of Alkali Hydroxides or Alkali Metal Carbonates. *Tetrahedron* **2009**, *65*, 2497–2505.
224. Liu, G.-B.; Tsukinoki, T.; Kanda, T.; Mitoma, Y.; Tashiro, M. Organic Reaction in Water. Part 2. A New Method for Dechlorination of Chlorobiphenyls Using a Raney Ni-Al Alloy in Dilute Aqueous Alkaline Solution. *Tetrahedron Lett.* **1998**, *39*, 5991–5994.
225. Massicot, F.; Schneider, R.; Fort, Y.; Illy-Cherrey, S.; Tillement, O. Synergistic Effect in Bimetallic Ni-Al Clusters. Application to Efficient Catalytic Reductive Dehalogenation of Polychlorinated Arenes. *Tetrahedron* **2000**, *56*, 4765–4768.
226. Tsukinoki, T.; Kakinami, T.; Iida, Y.; Ueno, M.; Ueno, Y.; Mashimo, T.; Tsuzuki, H.; Tashiro, M. Hydrogenation of Halophenols to Cyclohexanols Using Raney Nickel-Aluminium Alloy in Saturated Ba(OH)<sub>2</sub> Solution Under Mild Conditions. *J. Chem. Soc. Chem. Commun.* **1995**, 209–210.
227. Weidlich, T.; Prokes, L.; Pospisilova, D. Debromination of 2,4,6-Tribromophenol Coupled With Biodegradation. *Cent. Eur. J. Chem.* **2013**, *11*, 979–987.

228. Liu, G.-B.; Zhao, H.-Y.; Zhang, J.; Thiemann, T. Raney Ni-Al Alloy Mediated Hydrodehalogenation and Aromatic Ring Hydrogenation of Halogenated Phenols in Aqueous Medium. *J. Chem. Res.* **2009**, 342–344.
229. Wu, C.; Zhou, L.; Zhou, Y.; Zhou, C.; Xia, S.; Rittmann, B. E. Dechlorination of 2,4-Dichlorophenol in a Hydrogen-Based Membrane Palladium-Film Reactor: Performance, Mechanisms, and Model Development. *Water Res.* **2021**, 188, 116465.
230. Sohn, H.; Celik, G.; Gunduz, S.; Majumdar, S. S.; Dean, S. L.; Edmiston, P. L.; Ozkan, U. S. Effect of High-Temperature on the Swellable Organically-Modified Silica (SOMS) and Its Application to Gas-Phase Hydrodechlorination of Trichloroethylene. *Appl. Catal. B Environ.* **2017**, 209, 80–90.
231. Karpinski, Z.; Bonarowska, M.; Łomot, D.; Śrębowata, A.; Da Costa, P.; Rodrigues, J. A. Hydrogenolysis of Carbon–Halogen and Carbon–Carbon Bonds over Pd/Nb<sub>2</sub>O<sub>5</sub>–Al<sub>2</sub>O<sub>3</sub> Catalysts. *Catal. Commun.* **2009**, 10, 1757–1761.
232. Ha, J.-M.; Kim, D.; Kim, J.; Kim, S. K.; Ahn, B. S.; Kang, J. W. Supercritical-Phase-Assisted Highly Selective and Active Catalytic Hydrodechlorination of the Ozone-Depleting Refrigerant CHClF<sub>2</sub>. *Chem. Eng. J.* **2012**, 213, 346–355.
233. Bedia, J.; Arevalo-Bastante, A.; Grau, J. M.; Dosso, L. A.; Rodriguez, J. J.; Mayoral, A.; Diaz, I.; Gómez-Sainero, L. M. Effect of the Pt–Pd Molar Ratio in Bimetallic Catalysts Supported on Sulfated Zirconia on the Gas-Phase Hydrodechlorination of Chloromethanes. *J. Catal.* **2017**, 352, 562–571.
234. Kamiguchi, S.; Watanabe, M.; Kondo, K.; Kodomari, M.; Chihara, T. Catalytic Dehydrohalogenation of Alkyl Halides by Nb, Mo, Ta, and W Halide Clusters With an Octahedral Metal Framework and by a Re Chloride Cluster With a Triangular Metal Framework. *J. Mol. Catal. A Chem.* **2003**, 203, 153–163.
235. Donahue, N. M. Air Pollution and Air Quality. In *Green Chemistry: An Inclusive Approach*; Török, B., Dransfield, T., Eds.; Elsevier: Oxford, Cambridge, 2018.
236. Selvam, P.; Sonavane, S. U.; Mohapatra, S. K.; Jayaram, R. V. Selective Reduction of Alkenes,  $\alpha,\beta$ -Unsaturated Carbonyl Compounds, Nitroarenes, Nitroso Compounds, N,N-Hydrogenolysis of Azo and Hydrazo Functions as well as Simultaneous Hydrodehalogenation and Reduction of Substituted Aryl Halides Over PdMCM-41 catalyst Under Transfer Hydrogen Conditions. *Tetrahedron Lett.* **2004**, 45, 3071–3075.
237. Tsuzuki, H.; Iyama, H.; Mashimo, T.; Mukumoto, M.; Tsukinoki, T.; Mataka, S.; Tashiro, M. Reductive Dehalogenation and Ring Saturation of Halogenated Hydroquinones, Catechol, and Resorcinol With Raney Alloys in Aqueous Sodium Hydroxide. *Chem. Express* **1993**, 8, 495–498.
238. Tsuzuki, H.; Iyama, H.; Tsukinoki, T.; Mukumoto, M.; Yonemitsu, T.; Nagano, Y.; Thiemann, T.; Mataka, S.; Tashiro, M. Reductive Dehalogenation and Ring Saturation of Halogenated Hydroquinones, Pyrocatechol and Resorcinol With Raney Alloys in NaOD-D<sub>2</sub>O Solution Leading to Hydroquinones, Cyclohexane-1,4-Diol and Cyclohexane-1,3-Dione Labeled With Deuterium. *J. Chem. Res.* **1994**, 302–303.
239. Liu, G.-B.; Zhao, H.-Y.; Dai, L.; Thiemann, T. A Convenient Method for the Reductive Degradation of Mono-, Di-, and Tribromodiphenyl Ethers, Tetrabromo- and Tetrachlorobisphenol A with Raney Ni-Al Alloy. *ARKIVOC* **2009**, 211–226.
240. Liu, G.-B.; Dai, L.; Gao, X.; Li, M.-K.; Thiemann, T. Reductive Degradation of Tetrabromobisphenol A (TBBPA) in Aqueous Medium. *Green Chem.* **2006**, 8, 781–783.
241. Weidlich, T.; Krejcova, A.; Prokes, L. Study of Dehalogenation of Halogenoanilines Using Raney Al-Ni Alloy in Aqueous Medium at Room Temperature. *Monatsh. Chem.* **2010**, 141, 1015–1020.

**218** Heterogeneous catalysis in sustainable synthesis

242. Weidlich, T.; Prokes, L. Facile Dehalogenation of Halogenated Anilines and their Derivatives Using Al-Ni Alloy in Alkaline Aqueous Solution. *Cent. Eur. J. Chem.* **2011**, *9*, 590–597.
243. Orsy, G.; Fülöp, F.; Mándity, I. M. Continuous-Flow Catalytic Deuterodehalogenation Carried out in Propylene Carbonate. *Green Chem.* **2019**, *21*, 956–961.
244. Schäfer, C.; Zorigt, N.; Török, B. Selective Deuteration of a Broad Variety of Halogenated Compounds Using Pd/C-Al-D<sub>2</sub>O System as the Deuterium Source and Reaction Medium. *Appl. Catal. B Environ.* **2021**, submitted.
245. Li, J.; Li, M.; Li, J.; Wang, S.; Li, G.; Liu, X. Hydrodechlorination and Deep Hydrogenation on Single-Palladium-Atombased Heterogeneous Catalysts. *Appl. Catal. B Environ.* **2021**, *282*, 119518.
246. Cho, H.; Schäfer, C.; Török, B. Hydrogenations and Deuterium Labeling with Aluminum-Based Metal Alloys Under Aqueous Conditions. *Curr. Org. Synth.* **2016**, *13*, 255–277.
247. Baird, C.; Cann, M. *Environmental Chemistry*, 5th ed.; MacMillan Learning: New York, 2012.
248. Zupancic, S.; Svete, J.; Stanovnik, B. Reductive Ring Cleavage of 1-Alkyl-4-Benzoylamino-5-Phenyl-3-Pyrazolidinones with Raney-Nickel Alloy. Synthesis of N-Benzoyl-3-Alkylamino-3-Phenylalanine Amides From *rel*-(4*R*,5*R*)-4-Benzoylamino-5-Phenyl-3-Pyrazolidinone. *J. Heterocyclic Chem.* **1999**, *36*, 607–610.
249. Pacchioni, M.; Bega, A.; Fabretti, A. C.; Rovai, D.; Cornia, A. Post-Synthetic Isotopic Labeling of an Azamacrocyclic Ligand. *Tetrahedron Lett.* **2002**, *43*, 771–774.
250. Jnaneshwara, G. K.; Sudalai, A.; Deshpande, V. H. Palladium Catalyzed Transfer Hydrogenation of Azo Compounds and Oximes Using Ammonium Formate. *J. Chem. Res.* **1998**, 160–161.
251. Lunn, G.; Sansone, E. B. Destruction of Azo and Azoxy Compounds and 2-Aminoanthracene. *Appl. Occup. Environ.* **1991**, *6*, 1020–1026.
252. Srinivasa, G. R.; Abiraj, K.; Channe Gowda, D. Zinc-Catalyzed Hydrogenative Cleavage of Azo Compounds Using Triethylammonium Formate. *Synth. React. Inorg. Met.-Org. Chem.* **2004**, *34*, 223–231.
253. Gowda, S.; Abiraj, K.; Channe Gowda, D. Reductive Cleavage of Azo Compounds Catalyzed by Commercial Zinc Dust Using Ammonium Formate or Formic Acid. *Tetrahedron Lett.* **2002**, *43*, 1329–1331.
254. Meketa, M. L.; Weinreb, S. M. Total Synthesis of Ageladine A, an Angiogenesis Inhibitor From the Marine Sponge *Agelas nakamura*. *Org. Lett.* **2006**, *8*, 1443–1446.
255. Xie, Y.; Sun, M.; Zhou, H.; Cao, Q.; Gao, K.; Niu, C.; Yang, H. Enantiospecific Total Synthesis of (+)-Tanikolide via a Key [2,3]-Meisenheimer Rearrangement With an Allylic Amine N-Oxide- Directed Epoxidation and a One-Pot Trichloroisocyanuric Acid N-Debenzylation and N-Chlorination. *J. Org. Chem.* **2013**, *78*, 10251–10263.
256. Ghirardello, M.; Ledru, H.; Sau, A.; Galan, M. C. Chemo-Selective Rh-Catalysed Hydrogenation of Azides Into Amines. *Carbohydr. Res.* **2020**, *489*, 107948.
257. Tong, M. L.; Leusch, L. T.; Holzschneider, K.; Kirsch, S. F. Rubazonic Acids and Their Synthesis. *J. Org. Chem.* **2020**, *85*, 6008–6016.
258. Song, C. An Overview of New Approaches to Deep Desulfurization for Ultra-Clean Gasoline, Diesel Fuel and Jet Fuel. *Catal. Today* **2003**, *86*, 211–263.
259. EPA USA. *Control of Air Pollution From Motor Vehicles: Tier 3 Motor Vehicle Emission and Fuel Standards; Final Rule*; EPA USA, 2014. <https://www.epa.gov/regulations-emissions-vehicles-and-engines>(Accessed 11 October 2019).
260. Lindstad, H. E.; Rehn, C. F.; Eskeland, G. S. Sulphur Abatement Globally in Maritime Shipping. *Transp. Res. Part D: Transp. Environ.* **2017**, *57*, 303–313.

261. Schmitz, C.; Datsevitch, L.; Jess, A. Deep Desulfurization of Diesel Oil: Kinetic Studies and Process-Improvement by the Use of a Two-Phase Reactor with Pre-Saturator. *Chem. Eng. Sci.* **2004**, *59*, 2821–2829.
262. Grange, P. Catalytic Hydrodesulfurization. *Catal. Rev.* **1980**, *21*, 135–181.
263. Stanislaus, A.; Marafi, A.; Rana, M. S. Recent Advances in the Science and Technology of Ultra Low Sulfur Diesel (ULSD) Production. *Catal. Today* **2010**, *153*, 1–68.
264. Javadli, R.; de Klerk, A. Desulfurization of Heavy Oil. *Appl. Petrochem. Res.* **2012**, *1*, 3–19.
265. Puskas, J. E.; Barghi, S.; McIntyre, J. Practical Approach to Measure the Relative Activity of Heterogeneous Catalysts. *Appl. Catal. A Gen.* **2001**, *217*, 11–21.
266. Zhang, X.; Hayward, D. O. Applications of Microwave Dielectric Heating in Environment-Related Heterogeneous Gas-Phase Catalytic Systems. *Inorg. Chim. Acta* **2006**, *359*, 3421–3433.
267. Larabi, C.; Nielsen, P. K.; Helveg, S.; Thieuleux, C.; Johansson, F. B.; Brorson, M.; Quadrelli, E. A. Bulk Hydrodesulfurization Catalyst Obtained by Mo(CO)<sub>6</sub> Grafting on the Metal–Organic Framework Ni<sub>2</sub>(2,5-Dihydroxoterephthalate). *ACS Catal.* **2012**, *2*, 695–700.
268. Gándara, F.; Perles, J.; Snejko, N.; Iglesias, M.; Gómez-Lor, B.; Gutiérrez-Puebla, E.; Monge, M. A. Layered Rare-Earth Hydroxides: A Class of Pillared Crystalline Compounds for Intercalation Chemistry. *Angew. Chem. Int. Ed.* **2006**, *45*, 7998–8001.
269. Park, J. C.; Song, H. Synthesis of Polycrystalline Mo/MoO<sub>x</sub> Nanoflakes and Their Transformation to MoO<sub>3</sub> and MoS<sub>2</sub> Nanoparticles. *Chem. Mater.* **2007**, *19*, 2706–2708.
270. Nguyen, N.; Harrison, D. J.; Lough, A. J.; De Crisci, A. G.; Fekl, U. Molybdenum Dithiolene Complexes as Structural Models for the Active Sites of Molybdenum(IV) Sulfide Hydrodesulfurization Catalysts. *Eur. J. Inorg. Chem.* **2010**, 3577–3585.
271. Bataille, F.; Lemberon, J. L.; Michaud, P.; Pérot, G.; Vrinat, M.; Lemaire, M.; Schulz, E.; Breyse, M.; Kasztelan, S. Alkyldibenzothiophenes Hydrodesulfurization-Promoter Effect, Reactivity, and Reaction Mechanism. *J. Catal.* **2000**, *191*, 409–422.
272. Sun, Y.; Prins, R. Mechanistic Studies and Kinetics of the Hydrodesulfurization of Dibenzothiophene on Co–MoS<sub>2</sub>/γ–Al<sub>2</sub>O<sub>3</sub>. *J. Catal.* **2009**, *267*, 193–201.
273. Jang, J.-G.; Lee, Y.-K. Promotional Effect of Ga for Ni<sub>2</sub>P Catalyst on Hydrodesulfurization of 4,6-DMDBT. *Appl. Catal. B Environ.* **2019**, *250*, 181–188.
274. Li, H.; Li, M.; Chu, Y.; Liu, F.; Nie, H. Essential Role of Citric Acid in Preparation of Efficient NiW/Al<sub>2</sub>O<sub>3</sub> HDS Catalysts. *Appl. Catal. A Gen.* **2011**, *403*, 75–82.
275. Zhang, D.; Liu, X.-M.; Liu, Y.-X.; Yan, Z.-F. Impact of γ-Alumina Pore Structure on Structure and Performance of Ni–Mo/γ–Al<sub>2</sub>O<sub>3</sub> Catalyst for 4,6-Dimethyldibenzothiophene Desulfurization. *Microporous Mesoporous Mater.* **2021**, *310*, 110637.
276. Wang, H.; Liu, S.; Smith, K. J. Understanding Selectivity Changes during Hydrodesulfurization of Dibenzothiophene on Mo<sub>2</sub>C/Carbon Catalysts. *J. Catal.* **2019**, *369*, 427–439.
277. Rozanska, X.; Saintigny, X.; van Santen, R. A.; Clémendot, S.; Hutschka, F. A Theoretical Study of Hydrodesulfurization and Hydrogenation of Dibenzothiophene Catalyzed by Small Zeolitic Cluster. *J. Catal.* **2002**, *208*, 89–99.
278. Li, L.; Zhu, Y.; Lu, X.; Wei, M.; Zhuang, W.; Yang, Z.; Feng, X. Carbon Heterogeneous Surface Modification on a Mesoporous TiO<sub>2</sub>-Supported Catalyst and its Enhanced Hydrodesulfurization Performance. *Chem. Commun.* **2012**, *48*, 11525–11527.
279. Saleha, T. A.; AL-Hammadi, S. A. A Novel Catalyst of Nickel-Loaded Graphene Decorated on Molybdenumalumina for the HDS of Liquid Fuels. *Chem. Eng. J.* **2021**, *406*, 125167.
280. Muzic, M.; Sertic-Bionda, K. Alternative Processes for Removing Organic Sulfur Compounds from Petroleum Fractions. *Chem. Biochem. Eng. Q.* **2013**, *11*, 101–108.

**220** Heterogeneous catalysis in sustainable synthesis

281. Salnikov, O. G.; Burueva, D. B.; Barskiy, D. A.; Bukhtiyarova, G. A.; Kovtunov, K. V.; Kopyug, I. V. A Mechanistic Study of Thiophene Hydrodesulfurization by the Parahydrogen-Induced Polarization Technique. *ChemCatChem* **2015**, *7*, 3508–3512.
282. Zhou, X.; Li, X.; Prins, R.; Wang, A.; Wang, L.; Liu, S.; Sheng, Q. Desulfurization of 2-Phenylcyclohexanethiol Over Transition-Metal Phosphides. *J. Catal.* **2020**, *383*, 331–342.
283. Nasri, N. S.; Jones, J. M.; Dupont, V. A.; Williams, A. A Comparative Study of Sulfur Poisoning and Regeneration of Precious-Metal Catalysts. *Energy Fuel* **1998**, *12*, 1130–1134.
284. Bednar, T. N.; Resnikoff, A. R.; Gavenonis, J. Microwave-Assisted Cleavage of Cysteine Perfluoroaryl Thioethers. *Amino Acids* **2020**, *52*, 841–845.
285. Taoufik, M.; Cordonnier, M.-A.; Santini, C. C.; Basset, J.-M.; Candy, J.-P. Surface Organometallic Chemistry on Metals: Controlled Hydrogenolysis of Me<sub>4</sub>Sn, Me<sub>3</sub>SnR, Me<sub>2</sub>SnR<sub>2</sub>, MeSnBu<sub>3</sub> and SnBu<sub>4</sub> (R = Methyl, *n*-Butyl, *tert*-Butyl, Neopentyl, Cyclohexyl) onto Metallic Rhodium Supported on Silica. *New J. Chem.* **2004**, *28*, 1531–1537.
286. Pribanic, B.; Trincado, M.; Eiler, F.; Vogt, M.; Comas-Vives, A.; Grützmacher, H. Hydrogenolysis of Polysilanes Catalyzed by Low-Valent Nickel Complexes. *Angew. Chem. Int. Ed.* **2020**, *59*, 2–9.
287. Caes, B. R.; Teixeira, R. E.; Knapp, K. G.; Raines, R. T. Biomass to Furans: Renewable Routes to Chemicals and Fuels. *ACS Sustain. Chem. Eng.* **2015**, *3*, 2591–2605.
288. Wang, H.; Zhua, C.; Li, D.; Liu, Q.; Tan, J.; Wanga, C.; Cai, C.; Ma, L. Recent Advances in Catalytic Conversion of Biomass to 5-Hydroxymethylfurfural and 2, 5-Dimethylfuran. *Renew. Sust. Energ. Rev.* **2019**, *103*, 227–247.
289. Zhang, C.; Wang, F. Catalytic Lignin Depolymerization to Aromatic Chemicals. *Acc. Chem. Res.* **2020**, *53*, 470–484.
290. Kokel, A.; Török, B. Sustainable Production of Fine Chemicals and Materials Using Non-Toxic Renewable Sources. *Toxicol. Sci.* **2018**, *161*, 214–224.
291. May, A. S.; Biddinger, E. J. Strategies to Control Electrochemical Hydrogenation and Hydrogenolysis of Furfural and Minimize Undesired Side Reactions. *ACS Catal.* **2020**, *10*, 3212–3221.
292. Jenness, G. R.; Wan, W.; Chen, J. G.; Vlachos, D. G. Reaction Pathways and Intermediates in Selective Ring Opening of Biomass-Derived Heterocyclic Compounds by Iridium. *ACS Catal.* **2016**, *6*, 7002–7009.
293. Gilkey, M. J.; Mironenko, A. V.; Vlachos, D. G.; Xu, B. Adipic Acid Production Via Metal-Free Selective Hydrogenolysis of Biomass-Derived Tetrahydrofuran-2,5-Dicarboxylic Acid. *ACS Catal.* **2017**, *7*, 6619–6634.
294. Pisal, D. S.; Yadav, D. G. Single-Step Hydrogenolysis of Furfural to 1,2-Pentanediol Using a Bifunctional Rh/OMS-2 Catalyst. *ACS Omega* **2019**, *4*, 1201–1214.
295. Koley, P.; Chandra Shit, S.; Joseph, B.; Pollastri, S.; Sabri, Y. M.; Mayes, A. L. M.; Nakkal, L.; Tardio, J.; Mondal, J. Leveraging Cu/CuFe<sub>2</sub>O<sub>4</sub>-Catalyzed Biomass-Derived Furfural Hydrodeoxygenation: A Nanoscale Metal–Organic-Framework Template Is the Prime Key. *ACS Appl. Mater. Interfaces* **2020**, *12*, 21682–21700.
296. Cho, H. J.; Kim, D.; Xu, B. Selectivity Control in Tandem Catalytic Furfural Upgrading on Zeolite-Encapsulated Pt Nanoparticles through Site and Solvent Engineering. *ACS Catal.* **2020**, *10*, 4770–4779.
297. Wang, X.; Liang, X.; Li, J.; Li, Q. Catalytic Hydrogenolysis of Biomass-Derived 5-Hydroxymethylfurfural to Biofuel 2,5-Dimethylfuran. *Appl. Catal. A Gen.* **2019**, *576*, 85–95.
298. Jae, J.; Zheng, W.; Lobo, R. F.; Vlachos, D. G. Production of Dimethylfuran From Hydroxymethylfurfural Through Catalytic Transfer Hydrogenation With Ruthenium Supported on Carbon. *ChemSusChem* **2013**, *6*, 1158–1162.

299. Nagpure, A. S.; Venugopal, A. K.; Lucas, N.; Manikandan, M.; Thirumalaiswamy, R.; Chilukuri, S. Renewable Fuels From Biomass-Derived Compounds: Ru-Containing Hydrotalcites as Catalysts for Conversion of HMF to 2,5-Dimethylfuran. *Catal. Sci. Technol.* **2015**, *5*, 1463–1472.
300. Li, Q.; Man, P.; Yuan, L.; Zhang, P.; Li, P.; Ai, S. Ruthenium Supported on CoFe Layered Double Oxide for Selective Hydrogenation of 5-Hydroxymethylfurfural. *Mol. Catal.* **2017**, *431*, 32–38.
301. Luo, J.; Lee, J. D.; Yun, H.; Wang, C.; Monai, M.; Murray, C. B.; Fornasiero, P.; Gorte, R. J. Base Metal-Pt Alloys: A General Route to High Selectivity and Stability in the Production of Biofuels From HMF. *Appl. Catal. B Environ.* **2016**, *199*, 439–446.
302. Liu, L.; Gao, F.; Concepción, P.; Corma, A. A New Strategy to Transform Mono and Bimetallic Non-Noble Metal Nanoparticles into Highly Active and Chemoselective Hydrogenation Catalysts. *J. Catal.* **2017**, *350*, 218–225.
303. Hansen, T. S.; Barta, K.; Anastas, P. T.; Ford, P. C.; Riisager, A. One-Pot Reduction of 5-Hydroxymethylfurfural Via Hydrogen Transfer From Supercritical Methanol. *Green Chem.* **2012**, *14*, 2457–2461.
304. Bottari, G.; Kumalaputri, A. J.; Krawczyk, K. K.; Feringa, B. L.; Heeres, H. J.; Barta, K. Copper–Zinc Alloy Nanopowder: A Robust Precious-Metal-Free Catalyst for the Conversion of 5-Hydroxymethylfurfural. *ChemSusChem* **2015**, *8*, 1323–1327.
305. Li, J.; Liu, J.; Liu, H.; Xu, G.; Zhang, J.; Liu, J.; Zhou, G.; Li, Q.; Xu, Z.; Fu, Y. Selective Hydrodeoxygenation of 5-Hydroxymethylfurfural to 2,5-Dimethylfuran Over Heterogeneous Iron Catalysts. *ChemSusChem* **2017**, *10*, 1436–1447.
306. Zhang, Z.; Wang, C.; Gou, X.; Chen, H.; Chen, K.; Lu, X.; Ouyang, P.; Fu, J. Catalytic In-Situ Hydrogenation of 5-Hydroxymethylfurfural to 2,5-Dimethylfuran Over Cu-Based Catalysts With Methanol as a Hydrogen Donor. *Appl. Catal. A Gen.* **2019**, *570*, 245–250.
307. Gao, Z.; Li, C.; Fan, G.; Yang, L.; Li, F. Nitrogen-Doped Carbon-Decorated Copper Catalyst for Highly Efficient Transfer Hydrogenolysis of 5-Hydroxymethylfurfural to Convertibly Produce 2,5-Dimethylfuran or 2,5-Dimethyltetrahydrofuran. *Appl. Catal. B Environ.* **2018**, *226*, 523–533.
308. Chimentão, R. J.; Oliva, H.; Belmar, J.; Morales, K.; Mäki-Arvela, P.; Wärnåck, J.; Murzin, D. Y.; Fierrod, J. L. G.; Llorca, J.; Ruiz, D. Selective Hydrodeoxygenation of Biomass Derived 5-Hydroxymethylfurfural over Silica Supported Iridium Catalysts. *Appl. Catal. B Environ.* **2019**, *241*, 270–283.
309. Yang, P.; Cui, Q.; Zu, Y.; Liu, X.; Lu, G.; Wang, Y. Catalytic Production of 2,5-Dimethylfuran from 5-Hydroxymethylfurfural over Ni/Co<sub>3</sub>O<sub>4</sub> Catalyst. *Catal. Commun.* **2015**, *66*, 55–59.
310. An, Z.; Wang, W.; Dong, S.; He, J. Well-Distributed Cobalt-Based Catalysts Derived from Layered Double Hydroxides for Efficient Selective Hydrogenation of 5-Hydroxymethylfurfural to 2,5-Methylfuran. *Catal. Today* **2019**, *319*, 128–138.
311. Raut, A. B.; Nanda, B.; Parida, K. M.; Bhanage, B. M. Hydrogenolysis of Biomass-Derived 5-Hydroxymethylfurfural to Produce 2,5-Dimethylfuran Over Ru-ZrO<sub>2</sub>-MCM-41 Catalyst. *ChemistrySelect* **2019**, *4*, 6080–6089.
312. Sun, Y.; Xiong, C.; Liu, Q.; Zhang, J.; Tang, X.; Zeng, X.; Liu, S.; Lin, L. Catalytic Transfer Hydrogenolysis/Hydrogenation of Biomass-Derived 5-Formyloxymethylfurfural to 2, 5-Dimethylfuran Over Ni–Cu Bimetallic Catalyst With Formic Acid as a Hydrogen Donor. *Ind. Eng. Chem. Res.* **2019**, *58*, 5414–5422.
313. Guo, D.; Liu, X.; Cheng, F.; Zhao, W.; Wen, S.; Xiang, Y.; Xu, Q.; Yu, N.; Yin, D. Selective Hydrogenolysis of 5-Hydroxymethylfurfural to Produce Biofuel 2, 5-Dimethylfuran Over Ni/ZSM-5 Catalysts. *Fuel* **2020**, *274*, 117853.

222 Heterogeneous catalysis in sustainable synthesis

314. Liu, H.; Huang, Z.; Zhao, F.; Cui, F.; Li, X.; Xia, C.; Chen, J. Efficient Hydrogenolysis of Biomass-Derived Furfuryl Alcohol to 1,2- and 1,5-Pentanediols Over a Non-Precious Cu-Mg<sub>3</sub>AlO<sub>4.5</sub> Bifunctional Catalyst. *Catal. Sci. Technol.* **2016**, *6*, 668–671.
315. Tong, T.; Xia, Q.; Liu, X.; Wang, Y. Direct Hydrogenolysis of Biomass-Derived Furans over Pt/CeO<sub>2</sub> Catalyst with High Activity and Stability. *Catal. Commun.* **2017**, *101*, 129–133.
316. Gao, F.; Liu, H.; Hu, X.; Chen, J.; Huang, Z.; Xia, C. Selective Hydrogenolysis of Furfuryl Alcohol to 1,5- and 1,2-Pentanediol over Cu-LaCoO<sub>3</sub> Catalysts with Balanced Cu<sup>0</sup>-CoO Sites. *Chin. J. Catal.* **2018**, *39*, 1711–1723.
317. Shao, Y.; Wang, J.; Du, H.; Sun, K.; Zhang, Z.; Zhang, L.; Li, Q.; Zhang, S.; Liu, Q.; Hu, X. Importance of Magnesium in Cu-Based Catalysts for Selective Conversion of Biomass-Derived Furan Compounds to Diols. *ACS Sustain. Chem. Eng.* **2020**, *8*, 5217–5228.
318. Du, X.-L.; Bi, Q.-Y.; Liu, Y.-M.; Cao, Y.; He, H.-Y.; Fan, K.-N. Tunable Copper-Catalyzed Chemoselective Hydrogenolysis of Biomass-Derived  $\gamma$ -Valerolactone into 1,4-Pentanediol or 2-Methyltetrahydrofuran. *Green Chem.* **2012**, *14*, 935–939.
319. Guan, J.; Peng, G.; Cao, Q.; Mu, X. Role of MoO<sub>3</sub> on a Rhodium Catalyst in the Selective Hydrogenolysis of Biomass-Derived Tetrahydrofurfuryl Alcohol into 1,5-Pentanediol. *J. Phys. Chem. C* **2014**, *118*, 25555–25566.
320. Chia, M.; Pagan-Torres, Y. J.; Hibbitts, D.; Tan, Q.; Pham, H. N.; Datye, A. K.; Neurock, M.; Davis, R. J.; Dumesic, J. A. Selective Hydrogenolysis of Polyols and Cyclic Ethers over Bifunctional Surface Sites on Rhodium-Rhenium Catalysts. *J. Am. Chem. Soc.* **2011**, *133*, 12675–12689.
321. Bababrik, R.; Santharaj, D.; Resasco, D. E.; Wang, B. A Comparative Study of Thermal- and Electrocatalytic Conversion of Furfural: Methylfuran as a Primary and Major Product. *J. Appl. Electrochem.* **2021**, *15*, 19–26.
322. Huang, L.; Zhu, Y.; Zheng, H.; Dua, M.; Li, Y. Vapor-Phase Hydrogenolysis of Biomass-Derived Lactate to 1,2-Propanediol over Supported Metal Catalysts. *Appl. Catal. A Gen.* **2008**, *349*, 204–211.
323. Gabrysch, T.; Muhler, M.; Peng, B. The Kinetics of Glycerol Hydrodeoxygenation to 1,2-Propanediol over Cu/ZrO<sub>2</sub> in the Aqueous Phase. *Appl. Catal. A Gen.* **2019**, *576*, 47–53.
324. Wang, S.; Liu, H. Selective Hydrogenolysis of Glycerol to Propylene Glycol on Cu-ZnO Catalysts. *Catal. Lett.* **2007**, *117*, 62–67.
325. Pandhare, N. N.; Pudi, S. M.; Biswas, P.; Sinha, S. Selective Hydrogenolysis of Glycerol to 1,2-Propanediol over Highly Active and Stable Cu/MgO Catalyst in the Vapor Phase. *Org. Process. Res. Dev.* **2016**, *20*, 1059–1067.
326. Yuan, Z.; Wu, P.; Gao, J.; Lu, X.; Hou, Z.; Zheng, X. Pt/Solid-Base: A Predominant Catalyst for Glycerol Hydrogenolysis in a Base-Free Aqueous Solution. *Catal. Lett.* **2009**, *130*, 261–265.
327. Kim, N. D.; Park, J. R.; Park, D. S.; Kwak, B. K.; Yi, J. Promoter Effect of Pd in CuCr<sub>2</sub>O<sub>4</sub> Catalysts on the Hydrogenolysis of Glycerol to 1,2-Propanediol. *Green Chem.* **2012**, *14*, 2638–2646.
328. Kumar, P.; Shah, A. K.; Lee, J.-H.; Park, Y. H.; Stangar, U. L. Selective Hydrogenolysis of Glycerol Over Bifunctional Copper–Magnesium-Supported Catalysts for Propanediol Synthesis. *Ind. Eng. Chem. Res.* **2020**, *59*, 6506–6516.
329. Shan, J.; Liu, H.; Lu, K.; Zhu, S.; Li, J.; Wang, J.; Fan, W. Identification of the Dehydration Active Sites in Glycerol Hydrogenolysis to 1,2-Propanediol Over Cu/SiO<sub>2</sub> Catalysts. *J. Catal.* **2020**, *383*, 13–23.
330. Raso, R.; Garcia, L.; Ruiz, J.; Oliva, M.; Arauzo, J. Aqueous Phase Hydrogenolysis of Glycerol over Ni/Al-Fe Catalysts without External Hydrogen Addition. *Appl. Catal. B Environ.* **2021**, *283*, 119598.

331. García-Fernández, S.; Gandarias, I.; Requies, J.; Soulimani, F.; Arias, P. L.; Weckhuyzen, B. M. The Role of Tungsten Oxide in the Selective Hydrogenolysis of Glycerol to 1,3-Propanediol Over Pt/WO<sub>x</sub>/Al<sub>2</sub>O<sub>3</sub>. *Appl. Catal. B Environ.* **2017**, *204*, 260–272.
332. Priya, S. S.; Kumar, V. P.; Kantam, M. L.; Bhargava, S. K.; Chary, K. V. R. Vapour-Phase Hydrogenolysis of Glycerol to 1,3-Propanediol Over Supported Pt Catalysts: The Effect of Supports on the Catalytic Functionalities. *Catal. Lett.* **2014**, *144*, 129–2143.
333. Zhu, S.; Gao, X.; Zhu, Y.; Li, Y. Tailored Mesoporous Copper/Ceria Catalysts for the Selective Hydrogenolysis of Biomass-Derived Glycerol and Sugar Alcohols. *Green Chem.* **2016**, *18*, 782–791.
334. Niu, Y.; Zhao, B.; Liang, Y.; Liu, L.; Dong, J. Promoting Role of Oxygen Deficiency on a WO<sub>3</sub>-Supported Pt Catalyst for Glycerol Hydrogenolysis to 1,3-Propanediol. *Ind. Eng. Chem. Res.* **2020**, *59*, 7389–7397.
335. Zhu, S.; Zhu, Y.; Hao, S.; Zheng, H.; Mo, T.; Li, H. One-Step Hydrogenolysis of Glycerol to Biopropanols Over Pt–H<sub>4</sub>SiW<sub>12</sub>O<sub>40</sub>/ZrO<sub>2</sub> Catalysts. *Green Chem.* **2012**, *14*, 2607–2616.
336. Wang, M.; Yang, H.; Xie, Y.; Wu, X.; Chen, C.; Ma, W.; Dong, Q.; Hou, Z. Catalytic Transformation of Glycerol to 1-Propanol by Combining Zirconium Phosphate and Supported Ru Catalysts. *RSC Adv.* **2016**, *6*, 29769–29778.
337. Chaminand, J.; Djakovitch, L.; Gallezot, P.; Marion, P.; Pinel, C.; Rosier, C. Glycerol Hydrogenolysis on Heterogeneous Catalysts. *Green Chem.* **2004**, *6*, 359–361.
338. Huang, Z.; Chen, J.; Jia, Y.; Liu, H.; Xia, C.; Liu, H. Selective Hydrogenolysis of Xylitol to Ethylene Glycol and Propylene Glycol Over Copper Catalysts. *Appl. Catal. B Environ.* **2014**, *147*, 377–386.
339. Liu, H.; Huang, Z.; Kang, H.; Li, X.; Xia, C.; Chen, J.; Liu, H. Efficient Bimetallic NiCu-SiO<sub>2</sub> Catalysts for Selective Hydrogenolysis of Xylitol to Ethylene Glycol and Propylene Glycol. *Appl. Catal. B Environ.* **2018**, *220*, 251–263.
340. Sun, J.; Liu, H. Selective Hydrogenolysis of Biomass-Derived Xylitol to Ethylene Glycol and Propylene Glycol on Ni/C and Basic Oxide-Promoted Ni/C Catalysts. *Catal. Today* **2014**, *234*, 75–82.
341. Liu, H.; Huang, Z.; Xia, C.; Jia, Y.; Chen, J.; Liu, H. Selective Hydrogenolysis of Xylitol to Ethylene Glycol and Propylene Glycol over Silica Dispersed Copper Catalysts Prepared by a Precipitation–Gel Method. *ChemCatChem* **2014**, *6*, 2918–2928.
342. Sun, J.; Liu, H. Selective Hydrogenolysis of Biomass-Derived Xylitol to Ethylene Glycol and Propylene Glycol on Supported Ru Catalysts. *Green Chem.* **2011**, *13*, 135–142.
343. Li, S.; Zan, Y.; Sun, Y.; Tan, Z.; Miao, G.; Kong, L. Z.; Sun, Y. Efficient One-Pot Hydrogenolysis of Biomass-Derived Xylitol into Ethylene Glycol and 1,2-Propylene Glycol Over Cu–Ni–ZrO<sub>2</sub> Catalyst without Solid Bases. *J. Energy Chem.* **2019**, *28*, 101–106.
344. Liao, F.; Lo, T. W. B.; Sexton, D.; Qu, J.; Wu, C.-T.; Tsang, S. C. E. PdFe Nanoparticles as Selective Catalysts for C–C Cleavage in Hydrogenolysis of Vicinal Diol Units in Biomass-Derived Chemicals. *Catal. Sci. Technol.* **2015**, *5*, 887–896.
345. Chen, X.; Wang, X.; Yao, S.; Mu, X. Hydrogenolysis of Biomass-Derived Sorbitol to Glycols and Glycerol over Ni-MgO Catalysts. *Catal. Commun.* **2013**, *39*, 86–89.
346. Yin, B.; Jin, X.; Zhang, G.; Yan, H.; Zhang, W.; Liu, X.; Liu, M.; Yang, C.; Shen, J. Catalytic Transfer Hydrogenolysis of Bio-Polyols to Renewable Chemicals Over Bimetallic PtPd/C Catalysts: Size-Dependent Activity and Selectivity. *ACS Sustain. Chem. Eng.* **2020**, *8*, 5305–5316.
347. Hausoul, P. J. C.; Negahdar, L.; Schute, K.; Palkovits, R. Unravelling the Ru-Catalyzed Hydrogenolysis of Biomass-Based Polyols Under Neutral and Acidic Conditions. *ChemSusChem* **2015**, *8*, 3323–3330.

224 Heterogeneous catalysis in sustainable synthesis

348. Lv, M.; Xin, Q.; Yin, D.; Jia, Z.; Yu, C.; Wang, T.; Yu, S.; Liu, S.; Li, L.; Liu, Y. Magnetically Recoverable Bifunctional Catalysts for the Conversion of Cellulose to 1,2-Propylene Glycol. *ACS Sustain. Chem. Eng.* **2020**, *8*, 3617–3625.
349. Liu, L.; Asano, T.; Nakagawa, Y.; Tamura, M.; Tomishige, K. One-Pot Synthesis of 1,3-Butanediol by 1,4-Anhydroerythritol Hydrogenolysis over a Tungsten-Modified Platinum on Silica Catalyst. *Green Chem.* **2020**, *22*, 2375–2380.
350. Lin, B.; Li, R.; Shu, R.; Wang, C.; Cheng, Z.; Chen, Y. Hydrogenolysis and Hydrodeoxygenation of Lignin in a Two-Step Process to Produce Hydrocarbons and Alkylphenols. *J. Energy Inst.* **2020**, *93*, 784–791.
351. Si, X.-G.; Zhao, Y.-P.; Song, Q.-L.; Cao, J.-P.; Wang, R.-Y.; Wei, X.-Y. Hydrogenolysis of Lignin-Derived Aryl Ethers to Monomers Over a MOF-Derived Ni/N-C Catalyst. *React. Chem. Eng.* **2020**, *5*, 885–895.
352. Cheng, C.; Li, P.; Yu, W.; Shen, D.; Gu, S. Catalytic Hydrogenolysis of Lignin in Ethanol/Isopropanol Over an Activated Carbon Supported Nickel-Copper Catalyst. *Bioresour. Technol.* **2021**, *319*, 124238.
353. Cao, J.-P.; Xie, T.; Zhao, X.-Y.; Zhu, C.; Jiang, W.; Zhao, M.; Zhao, Y.-P.; Wei, X.-Y. Selective Cleavage of Ether C-O Bond in Lignin-Derived Compounds Over Ru System under Different H-Sources. *Fuel* **2021**, *284*, 119027.
354. Zhu, C.; Cao, J.-P.; Feng, X.-B.; Zhao, X.-Y.; Yang, Z.; Li, J.; Zhao, M.; Zhao, Y. P.; Bai, H. C. Theoretical Insight into the Hydrogenolysis Mechanism of Lignin Dimer Compounds Based on Experiments. *Renew. Energy* **2021**, *163*, 1831–1837.
355. Wang, M.; Liu, M.; Lu, J.; Wang, F. Photo Splitting of Bio-Polyols and Sugars to Methanol and Syngas. *Nat. Commun.* **2020**, *11*, 1083.
356. Carlier, S.; Gripekoven, J.; Philippo, M.; Hermans, S. Ru on N-Doped Carbon Supports for the Direct Hydrogenation of Cellobiose into Sorbitol. *Appl. Catal. B Environ.* **2021**, *282*, 119515.
357. Yan, P.; Mensah, J.; Drewery, M.; Kennedy, E.; Maschmeyer, T.; Stockenhuber, M. Role of Metal Support During Ru-Catalysed Hydrodeoxygenation of Biocrude Oil. *Appl. Catal. B Environ.* **2021**, *281*, 119470.
358. Kim, H.; Lee, S.; Won, W. System-Level Analyses for the Production of 1,6-Hexanediol From Cellulose. *Energy* **2021**, *214*, 118974.
359. Kokel, A.; Schäfer, C.; Török, B. Organic Synthesis Using Environmentally Benign Acid Catalysis. *Curr. Org. Synth.* **2019**, *16*, 615–649.
360. Ooi, X. Y.; Gao, W.; Ong, H. C.; Leeb, H. V.; Juan, J. C.; Chen, W. H.; Lee, K. T. Overview on Catalytic Deoxygenation for Biofuel Synthesis Using Metal Oxide Supported Catalysts. *Renew. Sust. Energy. Rev.* **2019**, *112*, 834–852.
361. Zhao, H. Y.; Li, D.; Bui, P.; Oyama, S. T. Hydrodeoxygenation of Guaiacol as Model Compound for Pyrolysis Oil on Transition Metal Phosphide Hydroprocessing Catalysts. *Appl. Catal. A Gen.* **2011**, *391*, 305–310.
362. Bui, V. N.; Laurenti, D.; Delichère, P.; Geantet, C. Hydrodeoxygenation of Guaiacol Part II: Support Effect for CoMoS Catalysts on HDO Activity and Selectivity. *Appl. Catal. B Environ.* **2011**, *101*, 246–255.
363. Yang, W.; Li, X.; Du, X.; Deng, Y.; Dai, H. Effective Low-Temperature Hydrogenolysis of Lignin Using Carbon-Supported Ruthenium and Formic Acid as Reducing Agent. *Catal. Commun.* **2019**, *126*, 30–34.
364. Bulut, S.; Siankevich, S.; van Muyden, A. P.; Alexander, D. T. L.; Savoglidis, G.; Zhang, J.; Hatzimanikatis, V.; Yan, N.; Dyson, P. J. Efficient Cleavage of Aryl Ether C-O Linkages by Rh-Ni and Ru-Ni Nanoscale Catalysts Operating in Water. *Chem. Sci.* **2018**, *9*, 5530–5535.

365. Sankaranarayanan, T. M.; Kreider, M.; Berenguer, A.; Gutiérrez-Rubio, S.; Moreno, I.; Pizarro, P.; Coronado, J. M.; Serrano, D. P. Cross-Reactivity of Guaiacol and Propionic Acid Blends During Hydrodeoxygenation Over Ni-Supported Catalysts. *Fuel* **2018**, *214*, 187–195.
366. Madsen, A. T.; Ahmed, E. H.; Christensen, C. H.; Fehrmann, R.; Riisager, A. Hydrodeoxygenation of Waste Fat for Diesel Production: Study on Model Feed With Pt/Alumina Catalyst. *Fuel* **2011**, *90*, 3433–3438.



## Chapter 3.3

# Heterogeneous catalytic oxidations

### 3.3.1 Introduction

The oxidation of organic molecules is undoubtedly one of the most important reactions in the area of synthetic chemistry. The term “oxidation” was coined by de Lavoisier in the 18th century for the formation of new compounds by the reaction with molecular oxygen. Both the definition of oxidation (now based on the movement of electrons) and the applied oxidizing agents have evolved since these early beginnings keeping pace with the need for new synthetic methods. There is probably no total synthesis of a chemically or biologically interesting organic molecule that does not contain at least one oxidation reaction. Oxidation allows for the introduction of (new) functional groups in a molecule, that is, by generating double bonds or converting C–H bonds into C–X bonds (C–H functionalization) thus creating new reactivity points needed for the architecture of complex molecules. Oxidation also allows for the interconversion of functional groups with different reactivities (i.e., alcohols and aldehydes) therefore giving the possibility to first mask the reactivity of a functional group to expose it at a later point. The importance of oxidation in total synthesis and the concept of late stage-oxidation have been reviewed previously.<sup>1–3</sup> In order for oxidation reactions to be useful in the concept of chemical synthesis the methods applied do not only need to be able to achieve the desired transformation, but they also need to accomplish this selectively without any undesirable transformation on other parts of the molecule.

Given the importance and the long history of oxidation reactions in organic chemistry it is no surprise that there are plenty of methodologies available in the literature for a broad variety of transformations and research is still being very active in the field.

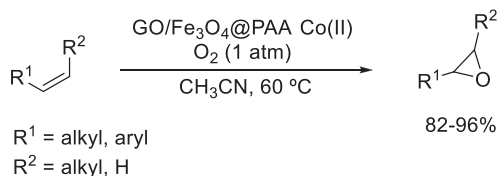
While the selectivity of oxidation reactions has been in the forefront of research in the synthesis field for over a century, the increasing societal and political pressure to use more environmentally friendly methods has led to an increased interest in the development of reactions following the principles of green chemistry.<sup>4,5</sup> In this chapter, the application of heterogeneous catalytic systems in oxidation reactions will be reviewed, with a focus on environmentally benign systems.

The presented selection of examples aims to represent a broad area of various transformations, focusing on examples from the recent (2000–21) literature.

### 3.3.2 Epoxidation reactions

Epoxides are of great importance in the chemical industry as they are versatile key intermediates for the production of fine chemicals including pharmaceuticals, cosmetics, plasticizer, etc.<sup>6,7</sup> The traditional ways to synthesize epoxides include the use of stoichiometric oxidizing agents such as organic peracids<sup>8</sup> or potassium monoperoxysulfate.<sup>9</sup> Although effective, these methods do not comply with the principles of green chemistry particularly due to the extensive amount of waste generated by the spent reagent. Therefore, the exploration of heterogeneous catalytic systems using environmentally benign terminal oxidants is of high interest.<sup>10</sup> A review on the use of heterogeneous catalytic systems for asymmetric epoxidation and dihydroxylation reactions has been published by Salvadori et al.<sup>11</sup> The examples given in this chapter will focus on methods complying with the principles of green chemistry.

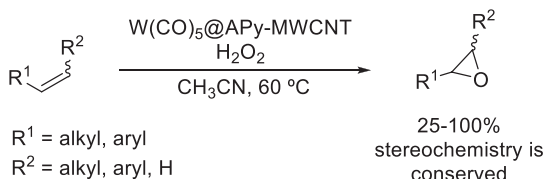
Kazemnejadi et al. developed a cobalt catalyst that was immobilized on magnetite-graphene oxide via complexation by a polyamino acid (GO/Fe<sub>3</sub>O<sub>4</sub>@PAA Co(II)).<sup>12</sup> A variety of terminal and internal alkenes were transformed with high conversions and selectivities for the corresponding epoxide (Scheme 1). A low catalyst loading of 0.2% and the use of molecular oxygen are the main green features of the reaction. The authors showed that the recycling of the catalyst is possible in six consecutive runs with only a minor decrease in activity. The reaction could be scaled up to a 700 mmol scale using styrene as a substrate with no loss in selectivity and only a small decrease in conversion. The disadvantage of the presented method is the need for acetonitrile as the solvent for the reaction.



**SCHEME 1** Epoxidation of alkenes using a magnetite-graphene oxide supported Co catalyst and O<sub>2</sub> as the oxidant.

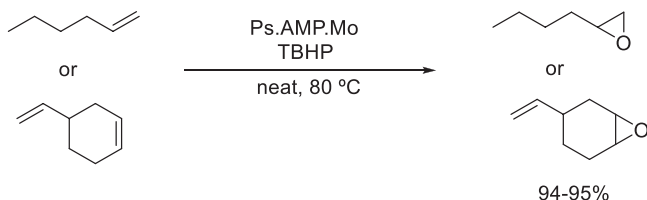
The group of Moghadam used multiwalled carbon nanotubes modified with 4-aminopyridine to anchor a tungsten catalyst and used the heterogenized system (W(CO)<sub>5</sub>@APy-MWCNT) for the epoxidation of alkenes.<sup>13</sup> The reaction performs well for different alkenes, typically delivering the epoxide in high yields and selectivities (Scheme 2). The stereochemistry of the alkene is conserved in the epoxide. The environmentally benign hydrogen peroxide is used

as an oxidant for the transformation and the catalyst can be reused eight times without decrease in product yield. Additionally, the authors showed that metal leaching is not a significant problem when reusing the catalyst. Drawback is that acetonitrile was the only solvent tested that gave the epoxidation product in high yields.



**SCHEME 2** Epoxidation of alkenes using a heterogeneous tungsten catalyst and  $\text{H}_2\text{O}_2$ .

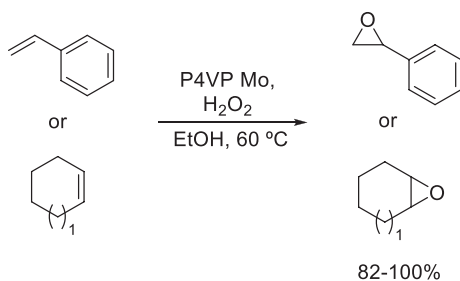
Using *tert*-butyl hydroperoxide (TBHP) as the final oxidant, Mohammed et al. developed a polymer-bound heterogeneous Mo(VI) catalyst (Ps.AMP.Mo) for the epoxidation of alkenes (Scheme 3).<sup>14</sup> Although only a limited number of substrates were examined, the authors revealed that the prediction of optimal reaction parameters was possible using an artificial neuronal network, thus opening the possibility to perform reaction optimization *in silico* instead of doing time consuming and expensive experimental studies in the laboratory. The products were obtained in excellent yields under optimized conditions. When investigating the reusability of the catalyst it was found that although possible, a relatively high drop in yield was observed even after the second run.



**SCHEME 3** Polymer-bound molybdenum-catalyzed epoxidation of alkenes.

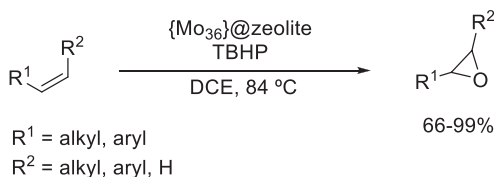
A similar system was developed by Cao and co-workers.<sup>15</sup> Using poly(4-vinylpyridine) microspheres as the support material for molybdenum (P4VP Mo) the authors could show that the oxidation of alkenes to the epoxide is possible with hydrogen peroxide as an oxidant in high yields (Scheme 4). Ethanol could be used as environmentally friendly solvent for the reaction and the catalyst was reused five times without showing a loss in activity or selectivity. A recent work focusing on the vapor phase epoxidation of cyclohexene as a test reaction applied an iron containing metal-organic framework-based catalyst.<sup>16</sup>

230 Heterogeneous catalysis in sustainable synthesis



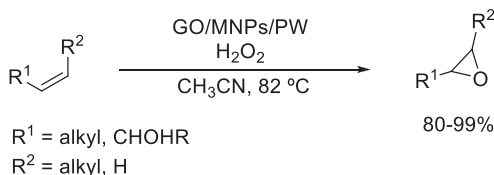
**SCHEME 4** Oxidation of alkenes by a polymer-supported molybdenum catalyst.

Polyoxomolybdates have also successfully been anchored to a zeolite support and subsequently used as heterogeneous catalyst ( $\{\text{Mo}_{36}\}@zeolite$ ) for the epoxidation of alkenes.<sup>17</sup> TBHP was used as the terminal oxidant giving the desired products in mostly high yields (Scheme 5). Lower yields were obtained for sterically hindered substrates (e.g.,  $\alpha$ -methylstyrene). Although very small loading of the catalyst is required and the catalyst is reusable seven times with only a small drop in yield, the drawback of the presented system is the need for dichloroethane (DCE) as a solvent.



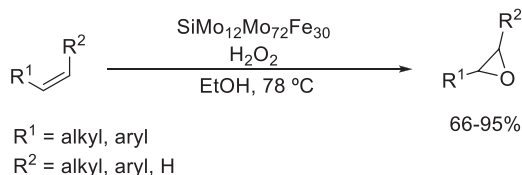
**SCHEME 5** Epoxidation of alkenes using a zeolite anchored polyoxomolybdate catalyst.

Changing from molybdenum to tungsten, Masteri-Farahani and Modarres developed a peroxopolyoxotungstate catalyst immobilized on the surface of clicked magnetite-graphene oxide nanocomposite (GO/MNPs/PW).<sup>18</sup> Using hydrogen peroxide as the oxidant, several alkenes and allylic alcohols were converted to the corresponding epoxide in high yields and excellent selectivities (Scheme 6). The catalyst was found to be recyclable five times without significant decrease in yield and no metal leaching was observed.



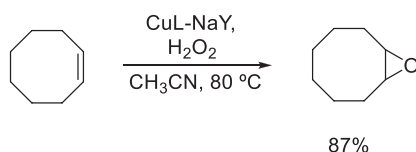
**SCHEME 6** The epoxidation of alkenes catalyzed by peroxopolytungstate containing magnetic nanoparticles.

Taghiyar and Yadollahi found that molybdenum-containing Keggin structures encapsulated in keplerate polyoxometalate ( $\text{SiMo}_{12}\text{Mo}_{72}\text{Fe}_{30}$ ) can be efficiently used for the epoxidation of different alkenes in good to high yields and selectivities (Scheme 7).<sup>19</sup> Ethanol was found to be the best solvent for the transformation and hydrogen peroxide was used as a green oxidant. The catalyst could be recovered and reused eight times with a small loss in activity.



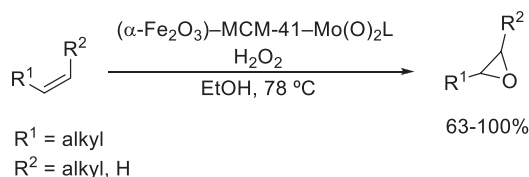
**SCHEME 7** Epoxidation of alkenes using a polyoxometalate encapsulated Keggin structure.

Rayati et al. used Na-Y zeolite to immobilize a copper pyrrole-phenylenediamine complex ( $\text{CuL-NaY}$ ) and investigated its activity in the epoxidation of cyclic alkenes.<sup>20</sup> Cyclohexene and cyclooctene were both oxidized, the allylic alcohol being the major product with cyclohexene. Interestingly, cyclooctene showed a different behavior and was converted into the corresponding epoxide in good yields with only a small amount of byproducts formed (Scheme 8). Hydrogen peroxide was used as the terminal oxidant, giving better results than TBHP. Acetonitrile proved to be the best solvent for the reaction. The recyclability of the catalyst was not tested.



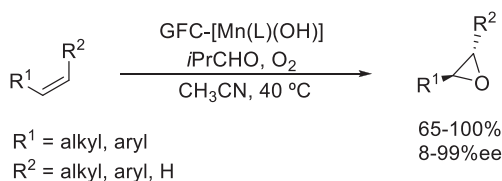
**SCHEME 8** Epoxidation of cyclooctene catalyzed by a zeolite-supported Cu complex.

Later, the same group developed a more versatile catalyst based on a molybdenum Schiff base complex bound to MCM-41 ( $(\alpha\text{-Fe}_2\text{O}_3)\text{-MCM-41-Mo(O)}_2\text{L}$ ).<sup>21</sup> A series of substrates was successfully transformed into the epoxide in good to excellent yields and excellent selectivities for the epoxide (Scheme 9). Ethanol as an environmentally friendly solvent could be employed and the catalyst was recyclable five times without significant drop in yield.



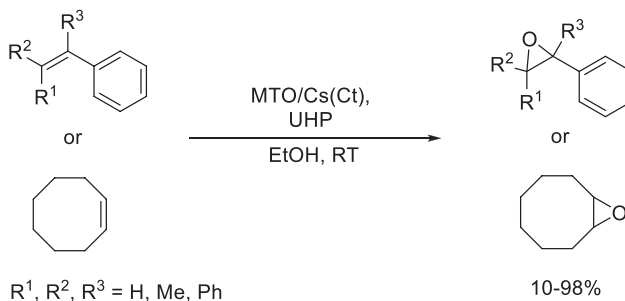
**SCHEME 9** Epoxidation of alkenes with hydrogen peroxide using magnetite-MCM-41 supported molybdenum complex as the catalyst.

The group of Hosseini-Monfared developed an epoxidation catalyst using manganese as the active metal. The manganese complex containing a chiral indanol ligand was anchored to a graphene oxide/Fe<sub>3</sub>O<sub>4</sub> hybrid support via an organic linker (GFC-[Mn(L)(OH)]).<sup>22</sup> Isobutyraldehyde was employed as a co-catalyst in acetonitrile as the solvent. Molecular oxygen was used as the final oxidant not generating any additional byproducts. Due to the chiral nature of the ligand employed, the epoxides were obtained with high enantiomeric excess with the exception of sterically hindered substrates (Scheme 10). Due to its magnetic properties, the catalyst could easily be recycled. Only a small drop in yield was observed while the enantiomeric excess seemed to improve upon reuse.



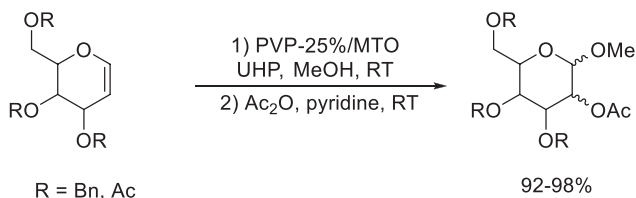
**SCHEME 10** Enantioselective epoxidation of alkenes using a chiral manganese complex immobilized on graphene oxide/Fe<sub>3</sub>O<sub>4</sub> hybrid support.

The group of Saladino synthesized several catalysts based on methyltrioxorhenium anchored to a modified chitosan matrix and used it for the epoxidation of substituted styrenes and cyclooctene.<sup>23</sup> The product yields obtained differ with the substrate and catalyst used but can reach excellent values (Scheme 11). Ethanol was used as the solvent and urea hydrogen peroxide (UHP) adduct was the terminal oxidant. While substituents in the *beta*-position are well tolerated, placing a methyl group in the *alpha*-position leads to an almost complete drop in conversion. Recycling of the catalyst was attempted and although the selectivity of the catalyst remained high, a notable decrease in yield was observed in the second run already.



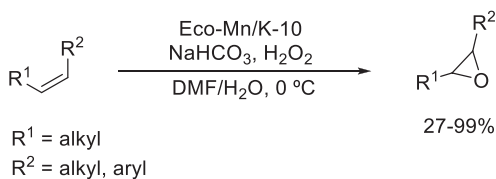
**SCHEME 11** Epoxidation of various alkenes using a chitosan matrix-supported methyltrioxorhenium catalysts.

The same group also performed the tandem epoxidation-methanolysis of glycols using a methyltrioxorhenium bound to a polymer matrix.<sup>24</sup> As for the chitosan-based catalysts UHP was used as the oxidant and the catalyst could be recovered and reused (Scheme 12). The stereoselectivity observed for the epoxidation varies with the exact catalyst-substrate combination.



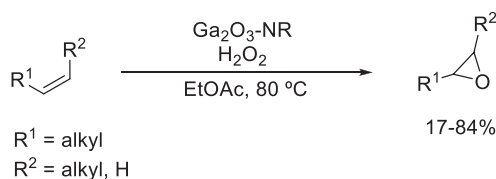
**SCHEME 12** Epoxidation-methanolysis of glycols catalyzed by methyltrioxorhenium bound to a polymer matrix.

Grison et al. generated an efficient epoxidation catalyst using the biomass from a Mn-hyperaccumulating plant.<sup>25</sup> The Eco-Mn catalyst was prepared from the plant biomass and incorporated into montmorillonite K-10 as the support material. The such prepared heterogeneous system (Eco-Mn/K-10) was found to be active in the epoxidation of various alkenes, including sterically demanding natural products (Scheme 13). The yields were high for most substrates with excellent selectivities observed. Hydrogen peroxide was applied as the oxidant and a DMF/water mixture was used as the solvent for the transformation. Catalyst recycling was reported to be possible four times without loss in catalytic activity.



**SCHEME 13** Biomass sourced manganese as an epoxidation catalyst.

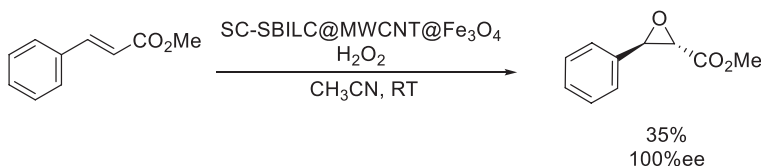
The group of Pescarmona showed that gallium oxide nanorods of small dimensions (Ga<sub>2</sub>O<sub>3</sub>-NR) can be used for the epoxidation of alkenes under transition metal-free conditions.<sup>26</sup> The method uses hydrogen peroxide as the oxidant and ethyl acetate as the solvent. Although the selectivity for the epoxide is high in all cases, the yield seems to be very substrate dependent (Scheme 14). The reaction was found to be truly heterogeneous as no leaching of the active species into solution was observed during the reaction. The catalyst could be recycled five times with only a slight decrease in its activity.



**SCHEME 14** Epoxidation of *cis*-alkenes using gallium oxide nanorods as a catalyst.

In a follow-up study the same group reported that Ga-MCM-41 nanoparticles were also able to catalyze the epoxidation of cyclooctene using hydrogen peroxide as the oxidant.<sup>27</sup> The desired product was obtained in 91% yield with exclusive selectivity. Unfortunately, a mixture of toluene with ethyl acetate was used as the solvent, which decreases the green value of the process.

The heterogenization of Shi's epoxidation catalyst was achieved by the groups of Parvulescu and Coman.<sup>28</sup> A slight modification of the original Shi catalyst allowed its immobilization to a multiwalled carbon nanotube/ $\text{Fe}_3\text{O}_4$  hybrid support (SC-SBILC@MWCNT@ $\text{Fe}_3\text{O}_4$ ). Additional decoration with an ionic liquid structure allowed the elimination of an inorganic base normally used in these systems. The catalytic activity was characterized by the catalysts' performance in the enantioselective epoxidation of *trans*-methylcinnamate. The reaction was performed in acetonitrile and hydrogen peroxide was used as the oxidant, delivering the desired product in 35% yield (Scheme 15). Although this appears relatively low, it should be noted that no by-products are formed, and the product is obtained with 100% ee. Recycling of the catalyst by magnetic separation was possible four times with only a small drop in yield.



**SCHEME 15** Enantioselective heterogeneous catalytic epoxidation of methyl cinnamate.

The same group later used levulinate-intercalated layered double hydroxides (LDH) (LEV@LDH-pp) as a catalyst for the same transformation.<sup>29</sup> Similar to their previous system (Scheme 15) the product was formed with 100% enantioselectivity but the observed yield was comparatively low (21%).

The epoxidation of fatty acid methyl esters was achieved by Ravasio et al. using titanium-grafted silicas as catalysts.<sup>30</sup> Using TBHP as the oxidant in ethyl acetate as the solvent, high conversion (76%–96%) and selectivity values (85%–96%) were observed. Unfortunately, no catalyst recycling studies were performed.

Turco, Di Serio and co-workers investigated the epoxidation of cardoon seed oil as alternative for soybean oil oxidation.<sup>31</sup> The authors found that the use of alumina and hydrogen peroxide is superior to other methods, for example, performic acid, with regard to both environmental concerns but also yield and selectivity of the transformation. Complete transformation of all three double bonds in the triglyceride was achieved with 88% selectivity at a conversion of 85%.

### 3.3.3 Dihydroxylation reactions

Dihydroxylation reactions are important tools in synthetic organic chemistry as they allow for the selective introduction of a dual functionality within a molecule. Although many protocols are based on the use of a homogeneous metal catalyst (including Sharpless' traditional catalysts for asymmetric dihydroxylation) there are efforts to perform the reaction under heterogeneous conditions. The first heterogeneous dihydroxylation was reported by Sharpless in 1990.<sup>32</sup> Since then a variety of new methods have been published. A general review on metal-catalyzed dihydroxylation was published by Beller et al.<sup>33</sup> while Jacobs et al. summarized the use of heterogeneous green osmium-catalyzed dihydroxylation.<sup>34</sup> The following part shall show examples of heterogeneous catalytic dihydroxylation that follow the principles of green chemistry.

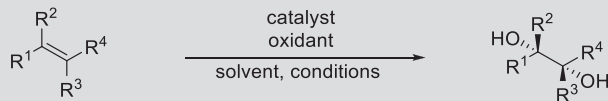
#### 3.3.3.1 Dihydroxylation with osmium

Despite its price and especially its toxicity osmium is still the metal of choice when it comes to choosing a catalyst for a dihydroxylation reaction, mainly due to its extraordinary selectivity. Many of the employed catalysts are homogeneous in nature. Alternative methods have been developed in order to prevent the contamination of the product mixture with the highly toxic osmium.<sup>35</sup> Even though this method can prevent the osmium contamination, from a green chemistry point of view the use of a fully heterogeneous catalyst should be preferred as not only the separation of the osmium could easily be achieved but in addition there is the possibility to recycle and reuse the catalyst. Several different osmium-based solid catalysts were applied in these transformations as summarized in Table 1.

Caps et al. developed a heterogenized dihydroxylation catalyst based on  $\text{Os}_3(\text{CO})_{12}$  immobilized on MCM-41 support ( $\text{Os}_3(\text{CO})_{12}/\text{MCM-41}$ ).<sup>36</sup> Using 4-methylmorpholine N-oxide (NMO) as the terminal oxidant the system was able to achieve the dihydroxylation of *trans*-stilbene in a water/acetone mixture as a solvent (Table 1 entry 1). While an excellent conversion and high selectivity was observed some results suggest that the catalyst can leach out into the reaction mixture.

Using a modified support material (Al-MCM-41) when preparing the catalyst the same group achieved the enantioselective dihydroxylation of *trans*-stilbene.<sup>51</sup> NMO as the oxidant in water/acetone (1:9) gave the (*S,S*) isomer in 64% yield and 90%*ee* (Scheme 16).

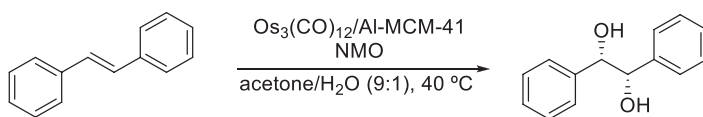
**TABLE 1** Heterogeneous osmium-catalyzed dihydroxylations.



| Entry | Catalyst   | Oxidant                            | Conditions   | R <sup>1</sup>                | R <sup>2</sup> | R <sup>3</sup> | R <sup>4</sup>                   | Yield (%) | Recycl. | Ref. |
|-------|--|------------------------------------|--|-------------------------------|----------------|----------------|----------------------------------|-----------|---------|------|
| 1     | Os <sub>3</sub> (CO) <sub>12</sub> /MCM-41       | NMO                                | H <sub>2</sub> O/acetone, 40°C                     | Ph                            | H              | H              | Ph                               | 84        | –       | 36   |
| 2     | Os@SiO <sub>2</sub>                              | NMO                                | <i>t</i> BuOH/CH <sub>2</sub> Cl <sub>2</sub> , RT | Alkyl, Ph                     | H              | H, alkyl       | H, alkyl, CO <sub>2</sub> Et     | 65–99     | 2 times | 37   |
| 3     | Os@SiO <sub>2</sub> , Ti-MCM-41                  | NMO, H <sub>2</sub> O <sub>2</sub> | <i>t</i> BuOH/CH <sub>2</sub> Cl <sub>2</sub> , RT | C <sub>4</sub> H <sub>9</sub> | H              | H              | H                                | 55        | –       | 38   |
| 4     | Os@Fe <sub>3</sub> O <sub>4</sub>                | NMO                                | <i>t</i> BuOH/CH <sub>2</sub> Cl <sub>2</sub> , RT | Alkyl, Ph                     | H              | H, alkyl       | H, alkyl                         | 84–99     | 5 times | 39   |
| 5     | OsO <sub>2</sub> -Fe <sub>3</sub> O <sub>4</sub> | NMO                                | H <sub>2</sub> O/acetone, 100°C                    | Alkyl, Ph                     | H, Ph          | H, alkyl       | H, alkyl, Ph, CO <sub>2</sub> Et | 65–99     | –       | 40   |
| 6     | LDH-OsO <sub>4</sub>                             | NMO                                | <i>t</i> BuOH/H <sub>2</sub> O, RT                 | Ph, alkyl                     | H, Me          | H, Me          | H, Ph, alkyl                     | 89–96     | *       | 41   |
| 7     | Resin-OsO <sub>4</sub>                           | O <sub>2</sub>                     | H <sub>2</sub> O/acetone, RT                       | Ph, alkyl                     | H, Me          | H, Me          | H, Me, CO <sub>2</sub> Me        | 20–99     | 5 times | 42   |
| 8     | MCM-(QN) <sub>2</sub> PHAL-OsO <sub>4</sub>      | O <sub>2</sub>                     | H <sub>2</sub> O/ <i>t</i> BuOH, 50°C              | Ph, alkyl                     | H, alkyl       | H              | H, alkyl, Ph                     | 15–99     | –       | 43   |

|    |  |                                    |   |           |          |              |                                  |       |         |    |
|----|--|------------------------------------|---|-----------|----------|--------------|----------------------------------|-------|---------|----|
| 9  | SGS-(DHQD) <sub>2</sub> PHAL-OsO <sub>4</sub> , TS-1 | NMO, H <sub>2</sub> O <sub>2</sub> | H <sub>2</sub> O/tBuOH, RT                  | Ph        | H, alkyl | H            | H, alkyl, Ph, CO <sub>2</sub> Me | 55–94 | –       | 44 |
| 10 | Resin-OsO <sub>4</sub> , (DHQN) <sub>2</sub> AQN     | K <sub>3</sub> Fe(CN) <sub>6</sub> | H <sub>2</sub> O/tBuOH, 10°C                | Alkyl     | H, Me    | H            | H, alkyl                         | 80–95 | 7 times | 45 |
| 11 | AP-Mg-OsO <sub>4</sub>                               | NMO                                | H <sub>2</sub> O/CH <sub>3</sub> CN/acetone | Ph, alkyl | H, alkyl | H            | H, alkyl, Ph, CO <sub>2</sub> Me | 85–94 | 5 times | 46 |
| 12 | Os@MS  | NMO                                | H <sub>2</sub> O/acetone, RT                | Ph, alkyl | H, Me    | H, alkyl     | H, alkyl, Ph                     | 94–99 | 4 times | 47 |
| 13 | Zeolite-Os   | H <sub>2</sub> O <sub>2</sub>      | H <sub>2</sub> O/acetone, RT                | Ph, alkyl | H        | alkyl, H, Ph | H, Ph                            | 30–98 | 5 times | 48 |
| 14 | I-APS-OsO <sub>4</sub>                               | NMO                                | H <sub>2</sub> O/acetone, RT                | Ph, alkyl | H, Me    | H, alkyl     | H, CO <sub>2</sub> R, Ph         | 68–89 | –       | 49 |
| 15 | OsO <sub>4</sub> -P4VP                               | NMO                                | H <sub>2</sub> O/acetone, RT                | Ph, alkyl | H, Me    | H            | H, alkyl, Ph                     | 92–95 | #       | 50 |

\*, Recyclability was mentioned by the authors but not specified. #, Reaction was performed under continuous flow conditions.



**SCHEME 16** The dihydroxylation of *trans*-stilbene using an Al modified MCM-41 supported osmium catalyst.

Jacobs' group immobilized osmium on a  $\text{SiO}_2$  surface modified with alkene containing side chains by the formation of an Os-diolate complex. The authors found that the diolate complex of a tetrasubstituted olefin does not undergo hydrolysis under standard reaction conditions and can therefore be used to anchor Os to a substrate.<sup>37</sup> The dihydroxylation reaction uses NMO as terminal oxidant in a *tert*-butanol/dichloromethane solvent mixture and delivers the desired products in high yields and selectivities (Table 1 entry 2). Exceptions to the high yields were found when crotonate or cinnamate was used as the substrate. The catalyst could be reused in a second reaction without losing its activity and selectivity. By performing heterogeneity tests it was found that no leaching of the osmium to the solution could be detected.

The same group also investigated the use of hydrogen peroxide as the terminal oxidant in the dihydroxylation reactions of alkenes. Although it was not possible to use  $\text{H}_2\text{O}_2$  to reoxidize the osmium-diolate complex directly the authors described the use of a two-vessel-system that still allowed for use of  $\text{H}_2\text{O}_2$  as overall terminal oxidant.<sup>38</sup> While the dihydroxylation reaction occurs in one vessel using the  $\text{Os@SiO}_2$  catalyst and NMO as oxidant, the regeneration of NMO by oxidation of 4-methylmorpholine (NMM) with  $\text{H}_2\text{O}_2$  and Ti-MCM-41 as a catalyst takes place in the second vessel. The heterogeneity of both catalysts allowed for the easy transfer of the solution between the two vessels. Each individual step gave low conversion towards the diol product, but the authors showed that higher conversions can be achieved by performing multiple iterations of the reaction sequence (Table 1 entry 3).

The concept of using osmium-diolate complex to anchor the metal to a support was also used by Fujita et al.<sup>39</sup> The authors anchored the osmium species on magnetic  $\text{Fe}_3\text{O}_4$  nanoparticles ( $\text{Os@Fe}_3\text{O}_4$ ) and could show that the catalyst efficiently performed the dihydroxylation of several alkenes in excellent yields (Table 1 entry 4). NMO was used as the oxidant in *t*BuOH- $\text{CH}_2\text{Cl}_2$  as a solvent. The catalytic system could be recycled five times with no decrease in yield, but the reaction time had to be increased. A small amount of osmium was found to leach into solution during the reaction.

Ramón and his co-workers showed that osmium can be deposited on commercial magnetite microparticles ( $\text{OsO}_2\text{-Fe}_3\text{O}_4$ ). The catalyst was able to perform the dihydroxylation of various substrates in acetone/water as a solvent with NMO as the oxidant.<sup>40</sup> The reaction gives high yields in general (including allyl esters and ethers) with the exception of sterically hindered substrates and cinnamates that only gave a medium yield (Table 1 entry 5). The authors

reported that the catalyst can be separated and reused but a much lower yield was observed, and substantial osmium leaching was also detected making the reuse of the catalyst impractical from a green point of view.

The research group of Choudary developed the heterogenization of osmium by the ion-exchange technique. Starting with ion-exchange in LDH<sup>41</sup> the method was extended to other substrates such as amine modified silica particles and polymer resins.<sup>42</sup> The researchers performed the dihydroxylations in the presence of (DHQD)<sub>2</sub>PHAL as chiral ligand and obtained the diols in high yields and very good enantioselectivities in most cases. Different oxidants such as NMO, also molecular oxygen, as a green alternative, performed well. Acetone/water or *t*BuOH/water mixtures were used as the solvent and the catalyst could be recycled up to five times without any decline in its performance (Table 1 entries 6 and 7).

The same researchers also investigated the immobilization of osmium via a cinchona alkaloid linker grafted onto the surface of MCM-41.<sup>43</sup> A series of alkenes were successfully submitted to the asymmetric dihydroxylation using molecular O<sub>2</sub> as oxidant amongst others. A water/*t*BuOH mixture was used as the solvent; both yields and enantiomeric excess were excellent for most substrates with the exception of highly conjugated systems such as stilbene (Table 1 entry 8). Although the use of oxygen gas as the oxidant is desirable from a green point of view, the system suffers from significant osmium leaching.

This method of osmium immobilization by a chiral complex was also applied to the two component oxidation system developed by Jacobs et al.<sup>38</sup> Silica gel particles were used as the substrate and the products were obtained in good yields (with the exception of styrene) and high enantiomeric excess (Table 1 entry 9).<sup>44</sup> Unfortunately the system showed a high osmium leaching making it not suitable for recycling.

In order to overcome the Os leaching issue Choudary et al. turned to their resin-bound osmium catalyst and added a chiral ligand to achieve the asymmetric dihydroxylation.<sup>45</sup> As oxidant K<sub>3</sub>Fe(CN)<sub>6</sub> was used in *t*BuOH/water (Table 1 entry 10). Both the product yields and enantiomeric excess were good for the examples shown. Recycling studies showed that the catalyst could be reused seven times before a notable drop in yield is observed, however, the chiral ligand had to be replenished after each reaction to maintain the level of enantioselectivity. In a similar example, K<sub>3</sub>Fe(CN)<sub>6</sub> and NaIO<sub>4</sub> served as catalytic co-oxidants with the osmium catalyst.<sup>52</sup>

Further investigations from the same research group indicated that osmium can be anchored on nanocrystalline MgO (AP-Mg-OsO<sub>4</sub>) to form an active dihydroxylation catalyst.<sup>46</sup> The reaction was performed in a combination of water/CH<sub>3</sub>CN/acetone as the solvent using NMO as the oxidant. The products were obtained in high yields and the catalyst was recycled five times with a small drop in yield (Table 1 entry 11). Experimental evidence revealed that the osmium was bound to the surface via a stable glycolate bond.

Rana et al. were able to immobilize osmium on poly-lysine/SiO<sub>2</sub>, inorganic-organic hybrid microspheres (Os@MS) and use this material as a catalyst for the dihydroxylation of alkenes with NMO as oxidant.<sup>47</sup> When (DHQD)<sub>2</sub>PHAL was added as a chiral ligand, the products were obtained in excellent yields and enantioselectivities in water/acetone as the solvent (Table 1 entry 12). The catalyst could be reused four times with no loss in activity.

Metin's group developed a new dihydroxylation catalyst that was based on osmium nanoclusters confined in zeolite-Y.<sup>48</sup> The catalyst is effective for a large variety of substrates including various functional groups (Table 1 entry 13). Mainly the *cis*-alkenes were tested and the yield obtained was high in all cases with the exception of *cis*-stilbene. This was rationalized by the large size of the *cis*-stilbene not allowing the molecule to enter the cavities of the zeolite catalyst. H<sub>2</sub>O<sub>2</sub> in water/acetone was used as the oxidant-solvent mixture and the catalyst could be reused five times with only a small decrease in yield.

Amine-functionalized imogolite nanorods were used by Xi et al. for the coordination of osmium and the thus prepared catalyst (I-APS-OsO<sub>4</sub>) was found to be effective in the dihydroxylation of alkenes.<sup>49</sup> The substrates were mostly styrene derivatives that gave the desired dihydroxylated compounds in high yields (Table 1 entry 14). NMO was used as the oxidant in acetone/water solvent mixture. Attempts to recycle the catalyst failed due to significant catalyst leaching causing a large drop in yield.

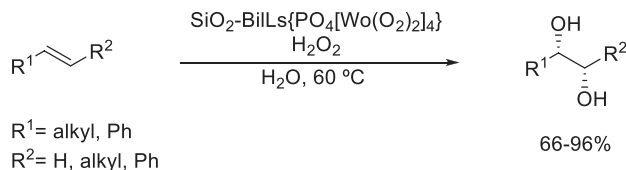
Kim and co-workers were able to immobilize OsO<sub>4</sub> within a P4VP nanobrush microreactor and successfully performed the dihydroxylation of alkenes under continuous flow conditions.<sup>50</sup> The desired products were obtained in excellent yields even after prolonged use of the microreactor (Table 1 entry 15). The same microreactor-catalyst system can be used to perform oxidative cleavage when NaIO<sub>4</sub> is used as oxidant instead of NMO.

### 3.3.3.2 Dihydroxylations with metals other than osmium

As described above, despite its toxicity, osmium is still the go-to metal when performing the dihydroxylation of alkenes, however, there are a few reports using other metals to perform this transformation.

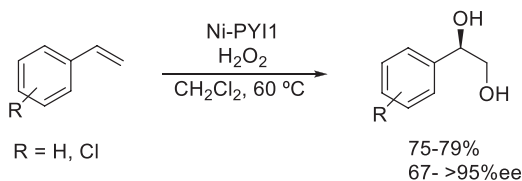
Shi et al. developed a dihydroxylation catalyst based on peroxophosphotungstate immobilized in an ionic liquid brush on a SiO<sub>2</sub> surface.<sup>53</sup> Using H<sub>2</sub>O<sub>2</sub> as the oxidant in water the desired products were obtained in mainly high yields (Scheme 17). Investigations on the recyclability of the system showed that reusing the catalyst eight times was possible with only a negligible decrease in yield. The authors also showed that the reaction could be scaled up to 100 mmol level without significant decline in performance.

Duan and his group synthesized chiral metal-organic frameworks (cMOFs) that incorporated Keggin-type tungsten-containing polyoxometallates. This system allowed for the asymmetric dihydroxylation of styrenes in a mixture



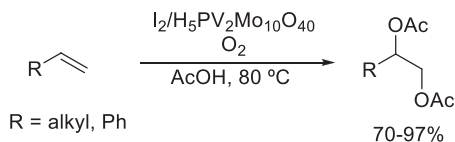
**SCHEME 17** The dihydroxylation of alkenes catalyzed by a heterogenized peroxophosphotungstate.

of  $\text{H}_2\text{O}_2$  (15%) and  $\text{CH}_2\text{Cl}_2$  (3:1) providing the diols in good yields.<sup>54</sup> The enantioselectivities obtained were excellent except for substrates possessing an *ortho*-substituent (Scheme 18). Filtration experiments showed that the reaction is indeed heterogeneous in nature and the catalyst could be recycled three times with a moderate loss in activity.



**SCHEME 18** Enantioselective dihydroxylation using a chiral MOF as catalyst.

Branyska and Neumann described the use of a mixed vanadium/molybdenum polyoxometalate and iodine for the diacetoxylation of alkenes.<sup>55</sup> The polyoxometalate first forms an electrophilic iodine species, which leads to the formation of a 1,2-iodoacetate. Hydrolysis and reaction with the solvent acetic acid leads to the formation of the final 1,2-diacetoxy compounds (Scheme 19). The use of molecular oxygen as green terminal oxidant is counterbalanced by the formation of 2 eq. hydrogen iodide during the reaction.



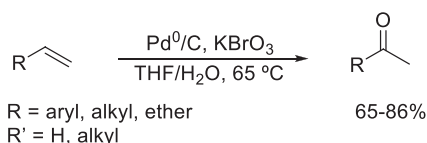
**SCHEME 19** Tandem hydroxylacetylation-acetylation reaction using and iodine polyoxometalate catalyst.

### 3.3.4 Wacker-type oxidation reactions

The Wacker oxidation or Wacker-Tsuji oxidation<sup>56</sup> was one of the first homogeneous catalytic reactions that was implemented on an industrial scale<sup>57</sup> and is still used today for the production of methyl ketones from terminal alkenes. Despite its high importance in the industry, the reaction is still mostly performed

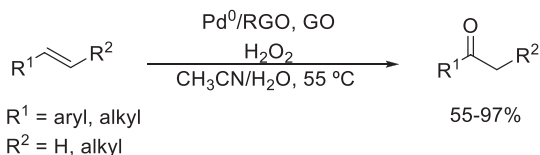
under homogeneous conditions, very few reports on the heterogenization of this transformation can be found. Examples on Wacker or Wacker-type oxidations using a heterogeneous catalytic system are summarized below.

The first report of a green, heterogeneous Wacker oxidation was presented by Kulkarni et al. Using palladium on carbon as the catalyst and  $\text{KBrO}_3$  as the oxidant the authors were not only able to heterogenize the system but also avoid the use of toxic copper co-catalysts.<sup>58</sup> A series of terminal alkenes could be converted into the corresponding methyl ketone in good yields using a THF-water mixture as solvent (Scheme 20). The substrates tested included aromatic and aliphatic alkenes containing a variety of functional groups including for example, ethers, esters, and aldehydes. It should be noted that the formyl group present in the substrate remained untouched by the catalytic system.



**SCHEME 20** Wacker-type oxidation of terminal alkenes catalyzed by a simple Pd/C-KBrO<sub>3</sub> system.

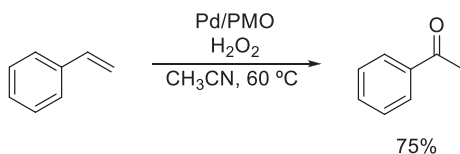
Gao et al. showed that palladium bound to reduced graphene oxide (RGO) can be used for the selective oxidation of terminal alkenes to the corresponding methyl ketones.<sup>59</sup> The reaction was suitable for styrene derivatives, as well as terminal and internal aliphatic alkenes. The catalyst ( $\text{Pd}^0/\text{RGO}$ ) showed good performance and gave the desired products in mostly good yields (Scheme 21). Exceptions are compounds with strong electron-withdrawing substituents. Hydrogen peroxide was used as the terminal oxidant in the system and graphene oxide was added as a weak solid acid. The catalyst was shown to be recyclable five times with a small drop in yield and hot filtration tests showed that the reaction is indeed heterogeneous in nature.



**SCHEME 21** Wacker oxidation of disubstituted alkenes catalyzed by reduced graphene oxide (RGO) supported Pd.

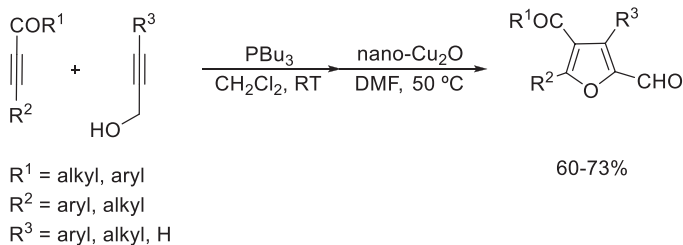
The same group showed previously that the oxidation of styrenes using a Pd/C catalyst with  $\text{H}_2\text{O}_2$  as oxidant is possible using sulfuric acid as the acid co-catalyst.<sup>60</sup> Medium to high yields were obtained with differently substituted styrene derivatives. Although reusing the catalyst is possible the use of sulfuric acid is not desirable from a green point of view.

Borah and Zhao used periodic mesoporous organosilicas (PMO) as a support to immobilize palladium via a diketimine linkage.<sup>61</sup> The obtained material (Pd/PMO) was used as a catalyst for the Wacker oxidation of styrene as a test reaction. Acetophenone was obtained with excellent selectivity and good yields (Scheme 22). The catalyst could be recycled five times with no loss in activity. While hydrogen peroxide was used as a green oxidant, the system suffers from the use of acetonitrile as the solvent. The authors could show that higher yields can be obtained when the reaction time is prolonged, but this causes deterioration of the catalyst, limiting its recyclability.



**SCHEME 22** Oxidation of styrene to acetophenone using hydrogen peroxide catalyzed by Pd on periodic mesoporous organosilicas.

A domino process for the synthesis of substituted  $\alpha$ -carbonyl-furans that involved a palladium-free Wacker-type oxidation was described by Jiang et al.<sup>62</sup> Starting from a propargylic alcohol and an electron-deficient alkyne a first  $\text{PBu}_3$ -catalyzed step forms an enyne intermediate, which then undergoes cyclization and oxidation catalyzed by  $\text{Cu}_2\text{O}$  nanoparticles. Oxygen is used as the terminal oxidant for the process and a large variety of substituents are tolerated in the reaction giving the desired products in moderate to good yields (Scheme 23).



**SCHEME 23** Domino C-C-coupling/oxidation reaction for the formation of substituted furans.

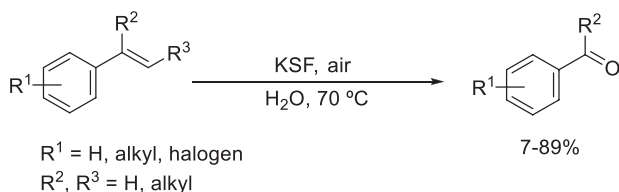
### 3.3.5 Oxidative cleavage of hydrocarbons

The oxidative cleavage of carbon-carbon (multiple) bonds is of immense importance in the field of synthetic chemistry as it allows for the specific alteration of the carbon framework of a compound, as well as the introduction of functional groups such as aldehydes, ketones, or carboxylic acids. Ozonolysis, one of the most well-known methods, had been first reported over a century ago and this transformation, at least the concept of the  $\text{C}=\text{C}$  bond cleavage, is still attracting

significant interest. Although there are a variety of methods available, many do not comply with the principles of green chemistry. Cousin et al. did provide a recent review on green cleavage reactions with  $\text{H}_2\text{O}_2$ .<sup>63</sup> Due to the practical value of these reactions, development of heterogeneous catalytic processes<sup>64</sup> as well as better understanding of the mechanism of such reactions<sup>65</sup> are in the forefront of research in this area. The following examples will focus on the use of heterogeneous catalysts for green cleavage reactions.

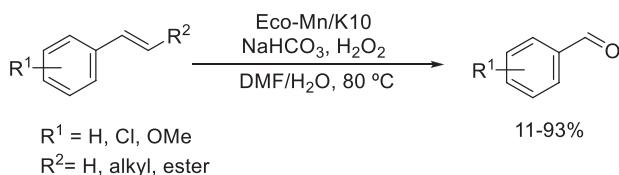
### 3.3.5.1 Cleavage to generate aldehydes and ketones

Schäfer et al. reported that styrenes can be easily cleaved to the corresponding aldehydes using montmorillonite KSF as a catalyst and oxygen from air as the oxidant.<sup>66</sup> The reaction is performed in water as the solvent and the products are mostly obtained in medium to good yields depending on the substitution pattern of the substrate (Scheme 24). The advantage of the method is in its simplicity and the absence of any harmful chemicals.



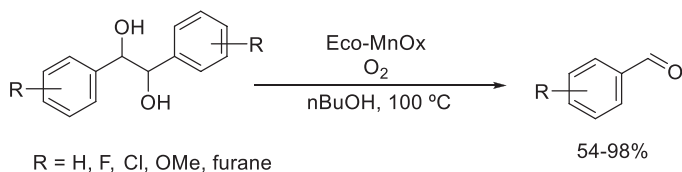
**SCHEME 24** A montmorillonite KSF-catalyzed oxidative cleavage of styrenes to aldehydes and ketones.

The Eco-Mn catalyst that was designed and applied by Grison and his group for the epoxidation of alkenes (vide supra) could also be used for the cleavage of  $\text{C}=\text{C}$  double bonds to form aldehydes.<sup>25</sup> In order to obtain the carbonyl function the reaction conditions were adjusted; an increase in the amount of the oxidant  $\text{H}_2\text{O}_2$  and higher temperatures were applied. Different styrene derivatives were cleaved with varying yields and selectivities (Scheme 25). The recycling of the catalyst was only shown for the epoxidation reaction, but it can be assumed that similar performance could be observed for the cleavage reaction.



**SCHEME 25** Cleavage of styrene derivatives using a biosourced manganese loaded montmorillonite K10.

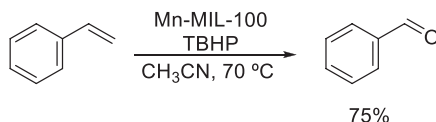
An oxidized version of this catalyst was applied by the same group for the cleavage of aromatic 1,2-diols to aldehydes and ketones.<sup>67</sup> Symmetric diols were converted into the expected carbonyl compounds with mostly excellent yields for the target compounds (Scheme 26). The catalyst showed no decrease in yield even after six consecutive runs.



**SCHEME 26** Oxidative cleavage of 1,2-diols with a biosourced manganese catalyst.

Anastas and his coworkers reported that the reaction could be performed under the same conditions as shown above using a catalyst made of Na-Mn-layered mixed oxides (Na-Mn LMO).<sup>68</sup> The scope of the reaction and the yields obtained were similar to the above shown results. Six consecutive reactions could be performed with the same catalyst before a notable decline in yield was observed. It was also shown that the reaction system is compatible with a variety of other reactions such as aldol-condensation, Wittig-reaction or imine formation, and their combination with the oxidative cleavage could be performed as one-pot operation. Additionally, the reaction is robust and easy to perform as it has been applied in teaching laboratories.<sup>69</sup>

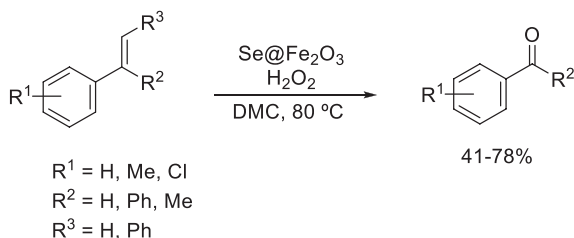
The group of Liu showed that metal organic frameworks of the Mn-MIL-100 type can be used for the cleavage of styrene to benzaldehyde (Scheme 27).<sup>70</sup> The researchers used *tert*-butyl hydroperoxide as the oxidant and showed that recycling of the catalyst was possible three times with only a minimal reduction in benzaldehyde yield. Unfortunately, styrene was the only substrate tested and acetonitrile had to be used as the solvent.



**SCHEME 27** Selective formation of benzaldehyde from styrene catalyzed by a Mn-containing metal-organic-framework.

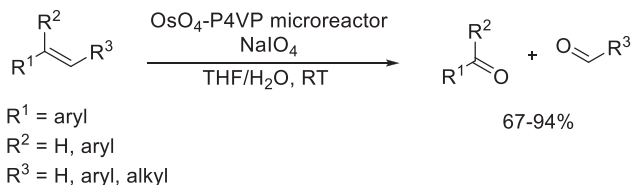
Yu, Zhang and co-workers developed an effective selenium-doped iron oxide (Se@Fe<sub>2</sub>O<sub>3</sub>) catalyst for the oxidative scission of the C=C double bond with hydrogen peroxide as the oxidant.<sup>71</sup> Several 1-aryl alkenes were successfully cleaved to form the corresponding ketone or aldehyde products in moderate to good yields (Scheme 28). The researchers were successful in recycling

the catalyst, it could be reused without deactivation. As an additional green feature, dimethylcarbonate (DMC) was used as solvent.



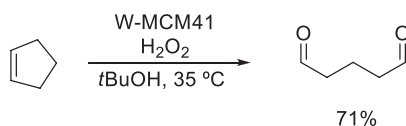
**SCHEME 28** Formation of 1-aryl carbonyl compounds via the selenium doped iron oxide-catalyzed oxidation of alkenes.

Kim et al. were able to extend the applicability of their microreactor system (immobilized OsO<sub>4</sub> within a P4VP nanobrush microreactor) for the continuous flow oxidative cleavage of styrene derivatives to aldehydes and ketones using NaIO<sub>4</sub> as the oxidant.<sup>50</sup> THF/water was used as the solvent and the products were obtained in good to excellent yields (Scheme 29).



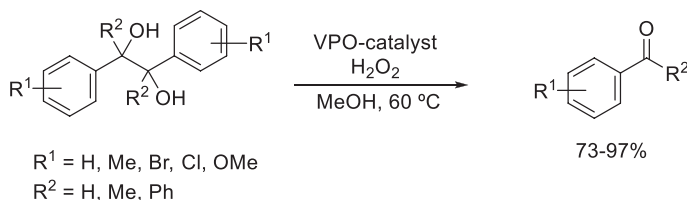
**SCHEME 29** Application of Os-loaded microreactors for the oxidative cleavage of alkenes.

Dai et al. were able to synthesize a tungsten-containing version of the popular MCM-41 catalyst (W-MCM41) and reported its use in the formation of glutaraldehyde from cyclopentene.<sup>72</sup> The reaction delivers the product under mild conditions using H<sub>2</sub>O<sub>2</sub> as the oxidant and *t*BuOH as the solvent (Scheme 30). The catalyst could be recycled and reused seven times without loss of activity or selectivity.



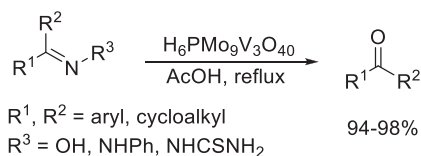
**SCHEME 30** Tungsten-containing MCM-41-catalyzed cleavage of cyclopentene with hydrogen peroxide as the oxidant.

Upadhyaya and Samant showed that the selection of solvent determines the outcome of the reaction of benzopinacol with vanadium phosphorous oxides (VPOs).<sup>73</sup> While performing the reaction in MeOH the cleavage product benzophenone was obtained (Scheme 31). In contrast, the use of a nonpolar solvent such as toluene favors the formation of the pinacol rearrangement product. A variety of starting materials was successfully transformed to the carbonyl product in good to excellent yields. The reusability of the catalyst was shown in four subsequent reactions without loss of activity.



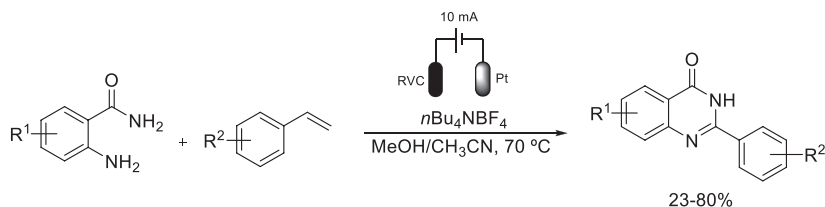
**SCHEME 31** Oxidative cleavage of symmetrical 1,2-diols using vanadium phosphorous oxides as catalyst.

Heravi and co-workers reported that the oxidative cleavage of different C=N-containing compounds to obtain ketones can be achieved with a vanadomolybdophosphate,  $\text{H}_6\text{PMo}_9\text{V}_3\text{O}_{40}$  as a catalyst in acetic acid as the solvent.<sup>74</sup> The applicability of the method was demonstrated by the cleavage of a variety of oximes, hydrazones, and semicarbazones in very high yields (Scheme 32). The catalyst was shown to be recyclable three times with only a small loss in yield.



**SCHEME 32** Oxidative cleavage of C=N bonds with vanadomolybdophosphate catalyst.

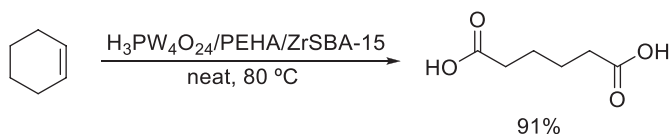
Using a one-pot electrochemical oxidative cleavage and oxidative cyclization the groups of Pan and Li were able to achieve the quinazolinone formation from styrenes and 2-aminobenzamides using a Pt electrode.<sup>75</sup> No additional oxidant was used and  $n\text{Bu}_4\text{NBF}_4$  was applied as the electrolyte in a MeOH/ $\text{CH}_3\text{CN}$  mixture. A variety of products was obtained in mainly medium to good yields (Scheme 33).



**SCHEME 33** One-pot electrochemical oxidative cleavage-cyclization sequence of amino-amides with styrenes on a solid Pt electrode.

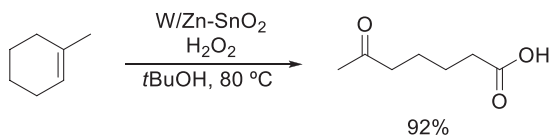
### 3.3.5.2 Cleavage to generate carboxylic acids and esters

The formation of adipic acid from cyclohexene was achieved by Zhai, An, and co-workers using a mixed  $\text{H}_3\text{PW}_4\text{O}_{24}/\text{PEHA}/\text{ZrSBA-15}$  catalyst system.<sup>76</sup> The reaction was performed with  $\text{H}_2\text{O}_2$  as the oxidant and no additional solvent was used, giving the product in 91% yield (Scheme 34). Recycling of the catalyst was attempted but it was found that although possible, a notable drop in yield was observed over five runs.



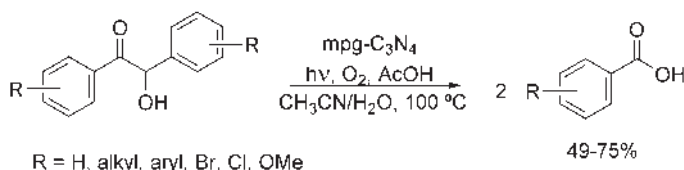
**SCHEME 34** Oxidative cleavage of cyclohexene to form adipic acid using a  $\text{H}_3\text{PW}_4\text{O}_{24}/\text{PEHA}/\text{ZrSBA-15}$  catalyst.

Mizuno et al. developed a “release and catch” system based on a tungstate species supported on zinc-modified tin oxide ( $\text{Zn-SnO}_2$ ) system for cleavage of alkenes to form carboxylic acids.<sup>77</sup> Hydrogen peroxide acted as the terminal oxidant and *tert*-butanol was chosen as the solvent. The tungstate species were thereby released from the support upon oxidation to peroxotungstate, which then oxidized the alkene. Upon returning into its original state the tungstate binds again to the  $\text{Zn-SnO}_2$  support. The catalyst could be reused in 10 reaction cycles without loss of activity and tungsten leaching was determined to be < 1% by ICP analysis. It should be noted that although a variety of substrates were subjected to the reaction conditions only 1-methylcyclohexene gave satisfactory product yield (Scheme 35).



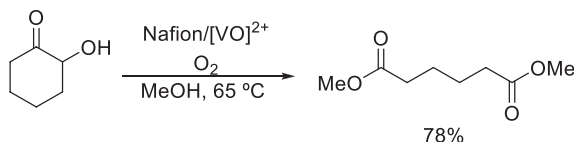
**SCHEME 35** Oxidative ring opening of 1-methylcyclohexene with hydrogen peroxide promoted by a tungstate supported on zinc-modified tin oxide catalyst.

Mesoporous carbon nitride (mpg-C<sub>3</sub>N<sub>4</sub>) was used by the group of Cao as an active photocatalyst to initiate the oxidative cleavage of  $\alpha$ -hydroxy ketones to acids.<sup>78</sup> Using visible light and molecular oxygen, a variety of substituted benzoin s were successfully converted into the corresponding benzoic acids (Scheme 36). CH<sub>3</sub>CN/H<sub>2</sub>O was used as the solvent mixture for the reaction. The authors reported that the catalytic activity remained stable when the catalyst was reused three times.



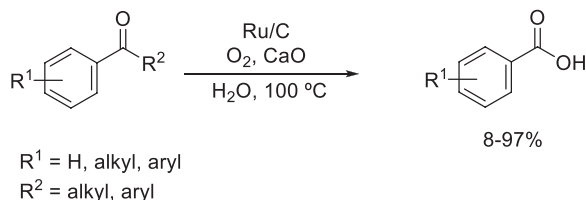
**SCHEME 36** An oxidative photocatalytic cleavage of benzoin s to form two molecules of benzoic acids.

The application of vanadium exchanged Nafion-H in the cleavage of  $\alpha$ -hydroxy ketones to form esters was reported by Aakel et al.<sup>79</sup> The reaction was performed in MeOH as a solvent and molecular oxygen served as the oxidizing agent (Scheme 37). Interestingly, the catalyst improved upon being reused as the recycled catalyst gave higher yields.



**SCHEME 37** Synthesis of diesters via the Nafion/[VO<sub>2</sub>]<sup>2+</sup>-catalyzed oxidative cleavage of cyclic  $\alpha$ -hydroxyketones.

The group of Sajiki and Monguchi described that a commercially available ruthenium on carbon catalyst can be used for the oxidative cleavage of aromatic ketones to generate the corresponding benzoic acids.<sup>80</sup> The authors used CaO to capture the CO<sub>2</sub> formed by degradation of R<sup>2</sup> and thereby increasing the yield of the reaction albeit with a low atom economy. The reaction is performed in water and uses molecular oxygen as the oxidant. With some exceptions the products are obtained in good to excellent yields (Scheme 38).

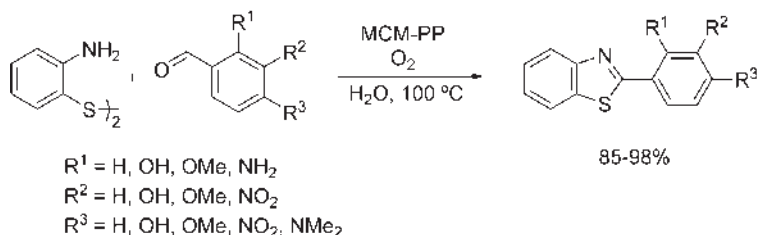


**SCHEME 38** A Ru/C-catalyzed oxidative cleavage of aryl ketones to benzoic acids with oxygen and the oxidant.

### 3.3.5.3 Other oxidative cleavage reactions

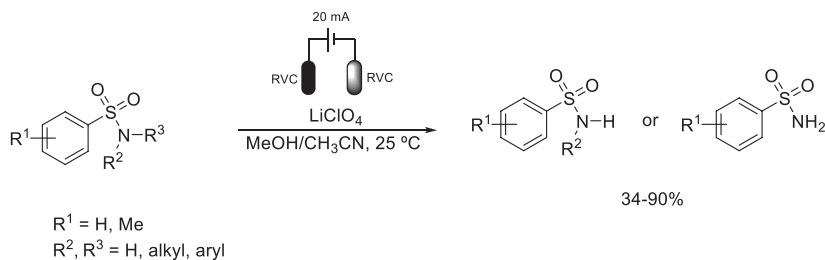
Several oxidative cleavage reactions serve environmental purposes, such as the degradation of certain pollutants. Ananthkrishnan et al. reported that an iron-phenanthroline hybrid resin can be used as a heterogeneous photocatalyst for the oxidative degradation of dyes with benzoic acid as the major product using molecular oxygen and visible light.<sup>81</sup> Using Rhodamin B as the model compound a good degree of degradation and reusability was achieved.

Mukhopadhyay and co-workers showed that the cleavage of disulfides is possible with molecular O<sub>2</sub> and piperazinylpyrimidine modified MCM-41 (MCM-PP) as catalyst.<sup>82</sup> The cleavage of *ortho*-aminothiophenol disulfide was performed in the presence of different benzaldehydes in order to obtain the corresponding benzothiazoles (Scheme 39). The yields obtained were excellent and only a minor decrease in yield was observed when the catalyst was reused in six consecutive runs.



**SCHEME 39** Synthesis of benzothiazoles by the catalytic oxidative cleavage of disulfides and the subsequent reaction of the intermediate with benzaldehydes.

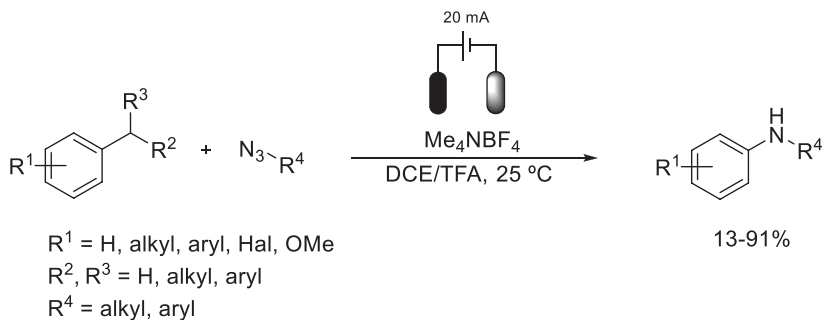
Wetzel and Jones used an electrochemical setup to perform the oxidative C-N cleavage of aromatic sulfonamides.<sup>83</sup> Using LiClO<sub>4</sub> as the electrolyte in MeOH/CH<sub>3</sub>CN solvent a variety of substrates can be converted to the desired products (Scheme 40). Depending on the amount of charge transferred, the controlled sequential cleavage of both alkyl-substituents can be achieved. The reaction can be performed either in batch or continuous-flow mode. No additional oxidants needed to be used and all unreacted reagents could be recovered.



**SCHEME 40** Electrochemical oxidative cleavage of C-N bonds.

The groups of Jiao and Zeng showed that substituted anilines can be obtained from alkylarenes using an electrochemical approach.<sup>84</sup> The researchers used azides as nitrogen source (Scheme 41). The advantage of the proposed

method is in the absence of an additional oxidant, although the use of the azide, as well as the solvent employed reduce the green rating of the reaction. The products are obtained mostly in medium to high yields.



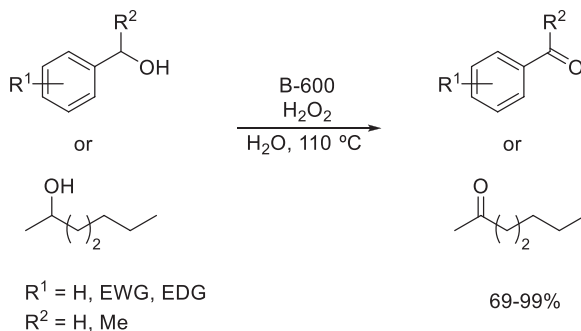
**SCHEME 41** Aniline formation by an oxidative electrochemical C–C cleavage.

### 3.3.6 Oxidation of C–O and C–N bonds

The selective transformation of carbon-heteroatom single bonds to multiple bonds by direct oxidation is of great importance in the field of synthetic organic chemistry. The following section will contain examples for the heterogeneous catalytic, controlled oxidation of C–O, and C–N bonds following the principles of green chemistry.

#### 3.3.6.1 Oxidation of C–O bonds

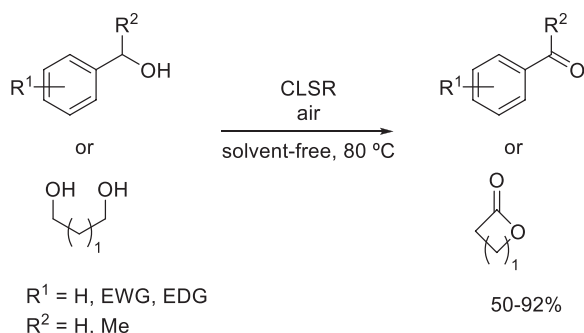
Chen, Li, and their co-workers developed an MOF-derived magnetic nanoparticles-based catalyst using iron as the catalytically active metal (B-600) for the selective oxidation of alcohols to aldehydes and ketones with  $\text{H}_2\text{O}_2$  as the oxidant and water as the solvent.<sup>85</sup> A variety of benzylic alcohols with both electron-withdrawing and -donating substituents, as well as several aliphatic alcohols were oxidized with high conversion and excellent selectivity (Scheme 42). Because of its magnetic properties the catalyst could be



**SCHEME 42** Synthesis of ketones by oxidation of secondary alcohols using an Fe-doped MOF catalyst.

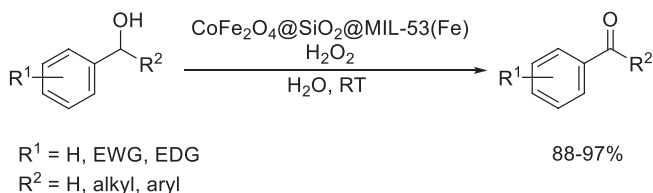
easily removed from the reaction mixture and reused in four subsequent reactions with only a small decrease in its activity.

The same transformation with a similar substrate scope was achieved using a ruthenate-based perovskite (CLSR) as a catalyst under solvent-free conditions.<sup>86</sup> Air was used as the oxidant and the desired products were obtained in high yields and with excellent selectivity for the aldehyde (Scheme 43). The authors showed that the catalyst was recyclable, albeit a drop in yield was noted over the course of four consecutive reactions. Interestingly, the catalyst could be reactivated by heating it to 400°C overnight. When a diol was used as the starting material, the corresponding lactone was obtained.



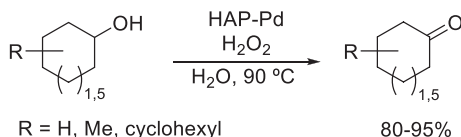
**SCHEME 43** Oxidation of alcohols to ketones and esters by a ruthenate-based perovskite catalyst.

A magnetically separable catalyst using a MOF was developed as the catalytic entity and was immobilized on a combined silica and cobalt-iron oxide support (CoFe<sub>2</sub>O<sub>4</sub>@SiO<sub>2</sub>@MIL-53(Fe)).<sup>87</sup> Benzylic alcohols were oxidized to their corresponding aldehydes and ketones with H<sub>2</sub>O<sub>2</sub> as the oxidant and water as the solvent (Scheme 44). Recycling of the catalyst was possible six times with only a minor decrease in yield while the selectivity was unchanged. The researchers could also show that the presented catalytic system was able to initiate the C–C bond cleavage of benzylic compounds if more hydrogen peroxide is used.



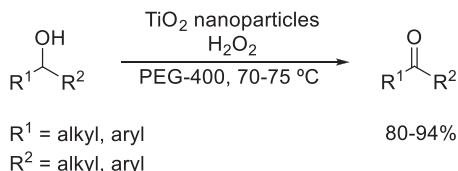
**SCHEME 44** Oxidation of benzylic alcohols with hydrogen peroxide using a magnetic MOF catalyst.

Varma and his team synthesized Pd-nanoparticles on a hydroxyapatite support (HAP-Pd) and applied it as a catalyst for the oxidation of secondary alcohols to ketones.<sup>88</sup> A series of cyclic aliphatic alcohols was transformed in high to excellent yields with H<sub>2</sub>O<sub>2</sub> using water as environmentally benign solvent (Scheme 45). The catalyst was recycled six times with only a minor decline in its performance.



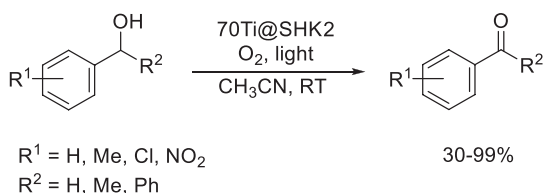
**SCHEME 45** Hydroxyapatite-supported Pd as a catalyst for the oxidation of cyclic alcohols to the corresponding ketones.

The same transformation was achieved by Kidwai et al. using nanocrystalline TiO<sub>2</sub> as a heterogeneous catalyst with H<sub>2</sub>O<sub>2</sub> as the oxidant in PEG-400.<sup>89</sup> Aliphatic as well as benzylic secondary alcohols provided the ketone in high yields (Scheme 46). Recycling studies showed that the catalyst could be reused, albeit with a slight decrease in yield after the second run.



**SCHEME 46** TiO<sub>2</sub> nanoparticles for the formation of ketones.

TiO<sub>2</sub> incorporated within a mesoporous MOF (70Ti@SHK2) was found to be an effective catalyst in the photocatalytic oxidation of primary and secondary alcohols with O<sub>2</sub> and sunlight to generate aldehydes and ketones.<sup>90</sup> Using acetonitrile as solvent, the products were obtained in mainly good yields with the exception of substrates possessing strong electron-withdrawing substituents (Scheme 47). The catalyst could be reused but a significant decrease in conversion was observed.



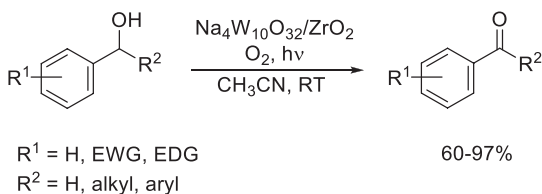
**SCHEME 47** Light-driven oxidation of benzylic alcohols catalyzed by a TiO<sub>2</sub> incorporated into a mesoporous metal-organic framework.

Farhadi et al. used a silica-encapsulated polyoxometalate ( $\text{H}_3\text{PW}_{12}\text{O}_{40}/\text{SiO}_2$ ) as a photocatalyst for the formation of aldehydes and ketones from benzylic alcohols.<sup>91</sup> Performing the reaction in acetonitrile in the presence of  $\text{O}_2$  and light resulted in the formation of the products in mostly good to excellent yields (Scheme 48). The catalyst could be reused eight times with only a slight decrease in yield. The authors could also show that scaling up the reaction by a factor of 100 was easily possible without any decline in the performance of the system. Similar photocatalytic systems have also been developed by other authors.<sup>92</sup>



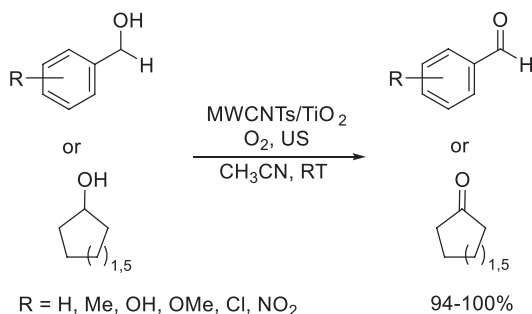
**SCHEME 48** Silica encapsulated polyoxometalate/light system for the oxidation of benzylic alcohols.

The same group also applied a zirconia-supported sodium decatungstate ( $\text{Na}_4\text{W}_{10}\text{O}_{32}/\text{ZrO}_2$ ) as a catalyst for the oxidation of benzylic alcohols with  $\text{O}_2$ /light.<sup>93</sup> As with the POM/ $\text{SiO}_2$ -system above (Scheme 48) the corresponding aldehydes and ketones were obtained in mostly high yields with the exception of substrates possessing strongly electron-withdrawing substituents on the aromatic ring (Scheme 49). The authors reported that the scale up (50-fold increase) of the system was possible. In addition, the recycling of the catalyst in seven cycles was tested and no deactivation was observed.



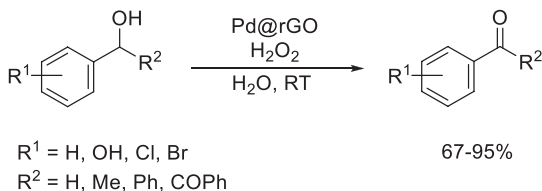
**SCHEME 49** Zirconia-supported sodium decatungstate-catalyzed light activated oxidation of benzylic alcohols.

A hybrid catalyst based on multiwalled carbon nanotubes and titanium dioxide ( $\text{MWCNTs}/\text{TiO}_2$ ) was developed and used in combination with ultrasounds for the oxidation of benzylic alcohols to aldehydes and cycloalkanols to the corresponding ketones.<sup>94</sup> The reaction was performed in acetonitrile as solvent and delivered the desired products in excellent yields with air as the oxidant (Scheme 50). The catalyst could be recycled in six consecutive reactions with only a minimal decrease in yield.



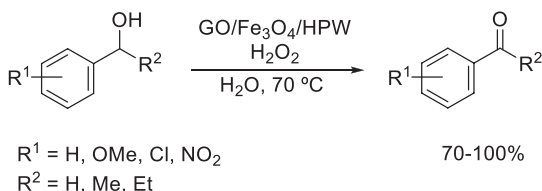
**SCHEME 50** Multiwalled carbon nanotubes/titanium dioxide system for the oxidation of benzylic alcohols and cyclic alcohols to aldehydes and ketones.

Pathak and Borah used piper leaf extract to generate reduced graphene oxide-supported Pd nanoparticles and used this catalyst (Pd@rGO) for the oxidation of benzylic alcohols.<sup>95</sup> Hydrogen peroxide was used as the oxidant in water as a solvent to obtain the desired aromatic aldehydes and ketones in mostly high yields (Scheme 51). No degradation of the catalyst was observed during the reaction and the catalyst could be reused five times without losing its activity.



**SCHEME 51** Oxidation of benzylic alcohols with an eco-sourced Pd nanoparticle-based catalyst.

Amani and co-workers used a magnetic nanocomposite as catalyst for the same transformation. Benzylic alcohols were oxidized to aldehydes and ketones with a catalyst based on a composite of graphene oxide-Fe<sub>3</sub>O<sub>4</sub>-NH<sub>3</sub><sup>+</sup>H<sub>2</sub>PW<sub>12</sub>O<sub>40</sub> (GO/Fe<sub>3</sub>O<sub>4</sub>/HPW) using H<sub>2</sub>O<sub>2</sub> as oxidant in water.<sup>96</sup> The products were obtained in high yields with substrates having both electron-donating and -withdrawing substituents present on the aromatic system (Scheme 52). When the alcohol substrate was not benzylic in nature the formation of the acid as by-product was



**SCHEME 52** Synthesis of aldehydes and ketones from benzylic alcohols promoted by a graphene oxide-Fe<sub>3</sub>O<sub>4</sub>-tungstophosphoric acid catalyst.

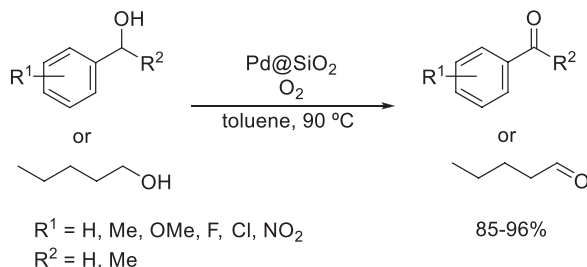
observed due to overoxidation. Recycling of the catalyst was possible five times but a notable drop in yield was already observed in the second reaction.

Naeimi et al. were able to immobilize a molybdenum complex on bio-based iron oxide nanofibers and use it as a catalyst for the oxidation of alcohols. The iron oxide was obtained from *Sesbania sesban* plant and modified with a Mo complex before depositing it on polyvinyl alcohol to form the active catalyst (PVA/Fe<sub>2</sub>O<sub>3</sub>/MoSB).<sup>97</sup> Formation of the aldehyde in excellent yields was achieved using H<sub>2</sub>O<sub>2</sub> as the oxidant under solvent-free conditions (Scheme 53). Changing the oxidant/solvent to *t*BuOOH led to the formation of the corresponding carboxylic acid instead. Although the recycling of the catalyst was possible with only a minor drop in yield when H<sub>2</sub>O<sub>2</sub> was used, a notable loss in activity was observed with *t*BuOOH as an oxidant.



**SCHEME 53** The oxidation of benzylic alcohols with hydrogen peroxide using a molybdenum modified bio-based iron oxide catalyst.

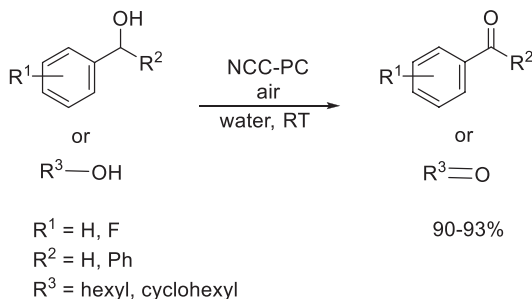
Oxygen as terminal oxidant was used in combination with a Pd-complex bound to SiO<sub>2</sub> (Pd@SiO<sub>2</sub>) as the catalyst for the oxidation of alcohols by Paul and co-workers.<sup>98</sup> Benzylic and aliphatic primary alcohols were converted to the corresponding aldehydes in high to excellent yields (Scheme 54). Air could also be used as the oxidant instead of pure oxygen without decreasing the selectivity of the reaction, however, longer reaction times were needed to achieve high yields. Drawback of the system is the limited reusability (a tremendous drop in yield occurred after the third run) and the need for toluene as the solvent.



**SCHEME 54** Oxidation of alcohols with a SiO<sub>2</sub>-bound Pd-complex.

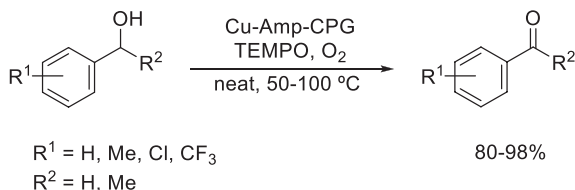
Chauhan and Yan synthesized a new oxidation catalyst based on copper phthalocyanine grafted on nanocrystalline cellulose (NCC-PC) for the oxidation

of alcohols to aldehydes and ketones in water as solvent using air as the oxidant.<sup>99</sup> The carbonyl compounds were obtained in high yields and the catalyst was shown to be recyclable in seven reactions with only a minor decrease in yield (Scheme 55). The authors investigated the stability of the catalyst and found that no copper leaching into the solution occurred.



**SCHEME 55** Oxidation of alcohols to aldehydes and ketones using a nanocrystalline cellulose-supported copper catalyst.

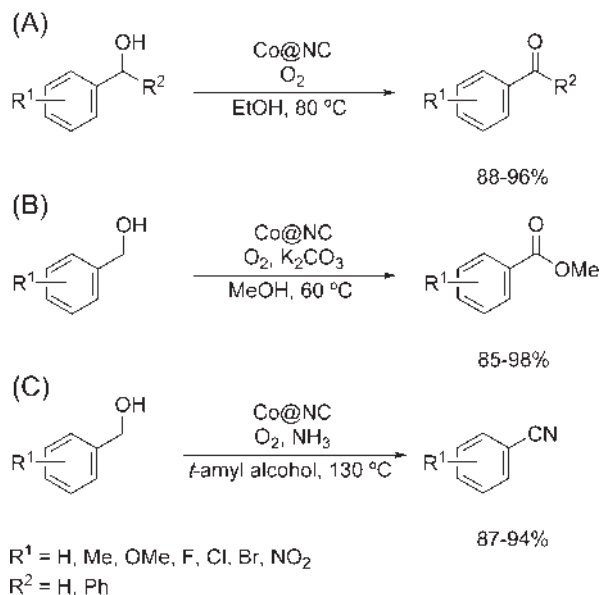
Ibrahim et al. used controlled pore glass as support material for the preparations of a copper nanoparticles-based catalyst (Cu-Amp-CPG) for the aerobic oxidation of alcohols using TEMPO/O<sub>2</sub> as oxidation system.<sup>100</sup> The system does not require a solvent and allows for a variety of benzylic alcohols to be efficiently oxidized into the corresponding aldehydes or ketones (Scheme 56). The catalyst was shown to be robust which ensured that it could be recycled and allowed the reaction to be performed seven consecutive times with only a minimal decrease in yield.



**SCHEME 56** The oxidation of benzylic alcohols on a glass-supported copper catalyst.

The Huang's group prepared a heterogeneous cobalt catalyst (Co@NC) by the pyrolysis of Co(OAc)<sub>2</sub> in an ionic liquid. This material was applied in the selective oxidation of alcohols with O<sub>2</sub> as the final oxidant.<sup>101</sup> The reaction outcome can thereby easily be directed via the applied reaction conditions. In order to obtain the aldehyde product the reaction should be performed using ethanol as the solvent (Scheme 57a) while in methanol, the process generates the methyl ester directly (Scheme 57b). Switching to *tert*-amyl alcohol and adding

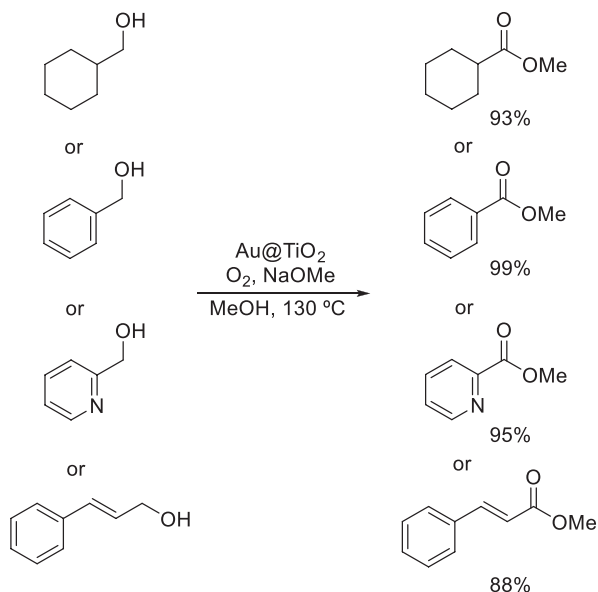
NH<sub>3</sub> into the reaction mixture delivers the corresponding nitrile as the product (Scheme 57c). All products are obtained in excellent yields and selectivities under their respective reaction conditions. Recycling of the catalyst was investigated for all three reaction pathways and proven to be possible eight times with only a minor decrease in yield.



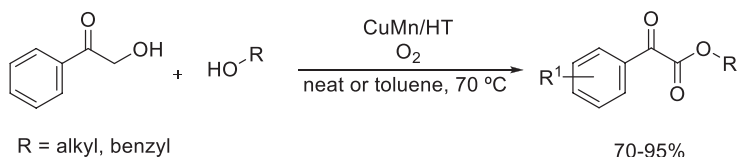
**SCHEME 57** A cobalt-catalyzed oxidation of benzylic alcohols to form (a) ketones/aldehydes, (b) esters or (c) nitriles depending on the reaction conditions.

In a similar process, Christensen et al. achieved the direct transformation of an alcohol to the corresponding methyl ester using a commercial heterogeneous gold-catalyst supported on TiO<sub>2</sub> (Au/TiO<sub>2</sub>).<sup>102</sup> Oxygen was used as the oxidant in the reaction system and the authors showed that aliphatic as well as benzylic alcohols can be transformed under these conditions (Scheme 58). The tested substrates allowed for the transformation to occur in high yields.

The same oxidative esterification was investigated by the groups of Meng and Zhao. Using an  $\alpha$ -hydroxy ketone as a starting material the authors targeted the hydroxyl part that was in situ oxidized and then participated in the esterification.<sup>103</sup> A copper-manganese hydrotalcite catalyst (CuMn-HT) was used and O<sub>2</sub> served as the oxidant. A series of alcohols was proven to be effective in the transformation and the ester products were obtained in high to excellent yields (Scheme 59). Furthermore, the authors also proved that the reaction could be performed with complicated molecules such as cholesterol or testosterone. The catalyst could be reused five times without showing a decrease in product yield and the reaction could also be easily scaled up to a multigram level.

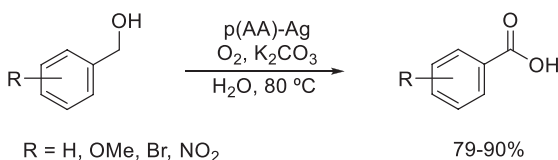


**SCHEME 58**  $\text{TiO}_2$ -supported gold catalyst for the formation of esters from primary alcohols.



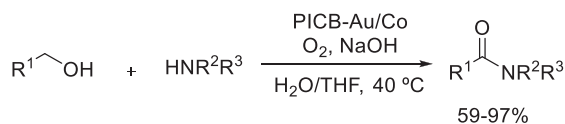
**SCHEME 59** Selective ester formation using a copper-manganese hydrocalcite catalyst.

Ghorbanloo et al. used silver nanoparticles embedded in poly(acrylic acid) hydrogels ( $\text{p(AA)-Ag}$ ) as a heterogeneous catalyst for the oxidation of primary alcohols to carboxylic acids using  $\text{O}_2$  as the oxidant in water.<sup>104</sup> Several benzylic alcohols were oxidized to the corresponding benzoic acid with only a minor amount of the aldehyde being formed (Scheme 60). The catalyst could be recycled four times without a notable change in its activity.



**SCHEME 60** The application of silver nanoparticles as catalyst for the oxidation benzylic alcohols of carboxylic acids.

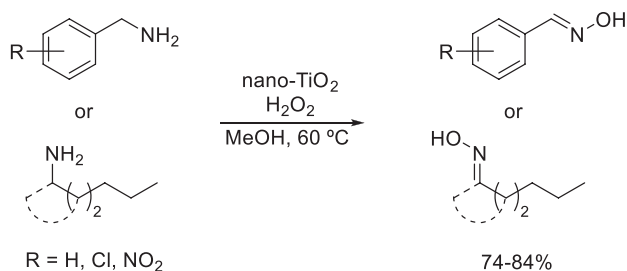
Kobayashi and co-workers reported the formation of amides from alcohols and amines by oxidative coupling using Au nanoparticles (PICB-Au/Co) in two studies.<sup>105, 106</sup> The reaction was performed with O<sub>2</sub> as oxidant in a THF/water mixture (Scheme 61). A large variety of primary alcohols was reacted with primary and secondary amines under the oxidative conditions to yield the desired amides in good to excellent yields. When optically active amines were employed, no racemization was observed. The recycling of the catalyst was shown to be possible, but it had to be reactivated by a heat treatment to restore its activity.



**SCHEME 61** Amide formation by oxidative coupling of alcohols and amines with a gold nanoparticle catalyst.

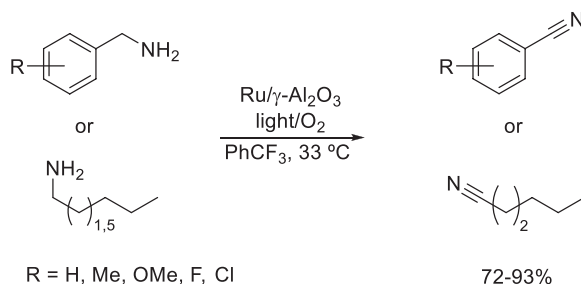
### 3.3.6.2 Oxidation of C–N bonds

Kidwai and Bhardwaj showed that nanocrystalline titanium dioxide (nano-TiO<sub>2</sub>) can be used for the oxidation of amines to oximes using H<sub>2</sub>O<sub>2</sub> as an oxidant.<sup>107</sup> The reaction was performed in MeOH as solvent and several benzylamines and aliphatic amines were transformed to the corresponding oximes in good yields (Scheme 62). The catalyst could be recycled in four consecutive runs without losing its activity.



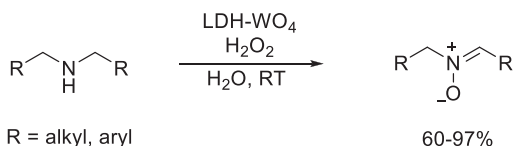
**SCHEME 62** Oxime formation from primary amines catalyzed by nanocrystalline TiO<sub>2</sub>.

The photocatalytic oxidation of amines to nitriles was demonstrated by the groups of Wang and Zheng using an alumina-supported heterogeneous ruthenium catalyst (Ru/γ-Al<sub>2</sub>O<sub>3</sub>).<sup>108</sup> Using a xenon lamp as a light source in combination with O<sub>2</sub> as the oxidant, a series of primary amines (benzylic and aliphatic) was converted to the corresponding nitriles (Scheme 63). Drawbacks of the presented methodology are that no information is given about the recyclability of the catalyst and that trifluoromethylbenzene was used as a solvent.



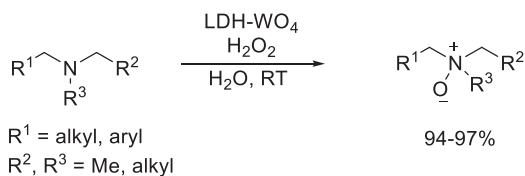
**SCHEME 63** A photocatalytic oxidation of primary amines to nitriles catalyzed by aluminum oxide-supported ruthenium.

Choudary et al. used tungstate exchanged layered double hydroxides (LDH- $\text{WO}_4$ ) as catalysts for the oxidation of secondary amines to nitrones.<sup>109</sup> The reactions were performed with  $\text{H}_2\text{O}_2$  as an oxidant in water as a green solvent. The desired products were obtained in excellent yields with the exception of dibenzylamine (Scheme 64). The catalyst could be reused six times without a significant drop in yield.



**SCHEME 64** Formation of nitrones by tungstate-exchanged layered double hydroxides-catalyzed oxidation of secondary amines.

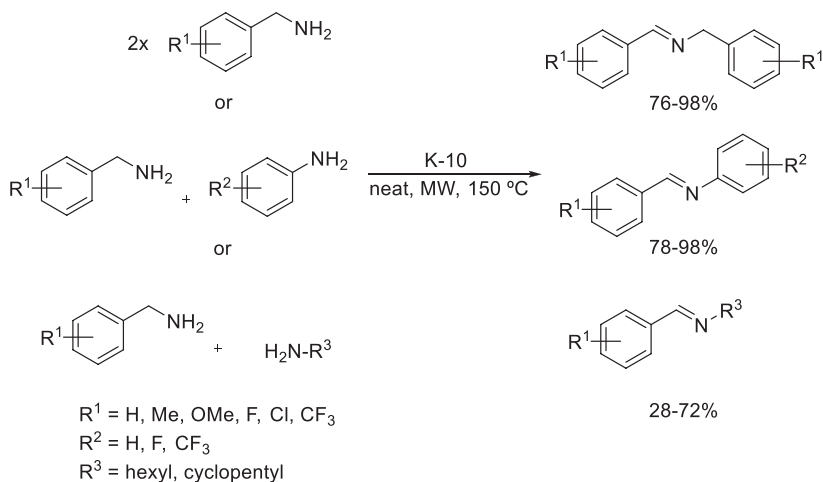
In addition to secondary amines the LDH- $\text{WO}_4$  catalyst could also be used for the oxidation of tertiary amines to the corresponding *N*-oxides.<sup>110</sup> The obtained yields were excellent for a variety of symmetric and nonsymmetric substrates (Scheme 65). As for the oxidation of secondary amines the catalyst was shown to be recyclable six times without showing any significant decrease in yield.



**SCHEME 65** Application of tungstate-exchanged layered double hydroxides as catalysts for the oxidation of tertiary amines to *N*-oxides.

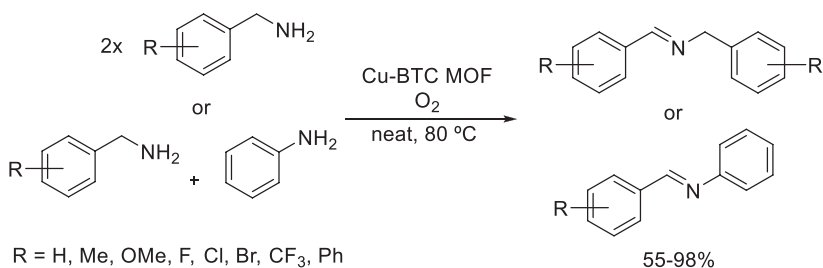
Török et al. reported that the use of the commercially available K-10 montmorillonite can facilitate the oxidative coupling of benzylic amines to imines

with different aliphatic, benzylic, and aromatic amines.<sup>111, 112</sup> The reaction does not require the use of a solvent and is performed under microwave irradiation giving the desired products in good to excellent yields and short reaction times. While benzylamines and anilines as coupling partners gave the products in high yields, lower yields were obtained in the case of aliphatic amines (Scheme 66).



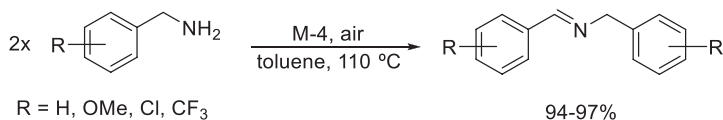
**SCHEME 66** The synthesis of imines via the oxidative coupling of benzylamines and other primary amines catalyzed by montmorillonite K-10.

Venugopal and co-workers used a copper-containing molecular organic framework (Cu-BTC MOF) as a catalyst for the oxidative coupling of benzylamines.<sup>113</sup> The reaction proceeded without the use of any solvent and generated either the product of self-coupling or in the case aniline is added the coupling with aniline is observed (albeit with lower yield, Scheme 67). The catalyst could be reused in five cycles with consistent product yield and the copper content of the catalyst did not decrease during the reaction indicating that no metal leaching took place.



**SCHEME 67** The solvent-free oxidative coupling of benzylamines and formation of imines using a copper-containing metal-organic framework as a catalyst.

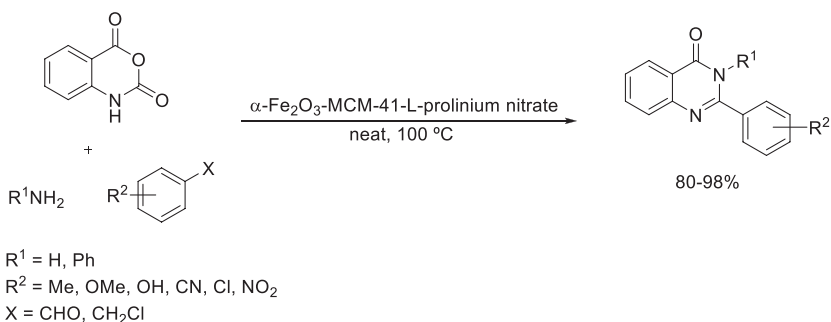
Chen et al. reported that the same reaction can be performed with manganese oxide (M-4) as a catalyst.<sup>114</sup> The reaction is performed in toluene as the solvent and uses air as the oxidant. The products are obtained in excellent yield and selectivity (Scheme 68). The recycling of the catalyst was possible with a slightly reduced selectivity.



**SCHEME 68** Homo-coupling of benzylamines toward imine formation using a manganese oxide catalyst.

The research group of Suib showed that the same transformation can be performed with Cs-doped manganese oxide (Cs/MnO<sub>x</sub>).<sup>115</sup> As described by Chen et al.<sup>114</sup> the reaction was performed in toluene with air as an oxidant. Recyclability of the catalyst was investigated in four cycles, although after prior reactivation of the catalyst.

The group of Rostamizadeh used an ionic liquid immobilized on  $\alpha$ -Fe<sub>2</sub>O<sub>3</sub>-MCM-41 as a catalyst for the synthesis of quinazolin-4(3*H*)-one derivatives from isatoic anhydride, primary amines, and aromatic aldehydes or halides.<sup>116</sup> The multicomponent reaction forms the desired products with different substitution patterns in high to excellent yields and includes the oxidation of a C–N single bond to a C=N double bond as one step during the catalytic cycle (Scheme 69). The catalyst was shown to be reusable three times with a slight loss in product yield.



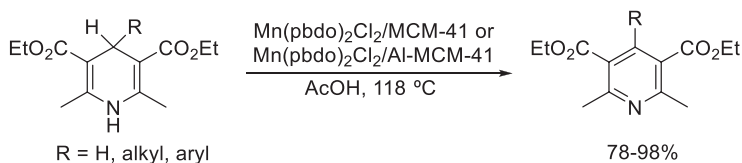
**SCHEME 69** The synthesis of quinazolin-4(3*H*)-ones via a multicomponent reaction catalyzed by an ionic liquid immobilized on iron oxide-MCM-41.

### 3.3.7 Dehydrogenation and aromatization of C–C and C–X bonds

The transformation of a C–X single-bond into a C=X multiple-bond (X = C, N, O) via dehydrogenation is another important transformation in organic chemistry as it allows the introduction of a new functional group in a formerly

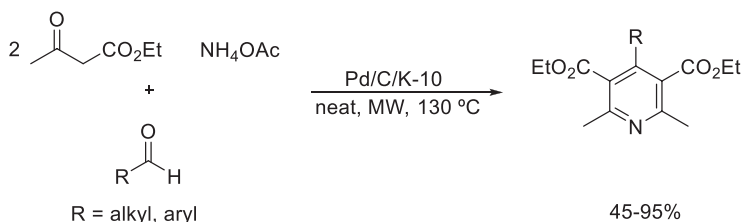
non- or low-functionalized molecule. In the following examples we will focus on dehydrogenation reactions leading to a new conjugated multiple bond systems. Dehydrogenations that form isolated double bonds have been treated earlier in the [Section 3.3.6](#).

Heravi et al. used a manganese complex anchored on a MCM-41 nanoreactor as a catalyst for the formation of pyridines from Hantzsch 1,4-dihydropyridines.<sup>117</sup> The authors used two slightly different systems to achieve the transformation with equally good results ([Scheme 70](#)). The desired products were obtained in high to excellent yields and the catalyst was shown to be recyclable with only a minor drop in yield. While the reaction could be performed without solvent, the use of acetic acid was able to substantially shorten the reaction times.



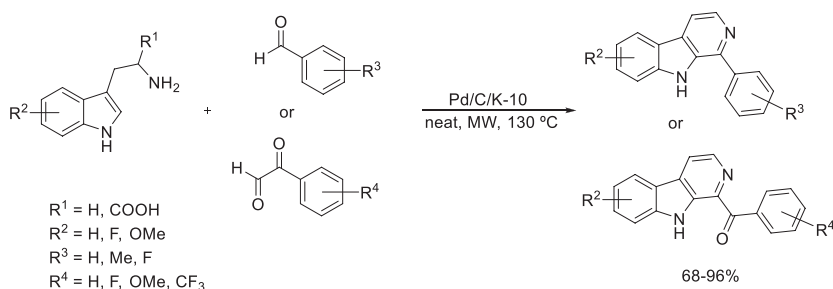
**SCHEME 70** The aromatization of 1,4-dihydropyridines catalyzed by an MCM-41-anchored manganese complex.

The synthesis of pyridines was also achieved by the group of Török using a bifunctional Pd/C/K-10 catalyst.<sup>118</sup> Using a multicomponent reaction and a domino cyclization-aromatization approach the desired products were obtained in good yields from ethyl acetoacetate, ammonium acetate, and substituted aldehydes ([Scheme 71](#)). The reaction was performed without the use of a solvent under microwave conditions allowing for short reaction times.



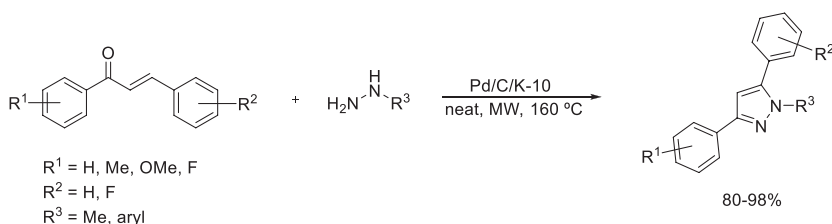
**SCHEME 71** Using a bifunctional Pd/C/K-10 catalyst in the three-component formation of pyridines.

Kulkarni et al. used the same catalytic system for the synthesis of  $\beta$ -carboline from tryptamines and aromatic aldehydes through a condensation-cyclization-aromatization sequence.<sup>119</sup> Similar to the above described protocol ([Scheme 71](#)), no solvent is needed and the use of microwaves allows for the formation of the desired products in good to excellent yields within short reaction times ([Scheme 72](#)).



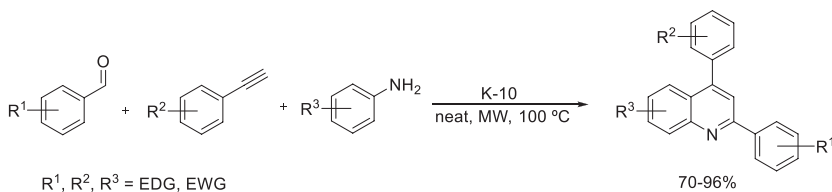
**SCHEME 72** Synthesis of  $\beta$ -carbolines with a bifunctional Pd/C/K-10 catalyst.

In a different study the same group could show that pyrazoles can be prepared by a tandem cyclization-dehydrogenation approach using Pd/C/K10.<sup>120</sup> Chalcones and hydrazones function as starting materials for the transformation giving the desired products in excellent yields under microwave-assisted conditions (Scheme 73). Other supported metals, such as Ni or Cu nanoparticles were also found to be effective in such tandem reactions that include oxidative steps.<sup>121</sup>



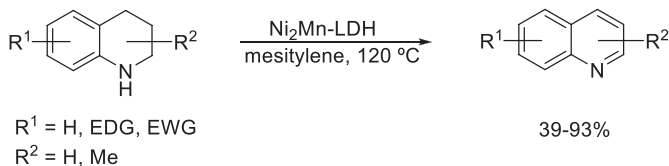
**SCHEME 73** Application of the Pd/C/K-10 bifunctional catalytic system for the synthesis of pyrazoles.

Kulkarni and Török showed that the use of palladium was not necessary for the formation of quinolines in a cascade reaction including an aromatization step.<sup>122</sup> Applying K-10 montmorillonite only as the catalyst under microwave conditions, the authors were able to achieve quinoline formation in a variation of the A3 reaction. The products were obtained in high to excellent yields with a variation of aromatic starting materials (Scheme 74).



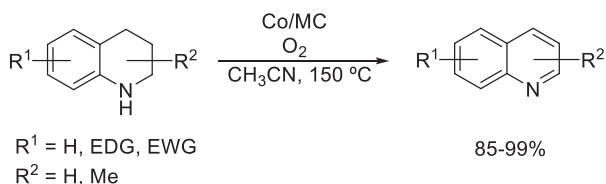
**SCHEME 74** Montmorillonite K-10-catalyzed variation of the A3-reaction to form quinolines.

Zhou et al. used a Ni-Mn layered double hydroxide (Ni<sub>2</sub>Mn-LDH) for the dehydrogenative aromatization of 1,2,3,4-tetrahydroquinolines, thus generating quinolines.<sup>123</sup> A variety of substituted tetrahydroquinolines was successfully oxidized with varying yields (Scheme 75). Although the authors could show that no apparent metal leaching took place, the recyclability of the catalyst is limited as prolonged reactions times are needed to achieve reasonable conversions when reusing the catalyst. Another drawback of the method is the use of mesitylene as solvent.



**SCHEME 75** Nickel-manganese layered double hydroxides as catalysts for the aromatization of 1,2,3,4-tetrahydroquinolines.

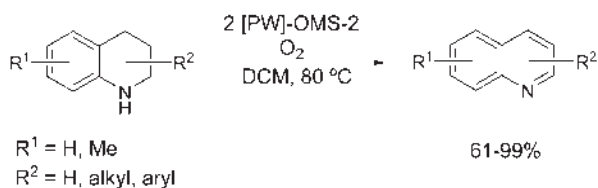
Zhang and co-workers used nitrogen-doped carbon-supported cobalt nanoparticles (Co/MC) for the dehydrogenation of 1,2,3,4-tetrahydroquinolines.<sup>124</sup> The desired products were obtained in high yields with acetonitrile as a solvent under O<sub>2</sub> atmosphere (Scheme 76). Reusing the catalyst was possible five times maintaining almost identical yield and selectivity.



**SCHEME 76** Aromatization of 1,2,3,4-tetrahydroquinolines with carbon-supported cobalt nanoparticles.

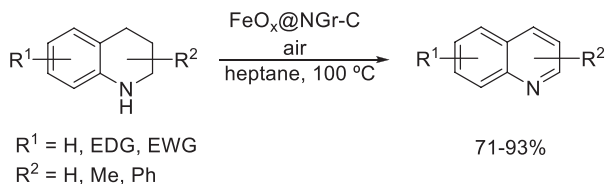
Manganese oxide octahedron molecular sieve doped with sodium phosphotungstate (2 [PW]-OMS-2) was used by Bi et al. for the dehydrogenation of tetrahydroquinolines in addition to some other N-heterocycles.<sup>125</sup> The reaction was performed in dichloromethane as the solvent and O<sub>2</sub> atmosphere was applied as the oxidant. A variety of substituted quinolines could be produced in mainly high yields using this methodology (Scheme 77). Other N-heterocycles that were synthesized by dehydrogenative aromatization using this protocol included quinazolines, indoles, or pyridines.

Beller and his co-workers developed an iron-nitrogen doped graphene core shell catalyst (FeO<sub>x</sub>@NGr-C) for the dehydrogenation of tetrahydroquinolines.<sup>126</sup> The catalyst performed well for a variety of different substituted starting materials and recycling of the catalyst was possible four times before a



**SCHEME 77** Tungstate on manganese oxide molecular sieves-catalyzed aromatization of tetrahydroquinolines to quinolines.

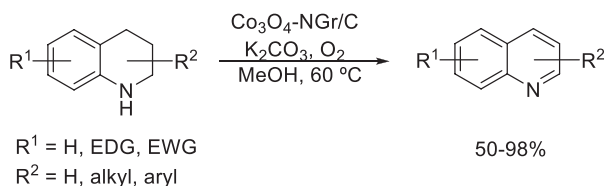
notable drop in yield was observed (Scheme 78). Oxygen from air was sufficient to reoxidize the catalyst. Drawback of the method is the use of the non-green solvent heptane.



**SCHEME 78** Formation of quinolines catalyzed by iron-nitrogen-doped graphene.

Gu, Cao, and their group reported the dehydrogenation of tetrahydroquinolines with Pt nanowire in their report as a proof of concept but only one basic example is given as their focus was on hydrogenation reactions.<sup>127</sup>

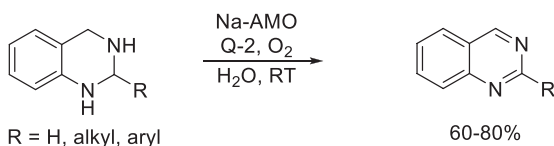
Iosub and Stahl also put their focus on the aromatization of tetrahydroquinolines but in addition, they investigated the reactivity of other N-heterocycles, as well.<sup>128</sup> The authors used cobalt oxide supported on nitrogen-doped carbon ( $\text{Co}_3\text{O}_4\text{-NGr/C}$ ) as the catalyst in methanol as a solvent and molecular oxygen as the oxidant. Besides quinolines (Scheme 79), the study showed that quinoxalines, indoles, pyridines, and imidazoles could also be synthesized by this method.



**SCHEME 79** Cobalt oxide supported on nitrogen-doped carbon catalyzed aromatization of tetrahydroquinolines.

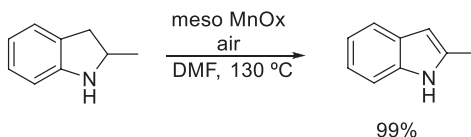
The oxidative dehydrogenation of different N-heterocycles on Na-doped manganese oxide (Na-AMO) catalyst was achieved by Tang et al.<sup>129</sup> The system uses a catechol derivative (Q-2) as a co-catalyst in water as a solvent and oxygen

as the reoxidizer. Quinolines, quinazolines (Scheme 80),  $\beta$ -carbolines, and pyridines were all successfully obtained under the reaction conditions. Recycling tests showed that the catalyst can be reused eight times with only a slight decrease in yield.



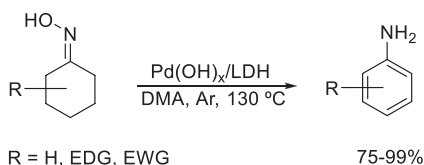
**SCHEME 80** The synthesis of quinazolines via Na-doped manganese oxide-catalyzed aromatization.

Mullick et al. used mesoporous manganese oxide (meso MnOx) for similar transformations.<sup>130</sup> Quinolines, indoles (Scheme 81), quinoxalines, and pyridines were obtained in good to excellent yields. The reactions were performed under air atmosphere using DMF as the solvent. Recycling of the catalyst was possible four times without loss in yield and selectivity, although the catalyst was reactivated by heating to 250°C before reusing.



**SCHEME 81** Aromatization of 2-methylindoline catalyzed by a mesoporous manganese oxide.

Mizuno's group showed that cyclohexanone oximes are suitable starting materials for the synthesis of anilines by oxidative aromatization.<sup>131</sup> The catalyst was Pd supported on a Mg-Al layered double hydroxide (Pd(OH)<sub>x</sub>/LDH). *N,N*-dimethylacetamide (DMA) was used as the solvent under argon atmosphere. Reusing of the catalyst was possible five times with unchanged results. Substrates with different electron-donating and -withdrawing substituents were readily aromatized in high yields (Scheme 82). The authors could also show that the one-pot reaction starting from the ketone in the presence of hydroxylamine was possible.



**SCHEME 82** Oxidative aromatization of oximes using a supported palladium catalyst.

### 3.3.8 Conclusions and outlook

The examples given in this chapter show that there is an increase in interest that brought significant progress in the application of heterogeneous oxidation catalysts to develop processes that adhere to the principles of green chemistry. Although there are many examples of using catalytic (metal)centers that are traditionally employed as oxidation catalysts in a more environmentally friendly form (i.e., immobilized manganese) there are also promising examples using naturally occurring materials (i.e., montmorillonite clays) in oxidative transformations. While this is an encouraging path to follow it is also obvious that the field is just at the beginning of this gradual change and there are still many challenges to solve. Several examples shown in this work are a step in the right direction, but do not yet fully comply with the recommendations of green and sustainable chemistry and engineering principles. They often have a limited substrate scope and the issue of chemoselectivity, when there are more than one oxidation sensitive groups present, is barely addressed. Future development in the field will likely continue to follow the path outlined and find solutions for the before mentioned problems to allow the broader application of these methods in synthetic organic chemistry and industrial applications.

### References

1. Gaich, T.; Baran, P. S. Aiming for the Ideal Synthesis. *J. Org. Chem.* **2010**, *75*, 4657–4673.
2. Young, I. S.; Baran, P. S. Protecting-Group-Free Synthesis as an Opportunity for Invention. *Nat. Chem.* **2009**, *1*, 193–205.
3. Ishihara, Y.; Baran, P. S. Two-Phase Terpene Total Synthesis: Historical Perspective and Application to the Taxol Problem. *Synthesis* **2010**, *12*, 1733–1745.
4. Anastas, P. T.; Warner, J. C. *Green Chemistry: Theory and Practice*; Oxford University Press: New York, 1998.
5. Török, B.; Dransfield, T., Eds. *Green Chemistry: An Inclusive Approach*; Elsevier: Oxford, Cambridge, MA, 2018.
6. Moschona, F.; Savvopoulou, I.; Tsitopoulou, M.; Tataraki, D.; Rassias, G. Epoxide Syntheses and Ring-Opening Reactions in Drug Development. *Catalysts* **2020**, *10*, 1117.
7. Marco-Contelles, J.; Molina, M. T.; Anjum, S. Naturally Occurring Cyclohexane Epoxides: Sources, Biological Activities, and Synthesis. *Chem. Rev.* **2004**, *104*, 2857–2899.
8. Swern, D. Epoxidation and Hydroxylation of Ethylenic Compounds with Organic Peroxides. In *Organic Reactions*; Denmark, S. E., Overman, L. E., Eds.; 2011.
9. Frohn, M.; Shi, Y. Chiral Ketone-Catalyzed Asymmetric Epoxidation of Olefins. *Synthesis* **2000**, *14*, 1979–2000.
10. Wang, R.; Liu, X.; Yang, F.; Gao, S.; Zhou, S.; Kong, Y. Neighboring Cu Toward Mn Site in Confined Mesopore to Trigger Strong Interplay for Boosting Catalytic Epoxidation of Styrene. *Appl. Surf. Sci.* **2021**, *537*, 148100.
11. Salvadori, P.; Pini, D.; Petri, A.; Mandoli, A. Catalytic Heterogeneous Enantioselective Dihydroxylation and Epoxidation. In *Chiral Catalyst Immobilization and Recycling*; DeVos, D. E., Vankelecom, I. F. J., Jacobs, P. A., Eds.; Wiley-VCH Verlag, 2000.

270 Heterogeneous catalysis in sustainable synthesis

12. Kazemnejadi, M.; Mahmoudi, B.; Sharafi, Z.; Nasserri, M. A.; Allahresani, A.; Esmaeilpour, M. Synthesis and Characterization of a New Poly  $\alpha$ -Amino Acid Co(II)-Complex Supported on Magnetite Graphene Oxide as an Efficient Heterogeneous Magnetically Recyclable Catalyst for Efficient Free-Coreductant Gram-Scale Epoxidation of Olefins With Molecular Oxygen. *J. Organomet. Chem.* **2019**, *896*, 59–69.
13. Nooraiepour, M.; Moghadam, M.; Tangestaninejad, S.; Mirkhani, V.; Mohammadpoor-Baltork, I.; Nabavizadeh, S. M. Highly Efficient Epoxidation of Alkenes With Hydrogen Peroxide Catalyzed by Tungsten Hexacarbonyl Supported on Multi-wall Carbon Nanotubes. *Transit. Met. Chem.* **2011**, *36*, 861–866.
14. Mohammed, M. L.; Patel, D.; Mbeleck, R.; Niyogi, D.; Sherrington, D. C.; Saha, B. Optimisation of Alkene Epoxidation Catalysed by Polymer Supported Mo(VI) Complexes And Application Of Artificial Neural Network for the Prediction of Catalytic Performances. *Appl. Catal. A Gen.* **2013**, *466*, 142–152.
15. Cao, L.; Yang, M.; Wang, G.; Wei, Y.; Sun, D. A Green Epoxidation System with Poly(4-vinylpyridine) Microsphere-Supported Molybdenum Catalyst. *J. Polym. Sci. A Polym. Chem.* **2010**, *48*, 558–562.
16. Ken-Ichi, O.; Sol, A.; Julia, K.; Hupp Joseph, T.; Notestein Justin, M.; Farha Omar, K. Vapor-Phase Cyclohexene Epoxidation by Single-Ion Fe(III) Sites in Metal-Organic Frameworks. *Inorg. Chem.* **2021**, *60*, 2457–2463.
17. Bagherzadeh, M.; Hosseini, H. Nanocluster Polyoxomolybdate Supported on Natural Zeolite: A Green and Recyclable Catalyst for Epoxidation of Alkenes. *J. Coord. Chem.* **2017**, *70*, 2212–2223.
18. Masteri-Farahani, M.; Modarres, M. Heterogenized Peroxopolyoxotungstate Catalyst on the Surface of Clicked Magnetite-Graphene Oxide Nanocomposite: Magnetically Recoverable Epoxidation Catalyst. *Appl. Organomet. Chem.* **2018**, *32*, e4142.
19. Taghiyar, H.; Yadollahi, B. New Perspective to Catalytic Epoxidation of Olefins by Keplerate Containing Keggin Polyoxometalates. *Polyhedron* **2018**, *156*, 98–104.
20. Lashanizadegan, M.; Rayati, S.; Dejarvar Derakhshan, Z. Heterogeneous Green Catalyst for Oxidation of Cyclohexene and Cyclooctene with Hydrogen Peroxide in the Presence of Host (Nanocavity of Y-zeolite)/Guest (N4-Cu(II) Schiff Base Complex) Nanocomposite Material. *Chin. J. Chem.* **2011**, *29*, 2439–2444.
21. Rayati, S.; Abdolalian, P. Heterogenization of a Molybdenum Schiff Base Complex as a Magnetic Nanocatalyst: An Eco-friendly, Efficient, Selective and Recyclable Nanocatalyst for the Oxidation of Alkenes. *C. R. Chimie* **2013**, *16*, 814–820.
22. Abbasi, V.; Hosseini-Monfared, H.; Hosseini, S. M. A Heterogenized Chiral Imino Indanol Complex of Manganese as an Efficient Catalyst for Aerobic Epoxidation of Olefins. *New J. Chem.* **2017**, *41*, 9866–9874.
23. Di Giuseppe, A.; Crucianelli, M.; Passacantando, M.; Nisi, S.; Saladino, R. Chitin- and Chitosan-Anchored Methyltrioxorhenium: An Innovative Approach for Selective Heterogeneous Catalytic Epoxidations of Olefins. *J. Catal.* **2010**, *276*, 412–422.
24. Goti, A.; Cardona, F.; Soldaini, G.; Crestini, C.; Fiani, C.; Saladino, R. Methyltrioxorhenium-Catalyzed Epoxidation-Methanolysis of Glycols under Homogeneous and Heterogeneous Conditions. *Adv. Synth. Catal.* **2006**, *348*, 476–486.
25. Escande, V.; Petit, E.; Garoux, L.; Boulanger, C.; Grison, C. Switchable Alkene Epoxidation/Oxidative Cleavage with  $H_2O_2/NaHCO_3$ : Efficient Heterogeneous Catalysis Derived from Biosourced Eco-Mn. *ACS Sustain. Chem. Eng.* **2015**, *3*, 2704–2715.
26. Lueangchaichaweng, W.; Brooks, N. R.; Fiorilli, S.; Gobechiya, E.; Lin, K.; Li, L.; Parres-Esclapez, S.; Javon, E.; Bals, S.; Van Tendeloo, G.; Martens, J. A.; Kirschhock, C. E. A.;

- Jacobs, P. A.; Pescarmona, P. P. Gallium Oxide Nanorods: Novel, Template-Free Synthesis and High Catalytic Activity in Epoxidation Reactions. *Angew. Chem. Int. Ed.* **2014**, *53*, 1585–1589.
27. Collard, X.; Li, L.; Lueangchaichaweng, W.; Bertrand, A.; Aprile, C.; Pescarmona, P. P. G-MCM-41 Nanoparticles: Synthesis and Application of Versatile Heterogeneous Catalysts. *Catal. Today* **2014**, *235*, 184–192.
28. Candu, N.; Rizescu, C.; Podolean, I.; Tudorache, M.; Parvulescu, V. I.; Coman, S. M. Efficient Magnetic and Recyclable SBILC (Supported Basic Ionic Liquid Catalyst)-Based Heterogeneous Organocatalysts for the Asymmetric Epoxidation Of Trans-Methylcinnamate. *Catal. Sci. Technol.* **2015**, *5*, 729–737.
29. Candu, N.; Paul, D.; Marcu, I.-C.; Parvulescu, V. I.; Coman, S. M. Levulinate-Intercalated LDH: A Potential Heterogeneous Organocatalyst for the Green Epoxidation of  $\alpha,\beta$ -Unsaturated Esters. *Catal. Today* **2018**, *306*, 154–165.
30. Guidotti, M.; Ravasio, N.; Psaro, R.; Gianotti, E.; Marchese, L.; Coluccia, S. Heterogeneous Catalytic Epoxidation of Fatty Acid Methyl Esters on Titanium-Grafted Silicas. *Green Chem.* **2003**, *5*, 421–424.
31. Turco, R.; Tesser, R.; Russo, V.; Vitiello, R.; Fagnano, M.; Di Serio, M. Comparison of Different Possible Technologies for Epoxidation of *Cynara cardunculus* Seed Oil. *Eur. J. Lipid Sci. Technol.* **2020**, *122*, 1900100.
32. Kim, B. M.; Sharpless, K. B. Heterogeneous Catalytic Asymmetric Dihydroxylation: Use of a Polymer-Bound Alkaloid. *Tetrahedron Lett.* **1990**, *31*, 3003–3006.
33. Tse, M. K.; Schröder, K.; Beller, M. Recent Developments in Metal-catalyzed Dihydroxylation of Alkenes. In *Modern Oxidation Methods*; Bäckvall, J.-E., Ed.; Wiley-VCH Verlag, 2010.
34. Severeys, A.; De Vos, D. E.; Jacobs, P. A. Towards Heterogeneous and Green Versions of Os Dihydroxylation. *Top. Catal.* **2002**, *19*, 125–131.
35. Köckritz, A.; Bartoszek, M.; Döbler, C.; Beller, M.; Mägerlein, W.; Militzer, H.-C. Development of Protocols for the Separation of Os Catalysts From Organic Products in the Catalytic Dihydroxylation of Olefins. *J. Mol. Catal. A Chem.* **2004**, *218*, 55–66.
36. Caps, V.; Paraskevas, I.; Tsang, S. C. A Surface and Catalytic Study Of Heterogenised  $\text{Os}_3(\text{CO})_{12}$  Species in MCM-41 Structures. *Appl. Catal. A Gen.* **2003**, *252*, 37–49.
37. Severeys, A.; De Vos, D. E.; Fiermans, L.; Verpoort, F.; Grobet, P. J.; Jacobs, P. A. A Heterogeneous *cis*-Dihydroxylation Catalyst with Stable, Site-Isolated Osmium  $\pm$  Diolate Reaction Centers. *Angew. Chem. Int. Ed.* **2001**, *40*, 586–589.
38. Severeys, A.; De Vos, D. E.; Jacobs, P. A. Development of a Heterogeneous *cis*-Dihydroxylation Process With Hydrogen Peroxide as Oxidant. *Green Chem.* **2002**, *4*, 380–384.
39. Fujita, K.; Umeki, S.; Yasuda, H. Magnetically Recoverable Osmium Catalysts with Osmium–Diolate Esters for Dihydroxylation of Olefins. *Synlett* **2013**, *24*, 947–950.
40. Cano, R.; Pérez, J. M.; Ramón, D. J. Osmium Impregnated on Magnetite as a Heterogeneous Catalyst for the *Syn*-Dihydroxylation of Alkenes. *Appl. Catal. A Gen.* **2014**, *470*, 177–182.
41. Choudary, B. M.; Chowdari, N. S.; Kantam, M. L.; Raghavan, K. V. Catalytic Asymmetric Dihydroxylation of Olefins with New Catalysts: The First Example of Heterogenization of  $\text{OsO}_4^2-$  by Ion-Exchange Technique. *J. Am. Chem. Soc.* **2001**, *123*, 9220–9221.
42. Choudary, B. M.; Chowdari, N. S.; Jyothi, K.; Kantam, M. L. Catalytic Asymmetric Dihydroxylation of Olefins with Reusable  $\text{OsO}_4^2-$  on Ion-Exchangers: The Scope and Reactivity Using Various Cooxidants. *J. Am. Chem. Soc.* **2002**, *124*, 5341–5349.
43. Choudary, B. M.; Chowdari, N. S.; Jyothi, K.; Kantam, M. L. MCM-41 Anchored Cinchona Alkaloid for Catalytic Asymmetric Dihydroxylation of Olefins: A Clean Protocol for Chiral Diols Using Molecular Oxygen. *Catal. Lett.* **2002**, *82*, 99–102.

44. Choudary, B. M.; Chowdari, N. S.; Jyothi, K.; Madhi, S.; Kantam, M. L. Silica Gel-Supported Cinchona Alkaloid-OsO<sub>4</sub> Complex for Catalytic Heterogeneous Asymmetric Dihydroxylation of Olefins by H<sub>2</sub>O<sub>2</sub> using a Titanium Silicalite-Based Coupled Catalytic System. *Adv. Synth. Catal.* **2002**, *344*, 503–506.
45. Choudary, B. M.; Jyothi, K.; Madhi, S.; Kantam, M. L. Catalytic Asymmetric Dihydroxylation of Aliphatic Olefins with Reusable Resin-Osmium Tetroxide. *Adv. Synth. Catal.* **2003**, *345*, 1190–1192.
46. Choudary, B. M.; Jyothi, K.; Kantam, M. L.; Sreedhar, B. Achiral Dihydroxylation of Olefins by Osmate (OsO<sub>4</sub><sup>2-</sup>) Stabilised on Nanocrystalline Magnesium Oxide. *Adv. Synth. Catal.* **2004**, *346*, 45–48.
47. Shilpa, N.; Manna, J.; Rana, R. K. Bioinspired Nanoparticle-Assembly Route to a Hybrid Scaffold: Designing a Robust Heterogeneous Catalyst for Asymmetric Dihydroxylation of Olefins. *Eur. J. Inorg. Chem.* **2015**, 4965–4970.
48. Metin, Ö.; Alp, N. A.; Akbayrak, S.; Biçer, A.; Gültekin, M. S.; Özkaz, S.; Bozkaya, U. Dihydroxylation of Olefins Catalyzed by Zeolite-Confined Osmium(0) Nanoclusters: An Efficient and Reusable Method for the Preparation of 1,2-cis-Diols. *Green Chem.* **2012**, *14*, 1488–1492.
49. Qi, X.; Yoon, H.; Lee, S.-H.; Yoon, J.; Kim, S.-J. Surface-Modified Imogolite by 3-APS–OsO<sub>4</sub> Complex: Synthesis, Characterization and Its Application in the Dihydroxylation of Olefins. *J. Ind. Eng. Chem.* **2008**, *14*, 136–141.
50. Basavaraju, K. C.; Sharma, S.; Maurya, R. A.; Kim, D.-P. Safe Use of a Toxic Compound: Heterogeneous OsO<sub>4</sub> Catalysis in a Nanobrush Polymer Microreactor. *Angew. Chem. Int. Ed.* **2013**, *52*, 6735–6738.
51. Caps, V.; Paraskevas, I.; Tsang, S. C. Unexpectedly Superior Enantioselectivity for Trans-Stilbene cis-Dihydroxylation Over Anchored Triosmium Carbonyl Species in Confined Al-MCM-41 Channels. *Chem. Commun.* **2005**, 1781–1783.
52. Blumberg, S.; Martin, S. F. Racemic or Enantioselective Osmium-Catalyzed Dihydroxylation of Olefins Under Near-Neutral Conditions. *ARKIVOC* **2021**, *5*, 7–14.
53. Shi, X.-Y.; Wang, P.-M.; Liu, K.-Y.; Dong, X.-F.; Han, X.-Y.; Wei, J.-F. Peroxophosphonate Held in an Ionic Liquid Brush: An Efficient and Reusable Catalyst for the Dihydroxylation of Olefins With H<sub>2</sub>O<sub>2</sub> in Neat Water. *Appl. Organomet. Chem.* **2014**, *28*, 760–763.
54. Han, Q.; He, C.; Zhao, M.; Qi, B.; Niu, J.; Duan, C. Engineering Chiral Polyoxometalate Hybrid Metal–Organic Frameworks for Asymmetric Dihydroxylation of Olefins. *J. Am. Chem. Soc.* **2013**, *135*, 10186–10189.
55. Branytska, O.; Neumann, R. Aerobic Oxidation of Alkenes to Esters of Vicinal Diols with a *syn*-Configuration Catalyzed by I<sub>2</sub> and the H<sub>3</sub>PV<sub>2</sub>Mo<sub>10</sub>O<sub>40</sub> Polyoxometalate. *Synlett* **2005**, *16*, 2525–2527.
56. Tsuji, J.; Nagashima, H.; Nemoto, H. A General Synthetic Method for the Preparation of Methyl Ketones from Terminal Olefins: 2-Decanone. *Org. Synth.* **1984**, *62*, 9.
57. Jira, R. Acetaldehyd aus Ethylen—Ein Rückblick auf die Entdeckung des Wacker-Verfahrens. *Angew. Chem.* **2009**, *121*, 9196–9199.
58. Kulkarni, M. G.; Shaikh, Y. B.; Borhade, A. S.; Chavhan, S. W.; Dhondge, A. P.; Gaikwad, D. D.; Desai, M. P.; Birhade, D. R.; Dhattrak, N. R. Greening the Wacker Process. *Tetrahedron Lett.* **2013**, *54*, 2293–2295.
59. Gao, X.; Zhou, J.; Peng, X. Efficient Palladium(0) Supported on Reduced Graphene Oxide for Selective Oxidation of Olefins Using Graphene Oxide as a ‘Solid Weak Acid’. *Catal. Commun.* **2019**, *122*, 73–78.

60. Xia, X.; Gao, X.; Xu, J.; Hu, C.; Peng, X. Selective Oxidation of Styrene Derivatives to Ketones over Palladium(0)/Carbon With Hydrogen Peroxide as the Sole Oxidant. *Synlett* **2017**, 28, 607–610.
61. Borah, P.; Zhao, Y.  $\beta$ -Diketimine Appended Periodic Mesoporous Organosilica as a Scaffold for Immobilization of Palladium Acetate: An Efficient Green Catalyst for Wacker Type Reaction. *J. Catal.* **2014**, 318, 43–52.
62. Cao, H.; Jiang, H.; Yuan, G.; Chen, Z.; Qi, C.; Huang, H. Nano-Cu O-Catalyzed Formation of C-C and C-O Bonds: One-Pot Domino Process for Regioselective Synthesis of  $\alpha$ -Carbonyl Furans from Electron-Deficient Alkynes and 2-Yn-1-ols. *Chem. Eur. J.* **2010**, 16, 10553–10559.
63. Cousin, T.; Chatel, G.; Kardos, N.; Andrioletti, B.; Draye, M. Recent Trends in the Development of Sustainable Catalytic Systems for the Oxidative Cleavage of Cycloalkenes by Hydrogen Peroxide. *Catal. Sci. Technol.* **2019**, 9, 5256–5278.
64. Inchaurredo, N.; di Luca, C.; Zerjav, G.; Grau, J. M.; Pintar, A.; Haure, P. Catalytic Ozonation of Azo-Dye Using Natural Aluminosilicate. *Catal. Today* **2021**, 361, 24–29.
65. Cousin, T.; Chatel, G.; Andrioletti, B.; Draye, M. Oxidative Cleavage of Cycloalkenes Using Hydrogen Peroxide and a Tungsten-Based Catalyst: Towards a Complete Mechanistic Investigation. *New J. Chem.* **2021**, 45, 235–242.
66. Schäfer, C.; Ellstrom, C. J.; Török, B. Heterogeneous Catalytic Aqueous Phase Oxidative Cleavage of Styrenes to Benzaldehydes: An Environmentally Benign Alternative to Ozonolysis. *Top. Catal.* **2018**, 61, 643–651.
67. Escande, V.; Lam, C. H.; Grison, C.; Anastas, P. T. EcoMnOx, a Biosourced Catalyst for Selective Aerobic Oxidative Cleavage of Activated 1,2-Diols. *ACS Sustain. Chem. Eng.* **2017**, 5, 3214–3222.
68. Escande, V.; Lam, C. H.; Coish, P.; Anastas, P. T. Heterogeneous Sodium-Manganese Oxide Catalyzed Aerobic Oxidative Cleavage of 1,2-Diols. *Angew. Chem. Int. Ed.* **2017**, 56, 9561–9565.
69. Lam, C. H.; Escande, V.; Mellor, K. E.; Zimmerman, J. B.; Anastas, P. T. Teaching Atom Economy and E-Factor Concepts through a Green Laboratory Experiment: Aerobic Oxidative Cleavage of meso-Hydrobenzoin to Benzaldehyde Using a Heterogeneous Catalyst. *J. Chem. Educ.* **2019**, 96, 761–765.
70. Ha, Y.; Mu, M.; Liu, Q.; Ji, N.; Song, C.; Ma, D. Mn-MIL-100 Heterogeneous Catalyst for the Selective Oxidative Cleavage of Alkenes to Aldehydes. *Catal. Commun.* **2018**, 103, 51–55.
71. Liu, C.; Mao, J.; Zhang, X.; Yu, L. Selenium-Doped Fe<sub>2</sub>O<sub>3</sub>-Catalyzed Oxidative Scission of C=C Bond. *Catal. Commun.* **2020**, 133, 105828.
72. Dai, W.-L.; Chen, H.; Cao, Y.; Li, H.; Xie, S.; Fan, K. Novel Economic and Green Approach to the Synthesis of Highly Active W-MCM41 Catalyst in Oxidative Cleavage of Cyclopentene. *Chem. Commun.* **2003**, 7, 892–893.
73. Upadhyaya, D. J.; Samant, S. D. New Insights Into the Bifunctionality of Vanadium Phosphorous Oxides: A Chemical Switch Between Oxidative Scission and Pinacol Rearrangement of Vicinal Diols. *Catal. Today* **2013**, 218, 60–65.
74. Heravi, M. M.; Ranjbar, L.; Derikvand, F.; Oskooie, H. A.; Bamoharram, F. F. Catalytic Oxidative Cleavage of C=N Bond in the Presence Of Mixed-Addenda Vanadomolybdophosphate, H<sub>6</sub>PMo<sub>9</sub>V<sub>3</sub>O<sub>40</sub> as a Green and Reusable Catalyst. *J. Mol. Catal. A Chem.* **2007**, 265, 186–188.
75. Teng, Q.-H.; Sun, Y.; Yao, Y.; Tang, H.-T.; Li, J.-R.; Pan, Y.-M. Metal- and Catalyst-Free Electrochemical Synthesis of Quinazolinones from Alkenes and 2-Aminobenzamides. *ChemElectroChem* **2019**, 6, 3120–3124.

76. Meng, L.; Zhai, S.; Sun, Z.; Zhang, F.; Xiao, Z.; An, Q. Green and Efficient Synthesis of Adipic Acid From Cyclohexene Over Recyclable  $\text{H}_3\text{PW}_4\text{O}_{24}/\text{PEHA}/\text{ZrSBA-15}$  With Platelet Morphology. *Microporous Mesoporous Mater.* **2015**, *204*, 123–130.
77. Yoshimura, Y.; Ogasawara, Y.; Suzuki, K.; Yamaguchi, K.; Mizuno, N. “Release and Catch” Catalysis by Tungstate Species for the Oxidative Cleavage of Olefins. *Catal. Sci. Technol.* **2017**, *7*, 1622–1670.
78. Zhan, H.; Liu, W.; Fu, M.; Cen, J.; Lin, J.; Cao, H. Carbon Nitride-Catalyzed Oxidative Cleavage of Carbon–Carbon Bond of  $\alpha$ -Hydroxy Ketones With Visible Light and Thermal Radiation. *Appl. Catal. A Gen.* **2013**, *468*, 184–189.
79. El Aakel, L.; Launay, F.; Brégeault, J.-M.; Atlamsani, A. Nafion®-Supported Vanadium Oxidation Catalysts: Redox Versus Acid-Catalysed Ring Opening of 2-Substituted Cycloalkanes by Dioxigen. *J. Mol. Catal. A Chem.* **2004**, *212*, 171–182.
80. Hattori, T.; Okami, H.; Ichikawa, T.; Mori, S.; Sawama, Y.; Monguchi, Y.; Sajiki, H. Ruthenium on Carbon Catalysed Carbon–Carbon Cleavage of Aryl Alkyl Ketones and Aliphatic Aldehydes in Aqueous Media. *Adv. Synth. Catal.* **2017**, *359*, 3490–3495.
81. Rakibuddin, M.; Gazi, S.; Ananthkrishnan, R. Iron(II) Phenanthroline-Resin Hybrid as a Visible Light-Driven Heterogeneous Catalyst for Green Oxidative Degradation of Organic Dye. *Catal. Commun.* **2015**, *58*, 53–58.
82. Ray, S.; Das, P.; Banerjee, B.; Bhaumik, A.; Mukhopadhyay, C. Piperazinylypyrimidine Modified MCM-41 for the Ecofriendly Synthesis of Benzothiazoles by the Simple Cleavage of Disulfide in the Presence of Molecular  $\text{O}_2$ . *RSC Adv.* **2015**, *5*, 72745–72754.
83. Wetzal, A.; Jones, A. M. Electrically Driven N ( $\text{sp}^2$ )–C( $\text{sp}^{2.3}$ ) Bond Cleavage of Sulfonamides. *ACS Sustain. Chem. Eng.* **2020**, *8*, 3487–3493.
84. Adeli, Y.; Huang, K.; Liang, Y.; Jiang, Y.; Liu, J.; Song, S.; Zeng, C.-C.; Jiao, N. Electrochemically Oxidative C–C Bond Cleavage of Alkylarenes for Anilines Synthesis. *ACS Catal.* **2019**, *9*, 2063–2067.
85. Yao, X.; Bai, C.; Chen, J.; Li, Y. Efficient and Selective Green Oxidation of Alcohols by MOF-Derived Magnetic Nanoparticles as a Recoverable Catalyst. *RSC Adv.* **2016**, *6*, 26921–26928.
86. Kumar, N.; Naveen, K.; Bhatia, A.; Muthaiah, S.; Siruguri, V.; Paul, A. K. Solvent and Additive-Free Efficient Aerobic Oxidation of Alcohols by a Perovskite Oxide-Based Heterogeneous Catalyst. *React. Chem. Eng.* **2020**, *5*, 1264–1271.
87. Tan, J.; Liu, X. B.; Chen, W. F.; Hu, Y. L. Synthesis of Magnetically Separable Nanocatalyst  $\text{CoFe}_2\text{O}_4@/\text{SiO}_2@/\text{MIL-53}(\text{Fe})$  for Highly Efficient and Selective Oxidation of Alcohols and Benzylic Compounds with Hydrogen Peroxide. *ChemistrySelect* **2019**, *4*, 8477–8481.
88. Shokouhimehr, M.; Yek, S. M.-G.; Nasrollahzadeh, M.; Kim, A.; Varma, R. S. Palladium Nanocatalysts on Hydroxyapatite: Green Oxidation of Alcohols and Reduction of Nitroarenes in Water. *Appl. Sci.* **2019**, *9*, 4183.
89. Kidwai, M.; Bhardwaj, S.; Jain, A. A Green Oxidation Protocol for the Conversion of Secondary Alcohols Into Ketones Using Heterogeneous Nanocrystalline Titanium (IV) Oxide in Polyethylene Glycol. *Green Chem. Lett. Rev.* **2012**, *5*, 195–202.
90. Abedi, S.; Morsali, A. Ordered Mesoporous Metal–Organic Frameworks Incorporated with Amorphous  $\text{TiO}_2$  As Photocatalyst for Selective Aerobic Oxidation in Sunlight Irradiation. *ACS Catal.* **2014**, *4*, 1398–1403.
91. Farhadi, S.; Afshari, M.; Maleki, M.; Babazadeh, Z. Photocatalytic Oxidation of Primary and Secondary Benzylic Alcohols to Carbonyl Compounds Catalyzed by  $\text{H}_3\text{PW}_{12}\text{O}_{40}/\text{SiO}_2$  under an  $\text{O}_2$  atmosphere. *Tetrahedron Lett.* **2005**, *46*, 8483–8486.

92. Auguliaro, V.; Palmisano, L. Green Oxidation of Alcohols to Carbonyl Compounds by Heterogeneous Photocatalysis. *ChemSusChem* **2010**, *3*, 1135–1138.
93. Farhadi, S.; Momeni, Z. Zirconia-Supported Sodium Decatungstate ( $\text{Na}_4\text{W}_{10}\text{O}_{32}/\text{ZrO}_2$ ): An Efficient, Green and Recyclable Photocatalyst for Selective Oxidation of Activated Alcohols to Carbonyl Compounds with  $\text{O}_2$ . *J. Mol. Catal. A Chem.* **2007**, *277*, 47–52.
94. Maleki, A. Green Oxidation Protocol: Selective Conversions of Alcohols and Alkenes to Aldehydes, Ketones and Epoxides by Using a New Multiwall Carbon Nanotube-Based Hybrid Nanocatalyst via Ultrasound Irradiation. *Ultrason. Sonochem.* **2018**, *40*, 460–464.
95. Pathak, C.; Borah, G. Green Synthesis of Pd@rGO Nanocomposite Using Piper (*Piper nigrum*) Leaf Extract and Its Catalytic Activity Towards Alcohol Oxidation in Water at Room Temperature. *Mater. Res. Express* **2019**, *6*, 125011.
96. Darvishi, K.; Amani, K.; Rezaei, M. Preparation, Characterization and Heterogeneous Catalytic Applications of  $\text{GO}/\text{Fe}_3\text{O}_4/\text{HPW}$  Nanocomposite in Chemoselective and Green Oxidation Of Alcohols With Aqueous  $\text{H}_2\text{O}_2$ . *Appl. Organomet. Chem.* **2018**, *32*, e4323.
97. Noghi, S. A.; Naeimi, A.; Hamidian, H. First Electrospun Immobilized Molybdenum Complex on Bio Iron Oxide Nanofiber for Green Oxidation of Alcohols. *Polymer* **2018**, *149*, 229–237.
98. Choudhary, D.; Paul, S.; Gupta, R.; Clark, J. H. Catalytic Properties of Several Palladium Complexes Covalently Anchored Onto Silica for the Aerobic Oxidation of Alcohols. *Green Chem.* **2006**, *8*, 479–482.
99. Chauhan, P.; Yan, N. Nanocrystalline Cellulose Grafted Phthalocyanine: A Heterogeneous Catalyst for Selective Aerobic Oxidation of Alcohols and Alkyl Arenes at Room Temperature in a Green Solvent. *RSC Adv.* **2015**, *5*, 37517–37520.
100. Ibrahim, I.; Iqbal, M. N.; Verho, O.; Eivazihollagh, A.; Olsén, P.; Edlund, H.; Tai, C.-W.; Norgren, M.; Johnston, E. V. Copper Nanoparticles on Controlled Pore Glass and TEMPO for the Aerobic Oxidation of Alcohols. *ChemNanoMat* **2018**, *4*, 71–75.
101. Mao, F.; Qi, Z.; Fan, H.; Sui, D.; Chen, R.; Huang, J. Heterogeneous Cobalt Catalysts for Selective Oxygenation of Alcohols to Aldehydes, Esters and Nitriles. *RSC Adv.* **2017**, *7*, 1498–1503.
102. Nielsen, I. S.; Taarning, E.; Egeblad, K.; Madsen, R.; Christensen, C. H. Direct Aerobic Oxidation of Primary Alcohols to Methyl Esters Catalyzed by a Heterogeneous Gold Catalyst. *Catal. Lett.* **2007**, *116*, 35–40.
103. Meng, X.; Bi, X.; Chen, G.; Chen, B.; Zhao, P. Heterogeneous Esterification from  $\alpha$ -Hydroxy Ketone and Alcohols through a Tandem Oxidation Process over a Hydrotalcite-Supported Bimetallic Catalyst. *Org. Process. Res. Dev.* **2018**, *22*, 1716–1722.
104. Ghorbanloo, M.; Heydari, A.; Yahiro, H. Ag-Nanoparticle Embedded p(AA) Hydrogel as an Efficient Green Heterogeneous Nano-Catalyst for Oxidation and Reduction of Organic Compounds. *Appl. Organomet. Chem.* **2018**, *32*, e3917.
105. Soulé, J. F.; Miyamura, H.; Kobayashi, S. Powerful Amide Synthesis from Alcohols and Amines under Aerobic Conditions Catalyzed by Gold or Gold/Iron, -Nickel or -Cobalt Nanoparticles. *J. Am. Chem. Soc.* **2011**, *133*, 18550–18553.
106. Soulé, J. F.; Miyamura, H.; Kobayashi, S. Direct Amidation from Alcohols and Amines through a Tandem Oxidation Process Catalyzed by Heterogeneous-Polymer-Incarcerated Gold Nanoparticles under Aerobic Conditions. *Chem. Asian J.* **2013**, *8*, 2614–2626.
107. Kidwai, M.; Bhardwaj, S. Transformation of Amines to Oximes Using Heterogeneous Nanocrystalline Titanium(IV) Oxide as a Green Catalyst. *Synth. Commun.* **2011**, *41*, 2655–2662.
108. Zhu, P.; Zhang, J.; Wang, J.; Kong, P.; Wang, J.; Zheng, Z. Photocatalytic Selective Aerobic Oxidation of Amines to Nitriles Over  $\text{Ru}/\gamma\text{-Al}_2\text{O}_3$ : The Role of the Support Surface and the Strong Imine Intermediate Adsorption. *Catal. Sci. Technol.* **2020**, *10*, 440–449.

276 Heterogeneous catalysis in sustainable synthesis

109. Choudary, B. M.; Bharathi, B.; Venkat Reddy, C.; Lakshmi Kantam, M. The First Example Of Heterogeneous Oxidation of Secondary Amines by Tungstate-Exchanged Mg–Al Layered Double Hydroxides: A Green Protocol. *Green Chem.* **2002**, *4*, 279–284.
110. Choudary, B. M.; Bharathi, B.; Venkat Reddy, C.; Lakshmi Kantam, M.; Raghavan, K. V. The First Example of Catalytic N-Oxidation of Tertiary Amines by Tungstate-Exchanged Mg–Al Layered Double Hydroxide in Water: A Green Protocol. *Chem. Commun.* **2001**, *18*, 1736–1737.
111. Landge, S. M.; Atanassova, V.; Thimmaiah, M.; Török, B. Microwave-Assisted Oxidative Coupling of Amines to Imines on Solid Acid Catalysts. *Tetrahedron Lett.* **2007**, *48*, 5161–5164.
112. Atanassova, V.; Ganno, K.; Kulkarni, A.; Landge, S. M.; Curtis, S.; Foster, M.; Török, B. Mechanistic Study on the Oxidative Coupling of Amines to Imines on K-10 Montmorillonite. *Appl. Clay Sci.* **2011**, *53*, 220–226.
113. Venu, B.; Shirisha, V.; Vishali, B.; Naresh, G.; Kishore, R.; Sreedhar, I.; Venugopal, A. Cu-BTC Metal-Organic Framework (MOF) as an Efficient Heterogeneous Catalyst for Aerobic Oxidative Synthesis of Imines From Primary Amines Under Solvent Free Conditions. *New J. Chem.* **2020**, *44*, 5972–5979.
114. Chen, F.; Yang, T.; Zhao, S.; Jiang, T.; Yu, L.; Xiong, H.; Guo, C.; Rao, Y.; Liu, Y.; Liu, L.; Zhou, J.; Tu, P.; Ni, J.; Zhang, Q.; Li, X. Highly Selective Oxidation of Amines to Imines by Mn<sub>2</sub>O<sub>3</sub> Catalyst Under Eco-friendly Conditions. *Chin. Chem. Lett.* **2019**, *30*, 2282–2286.
115. Biswas, S.; Dutta, B.; MULLICK, K.; Kuo, C.-H.; Poyraz, A. S.; Suib, S. L. Aerobic Oxidation of Amines to Imines by Cesium-Promoted Mesoporous Manganese Oxide. *ACS Catal.* **2015**, *5*, 4394–4403.
116. Rostamizadeh, S.; Nojavan, M.; Aryan, R.; Isapoor, E.; Azad, M. Amino Acid-Based Ionic Liquid Immobilized on  $\alpha$ -Fe<sub>2</sub>O<sub>3</sub>-MCM-41: An Efficient Magnetic Nanocatalyst and Recyclable Reaction Media for the Synthesis of Quinazolin-4(3H)-One Derivatives. *J. Mol. Catal. A Chem.* **2013**, *374*-375, 102–110.
117. Heravi, M. M.; Oskooie, H. A.; Malakooti, R.; Alimadadi, B.; Alinejad, H.; Behbahani, F. K. Oxidative Aromatization of Hantzsch 1,4-Dihydropyridines in the Presence of a Catalytic Amount of Mn(pbdo)<sub>2</sub>Cl<sub>2</sub>/MCM-41 or Mn(pbdo)<sub>2</sub>Cl<sub>2</sub>/Al-MCM-41 as Reusable and Green Catalysts. *Catal. Commun.* **2009**, *10*, 819–822.
118. De Paolis, O.; Baffoe, J.; Landge, S. M.; Török, B. Multicomponent Domino Cyclization–Oxidative Aromatization on a Bifunctional Pd/C/K-10 Catalyst: An Environmentally Benign Approach toward the Synthesis of Pyridines. *Synthesis* **2008**, *21*, 3423–3428.
119. Kulkarni, A.; Abid, M.; Török, B.; Huang, X. A Direct Synthesis of  $\beta$ -Carbolines Via a Three-Step One-Pot Domino Approach With a Bifunctional Pd/C/K-10 Catalyst. *Tetrahedron Lett.* **2009**, *50*, 1791–1794.
120. Landge, S. M.; Schmidt, A.; Outerbridge, V.; Török, B. Synthesis of Pyrazoles by a One-Pot Tandem Cyclization–Dehydrogenation Approach on Pd/C/K-10 Catalyst. *Synthesis* **2007**, *10*, 1600–1604.
121. Hajjami, M.; Sheikhaei, S.; Gholamian, F.; Yousofvand, Z. Synthesis and Characterization of Magnetic Functionalized Ni and Cu Nano Catalysts and Their Application in Oxidation, Oxidative Coupling and Various Multi-Component Reactions. *Catal. Lett.* **2021**, *151*, 2420–2435.
122. Kulkarni, A.; Török, B. Microwave-Assisted Multicomponent Domino Cyclization–Aromatization: An Efficient Approach for the Synthesis of Substituted Quinolines. *Green Chem.* **2010**, *12*, 875–878.

123. Zhou, W.; Tao, Q.; Sun, F.; Cao, X.; Qian, J.; Xu, J.; He, M.; Chen, Q.; Xiao, J. Additive-Free Aerobic Oxidative Dehydrogenation of N-Heterocycles Under Catalysis by NiMn Layered Hydroxide Compounds. *J. Catal.* **2018**, *361*, 1–11.
124. Liao, C.; Li, X.; Yao, K.; Yuan, Z.; Chi, Q.; Zhang, Z. Efficient Oxidative Dehydrogenation of N-Heterocycles over Nitrogen-Doped Carbon-Supported Cobalt Nanoparticles. *ACS Sustainable Chem. Eng.* **2019**, *7*, 13646–13654.
125. Bi, X.; Tang, T.; Meng, X.; Gou, M.; Liu, X.; Zhao, P. Aerobic Oxidative Dehydrogenation of N-Heterocycles over OMS-2-Based Nanocomposite Catalysts: Preparation, Characterization and Kinetic Study. *Catal. Sci. Technol.* **2020**, *10*, 360–371.
126. Cui, X.; Li, Y.; Bachmann, S.; Scalone, M.; Surkus, A.-E.; Junge, K.; Topf, C.; Beller, M. Synthesis and Characterization of Iron–Nitrogen-Doped Graphene/Core–Shell Catalysts: Efficient Oxidative Dehydrogenation of N-Heterocycles. *J. Am. Chem. Soc.* **2015**, *137*, 10652–10658.
127. Ge, D.; Hu, L.; Wang, J.; Li, X.; Qi, F.; Lu, J.; Cao, X.; Gu, H. Reversible Hydrogenation–Oxidative Dehydrogenation of Quinolines over a Highly Active Pt Nanowire Catalyst under Mild Conditions. *ChemCatChem* **2013**, *5*, 2183–2186.
128. Iosub, A. V.; Stahl, S. S. Catalytic Aerobic Dehydrogenation of Nitrogen Heterocycles Using Heterogeneous Cobalt Oxide Supported on Nitrogen-Doped Carbon. *Org. Lett.* **2015**, *17*, 4404–4407.
129. Tang, T.; Bi, X.; Meng, X.; Chen, G.; Gou, M.; Liu, X.; Zhao, P. MnOx/Catechol/H<sub>2</sub>O: A Cooperative Catalytic System for Aerobic Oxidative Dehydrogenation of N-Heterocycles at Room Temperature. *Tetrahedron Lett.* **2020**, *61*, 151425.
130. Mullick, K.; Biswas, S.; Angeles-Boza, A. M.; Suib, S. L. Heterogeneous Mesoporous Manganese Oxide Catalyst for Aerobic and Additive-Free Oxidative Aromatization of N-Heterocycles. *Chem. Commun.* **2017**, *53*, 2256–2259.
131. Jin, X.; Koizumi, Y.; Yamaguchi, K.; Nozaki, K.; Mizuno, N. Selective Synthesis of Primary Anilines from Cyclohexanone Oximes by the Concerted Catalysis of a Mg–Al Layered Double Hydroxide Supported Pd Catalyst. *J. Am. Chem. Soc.* **2017**, *139*, 13821–13829.



## Chapter 3.4

# Metathesis by heterogeneous catalysts

### 3.4.1. Introduction

Metathesis constitutes a group of reactions during which unsaturated carbon-carbon bonds are rearranged, thus creating new carbon-carbon multiple bonds and/or breaking existing carbon-carbon bonds in the presence of a metal catalyst. The bond cleavage and bond forming processes are highly energy demanding, particularly those of the carbon-carbon bond, one of the most stable chemical bonds. Therefore the discovery of a method that could promote the formation of carbon-carbon bonds under mild conditions was a breakthrough in organic chemistry. The first catalyst capable of initiating alkene metathesis was discovered by Ziegler in 1952 while he was working on the oligomerization of ethylene and observed the formation of 1-butene.<sup>1</sup> However, the Ziegler catalyst exhibited poor tolerance toward the polar functional group containing substrates that are incompatible with the strong Lewis acid and alkylating properties of the metal complexes.<sup>1</sup> Later, more versatile catalysts, the metal alkylidene complexes, were introduced by Grubbs, Chauvin, and Schrock opening up an avenue of new applications in the field of metal-catalyzed reactions. As an evidence of the importance of their discovery, they were awarded the Nobel prize in chemistry in 2005.<sup>2-4</sup> Extensive studies led to several generations of catalyst with the tungsten or molybdenum alkylidene complexes developed by Schrock and coworkers<sup>5</sup> as well as the ruthenium carbene complexes developed by Grubbs and coworkers<sup>6</sup> being the most widely used. One of the remarkable industrial applications of olefin metathesis is the solvent-free transformation of seed oils to compounds that can serve as renewable sources replacing the petroleum-based products.<sup>3</sup>

Mechanistic studies led to a generally accepted reaction mechanism, also called the Chauvin mechanism, involving a series of metallocyclobutanes and carbene complexes.<sup>7</sup> In regard to the Hoveyda-Grubbs catalyst, one of the most versatile olefin metathesis catalyst, a so-called release-return (or boomerang) mechanism is believed to be involved. In the initiation step, the ligand 2-(isopropoxy)benzylidene dissociates from the metal complex and after the metathesis reaction, the released 2-(isopropoxy)styrene reacts back with the unstable  $14e^-$  ruthenium species to recreate the precatalyst.<sup>8</sup>

The numerous advantages of metathesis include: (i) low catalyst loading (typically between 1 and 5 mol%), (ii) high yields under mild conditions and relatively short times, (iii) tunable selectivity of the reaction depending on the catalyst employed, (iv) high substrate tolerance, (v) good atom economy.<sup>9</sup> In combination with heterogeneous catalysis, metathesis reactions are further improved by making possible the recyclability and higher stability of the catalytic system as well as potential applicability in continuous flow systems.<sup>10</sup> Due to its unambiguous benefits, metathesis reactions remain in the forefront of synthesis research and were frequently reviewed.<sup>1, 5, 9, 11–16</sup>

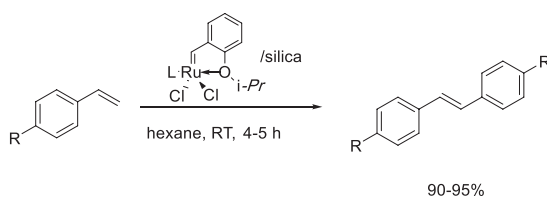
This chapter aims to review selected examples of metathesis in the context of heterogeneous catalysis. The material will be discussed in five parts according to the major types of metathesis: cross-metathesis, ring-opening and ring-closing metatheses, and alkyne metathesis; and an additional part will be dedicated to the conversion of biomass by metathesis-based transformations, a discussion that is particularly relevant in the current environmental context. It should be noted that due to the specificity of the catalysts employed for this reaction type, the literature about heterogeneous catalytic metathesis mostly utilize the well-established metal complexes immobilized on solid supports.

### 3.4.2. Cross-metathesis

Olefin cross-metathesis (CM) is defined as the intermolecular exchange of alkylidene moiety aided by a metal-carbene complex. Industrial applications of cross-metathesis, underscoring its importance, include the Shell Higher Olefin Process producing linear  $\alpha$ -olefins and the Phillips Triolefin Process producing propylene in large scale.<sup>7</sup> The earlier developed molybdenum-based catalysts were highly active for CM but lacked functional group tolerance. The second generation of catalysts now combines high activity with high substrate tolerance allowing their broad application for multiple CMs.<sup>7</sup> Given the price of ruthenium and the need for product purity, the efficient separation of the catalyst from the reaction mixture and its recycling are of key importance. Although the recycling of these catalysts has already been explored using chromatography due to their sufficient stability, the process requires organic solvent and generates significant amount of waste.<sup>17</sup> A simpler way to allow the recovery and reuse of these catalysts is to graft them onto solid supports and use a simple filtration as a separation. While the immobilization of homogeneous catalysts sometimes results in at least partial loss of activity, some methods reported efficient immobilized catalysts that retained their full potential after immobilization.

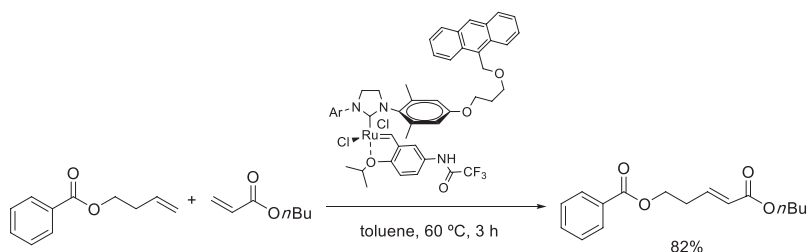
The Hoveyda-Grubbs catalysts and their derivatives are among the most employed catalysts for the adaptation of CM into heterogeneous systems. Multiple supports have been employed and involve either covalent or noncovalent bonding depending on the nature of the support and the method of preparation. The wide range of available immobilized Hoveyda-Grubbs catalysts offers different activity, stability, and recyclability profiles.

Silica-supported catalysts have been studied extensively. For instance, the second generation Hoveyda-Grubbs catalyst was immobilized on silica. It was prepared in a straightforward method either using silica pellets or silica powder in one step, and was efficient for various CM reactions and the products obtained revealed very low Ru contamination (ppb level) (Scheme 1).<sup>18</sup> A continuous flow reaction further demonstrated the robustness of the catalyst. Although the anchoring mechanism was not fully elucidated, it was suggested that the catalyst was attached to the surface of silica via ligand exchange.



**SCHEME 1** Heterogeneous catalytic cross-metathesis using a silica-supported Hoveyda-Grubbs catalyst.

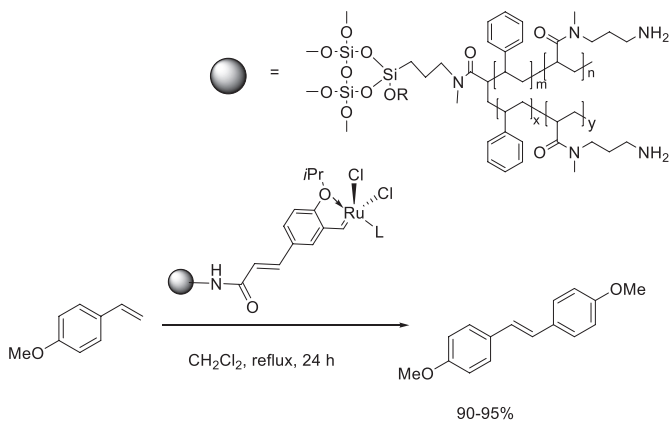
A more complex catalyst structure derived from the Hoveyda-Grubbs catalyst, possessing an anthracene group linked to the *N*-heterocyclic carbene moiety of the Ru complex, was immobilized by charge-transfer interactions to a 2,4,7-trinitrofluoren-9-one-grafted on passivated silica.<sup>19</sup> The resulting solid catalyst was active in the CM of but-3-en-1-yl benzoate with butyl acrylate (Scheme 2). It was recyclable in three cycles after which deactivation was observed; the support, however, could be washed and used for another three cycles after loading a new batch of fresh catalyst.



**SCHEME 2** Heterogeneous catalytic cross-metathesis using a silica-supported anthracene-tagged Ru complex.

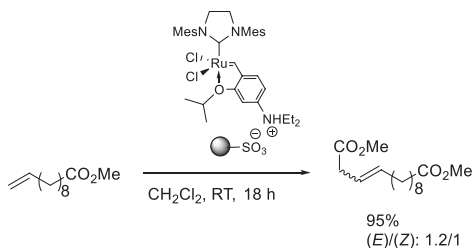
An interesting study by Michalek et al. compared the activity of Hoveyda-Grubbs catalyst when bound to different supports.<sup>20</sup> The metal complex was covalently attached via an amide bond to four selected supports: a hybrid polymer-silica support, HypoGel400 which is a polystyrene, bearing oligomeric units, PEGA—a poly(acrylamide) interspaced with poly(ethylene glycol) units, and Trisoperl—an aminopropylated silica gel. It was reported that the

performance of the catalysts was highly dependent on the nature of the solid support employed. The hybrid silica-based material successfully catalyzed the CM reaction of substituted aromatic alkenes and provided the best results (Scheme 3). It should be noted that low catalyst leaching was observed.



**SCHEME 3** Heterogeneous catalytic cross-metathesis 4-methoxy-styrene on a hybrid silica-supported Hoveyda-Grubbs catalyst.

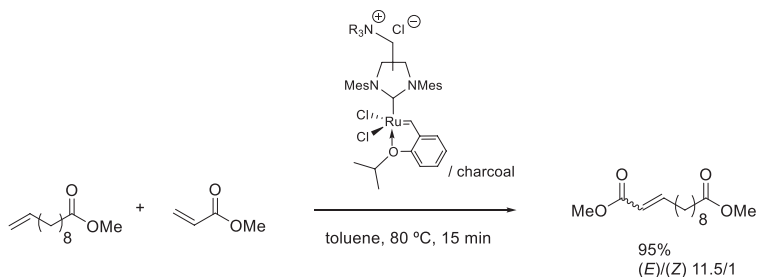
Noncovalent immobilization of a Hoveyda-Grubbs catalyst analog was also achieved by means of electrostatic binding after introduction of amino groups and subsequent treatment with sulfonated polystyrene (Scheme 4).<sup>21</sup> For industrial application purposes, the polymerization process could be carried out inside porous Raschig glass rings, protecting the polymeric phase from mechanical stress. In addition, the rings allowed easy removal of the solid phase. The homo CM of alkenes was successfully achieved and yielded 95% product.



**SCHEME 4** Heterogeneous catalytic cross-metathesis of long chain alkenes by a sulfonated polystyrene-supported Hoveyda-Grubbs catalyst.

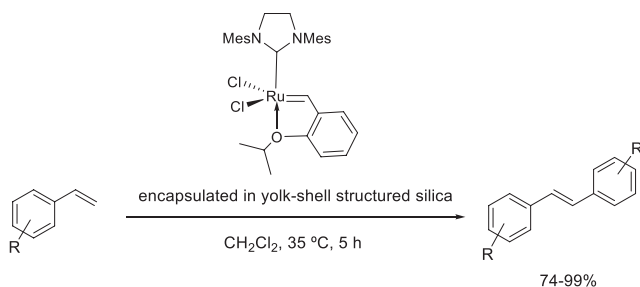
An ammonium-tagged NHC ligand bound to the catalytic complex deposited on various supports provided interesting properties depending on the nature of the solid support (Scheme 5).<sup>22</sup> Both organic and inorganic supports were

considered, including activated carbon, silica, alumina, cotton, paper, and magnetic nanoparticles. The most efficient immobilized catalysts were found to be silica and charcoal-supported Ru complexes. While the iron powder-supported counterpart was slightly less effective, it allowed for easy recovery upon application of a magnet, an important feature worth considering when taking separability and recyclability into account.



**SCHEME 5** Cross-metathesis catalyzed by a Ru complex bearing a quaternary ammonium-tagged NHC ligand supported on charcoal.

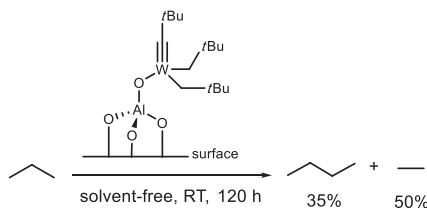
The same Ru complex was also successfully encapsulated within yolk-shell structured silica.<sup>23</sup> Excellent activity was observed due in part to the combination of a hollow structure in the core and the microporous permeable shell. The CM of various aromatic alkenes was achieved in high yields under mild temperature (Scheme 6). In addition, the catalyst was recovered and recycled for eight consecutive reactions. The preparation of yolk-shell structured mesoporous silica as well as the encapsulation of the catalyst required minimal amount of toxic chemicals, involved moderate temperatures, and were completed in a reasonable timeframe. Thus the yolk-shell structure silica scaffold appears to be a promising material to produce solid catalyst from the homogeneous form of metal complexes.



**SCHEME 6** Cross-metathesis reaction of various aromatic alkenes over the yolk-shell structure silica-encapsulated Ru catalyst.

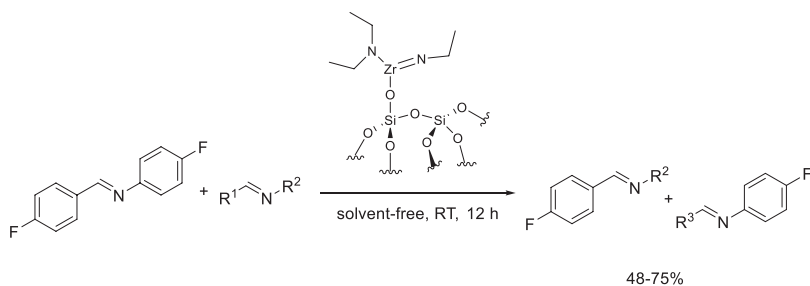


Another common strategy to immobilize homogeneous catalysts is to graft the metal complex to silica or alumina via direct covalent bond between the metal and metal oxide. The grafting of a tungsten-based complex on alumina proved to be highly efficient to perform the uncommon alkane metathesis of propane (Scheme 9).<sup>26</sup> The catalyst also provided good product selectivity in favor of ethane. It was proposed that alkane metathesis proceeded via carbene and metallacyclobutane intermediates. The same group later further extended these investigations to a comparative study with alumina and silica-supported tungsten-based Schrock catalyst, reporting similar observations in greater details.<sup>27, 28</sup> In addition, in a follow-up investigation, a partially dehydrated (at 700°C) silica-supported tungsten-imido carbene complex was found to be a well-defined heterogeneous alkene metathesis catalyst.<sup>29</sup> It was characterized by mass balance analysis, IR and <sup>1</sup>H and <sup>13</sup>C-MAS NMR spectroscopies, EXAFS, as well as DFT calculations. The performance of the catalyst was reported to be excellent in the cross-metathesis of propene, providing a TON of 16,000 in a 100 h reaction and only a slow deactivation of the catalyst was observed.<sup>30</sup> A related study describes the characterization of such surface-anchored organometallic complex-based catalysts via resolution enhancement in <sup>1</sup>H solid state NMR spectroscopy.<sup>31</sup> Later it was found that the introduction of bulky 2,6-diadamantylaryloxy ligands stabilized the immobilized complex and the improved catalyst was able to produce over 75,000 TON when ethylene was continuously removed from the system.<sup>32</sup> Further characterization of these silica-supported catalysts was carried out by the combination of solid state NMR spectroscopy and DFT calculations.<sup>33, 34</sup>



**SCHEME 9** Heterogeneous catalytic propane metathesis by an alumina-supported W complex.

Hamzaoui et al. reported the use of silica-supported zirconium-imido complexes to catalyze the little known heterogeneous imine metathesis using the metal/metal oxide bonding strategy (Scheme 10).<sup>35</sup> The reaction of the complex with an imine resulted in the exchange of the imide/imine groups leading to the metathesis products. The catalyst could be recycled for several cycles; however, it required a washing and vacuum drying steps in between each cycle.



**SCHEME 10** Heterogeneous catalytic imine metathesis by a silica-supported Zr catalyst.

Highly active heterogeneous metathesis catalysts based on Re, W, or Mo complexes were grafted on silica with a similar strategy relying on surface organometallic chemistry.<sup>36–39</sup> Mixing  $\text{SiO}_{2-700}$  and the  $\text{Re}(\text{CBu-}t)(\text{CH Bu-}t)(\text{CH}_2\text{Bu-}t)_2$  complex in pentane for 2 h at ambient temperature afforded the immobilized catalyst after washing the compound obtained and drying it under vacuum.<sup>38</sup> Similar Mo and W heterogeneous catalysts were prepared by substituting the hydroxyl groups of silica by hydroquinone moieties via a simple two-step synthesis from a tungsten perhydrocarbenyl and molybdenum bispyrrolide alkylidene complex and  $\text{SiO}_{2-700}$  as precursors as well as other inexpensive and readily available reagents.<sup>39</sup> The solid catalysts, depicted in Fig. 1, were highly active for the metathesis of propene. The Re-based catalyst achieved equilibrium within less than an hour in presence of 500 equivalent of propene.<sup>38</sup> The other two catalysts containing a phenolic spacer between the active metal center and the surface of silica showed enhanced stereoselectivity toward the (*Z*)-isomer and improved catalytic activity compared to the homogeneous counterparts.<sup>39</sup> A similar series of catalysts was prepared by using tungsten-imido-carbene complexes immobilized on silica that was partially dehydroxylated at significantly lower temperature ( $200^\circ\text{C}$ )<sup>40</sup> as

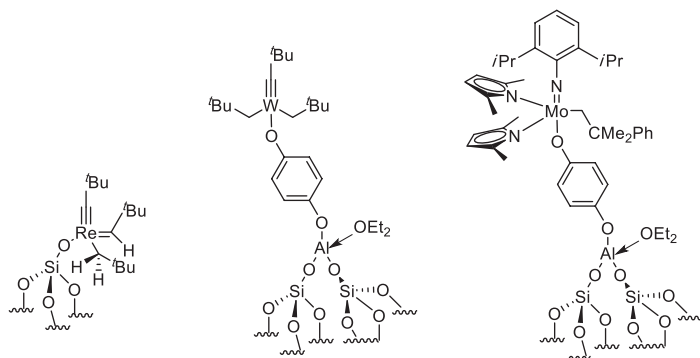


**FIG. 1** Heterogeneous catalysts for olefin metathesis prepared via surface organometallic chemistry.

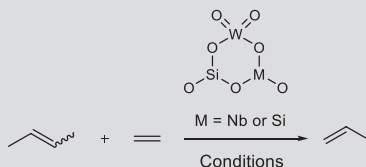
compared to some earlier examples.<sup>30,39</sup> This process led to the expected digrafted carbene species, as well as to the monografted carbene complex and to a bis-neopentyl surface species as determined by IR-, 1D and 2D solid state NMR spectroscopies, elemental analysis, and molecular models. The grafting mechanism, used during the preparation of these silica-supported Mo complex catalysts, and their activity in olefin metathesis were also studied.<sup>41</sup>

In an interesting mechanistic study, Salameh et al. described a simple alumina-supported Re(VII) oxide catalyst ( $\text{Re}_2\text{O}_7/\text{Al}_2\text{O}_3$ ) that efficiently catalyzed the metathesis of several alkenes, including the self-metathesis of (*Z*)-stilbene, and its CM with ethylene. It was observed that the initiation of the reaction did not necessitate an allyl positioned C–H bond. In the CM reaction of (*Z*)-2-butene with di-<sup>13</sup>C-ethylene the ratio of the active sites of the catalyst was also determined.<sup>42</sup>

Wu et al. reported the preparation of catalysts based on tungsten- and niobium-complexes, grafted on mesoporous silica (KIT-6) by a one-pot sol-gel method (Table 1, entry 1).<sup>43</sup> When applied to the CM of butene and ethylene, the highest yield of propene was obtained with a tuned metal composition of 20 wt% tungsten and 1 wt% niobium. The reaction was performed at 450°C under 1 atm. It was demonstrated that the incorporation of Nb contributes to an optimum dispersion of W species on the surface of the catalyst and forms new active site precursors ( $\text{O}=\text{W}(\text{OSi})(\text{ONb})$ ). Interestingly, a significant effect of the O–Nb moiety on the electronic environment around the tungsten atom was also observed, which played a role in the  $\text{O}=\text{W}=\text{O}$  bond angle correlated to enhanced yield of propene. The performance of the catalyst in this work surpassed the results obtained in a previous study reported by the same group<sup>45</sup>; however, it did not match the results of a similar method employing  $\text{WO}_2/\text{SiO}_2$  synthesized via an impregnation/calcination approach (Table 1, entry 2).<sup>44</sup> The yield of propene was in fact superior, and the reaction was performed at significantly lower temperature but significantly higher pressure.

**TABLE 1** Synthesis of propene via olefin CM catalyzed by heterogeneous tungsten-based catalysts.

| Entry | Catalyst/conditions                               | Yield | Ref. |
|-------|---|-------|------|
| 1     | $\text{W}_{10}\text{Nb}_1$ -KIT-6, 450°C, 1 atm   | 70    | 43   |
| 2     | $\text{WO}_2/\text{SiO}_2$ (8 wt%), 200°C, 29 atm | 80    | 44   |



### 3.4.3. Ring-closing metathesis

Ring-closing metathesis (RCM), one of the major metathesis types involving a diene treated with a metal alkylidene complex, was first exploited in organic synthesis by Tsuji for the synthesis of macrocycles.<sup>46</sup> Although the yields obtained in this study were low, advances in catalyst development allowed the achievement of both high yields and good tolerance toward multiple functional groups rendering RCM a useful and popular strategy for the preparation of multiple heterocycles including the synthesis of natural products.<sup>46</sup> However, the pathway leading to the RCM products is often in competition with a second pathway forming polymeric adducts.

Similarly to the heterogeneous catalytic CM, the most commonly used heterogeneous catalysts are immobilized Hoveyda-Grubbs Ru complexes. The supports employed include silanol functionalized silica,<sup>47</sup> fluorosilica gel,<sup>48</sup> sulfonated silica,<sup>49</sup> mesoporous molecular sieves SBA-15,<sup>50–52</sup> SBA-1<sup>53</sup> and MCM-41,<sup>54</sup> mesocellular siliceous foam,<sup>55</sup> MOFs,<sup>56–59</sup> or PEGA resin.<sup>24</sup> While supported Hoveyda-Grubbs Ru catalysts generally exhibit somewhat similar activities, their recyclability, stability, as well as their method of preparation substantially vary. Examples of RCM catalyzed by such solid catalysts are summarized in Table 2. Due to the wide variety of reactants employed and resulting products, a few examples, selected according to the performance, will be presented for each study.

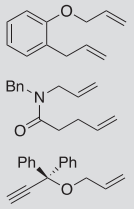
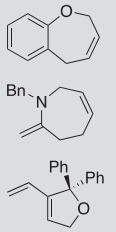
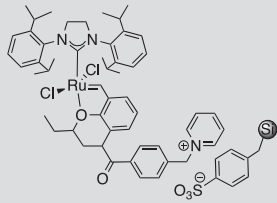
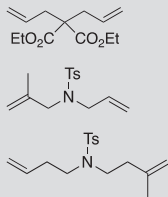
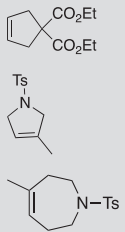
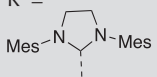
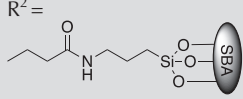
Silica-based mesoporous materials have been widely used as support for the Grubbs-type catalysts mainly due to the high affinity of silica toward the Ru complexes, the large surface area of the materials, and their ordered structure that can easily accommodate metal complexes. The nature of the silica-based support, its pore size, as well as the type of bonding involved in the immobilization influence the activity, the recyclability, and the metal leaching of the catalyst. Direct immobilization of the Ru complex on silica by simple impregnation resulting in hydrogen bonding between the ligand of the phenyl group of the metal complex and the silanol is a possible approach (Table 2, entry 1).<sup>47</sup> An enhanced reactivity was observed in presence of the support compared to the homogeneous system. In addition, the immobilized catalyst could be recycled in five runs while retaining more than 80% of its original activity. Michalek et al. reported a noncovalent fluorosilica gel catalyst, prepared by mixing the fluorinated ligand with the metal complex before purification and immobilization. The resulting catalytic material was highly active for the RCM of various substrates (Table 2, entry 2). It was subjected to an interesting reactivation method involving a solvent switch (methanol/water) to reattach the catalyst to the fluorosilica material which allowed recovery by filtration and reuse in further three cycles.<sup>48</sup> Sulfonated silica as a support for a pyridinium-tagged Hoveyda-Grubbs-type catalyst formed a highly active metathesis catalyst as well (Table 2, entry 3).<sup>49</sup> Further modification with an oxazine-benzylidene ligand provided steric and electronic activation which translated into improved reaction rates. Although the steps involved in the synthesis of the catalyst afforded high yields,

**TABLE 2** Heterogeneous catalytic ring-closing metathesis by immobilized Hoveyda-Grubbs-type catalysts.

| Entry | Reactants | Products | Catalyst/conditions  | Yield (%) | Ref. |
|-------|-----------|----------|--|-----------|------|
| 1     |           |          | <p>Conditions</p> <p> <math>R^1 =</math> <br/> <math>R^2 =</math> <br/> <math>\text{CH}_2\text{Cl}_2</math>, RT, 45 min         </p> | 89–96     | 47   |
| 2     |           |          | <p> <math>R^1 =</math> <br/> <math>R^2 =</math> <br/> <math>\text{CH}_2\text{Cl}_2</math>, 60°C, 2 h         </p>                    | 98        | 48   |

Continued

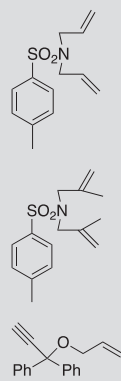
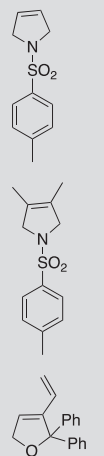
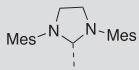
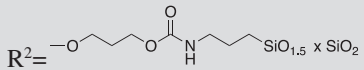
**TABLE 2** Heterogeneous catalytic ring-closing metathesis by immobilized Hoveyda-Grubbs-type catalysts—cont'd

| Entry | Reactants   | Products  | Catalyst/conditions   | Yield (%) | Ref. |
|-------|---|---|---|-----------|------|
| 3     |  |  |  <p>CH<sub>2</sub>Cl<sub>2</sub>, RT, 1–5 h</p>   | 79–86     | 49   |
| 4     |  |  | <p>R<sup>1</sup> =</p>  <p>R<sup>2</sup> =</p>  <p>@SBA-15<br/>CH<sub>2</sub>Cl<sub>2</sub>, 38°C, Ar atmosphere</p> | 92–93     | 50   |

|   |  |  |  |       |    |
|---|--|--|--|-------|----|
| 5 |  |  | <p><math>R^1 =</math></p> <p>Mes-N-Mes</p> <p>@SBA-15 or MCM-41<br/>Toluene, 20–80°C, 1–5 h, Ar atmosphere</p> | 50–85 | 51 |
| 6 |  |  | <p><math>R^1 =</math></p> <p><math>R^2 =</math></p> <p>@SBA-15<br/>Toluene, 30–80°C, 5 h</p>                   | 90–93 | 52 |
| 7 |  |  | <p><math>R^1 =</math></p> <p>Mes-N-Mes</p> <p>@SBA-1<br/>Hexane, 25°C</p>                                      | 90–99 | 53 |

Continued

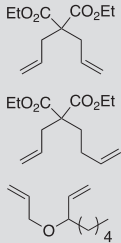
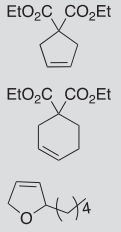
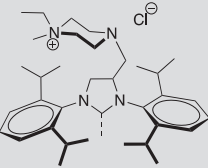
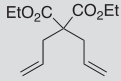
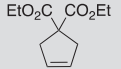
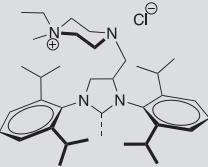
**TABLE 2** Heterogeneous catalytic ring-closing metathesis by immobilized Hoveyda-Grubbs-type catalysts—cont'd

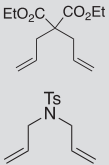
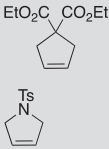
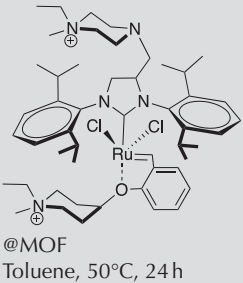
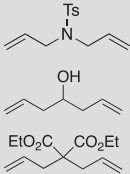
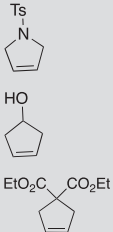
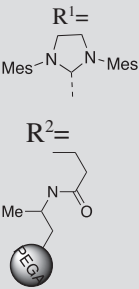
| Entry | Reactants   | Products  | Catalyst/conditions  | Yield (%) | Ref. |
|-------|---|---|--|-----------|------|
| 8     |  |  | <p>R<sup>1</sup>=</p>  <p>R<sup>2</sup>=</p>  <p>CH<sub>2</sub>Cl<sub>2</sub>, RT-80 °C, 24 h</p> | 98        | 54   |

|    |  |  |  |       |        |
|----|--|--|--|-------|--------|
| 9  |  |  | <p> <math>R^1 =</math><br/> </p> <p> <math>R^2 =</math><br/> </p> <p> <math>CH_2Cl_2, 50^\circ C, 30-90 \text{ min}</math> </p>  | 91-99 | 55, 60 |
| 10 |  |  | <p> <math>R^1 =</math><br/> </p> <p> <math>R^2 =</math><br/> </p> <p>           Entrapped in MOF "MIL-101-NH<sub>2</sub>(Al)"<br/> <math>CH_2Cl_2, RT, 24 \text{ h, Ar atmosphere}</math> </p> | 98    | 56     |

Continued

**TABLE 2** Heterogeneous catalytic ring-closing metathesis by immobilized Hoveyda-Grubbs-type catalysts—cont'd

| Entry | Reactants   | Products  | Catalyst/conditions  | Yield (%) | Ref. |
|-------|---|---|--|-----------|------|
| 11    |  |  | <p><math>R^1 =</math></p>  <p>@(Cr)MIL-101 <math>SO_3^- Na^+</math> MOF<br/>Dimethyl carbonate, 50°C, 24 h</p> | 93–99     | 57   |
| 12    |  |  | <p><math>R^1 =</math></p>  <p>@(Cr) MIL-101-<math>SO_3H</math> MOF<br/>dimethyl carbonate, RT, 24 h</p>        | 99        | 58   |

|    |   |   |   |       |    |
|----|---|---|---|-------|----|
| 13 |  |  |  <p>@MOF<br/>Toluene, 50°C, 24 h</p>    | 86–95 | 59 |
| 14 |  |  |  <p>Methanol or water, RT-45°C, 12 h</p> | 71–96 | 24 |

multiple reagents and organic solvents were employed. It is worth noting that upon immobilization of the precatalyst onto a silica-based cationic-exchange resin, a flow system could be generated. Both the batch and flow systems showed similar leaching profiles ranging from low to moderate. The recyclability of the catalyst was sufficient under batch conditions; it was proved, however, inefficient under continuous flow conditions, questioning the utility of the catalyst in fixed-bed systems. Other silica-based mesoporous materials SBA-15, with variable pore size, served as a support for the Grubbs-type catalysts (Table 2, entry 4).<sup>50</sup> The activity of the supported metal complex was highly dependent on the porosity of the support. The highest activity occurred with the largest pore sizes due to a better diffusion of the reactants and products. Increased pore size also coincided with shorter reaction times and greater number of recycling attempts (up to nine). In regard to the catalyst preparation, several steps were required to achieve functionalization of the support with amino groups followed by the immobilization of the metal complex under controlled atmosphere and moderate temperatures. Another modified Hoveyda-Grubbs catalyst supported on silica and siliceous mesoporous molecular sieves entailed a simple deposition of the homogeneous catalyst by addition to a suspension of precalcined support (Table 2, entry 5).<sup>51</sup> In contrast, the preparation of the catalyst itself was performed using multiple reagents and organic solvents to afford the Ru complex bearing a polar quaternary ammonium group in the *N*-heterocyclic ligand. The highest activity was obtained with SBA-15 as a support and in presence of chloride-containing counter ions. The effect of the pore size corroborated with the aforementioned studies. A different version of the catalyst, bearing 2,6-diisopropylphenyl group as a substituent in lieu of 2,4,6-trimethylphenyl (Mes), was shown to improve the stability of the immobilized metal complex as well as its recyclability.<sup>61</sup> It is noteworthy that the developed heterogeneous catalysts could be used in a tube-in-tube reactor under continuous flow mode.<sup>62</sup> The innovative flow system allows the removal of ethylene as it is produced thanks to a vacuum pump connected to the apparatus. Because ethylene is believed to have a negative influence on the catalytic activity, the tube-in-tube system constitutes a better scale-up option than the usual fixed-bed system where the catalyst suffers from the accumulation of ethylene. Pastva et al. also selected SBA-15 as the support for the first generation Hoveyda-Grubbs complex (Table 2, entry 6).<sup>51</sup> In this study, the catalyst could easily be separated and reused; in addition, the Ru leaching was very low compared to other immobilized catalysts (below 0.4%). Immobilization of Grubbs-type catalyst onto the same type of mesoporous materials including SBA-15, MCM-41, and SBA-1 was described by Yang et al.<sup>53</sup> The immobilization of the Ru complex was achieved via a simple adsorption and led to a highly recyclable catalyst (Table 2, entry 7). SBA-1 was found to exhibit the largest adsorption capacity for the Ru complex. The deactivation of the catalyst was observed only after eight consecutive reaction cycles. Interestingly, the leaching of the metal decreased from one cycle to another going from around 1% in the first cycle to less than 0.5% for the following cycles while the yield remained consistent (98%–99%) until the seventh cycle. Elias et al. reported a

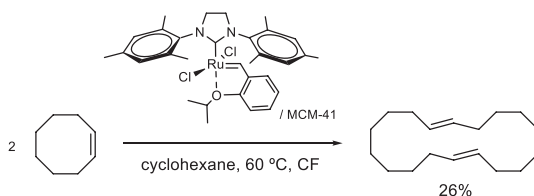
hybrid MCM-41/bis-silylated Ru prepared by a multiple step protocol involving a sol-gel method followed by the anchoring of the organic ligand on the solid support and finally the addition of the Ru moiety (Table 2, entry 8). Despite the tedious preparation method, the catalyst exhibited excellent recyclability.<sup>54</sup> Ruthenium-based metathesis catalysts immobilized on mesocellular siliceous foam (MCF) bearing large nanopores showed remarkable selectivity particularly for the formation of macrocycles, greater than 20-membered rings, which was enhanced by increasing the pore size of the support (Table 2, entry 9).<sup>55</sup> Thus the synthesis of the supported Ru-based metathesis catalysts included the adjustment of the pore size by varying the temperature and adding ammonium fluoride, as well as the modification of 2-isopropoxystyrenyl ligand via click chemistry for covalent attachment to the silica wall surface. The recyclability of a similar immobilized catalyst was investigated in a different work, which reported good performances.<sup>63</sup> It was also tested in circulating flow reactors and it exhibited good activity for substrates such as diethyl 2,2-diallylmalonate.<sup>60</sup> Further studies revealed that the in situ-generated ethylene contributed to the process of catalytic deactivation, thus impacting catalyst recyclability.

Similarly to silica-supported Hoveyda-Grubbs-type catalysts, the immobilization of these homogeneous complexes on MOFs can be achieved by different approaches. Spekrijse et al. proposed the immobilization by mechanochemical means demonstrating the effect of the ball mill activation on the MOF structure ultimately breaking open and forming new bonds upon grinding together with the catalyst (Table 2, entry 10).<sup>56</sup> This original grinding method could also be applied to the Zhan catalyst. The catalyst was however inactive after the first catalytic cycle. Choluj et al. reported a noncovalent immobilization of an olefin metathesis catalyst inside an MOF. The Hoveyda-Grubbs alkylidene catalyst bearing an ammonium-tagged NHC ligand was immobilized on a robust (Cr)MIL-101SO<sub>3</sub><sup>-</sup>Na<sup>+</sup> MOF (modified version of (Cr)MIL-101-SO<sub>3</sub>H in which H<sup>+</sup> were replaced by Na<sup>+</sup>) via ion exchange (Table 2, entry 11).<sup>57</sup> The remaining traces of water, used as a solvent during immobilization, were found to have a detrimental effect on the activity of the heterogeneous catalyst; thus a specially prepared MOF with sodium cations complexed by 15-crown-5 ether molecules allowed the use of methanol as an alternative solvent. The resulting material exhibited high activity and selectivity in a wide range of solvents including polar solvents such as dimethyl carbonate, which is considered as a green solvent. In addition, the method can easily be scaled up and catalyst leaching is expected to be minimal as long as there are no other cations in solution that have a higher affinity with the sulfonic group of the MOF. The same research group also reported the immobilization of amino-tagged Hoveyda-Grubbs-type ruthenium catalyst inside Brønsted acidic (Cr)MIL-101-SO<sub>3</sub>H MOF by an acid-base reaction (Table 2, entry 12).<sup>58</sup> The high acidity of the solid support was essential to provide a stable heterogeneous catalyst that essentially led ruthenium-free products upon filtration. Here again, polar solvents such as dimethyl carbonate and 2-propanol could be employed. Furthermore, the immobilized catalyst showed higher activity than the unsupported counterpart and no acid-catalyzed side reactions were observed. However, preliminary recycling studies revealed a gradually

decreasing activity. A third work authored by Choluj et al. focused on probing the heterogeneous *boomerang effect* employing ammonium-tagged Ru-benzylidene complexes on different supports including a MOF (Table 2, entry 13).<sup>59</sup> A non-covalent immobilization strategy was adopted so that both the precatalyst and the benzylidene ligand precursor were immobilized on the support close to each other with a sufficient flexibility to allow their subsequent coupling. The ammonium-tagged styrene derivative (a precursor of benzylidene ligand) was employed as a doping agent in order to enhance precatalyst regeneration via release-return effect. Although the effect was indeed observed inside the solid support, it was found that nondoped systems gave better results in terms of turnover number. Despite an interesting mechanistic insight provided by the study, the approach seems to suffer from a tedious catalyst synthesis, a mediocre catalyst recycling, and a limited substrate scope.

It should be noted that all reactions presented in Table 2 are performed with organic solvents except the Ru complex on PEGA resin that comparatively afforded inferior results, nonetheless remaining above 70% yield (Table 2, Entry 14).<sup>24</sup> While for most examples presented, the immobilization of the catalysts did not impact their activity, the decrease of catalytic activity upon immobilization was observed in the literature such as the RCM of diethyl diallyl malonate catalyzed by the second generation Hoveyda-Grubbs complex directly attached to silica through covalent Ru–O–Si bonds; a 50% activity decrease was noted compared to the homogeneous catalytic system (data not shown).<sup>64</sup>

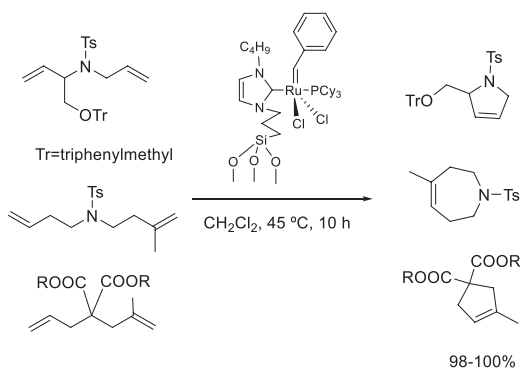
A specific type of ring-closing metathesis is the ring-opening/ring-closing metathesis of cycloalkenes leading to large rings.<sup>65</sup> The metathesis of *cis*-cyclooctene was achieved with the aid of a heterogenized Hoveyda-Grubbs complex. The longevity and selectivity of the catalyst increased when performing the reaction under continuous flow conditions (Scheme 11). The optimum conditions obtained with MCM-41 as the support at 60°C led to a maximum of 75% conversion and 35% selectivity for the cyclic dimer, a range of small oligomers accounting for the other 65%. It must be noted that temperatures higher than 50°C caused the catalyst to become deactivated after short reaction times while lower temperatures such as 40°C preserved the catalytic activity for several hours but achieved lower conversion.



**SCHEME 11** Heterogeneous catalytic ring-opening/ring-closing metathesis of *cis*-cyclooctene under continuous flow (CF) conditions with an immobilized Ru complex.

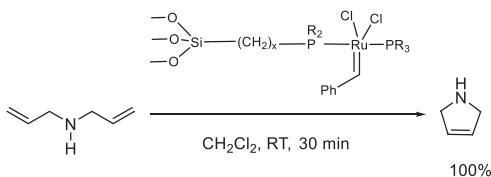
In addition to the Hoveyda-Grubbs immobilized catalyst, other Ru-based catalysts account for a large part of solid supported complexes in RCM. Here again, the solid supports used are the common mesoporous SBA-15<sup>66</sup> and MCM-41,<sup>67</sup> and the less common perfluoroglutaric acid derivatized polystyrene-divinylbenzene.<sup>68</sup>

In the case of the Ru-based complex grafted on mesoporous SBA-15, the immobilization prevented the decomposition of the catalyst and allowed its recyclability while preserving high yields; after the fifth cycle a yield as high as 95% was reported (Scheme 12).<sup>66</sup>



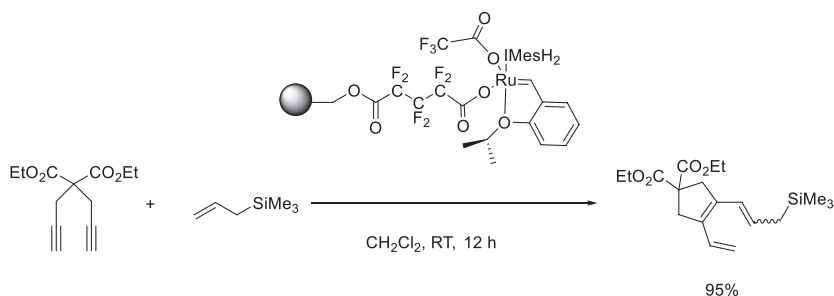
**SCHEME 12** Heterogeneous catalytic ring-closing metathesis by a silica-anchored Ru complex.

The MCM-41-supported Grubbs-type catalyst demonstrated high activity in the RCM of dienes (Scheme 13).<sup>67</sup> Analysis with Raman spectroscopy confirmed the hypothesis postulating that a fraction of the catalyst is detached from the solid support during the metathesis reaction and is then recaptured by the free phosphine group after completion of the reaction.



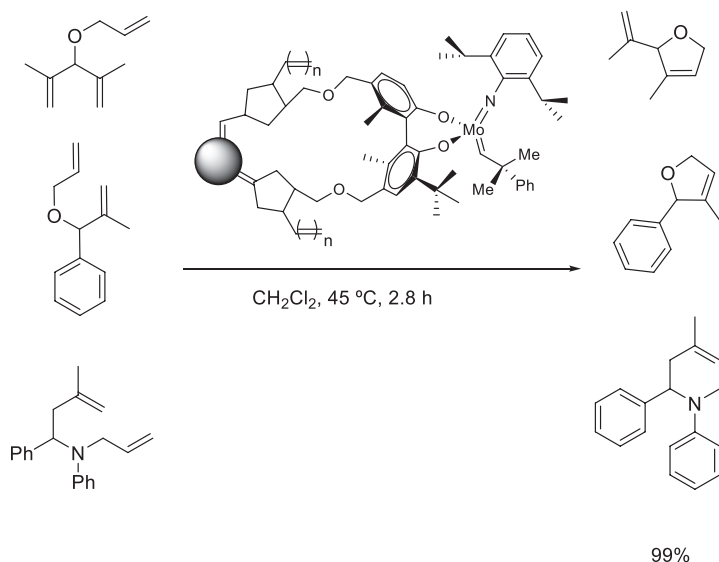
**SCHEME 13** Heterogeneous catalytic ring-closing metathesis by MCM-41-supported Grubbs-type catalyst.

Heterogenization of a Grubbs-Herrmann catalyst on a macroreticular poly(styrene-*co*-divinylbenzene) resin appears to be a viable option to catalyze RCM effectively (Scheme 14).<sup>68</sup> The heterogeneous catalyst was found to be equally or more active than its homogeneous version.



**SCHEME 14** Heterogeneous catalytic ring-closing metathesis/cross-metathesis using a Ru complex on resin.

Finally, the activity of heterogeneous Mo complexes has been reported for the RCM of multiple dienes. Interesting studies described a synthetic approach that grafts chiral Schrock catalysts as well as Grubbs-Herrmann catalyst on polymeric, monolithic discs (Scheme 15).<sup>69,70</sup> The synthesis of the solid materials proceeded through a surface derivatization of the support via ring-opening metathesis polymerization followed by the catalyst immobilization. Several washing steps with organic solvents were necessary to provide the ready to use, immobilized Mo complex. The advantage of the approach lies in the practicality of the disc-like nature of the heterogeneous catalyst that can be used in combinatorial chemistry, parallel synthesis, and high-throughput screening. However, despite excellent yields obtained for the RCM of various substrates, the monolithic discs loaded with catalyst were designed to be used for a single cycle.

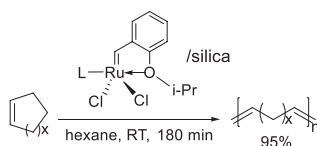


**SCHEME 15** Ring-closing metathesis catalyzed by a monolithic disk-supported Mo complex.

### 3.4.4. Ring-opening metathesis

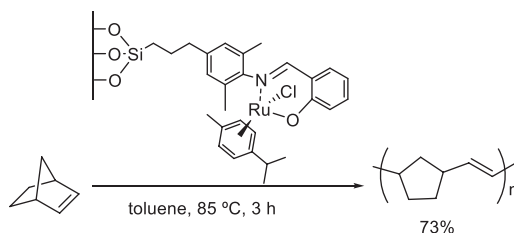
Ring-opening metathesis (ROM) can be separated into two major types: the simple ring opening of cycloalkenes and the ring-opening metathesis polymerization (ROMP).<sup>71</sup> Ru and Re-based homogeneous catalysts are the most studied in this field while their heterogeneous counterparts immobilized on alumina or silica are the most investigated systems and constitute an important class of catalysts due to the practicability they offer in industrial settings.<sup>18, 72, 73</sup>

The second generation Hoveyda-Grubbs catalyst immobilized on silica, described above in the CM section, also performed well in catalyzing ROMP (Scheme 16).<sup>18</sup> Here again, the reaction is performed in hexane. Although it is not ideal from an environmental point of view, the advantages of such nonpolar solvents were clearly identified; they contribute to the stability (nonleaching) of the catalyst from the support and ensure a metal-free product.



**SCHEME 16** Heterogeneous catalytic ring-opening metathesis polymerization by the Hoveyda-Grubbs Ru-based catalyst immobilized on silica.

Another silica-supported Ru catalyst showed acceptable activity in the ROMP of norbornene producing 73% yield (Scheme 17). While the homogeneous catalyst performed significantly better (98% yield), the solid catalyst exhibited negligible levels of leaching to the reaction mixture and exhibited good recyclability.<sup>72</sup>

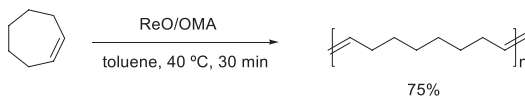


**SCHEME 17** Heterogeneous catalytic ring-opening metathesis polymerization of norbornene with silica-supported Ru catalyst.

Although Ru complexes are undeniably the most commonly used catalysts in this field and it is no exception for ROM, there are a few examples of other metal-based catalyst such as Re. Re oxide supported on organized mesoporous alumina (OMA) showed higher activity in the ROMP of cycloalkenes than other alumina-supported catalysts (Scheme 18).<sup>73</sup> The high activity was attributed to

302 Heterogeneous catalysis in sustainable synthesis

the organized structure of the support. Additionally, the solid-supported Re oxide was easily separated from the reaction mixture and reused after an activation step (drying under Ar).

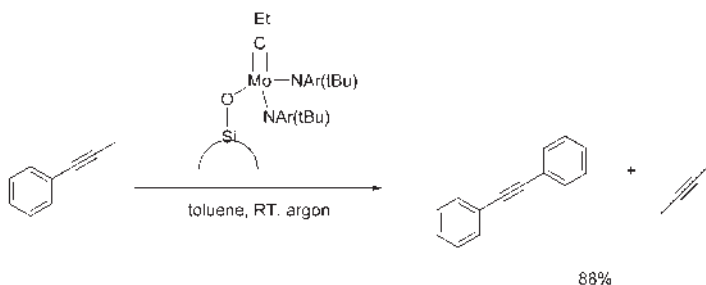


**SCHEME 18** Heterogeneous catalytic ring-opening metathesis polymerization of cycloheptene by Re oxide on OMA.

### 3.4.5. Alkyne metathesis

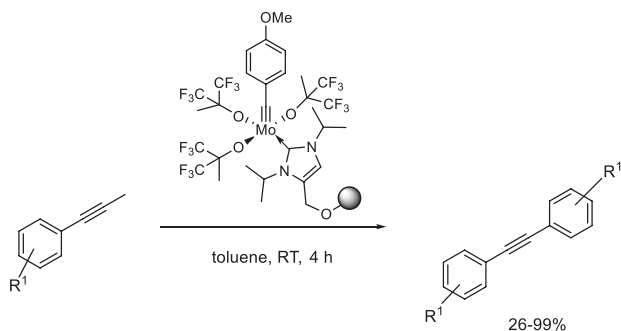
The alkyne metathesis is less developed than the highly versatile and chemo- and stereoselective alkene metathesis. Similarly to the alkene metathesis mechanism, alkyne metathesis involves the exchange of alkylidyne units between a pair of acetylenes through a metallacyclobutadiene intermediate.<sup>15</sup> Three decades ago, the first catalytic system capable of catalyzing the alkyne metathesis was a heterogeneous mixture of tungsten oxide and silica applied at high temperatures.<sup>74</sup> Later, Mo and W-based catalysts were developed allowing milder reaction conditions.

A silica-supported Mo catalyst, prepared by mixing triamide with a suspension of silica in toluene at room temperature, showed good activity in the metathesis of 1-phenyl-1-propyne under vacuum at room temperature. The immobilization appeared to have prevented the catalyst deactivation as well as the often observed polymerization side reaction (Scheme 19).<sup>75</sup>



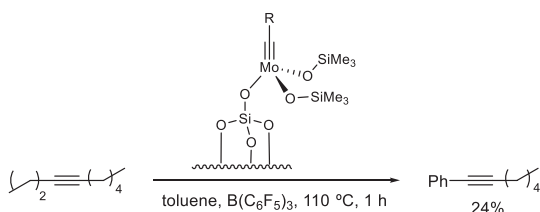
**SCHEME 19** Heterogeneous catalytic alkyne metathesis of 1-phenyl-1-propyne by a silica-supported Mo complex.

Silica-supported Mo-alkylidyne-*N*-heterocyclic carbene catalyzed the alkyne metathesis of substituted aryl-methyl internal alkynes in excellent yields (Scheme 20).<sup>76</sup> The heterogeneous catalyst allowed the decrease of the catalyst loading by a factor of two compared to the homogeneous form of the complex while resulting in higher productivity attributed to the prevention of the catalyst decomposition due to its immobilization.



**SCHEME 20** Heterogeneous catalytic alkyne metathesis of aryl-methyl alkynes by a silica-supported Mo complex.

Other silica-grafted Mo catalyst demonstrated activity in the CM of alkynes.<sup>77</sup> In one example, the study of the fluorine-bearing Mo catalysts showed that their activity was highly dependent on the number of fluorine atoms (Scheme 21).<sup>78</sup> The optimum number of fluorine ligands was reached when the Mo sites became more and more electrophilic with increasing number of fluorine atoms until it led to an overly stable complex unable to catalyze the reaction. Due to the loss of electrophilicity upon immobilization, corroborating with the previous postulate, the silica-supported catalyst was significantly less active than the homogeneous Mo complex. In another example, only about 20% yield was obtained despite the presence of a boron Lewis acid cocatalyst although the results were superior to those obtained with the homogeneous analogue.

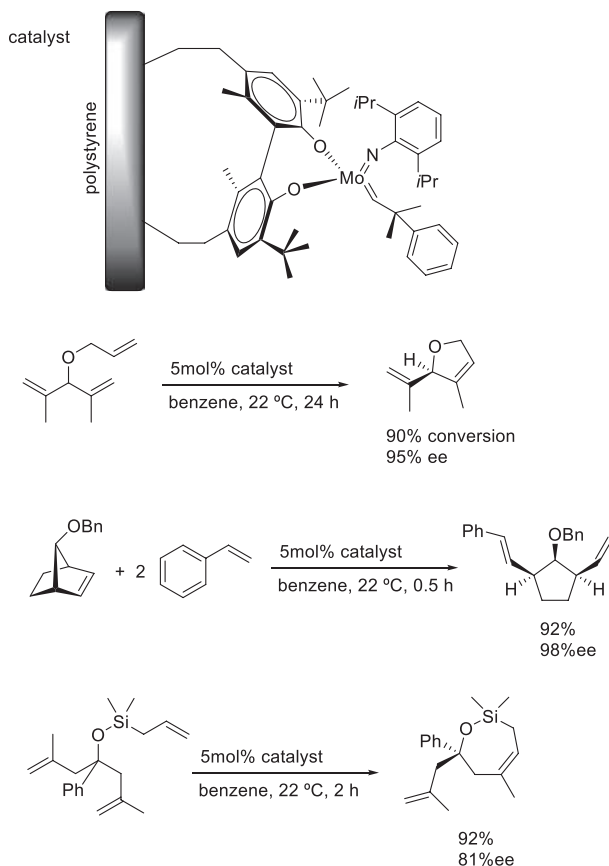


**SCHEME 21** Heterogeneous catalytic alkyne metathesis using a silica-grafted Mo complex.

### 3.4.6. Heterogeneous catalytic asymmetric metathesis

The synthesis of chiral compounds via asymmetric catalysis is one of the most active areas in synthetic organic chemistry.<sup>79</sup> Using chiral metathesis catalysts enables us to produce chiral molecules via a variety of alkene metathesis pathways. Although there is a broad variety of such homogeneous applications in the literature,<sup>80-83</sup> the available heterogeneous catalytic examples are quite limited.

In 2002 Hultzsch et al. described the first polymer-supported and recyclable catalyst for application in enantioselective alkene metathesis, in particular, in CM, ROM, and RCM type reactions.<sup>84</sup> The synthesis of the catalyst is straightforward and is based on a chiral biphenyl moiety. The molybdenum complex is covalently bound to the polystyrene backbone. Although the synthesis of the catalyst includes six steps and involves several, generally undesirable chemicals (HCl, Grignard reagent, chlorinated solvents, etc.), the catalyst itself is recyclable in three consecutive reaction cycles with a consistently stable, high ee, and only a moderate drop in activity, which partially alleviates the negative aspects. The catalyst appeared to be active and highly enantioselective in various transformations. The structure of the catalyst and a few representative examples are shown in Scheme 22.



**SCHEME 22** Heterogeneous catalytic enantioselective alkene metathesis with a polystyrene-bound Mo complex.

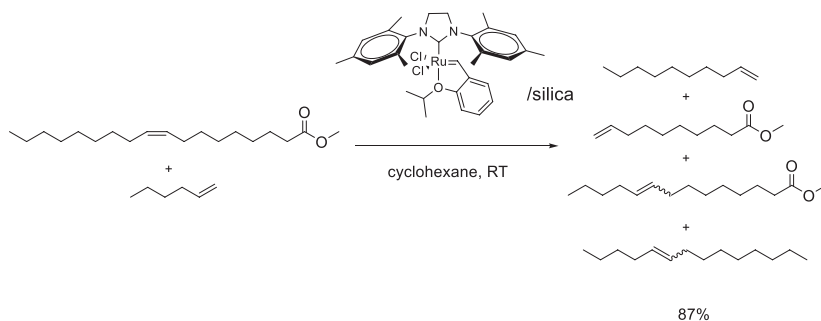
Later the authors extended their study to seven new chiral metathesis catalysts based on polymer-bound Mo complexes.<sup>85</sup> Four of these samples possessed polystyrene and three poly-norbornene backbones. The chiral information was introduced by a binaphthyl unit. Most catalysts provided high yields and enantioselectivities in several applications, including those depicted in [Scheme 22](#).

### 3.4.7. Metathesis applied to bioderived alkenes

Due to the current ever strengthening environmental context of chemistry research, efforts have been devoted in the field to rely on renewable feedstock rather than fossil fuel-based resources as much as possible.<sup>86</sup> Therefore plant oils are becoming attractive substrates because of their versatility as starting materials, generating a wide scope of fine chemicals and building blocks. Although carbohydrates are currently more widely used than fatty acids in the chemical industry, the unique properties of fatty acids and their derivatives make them suitable for a range of specific applications. For instance, their amphiphilic property is the basis for their long-standing application as soaps. Their tunable backbone also allows for multiple functionalization opening up other application possibilities, such as the epoxidation of triglycerides producing multifunctional cross-linkers in polyurethanes.<sup>86</sup> In addition, unsaturated fatty acids can readily undergo catalytic C–C linkage reactions and cleavage reactions. Olefin metathesis is an outstanding example of processes that produce valuable chemicals and key intermediates notably from fatty acid methyl esters, easily obtained from the transesterification of natural oils and fats.<sup>87, 88</sup> While homogeneous catalytic metathesis processes are well established and efficient, the development of industrial-scale reactions was accompanied by the emergence of issues related to the separation of the catalyst and its stability. Designing immobilized catalysts can potentially address these issues and eliminate cumbersome purifications steps.<sup>87</sup> Ru or Re complexes immobilized on different supports have shown to prevent the contamination of products with metal particles as well as to ease the separation of the catalyst from the reaction mixture.

A second generation Hoveyda-Grubbs catalyst was successfully immobilized on commercially available silica and demonstrated high activity in the cross-metathesis of methyl oleate with 1-hexene to obtain 1-decene, methyl 9-tetradecenoate, 5-tetradecene, and methyl 9-decenoate, medium-chain fatty acid esters that are valuable intermediates in the synthesis of fine chemicals ([Scheme 23](#)).<sup>89</sup> Competitive side reactions included the self-metathesis of methyl oleate and the self-metathesis of 1-hexene giving rise to by-products such as 5-decene and 9-octadecene. The yield of cross-metathesis products reached 47% when the reactants were introduced in stoichiometric proportions

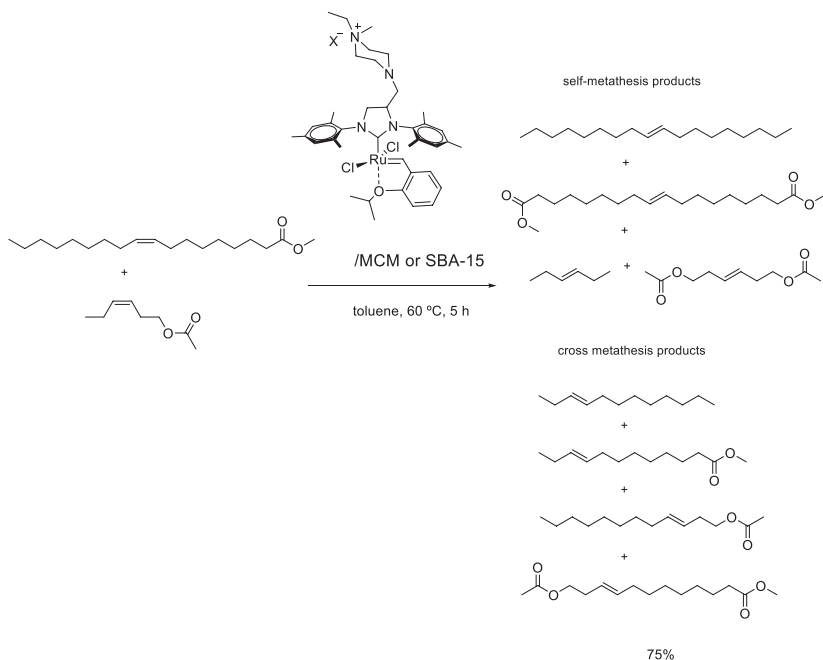
and 87% when the ratio of 1-hexene to methyl oleate attained seven. The same observation was made in a different work reporting the cross-metathesis of methyl oleate with ethylene in gaseous state.<sup>90</sup> The use of excess ethylene compared to methyl oleate seems to shift the equilibrium to high CM yields while suppressing the formation of self-metathesis by-products. However, using ratios higher than 2.5 in this work resulted in catalyst deactivation. The highest yield of 63% was obtained by employing a ratio of ethylene/methyl oleate of 2.5 at 40°C for 180 min with an ethylene pressure of 0.125 bar.



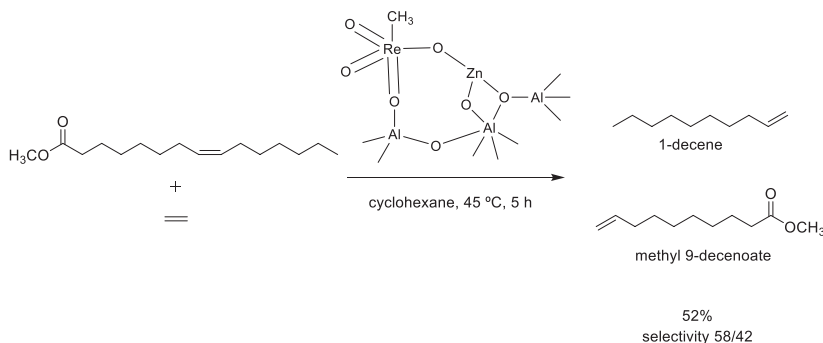
**SCHEME 23** Heterogeneous catalytic cross-metathesis of 1-hexene and methyl oleate by a silica-supported Hoveyda-Grubbs catalyst.

Cross-metathesis of methyl oleate with *cis*-3-hexenyl acetate was performed with Hoveyda-Grubbs-type catalysts bearing cationic tags on NHC ligands and immobilized on the surface of lamellar zeolitic supports without linkers (Scheme 24).<sup>91</sup> Several mesoporous molecular sieves were tested and exhibited different activities depending on the type of metathesis. Both catalysts, immobilized on MCM-22 and SBA-15, provided rapid conversion of the fatty acid methyl ester. At equilibrium, the consumption of both reactants reached 75%. The remaining 25% of the conversion accounted for the yield of self-metathesis products according to Scheme 24. No leaching of catalytically active species into the liquid phase was observed.

Alternatives to the expensive Hoveyda-Grubbs catalysts are methyltrioxorhenium (MTO) catalysts which have been successfully immobilized as well. For instance, the high catalytic activity of methyltrioxorhenium on ZnCl<sub>2</sub>-modified mesoporous alumina is well-known for the metathesis of olefin esters bearing functional groups.<sup>92, 93</sup> The highly active heterogeneous catalyst allows bypassing the use of additional promoters. However, the leaching of the surface chlorine sites constitutes a potential source of product contamination. Lee et al. developed a chloride-free and cocatalyst-free catalytic system based on MTO grafted to the spinel-type mesoporous zinc aluminate (ZnAl<sub>2</sub>O<sub>4</sub>).<sup>94</sup> The catalyst exhibited good catalytic activity and selectivity, affording only the desired cross-metathesis products of 1-decene and methyl 9-decenoate (Scheme 25).



**SCHEME 24** Cross-metathesis of methyl oleate with *cis*-3-hexenyl acetate catalyzed by a Hoveyda-Grubbs-type catalyst immobilized on lamellar zeolites.



**SCHEME 25** Heterogeneous catalytic cross-metathesis of methyl oleate with ethylene for production of 1-decene and methyl 9-decenoate from seed oil.

The self-metathesis of the same fatty acid methyl ester has been extensively studied under homogeneous catalytic conditions with well-known catalysts.<sup>95–97</sup> Multiple heterogeneous catalysts consisting of Ru or Re complexes supported on alumina or silica have been designed to provide catalysts with prolonged activity and good recyclability, which homogeneous systems lack. Representative examples regarding the self-metathesis of methyl oleate are tabulated in [Table 3](#).

**TABLE 3** Heterogeneous catalytic self-metathesis of methyloleate.

| Entry | Catalyst/conditions  | Yield (%) | Ref. |
|-------|--|-----------|------|
| 1     | Methyltrioxorhenium-ZnCl <sub>2</sub> on mesoporous alumina, hexane, 45°C, 5 h                   | 52        | 93   |
| 2     | Methyltrioxorhenium-ZnCl <sub>2</sub> on mesoporous alumina, [bmim][PF <sub>6</sub> ], 45°C, 5 h | 27        | 98   |
| 3     | Methyltrioxorhenium on mesoporous hexagonal zinc-doped alumina, hexane, 45°C, 90 min             | 57        | 99   |
| 4     | Second generation Hoveyda-Grubbs/silica, cyclohexane, 30°C, 80 min                               | 50        | 100  |
| 5     | Magnetite nanoparticles supported second generation Hoveyda-Grubbs catalyst, neat, 50°C, 3 h     | 73        | 101  |
| 6     | Rhenium oxide supported on borated silica-alumina, heptane, 40°C, 90 min                         | –         | 102  |

The self-metathesis of methyloleate was performed with a methyltrioxorhenium catalyst incorporated on ZnCl<sub>2</sub>-modified mesoporous alumina (Table 3, entry 1).<sup>93</sup> It was found that a ratio of 8–12 for the content of Al/Zn was optimal. Surprisingly, the use of other zinc halides or metal chlorides did not promote the catalytic activity; thus it is thought that the formation of active sites is related to the combined Zn–Cl bond with the alumina support. A conversion of 92% was observed and 52% yield of the desired products was obtained at 45°C in 5 h, which are results comparable to those obtained with the homogeneous second generation Grubb catalyst. In a different study, the same solid catalyst was employed under similar conditions except that hexane was replaced with an ionic liquid, the 1-butyl-3-methylimidazolium hexafluorophosphate ([bmim][PF<sub>6</sub>]) (Table 3, entry 2).<sup>98</sup> The catalyst leaching was lower in the ionic liquid-based reaction than in the hexane-based reaction and the recyclability of the catalyst was made possible for two runs whereas poor recyclability was observed for the reaction performed in hexane. However, these improvements were made at the expense of the reaction rate and selectivity; lower yields toward the desired products as well as more by-products were obtained. The activity of a series of methyltrioxorhenium-based catalysts supported on highly ordered hexagonal mesoporous alumina and zinc-modified mesoporous alumina, prepared by

a sol-gel method, was investigated and compared to the aforementioned studies (Table 3, entry 3).<sup>99</sup> The hexagonal structure of the support demonstrated to be suitable for the reaction of bulky fatty acid molecules reducing the mass transfer limitations observed when using wormhole-like structures. Therefore a slightly higher yield of the desired metathesis products was obtained in a shorter reaction time.

The second generation Hoveyda-Grubbs catalyst immobilized on mesoporous silica afforded similar results to that of the rhenium-driven reaction in hexane, though at lower temperature in shorter time (Table 3, entry 4).<sup>100</sup> The successful immobilization of the catalyst was proven by detecting negligible metal-complex leaching. However, low catalyst loading led to rapid deactivation of the catalyst although higher loadings allowed for good catalytic activity for two consecutive cycles.

Significant recyclability improvements were provided by magnetic nanoparticles as a support for the second generation Hoveyda-Grubbs catalyst (Table 3, entry 5).<sup>101</sup> Not only was the catalyst remarkably active in olefin self-metathesis, but it could also be efficiently dispersed in the organic reaction mixture to mimic a homogeneous system with the recyclability feature of a heterogeneous system owing it to the magnetic properties of the support. Five consecutive cycles could be performed with negligible loss of activity. The synthesis of the immobilized catalyst required several steps including the preparation of the linkers and the functionalization of the nanoparticles by starch and the final linkage with the ruthenium complex. Continuing on the evaluation of the recyclability of catalysts, it is worth mentioning the study that applied a rhenium oxide catalyst supported on borated silica-alumina with tetrabutyltin as a cocatalyst (Table 3, entry 6).<sup>102</sup> The performance of the catalyst was only reported in terms of turnover numbers. After as many as 25 cycles, the turnover numbers remained constant and the selectivity was preserved. Only after the thirtieth cycle, the catalyst became inactive likely due to the interactions of the tin with the active sites. It must be noted that the catalyst was reactivated after each cycle by means of washing and calcination; fresh tetrabutyltin was added before each cycle as well.

### 3.4.8. Conclusions and outlook

In conclusion, typical examples of heterogeneous catalytic cross-metathesis, ring-opening and ring-closing metathesis, alkyne metathesis, and metathesis applied to the conversion of biorenewable biomass sourced alkenes were reviewed. In light of the efficiency of the reactions described throughout the chapter, it is safe to conclude that heterogeneous catalysis contributes to the broad use of metathesis as a tool to produce all types of value-added chemicals in one single, highly atom-economic, step. While solid catalyst-based metathesis has not reinvented the field because it mainly applies the well-established metal complexes on various supports via different strategies, it certainly has improved the environmental impact of metathesis reactions as well as its practical use

notably in industrial settings (e.g., continuous flow beds). Generally, the immobilization of those catalysts did not hinder their catalytic activity and often allowed their recycling for several consecutive cycles, a major advantage over homogeneous catalytic systems.

## References

1. Fürstner, A. Olefin Metathesis and Beyond. *Angew. Chem. Int. Ed.* **2000**, *39*, 3012–3043.
2. Chauvin, Y. Olefin Metathesis: The Early Days (Nobel Lecture). *Angew. Chem. Int. Ed.* **2006**, *45*, 3740–3747.
3. Grubbs, R. Olefin-Metathesis Catalysts for the Preparation of Molecules and Materials (Nobel Lecture). *Angew. Chem. Int. Ed.* **2006**, *45*, 3760–3765.
4. Schrock, R. R. Multiple Metal–Carbon Bonds for Catalytic Metathesis Reactions (Nobel Lecture). *Angew. Chem. Int. Ed.* **2006**, *45*, 3748–3759.
5. Schrock, R.; Hoveyda, A. Molybdenum and Tungsten Imido Alkylidene Complexes as Efficient Olefin–Metathesis Catalysts. *Angew. Chem. Int. Ed.* **2003**, *42*, 4592–4633.
6. Ulman, M.; Belderrain, T.; Grubbs, R. A Series of Ruthenium(II) Ester–Carbene Complexes as Olefin Metathesis Initiators: Metathesis of Acrylates. *Tetrahedron Lett.* **2000**, *41*, 4689–4693.
7. Grubbs, R.; Chang, S. Recent Advances in Olefin Metathesis and its Application in Organic Synthesis. *Tetrahedron* **1998**, *54*, 4413–4450.
8. Bates, J. M.; Lummiss, J. A. M.; Bailey, G. A.; Fogg, D. E. Operation of the Boomerang Mechanism in Olefin Metathesis Reactions Promoted by the Second-Generation Hoveyda Catalyst. *ACS Catal.* **2014**, *4*, 2387–2394.
9. Connon, S.; Blechert, S. Recent Developments in Olefin Cross-Metathesis. *Angew. Chem. Int. Ed.* **2003**, *42*, 1900–1923.
10. Dewaele, A.; Verpoort, F.; Sels, B. Opportunities of Immobilized Homogeneous Metathesis Complexes as Prominent Heterogeneous Catalysts. *ChemCatChem* **2016**, *8*, 3010–3030.
11. Nicolaou, K.; Bulger, P.; Sarlah, D. Metathesis Reactions in Total Synthesis. *Angew. Chem. Int. Ed.* **2005**, *44*, 4490–4527.
12. Schrock, R. R.; Czekelius, C. Recent Advances in the Syntheses and Applications of Molybdenum and Tungsten Alkylidene and Alkylidyne Catalysts for the Metathesis of Alkenes and Alkynes. *Adv. Synth. Catal.* **2007**, *349*, 55–77.
13. Grubbs, R. H. Realizing the Promise of Olefin Metathesis. *Adv. Synth. Catal.* **2007**, *349*, 23–24.
14. Schrock, R. R. High Oxidation State Molybdenum and Tungsten Alkene and Alkyne Metathesis Catalysts: Where We Are and Where We Want to Go. *Adv. Synth. Catal.* **2007**, *349*, 25.
15. Zhang, W.; Moore, J. S. Alkyne Metathesis: Catalysts and Synthetic Applications. *Adv. Synth. Catal.* **2007**, *349*, 93–120.
16. Jeong, H.; Axtell, J.; Török, B.; Schrock, R. R.; Müller, P. Syntheses of Tungsten *t*-Butylimido and Adamantylimido Alkylidene Complexes Employing Pyridinium Chloride as the Acid. *Organometallics* **2012**, *31*, 6522–6525.
17. Kingsbury, J.; Harrity, J.; Bonitatebus, P.; Hoveyda, H. A Recyclable Ru-Based Metathesis Catalyst. *J. Am. Chem. Soc.* **1999**, *121* (4), 791–799.
18. Van Berlo, B.; Houthoofd, K.; Sels, B. F.; Jacobs, P. A. Silica Immobilized Second Generation Hoveyda-Grubbs: A Convenient, Recyclable and Storageable Heterogeneous Solid Catalyst. *Adv. Synth. Catal.* **2008**, *350*, 1949–1953.

- Nasrallah, H.; Pagnoux, A.; Didier, D.; Magnier, C.; Toupet, L.; Guillot, R.; Crevisy, C.; Mauduit, M.; Schulz, E. Immobilization of an Anthracene-Tagged Ruthenium Complex on a 2,4,7-Trinitrofluoren-9-One-Grafted Silica: Efficiency and Recyclability in Olefin Metathesis Reactions. *Eur. J. Org. Chem.* **2014**, 7781–7787.
- Michalek, F.; Maedge, D.; Ruehe, J.; Bannwarth, W. The Activity of Covalently Immobilized Grubbs-Hoveyda Type Catalyst Is Highly Dependent on the Nature of the Support Material. *J. Organomet. Chem.* **2006**, 691, 5172–5180.
- Michrowska, A.; Mennecke, K.; Kunz, U.; Kirschning, A.; Grela, K. A New Concept for the Noncovalent Binding of a Ruthenium-Based Olefin Metathesis Catalyst to Polymeric Phases: Preparation of a Catalyst on Raschig Rings. *J. Am. Chem. Soc.* **2006**, 128, 13261–13267.
- Skowerski, K.; Bialecki, J.; Czarnocki, S. J.; Zukowska, K.; Grela, K. Effective Immobilisation of a Metathesis Catalyst Bearing an Ammonium-Tagged NHC Ligand on Various Solid Supports. *Beilstein J. Org. Chem.* **2016**, 12, 5–15.
- Li, Q.; Zhou, T.; Yang, H. Encapsulation of Hoveyda-Grubbs(2nd) Catalyst within Yolk-Shell Structured Silica for Olefin Metathesis. *ACS Catal.* **2015**, 5, 2225–2231.
- Connon, S.; Blechert, S. A Solid-Supported Phosphine-Free Ruthenium Alkylidene for Olefin Metathesis in Methanol and Water. *Bioorg. Med. Chem. Lett.* **2002**, 12, 1873–1876.
- Balcar, H.; Zilkova, N.; Sedlacek, J.; Zednik, J. MCM-41 Anchored Schrock Catalyst  $\text{Mo}(\text{=CHCMe}_2\text{Ph})(\text{=N-2,6-I-Pr}_2\text{C}_6\text{H}_3)[\text{OCMe}(\text{CF}_3)_2]_2$ -Activity in 1-Heptene Metathesis and Cross-Metathesis Reactions. *J. Mol. Catal. A Chem.* **2005**, 232, 53–58.
- Le Roux, E.; Taoufik, M.; Coperet, C.; de Mallmann, A.; Thivolle-Cazat, J.; Basset, J.; Maunders, B.; Sunley, G. Development of Tungsten-Based Heterogeneous Alkane Metathesis Catalysts Through a Structure-Activity Relationship. *Angew. Chem. Int. Ed.* **2005**, 44, 6755–6758.
- Le Roux, E.; Taoufik, M.; Baudouin, A.; Coperet, C.; Thivolle-Cazat, J.; Basset, J.; Maunders, B.; Sunley, G. Silica-Alumina-Supported, Tungsten-Based Heterogeneous Alkane Metathesis Catalyst: Is it Closer to a Silica- or an Alumina-Supported System? *Adv. Synth. Catal.* **2007**, 349, 231–237.
- Yuan, J.; Townsend, E. M.; Schrock, R. R.; Goldman, A. S.; Müller, P.; Takase, M. Preparation of Tungsten-Based Olefin Metathesis Catalysts Supported on Alumina. *Adv. Synth. Catal.* **2011**, 353, 1985–1992.
- Conley, M. P.; Mougél, V.; Peryshkov, D. V.; Forrest, W. P.; Gajan, D.; Lesage, A.; Emsley, L.; Copéret, C.; Schrock, R. R. A Well-Defined Silica-Supported Tungsten Oxo Alkylidene Is a Highly Active Alkene Metathesis Catalyst. *J. Am. Chem. Soc.* **2013**, 135, 19069–19070.
- Rhers, B.; Salameh, A.; Baudouin, A.; Quadrelli, E. A.; Taoufik, M.; Copéret, C.; Lefebvre, F.; Basset, J.-M.; Solans-Monfort, X.; Eisenstein, O.; Lukens, W. W.; Lopez, L. P. H.; Sinha, A.; Schrock, R. R. A Silica Supported W Imido Carbene Complex: A Well-Defined Heterogeneous Olefin Metathesis Catalyst. *Organometallics* **2006**, 25, 3554–3557.
- Blanc, F.; Copéret, C.; Thivolle-Cazat, J.; Basset, J.-M.; Lesage, A.; Emsley, L.; Sinha, A.; Schrock, R. R. Better Characterization of Surface Organometallic Catalysts through Resolution Enhancement in Proton Solid State NMR Spectra. *Inorg. Chem.* **2006**, 45, 9587–9592.
- Conley, M. P.; Forrest, W. P.; Mougél, V.; Siddiqi, G.; Safonova, O. V.; Copéret, C.; Schrock, R. R. Bulky Aryloxide Ligand Stabilizes a Heterogeneous Metathesis Catalyst. *Angew. Chem. Int. Ed.* **2014**, 53, 14221–14224.
- Blanc, F.; Basset, J.-M.; Copéret, C.; Sinha, A.; Tonzetich, Z. J.; Schrock, R. R.; Solans-Monfort, X.; Clot, E.; Eisenstein, O.; Lesage, A.; Emsley, L. Dynamics of Silica Supported Catalysts Determined by Combining Solid State NMR Spectroscopy and Periodic DFT Calculations. *J. Am. Chem. Soc.* **2008**, 130, 5886–5990.

312 Heterogeneous catalysis in sustainable synthesis

34. Blanc, F.; Berthoud, R.; Copéret, C.; Lesage, A.; Emsley, L.; Singh, R.; Kreickmann, T.; Schrock, R. R. A Heterogeneous Alkene Metathesis Catalyst “Caught in the Act:” Direct Observation of the Key Reaction Intermediates by Solid State NMR Spectroscopy. *Proc. Natl. Acad. Sci.* **2008**, *105*, 12123–12127.
35. Hamzaoui, B.; Pelletier, J. D. A.; Abou-Hamad, E.; Basset, J. Well-Defined Silica-Supported Zirconium-Imido Complexes Mediated Heterogeneous Imine Metathesis. *Chem. Commun.* **2016**, *52*, 4617–4620.
36. Blanc, R.; Berthoud, R.; Salameh, A.; Basset, J.-M.; Copéret, C.; Singh, R.; Schrock, R. R. Dramatic Improvements of Well-Defined Silica Supported Mo-Based Olefin Metathesis Catalysts by Tuning the N-Containing Ligands. *J. Am. Chem. Soc.* **2007**, *129*, 8434–8435.
37. Rendón, N.; Berthoud, R.; Blanc, F.; Gajan, D.; Maishal, T.; Basset, J.-M.; Copéret, C.; Lesage, A.; Emsley, L.; Marinescu, S. C.; Singh, R.; Schrock, R. R. Well-Defined Silica-Supported Mo-Alkylidene Catalyst Precursors Containing One RO Substituent: Methods of Preparation and Structure-Reactivity Relationship in Alkene Metathesis. *Chem. Eur. J.* **2009**, *15*, 5083–5089.
38. Chabanas, M.; Baudouin, A.; Coperet, C.; Basset, J. A Highly Active Well-Defined Rhenium Heterogeneous Catalyst for Olefin Metathesis Prepared Via Surface Organometallic Chemistry. *J. Am. Chem. Soc.* **2001**, *123*, 2062–2063.
39. Popoff, N.; Szeto, K. C.; Merle, N.; Espinas, J.; Pelletier, J.; Lefebvre, F.; Thivolle-Cazat, J.; Delevoye, L.; De Mallmann, A.; Gauvin, R. M.; Taoufik, M. Enforcing Z-Selectivity in Olefin Metathesis through Use of Catalysts Grafted on Well-Defined Phenolic Hybrid Material. *Catal. Today* **2014**, *235*, 41–48.
40. Rhers, B.; Quadrelli, E. A.; Baudouin, A.; Taoufik, M.; Copéret, C.; Lefebvre, F.; Basset, J.-M.; Fenet, B.; Sinha, A.; Schrock, R. R. Understanding the Reactivity of  $W=NAr(CH_2tBu)_2(=CHtBu)$  ( $Ar=2,6-iPrC_6H_3$ ) with Silica Partially Dehydroxylated at Low Temperatures through a Combined Use of Molecular and Surface Organometallic Chemistry. *J. Organomet. Chem.* **2006**, *691*, 5448–5455.
41. Blanc, F.; Salameh, A.; Thivolle-Cazat, J.; Basset, J.-M.; Copéret, C.; Sinha, A.; Schrock, R. R. Grafting Mechanism and Olefin Metathesis Activity of Well-Defined Silica-Supported Mo Imido Alkyl Alkylidene Complexes. *C. R. Chim.* **2008**, *11*, 137–146.
42. Salameh, A.; Copéret, C.; Basset, J. M.; Böhm, V. P. W.; Röper, M. Rhenium(VII) Oxide/Aluminum Oxide: more Experimental Evidence for an Oxametallacyclobutane Intermediate and a Pseudo-Wittig Initiation Step in Olefin Metathesis. *Adv. Synth. Catal.* **2007**, *349*, 238–242.
43. Wu, J.; Ramanathan, A.; Kersting, R.; Jystad, A.; Zhu, H.; Hu, Y.; Marshall, C. P.; Caricato, M.; Subramaniam, B. Enhanced Olefin Metathesis Performance of Tungsten and Niobium Incorporated Bimetallic Silicates: Evidence of Synergistic Effects. *ChemCatChem* **2020**, *12*, 2004–2013.
44. Zhao, Q.; Chen, S.; Gao, J.; Xu, C. Effect of Tungsten Oxide Loading on Metathesis Activity of Ethene and 2-Butene over  $WO_3/SiO_2$  Catalysts. *Transit. Met. Chem.* **2009**, *34*, 621–627.
45. Wu, J.; Ramanathan, A.; Subramaniam, B. Novel Tungsten-Incorporated Mesoporous Silicates Synthesized Via Evaporation-Induced Self-Assembly: Enhanced Metathesis Performance. *J. Catal.* **2017**, *350*, 182–188.
46. Grubbs, R.; Miller, S.; FU, G. Ring-Closing Metathesis and Related Processes in Organic-Synthesis. *Acc. Chem. Res.* **1995**, *28*, 446–452.
47. Nasrallah, H.; Drago, D.; Magnier, C.; Crevisy, C.; Mauduit, M.; Schulz, E. Direct Immobilization of Ru-Based Catalysts on Silica: Hydrogen Bonds as Non-Covalent Interactions for Recycling in Metathesis Reactions. *ChemCatChem* **2015**, *7*, 2493–2500.

48. Michalek, F.; Bannwarth, W. Application of a Grubbs-Hoveyda Metathesis Catalyst Noncovalently Immobilized by Fluorous-Fluorous Interactions. *Helv. Chim. Acta* **2006**, *89*, 1030–1037.
49. Borre, E.; Rouen, M.; Laurent, I.; Magrez, M.; Caijo, F.; Crevisy, C.; Solodenko, W.; Toupet, L.; Frankfurter, R.; Vogt, C.; Kirschning, A.; Mauduit, M. A Fast-Initiating Ionically Tagged Ruthenium Complex: A Robust Supported Pre-Catalyst for Batch-Process and Continuous-Flow Olefin Metathesis. *Chem. Eur. J.* **2012**, *18*, 16369–16382.
50. Zhang, H.; Li, Y.; Shao, S.; Wu, H.; Wu, P. Grubbs-Type Catalysts Immobilized on SBA-15: A Novel Heterogeneous Catalyst for Olefin Metathesis. *J. Mol. Catal. A Chem.* **2013**, *372*, 35–43.
51. Pastva, J.; Skowerski, K.; Czarnocki, S. J.; Zilkova, N.; Cejka, J.; Bastl, Z.; Balcar, H. Ru-Based Complexes with Quaternary Ammonium Tags Immobilized on Mesoporous Silica as Olefin Metathesis Catalysts. *ACS Catal.* **2014**, *4*, 3227–3236.
52. Pastva, J.; Cejka, J.; Zilkova, N.; Mestek, O.; Rangus, M.; Balcar, H. Hoveyda-Grubbs First Generation Type Catalyst Immobilized on Mesoporous Molecular Sieves. *J. Mol. Catal. A Chem.* **2013**, *378*, 184–192.
53. Yang, H.; Ma, Z.; Wang, Y.; Fang, L. Hoveyda-Grubbs Catalyst Confined in the Nanocages of SBA-1: Enhanced Recyclability for Olefin Metathesis. *Chem. Commun.* **2010**, *46*, 8659–8661.
54. Elias, X.; Pleixats, R.; Man, M.; Moreau, J. Hybrid-Bridged Silsesquioxane as Recyclable Metathesis Catalyst Derived from a Bis-Silylated Hoveyda-Type Ligand. *Adv. Synth. Catal.* **2006**, *348*, 751–762.
55. Jee, J.; Cheong, J. L.; Lim, J.; Chen, C.; Hong, S. H.; Lee, S. S. Highly Selective Macrocyclic Formations by Metathesis Catalysts Fixated in Nanopores. *J. Org. Chem.* **2013**, *78*, 3048–3056.
56. Spekrijse, J.; Ohlstrom, L.; Sanders, J. P. M.; Bitter, J. H.; Scott, E. L. Mechanochemical Immobilisation of Metathesis Catalysts in a Metal-Organic Framework. *Chem. Eur. J.* **2016**, *22*, 15437–15443.
57. Choluj, A.; Krzesinski, P.; Ruszczynska, A.; Bulska, E.; Kajetanowicz, A.; Grela, K. Noncovalent Immobilization of Cationic Ruthenium Complex in a Metal-Organic Framework by Ion Exchange Leading to a Heterogeneous Olefin Metathesis Catalyst for Use in Green Solvents. *Organometallics* **2019**, *38*, 3397–3405.
58. Choluj, A.; Karczykowski, R.; Chmielewski, M. J. Simple and Robust Immobilization of a Ruthenium Olefin Metathesis Catalyst inside MOFs by Acid-Base Reaction. *Organometallics* **2019**, *38*, 3392–3396.
59. Choluj, A.; Nogas, W.; Patrzalek, M.; Krzesinski, P.; Chmielewski, M. J.; Kajetanowicz, A.; Grela, K. Preparation of Ruthenium Olefin Metathesis Catalysts Immobilized on MOF, SBA-15, and 13X for Probing Heterogeneous Boomerang Effect. *Catalysts* **2020**, *10*, 438.
60. Lim, J.; Lee, S. S.; Ying, J. Y. Mesoporous Silica-Supported Catalysts for Metathesis: Application to a Circulating Flow Reactor. *Chem. Commun.* **2010**, *46*, 806–808.
61. Skowerski, K.; Pastva, J.; Czarnocki, S. J.; Janoscova, J. Exceptionally Stable and Efficient Solid Supported Hoveyda-Type Catalyst. *Org. Process Res. Dev.* **2015**, *19*, 872–877.
62. Skowerski, K.; Czarnocki, S. J.; Knapkiewicz, P. Tube-in-Tube Reactor as a Useful Tool for Homo- and Heterogeneous Olefin Metathesis under Continuous Flow Mode. *ChemSusChem* **2014**, *7*, 536–542.
63. Lim, J.; Lee, S. S.; Ying, J. Y. Silica-Supported Catalysts for Ring-Closing Metathesis: Effects of Linker Group and Microenvironment on Recyclability. *Chem. Commun.* **2008**, 4312–4314.

314 Heterogeneous catalysis in sustainable synthesis

64. Marciniak, B.; Rogalski, S.; Potrzebowski, M. J.; Pietraszuk, C. Ruthenium Carbene Siloxide Complexes Immobilized on Silica: Synthesis and Catalytic Activity in Olefin Metathesis. *ChemCatChem* **2011**, *3*, 904–910.
65. Bru, M.; Dehn, R.; Teles, J. H.; Deuerlein, S.; Danz, M.; Mueller, I. B.; Limbach, M. Ruthenium Carbenes Supported on Mesoporous Silicas as Highly Active and Selective Hybrid Catalysts for Olefin Metathesis Reactions under Continuous Flow. *Chem. Eur. J.* **2013**, *19*, 11661–11671.
66. Li, L.; Shi, J. A Highly Active and Reusable Heterogeneous Ruthenium Catalyst for Olefin Metathesis. *Adv. Synth. Catal.* **2005**, *347*, 1745–1749.
67. Melis, K.; De Vos, D.; Jacobs, P.; Verpoort, F. ROMP and RCM Catalysed by (R<sub>3</sub>P)(2) Cl<sub>2</sub>Ru=CHPh Immobilised on a Mesoporous Support. *J. Mol. Catal. A Chem.* **2001**, *169*, 47–56.
68. Krause, J.; Nuyken, O.; Wurst, K.; Buchmeiser, M. Synthesis and Reactivity of Homogeneous and Heterogeneous Ruthenium-Based Metathesis Catalysts Containing Electron-Withdrawing Ligands. *Chem. Eur. J.* **2004**, *10*, 777–784.
69. Mayr, M.; Wang, D.; Kroll, R.; Schuler, N.; Pruhs, S.; Furstner, A.; Buchmeiser, M. Monolith-Disk-Supported Metathesis Catalysts for Use in Combinatorial Chemistry. *Adv. Synth. Catal.* **2005**, *347*, 484–492.
70. Krause, J.; Lubbad, S.; Nuyken, O.; Buchmeiser, M. Monolith- and Silica-Supported Carboxylate-Based Grubbs-Herrmann-Type Metathesis Catalysts. *Adv. Synth. Catal.* **2003**, *345*, 996–1004.
71. Weck, M.; Jackiw, J.; Rossi, R.; Weiss, P.; Grubbs, R. Ring-Opening Metathesis Polymerization from Surfaces. *J. Am. Chem. Soc.* **1999**, *121*, 4088–4089.
72. De Clercq, B.; Lefebvre, F.; Verpoort, F. A New Heterogeneous Hybrid Ruthenium Catalyst Being an Eco-Friendly Option for the Production of Polymers and Organic Intermediates. *New J. Chem.* **2002**, *26*, 1201–1208.
73. Hamtil, R.; Zilkova, N.; Balcar, H.; Cejka, J. Rhenium Oxide Supported on Organized Mesoporous Alumina—A Highly Active and Versatile Catalyst for Alkene, Diene, and Cycloalkene Metathesis. *Appl. Catal. A Gen.* **2006**, *302*, 193–200.
74. Mori, M.; Kitamura, K. Ene–Yne and Alkyne Metathesis. In *Comprehensive Organometallic Chemistry III*; Michael, D., Mingos, P., Crabtree, R., Eds.; Elsevier, 2007.
75. Weissman, H.; Plunkett, K.; Moore, J. A Highly Active, Heterogeneous Catalyst for Alkyne Metathesis. *Angew. Chem. Int. Ed.* **2006**, *45*, 585–588.
76. Hauser, P. M.; Hunger, M.; Buchmeiser, M. R. Silica-Supported Molybdenum Alkylidyne N-Heterocyclic Carbene Catalysts: Relevance of Site Isolation to Catalytic Performance. *ChemCatChem* **2018**, *10*, 1829–1834.
77. Genelot, M.; Cheval, N. P.; Vitorino, M.; Berrier, E.; Weibel, J.; Pale, P.; Mortreux, A.; Gauvin, R. M. Well-Defined Silica-Supported Molybdenum Nitride Species: Silica Grafting Triggers Alkyne Metathesis Activity. *Chem. Sci.* **2013**, *4*, 2680–2685.
78. Estes, D. P.; Gordon, C. P.; Fedorov, A.; Liao, W.; Ehrhorn, H.; Bittner, C.; Zier, M. L.; Bockfeld, D.; Chan, K. W.; Eisenstein, O.; Raynaud, C.; Tamm, M.; Coperet, C. Molecular and Silica-Supported Molybdenum Alkyne Metathesis Catalysts: Influence of Electronics and Dynamics on Activity Revealed by Kinetics, Solid-State NMR, and Chemical Shift Analysis. *J. Am. Chem. Soc.* **2017**, *139*, 17597–17607.
79. Giacalone, F.; Gruttadauria, M. *Catalytic Methods in Asymmetric Synthesis: Advanced Materials, Techniques, and Applications*; Wiley: Hoboken, NJ, 2011.
80. Hoveyda, A. H.; Schrock, R. R. Catalytic Asymmetric Olefin Metathesis. *Chem. Eur. J.* **2001**, *7*, 945–950.

81. Hoveyda, A. H.; Malcolmson, S. J.; Meek, S. J.; Zhugralin, A. R. Catalytic Enantioselective Olefin Metathesis in Natural Product Synthesis. Chiral Metal-Based Complexes That Deliver High Enantioselectivity and More. *Angew. Chem. Int. Ed.* **2009**, *49*, 34–44.
82. Hartung, J.; Dornan, P. K.; Grubbs, R. H. Enantioselective Olefin Metathesis with Cyclo-metallated Ruthenium Complexes. *J. Am. Chem. Soc.* **2014**, *136*, 13029–13037.
83. Meek, S. J.; Malcolmson, S. J.; Li, B.; Schrock, R. R.; Hoveyda, A. H. The Significance of Degenerate Processes to Enantioselective Olefin Metathesis Reactions Promoted by Stereogenic-at-Mo Complexes. *J. Am. Chem. Soc.* **2009**, *131*, 16407–16409.
84. Hultsch, K. C.; Jernelius, J. A.; Hoveyda, A. H.; Schrock, R. R. The First Polymer-Supported and Recyclable Chiral Catalyst for Enantioselective Olefin Metathesis. *Angew. Chem. Int. Ed.* **2002**, *41*, 589–593.
85. Dolman, S. J.; Hultsch, K. C.; Pezet, F.; Teng, X.; Hoveyda, A. H.; Schrock, R. R. Supported Chiral Mo-Based Complexes as Catalysts for Enantioselective Olefin Metathesis. *J. Am. Chem. Soc.* **2004**, *126*, 10945–10953.
86. Chikkali, S.; Mecking, S. Refining of Plant Oils to Chemicals by Olefin Metathesis. *Angew. Chem. Int. Ed.* **2012**, *51*, 5802–5808.
87. Nieres, P. D.; Zelin, J.; Trasarti, A. F.; Apesteguia, C. R. Valorisation of Vegetable Oils by Heterogeneous Catalysis Via Metathesis Reactions. *Curr. Opinion Green Sust. Chem.* **2018**, *10*, 1–5.
88. Rybak, A.; Meier, M. A. R. Cross-Metathesis of Fatty Acid Derivatives With Methyl Acrylate: Renewable Raw Materials for the Chemical Industry. *Green Chem.* **2007**, *9*, 1356–1361.
89. Zelin, J.; Nieres, P. D.; Trasarti, A. F.; Apesteguia, C. R. Valorisation of Vegetable Oils Via Metathesis Reactions on Solid Catalysts: Cross-Metathesis of Methyloleate with 1-Hexene. *Appl. Catal. A. Gen.* **2015**, *502*, 410–441.
90. Nieres, P. D.; Zelin, J.; Trasarti, A. F.; Apesteguia, C. R. Heterogeneous Catalysis for Valorisation of Vegetable Oils Via Metathesis Reactions: Ethenolysis of Methyl Oleate. *Cat. Sci. Technol.* **2016**, *6*, 6561–6568.
91. Balcar, H.; Zilkova, N.; Kubo, M.; Mazur, M.; Bastl, Z.; Cejka, J. Ru Complexes of Hoveyda-Grubbs Type Immobilized on Lamellar Zeolites: Activity in Olefin Metathesis Reactions. *Beilstein J. Org. Chem.* **2015**, *11*, 2087–2096.
92. Pillai, S. K.; Hamoudi, S.; Belkacemi, K. Metathesis of Methyloleate over Methyltrioxorhenium Supported on ZnCl<sub>2</sub>-Promoted Mesoporous Alumina. *Appl. Catal. A Gen.* **2013**, *455*, 155–163.
93. Pillai, S. K.; Hamoudi, S.; Belkacemi, K. Functionalized Value-Added Products Via Metathesis of Methyloleate over Methyltrioxorhenium Supported on ZnCl<sub>2</sub>-Promoted Mesoporous Alumina. *Fuel* **2013**, *110*, 32–39.
94. Lee, M.; Han, Y. H.; Hwang, D. W. Cross-Metathesis of Methyl Oleate with Ethylene over Methyltrioxorhenium Supported on ZnAl<sub>2</sub>O<sub>4</sub> as a Heterogeneous Catalyst. *Catal. Commun.* **2020**, *144*, 106088.
95. Kajetanowicz, A.; Sytniczuk, A.; Grela, K. Metathesis of Renewable Raw Materials-Influence of Ligands in the Indenylidene Type Catalysts on Self-Metathesis of Methyl Oleate and Cross-Metathesis of Methyl Oleate with (Z)-2-butene1,4-Diol Diacetate. *Green Chem.* **2014**, *16*, 1579–1585.
96. Forman, G. S.; Bellabarba, R. M.; Tooze, R. P.; Slawin, A. M. Z.; Karch, R.; Winde, R. Metathesis of Renewable Unsaturated Fatty Acid Esters Catalysed by a Phoban-Indenylidene Ruthenium Catalyst. *J. Organomet. Chem.* **2006**, *691*, 5513–5516.
97. Kadyrov, R.; Azap, C.; Weidlich, S.; Wolf, D. Robust and Selective Metathesis Catalysts for Oleochemical Applications. *Top. Catal.* **2012**, *55*, 538–542.

**316** Heterogeneous catalysis in sustainable synthesis

98. Hasib-ur-Rahman, M.; Hamoudi, S.; Belkacemi, K. Fatty Acid Methyl Ester Heterogeneous Self-Metathesis in Hydrophobic Green Solvent: Mass Transfer Limitations, Catalyst Recyclability, and Stability. *Can. J. Chem. Eng.* **2018**, *96*, 223–230.
99. Abidli, A.; Hamoudi, S.; Belkacemi, K. Synthesis, Characterization and Insights into Stable and Well Organized Hexagonal Mesoporous Zinc-Doped Alumina as Promising Metathesis Catalysts Carrier. *Dalton Trans.* **2015**, *44*, 9823–9838.
100. Zelin, J.; Trasarti, A. F.; Apesteguia, C. R. Self-Metathesis of Methyl Oleate on Silica-Supported Hoveyda-Grubbs Catalysts. *Catal. Commun.* **2013**, *42*, 84–88.
101. Yinghuai, Z.; Kuijin, L.; Huimin, N.; Chuanzhao, L.; Stubbs, L. P.; Siong, C. F.; Muihua, T.; Peng, S. C. Magnetic Nanoparticle Supported Second Generation Hoveyda-Grubbs Catalyst for Metathesis of Unsaturated Fatty Acid Esters. *Adv. Synth. Catal.* **2009**, *351*, 2650–2656.
102. Rodella, C.; Cavalcante, J.; Buffon, R. Metathesis of Methyl Oleate over Rhenium Oxide-Based Catalysts Supported on Borated Silica-Alumina: Catalyst Recycling. *Appl. Catal. A Gen.* **2004**, *274*, 213–217.

## Chapter 3.5

# Friedel-Crafts and related reactions catalyzed by solid acids

### 3.5.1 Introduction

The Friedel-Crafts and related transformations are likely one of the most common and important transformations in synthetic chemistry, both at the laboratory as well as the industrial level.<sup>1</sup> These processes occur by the common electrophilic aromatic substitution ( $S_{EAr}$ ) pathway.<sup>2</sup> The target reactions include a large group of transformations; the most common are alkylation and hydroxy/amino-alkylation, acylation, halogenation, nitration, sulfonation, etc. The original reactions were developed by Friedel and Crafts in the 1870s when they reported the alkylation of benzene with alkyl chlorides as alkylating agents using  $AlCl_3$  to promote the reaction<sup>3</sup> followed by several related applications, such as acylation, carboxylation, just to name a few.<sup>4</sup> Their pioneering efforts launched a new field in synthetic chemistry. One cannot overstate the overwhelming impact Friedel-Crafts chemistry had and continues to have on organic synthesis. Due to its applicability and importance, the field generated considerable attention and thus its continued progress had been the target of regular reviews and books. Olah's extensive series on these reactions<sup>5,6</sup> was the first major effort to organize related reports to a framework of reactions. Over the nearly 150 years of progress, Friedel-Crafts reactions became one of the most important C–C bond forming transformations in organic synthesis, both at the laboratory level and in the chemical/pharmaceutical industries.<sup>7</sup> These reactions are typically carried out by either Brønsted or Lewis acid catalysis. The traditional catalysts for Friedel-Crafts chemistry include the well-known Lewis acids such as  $AlCl_3$  or  $BF_3$  and protic mineral acids such as  $HCl$ ,  $H_2SO_4$  or  $HNO_3$ . The use of these acids, especially the Lewis acids, as promoters/catalysts has several drawbacks: they are often applied in stoichiometric (even superstoichiometric) amounts, they are moisture sensitive, and they often form a covalent bond with the oxygen atoms of the products. These products have to be hydrolyzed; therefore, a considerable amount of toxic waste is generated. In addition, mostly all possible product isomers form, and the reactions exhibit poor regioselectivity.<sup>8</sup> The previously mentioned mineral Brønsted acids are highly corrosive and most of

them discharge toxic fumes that represent safety and health hazards. The regeneration and recycling of both groups are practically impossible. In conclusion, these catalysts/promoters and the reactions they catalyze do not comply with the principles of green chemistry and green engineering.<sup>9–11</sup> Solid acid catalysts appear to be favorable replacements to the traditional Lewis and Brønsted acids in many acid-catalyzed reactions, including Friedel-Crafts chemistry.<sup>12, 13</sup> In addition to being effective catalysts for these transformations, they possess distinct advantages. Among the many benefits they offer, they are stable under the experimental conditions, can be easily removed from the product mixture, and are commonly recyclable, and due to their unique structures they exhibit high selectivities, often called shape selective catalysis.<sup>14</sup> Both solid Lewis and Brønsted acids became mainstream catalyst for Friedel-Crafts and related reactions, and thus are the subject of numerous books and reviews.<sup>15–19</sup> In fact, a large part of the current efforts in the development of environmentally benign aromatic electrophilic substitution is focused on the design of novel, moisture-resistant, and recyclable catalysts.<sup>20, 21</sup> Many of these catalysts could be applied under microwave-assisted conditions that commonly resulted in significant reduction in reaction times, while maintaining or increasing yields.<sup>22–24</sup>

In this chapter the applications of solid acids in Friedel-Crafts chemistry and other related electrophilic reactions will be reviewed, focusing on environmentally benign transformations. As this field has been thoroughly and regularly reviewed, while providing references for the major earlier reviews and books on the specific areas, the focus of this chapter will be placed on advancement made in the past two decades, thus most of the original work surveyed was published between 1996 and 2021. Despite this limitation, the number of related published works is still extensive, thus the major goal is to provide the broadest possible scope by citing representative examples and not to attempt a fully comprehensive treatment of the material.

## 3.5.2 Alkylation, hydroxyalkylation

Aromatic electrophilic alkylation was one of the classical reactions that Friedel and Crafts originally developed.<sup>3, 4</sup> It is one of the most fundamental C–C bond forming reactions that results in the formation of a broad variety of alkylated aromatic compounds. These synthetic procedures utilize diverse alkylating agents, including mostly alkenes, alcohols, or alkyl halides for the introduction of alkyl groups, and aldehydes, ketones, or imines to introduce a hydroxyl-alkyl or amino-alkyl substituent. These processes are widely used at the laboratory as well as at the industrial scale to produce fine chemicals or pharmaceutical intermediates.

### 3.5.2.1 Alkylations with hydrocarbons

Hydrocarbons, particularly, alkenes are the environmentally most preferable alkylating agents. Using these reactants the atom economy of the reaction is 100%, namely both the substrate and the alkylating agent are fully incorporated

into the final product. This also means that, at least theoretically, the reaction will not produce any waste, eliminating the need for waste disposal. In a few cases, aromatic hydrocarbons, usually presubstituted with *tert*-butyl or adamantyl substituents, or occasionally simple alkanes are also used in transalkylation and alkylation reactions. The most common applications of simple alkenes in heterogeneous catalytic Friedel-Crafts alkylations are summarized in Table 1.

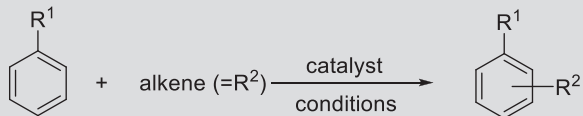
Table 1 presents several applications that use simple alkenes with heterocyclic and carbocyclic aromatics. The reactions mostly provide good to excellent conversions using a variety of solid acids. Although most of the reactions progressed with high yields, they often suffer from the lack of regioselectivity and accordingly, their synthetic potential is limited. Most of the products are large-scale industrial materials and commonly used as mixtures, thus not requiring separation. There are, however, several specialized synthetic processes that employ more complicated substrates as well as reagents, and result in the selective formation of valuable synthons with considerable structural diversity. The typical catalysts used are zeolites, sulfonic acid-based resins, supported heteropoly acids, and acidic clays.

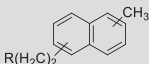
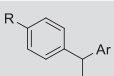
A synthetically more relevant transformation is the reaction of nitroalkanes with benzene derivatives and common heterocyclic building blocks. Table 2 summarizes these reactions depicting the structure of the products.

The earlier mentioned reactions are of synthetic importance, and the depicted yields are commonly isolated yields. The typical solid acids used in these alkylations are ion-exchange resins (Amberlyst 15) and acidic montmorillonites, such as K-10. As a significant shift in the application of catalysts, the most recent examples are dominated by metal-organic framework (MOF)-based solids. In an example (Table 2, entry 3) an MOF material prepared from V-shaped dicarboxylate ligands and dicopper units was applied. These materials are often functionalized in order to improve their performance. Urea-containing MOFs have been applied to catalyze the alkylation of indoles with nitroalkenes in several examples (Table 2 entries 4–6). Although some applications have shortcomings from the environmental/sustainability perspective (e.g. Table 2 entries 1, 3–6) using dichloromethane, acetonitrile, or toluene as the solvent, some processes use solvent-free conditions during the reaction itself (Table 2 entry 2). In most cases, the catalysts are reusable through more than three to four consecutive reactions without a meaningful drop in their activity. The reactions usually readily take place at moderate temperatures (RT–80°C) and provide the products in good to excellent yields often with exclusive selectivity.

There is a wealth of information available for alkylations of synthetic importance when specific alkylating agents where the alkylating unit is an alkene are used. The regioselective alkylation of indoles with  $\alpha,\beta$ -unsaturated ketones was achieved by Amberlyst as a catalyst (Scheme 1). The products were isolated in good to excellent yields up to 96%. The catalyst was found to be recyclable in a number of consecutive reactions even without reactivation; decline in activity was not observed.<sup>20</sup>

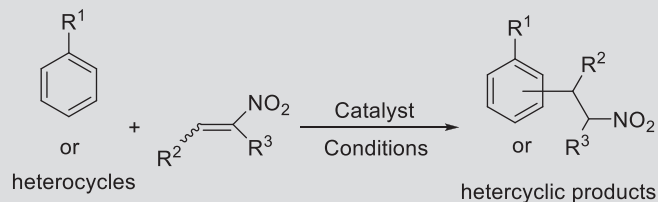
**TABLE 1** Heterogeneous catalytic alkylation of aromatics with simple alkenes.



| Entry | Aromatics                    | Alkene  | Catalysts/conditions   | Product  | Yield (%)       | Selectivity  | Ref. |
|-------|------------------------------|---|--|--|-----------------|--|------|
| 1     | Toluene                      | Octene  | Amberlyst-15/80°C, 4 h, liquid phase   | 2-Octyl-toluene (plus a variety of products due to rearrangement)                  | 75 <sup>a</sup> | 65% (2/3/4 = 56/17/2)                                    | 25   |
| 2     | 4-Methoxy-phenol             | Isobutylene   | Filtrol (acidic activated clay)/1,4-dioxane, 150°C, 3 h  | Mono- and di- <i>tert</i> -butylated methoxyphenols                                | 75 <sup>a</sup> | Mono/di = 7/3  | 26   |
| 3     | Diphenyl ether               | 1-Decene  | Sulfated zirconia <sup>b</sup> /150°C, 2 h   | A variety of 2- and 4-alkylated products due to rearrangement                      | 89 <sup>a</sup> | 18%–40%  | 27   |
| 4     | Guaiacol                     | Cyclohexene   | Amberlyst-15 <sup>c</sup> /80°C, 2 h, in excess cyclohexene  | A mixture of monoalkylated products  | 94              | –  | 28   |
| 5     | $\alpha$ -Methylnaphthalenes | Long chain C <sub>11</sub> –C <sub>12</sub> alkenes | HY and H $\beta$ zeolites/180–200°C, 4 h   |  | 90              | 100%   | 29   |
| 6     | Electron-rich arenes         | Styrene derivatives                                 | Sulfonic acid resin D072 <sup>c</sup> /reflux in DCE <sup>d</sup> , 4 h                                    |  | 81–100          | 60%–100%   | 30   |
| 7     | Benzene                      | 1-Dodecene  | H <sub>3</sub> PW <sub>12</sub> O <sub>40</sub> /IL <sup>e</sup> /SBA-15 <sup>f</sup> , 100°C, flow system | Linear alkylbenzenes   | 30–87           | 2-Selectivity is 50%, 3-, 4-, 5-, 6-products also formed | 31   |

a, conversion; b, deactivation, regeneration necessary; c, reusable catalyst; d, DCE-1,2-dichloroethane; e, IL, ionic liquid; f, SBA-15-Santa Barbara amorphous silica.

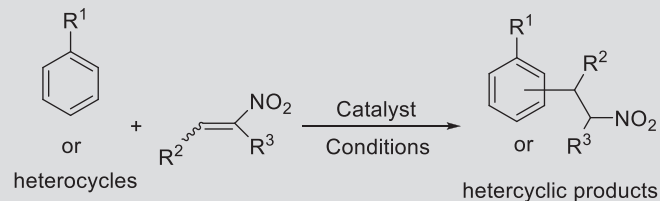
**TABLE 2** Solid acid-catalyzed alkylation of aromatics with nitroalkenes.



| Entry | Aromatics            | Nitro-alkene       | Catalysts/conditions  | Product | Yield (%)                           | Ref.                  |
|-------|----------------------|--------------------|---|---------|-------------------------------------|-----------------------|
| 1     | Indoles              | Nitrostyrene       | Amberlyst-15/RT, 24 h, ether or CH <sub>2</sub> Cl <sub>2</sub> ; Zr-UiO-67 MOF<br>Zr-MOF |         | 55–97                               | <a href="#">32–34</a> |
| 2     | Indoles and pyrroles | Aryl-nitroalkanes  | K-10/neat, 60°C, 20–35 min (pyrroles), 15–75 min (indoles)                                |         | 84–93 (pyrroles)<br>81–94 (indoles) | <a href="#">35</a>    |
| 3     | Indoles              | Alkyl-nitroalkenes | Cu-MOF-urea/acetonitrile, 60°C, 18 h  |         | 81–98                               | <a href="#">36</a>    |

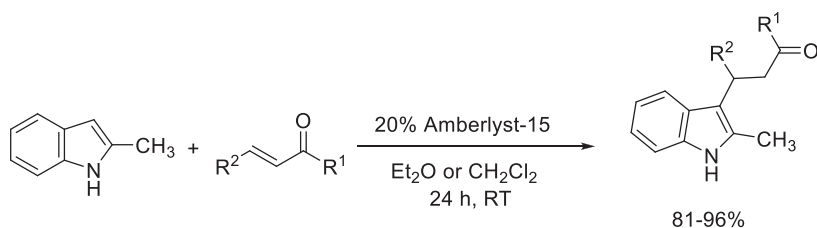
*Continued*

**TABLE 2** Solid acid-catalyzed alkylation of aromatics with nitroalkenes—cont'd



| Entry | Aromatics                                | Nitro-alkene           | Catalysts/conditions  | Product  | Yield (%) | Ref.   |
|-------|--|------------------------|---|--|-----------|--------|
| 4     | <i>N</i> -alkyl-indoles                  | Alkyl-nitroalkenes     | Zn-MOF-urea/toluene, 60°C, 24 h   |  | 80–92     | 37, 38 |
| 5     | Indoles, pyrrole, electron-rich benzenes | $\beta$ -nitro-styrene | $\text{Cu}_3(\text{BTC})_2$ /toluene, 55°C, 24 h  | Indoles: 3-substitution<br>Pyrrole: 2-substitution | 17–98     | 39     |
| 6     | Indole                                   | $\beta$ -nitro-styrene | MIL101(Cr)@thiourea <sub>3</sub> /CH <sub>3</sub> CN or toluene as solvents, RT–80°C, 18–48 h | Major product: 3-substitution                      | 16–85     | 40     |

BTC, 1,3,5-benzenetricarboxylic acid; MOF, metal-organic framework.

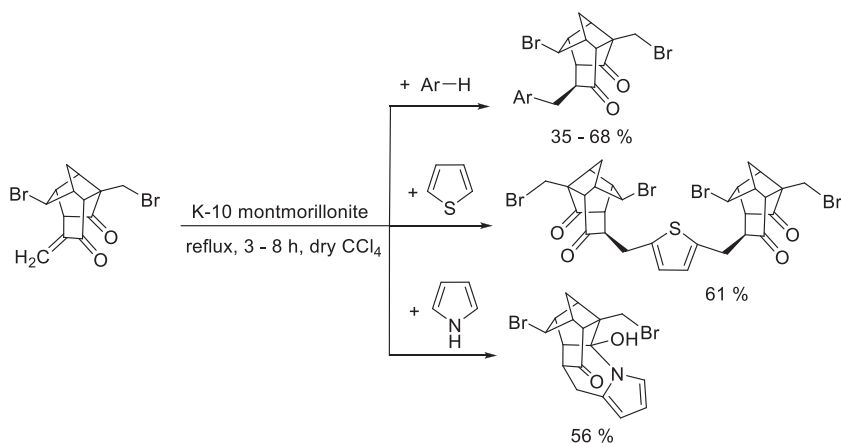


**SCHEME 1** Alkylation of indoles with  $\alpha,\beta$ -unsaturated ketones by Amberlyst 15.

The Friedel-Crafts alkylation of carbocyclic and heterocyclic compounds with a polycyclic caged enone was developed using K-10 montmorillonite as a solid acid catalyst at relatively modest temperatures (Scheme 2). The reaction was highly sensitive to the structure of the aromatic substrate; benzene derivatives gave the expected monoalkylated products; however, highly activated heterocycles such as thiophene afforded 2,5-bis-alkylthiophene. Although pyrrole provided selective monoalkylation, the intermediate underwent an intramolecular cyclization via the reaction of the pyrrole NH with a carbonyl group.<sup>41</sup>

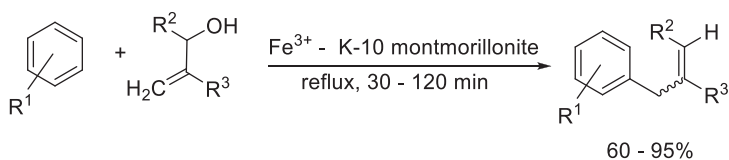
Several Baylis-Hillman adducts were used as alkylating agents in the iron(III)-exchanged montmorillonite K-10-catalyzed Friedel-Crafts alkylation of substituted benzenes (Scheme 3). The reaction provided good to excellent yields in short reaction times and the catalyst was found to be recyclable as it showed no decline in its activity after several consecutive reactions.<sup>42</sup>

A microwave-assisted solvent-free Cu-triflate-catalyzed protocol was developed for the synthesis of fused chromenopyridines. The transformation required an oxidation step and air was used as a green oxidant.<sup>43</sup> The copper-based

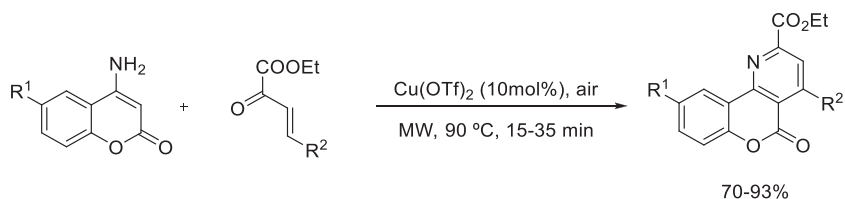


**SCHEME 2** Alkylation of aromatics with a polycyclic caged enone using K-10 montmorillonite catalysis.

324 Heterogeneous catalysis in sustainable synthesis



**SCHEME 3** Alkylation of aromatics with Baylis-Hillman adducts using  $\text{Fe}^{3+}$ -doped K-10 montmorillonite as catalyst.

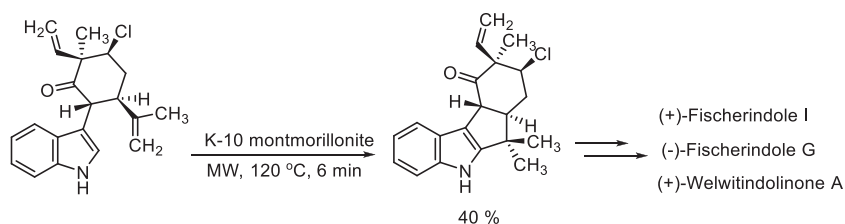


**SCHEME 4** Synthesis of chromenopyridines by  $\text{Cu}(\text{OTf})_2$ -catalyzed alkylations.

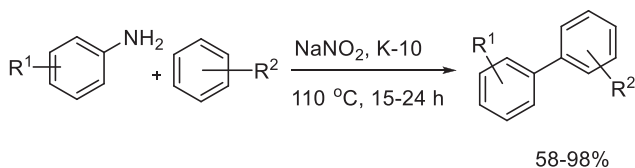
catalyst was found to be a multifunctional promoter in this reaction due to its redox properties; it catalyzed the Michael addition as well as the oxidation of the intermediate to the final product (Scheme 4). Although the reaction, including the last aromatization step, can occur in a catalyst-free system, the catalyst significantly enhanced the reaction rate and overall yield of the products.

Commonly Friedel-Crafts alkylations are applied as one of the steps in complicated total synthetic pathways. The cyclization of an important intermediate in the synthesis of welwitindolinone A, fischerindole I and G was carried out by a montmorillonite K-10-catalyzed microwave-assisted intramolecular alkylation (Scheme 5).<sup>44, 45</sup> The reaction occurred via the alkylation of the C-2 of indole with a terminal  $\text{C}=\text{C}$  bond to form the new five-membered ring.

Although the traditional coupling reactions, such as the Heck, Suzuki, or Negishi couplings, are typically metal-catalyzed transformations,<sup>46-48</sup> acid-catalyzed approaches that occur via a different mechanism can also be applied to synthesize similar products. K-10 montmorillonite was found to be an environmentally benign solid acid catalyst for several solid-phase diazotization



**SCHEME 5** Synthesis of indole alkaloids via a K-10-catalyzed intramolecular cyclialkylation.

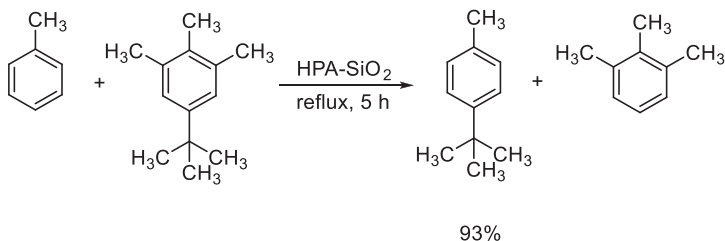


**SCHEME 6** K-10-catalyzed metal-free coupling of aromatics via solid-phase diazotization.

reactions, one being the synthesis of biphenyls. The reaction generates the diazonium salt that undergoes a nucleophilic attack by the aromatic hydrocarbons to yield a new C–C bond connecting the two rings (Scheme 6).<sup>49</sup> The process appears to have a broad substituent tolerance and provided excellent yield for most substrates. As another environmentally beneficial feature, the catalyst can be recycled several times without loss in its activity.

The Friedel-Crafts transalkylation of aromatics is mostly carried out by reagents that can supply the *tert*-butyl or adamantyl cations.<sup>50</sup> The *tert*-butylation of toluene with 5-*tert*-butyl-1,2,3-trimethylbenzene was achieved by using silica-supported and silica-included phosphotungstic ( $H_3[PW_{12}O_{40}]$ ) and silicotungstic ( $H_4[SiMo_{12}O_{40}]$ ) acids (HPA) (Scheme 7). The silica-included heteropoly acids achieved 93% conversion, while the surface-bound silica-supported counterparts only provided 62% conversion. An excess of toluene was used to ensure the complete capture of the released *tert*-butyl cations. The catalysts were found to be recyclable, although the activity declined in the successive reactions.<sup>51,52</sup> The acidic Cs salts of the phosphotungstic acid were also applied in different designs, such as neat, or silica- and MCM-41-supported samples to catalyze the transalkylation providing high activity (up to 100% conversion).<sup>12</sup>

Reactions using simple alkanes are relatively scarce due to the low reactivity of alkanes, a few examples can still be found. A process applying a simple alkane, heptane over various montmorillonite catalysts readily yielded the expected 2-phenyl-heptanes, with low conversion, but high selectivities (up to 80%).<sup>53</sup>



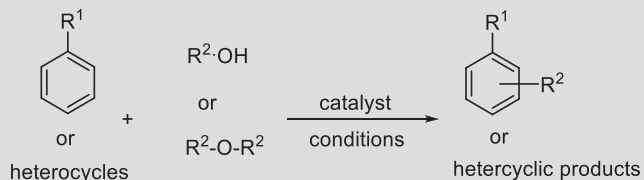
**SCHEME 7** Transalkylation of toluene by silica-supported heteropoly acid catalysis.

### 3.5.2.2 Alkylations with alcohols, ethers, aldehydes, and ketones

As mentioned before, the greenest alkylating reagents are alkenes as those reactions occur with 100% atom economy and the reactions theoretically do not generate any waste. Several oxygen-containing compounds, such as alcohols, ethers, and carbonyl compounds (hydroxyalkylations), are also applied as alkylating agents. These compounds are also considered as green reactants. Although the atom economy of these reactions is not perfect, for alkylations with alcohols and ethers, the fact that the waste, water (or alcohol) is not or only minimally toxic is an inherent advantage of these reactions. These reagents, however, would cause problems when using some of the traditional catalysts. The water or alcohol that is being produced as a by-product would hydrolyze and decompose the traditional moisture-sensitive catalysts such as aluminum halides, which inhibited the past use of these green alkylating agents. The commonly used solid acids are not only just safer, less corrosive, and easier to use but they are also moisture stable and can be used with these alkylating agents. **Table 3** summarizes applications that make use of the most common alcohols and ethers for alkylation of aromatics.

As shown, a variety of catalysts can be applied for these alkylation reactions.  $\text{Ga}(\text{OTf})_3$  and rare earth metal triflates remained stable in the presence of isopropanol and provided moderate to excellent yields and selectivities (**Table 3**, entry 1) although the reaction was sluggish with substrates bearing electron-withdrawing substituents.<sup>54</sup> While the monoalkylated derivative was the dominant product, overalkylation was also observed with low selectivities. Isopropanol has also been an alkylating agent of choice in several other reactions as well (**Table 3**, entries 2–3). *p*-Cymene (**Table 3**, entry 3) was prepared by the alkylation of toluene with propan-2-ol using a catalyst UDCaT-4, which is made by combining hexagonal mesoporous alumina as an inert support for persulfated alumina and zirconia.<sup>60,63</sup> The catalyst was recycled in multiple cycles without a decrease in its activity. It is worth mentioning that the predominantly *ortho*-product often undergoes a secondary isomerization over longer reaction times to the sterically more stable *para*-compound on sulfonic acid-doped MCM41.<sup>73</sup> *Tert*-butanol is also a common *tert*-butylating agent for aromatics with catalyst such as zeolites, MCM-41-supported heteropoly acids, and rare-earth metal triflates, often in supercritical carbon dioxide ( $\text{scCO}_2$ , **Table 3**, entry 5). However, in this case 2,4-di-*tert*-butylphenol (using HY zeolite) or 2,4,6-tri-*tert*-butylphenol (with  $\text{Sc}(\text{OTf})_3/\text{MCM-41}$ ) were the major products. All catalysts were found to be recyclable with maintaining their activity. In a similar reaction, UDCaT-5, a modified zirconium dioxide catalyst containing 9% sulfate (w/w), selectively gave a monoalkylated 2-*tert*-butyl product (**Table 3** entry 6); however, using *tert*-amylalcohol a mixture of 2 and 4 alkylated products formed (**Table 3** entry 7). Another alcohol that is commonly used in alkylations is benzyl alcohol (**Table 3**, entries 8–13). This alkylating agent is proven to be

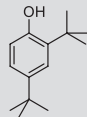
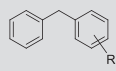
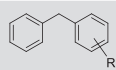
**TABLE 3** Heterogeneous catalytic alkylation of aromatics with alcohols and ethers.

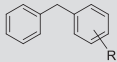
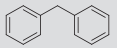
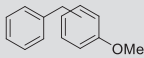
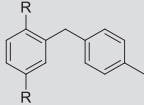
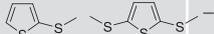
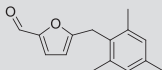
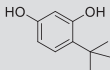


| Entry | Aromatics            | Alcohol/ether        | Catalysts/conditions                                   | Product                | Yield (%)                         | Ref. |
|-------|----------------------|----------------------|--|------------------------|-----------------------------------|------|
| 1     | Substituted benzenes | <i>i</i> Pr-OH       | Ga(OTf) <sub>3</sub> /80–110°C, 4–6 h                  |                        | 38–97 (22%–100% selectivity)      | 54   |
| 2     | Phenol               | <i>i</i> Pr-OH       | Sulfonic acid functionalized MCM-41/60°C, 20–35 min    |                        | up to 100 <sup>a</sup>            | 50   |
|       |                      | Cyclic alcohols      | H-BEA, HY zeolites                                     |                        | 77–85, overalkylation is possible | 55   |
|       |                      | Aliphatic alcohols   | Pd/C   | Selective 2-alkylation |                                   | 56   |
| 3     | Toluene              | <i>i</i> Pr-OH       | UDCaT-4 <sup>c</sup> /vapor phase reaction, 60°C, 18 h |                        | –                                 | 57   |
| 4     | Phenol               | <i>Tert</i> -butanol | Sulfonic acid functionalized MCM-41/60°C, 20–35 min    |                        | –                                 | 51   |

Continued

**TABLE 3** Heterogeneous catalytic alkylation of aromatics with alcohols and ethers—cont'd

| Entry | Aromatics                     | Alcohol/ether             | Catalysts/conditions   | Product   | Yield (%)                            | Ref.   |
|-------|-------------------------------|---------------------------|--|---|--------------------------------------|--------|
| 5     | Phenol                        | <i>Tert</i> -butanol      | Heteropoly acid functionalized MCM-41, zeolites or rare-earth-metal triflates <sup>c</sup> /scCO <sub>2</sub> , 130°C, 6 h |    | –                                    | 58, 59 |
| 6     | <i>m</i> -Cresol              | <i>Tert</i> -butanol      | UDCaT-5/120°C, 6 h   |    | 90 (93% selectivity)                 | 60     |
|       |                               | Methanol                  | Zeolites, Zr oxides<br>WO <sub>3</sub> /t-ZrO <sub>2</sub> , gas phase reaction  |    | 30                                   | 61     |
| 7     | <i>p</i> -Cresol              | <i>Tert</i> -butanol      | D3-MMT, 100°C, 10 min  |    | 73% conversion, 94%<br>2-selectivity | 62     |
| 8     | Phenol                        | <i>Tert</i> -amyl-alcohol | UDCaT-5/120°C, 6 h   | <br>2- and 4-products                            | 85 (2 vs 4 = (65:35))                | 63     |
| 9     | Benzene, substituted benzenes | Benzyl alcohol            | Polytrifluoromethanesulfoniloxane solid superacid (SiO <sub>2</sub> -SO <sub>3</sub> CF <sub>3</sub> )/110°C, 1.5–5 h      |    | 97–100                               | 64     |
| 10    | Benzene, substituted benzenes | Benzyl alcohol            | Propanesulfonic acid or benzenesulfonic acid on MCM-41, HMS and SBS-15/110°C, 1.5–5 h                                      | <br>(+ diphenyl ether as major (30%) by-product) | –                                    | 65     |

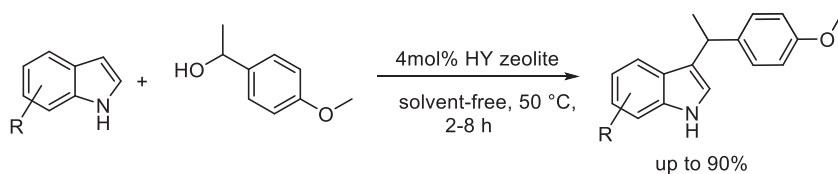
|    |                               |                                 |   |  |   |    |
|----|-------------------------------|---------------------------------|---|--|---|----|
| 11 | Benzene, substituted benzenes | Benzyl alcohol                  | Silica-supported heteropoly acids and Nafion-H  |                             | –   | 66 |
| 12 | Benzene                       | Benzyl alcohol                  | H <sub>3</sub> [PW <sub>12</sub> O <sub>40</sub> ].H <sub>2</sub> O on MCM-41, FSM-16, SBA-15 <sup>c</sup> /90°C, 4 h |                             | 80  | 67 |
| 13 | Anisole                       | Benzyl alcohol                  | M-ZrPMo/–   |                             | –   | 68 |
| 14 | Benzene, xylene               | 4-Methylbenzyl alcohol          | Nafion-H/gas phase, 80–100°C  |                             | 66–71   | 69 |
| 15 | Thiophene                     | Dimethyl disulfide              | Acid catalysts/160–350°C, flow system, gas phase  | <br>and methylated products | –   | 70 |
| 16 | Mesitylene                    | Hydroxymethyl-furfural          | Zr-montmorillonite, 110°C, 16 h   |                             | –   | 71 |
| 17 | Resorcinol                    | <i>Tert</i> -butyl-methyl ether | H <sub>3</sub> PW <sub>12</sub> O <sub>40</sub> /SBA-15   |                             | Nearly exclusive 4-selectivity, 20% conversion, 40% selectivity | 72 |

a, Conversion; b, deactivation, regeneration necessary; c, reusable catalyst; d, dichloroethane; M-ZrPMo, mesoporous molybdate-zirconium oxophosphate; D3-MMT, dealuminated montmorillonite; SBA-15, Santa Barbara amorphous silica; MCM-41, mobil composition of matter No.41), a mesoporous material; FSM-16, folding sheet materials using C16 surfactant, a mesoporous material.

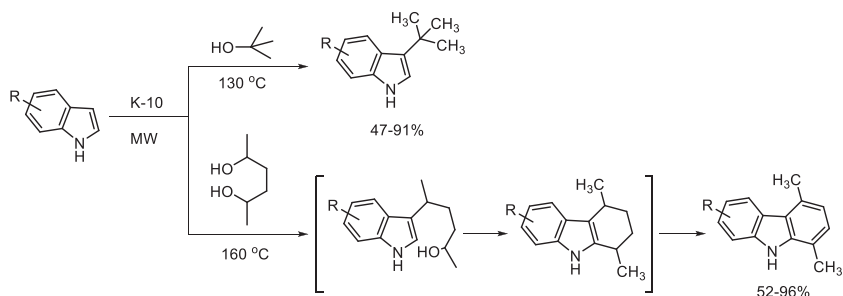
active in the presence of a broad variety of catalysts, from a silica-supported polytrifluoromethanesulfosiloxane solid superacid ( $\text{SiO}_2\text{-SO}_3\text{CF}_3$ ) to propane-sulfonic acid or benzenesulfonic acid on mesoporous silica MCM-41, HMS and SBS-15 or silica-supported heteropoly acids and Nafion-H all were found to be effective catalysts for this transformation and many showed recyclable character even after eight consecutive runs. The gas-phase thiomethylation and methylation of thiophene with dimethyl disulfide are readily catalyzed by a variety of solid acid catalysts under atmospheric pressure at 160–350°C (Table 3, entry 14). Catalysts that possess strong protic and Lewis acid sites, as well as basic sites of moderate strength, were found to show the best performance. In a somewhat difficult to classify method, the methylation of benzene and toluene was described by using syngas (mainly  $\text{H}_2$  and  $\text{CO}$ ) as a methyl source on bifunctional catalysts such as  $\text{Ce-Pt/ZSM-5}$  and  $\text{Cr}_2\text{O}_3/\text{ZnO}$ . In a flow process, the yield reached about 30% for both toluene (from benzene) and xylenes (from toluene). It was suggested that in the first step of the reaction the syngas was in situ converted to methanol, which was immediately consumed by the aromatic reactants to prevent large-scale side reactions of methanol.<sup>74–76</sup>

In synthesis of methylbenzyl-indoles, the solvent-free Friedel-Crafts alkylation of indoles was carried out with alcohols (Scheme 8).<sup>77</sup> In a comparative study, the catalytic activity, selectivity, and recyclability of ionic liquids and several solid acid catalysts (metal-organic frameworks and zeolites) were investigated. Although ionic liquids appeared to show the highest activity, the microporous frameworks provided better recyclability and selectivity. In addition, the use of these catalysts improved the monoalkylation selectivity. Combining all observations and weighing catalyst performances it was concluded that the HY zeolite is the most preferred option for these reactions. A similar application using bis(hydroxymethyl)-benzene or -naphthalene led to the formation of a polymeric material.<sup>78</sup>

K-10 montmorillonite was also found efficient in the solvent-free one-step alkylation of indoles with *tert*-butyl alcohol and the multistep alkylation/electrophilic annulation of indoles using 2,5-pentanediol (Scheme 9).<sup>79</sup> The *tert*-butylation provided moderate to high yields with excellent selectivity toward the C-3 position of indole. The solid acid showed remarkable resistance to the water that formed as a by-product in the reaction. The reaction with the diol took place in a three-step domino sequence; first the alkylation occurred



**SCHEME 8** HY zeolite-catalyzed alkylation of indoles with substituted methylbenzyl alcohol.



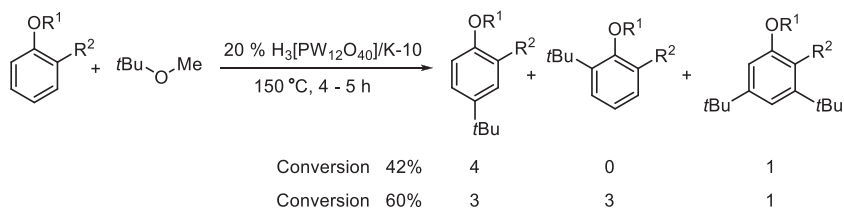
**SCHEME 9** K-10 montmorillonite-catalyzed *tert*-butylation and cyclialkylation/aromatization of indoles.

then the annulation took place by a second alkylation in the C2 position of indole. The last step was the aromatization of the cyclized product that yielded 1,4-dimethylcarbazoles in good to excellent yields. Although K-10 is most well known as a solid acid catalyst, it is also known to catalyze mild oxidations yielding aromatic products.<sup>80–82</sup>

Although ethers and esters are not commonly used alkylating agents, there are reports that indicate that these compound classes might be somewhat overlooked in alkylations. For instance, methyl-*tert*-butyl ether was used as a *tert*-butylating agent in the transalkylation of phenols. The product *tert*-butylated phenols are important industrial precursors. The catalyst used was a clay-supported heteropoly acid ( $\text{H}_3[\text{PW}_{12}\text{O}_{40}]$ ) (20% w/w) on K-10 montmorillonite), which performed well in the synthesis of *tert*-butylated dihydroxy and alkoxy benzenes using common starting materials such as catechol, resorcinol, and anisole.<sup>83</sup> The reaction was carried out without any additional solvent and the catalyst was recyclable without loss of activity (Scheme 10).

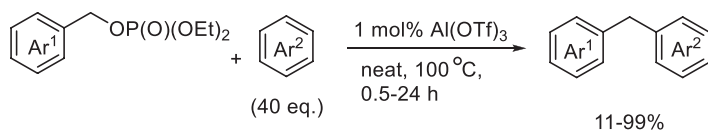
Neat (unsupported) heteropoly acids, such as the commercially available  $\text{H}_3[\text{PW}_{12}\text{O}_{40}]$  and  $\text{H}_4[\text{SiW}_{12}\text{O}_{40}]$ , were found to be effective and reusable solid acids for the alkylation of mesitylene with  $\gamma$ -butyrolactone. The product 4-(2,4,6-trimethylphenyl)butyric acid (Scheme 11) was obtained with excellent selectivity although only in moderate yield.<sup>84</sup>

The alkylation of a tetra-substituted benzene with a carvone derivative was a key step in the total synthesis of Adunctin B, a natural product.<sup>85</sup> Several

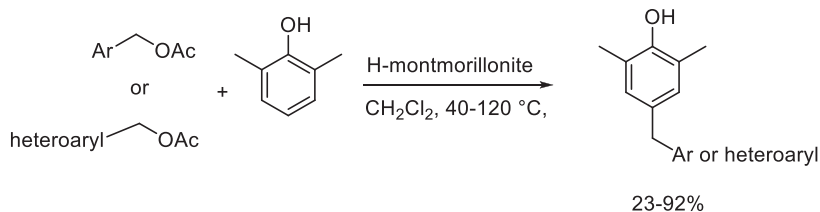


**SCHEME 10** Heterogeneous catalytic alkylation of substituted anisoles with *tert*-Bu-methyl ether.





**SCHEME 13** Benzylation of aromatics with benzylic phosphates in  $\text{Al}(\text{OTf})_3$ -catalyzed reactions.



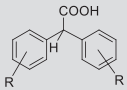
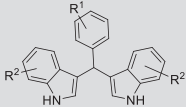
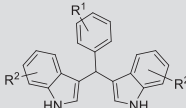
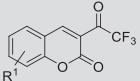
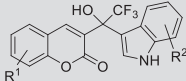
**SCHEME 14** A H-montmorillonite-catalyzed alkylation of a dimethyl phenol with benzyl or hetero-benzyl acetates during the synthesis of zafirlukast.

better results for the conversion of acetone and phenol to give bisphenol A and its regioisomer (Table 4, entry 1). In addition, this catalyst could be regenerated with no loss of activity.<sup>88</sup> Large pore zeolites were also investigated in this reaction and gave promising results for the synthesis of bisphenols.<sup>96, 97</sup> Zeolite Y resulted in good selectivity toward the formation of methylenedianiline in the reaction of aniline and formaldehyde (Table 4, entry 2). However, the intermediate partially rearranged to yield a product mixture, although the by-product formation was only 2%–3%.<sup>88</sup> The perfluorinated resin sulfonic acid, Nafion-H, efficiently catalyzed the synthesis of di- and triarylmethanes from benzaldehydes and arenes under solvent-free microwave-assisted conditions (Table 4, entry 3). The reaction conditions resulted in high yields in short reactions. It was observed that microwave irradiation favored the formation of *ortho-ortho* products; however, conventional heating resulted in primarily *para-para* products. Although the reaction conditions are green, the reusability of Nafion H was not studied. When using the significantly more active indoles in a reaction with benzaldehydes, weak acid catalysts, such as silica or alumina, also provided good yields for the product bis(indolyl)methanes (Table 4, entry 4). HY zeolite was able to catalyze the same transformation at room temperature in short reactions (Table 4, entry 5) still providing good yields. Although the process appears to have many green features the use of dichloromethane is undesirable. Other indoles were alkylated with benzaldehydes and a trifluoromethyl ketone, providing good to excellent yields (Table 4, entries 6, 7). HY zeolite and scandium triflate were used as catalysts, respectively. These processes also suffer from the use of dichloromethane, which represents potential harm to the ozone layer, when reaching the stratosphere.

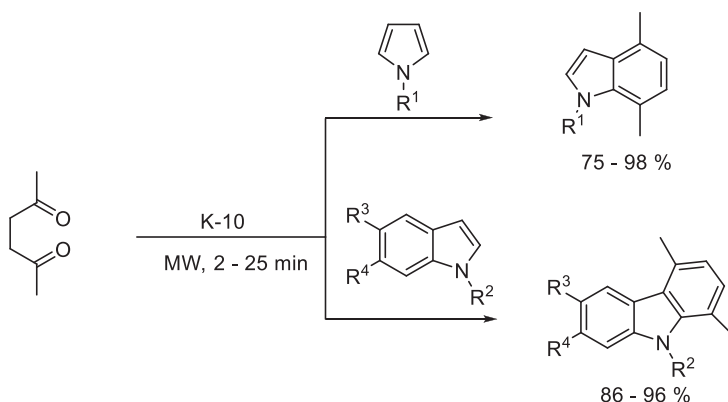
One of the more synthetically relevant examples includes a multistep domino process that is based on a double alkylation of pyrroles and indoles with 2,5-hexanedione that led to a cyclialkylation via the electrophilic annulation

**TABLE 4** Heterogeneous catalytic alkylation of aromatics with carbonyl compounds and their derivatives.

| Entry | Aromatics   | Carbonyl-compound         | Catalysts/conditions                 | Product  | Yield (%)                           | Ref. |
|-------|---|---------------------------|--------------------------------------|--|-------------------------------------|------|
|       | <p style="text-align: center;"> <math>\text{Aromatic ring with } R^1 + \text{Carbonyl compound } (R^2-C(=O)-R^3) \xrightarrow{\text{catalyst conditions}} \text{Mono-alkylated product or Hydroxylated product}</math> </p> |                           |                                      |  |                                     |      |
| 1     | Phenol and aniline  | Acetone                   | $\beta$ -zeolite/180°C, 12 h         | <p style="text-align: center;">Bisphenol A<br/>+<br/>2,4-Bisphenol A<br/>and methylenedianilines</p> | 49<br>27                            | 88   |
| 2     | Aniline   | Formaldehyde              | Zeolite Y/neat, 150°C, 6 h           |  | 97 (conversion)<br>89 (selectivity) | 88   |
| 3     | Arenes  | Substituted benzaldehydes | Nafion H/neat, 150°C, 25–190 min, MW | <p style="text-align: center;">and triarylmethanes</p>   | 21–100                              | 89   |

|   |         |   |   |  |                                   |       |
|---|---------|---|---|--|-----------------------------------|-------|
| 4 | Arenes  | Glyoxylic acid  | TfOH-PVP, 80°C,<br>4–72 h   |   | 40–95 yield, various regioisomers | 90    |
| 5 | Indoles | Benzaldehydes   | SiO <sub>2</sub> or<br>Al <sub>2</sub> O <sub>3</sub> /90°C,<br>5–15 min, MW<br>BAIL gel, solvent-<br>free sonication,<br>Cu-Al LDH |  | 59–98                             | 91–93 |
| 6 | Indoles | Benzaldehydes   | HY zeolite/rt,<br>CH <sub>2</sub> Cl <sub>2</sub> , 1–1.5 h   |  | 65–85                             | 94    |
| 7 | Indoles |  | 5 mol% Sc(OTf) <sub>3</sub> ,<br>CH <sub>2</sub> Cl <sub>2</sub> , reflux   |  | 72–95                             | 95    |

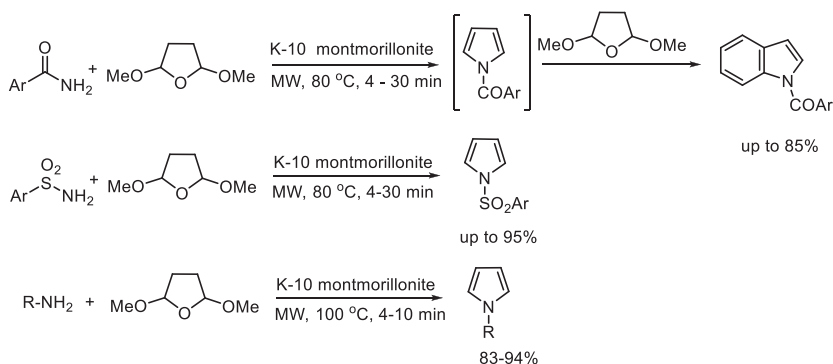
PVP, polyvinyl pyridine; BAIL, Brønsted acidic ionic liquid; LDH, layered double hydroxide; MW, microwave irradiation.



**SCHEME 15** K-10 montmorillonite-catalyzed cyclialkylation and aromatization of indoles and pyrrole with 2,5-hexanedione.

of these activated N-heterocycles. The solvent-free microwave-assisted method was catalyzed by K-10 montmorillonite (Scheme 15) and appeared to be a high yielding and selective new protocol for the synthesis of indoles and carbazoles.<sup>98, 99</sup>

Essentially the same idea was extended for the synthesis of non-*N*-methylated heterocycles by using 2,5-dimethoxytetrahydrofuran (an 1,4-butanediol derivative) as the cyclialkylating agent (Scheme 16).<sup>100, 101</sup> In a double cyclialkylation sequence (first with the N of the amides and then the formed pyrroles), *N*-acylindoles were obtained from arylbenzoic acid amides via a pyrrole intermediate in good yields and with nearly 100% selectivity. When using anilines or arylsulfonamides, however, the decreased reactivity of the pyrrole obtained after the first reaction terminated the process at this phase and *N*-arylamines and *N*-arylsulfonylpyrroles were obtained in good yields. The product *N*-sulfonylpyrroles were effective FBPase enzyme inhibitors ( $IC_{50}=32-135$  nM) and were proposed as potential drug candidates for type 2 diabetes.<sup>102</sup>

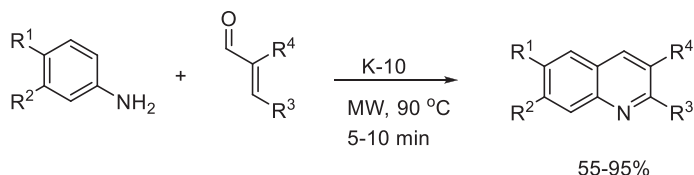


**SCHEME 16** K-10 montmorillonite-catalyzed cyclialkylations with 2,5-dimethoxytetrahydrofuran.

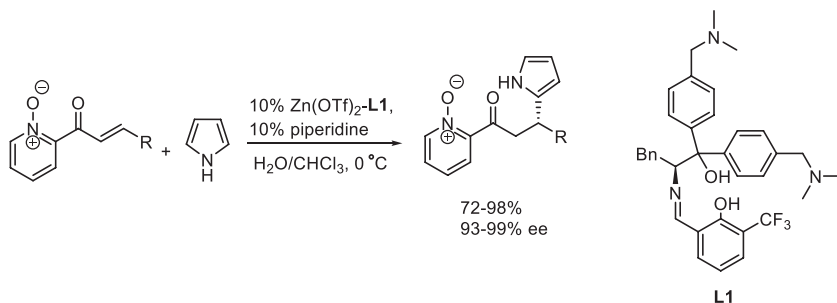
Using  $\alpha,\beta$ -unsaturated carbonyl compounds, such as cinnamaldehydes, as bifunctional alkylating agents, the K-10-catalyzed microwave-assisted process provided quinolines through reactions with anilines (Scheme 17).<sup>103</sup> The reaction times were within few minutes and the yields were excellent. It was observed, however, that substrates with strong electron-donating ability, e.g., methoxy, reacted sluggishly and provided the products in moderate yields. The complex formation between the lone pairs and the Lewis acid centers of the catalyst appeared to, at least partially, deactivate the catalyst in these cases.

The enantioselective Friedel-Crafts alkylation of pyrroles with  $\alpha,\beta$ -unsaturated carbonyl compounds was described by using zinc triflate as the catalyst.<sup>104</sup> As customary, the zinc-based Lewis acid was used to initiate the enantioselection in the process. The reaction provided the products in good to excellent yields and excellent enantioselectivities (Scheme 18).

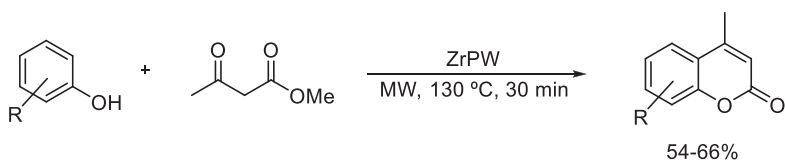
The solvent-free Pechmann condensation yielded substituted coumarins via an acylation-cyclization sequence of phenols with methyl acetoacetate in the presence of zirconium(IV) phosphotungstate (ZrPW)<sup>105</sup> in short reaction times, albeit in moderate yields (Scheme 19). The catalyst appeared to be recyclable, although it required an acid recovery treatment to restore its original activity. A similar study applied Envirocat EPZ-10 as a catalyst for this reaction.<sup>106</sup> The reaction conditions were about the same; however, the new catalyst appeared to make a significant difference and resulted in good yields. The same reaction was also carried out using high loadings of 12-tungstophosphoric acid ( $H_3PW_{12}O_{40}$ ) introduced into a highly porous metal-organic framework MIL-101.<sup>107</sup>



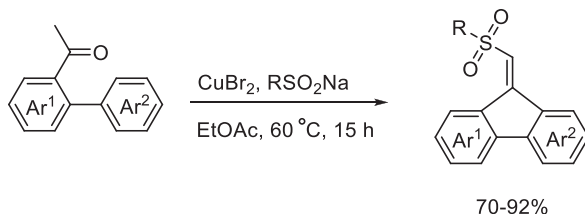
**SCHEME 17** Microwave-assisted K-10 montmorillonite-catalyzed condensation-cyclialkylation of anilines with cinnamaldehydes.



**SCHEME 18** Enantioselective alkylation of pyrroles using a chiral modified  $Zn(OTf)_2$  catalyst.



**SCHEME 19** Heterogeneous catalytic Pechmann condensation of phenols with methyl acetoacetate.



**SCHEME 20** Synthesis of sulfonyl 9-fluorenylidene by a  $\text{CuBr}_2$ -catalyzed process.

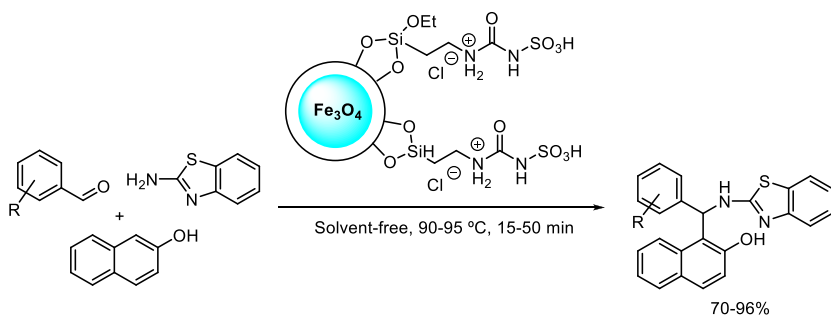
The catalytic performance of this solid acid was tested in other reactions as well, such as esterification and Friedel-Crafts acylation reactions (*vide infra*). Based on the data, 70 wt% of  $\text{H}_3\text{PW}_{12}\text{O}_{40}$  loading resulted in the maximum catalyst activity and a correlation between dispersion, mesoporosity, and acid strength was demonstrated and attributed as a major factor in the catalyst's resistance to deactivation.

A one-pot three-step reaction that included a final Friedel-Crafts alkylation step resulted in the formation of sulfonyl 9-fluorenylidene (Scheme 20).<sup>108</sup> The reaction was catalyzed by  $\text{CuBr}_2$  and resulted in the product in good to excellent yields. The cyclization occurred with activated aromatic rings, while the R group on the sulfonyl group could include groups with electron-donating or electron-withdrawing substituents.

A magnetically separable magnetite-supported solid acid [ $\text{Fe}_3\text{O}_4@\text{SiO}_2@(\text{CH}_2)_3\text{-Urea-SO}_3\text{H/HCl}$ ] was found to be an efficient catalyst for the synthesis of 2'-aminobenzothiazolomethylnaphthol derivatives (Scheme 21).<sup>109</sup> The catalyst showed high activity, producing good to excellent yields and could be recovered and reused after the completion of the reaction. Even after eight reactions the catalyst showed no signs of deactivation.

### 3.5.2.3 Alkylations with alkyl halides

Alkyl halogenides are one of the oldest and most established alkylating agents in aromatic electrophilic substitution. Using these compounds is also very convenient and practical as many of them are highly active and their physical properties (boiling point, melting point, solubility, etc.) make them well suited for the traditional Friedel-Crafts chemistry. Their application as alkylating agents

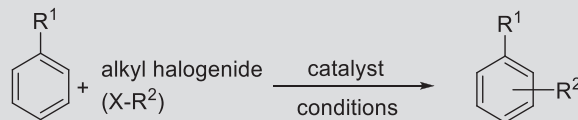


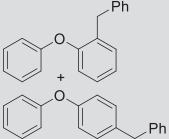
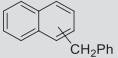
**SCHEME 21** Synthesis of 2'-aminobenzothiazolomethylnaphthol derivatives by a magnetically separable solid acid.

vastly dominated the field of Friedel-Crafts alkylations or alkyl-arene synthesis in the past. However, with the emergence of green chemistry,<sup>8</sup> these reagents became somewhat undesirable. One cannot overlook several issues that arise when analyzing their reactions from a sustainability point of view. First of all, alkyl halides are not sustainable reagents as opposed to several alcohols. They are commonly synthesized from alkenes by halogen or hydrogen halogenide addition, a process that applies environmentally unfriendly halogens ( $X_2$ ) or their HX derivatives. It is well known that halogens and organohalogen compounds are the most likely to cause the development of the ozone hole in Earth's stratosphere. During the alkylation reactions the same problems occurs, the generation of HX has the same effect. In addition, the HX by-products significantly decrease the atom economy, they are corrosive and if a base is applied to capture them, large amount of waste is generated. It is apparent that despite the positive impacts of solid acid catalysis on these reactions, the use of alkyl halogenides, if possible, should be avoided, especially in industrial practice. With the potential negative impact in mind we still summarize alkylations carried out using alkyl halides, as at the moment a number of procedures are still based on these reagents and greener alternatives are not yet available. There are several common alkyl halides that are often used in Friedel-Crafts reactions. The most common applications are tabulated in [Table 5](#).

Considering the traditional mechanism of the reaction, it often occurs through carbocationic mechanism. Thus the best alkylating agents form stable carbocations. It is important not only to ensure sufficient activity, but to make sure that the carbocation will not rearrange and the reaction would not produce an undesired rearranged product. Accordingly, the most popular alkylating agents are the benzyl and tertiary halides. Benzylchloride and bromide are the most commonly applied alkylhalide alkylating agents. They are highly reactive and commercially readily available and relatively inexpensive. The application of tertiary halides is also common; however, the alkylated products are susceptible to transalkylation reactions often resulting in the formation of undesired overalkylated by-products.

**TABLE 5** Solid acid-catalyzed alkylation of aromatics with simple alkylhalogenides.



| Entry | Aromatics                      | Alkyl halogenide                    | Catalysts/conditions  | Product   | Yield (%)               | Selectivity                    | Ref.     |
|-------|--------------------------------|-------------------------------------|---|---|-------------------------|--------------------------------|----------|
| 1     | Activated substituted benzenes | Benzyl chloride                     | Inorganic aluminosilicate polymer <sup>b</sup> /110°C, 3 h, liquid phase; AlCl <sub>3</sub> -ionic liquid complex | 2- and 4-monobenzylated aromatics   | > 90 <sup>a</sup>       | 100% (2/4 = varied around 1:1) | 110, 111 |
| 2     | Benzyl chlorides               | Benzyl chlorides (self benzylation) | NaY zeolite/RT, 24 h  | Dimers, oligomers, polymers   | 33 <sup>a</sup> (dimer) | 2/3/4 = 25/65/10               | 112      |
| 3     | Toluene                        | Benzyl chloride                     | M-ZrPMo <sup>c,e</sup> /-   |   | -                       | -                              | 68       |
| 4     | Substituted benzenes           | Adamantyl bromide                   | Broad variety of solid acids <sup>d</sup> /80–130°C, 1–2 h, in excess aromatic                                    | <br>a mixture of monoadamantylated products | 85–98                   | 2/3/4 = --                     | 113      |
| 5     | Diphenyl ether                 | Benzyl chloride                     | Sulfated zirconia/90°C  |   | 66                      | -                              | 30       |
| 6     | Naphthalene                    | Benzyl chloride                     | UDCaT-4 <sup>b</sup> cyclohexane, 80°C, 4 h   |   | 82                      | Not discussed                  | 114      |
| 7     | Substituted benzenes           | Alkyl halides                       | Metal accumulating plant based catalyst <sup>b</sup> with K-10/neat, RT, 1 h                                      | Various monoalkylated products  | 52–100                  | 2/3/4 = 15–30/0/85–70          | 115, 116 |

*a*, conversion; *b*, reusable catalyst; *c*, deactivation, regeneration necessary; *d*, HY zeolite, HY-supported triflic acid, Nafion H, Nafion H-silica nanocomposite, Amberlyst, silica-supported heteropoly acids, benzenetricarboxylic acid; *e*, mesoporous molybdate-zirconium oxophosphate (M-ZrPMo).

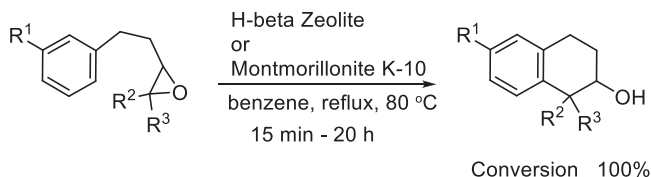
Adamantyl bromide is a representative of the tertiary alkyl halide group. It was applied in the regioselective adamantylation of substituted benzenes using a wide variety of solid acid catalysts, including acidic ion exchange and ionomer resins, HY zeolites, sulfated zirconia, and supported superacids on HY zeolite and SiO<sub>2</sub> (Table 5, entry 4).<sup>113</sup> The reaction generally occurred with high yields; the selectivity strongly depended upon the acid strength of the catalyst. Amberlyst, a cross-linked polystyrene resin sulfonic acid of moderate acid strength, provided excellent regioselectivity toward the formation of 4-adamantylated substituted benzenes. In contrast, much stronger acids, such as Nafion-H, resulted in the formation of the 3-adamantylated compounds as the major product. This suggested that the reaction could be used to characterize the acid strength of solid acids. This study was further extended to the applications of heteropoly acids (Hn[XM<sub>12</sub>O<sub>40</sub>]; n = 3, 4; X = Si, P; M = Mo, W),<sup>117, 118</sup> their silica-inclusion complexes, Nafion-H silica nanocomposite,<sup>119</sup> and a broad array of metal (lanthanide and gallium) triflates.<sup>120</sup> As a general observation, weaker acids (H<sub>0</sub> ≈ -5 to -8, such as Amberlyst, H<sub>4</sub>[SiMo<sub>12</sub>O<sub>40</sub>], H<sub>3</sub>[PM<sub>12</sub>O<sub>40</sub>]) favored the formation of 4-substituted products. Stronger acids (H<sub>0</sub> ≈ -9 to -12, e.g., Nafion-H, H<sub>4</sub>[SiW<sub>12</sub>O<sub>40</sub>], H<sub>3</sub>[PW<sub>12</sub>O<sub>40</sub>]), however, catalyzed a secondary isomerization reaction and resulted in the thermodynamic mixture of 3- and 4-adamantylated products in a ~70:30 = 3-substitution/4-substitution ratio. The 2-substituted product was never observed likely due to significant steric demand of the adamantyl group.

Several works describe the preparation of catalysts from nonconventional biomass, such as metal hyperaccumulator plants, and their use in alkylations in combination with K-10 montmorillonite (Table 5 entry 7).<sup>73, 74</sup> The catalysts provided high yields and were found to be reusable.

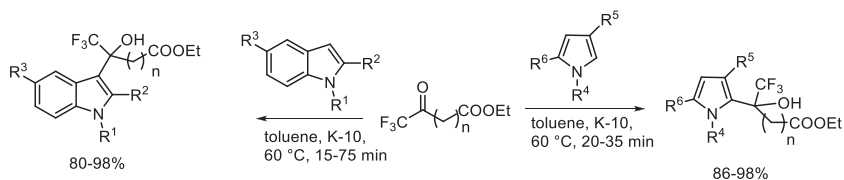
### 3.5.2.4 Hydroxyalkylations

Hydroxyalkylation reactions are a special type among Friedel-Crafts reactions. The reaction formally is an addition of the aromatic C-H bond to the carbonyl (C=O) group of aldehydes and ketones (carboxylic acid derivatives will react via the traditional acylation mechanism) or can occur via epoxide ring opening, forming the -CH(OH)R unit as a side chain on the parent aromatic ring. Hydroxyalkylation is a great example for environmentally benign synthesis; the alkylating reagents (aldehydes ketones) are green, it occurs with 100% atom economy, (theoretically) there is no waste production, and often the reactions do not even require the use of catalysts or elevated temperatures.<sup>121</sup>

Environmentally benign solid acid catalysts, such as zeolites and K-10 montmorillonite, readily catalyzed the intramolecular hydroxyalkylation of arylalkyl epoxides via the epoxide ring opening.<sup>122</sup> Although the catalysts could be reactivated and performed well in at least three consecutive reactions and excellent conversions of the starting materials were reported, the selectivities were rather low (25%–30%) (Scheme 22).



**SCHEME 22** Solid acid-catalyzed intramolecular cyclization of epoxides.

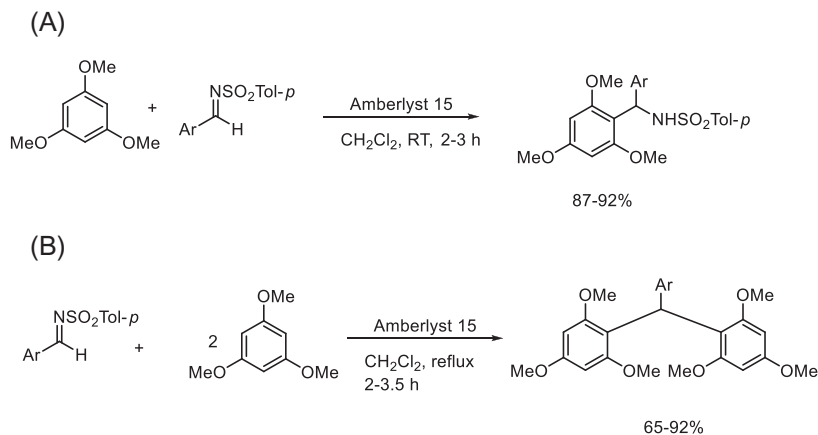


**SCHEME 23** K-10 montmorillonite-catalyzed hydroxyalkylations of pyrroles and indoles with ethyl trifluoropyruvate and ethyl trifluoroacetate.

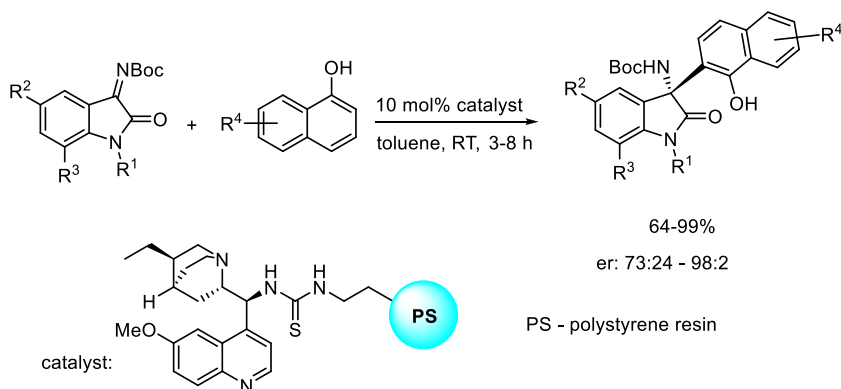
K-10 montmorillonite was found to be an excellent catalyst for the hydroxyalkylation of substituted indoles and pyrroles with ethyl 3,3,3-trifluoropyruvate and ethyl 4,4,4-trifluoroacetate (Scheme 23) in high yields and selectivity.<sup>123</sup> The same group developed the highly enantioselective version of the trifluoropyruvate reaction by using cinchona alkaloids as chiral catalysts.<sup>124</sup> The products of these syntheses as well as their extension to carbocyclic aromatics<sup>125</sup> were applied as inhibitors of the fibril and oligomer formation of the amyloid  $\beta$  peptide that has a prominent role in the development of Alzheimer's disease.<sup>126, 127</sup>

A special case of hydroxyalkylations is when the alkylating agent contains a C=N double bond, such as aldimine or ketimines, when the reaction is called aminoalkylation. The alkylation of activated arenes with *N*-sulfonyl aldimines was carried out by Thirupathi et al.<sup>128</sup> The reaction was successfully achieved by using Amberlyst-15, an acidic ion-exchange resin, which was found to be a recyclable catalyst in this reaction. The alkylation was carried out in two different stoichiometric ratios; when the alkylating agent/arene ratio was 1 a simple aminoalkylation occurred (Scheme 24A); however, doubling the amount of arene (ratio=0.5) resulted in the formation of triarylmethanes (Scheme 24B). Although the protocol has several green features, one must not overlook that dichloromethane, a highly undesirable compound, was used as solvent. Using chiral amines to synthesize chiral imines and apply the chiral imines in similar aminoalkylations, the same strategy leads to highly selective asymmetric aminoalkylations.<sup>129</sup>

Polystyrene-anchored cinchonide-modified bifunctional thioureas have been found as an excellent catalyst for the highly enantioselective aza-Friedel-Crafts aminoalkylation of naphthol derivatives and *N*-Boc ketimines that were obtained from isatin.<sup>130</sup> The reaction was carried out under flow condition to



**SCHEME 24** Amberlyst 15-catalyzed aminoalkylations of activated arenes with *N*-sulfonyl aldimines.



**SCHEME 25** Enantioselective aminoalkylation of naphthyl derivatives with isatin-derived ketimines on polystyrene-supported cinchona alkaloid-modified thiourea catalysts.

produce the products in good to excellent yield (70%–99%) and moderate to excellent enantioselectivities (50%–96%*ee*) (Scheme 25).

### 3.5.2.5 Intramolecular transalkylations—Rearrangements

Transalkylation reactions involve the removal of an alkyl group from a compound with the subsequent transfer of that alkyl group to either the same (intramolecular) or an additional molecule (intermolecular). The purpose could be direct synthesis or using the alkyl group as a blocking group before additional steps. The *ortho*-Claisen rearrangement of phenol-allyl ethers, a 1,3 O → C shift of the allyl group from the phenolic O to the aromatic ring can formally be considered as an intramolecular transalkylation, is a useful method for the synthesis

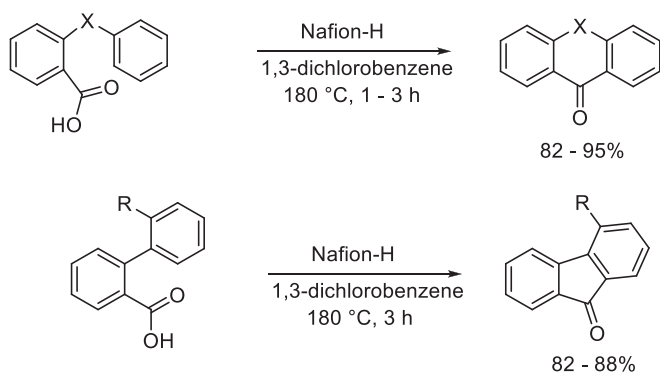


be hydrolyzed to isolate the products, a process that decomposes the moisture-sensitive Lewis acids and yields significant amount of waste. Unlike these acids, solid acids either do not bind strongly with carbonyl compounds thus either no hydrolysis is necessary, or these materials do not decompose upon hydrolysis with water and therefore, in principle, are recyclable. In other words, traditional Lewis acids rather act as reagents and have to be used in stoichiometric amount. In contrast, the solid acids work as real catalysts. Recyclability is a major advantage of solid acids in Friedel-Crafts acylations. In addition, solid acids can be utilized in reactions with environmentally more benign reagents, such as carboxylic acids or anhydrides unlike the traditional Lewis acids that often decompose in the presence of such reagents.

### 3.5.3.1 Acylations with carboxylic acids

Carboxylic acids are the environmentally most benign acylating reagents, given the relatively high atom economy and the formation of water as the only theoretically plausible by-product. Unfortunately, carboxylic acids are considered to be relatively low activity reagents in acylation reactions. As a potential solution to this problem, the application of strong, often superacidic, solid acids (such as Nafion-H or  $\text{Cs}_{2.5}\text{H}_{0.5}[\text{PW}_{12}\text{O}_{40}]$ ) and elevated temperatures are recommended. Due to their low reactivity, carboxylic acids are not frequently considered as acylating agents indicated by the limited number of processes described; however, due to their green character their application is desirable.

Nafion-H, a superacidic perfluorinated resin sulfonic acid, was found to be an excellent catalyst to promote the intramolecular Friedel-Crafts acylation of benzoic acid derivatives having aromatic substituents in *ortho* position to the carboxylic group (Scheme 28). A broad variety of three ring systems, such as anthraquinone, anthrone, fluorenone,  $\alpha$ -tetralone, 1-benzosuberone and various heterocycles like acridone and xanthone, were obtained in excellent yields by using this protocol. As expected, the reaction occurred most efficiently at high

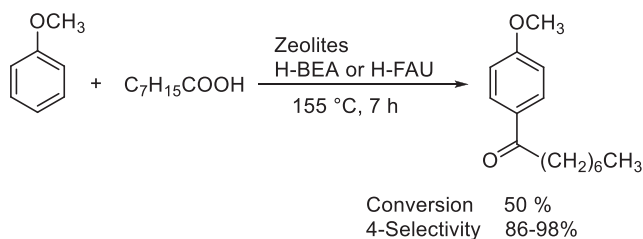


**SCHEME 28** Nafion-H-catalyzed intramolecular acylations with benzoic acid derivatives.

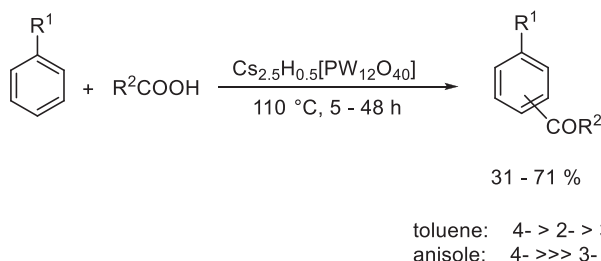
temperatures (180°C).<sup>136</sup> In addition to the high temperature, the use of the halogenated solvents is also a drawback of the method from green point of view.

Another alternative to solid superacids and high temperatures is to apply highly activated aromatic compounds for acylation. Anisole can be acylated by octanoic acid in the presence of several zeolite catalysts, such as zeolite H-BEA, H-FAU, and also the high surface area Nafion-H/silica nanocomposite<sup>137</sup> (Scheme 29). Zeolites H-BEA and H-FAU exhibited the best overall catalytic performance, providing excellent 4-selectivities, albeit moderate yields.<sup>138</sup> In a similar study, anisole was acylated with propanoic acid. The zeolites tested were ZSM-5 and BEA and their nickel, silver, or iron-loaded derivatives: pristine ZSM-5 being the most efficient with 70% conversion and 80% selectivity.<sup>139</sup> In each reaction, the 2- and 4-products dominated, the catalysts made no difference in terms of selectivity; however, the modifications appeared to decrease catalytic activity. The same acylation was also achieved using MOF-based catalysts with high phosphotungstic acid loading.<sup>107</sup> The zeolite-catalyzed acylation of aromatics with alkylcarboxylic acids can also be carried out by microwave activation as well.<sup>16, 140</sup> The microwave-assisted reactions produced higher yields, which was attributed to the rapid evaporation of water from the surface.

A similar acylation of toluene and anisole was carried out with aliphatic carboxylic acids from acetic acid to tridecanoic acid by heteropoly acid catalysis. The superacidic partial cesium salt of phosphotungstic acid ( $\text{Cs}_{2.5}\text{H}_{0.5}[\text{PW}_{12}\text{O}_{40}]$ )



**SCHEME 29** Microwave-assisted zeolite-catalyzed acylation of anisole with octanoic acid.



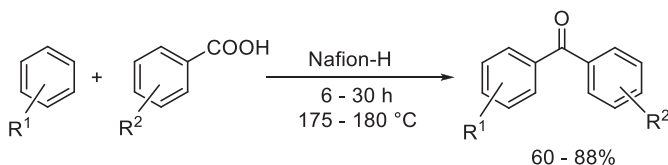
**SCHEME 30** Acylation of toluene and anisole with aliphatic carboxylic acids catalyzed by  $\text{Cs}_{2.5}\text{H}_{0.5}[\text{PW}_{12}\text{O}_{40}]$ .

appeared to efficiently catalyze the reaction at a relatively moderate temperature (Scheme 30) while also being recyclable in consecutive experiments.<sup>141</sup>

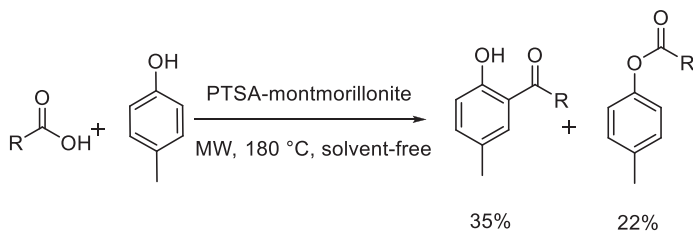
Benzoic acid was applied in the arylation of substituted benzenes with Nafion-H catalysis. The product benzophenones were obtained in moderate to good yields (Scheme 31).<sup>142</sup> Interestingly, toluene was an exception, as the benzylation resulted in the formation of benzophenone isomers and only in low yields (~5%).

A *p*-toluenesulfonic acid (PTSA) treated montmorillonite catalyst was applied in the acylation of *p*-cresol with aliphatic carboxylic acids in a microwave-assisted reaction (Scheme 32).<sup>143</sup> Albeit the yields were only moderate, it was observed that the microwave irradiation prevented the catalyst deactivation that was typically observed in conventionally heated systems. It was suggested that the electromagnetic field positively moderated the orientation of the acylium ions and favored the reaction with cresol.

As an example for the application of highly activated aromatics in acylations with carboxylic acids, Montanez Valencia et al. reported the gas-phase acylation of guaiacol with acetic acid using commercially available HZSM-5, HBEA zeolites, and tailored ZnZSM-5 and TPA (tungstophosphoric acid)/SiO<sub>2</sub> catalysts, respectively. The authors described the reaction as effective, however, obtained a product mixture that required extensive separation.<sup>144</sup> The same reaction was investigated using micro-, nano-, and hierarchical MFI and BEA zeolites in a continuous flow reactor. The authors obtained similar results as the previously mentioned work with the additional observation of the O-acylated product and its subsequent Fries rearrangement.<sup>145</sup>



**SCHEME 31** Nafion-H-catalyzed acylation of aromatics with substituted benzoic acids.



**SCHEME 32** Acylation of *p*-cresol with aliphatic carboxylic acids catalyzed by *p*-toluenesulfonic acid (PTSA) treated montmorillonite.

### 3.5.3.2 Acylations with activated carboxylic acid derivatives

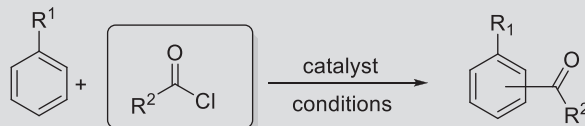
Due to their enhanced reactivity carboxylic acid chlorides and anhydrides are the most popular acylating reagents in common synthetic procedures. Despite their overwhelming popularity one must not overlook that their application also raises some issues that do not conform to the green chemistry principles. First of all, acid chlorides upon reaction release HCl, and similarly anhydrides release an organic acid. HCl is particularly problematic, but both by-products are corrosive, significantly decrease the atom economy (highly unfavorable for anhydrides), and generate waste that should be dealt with. Therefore the application of acid chlorides and anhydrides should be avoided whenever it is possible.

Despite these concerns these reagents are the most commonly used acylating agents. Acetyl chloride, benzoyl chloride, and acetic anhydride are the most regular reagents with a plethora of applications featuring a broad variety of heterogeneous catalysts. Tables 6–8 include several representative applications.

Tables 6–8 indicate that acylation reactions are carried out by using a relatively limited number of acylating agents; acetyl chloride and some higher aliphatic acid chlorides, benzoyl chloride and its substituted derivatives, and anhydrides were overwhelmingly dominated by acetic anhydride. In contrast, the number and variety of catalysts used and specifically developed for these reactions is great and ever growing. They include traditional solid acid catalysts such as metal oxides ( $\alpha$ -Fe<sub>2</sub>O<sub>3</sub>, Bi<sub>2</sub>O<sub>3</sub>, ZnO), zeolites (HY, H $\beta$ , etc.), mesoporous aluminum silicates (HMCM-48-SH and HMCM-41-S), acidic clays (K-10), sulfated zirconia, heteropoly acids (H<sub>3</sub>PW<sub>12</sub>O<sub>40</sub>), acidic ion-exchange resins (Amberlyst, Nafion-H) derivatives. Several works have also investigated the catalytic potential of newly developed innovative catalysts, such as a biomass-based material often in combination with a well-known porous support, K-10 montmorillonite, modified zeolites or clays (microcrystalline  $\beta$ -zeolite, PTFMSS-bentonite-supported polytrifluoromethane sulfosiloxane), supported heteropoly acids or the partial Cs-salt of HPAs, or sulfated mesoporous aluminum silicates demonstrating the benefits of the derivatized forms of the traditional catalysts. Many of these catalysts produced high yields and were found to be recyclable.

There are several applications when a variety of other acid anhydrides were used for acylation. For instance, heteropoly acid-based solid acids, mainly H<sub>3</sub>[PW<sub>12</sub>O<sub>40</sub>] and Cs<sub>2.5</sub>H<sub>0.5</sub>[PW<sub>12</sub>O<sub>40</sub>], were applied for the Friedel-Crafts acylation reaction of substituted benzenes with acid anhydrides (Scheme 33).<sup>183</sup> The catalysts provided moderate to high yields with high selectivity. The 2- to 4-regioselectivity was strongly dependent upon the R<sup>1</sup> substituent (2:2%–56%; 4:44%–98%). Kobayashi's group recently reported the application of trifluoromethanesulfonic acid immobilized on nitrogen-doped carbon-incarcerated titanium nanoparticle catalysts in the same reaction using a variety of acid anhydrides as acylating agents describing similar yields (70%–96%).<sup>184</sup>

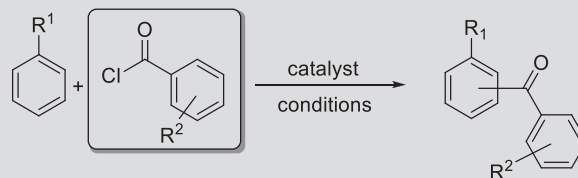
**TABLE 6** Solid acid-catalyzed acylation of aromatics with alkylcarboxylic acid chlorides.



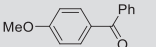
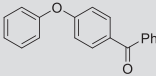
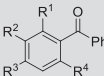
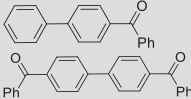
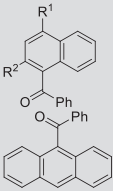
| Entry | Aromatics  | Catalysts/conditions   | Product | Yield (%) | Selectivity   | Ref.     |
|-------|--|--|---------|-----------|---|----------|
| 1     | 1,2-Dimethoxybenzene                             | H-beta zeolite/130°C, 1 h chlorobenzene with propionyl chloride (recyclable catalyst)  |         | 43        | 94  | 146      |
| 2     | Anisole  | H-beta zeolite/60°C, 2 h acetyl chloride (gas phase)   |         | n.d.      | Not determined, mechanistic study on surface adsorption         | 147      |
|       |  | HMCM-48-SH and HMCM-41-S, 155°C, 1 h with octanoyl chloride  |         | 90–99     | 100% 4-selectivity  | 148      |
| 3     | N-ethyl-carbazole                                | ZnCl <sub>2</sub> , 20°C, 6 h, acetylchloride, dichloromethane   |         | 80        | High selectivity for the product, no other regioisomer detected | 149      |
| 4     | Substituted dimethoxybenzenes                    | Variety of zeolites, mainly HY, 65°C, 1 h, N <sub>2</sub> atm., various straight chain (C <sub>2</sub> -C <sub>4</sub> and C <sub>6</sub> -C <sub>10</sub> ) acylchlorides |         | Up to 48  | High selectivity for the expected products                      | 150      |
| 5     | Ferrocene  | B-PTFMSS or sulfated zirconia, 80°C (reflux), 4 h, 1,2-diCl-ethane (solvent), (recyclable catalyst)  |         | 76–85     | Conversion: 21–82   | 151, 152 |
| 6     | Activated and nonactivated aromatic hydrocarbons | ZnO, RT, 5-120 min, solvent-free, (recyclable catalyst)  |         | 67–95     | Not discussed   | 153      |

n.d., not determined; B-PTFMSS, bentonite-supported polytrifluoromethane sulfosiloxane; HMCM, H-exchanged forms of synthetic mesoporous aluminosilicates.

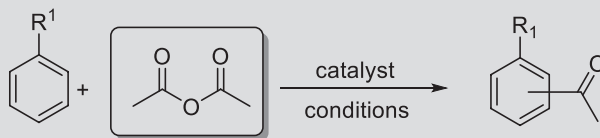
**TABLE 7** Solid acid-catalyzed benzoylation of aromatics with benzoyl chloride and its substituted derivatives.



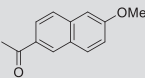
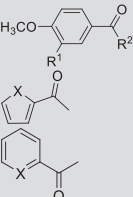
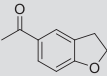
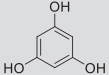
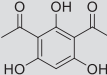
| Entry | Aromatics             | Catalysts/conditions  | Product                    | Yield (%)     | Selectivity                                   | Ref.                |
|-------|-----------------------|---|----------------------------|---------------|---|---------------------|
| 1     | Toluene               | Sulfated zirconia/100°C, 3 h (benzoic anhydride as well)  |                            | Up to 92      | 70%–80% 4-product                             | <a href="#">154</a> |
|       |                       | Mesoporous zirconium trifluoromethylsulfonate (Zr-O-SO <sub>2</sub> -CF <sub>3</sub> ), 15–30 wt% triflic acid, 130°C, 24 h, nitrobenzene (solvent) | 4,4'-Dimethyl-benzophenone | 73–74         | Selective, conversion: 72–85                  | <a href="#">155</a> |
| 2     | m-Xylene              | Core shell Bi <sub>2</sub> O <sub>3</sub> /SiO <sub>2</sub> catalyst RT-100°C, 40–270 min, recyclable catalyst                                      |                            | 68–91         | Nearly exclusive                              | <a href="#">156</a> |
| 3     | 1,2-Dimethoxy benzene | H-Y and H-BEA zeolites chlorobenzene, 130°C, 8 h, (substituted benzoyl chlorides as well)   |                            | 23–75 (conv.) | Nearly 100% selectivity for the major product | <a href="#">157</a> |

|   |                                      |  |  |                 |   |          |
|---|--------------------------------------|--|--|-----------------|---|----------|
| 4 | Anisole                              | H <sub>3</sub> PW <sub>12</sub> O <sub>40</sub> /Zr-based MOF, 120°C, 6 h, H-BEA/SiC, 120°C, 10 h  |   | 60–99.4 (conv.) | 95%–99% selectivity for the major product | 158, 159 |
| 5 | Diphenyl oxide                       | 15 wt. % H <sub>3</sub> [PW <sub>12</sub> O <sub>40</sub> ]/ZrO <sub>2</sub> , (calcined at 750°C), 120°C, 3 h   |   | 39 (conv.)      | 97%                                       | 160      |
| 6 | Substituted benzene derivatives      | Sulfated zirconia, 100–200°C, 1.5–20 h   |  |                 |   |          |
|   |                                      | Al <sub>2</sub> O <sub>3</sub> -ZrO <sub>2</sub> /S <sub>2</sub> O <sub>8</sub> <sup>2-</sup> , 100–150°C, 2–6 h with benzoyl chloride and its substituted derivatives |   | 16–99           | n/a                                       | 161–163  |
|   |                                      | Fe <sub>x</sub> C nanocomposite 130°C 2–7 h  |  |                 |   |          |
| 7 | Biphenyl                             | Sulfated mesoporous MCM-41 (SO <sub>4</sub> -AlMCM-41), 180°C, 24 h  |  | 94 (conv.)      | 83%<br>11%                                | 164      |
| 8 | Substituted naphthalenes, anthracene | Sulfated zirconia, 1,2-dichloroethane or chlorobenzene, 70–130°C, 4–20 h   |   | 70–93<br>61–67  | n/a                                       | 165      |

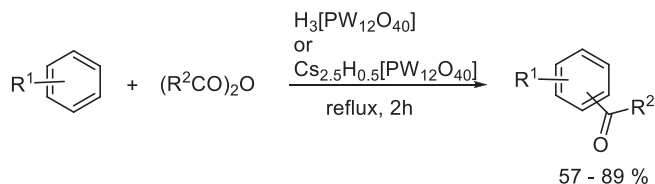
**TABLE 8** Solid acid-catalyzed acetylation of aromatics with acetic anhydride.



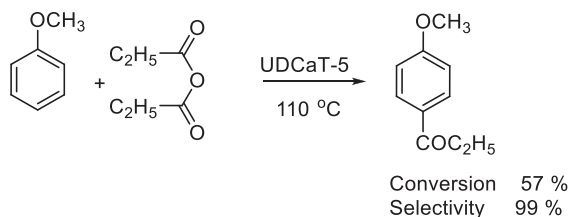
| Entry | Aromatics       | Catalysts/conditions  | Product | Yield (%) | Selectivity   | Ref.  |
|-------|-----------------|---|---------|-----------|---|---|
| 1     | Anisole         | Zn-hyper-accumulative plants/K-10/Solvent-free, rt, 1 h<br>high silica mordenite zeolite<br>sulfated zirconia, 100°C, 1.5 h<br>β-zeolite, 120°C, 24 h<br>Nafion-H/mesoporous support, 70% HPA/SiO <sub>2</sub> , Cs <sub>2.5</sub> -HPA/SiO <sub>2</sub> , 70°C   |         | 40–100    | 2/3/4: 10–30/0/85–98                                    | <a href="#">115</a> , <a href="#">116</a> , <a href="#">161</a> , <a href="#">166–169</a> |
| 2     | Anisole         | Amberlyst-36, or H <sub>3</sub> PW <sub>12</sub> O <sub>40</sub> /SiO <sub>2</sub> /50°C, 5 h (A36) or 90–110°C, 2 h (PW/SiO <sub>2</sub> )   |         | 35–98     | 98  | <a href="#">170</a> , <a href="#">171</a>   |
| 3     | Aromatic ethers | Amberlyst 15, 80°C, 10 h, ethylene dichloride (solvent) (other anhydrides as well)<br>Zr-β-zeolite, 70–100°C, flow system<br>α-Fe <sub>2</sub> O <sub>3</sub> and CaCO <sub>3</sub> NPs<br>HY, Hβ zeolite, 90–120°C, 2–24 h<br>H <sub>3</sub> PW <sub>12</sub> O <sub>40</sub> /HMS, diCl-ethane, 60°C, 30 min<br>15 wt% H <sub>3</sub> [PW <sub>12</sub> O <sub>40</sub> ]-22.4 wt% ZrO <sub>2</sub> , 80°C, 1 h |         | 27–100    | High selectivity for the expected 4-acetylated products | <a href="#">172–179</a>   |

|   |   |  |  |                                    |  |     |
|---|---|--|--|------------------------------------|--|-----|
| 4 | 2-Methoxy-naphthalene   | H $\beta$ zeolite, chlorobenzene, 80°C, 4 h                                    |  | 7–22                               | 2-Methoxy-1-naphthophenone<br>(5%–12%) | 180 |
| 5 | Aromatic and hetero-aromatic compounds<br>(X = O, S)                              | Microcrystalline $\beta$ -zeolite, nitrobenzene (standard), 90–130°C, 2.5–12 h |  | 70–98<br>26–91<br>20–30<br>(conv.) | N/a<br>64%–100%<br>100%                | 181 |
| 6 | Benzo-dihydrofuran  | HY, H $\beta$ zeolite, 120°C, 1.5 h  |  | 95                                 | Nearly 100%                            | 177 |
| 7 |  | Silica-immobilized sulfuric acid (SSA), 60°C<br>15–20 min sonication           |  | 94–95                              | n/a                                    | 182 |

HMS, hexagonal mesoporous silica; HPA, heteropoly acid; NP, nanoparticle.



**SCHEME 33** Phosphotungstic acid and its Cs salt-catalyzed acetylation of substituted benzenes with acid anhydrides.

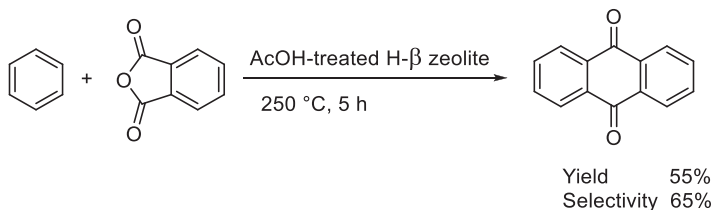


**SCHEME 34** A modified zeolite-catalyzed acetylation of anisole.

The acylation of anisole with propionic anhydride was studied with a variety of solid acid catalysts, such as UDCaT-5, UDCaT-6,  $\text{Cs}_{2.5}\text{H}_{0.5}\text{PW}_{12}\text{O}_{40}$  on K-10 montmorillonite, etc. The mesoporous UDCaT-5 was found to be the most effective catalyst for the synthesis of 4-methoxypropionophenone.<sup>185</sup> The reaction was carried out under solvent-free conditions at 110°C and provided moderate yield with excellent selectivity (Scheme 34).

Yadav and Kamble developed a new solid superacidic mesoporous UDCat-5 catalyst for the similar acylation of toluene with propionic anhydride.<sup>186</sup> The reaction occurred at 180°C, with relatively moderate yield (68%), however, with exclusive regioselectivity. The reaction was carried out under solvent-free condition.

The synthesis of anthraquinone has been achieved by a double acylation reaction carried out using phthalic anhydride and benzene (Scheme 35).<sup>187</sup> The catalyst applied in the reaction was a modified H $\beta$  zeolite that was treated by acetic acid under microwave-assisted conditions. The catalyst provided



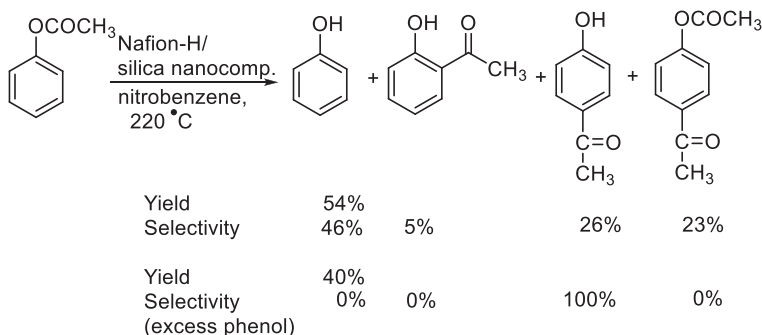
**SCHEME 35** H $\beta$  zeolite-catalyzed microwave-assisted synthesis of anthraquinone by the double acylation of benzene with phthalic anhydride.

moderate yields (up to 55%) and selectivity (65%). It was also found to be recyclable after regeneration; while the yields show continuous drop during reuse, after a simple regeneration by a treatment with acetic acid, the yields remained stable at the original value even after five subsequent reactions.

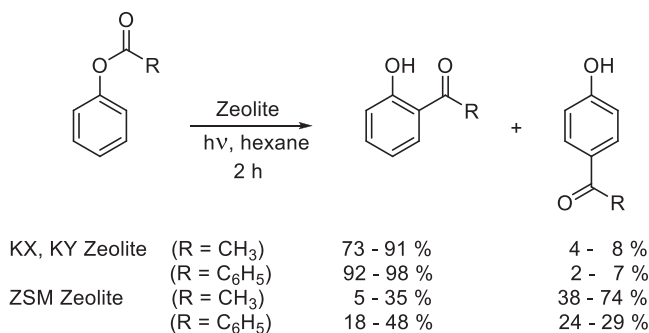
### 3.5.3.3 Intramolecular transacylations—Rearrangements

There are several rearrangement reactions that occur, at least partially, via an aromatic electrophilic substitution mechanism. The Fries rearrangement is a well-known acid-catalyzed transformation of phenol esters resulting in the formation of 2- and 4-hydroxyacetophenones.<sup>188</sup> The ester group is usually activated by a strong acid to yield an acetyl cation that is initiating the acylation on the aromatic ring. Several solid Brønsted acid catalysts were able to efficiently catalyze this reaction; the most recent examples use Nafion-H/silica-nanocomposite.<sup>119</sup> The catalyst showed significantly higher activity than its precursor Nafion-H or the simple Nafion-H/SiO<sub>2</sub> catalyst. Another significant difference is that while Nafion-H produced only phenol (95%) and 4-hydroxyacetophenone (5%), the nanocomposite material gave all possible rearranged products (Scheme 36). More importantly, 4-hydroxyacetophenone was formed in moderate yield but with exclusive selectivity using the nanocomposite catalyst in the presence of excess phenol. The same reaction was later studied on bridged periodic mesoporous organosilica structure (PMO) functionalized with anchored sulfonic acid. The catalysts afforded high reaction rates usually yielding high *para/ortho* ratios.<sup>59</sup>

The photo-induced Fries rearrangement of phenolacetate and benzoate was catalyzed by zeolites (X, Y, ZSM-5 and ZSM-11) in order to obtain hydroxyacetophenones and hydroxybenzophenones (Scheme 37). The X and Y zeolites gave the 2-isomer as the predominant product. In contrast, ZSM-5 zeolite gave substantial amount of the 4-isomer. Moreover, in the case of hydroxyacetophenone the 4-substituted isomer became the major product.<sup>133</sup>



**SCHEME 36** Nafion-H/silica nanocomposite-catalyzed Fries rearrangement.

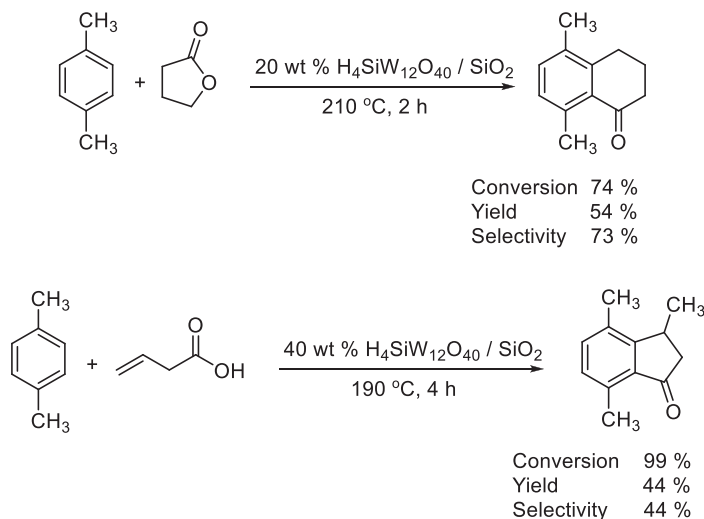


**SCHEME 37** A zeolite-catalyzed photochemical Fries rearrangement.

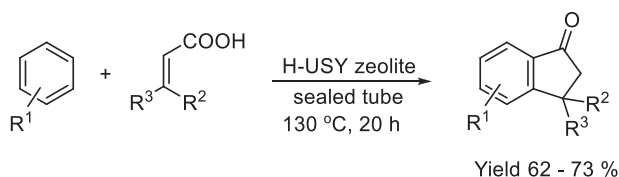
### 3.5.4 Friedel-Crafts cycliacylations

The cycliacylation reactions are a unique combination of separate alkylation and acylation reactions carried out on the same aromatic ring with a bidentate substrate that can facilitate both types of reactions. Such reactions are well known under superacidic conditions.<sup>189</sup> In recent attempts, however, solid acids were also able to catalyze such reactions providing a *green* tool for the synthesis of bicyclic compounds.

Silica-supported silicotungstic acid (H<sub>4</sub>SiW<sub>12</sub>O<sub>40</sub>/SiO<sub>2</sub>, approximately 20–40 wt%) appeared to be an efficient catalysts in the reaction of *p*-xylene with  $\gamma$ -butyrolactone or vinyl acetic acid for the formation of 5,8-dimethyl- $\alpha$ -tetralone or 3,4,7-tetramethyl- $\alpha$ -indanone, respectively (Scheme 38).<sup>190</sup> The authors proposed a step-by-step mechanism, involving an initial alkylation of *p*-xylene with the C=C double bond, followed by an intramolecular cycliacylation reaction.



**SCHEME 38** Silica supported heteropoly acid-catalyzed cycliacylations.



**SCHEME 39** A zeolite-catalyzed cycliacylation.

In another example, the Friedel-Crafts cycliacylation between different aromatic compounds and  $\alpha,\beta$ -unsaturated carboxylic acids was investigated in the presence of H-USY zeolite (Scheme 39). As the zeolite also served as a solid medium for the reaction, an excess of it was required and the cyclic ketones were isolated in moderate to good yields. The catalysts could be recycled up to three times.<sup>191</sup>

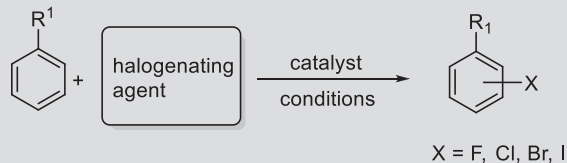
### 3.5.5 Halogenation

The direct halogenation of aromatic compounds by molecular halogens is a convenient way to prepare halogenated aromatics.<sup>192</sup> The reaction is commonly catalyzed by Lewis and Brønsted acids; however, the halogens are typically restricted to chlorine and bromine. Iodine exhibits low activity in such reactions, while fluorine is too active and fluorinated aromatics are mostly prepared by indirect methods. Halogenating agents include molecular  $\text{Cl}_2$ , and  $\text{Br}_2$ , and several activated derivatives such as *N*-chloro- and *N*-bromosuccinimide (NCS, NBS), trichloroisocyanuric acid (TCCA), tribromoisocyanuric acid (TBCA), and many others.<sup>193</sup> It is worth noting that while elemental  $\text{I}_2$  or  $\text{F}_2$  is not sufficient for direct halogenation, activated I-containing or tamed F-containing reagents (e.g., *N*-iodosuccinamide (NIS) or Selectfluor) are available for the preparation of iodinated and fluorinated aromatics. Table 9 summarizes relevant representative examples of aromatic halogenations.

As Table 9 indicates, a broad variety of aromatics from simple benzene derivatives to multiring systems and heteroaromatic compounds can be halogenated by heterogeneous catalytic methods. It is worth noting that in contemporary halogenation reactions, the halogenating agent is scarcely molecular halogen, the use of different activated halogen-containing compounds dominates these protocols. The catalysts also belong to a wide range of materials. These include zeolites, natural, synthetic, and modified alike, mesoporous molecular sieves, surface-modified silica-based materials, and neat metals, metal salts, and complexes. In most cases the reactions yield monohalogenated products, with varying selectivities. Monosubstituted benzenes typically afford the *para*-isomer as a major product; the selectivity is dependent upon electronic and steric effects.

As of individual examples, the chlorination of aromatic compounds was performed using various types of zeolites. One of them, the proton-exchanged zeolite X, catalyzed the chlorination of toluene at ambient temperature in different

**TABLE 9** Solid acid-catalyzed halogenation of aromatics.



| Entry | Aromatics   | Catalysts/conditions  | Product   | Yield (%) | Selectivity  | Ref.     |
|-------|---|---|---|-----------|--|----------|
| 1     | Aromatics (toluene, nitrobenzene)                 | FAU, EMT zeolites, TCCA, gas phase, N <sub>2</sub> flow, 150°C  | <br>Me or NO <sub>2</sub>                       | Up to 100 | Toluene: <i>o/p</i> : 0.95–1.22<br>Nitrobenzene: up to 97% for monochlorinated product | 194      |
| 2     | Substituted benzenes                              | H-BEA, H-Beta zeolites, TCCA, NBS, NCS, NIC, 20–120°C, 30 min   | Substituted chloro-, bromo-, and iodo-benzenes  | 37–100    | 84%–100% monohalogenation, <i>p/o</i> ratio: 3 to 0.5                                  | 195, 196 |
| 3     | Anthracene, substituted naphthalenes and benzenes | TCCA, TBCA, 0.5–6 h, solvent-free mechanochemical activation  | Mono- and dihalogenated (mixed Br, Cl) products | 31–96     | High selectivity for the expected products   | 197      |
| 4     | Substituted benzenes and naphthalene              | Ag/HMB <sup>+</sup> NBS, 25–100°C, 16 h, dichloroethane   | Monobrominated product                          | 81–100    | 2/4 = 1/3 to 1/18; 3/4 = 4/1   | 198      |
| 5     | Substituted benzenes, naphthalene, pyridine       | CuAl <sub>2</sub> F <sub>8</sub> , HF and O <sub>2</sub> , 500°C  | Monofluorinated products                        | 4–61      | High monofluorination selectivity  | 199      |
| 6     | Substituted benzenes                              | NH <sub>4</sub> VO <sub>3</sub> , H <sub>2</sub> O <sub>2</sub> , TBAB, CHCl <sub>3</sub> , RT, 15 min–5 days                         | Various monobrominated products                 | 80–99     | High monobromination selectivity and regioselectivity                                  | 200      |
| 7     | Substituted aromatics, hetero-aromatics           | Sulfonic acid functionalized silica, NBS, neat, RT, 5–180 min   | Various monobrominated products                 | 69–99     | Often exclusive selectivity for 4-Br products  | 201      |
| 8     | Substituted phenols                               | {[Mn <sub>2</sub> Cu(idbt) <sub>2</sub> (H <sub>2</sub> O) <sub>2</sub> ]·3H <sub>2</sub> O} <sub>n</sub> , NBS, NCS, MeCN, 90°C, 6 h | Monohalogenated products                        | 91–95     | The 4-halogenated product formed selectively in all cases                              | 202      |

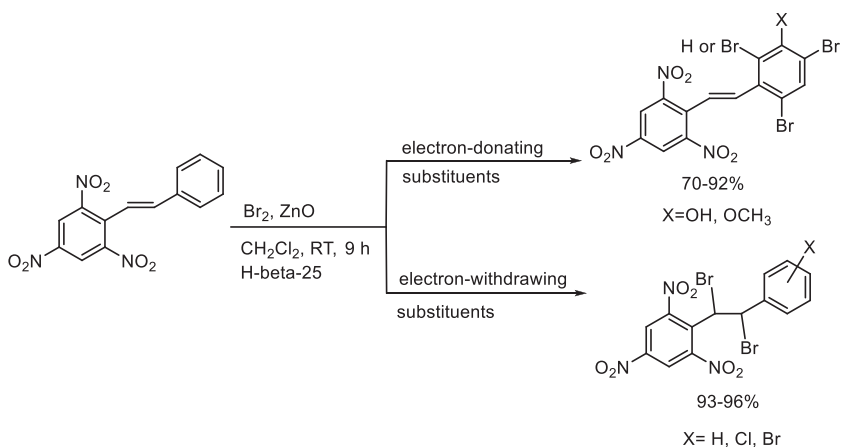
TCCA, trichloroisocyanuric acid; TBCA, tribromoisocyanuric acid; NBS, *N*-bromosuccinimide; NCS, *N*-chlorosuccinimide; NIS, *N*-iodosuccinimide; HMB, mesoporous molecular sieve; TBAB, tetrabutyl ammonium bromide; idbt, 5,5-(1H-imidazole-4,5-diyl)-bis(2H-tetrazole).



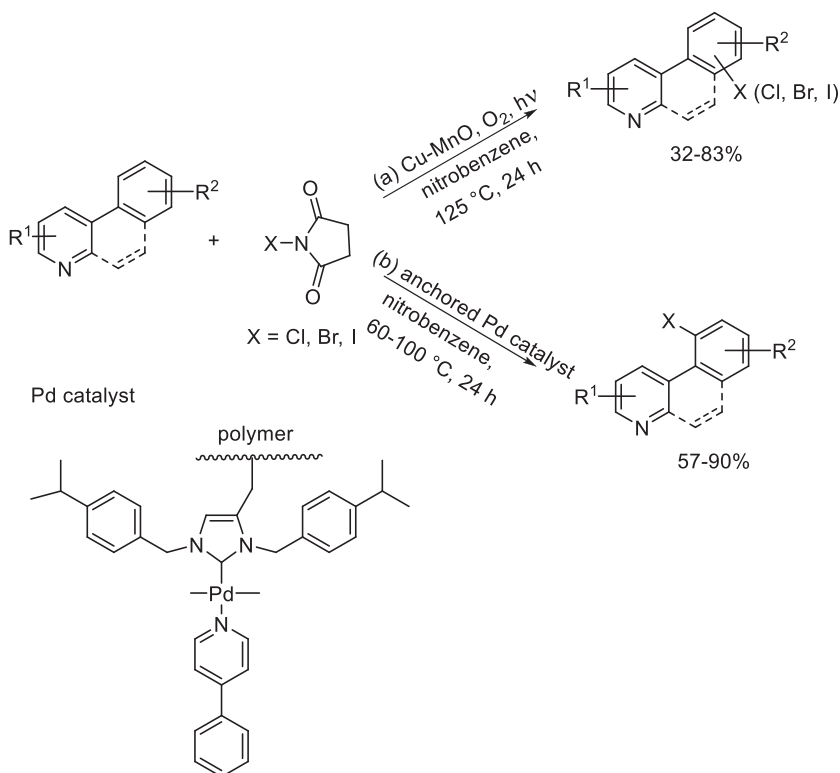
**SCHEME 40** Zeolite-catalyzed chlorination of toluene.

solvents using *tert*-butyl hypochlorite as a halogenating agent (Scheme 40).<sup>203</sup> The solvent effect appeared to be an important factor for the selectivity as well as the conversion. The best results in terms of both yield and selectivity were obtained in ether, probably due to its polarity that is believed to stabilize the oxonium intermediate and aid the selectivity. Tetrachloromethane also provided high yields; however, both solvents cause many health and environmental issues that tempers the enthusiasm toward their use. A similar electrophilic chlorination of arenes with trichloroisocyanuric acid over acidic zeolites has been described by Mendon et al. Trichloroisocyanuric acid (TCCA) reacted with arenes and its reactivity was highly affected by the acid strength of the reaction medium.<sup>204</sup> Deactivated arenes were also efficiently chlorinated.

A ZnO-H-beta-25 catalyst mixture was effectively applied for the bromination of di- and trinitro-stilbenes, under mild conditions using Br<sub>2</sub> as a brominating agent.<sup>205</sup> Commonly, one ring of the stilbene contained the nitro groups, highly deactivating that ring where bromination never occurred. The site of bromination depended on the substituents on the other ring. In the case of activating substituents the bromination occurred on the aromatic ring, while deactivating substituents (even as weak as halogens) will inhibit the electrophilic aromatic substitution and electrophilic addition to the C=C was the dominant outcome (Scheme 41).



**SCHEME 41** Heterogeneous catalytic bromination of polynitro-stilbenes.



**SCHEME 42** Halogenation of 2-arylpyridines catalyzed by Cu-MnO (A) and a polymer-anchored Pd complex (B).

The halogenation of aromatics, focusing on 2-arylpyridines, with *N*-halosuccinimides was successfully achieved by Pal et al. using a Cu-MnO catalyst, in a photonic activated reaction (Scheme 42).<sup>206</sup> The halogenation could be carried out by the three common succinimide derivatives, NCS, NBS, and NIS. The halogen introduction occurred in the 2-position of the aryl group, in contrast, the pyridine ring did not undergo halogenation. The same group extended the use of this process to halogenation of anilides and quinoline derivatives. In the latter case, the halogen was selectively introduced to the carbocyclic ring, the heterocycle appeared resistant to the reaction, in agreement with the arylpyridine starting materials.<sup>207</sup> A similar process with arylpyridine derivatives has also been carried out by using a polymer (mainly divinyl-benzene-styrene copolymer) anchored Pd complex.<sup>208</sup> The yields in both cases were moderate to high and the catalysts could be recycled.

### 3.5.6 Nitration

Nitration is an important reaction as it opens up new synthetic pathways to, for example, amines and other fine chemicals.<sup>209-212</sup> Several works have reported

successful nitration of aromatics over a broad variety of solid acid catalyst, including zeolites and metal oxides, in attempts to substitute the concentrated acidic solution mixture (nitric and sulfuric acids) that is traditionally employed for this reaction type.<sup>213, 214</sup> Representative examples for the heterogeneous catalytic nitration of aromatic compounds are presented in Table 10.

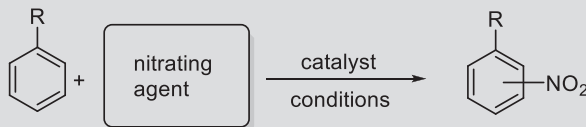
As Table 10 indicates, a notoriously dangerous and corrosive reaction medium, the HNO<sub>3</sub> - concentrated (cc) H<sub>2</sub>SO<sub>4</sub> mixture, has been successfully replaced by a broad variety of solid acid-catalyzed protocols. It is worth noting that while the reagents used in these methods are less harmful or dangerous, e.g., simple aqueous nitric acid or variety of nitrous gases, they still represent considerable problems environmentally. The use of nitrate salts, such as Cu(NO<sub>3</sub>)<sub>2</sub> or AgNO<sub>3</sub>, is a step in the right direction (Table 10, entries 1, 4). They are mostly used in excess and the recycling of the unspent acid or gas is challenging. The most commonly used catalysts include metal oxides, zeolites, clays, heteropoly acids and their salts, in addition to a large group of immobilized acids on a variety of supports. A few current examples later indicate that nitration is still of interest, and the search for greener methods is currently ongoing.

Kumar et al. developed a microwave-assisted solvent-free solid acid-catalyzed nitration protocol for the synthesis of nitroaromatics. The authors used a silica-supported perchloric acid or bisulfate as their catalysts of choice (Scheme 43).<sup>236</sup> A forward-looking aspect of the methodology is the application of NaNO<sub>2</sub> as the nitrating agent, which provided excellent yields in short reactions. The data showed that the perchloric acid-based catalyst performed better than the bisulfate one due to its low nucleophilicity and higher acidity. The catalyst was prepared by a simple procedure and was reused in four consecutive cycles without a significant drop in its activity.

Wang et al. prepared a series of Keggin heteropoly acid anion-based amphiphilic salts supported on nanosize metal oxides to be applied as catalysts in the nitration of aromatics. Aqueous HNO<sub>3</sub> served as the nitrating reagent. The nitration of toluene was used as a test reaction to optimize the reaction conditions, producing 93% conversion and good *para* selectivity (*o:p* = 1:9).<sup>223</sup> The protocol appeared to have a broad substrate scope, including aromatics with electron-donating and electron-withdrawing substituents alike. It is worth noting that even nitrotoluene and nitrochlorobenzene afforded acceptable yields. The overall conversion range was 60%–100%. The lowest yield (12%, with 90% *para*-selectivity) was obtained with the notoriously unreactive nitrobenzene.

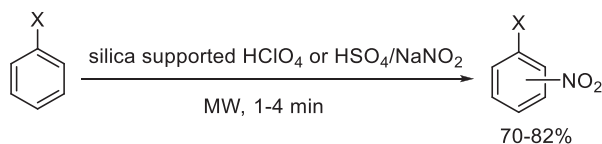
A sol-gel method was used for the preparation of several WO<sub>3</sub>/SiO<sub>2</sub> catalysts. Ammonium metatungstate (a WO<sub>3</sub> precursor) and ethyl silicate-40 (ES-40, a SiO<sub>2</sub> precursor) were applied during the synthesis.<sup>237</sup> The procedure resulted in the formation of well-dispersed WO<sub>3</sub> nanoparticles with the average size of 2–5 nm on the surface of the mesoporous silica. The 20 wt% WO<sub>3</sub>/SiO<sub>2</sub> catalyst was found to exhibit the strongest acidity, which was characterized as a combination of both Lewis and Brønsted acid centers. The catalysts were highly active in the liquid-phase nitration of aromatics when 70% nitric acid was used as the nitrating agent. The conversion was close to quantitative (99%)

**TABLE 10** Solid acid-catalyzed nitration of aromatics.



| Entry | Aromatics               | Catalysts/conditions   | Product                        | Yield (%)           | Selectivity   | Ref.                     |
|-------|-------------------------|--|--------------------------------|---------------------|---|--------------------------|
| 1     | Activated aromatics     | WO <sub>3</sub> /SiO <sub>2</sub> , or PdO <sub>2</sub> /SiO <sub>2</sub> , 70% aq. HNO <sub>3</sub> or Cu(NO <sub>3</sub> ) <sub>2</sub> 90°C, ethylene dichloride, 5.3–8 h                       | Mononitro products             | 55–100              | The 2-NO <sub>2</sub> products dominate (WO <sub>3</sub> ), 2/4 ratio ~ 1 except tertbutylbenzene | <a href="#">215–217</a>  |
| 2     | Substituted benzenes    | SO <sub>4</sub> <sup>2-</sup> /ZrO <sub>2</sub> -M <sub>x</sub> O <sub>y</sub> -Fe <sub>3</sub> O <sub>4</sub> , 95% aq. HNO <sub>3</sub> , CCl <sub>4</sub> , Ac <sub>2</sub> O, 100–700°C, 1.5 h | Substituted mononitro benzenes | 70–100 (conversion) | Selective mononitration, high 4-NO <sub>2</sub> selectivity                                       | <a href="#">218</a>      |
| 3     | Xylenes                 | MoO <sub>3</sub> /SiO <sub>2</sub> supported H <sub>3</sub> PO <sub>4</sub> , 65% aq. HNO <sub>3</sub> , RT-80°C, 2.5 h  | Mononitro-xylenes              | 62–100              | High selectivity for the 2-NO <sub>2</sub> products   | <a href="#">219</a>      |
| 4     | <i>N</i> -aryl anilines | Co(OAc) <sub>4</sub> × 4 H <sub>2</sub> O, AgNO <sub>3</sub> , 80°C, 60 h, THF   | Mononitrated products          | 70–92               | Exclusive 2-nitration on the aniline ring   | <a href="#">220</a>      |
| 5     | Toluene                 | Cs <sub>2.5</sub> H <sub>0.5</sub> PMoO <sub>40</sub> , 70°C, 10 h; 20 wt% KHSO <sub>4</sub> /diatomite, nitric acid   | Mononitrated products          | Up to 100           | 2-/4-nitro = 1.3<br>2/3/4 = 40:5:55   | <a href="#">221, 222</a> |
| 6     | Substituted benzenes    | [bmim] <sub>3</sub> PW <sub>12</sub> O <sub>40</sub> on SiO <sub>2</sub> , 65% aq. HNO <sub>3</sub> , 50°C, 3 h  | Mononitro products             | 61–99               | High 4-NO <sub>2</sub> selectivity except phenol  | <a href="#">223</a>      |

|    |   |   |                               |                      |   |                         |
|----|---|---|-------------------------------|----------------------|---|-------------------------|
| 7  | Substituted aromatics                           | PEG200-based dicationic acidic ionic liquid, N <sub>2</sub> O <sub>5</sub> , CCl <sub>4</sub> , 50°C, 2 h   | Various mononitrated products | 78–97                | High 2- and 4-NO <sub>2</sub> selectivity, depending on the aromatic compound   | <a href="#">224</a>     |
| 8  | Substituted benzenes, naphthalenes, anthracenes | H <sub>3</sub> PO <sub>4</sub> modified montmorillonite, 65% aq. HNO <sub>3</sub> , RT-50°C, 0.5–24 h   | Mononitrated products         | 35–97                | 2–4 ratio = 0.92–0.11   | <a href="#">225</a>     |
| 9  | Benzene   | Mesoporous silica-immobilized FeCl <sub>3</sub> , NO <sub>2</sub> gas, 60–120°C, 0.5–24 h   | Nitrobenzene                  | Up to 99% conversion | > 99% for nitro-benzene   | <a href="#">226</a>     |
| 10 | Phenol  | Zeolites H-beta, ZSM-5, NaY, silicotungstic acid supported zirconia, H <sub>3</sub> +xPMo <sub>12-x</sub> VxO <sub>40</sub> , sulfated titania, nanosized tungsten oxide supported on sulfated SnO <sub>2</sub> , TiO <sub>2</sub> -SiO <sub>2</sub> mixed oxide supported MoO <sub>3</sub> dilute or fuming HNO <sub>3</sub> , RT-400°C, 1–2 h | Mononitrated products         | Up to 99% conversion | 4-NO <sub>2</sub> product dominates, in many cases remarkable 2-selectivity<br>2 vs 4 selectivity depends on the reaction temperature | <a href="#">227–235</a> |



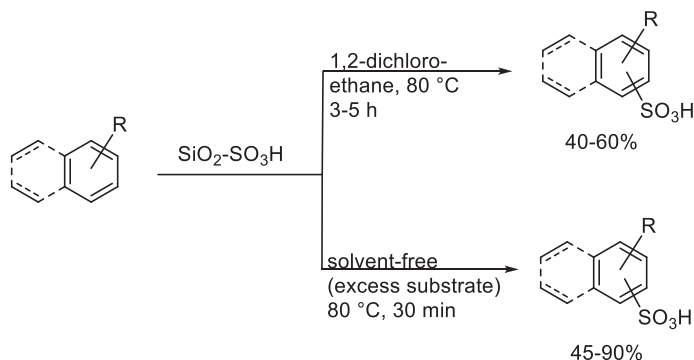
**SCHEME 43** Nitration of aromatics by silica-supported nitrating reagents.

and the product 2-nitro-*p*-cresol was obtained with very high selectivity (99%). The water formed during the reaction was removed azeotropically. Applying *o*-xylene as a substrate, 74% conversion was observed and the product 4-nitro *o*-xylene formed with 54% selectivity.

### 3.5.7 Sulfonation

Sulfonation of organic compounds is an important process, as many aryl sulfonic acids fulfill vital roles in organic chemistry as acid catalysts that are soluble in typical organic solvents, or they are used in the preparation of solid acids, sulfonic acid chlorides, and sulfonamides or simply as easily removable placeholders in synthesis design.<sup>238-240</sup> Although the overwhelming majority of sulfonation reactions is carried out with simple cc. H<sub>2</sub>SO<sub>4</sub>, several alternative processes have been developed that can serve as greener replacements to the corrosive and dangerous sulfuric acid. Many of these processes apply solid catalysts to address these problems.

A green sulfonation of substituted benzenes was developed by Hajipour et al., using a silica-bound sulfuric acid complex material, SiO<sub>2</sub>-SO<sub>3</sub>H (Scheme 44). As one of the least green features of the protocol, 1,2-dichloroethane was used as a solvent. It is worth mentioning that the reaction readily occurs under solvent-free conditions as well. In fact, the solvent-free reaction was much more effective than the one carried out in solvent. A broad scope of aromatics (benzene derivatives and naphthalene) with electron-donating and moderately electron-withdrawing substituent were evaluated in the reaction. As a drawback,



**SCHEME 44** Sulfonation of benzene derivatives and naphthalene with SiO<sub>2</sub>-SO<sub>3</sub>H.

the silica-bound solid sulfuric acid was rather a reagent than a catalyst as it was consumed in stoichiometric amount.<sup>241</sup> A similar silica-supported HClO<sub>4</sub> and KHSO<sub>4</sub> catalysts were applied in the green sulfonation of aromatics under a solvent-free microwave-assisted protocol. The microwave reactions occurred in significantly shorter times (3–5 min) than the reactions under conventional conditions (3–5 h). The catalyst was found to be recyclable up to four times.<sup>242</sup>

As a general trend, a sulfuric acid derivative commonly serves as the reagent, and the main focus of the new advances is to develop new catalysts via sulfonation. Many of these catalysts are green alternatives, such as carbon-bound SO<sub>3</sub>Cu<sup>243</sup> or sulfonated graphitic nitride.<sup>244</sup>

### 3.5.8 Conclusions and outlook

The earlier presented results clearly indicate that the aromatic electrophilic substitution, including Friedel-Crafts and related reactions, is an essential, important part of contemporary organic synthesis whether it is about a C–C bond forming reaction or the introduction of halogen or nitro substituents. The trends, however, appear to change. A large majority of the protocols published in the past two decades apply solid acids as catalysts for these reactions following the worldwide push for the development of green and environmentally more benign industrial practices. A future extension on the development of these green protocols is anticipated with the parallel decline in the application of traditional catalysts and gradually, the outdated processes will be replaced by more environmentally benign methods that fulfill the current needs.

### References

1. Lewis, D. Charles Friedel (1832–1899) and James Mason Crafts (1839–1917): The Friedel-Crafts Alkylation and Acylation Reactions. *Synform* **2018**, *4*, A49–A52.
2. Smith, M. B.; March, J. *March's Advanced Organic Chemistry: Reactions, Mechanisms, and Structure*, 6th ed.; Wiley: Hoboken, NJ, 2007; pp. 657–751 (chapter 11).
3. Friedel, C.; Crafts, J. M. Sur une nouvelle méthode générale de synthèse d'hydrocarbures, d'acétones etc. Deuxieme note. *Compt. Rend.* **1877**, *84*, 1450–1454.
4. Friedel, C.; Crafts, J. M. Sur une nouvelle méthode générale de synthèse d'hydrocarbures, d'acétones etc. Troisieme note. *Compt. Rend.* **1877**, *85*, 74–77.
5. Olah, G. A., Ed. *Friedel-Crafts and Related Reactions*; Wiley: New York, 1964.
6. Olah, G. A. *Friedel-Crafts Chemistry*, Wiley-Interscience: New York, 1973.
7. Dasgupta, S.; Török, B. Environmentally Benign Contemporary Friedel-Crafts Chemistry by Solid Acids. *Curr. Org. Synth.* **2008**, *5*, 321–342.
8. El-Hiti, G. A.; Smith, K.; Hegazy, A. S. Catalytic, Green and Regioselective Friedel-Crafts Acylation of Simple Aromatics and Heterocycles Over Zeolites. *Curr. Org. Chem.* **2015**, *19*, 585–598.
9. Anastas, P. T.; Warner, J. C. *Green Chemistry: Theory and Applications*, Oxford University Press: Oxford, 1998.
10. Li, C.-J., Ed. *Green Synthesis*, Vol. 7; *Handbook of Green Chemistry-Green Processes*; Wiley-VCH: Weinheim, 2012.

11. Török, B.; Dransfield, T., Eds. *Green Chemistry: An inclusive approach*; Elsevier: Cambridge, Oxford, 2018.
12. Olah, G. A.; Mathew, T.; Goepfert, A.; Török, B.; Bucsi, I.; Li, X.-Y.; Wang, Q.; Marinez, E. R.; Batamack, P.; Aniszfeld, R.; Prakash, G. K. S. Ionic Liquid and Solid HF Equivalent Amine-Poly(Hydrogen Fluoride) Complexes Effecting Efficient Environmentally Friendly Isobutane-Isobutylene Alkylation. *J. Am. Chem. Soc.* **2005**, *127*, 5964–5969.
13. Liu, N.; Yao, J.; Shi, L. A novel method to anchor methanesulfonic acid in silica matrix. *Sci. China* **2016**, *59*, 370–379.
14. Yamamoto, H.; Ishihara, K., Eds. *Acid Catalysis in Modern Organic Synthesis*; Wiley-VCH: Weinheim, 2008.
15. Molnár, Á. Acids and Acid Catalysis—Homogeneous. In *Encyclopedia of Catalysis*; Horvath, I. T., Ed.; Vol. 1; Wiley: New York, 2003; pp. 40–86.
16. Bag, S.; Dasgupta, S.; Török, B. Microwave-Assisted Heterogeneous Catalysis: An Environmentally Benign Tool for Contemporary Organic Synthesis. *Curr. Org. Synth.* **2011**, *8*, 237–261.
17. Kokel, A.; Schäfer, C.; Török, B. Organic Synthesis using Environmentally Benign Acid Catalysis. *Curr. Org. Synth.* **2019**, *16*, 615–649.
18. Dasgupta, S.; Török, B. Application of Clay Catalysts in Organic Synthesis. A Review. *Org. Prep. Proced. Int.* **2008**, *40*, 1–65.
19. Xu, X.-L.; Li, Z. Deciphering the Redox Chain Mechanism in the Catalytic Alkylation of Quinones. *Synlett* **2018**, *29*, 1807–1813.
20. Carraro, P. M.; Goldani, B. S.; Alves, D.; Sathicq, A. G.; Eimer, G. A.; Romanelli, G. P.; Luque, R. Stability and Activity of Zn/MCM-41 Materials in Toluene Alkylation: Microwave Irradiation vs Continuous Flow. *Catalysts* **2019**, *9*, 136.
21. Zhang, K.; Yang, T.-Q.; Shan, B.-Q.; Liu, P.-C.; Peng, B.; Xue, Q.-S.; Yuan, E.-H.; Wu, P.; Albela, B.; Bonneviot, L. Dendritic and Core–Shell–Corona Mesoporous Sister Nanospheres from Polymer–Surfactant–Silica Self-Entanglement. *Chem. Eur. J.* **2018**, *24*, 478–486.
22. Abid, M.; Török, B.; Huang, X. Microwave-Assisted Tandem Processes for the Synthesis of N-Heterocycles. *Aust. J. Chem.* **2009**, *62*, 208–222.
23. Daştan, A.; Kulkarni, A.; Török, B. Environmentally Benign Synthesis of Heterocyclic Compounds by Combined Microwave-assisted Heterogeneous Catalytic Approaches. *Green Chem.* **2012**, *14*, 17–37.
24. Kokel, A.; Schäfer, C.; Török, B. Application of Microwave-assisted Heterogeneous Catalysis in Sustainable Synthesis Design. *Green Chem.* **2017**, *19*, 3729–3751.
25. Lachter, E. R.; da Silva San Gil, R. A.; Tabak, D.; Costa, V. G.; Chaves, C. P. S.; dos Santos, J. A. Alkylation of Toluene With Aliphatic Alcohols and 1-Octene Catalyzed by Cation-exchange Resins. *React. Funct. Polym.* **2000**, *44*, 1–7.
26. Yadav, G. D.; Rahuman, M. S. M. M. Efficacy of Solid Acids in the Synthesis of Butylated Hydroxy Anisoles by Alkylation of 4-Methoxyphenol with MTBE. *Appl. Catal. A* **2003**, *253*, 113–123.
27. Yadav, G. D.; Kundu, B. Friedel-Crafts Alkylation of Diphenyl Oxide With 1-Decene Over Sulfated Zirconia as Catalyst. *Can. J. Chem. Eng.* **2001**, *79*, 805–811.
28. Yadav, G. D.; Pathre, G. S. Selectivity Engineering of Cation-Exchange Resins over Inorganic Solid Acids in C-Alkylation of Guaiacol with Cyclohexene. *Ind. Eng. Chem. Res.* **2007**, *46*, 3119–3127.
29. Zlao, Z.; Wang, W.; Qiao, W.; Wang, G.; Li, Z.; Cheng, L. HY Zeolite Catalyst for Alkylation of  $\alpha$ -Methylnaphthalene With Long-chain Alkenes. *Microporous Mesoporous Mater.* **2006**, *93*, 164–170.

30. Wen, J.; Qi, H.; Kong, X.; Chen, L.; Yan, X. Hydroarylation of Styrenes with Electron-Rich Arenes Over Acidic Ion-Exchange Resins. *Synth. Commun.* **2014**, *44*, 1893–1903.
31. Hung, C.-T.; Liu, L.-L.; Wang, J.-J.; Wu, P.-H.; Wang, C.-B.; Tsai, T.-C.; Liu, S.-B. Acidity and Alkylation Activity of 12-Tungstophosphoric Acid Supported on Ionic Liquid-functionalized SBA-15. *Catal. Today* **2019**, *327*, 10–18.
32. Bandini, M.; Fagioli, M.; Umani-Ronchi, A. Solid Acid-Catalysed Michael-Type Conjugate Addition of Indoles to Electron-Poor C=C Bonds: Towards High Atom Economical Semi-continuous Processes. *Adv. Synth. Catal.* **2004**, *346*, 545–548.
33. Das, A.; Anbu, N.; SK, M.; et al. Highly Active Urea-Functionalized Zr(IV)-UiO-67 Metal – Organic Framework as Hydrogen Bonding Heterogeneous Catalyst for Friedel – Crafts Alkylation. *Inorg. Chem.* **2019**, *58*, 5163–5172.
34. Nguyen, K. D.; Ehrling, S.; Senkovska, I.; Bon, V.; Kaskel, S. New 1D Chiral Zr-MOFs Based on In Situ Imine Linker Formation as Catalysts for Asymmetric CAC Coupling Reactions. *J. Catal.* **2020**, *386*, 106–116.
35. An, L.; Zhang, L.; Zou, J.; Zhang, G. Montmorillonite K10: Catalyst for Friedel-Crafts Alkylation of Indoles and Pyrrole with Nitroalkenes Under Solventless Conditions. *Synth. Commun.* **2010**, *40*, 1978–1984.
36. Zhu, C.; Mao, Q.; Li, D.; Li, C.; Zhou, Y.; Wu, X.; Luo, Y.; Li, Y. A Readily Available Urea Based MOF That Act as a Highly Active Heterogeneous Catalyst for Friedel-Crafts Reaction of Indoles and Nitrostyrenes. *Catal. Commun.* **2018**, *104*, 123–127.
37. Rao, P. C.; Mandal, S. Friedel-Crafts Alkylation of Indoles with Nitroalkenes through Hydrogen-Bond-Donating Metal-Organic Framework. *ChemCatChem* **2017**, *9*, 1172–1176.
38. Markad, D.; Mandal, S. K. Design of a Primary-Amide-Functionalized Highly Efficient and Recyclable Hydrogen-Bond-Donating Heterogeneous Catalyst for the Friedel–Crafts Alkylation of Indoles with  $\beta$ -Nitrostyrenes. *ACS Catal.* **2019**, *9*, 3165–3173.
39. Anbu, N.; Dhakshinamoorthy, A.  $\text{Cu}_3(\text{BTC})_2$  as a Viable Heterogeneous Solid Catalyst for Friedel-Crafts Alkylation of Indoles With Nitroalkenes. *J. Colloid Interface Sci.* **2017**, *494*, 282–289.
40. Mohammadian, R.; Amini, M. M.; Shaabani, A. Thiourea-functionalized MIL-101(Cr) Metal-organic Framework as a Hydrogen-Bond-Donating Heterogeneous Organocatalyst for the Friedel-Crafts Alkylation and Biginelli Reactions. *Catal. Commun.* **2020**, *136*, 105905.
41. James, B.; Suresh, E.; Nair, M. S. Friedel–Crafts Alkylation of a Cage Enone: Synthesis of Aralkyl Substituted Tetracyclo[5.3.1.0[2,6].0[4,8]]Undeca-9,11-Diones and the Formation of Fascinating Novel Cage Compounds With Pyrrole and Thiophene Using Montmorillonite K-10. *Tetrahedron Lett.* **2007**, *48*, 6059–6063.
42. Das, B.; Majhi, A.; Banerjee, J.; Chowdhury, N.; Venkateswarlu, K.  $\text{Fe}^{3+}$ -K-10 Montmorillonite Clay Catalyzed Friedel–Crafts Reaction of Unactivated Baylis–Hillman Adducts: An Efficient Stereoselective Synthesis of Trisubstituted Alkenes Containing a Benzyl Substituent. *Chem. Lett.* **2005**, *34*, 1492–1493.
43. Yadav, A.; Biswas, S.; Mobin, S. M.; Samanta, S. Efficient  $\text{Cu}(\text{OTf})_2$ -Catalyzed and Microwave-Assisted Rapid Synthesis of 3,4-Fused Chromenopyridinones Under Neat Conditions. *Tetrahedron Lett.* **2017**, *58*, 3634–3639.
44. Baran, P. S.; Richter, J. M. Enantioselective Total Syntheses of Welwitindolinone A and Fischerindoles I and G. *J. Am. Chem. Soc.* **2005**, *127*, 15394–15396.
45. Baran, P. S.; Maimone, T. J.; Richter, J. M. Total Synthesis of Marine Natural Products Without Using Protecting Groups. *Nature* **2007**, *446*, 404–408.
46. Heck, R. F. Acylation, Methylation, and Carboxyalkylation of Olefins by Group VIII Metal Derivatives. *J. Am. Chem. Soc.* **1968**, *90*, 5518–5526.

47. Molnár, Á., Ed. *Palladium-Catalyzed Coupling Reactions: Practical Aspects and Future Developments*; Wiley-VCH: Weinheim, 2013.
48. [https://www.nobelprize.org/nobel\\_prizes/chemistry/laureates/2010/](https://www.nobelprize.org/nobel_prizes/chemistry/laureates/2010/) (Accessed 15 February 2021).
49. Pandey, G.; Török, B. K-10 Montmorillonite-Catalyzed Solid Phase Diazotizations: Environmentally Benign Coupling of Diazonium Salts With Aromatic Hydrocarbons to Biaryls. *Green Chem.* **2017**, *19*, 2515–2519.
50. Tashiro, M.; Yamato, T.; Fukata, G. Studies on Selective Preparation of Aromatic Compounds. 15. The Lewis Acid Catalyzed Transalkylation of Some Tert-butylidiphenylmethanes and -Ethanes in Aromatic Solvents. *J. Org. Chem.* **1978**, *43*, 1413–1420.
51. Molnár, Á.; Kereszszegi, C.; Török, B. Heteropoly Acids Immobilized Into a Silica Matrix: Characterization and Catalytic Applications. *Appl. Catal. A: Gen.* **1999**, *189*, 217–224.
52. Molnár, Á.; Beregszászi, T.; Fudala, A.; Lentz, P.; Nagy, J. B.; Kónya, Z.; Kiricsi, I. The Acidity and Catalytic Activity of Supported Acidic Cesium Dodecatungstophosphates Studied by MAS NMR, FTIR, and Catalytic Test Reactions. *J. Catal.* **2001**, *202*, 379–386.
53. Takabatake, M.; Nambo, M.; Manaka, Y.; Motokura, K. Direct Alkylation of Benzene at Lower Temperatures in the Liquid Phase: Catalysis by Montmorillonites as Noble-Metal-Free Solid Acids. *ChemPlusChem* **2020**, *85*, 450–453.
54. Prakash, G. K. S.; Yan, P.; Török, B.; Bucsi, I.; Tanaka, M.; Olah, G. A. Gallium(III) Tri-fluoromethanesulfonate: A Water-tolerant, Reusable Lewis Acid Catalyst for Friedel–Crafts Reactions. *Catal. Lett.* **2003**, *85*, 1–6.
55. Liu, Y.; Cheng, G.; Barath, E.; Shia, H.; Lercher, J. A. Alkylation of Lignin-Derived Aromatic Oxygenates With Cyclic Alcohols on Acidic Zeolites. *Appl. Catal. B Environ.* **2021**, *281*, 119424.
56. Yu, J.; Li, C.-J.; Zeng, H. Dearomatization-Rearomatization Strategy for ortho-Selective Alkylation of Phenols with Primary Alcohols. *Angew. Chem. Int. Ed.* **2021**, *60*, 4043–4048.
57. Yadav, G. D.; Purandare, S. A. Vapor Phase Alkylation of Toluene With 2-Propanol to Cymenes With a Novel Mesoporous Solid acid UDCaT-4. *Microporous Mesoporous Mater.* **2007**, *103*, 363–372.
58. Kamalakar, G.; Kommura, K.; Sugi, Y. tert-Butylation of Phenol over Ordered Solid Acid Catalysts in Supercritical Carbon Dioxide: Efficient Synthesis of 2,4-Di-tert-butylphenol and 2,4,6-Tri-tert-butylphenol. *Ind. Eng. Chem. Res.* **2006**, *45*, 6118–6126.
59. Rác, B.; Hegyes, P.; Forgó, P.; Molnár, Á. Sulfonic Acid-Functionalized Phenylene-Bridged Periodic Mesoporous Organosilicas as Catalyst Materials. *Appl. Catal. A* **2006**, *299*, 193–201.
60. Yadav, G. D.; Pathere, G. S. Novel Mesoporous Solid Superacids for Selective C-alkylation of *m*-cresol with tert-Butanol. *Microporous Mesoporous Mater.* **2006**, *89*, 16–24.
61. Einemann, M.; Schroeter, F.; Roessner, F. Alkylation of Phenol Derivatives Catalyzed by Zeolites and Zirconia Based Oxides. *React. Kinet. Mech. Catal.* **2020**, *130*, 477–491.
62. Muraleedharan, L.; Bellundagere; Chandrashekhara, M.; Bangalore; Prakash, S. J.; Yajnavalkya; Bhat, S. Clay-Based Solid Acid Catalyst for the Alkylation of *p*-Cresol with tert-Butyl Alcohol. *ChemistrySelect* **2018**, *3*, 801–808.
63. Yadav, G. D.; Pathre, G. S. Novelities of a Superacidic Mesoporous Catalyst UDCaT-5 in Alkylation of Phenol with tert-Amyl Alcohol. *Appl. Catal. A Gen.* **2006**, *297*, 237–246.
64. Zhou, D.-Q.; Yang, J.-H.; Dong, G.-M.; Huang, M.-Y.; Jiang, Y.-Y. Solid Superacid, Silica-supported Polytrifluoromethanesulfosiloxane Catalyzed Friedel–Crafts Benzoylation of Benzene and Substituted Benzenes. *J. Mol. Catal. A* **2000**, *159*, 85–87.
65. Rác, B.; Molnár, Á.; Forgó, P.; Mohai, M.; Bertóti, I. A Comparative Study of Solid Sulfonic Acid Catalysts Based on Various Ordered Mesoporous Silica Materials. *J. Mol. Catal. A Chem.* **2006**, *244*, 46–57.

66. Rác, B.; Mulas, G.; Csongrádi, A.; Lóki, K.; Molnár, Á. SiO<sub>2</sub>-supported Dodecatungstophosphoric Acid and Nafion-H Prepared by Ball-milling for Catalytic Application. *Appl. Catal. A Gen.* **2005**, *282*, 255–265.
67. Kamalakar, G.; Komura, K.; Kubota, Y.; et al. Friedel–Crafts benzylation of aromatics with benzyl alcohols catalyzed by heteropoly acids supported on mesoporous silica. *J. Chem. Technol. Biotechnol.* **2006**, *81*, 981–988.
68. Miao, Z.; Li, Z.; Liu, D.; Zhao, J.; Chou, L.; Zhou, J.; Zhuo, S. An Efficient Ordered Mesoporous Molybdate-Zirconium Oxophosphate Solid Acid Catalyst With Homogeneously Dispersed Active Sites: Synthesis, Characterization and Application. *J. Coll. Interface Sci.* **2018**, *526*, 145–157.
69. Sun, Q.; Harmer, M. A.; Farneth, W. E. An Extremely Active Solid Acid Catalyst, Nafion Resin/Silica Composite, for the Friedel–Crafts Benzylation of Benzene and *p*-Xylene with Benzyl Alcohol. *Ind. Eng. Chem. Res.* **1997**, *36*, 5541–5544.
70. Mashkina, A. V.; Khairulina, L. N. Catalytic Reactions of Dimethyl Disulfide with Thiophene and Benzene. *Kinet. Catal.* **2016**, *57*, 72–81.
71. Shinde, S. H.; Rode, C. V. Friedel–Crafts Alkylation over Zr-Mont Catalyst for the Production of Diesel Fuel Precursors. *ACS Omega* **2018**, *3*, 5491–5501.
72. Pezzotta, C.; Fleury, G.; Soetens, M.; Van der Perre, S.; Denayer, J. F. M.; Riant, O.; Gaigneaux, E. M. Improving the Selectivity to 4-*tert*-Butylresorcinol by Adjusting the SURFACE chemistry of Heteropolyacid-based Alkylation Catalysts. *J. Catal.* **2018**, *359*, 198–211.
73. Rác, B.; Nagy, M.; Pálinkó, I.; Molnár, Á. Application of Sulfonic Acid Functionalized MCM-41 Materials—Selectivity Changes in Various Probe Reactions. *Appl. Catal. A* **2007**, *316*, 152–159.
74. Yang, F.; Zhong, J.; Liu, X.; Zhu, X. A Novel Catalytic Alkylation Process of Syngas With Benzene Over the Cerium Modified Platinum Supported on HZSM-5 Zeolite. *Appl. Energy* **2018**, *226*, 22–30.
75. Lee, S.; Kim, D.; Lee, J.; et al. An In Situ Methylation of Toluene Using Syngas Over Bifunctional Mixture of Cr<sub>2</sub>O<sub>3</sub>/ZnO and HZSM-5. *Appl. Catal. A* **2013**, *466*, 90–97.
76. Xua, Y.; Liu, J.; Ma, G.; Wang, J.; Lin, J.; Wang, H.; Zhang, C.; Ding, M. Effect of IRON LOADING on acidity and Performance of Fe/HZSM-5 Catalyst for Direct Synthesis of Aromatics From Syngas. *Fuel* **2018**, *228*, 1–9.
77. Cirujano, F. G.; Stalpaert, M.; De Vos, D. E. Ionic Liquids vs. Microporous Solids as Reusable Reaction Media for the Catalytic C-H Functionalization of Indoles With Alcohols. *Green Chem.* **2018**, *20*, 2481–2485.
78. Song, W.; Zhang, Y.; Varyambath, A.; Kim, J. S.; Kim, I. Sulfonic Acid Modified Hollow Polymer Nanospheres With Tunable Wall-thickness for Improving Biodiesel Synthesis Efficiency. *Green Chem.* **2020**, *22*, 3572–3583.
79. Kulkarni, A.; Quang, P.; Török, B. Microwave-Assisted Solid Acid-Catalyzed Friedel–Crafts Alkylation and Electrophilic Annulation of Indoles Using Alcohols as Alkylating Agents. *Synthesis* **2009**, 4010–4014.
80. Landge, S. M.; Atanassova, V.; Thimmaiah, M.; Török, B. Microwave-Assisted Oxidative Coupling of Amines to Imines on Solid Acid Catalysts. *Tetrahedron Lett.* **2007**, *48*, 5161–5164.
81. Atanassova, V.; Ganno, K.; Kulkarni, A.; Landge, S. M.; Curtis, S.; Foster, M.; Török, B. Oxidative Coupling of Amines to Imines on K-10 Montmorillonite: A Mechanistic Study. *Appl. Clay Sci.* **2011**, *53*, 220–226.
82. Schäfer, C.; Ellstrom, C. J.; Török, B. Heterogeneous Catalytic Aqueous Phase Oxidative Cleavage of Styrenes to Benzaldehydes: An Environmentally Benign Alternative to Ozonolysis. *Top. Catal.* **2018**, *61*, 643–651.

370 Heterogeneous catalysis in sustainable synthesis

83. Yadav, G. D.; Goel, P. K.; Joshi, A. V. Alkylation of Dihydroxybenzenes and Anisole with Methyl-*tert*-Butyl Ether (MTBE) Over Solid Acid Catalysts. *Green Chem.* **2001**, *3*, 92–99.
84. Mao, J.; Kamiyo, Y.; Okuhara, T. Alkylation of 1,3,5-Trimethylbenzene With  $\gamma$ -Butyrolactone Over Heteropolyacid Catalysts. *Appl. Catal. A* **2003**, *255*, 337–344.
85. Dethé, D. H.; Dherange, B. D. Total Synthesis of Adunctin B. *J. Org. Chem.* **2018**, *83*, 3392–3396.
86. Yurino, T.; Hachiya, A.; Suzuki, K.; Ohkuma, T. Selective Conversion of Benzylic Phosphates into Diarylmethanes Through Al(OTf)<sub>3</sub>-Catalyzed Friedel–Crafts-Type Benzylolation. *Eur. J. Org. Chem.* **2020**, 2225–2232.
87. Yang, L.; Chen, X.; Ni, K.; Li, Y.; Wu, J.; Chen, W.; Ji, Y.; Feng, L.; Li, F.; Chen, D. Proton-Exchanged Montmorillonite-mediated Reactions of Hetero-benzylacetates: Application to the Synthesis of Zafirlukast. *Tetrahedron Lett.* **2020**, *61*, 152123.
88. de Angelis, A.; Ingallina, P.; Perego, C. Solid Acid Catalysts for Industrial Condensations of Ketones and Aldehydes with Aromatics. *Ind. Eng. Chem. Res.* **2004**, *43*, 1169–1178.
89. Prakash, G. K. S.; Fogassy, G.; Olah, G. A. Microwave-Assisted Nafion-H Catalyzed Friedel–Crafts Type Reaction of Aromatic Aldehydes with Arenes: Synthesis of Triarylmethanes. *Catal. Lett.* **2010**, *138*, 155–159.
90. Prakash, G. K. S.; Paknia, F.; Kulkarni, A.; Narayanan, A.; Wang, F.; Rasul, G.; Mathew, T.; Olah, G. A. Taming of Superacids: PVP-triflic acid as an Effective Solid Triflic Acid Equivalent for Friedel–Crafts Hydroxyalkylation and Acylation. *J. Fluor. Chem.* **2015**, *171*, 102–112.
91. Zhang, D. W.; Zhang, Y. M.; Zhang, Y. L.; Zhao, T. Q.; Liu, H. W.; Gan, Y. M.; Gu, Q. Efficient Solvent-free Synthesis of Bis(indolyl)methanes on SiO<sub>2</sub> Solid Support Under Microwave Irradiation. *Chem. Pap.* **2015**, *69*, 470–478.
92. Tran, P. H.; Nguyen, X.-T. T.; Chau, D.-K. N. A Brønsted-Acidic Ionic Liquid Gel as an Efficient and Recyclable Heterogeneous Catalyst for the Synthesis of Bis(indolyl)methanes Under Solvent-Free Sonication. *Asian J. Org. Chem.* **2018**, *7*, 232–239.
93. Nguyen, T.-T. H.; Nguyen, X.-T. T.; Nguyen, C. Q.; Tran, P. H. Porous Metal Oxides Derived From Cu–Al Layered Double Hydroxide as an Efficient Heterogeneous Catalyst for the Friedel–Crafts Alkylation of Indoles With Benzaldehydes Under Microwave Irradiation. *Heliyon* **2018**, *4*, e00966.
94. Reddy, A. V.; Ravinder, K.; Reddy, V. L. N.; Goud, T. V.; Ranikanth, V.; Venkateshwar, Y. Zeolite Catalyzed Synthesis of *bis*(Indolyl) Methanes. *Synth. Commun.* **2003**, *33*, 3687–3694.
95. Shi, L.; Liu, Y.; Wang, C.; Yuan, X.; Liu, X.; Wu, L.; Pan, Z.; Yu, Q.; Xu, C.; Yang, G. Synthesis of 1-(*b*-coumarinyl)-1-(*b*-indolyl) Trifluoroethanols Through Regioselective Friedel–Crafts Alkylation of Indoles with  $\beta$ -(trifluoroacetyl) Coumarins Catalyzed by Sc(OTf)<sub>3</sub>. *RSC Adv.* **2020**, *10*, 13929–13935.
96. Weitkamp, J.; Ernst, S. Probing the shape selective properties of zeolites by catalytic hydrocarbon reactions. *Catal. Today* **1988**, *3*, 451–457.
97. Unverricht, S.; Hunger, M.; Ernst, S.; Karge, H. G.; Weitkamp, J. Zeolite MCM-22: Synthesis, Dealumination and Structural Characterization. *Stud. Surf. Sci. Catal.* **1994**, *84*, 37–44.
98. Abid, M.; Spaeth, A.; Török, B. Solvent-Free Solid Acid-Catalyzed Electrophilic Annulations: A New Green Approach for the Synthesis of Substituted Five-Membered N-Heterocycles. *Adv. Synth. Catal.* **2006**, *348*, 2191–2196.
99. Cho, H.; Török, F.; Török, B. Energy efficiency of heterogeneous catalytic microwave-assisted organic reactions. *Green Chem.* **2014**, *16*, 3623–3634.
100. Abid, M.; Landge, S. M.; Török, B. An Efficient and Rapid Synthesis of N-substituted Pyrroles by Microwave Assisted Solid Acid Catalysis. *Org. Prep. Proced. Int.* **2006**, *35*, 495–500.

101. Abid, M.; De Paolis, O.; Török, B. A Novel One-pot Synthesis of N-acylindoles From Primary Aromatic Amides. *Synlett* **2008**, 410–413.
102. Rudnitskaya, A.; Borkin, D. A.; Huynh, K.; Török, B.; Stieglitz, K. Rational Design, Synthesis and Potency of N-substituted Indoles, Pyrroles and Triarylpyrazoles as Potential Fructose 1,6-biphosphatase Inhibitors. *ChemMedChem* **2010**, *5*, 384–389.
103. De Paolis, O.; Teixeira, L.; Török, B. Synthesis of Quinolines by a Solid Acid-Catalyzed Microwave-Assisted Domino Cyclization-aromatization Approach. *Tetrahedron Lett.* **2009**, *50*, 2939–2942.
104. Sun, J.; Gui, Y.; Huang, Y.; Li, J.; Zha, Z.; Yang, Y.; Wang, Z. Lewis Acid-Catalyzed Enantioselective Friedel–Crafts Alkylation of Pyrrole in Water. *ACS Omega* **2020**, *5*, 11962.
105. Ghodke, S.; Chudasama, U. Solvent Free Synthesis Of Coumarins Using Environment Friendly Solid Acid Catalysts. *Appl. Catal. A Gen.* **2013**, *453*, 219–226.
106. Chavan, O. S.; Shioorkar, M. G.; Jadhav, S. A.; Sakhare, M. A.; Pawar, Y. M.; Shivaji, B.; Chavan, S. B.; Baseer, M. A. Envirocat EPZ-10: An Efficient Catalyst for Synthesis of Coumarins by Pechmann Reactin Under Solvent Free Microwave Irradiation Method. *Heterocyclic Lett.* **2017**, *7*, 377–380.
107. Abd El Rahman, S. K.; Hassan, M. A. H.; El-Shalld, M. S. Metal-organic Frameworks With High Tungstophosphoric acid Loading as Heterogeneous Acid Catalysts. *Appl. Catal. A: Gen.* **2014**, *487*, 110–118.
108. Chang, M. Y.; Tsai, Y.-L.; Chen, H.-Y. CuBr<sub>2</sub>-Mediated One-Pot Synthesis of Sulfonyl 9-Fluorenylidenes. *J. Org. Chem.* **2020**, *85*, 6897–6909.
109. Zolfigol, M. A.; Yarie, M. N. M.; Ayazi-Nasrabadi, R. Catalytic Application of [Fe<sub>3</sub>O<sub>4</sub>@SiO<sub>2</sub>@(CH<sub>2</sub>)<sub>3</sub>-Urea-SO<sub>3</sub>H/HCl] as a Magnetically Recoverable Solid Acid at the Synthesis of 20-Aminobenzothiazolomethylnaphthols. *Res. Chem. Intermed.* **2018**, *44*, 191–200.
110. Alzeer, M. I. M.; MacKenzie, K. J. D.; Keyzers, R. A. Facile Synthesis of New Hierarchical Aluminosilicate Inorganic Polymer Solid Acids and Their Catalytic Performance in Alkylation Reactions. *Microporous Mesoporous Mater.* **2017**, *241*, 316–325.
111. Kore, R.; Kelley, S. P.; Sawant, A. D.; Mishra, M. K.; Rogers, R. D. Are Ionic Liquids and Liquid Coordination Complexes Really Different?—Synthesis, Characterization, and Catalytic Activity of AlCl<sub>3</sub>/Base Catalysts. *Chem. Commun.* **2020**, *56*, 5362–5365.
112. Van Herwijnen, H. W. G.; Brinker, U. H. Meta Selectivity in the Friedel-Crafts Reaction Induced by a Faujasite-Type Zeolite. *J. Org. Chem.* **2001**, *66*, 2874–2876.
113. Olah, G. A.; Török, B.; Shamma, T.; Török, M.; Prakash, G. K. S. Solid Acid (Superacid) Catalyzed Regioselective Adamantylation of Substituted Benzenes. *Catal. Lett.* **1996**, *42*, 5–13.
114. Yadav, G. D.; Purandare, S. A. Efficacy of a Novel Mesoporous Solid Acid Catalyst UDCaT-4 in Liquid Phase Benzoylation of Naphthalene. *J. Mol. Catal. A* **2007**, *263*, 26–31.
115. Hechelski, M.; Ghinet, A.; Louvel, B.; Dufrenoy, P.; Rigo, B.; Daich, A.; Waterlot, C. From Conventional Lewis Acids to Heterogeneous Montmorillonite K10: Eco-Friendly Plant-Based Catalysts Used as Green Lewis Acids. *ChemSusChem* **2018**, *11*, 1249–1277.
116. Losfeld, G.; Escande, V.; de La Blache, P. V.; L'Huillier, L.; Grison, C. Design and Performance of Supported Lewis Acid Catalysts Derived From Metal Contaminated Biomass for Friedel-Crafts Alkylation and Acylation. *Catal. Today* **2012**, *189*, 111–116.
117. Beregszászi, T.; Török, B.; Molnár, Á.; Olah, G. A.; Prakash, G. K. S. Friedel-Crafts Reactions Induced by Heteropoly Acids. Regioselective Adamantyl Substitution of Aromatic Compounds. *Catal. Lett.* **1997**, *48*, 83–87.
118. Török, B.; Molnár, Á. Electrophilic Transformations Induced by Heteropoly Acids: Applications and Structural Studies. *Compt. Rend. Acad. Sci. Paris, Serie II c.* **1998**, *1*, 381–396.

372 Heterogeneous catalysis in sustainable synthesis

119. Török, B.; Kiricsi, I.; Molnár, Á.; et al. Acidity and Catalytic Activity of a Nafion-H/Silica Nanocomposite Catalyst Compared with a Silica-Supported Nafion Sample. *J. Catal.* **2000**, *193*, 132–138.
120. Prakash, G. K. S.; Yan, P.; Török, B.; Bucsi, I.; Tanaka, M.; Olah, G. A. Gallium(III) Trifluoromethanesulfonate: A Water Tolerant, Reusable Lewis Acid Catalyst for Friedel-Crafts Reactions. *Catal. Lett.* **2003**, *85*, 1–6.
121. Fuson, R. C.; Weinstock, H. H., Jr.; Ulliyot, G. E. A New Synthesis of Benzoin. 2',4',6'-Trimethylbenzoin. *J. Am. Chem. Soc.* **1935**, *57*, 1803–1804.
122. Elings, J. A.; Downing, R. S.; Sheldon, R. A. Cyclialkylation of Arylalkyl Epoxides with Solid Acid Catalysts. *Eur. J. Org. Chem.* **1999**, 837–846.
123. Abid, M.; Török, B. Synthesis of *N*-Heteroaryl-Trifluoromethyl-Hydroxyl Alkanoic Acid Esters by Highly Efficient Solid Acid Catalyzed Hydroxyalkylation of Indoles and Pyrroles with Activated Trifluoromethyl Ketones. *Adv. Synth. Catal.* **2005**, *347*, 1797–1803.
124. Török, B.; Abid, M.; London, G.; Esquibel, J.; Török, M.; Mhadgut, S. C.; Yan, P.; Prakash, G. K. S. Highly Enantioselective Organocatalytic Hydroxyalkylation of Indoles With Ethyl Trifluoropyruvate. *Angew. Chem. Int. Ed.* **2005**, *44*, 3086–3089.
125. Prakash, G. K. S.; Yan, P.; Török, B.; Olah, G. A. Superacid Catalyzed Hydroxyalkylation of Aromatics with Ethyl Trifluoropyruvate: A New Synthetic Route to Mosher's Acid Analogs. *Synlett* **2003**, 527–531.
126. Török, M.; Abid, M.; Mhadgut, S. C.; Török, B. Organofluorine Inhibitors of Amyloid Fibrillogenesis. *Biochemistry* **2006**, *45*, 5377–5383.
127. Török, B.; Sood, A.; Bag, S.; Kulkarni, A.; Borkin, D.; Lawler, E.; Dasgupta, S.; Landge, S. M.; Abid, M.; Zhou, W.; Foster, M.; LeVine, H., III; Török, M. Structure-activity Relationship of Organofluorine Inhibitors of Amyloid-beta Self-assembly. *ChemMedChem* **2012**, *7*, 910–919.
128. Thirupathi, P.; Venkatagiri, N.; Reddy, C. K. Amberlyst-15 as a Green and Efficient Reusable Catalyst for Friedel-Crafts Alkylation of Activated Arenes with *N*-Sulfonyl Aldimines and Synthesis of Bis-triarylmethanes. *ChemistrySelect* **2018**, *3*, 9911–9915.
129. Abid, M.; Teixeira, L.; Török, B. Triflic Acid-Catalyzed Highly Stereoselective Friedel-Crafts Aminoalkylation of Indoles and Pyrroles. *Org. Lett.* **2008**, *10*, 933–935.
130. Rodríguez-Rodríguez, M.; Maestro, A.; Andrés, J. M.; Pedrosa, R. Supported Bifunctional Chiral Thioureas as Catalysts in the Synthesis of 3-Amino-2-Oxindoles through Enantioselective aza-Friedel-Crafts Reaction: Application in Continuous Flow Processes. *Adv. Synth. Catal.* **2020**, *362*, 1–12.
131. Wipf, P. In *Comprehensive Organic Synthesis*; Trost, B. M., Fleming, I., Eds.; *Combining C–C  $\pi$ -Bonds*, Paquette, L.A. Ed, Vol. 5; Pergamon Press: Oxford, 1991; p. 834.
132. Sheldon, R. A.; Elings, J. A.; Lee, S. K.; Lempers, H. E. B.; Downing, R. S. Zeolite-catalysed Rearrangements in Organic Synthesis. *J. Mol. Catal. A Chem.* **1999**, *134*, 129–135.
133. Pitchumani, K.; Warriar, M.; Ramamurthy, V. Remarkable Product Selectivity During Photo-Fries and Photo-Claisen Rearrangements within Zeolites. *J. Am. Chem. Soc.* **1996**, *118*, 9428–9429.
134. Sartori, G.; Maggi, R. Use of Solid Catalysts in Friedel-Crafts Acylation Reactions. *Chem. Rev.* **2006**, *106*, 1077–1104.
135. Sartori, G.; Maggi, R. Update of 1: Use of Solid Catalysts in Friedel-Crafts Acylation Reactions. *Chem. Rev.* **2011**, *111*, PR181–PR214.
136. Olah, G. A.; Mathew, T.; Farnia, M.; Prakash, G. K. S. Nafion-H Catalysed Intramolecular Friedel-Crafts Acylation: Formation of Cyclic Ketones and Related Heterocycles. *Synlett* **1999**, 1067–1068.

137. Harmer, M. A.; Farneth, W. E.; Sun, Q. High Surface Area Nafion Resin/Silica Nanocomposites: A New Class of Solid Acid Catalyst. *J. Am. Chem. Soc.* **1996**, *118*, 7708–7715.
138. Beers, A. E. W.; Nijhuis, T. A.; Kapteijn, F.; Moulijn, J. A. Zeolite Coated Structures for the Acylation of Aromatics. *Microporous Mesoporous Mater.* **2001**, *48*, 279–284.
139. Bernardon, C.; Ben Osman, M.; Laugel, G.; Louis, B.; Pale, P. Acidity Versus Metal-induced Lewis Acidity in Zeolites for Friedel-Crafts Acylation. *C. R. Chim.* **2017**, *20*, 20–29.
140. Yamashita, H.; Mitsukura, Y.; Kobashi, H. Microwave-assisted Acylation of Aromatic Compounds Using Carboxylic Acids and Zeolite Catalysts. *J. Mol. Catal. A-Chem.* **2010**, *327*, 80–86.
141. Kaur, J.; Kozhevnikov, I. V. Efficient Acylation of Toluene and Anisole With Aliphatic Carboxylic Acids Catalysed by Heteropoly Salt  $\text{Cs}_{2.5}\text{H}_{0.5}\text{PW}_{12}\text{O}_{40}$ . *Chem. Commun.* **2002**, 2508.
142. Prakash, G. K. S.; Mathew, T.; Mandal, M.; Farnia, M.; Olah, G. A. Aroylation of Aromatics With Arylcarboxylic Acids Over Nafion-H (Polymeric Perfluoroalkanesulfonic Acid), an Environmentally friendly solid acid catalyst. *ARKIVOC* **2004**, 103–110.
143. Venkatesha, N. J.; Chandrashekhara, B. M.; Prakash, B. S. J.; Bhat, Y. S. Active and Deactive Modes of Modified Montmorillonite in p-Cresol Acylation. *J. Mol. Catal. A-Chem.* **2014**, *392*, 181–187.
144. Montañez Valencia, M. K.; Padró, C. L.; Sad, M. E. Gas phase Acylation of Guaiacol With Acetic Acid on Acid Catalysts. *Appl. Catal. B Environ.* **2020**, *278*, 119317.
145. Gutiérrez-Rubio, S.; Shamzhy, M.; Čejka, J.; Serrano, D. P.; Moreno, I.; Coronado, J. M. Vapor Phase Acylation of Guaiacol With Acetic Acid Over Micro, Nano and Hierarchical MFI and BEA Zeolites. *Appl. Catal. B Environ.* **2021**, *285*, 119826.
146. Jaimol, T.; Moreau, P.; Finiels, A.; Ramaswamy, A. V.; Singh, A. P. Selective Propionylation of Veratrole to 3,4-Dimethoxypropiofenone Using Zeolite H-beta Catalysts. *Appl. Catal. A* **2001**, *214*, 1–10.
147. Lezcano-González, I.; Vidal-Moya, J. A.; Boronat, M.; Blasco, T.; Corma, A. Identification of Active Surface Species for Friedel–Crafts Acylation and Koch Carbonylation Reactions by In Situ Solid-State NMR. *Angew. Chem. Int. Ed.* **2013**, *52*, 5138–5141.
148. Shih, P.-C.; Wang, J.-H.; Mou, C.-Y. Strongly Acidic Mesoporous Aluminosilicates Prepared From Zeolite Seeds: Acylation of Anisole With Octanyl Chloride. *Catal. Today* **2004**, *93–95*, 365–370.
149. Tang, R. R.; Zhang, W. Facile Procedure for the Synthesis of 3-Acetyl-9-Ethylcarbazole and Corresponding Functionalized bis-b-Diketone Compounds. *Synth. Commun.* **2010**, *40*, 601–606.
150. Bigi, F.; Carloni, S.; Flego, C.; et al. HY Zeolite-Promoted Electrophilic Acylation of Methoxyarenes With Linear Acid Chlorides. *J. Mol. Catal. A-Chem.* **2002**, *178*, 139–146.
151. Hu, R.-J.; Li, B.-G. Novel Solid Acid Catalyst, Bentonite-Supported polytrifluoromethanesulfoniloxane for Friedel–Crafts acylation of ferrocene. *Catal. Lett.* **2004**, *98*, 43–47.
152. Bian, Z.; Li, J.; Chen, S. Rare Earth Solid Supercid Catalyzed Friedel-Crafts Acylation of Ferrocene. *Synth. Commun.* **2012**, *42*, 1053–1058.
153. Sarvari, M. H.; Sharghi, H. Reactions on a Solid Surface. A Simple, Economical and Efficient Friedel-Crafts Acylation Reaction over Zinc Oxide (ZnO) as a New Catalyst. *J. Org. Chem.* **2004**, *69*, 6953–6956.
154. Arata, K.; Nakamura, H.; Shonji, M. Friedel–Crafts Acylation of Toluene Catalyzed by Solid Supercids. *Appl. Catal. A* **2000**, *197*, 213–219.
155. Landge, S. M.; Chidambaran, M.; Singh, A. P. Benzoylation of Toluene With p-Toluoyl Chloride over Triflic Acid Functionalized Mesoporous Zr-TMS Catalyst. *J. Mol. Catal. A-Chem.* **2004**, *213*, 257–266.

156. Jain, P. U.; Samant, S. D.  $\text{Bi}_2\text{O}_3@m\text{SiO}_2$  as an Environmentally Benign and Sustainable Solid Acid Catalyst for Benzoylation of Aromatics: Impact of Silica Encapsulation on Catalyst Leaching and Reaction Synergy. *ChemistrySelect* **2020**, *5*, 4437–4446.
157. Raja, T.; Singh, A. P.; Ramaswamy, A. V.; Finiels, A.; Moreau, P. Benzoylation of 1,2-Dimethoxybenzene with Benzoic Anhydride and Substituted Benzoyl Chlorides Over Large Pore Zeolites. *Appl. Catal. A* **2001**, *211*, 31–39.
158. Ullah, L.; Zhao, G.; Xu, Z.; He, H.; Usman, M.; Zhang, S. 12-Tungstophosphoric acid Nixed in Zr-Based Metal-organic Framework: A Stable and Efficient Catalyst for Friedel-Crafts acylation. *Sci. China Chem.* **2018**, *61*, 402–411.
159. Winé, G.; Tessonnier, J.-P.; Rigolet, S.; et al. Beta Zeolite Supported on a  $\beta$ -SiC Foam Monolith: A Diffusionless Catalyst for Fixed-bed Friedel–Crafts Reactions. *J. Mol. Catal. A-Chem.* **2006**, *248*, 113–120.
160. Sawant, D. P.; Devassy, B. M.; Halligudi, S. B. Friedel–Crafts Benzoylation of Diphenyl Oxide Over Zirconia Supported 12-Tungstophosphoric Acid. *J. Mol. Catal. A-Chem.* **2004**, *217*, 211–217.
161. Deutsch, J.; Trunschke, A.; Müller, D.; et al. Acetylation and Benzoylation of Various Aromatics on Sulfated Zirconia. *J. Mol. Catal. A-Chem.* **2004**, *207*, 51–57.
162. Jin, T.-S.; Yang, M.-N.; Feng, G.-L.; Li, T.-S. Synthesis of Diaryl Ketones Catalyzed by  $\text{Al}_2\text{O}_3\text{-ZrO}_2/\text{S}_2\text{O}_8^{2-}$  Solid Superacid. *Synth. Commun.* **2004**, *34*, 479–485.
163. Zhang, H.; Song, X.; Zhao, C.; Hu, D.; Zhang, W.; Jia, M. N-Doped Porous Carbon– $\text{Fe}_3\text{C}$  Nanoparticle Composites as Catalysts for Friedel–Crafts Acylation. *ACS Appl. Nano Mater.* **2020**, *3*, 6664–6674.
164. Poh, N. E.; Nur, H.; Muhid, M. N. M.; Hamdan, H. Sulphated AlMCM-41: Mesoporous solid Brønsted Acid Catalyst for Dibenzoylation of Biphenyl. *Catal. Today* **2006**, *114*, 257–262.
165. Deutsch, J.; Prescott, H. A.; Müller, D.; Kemnitz, E.; Lieske, H. Acylation of Naphthalenes and Anthracene on Sulfated Zirconia. *J. Catal.* **2005**, *231*, 269–278.
166. Makihara, M.; Aoki, H.; Komura, K. Reaction Profiles of High Silica MOR Zeolite Catalyzed Friedel–Crafts Acylation of Anisole Using Acetic Anhydride in Acetic Acid. *Catal. Lett.* **2018**, *148*, 2974–2979.
167. Winé, G.; Pham-Huu, C.; Ledoux, M.-J. Acylation of Anisole by Acetic Anhydride Catalysed by BETA Zeolite Supported on Pre-shaped Silicon Carbide. *Catal. Commun.* **2006**, *7*, 768–772.
168. Sarsani, V. S. R.; Lyon, C. J.; Hutchenson, K. W.; Harmer, M. A.; Subramaniam, B. Continuous Acylation of Anisole by Acetic Anhydride in Mesoporous Solid Acid Catalysts: Reaction Media Effects on Catalyst Deactivation. *J. Catal.* **2007**, *245*, 184–190.
169. Zaccheria, F.; Shaikh, N. I.; Scotti, N.; Psaro, R.; Ravasio, N. New Concepts in Solid Acid Catalysis: Some Opportunities Offered by Dispersed Copper Oxide. *Top. Catal.* **2014**, *57*, 1085–1093.
170. Yadav, G. D.; Rahuman, M. S. M. M. Cation-Exchange Resin-Catalysed Acylations and Esterifications in Fine Chemical and Perfumery Industries. *Org. Process. Res. Dev.* **2002**, *6*, 706–713.
171. Kaur, J.; Griffin, K.; Harrison, B.; Kozhevnikov, I. V. Friedel–Crafts Acylation Catalysed by Heteropoly Acids. *J. Catal.* **2002**, *208*, 448–455.
172. Pande, M. A.; Samant, S. D. Acylation of Aromatic Ethers Using Different Carboxylic Acid Anhydrides as Acylating Agents in the Presence of Nontoxic, Noncorrosive Resin Amberlyst 12 as a Solid Acid Catalyst. *Synth. Commun.* **2011**, *41*, 754–761.
173. Rao, X.; Ishitani, H.; Yoo, W.-J.; Kobayashi, S. Zirconium- $\beta$  Zeolite-Catalyzed Continuous-Flow Friedel-Crafts Acylation Reaction. *Asian J. Org. Chem.* **2019**, *8*, 316–319.

174. Fang, W.; He, W.; Tu, T.; Lv, N.; Qiu, C.; Li, X.; Zhu, N.; Wan, L.; Guo, K. An Efficient and Green Pathway For Continuous Friedel-Crafts Acylation over  $\alpha$ -Fe<sub>2</sub>O<sub>3</sub> and CaCO<sub>3</sub> Nanoparticles Prepared in the Microreactors. *Chem. Eng. J.* **2018**, *331*, 443–449.
175. Guignard, C.; Pédrón, V.; Richard, F.; Jacquot, R.; Spagnol, M.; Coustard, J. M.; Pérot, G. Acylation of Veratrole by Acetic Anhydride over H and HY Zeolites Possible Role of di- and Triketone By-products in the Deactivation Process. *Appl. Catal. A* **2002**, *234*, 79–90.
176. Yadav, G. D.; Manyar, H. G. Novelities of Synthesis of Acetoveratrone Using Heteropoly Acid Supported on Hexagonal Mesoporous Silica. *Microporous Mesoporous Mater.* **2003**, *63*, 85–96.
177. Smith, K.; El-Hiti, G. A.; Jayne, A. J.; Butters, M. Acetylation of Aromatic Ethers Using Acetic Anhydride Over Solid Acid Catalysts in a Solvent-free System. Scope of the Reaction for Substituted Ethers. *Org. Biomol. Chem.* **2003**, *1*, 1560–1564.
178. Sawant, D. P.; Vinu, A.; Lefebvre, F.; et al. Tungstophosphoric Acid Supported Over Zirconia in Mesoporous Channels of MCM-41 as Catalyst in Veratrole Acetylation. *J. Mol. Catal. A-Chem.* **2007**, *262*, 98–108.
179. Yadav, G. D.; Pimparkar, K. P. Insight into Friedel-Crafts Acylation of 1,4-Dimethoxybenzene to 2,5-Dimethoxyacetophenone Catalysed by Solid acids—Mechanism, Kinetics and Remedies for Deactivation. *J. Mol. Catal. A-Chem.* **2007**, *264*, 179–191.
180. Moreau, P.; Finiels, A.; Meric, P.; Fajula, F. Acetylation of 2-Methoxynaphthalene in the Presence of Beta Zeolites: Influence of Reaction Conditions and Textural Properties of the Catalysts. *Catal. Lett.* **2003**, *85*, 199–203.
181. Kantam, M. L.; Ranganath, K. V. S.; Sateesh, M.; et al. Friedel–Crafts Acylation of Aromatics and Heteroaromatics by Beta Zeolite. *J. Mol. Catal. A-Chem.* **2005**, *225*, 15–20.
182. Kusumaningsih, T.; Prasetyo, W. E.; Firdaus, M. A Greatly Improved Procedure for the Synthesis of an Antibiotic-drug Candidate 2,4-Diacetylphloroglucinol Over Silica Sulphuric Acid Catalyst: Multivariate Optimisation and Environmental Assessment Protocol Comparison by Metrics. *RSC Adv.* **2020**, *10*, 31824–31837.
183. Kozhevnikov, I. V. Friedel–Crafts Acylation and Related Reactions Catalysed by Heteropoly Acids. *Appl. Catal. A* **2003**, *256*, 3–18.
184. Yang, X.; Yasukawa, T.; Maki, T.; Yamashita, Y.; Kobayashi, S. Well-Dispersed Trifluoromethanesulfonic Acid-Treated Metal Oxide Nanoparticles Immobilized on Nitrogen-Doped Carbon as Catalysts for Friedel–Crafts Acylation. *Chem. Asian J.* **2021**, *16*, 232–236.
185. Yadav, G. D.; George, G. Friedel–Crafts Acylation of Anisole With Propionic Anhydride Over Mesoporous Superacid Catalyst UDCaT-5. *Microporous Mesoporous Mater.* **2006**, *96*, 36–43.
186. Yadav, G. D.; Kamble, S. B. Atom Efficient Friedel-Crafts Acylation of Toluene With Propionic Anhydride Over Solid Mesoporous Superacid UDCaT-5. *Applied Catal. A* **2012**, *433-434*, 265–274.
187. Wang, T.; Yu, H.; Bian, B.; Liu, Y.; Liu, S.; Yu, S.; Wang, Z. One-Pot Synthesis of Anthraquinone Catalyzed by Microwave Acetic Acid Modified H $\beta$  Zeolite. *Catal. Lett.* **2020**, *150*, 3007–3016.
188. Heaney, H. In *Comprehensive Organic Synthesis*; Trost, B. M., Fleming, I., Eds.; Additions to C–X  $\pi$ -Bonds, Part 2, Heathcock, C.H. Ed, Vol. 2; Pergamon Press: Oxford, 1991; p. 745.
189. Prakash, G. K. S.; Yan, P.; Török, B.; Olah, G. A. Superacidic Trifluoromethanesulfonic Acid-induced Cycli-acyalkylation of Aromatics. *Catal. Lett.* **2003**, *87*, 109–112.
190. Kamiya, Y.; Ooka, Y.; Obara, C.; et al. Alkylation–Acylation of *p*-Xylene with  $\gamma$ -Butyrolactone or Vinylacetic Acid Catalyzed by Heteropolyacid Supported on Silica. *J. Mol. Catal. A-Chem.* **2007**, *262*, 77–85.

376 Heterogeneous catalysis in sustainable synthesis

191. Chassaing, S.; Kumarraja, M.; Pale, P.; Sommer, J. Zeolite-Directed Cascade Reactions: Cyclacyarylation Versus Decarboxyarylation of  $\alpha,\beta$ -Unsaturated Carboxylic Acids. *Org. Lett.* **2007**, *9*, 3889–3892.
192. Mackie, R. K.; Smith, D. M.; Aitken, R. A. *Guidebook to Organic Synthesis*, 3rd ed.; Pearson Ed Ltd: Harlow, 1999.
193. Saikia, I.; Borah, A. J.; Phukan, P. Use of Bromine and Bromo-Organic Compounds in Organic Synthesis. *Chem. Rev.* **2016**, *116*, 6837–7042.
194. Daou, T. J.; Boltz, M.; Tzanis, L.; Michelin, L.; Louis, B. Gas-phase Chlorination of Aromatics over FAU- and EMT-type Zeolites. *Catal. Commun.* **2013**, *39*, 10–13.
195. Losch, P.; Kolb, J. F.; Astafan, A.; Daou, T. J.; Pinard, L.; Palea, P.; Louis, B. Eco-compatible Zeolite-catalysed Continuous Halogenation of Aromatics. *Green Chem.* **2016**, *18*, 4714–4724.
196. Singh, A. P.; Mirajkar, S. P.; Sharma, S. Liquid Phase Bromination of Aromatics Over Zeolite H-beta Catalyst. *J. Mol. Catal. A-Chem.* **1999**, *150*, 241–250.
197. Mishra, A. K.; Nagarajaiah, H.; Moorthy, J. N. Trihaloisocyanuric Acids as Atom-Economic Reagents for Halogenation of Aromatics and Carbonyl Compounds in the Solid State by Ball Milling. *Eur. J. Org. Chem.* **2015**, 2733–2738.
198. Zhang, R.; Huang, L.; Zhang, Y.; Chen, X.; Xing, W.; Huang, J. Silver Catalyzed Bromination of Aromatics with N-Bromosuccinimide. *Catal. Lett.* **2012**, *142*, 378–383.
199. Janmanchi, K. M.; Dolbier, W. R., Jr. Highly Reactive and Regenerable Fluorinating Agent for Oxidative Fluorination of Aromatics. *Org. Process. Res. Dev.* **2008**, *12*, 349–354.
200. Mendoza, F.; Ruíz-Guerrero, R.; Hernández-Fuentes, C.; Molina, P.; Norzagaray-Campos, M.; Reguera, E. On the Bromination of Aromatics, Alkenes and Alkynes Using Alkylammonium Bromide: Towards the Mimic of Bromoperoxidases Reactivity. *Tetrahedron Lett.* **2016**, *57*, 5644–5648.
201. Das, B.; Venkateswarlu, K.; Krishnaiah, M.; Holla, H. An Efficient, Rapid and Regioselective Nuclear Bromination of Aromatics and Heteroaromatics with NBS Using Sulfonic-acid-Functionalized Silica as a Heterogeneous Recyclable Catalyst. *Tetrahedron Lett.* **2006**, *47*, 8693–8697.
202. Huang, C.; Zhu, K.; Zhang, Y.; Shao, Z.; Wang, D.; Mi, L.; Hou, H. Directed Structural Transformations of Coordination Polymers Supported Single-Site Cu(II) Catalysts To Control the Site Selectivity of C–H Halogenation. *Inorg. Chem.* **2019**, *58*, 12933–12942.
203. Smith, K.; El-Hiti, G. A. Use of Zeolites for Greener and More Para-selective Electrophilic Aromatic Substitution Reactions. *Green Chem.* **2011**, *11*, 1579–1608.
204. Mendon, G. F.; Bastosa, A. R.; Boltz, M.; et al. Electrophilic Chlorination of Arenes With Trichloroisocyanuric Acid Over Acid Zeolites. *Appl. Catal. A* **2013**, *460–461*, 46–51.
205. Hao, Z.; Xu, J.; Huang, J.; Peng, X. Highly Competitive and Selective Electrophilic Catalytic Bromination of Polynitro Stilbenes With Molecular Bromine in the Presence of ZnO/H-beta-25. *Catal. Commun.* **2017**, *91*, 25–29.
206. Pal, P.; Singh, H.; Panda, A. B.; Ghosh, S. C. Heterogeneous Cu-MnO Catalyzed Monoselective Ortho-Halogenation of Aromatic C–H Bonds under Visible Light. *Asian J. Org. Chem.* **2015**, *4*, 879–883.
207. Singh, H.; Sen, C.; Sahoo, T.; Ghosh, S. C. A Visible Light-Mediated Regioselective Halogenation of Anilides and Quinolines by Using a Heterogeneous Cu-MnO Catalyst. *Eur. J. Org. Chem.* **2018**, 4748–4753.
208. Majeed, M. H.; Shayesteh, P.; Tun, P.; Persson, A. R.; Gritcenko, R.; Wallenberg, R. L.; Ye, L.; Hultberg, C.; Schnadt, J.; Wendt, O. F. Directed C–H Halogenation Reactions Catalysed by PdII Supported on Polymers under Batch and Continuous Flow Conditions. *Chem. Eur. J.* **2019**, *25*, 13591–13597.

209. Ono, N. *The Nitro Group in Organic Synthesis*, Wiley-VCH: New York, 2001.
210. Olah, G. A.; Malhotra, R.; Narang, S. C. In *Nitration: Methods and Mechanism*; Feuer, H., Ed.; VCH: New York, 1989.
211. Hoggett, J. G.; Moodie, R. B.; Penton, J. R.; et al. *Nitration and Aromatic Reactivity*, Cambridge University Press: London, 1971.
212. Schofield, K. *Aromatic Nitration*, Cambridge University Press: London, 1980.
213. Smith, K.; El-Hiti, G. A. Use of Zeolites for Greener and More *para*-Selective Electrophilic Aromatic Substitution Reactions. *Green Chem.* **2011**, *13*, 1579–1608.
214. Patel, S. S.; Patel, D. B.; Patel, H. D. Synthetic Protocols for Aromatic Nitration: A Review. *ChemistrySelect* **2021**, *6*, 1337–1356.
215. Kulal, A. B.; Dongare, M. K.; Umbarkar, S. B. Sol-gel Synthesised WO<sub>3</sub> Nanoparticles Supported on Mesoporous Silica for Liquid Phase Nitration of Aromatics. *Appl. Catal. B Environ.* **2016**, *182*, 142–152.
216. Kulala, A. B.; Kasabea, M. M.; Jadhava, P. V.; et al. Hydrophobic WO<sub>3</sub>/SiO<sub>2</sub> Catalyst for the Nitration of Aromatics in Liquid Phase. *Appl. Catal. A* **2019**, *574*, 105–113.
217. Huang, B.; Fan, C.; Yu, H.; Ma, J.; Pan, C.; Zhang, D.; Zheng, A.; Li, Y.; Sun, Y. Sol-gel Preparation of Helical Silicate Containing Palladium Oxidene nanoparticles and the Application for Nitration of Aromatic Compound. *Mol. Catal.* **2018**, *446*, 140–151.
218. Wang, P. C.; Zhu, J.; Liu, X.; Lu, T. T.; Lu, M. Regioselective Nitration of Aromatics with Nanomagnetic Solid Superacid SO<sub>4</sub><sup>2-</sup>/ZrO<sub>2</sub>-M<sub>x</sub>O<sub>y</sub>-Fe<sub>3</sub>O<sub>4</sub> and Its Theoretical Studies. *ChemPlusChem* **2013**, *78*, 310–317.
219. Adamiak, J.; Chmielarek, M. Efficient and Selective Nitration of Xylenes Over MoO<sub>3</sub>/SiO<sub>2</sub> Supported Phosphoric Acid. *J. Ind. Eng. Chem.* **2015**, *27*, 175–181.
220. Rao, D. N.; Rasheed, S.; Raina, G.; Ahmed, Q. N.; Jaladanki, C. K.; Bharatam, P. V.; Das, P. Cobalt-Catalyzed Regioselective Ortho C(sp<sup>2</sup>)-H Bond Nitration of Aromatics through Proton-Coupled Electron Transfer Assistance. *J. Org. Chem.* **2017**, *82*, 7234–7244.
221. Gong, S.; Liu, L.; Zhang, J.; Cui, Q. Stable and Eco-friendly Solid Acids as Alternative to Sulfuric Acid in the Liquid Phase Nitration of Toluene. *Process Saf. Environ. Prot.* **2014**, *92*, 577–582.
222. Yue, C.-J.; Yao, S.-S.; Gu, L.-P. Diatomite-entrapped Hydrosulfate Catalysts for the Efficient Nitration of Toluene With Nitric Acid. *J. Porous. Mater.* **2015**, *22*, 455–464.
223. Wang, P.; Yao, K.; Lu, M. Preparation of Heteropoly Acid Based Amphiphilic Salts Supported by Nano Oxides and Their Catalytic Performance in the Nitration of Aromatics. *RSC Adv.* **2013**, *3*, 2197–2202.
224. Wang, P.-C.; Lu, M. Regioselectivity Nitration of Aromatics With N<sub>2</sub>O<sub>5</sub> in PEG-based Dicationic Ionic Liquid. *Tetrahedron Lett.* **2011**, *52*, 1452–1455.
225. Bharadwaj, S. K.; Boruah, P. K.; Gogoi, P. K. Phosphoric Acid Modified Montmorillonite Clay: A New Heterogeneous Catalyst for Nitration of Arenes. *Catal. Commun.* **2014**, *57*, 124–128.
226. Zhou, S.; You, K.; Gao, H.; Deng, R.; Zhao, F.; Liu, P.; Ai, Q.; Luo, H. Mesoporous Silica-immobilized FeCl<sub>3</sub> as a Highly Efficient and Recyclable Catalyst for the Nitration of Benzene with NO<sub>2</sub> to Nitrobenzene. *Mol. Catal.* **2017**, *433*, 91–99.
227. Dagade, S. P.; Kadam, V. S.; Dongare, M. K. Regioselective Nitration of Phenol Over Solid Acid Catalysts. *Catal. Commun.* **2002**, *3*, 67–70.
228. Heravi, M. M.; Benmorad, T.; Bakhtiari, K.; et al. H<sub>3</sub>+<sub>x</sub>PMO<sub>12-x</sub>V<sub>x</sub>O<sub>40</sub> (Heteropolyacids)-catalyzed Regioselective Nitration of Phenol to *o*-Nitrophenol in Heterogeneous System. *J. Mol. Catal. A-Chem.* **2007**, *264*, 318–321.
229. Esakkidurai, T.; Pitchumani, K. Zeolite-Mediated Regioselective Nitration of Phenol in Solid State. *J. Mol. Catal. A-Chem.* **2002**, *185*, 305–309.

378 Heterogeneous catalysis in sustainable synthesis

230. Mallick, S.; Parida, K. M. Selective Nitration of Phenol Over Silicotungstic Acid Supported Zirconia. *Catal. Commun.* **2007**, *8*, 1487–1492.
231. Sunajadevi, K. R.; Sugunan, S. Sulfated Titania Mediated Regioselective Nitration of Phenol in Solid State. *Catal. Commun.* **2005**, *6*, 611–616.
232. Arshadi, M.; Ghiaci, M.; Gil, A. Nitration of Phenol over a ZSM-5 Zeolite. *Ind. Eng. Chem. Res.* **2010**, *49*, 5504–5510.
233. Sunajadevi, K. R.; Sugunan, S. Selective Nitration of Phenol Over Sulfated Titania Systems Prepared Via Sol–gel Route. *Mater. Lett.* **2006**, *60*, 3813–3817.
234. Khder, A. S.; Ahmed, A. I. Selective Nitration Of Phenol Over Nanosized Tungsten Oxide Supported on Sulfated SnO<sub>2</sub> as a Solid Acid Catalyst. *Appl. Catal. A Gen.* **2009**, *354*, 153–160.
235. Kemdeo, S. M.; Sapkal, V. S.; Chaudhari, G. N. TiO<sub>2</sub>-SiO<sub>2</sub> Mixed Oxide Supported MoO<sub>3</sub> Catalyst: Physicochemical Characterization and Activities in Nitration of Phenol. *J. Mol. Catal. A-Chem.* **2010**, *323*, 70–77.
236. Satish Kumar, M.; Hemanth Sriram, Y.; Venkateswarlu, M.; Rajanna, S. S. M.; Saiprakash, P. V. K. Silica-supported Perchloric Acid and Potassium Bisulfate as Reusable Green Catalysts for Nitration of Aromatics Under Solvent-free Microwave Conditions. *Synth. Commun.* **2017**, *48*, 59–67.
237. Kulala, A. B.; Dongarea, M. K.; Umbarkar, S. B. Sol–gel Synthesised WO<sub>3</sub> Nanoparticles Supported on Mesoporous Silica for Liquid Phase Nitration of Aromatics. *Appl. Catal. B: Env.* **2016**, *182*, 142–152.
238. Gilbert, E. E. *Sulfonation and Related Reactions*, Wiley: New York, 1965; p. 62.
239. Moors, S. L. C.; Deraet, X.; Van Assche, G.; Geerlings, P.; De Proft, F. Aromatic Sulfonation With Sulfur Trioxide: Mechanism and Kinetic Model. *Chem. Sci.* **2017**, *8*, 680–688.
240. Koleva, G.; Galabov, B.; Kong, J.; Schaefer, H. F., III; Schleyer, P. V. R. Electrophilic Aromatic Sulfonation with SO<sub>3</sub>: Concerted or Classic S<sub>E</sub>Ar Mechanism? *J. Am. Chem. Soc.* **2011**, *133*, 19094–19101.
241. Hajipour, A. R.; Mirjalili, B. B. F.; Zarei, A.; Khazdooz, L.; Ruoho, A. E. A Novel Method for Sulfonation of Aromatic Rings With Silica Sulfuric Acid. *Tetrahedron Lett.* **2004**, *45*, 6607–6609.
242. Touheeth, F.; Hemanth Sriram, Y.; Satish Kumar, M.; Marri, V.; Chinna, R. K. Silica-supported HClO<sub>4</sub> and KHSO<sub>4</sub> as Reusable Green Catalysts for Sulfonation of Aromatic Compounds Under Solvent-Free Conditions. *Asian J. Green Chem.* **2017**, *2*, 69–77.
243. Rani, G. S.; Vijay, M.; Prabhavathi Devi, B. L. A. SO<sub>3</sub>Cu-Carbon: A Novel Heterogeneous Catalyst for the Synthesis of β-Hydroxy 1,2,3-Triazoles by One Pot Cycloaddition Reaction. *ChemistrySelect* **2019**, *4*, 10133–10142.
244. Chhabra, T.; Bahuguna, A.; Dhankhar, S. S.; Nagarajab, C. M.; Krishnan, V. Sulfonated Graphitic Carbon Nitride as a Highly Selective and Efficient Heterogeneous Catalyst for the Conversion of Biomass-derived Saccharides to 5-Hydroxymethylfurfural in Green Solvents. *Green Chem.* **2019**, *21*, 6012–6026.

## Chapter 3.6

# Cross-coupling reactions for environmentally benign synthesis

### 3.6.1 Introduction

In this chapter we will focus on coupling reactions that by the assistance of a metal catalyst selectively fuse together two different reaction partners, hence the name cross-coupling reactions. Cross-coupling reactions have been in the focus of attention and have experienced a series of improvements since their first discoveries in 1970s.<sup>1,2</sup> A large array of substrates was explored since these initial reports opened new vistas for the selective transformation of one functional group in the presence of others. As these reactions allow for the selective placement of a C–C bond, they have earned their place as an indispensable tool for the synthesis of organic compounds. These developments have culminated in the 2010 Nobel prize being awarded to Heck,<sup>3</sup> Negishi,<sup>4</sup> and Suzuki<sup>5</sup> for their work on palladium-catalyzed cross-coupling reactions.<sup>6,7</sup>

From the point of view of green chemistry applications, some cross-coupling reactions are more interesting than others. While all benefit from the fact that they are catalytic reactions, the nature of the substrate makes some of the reactions, such as the Stille coupling producing toxic tin waste, less attractive compared to, e.g., the Heck reaction that produces 1 mol of hydrogen halogenide by product. With the recent development toward more and more environmentally benign methods, other aspects of cross-coupling reactions do attract increasing focus of attention. This includes factors such as the choice of the catalyst, the solvent, or the heating method. Traditionally performed cross-coupling reactions use a homogeneous catalyst, mostly a metal complex with palladium as the active metal center. While these catalyst benefit from a relatively easy tuning of the catalytic properties by ligand exchange, they are sensitive and often suffer from catalyst degradation and thus catalyst recovery and recyclability are limited. Heterogeneous catalysts, in contrast, often exhibit enhanced stability and can be more easily separated and recycled although their tunability is often challenging. Another benefit of using solid catalysts is the possibility of applying continuous flow reactor systems that are common in the chemical industry and allow uninterrupted production.

The present chapter focuses exclusively on the application of heterogeneous catalytic systems for cross-coupling reactions and examples that appeal to the concept of green chemistry were selected. Due to the large number of publications in the field an exhaustive summary is not possible, rather selected examples from the last two decades are presented here. More examples for the use of heterogeneous catalysts in cross-coupling chemistry can be found in previously published review and opinion articles.<sup>8-19</sup>

### 3.6.2 The Heck coupling

The Heck or Mizoroki-Heck reaction was among the first cross-coupling reactions being described.<sup>1</sup> The reaction is used to create a bond between an aromatic carbon and the terminal carbon of an alkene using a palladium catalyst. While the traditional Heck coupling applies homogeneous systems with metal complex catalyst, the growing environmental consciousness initiated a push for the development of greener reaction systems. These changes generated more attention toward heterogeneous catalytic processes and in this particular case, the heterogenization of the traditional catalysts to improve stability and promote recyclability.<sup>16, 18, 20</sup> The catalysts used range from relatively simple palladium nanoparticles to more complex systems where palladium ions are tethered to a support such as MCM-41. In addition to the choice of the catalyst, the solvent used plays another important role. Often used solvents such as dimethylformamide (DMF) do not conform with the principles of green chemistry and other, greener alternatives are being considered.<sup>21</sup> Alternatively, research to omit the solvent completely and carry out the reaction under neat or solvent-free conditions has been performed and the results are presented later in the chapter.

#### 3.6.2.1 Heck reactions using a heterogeneous catalyst in solution

When carried out in solvents, the solubility of the substrates can significantly affect the outcome of the reactions. Roberts et al. completed a study on the reactivity of different acrylates for the Heck reaction in water as the solvent.<sup>22</sup> Using a Pd-phosphine-cholate aggregate with a large hydrophobic area as the catalyst the authors found that acrylates with lower water solubility perform better than those with high solubility, probably due to the surfactant effect of the catalyst. Substrates with a lower water solubility are expected to have a higher local concentrations in the vicinity of the catalyst and thus exhibit better reactivity. A variety of substrates with more lipophilic properties were tested and good yields were obtained.

In general, the solvent-based approach is the most common in executing the Heck reactions using a broad group of substrates and catalysts. Relevant selected examples are tabulated in [Table 1](#).

**TABLE 1** Heterogeneous catalytic Heck reactions in solvents.



| Entry | Catalyst   | Additive                        | Conditions                                | Halide (X) | R <sup>2</sup>  | % Yield | Recycl. (times) | Ref.               |
|-------|--|---------------------------------|---|------------|---|---------|-----------------|--------------------|
| 1     | Pd/CuFe <sub>2</sub> O <sub>4</sub>                    | K <sub>2</sub> CO <sub>3</sub>  | DMSO, 120°C                               | I          | CO <sub>2</sub> Me, CO <sub>2</sub> Et, CO <sub>2</sub> tBu, Ph, 4-BrPh | 62–99   | 5               | <a href="#">23</a> |
| 2     | Pd-Ni NPs  | K <sub>2</sub> CO <sub>3</sub>  | H <sub>2</sub> O/EtOH, 120°C, MW          | I, Br, Cl  | CO <sub>2</sub> Et, Ph  | 81–88   | 5               | <a href="#">24</a> |
| 3     | Tetraimine-Pd NPs                                      | K <sub>2</sub> CO <sub>3</sub>  | H <sub>2</sub> O, 90°C                    | I, Br      | CO <sub>2</sub> Bu, Ph  | 84–96   | 8               | <a href="#">25</a> |
| 4     | Pd-imi@MCM-41/Fe <sub>3</sub> O <sub>4</sub>           | Na <sub>2</sub> CO <sub>3</sub> | PEG-400, 120°C                            | I          | CO <sub>2</sub> Me, CO <sub>2</sub> Bu, CN                              | 88–98   | 6               | <a href="#">26</a> |
| 5     | Pd(II)@MCM-41  | NEt <sub>3</sub>                | NMP, 110°C                                | I          | CO <sub>2</sub> Me  | 92      | 6               | <a href="#">27</a> |
| 6     | IRMOF-3-Pd   | NEt <sub>3</sub>                | DMA, 140°C                                | I          | CO <sub>2</sub> Me  | 100     | 3               | <a href="#">28</a> |
| 7     | Pd NPs@NHC@ZIF-8                                       | NEt <sub>3</sub>                | DMF/H <sub>2</sub> O, 110°C               | I, Br, Cl  | CO <sub>2</sub> Me, CO <sub>2</sub> Et, CO <sub>2</sub> Bu, Ph, CN      | 54–95   | 3               | <a href="#">29</a> |
| 8     | PdNP/α-ZrPK  | NEt <sub>3</sub>                | H <sub>2</sub> O/CH <sub>3</sub> CN, 80°C | I          | CO <sub>2</sub> Me, Ph  | 67–98   | 6               | <a href="#">30</a> |
| 9     | TiO <sub>2</sub> @Pd NPs                               | NEt <sub>3</sub>                | DMF, 140°C                                | I, Br      | CO <sub>2</sub> Me, CO <sub>2</sub> Et, CO <sub>2</sub> Bu, Ph          | 56–94   | 5               | <a href="#">31</a> |
| 10    | Fe <sub>3</sub> O <sub>4</sub> @Silica-Threonine-Pd(0) | NEt <sub>3</sub>                | H <sub>2</sub> O, 80°C                    | I, Br      | CO <sub>2</sub> Me, CO <sub>2</sub> Et, CO <sub>2</sub> Bu              | 85–96   | 6               | <a href="#">32</a> |

*Continued*

**TABLE 1** Heterogeneous catalytic Heck reactions in solvents—cont'd

| Entry | Catalyst   | Additive                              | Conditions                   | Halide (X)  | R <sup>2</sup>                                      | % Yield | Recycl. (times) | Ref. |
|-------|--|---------------------------------------|------------------------------|---|---|---------|-----------------|------|
| 11    | Pd@Fe <sub>3</sub> O <sub>4</sub> @PCA- <i>b</i> -PEG      | K <sub>2</sub> CO <sub>3</sub>        | H <sub>2</sub> O, 90°C       | I, Br   | CO <sub>2</sub> H, CO <sub>2</sub> Me               | 85–99   | 10              | 33   |
| 12    | γ-Fe <sub>2</sub> O <sub>3</sub> /AEPH <sub>2</sub> -TC-Pd | K <sub>2</sub> CO <sub>3</sub> , TBAB | H <sub>2</sub> O, 65°C       | I, Br   | CO <sub>2</sub> Me, CO <sub>2</sub> Bu              | 79–98   | 8               | 34   |
| 13    | Pd-phosphinite   | NaOH                                  | H <sub>2</sub> O, 80 or 95°C | I, Br   | CO <sub>2</sub> Bu, Ph                              | 72–90   | 6               | 35   |
| 14    | Biohybrid catalyst   | NEt <sub>3</sub>                      | DMF/H <sub>2</sub> O, 80°C   | I   | CO <sub>2</sub> Et                                  | 99      | 5               | 36   |
| 15    | Pd-NHC-surfactant  | NEt <sub>3</sub>                      | H <sub>2</sub> O, 70°C       | I, Br   | CO <sub>2</sub> Me, Ph                              | 35–91   | –               | 37   |
| 16    | Corn-cellulose-Pd  | NEt <sub>3</sub>                      | DMF or EtOH, 130°C or RT     | I, Br, N <sub>2</sub> <sup>+</sup> BF <sub>4</sub> <sup>-</sup> | CO <sub>2</sub> Me, CO <sub>2</sub> Bu, CONHiPr, Ph | 77–97   | 5               | 38   |
| 17    | Sporopollenin-Pd   | NEt <sub>3</sub>                      | NMP, 100°C                   | I, Br   | CO <sub>2</sub> Me, CO <sub>2</sub> Bu              | 75–99   | –               | 39   |
| 18    | MPCS-TI/Pd   | NEt <sub>3</sub>                      | DMF/H <sub>2</sub> O, 110°C  | Br, Cl  | CO <sub>2</sub> Me, CO <sub>2</sub> Et, Ph, Ph-R    | 69–96   | 6               | 40   |
| 19    | Pd-CS/PVA nanofibers                                       | NEt <sub>3</sub>                      | DMSO, 110°C                  | I   | CO <sub>2</sub> Me, CO <sub>2</sub> Bu, Ph          | 89–98   | 18              | 41   |
| 20    | PNP-SSS  | K <sub>2</sub> CO <sub>3</sub>        | H <sub>2</sub> O, reflux     | I, Br, Cl   | CO <sub>2</sub> Et, CO <sub>2</sub> tBu, Ph, Ph-R   | 55–95   | 5               | 42   |

|    |   |                                 |                                |        |   |            |   |                    |
|----|---|---------------------------------|--------------------------------|--------|---|------------|---|--------------------|
| 21 | PS-PEG-terpyridine Pd                           | DBU                             | H <sub>2</sub> O, reflux       | I, Br  | Ph, Ph-R  | 37–99      | 3 | <a href="#">43</a> |
| 22 | Pd/HNT  | NEt <sub>3</sub>                | EtOH, 100°C                    | I      | CO <sub>2</sub> Bu, Ph, Ph-R  | 58–81      | 4 | <a href="#">44</a> |
| 23 | Pd@rGO  | K <sub>2</sub> CO <sub>3</sub>  | DMF/H <sub>2</sub> O,<br>120°C | I, Br  | CO <sub>2</sub> Me, CO <sub>2</sub> Et, Ph                                  | 89–99      | 5 | <a href="#">45</a> |
| 24 | Pd/salen@MWCNTs                                 | NEt <sub>3</sub>                | DMF, 130°C                     | I, Br  | CO <sub>2</sub> Me, CO <sub>2</sub> Et, CO <sub>2</sub> Bu,<br>Ph, Ph-R, CN | 76–96      | 3 | <a href="#">46</a> |
| 25 | Pd/SiO <sub>2</sub> modified with chlorosilanes | NaOAc                           | NMP, 150°C                     | Br, I  | Ph, CO <sub>2</sub> Me  | 19–<br>100 | 3 | <a href="#">47</a> |
| 26 | Pd/montmorillonite                              | Na <sub>2</sub> CO <sub>3</sub> | 150–160°C,<br>3 h              | Cl, Br | Ph,   | 55–89      | 3 | <a href="#">48</a> |

CS, chitosan; HNT, halloysite nanotubes; MOF, metal-organic framework; NP, nanoparticle; PNP-SSS, palladium nanoparticles on silica-starch substrate; PVA, poly(vinylalcohol); rGO, reduced graphene oxide.

Subrahmanyam et al. designed a catalyst based on Pd/CuFe<sub>2</sub>O<sub>4</sub> hybrid nanowires and used it for the Heck reaction between aryl iodides and styrenes/acrylates in DMSO.<sup>23</sup> Several electron-donating and electron-withdrawing substituents are well tolerated and the products are formed in high yields (Table 1, entry 1). Although the electronic nature of the substituents seems to be less important with regard to the product yield, it was found that substituents in the *ortho* position of the aryl halide dramatically decrease the yield of the transformation. The catalyst could be recycled five times with only a small drop in yield. In an extension of the work, the catalytic system was also used for the formation of dihydrochalcones via the Jeffrey-Heck reaction of phenylvinyl alcohol with iodoarenes.

Using a related catalyst system, the group of Chaudhary was able to perform the Heck reaction in a water-ethanol mixture.<sup>24</sup> The authors generated well-defined Pd-Ni alloy nanoparticles using a surfactant methodology. High product yields were obtained for the coupling of styrene or ethyl acrylate with haloarenes. Iodo-, bromo-, and chloroarenes were suitable substrates and substituents with varying electronic nature were tolerated (Table 1, entry 2). In addition to the use of a green solvent mixture and the recyclability of the catalyst (five times), the use of microwave heating and short reaction times also helps to reduce the energy consumption of the reaction.

Asadi and coworkers used palladium nanoparticles with tetraimine ligand system for the Heck reaction.<sup>25</sup> The variety of aryl iodides and aryl bromides was coupled with either butyl acrylate or styrene using water as the solvent. The yield for the reaction was high for all examples shown and neither the electronic nature nor the position of the substituent resulted in significant variations in the product yield (Table 1, entry 3). The product yield appears stable when the catalyst is recycled; the authors showed that a notable amount of palladium leaches into the reaction mixture after several reuses of the catalyst.

Acrylonitrile, methyl and butyl acrylate were successfully coupled with aryl iodides in the presence of a Pd-imidazole complex supported on magnetic MCM-41 (Pd-imi@MCM-41/Fe<sub>3</sub>O<sub>4</sub>).<sup>26</sup> PEG-400 was used as the solvent and the catalyst could be recycled six times with only a slight decrease in yield (Table 1, entry 4). Unfortunately, only substrates bearing electron-donating substituents were reported by the authors.

Fan and coworkers showed that the Heck reaction between iodobenzene and methyl acrylate can be catalyzed using PdCl<sub>2</sub> immobilized on functionalized MCM-41.<sup>27</sup> The reaction is performed in NMP as solvent using NEt<sub>3</sub> as the base (Table 1, entry 5). Even though no other substrate examples were reported for this catalyst and NMP is not considered a green solvent, the system benefits from a high catalyst stability with no significant loss in catalytic activity and no significant Pd leaching observed. A similar report also used NMP as a solvent, with organically derivatized silica-supported Pd catalyst (Table 1, entry 25), confirming that although NMP is not a green solvent, it does not promote the leaching

of Pd into the solution. Later, the same group reported the extensive characterization of the catalysts, and found that the introduced surface functional groups significantly affected the catalytic activity.<sup>49</sup> Another related report described the preparation and application of ligand-free MCM-41-supported Pd catalysts in the Heck reaction. Unlike the above-mentioned MCM-supported sample, these catalysts had a broad substrate scope, including deactivated aryl bromides. As additional benefits, the catalysts gave high yields and selectivities; showed unprecedented stability under regular conditions (air, moisture) and could be recycled 20 times with stable activity and selectivity, without applying any reactivation treatment.<sup>50</sup> The same group extended these studies to silica-immobilized Pd nanoparticle-based catalyst as well that were deposited in the presence of an ionic liquid. The catalyst gave mostly excellent yields and selectivity.<sup>51</sup>

Murzin et al. used IRMOF-3 to stabilize palladium nanoparticles (IRMOF-3-Pd) and showed its applicability by performing the coupling of iodobenzene and methyl acrylate.<sup>28</sup> The reaction had to be performed in dimethylacetamide (DMA) as the solvent and high reaction temperatures were required (Table 1, entry 6). Although the base reaction delivers the product in quantitative yield and the catalyst could be recycled for three times without losing its activity, the scope of the presented method is drastically limited by the fact that no other substrates were tested.

A more widely applicable system was developed by the group of Azad et al.<sup>29</sup> The authors used palladium nanoparticles stabilized in a zeolitic imidazolate framework (Pd NPs@NHC@ZIF-8) for the Heck coupling between various aryl halides and acrylates as well as styrene in a DMF/H<sub>2</sub>O solvent mixture (Table 1, entry 7). The array of substituents contains electron-withdrawing and electron-donating groups for the aryl halide. Although the electronic nature of the substituents only plays a minor role in determining the product yield, it was found that aryl chlorides require substantially longer reaction times and deliver lower yields than iodides or bromides.

Vaccaro et al. used a new catalyst based on palladium nanoparticles deposited on layered potassium  $\alpha$ -zirconium phosphate (PdNP/ $\alpha$ -ZrPK) for the Heck reaction.<sup>30</sup> Different aryl iodides with electron-donating and electron-withdrawing substituents are efficiently coupled to methyl acrylate or styrene in high yields (Table 1, entry 8). The reaction uses a H<sub>2</sub>O/CH<sub>3</sub>CN solvent system and was operated under flow conditions allowing for an easy catalyst recycling (six times without loss of activity).

A conceptionally more simple catalyst prepared from TiO<sub>2</sub>@Pd nanoparticles was employed for the Heck coupling as well.<sup>31</sup> No ligand for the palladium was needed when aryl iodides and aryl bromides were reacted with styrene and different acrylates (Table 1, entry 9). The products are mostly obtained in high yields and the catalyst could be recycled five times while maintaining its activity. Unfortunately DMF had to be used, and thus the solvent increases the environmental impact of the reaction.

A magnetically separable  $\text{Fe}_3\text{O}_4$ @Silica-Threonine-Pd(0) nanoparticle-based catalyst was also found to be effective in the Heck reaction.<sup>32</sup> A variety of substituted aryl iodides and bromides are easily coupled with different acrylates using water as the solvent (Table 1, entry 10). While there was little difference in the use of bromide vs iodide derivatives, the authors showed that chlorides react poorly under the employed conditions. The products are obtained in high to excellent yields in all cases. Recycling experiments showed that a notable drop in yield is observed after the sixth reuse of the catalyst.

A new magnetite-based semiheterogeneous catalyst was developed for the Mizoroki-Heck reaction. The  $\text{Fe}_3\text{O}_4$  nanoparticles were modified with a poly(ethylene glycol)-*block*-poly(citric acid) copolymer which could incorporate and stabilize the palladium nanoparticles and also served to solubilize the particles in a variety of solvents.<sup>33</sup> The heterogeneous aspect is generated by the magnetic properties of the core material, allowing for an easy separation by application of an external magnetic field. Aryl halides with a variety of electron-withdrawing and electron-donating substituents were reacted with methyl acrylate or acrylic acid in water as solvent (Table 1, entry 11). The products were obtained in high to excellent yields in the case of iodides and bromides; it was found that when chlorides were used only low product yields were obtained. Recycling of the catalyst could be easily achieved 10 times with only a slight loss in activity.

A similar magnetic nanoparticle-based catalyst was developed by using  $\text{Fe}_2\text{O}_3$ . A thiophene methanimine Schiff base was tethered to the particle and used to complex a palladium ion and form the active catalyst ( $\gamma\text{-Fe}_2\text{O}_3/\text{AEPH}_2\text{-TC-Pd}$ ).<sup>34</sup> A variety of aryl iodides and bromides with substituents of different electronic nature were coupled with methyl and butyl acrylate in water as the solvent (Table 1, entry 12). The products were obtained in high yields and the catalyst could be recycled eight times with only a slight loss in activity. Unfortunately the use of chlorides gave significantly lower yields and required much longer reaction time. More importantly, a phase transfer agent had to be used, thus increasing the environmental impact of the reaction.

A heterogeneous catalyst was formed by Firouzabadi et al. through the reaction of  $\text{Pd}(\text{OAc})_2$  with a phosphinite ligand in water.<sup>35</sup> The obtained black material was able to facilitate the coupling of aryl halides with butyl acrylate and styrene in good yields in water as the solvent (Table 1, entry 13). The authors could demonstrate that iodides, bromides, and chlorides can be used as substrates but the latter ones usually only give low yield. The catalyst was recycled six times with only a minimal decrease in product yield.

Palomo et al. designed a catalyst based on palladium nanoparticles incorporated in semisynthetic lipase.<sup>36</sup> This biohybrid catalyst was tested for its activity by performing the Heck coupling of iodobenzene and ethyl acrylate (Table 1, entry 14). The reaction was carried out in a DMF/ $\text{H}_2\text{O}$  mixture at a moderate temperature ( $65^\circ\text{C}$ ). Although the reaction could be performed with various DMF-water ratios, it was found that 10% water gives the best yield. Recycling of the catalyst was possible five times with only a slight loss in yield.

A surface-active Pd-NHC complex was used as catalyst by Taira et al. as a catalyst for the Heck reaction.<sup>37</sup> The unusual combination of substituents for the NHC complex was chosen to ensure high solubility of the organic substrates in water. Aryl iodides with different substituents were successfully coupled to styrene and methyl acrylate in good yields (Table 1, entry 15). The use of other halides proved to be less successful. While bromides could be converted (albeit with a dramatically decreased yield), no reaction was observed when aryl chlorides were employed. A drawback of the reaction is the decomposition of the catalyst during the reaction; it was not possible to recycle the catalytic system. A similar complex has been immobilized on silica support as well, providing comparable characteristics.<sup>52</sup>

Cellulose, derived from corn-cob biowaste, was used as support for a poly(hydroxamic acid) palladium complex to generate an efficient catalyst for the Heck and Heck-Matsuda reaction.<sup>38</sup> Aryl iodides and bromides were efficiently coupled with different acrylates or styrene using DMF as the solvent (Table 1, entry 16). The catalyst can be recycled five times before a notable drop in yield is observed. The catalyst system is also suitable for the Heck-Matsuda reaction of diazonium tetrafluoroborates using ethanol as solvent. Both systems tolerate electron-withdrawing and electron-donating substituents on the haloarene reaction partner.

A different natural support was used by Keles. Sporopollenin was functionalized with a Schiff base that served to complex and heterogenize Pd(II) ions.<sup>39</sup> The obtained catalytic system was effective for the coupling of iodo- and bromobenzene and bromotoluene with methyl/butyl acrylate (Table 1, entry 17). The disadvantage of the system is that NMP was used as the solvent and the catalyst showed poor recyclability (15%–20% drop in yield after first run).

Movassagh and Rezaei were able to generate a catalyst from another natural polysaccharide chitosan. A functionalized chitosan system was tethered to an iron oxide core to allow for the catalyst to be magnetically recoverable (MPCS-TI/Pd).<sup>40</sup> Different substituted styrenes and acrylates were coupled with substituted bromo- and chloroarenes in a DMF-water mixture (Table 1, entry 18). The products were obtained with high yield in the case of bromides; chlorides gave somewhat lower yields. Recycling of the catalyst was possible six times with only a slight drop in yield.

A similar support material was used by Shao et al. who embedded palladium nanoparticles into chitosan/poly(vinyl alcohol) composite nanofibers (Pd-CS/PVA nanofibers).<sup>41</sup> The Heck reaction between aryl iodides and acrylates/styrene was catalyzed in DMSO as the solvent to yield the products in excellent yields (Table 1, entry 19). Although the use of DMSO is not desirable from an environmental point of view, it is balanced by the fact that the catalyst could be recycled a remarkable amount of 18 times without losing its activity.

A silica starch composite material also proved to be a suitable substrate for the immobilization of Pd nanoparticles (PNP-SSS) as shown by Khalafi-Nezhad and Panahi.<sup>42</sup> The catalyst was used for the coupling of aryl halides and various acrylates/styrenes in

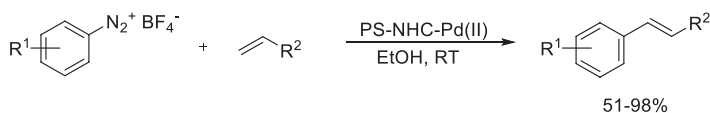
water (Table 1, entry 20). It was found that aryl bromides and iodides work significantly better than the corresponding chlorides. Electron-donating and electron-withdrawing substituents performed similar when placed on the aryl halide. Catalyst recycling was not shown for the Heck reaction but the catalyst could be recycled five times when used in the Sonogashira coupling (*vide infra*).

Styrenes have been coupled with aryl iodides and bromides under Heck conditions using a polymer-supported palladium complex (PS-PEG-terpyridine Pd).<sup>43</sup> While there is little difference with respect to the nature of the substituent, it was found that bromides do not give as high yields as those observed for iodides (Table 1, entry 21). Catalyst recycling was tested in three runs and no loss in activity was observed.

Using aryl dihalides as substrates the synthesis of *p*-phenylenevinylene oligomers was achieved via the Heck reaction.<sup>44</sup> The catalyst used consists of palladium immobilized on halloysite nanotubes (Pd/HNT) and ethanol was used as the solvent (Table 1, entry 22). The yields obtained varied depending on the substrate, but usually surpassed previously known synthetic methods to prepare the compounds. Recycling of the catalyst was possible in four consecutive runs with only a slight decrease in yield.

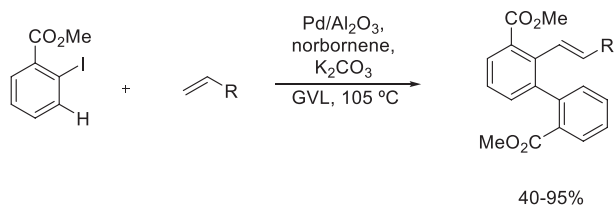
Palladium nanoclusters were deposited on reduced graphene oxide nanosheets to obtain a catalytic system for the Heck reaction.<sup>45</sup> The system proved to be highly efficient for the coupling of aryl iodides and bromides with styrene and acrylates in a DMF-water mixture as the solvent (Table 1, entry 23). Both substrates with electron-withdrawing or electron-donating substituents gave the desired product in excellent yield. The authors could recycle the catalyst five times with only a slight decrease in yield.

Movassagh and coworkers used multiwalled carbon nanotubes as support to anchor a palladium-salen complex (Pd/salen@MWCNTs) and applied this system to the reaction of aryl halides with styrenes or acrylates.<sup>46</sup> While a variety of aryl iodides and bromides with substituents of varying electronic nature form the products in high yields, the use of aryl chlorides only gave low conversions (Table 1, entry 24). Although it was necessary to use DMF as the solvent, the system benefits from a relatively wide range of alkene substrates that were tested and gave the products in high yield. The same group also worked on the development of another heterogeneous catalyst for the Heck-Matsuda reaction.<sup>53</sup> Anchoring a NHC-palladium complex on polystyrene resin allowed the transformation of arenediazonium salts with acrylates and styrenes to form the corresponding coupling product (Scheme 1). Ethanol was used as the solvent and the catalyst was recyclable for six times before a notable drop in yield was observed.



**SCHEME 1** A Pd/PS-NHC-catalyzed Heck reaction of diazonium salts with alkenes.

Vaccaro's group used the simple Pd/Al<sub>2</sub>O<sub>3</sub> as catalyst for the Heck-terminated Catellani reaction of 2-iodomethyl benzoate and several different alkenes.<sup>54</sup> The reaction yield is highly dependent on the alkene used with methyl acrylate working especially well, while acrylonitrile, for example, gives a low yield (Scheme 2). The biomass derived and sustainable  $\gamma$ -valerolactone (GVL) was chosen as green solvent for the reaction.

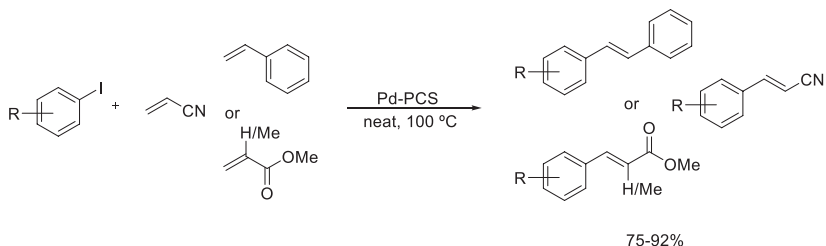


**SCHEME 2** The Heck-terminated Catellani reaction of 2-iodomethyl benzoate and several different alkenes catalyzed by Pd/Al<sub>2</sub>O<sub>3</sub>.

### 3.6.2.2 Solvent-free Heck reactions

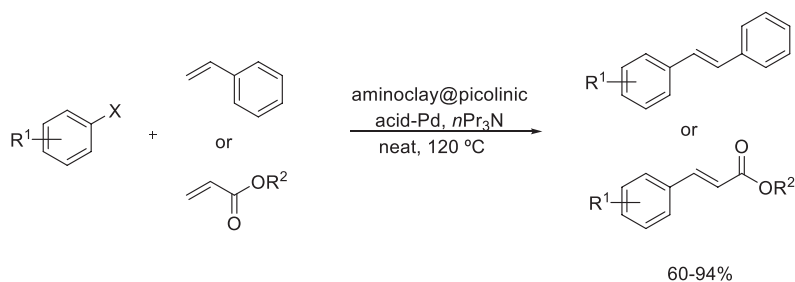
While most Heck reactions require the use of a solvent to be effective, there are also a number of examples that show that a solvent is not absolutely necessary. Reactions that do not require solvent are considered green even if solvent is used for product isolation. Avoiding the use of flammable solvents during a heated reaction creates less hazard for the systems and operators. In addition, the solvent-free feature results in another potential benefit, particularly in heterogeneous catalysis; when, due to the lack of solvent, the substrates are concentrated on the surface of the catalyst, the higher concentration commonly brings about higher reaction rates.

The use of an inorganic support material for palladium ions as catalyst in the solvent-free Heck reaction was developed by Mangala et al.<sup>55</sup> Pd(OAc)<sub>2</sub> was successfully immobilized on polycarbosilane (Pd-PCS) and used for the reaction between several iodoarenes and acrylonitrile, styrene, or methyl acrylate and methacrylate as the reaction partners. The corresponding products were obtained in good to high yields (Scheme 3) and the catalyst was found to be recyclable three times with negligible drop in product yield.



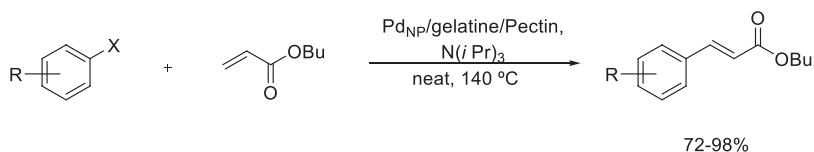
**SCHEME 3** A solvent-free Heck coupling catalyzed by polycarbosilane (Pd-PCS)-immobilized Pd(OAc)<sub>2</sub>.

Fahimi and Sardarian developed an aminoclay decorated with palladium nanoparticles stabilized by picolinic acid as efficient catalyst for the solvent-free Heck reaction.<sup>56</sup> A variety of iodo- and bromoarenes were coupled to different acrylates and styrene. Yields were high in most examples, independent of the nature of the substituents and the halide used (Scheme 4). While the product yield for different aryl halides was not substantially different, it was found that bromides and chlorides require a vastly extended reaction time compared to iodides. The catalyst could be recycled seven times before a notable loss in activity was observed after the 8th run.



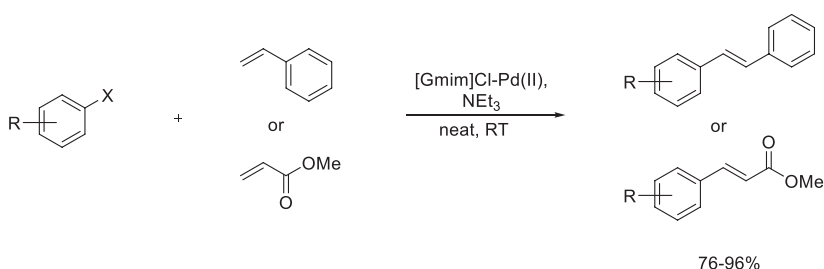
**SCHEME 4** The aminoclay immobilized, picolinic acid stabilized palladium nanoparticles catalyzed solvent-free Heck coupling.

A support material for palladium nanoparticles based on renewable resources was developed by Khazaei et al.<sup>57</sup> A mixture of dissolved gelatin and pectin was treated with  $\text{PdCl}_2$  to form the desired Pd nanoparticles and the final catalyst ( $\text{Pd}_{\text{NP}}/\text{gelatin}/\text{pectin}$ ) was obtained after drying of the material. The Heck reaction between aryl halides (I, Br) with electron-donating and electron-withdrawing substituents and butyl acrylate under solvent-free conditions gave the desired products in high yields (Scheme 5). Recycling of the catalyst was possible three times before a notable drop in yield was observed. The same group later showed that a mixture of gum Arabic and pectin can also act as a support material for Pd nanoparticles and the obtained catalysts exhibited similar performance to the earlier sample in the Mizoroki-Heck reaction under nearly identical conditions.<sup>58</sup>



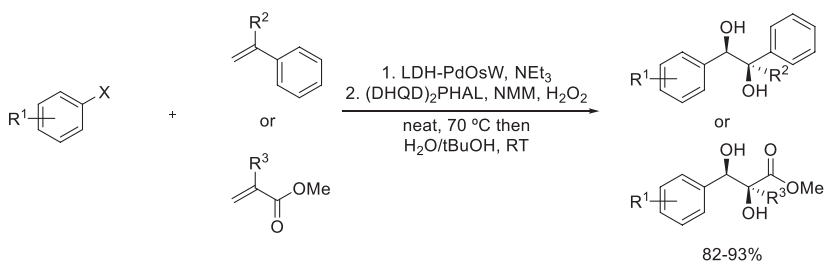
**SCHEME 5** A solvent-free Mizoroki-Heck reaction catalyzed by Pd nanoparticles supported on gelatin/pectin mixture.

Karthikeyan et al. utilized an interesting method to combine the features of heterogeneous and homogeneous catalysis. Complexation of an amino acid-ionic liquid hybrid molecule with Pd(II) generated a catalyst that was soluble in the reaction mixture but not in the solvent used for extraction and could thus be easily separated after the reaction was complete.<sup>59</sup> Using this complex the authors were able to couple aryl bromides and chlorides with alkenes such as styrene and methyl acrylate (Scheme 6). Substituents on the aryl halide substrate included both electron-donating and electron-withdrawing groups. A slight decrease in yield was observed when comparing aryl chlorides with the corresponding bromides. The catalyst could be reused seven times before a notable drop in yield did occur.



**SCHEME 6** A combined heterogeneous-homogeneous solvent-free Heck reaction of aryl bromides and chlorides with styrene and methyl acrylate.

Choudary and coworkers used a layered double hydroxides (LDH)-based material as support for palladium as well as osmium- and tungsten oxides to form a trifunctional catalyst.<sup>60</sup> This catalyst (LDH-PdOsW) could be used for the one-pot tandem Heck—N-oxidation-asymmetric dihydroxylation reaction (Scheme 7). The Heck reaction was performed with aryl iodides and bromides as one reaction partner and  $\alpha$ -substituted styrenes and acrylates as second reagent. Following the coupling reaction the dihydroxylation is performed using the same catalyst after addition of the oxidizing agent. The products were obtained in high yields for the two-step procedure and the catalyst could be recycled five times with only a slight decrease in yield.

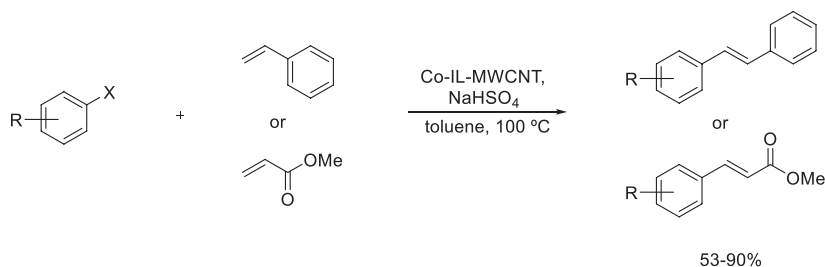


**SCHEME 7** A multistep one-pot tandem Heck coupling-N-oxidation-asymmetric dihydroxylation reaction catalyzed by layered double hydroxide (LDH)-based Pd-Os-oxide-W-oxide catalyst.

### 3.6.2.3 Heck reactions without palladium

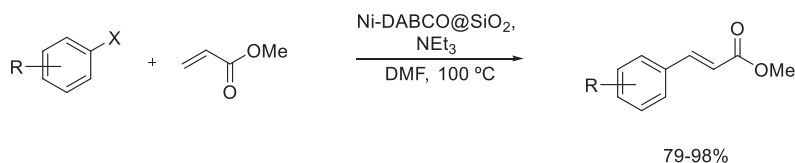
With palladium being the most commonly used catalytic metal in Heck coupling reactions, there are only a few examples employing other metal centers for this transformation. While the applications are scarce, this is an important new direction as it may provide more economic alternatives to the quite expensive Pd-based catalysts.

Hajipour et al. used cobalt nanoparticles on ionic liquid functionalized multi-wall carbon nanotubes (Co-IL-MWCNT) as catalyst for the Heck reaction between aryl halides and acrylates or styrenes.<sup>61</sup> Both iodo- and bromoarenes were suitable substrates for the transformation with the former delivering the product in much better yields (Scheme 8). It was found that substrates with electron-withdrawing substituents, in general, performed better than electron-donating ones. Although the catalyst could be recycled four times, a drawback of the proposed system is the need for toluene as solvent and high reaction temperatures.



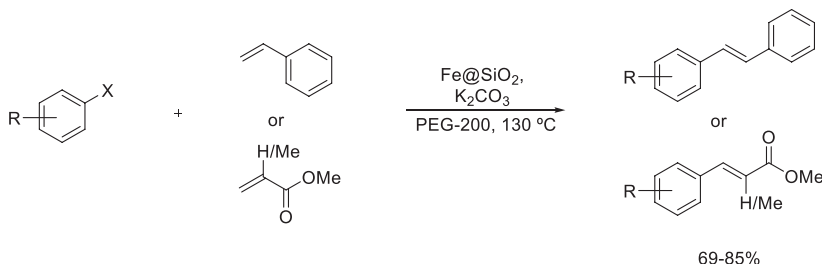
**SCHEME 8** The Heck coupling of haloarenes with acrylates or styrene catalyzed by immobilized Co nanoparticles.

The same group also published the use of a nickel-based catalyst for the Heck reaction.<sup>62</sup> A nickel DABCO complex was anchored to the surface of silica gel particles (Ni-DABCO@SiO<sub>2</sub>) to form the active catalyst which is able to catalyze the coupling of aryl halides with methyl acrylate in DMF (Scheme 9). No difference in yield was observed for aryl halides with electron-donating or electron-withdrawing substituents. When comparing the nature of the halide atom, the authors found that chlorides gave slightly lower yields compared to bromides and iodides. The catalyst could be reused three times before a notable drop in yield occurred.



**SCHEME 9** The Heck coupling of haloarenes with methyl acrylate catalyzed by a silica-immobilized Ni-DABCO complex.

In a further extension of their work toward a more sustainable system, Hajipour and coworkers showed that iron(III) immobilized on SiO<sub>2</sub> (Fe@SiO<sub>2</sub>) can act as an efficient catalyst for the Heck reaction.<sup>63</sup> Aryl iodides were coupled to styrene and methyl acrylates in good yields using PEG-200 as environmentally benign solvent (Scheme 10). Substrates with electron-donating and electron-withdrawing substituents gave nearly identical yields and the catalyst could be recycled five times before a minor drop in yield was observed.



**SCHEME 10** The Heck coupling of aryl iodides with acrylates or styrene catalyzed by a silica-immobilized Fe in poly(ethylene glycol).

### 3.6.3 The Suzuki coupling

The Suzuki or Suzuki-Miyaura coupling is another prominent example of palladium-catalyzed cross-coupling reactions. In general, it involves the coupling of arylboronic acids with aryl halides to provide biaryl systems. Its prominence and importance is manifested by the award of the Nobel prize in 2010 for cross-coupling reactions.<sup>6</sup> Early work on the reaction applied homogeneous palladium(0) catalysts for this transformation in mostly organic solvents. Although the developments achieved using homogeneous systems allow for the product formation from the less reactive chloride precursors, this still remains challenging in heterogeneous systems. With regard to the solvent choice an increasing number of publications investigate the use of environmentally friendly solvents such as water using heterogeneous systems. The work in this field has previously been reviewed.<sup>64, 65</sup>

This section focuses on the application of heterogeneous catalysts in the Suzuki coupling for the formation of biaryl compounds as part of the exciting new developments made in this field.

#### 3.6.3.1 Palladium-catalyzed heterogeneous Suzuki coupling reactions

The following section summarizes Suzuki coupling reactions that, following the original procedure, use palladium as the catalyst. Examples were chosen with regard to environmental considerations and the application of green chemistry

principles. Examples using catalysts that apply metals other than palladium will be treated in a separate section later in this chapter.

Wei et al. synthesized a heterogeneous palladium organosilane complex using an aerosol-based method and used it in different transformations, including the Suzuki coupling.<sup>66</sup> The catalyst (PdDPP-SHCs-HP-2) consists of nanoparticles mainly made of an organosilane using benzene linkers to bridge the silane units and is decorated with phosphine pincers complexing a Pd(II) center. *Para*-methylbenzylboronic acid and different iodoarenes were coupled in high yields in water as solvent at 50°C (Table 2 entry 1). When other haloarenes were used, lower yields were obtained, somewhat limiting the utility of the reaction. The catalytic system was shown to be recyclable up to nine times when applied to the Tsuji-Trost reaction (vide infra).

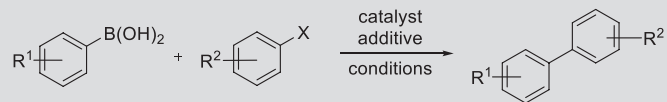
Ghorbani-Choghamarani et al. used the catalyst they developed for the Heck reaction (vide supra), a Pd complex supported on magnetic MCM-41 (Pd-imi@MCM-41/Fe<sub>3</sub>O<sub>4</sub>) also as catalyst for the Suzuki coupling of a variety of aryl halides and phenylboronic acids.<sup>26</sup> PEG-400 was used as the solvent for the reaction and high yields were obtained with substrates possessing both electron-donating and electron-withdrawing substituents on the halide reagent (Table 2 entry 2). On the boronic acid reagent, only phenyl and 3,4-difluorophenyl was used. The catalyst could be reused up to seven times with only a slight loss in reactivity.

The same group also developed a magnetically recoverable catalyst based on Fe<sub>3</sub>O<sub>4</sub>-serine as a support for palladium nanoparticles (Pd-Fe<sub>3</sub>O<sub>4</sub>-Serine-Pd(0)). Different iodo-, bromo-, and chloro-arylhalides were successfully coupled with phenylboronic acid in PEG as the reaction medium (Table 2 entry 3).<sup>67</sup> High yields were obtained for substrates having both electron-withdrawing and electron-donating substituents on the aryl halide. Although the yield increases from the chloride to the iodide, the difference is not significant.

Jahanshahi and Akhlaghinia showed that the anchored thiophene methanimine-palladium Schiff base ( $\gamma$ -Fe<sub>2</sub>O<sub>3</sub>/AEPH<sub>2</sub>-TC-Pd) can also be used for the Suzuki-Miyaura coupling between different aryl iodides/bromides and two phenyl boronic acids (Table 2 entry 4).<sup>34</sup> The reaction is performed in water as the reaction medium applying a phase transfer reagent to enable the transformation. The catalyst could be recovered magnetically and reused eight times with only a slight loss in activity. The authors also investigated the use of aryl chlorides as substrates but noted a dramatic drop in product yield.

Gholinejad and his group developed a heterogeneous catalyst based on a modified polyacrylamide as support for Pd nanoparticles (PAA-Pd-NP).<sup>68</sup> The Suzuki reaction between different (hetero)aryl iodides, bromides, chlorides, and several phenyl boronic acids was effectively catalyzed in water as the solvent (Table 2 entry 5). Even though it was possible to use aryl chlorides as the substrate, the yield was about 20% lower compared to bromides and iodides. The catalyst could be recycled four times before a drop in yield was observed.

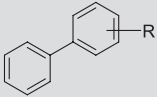
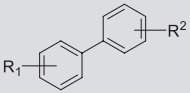
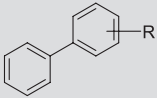
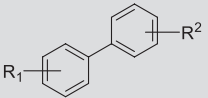
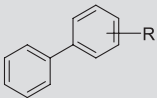
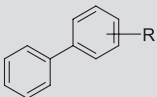
**TABLE 2** Representative examples of the Suzuki reaction using palladium-based heterogeneous catalysts.

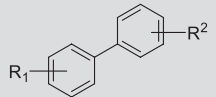
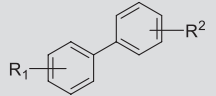
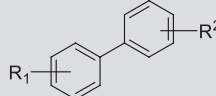
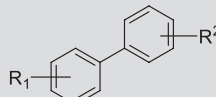
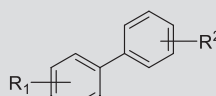
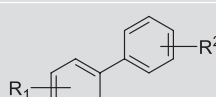


| Entry | Catalyst  | Additive                              | Conditions             | Halide    | Product | Yield (%) | Recycl. (times) | Ref.               |
|-------|---|---------------------------------------|------------------------|-----------|---------|-----------|-----------------|--------------------|
| 1     | PdDPP-SHCs-HP-2                                 | K <sub>2</sub> CO <sub>3</sub>        | H <sub>2</sub> O, 50°C | I         |         | 86–98     | 9               | <a href="#">66</a> |
| 2     | Pd-imi@MCM-41/Fe <sub>3</sub> O <sub>4</sub>    | Na <sub>2</sub> CO <sub>3</sub>       | PEG-400, 80°C          | I, Br, Cl |         | 63–98     | 7               | <a href="#">26</a> |
| 3     | Pd-Fe <sub>3</sub> O <sub>4</sub> -Serine-Pd(0) | Na <sub>2</sub> CO <sub>3</sub>       | PEG, 110°C             | I, Br, Cl |         | 70–100    | 3               | <a href="#">67</a> |
| 4     | γ-Fe <sub>2</sub> O <sub>3</sub> /AEPH2-TC-Pd   | K <sub>2</sub> CO <sub>3</sub> , TBAB | H <sub>2</sub> O, 40°C | I, Br     |         | 80–98     | 8               | <a href="#">34</a> |
| 5     | PAA-Pd-NP                                       | <i>t</i> BuOK                         | H <sub>2</sub> O, 25°C | I, Br, Cl |         | 71–99     | 4               | <a href="#">68</a> |

*Continued*

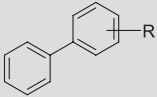
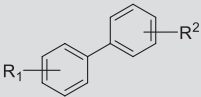
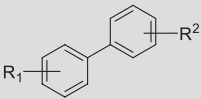
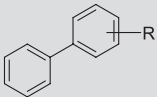
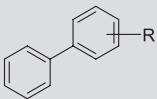
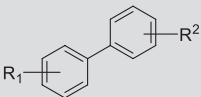
**TABLE 2** Representative examples of the Suzuki reaction using palladium-based heterogeneous catalysts—cont'd

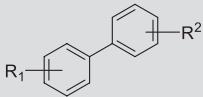
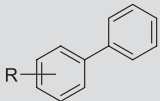
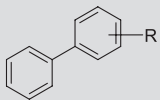
| Entry | Catalyst   | Additive                        | Conditions                  | Halide    | Product  | Yield (%) | Recycl. (times) | Ref. |
|-------|--|---------------------------------|-----------------------------|-----------|--|-----------|-----------------|------|
| 6     | Fe <sub>3</sub> O <sub>4</sub> @-NH <sub>2</sub> @ Murexide@Pd | K <sub>2</sub> CO <sub>3</sub>  | H <sub>2</sub> O/EtOH, 60°C | I, Br, Cl |  | 60–100    | 3               | 69   |
| 7     | Fe <sub>3</sub> O <sub>4</sub> @SiO <sub>2</sub> -Pd           | CaO                             | H <sub>2</sub> O/EtOH, 85°C | I, Br     |  | 85–96     | 5               | 70   |
| 8     | Pd-γ-Fe <sub>2</sub> O <sub>3</sub> -2-ATP-TEG-MME             | NEt <sub>3</sub>                | H <sub>2</sub> O, 80°C      | I, Br, Cl |  | 80–98     | 9               | 71   |
| 9     | PS-Pd-salen  | K <sub>2</sub> CO <sub>3</sub>  | H <sub>2</sub> O, RT        | I, Br     |  | 60–89     | 4               | 72   |
| 10    | Poly(AAm-AMPs) NHC-Pd  | K <sub>2</sub> CO <sub>3</sub>  | H <sub>2</sub> O, 60°C      | Br        |  | 91–99     | 5               | 73   |
| 11    | CelFemImiNHC@Pd  | Cs <sub>2</sub> CO <sub>3</sub> | EtOH, RT                    | I, Br     |  | 73–87     | 5               | 74   |

|    |   |                                |                                    |           |  |        |   |    |
|----|---|--------------------------------|------------------------------------|-----------|--|--------|---|----|
| 12 | MNP@SPGMA@<br>AP@Pd                     | K <sub>2</sub> CO <sub>3</sub> | H <sub>2</sub> O/DMF,<br>70°C      | I, Br, Cl |  | 48–99  | 7 | 75 |
| 13 | APPd(0)@Si                              | K <sub>2</sub> CO <sub>3</sub> | H <sub>2</sub> O, 80°C             | Br        |  | 43–100 | 8 | 76 |
| 14 | PdNP-NMe <sub>2</sub> @SiO <sub>2</sub> | K <sub>2</sub> CO <sub>3</sub> | H <sub>2</sub> O,<br>50–90°C       | Br, Cl    |  | 52–98  | 3 | 77 |
| 15 | Pd/ZnO                                  | K <sub>2</sub> CO <sub>3</sub> | H <sub>2</sub> O, 100°C            | I, Br, Cl |  | 84–96  | 7 | 78 |
| 16 | IRMOF-3-BI-Pd                           | K <sub>2</sub> CO <sub>3</sub> | H <sub>2</sub> O/EtOH,<br>RT       | I, Br, Cl |  | 92–98  | 5 | 79 |
| 17 | PdNPs@NHC@<br>ZIF-8                     | NEt <sub>3</sub>               | H <sub>2</sub> O/EtOH,<br>90–120°C | I, Br, Cl |  | 54–99  | – | 80 |

*Continued*

**TABLE 2** Representative examples of the Suzuki reaction using palladium-based heterogeneous catalysts—cont'd

| Entry | Catalyst               | Additive                       | Conditions                     | Halide    | Product  | Yield (%) | Recycl. (times) | Ref.               |
|-------|------------------------|--------------------------------|--------------------------------|-----------|--|-----------|-----------------|--------------------|
| 18    | LDH/Tris/Pd            | K <sub>2</sub> CO <sub>3</sub> | H <sub>2</sub> O/EtOH, RT      | I, Br, Cl |  | 60–98     | 3               | <a href="#">81</a> |
| 19    | PCIL-1                 | K <sub>2</sub> CO <sub>3</sub> | H <sub>2</sub> O/iPrOH, RT     | I, Br     |  | 70–98     | 5               | <a href="#">82</a> |
| 20    | Pd <sup>0</sup> -Mont. | K <sub>2</sub> CO <sub>3</sub> | H <sub>2</sub> O, 60°C         | I, Br, Cl |  | 80–94     | 3               | <a href="#">83</a> |
| 21    | MNPs@SB-Pd             | K <sub>2</sub> CO <sub>3</sub> | H <sub>2</sub> O/EtOH, RT      | Br        |  | 61–88     | 6               | <a href="#">84</a> |
| 22    | GO-Met-Pd              | K <sub>2</sub> CO <sub>3</sub> | H <sub>2</sub> O/EtOH, 60°C    | I, Br     |  | 85–98     | 9               | <a href="#">85</a> |
| 23    | GONS-NHC-Pd            | K <sub>2</sub> CO <sub>3</sub> | H <sub>2</sub> O/EtOH, RT-50°C | Br, Cl    |  | 83–99     | 10              | <a href="#">86</a> |

|    |                            |                                |                        |        |  |       |    |    |
|----|----------------------------|--------------------------------|------------------------|--------|--|-------|----|----|
| 24 | Pd(0)-PzC                  | KOH, TBAB                      | H <sub>2</sub> O, 90°C | Br     |  | 84–98 | 3  | 87 |
| 25 | Pd@MCM-Calix <sub>ox</sub> | K <sub>2</sub> CO <sub>3</sub> | H <sub>2</sub> O, 80°C | I      |  | 85–99 | 5  | 88 |
| 26 | Pd/CoO-C                   | K <sub>2</sub> CO <sub>3</sub> | H <sub>2</sub> O, 80°C | Br, Cl |  | 19–97 | 10 | 89 |

AAm-AMPs, acrylamide-aminomethylphenol; ATP-TEG-MME, aminothiophenol/triethyleneglycol-monomethylether; Calix, calixarene; CS, chitosan; GO-Met, graphene oxide modified by metformin; GONS, graphene oxide nanosheets; HNT, halloysite nanotubes; LDH, layered double hydroxides; MNP, magnetic nanoparticle; MOF, metal-organic framework; NP, nanoparticle; PAA, polyacrylamide; PdDPP-SHCs-HP-2-a Pd organosilane complex; PNP-SSS, palladium nanoparticles on silica-starch substrate; PS, polystyrene; PVA, poly(vinylalcohol); rGO, reduced graphene oxide; SB, Schiff base;  $\gamma$ -Fe<sub>2</sub>O<sub>3</sub>/AEPH<sub>2</sub>-TC-Pd-anchored thiophene methanimine-palladium Schiff base.

Adib et al. immobilized palladium on magnetical support, ( $\text{Fe}_3\text{O}_4$ ) functionalized with Murexide as anchor ( $\text{Fe}_3\text{O}_4\text{-NH}_2\text{-Murexide-Pd}$ ). The so-generated catalyst was used for the Suzuki reaction between differently substituted aryl halides and phenylboronic acid.<sup>69</sup> A water-ethanol mixture was used as the solvent for the reaction and the authors demonstrated that iodo-, bromo-, and chloroarenes can all be used as the substrate (Table 2 entry 6). It should be noted that substrates bearing a substituent in the *ortho* position show significantly lower yields. Although it was shown that the catalyst can be recycled up to six times, there is a notable drop in yield after the third reuse.

Khazaei and coworkers generated a magnetically recoverable catalyst ( $\text{Fe}_3\text{O}_4\text{-SiO}_2\text{-Pd}$ ) using renewable resources. Rice husk was used as the starting material to produce the  $\text{SiO}_2$  nanoparticles needed and the base used during the reaction was provided by waste eggshells.<sup>70</sup> This allowed for the coupling of aryl iodides and bromides with phenylboronic acid and *p*-ethylphenylboronic acid, respectively, in water-ethanol mixture in high yields (Table 2 entry 7). The catalyst was recycled five times with only a minimal decrease in activity.

Sobhani et al. developed a magnetically recyclable heterogeneous Pd-catalyst (Pd- $\gamma$ - $\text{Fe}_2\text{O}_3$ -2-ATP-TEG-MME) which was used for the coupling of aryl halides with phenyl boronic acid.<sup>71</sup> The reaction could be performed with iodo-, bromo-, and chloro-substituted arenes bearing both electron-donating and electron-withdrawing substituents (Table 2 entry 8). The catalyst consists of a 2-amino-thiophenol unit to complex a Pd(II) center which is linked to the  $\text{Fe}_2\text{O}_3$  nanoparticles. The additional triethyleneglycol unit allows for a better dispersion of the catalyst and thus a better contact with the reactants in the reaction medium water. The yields obtained are high for all cases and the catalyst could be easily recycled up to nine times with only a slight loss in product yield.

A functionalized polystyrene polymer was used as support material for a Pd salen-complex (PS-Pd-salen) as catalyst for Suzuki reactions between aryl iodides/bromides and phenylboronic acids in neat water.<sup>72</sup> Substrates with electron-donating and electron-withdrawing substituents are well tolerated on both reactants and the products are obtained in high yields (Table 2 entry 9). Interestingly, the reaction does not require the use of high reaction temperatures and can be performed at room temperature. Recyclability of the catalyst was reported for four consecutive cycles before a significant drop in yield was noted.

A similar polymer-based approach was developed by Künkül et al. using acrylamide as the support for a NHC palladium complex (Poly(AAm-AMPs) NHC-Pd).<sup>73</sup> The Suzuki coupling between several aryl bromides and phenylboronic acid was catalyzed efficiently in water as the reaction medium (Table 2 entry 10). The catalyst was reused five times without any decrease in yield being observed.

Salunkhe and coworkers used the natural polymer cellulose as support material for the fixation of a palladium center via a ferrocene tether (CelFemImiNHC@Pd).<sup>74</sup> Although iodides and bromides are good substrates for the Suzuki coupling between aryl halides and phenylboronic acid (Table 2

entry 11), the corresponding chlorides gave the product in a very limited amount. The reaction was performed in ethanol and the catalyst could be recycled up to five times before a notable drop in yield was observed.

Pourjavadi et al. combined the concept of magnetic nanoparticles with the use of a natural polysaccharide to stabilize the palladium nanoparticles (MNP@SPGMA@AP@Pd).<sup>75</sup> A variety of substrates were used for the Suzuki coupling and high yields were obtained with aryl iodides and bromides while aryl chlorides delivered the products in lower yields (Table 2 entry 12). Catalyst recycling was easily possible seven times. The positive effect of using a natural polymer as support is partially negated by the fact that DMF had to be used as a cosolvent to water to ensure high yields.

Rhee et al. used reverse phase silica gel as support for palladium nanoparticles (APPd(0)@Si) and showed that the produced material could serve as an effective catalyst for the Suzuki coupling of aryl bromides and phenylboronic acids in water.<sup>76</sup> With the exception of both reaction partners bearing a strong electron-withdrawing group, the products are generally obtained in high yields indifferent of the electronic nature of the substituent (Table 2 entry 13). The catalyst can be reused eight times without losing significant activity.

Very similar results were obtained by Das and coworkers. Using silica and an amine linker the authors were able to stabilize Pd nanoparticles (PdNP-NMe<sub>2</sub>@SiO<sub>2</sub>) and use them to catalyze the Suzuki coupling between a variety of (hetero)aryl bromides and chlorides and different phenylboronic acids (Table 2 entry 14).<sup>77</sup> The reactions were performed in water and generally gave the products in high yields. It was reported that higher temperatures were needed for the transformation of aryl chlorides than for the corresponding bromides.

Hosseini-Sarvari and Razmi showed that the coupling of arylboronic acids with haloarenes can be achieved by using a Pd/ZnO nanoparticle as catalyst.<sup>78</sup> The reaction is best performed in water as the solvent and provides the desired products in high yields. Electron-donating and electron-withdrawing substituents are well tolerated for chloro-, bromo-, and iodoaryl starting materials as well as the arylboronic acid (Table 2 entry 15). It was shown that the catalyst could be recycled up to seven times without losing its activity.

Metal-organic frameworks can also be used to stabilize a palladium complex for the use as a heterogeneous catalyst. Postsynthetic modification of IRMOF-3 with an imidopalladacycle complex allowed the successful coupling of different electron-withdrawing and electron-donating groups-containing aryl halides with substituted phenylboronic acids (Table 2 entry 16).<sup>79</sup> Excellent yields were obtained under mild conditions in a water-ethanol solvent mixture. The catalyst could be recycled five times without substantial loss of activity.

In a similar way to MOFs, zeolitic imidazolate framework has been functionalized with NHCs and used to stabilize palladium nanoparticles (PdNPs@NHC@ZIF-8). Azad et al. used this material as a catalyst for the Suzuki reaction between substituted aryl halides and phenylboronic acids in water-ethanol mixture.<sup>80</sup> It was reported that aryl chlorides could be used as substrates but

higher temperatures and higher catalyst loading had to be used compared to aryl iodides and bromides (Table 2 entry 17). Unfortunately no catalyst recycling studies were carried out in this work.

Ghorbani-Vaghei and his group used layered double hydroxides (LDH) as support for Pd nanoparticles (LDH/Tris/Pd) in the Suzuki reaction of aryl halides with phenylboronic acid (Table 2 entry 18).<sup>81</sup> The products were obtained in mostly excellent yields with the exception of aryl chlorides and *ortho*-substituted molecules afforded lower yields.

Sarma et al. applied montmorillonite K-10 as a support for Pd(OAc)<sub>2</sub>.<sup>82</sup> The immobilization was achieved by the impregnation with an ionic liquid. The active catalyst (PCIL-1) was able to facilitate the Suzuki coupling between aryl bromides and iodides and phenylboronic acids (Table 2 entry 19). Aryl halides with electron-withdrawing and electron-donating substituents as well as heteroaryl bromides could be converted. While bromides and iodides furnished the products in good yields using a water-isopropanol mixture as the solvent, the use of chlorides resulted in significantly lower yields.

Another montmorillonite clay was used as a support material for depositing Pd nanoparticles on its surface by the group of Dutta. The clay was activated by acid treatment and the nanoparticles formed on the support.<sup>83</sup> The catalyst (Pd(0)-Mont.) effectively coupled aryl halides (I, Br, Cl) and different phenylboronic acids in water-ethanol mixture (Table 2 entry 20). The yields obtained were high in all cases, only slight variations were observed with the change of substituent or the halide used. The catalyst could be reused three times with significant changes in yield and catalyst structure.

Patil et al developed Schiff base-palladium(II) complex tethered to a magnetic nanoparticle on iron oxide basis (MNPs@SB-Pd) for the Suzuki reaction.<sup>84</sup> Aryl bromides and phenylboronic acid were successfully coupled in ethanol-water mixture in good to high product yields (Table 2 entry 21). When aryl chlorides were used a notable drop in yield was observed. The authors showed that the catalyst could be recycled six times while maintaining stable activity.

Another suitable support material for palladium nanoparticles is graphene oxide. After modification of the graphene oxide with metformin it was possible to anchor palladium nanoparticles to the surface and use the new material (GO-Met-Pd) for the Suzuki coupling between aryl halides and phenylboronic acid.<sup>85</sup> Aryl bromides and iodides with mainly electron-donating substituents formed the products in high yields in water-ethanol mixture (Table 2 entry 22). When chlorides were employed as the starting material an about 30% decrease in yield was observed. The catalyst was recyclable nine times with only a slight loss in activity.

Graphene oxide was also used by Shim and coworkers. They functionalized graphene oxide nanosheets with a NHC-containing tether that then complexed a palladium ion (GONS-NHC-Pd).<sup>86</sup> The thus generated material acted as catalyst for the coupling of (hetero)aryl bromides with phenylboronic acids using ethanol-water as the solvent. While aryl and heteroaryl bromides were easily transformed at room temperature, the conversion of aryl chlorides required elevated

temperature (50°C) to achieve high yields (Table 2 entry 23). The catalyst only showed a slight decrease in product yield even after having been used 10 times.

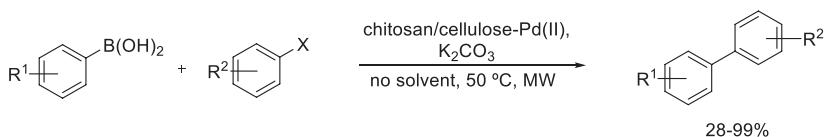
The work described by Bharadwaj et al. used a cryptand to stabilize Pd nanoparticles (Pd(0)-PzC).<sup>87</sup> Aryl bromides with several different substituents have been coupled to various phenylboronic acids using water as the solvent (Table 2 entry 24). The products are obtained in high yields and the catalyst could be recycled three times without significant loss in activity. Drawback of the methodology is the need for the strong base KOH and the use of a phase transfer catalyst (TBAB).

Rao et al. used calixarenes bound to MCM-41 as support for Pd nanoparticles (Pd@MCM-Calix<sub>ox</sub>) and used this system for a variety of reactions including the coupling of iodobenzene and phenylboronic acids in water.<sup>88</sup> The phenylboronic acids used could bear a variety of electron-withdrawing and electron-donating substituents (Table 2 entry 25). Most products were obtained in excellent yield, with the exception of sterically hindered substrates. The catalyst could be recycled five times with only a slight decrease in product yield.

A similar study also reported the use of MCM-41 as support (as well as SBA-15), giving low to excellent yields for a broad variety of substrates.<sup>90</sup>

A catalyst based on palladium supported on CoO-carbon nanocomposites (Pd/CoO-C) was employed in the coupling of aryl chlorides and bromides with phenylboronic acid in water (Table 2 entry 26).<sup>89</sup> Several different substituents on the aryl halide were tested and it was found that aryl chlorides only gave high yields if strong electron-withdrawing substituents such as CN or NO<sub>2</sub> were present. Recycling of the catalyst was possible 10 times without any decrease in activity.

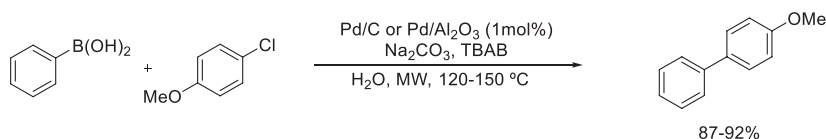
Baran et al. developed a heterogeneous catalyst system based on the use of a support that was derived from a renewable resource. The authors used a natural carbohydrate, chitosan-based<sup>91</sup> catalyst, namely cross-linked chitosan-cellulose beads to support Pd(II) ions and applied it to the Suzuki coupling between aryl bromides and iodides and phenylboronic acid.<sup>92</sup> The reaction was performed using microwave heating, required no solvent, and a variety of different substituents were tolerated (Scheme 11). While it is not surprising that chlorides show a poor performance in the coupling reaction it was also found that iodides gave lower yields than the corresponding bromides. Unfortunately the authors did not give an explanation for this interesting finding. While the catalyst was found to be reusable nine times, a significant drop in yield was observed after the third run.



**SCHEME 11** The Suzuki coupling catalyzed by cross-linked chitosan-cellulose beads-supported Pd(II) ions.

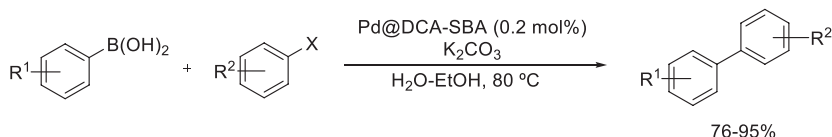
404 Heterogeneous catalysis in sustainable synthesis

While investigating the heating profile of several catalysts, Kappe and his group found that simple Pd/C or Pd/Al<sub>2</sub>O<sub>3</sub> could serve as catalyst for the coupling of *p*-chloroanisole and phenylboronic acid (Scheme 12).<sup>93</sup> The advantage of the described reaction condition lied in the use of microwave heating and short reaction times, therefore decreasing the amount of energy consumed. Water could be used as the reaction medium.



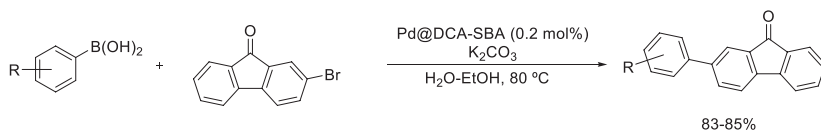
**SCHEME 12** A microwave-assisted Suzuki coupling catalyzed by commercially available Pd/C and Pd/Al<sub>2</sub>O<sub>3</sub> catalysts.

Mohammadkhanni and Bazgir synthesized a SBA-based material functionalized with a dicarboxylic acid as support for Pd centers and used it as a catalyst in the synthesis of fluorenones using the Suzuki reaction. Chloro-, bromo-, and iodoarenes could be coupled with phenylboronic acids to yield the corresponding biaryl product.<sup>94</sup> While both electron-donating and electron-withdrawing substituents were tolerated on the haloarenes coupling partner, only electron-donating substituents were tested regarding the phenylboronic acid starting materials (Scheme 13). The reaction was performed in a water-ethanol mixture and the catalyst could be reused five times without significant loss in activity. Similar results were obtained when a catalyst with MCM was used as the support material instead of SBA.<sup>95</sup>



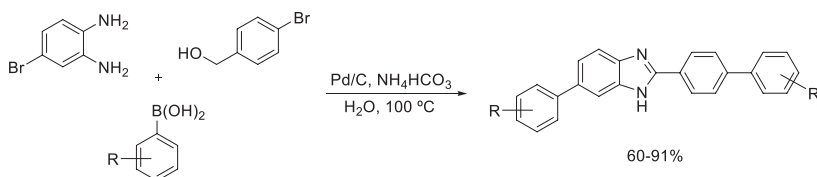
**SCHEME 13** A modified SBA-supported Pd-catalyzed Suzuki coupling in water-ethanol solvent mixture.

The same catalytic system was also employed for the synthesis of a variety of fluorenones under the same conditions (Scheme 14). Both electron-donating and electron-withdrawing substituents were tolerated on the phenylboronic acid for these transformations.



**SCHEME 14** Synthesis of arylated fluorenones using an SBA-supported Pd-catalyzed Suzuki coupling.

Xu and coworkers showed that simple Pd/C could be used as a catalyst for the synthesis of aryl-substituted benzimidazoles through a combination of hydrogen transfer and the Suzuki reaction.<sup>96</sup> A variety of aryl-1,2-diamines were coupled with benzyl alcohols to form the benzimidazoles that when bearing a bromo-substituent underwent simultaneous Suzuki coupling (Scheme 15). Phenylboronic acids bearing electron-withdrawing and electron-donating substituents could be used for the reaction with electron-donating substituents giving a slightly higher yield. The environmentally friendly method used water as the solvent and did not require the use of an additional ligand for the metal.

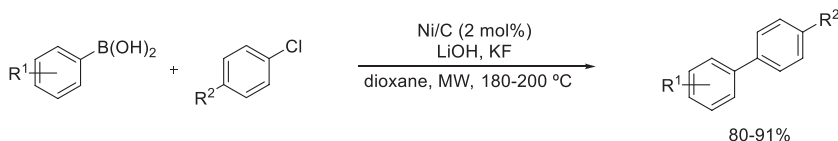


**SCHEME 15** A ligand-free Pd/C-catalyzed synthesis of arylated benzimidazoles with a one-pot cyclization-Suzuki coupling approach.

### 3.6.3.2 Palladium-free heterogeneous catalytic Suzuki coupling reactions

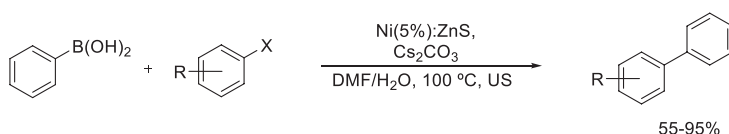
Similarly to the Heck couplings, there has been an increasing interest in investigations regarding the use of other metals besides palladium as a catalytically active metal. This is in part due to economic reasons but also environmental concerns due to, e.g., the toxicity of palladium. The following section focuses on Suzuki-Miyaura coupling reactions using metals other than palladium.

Lipshutz and his group used Ni/C under microwave conditions for the coupling of aryl chlorides with aryl boronic acids (Scheme 16).<sup>97</sup> High product yields were obtained when aryl chlorides with an electron-withdrawing substituent were used. The need for a strong base and a fluoride source in most examples counterbalances the advantage of the comparably very short reaction times achieved by the microwave heating.



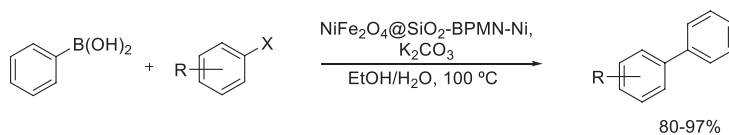
**SCHEME 16** A microwave-assisted Ni/C-catalyzed Suzuki coupling.

Labiadh et al. used zinc sulfide doped with nickel (Ni(5%):ZnS) as a catalyst for the Suzuki reaction.<sup>98</sup> The authors found that the reaction between aryl iodides and bromides with phenylboronic acid could be performed in DMF/water as the solvent and the use of ultrasounds increases the product yield (Scheme 17). Although the majority of their examples used aryl bromide it was reported that iodides work equally well. Chloroarenes were also tested but gave substantially lower yields. In regard to the substitution of the aryl halides the authors found that electron-withdrawing substituents perform notably better than substrates bearing an electron-donating substituent. Unfortunately, no catalyst recycling study was performed.



**SCHEME 17** Synthesis of biaryls using the Suzuki reaction catalyzed by Ni-doped zinc sulfide heterogeneous catalysts.

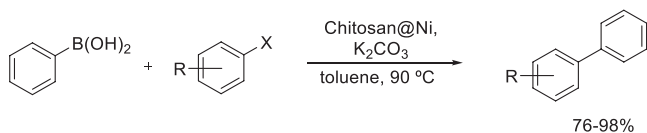
The synthesis of an inorganic-organic hybrid material using nickel ferrite as core and an organic linker to anchor a nickel(II) ion was reported by Naeimi and Kiani.<sup>99</sup> This nano magnetic complex (NiFe<sub>2</sub>O<sub>4</sub>@SiO<sub>2</sub>-BPMN-Ni) acted as catalyst for the Suzuki coupling between aryl halides and phenylboronic acid in water-ethanol mixture (Scheme 18). Iodides, bromides, and chlorides all gave the products in high yields with the chlorides only giving a slightly lower yield. No significant difference was observed between electron-withdrawing and electron-donating substituents. Due to its magnetic properties, the catalyst was easily recyclable six times without losing its activity.



**SCHEME 18** A Ni-ferrite-based magnetic nanoparticle-catalyzed synthesis of biaryls via the Suzuki coupling of aryl halides with phenylboronic acid.

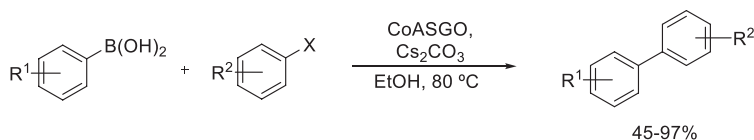
Hajipour and Abolfathi developed a nanoparticle catalyst from chitosan that is decorated with nickel ions (Chitosan@Ni).<sup>100</sup> Phenylboronic acid was coupled with aryl halides in toluene in high yields (Scheme 19). While iodides and bromides performed equally well, the use of chlorides resulted in around 10% drop in product yields. No difference in product formation was observed when using substrates with electron-donating or electron-withdrawing substituents.

When the catalyst was tested for recyclability, a small drop in yield was observed after three runs.



**SCHEME 19** The Suzuki coupling catalyzed by a chitosan-supported Ni catalyst.

In addition to Ni, cobalt-based catalysts can also be used to catalyze the reaction as described by Saroja and Bhat for the coupling of aryl bromides and different phenylboronic acids.<sup>101</sup> Cobalt particles were immobilized on graphene nanosheets via a Schiff base formation to generate the active catalyst (CoASGO). Although electron-donating and electron-withdrawing substituents were tolerated on both substrates, a substantially lower yield was observed with electron-donating substituents (Scheme 20). The reactivity of aryl chlorides was also tested but only negligible product formation was observed. The reaction was performed in ethanol as an environmentally friendly solvent and the catalyst could be reused three times before a notable decrease in yield was observed.



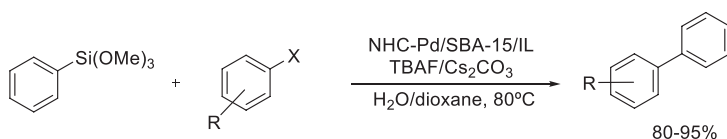
**SCHEME 20** The Suzuki coupling catalyzed by a graphene-supported Co nanoparticle catalyst.

### 3.6.4 The Hiyama coupling

The Hiyama coupling<sup>102</sup> is conceptionally similar to the Suzuki coupling but uses an organo-silicon substrate instead of the organoboron compound used in the Suzuki reaction. The recent developments with regard to the application of heterogeneous catalysts in these reactions are summarized here.

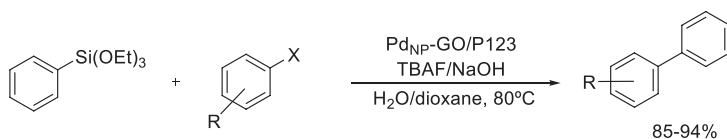
Rostamnia et al. developed a Pd-NHC complex that was immobilized within the pores of an SBA-15/ionic liquid material (NHC-Pd/SBA-15/IL) for the Hiyama coupling of phenyltrimethoxysilane with a variety of haloarenes.<sup>103</sup> Aryl bromides and iodides with both electron-donating and electron-withdrawing substituents were suitable substrates and gave the biaryl compounds in high yields (Scheme 21). The catalyst could be recycled five times before the yield began to drop due to the disintegration of the support material caused by the fluoride additive. A mixture of water and dioxane was used as the solvent allowing for an easy separation of the catalyst and the product by filtration and extraction.

408 Heterogeneous catalysis in sustainable synthesis



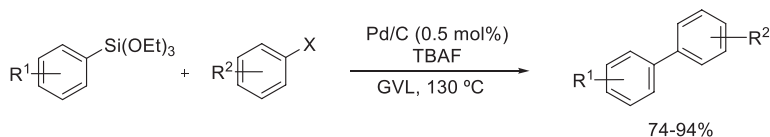
**SCHEME 21** The synthesis of biaryls via the Hiyama coupling catalyzed by an ionic liquid-doped SBA-supported Pd catalyst.

The same group also showed that Pd nanoparticles can be immobilized on graphene oxide nanosheets and used as the catalyst for Hiyama coupling reactions.<sup>104</sup> The researchers found that by using a surfactant (P123) the product yield could be dramatically increased, most likely due to the surface cleaning effect of the surfactant. The ligand-free catalytic system can be reused four times before a drop in product yield is noted. A variety of different substituted haloarenes were suitable substrates for the reaction, including those with electron-withdrawing and electron-donating substituents (Scheme 22).



**SCHEME 22** The Hiyama coupling catalyzed by graphene oxide nanosheet-immobilized Pd nanoparticles.

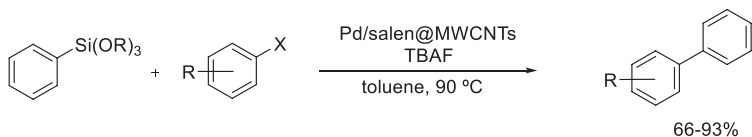
Vaccaro's group described the use of a simple, commercially available Pd/C catalyst in  $\gamma$ -valerolactone (GVL) as the solvent for the coupling of a variety of aryl chlorides and bromides with triethoxyphenylsilanes.<sup>105</sup> Although the substituents on the halide could be electron-donating and electron-withdrawing, only the methoxy group was tolerated as a substituent on the arylsilane reagent (Scheme 23). The major advantage of the reaction system is the use of the renewable solvent GVL and the simplicity of the employed catalyst. Unfortunately, no studies on the recyclability of the catalyst were performed.



**SCHEME 23** The synthesis of biaryls via the Hiyama coupling catalyzed by a commercially available simple Pd/C catalyst carried out in a renewable solvent  $\gamma$ -valerolactone (GVL).

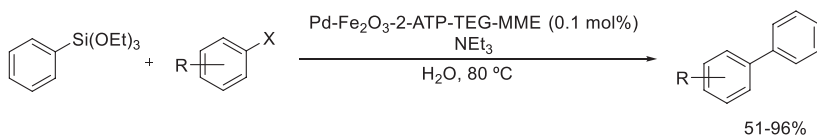
Movassagh et al. described the use of a Pd-salen complex anchored to multiwalled carbon nanotubes for the coupling of trialkoxysilanes with aryl iodides

and aryl bromides.<sup>46</sup> The products were obtained with both electron-rich and electron-poor haloarenes in mostly high yields (Scheme 24). Unfortunately, the reaction had to be performed in toluene as the solvent and TBAF had to be used as an additive, overcoming the positive effect of the recyclability of the catalyst.



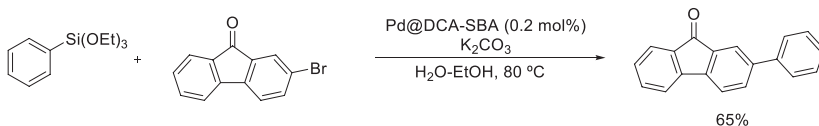
**SCHEME 24** A multiwall carbon nanotubes-supported Pd-salen complex-catalyzed Hiyama coupling.

Sobhani et al. also used their magnetically separable catalyst for the fluoride-free Hiyama coupling of chloro-, bromo-, and iodobenzenes with triethoxyphenylsilane in water as the reaction medium.<sup>71</sup> Similarly to the Suzuki reactions described earlier, the products are generally obtained in high yields and a variety of electron-donating and electron-withdrawing substituents can be used (Scheme 25). A notably lower yield was observed only when the strong electron-withdrawing nitro group was present. As reported before, catalyst recycling was easily carried out with a decrease in yield becoming notable after the seventh run.



**SCHEME 25** The synthesis of biaryls via the Hiyama coupling catalyzed by a water-dispersible, magnetically recyclable Pd catalyst.

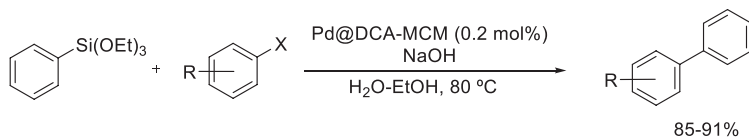
During their studies for the synthesis of fluorenones, Mohammadkhanni and Bazgir also examined the synthesis via the Hiyama coupling using the same catalytic system that was developed for other cross-coupling reactions.<sup>94</sup> The synthesis of the arylfluorenone was achieved in a reasonable yield of 65% under environmentally friendly conditions using water-ethanol as the solvent (Scheme 26).



**SCHEME 26** An environmentally benign synthesis of the arylfluorenone in water-ethanol mixture via a Pd-catalyzed Hiyama coupling.

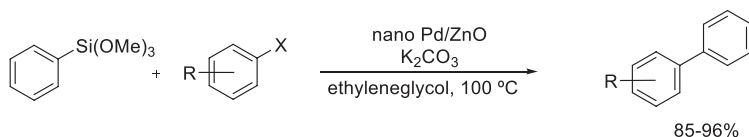
410 Heterogeneous catalysis in sustainable synthesis

A very similar catalyst using MCM as the support instead of SBA was employed under nearly identical experimental conditions for the Hiyama coupling of triethoxyphenylsilane and iodo- and bromoarenes.<sup>95</sup> The products were obtained in high yields with a broad scope including a variety of electron-donating and electron-withdrawing substituents in the haloarene starting material (Scheme 27).



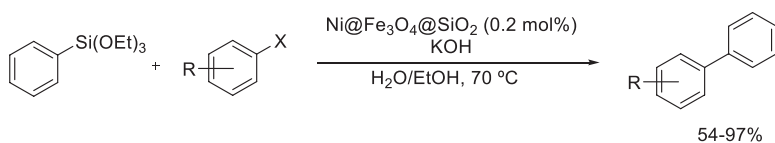
**SCHEME 27** The Hiyama coupling catalyzed by an MCM-supported Pd catalyst.

A simple Pd/ZnO catalyst was used by Hosseini-Sarvari and Razmi for the Hiyama coupling in ethylene glycol as the solvent.<sup>78</sup> Iodo-, bromo-, and chloroarenes were suitable substrates for the coupling with trimethoxyphenylsilane and a variety of additional substituents ranging from strongly electron-withdrawing to electron-donating gave the products in high yields (Scheme 28). It should be noted that only aryl chlorides and bromides with electron-withdrawing substituents were tested. Although no catalyst recycling studies were conducted for the Hiyama coupling, it can be expected that the recyclability of the catalyst shown for the Suzuki coupling (seven times without loss of activity, *vide supra*) will also be applicable in the case of the Hiyama coupling.



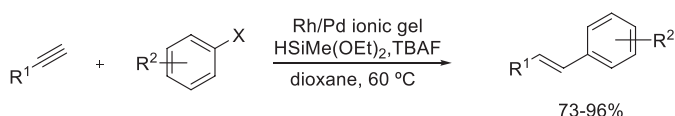
**SCHEME 28** Synthesis of biaryls with a Pd/ZnO-catalyzed Hiyama coupling.

Similarly to the Heck or Suzuki coupling reactions effort has been made to develop alternative catalysts to replace the expensive and quite toxic Pd as the catalytic metal with more economic and potentially less toxic metals in the Hiyama coupling as well. Hajipour and Abolfathi designed a heterogeneous Ni catalyst for the coupling of triethoxyphenylsilane with a variety of aromatic halides.<sup>106</sup> The catalytically active Ni center is coordinated by a triazole unit tethered to a magnetic nanoparticle. Different haloarenes are transformed in high yield, only compounds with sterically demanding *ortho*-substituents gave lower yields (Scheme 29). It was reported that the environmentally friendly solvent water-ethanol mixture was superior to the traditionally employed DMF. It should be noted that no fluoride additives were necessary for the reaction.



**SCHEME 29** The Hiyama coupling with a triazole-coordinated nickel catalyst immobilized on a magnetic support.

Wagner and his group developed a heterogeneous bimetallic Rh/Pd catalyst with a polyionic gel as support.<sup>107</sup> The catalyst showed good activity for the one-pot hydrosilylation-Hiyama-coupling reaction of acetylenes with aryl iodides. The reaction occurs with almost exclusive *E* selectivity and the products are obtained in high yields (Scheme 30). Even though the reagents used are not necessarily considered green, the one-pot process can be seen as a significant improvement over the traditional synthetic pathway involving multiple steps and other hazardous reagents. While the authors attempted to reuse the catalyst, a significant drop in yield was observed starting with the third run.



**SCHEME 30** A polyionic gel-supported bimetallic Rh/Pd-catalyzed one-pot hydrosilylation-Hiyama-coupling reaction of acetylenes with aryl iodides.

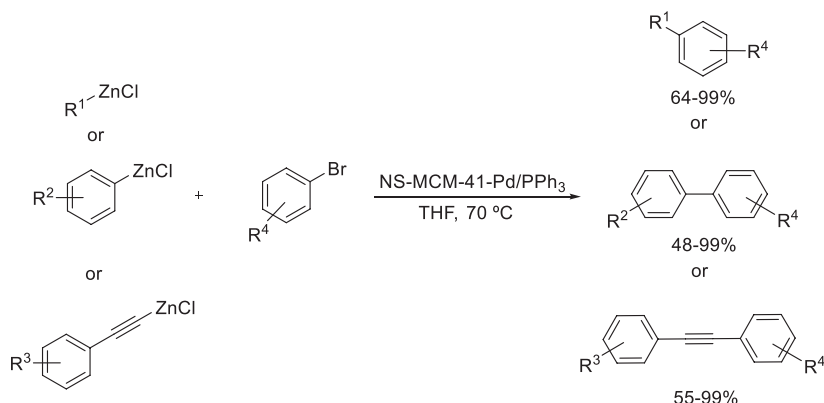
### 3.6.5 The Negishi coupling

While both the Suzuki and Hiyama coupling reactions use fairly stable nucleophiles, this is no longer the case for the Negishi coupling when the more reactive organozinc substrates are used. This increased reactivity is often appreciated when hard-to-couple substrates are employed. On the other hand, this advantage does often bring about a limited choice concerning the solvents that can be used as most organozinc reagents are not compatible with protic solvents.

The next section describes selected examples applying heterogeneous catalytic systems for the Negishi reaction that comply with the principles of green chemistry.

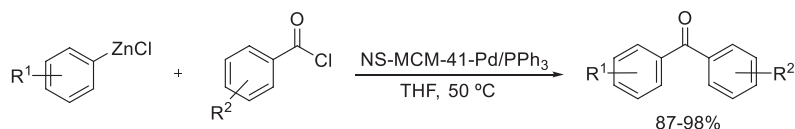
Wu et al. showed that a variety of aryl bromides can undergo the Negishi coupling with different organozinc reagents to yield the desired products in medium to high yields (Scheme 31).<sup>108</sup> The catalyst used consists of a nano-sized MCM-41 support material having a Pd ion immobilized through complex formation by a covalently-bound linker molecule. For the organozinc reaction partner, alkyl, aryl, heteroaryl, and alkynyl reagents were proven suitable for the transformation. The arylbromide reaction partner could be substituted with a variety of substituents, including electron-withdrawing and electron-donating ones. Recycling of the catalyst was possible up to four times with only a slight

decrease in yield. Unfortunately the reaction requires the addition of a phosphine to stabilize the palladium species as well as THF as the solvent.



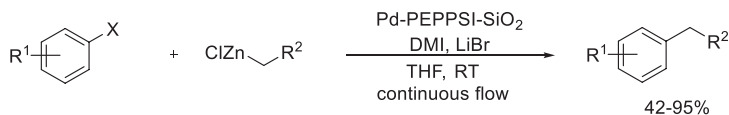
**SCHEME 31** The Negishi coupling catalyzed by a nanosized MCM-41-supported Pd catalyst.

In the same study<sup>108</sup> the authors could also show that aromatic acyl chlorides can serve as the reaction partner for aryl zinc compounds giving the corresponding diaryl ketones in high yields (Scheme 32). Although the reaction can be performed without PPh<sub>3</sub>, it was shown that by using the ligand the reaction yield increases by 10% and the catalyst loading can be lowered by a factor of 10.



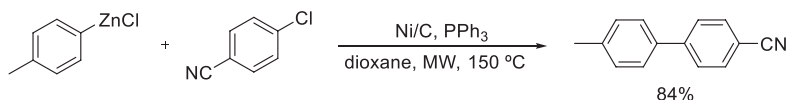
**SCHEME 32** The Negishi coupling of aryl zinc substrates with acyl chlorides catalyzed by a nanosized MCM-41-supported Pd catalyst.

The group of Organ successfully immobilized a Pd-PEPPSI complex onto silica gel and used it as heterogeneous catalyst for the Negishi coupling applying a variety of aryl halides with different alkyl zinc reagents under flow conditions (Scheme 33).<sup>109</sup> Application of the flow conditions allowed to obtain the same yields in extremely reduced reactions times compared to the batch system under otherwise identical conditions. When performing tests about the recyclability of the catalyst, it was noted that the activity constantly and gradually decreased over time. This was attributed to a relatively high amount of unbound catalyst rather than actual leaching out of the immobilized catalyst. While this decrease in activity required longer reaction times, no significant drop in product yield was observed for the first four reuses in the batch process.



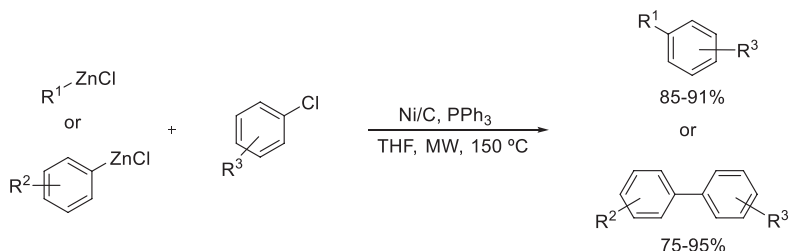
**SCHEME 33** A silica-supported Pd-catalyzed Negishi coupling.

Kappe and his group also investigated the Negishi coupling for their catalyst heating study mentioned earlier.<sup>93</sup> Using microwave heating in dioxane a simple Ni/C catalyst was shown to be able to perform the coupling reaction of *p*-tolyl-zinc chloride and *p*-cyanochlorobenzene in high yield and short reaction time (Scheme 34). As previously mentioned the use of dioxane at high reaction temperature is a major drawback of the method.



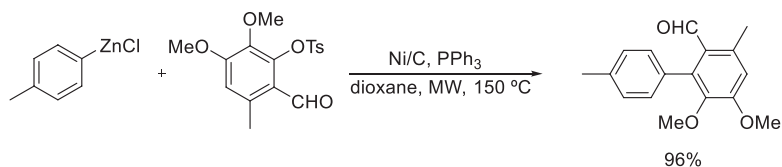
**SCHEME 34** A Ni/C-catalyzed Negishi reaction under flow conditions.

Using similar conditions, Lipshutz et al. were able to show that a broad range of organozinc reagents can be coupled with different aryl chlorides in high yields.<sup>97</sup> The major advantage of the developed method is the application of a simple Ni/C catalyst as well as the extremely shortened reaction time of the microwave reaction when compared to other systems known in the literature. Both the organozinc reagent as well as the aryl chloride could possess electron-donating or electron-withdrawing substituents, thus allowing the synthesis of biaryls with a broad combination of substituents (Scheme 35).



**SCHEME 35** A microwave-assisted Negishi coupling.

The earlier described reaction conditions also allowed the transformation of a sterically crowded tosylate into the diaryl compound (Scheme 36).<sup>97</sup>



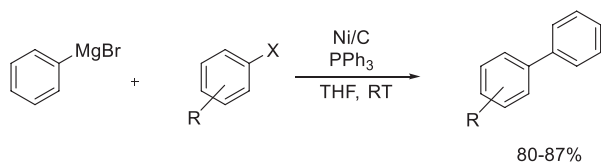
**SCHEME 36** Application of sterically crowded aryl tosylate in a microwave-assisted Negishi coupling

### 3.6.6 The Kumada coupling

When moving from the Hiyama to the Kumada coupling<sup>2</sup> the problematic issue of the high reactivity of the organometallic substrate becomes even more dominant, especially from the green chemistry point of view. The employed Grignard reagents are only compatible with a very limited solvent selection, mainly diethyl ether and THF: both of those are flammable and explosive not to mention that they easily undergo peroxidation and their shelf life is relatively short. In addition, there is also the risk that the Grignard reagent reacts with the substrate in side reactions or the formation of the Grignard reagent itself cannot be easily achieved due to functional group incompatibilities on the aromatic ring. The question could be raised whether a reaction using a Grignard reagent can be brought into compliance with the principles of green chemistry?

Nonetheless, the examples shown later do take some steps toward a more environmentally friendly reaction by using heterogeneous catalysts and reducing the amount of additives needed for the reaction.

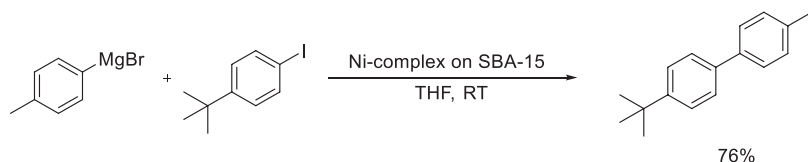
During a study of amination reactions, Lipshutz and Tasler showed that the Kumada coupling can be performed by using a Ni on charcoal catalyst.<sup>110</sup> The reaction works well for chlorotoluene and chloroanisole but 2 equiv. (compared to the amount of Ni) of a phosphine ligand had to be used (Scheme 37). Although the use of the heterogeneous catalyst is desirable, the need for the ligand and THF as a solvent are detrimental for the environmental impact of the reaction.



**SCHEME 37** A Ni/C-catalyzed Kumada coupling.

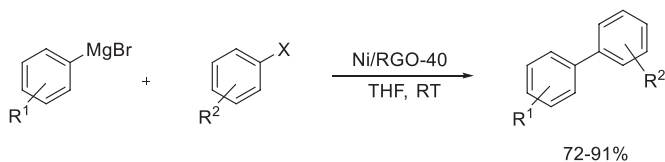
A collaboration of different research groups resulted in the development of a heterogeneous catalyst for the Kumada coupling of *p*-iodo-*t*-butylbenzene and *p*-tolyl magnesium bromide.<sup>111</sup> The catalyst was obtained by reacting a Ni salt with a diphosphine ligand-containing silanol ester unit, able to connect with the

heterogeneous support (SBA-15). Even though THF had to be used as a solvent, the authors could show that using their heterogeneous system, the amount of THF needed could be dramatically reduced compared to the homogeneous system (0.8 vs 3.0 mL) while still obtaining the desired product in good yields and high selectivities (Scheme 38). The catalyst could be recycled four times before losing its activity.



**SCHEME 38** The Kumada coupling catalyzed by an SBA-supported Ni complex.

A variety of haloaryls and aryl Grignard reagents could be reacted to the corresponding biphenyl compounds using a heterogeneous Ni catalyst developed by Bhowmik et al.<sup>112</sup> The catalyst Ni/RGO-40 is formed by depositing Ni on graphene oxide using a hydrothermal method followed by heating in H<sub>2</sub> to perform the reduction. The biphenyl products could be obtained from compounds containing different halogen substituents in good yields with both electron-donating and electron-withdrawing substituents on the aryl halide being well tolerated (Scheme 39). Dihaloaryl compounds were successfully used as substrates yielding the coupling reaction on both halogenated positions. The catalyst was recyclable six times with only a slight loss in yield.

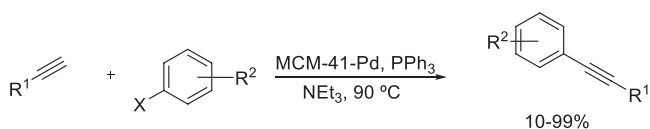


**SCHEME 39** The Kumada reaction catalyzed by a graphene oxide-supported Ni catalyst.

### 3.6.7 The Sonogashira coupling

The Sonogashira coupling reaction forms a C–C bond between an aryl halide and the terminal carbon of an alkyne. Originally published in 1975,<sup>113</sup> the reaction is traditionally performed with a palladium catalyst using a phosphine ligand, a copper cocatalyst, and a strong base to activate the alkyne. As with other cross-coupling reactions the recent developments are focused on the replacement of the traditional homogeneous system with a heterogeneous one.<sup>114</sup> The following section gives an overview over recent developments in the field.

One example that uses a heterogeneous version of the traditional conditions is reported by Lin and coworkers.<sup>115</sup> The authors used MCM-41 as a support for a bipyridine linker unit coordinating a Pd ion. Triphenylphosphine as the ligand and CuI as a cocatalyst were used in triethylamine as the solvent. The reaction works well for a large combination of substrates with only a few exceptions giving low yields (Scheme 40). Surprisingly, unsubstituted bromobenzene gives the lowest yields with all coupling partners while both electron-donating and electron-withdrawing substituents furnish higher yields of the desired products. The catalyst was shown to be recyclable three times with only a slight drop in yield.



**SCHEME 40** The Sonogashira reaction catalyzed by an MCM-41-supported Pd catalyst.

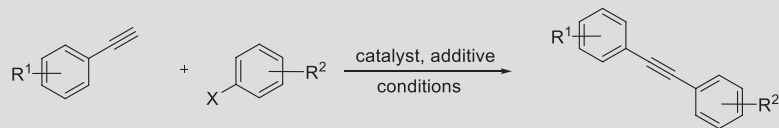
Even though the heterogenization of the metal complexes to solid catalysts is generally considered a step toward environmentally friendly reactions, the use of ligands and cocatalysts should be avoided. A variety of copper- and ligand-free heterogeneous catalytic applications of the Sonogashira reactions is given as follows (Table 3).

Vaccaro et al. used a combination of a heterogeneous catalyst and a heterogeneous base for the Sonogashira coupling of aryl iodides with phenylacetylenes (Table 3 entry 1).<sup>116</sup> The catalyst is based on a highly cross-linked thiazolium-based material that is used to immobilize palladium (Pd/polythiazolium/SBA-15). The desired coupling products were obtained in high yields with the exception of substrates bearing electron-donating groups. The use of a heterogeneous base has the advantage that both catalyst and base can be easily recovered as well as stabilizing the catalytic system, allowing for better results when recycling the catalyst. The water-acetonitrile azeotrope used as a solvent could be easily distilled off and reused after completion of the reaction.

Khalafi-Nezhad and Panahi reported that the PNP-SSS catalyst they developed for the Heck reaction could also be used for the copper-free Sonogashira reaction of aryl halides and alkynes in water (Table 3 entry 2).<sup>42</sup> The reaction was performed in water as the solvent and  $\text{K}_2\text{CO}_3$  as base. The catalyst could be recycled five times without losing its activity and investigations of the reused catalyst showed only a slight leaching of palladium content.

Li, Zhang, and coworkers used their catalytic system (PdDPP-SHCs-HP-2) also for the Sonogashira reaction.<sup>66</sup> Although the reaction between phenylacetylene and iodobenzene was achieved with 92% yield (Table 3 entry 3), switching to bromobenzene dramatically decreased the yield obtained. Water was used as the solvent and the reaction is performed at 60°C. As mentioned before the

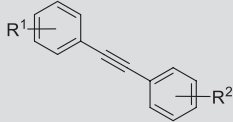
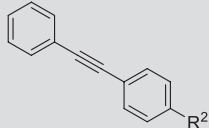
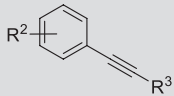
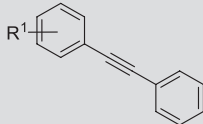
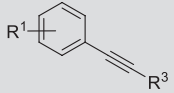
**TABLE 3** Copper-free Sonogashira reactions.

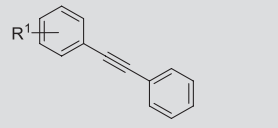
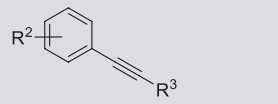
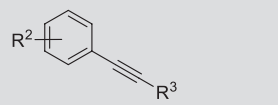
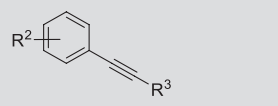
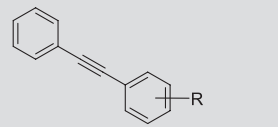
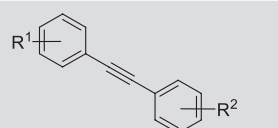


| Entry | Catalyst                            | Base                           | Conditions                                | Product | % Yield | Recycl. (times) | Ref. |
|-------|-------------------------------------|--------------------------------|---|---------|---------|-----------------|------|
| 1     | Pd/polythiazolium/SBA-15 (0.4 mol%) | PS-piperazine                  | CH <sub>3</sub> CN/H <sub>2</sub> O, 90°C |         | 62–95   | 5               | 116  |
| 2     | PNP-SSS (1.2 mol%)                  | K <sub>2</sub> CO <sub>3</sub> | H <sub>2</sub> O, reflux                  |         | 81–97   | 6               | 42   |
| 3     | PdDPP-SHCs-HP-2 (5 mol%)            | NEt <sub>3</sub>               | H <sub>2</sub> O, 60°C                    |         | 92      | 9               | 66   |
| 4     | MWCNT/HL2-Pd                        | NEt <sub>3</sub>               | H <sub>2</sub> O, 50°C                    |         | 94      | 2               | 117  |

*Continued*

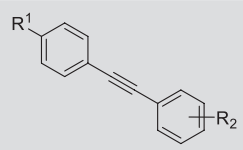
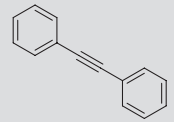
**TABLE 3** Copper-free Sonogashira reactions—cont'd

| Entry | Catalyst                    | Base                           | Conditions                  | Product  | % Yield | Recycl. (times) | Ref. |
|-------|-----------------------------|--------------------------------|-----------------------------|--|---------|-----------------|------|
| 5     | Pd@DCA-MCM (0.2 mol%)       | NaOH                           | H <sub>2</sub> O/EtOH, 80°C |  | 85–93   | 5               | 95   |
| 6     | Pd(II)-PMO-P-2              | NEt <sub>3</sub>               | H <sub>2</sub> O, 60°C      |  | 84–98   | 7               | 118  |
| 7     | PAA-Pd-NP                   | DABCO                          | H <sub>2</sub> O, 60°C      |  | 77–99   | 5               | 68   |
| 8     | SiO <sub>2</sub> -acac-PdNP | Piperidine                     | H <sub>2</sub> O, reflux    |  | 40–93   | 5               | 119  |
| 9     | Pd@HNTs-T-CD                | K <sub>2</sub> CO <sub>3</sub> | H <sub>2</sub> O/EtOH, 60°C |  | 45–95   | 5               | 120  |

|    |   |                                   |                             |  |       |   |                     |
|----|---|-----------------------------------|-----------------------------|--|-------|---|---------------------|
| 10 | Fe <sub>3</sub> O <sub>4</sub> @-NH <sub>2</sub> @Murexide@Pd | K <sub>2</sub> CO <sub>3</sub>    | H <sub>2</sub> O/EtOH, 60°C |  | 79–99 | 4 | <a href="#">69</a>  |
| 11 | Pd-CoFe <sub>2</sub> O <sub>4</sub> -MNP                      | K <sub>2</sub> CO <sub>3</sub>    | EtOH, 70°C                  |  | 60–95 | 5 | <a href="#">121</a> |
| 12 | Pd@Hal-2N-TCT-EDA   | K <sub>2</sub> CO <sub>3</sub>    | EtOH, 90°C                  |  | 72–97 | 5 | <a href="#">122</a> |
| 13 | Pd-MCM-48   | K <sub>2</sub> CO <sub>3</sub>    | EtOH, 80°C                  |  | 72–90 | – | <a href="#">123</a> |
| 14 | NS-ADP-TiO <sub>2</sub>                                       | K <sub>2</sub> CO <sub>3</sub>    | EtOH or DMF, 85°C           |  | 28–99 | 3 | <a href="#">124</a> |
| 15 | CS/MMT/Pd   | CH <sub>3</sub> CO <sub>2</sub> K | DMSO/ethylene glycol, 110°C |  | 69–94 | 8 | <a href="#">125</a> |

*Continued*

**TABLE 3** Copper-free Sonogashira reactions—cont'd

| Entry | Catalyst                                   | Base                           | Conditions    | Product  | % Yield | Recycl. (times) | Ref.                |
|-------|--|--------------------------------|---------------|--|---------|-----------------|---------------------|
| 16    | MNPFEMTriaz<br>NHC@Ag complex              | K <sub>2</sub> CO <sub>3</sub> | DMF, 100°C    |  | 54–92   | 8               | <a href="#">126</a> |
| 17    | Pd <sub>6</sub> L <sub>6</sub> nanocluster | NEt <sub>3</sub>               | Toluene, 80°C |  | 85–96   | 4               | <a href="#">127</a> |

MWCNT/HL2-Pd, multiwalled carbon nanotubes with Pd (II) complexes of azamacrocycles; PAA-Pd-NP, modified polyacrylamide nanoparticles with incorporated Pd centers; PdDPP-SHCs-HP-2, a Pd organosilane complex; PNP-SSS, palladium nanoparticles on silica-starch substrate; SBA, Santa Barbara Amorphous silica.

catalyst recycling was shown for the Tsuji-Trost reaction. Unfortunately, no other substrates were tested.

Savastano et al. demonstrated that azamacrocycles could be noncovalently fixed to a carbon nanotube and serve as ligand for a Pd ion. The catalyst was used to generate diphenylacetylene from iodobenzene and phenylacetylene (Table 3 entry 4).<sup>117</sup> The authors attempted to reuse the catalyst but a notable drop in yield was observed after the second run. Although the obtained yield is comparable to other catalysts, the lack of recyclability and more importantly substrate diversity limits the usefulness of this system.

The catalytic system developed by Bazgir et al. for Suzuki reactions could also be used for the Sonogashira coupling under environmentally benign conditions (Table 3 entry 5).<sup>95</sup> The coupling products were obtained in high yields using water-ethanol as reaction mixture and electron-donating and electron-withdrawing substituents are tolerated on the phenylalkyne reagent. While the catalyst recycling was only tested for the Suzuki reactions it can be assumed that similar recyclability (five times without significant loss in activity) can be achieved in the case of the Sonogashira reaction as well.

The group of Zhao developed a mesoporous silica catalyst bridged by Pd(II) centers (Pd(II)-PMO-P-2) for the reaction of phenylacetylene with aryl iodides and bromides (Table 3 entry 6).<sup>118</sup> The catalyst allows the transformation of the starting materials with both electron-donating and electron-withdrawing substituents on the halide in high yields using water as a solvent. The authors showed that the catalyst could be recycled up to seven times without significant decrease in yield and that no palladium ions were leaching out of the catalyst.

The modified polyacrylamide nanoparticles with incorporated Pd centers (PAA-Pd-NP) developed by Gholinejad could not only be used for the Suzuki reaction (*vide supra*), but also for the Sonogashira reaction (Table 3 entry 7).<sup>68</sup> A variety of aromatic iodides and bromides were successfully coupled to terminal alkynes with aryl as well as alkyl substituents. The products were obtained in high yields irrespective of the nature of the substituent on the aryl halide. Catalyst recycling experiments were not performed for the Sonogashira reaction but the same catalyst was recyclable five times before a significant drop in yield was observed under Suzuki conditions.

A catalyst based on SiO<sub>2</sub> particles decorated with acetylacetone as anchor for Pd nanoparticles was developed for and used in the Sonogashira reaction (Table 3 entry 8).<sup>119</sup> The reaction can be carried out using water and electron-donating and electron-withdrawing substituents can be present on the aryl halide. Although iodoarenes gave the products in high yields and short reaction times, the application of aryl bromides and chlorides resulted in substantially lower yields and longer reaction times. The catalyst could be recycled five times before a notable drop in yield was observed.

Sajadi found that when halloysite nanotubes were decorated with cyclodextrin they could bind a Pd ion and act as a catalyst for the coupling of various terminal alkynes and aryl halides (Table 3 entry 9).<sup>120</sup> It was found that aryl

iodides give much higher yields than bromides or chlorides. No difference was found with regard to the nature of the substituent on the aryl halide and both aromatic and aliphatic alkynes could be used. The catalyst could be reused and only exhibited a decrease in activity after the fifth consecutive reaction.

A magnetically separable catalyst ( $\text{Fe}_3\text{O}_4@-\text{NH}_2@$ Murexide@Pd) was used by Abid et al. to couple bromo- and iodoarenes with phenylacetylene (Table 3 entry 10).<sup>69</sup> Substituents with both electron-donating and electron-withdrawing effects were well tolerated and the products were obtained in high yields using a water-ethanol mixture as a solvent. Recycling of this catalyst was only tested using the Suzuki reaction and a significant drop in yield after the fourth run was noted.

Similar results were obtained by Roy et al. using a Pd-doped  $\text{CoFe}_2\text{O}_4$  nanoparticle-based catalyst (Table 3 entry 11).<sup>121</sup> While a variety of substrates did undergo the desired Sonogashira coupling, the authors found that aromatic alkynes, in general, worked better than aliphatic alkynes and placing a substituent into the *ortho* position of the halide also decreased the yield. The catalyst could be recycled five times with a small decrease in yield.

Another example of palladium combined with a ferrite material was reported by Gholinejad and Ahmadi.<sup>128</sup> The authors used  $\text{SiO}_2$  microparticles to anchor both palladium and copper ferrite nanoparticles and use this as catalyst for the Sonogashira reaction. Both substrate scope and yields are comparable to other reported methods but the reaction has to be performed in the uncommon solvent dimethyl acetamide (DMA).

Nitrogen functionalized halloysite was also used to immobilize palladium and then this material was applied as a catalyst for the Sonogashira reaction using ethanol as solvent (Table 3 entry 12).<sup>122</sup> Terminal alkynes with aromatic and aliphatic side chain could be used in combination with a variety of iodo-, bromo-, and chloroarenes. Although the nature of an additional substituent on the aromatic ring appeared mainly unimportant in determining the product yield, it was found that significantly less product formed when arylchlorides and -bromides were used. The catalyst could be reused five times before losing its activity.

Banerjee et al. showed that MCM-48 impregnated with Pd nanoparticles could be used for a variety of reactions, including the Sonogashira coupling.<sup>123</sup> The reaction was performed in ethanol as a solvent and a variety of terminal alkynes and substituted haloarenes were suitable substrates (Table 3 entry 13). Although with aryl iodides generally high yields were obtained, aryl bromides gave the desired products in lower amounts. Unfortunately the recycling of the catalyst was not tested.

An extremely low palladium loading of 0.005 mol% was used by Karami et al. for the coupling of aryl iodides with phenylacetylene (Table 3 entry 14).<sup>124</sup> The reactions worked very well for aryl iodides; however, when switching to bromides and chlorides the solvent had to be changed from ethanol to DMF and the catalyst loading had to be increased as well, to ensure product formation.

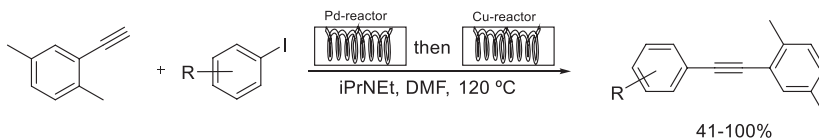
The catalyst consists of an Auramine-palladacycle tethered to the surface of a TiO<sub>2</sub> nanoparticle.

Qi and his group used chitosan-montmorillonite-palladium hybrid nanospheres to couple phenylacetylenes with aryl iodides (Table 3 entry 15).<sup>125</sup> The aryl iodides could bear electron-donating and electron-withdrawing substituents with similar results but it was noted that substituents in the *ortho* position lowered the yield, most likely due to steric hindrance. Although the original catalyst used only gave satisfactory results in eight consecutive uses, in terms of recyclability, a slight alteration in the support composition toward more montmorillonite content allowed for up to 10 runs using the same catalyst without a drop in activity. Likewise, only minimal Pd leaching was observed when reusing the catalyst.

Rashinkar et al. showed that a silver-NHC complex tethered to magnetic nanoparticles (MNPFeTriazNHC@Ag) could be used for the coupling of phenylacetylenes and different haloarenes (Table 3 entry 16).<sup>126</sup> Although aryl iodides and aryl bromides gave the desired products in high yield, the use of aryl chlorides yielded significantly lower product formation. Both electron-donating and electron-withdrawing substituents were well tolerated on the aryl halide, and only electron-donating substituents were tested on the phenylacetylene. It was shown that the catalyst could be recycled eight times before a significant drop in yield occurs.

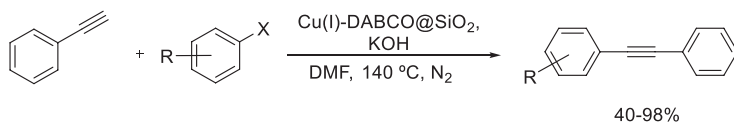
John et al. developed a Pd<sub>6</sub>L<sub>6</sub> nanocluster that could act as a catalyst for the Sonogashira coupling.<sup>127</sup> Although the authors originally used the clusters as a homogeneous catalyst in water as the solvent, it was found that the catalyst became heterogeneous when changing the solvent to toluene (Table 3 entry 17). While this is beneficial in terms of catalyst recovery and recycling, it is detrimental from an environmental point of view as a green solvent (water) is changed into the not green solvent toluene.

Lee and his coworkers developed a catalyst for the Sonogashira reaction to be applied in a continuous flow system.<sup>129</sup> A dual reactor with a Pd and Cu inner coating furnished the coupling products for a variety of aryl iodides with 2,5-dimethyl phenylacetylene in mostly high yields (Scheme 41). Both electron-donating and electron-withdrawing substituents were tolerated in the aryl iodide and the catalyst could be used in up to 10 runs of the flow system without decreased performance. Unfortunately high temperature and DMF as the solvent were needed.



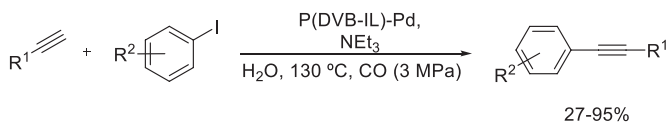
**SCHEME 41** The Sonogashira reaction of 2,5-dimethyl phenylacetylene with aryl iodides carried out in a continuous flow system.

Hajipour and his coworkers also developed a heterogeneous, palladium-free version of the Sonogashira reaction.<sup>130</sup> Phenylacetylene was coupled with a variety of aryl iodides in high yields. Although aryl bromides did give the coupling product as well, notably lower yields were obtained (Scheme 42). The catalyst used was formed from SiO<sub>2</sub> functionalized with DABCO that coordinated a Cu ion. Unfortunately a strong base in DMF at high temperatures had to be used, negating the positive effect of not needing a palladium catalyst.



**SCHEME 42** The Sonogashira coupling catalyzed by an immobilized Cu catalyst.

An interesting variation of the Sonogashira reaction was developed by Xia et al.<sup>131</sup> A cross-linked polymer-supported ionic liquid was used to immobilize palladium and employed in the carbonylative Sonogashira coupling using terminal alkynes, aryl iodides, and carbon monoxide (Scheme 43). The reaction is performed in water under 3 MPa CO pressure at 130°C. High yields were obtained for a variety of substrates with the exception of butylacetylene giving a low yield. Recycling of the catalyst was possible five times with only a slight decrease in yield.



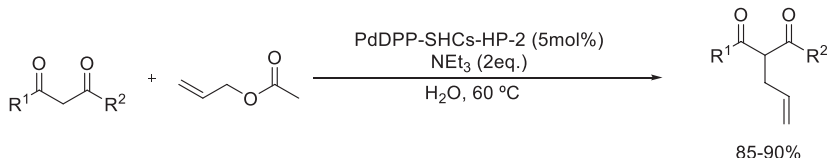
**SCHEME 43** The Sonogashira reaction catalyzed by a cross-linked polymer-supported ionic liquid-immobilized palladium.

### 3.6.8 The Tsuji-Trost allylation

The Tsuji-Trost allylation<sup>132, 133</sup> is another example of the palladium-catalyzed coupling reactions that has originated as a homogeneous catalytic reaction and experiences a trend toward the application of heterogeneous catalytic systems. This coupling has not been as widely used as the other systems mentioned before; however, a few examples using a heterogeneous catalytic systems have been developed as summarized below.

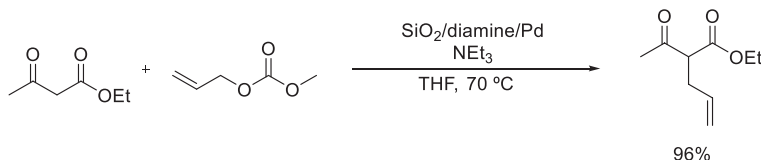
Further extending their investigations Li, Zhang and coworkers demonstrated the applicability of their new catalytic system (PdDPP-SHCs-HP-2) in the Tsuji-Trost reaction between various 1,3-dicarbonyl compounds and allylacetate.<sup>66</sup> Cyclic and acyclic substrates, both 1,3-diketones and diester were suitable substrates for the transformation (Scheme 44). The reaction is performed in water as solvent and yields the products in high yields with excellent

selectivities for the monoallylated product. The recycling of the catalyst was possible nine times and ICP analysis showed only a slight decrease in Pd content (1.3 wt% vs 1.4 wt%) of the catalyst.



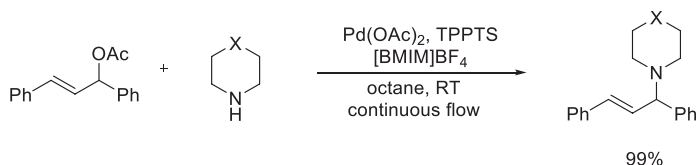
**SCHEME 44** The Tsuji-Trost reaction between various 1,3-dicarbonyl compounds and allyl acetate catalyzed by an organosilane nanoparticle-supported Pd catalyst.

Noda et al. developed a heterogeneous catalyst by grafting Pd(II) to a silica surface using a diamine tether and tested this catalytic system in a similar reaction as described before.<sup>134</sup> The Tsuji-Trost reaction between ethyl acetoacetate and allyl methylcarbonate could be performed in excellent yields and high selectivities for the monoallylated product (Scheme 45). The reaction could be performed with a very low amount of the metal catalyst (0.6 mol% Pd) but unfortunately THF had to be used as the solvent for the reaction to ensure optimum performance.



**SCHEME 45** The Tsuji-Trost reaction of ethyl acetoacetate and allyl methylcarbonate catalyzed by a silica-supported Pd catalyst.

Yang et al. used an ionic liquid to trap a palladium complex as a heterogeneous catalyst in the continuous flow Tsuji-Trost allylation of (*E*)-1,3-diphenylallylacetate and amine-based nucleophiles.<sup>135</sup> Excellent conversion toward the products was obtained (Scheme 46) and it was shown that the continuous flow system performed significantly better than a corresponding batch process. No traces of the catalyst could be detected in the product even after prolonged reaction times.



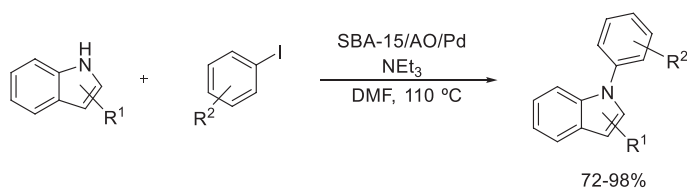
**SCHEME 46** The Tsuji-Trost reaction of (*E*)-1,3-diphenylallylacetate and amine-based nucleophiles catalyzed by an ionic liquid-immobilized Pd catalyst.

### 3.6.9 Coupling reactions not involving a C–C bond formation

In addition to the C–C bond forming reactions presented before, a variety of other coupling reactions are found in the literature. The Ullmann or Buchwald-Hartwig couplings are the most prominent examples for C–N bond formation but C–O and C–S bonds can be formed by cross-coupling reactions as well. The following section describes selected examples for the formation of carbon-heteroatom bonds using a heterogeneous catalyst that follow the principles of green chemistry.

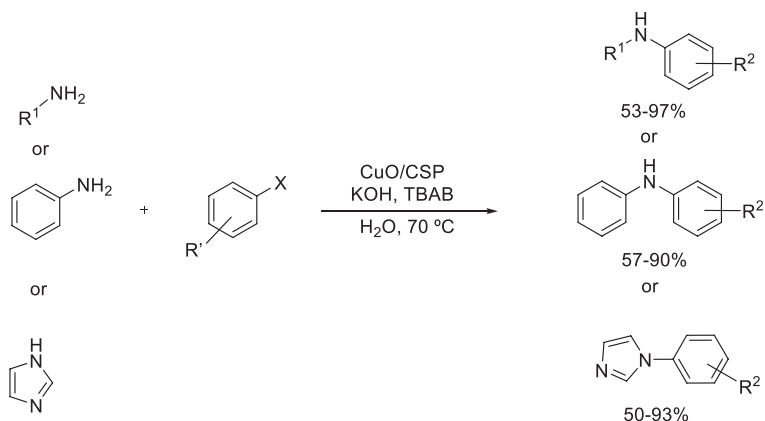
#### 3.6.9.1 C–N bond-forming reactions

Ghorbani-Vaghei et al. reported that amidoxime-functionalized SBA-15 could immobilize palladium and serve as a heterogeneous catalyst for the N-arylation of indoles.<sup>136</sup> Indoles with different substitution patterns were reacted with a selection of iodoarenes containing both electron-donating and electron-withdrawing substituents and the corresponding products were obtained in high yields (Scheme 47). The catalyst could be recycled six times by simple filtration without losing its activity. While the authors claim the reaction to be superior to a number of known literature protocols in terms of yield and conversion, from a green point of view, the use of DMF and elevated temperature is a drawback.



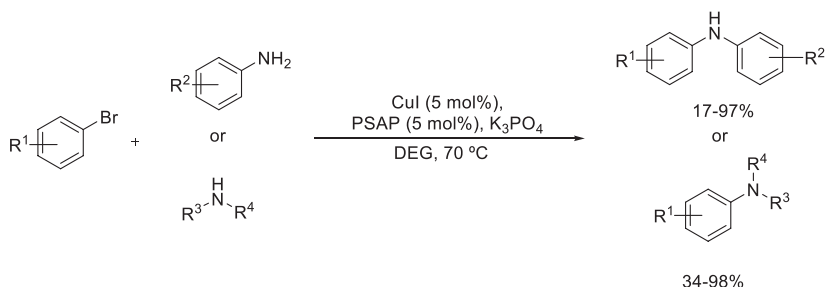
**SCHEME 47** N-arylation of indoles with an SBA-15 immobilized Pd catalyst.

Zhu et al. developed a functionalized chitosan as a support for a copper salt to form a heterogeneous catalyst that was able to efficiently catalyze the arylation of a variety of nitrogen-containing molecules, commonly known as the Ullmann coupling, using water as the solvent.<sup>137</sup> Aliphatic and aromatic amines as well as imidazoles were easily arylated in good to excellent yields (Scheme 48). Although electron-donating and electron-withdrawing substituents on the aryl halide are tolerated, lower yields are obtained for strongly electron-withdrawing groups on the amine. The greenness of the reaction was reduced by the fact that a phase transfer agent and a strong base had to be used to obtain high conversions.



**SCHEME 48** The Ullmann C–N coupling catalyzed by a chitosan-supported CuO catalyst.

Yi and coworkers used a polystyrene-bound diamine (PSAP) as ligand system to complex a copper ion and create a heterogeneous catalytic system for the C–N bond formation between amines (aromatic as well as aliphatic) and bromoarenes.<sup>138</sup> The yield of the reaction was highly dependent on the nature of the substituent on the aromatic systems. When electron-withdrawing substituents were present on either reaction partner a dramatic decrease in yield was observed (Scheme 49). Diethylene glycol was used as the solvent for the reaction. While the catalyst could, in principle, be reused, it was found that the copper salt is leaching out and had to be replenished to maintain the catalytic activity.

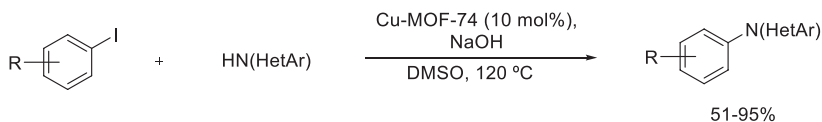


**SCHEME 49** A polystyrene-bound diamine (PSAP)-immobilized copper-catalyzed Ullmann C–N coupling.

Xie et al. described the coupling of nitrogen-containing heterocycles with aryl iodides using Cu-MOF-74 as a heterogeneous catalyst.<sup>139</sup> Although the desired products were obtained with a variety of different substituted aromatic iodides, it was found that when electron-withdrawing groups were present the yield was notably lower than in the case of electron-donating substituents, in

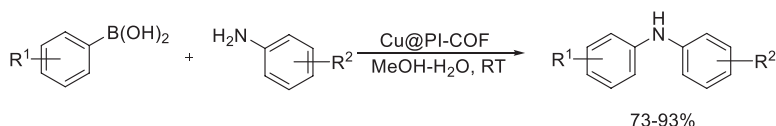
428 Heterogeneous catalysis in sustainable synthesis

agreement with the earlier examples. Likewise, the presence of a substituent in the *ortho* position on the aromatic substrate inhibited product formation and lower yields were obtained (Scheme 50). The authors showed that the catalyst could be reused six times with only a slight drop in yield.



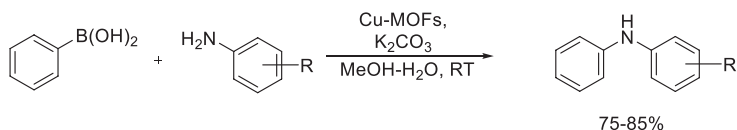
**SCHEME 50** The coupling reaction of nitrogen-containing heterocycles with aryl iodides using a Cu-containing metal-organic framework MOF-74.

The Chan-Lam coupling between aromatic amines and aryl boronic acids was performed by Zhang and coworkers using a copper catalyst immobilized on a polyimide covalent organic framework (Cu@PI-COF).<sup>140</sup> A large variety of substituents of both electronic natures were tolerated on the starting materials giving the desired products in high yields (Scheme 51). The reaction is performed in a water-methanol mixture as environmentally benign solvent and the catalyst could be recycled eight times with only a slight decrease in product yield.



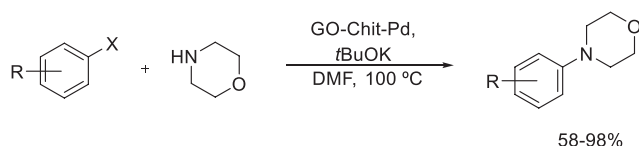
**SCHEME 51** The Chan-Lam coupling between aromatic amines and aryl boronic acids catalyzed by a polyimide covalent organic framework-immobilized Cu (Cu@PI-COF).

Mokhtari et al. performed the Chan-Lam coupling using a copper-based metal-organic framework as catalyst prepared via a ball-milling strategy (Cu<sub>2</sub>(BDC)<sub>2</sub>(BPY)-MOF).<sup>141</sup> The products of the coupling of phenylboronic acid with aniline derivatives were obtained in good yields (Scheme 52). The authors claimed the catalyst to be recyclable several times but no exact data was given in the report.



**SCHEME 52** The Chan-Lam coupling catalyzed by a copper-based metal-organic framework (Cu<sub>2</sub>(BDC)<sub>2</sub>(BPY)-MOF).

Sarvestani and Azadi showed that the Buchwald-Hartwig coupling could also be performed using heterogeneous catalysis. The catalyst was prepared by functionalizing graphene oxide with chitosan that acted as support for palladium nanoparticles (GO-Chit-Pd).<sup>142</sup> Morpholine as well as a few other amines were coupled with aryl halides in good yields (Scheme 53). It was found that secondary amines perform better than primary ones and chlorides give a slightly lower yield than the corresponding bromides or iodides. The nature of the aromatic substituent was found to be negligible as only a slight decrease in yield was observed for strongly electron-withdrawing substituents.

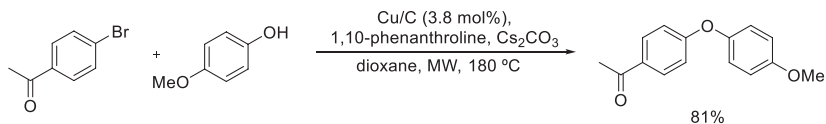


**SCHEME 53** A graphene oxide-chitosan-immobilized Pd nanoparticles (GO-Chit-Pd)-catalyzed Buchwald-Hartwig coupling.

Although the reported examples include a broad variety of support materials, as of the metal component, copper and palladium dominated the applications mostly in the form of immobilized metal complexes or nanoparticles.

### 3.6.9.2 C–O bond-forming reactions

Kappe et al. showed that an Ullmann-type reaction to form a biaryl ether is possible using simple Cu/C as the catalyst.<sup>93</sup> Although the product is obtained in high yield, the solvent used (dioxane) and the high reaction temperature have a negative impact on the greenness of the reaction (Scheme 54). The simplicity of the catalyst as well as the use of microwave heating and short reaction times can be positively noted from a green point of view.

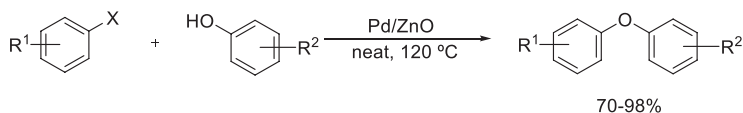


**SCHEME 54** Synthesis of biaryl ethers by a microwave-assisted Cu/C-catalyzed Ullmann coupling.

Hosseini-Sarvari and Razmi reported that palladium supported on zinc oxide nanoparticles promoted the coupling of phenols and aryl halides under solvent-free

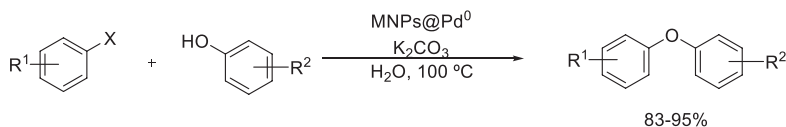
### 430 Heterogeneous catalysis in sustainable synthesis

conditions.<sup>143</sup> The reaction performed well for a variety of substituents on both the aryl halide and the phenol reaction partner (Scheme 55). No significant difference in yield was observed depending on the electronic nature of the substituent or the halide used. The authors showed that the catalyst could be recycled five times with only a minimal decrease in yield but also found that the repeated reactions required significantly longer times to reach high conversions.



**SCHEME 55** A solvent-free synthesis of biaryl ethers catalyzed by a ZnO nanoparticle-immobilized Pd catalyst.

A similar range of products was prepared by Moghaddam and Eslami using a magnetically recoverable palladium catalyst. The catalytically active palladium complex was tethered to magnetic Fe<sub>3</sub>O<sub>4</sub> nanoparticles.<sup>144</sup> Aryl iodides, bromides, and chlorides were coupled with substituted phenols and the products were obtained in high yields (Scheme 56). Water was used as the solvent and catalyst recycling was possible seven times with only a slight decrease in yield.

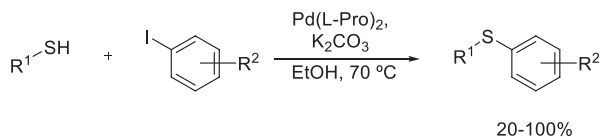


**SCHEME 56** Synthesis of biaryl ethers by magnetically recoverable immobilized Pd nanoparticles (MNP, magnetic nanoparticle).

#### 3.6.9.3 C–S bond-forming reactions

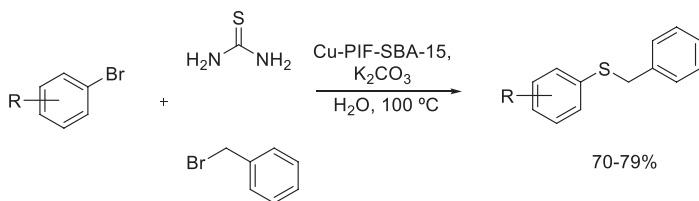
While rare, there are some reports that describe the formation of C–S bonds by heterogeneous catalytic coupling reactions.

The C–S cross-coupling between different thiols and aryl iodides was successfully achieved using a palladium proline complex (Pd(L-Pro)<sub>2</sub>).<sup>145</sup> The palladium complex acted as heterogeneous catalyst in ethanol as the solvent and the products were obtained in good yields when the aryl halide used possessed an electron-withdrawing substituent. On the thiol moiety mostly aromatic thiols were tested (Scheme 57). When a strongly electron-withdrawing substituent (such as fluoride) was placed on the thiol, the reactivity is shut down and no product was obtained. The catalyst could be recycled five times with only a slight decrease in yield.



**SCHEME 57** The C–S cross-coupling of thiols with aryl iodides catalyzed by palladium prolinato complex (Pd(L-Pro)<sub>2</sub>).

In another example, a catalyst based on copper grafted onto SBA-15 (Cu-PIF-SBA-15) was used by Bhaumik et al. for the C–S bond formation reaction of aryl bromides and chlorides with thiourea and benzyl bromide.<sup>146</sup> The three-component coupling provided the desired products in good yields with aryl halides bearing substituents of all electronic nature (Scheme 58). Water was used as the solvent and the catalyst was recyclable six times with negligible decrease in yield.



**SCHEME 58** Synthesis of aryl-thioethers by a three-component coupling with SBA-15 grafted copper catalyst.

### 3.6.10 Conclusions and outlook

As can be seen by the examples described in this chapter, the application of heterogeneous catalytic systems became a frequently researched topic in the field of cross-coupling reactions. There are a multitude of driving forces for this development but the increasing environmental concerns are often the most important initiative in the progress. Heterogeneous catalytic applications carry the promise of being environmentally friendly due to the potentially reduced release of heavy metals into the product and environment or the common possibility to reuse the catalyst. Although these are valid points, it is often necessary to take a closer look at the performance of the catalyst as well as the preparation of the catalyst before a heterogeneous system can be claimed to be environmentally friendly. Most studies dealing with a new heterogeneous catalyst perform some tests for recyclability. Often a slight decrease in product yield is noted without further investigation on the reason of that decrease. It is only in rare cases that, e.g., leaching of the catalyst is discussed by measuring

the metal content of the catalyst (and the product solution). Many catalytic systems require some sort of treatment or reactivation before they can be reused, thus increasing the environmental impact. Another often overlooked point is the synthesis of the catalyst itself. The preparation of many of the discussed catalysts requires multistep synthesis using harmful reactions and producing extended amount of waste. This should be factored in when evaluating the greenness of a new catalytic system. In short, a holistic evaluation of a process is needed to determine its overall greenness or environmental sustainable nature.

Even though there are still many challenges to overcome, the use of heterogeneous systems for cross-coupling reactions is becoming more and more prominent and the research in this field is growing. The potential and the advantages of heterogeneous catalytic systems will become increasingly important with the continued demand and necessity to implement greener synthetic methods. The examples described in the chapter provide an overview on what can already be done using heterogeneous catalysis in cross-coupling reactions and also shine some light on what problems remain to be solved and finally indicate the directions of future research in this field.

## References

1. Heck, R. F.; Nolley, J. P. Palladium-Catalyzed Vinylic Hydrogen Substitution Reactions With Aryl, Benzyl, and Styryl Halides. *J. Org. Chem.* **1972**, *37*, 2320–2322.
2. Tamao, K.; Sumitani, K.; Kumada, M. Selective Carbon-Carbon Bond Formation by Cross-Coupling of Grignard Reagents With Organic Halides. Catalysis by Nickel-Phosphine Complexes. *J. Am. Chem. Soc.* **1972**, *94*, 4374–4376.
3. <https://www.nobelprize.org/prizes/chemistry/2010/heck/lecture/> (accessed 5 January 2021).
4. Negishi, E. Magical Power of Transition Metals: Past, Present, and Future (Nobel Lecture). *Angew. Chem. Int. Ed.* **2011**, *50*, 6738–6764.
5. Suzuki, A. Cross-Coupling Reactions of Organoboranes: An Easy Way to Construct C-C Bonds (Nobel Lecture). *Angew. Chem. Int. Ed.* **2011**, *50*, 6722–6737.
6. Johansson Seechurn, C. C. C.; Kitching, M. O.; Colacot, T. J.; Snieckus, V. Palladium-Catalyzed Cross-Coupling: A Historical Contextual Perspective to the 2010 Nobel Prize. *Angew. Chem. Int. Ed.* **2012**, *51*, 5062–5085.
7. *The Nobel Prize in Chemistry 2010—Richard F. Heck, Ei-ichi Negishi, Akira Suzuki*. Nobel-Prize.org (accessed 10 January 2021).
8. Lamblin, M.; Nassar-Hardy, L.; Hierso, J.-C.; Fouquet, E.; Felpin, F.-X. Recyclable Heterogeneous Palladium Catalysts in Pure Water: Sustainable Developments in Suzuki, Heck, Sonogashira and Tsuji–Trost Reactions. *Adv. Synth. Catal.* **2010**, *352*, 33–79.
9. Astruc, D. Palladium Nanoparticles as Efficient Green Homogeneous and Heterogeneous Carbon–Carbon Coupling Precatalysts: A Unifying View. *Inorg. Chem.* **2007**, *46*, 1884–1894.
10. Díaz-Sánchez, M.; Díaz-García, D.; Prashar, S.; Gómez-Ruiz, S. Palladium Nanoparticles Supported on Silica, Alumina or Titania: Greener Alternatives for Suzuki–Miyaura and Other C–C Coupling Reactions. *Environ. Chem. Lett.* **2019**, *17*, 1585–1602.

11. Yin, L.; Liebscher, J. Carbon–Carbon Coupling Reactions Catalyzed by Heterogeneous Palladium Catalysts. *Chem. Rev.* **2007**, *107*, 133–173.
12. Heravi, M. M.; Heidari, B.; Ghavidel, M.; Ahmadi, T. Non-Conventional Green Strategies for NHC Catalyzed Carbon-Carbon Coupling Reactions. *Curr. Org. Chem.* **2017**, *21*, 2249–2313.
13. Kerru, N.; Maddila, S.; Jonnalagadda, S. B. Design of Carbon-Carbon and Carbon-Heteroatom Bond Formation Reactions Under Green Conditions. *Curr. Org. Chem.* **2019**, *23*, 3154–3190.
14. Karimi, B.; Behzadnia, B.; Farhangi, E.; Jafari, E.; Zamani, A. Recent Application of Polymer Supported Metal Nanoparticles in Heck, Suzuki and Sonogashira Coupling Reactions. *Curr. Org. Synth.* **2010**, *7*, 543–567.
15. Vargas, C.; Balu, A. M.; Campelo, J. M.; Gonzalez-Arellano, C.; Luque, R.; Romero, A. A. Towards Greener and More Efficient C-C and C-Heteroatom Couplings: Present and Future. *Curr. Org. Synth.* **2010**, *7*, 568–586.
16. Molnár, Á. Sustainable Heck Chemistry With New Palladium Catalysts. *Curr. Org. Synth.* **2011**, *8*, 172–186.
17. Molnár, Á. Efficient, Selective, and Recyclable Palladium Catalysts in Carbon-Carbon Coupling Reactions. *Chem. Rev.* **2011**, *111*, 2251–2320.
18. Polshettivar, V.; Molnár, Á. Silica-Supported Pd Catalysts for Heck Coupling Reactions. *Tetrahedron* **2007**, *30*, 6949–6976.
19. Molnár, Á., Ed. *Palladium-Catalyzed Coupling Reactions: Practical Aspects and Future Developments*; Wiley-VCH: Weinheim, 2013.
20. Molnár, Á. Catalyst Recycling in Palladium-Catalyzed Carbon-Carbon Coupling Reactions. In *Palladium-Catalyzed Coupling Reactions: Practical Aspects and Future Developments*; Molnár, Á., Ed.; Wiley-VCH: Weinheim, 2013; pp. 333–386 (chapter 9).
21. Shaughnessy, K. H. Cross-Coupling Reactions in Aqueous Media. In *Palladium-Catalyzed Coupling Reactions: Practical Aspects and Future Developments*; Molnár, Á., Ed.; Wiley-VCH: Weinheim, 2013; pp. 235–286 (chapter 7).
22. Roberts, G. M.; Zhang, S.; Zhao, Y.; Woo, L. K. Improving Reactivity and Selectivity of Aqueous-Based Heck Reactions by the Local Hydrophobicity of Phosphine Ligands. *Tetrahedron* **2015**, *71*, 8263–8270.
23. Lakshminarayana, B.; Mahendar, L.; Ghosal, P.; Sreedhar, B.; Satyanarayana, G.; Subrahmanyam, C. Fabrication of Pd/CuFe<sub>2</sub>O<sub>4</sub> Hybrid Nanowires: A Heterogeneous Catalyst for Heck Couplings. *New J. Chem.* **2018**, *42*, 1646–1654.
24. Kaur, N.; Kaur, G.; Bhalla, A.; Dhau, J. S.; Chaudhary, R. G. Metallosurfactant Based Pd–Ni Alloy Nanoparticles as a Proficient Catalyst in the Mizoroki Heck Coupling Reaction. *Green Chem.* **2018**, *20*, 1506–1514.
25. Mandegani, Z.; Asadi, M.; Asadi, Z.; Mohajeri, A.; Iranpoor, N.; Omidvar, A. A Nano Tetraimine Pd(0) Complex: Synthesis, Characterization, Computational Studies and Catalytic Applications in the Heck–Mizoroki Reaction in Water. *Green Chem.* **2015**, *17*, 3326–3337.
26. Ghorbani-Choghmarani, A.; Tahmasbi, B.; Hudson, R. E. H.; Heidari, A. Supported Organometallic Palladium Catalyst Into Mesoporous Channels of Magnetic MCM-41 Nanoparticles for Phosphine-Free C-C Coupling Reactions. *Microporous Mesoporous Mater.* **2019**, *284*, 366–377.
27. Fan, G.-Z.; Cheng, S.-Q.; Zhu, M.-F.; Gao, X.-L. Palladium Chloride Anchored on Organic Functionalized MCM-41 as a Catalyst for the Heck Reaction. *Appl. Organomet. Chem.* **2007**, *21*, 670–675.

434 Heterogeneous catalysis in sustainable synthesis

28. Nuri, A.; Vucetic, N.; Småt, J.-H.; Mansoori, Y.; Mikkola, J.-P.; Murzin, D. Y. Pd Supported IRMOF-3: Heterogeneous, Efficient and Reusable Catalyst for Heck Reaction. *Catal. Lett.* **2019**, *147*, 1941–1951.
29. Azad, M.; Rostamizadeh, S.; Estiri, H.; Nouri, F. Ultra-Small and Highly Dispersed Pd Nanoparticles Inside the Pores of ZIF-8: Sustainable Approach to Waste-Minimized Mizoroki–Heck Cross-Coupling Reaction Based on Reusable Heterogeneous Catalyst. *Appl. Organomet. Chem.* **2019**, *33*, e4952.
30. Petrucci, C.; Cappelletti, M.; Piermatti, O.; Nocchetti, M.; Pica, M.; Pizzo, F.; Vaccaro, L. Immobilized Palladium Nanoparticles on Potassium Zirconium Phosphate as an Efficient Recoverable Heterogeneous Catalyst for a Clean Heck Reaction in Flow. *J. Mol. Catal. A Chem.* **2015**, *401*, 27–34.
31. Nasrollahzadeh, M.; Azarian, A.; Ehsani, A.; Khalaj, M. Preparation, Optical Properties and Catalytic Activity of TiO<sub>2</sub>@Pd Nanoparticles as Heterogeneous and Reusable Catalysts for Ligand-Free Heck Coupling Reaction. *J. Mol. Catal. A Chem.* **2014**, *394*, 205–210.
32. Sarvi, I.; Gholizadeh, M.; Izadyar, M. Threonine Stabilizer-Controlled Well-Dispersed Small Palladium Nanoparticles on Modified Magnetic Nanocatalyst for Heck Cross-Coupling Process in Water. *Appl. Organomet. Chem.* **2019**, *33*, e4645.
33. Tabatabaei Rezaei, S. J.; Shamseddin, A.; Ramazani, A.; Malekzadeh, A. M.; Asiabi, P. A. Palladium Nanoparticles Immobilized on Amphiphilic and Hyperbranched Polymer-Functionalized Magnetic Nanoparticles: An Efficient Semi-Heterogeneous Catalyst for Heck Reaction. *Appl. Organomet. Chem.* **2017**, *31*, e3707.
34. Jahanshahi, R.; Akhlaghinia, B. Thiophene Methanimine–Palladium Schiff Base Complex Anchored on Magnetic Nanoparticles: A Novel, Highly Efficient and Recoverable Nanocatalyst for Cross-Coupling Reactions in Mild and Aqueous Media. *Catal. Lett.* **2017**, *147*, 2640–2655.
35. Firouzabadi, H.; Iranpoor, N.; Gholinejad, M. 2-Aminophenyl Diphenylphosphinite as a New Ligand for Heterogeneous Palladium-Catalyzed Heck–Mizoroki Reactions in Water in the Absence of Any Organic Co-Solvent. *Tetrahedron* **2009**, *65*, 7079–7084.
36. Lopez-Tejedor, D.; de las Rivas, B.; Palomo, J. M. Ultra-Small Pd(0) Nanoparticles Into a Designed Semisynthetic Lipase: An Efficient and Recyclable Heterogeneous Biohybrid Catalyst for the Heck Reaction Under Mild Conditions. *Molecules* **2018**, *23*, 2358.
37. Taira, T.; Yanagimoto, T.; Sakai, K.; Sakai, H.; Endo, A.; Imura, T. Synthesis of Surface-Active N-Heterocyclic Carbene Ligand and its Pd-Catalyzed Aqueous Mizoroki–Heck Reaction. *Tetrahedron* **2016**, *72*, 4117–4122.
38. Sarkar, S. M.; Rahman, M. L.; Chong, K. F.; Yusoff, M. M. Poly(Hydroxamic Acid) Palladium Catalyst for Heck Reactions and Its Application in the Synthesis of Ozagrel. *J. Catal.* **2017**, *350*, 103–110.
39. Keles, M. Preparation of Heterogeneous Palladium Catalysts Supported on Sporopollenin for Heck Coupling Reactions. *Synth. React. Inorg., Met.-Org., Nano-Met. Chem.* **2013**, *43*, 575–579.
40. Movassagh, B.; Rezaei, N. A Magnetic Porous Chitosan-Based Palladium Catalyst: a Green, Highly Efficient and Reusable Catalyst for Mizoroki–Heck Reaction in Aqueous Media. *New J. Chem.* **2015**, *39*, 7988–7997.
41. Ye, Z.; Zhang, B.; Shao, L.; Xing, G.; Qi, C.; Tao, H. Palladium Nanoparticles Embedded Chitosan/Poly(Vinyl Alcohol) Composite Nanofibers as an Efficient and Stable Heterogeneous Catalyst for Heck Reaction. *J. Appl. Polym. Sci.* **2019**, *136*, 48026.

42. Khalafi-Nezhad, A.; Panahi, F. Immobilized Palladium Nanoparticles on a Silica–Starch Substrate (PNP–SSS): As an Efficient Heterogeneous Catalyst for Heck and Copper-Free Sonogashira Reactions in Water. *Green Chem.* **2011**, *13*, 2408–2415.
43. Suzuka, T.; Nagamine, T.; Ogihara, K.; Higa, M. Mizoroki–Heck Reaction in Water With Polymer-Supported Terpyridine–Palladium Complex Under Aerobic Conditions. *Trans. Mater. Res. Soc. Jpn.* **2010**, *35*, 889–892.
44. Molano, W. A.; Cárdenas, J. C.; Sierra, C. A.; Carriazo, J. G.; Ochoa-Puentes, C. Pd/Halloysite as a Novel, Efficient and Reusable Heterogeneous Nanocatalyst for the Synthesis of *p*-Phenylenevinylene Oligomers. *ChemistrySelect* **2018**, *3*, 4430–4438.
45. Wang, Y.; Dou, L.; Zhang, H. Nanosheet Array-like Palladium-Catalysts Pd,*r*GO@CoAl-LDH Via Lattice Atomic-Confined In Situ Reduction for Highly Efficient Heck Coupling Reaction. *ACS Appl. Mater. Interfaces* **2017**, *9*, 38784–38795.
46. Movassagh, B.; Parvis, F. S.; Navidi, M. Pd(II) Salen Complex Covalently Anchored to Multi-Walled Carbon Nanotubes as a Heterogeneous and Reusable Precatalyst for Mizoroki–Heck and Hiyama Cross-Coupling Reactions. *Appl. Organomet. Chem.* **2015**, *29*, 40–44.
47. Molnár, Á.; Papp, A.; Miklos, K.; Forgó, P. Organically Modified Pd-Silica Catalysts Applied in Heck Coupling. *Chem. Commun.* **2003**, 2626–2627.
48. Molnár, Á.; Papp, A. Efficient Heterogeneous Palladium-Montmorillonite Catalysts for Heck Coupling of Aryl Bromides and Chlorides. *Synlett* **2006**, 3130–3134.
49. Papp, A.; Miklos, K.; Forgó, P.; Molnár, Á. Heck Coupling by Pd Deposited Onto Organic-Inorganic Hybrid Supports. *J. Mol. Catal. A Chem.* **2005**, *229*, 107–116.
50. Papp, A.; Galbács, G.; Molnár, Á. Recyclable Ligand-Free Mesoporous Heterogeneous Pd Catalysts for Heck Coupling. *Tetrahedron Lett.* **2005**, *46*, 7725–7728.
51. Bucsi, I.; Mastalir, Á.; Molnár, Á.; Juhász, K. L.; Kunfi, A. Heck Coupling Reactions Catalysed by Pd Particles Generated In Silica in the Presence of an Ionic Liquid. *Struct. Chem.* **2017**, *28*, 501–509.
52. Khajehzadeh, M.; Moghadam, M. A New Poly(N-Heterocyclic Carbene Pd Complex) Immobilized on Nano Silica: An Efficient and Reusable Catalyst for Suzuki-Miyaura, Sonogashira and Heck-Mizoroki C–C Coupling Reactions. *J. Organomet. Chem.* **2018**, *863*, 60–69.
53. Mohammadi, E.; Movassagh, B. Synthesis of Polystyrene-Supported Pd(II)-NHC Complex Derived From Theophylline as an Efficient and Reusable Heterogeneous Catalyst for the Heck-Matsuda Cross-Coupling Reaction. *J. Mol. Catal. A Chem.* **2016**, *418–419*, 158–167.
54. Rasina, D.; Kahler-Quesada, A.; Ziarelli, S.; Warratz, S.; Cao, H.; Santoro, S.; Ackermann, L.; Vaccaro, L. Heterogeneous Palladium-Catalysed Catellani Reaction in Biomass-Derived  $\gamma$ -Valerolactone. *Green Chem.* **2016**, *18*, 5025–5030.
55. Mangala, K.; Sinija, P. S.; Sreekumar, K. Palladium(II) Supported on Polycarbosilane: Application as Reusable Catalyst for Heck Reaction. *J. Mol. Catal. A Chem.* **2015**, *407*, 87–92.
56. Fahimi, N.; Sardarian, A. R. Aminoclay Decorated With Nano-Pd(0) Picolinic Acid Complex as a Novel Efficient, Heterogeneous, and Phosphine Ligand-Free Catalyst in Heck Reaction Under Solvent-Free Conditions. *Res. Chem. Intermed.* **2017**, *43*, 4923–4941.
57. Khazaei, A.; Khazaei, M.; Rahmati, S. A Green Method for the Synthesis of Gelatin/Pectin Stabilized Palladium Nano-Particles as Efficient Heterogeneous Catalyst for Solvent-Free Mizoroki–Heck Reaction. *J. Mol. Catal. A Chem.* **2015**, *398*, 241–247.
58. Rahmati, S.; Arabi, A.; Khazaei, A.; Khazaei, M. In Situ Stabilization of Pd(0) Nanoparticles Into a Mixture of Natural Carbohydrate Beads: A Novel and Highly Efficient Heterogeneous Catalyst System for Heck Coupling Reactions. *Appl. Organomet. Chem.* **2017**, *31*, e3588.

59. Karthikeyan, P.; Muskawar, P. N.; Aswar, S. A.; Bhagat, P. R.; Sythana, S. K. Development of an Efficient Solvent Free One-Pot Heck Reaction Catalyzed by Novel Palladium (II) Complex-Via Green Approach. *J. Mol. Catal. A Chem.* **2012**, *358*, 112–120.
60. Choudary, B. M.; Chowdari, N. S.; Madhi, S.; Kantam, M. L. A Trifunctional Catalyst for One-Pot Synthesis of Chiral Diols Via Heck Coupling-N-Oxidation-Asymmetric Dihydroxylation: Application for the Synthesis of Diltiazem and Taxol Side Chain. *J. Org. Chem.* **2003**, *68*, 1736–1746.
61. Hajipour, A. R.; Khorsandi, Z.; Karimi, H. Cobalt Nanoparticles Supported on Ionic Liquid- Functionalized Multiwall Carbon Nanotubes as an Efficient and Recyclable Catalyst for Heck Reaction. *Appl. Organomet. Chem.* **2015**, *29*, 805–808.
62. Hajipour, A. R.; Abolfathi, P. Silica-Supported Ni(II)–DABCO Complex: An Efficient and Reusable Catalyst for the Heck Reaction. *Catal. Lett.* **2017**, *147*, 188–195.
63. Hajipour, A. R.; Azizi, G. Iron-Catalyzed Cross-Coupling Reaction: Recyclable Heterogeneous Iron Catalyst for Selective Olefination of Aryl Iodides in Poly(Ethylene Glycol) Medium. *Green Chem.* **2013**, *15*, 1030–1034.
64. Paul, S.; Islam, M. M.; Islam, S. M. Suzuki–Miyaura Reaction by Heterogeneously Supported Pd in Water: Recent Studies. *RSC Adv.* **2015**, *5*, 42193–42221.
65. Len, C.; Bruniaux, S.; Delbecq, F.; Parmar, V. S. Palladium-Catalyzed Suzuki–Miyaura Cross-Coupling in Continuous Flow. *Catalysts* **2017**, *7*, 146–168.
66. Wei, Y.; Mao, Z.; Li, Z.; Zhang, F.; Li, H. Aerosol-Assisted Rapid Fabrication of a Heterogeneous Organopalladium Catalyst With Hierarchical Bimodal Pores. *ACS Appl. Mater. Interfaces* **2018**, *10*, 13914–13923.
67. Tamoradi, T.; Ghorbani-Choghamarani, A.; Ghadermazi, M. Synthesis of a New Pd(0)-Complex Supported on Magnetic Nanoparticles and Study of its Catalytic Activity for Suzuki and Stille Reactions and Synthesis of 2,3-Dihydroquinazolin-4(1H)-One Derivatives. *Polyhedron* **2018**, *145*, 120–130.
68. Gholinejad, M.; Hamed, F.; Biji, P. A Novel Polymer Containing Phosphorus–Nitrogen Ligands for Stabilization of Palladium Nanoparticles: An Efficient and Recyclable Catalyst for Suzuki and Sonogashira Reactions in Neat Water. *Dalton Trans.* **2015**, *44*, 14293–14303.
69. Adib, M.; Yasaei, Z.; Karimi-Nami, R.; Khakyzadeh, V.; Veisi, H. Facile Preparation of Highly Stable and Active Hybrid Palladium Nanoparticles: Effectual, Reusable and Heterogeneous Catalyst for Coupling Reactions. *Appl. Organomet. Chem.* **2016**, *30*, 748–752.
70. Khazaei, A.; Khazaei, M.; Nasrollahzadeh, M. Nano-Fe<sub>3</sub>O<sub>4</sub>@SiO<sub>2</sub> Supported Pd(0) as a Magnetically Recoverable Nanocatalyst for Suzuki Coupling Reaction in the Presence of Waste Eggshell as Low-Cost Natural Base. *Tetrahedron* **2017**, *73*, 5624–5633.
71. Sobhani, S.; Habibollahi, A.; Zeraatkar, Z. A Novel Water-Dispersible/Magnetically Recyclable Pd Catalyst for C–C Cross-Coupling Reactions in Pure Water. *Org. Process Res. Dev.* **2019**, *23*, 1321–1332.
72. Balinge, K. R.; Khiratkar, A. G.; Bhagat, P. R. A Highly Recoverable Polymer-Supported Ionic Salen-Palladium Complex as a Catalyst for the Suzuki-Miyaura Cross Coupling in Neat Water. *J. Organomet. Chem.* **2018**, *854*, 131–139.
73. Boztepe, C.; Künkül, A.; Yasar, S.; Gürbüz, N. Heterogenization of Homogeneous NHC-Pd-Pyridine Catalysts and Investigation of Their Catalytic Activities in Suzuki-Miyaura Coupling Reactions. *J. Organomet. Chem.* **2018**, *872*, 123–134.
74. Kale, D.; Rashinkar, G.; Kumbhar, A.; Salunkhe, R. Facile Suzuki-Miyaura Cross Coupling Using Ferrocene Tethered N- Heterocyclic Carbene-Pd Complex Anchored on Cellulose. *React. Funct. Polym.* **2017**, *116*, 9–16.

75. Pourjavadi, A.; Motamedi, A.; Marvdashti, Z.; Hosseini, S. H. Magnetic Nanocomposite Based on Functionalized Salep as a Green Support for Immobilization of Palladium Nanoparticles: Reusable Heterogeneous Catalyst for Suzuki Coupling Reactions. *Catal. Commun.* **2017**, *97*, 27–31.
76. Shabbir, S.; Lee, S.; Lim, M.; Lee, H.; Ko, H.; Lee, Y.; Rhee, H. Pd Nanoparticles on Reverse Phase Silica Gel as Recyclable Catalyst for Suzuki-Miyaura Cross Coupling Reaction and Hydrogenation in Water. *J. Organomet. Chem.* **2017**, *846*, 296–304.
77. Sahu, D.; Silva, A. R.; Das, P. Facile Synthesis of Palladium Nanoparticles Supported on Silica: An Efficient Phosphine-Free Heterogeneous Catalyst for Suzuki Coupling in Aqueous Media. *Catal. Commun.* **2016**, *86*, 32–35.
78. Hosseini-Sarvari, M.; Razmi, Z. Palladium Supported on Zinc Oxide Nanoparticles as Efficient Heterogeneous Catalyst for Suzuki-Miyaura and Hiyama Reactions Under Normal Laboratory Conditions. *Helv. Chim. Acta* **2015**, *98*, 805–818.
79. Nouri, F.; Rostamizadeh, S.; Azad, M. Post-Synthetic Modification of IRMOF-3 With an Iminopalladacycle Complex and its Application as an Effective Heterogeneous Catalyst in Suzuki-Miyaura Cross-Coupling Reaction in H<sub>2</sub>O/EtOH Media at Room Temperature. *Mol. Catal.* **2017**, *443*, 286–293.
80. Azad, M.; Rostamizadeh, S.; Nouri, F.; Estiri, H.; Fadakar, Y. Pd Nanoparticles at N-Heterocyclic Carbene at ZIF-8 as an Ultrafine, Robust and Sustainable Heterogeneous System for Suzuki-Miyaura Cross Coupling Processes. *Mater. Lett.* **2019**, *236*, 757–760.
81. Ghorbani-Vaghei, R.; Sarmast, N.; Rahmatpour, F. Immobilization of Palladium Nanoparticles as a Recyclable Heterogeneous Catalyst for the Suzuki-Miyaura Coupling Reaction. *C. R. Chim.* **2018**, *21*, 644–651.
82. Boruah, P. R.; Gehlot, P. S.; Kumar, A.; Sarma, D. Palladium Immobilized on the Surface of MMT K 10 With the Aid of [BMIM][BF<sub>4</sub>]: An Efficient Catalyst for Suzuki-Miyaura Cross-Coupling Reactions. *Mol. Catal.* **2018**, *461*, 54–59.
83. Borah, B. J.; Borah, S. J.; Saikia, K.; Dutta, D. K. Efficient Suzuki-Miyaura Coupling Reaction in Water: Stabilized Pd<sup>0</sup>-Montmorillonite Clay Composites Catalyzed Reaction. *Appl. Catal., A Gen.* **2014**, *469*, 350–356.
84. Kandathil, V.; Koley, T. S.; Manjunatha, K.; Dateer, R. B.; Keri, R. S.; Sasidhar, B. S.; Patil, S. A.; Patil, S. A. A New Magnetically Recyclable Heterogeneous Palladium(II) as a Green Catalyst for Suzuki-Miyaura Cross-Coupling and Reduction of Nitroarenes in Aqueous Medium at Room Temperature. *Inorg. Chim. Acta* **2018**, *478*, 195–210.
85. Hemmati, S.; Mehrazin, L.; Pirhayati, M.; Veisi, H. Immobilization of Palladium Nanoparticles on Metformin-Functionalized Graphene Oxide as a Heterogeneous and Recyclable Nanocatalyst for Suzuki Coupling Reactions and Reduction of 4-Nitrophenol. *Polyhedron* **2019**, *158*, 414–422.
86. Qian, Y.; So, J.; Jung, S.-Y.; Hwang, S.; Jin, M.-J.; Shim, S. E. A Graphene Oxide Nanosheet Supported NHC-Palladium Complex as a Highly Efficient and Recyclable Suzuki Coupling Catalyst. *Synthesis* **2019**, *51*, 2287–2292.
87. Verma, A.; Tomar, K.; Bharadwaj, P. K. Nanosized Bispyrazole-Based Cryptand-Stabilized Palladium(0) Nanoparticles: A Reusable Heterogeneous Catalyst for the Suzuki-Miyaura Coupling Reaction in Water. *Inorg. Chem.* **2019**, *58*, 1003–1006.
88. Narkhede, N.; Uttam, B.; Rao, C. P. Calixarene-Assisted Pd Nanoparticles in Organic Transformations: Synthesis, Characterization, and Catalytic Applications in Water for C–C Coupling and for the Reduction of Nitroaromatics and Organic Dyes. *ACS Omega* **2019**, *4*, 4908–4917.

**438** Heterogeneous catalysis in sustainable synthesis

89. Duan, L.; Fu, R.; Xiao, Z.; Zhao, Q.; Wang, J.-Q.; Chen, S.; Wan, Y. Activation of Aryl Chlorides in Water Under Phase-Transfer Agent- Free and Ligand-Free Suzuki Coupling by Heterogeneous Palladium Supported on Hybrid Mesoporous Carbon. *ACS Catal.* **2015**, *5*, 575–586.
90. Papp, A.; Tóth, D.; Molnár, Á. Suzuki–Miyaura Coupling on Heterogeneous Palladium Catalysts. *React. Kinet. Catal. Lett.* **2006**, *87*, 335–342.
91. Molnár, Á. The Use of Chitosan-Based Metal Catalysts in Organic Transformations. *Coord. Chem. Rev.* **2019**, *388*, 126–171.
92. Baran, T.; Sargin, I.; Kaya, M.; Mentés, A. Green Heterogeneous Pd(II) Catalyst Produced from Chitosan-Cellulose Micro Beads for Green Synthesis of Biaryls. *Carbohydr. Polym.* **2016**, *152*, 181–188.
93. Irfan, M.; Fuchs, M.; Glasnov, T. N.; Kappe, C. O. Microwave-Assisted Cross-Coupling and Hydrogenation Chemistry by Using Heterogeneous Transition-Metal Catalysts: An Evaluation of the Role of Selective Catalyst Heating. *Chem. A Eur. J.* **2009**, *15*, 11608–11618.
94. Mohammadkhani, A.; Bazgir, A. Palladium Supported SBA-Functionalized 1,2-Dicarboxylic Acid: The First Pd-Based Heterogeneous Synthesis of Fluorenones. *Mol. Catal.* **2018**, *447*, 28–36.
95. Amini, M. M.; Mohammadkhani, A.; Bazgir, A. Dicarboxylic Acid-Functionalized MCM-41 With Embedded Palladium Nanoparticles as an Efficient Heterogeneous Catalyst for C–C Coupling Reactions. *ChemistrySelect* **2018**, *3*, 1439–1444.
96. Xu, C.; Xiao, Z.-Q.; Li, H.-M.; Han, X.; Wang, Z.-Q.; Fu, W.-J.; Ji, B.-M.; Hao, X.-Q.; Song, M.-P. Ligand-Free Pd/C-Catalyzed One-Pot, Three-Component Synthesis of Aryl-Substituted Benzimidazoles by Hydrogen-Transfer and Suzuki Reactions in Water. *Eur. J. Org. Chem.* **2015**, *34*, 7427–7432.
97. Lipshutz, B. H.; Frieman, B. A.; Lee, C.-T.; Lower, A.; Nihan, D. M.; Taft, B. R. Microwave-Assisted Heterogeneous Cross-Coupling Reactions Catalyzed by Nickel-in-Charcoal (Ni/C). *Chem. Asian J.* **2006**, *1*, 417–429.
98. Labiadh, H.; Said, K.; Ben Chaabane, T.; Ben Salem, R. Development of a Highly Active and Reusable Heterogeneous Catalyst Based on ZnS-Doped Ni (5%) for Suzuki Cross-Coupling Reactions. *J. Mater. Environ. Sci.* **2016**, *7*, 4570–4579.
99. Naeimi, H.; Kiani, F. Inorganic–Organic Hybrid Nano Magnetic Based Nickel Complex as a Novel, Efficient and Reusable Nanocomposite for the Synthesis of Biphenyl Compounds in Green Condition. *Polyhedron* **2019**, *160*, 163–169.
100. Hajipour, A. R.; Abolfathi, P. Novel Triazole-Modified Chitosan@Nickel Nanoparticles: Efficient and Recoverable Catalysts for Suzuki Reaction. *New J. Chem.* **2017**, *41*, 2386–2391.
101. Saroja, A.; Bhat, B. R. Cobalt Schiff Base Immobilized on a Graphene Nanosheet With N, O Linkage for Cross-Coupling Reaction. *Ind. Eng. Chem. Res.* **2019**, *58*, 590–601.
102. Hatanaka, Y.; Hiyama, T. Cross-Coupling of Organosilanes With Organic Halides Mediated by a Palladium Catalyst and Tris(Diethylamino)Sulfonium Difluorotrimethylsilicate. *J. Org. Chem.* **1988**, *53*, 918–920.
103. Rostamnia, S.; Hossieni, H. G.; Doustkhah, E. Homoleptic Chelating N-Heterocyclic Carbene Complexes of Palladium Immobilized Within the Pores of SBA-15/IL (NH<sub>4</sub>CePd@SBA-15/IL) as Heterogeneous Catalyst for Hiyama Reaction. *J. Organomet. Chem.* **2015**, *791*, 18–23.
104. Rostamnia, S.; Zeynizadeh, B.; Doustkhah, E.; Hosseini, H. G. Exfoliated Pd Decorated Graphene Oxide Nanosheets (Pd<sub>NP</sub>-GO/P123): Non-toxic, Ligandless and Recyclable in Greener Hiyama Cross-Coupling Reaction. *J. Colloid Interface Sci.* **2015**, *451*, 46–52.

105. Ismalaj, E.; Strappaveccia, G.; Ballerini, E.; Elisei, F.; Piermatti, O.; Gelman, D.; Vaccaro, L.  $\gamma$ -Valerolactone as a Renewable Dipolar Aprotic Solvent Deriving From Biomass Degradation for the Hiyama Reaction. *ACS Sustain. Chem. Eng.* **2014**, *2*, 2461–2464.
106. Hajipour, A. R.; Abolfathi, P. Nickel Embedded on Triazole-Modified Magnetic Nanoparticles: A Novel and Sustainable Heterogeneous Catalyst for Hiyama Reaction in Fluoride-Free Condition. *Catal. Commun.* **2018**, *103*, 92–95.
107. Thiot, C.; Schmutz, M.; Wagner, A.; Mioskowski, C. A One-Pot Synthesis of (*E*)-Disubstituted Alkenes by a Bimetallic [Rh–Pd]-Catalyzed Hydrosilylation/Hiyama Cross-Coupling Sequence. *Chem. A Eur. J.* **2007**, *13*, 8971–8978.
108. Wu, W.-Y.; Lin, T.-C.; Takahashi, T.; Tsai, F.-Y.; Mou, C. Y. A Palladium Bipyridyl Complex Grafted Onto Nanosized MCM-41 as a Heterogeneous Catalyst for Negishi Coupling. *ChemCatChem* **2013**, *5*, 1011–1019.
109. Price, G. A.; Bogdan, A. R.; Aguirre, A. L.; Iwai, T.; Djuric, S. W.; Organ, M. G. Continuous Flow Negishi Cross-Couplings Employing Silica-Supported Pd-PEPPSI-IPr Precatalyst. *Cat. Sci. Technol.* **2016**, *6*, 4733–4742.
110. Tasler, S.; Lipshutz, B. H. Nickel-on-Charcoal-Catalyzed Aromatic Aminations and Kumada Couplings: Mechanistic and Synthetic Aspects. *J. Org. Chem.* **2003**, *68*, 1190–1199.
111. Stamatopoulos, I.; Giannitsios, D.; Psycharis, V.; Raptopoulou, C. P.; Balcar, H.; Zukal, A.; Svoboda, J.; Kyritsis, P.; Vohlidal, J. A Kumada Coupling Catalyst, [Ni{(Ph<sub>2</sub>P)<sub>2</sub>N(CH<sub>2</sub>)<sub>3</sub>Si(OCH<sub>3</sub>)<sub>3</sub>-P-P<sup>+</sup>}Cl<sub>2</sub>], Bearing a Ligand for Direct Immobilization Onto Siliceous Mesoporous Molecular Sieves. *Eur. J. Inorg. Chem* **2015**, *18*, 3028–3044.
112. Bhowmik, K.; Sengupta, D.; Basu, B.; De, G. Reduced Graphene Oxide Supported Ni Nanoparticles: A High Performance Reusable Heterogeneous Catalyst for Kumada–Corriu Cross-Coupling Reactions. *RSC Adv.* **2014**, *4*, 35442–35448.
113. Sonogashira, K.; Tohda, Y.; Hagiwara, N. A Convenient Synthesis of Acetylenes: Catalytic Substitutions of Acetylenic Hydrogen With Bromoalkenes, Iodoarenes and Bromopyridines. *Tetrahedron Lett.* **1975**, *50*, 4467–4470.
114. Nasrollahzadeh, M.; Atarod, M.; Alizadeh, M.; Hatamifard, A.; Sajadi, S. M. Recent Advances in the Application of Heterogeneous Nanocatalysts for Sonogashira Coupling Reactions. *Curr. Org. Synth.* **2017**, *21*, 708–749.
115. Lin, B.-N.; Huang, S.-H.; Wu, W.-Y.; Mou, C.-Y.; Tsai, F.-Y. Sonogashira Reaction of Aryl and Heteroaryl Halides With Terminal Alkynes Catalyzed by a Highly Efficient and Recyclable Nanosized MCM-41 Anchored Palladium Bipyridyl Complex. *Molecules* **2010**, *15*, 9157–9173.
116. Kozell, V.; McLaughlin, M.; Strappaveccia, G.; Santoro, S.; Bivona, L. A.; Aprile, C.; Gruttadauria, M.; Vaccaro, L. Sustainable Approach to Waste-Minimized Sonogashira Cross-Coupling Reaction Based on Recoverable/Reusable Heterogeneous Catalytic/Base System and Acetonitrile Azeotrope. *ACS Sustain. Chem. Eng.* **2016**, *4*, 7209–7216.
117. Savastano, M.; Arranz-Mascarós, P.; Bazzicalupi, C.; Clares, M. P.; Godino-Salido, M. L.; Gutiérrez-Valero, M. D.; Inclán, M.; Bianchi, A.; García-España, E.; López-Garzón, R. Construction of Green Nanostructured Heterogeneous Catalysts Via Non-Covalent Surface Decoration of Multi-Walled Carbon Nanotubes With Pd (II) Complexes of Azamacrocycles. *J. Catal.* **2017**, *353*, 239–249.
118. Zhu, F.; Zhao, P.; Li, Q.; Yang, D. Synthesis and Characterization of Mesoporous Pd(II) Organometal Nanoplatelet Catalyst for Copper-Free Sonogashira Reaction in Water. *J. Organomet. Chem.* **2018**, *859*, 92–98.

**440** Heterogeneous catalysis in sustainable synthesis

119. Hajipour, A. R.; Shirdashtzade, Z.; Azizi, G. Copper- and Phosphine-Free Sonogashira Coupling Reaction Catalyzed by Silica-(Acac)-Supported Palladium Nanoparticles in Water. *Appl. Organomet. Chem.* **2014**, *28*, 696–698.
120. Sadjadi, S. Palladium Nanoparticles Immobilized on Cyclodextrin- Decorated Halloysite Nanotubes: Efficient Heterogeneous Catalyst for Promoting Copper- and Ligand-Free Sonogashira Reaction in Water–Ethanol Mixture. *Appl. Organomet. Chem.* **2018**, *32*, e4211.
121. Roy, R.; Senapati, K. K.; Phukan, P. Direct Use of Nanoparticles as a Heterogeneous Catalyst: Pd<sup>0</sup>-Doped CoFe<sub>2</sub>O<sub>4</sub> Magnetic Nanoparticles for Sonogashira Coupling Reaction. *Res. Chem. Intermed.* **2015**, *41*, 5753–5767.
122. Sadjadi, S.; Heravi, M. M.; Masoumi, B.; Kazemi, S. S. Pd(0) Nanoparticles Immobilized on Multinitrogen Functionalized Halloysite for Promoting Sonogashira Reaction: Studying the Role of the Number of Surface Nitrogens in Catalytic Performance. *J. Coord. Chem.* **2019**, *72*, 119–134.
123. Banerjee, S.; Khatri, H.; Balasanthiran, V.; Koodali, R. T.; Sereda, G. Synthesis of Substituted Acetylenes, Arylealkyl Ethers, 2-Alkene-4-Ynoates and Nitriles Using Heterogeneous Mesoporous Pd-MCM-48 as Reusable Catalyst. *Tetrahedron* **2011**, *67*, 5717–5724.
124. Karami, K.; Abedanzadeh, S.; Hervés, P. Synthesis and Characterization of Functionalized Titania-Supported Pd Catalyst Deriving From New Orthopalladated Complex of Benzophenone Imine: Catalytic Activity in the Copper-Free Sonogashira Cross-Coupling Reactions at Low Palladium Loadings. *RSC Adv.* **2016**, *6*, 93660–93672.
125. Zeng, M.; Yuan, X.; Zuo, S.; Qi, C. Novel Chitosan-Based/Montmorillonite/Palladium Hybrid Microspheres as Heterogeneous Catalyst for Sonogashira Reactions. *RSC Adv.* **2015**, *5*, 37995–38000.
126. Naikwade, A.; Bansode, P.; Rashinkar, G. Magnetically Retrievable *N*-Heterocyclic Carbene-Silver Complex With Wingtip Ferrocenyl Group for Sonogashira Coupling. *J. Organomet. Chem.* **2018**, *866*, 112–122.
127. Pradhan, S.; Dutta, S.; John, R. P. A Coordination Driven Self-Assembled Pd<sub>6</sub>L<sub>8</sub> Nanoball Catalyses Copper and Phosphine-Free Sonogashira Coupling Reaction in Both Homogeneous and Heterogeneous Formats. *New J. Chem.* **2016**, *40*, 7140–7147.
128. Gholinejad, M.; Ahmadi, J. Assemblies of Copper Ferrite and Palladium Nanoparticles on Silica Microparticles as a Magnetically Recoverable Catalyst for Sonogashira Reaction Under Mild Conditions. *ChemPlusChem* **2015**, *80*, 973–979.
129. Tan, L.-M.; Sem, Z.-Y.; Chong, W.-Y.; Liu, X.; Hendra; Kwan, W. L.; Ken Lee, C.-L. Continuous Flow Sonogashira CC Coupling Using a Heterogeneous Palladium Copper Dual Reactor. *Org. Lett.* **2013**, *15*, 65–67.
130. Hajipour, A. R.; Hosseini, S. M.; Mohammadsaleh, F. DABCO-Functionalized Silica-Copper(I) Complex: A Novel and Recyclable Heterogeneous Nanocatalyst for Palladium-Free Sonogashira Cross-Coupling Reactions. *New J. Chem.* **2016**, *40*, 6939–6945.
131. Wang, Y.; Liu, J.; Xia, C. Cross-Linked Polymer Supported Palladium Catalyzed Carbonylative Sonogashira Coupling Reaction in Water. *Tetrahedron Lett.* **2011**, *52*, 1587–1591.
132. Trost, B. M. Transition Metal Templates for Selectivity in Organic Synthesis. *Pure Appl. Chem.* **1981**, *53*, 2357–2370.
133. Tsuji, J. Catalytic Reactions Via  $\pi$ -Allylpalladium Complexes. *Pure Appl. Chem.* **1982**, *54*, 197–206.
134. Noda, H.; Motokura, K.; Miyaji, A.; Baba, T. Heterogeneous Synergistic Catalysis by a Palladium Complex and an Amine on a Silica Surface for Acceleration of the Tsuji–Trost Reaction. *Angew. Chem. Int. Ed.* **2012**, *51*, 8017–8020.

135. Xiaoming Zhang, X.; Hou, Y.; Ettelaie, R.; Guan, R.; Zhang, M.; Zhang, Y.; Yang, H. Pickering Emulsion-Derived Liquid–Solid Hybrid Catalyst for Bridging Homogeneous and Heterogeneous Catalysis. *J. Am. Chem. Soc.* **2019**, *141*, 5520–5530.
136. Ghorbani-Vaghei, R.; Hemmati, S.; Hamelian, M.; Veisi, H. An Efficient, Mild and Selective Ullmann-Type N-Arylation of Indoles Catalysed by Pd Immobilized on Amidoxime-Functionalized Mesoporous SBA-15 as Heterogeneous and Recyclable Nanocatalyst. *Appl. Organomet. Chem.* **2015**, *29*, 195–199.
137. Yang, B.; Mao, Z.; Zhu, X.; Wan, Y. Functionalised Chitosan as a Green, Recyclable, Supported Catalyst for the Copper-Catalysed Ullmann C–N Coupling Reaction in Water. *Catal. Commun.* **2015**, *60*, 92–95.
138. Yi, Z.; Huang, M.; Wan, Y.; Zhu, X. An Effective Heterogeneous Copper Catalyst System for C–N Coupling and Its Application in the Preparation of 2-Methyl-4-Methoxydiphenylamine (MMDPA). *Synthesis* **2018**, *50*, 3911–3920.
139. Ma, P.; Meng, F.; Wang, N.; Zhang, J.; Xie, J.; Dai, B. Heterogeneous Amorphous Cu–MOF-74 Catalyst for C–N Coupling Reaction. *ChemistrySelect* **2018**, *3*, 10694–10700.
140. Han, Y.; Zhang, M.; Zhang, Y.-Q.; Zhang, Z.-H. Copper Immobilized at a Covalent Organic Framework: An Efficient and Recyclable Heterogeneous Catalyst for the Chan–Lam Coupling Reaction of Aryl Boronic Acids and Amines. *Green Chem.* **2018**, *20*, 4891–4900.
141. Khosravi, A.; Mokhtari, J.; Naimi-Jamal, M. R.; Tahmasebi, S.; Panahi, L. Cu<sub>2</sub>(BDC)<sub>2</sub>(BPY)–MOF: An Efficient and Reusable Heterogeneous Catalyst for the Aerobic Chan–Lam Coupling Prepared Via Ball-Milling Strategy. *RSC Adv.* **2017**, *7*, 46022–46027.
142. Sarvestani, M.; Azadi, R. Buchwald-Hartwig Amination Reaction of Aryl Halides Using Heterogeneous Catalyst Based on Pd Nanoparticles Decorated on Chitosan Functionalized Graphene Oxide. *Appl. Organomet. Chem.* **2018**, *32*, e3906.
143. Hosseini-Sarvari, M.; Razmi, Z. Highly Active Recyclable Heterogeneous Pd/ZnO Nanoparticle Catalyst: Sustainable Developments for the C–O and C–N Bond Cross-Coupling Reactions of Aryl Halides Under Ligand-Free Conditions. *RSC Adv.* **2014**, *4*, 44105–44116.
144. Moghaddam, F. M.; Eslami, M. Immobilized Palladium Nanoparticles on MNPs@A–N–AEB as an Efficient Catalyst for C–O Bond Formation in Water as a Green Solvent. *Appl. Organomet. Chem.* **2018**, *32*, e4463.
145. Santos, B. F.; da Silva, C. D. G.; da Silva, B. A. L.; Katla, R.; Oliveira, A. R.; Kupfer, V. L.; Rinaldi, A. W.; Domingues, N. L. C. C–S Cross-Coupling Reaction Using a Recyclable Palladium Prolinate Catalyst Under Mild and Green Conditions. *ChemistrySelect* **2017**, *2*, 9063–9068.
146. Mondal, J.; Borah, P.; Modak, A.; Zhao, Y.; Bhaumik, A. Cu-Grafted Functionalized Mesoporous SBA-15: A Novel Heterogeneous Catalyst for Facile One-Pot Three-Component C–S Cross-Coupling Reaction of Aryl Halides in Water. *Org. Process Res. Dev.* **2014**, *18*, 257–265.



## Chapter 3.7

# Multicomponent reactions

### 3.7.1. Introduction

Multicomponent reactions (MCRs) are synthetic processes that produce a single product from three or more reactants in a one-pot fashion through a cascade of elementary reactions.<sup>1</sup> The popularity of MCRs lies in the simplicity and versatility of the experimental procedures that unlock the access to a wide range of products through the manifold possibilities of reagent combinations. The first reported example of such reactions, the Strecker synthesis of aminonitriles from aldehydes, emerged as early as 1850 and was soon after industrially developed to produce methionine, a common amino acid used notably as a raw material for drug synthesis.<sup>2</sup> It was not long before the development of other carbonyl-based MCRs followed. Among them are the well-known Mannich reaction that affords  $\beta$ -aminocarbonyls from a nonenolizable aldehyde, a primary or secondary amine and formaldehyde via an iminium intermediate<sup>3</sup>; and the Biginelli reaction that produces dihydropyrimidones from an aldehyde, a  $\beta$ -ketoester, and urea.<sup>4</sup> Both reaction types produce important synthetic building blocks for medicinal chemistry and fine chemicals synthesis.<sup>5, 6</sup> In parallel, isocyanide-based MCRs, first introduced by Passerini in 1921, also became a highly useful tool in the pharmaceutical industry.<sup>7</sup> Another isocyanide-based MCR, the Ugi condensation involving an aldehyde, an amine, a carboxylic acid, and an isocyanide allows the rapid preparation of  $\alpha$ -aminoacyl amide derivatives, essentially serving the purpose of drug discovery by generating large compound libraries.<sup>8</sup>

Due to the straightforward nature of the approach that eliminates multiple isolation/purification steps, provides a high atom economy, limits the generation of potentially toxic intermediates, and minimizes the waste produced, MCRs have emerged as a powerful tool for sustainable organic synthesis gaining increasing interests in the ongoing search for environmentally friendly methods.<sup>6</sup> As of today, hundreds of MCRs are known in the literature and the number is growing steadily. Although some traditional catalyst-free MCRs rely solely on the inherent reactivity of the reagents,<sup>9</sup> efforts have intensified to develop novel and versatile MCRs that often require a catalyst.<sup>10–12</sup> Evidently, the association of this reaction type with heterogeneous catalysis results in a range of methods that combine the advantages of the highly atom-efficient MCRs and the potentially recyclable heterogeneous catalytic systems.<sup>13</sup>

In this chapter the applications of heterogeneous/solid catalysts for MCRs will be reviewed with an emphasis placed on the sustainability of the methods. Sustainable multicomponent syntheses will be thematically discussed based on the nature of the starting materials: carbonyl-based MCRs and isocyanide-based MCRs.

### 3.7.2. Carbonyl-based multicomponent reactions

Carbonyl-based MCRs are widely used in organic chemistry due, in part, to the commercial availability of a large number and variety of aldehydes, but mostly to the reactivity of the C=O bond that requires low activation energy to undergo polarization, thus making it prone to nucleophilic attacks. Carbonyl-based MCRs allow the preparation of a diverse group of heterocycles<sup>14</sup> via cyclization and various other compounds through the formation of aliphatic bonds,<sup>15, 16</sup> often using dearomatization strategies.<sup>17</sup> Both product types will be reviewed separately in this chapter with the heterocycles being sorted according to the size of the ring generated which will be limited up to 6-membered rings.

#### 3.7.2.1 Formation of 6-membered rings with multicomponent reactions

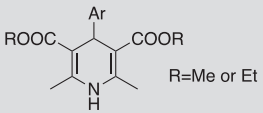
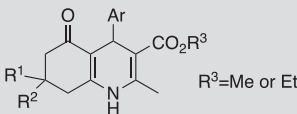
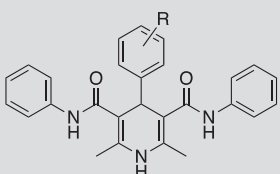
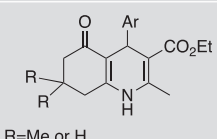
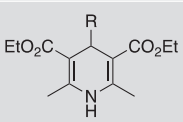
Given the remarkable stability of the 6-membered rings due to the lack of ring strain, these reactions dominate all cyclizations, including MCRs. The Hantzsch synthesis is a widely used strategy to produce pyridine or dihydropyridine derivatives, that are of great medicinal relevance, from an aldehyde, two equivalents of  $\beta$ -ketoester and a nitrogen donor, often ammonium acetate.<sup>18</sup> The reaction proceeds through a series of condensation reactions via two key intermediates—a Knoevenagel product and an ester enamine—leading to the pyridine or dihydropyridine product after the final cyclization step occurring via a third condensation.<sup>18</sup> The reactivity and solubility of the starting materials allow the use of water as the solvent and the application of mild conditions, as reported in some traditional protocols. Despite the apparent environmentally friendly features of these methods, some drawbacks still exist such as the potential toxicity of the commonly used catalysts or the low yields observed. However, heterogeneous catalytic systems have the potential to further decrease the environmental impact of the Hantzsch reaction mainly by employing nontoxic and recyclable catalysts while maintaining mild conditions.<sup>19–30</sup> In addition, most sustainable Hantzsch methods have several other advantages in common, namely, short reaction times, easy reaction workup, and excellent yields. Various clays,<sup>19, 20</sup> silica,<sup>21–23</sup> metal nanoparticles,<sup>24, 25</sup> zeolites,<sup>26</sup> MOF,<sup>27</sup> and ion exchange resins<sup>28–30</sup> have been demonstrated to meet the above-mentioned sustainability criteria. However, these heterogeneous catalysts often have to be combined with a transition metal or a metal oxide.<sup>19–21, 26</sup> Table 1 summarizes multiple examples of the Hantzsch-type multicomponent syntheses to prepare pyridine and dihydropyridine derivatives by heterogeneous catalysis.

**TABLE 1** Heterogeneous catalytic multicomponent Hantzsch reactions.

| Entry  | Catalyst/<br>conditions  | Product | Yield (%) | Ref.   |
|--|--|---------|-----------|--------|
| $\text{XNH}_4 + 2 \text{R}^2\text{C(=O)CH}_2\text{C(=O)OR}^3 + \text{R}^1\text{-CHO} \xrightarrow[\text{conditions}]{\text{catalyst}} \text{R}^3\text{O}_2\text{C-C}_6\text{H}_2\text{(R}^1\text{, R}^2\text{)-CO}_2\text{R}^3$ <p>X=OH, Cl or OAc</p> |  |         |           |        |
| 1  | Montmorillonite-supported Ni <sup>0</sup> -NPs, solvent free, RT, 10–25 min                              |         | 85–95     | 19     |
| 2  | 10% Pd/C/ K10, methanol, MW, 130°C, 90–120 min   |         | 45–95     | 20     |
| 3  | FeCl <sub>3</sub> /SiO <sub>2</sub> NPs, ethanol, reflux, 20–40 min                                      |         | 85–93     | 21     |
| 4  | SiO <sub>2</sub> -SO <sub>3</sub> H, solvent free, 60°C, 4–7 h<br>USY zeolite, ethanol, MW, 110°C 20 min |         | 72–96     | 22, 31 |
| 5  | Silica sulfuric acid, solvent free, 60°C, 25–90 min  |         | 89–96     | 23     |
| 6  | Ni-NPs, solvent free, MW, 60–90 min  |         | 85–96     | 24     |
| 7  | Nano-ZnO, water, 120°C, 1–3 min  |         | 94–96     | 25     |
| 8  | ZnO-beta zeolite, ethanol, RT, 30–60 min   |         | 86–95     | 26     |

Continued

**TABLE 1** Heterogeneous catalytic multicomponent Hantzsch reactions—cont'd

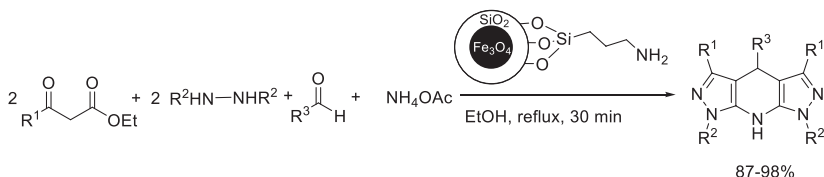
| Entry | Catalyst/<br>conditions                                    | Product  | Yield (%) | Ref. |
|-------|--|--|-----------|------|
| 9     | Isorecticular MOF-3, solvent free, reflux, 4–6 h           |   | 76–94     | 27   |
| 10    | Wang-OSO <sub>3</sub> H, water, 100°C, 60–90 min           |   | 85–96     | 28   |
| 11    | Hydrotalcite, water, 60°C, 120–180 min                     |   | 85–93     | 29   |
| 12    | Nafion-H, PEG 400 water, 50°C, 70–100 min                  |   | 90–96     | 30   |
| 13    | Chitosan-SO <sub>3</sub> H, solvent free, 80°C, 60–240 min |  | 80–95     | 32   |

MOF, metal-organic framework; MW, microwave-assisted reaction; NP, nanoparticles; PEG, poly(ethylene glycol).

A typical example is the one-pot synthesis of polyhydroquinones catalyzed by a ZnO-beta zeolite in ethanol at room temperature leading to excellent yields (Table 1, entry 8).<sup>26</sup> Similarly, the bifunctional catalytic system composed of K-10 montmorillonite and Pd/C efficiently yielded substituted pyridines via an interesting domino cyclization-oxidative aromatization approach (Table 1, entry 2).<sup>20</sup> Metal-free methods have shown similar performances as well, for instance the covalently anchored sulfuric acid on silica gel successfully catalyzed the preparation of Hantzsch 1,4-dihydropyridines under neat conditions (Table 1, entry 5).<sup>22</sup> Nontraditional heterogeneous catalysts that offer additional benefits are also available in the literature. A biocompatible and biodegradable sulfonic acid functionalized chitosan (CS-SO<sub>3</sub>H), easily prepared by the reaction of

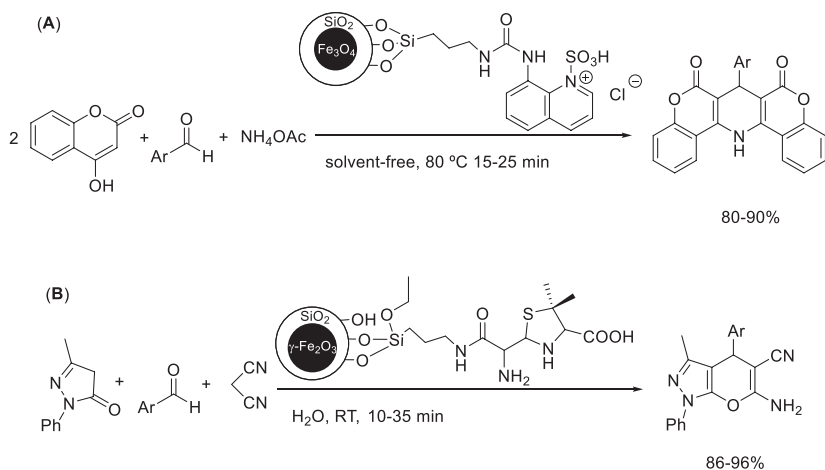
chitosan with chlorosulfonic acid, was employed to catalyze the Hantzsch reaction affording 1,4-dihydropyridines in high yields (Table 1, entry 13).<sup>32</sup> The economical and biosourced catalyst was also found recyclable and retained its activity after five consecutive cycle.

Other than the Hantzsch multicomponent reaction, the preparation of pyridine derivatives can be performed via a one-pot approach starting from four components. A paramagnetic dendritic fibrous nano-silica catalyst functionalized by an amino-bearing ligand was applied to the preparation of tetrahydrodipyrzolo-pyridines via a 6-membered ring cyclization of 1,2-diphenylhydrazine, ethyl acetoacetate, ammonium acetate, and different substituted aromatic aldehydes.<sup>33</sup> Conventional heating under reflux using ethanol as the solvent appeared to be the optimum conditions for the four-component cyclization reaction (Scheme 1). For most reactions, 30 min was necessary to reach completion, which corresponded to a yield of 90% and above. The magnetic catalyst demonstrated excellent recyclability with a slight decrease from 97% to 88% yield after the 10th cycle. The eco-friendliness of this one-pot synthesis of pyrazolopyridine derivatives is only hindered by the laborious synthesis of this catalyst type that requires a step of hydroxylation of the magnetite particles followed by a step of aminoalkylation of the newly attached hydroxyl groups.



**SCHEME 1** Heterogeneous catalytic synthesis of tetrahydrodipyrzolo-pyridines catalyzed by amino propyl-functionalized nano-silica catalyst supported on magnetic, iron oxide-based nanoparticles.

A specialized version of the Hantzsch reaction was applied for the synthesis of 1,4-dihydropyridines by replacing the typical ethyl acetoacetate with the appropriate coumarin derivatives (Scheme 2A) under solvent-free conditions.<sup>34</sup> The authors prepared a magnetic  $\text{Fe}_3\text{O}_4@(\text{CH}_2)_3\text{-urea-quinoline sulfonic acid chloride}$  catalyst for this purpose by immobilizing the sulfonic acid chloride on the surface of the nanoparticles using the urea linkers. The catalyst provided the products in good to excellent yields and was reported to be recyclable, maintaining its activity in three reactions and showing only a minor decline in yields in six consecutive reactions (from 85% to 75%). A similar catalyst ( $6\text{-APA}/\gamma\text{-Fe}_2\text{O}_3@(\text{SiO}_2)$ ), where 6-aminopenicillanic acid (6-APA) was immobilized onto superparamagnetic  $\gamma\text{-Fe}_2\text{O}_3@(\text{SiO}_2)$  nanocomposites was prepared by Saberi et al. (Scheme 2B).<sup>35</sup> The performance of the catalyst was assessed in the multicomponent synthesis of 1,4-dihydropyrano[2,3-*c*]pyrazole derivatives, affording the products in good to excellent yields. The catalyst could be reused in 10 successive reactions without a notable loss of activity.



**SCHEME 2** (A)  $\text{Fe}_3\text{O}_4@ \text{SiO}_2@ (\text{CH}_2)_3$ -urea-quinoline sulfonic acid chloride-catalyzed synthesis of coumarin-based 1,4-dihydropyridines and (B) 6-APA/ $\gamma$ - $\text{Fe}_2\text{O}_3@ \text{SiO}_2$ -catalyzed preparation of substituted 1,4-dihydropyrazolo[2,3-*c*]pyrazoles.

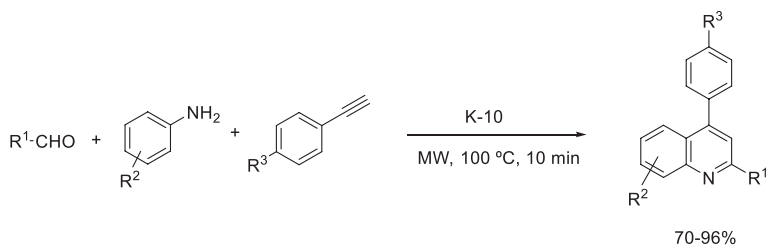
Among the 6-membered ring heterocycles, quinoline derivatives are considered to be one of the most promising biologically relevant compounds. They have demonstrated anticonvulsant, anticancer, and antibacterial properties, to mention but a few.<sup>36</sup> Modified zeolites provided advantageous reaction features for the multicomponent synthesis of complex quinolone derivatives. For instance, copper-containing zeolites catalyzed a regio- and stereoselective [2+2+2] cyclotrimerization cascade of sulfonyl azide, an alkyne, and quinoline, to prepare pyrimido[1,6-*a*]quinolones at room temperature resulting in moderate to high yields: a better performance than its homogeneous counterpart.<sup>36</sup> It should be noted that despite the obvious green aspects of the method, the solvent employed is the toxic and environmentally harmful dichloromethane (Scheme 3).



**SCHEME 3** Multicomponent synthesis of pyrimido[1,6-*a*]quinolones by copper-modified Y-zeolite.

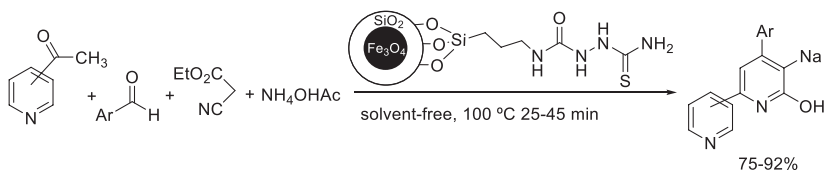
Substituted quinolines can also be prepared by a multicomponent domino reaction of anilines, aldehydes, and terminal alkynes.<sup>37</sup> A reactive imine is formed as a reaction intermediate and reacts further with the alkyne via an

intramolecular addition to finally undergo ring closure and oxidative aromatization. The method combines microwave irradiation with a strong microwave absorber heterogeneous catalyst, montmorillonite K-10. This powerful approach affords the products with high yields in a matter of minutes (Scheme 4).



**SCHEME 4** Microwave-assisted multicomponent synthesis of substituted quinolines by montmorillonite K-10.

The synthesis of bipyridine-5-carbonitriles was achieved by a solvent-free multicomponent reaction of an aromatic aldehyde (substituted benzaldehydes and heterocyclic aldehydes), acetylpyridine, ethylcyanoacetate, and ammonium acetate (Scheme 5).<sup>38</sup> The reaction was catalyzed by a novel magnetic immobilized organocatalyst  $\text{Fe}_3\text{O}_4@(\text{CH}_2)_3\text{-urea-thiourea}$ , which was characterized by a broad range of instrumental methods such as transmission electron microscopy (TEM), thermogravimetric analysis (TGA-DTG), vibrating sample magnetometer (VSM), FT-IR spectroscopy, field emission scanning electron microscopy (FESEM), energy dispersive spectroscopy (EDS), and elemental mapping analysis. The catalyst provided the products in moderate to excellent yields and was also found to be recyclable; in four subsequent reactions the catalytic activity remained stable.



**SCHEME 5**  $\text{Fe}_3\text{O}_4@(\text{CH}_2)_3\text{-urea-thiourea}$ -catalyzed synthesis of bipyridine-5-carbonitriles.

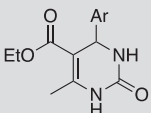
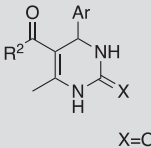
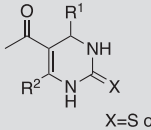
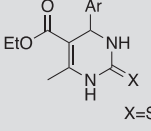
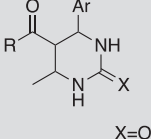
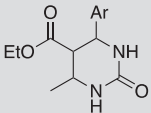
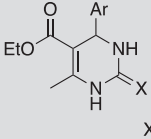
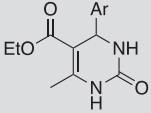
Another one of the established MCRs producing 6-membered rings is the Biginelli reaction, a simple one-pot synthesis involving an aldehyde, an  $\alpha$ -ketoester (or a ketone), and urea for the preparation of dihydropyrimidones.<sup>39</sup> The first step of the mechanism is a condensation step between the aldehyde and urea. The resulting iminium intermediate acts as an electrophile for the nucleophilic addition of the ketoester enol, and the ketone carbonyl finally undergoes

condensation with the amino group of the urea to lead to the cyclized end-product. Conventional methods often suffer from a lack of conversion, employ stoichiometric amount of toxic reagents, and have long reaction times.<sup>40</sup> Thus the Biginelli reaction has received renewed interest in contemporary organic synthesis in order to develop improved protocols in terms of yields and reaction conditions. Heterogeneous catalysis is a potentially great solution to provide high yields under mild reaction conditions. Various methods propose silica- or alumina-supported materials such as heteropolyacids,<sup>41</sup> other Brønsted acids,<sup>42,43</sup> and metal oxide nanoparticles<sup>44,45</sup> as potential catalysts for the Biginelli reactions. Several examples of heterogeneous catalytic Biginelli reactions are presented in Table 2.

A typical example is the solvent-free microwave-driven alumina sulfuric acid-catalyzed Biginelli reaction that provides high yields in short reaction times while avoiding the use of toxic solvents (Table 2, entry 1). However, although the catalyst is recyclable for several cycles, its environmental friendliness can be regarded as controversial because its synthesis uses both sulfuric acid and hydrogen chloride, sources of hazardous waste.<sup>42</sup> ZnO nanoparticles supported on SBA-15,<sup>44</sup> silica-coated magnetite nanoparticles,<sup>45</sup> silica-supported perchloric acid,<sup>43</sup> and magnetic mesoporous MCM-41, silica-supported boric acid<sup>46</sup> also efficiently catalyzed the reaction in relatively short reaction times (Table 2, entries 2–5). Despite the remarkable advantages these methods have to offer,

**TABLE 2** Heterogeneous catalytic Biginelli multicomponent reactions.

| Entry | Catalyst/conditions  | Product | Yield (%) | Ref. |
|-------|--|---------|-----------|------|
|       |  |         |           |      |
| 1     | Al <sub>2</sub> O <sub>3</sub> -SO <sub>3</sub> H, solvent free, MW, 1–3 min |         | 69–92     | 42   |
| 2     | HClO <sub>4</sub> -SiO <sub>2</sub> , solvent free, 80°C, 2 h                |         | 70–82     | 43   |
| 3     | MNPs-BSAT, solvent free, 100°C 40–80 min                                     |         | 80–95     | 44   |
|       |  | X=O, S  |           |      |

| Entry | Catalyst/conditions   | Product   | Yield (%) | Ref. |
|-------|---|---|-----------|------|
| 4     | ZnO NPs/SBA-15, ethanol, 65°C, 150–210 min  |    | 75–96     | 45   |
| 5     | Fe <sub>3</sub> O <sub>4</sub> /MCM41-OB(OH) <sub>2</sub> , solvent free, 50°C, US, 15–50 min                       |    | 88–96     | 46   |
| 6     | Silica-supported H <sub>3</sub> PW <sub>12</sub> O <sub>40</sub> , acetonitrile, 80°C, 50–100 min                   |    | 50–95     | 41   |
| 7     | Scolecite, acetonitrile, reflux temperature, 30–60 min  |    | 65–91     | 47   |
| 8     | g-C <sub>3</sub> N <sub>4</sub> , visible light, 70°C, 60–120 min   |    | 44–57     | 48   |
| 9     | C <sub>3</sub> N <sub>4</sub> /SO <sub>3</sub> H, ethanol, reflux, 20–50 min  |  | 76–98     | 49   |
| 10    | White marble, ethanol, reflux, 25–55 min  |  | 88–96     | 50   |
| 11    | Montmorillonite KSF supported H <sub>5</sub> PV <sub>2</sub> W <sub>10</sub> O <sub>40</sub> , ethanol, reflux, 1 h |  | 79–97     | 51   |

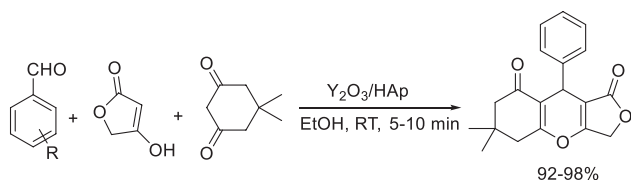
MCM41, a special mesoporous silica; MNPs-BSAT, bis(*p*-sulfoanilino)triazine-functionalized silica-coated magnetite nanoparticles; Ps/SBA, nanoparticles on Santa Barbara amorphous support; US, ultrasound.

the synthesis of the catalyst should also be carefully assessed from an environmental point of view before labeling the reaction it catalyzes as “green.” It should be considered that the preparation of these silica-supported catalysts requires the use of potentially toxic reagents and/or organic solvent and/or harsh conditions. Another example of heterogeneous catalytic Biginelli reaction with a silica-supported catalyst is the one-pot synthesis of dihydropyrimidones using a silica-supported heteropoly acid (Table 2, entry 6).<sup>41</sup> Here, the efficient and reusable catalyst was prepared via simple impregnation of the silica with an aqueous solution of the heteropoly acid. The additional benefits of the method revolve around the good tolerance toward a variety of substituents for all three components. On the negative side, the use of acetonitrile as the reaction solvent is against the eco-friendliness of the method. The same comment can be made for another method employing scolecite, a natural zeolite possessing both Lewis and Brønsted acidity (Table 2, entry 7).<sup>47</sup> However, in this case the catalyst is employed directly in its original form, eliminating the use of extra reagents that are often required during the preparation of solid acid catalysts.

Other metal-free catalysts include graphitic carbon nitride<sup>48</sup> and its sulfonated version (Table 2, entries 8 and 9).<sup>49</sup> Although the former is activated by visible light, which is a greener concept compared to the sulfonic acid functionalization of the latter, the yields obtained are significantly lower.

The uncommon white marble catalyst, a naturally occurring metamorphic rock composed of recrystallized carbonate minerals, demonstrated high activity for the Biginelli reaction (Table 2, entry 10).<sup>50</sup> The catalyst actually derives from the waste generated during the cutting of white marble pieces. The collected powder was subjected to washing and drying treatments before its use in the synthesis of dihydropyrimidinones/thiones, which are particularly difficult to synthesize via alternative pathways. It was also successfully recovered from the reaction mixture and reused for several consecutive cycles.

The following example illustrates a multicomponent reaction forming a 6-membered heterocycle-containing oxygen as the heteroatom in lieu of nitrogen.<sup>52</sup> Furo[3,4-*b*]chromene derivatives were prepared from the MCR of an aldehyde, 4-hydroxyfuran-2(5H)-one, and 5,5-dimethylcyclohexane-1,3-dione in the presence of heterogeneous yttria-doped hydroxyapatite, obtained via a multistep synthesis (Scheme 6). The MCR protocol proposed employs ethanol at room temperature and allows the recycling of the catalyst.

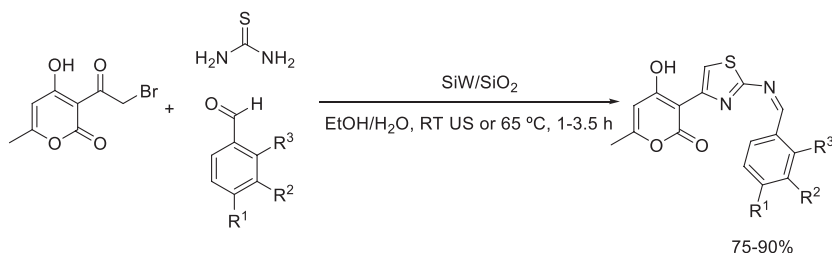


**SCHEME 6** Multicomponent synthesis of furo[3,4-*b*]chromene derivatives with Y<sub>2</sub>O<sub>3</sub>/HAp heterogeneous catalyst.

It is worth noting that one of the most characteristic trends in designing new catalysts for Hantzsch or Biginelli-type multicomponent reactions, whether dihydropyridine or 4*H*-pyrans are the target products, is the use of magnetic nanoparticles often combined with silica that are commonly designed as a core-shell. These core-shells are modified on their surface by natural products such as cellulose or other carbohydrates, or synthetic entities, that either act as an immobilized organocatalyst, or as a binding unit for metal active centers. Mostly Fe<sub>3</sub>O<sub>4</sub> is applied as magnetic species, but in some cases superparamagnetic Fe<sub>2</sub>O<sub>3</sub> has also been used. The catalysts have been found recyclable in every case. Several of these applications are using the multicomponent reactions as assessment of catalytic activity mostly providing high yields.<sup>33, 34, 38, 53–56</sup>

### 3.7.2.2 Formation of 5-membered rings with multicomponent reactions

Although the Hantzsch reaction is mostly known for the preparation of pyridines and their derivatives, it is also a reliable method to produce thiazoles, another type of heterocycle that is equally important in medicinal chemistry and also finds applications in material science.<sup>57</sup> Only a few green Hantzsch thiazole synthetic methods are available in the literature. As a representative example, silica-supported silicotungstic acid was applied to the one-pot synthesis involving 3-(bromoacetyl)-4-hydroxy-6-methyl-2*H*-pyran-2-one, thiourea, and substituted benzaldehydes under ultrasonic irradiation or under mild conventional heating (65°C).<sup>57</sup> The environmentally benign reusable catalyst constitutes a superior alternative to most homogeneous catalysts, affording thiazoles in no less than 80% yield (Scheme 7). The resulting products were compared to amoxicillin and ciprofloxacin for their antibacterial activity; the synthesized compounds demonstrated significantly higher activity than the controls.

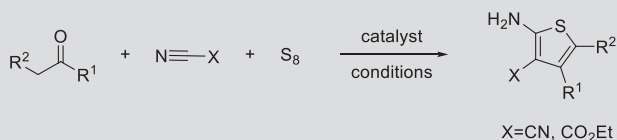


**SCHEME 7** Silica-supported silicotungstic acid-catalyzed Hantzsch synthesis of thiazole derivatives.

The Gewald synthesis, although less documented in the literature than the Hantzsch reaction, is a useful method to prepare sulfur-containing 5-membered rings from sulfur, an  $\alpha$ -methylene carbonyl compound, and an  $\alpha$ -cyanoester.<sup>58</sup> The reaction mechanism is initiated by a Knoevenagel condensation and is

**TABLE 3** Heterogeneous catalytic Gewald reactions.

| Entry | Catalyst/conditions                        | Yield (%) | Ref. |
|-------|--|-----------|------|
| 1     | NaAlO <sub>2</sub> , ethanol, 60°C, 6–16 h | 26–97     | 59   |
| 2     | KG-60-piperazine, ethanol, reflux, 4 h     | 41–89     | 60   |
| 3     | ZnO, solvent free, 100°C, 6 h              | 45–75     | 61   |

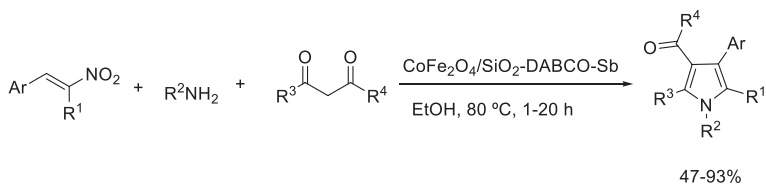


terminated by a cyclization step driven by the force of aromatization. Three examples are selected to illustrate the applications of this MCR type in Table 3.

Two of the methods use a solid base catalyst, one is sodium aluminate<sup>59</sup> and the other is a piperazine supported on amorphous silica heterogeneous catalyst (Table 3, entries 1 and 2).<sup>60</sup> It should be noted that both of these methods exhibit some limitations in regard to the substrates. It appears that the yield is significantly dependent on the nature of the substituents on the ketone especially for the sodium-aluminate-catalyzed reaction.

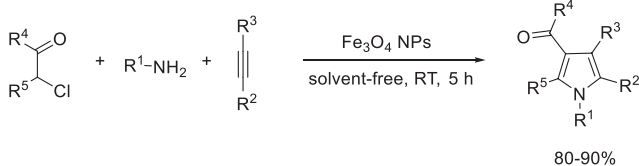
Commercial zinc oxide constitutes an eco-friendly and simple option to catalyze the Gewald reaction (Table 3, entry 3).<sup>61</sup> Here again, the yields range from moderate to high depending on the substrates. Unlike the other two methods that employ ethanol as the solvent under mild temperatures, the metal-catalyzed reaction is performed under neat conditions at a higher temperature.

Another important class of 5-membered aromatic heterocycles is pyrrole and its derivatives. They are valuable precursors in materials science and medicinal chemistry due to the interesting properties they exhibit.<sup>62</sup> Various methods exist for the preparation of pyrroles depending on the available starting materials and continuous progress is being made to develop more efficient and sustainable syntheses. Multicomponent one-pot syntheses catalyzed by solid acids have been applied to the synthesis of pyrroles for this purpose. In fact, a wide range of heterogeneous catalysts have been reported to efficiently catalyze this transformation. Particularly, magnetic nanoparticles employed under mild conditions demonstrated versatile properties in addition to their great stability and easy recovery with the aid of an external magnet. Applying nano CoFe<sub>2</sub>O<sub>4</sub>-supported antimony complex in ethanol at 80°C was a powerful protocol to afford 48 different multisubstituted pyrroles (Scheme 8).<sup>63</sup> It is important to mention that the synthesis of the catalytic material prepared by chemical coprecipitation was relatively green, involving minimal reagents and mild reaction conditions.



**SCHEME 8** Nano  $\text{CoFe}_2\text{O}_4$ -supported Sb-catalyzed synthesis of multisubstituted pyrroles.

Simple nanosized magnetite exhibited catalytic activity for the synthesis of pyrroles as well, although the method was successful only for a limited range of pyrrole derivatives (Scheme 9).<sup>56</sup> Nonetheless, the magnetic properties of the catalyst allowed its easy recovery and reuse.



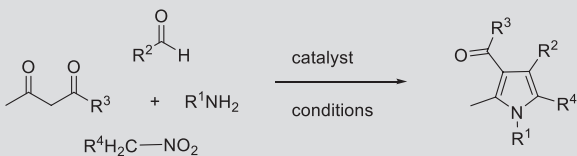
**SCHEME 9**  $\text{Fe}_3\text{O}_4$ -catalyzed synthesis of multisubstituted pyrroles.

The four-component reaction of amines, aldehydes,  $\alpha$ -methylene ketones, and nitroalkanes is another common way to prepare pyrroles and has been the subject of multiple works proposing various protocols as summarized in Table 4.

One of the methods also uses a magnetic catalyst, a copper Schiff-base complex immobilized on silica-coated  $\text{Fe}_3\text{O}_4$ , under solvent-free conditions (Table 4, entry 1).<sup>56</sup> In spite of a relatively long catalyst synthesis, superior results were obtained as compared to the other methods in addition to the use of milder reaction conditions. Lower yields were obtained for the method employing heterogenized tungsten catalyst, which too, required several preparation steps involving organic solvents (Table 4, entry 2).<sup>64</sup> While the NiO nanoparticle-catalyzed reaction possessed obvious advantages, the results obtained vary greatly depending on the substrates (Table 4, entry 3).<sup>65</sup> The same metal, complexed with ferrite provided higher and more consistent yields (Table 4, entry 4).<sup>66</sup> The two other methods involving a polymer-supported acid<sup>67</sup> and an ion exchange resin,<sup>68</sup> using either microwave irradiation or ultrasounds as activation energy, provided good to excellent yields (Table 4, entries 5 and 6).

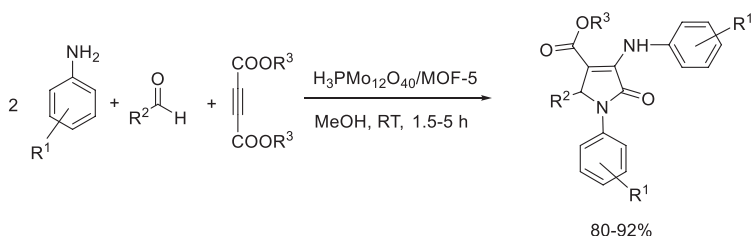
A similar, pseudo-four-component reaction was developed for the synthesis of poly-substituted 3-pyrrolin-2-ones by Zhang's group by using dialkyl acetylenedicarboxylate, amines, and aromatic aldehydes (Scheme 10).<sup>69</sup> The authors developed an MOF (metal-organic framework)-immobilized phosphomolybdic acid ( $\text{H}_3\text{PMO}_{12}\text{O}_{40}$ ) catalyst for this reaction. The reuse of the catalyst was attempted and it was found to show stable activity even after five consecutive runs.

**TABLE 4** Heterogeneous catalytic four-component syntheses of multisubstituted pyrroles.



| Entry | Catalyst/conditions   | Yield (%) | Ref. |
|-------|---|-----------|------|
| 1     | SB Cu/silica Fe <sub>3</sub> O <sub>4</sub> , solvent free, RT, 20–40 min | 80–93     | 56   |
| 2     | WO <sub>4</sub> H/SiO <sub>2</sub> , solvent free, reflux, 4 h            | 60–88     | 64   |
| 3     | NiO NPs, solvent free, RT, N <sub>2</sub> atmosphere, 4 h                 | 28–88     | 65   |
| 4     | NiFe <sub>2</sub> O <sub>4</sub> NPs, solvent free, 100°C, 3–4 h          | 80–96     | 66   |
| 5     | <i>p</i> -TSA doped polystyrene, MW, 80°C, 50–70 min                      | 78–90     | 67   |
| 6     | Amberlyst 15, RT, US, 4–6 h   | 60–80     | 68   |

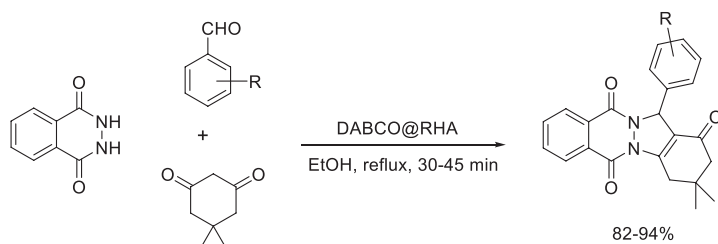
MW, microwave; *p*-TSA, *p*-toluenesulfonic acid; US, ultrasound; NPs, nanoparticles.



**SCHEME 10** Synthesis of poly-substituted 3-pyrrolin-2-ones by an H<sub>3</sub>PMo<sub>12</sub>O<sub>40</sub>/MOF-5-catalyzed pseudo-four-component reaction.

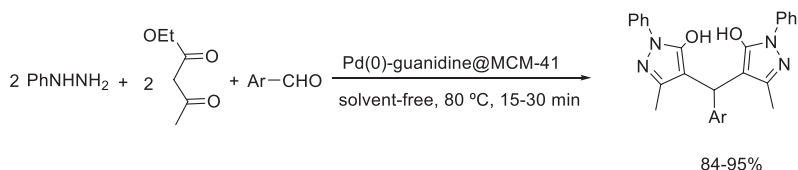
Besides pyrroles, certain fused phthalazines also belong to nitrogen-containing five-membered-ring heterocycles that exhibit interesting biological properties such as anticonvulsant,<sup>70</sup> antimicrobial,<sup>71</sup> cardiotoxic,<sup>70</sup> and vasorelaxant<sup>70</sup> properties as well as unique optical and electrical properties.<sup>72,73</sup> These molecules can easily be prepared in a single step MCR catalyzed by the highly nucleophilic organic base 1,4-diazabicyclo[2.2.2]octane (DABCO). The major disadvantage of a DABCO-based catalyst is its difficult separation from the products after the completion of the reaction. A heterogeneous and recyclable DABCO catalyst is therefore of great interest to solve the recovery issue. Silica-supported DABCO was proposed as a heterogeneous recyclable catalyst for the conversion of phthalhydrazide, dimedone, and substituted benzaldehyde to phthalazine-trione derivatives (Scheme 11).<sup>74</sup> The reaction proceeded in refluxing ethanol in less than an hour and the yields reached

above 80% independently of the substituent on the phenyl ring of benzaldehyde. The unique aspect of this method is the origin of the silica, obtained from rice husk, an inexpensive and eco-friendly source of silica. The preparation of the material, however, requires a combined acid and heat treatment while a single acid or a single heat treatment is sufficient when producing silica from sodium silicate or organosilicon compounds, two common sources of silica.<sup>75</sup>



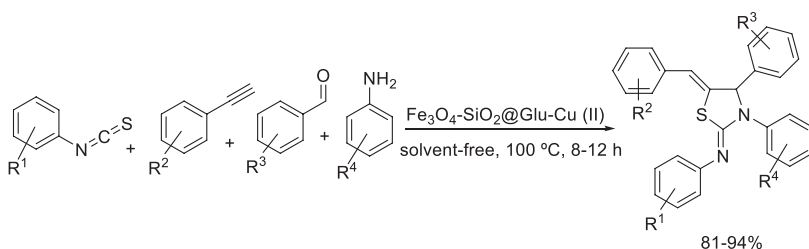
**SCHEME 11** Synthesis of phthalazine-trione derivatives by the silica-supported DABCO-catalyzed MCR (RHA-rice husk based silica).

Pyrazoles and pyrazolones constitute another significant class of bioactive nitrogen-containing heterocycles.<sup>76</sup> The earlier developed methods for the synthesis of pyrazoles, involving refluxing the reagents for several hours,<sup>77</sup> were progressively replaced by newer synthetic routes, such as one-pot multicomponent syntheses, solvent-free syntheses, and heterogeneous-catalytic processes providing higher yields in shorter reaction times.<sup>78</sup> For instance, the synthesis of bis(pyrazolyl)methane derivatives was conducted in the presence of Pd(0)-guanidine@MCM-41 catalyst under solvent-free conditions (Scheme 12). The nanocatalyst was prepared by grafting guanidine onto the surface of MCM-41, previously functionalized with (3-chloropropyl)-trimethoxysilane, via a substitution reaction of the amino group of guanidine with terminal Cl groups of the mesoporous material. This step was followed by the reaction of guanidine@MCM-41 with Pd(OAc)<sub>2</sub>. It was demonstrated that this catalyst was superior in efficiency as compared to other reported catalysts such as CuFe<sub>2</sub>O<sub>4</sub> or [pyridine-SO<sub>3</sub>H]Cl for the synthesis of bis(pyrazolyl)methanes. The one-pot three-component reaction between 3-methyl-1-phenyl-1*H*-pyrazol-5(4*H*)-one and aromatic aldehydes in presence of the nanocatalyst exhibits several notable advantages, including green conditions, short reaction times, high yields, easy workup, and good recyclability of the catalyst.



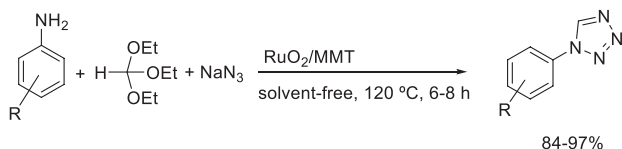
**SCHEME 12** Pd(0)-guanidine@MCM-41-catalyzed synthesis of bis(pyrazolyl)methanes.

Yielzoleh and Nikoofar described the preparation of a multilayered inorganic-bioorganic nanosized hybrid catalyst on a magnetite silica support by embedding glutamic acid into the magnetized silica followed by anchoring Cu(II) (nano  $\text{Fe}_3\text{O}_4\text{-SiO}_2\text{@Glu-Cu (II)}$ ). In addition to the extensive characterization of the catalyst by FT-IR, field-emission scanning electron microscopy (FESEM), energy dispersive X-ray analysis (EDAX), transmission electron microscopy (TEM), X-ray fluorescence (XRF), thermogravimetric analysis (TGA-DTG), vibrating sample magnetometer (VSM), X-ray photoelectron spectroscopy (XPS), and Brunauer-Emmett-Teller (BET) techniques, the authors applied this newly prepared material for the solvent-free synthesis of thiazolidin-2-imines (Scheme 13).<sup>79</sup> The products were obtained in good to excellent yields. The authors evaluated the recyclability of the catalyst as well. It was found that, as expected, the magnetic separation of the catalyst occurred readily using methanol to isolate the product. Although the catalyst maintained its activity, a slight decrease in yields was observed in three consecutive reactions (90%–88%–86% yield).



**SCHEME 13** A nano  $\text{Fe}_3\text{O}_4\text{-SiO}_2\text{@Glu-Cu (II)}$ -catalyzed synthesis of thiazolidin-2-imines.

A one-pot, three-component method has been developed for the  $\text{RuO}_2/\text{MMT}$  (K-10 montmorillonite)-catalyzed synthesis of *N*-aryl tetrazoles from substituted anilines, triethyl-ortho-formate, and sodium azide (Scheme 14).<sup>80</sup> The X-ray analysis indicated that the geometry of the  $\text{RuO}_2$  nanoparticles was spherical and they appeared to have a homogeneous distribution on the surface of the montmorillonite. The solvent-free conditions resulted in good to excellent yields for the products. The catalyst was found to exhibit excellent recyclability; there was only 5% decrease in its activity even after the fifth reaction.



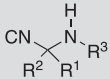
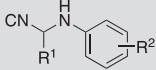
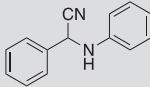
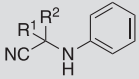
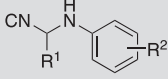
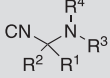
**SCHEME 14** A  $\text{RuO}_2/\text{MMT}$ -catalyzed synthesis of *N*-aryl-tetrazoles.

### 3.7.2.3 Formation of aliphatic bonds

The Strecker synthesis, occurring between a carbonyl compound, an amine, and a cyanide, is one of the oldest and most important multicomponent reactions because it produces the useful intermediates,  $\alpha$ -aminonitrile derivatives, that can be further transformed to generate  $\alpha$ -amino acids, nitrogen-containing heterocycles, or other value-added chemicals.<sup>81</sup> To avoid the use of hazardous alkali metal cyanides<sup>82</sup> or HCN,<sup>83</sup> multicomponent Strecker reactions can take advantage of other sources of cyanide, such as trimethylsilyl cyanide, a relatively safe and easy to handle chemical. In addition to employing a safer cyanide source, heterogeneous catalysis can be applied to further decrease the environmental impact of the one-pot multicomponent Strecker reactions. Representative examples are tabulated in Table 5.

While some heterogeneous catalysts, such as mesoporous aluminosilicates, Al-MCM-41,<sup>84</sup> chitosan,<sup>85</sup> and MOFs<sup>86, 87</sup> resulted in the formation of the products in high yields without prior modification/functionalization, others such

**TABLE 5** Heterogeneous catalytic Strecker MCRs.

| $\text{R}^1\text{C}(=\text{O})\text{R}^2 + \text{R}^3\text{-NH-R}^4 + \text{TMSCN} \xrightarrow[\text{conditions}]{\text{catalyst}} \text{CN-C(R}^1\text{)(R}^2\text{)-N(R}^3\text{)-R}^4$ |   |   |           |      |
|--|---|---|-----------|------|
| Entry  | Catalyst/conditions   | Product   | Yield (%) | Ref. |
| 1  | Al-MCM-41, dichloromethane, RT, Ar atmosphere, 2–24 h         |   | 40–100    | 84   |
| 2  | Chitosan, solvent free, RT, 3 min–12 h                        |  | 80–95     | 85   |
| 3  | Ga, In-MOFs, solvent free, RT, 5–80 min                       |  | 91–99     | 86   |
| 4  | In-MOF, water, methanol or ethanol, N2 atmosphere, RT, 3–48 h |  | 64–99     | 87   |
| 5  | MCM-41-SO3H, ethanol, RT, 15–250 min                          |  | 85–97     | 88   |
| 6  | Silica-supported H3PW12O40, acetonitrile, RT, 1–120 min       |  | 50–98     | 89   |

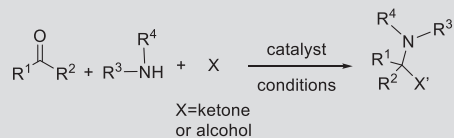
as silica-supported heteropolyacids<sup>88</sup> and MCM-41 anchored sulfonic acid<sup>89</sup> were functionalized before being successfully applied to the Strecker MCR. It is worth noting that the chitosan-catalyzed reaction was performed under truly green conditions (Table 5, entry 2) and yet afforded yields equivalent to those of other reported methods (Table 5, entries 1, 4–6). The great potential of chitosan is mainly due to the presence of free amino groups at the surface of the material and its insoluble nature allowing an easy recovery and reuse. Another outstanding work reported the synthesis of novel MOFs with Ga and In under neat conditions (Table 5, entry 3).<sup>86</sup> Interestingly, it was found that the catalysts exhibited different behavior as a function of the ratio of the metals in the organic framework. Two of the MOFs synthesized resulted in high selectivity in the cyanosilylation and the imine formation products instead of the expected aminonitrile product.

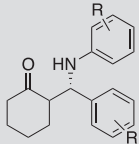
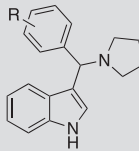
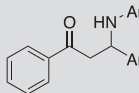
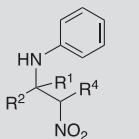
Another MCR for the synthesis of aliphatic products, the Mannich reaction, dating back to 1912, is a useful method for the construction of carbon-carbon bonds affording  $\beta$ -aminocarbonyl compounds.<sup>3</sup> The reaction is initiated by the carbonyl-containing starting material that reacts with an amine to form an iminium ion as the intermediate; this ion further reacts with a compound containing an acidic proton (which is, or had become an enol). Usually performed with the aid of transition metal catalysts, Brønsted or Lewis acids, the Mannich reaction proved to be valuable in the total synthesis of natural products.<sup>90</sup> It is notably crucial to produce precursors of  $\beta$ -lactams,  $\beta$ -amino acid derivatives, and other biologically active compounds. In the past years, the Mannich reaction has been revisited and extensive efforts have been made to apply heterogeneous catalytic systems in order to comply with the green chemistry principles. Sustainable protocols of heterogeneous catalysis-driven Mannich and Mannich-type reactions are described in Table 6.

Silica-supported metal,<sup>91, 92</sup> or silica supported acid,<sup>93</sup> ion exchange resin,<sup>94</sup> metal nanoparticle<sup>95</sup> or metal oxide nanoparticle<sup>96, 97</sup> and clay<sup>98</sup>-catalyzed Mannich reactions offer various advantages. Essentially, due to the large surface area of the diverse catalysts employed they provided excellent yields in relatively short reaction times. Moreover, their solid nature enabled a good recyclability of the catalytic system (Table 6, entries 1–8). In regard to the reaction conditions, most reactions were performed at ambient temperature apart from the Amberlyst-catalyzed reaction requiring temperatures above 100°C to achieve acceptable activity (Table 6, entry 4). On a similar note, while most methods employed a green solvent or no solvent, the SiO<sub>2</sub>-I-catalyzed reaction provided optimum results in acetonitrile, a not truly green solvent (Table 6, entry 2). It should be noted that for the selected examples, the yields reported are isolated yields.

Interestingly, the silica ferric hydrogensulfate catalyst applied for the Mannich reaction of aromatic amines, aldehydes and cyclohexanone, is believed to govern the diastereoselectivity of the reaction by controlling the stereochemistry of the transition state (Table 6, entry 1). As a result, the major

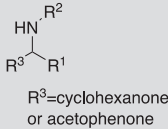
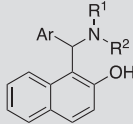
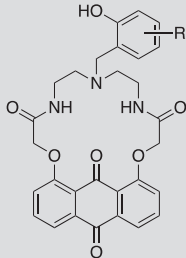
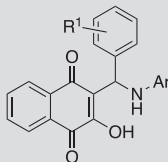
**TABLE 6** Heterogeneous catalytic multicomponent Mannich reactions.



| Entry | Catalyst/conditions   | Starting materials   | Product  | Yield (%) (e.r) | Ref. |
|-------|---|--|--|-----------------|------|
| 1     | Ferric hydrogensulfate/SiO <sub>2</sub> , ethanol, RT, 1–24 h | Substituted anilines, substituted benzaldehydes, cyclohexanone |  | 65–86<br>(99:1) | 91   |
| 2     | SiO <sub>2</sub> -I, acetonitrile, RT, 3 h                    | Substituted benzaldehyde, indole, pyrrolidine                  |  | 88–92           | 92   |
| 3     | HClO <sub>4</sub> -SiO <sub>2</sub> , ethanol, RT, 10–17 h    | Aromatic aldehydes, aromatic amines, acetophenone              |  | 75–95           | 93   |
| 4     | CuI-Amberlyst-21, solvent free, 110°C, 1–8 h                  | Aldehydes, aniline, nitromethane                               |  | 34–88           | 94   |

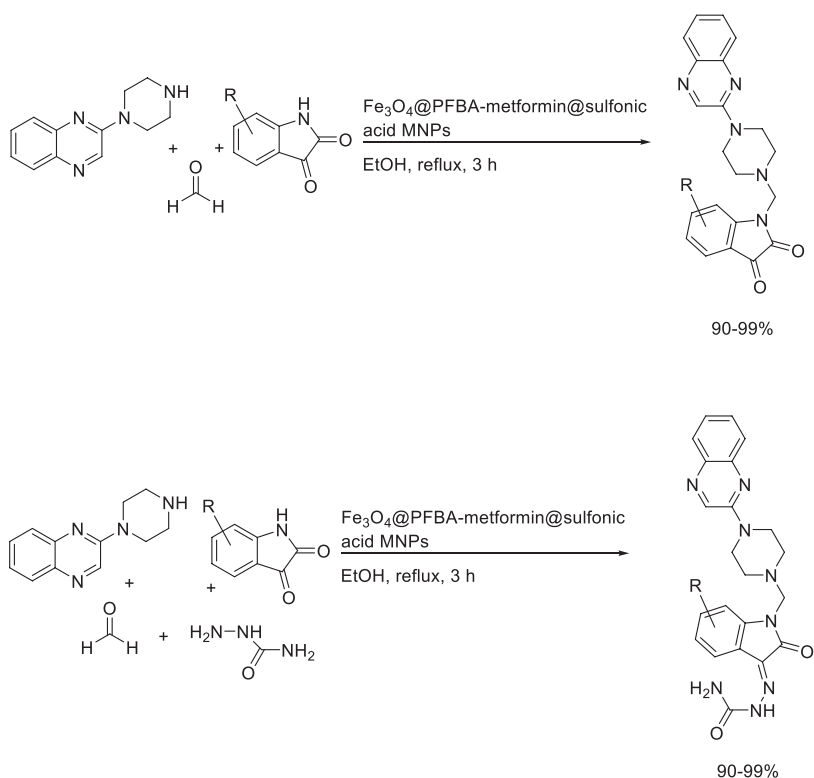
*Continued*

**TABLE 6** Heterogeneous catalytic multicomponent Mannich reactions—cont'd

| Entry | Catalyst/conditions                           | Starting materials   | Product   | Yield (%) (e.r) | Ref. |
|-------|---|--|---|-----------------|------|
| 5     | Cu NPs, methanol, RT, N <sub>2</sub> , 8–12 h | Aromatic aldehydes, aromatic amines, cyclohexanone or acetophenone |  <p>R<sup>3</sup>=cyclohexanone or acetophenone</p> | 73–97           | 95   |
| 6     | Nano MgO, water, RT, 120–200 min              | Aromatic aldehydes, amines and 2-naphtol                           |   | 82–90           | 96   |
| 7     | ZnO NPs, solvent free, 100°C, 10–60 min       | Phenols, anthraquinone aza crown ether, paraformaldehyde           |   | 87–97           | 97   |
| 8     | Montmorillonite K10, ethanol, RT, 8–10 h      | Substituted benzaldehydes, aromatic amines and                     |   | 81–93           | 98   |

product is not the most sterically favored but the most electronically favored due to the interaction with the iron center—the antiisomer.<sup>91</sup>

The combination of 2-piperazinyl quinoxaline or 2-(piperazin-1-ylmethyl)-benzimidazole and various isatin derivatives via bridging reaction using formaldehyde (Scheme 15) was achieved by Esam et al.<sup>99</sup> The authors used this multicomponent Mannich type reaction as a test system to characterize a newly developed superparamagnetic Fe<sub>3</sub>O<sub>4</sub> core-shell supported sulfonic acid nanoparticles (Fe<sub>3</sub>O<sub>4</sub>@PFBA-metformin@sulfonic acid MNPs (magnetic nanoparticles)) as a novel acid nanocatalyst. The material has been thoroughly characterized by FTIR, X-ray diffraction (XRD), energy dispersive X-ray spectroscopy (EDS), field-emission scanning electron microscopy (FESEM), transmission electron microscopy (TEM), thermogravimetric analysis analysis (TGA-DTA), atomic force microscopy (AFM), dynamic light scattering (DLS), Brunauer-Emmett-Teller (BET), and vibrating sample magnetometer (VSM) techniques. The products were obtained in excellent yields independently of the substituent on the isatin. It has been reported that the catalyst could be recycled in six consecutive reactions with only minor decrease in product yields.



**SCHEME 15** A Fe<sub>3</sub>O<sub>4</sub>@PFBA-metformin@sulfonic acid-catalyzed coupling of 2-piperazinyl quinoxaline or 2-(piperazin-1-ylmethyl)-benzimidazole with formaldehyde and various isatin derivatives.

Propargylamines are versatile compounds that can serve as building blocks for nitrogen-containing drugs such as alkaloids<sup>100</sup> or polycyclic pyrroles,<sup>101</sup> and other useful synthetic precursors.<sup>102</sup> While some preparation methods of propargylamines require high temperatures, inert atmospheres, and long reaction times,<sup>103</sup> multicomponent reactions with appropriate heterogeneous catalysts offer an efficient way to produce these compounds in high yields under mild reaction conditions. Representative data are presented in Table 7.

Multiple reports in the literature proposed the synthesis of propargylamines via the coupling of an aldehyde, amine, and alkyne using supported copper catalysts. Zeolites,<sup>104</sup> polymers,<sup>105, 106</sup> resins,<sup>107, 108</sup> mesoporous organosilica,<sup>109</sup> or graphene oxide<sup>110</sup> materials have all been considered to serve as support for the copper salt in order to improve its properties as a catalyst. The functionalization of these solid materials involves a multistep synthesis that should be evaluated before claiming an environmentally friendly catalyzed MCR. Indeed, simple syntheses requiring a minimum amount of organic solvent and few additional reagents are preferable. For instance, although the graphene-oxide-supported CuCl<sub>2</sub> catalyst provided high yields, good recyclability, and a possible scale-up of the reaction, the preparation of the catalyst employing *N,N*-dimethylformamide and overnight reaction time at 90°C should be taken into consideration for a holistic assessment of the environmental impact.<sup>110</sup> Similarly, copper nanoparticles supported on a zinc oxide-polythiophene support were prepared via three stages: the preparation of the zinc oxide nanorods, the synthesis of the zinc oxide polythiophene nanocomposite, and finally the deposition of copper nanoparticles on the support.<sup>106</sup> It could be argued that the advantages of the MCR it catalyzes, namely the short reaction times and the use of a green solvent, are somewhat tempered by the laborious and chemical intensive preparation of the catalyst. To the contrary, the synthesis of copper nanoparticles stabilized onto a polystyrene resin was performed in a two-step process involving green solvents, methanol, and water, under mild temperatures.<sup>114</sup>

Other efficient catalysts include gold nanoparticles,<sup>111</sup> graphene oxide-supported magnetite,<sup>112</sup> and nano Fe<sub>2</sub>O<sub>3</sub>/silica/ionic liquid/Ag.<sup>113</sup> The first two catalysts provided interesting results and were prepared through simple methods (Table 7, entries 8 and 9). Regarding the latter mentioned catalyst, despite the long synthesis due to the presence of several constituents, efforts were made to include green chemistry principles such as the preparation of silver nanoparticles using biosynthesis (Table 7, entry 10). In addition, the catalyst afforded high yields in short reaction times in water and demonstrated high versatility as 40 examples of propargylamines were synthesized. As a significant advantage, the catalysts reported in Table 7 were successfully recycled with no exception.

### 3.7.3. Isocyanide-based reactions

Isocyanides, also called isonitriles, are compounds with a zwitterionic structure composed of a divalent carbon stabilized by an electron-donor nitrogen atom. Due to their unusual structure subject to resonance, they possess an interesting reactivity

**TABLE 7** Heterogeneous catalytic multicomponent synthesis of propargylamines.

| Entry  | Catalyst/conditions   | Product | Yield | Ref. |
|--|---|---------|-------|------|
| $R^1-\overset{\text{O}}{\parallel}{C}-H + R^2-\overset{\text{R}^3}{\text{N}}-H + R^4-\equiv \xrightarrow[\text{conditions}]{\text{catalyst}} R^3-\overset{\text{R}^2}{\text{N}}-\overset{\text{R}^1}{\text{C}}-\equiv R^4$ |   |         |       |      |
| 1  | Cu(N <sub>2</sub> S <sub>2</sub> )Cl/Y-zeolite, dichloroethane, 70°C, 12–20 h     |         | 80–91 | 104  |
| 2  | Polymer-anchored copper (II) complex, toluene, 110°C, 6 h                         |         | 64–90 | 105  |
| 3  | CuNPs/ZnO-polythiophene, ethylene glycol, MW, 80°C, 15 min                        |         | 71–99 | 106  |
| 4  | CuI A-21, solvent free, N <sub>2</sub> atmosphere, 100°C, 2–6 h                   |         | 87–96 | 107  |
| 5  | Cu NPs/resin, toluene, MW, 100°C, 25 min  |         | 65–99 | 108  |
| 6  | Cu/periodic mesoporous organosilica, chloroform, 60°C, 24 h                       |         | 82–99 | 109  |
| 7  | Graphene oxide-CuCl <sub>2</sub> , MW, solvent free, 90°C, 20 min                 |         | 85–98 | 110  |
| 8  | Au NPs, water, RT, 3 h  |         | 70–94 | 111  |
| 9  | Fe <sub>3</sub> O <sub>4</sub> -graphene oxide, water, 90°C, 16 h                 |         | 37–93 | 112  |
| 10   | Fe <sub>2</sub> O <sub>3</sub> /SiO <sub>2</sub> -IL/Ag, water, MW, RT, 10–25 min |         | 79–95 | 113  |

IL, ionic liquid.

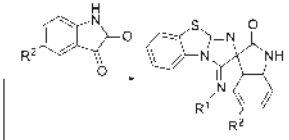
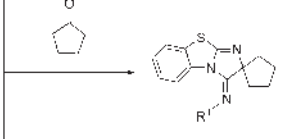
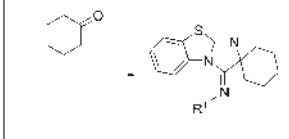
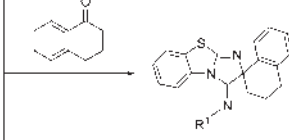
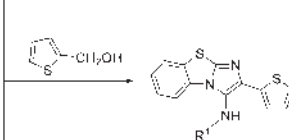
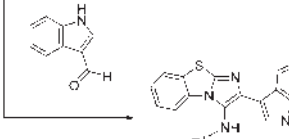
based on three main properties: the  $\alpha$ -acidity, the  $\alpha$ -addition, and the ease of radical formation.<sup>115</sup> They are therefore excellent candidates for MCRs as they are prone to irreversible ring-closure reaction, aromatization, or electrophilic addition.<sup>116</sup>

### 3.7.3.1 Isocyanide-based MCRs for the preparation of 5-membered rings

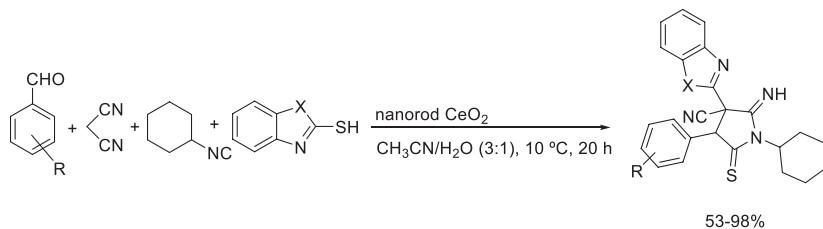
Isocyanide-based multicomponent reactions have emerged as a powerful tool for the synthesis of complex, drug-like molecules often possessing a 5-membered ring formed as a result of the reaction.<sup>117</sup> In fact, when using isocyanides as a starting material, MCRs appear to commonly lead to a 5-membered ring cyclization. Many examples of such reactions in the literature employ 2-aminobenzothiazole as a second reagent. Fig. 1 exhibits the possible products and the corresponding yields of the MCRs of isocyanide and 2-aminobenzothiazole combined with a third reagent for the heterogeneous catalytic synthesis of multiple heterocycles. Interestingly, only a few heterogeneous catalyst types have been shown to successfully drive those reactions; metal oxides, in their regular or nanoparticle forms, are among of them. For instance, spiroheterocycles were obtained with structural diversity by reacting 2-aminobenzothiazole with cyclohexyl/*tert*-butyl isocyanides and isatins/cyclic carbonyl compounds in the presence of TiO<sub>2</sub> nanoparticles in aqueous ethanol (Fig. 1, entries 1–4).<sup>118</sup> The excellent yields of the reaction were not the only benefits of the environmentally benign method; the nanocatalyst employed also demonstrated superior recyclability compared to the commercially available counterpart. In addition, their synthesis entailed a simple and mild chemical precipitation method. Modified TiO<sub>2</sub> nanoparticles with *p*-TSA also offered a cost-effective and green catalytic system to synthesize spirooxindoles in aqueous medium (Fig. 1, entry 5).<sup>119</sup> When combined with indole-3-carbaldehyde, and 2-aminobenzothiazole, phenyl isocyanide afforded biologically active 3-aminoimidazo-benzothiazole derivatives in a polar protic solvent using P<sub>2</sub>O<sub>5</sub>/SiO<sub>2</sub> as a catalyst (Fig. 1, entry 6).<sup>120</sup> The aforementioned catalysts demonstrated good recyclability.

CeO<sub>2</sub>, in its nanorod form, is another promising metal oxide candidate for the catalysis of isocyanide-based MCRs due, in part, to its porous structure. Highly functionalized imino-pyrrolidine-thiones were produced in high yields from a four-component reaction using benzaldehyde, malononitrile, 2-mercaptobenzoxazole, and isocyanide (Scheme 16).<sup>121</sup> It is noteworthy that the aqueous medium played an important role in the reaction as it is believed to gather the organic reagents at the surface of the catalyst, due to hydrophobic effect, thus promoting their interaction.

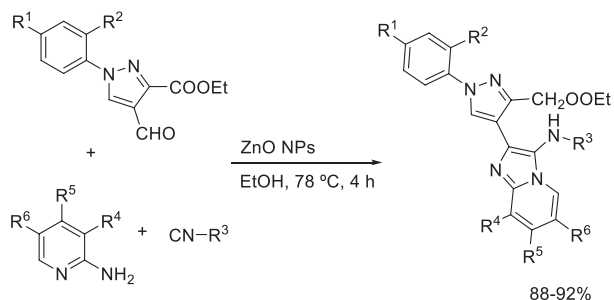
Continuing the illustration of metal oxide nanoparticle-catalyzed isocyanide based-MCRs, ZnO demonstrated high activity in the one-pot three-component synthesis of imidazo-fused polyheterocycles, a class of compound that is not only used for its drug-like properties but also as bioimaging probes due to distinctive structural features.<sup>122</sup> The reaction was performed in ethanol at 70°C in short reaction times (Scheme 17). The catalyst could be recycled for up to eight consecutive cycles with retention of its initial catalytic activity.

|  | Entry | Catalyst/<br>conditions  | Yield (%) | Ref. |
|--|-------|--|-----------|------|
|   | 1     | TiO <sub>2</sub> NPs,<br>ethanol, 90 °C,<br>2-3 h                            | 92-96     | 118  |
|   | 2     | TiO <sub>2</sub> NPs,<br>ethanol, 90 °C,<br>3.5 h                            | 90-92     | 118  |
| <p>R<sup>1</sup> =<br/>C<sub>6</sub>H<sub>5</sub><br/>or C<sub>6</sub>H<sub>13</sub></p>  | 3     | TiO <sub>2</sub> NPs,<br>ethanol, 90 °C,<br>3.5 h                            | 90        | 118  |
|   | 4     | TiO <sub>2</sub> NPs,<br>ethanol, 90 °C,<br>2.5-3 h                          | 91-92     | 118  |
| <p>R<sup>1</sup> =<br/>C<sub>6</sub>H<sub>5</sub></p>                                    | 5     | p-TSA-TiO <sub>2</sub> NPs,<br>water, 70 °C,<br>90 min                       | 90        | 119  |
| <p>R<sup>1</sup> =<br/>C<sub>6</sub>H<sub>5</sub></p>                                   | 6     | P <sub>2</sub> O <sub>5</sub> /SiO <sub>2</sub> ,<br>methanol, 70 °C,<br>5 h | 86        | 120  |

**FIG. 1** Heterogeneous catalytic synthesis of diverse 5-membered heterocycles.



**SCHEME 16** The synthesis of imino-pyrrolidine-thiones by a nanorod CeO<sub>2</sub>-catalyzed MCR.



**SCHEME 17** ZnO-catalyzed MCR producing imidazo-fused polyheterocycles.

A less complex, yet biologically relevant group of compounds, 3-aminoimidazo[1,2-*a*]pyridines can be prepared through the Groebke-Blackburn-Bienaymé reaction<sup>123</sup> of 2-aminopyridine, an aldehyde and an alkyl or aryl isocyanide in presence of a catalytic amount of cellulose-supported Fe<sub>2</sub>O<sub>3</sub>,<sup>124</sup> sulfuric acid supported on multiwalled carbon nanotubes,<sup>125</sup> or by using a mesoporous silica immobilized lipase enzyme (Table 8).<sup>126</sup>

Each catalytic method possesses its own advantages. The iron oxide-based material exhibits a magnetically recoverable potential and is prepared via a simple two-step procedure involving aqueous iron chloride solutions and a thiourea/urea-containing cellulose solution under ambient conditions

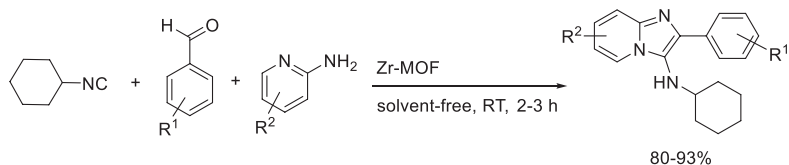
**TABLE 8** Heterogeneous catalytic multicomponent synthesis of 3-aminoimidazo[1,2-*a*]pyridines by the Groebke-Blackburn-Bienaymé reaction.

| Entry | Catalyst/conditions  | Yield (%) | Ref. |
|-------|--|-----------|------|
| 1     | Cellulose/Fe <sub>2</sub> O <sub>3</sub> , methanol, reflux, 3 h | 78–96     | 124  |
| 2     | MWCNTs-OSO <sub>3</sub> H, methanol, RT, 40 min                  | 71–91     | 125  |
| 3     | CALB@SiO <sub>2</sub> , ethanol, RT, overnight                   | 55–91     | 126  |

CALB@SiO<sub>2</sub>, *Candida antarctica* lipase B immobilized on mesoporous silica; MWCNT, multiwalled carbon nanotubes.

(Table 8, entry 1). The MC reaction it catalyzes is, however, performed under reflux. In contrast, the carbon-nanotube-based material catalyzes the reaction at room temperature in short times but its synthesis requires the use of chlorosulfonic acid in hexane. Both methods provide high yields and good catalyst recyclability (Table 8, entries 1 and 2). The third method is the first application of an immobilized enzyme catalyst (CALB@SiO<sub>2</sub>, Table 8, entry 3) in this reaction, thus the catalyst is environmentally compatible. The method also applies a green solvent, and the catalyst is recyclable in five consecutive reactions, although the yields decrease significantly by the end of the fifth run (91%–60%).

Zirconium metal-organic framework (UiO-66) demonstrated high activity for the preparation of various nitrogen-containing heterocyclic scaffolds, including imidazopyridine, pyridine, and quinoxaline moieties.<sup>127</sup> These compounds were obtained in high yields under solvent-free conditions (Scheme 18). Another notable advantage of this environmentally friendly protocol is the reusability of the catalyst that provided consistent results in at least three consecutive cycles. Scheme 18 shows a representative reaction performed via this approach; it should be noted that other products such as 2,4,6-triphenyl pyridine, *N*-cyclohexyl-3,4-dihydro-3,3-dimethyl quinoxalin-2 amine, and 3,4-dihydroquinoxaline-2-amines could be prepared under the same solvent-free conditions but at different temperatures.



**SCHEME 18** Heterogeneous catalytic MCR-based one-pot synthesis of imidazo[1, 2-*a*]pyridines using UiO-66 nanocatalyst.

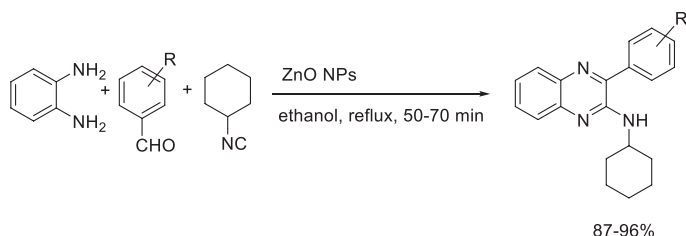
### 3.7.3.2 Isocyanide-based MCRs for the preparation of 5- and 6-membered heterocycles

Examples of reactions leading to the formation of 5- and 6-membered heterocycles and involving isocyanides are the synthesis of quinoxaline, pyridine, pyran, and pyrazole derivatives. These heterocycles possess a variety of biological and pharmaceutical properties, including antibacterial,<sup>128</sup> antiinflammatory,<sup>129</sup> antiviral,<sup>130</sup> antiproliferative,<sup>131</sup> and antioxidant<sup>132</sup> activities among others. Their synthesis and characterization are commonly performed and the search for efficient and recyclable catalysts is of growing interest.

One example illustrating the production of quinoxaline derivatives involves the use of aldehydes, *o*-phenylenediamine and cyclohexyl isocyanide as starting

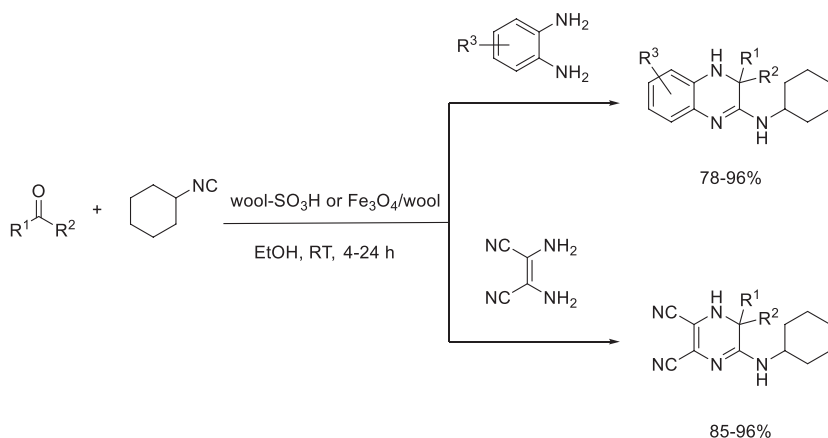
470 Heterogeneous catalysis in sustainable synthesis

materials. The resulting *N*-cyclohexyl-3-aryl-quinoxaline-2-amines were obtained in high yields under environmentally friendly conditions aided by ZnO nanoparticles (Scheme 19).<sup>133</sup> Employing ZnO nanoparticles as a catalyst in the present reaction appears to offer several advantages, namely, a simple catalyst preparation, a yield enhancement, the ease of workup, and the possibility to recover and reuse the catalyst in six cycles without significant decrease in yields.



**SCHEME 19** Heterogeneous catalytic synthesis of *N*-cyclohexyl-3-aryl-quinoxaline-2-amines using ZnO nanoparticles.

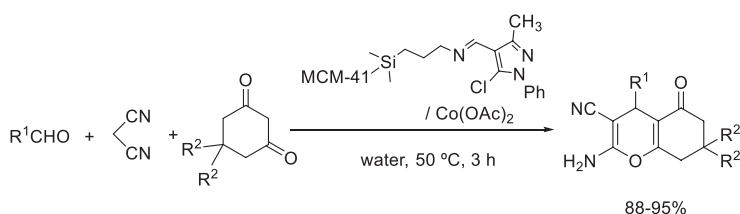
Other materials have also been considered as heterogeneous catalyst precursor for the synthesis of quinoxaline or pyrazine derivatives such as natural biopolymers, e.g., white wool. The approach is an alternative to the methods involving the sulfonation of supports with sulfuric acids or chlorosulfuric acid.<sup>134</sup> Instead, due to the presence of S–S bonds in wool, an oxidation step affords the –SO<sub>3</sub>H groups that can potentially play the role of a solid acid catalyst. Wool-SO<sub>3</sub>H demonstrated high activity in one-pot isocyanide-based multi-component reactions from a carbonyl compound, an amine, and isocyanide (Scheme 20).<sup>135</sup> The catalyst was recyclable after a filtration step that could be



**SCHEME 20** Wool-SO<sub>3</sub>H or Fe<sub>3</sub>O<sub>4</sub>/wool-catalyzed synthesis of pyrazine- and quinoxaline derivatives.

bypassed by using a magnetic version of the catalyst (wool/Fe<sub>3</sub>O<sub>4</sub>). However, even though the synthesis of the catalyst did not involve sulfuric acid; the multiple wash steps, the use of potassium permanganate, sodium sulfite, and acetic acid were all necessary to obtain sufficient number of active sites.

A third example illustrating 6-membered ring multicomponent cyclization is the one-pot synthesis of 2-amino-4H-pyran derivatives via MCM-41@Schiff base-Co(OAc)<sub>2</sub>-mediated reaction of cyclohexane-1,3-diones, an aldehyde, and malononitrile (Scheme 21).<sup>136</sup> Pyrans are oxygen-containing heterocyclic compounds which skeletons are widely found as structural unit of natural products, including sugars and coumarins. As most heterocycles, pyran derivatives exhibit bioactive properties that have notably been evaluated for their anticancer potential.<sup>137</sup> The catalyst exhibited excellent performance; it afforded the products with yields around 90% in water at 50°C in a 3 h long reaction. The mesoporous silica-based catalyst showed good recyclability, it was recovered and reused in at least six cycles while maintaining a yield above 80%.

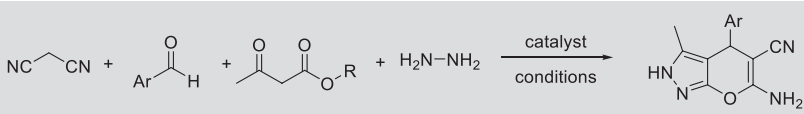


**SCHEME 21** Heterogeneous catalytic MCR-based synthesis of 2-amino-4H-pyran derivatives using MCM-41@Schiff base-Co(OAc)<sub>2</sub>.

Pyrazole derivatives, another useful group of biologically active heterocyclic compounds, can also be prepared from malononitrile as one of the starting materials. Various nanocomposite catalysts, exhibiting apparent synergetic effect provided by the different nanomaterials that compose them, have shown remarkable activity for the production of pyrano[2,3-*c*]pyrazole derivatives (Table 9).<sup>128, 138, 139</sup>

A magnetic nanocomposite catalyst based on melamine-functionalized graphene oxide nano-sheets, iron oxide nanoparticles, and zinc oxide, prepared via a multistep synthesis, efficiently catalyzed the one-pot four-component reaction in short reaction times with excellent yields (Table 9, entry 1).<sup>138</sup> The reaction mechanism appears to be initiated by effective electronic interactions between the Lewis acid sites of the ZnO nanoparticles and the heteroatoms of the carbonyl-containing starting materials. In addition to excellent catalytic activity, the catalyst demonstrated facilitated recovery upon magnetic separation and collection and good recyclability in at least eight consecutive cycles after which a noticeable drop in yield was observed. Another nanocomposite material based on SiO<sub>2</sub> nanoparticles and the combination of Co<sub>3</sub>O<sub>4</sub> nanoparticles and amino groups successfully catalyzed

**TABLE 9** Heterogeneous catalytic synthesis of 1,4-dihydropyrano[2,3-*c*]pyrazoles.

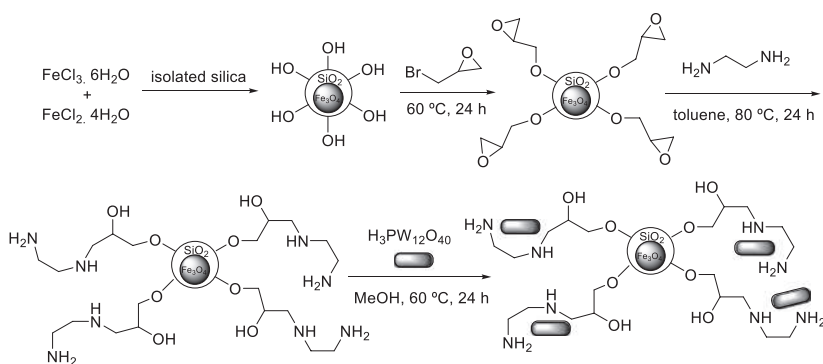


| Entry | Catalyst/conditions  | Yield (%) | Ref. |
|-------|--|-----------|------|
| 1     | Fe <sub>3</sub> O <sub>4</sub> /graphene oxide@melamine-ZnO, EtOH, RT, 10 min                            | 89–96     | 138  |
| 2     | Co <sub>3</sub> O <sub>4</sub> @SiO <sub>2</sub> -NH <sub>2</sub> , H <sub>2</sub> O/EtOH, RT, 35–55 min | 88–95     | 128  |
| 3     | Fe <sub>3</sub> O <sub>4</sub> @halloysite nanotubes-poly(ethylene imine), EtOH, RT, 10–20 min           | 89–96     | 139  |
| 4     | Fe <sub>3</sub> O <sub>4</sub> @SiO <sub>2</sub> EP-NH-HPA, H <sub>2</sub> O, RT, 3–11 min               | 89–98     | 140  |

the synthesis of 1,4-dihydropyrano[2,3-*c*]pyrazoles from ethyl acetoacetate, hydrazine hydrate, aldehydes, and malononitrile (Table 9, entry 2).<sup>128</sup> This approach ensured high yields in short reaction times. The high catalytic activity was attributed to the Brønsted base properties in addition to the high surface area. Unlike the graphene oxide-based catalyst, the recyclability of this nanocomposite was not investigated although the replacement of Co<sub>3</sub>O<sub>4</sub> with the magnetic Fe<sub>3</sub>O<sub>4</sub> nanoparticles was discussed. A third nanomaterial served as a backbone to generate a nanocomposite catalyst: halloysite nanotubes, naturally occurring aluminosilicate clay minerals that have the particular capability to hold both negative and positive charges within their structure (Table 9, entry 3).<sup>139</sup> In fact, the silica groups contained in the material rendered the external surface negatively charged while the alumina groups turned the core of the nanotubes into a positively charged internal surface. Like the two other nanocomposites reviewed, these halloysite nanotubes were functionalized with an imino group-containing compound, poly(ethylene imine), and magnetite. The desired products were obtained in high yields under mild reaction conditions. The catalyst presented similar behavior as the graphene oxide-based catalyst in terms of recyclability; it could be easily recovered upon application of an external magnet and it was reused in eight consecutive cycles before detecting a significant loss in activity.

Keggin-type heteropolyacids, specifically H<sub>3</sub>PW<sub>12</sub>O<sub>40</sub>, well known for their high acidity and thus their great catalytic activity, were heterogenized over amine-functionalized Fe<sub>3</sub>O<sub>4</sub>@SiO<sub>2</sub> nanoparticles and applied in the synthesis of pyrano[2,3-*c*]pyrazole derivatives.<sup>140</sup> In addition to making possible the recycling of the heteropolyacid catalyst, the immobilization increased its stability

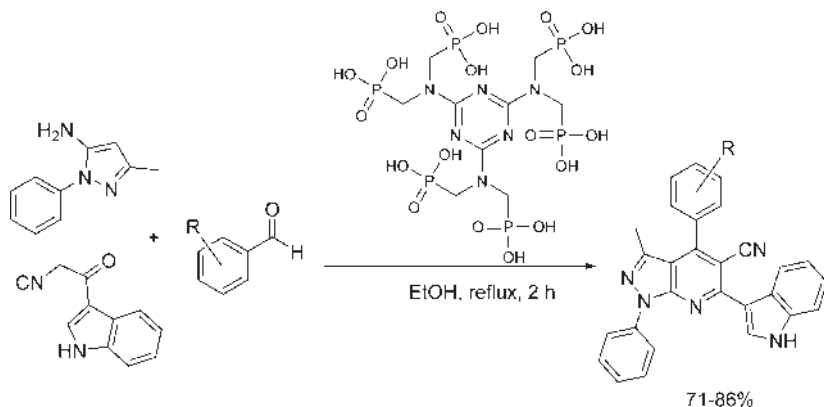
and also surprisingly increased its activity. In addition, the particular advantage of the catalyst lies in the origin of the silica nanoparticles that were extracted from the densely silicified horsetail plant defined as a cheap, highly reactive silicon source. The resulting heterogeneous catalyst exhibited excellent performance in the MCR. It should be noted that the synthesis of the catalyst requires three steps in addition to the extraction process to collect the silica from the horsetail plant. While the reaction steps were performed under relatively mild temperatures (60–80°C), the reactants were stirred for 24 h for each of the three steps. Moreover, a few organic solvents were employed, and several washing steps were required (Scheme 22).



**SCHEME 22** Schematic representation of the synthesis of  $\text{Fe}_3\text{O}_4@ \text{SiO}_2\text{-EP-NH-HPA}$  (IV) nanocatalyst.

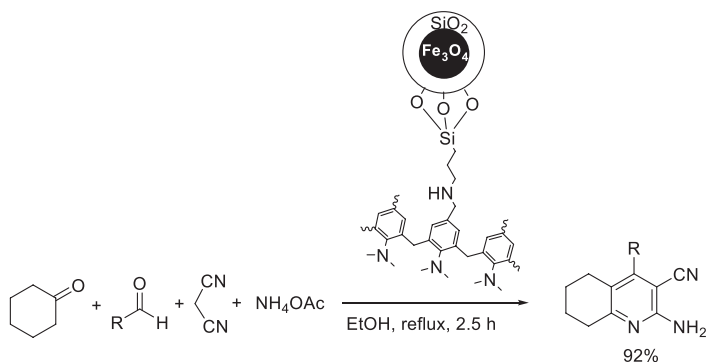
All four methods presented in Table 9 determined ethanol, water, or a mixture of the two to be the preferred solvents which, in addition to mild conditions, contribute to the environmentally benign features of the reactions.

It was already shown in the previous section that pyridine derivatives are commonly synthesized via one-pot multicomponent reactions; it will be demonstrated this time that they can be prepared specifically via MCRs involving isocyanides. As a representative example, the novel nanostructured melamine-based organic solid acid with phosphorus acid tags served as a heterogeneous catalyst for the synthesis of (3'-indolyl)pyrazolo[3,4-*b*] pyridines from cyano-acetylindole, 3-methyl-1-phenyl-1*H*-pyrazol-5-amine, and an aromatic aldehyde (Scheme 23).<sup>141</sup> The synthesis of the catalyst was relatively simple, entailing a one-step reaction of paraformaldehyde, 1,3,5-triazine-2,4,6-triamine, phosphorous acid in ethanol with a minimal amount of hydrochloric acid. More importantly, it yielded above 90% of solid catalyst that was collected after a simple filtration. The synthesized melamine hexakis(methylene)-hexakis(phosphonic acid) (MHMHPA) successfully catalyzed the four-component reaction in good yields in ethanol under reflux conditions. The solid catalyst could be recovered and reused in six consecutive cycles while still retaining satisfactory catalytic activity.



**SCHEME 23** Heterogeneous catalytic synthesis of (3'-indolyl)pyrazolo[3,4-*b*] pyridines using melamine hexakis(methylene)hexakis(phosphonic acid) as catalyst.

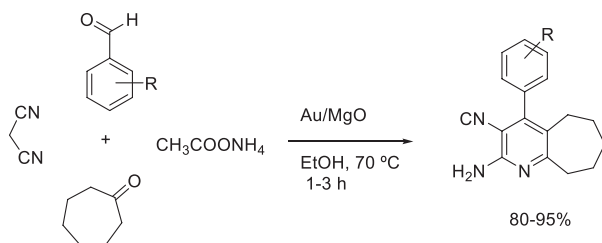
Another eco-friendly method affording pyridine derivatives from cyclohexanone, an aldehyde, malononitrile, and ammonium acetate in a one-pot fashion was reported by Asadbegi et al. (Scheme 24).<sup>142</sup> The preparation, characterization, and catalytic activity of the novel and reusable heterogeneous catalyst employed, a poly(*N,N*-dimethylaniline-formaldehyde) supported on silica-coated Fe<sub>3</sub>O<sub>4</sub> magnetic nanoparticles, was studied. The catalytic performance of this organic-inorganic hybrid nanomaterial was excellent, affording higher than 90% product yield in 2.5 h in refluxing ethanol. After reusing the same initial catalyst in six cycles, the yield was still around 85%.



**SCHEME 24** Heterogeneous catalytic synthesis of 2-amino-3-cyanopyridine derivatives using poly(*N,N*-dimethylaniline-formaldehyde) supported on silica-coated Fe<sub>3</sub>O<sub>4</sub> magnetic nanoparticles as a catalyst.

In another study, similar products were obtained, this time using cyclooctanone as a reagent in lieu of cyclohexanone. The eco-friendly and efficient method used Au/MgO as the catalyst and ethanol as the solvent.<sup>143</sup> In a similar

way to the Hantzsch mechanism, presented as a common synthetic route to form pyridines in the carbonyl-based reaction section before, the isocyanide-based reaction is initiated by a Knoevenagel condensation. The reaction then proceeds through a Michael-type addition of the ketone to the activated double bond of the arylidene intermediate before undergoing intramolecular cyclization and subsequent oxidation. The resulting products were obtained with high yields in under 3 h reaction time. The catalyst could be recovered and reused in up to six cycles with only slight loss in activity making the method a truly green synthesis given that the catalyst preparation also possesses minimal impact on the environment (Scheme 25).

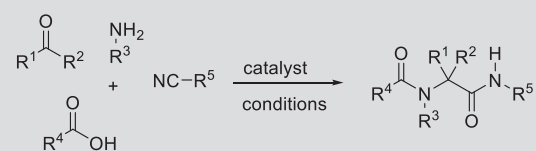
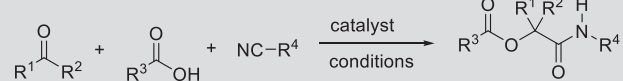
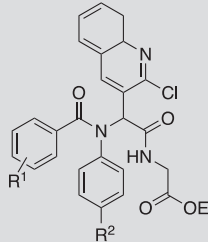
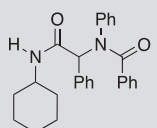


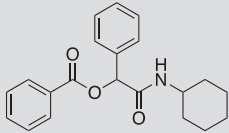
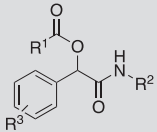
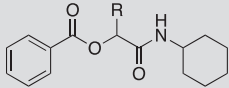
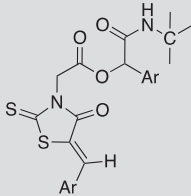
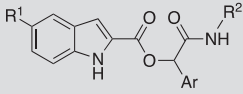
**SCHEME 25** Synthesis of multisubstituted pyridines by Au/MgO heterogeneous catalyst.

### 3.7.3.3 Aliphatic bond formation

The most well-known isocyanide-based multicomponent reactions are the Ugi and the Passerini reactions that produce peptidomimetic compounds of great importance notably as lead compounds in the drug discovery process or polymeric nanomaterials.<sup>116, 144, 145</sup> Both reactions deal with the same starting materials, namely an isocyanide, a carboxylic acid, and an aldehyde (or ketone), except that the Ugi reaction involves a fourth reagent—an amine.<sup>146</sup> Therefore their respective mechanism is essentially different. The Ugi reaction proceeds through the condensation of the amine with the aldehyde followed by the nucleophilic addition of the isocyanide to the previously formed imine intermediate. Then a second nucleophilic addition, initiated by the activated oxygen of the carboxylic acid to the carbon of the isocyanide, takes place before a rearrangement leads to an  $\alpha$ -aminoacyl amide derivative as the final product. In contrast, the Passerini reaction is initiated by a nucleophilic addition of the isocyanide to the carbonyl of the aldehyde (or ketone) followed by the addition of the carboxylate anion forming an  $\alpha$ -acyloxyamide after tautomerization.<sup>147</sup> The high reactivity of the starting materials involved in these reactions usually allow them to proceed without the need for a catalyst.<sup>148, 149</sup> However, when less activated substrates are employed, in order to obtain high yields and shorten the reaction times, the use of a catalyst becomes necessary. Selected examples of heterogeneous catalytic Ugi and Passerini multicomponent reactions are presented in Table 10 with various solid catalysts of proven performance.

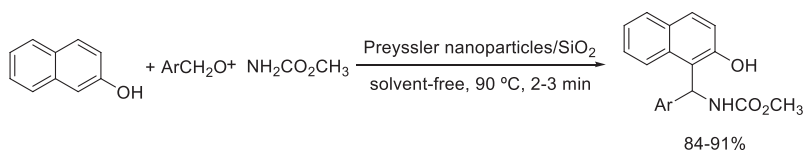
**TABLE 10** Heterogeneous catalytic Ugi and Passerini multicomponent reactions.

| Entry   | Reaction type | Catalyst/conditions             | Product   | Yield (%) | Ref.                |
|---|---------------|---------------------------------|---|-----------|---------------------|
| <p>Ugi</p>  <p>Passerini</p>  |               |                                 |   |           |                     |
| 1   | Ugi           | Fluorite, ethanol, MW, 2–10 min |   | 89–95     | <a href="#">150</a> |
| 2   | Ugi           | Indium-MOF, RT, 30–120 min      |  | 92        | <a href="#">151</a> |

|   |           |   |  |       |     |
|---|-----------|---|--|-------|-----|
|   | Passerini | Solvent free  |  | 89    |     |
| 3 | Passerini | Magnetic core-shell NPs supported TEMPO, O <sub>2</sub> (1atm), toluene, RT, 24 h |  | 53–92 | 152 |
| 4 | Passerini | Zr-MOF-Fe pyridine carboxaldehyde, acetonitrile, <i>hν</i> , RT, 24–30 h,         |  | 73–81 | 153 |
| 5 | Passerini | TMG-nanoSiO <sub>2</sub> , THF, reflux, 3–24 h                                    |  | 67–85 | 154 |
| 6 | Passerini | GO@lipase, THF, 40°C, 4–10 h  |  | 90–95 | 155 |

One of these catalysts is fluorite, a natural halide mineral, composed of calcium fluoride. It has inherent acidic properties that were exploited for the catalysis of a four-component Ugi reaction. The microwave-mediated synthesis provided excellent yields in a matter of minutes (Table 10, entry 1).<sup>150</sup> An environmentally friendly indium-MOF catalyst demonstrated high performance when applied to both the Ugi and the Passerini reactions (Table 10, entry 2).<sup>151</sup> The preparation of the catalysts was carried out by a straightforward microwave-assisted hydrothermal synthesis and their characterization revealed the presence of Lewis acid and base sites responsible for their high activity. Other examples, such as the magnetic core-shell nanoparticle-supported TEMPO<sup>152</sup> and the zirconium-based MOF<sup>153</sup>-driven oxidative three-component reactions, exhibit interesting advantages despite the use of a rather environmentally unfriendly solvent (Table 10, entries 3 and 4). The magnetic feature of the former catalyst allows its recyclability in no less than 14 cycles which is a major benefit in terms of cost and environmental friendliness. The latter catalyst possesses photoactive properties making the tandem oxidative Passerini reaction possible in a one-pot fashion upon irradiation with light. Finally, catalysts based on bio-derived compounds, such as nucleobase derivatives or enzymes, were explored for the Passerini MCR (Table 10, entries 5 and 6). The Passerini reaction of rhodanine-*N*-acetic acid with aromatic aldehydes and *tert*-butyl isocyanide was facilitated by tetramethylguanidine immobilized on silica nanoparticles (TMG-nanoSiO<sub>2</sub>) as a heterogeneous base catalyst.<sup>154</sup> Interestingly, while the presence of excess amount of aldehyde afforded the Passerini product, the use of equivalent amount of the aldehyde yielded a product resulting from the condensation of the aldehyde and rhodamine-*N*-acetic acid. Also worth mentioning, that the reaction of aldehydes possessing electron withdrawing groups afforded high yields in short reaction times, whereas aldehydes bearing strong electron donating groups were left unreacted. Another green and efficient Passerini reaction of indole-2-carboxylic acids, aromatic aldehydes, and alkyl isocyanides in presence of lipase immobilized on graphene oxide as a heterogeneous catalyst was reported by Rassi et al. (Table 10, entry 6).<sup>155</sup> The biocatalyst owes its remarkable activity to its acid-base amphoteric nature; it acts both as a proton donor and proton acceptor entity during the course of the reaction. Thus excellent yields were observed for most substrates, although it should be mentioned that the reaction, involving aldehydes containing electron donor groups at the 4-position, did not proceed. Both the tetramethylguanidine immobilized on silica nanoparticles and the lipase immobilized on graphene oxide were recyclable in five cycles after which a significant loss in activity was detected. In addition, the preparation of both required a rather laborious multistep synthesis.

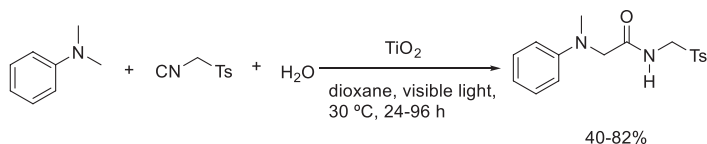
Another condensation-based one-pot multicomponent reaction using aryl aldehydes, beta-naphthol, and methyl carbamate led to the formation of carbamato-alkyl naphthols in the presence of silica-supported Preyssler nanoparticles (H<sub>14</sub>[NaP<sub>5</sub>W<sub>30</sub>O<sub>110</sub>]), a type of nanosized heteropolyacids (Scheme 26).<sup>156</sup> The catalyst benefits both from the solid nature of the heteropolyacids and the



**SCHEME 26** Silica-supported Preyssler nanoparticle-catalyzed synthesis of carbamatoalkyl naphthols.

large surface area provided by the nanoparticles. Therefore it allows an easy recovery while exhibiting enhanced activity. Excellent yields were reported under solvent-free conditions in a matter of a few minutes and the catalyst could be recycled and reused in three cycles with consistent yields. The supported catalyst possessed a better catalytic activity than its unsupported counterpart, likely due to the better dispersion of the active component on the surface of the nanoparticles.

The synthesis of  $\alpha$ -amino-amides from an isocyanide, an amine, and water, an Ugi-like reaction, is another example of multicomponent reactions leading to aliphatic bond formation. An interesting study focused on the visible light-mediated titanium dioxide-catalyzed synthesis of  $\alpha$ -amino-amides (Scheme 27).<sup>157</sup> It was proposed that the first step of the mechanism was the light-induced oxidation of the amine to produce an iminium ion that reacts in turn with the isocyanide to form a nitrilium ion affording the product upon tautomerization. Moderate to high yields were obtained after several days at 30°C in dioxane. Although the conditions do not seem ideal from an environmental point of view, the fact that this reaction type is underexplored makes the method an interesting new alternative for the production of essential building blocks.



**SCHEME 27** Heterogeneous catalytic synthesis of  $\alpha$ -amino-amides by  $\text{TiO}_2$  catalysis.

### 3.7.4. Conclusions and outlook

In light of the multiple examples reviewed in this chapter, it is unambiguous that heterogeneous catalysis has played and continues to play a major role in the development of environmentally benign MCR-based synthesis. Both carbonyl-based and isocyanide-based heterogeneous catalytic MCRs were extensively reviewed offering various synthetic routes to prepare heterocycles and other useful products through green approaches. Heterogeneous catalysis notably unlocked the access to mild reaction conditions and the possibility to recycle the catalysts. Finally, in spite of these obvious benefits, it should be stressed that

some solid acid catalysts require more laborious preparation than others, ranging from simple washing/drying treatments to multistep syntheses. It is important to take this factor into consideration for each process, in order to conscientiously determine the environmental impact of these heterogeneous catalytic reactions.

## References

1. Domling, A.; Wang, W.; Wang, K. Chemistry and Biology of Multicomponent Reactions. *Chem. Rev.* **2012**, *112*, 3083–3135.
2. Strecker, A. Ueber die künstliche Bildung der Milchsäure und einen neuen, dem Glycocoll homologen Körper. *Annal. Chem. Pharm.* **1850**, *75*, 27–45.
3. Mannich, C.; Krösche, W. Ueber ein Kondensationsprodukt aus Formaldehyd, Ammoniak und Antipyrin. *Archiv. Pharm.* **1912**, *250*, 647–667.
4. Biginelli, P. Ueber Aldehyduramide des Acetessigäthers. *Chem. Ber.* **1891**, *24*, 1317–1319.
5. Graebin, C. S.; Ribeiro, F. V.; Rogerio, K. R.; Kummerle, A. E. Multicomponent Reactions for the Synthesis of Bioactive Compounds: A Review. *Curr. Org. Synth.* **2019**, *16*, 855–899.
6. Alvim, H. G. O.; da Silva Junior, E. N.; Neto, B. A. D. What Do We Know About Multicomponent Reactions? Mechanisms and Trends for the Biginelli, Hantzsch, Mannich, Passerini and Ugi MCRs. *RSC Adv.* **2014**, *4*, 54282–54299.
7. Passerini, M.; Simone, L. Sopra gli isonitrili (I). Composto del *p*-isonitril-azobenzolo con acetone ed acido acetico. *Gazz. Chim. Ital.* **1921**, *51*, 126–129.
8. Ugi, I.; Meyr, R.; Fetzer, U.; Steinbrückner, C. Versuche mit Isonitrilen. *Angew. Chem.* **1959**, *71*, 386.
9. Gu, Y. Multicomponent Reactions in Unconventional Solvents: State of the Art. *Green Chem.* **2012**, *14*, 2091–2128.
10. Shirini, F.; Abedini, M. Application of Nanocatalysts in Multi-Component Reactions. *J. Nanosci. Nanotechnol.* **2013**, *13*, 4838–4860.
11. Treesa, G. S. S.; Saranya, S.; Meera, G.; Anilkumar, G. Recent Advances and Perspectives in the Silver-Catalyzed Multi-Component Reactions. *Curr. Org. Chem.* **2020**, *24*, 291–313.
12. Treesa, G. S.; Neetha, M.; Saranya, S.; Anilkumar, G. Cobalt-Catalyzed Multi-Component Reactions: Recent Advances and Perspectives in Organic Synthesis. *ChemistrySelect* **2020**, *5*, 7400–7416.
13. Climent, J. M.; Corma, A.; Iborra, S. Homogeneous and Heterogeneous Catalysts for Multi-component Reactions. *RSC Adv.* **2012**, *2*, 16–58.
14. D'Souza, D. M.; Mueller, T. J. J. Multi-Component Syntheses of Heterocycles by Transition-Metal Catalysis. *Chem. Soc. Rev.* **2007**, *36*, 1095–1108.
15. Iwanejko, J.; Wojaczynska, E.; Olszewski, T. K. Green Chemistry and Catalysis in Mannich Reaction. *Curr. Opin. Green Sustain. Chem.* **2018**, *10*, 27–34.
16. Jesin, I.; Nandi, G. C. Recent Advances in the A(3) Coupling Reactions and their Applications. *Eur. J. Org. Chem.* **2019**, *2019*, 2704–2720.
17. Sharma, U. K.; Ranjan, P.; Van der Eycken, E. V.; You, S.-L. *Sequential and Direct Multicomponent Reaction (MCR)-Based Dearomatization Strategies*; 2021. <https://doi.org/10.1039/d0cs00128g>.
18. Simon, L.; Goodman, J. M. Theoretical Study of the Mechanism of Hantzsch Ester Hydrogenation of Imines Catalyzed by Chiral BINOL-Phosphoric Acids. *J. Am. Chem. Soc.* **2008**, *130*, 8741–8747.
19. Saikia, L.; Dutta, D.; Dutta, D. K. Efficient Clay Supported Ni-0 Nanoparticles as Heterogeneous Catalyst for Solvent-Free Synthesis of Hantzsch Polyhydroquinoline. *Catal. Commun.* **2012**, *19*, 1–4.

- de Paolis, O.; Baffoe, J.; Landge, S. M.; Török, B. Multicomponent Domino Cyclization-Oxidative Aromatization on a Bifunctional Pd/C/K-10 Catalyst: an Environmentally Benign Approach toward the Synthesis of Pyridines. *Synthesis* **2008**, 3423–3428.
- Safaei-Ghomi, J.; Ziarati, A.; Zahedi, S. Silica (NPs) Supported Fe (III) as a Reusable Heterogeneous Catalyst for the One-Pot Synthesis of 1, 4-Dihydropyridines under Mild Conditions. *J. Chem. Sci.* **2012**, *124*, 933–939.
- Gupta, R.; Gupta, R.; Paul, S.; Loupy, A. Covalently Anchored Sulfonic Acid on Silica Gel as an Efficient and Reusable Heterogeneous Catalyst for the One-Pot Synthesis of Hantzsch 1,4-Dihydropyridines under Solvent-Free Conditions. *Synthesis* **2007**, 2835–2838.
- Mobinikhaledi, A.; Foroughifar, N.; Fard, M. A. B.; Moghanian, H.; Ebrahimi, S.; Kalhor, M. Efficient One-Pot Synthesis of Polyhydroquinoline Derivatives Using Silica Sulfuric Acid as a Heterogeneous and Reusable Catalyst Under Conventional Heating and Energy-Saving Microwave Irradiation. *Synth. Commun.* **2009**, *39*, 1166–1174.
- Sapkal, S. B.; Shelke, K. F.; Shingate, B. B.; Shingare, M. S. Nickel Nanoparticle-Catalyzed Facile and Efficient One-Pot Synthesis of Polyhydroquinoline Derivatives Via Hantzsch Condensation under Solvent-Free Conditions. *Tetrahedron Lett.* **2009**, *50*, 1754–1756.
- Tamaddon, F.; Moradi, S. Controllable Selectivity in Biginelli and Hantzsch Reactions Using nanoZnO as a Structure Base Catalyst. *J. Mol. Catal. A. Chem.* **2013**, *370*, 117–122.
- Katkar, S. S.; Mohite, P. H.; Gadekar, L. S.; Arbad, B. R.; Lande, M. K. ZnO-Beta Zeolite: as an Effective and Reusable Heterogeneous Catalyst for the One-Pot Synthesis of Polyhydroquinolines. *Green Chem. Lett. Rev.* **2010**, *3*, 287–292.
- Rostamnia, S.; Morsali, A. Basic Isoreticular Nanoporous Metal-Organic Framework for Biginelli and Hantzsch Coupling: IRMOF-3 as a Green and Recoverable Heterogeneous Catalyst in Solvent-Free Conditions. *RSC Adv.* **2014**, *4*, 10514–10518.
- Rao, A. V. D.; Surasani, R.; Vykuteswararao, B. P.; Bhaskarkumar, T.; Srikanth, B.; Jogdand, N. R.; Kalita, D.; Lilakar, J. K. D.; Siddaiah, V.; Sanasi, P. D.; Raghunadh, A. Sulfonic Acid-Functionalized Wang Resin (Wang-OSO<sub>3</sub>H) as Polymeric Acidic Catalyst for the Ecofriendly Multicomponent Synthesis of Polyhydroquinolines Via Hantzsch Condensation. *Synth. Commun.* **2016**, *46*, 1519–1528.
- Pagadala, R.; Maddila, S.; Dasireddy, V. D. B. C.; Jonnalagadda, S. B. Zn-VCO<sub>3</sub> Hydroxalcite: A Highly Efficient and Reusable Heterogeneous Catalyst for the Hantzsch Dihydropyridine Reaction. *Catal. Commun.* **2014**, *45*, 148–152.
- Kidwai, M.; Chauhan, R.; Bhatnagar, D.; Singh, A. K.; Mishra, B.; Dey, S. Nafion-H-A (R)-Catalyzed Synthesis of Polyhydroquinolines Via the Hantzsch Multicomponent Reaction. *Monatsh. Chem.* **2012**, *143*, 1675–1680.
- Alponti, L. H. R.; Picinini, M.; Urquieta-Gonzalez, E. A.; Corrêa, E. G. USY-Zeolite Catalyzed Synthesis of 1,4-Dihydropyridines Under Microwave Irradiation: Structure and Recycling of the Catalyst. *J. Mol. Struct.* **2021**, <https://doi.org/10.1016/j.molstruc.2020.129430>.
- Safari, J.; Zarnegar, Z.; Sadeghi, M.; Azizi, F. Chitosan-SO<sub>3</sub>H: An Efficient and Biodegradable Catalyst for the Green Syntheses of 1,4-Dihydropyridines. *Curr. Org. Chem.* **2016**, *20*, 2926–2932.
- Azizi, S.; Soleymani, J.; Hasanzadeh, M. Iron Oxide Magnetic Nanoparticles Supported on Amino Propyl-Functionalized KCC-1 as Robust Recyclable Catalyst for One Pot and Green Synthesis of Tetrahydropyrazolopyridines and Cytotoxicity Evaluation. *Appl. Organomet. Chem.* **2020**, *34*, e5440.
- Saffarian, H.; Karimi, F.; Yarie, M.; Zolfigol, M. A. Fe<sub>3</sub>O<sub>4</sub>@SiO<sub>2</sub>@(CH<sub>2</sub>)<sub>3</sub>-Urea-Quinoline Sulfonic Acid Chloride: A Novel Catalyst for the Synthesis of Coumarin Containing 1,4 Dihydropyridines. *J. Mol. Struct.* **2021**, *1224*, 129294.

35. Saberi, F.; Ostovar, S.; Behazin, R.; Rezvani, A.; Ebrahimi, A.; Shaterian, H. R. Insight into 6-Aminopenicillanic Acid Structure and Study of the Quantum Mechanical Calculations of the Acid–Base Site on  $\gamma\text{-Fe}_2\text{O}_3\text{/SiO}_2$  Core–Shell Nanocomposites and as Efficient Catalysts in Multicomponent Reactions. *New J. Chem.* **2020**, *44*, 20688–20696.
36. Ramanathan, D.; Pitchumani, K. Copper(I)-Y Zeolite-Catalyzed Regio- and Stereoselective [2+2+2] Cyclotrimerization Cascade: An Atom- and Step-Economical Synthesis of Pyrimido[1,6-a]Quinoline. *J. Org. Chem.* **2015**, *80*, 10299–10308.
37. Kulkarni, A.; Török, B. Microwave-Assisted Multicomponent Domino Cyclization-Aromatization: An Efficient Approach for the Synthesis of Substituted Quinolines. *Green Chem.* **2010**, *12*, 875–878.
38. Karimi, F.; Yarie, M.; Zolfigol, M. A.  $\text{Fe}_3\text{O}_4\text{/SiO}_2\text{@(CH}_2\text{)}_3\text{-Urea-Thiourea}$ : a Novel Hydrogen-Bonding and Reusable Catalyst for the Construction of Bipyridine-5-Carbonitriles via a Cooperative Vinylogous Anomeric Based Oxidation. *Mol. Catal.* **2020**, *497*, 111201.
39. De Souza, R. O. M. A.; da Penha, E. T.; Milagre, H. M. S.; Garden, S. J.; Esteves, P. M.; Eberlin, M. N.; Antunes, O. A. C. The Three-Component Biginelli Reaction: A Combined Experimental and Theoretical Mechanistic Investigation. *Chem. Eur. J.* **2009**, *15*, 9799–9804.
40. Heravi, M. M.; Zadsirjan, V. Recent Advances in Biginelli-Type Reactions. *Curr. Org. Chem.* **2020**, *24*, 1331–1366.
41. Rafiee, E.; Shahbazi, F. One-Pot Synthesis of Dihydropyrimidones Using Silica-Supported Heteropoly Acid as an Efficient and Reusable Catalyst: Improved Protocol Conditions for the Biginelli Reaction. *J. Mol. Catal. A. Chem.* **2006**, *250*, 57–61.
42. Shaterian, H. R.; Hosseinian, A.; Ghashang, M. An Efficient Synthesis of Multi-Substituted 3,4-Dihydropyrimidin-2(1H)-Ones/Thiones Under Solvent-Free Microwave Irradiation Using Alumina Sulfuric Acid. *Phosphorus Sulfur Silicon Relat. Elem.* **2009**, *184*, 197–205.
43. Chanu, L. V.; Singh, T. P.; Devi, L. R.; Singh, O. M. Synthesis of Bioactive Heterocycles Using Reusable Heterogeneous Catalyst  $\text{HClO}_4\text{-SiO}_2$  under Solvent-Free Conditions. *Green Chem. Lett. Rev.* **2018**, *11*, 352–360.
44. Bhuyan, D.; Saikia, M.; Saikia, L. ZnO Nanoparticles Embedded in SBA-15 as an Efficient Heterogeneous Catalyst for the Synthesis of Dihydropyrimidinones Via Biginelli Condensation Reaction. *Microporous Mesoporous Mater.* **2018**, *256*, 39–48.
45. Moghanian, H.; Fard, M. A. B.; Mobinikhaledi, A.; Ahadi, N. Bis(P-Sulfoanilino)Triazine-Functionalized Silica-Coated Magnetite Nanoparticles as an Efficient and Magnetically Reusable Nano-Catalyst for Biginelli-Type Reaction. *Res. Chem. Intermed.* **2018**, *44*, 4083–4101.
46. Ramazani, Z.; Elhamifar, D.; Norouzi, M.; Mirbagheri, R. Magnetic Mesoporous MCM-41 Supported Boric Acid: A Novel, Efficient and Ecofriendly Nanocomposite. *Compos. Part B Eng.* **2019**, *164*, 10–17.
47. Shinde, S. V.; Jadhav, W. N.; Lande, M. K.; Gadekar, L. S.; Arbad, B. R.; Kondre, J. M.; Karade, N. N. Scolecite as a Novel Heterogeneous Acid Catalyst for an Efficient Synthesis of 3,4-Dihydropyrimidin-2(1H)-Ones Via Multi-Component Biginelli Reaction. *Catal. Lett.* **2008**, *125*, 57–61.
48. Devthade, V.; Kamble, G.; Ghugal, S. G.; Chikhaliya, K. H.; Umare, S. S. Visible Light-Driven Biginelli Reaction over Mesoporous  $\text{g-C}_3\text{N}_4$  Lewis-Base Catalyst. *ChemistrySelect* **2018**, *3*, 4009–4014.
49. Fard, M. A. D.; Ghafari, H.; Rashidizadeh, A. Sulfonated Highly Ordered Mesoporous Graphitic Carbon Nitride as a Super Active Heterogeneous Solid Acid Catalyst for Biginelli Reaction. *Microporous Mesoporous Mater.* **2019**, *274*, 83–93.

50. El Mejdoubi, K.; Sallek, B.; Cherkaoui, H.; Chaair, H.; Oudadesse, H. One-Pot Synthesis of Dihydropyrimidinones/Thiones Catalyzed by White Marble a Metamorphic Rock: An Efficient and Reusable Catalyst for the Biginelli Reaction. *Kinet. Catal.* **2018**, *59*, 290–295.
51. Farooq, S.; Alharthi, F. A.; Alsahme, A.; Hussain, A.; Dar, B. A.; Hamid, A.; Koul, S. Dihydropyrimidinones: Efficient One-Pot Green Synthesis Using Montmorillonite-KSF and Evaluation of their Cytotoxic Activity. *RSC Adv.* **2020**, *10*, 42221–42234.
52. Ganja, H.; Robert, A. R.; Lavanya, P.; Chinnam, S.; Maddila, S.; Jonnalagadda, S. B.  $Y_2O_3/HAP$ , a Sustainable Catalyst for Novel Synthesis of Furo[3,4-b] Chromenes Derivatives Via Green Strategy. *Inorg. Chem. Commun.* **2020**, *114*, 107807.
53. Kargar, P. G.; Bagherzade, G.; Eshghi, H. Novel Biocompatible Core/Shell  $Fe_3O_4@NFC@Co(II)$  as a New Catalyst in a Multicomponent Reaction: An Efficient and Sustainable Methodology and Novel Reusable Material for One-Pot Synthesis of 4H-Pyran and Pyranopyrazole in Aqueous Media. *RSC Adv.* **2020**, *10*, 37086–37097.
54. Tailor, Y. K.; Khandelwal, S.; Verma, K.; Gopal, R.; Kumar, M. Multicomponent Synthesis of Dispiroheterocycles Using a Magnetically Separable and Reusable Heterogeneous Catalyst. *RSC Adv.* **2020**, *10*, 36713–36722.
55. Kamalzare, M.; Bayat, M.; Maleki, A. Green and Efficient Three Component Synthesis of 4H-Pyran Catalysed by  $CuFe_2O_4@Starch$  as a Magnetically Recyclable Bionanocatalyst. *R. Soc. Open Sci.* **2020**, *7*, 200385.
56. Babaei, S. E.; Hossaini, Z.; Besheli, R. R.; Tavakkoli, V.  $Fe_3O_4$  Nanoparticles as an Efficient and Reusable Catalyst for the Solvent-Free Synthesis of 1H-Indole and 1H-Pyrrole Derivatives. *Chem. Heterocycl. Comp.* **2016**, *52*, 294–298.
57. Bouherrou, H.; Saidoun, A.; Abderrahmani, A.; Abdellaziz, L.; Rachedi, Y.; Dumas, F.; Demenceau, A. Synthesis and Biological Evaluation of New Substituted Hantzsch Thiazole Derivatives from Environmentally Benign One-Pot Synthesis Using Silica Supported Tungstosilicic Acid as Reusable Catalyst. *Molecules* **2017**, *22*, 757.
58. Gewalt, K.; Schinke, E.; Böttcher, H. 2-Amino-Thiophene Aus Methyleneaktiven Nitrilen Carbonylverbindungen und Schwefel. *Chem. Ber.* **1966**, *99*, 94–100.
59. Bai, R.; Liu, P.; Yang, J.; Liu, C.; Gu, Y. Facile Synthesis of 2-Aminothiophenes Using  $NaAlO_2$  as an Eco-Effective and Recyclable Catalyst. *ACS Sustain. Chem. Eng.* **2015**, *3*, 1292–1297.
60. Rezaei-Seresht, E.; Tayebee, R.; Yasemi, M. KG-60-Piperazine as a New Heterogeneous Catalyst for Gewalt Three-Component Reaction. *Synth. Commun.* **2013**, *43*, 1859–1864.
61. Tayebee, R.; Ahmadi, S. J.; Seresht, E. R.; Javadi, F.; Yasemi, M. A.; Hosseinpour, M.; Maleki, B. Commercial Zinc Oxide: A Facile, Efficient, and Eco-Friendly Catalyst for the One-Pot Three-Component Synthesis of Multisubstituted 2-Aminothiophenes Via the Gewalt Reaction. *Ind. Eng. Chem. Res.* **2012**, *51*, 14577–14582.
62. Iqbal, S.; Rasheed, H.; Awan, R. J.; Awan, R. J.; Mukhtar, A.; Moloney, M. G. Recent Advances in the Synthesis of Pyrroles. *Curr. Org. Chem.* **2020**, *24*, 1196–1229.
63. Li, B.; Hu, H.; Mo, L.; Zhang, Z. Nano  $CoFe_2O_4$  Supported Antimony(III) as an Efficient and Recyclable Catalyst for One-Pot Three-Component Synthesis of Multisubstituted Pyrroles. *RSC Adv.* **2014**, *4*, 12929–12943.
64. Atar, A. B.; Jeong, Y. T. Heterogenized Tungsten Complex: an Efficient and High Yielding Catalyst for the Synthesis of Structurally Diverse Tetra Substituted Pyrrole Derivatives Via Four-Component Assembly. *Tetrahedron Lett.* **2013**, *54*, 5624–5628.
65. Gajengi, A. L.; Bhanage, B. M. NiO Nanoparticles: Efficient Catalyst for Four Component Coupling Reaction for Synthesis of Substituted Pyrroles. *Catal. Lett.* **2016**, *146*, 1341–1347.

66. Moghaddam, F. M.; Foroushani, B. K.; Rezvani, H. R. Nickel Ferrite Nanoparticles: An Efficient and Reusable Nanocatalyst for a Neat, One-Pot and Four-Component Synthesis of Pyrroles. *RSC Adv.* **2015**, *5*, 18092–18096.
67. Shinde, V. V.; Lee, S. D.; Jeong, Y. S.; Jeong, Y. T. P-Toluenesulfonic Acid Doped Polystyrene (PS-PTSA): Solvent-Free Microwave Assisted Cross-Coupling-Cyclization-Oxidation to Build One-Pot Diversely Functionalized Pyrrole from Aldehyde, Amine, Active Methylene, and Nitroalkane. *Tetrahedron Lett.* **2015**, *56*, 859–865.
68. Murthi, P. R. K.; Rambabu, D.; Rao, M. V. B.; Pal, M. Synthesis of Substituted Pyrroles Via Amberlyst-15 Mediated MCR under Ultrasound. *Tetrahedron Lett.* **2014**, *55*, 507–509.
69. Li, B.-L.; Zhang, H.-Y.; Di, J.-Q.; Zhang, Z. H. Polyoxometalate Immobilized on MOF-5 as an Environment-Friendly Catalyst for the Synthesis of Poly-Functionalized 3-Pyrrolin-2-Ones. *Appl. Organomet. Chem.* **2021**, *35*, e6064.
70. Turkes, C.; Arslan, M.; Demir, Y.; Cocaj, L.; Nixha, A. R.; Beydemir, S. Synthesis, Biological Evaluation and In Silico Studies of Novel N-Substituted Phthalazine Sulfonamide Compounds as Potent Carbonic Anhydrase and Acetylcholinesterase Inhibitors. *Bioorg. Chem.* **2019**, *89*, 103004.
71. Mourad, A. K.; Makhlof, A. A.; Soliman, A. Y.; Mohamed, S. A. Phthalazines and Phthalazine Hybrids as Antimicrobial Agents: Synthesis and Biological Evaluation. *J. Chem. Res.* **2020**, *44*, 31–41.
72. Mei, Q.; Wang, L.; Tian, B.; Tong, B.; Weng, J.; Zhang, B.; Jiang, Y.; Huang, W. Highly Efficient Red Iridium(III) Complexes Based on Phthalazine Derivatives for Organic Light-Emitting Diodes. *Dyes Pigments* **2013**, *97*, 43–51.
73. Martins, F. T.; Queiroz Maia, L. J.; Gasparotto, G.; Silva Medanha Valdo, A. K.; Nascimento Neto, J. A.; Ribeiro, L.; Rego, Y. D. F.; da Silva, C. M.; de Fatima, A. Phthalazine-Trione as a Blue-Green Light-Emitting Moiety: Crystal Structures, Photoluminescence and Theoretical Calculations. *New J. Chem.* **2019**, *43*, 1313–1321.
74. Ghahremani, M.; Davarpanah, J.; Rezaee, P.; Davoodi, G. Synthesis of Phthalazine Compounds Using Heterogeneous Base Catalyst Based on Silica Nanoparticles Obtained from Rice Husk. *Res. Chem. Intermed.* **2020**, *46*, 2683–2704.
75. Greenwood, N.; Earnshaw, A. *Chemistry of the Elements*; Pergamon Press: Oxford, 1984; pp. 393–399.
76. Sabale, P. M.; Patel, R. S. Synthesis, Characterization and Biological Evaluation of Substituted Novel Pyrazolone and Pyrazole Derivatives. *Indian J. Heterocycl. Chem.* **2013**, *23*, 143–148.
77. Schiel, M.; Chopra, A.; Silbestri, G.; Alvarez, M.; Lista, A.; Domini, C. Use of Ultrasound in the Synthesis of Heterocycles of Medicinal Interest. In *Green Synthetic Approaches for Biologically Relevant Heterocycles*; Brahmachari, G., Ed.; Elsevier: Boston, MA, 2015; pp. 571–601 (chapter 21).
78. Filian, H.; Kohzadian, A.; Mohammadi, M.; Ghorbani-Choghamarani, A.; Karami, A. Pd(0)-Guanidine@MCM-41: A Very Effective Catalyst for Rapid Production of Bis (Pyrazolyl) Methanes. *Appl. Organomet. Chem.* **2020**, *34*, e5579.
79. Yielzoleh, F. M.; Nikoofar, K. Magnetized Inorganic–Bioorganic Nanohybrid [nano Fe<sub>3</sub>O<sub>4</sub>-SiO<sub>2</sub>@Glu-Cu (II)]: A Novel Nanostructure for the Efficient Solvent-Free Synthesis of Thiazolidin-2-Imines. *Appl. Organomet. Chem.* **2021**, *35*, e6043.
80. Pawar, H. R.; Chikate, R. C. One Pot Three Component Solvent Free Synthesis of N-Substituted Tetrazoles Using RuO<sub>2</sub>/MMT Catalyst. *J. Mol. Struct.* **2021**, *1225*, 128985.
81. Cai, X.; Xie, B. Recent Advances in Asymmetric Strecker Reactions. *Arkivoc* **2014**, 205–248.

82. Abell, J. P.; Yamamoto, H. Dual-Activation Asymmetric Strecker Reaction of Aldimines and Ketimines Catalyzed by a Tethered Bis(8-Quinolinolato) Aluminum Complex. *J. Am. Chem. Soc.* **2009**, *131*, 15118–15119.
83. Zuend, S. J.; Coughlin, M. P.; Lalonde, M. P.; Jacobsen, E. N. Scaleable Catalytic Asymmetric Strecker Syntheses of Unnatural Alpha-Amino Acids. *Nature* **2009**, *461*, 968–970.
84. Iwanami, K.; Seo, H.; Choi, J.; Sakakura, T.; Yasuda, H. Al-MCM-41 Catalyzed Three-Component Strecker-Type Synthesis of Alpha-Aminonitriles. *Tetrahedron* **2010**, *66*, 1898–1901.
85. Dekamin, M. G.; Azimoshan, M.; Ramezani, L. Chitosan: a Highly Efficient Renewable and Recoverable Bio-Polymer Catalyst for the Expeditious Synthesis of Alpha-Amino Nitriles and Imines under Mild Conditions. *Green Chem.* **2013**, *15*, 811–820.
86. Maria Aguirre-Diaz, L.; Gandara, F.; Iglesias, M.; Snejko, N.; Gutierrez-Puebla, E.; Angeles Monge, M. Tunable Catalytic Activity of Solid Solution Metal-Organic Frameworks in One-Pot Multicomponent Reactions. *J. Am. Chem. Soc.* **2015**, *137*, 6132–6135.
87. Reinares-Fisac, D.; Maria Aguirre-Diaz, L.; Iglesias, M.; Snejko, N.; Gutierrez-Puebla, E.; Angeles Monge, M.; Gandara, F. A Mesoporous Indium Metal-Organic Framework: Remarkable Advances in Catalytic Activity for Strecker Reaction of Ketones. *J. Am. Chem. Soc.* **2016**, *138*, 9089–9092.
88. Rafiee, E.; Rashidzadeh, S.; Azad, A. Silica-Supported Heteropoly Acids: Highly Efficient Catalysts for Synthesis of Alpha-Aminonitriles, Using Trimethylsilyl Cyanide or Potassium Cyanide. *J. Mol. Catal. A. Chem.* **2007**, *261*, 49–52.
89. Dekamin, M. G.; Mokhtari, Z. Highly Efficient and Convenient Strecker Reaction of Carbonyl Compounds and Amines with TMSCN Catalyzed by MCM-41 Anchored Sulfonic Acid as a Recoverable Catalyst. *Tetrahedron* **2012**, *68*, 922–930.
90. Arend, M.; Westermann, B.; Risch, N. Modern Variants of the Mannich Reaction. *Angew. Chem. Int. Ed.* **1998**, *37*, 1044–1070.
91. Eshghi, H.; Rahimizadeh, M.; Hosseini, M.; Javadian-Saraf, A. Diastereoselective Three-Component Mannich Reaction Catalyzed by Silica-Supported Ferric Hydrogensulfate. *Monatsh. Chem.* **2013**, *144*, 197–203.
92. Ahad, A.; Farooqui, M. An Efficient Synthesis of 3-Amino-Alkylated Indoles Via a Mannich-Type Reaction Catalyzed by SiO<sub>2</sub>-I. *Heterocycl. Lett.* **2017**, *7*, 953–958.
93. Bigdeli, M. A.; Nemati, F.; Mahdavinia, G. H. HClO<sub>4</sub>-SiO<sub>2</sub> Catalyzed Stereoselective Synthesis of Beta-Amino Ketones Via a Direct Mannich-Type Reaction. *Tetrahedron Lett.* **2007**, *48*, 6801–6804.
94. Bosica, G.; Zammit, R. One-Pot Multicomponent Nitro-Mannich Reaction Using a Heterogeneous Catalyst under Solvent-Free Conditions. *PeerJ* **2018**, *6*, 1–29.
95. Kidwai, M.; Mishra, N. K.; Bansal, V.; Kumar, A.; Mozumdar, S. Novel One-Pot Cu-Nanoparticles-Catalyzed Mannich Reaction. *Tetrahedron Lett.* **2009**, *50*, 1355–1358.
96. Karmakar, B.; Banerji, J. A Competent Pot and Atom-Efficient Synthesis of Betti Bases over Nanocrystalline MgO Involving a Modified Mannich Type Reaction. *Tetrahedron Lett.* **2011**, *52*, 4957–4960.
97. Sharghi, H.; Khoshnood, A.; Doroodmand, M. M.; Khalifeh, R. Rapid, Eco-Friendly, and One-Pot Synthesis of New Lariat Ethers Based on Anthraquinone by Using ZnO Nanoparticles Via "Mannich" Reaction under Solvent-Free Condition. *J. Heterocyclic Chem.* **2016**, *53*, 164–174.
98. Jayashree, S.; Shivashankar, K. Montmorillonite K-10 Catalyzed Mannich Reaction: Synthesis of Aminonaphthoquinone Derivatives from Lawsone. *Synth. Commun.* **2018**, *48*, 1805–1815.

99. Esam, Z.; Akhavan, M.; Bekhradnia, A. One-Pot Multicomponent Synthesis of Novel 2-(Piperazin-1-yl) Quinoxaline and Benzimidazole Derivatives, Using a Novel Sulfamic Acid Functionalized Fe<sub>3</sub>O<sub>4</sub> MNPs as Highly Effective Nanocatalyst. *Appl. Organomet. Chem.* **2021**, *35*, e6005.
100. Ermolat'ev, D. S.; Bariwal, J. B.; Steenackers, H. P. L.; De Keersmaecker, S. C. J.; Van der Eycken, E. V. Concise and Diversity-Oriented Route toward Polysubstituted 2-Aminoimidazole Alkaloids and their Analogues. *Angew. Chem. Int. Ed.* **2010**, *49*, 9465–9468.
101. Yamamoto, Y.; Hayashi, H.; Saigoku, T.; Nishiyama, H. Domino Coupling Relay Approach to Polycyclic Pyrrole-2-Carboxylates. *J. Am. Chem. Soc.* **2005**, *127*, 10804–10805.
102. Kauffman, G.; Harris, G.; Dorow, R.; Stone, B.; Parsons, R.; Pesti, J.; Magnus, N.; Fortunak, J.; Confalone, P.; Nugent, W. An Efficient Chiral Moderator Prepared from Inexpensive (+)-3-Carene: Synthesis of the HIV-1 Non-nucleoside Reverse Transcriptase Inhibitor DPC 963. *Org. Lett.* **2000**, *2*, 3119–3121.
103. Zani, L.; Bolm, C. Direct Addition of Alkynes to Imines and Related C=N Electrophiles: a Convenient Access to Propargylamines. *Chem. Commun.* **2006**, 4263–4275.
104. Naeimi, H.; Moradian, M. Encapsulation of Copper(I)-Schiff Base Complex in NaY Nanoporosity: an Efficient and Reusable Catalyst in the Synthesis of Propargylamines Via A(3)-Coupling (Aldehyde-Amine-Alkyne) Reactions. *Appl. Catal. A Gen.* **2013**, *467*, 400–406.
105. Kodicherla, B.; Perumgani, P. C.; Mandapati, M. R. Polymer-Anchored Copper(II) Complex: An Efficient Reusable Catalyst for the Synthesis of Propargylamines. *Appl. Organomet. Chem.* **2014**, *28*, 756–759.
106. Shah, A. P.; Sharma, A. S.; Jain, S.; Shimpi, N. G. Microwave Assisted One Pot Three Component Synthesis of Propargylamine, Tetra Substituted Propargylamine and Pyrrolo[1,2-a] Quinolines Using CuNPs@ZnO-PTh as a Heterogeneous Catalyst. *New J. Chem.* **2018**, *42*, 8724–8737.
107. Bosica, G.; Gabarretta, J. Unprecedented One-Pot Multicomponent Synthesis of Propargylamines Using Amberlyst A-21 Supported CuI under Solvent-Free Conditions. *RSC Adv.* **2015**, *5*, 46074–46087.
108. Sharma, A. S.; Kaur, H.; Barot, N. Microwave-Assisted Facile Synthesis of Propargylamine Library by Robust Nitro Functionalized Cross-Linked Polystyrene Resin Supported Cu NPs. *J. Phys. Org. Chem.* **2018**, *31*, e3749.
109. Gholinejad, M.; Karimi, B.; Aminianfar, A.; Khorasani, M. One-Pot Preparation of Propargylamines Catalyzed by Heterogeneous Copper Catalyst Supported on Periodic Mesoporous Organosilica with Ionic Liquid Framework. *ChemPlusChem* **2015**, *80*, 1573–1579.
110. Xiong, X.; Chen, H.; Zhu, R. Highly Efficient and Scale-Up Synthesis of Propargylamines Catalyzed by Graphene Oxide-Supported CuCl<sub>2</sub> Catalyst under Microwave Condition. *Catal. Commun.* **2014**, *54*, 94–99.
111. Moghaddam, F. M.; Pourkaveh, R. Efficient Synthesis of Propargylamines in Aqueous Media Catalyzed by Au Nanoparticles under Ambient Temperature. *ChemistrySelect* **2018**, *3*, 2053–2058.
112. Mandal, P.; Chattopadhyay, A. P. Excellent Catalytic Activity of Magnetically Recoverable Fe<sub>3</sub>O<sub>4</sub>-Graphene Oxide Nanocomposites Prepared by a Simple Method. *Dalton Trans.* **2015**, *44*, 11444–11456.
113. Sadjadi, S.; Heravi, M. M.; Malmir, M. Green Bio-Based Synthesis of Fe<sub>2</sub>O<sub>3</sub>@SiO<sub>2</sub>-IL/Ag Hollow Spheres and their Catalytic Utility for Ultrasonic-Assisted Synthesis of Propargylamines and Benzo[b]Furans. *Appl. Organomet. Chem.* **2018**, *32*, e4029.
114. Barot, N.; Patel, S. B.; Kaur, H. Nitro Resin Supported Copper Nanoparticles: An Effective Heterogeneous Catalyst for C-N Cross Coupling and Oxidative C-C Homocoupling. *J. Mol. Catal. A. Chem.* **2016**, *423*, 77–84.

115. Giustiniano, M.; Basso, A.; Mercalli, V.; Massarotti, A.; Novellino, E.; Tron, G. C.; Zhu, J. To each his Own: Isonitriles for all Flavors. Functionalized Isocyanides as Valuable Tools in Organic Synthesis. *Chem. Soc. Rev.* **2017**, *46*, 1295–1357.
116. Domling, A.; Ugi, I. Multicomponent Reactions with Isocyanides. *Angew. Chem. Int. Ed.* **2000**, *39*, 3168–3210.
117. Rudick, J. G.; Shaabani, S.; Doemling, A. Editorial: Isocyanide-Based Multicomponent Reactions. *Front. Chem.* **2020**, *7*, 918.
118. Tailor, Y. K.; Khandelwal, S.; Kumari, Y.; Awasthi, K.; Kumar, M. An Efficient One Pot Three-Component Nanocatalyzed Synthesis of Spiroheterocycles Using TiO<sub>2</sub> Nanoparticles as a Heterogeneous Catalyst. *RSC Adv.* **2015**, *5*, 46415–46422.
119. Tailor, Y. K.; Khandelwal, S.; Verma, K.; Gopal, R.; Kumar, M. Diversity-Oriented Synthesis of Spirooxindoles Using Surface-Modified TiO<sub>2</sub> Nanoparticles as Heterogeneous Acid Catalyst. *ChemistrySelect* **2017**, *2*, 5933–5941.
120. Khan, T.; Yadav, R. Silica-Supported P<sub>2</sub>O<sub>5</sub> as an Efficient Heterogeneous Catalyst for the One Pot Synthesis of 3-Amino-Imidazo[2,1-b](1,3)Benzothiazole under Green Conditions. *J. Heterocyclic Chem.* **2019**, *56*, 11–17.
121. Wang, Y.; Ge, W.; Fang, Y.; Ren, X.; Cao, S.; Liu, G.; Li, M.; Xu, J.; Wan, Y.; Han, X.; Wu, H. Porous CeO<sub>2</sub> Nanorod-Catalyzed Synthesis of Poly-Substituted Imino-Pyrrolidine-Thiones. *Res. Chem. Intermed.* **2017**, *43*, 631–640.
122. Swami, S.; Devi, N.; Agarwala, A.; Singh, V.; Shrivastava, R. ZnO Nanoparticles as Reusable Heterogeneous Catalyst for Efficient One Pot Three Component Synthesis of Imidazo-Fused Polyheterocycles. *Tetrahedron Lett.* **2016**, *57*, 1346–1350.
123. Boltjes, A.; Dömling, A. The Groebke-Blackburn-Bienaymé Reaction. *Eur. J. Org. Chem.* **2019**, 7007–7049.
124. Shaabani, A.; Seyyedhamzeh, M.; Shaabani, S.; Ganji, N. Multi-Walled Carbon Nanotubes Sulfuric Acid as a Reusable Heterogeneous Solid Acid Catalyst for the Rapid Synthesis of Imidazo[1,2-a]Pyridines. *Res. Chem. Intermed.* **2015**, *41*, 2377–2383.
125. Shaabani, A.; Nosrati, H.; Seyyedhamzeh, M. Cellulose@Fe<sub>2</sub>O<sub>3</sub> Nanoparticle Composites: Magnetically Recyclable Nanocatalyst for the Synthesis of 3-Aminoimidazo[1,2-a]Pyridines. *Res. Chem. Intermed.* **2015**, *41*, 3719–3727.
126. Budhiraja, M.; Kondabala, R.; Ali, A.; Tyagi, V. First Biocatalytic Groebke-Blackburn-Bienaymé Reaction to Synthesize Imidazo[1,2-a]Pyridine Derivatives Using Lipase Enzyme. *Tetrahedron* **2020**, *76*, 131643.
127. Shaabani, A.; Mohammadian, R.; Hooshmand, S. E.; Hashemzadeh, A.; Amini, M. M. Zirconium Metal-Organic Framework (UiO-66) as a Robust Catalyst toward Solvent-Free Synthesis of Remarkable Heterocyclic Rings. *ChemistrySelect* **2017**, *2*, 11906–11911.
128. Shahbazi, S.; Ghasemzadeh, M. A.; Shakib, P.; Zolfaghari, M. R.; Bahmani, M. Synthesis and Antimicrobial Study of 1,4-Dihydropyrano[2,3-c]Pyrazole Derivatives in the Presence of Amino-Functionalized Silica-Coated Cobalt Oxide Nanostructures as Catalyst. *Polyhedron* **2019**, *170*, 172–179.
129. Abdellatif, K. R. A.; Abdelall, E. K. A.; Fadaly, W. A. A.; Kamel, G. M. Synthesis, Cyclooxygenase Inhibition, and Anti-Inflammatory Evaluation of Novel Diarylheterocycles with a Central Pyrazole, Pyrazoline, or Pyridine Ring. *Med. Chem. Res.* **2015**, *24*, 2632–2644.
130. Xia, R.; Guo, T.; Chen, M.; Su, S.; He, J.; Tang, X.; Jiang, S.; Xue, W. Synthesis, Antiviral and Antibacterial Activities and Action Mechanism of Penta-1,4-Dien-3-One Oxime Ether Derivatives Containing a Quinoxaline Moiety. *New J. Chem.* **2019**, *43*, 16461–16467.
131. Akhtar, J.; Khan, A. A.; Ali, Z.; Haider, R.; Yar, M. S. Structure-Activity Relationship (SAR) Study and Design Strategies of Nitrogen-Containing Heterocyclic Moieties for their Anticancer Activities. *Eur. J. Med. Chem.* **2017**, *125*, 143–189.

132. Aghajani, M.; Asghari, S.; Pasha, G. F.; Mohseni, M. Study of Three-Component Reaction of Alpha-Ketoesters and Active Methylenes with OH-Acids to Synthesize New 2-Amino-4H-Pyran Derivatives and Evaluation of their Antibacterial and Antioxidant Activities. *Res. Chem. Intermed.* **2020**, *46*, 1841–1855.
133. Ziarati, A.; Safaei-Ghomi, J.; Rohani, S. A One-Pot Multi-Component Synthesis of N-Cyclohexyl-3-Aryl-Quinoxaline-2-Amines Using ZnO Nanoparticles as a Heterogeneous Reusable Catalyst. *Lett. Org. Chem.* **2013**, *10*, 47–52.
134. Sekerova, L.; Brezinova, P.; Do, T. T.; Vyskocilova, E.; Krupka, J.; Cerveny, L.; Havelkova, L.; Bashta, B.; Sedlacek, J. Sulfonated Hyper-Cross-Linked Porous Polyacetylene Networks as Versatile Heterogeneous Acid Catalysts. *ChemCatChem* **2020**, *12*, 1075–1084.
135. Shaabani, A.; Hezarkhani, Z.; Faroghi, M. T. Wool-SO<sub>3</sub>H and Nano-Fe<sub>3</sub>O<sub>4</sub>@Wool as Two Green and Natural-Based Renewable Catalysts in One-Pot Isocyanide-Based Multicomponent Reactions. *Monatsh. Chem.* **2016**, *147*, 1963–1973.
136. Pan, S.; Li, P.; Xu, G.; Guo, J.; Ke, L.; Xie, C.; Zhang, Z.; Hui, Y. MCM-41@Schiff Base-co(OAc)(2) as an Efficient Catalyst for the Synthesis of Pyran Derivatives. *Res. Chem. Intermed.* **2020**, *46*, 1353–1371.
137. Kumar, D.; Sharma, P.; Singh, H.; Nepali, K.; Gupta, G. K.; Jain, S. K.; Ntie-Kang, F. The Value of Pyrans as Anticancer Scaffolds in Medicinal Chemistry. *RSC Adv.* **2017**, *7*, 36977–36999.
138. Eivazzadeh-Keihan, R.; Taheri-Ledari, R.; Khosropour, N.; Dalvand, S.; Maleki, A.; Mousavi-Khoshdel, S. M.; Sohrabi, H. Fe<sub>3</sub>O<sub>4</sub>/GO@Melamine-ZnO Nanocomposite: a Promising Versatile Tool for Organic Catalysis and Electrical Capacitance. *Colloids Surf. A Physicochem. Eng. Asp.* **2020**, *587*, 124335.
139. Hajizadeh, Z.; Maleki, A. Poly(Ethylene Imine)-Modified Magnetic Halloysite Nanotubes: a Novel, Efficient and Recyclable Catalyst for the Synthesis of Dihydropyrano [2,3-c] Pyrazole Derivatives. *Mol. Catal.* **2018**, *460*, 87–93.
140. Mohtasham, N.; Gholizadeh, M. Nano Silica Extracted from Horsetail Plant as a Natural Silica Support for the Synthesis of H<sub>3</sub>PW<sub>12</sub>O<sub>40</sub> Immobilized on Aminated Magnetic Nanoparticles (Fe<sub>3</sub>O<sub>4</sub>@SiO<sub>2</sub>-EP-NH-HPA): A Novel and Efficient Heterogeneous Nanocatalyst for the Green One-Pot Synthesis of Pyrano[2,3-c]Pyrazole Derivatives. *Res. Chem. Intermed.* **2020**, *46*, 3037–3066.
141. Afsar, J.; Zolfigol, M. A.; Khazaei, A.; Zarei, M.; Gu, Y.; Alonso, D. A.; Khoshnood, A. Synthesis and Application of Melamine-Based Nano Catalyst with Phosphonic Acid Tags in the Synthesis of (3'-Indolyl)Pyrazolo[3,4-b] Pyridines Via Vinylogous Anomeric Based Oxidation. *Mol. Catal.* **2020**, *482*, 110666.
142. Asadbegi, S.; Bodaghifard, M. A.; Mobinikhaledi, A. Poly N,N-Dimethylaniline-Formaldehyde Supported on Silica-Coated Magnetic Nanoparticles: A Novel and Retrievable Catalyst for Green Synthesis of 2-Amino-3-Cyanopyridines. *Res. Chem. Intermed.* **2020**, *46*, 1629–1643.
143. Pagadala, R.; Maddila, S.; Moodley, V.; van Zyl, W. E.; Jonnalagadda, S. B. An Efficient Method for the Multicomponent Synthesis of Multisubstituted Pyridines, a Rapid Procedure Using Au/MgO as the Catalyst. *Tetrahedron Lett.* **2014**, *55*, 4006–4010.
144. Gordon, A.; Landge, S. Recent Advances in Multicomponent Microwave-Assisted Ugi Reactions. In *Non-traditional Activation Methods in Green and Sustainable Applications: Microwaves, Ultrasounds, Photo, Electro and Mechanochemistry and High Hydrostatic Pressure*; Török, B., Schäfer, C., Eds.; Elsevier: Cambridge, Oxford, 2021 Chp. 3, pp. 71–99.
145. Huang, H.; Jiang, R.; Ma, H.; Li, Y.; Zeng, Y.; Zhou, N.; Liu, L.; Zhang, X.; Wei, Y. Fabrication of Claviform Fluorescent Polymeric Nanomaterials Containing Disulfide Bond

- through an Efficient and Facile Four-Component Ugi Reaction. *Mater. Sci. Eng. C* **2021**, *118*, 111437.
146. Liu, Z. Ugi and Passerini Reactions as Successful Models for Investigating Multicomponent Reactions. *Curr. Org. Chem.* **2014**, *18*, 719–739.
  147. Maeda, S.; Komagawa, S.; Uchiyama, M.; Morokuma, K. Finding Reaction Pathways for Multicomponent Reactions: The Passerini Reaction Is a Four-Component Reaction. *Angew. Chem. Int. Ed.* **2011**, *50*, 644–649.
  148. Pharande, S. G.; Renteria-Gomez, M. A.; Gamez-Montano, R. Isocyanide Based Multicomponent Click Reactions: A Green and Improved Synthesis of 1-Substituted 1H-1,2,3,4-Tetrazoles. *New J. Chem.* **2018**, *42*, 11294–11298.
  149. Gohel, J. N.; Lunagariya, K. S.; Kapadiya, K. M.; Khunt, R. C. An Efficient Protocol for the Synthesis of 1, 5-Disubstituted Tetrazole Derivatives Via a TMS-N-3 Based Ugi Reaction and their Anti-Cancer Activity. *ChemistrySelect* **2018**, *3*, 11657–11662.
  150. Mohanram, I.; Meshram, J.; Shaikh, A.; Kandpal, B. Microwave-Assisted One-Pot Synthesis of Bioactive UGI-4CR Using Fluorite as Benign and Heterogeneous Catalyst. *Synth. Commun.* **2013**, *43*, 3322–3328.
  151. Maria Aguirre-Diaz, L.; Iglesias, M.; Snejko, N.; Gutierrez-Puebla, E.; Angeles Monge, M. Synchronizing Substrate Activation Rates in Multicomponent Reactions with Metal-Organic Framework Catalysts. *Chem. Eur. J.* **2016**, *22*, 6654–6665.
  152. Karimi, B.; Farhangi, E. One-Pot Oxidative Passerini Reaction of Alcohols Using a Magnetically Recyclable TEMPO under Metal- and Halogen-Free Conditions. *Adv. Synth. Catal.* **2013**, *355*, 508–516.
  153. Azarifar, D.; Ghorbani-Vaghei, R.; Daliran, S.; Oveisi, A. R. A Multifunctional Zirconium-Based Metal-Organic Framework for the One-Pot Tandem Photooxidative Passerini Three-Component Reaction of Alcohols. *ChemCatChem* **2017**, *9*, 1992–2000.
  154. Baharfar, R.; Azimi, R.; Barzegar, S.; Mohseni, M. Efficient Synthesis of Rhodanine-Based Amides Via Passerini Reaction Using Tetramethylguanidine-Functionalized Silica Nanoparticles as Reusable Catalyst. *J. Braz. Chem. Soc.* **2015**, *26*, 1396–1404.
  155. Rassi, S.; Baharfar, R. Synthesis of Indole-Based Amides Using Immobilized Lipase on Graphene Oxide (GO@Lipase) as a Retrievable Heterogeneous Nano Biocatalyst. *Polyhedron* **2019**, *174*, 114153. UNSP.
  156. Heravi, M. M.; Tavakoli-Hoseini, N.; Bamoharram, F. F. Silica-Supported Preyssler Nano Particles: a Green, Reusable and Highly Efficient Heterogeneous Catalyst for the Synthesis of Carbamatoalkyl Naphthols. *Green Chem. Lett. Rev.* **2010**, *3*, 263–267.
  157. Vila, C.; Rueping, M. Visible-Light Mediated Heterogeneous C-H Functionalization: Oxidative Multi-Component Reactions Using a Recyclable Titanium Dioxide (TiO<sub>2</sub>) Catalyst. *Green Chem.* **2013**, *15*, 2056–2059.



## Chapter 3.8

# Ring transformations by heterogeneous catalysis

### 3.8.1. Introduction

Cyclization reactions provide an instant and effective path to generate molecular complexity. In fact, the vast majority of the synthesis of complex molecules involve one or more cyclizations. One of the first ring formation reactions in the history of organic chemistry was reported back in 1884 by the German chemists Carl Paal and Ludwig Knorr. The original Paal-Knorr cyclization prepares furans from 1,4-diketones.<sup>1</sup> Later the reaction was also adapted to the cyclization of pyrroles<sup>2</sup> and thiophenes.<sup>3</sup> Another famous example, the Diels-Alder cyclization, occurring between a conjugated diene and a substituted alkene (often referred as “a dienophile”) was a second breakthrough in the discovery of cyclization reactions that won the two scientists, whom the reaction is named after, the Nobel Prize in Chemistry in 1950.<sup>4</sup> Now a large number of cyclization reaction-types exist and while some are self-driven,<sup>5-7</sup> others require a catalyst to be initiated.<sup>8-10</sup> Porous materials with abundant active sites are of particular interest when dealing with heteroatom-containing starting materials for the preparation of heterocycles due to multiple potential electrochemical interactions.<sup>11-13</sup>

Although ring opening reactions are less commonly employed for the synthesis of complex molecules than cyclization reactions, they undeniably remain important in organic chemistry. For instance, the electrophilic ring opening of small heterocycles such as epoxides or aziridines allow the introduction of various electrophilic functional groups.<sup>14</sup> The same is true for the formation and ring opening of cyclopropanes.<sup>15, 16</sup> Similarly, ring opening polymerization is one of the many paths leading to the formation of polymers which are of prominent importance in the 20th and 21st centuries due to their multiple and highly practical applications.<sup>17</sup> Whether this group of reactions is initiated by a radical, an electrophilic or a nucleophilic route, catalysis constitutes a critical tool to increase the reaction rate and allow the tolerance of various functional groups.<sup>14, 17</sup> Commonly used catalysts include transition metals, metal salts, a variety of acids and organocatalysts.<sup>14, 17</sup> Here again, heterogeneous catalysis can bring its unique set of assets<sup>18-23</sup>; it has a high potential to contribute to the expansion of

the applicability of ring opening reactions as well as to ensure that the catalytic processes are conform to the recent environmental and safety requirements.<sup>24–28</sup>

This subchapter describes representative examples of various heterogeneous catalytic cyclization and ring opening (with possible subsequent cycloaddition) reactions thus revealing the wide application scope of heterogeneous catalysis to ring transformations. The examples will be selected and evaluated based on their green synthesis potential, and mechanistic insights will also be provided.

The reactions presented will be discussed according to the type of the ring transformation: ring formation (cyclization) and ring opening.

### 3.8.2. Cyclization

Due to the diversity of applications of cyclic molecules and their importance in many fields, notably in medicinal chemistry, the development of cyclization reactions has been ongoing since the emergence of organic chemistry as a discipline.<sup>1, 4</sup> There are two distinct strategies to achieve cyclization; the intramolecular and intermolecular cyclizations. Cyclization can occur as a step-wise process that uses multiple linear substrates as starting materials, which are nucleophiles, electrophiles, or radicals; and the ring closure step gives rise to a new bond.<sup>29</sup> On the other hand, the cyclization mechanism could also be concerted, and two bonds are formed during the process. Both cyclization strategies can produce either two C–X bonds (X being a heteroatom), two C–C bonds or one bond of each type.<sup>29, 30</sup>

#### 3.8.2.1 Intermolecular cyclization reactions

##### 3.8.2.1.1 *Diels-Alder and hetero-Diels-Alder reactions*

The [4+2] cycloaddition forming new C–C bonds from a diene and a dienophile, widely known as the Diels-Alder reaction, is a well-established synthetic transformation providing a perfect 100% atom economy.<sup>31, 32</sup> Hetero-Diels-Alder reactions are regular Diels-Alder reactions that include substrates with heteroatoms. The reaction allows for the formation of two or more rings in a simultaneous manner avoiding sequential chemical reactions that require multiple separation and purification steps. Therefore, they represent a highly efficient synthetic pathway for the formation of complex, often heterocyclic compounds, especially natural products. Although Diels-Alder reactions can occur as self-driven organic transformations due to the complementary reactivity of the reagents, the diene, and the dienophile,<sup>33, 34</sup> several substrates are not sufficiently activated to undergo the reaction spontaneously and would require harsh reaction conditions.<sup>35, 36</sup> Harsh conditions, however, often result in low selectivity due to undesired side reactions. The use of a suitable catalyst can afford high yields under mild conditions even with deactivated substrates. Highly porous solid acid catalysts are promising candidates to perform the challenging task. It is mainly due to their unique framework, in which the reactants can reorganize

and ultimately cyclize.<sup>37–45</sup> The catalyst can offer additional benefits to the obvious green advantages that the perfect atom economy of the transformation provides, such as potential recyclability. A broad array of heterogeneous catalysts has been developed for the Diels-Alder reaction including heteropolyacids,<sup>37, 38</sup> metal oxides,<sup>39, 40</sup> clays,<sup>41, 42</sup> zeolites,<sup>43, 44</sup> and MOFs.<sup>45–47</sup> Naturally, each catalyst demonstrates efficiency for different types of substrates. The corresponding representative examples are presented in Table 1.

Tungstophosphoric acid ( $H_3PW_{12}O_{40}$ ) supported on silica gel is a well-known heterogeneous catalyst that efficiently catalyze the Diels-Alder reactions. It proved to significantly accelerate the reaction rate of Diels-Alder reactions of enones with various dienes<sup>37</sup> as well as quinones with butadienes (Table 1, entries 1 and 2).<sup>38</sup> The catalyst was active under mild conditions and its solid nature theoretically allows its recovery and reuse although it has not been investigated experimentally in the referenced works.

Another tungsten-containing catalyst, tin-tungsten mixed oxide, prepared by calcination at high temperature (800°C), was found to be highly effective in the regular Diels-Alder reaction of various dienes and dienophiles and it also demonstrated good recyclability (Table 1, entry 3).<sup>39</sup> Mild reaction conditions, short reaction times and ambient temperatures, were sufficient to achieve excellent yields.

Kiamehr et al. developed a protocol based on a zinc oxide catalyst, that showed high activity for the synthesis of inactivated alkynes with indole-2-thiones for the preparation of pentacyclic indole derivatives (Table 1, entry 4).<sup>40</sup> The role of the catalyst was dual and the reaction proceeded via domino Knoevenagel-condensation/hetero-Diels-Alder cyclization sequence.

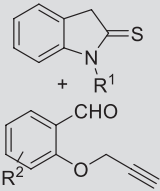
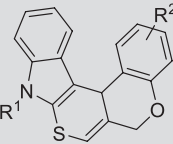
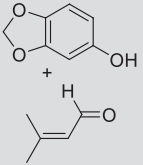
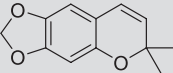
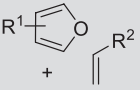
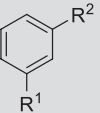
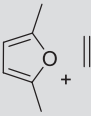
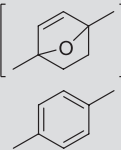
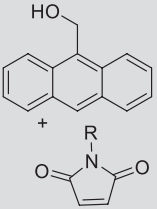
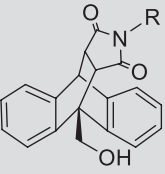
Similarly, a microwave-assisted montmorillonite K-10 catalyzed hetero-Diels Alder reaction successfully resulted in the synthesis of methylenedioxyprococene, a natural insecticide (Table 1, entry 5).<sup>41</sup> Here again, the catalyst successfully catalyzed both an electrophilic addition of 3-methyl-2-butenal to sesamol and the subsequent intramolecular hetero-Diels-Alder cyclization.

Zeolites such as ZMS-5 can also be used to produce aromatic compounds from furans and dienes in a continuous flow fixed-bed reactor at a temperature range of 450–600°C (Table 1, entry 6).<sup>43</sup> Co-feeding propylene with furan afforded a selectivity of 57% toward toluene, whereas co-feeding propylene with 2-methylfuran increased the formation of xylene. The selectivity of the reaction was highly dependent on the furan/diene ratio; for instance, the higher production of xylene (45%) was obtained with a molar ratio of propylene to 2-methyl-furan of 1 at 450°C. Although the selectivities are not excellent and the reaction conditions are harsh, the goal of the study was to demonstrate the potential of zeolites to catalyze Diels-Alder reactions from furan-based compounds and olefins in continuous mode in order to convert lignocellulosic biomass feedstock to useful aromatics.

For the same purpose, the selective conversion of biomass-derived 2,5-dimethylfurantop-xylene was achieved through Diels-Alder cycloaddition and

**TABLE 1** Heterogeneous catalytic Diels-Alder and hetero-Diels-Alder reactions.

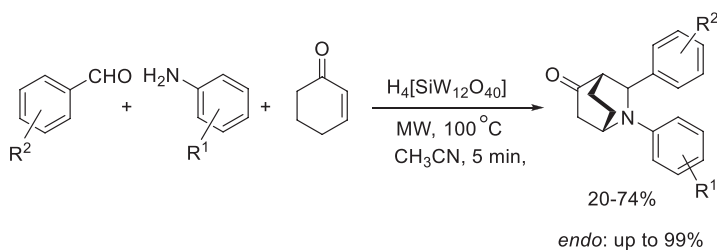
| Entry | Starting material   | Catalyst/conditions   | Product          | Yield (%)                                       | Ref.      |
|-------|---|---|------------------|---|-----------|
|       |   |   |                  |   |           |
| 1     |   | <p>H<sub>3</sub>PW<sub>12</sub>O<sub>40</sub>/silica, CH<sub>2</sub>Cl<sub>2</sub>,<br/>0–4°C, 5–27 h</p> |                  | <p>37–82<br/>Selectivity: 84–97 to<br/>3–16</p> | <p>37</p> |
| 2     |   | <p>H<sub>3</sub>PW<sub>12</sub>O<sub>40</sub>/silica, toluene,<br/>RT, 20 h</p>                           |                  | <p>70</p>                                       | <p>38</p> |
| 3     | <p>Various cyclic and<br/>linear dienes and<br/>dienophiles</p> | <p>Sn-W<sub>2</sub>-800 (tin-tungsten<br/>mixed oxide), CH<sub>2</sub>Cl<sub>2</sub>, RT,<br/>0.5–1 h</p> | <p>Examples:</p> | <p>86–97</p>                                    | <p>39</p> |

|   |  |   |  |                                    |    |
|---|--|---|--|------------------------------------|----|
| 4 |   | ZnO, CH <sub>3</sub> CN, reflux, 3 h                          |  | 85–95                              | 40 |
| 5 |   | Montmorillonite K-10-K <sup>+</sup> , solvent-free, MW, 8 min |  | Not specified                      | 41 |
| 6 |   | ZSM-5, 450–600°C  |   | Depending on furan/<br>diene ratio | 43 |
| 7 |   | Silica-alumina aerogel, 1,4-dioxane, 250°C, 4 h               |   | 60                                 | 44 |
| 8 |  | MOF, EtOH, 40–50°C, 24 h                                      |   | 60–86                              | 45 |

subsequent dehydration with silica-alumina aerogel catalysts (Table 1, entry 7).<sup>44</sup> The yield indicated in Table 1 corresponds to the yield of the final product obtained after dehydration of the cycloadduct. Interestingly, it was observed that the reaction rate of the dehydration step was dependent on the concentration of the Brønsted acid sites on the surface of the catalyst; in contrast, the cycloaddition was rather dependent on the Lewis acid sites. Because most zeolites comprise a diminished Lewis acidity due to the electron density transfer from the oxygen atoms present in the framework, their catalytic activity in the Diels-Alder cycloaddition was questioned in this work. It is probable that the zeolites promote the formation of the cycloadduct on account of a simple charge transfer and confinement matter. These observations corroborated with the conclusions drawn in a similar work studying the production of toluene from 2-methylfuran and ethylene.<sup>48</sup>

Last, a highly porous electron rich metal-organic framework (MOF), prepared from a tetracarboxylic acid, showed excellent performances in the Diels-Alder reaction of reactive and less reactive starting materials such as polyaromatic compounds and maleimides under mild conditions (Table 1, entry 8).<sup>45</sup> Evidently, the high surface area combined with the porous nano-channels of the catalyst created a confined environment where the reactants, thus encapsulated, easily underwent reorganization subsequently followed by the adduct formation. It was observed that the aliphatic substrates, having lower affinity to the catalyst framework, were subject to diminished reactivity. Nonetheless, the advantages of the heterogeneous material were further demonstrated by reusing it in several cycles.

Several multicomponent reactions (MCRs) also include the Diels-Alder reaction as their cyclization step. A heteropolyacid-catalyzed condensation/hetero Diels-Alder domino reaction sequence produced azabicyclo[2.2.2]octan-5-ones, in a microwave-assisted reaction with moderate to good yields (Scheme 1).<sup>49</sup> Among the several commercially available heteropoly acids tested in the transformation,  $H_4[SiW_{12}O_{40}]$  provided the best yields and highest diastereoselectivities for the *endo* products.



**SCHEME 1** A microwave-assisted heteropoly acid-catalyzed condensation-hetero Diels-Alder domino reaction sequence for the synthesis of azabicyclo[2.2.2]octan-5-ones.

### 3.8.2.1.2 *Heterogeneous catalytic synthesis of six-membered rings*

Many heterocyclic compounds are regularly synthesized by MCRs that occur in a several steps-one pot fashion including a cyclization step in their sequence of reactions. One such reaction is the Hantzsch synthesis using an aldehyde, two equivalents of  $\beta$ -ketoester and a nitrogen donor.<sup>50</sup> The reaction can be catalyzed by a broad array of heterogeneous catalysts such as clays,<sup>51, 52</sup> silica,<sup>53–55</sup> metal nanoparticles,<sup>56, 57</sup> zeolites,<sup>58</sup> MOF,<sup>59</sup> and ion exchange resins.<sup>60–62</sup> Another well-known transformation is the Biginelli reaction that produces dihydropyrimidones from an aldehyde, an  $\alpha$ -ketoester (or a ketone) and urea.<sup>63, 64</sup> The various heterogeneous catalytic protocols apply silica or alumina supported catalysts such as heteropolyacids,<sup>65</sup> other Brønsted acids,<sup>66, 67</sup> and metal oxide nanoparticles.<sup>68, 69</sup> Other examples that are commonly used for the synthesis of cyclic compounds catalyzed by a wide selection of solid catalysts include the Gewald reaction,<sup>70</sup> isocyanide based MCRs,<sup>71</sup> the Groebke-Blackburn-Bienaymé reaction,<sup>72</sup> just to name a few. MCRs are the focus of another chapter in this book, thus, here we focus on processes that are not covered there.

### Pyrazines and piperazines

Pyrazines are two-nitrogen-containing six-membered ring compounds. They are of particular importance for the synthesis of pharmaceuticals<sup>73</sup> and fragrances.<sup>74</sup> Among them, 2-methylpyrazine is used as a precursor in the synthesis of the antituberculosis drug pyrazinamide.<sup>75</sup> To date, the most effective pathway for the synthesis of 2-methylpyrazine is a cyclodehydration/dehydrogenation route starting from ethylenediamine and propylene glycol, a reaction that occurs at high temperatures in presence of a catalyst.<sup>75</sup> Homogeneous catalytic systems based on transition metals such as Zn, Cu, Cr have proved their efficiency in the synthesis of pyrazines.<sup>75–77</sup> Although heterogeneous catalytic systems have been less explored, they offer numerous benefits compared to their homogeneous counterparts, such as the possibility to perform the reaction in a continuous bed flow system, or the recycling of the catalyst. Notably, Cu and Zn-modified zeolites demonstrated excellent performance by suitably tuning the reaction conditions and catalyst composition and structure.<sup>78, 79</sup> The reaction conditions and results of representative examples are presented in [Table 2](#).

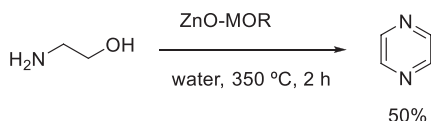
The activity of CuO/ZnO/meso-SiO<sub>2</sub> catalysts possessing different pore diameters were compared in the synthesis of 2-methylpyrazine using a continuous fixed-bed reactor at 380°C for 1 h ([Table 2](#), entry 1).<sup>78</sup> It was found that the sample CZ/S1, possessing the smallest pore size (17.8 nm)—which appeared to be a critical factor—was the most efficient catalyst, converting the starting materials to the desired product in 69% yield. It was also observed that the surface acid strength of CZ/S1 was moderate; while high acid strength led to more by-products and low acidic strength resulted in decreased yields. Another comparative study examined the activity of Zn-modified zeolite for the same

**TABLE 2** Modified-zeolite-catalyzed synthesis of 2-methylpyrazine.

| Entry | Catalyst/conditions                                      | Yield (%) | Ref. |
|-------|--|-----------|------|
| 1     | CuO/ZnO/meso-SiO <sub>2</sub> (CZ/S1), water, 380°C, 2 h | 69        | 78   |
| 2     | ZSM-5, water, 450°C, 2 h                                 | 63        | 79   |

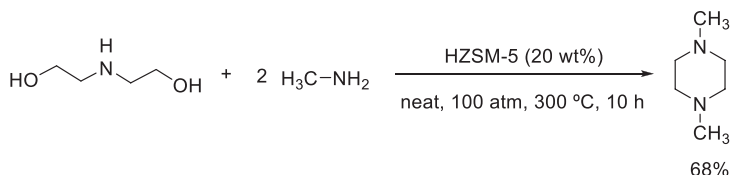
reaction.<sup>79</sup> ZSM-5 afforded the highest yield of 2-methylpyrazine at 450°C, its activity was attributed to the high density of Lewis acid sites (Table 2, entry 2).

Another type of zeolites, ZnO-modified samples, were investigated for the condensation reaction of mono-ethanolamine on a continuous flow bed to produce pyrazine and alkyl substituted pyrazines as a function of temperature and time.<sup>80</sup> The highest yield of pyrazine was obtained with catalyst type ZnO-MOR after 2 h at 350°C (Scheme 2).



**SCHEME 2** Condensation of monoethanolamine over ZnO-modified zeolite in a continuous bed flow reactor.

The fully hydrogenated derivatives of pyrazines, piperazines, are also important intermediates for drug syntheses and particularly for quinoline-type antibacterial drugs. They also serve as precursors for the synthesis of pyrazines. The synthesis of *N,N'*-dimethylpiperazine via intermolecular cyclization of diethanolamine was studied under high pressure and high temperature conditions using zeolites and montmorillonite K-10 as catalysts (Scheme 3).<sup>81</sup> The study specifically revealed the potential of the zeolite HZSM-5 which was found to achieve good yields and recyclability. However, in addition to harsh reaction conditions, the catalyst loads employed were relatively high.

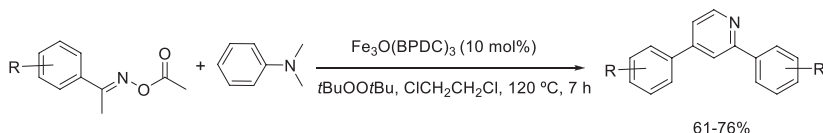


**SCHEME 3** Zeolite-catalyzed synthesis of *N,N*-dimethylpiperazine via the intermolecular cyclization of diethanolamine with methylamine.

## Pyridines

Pyridines<sup>82</sup> constitute another important class of six-membered nitrogen-containing heterocycles that offers a wide range of applications in pharmaceutical,<sup>83</sup> and fine chemical industries.<sup>84–86</sup> The synthesis of pyridines along with their condensed derivatives, quinolines or isoquinolines or their hydrogenated products, piperidines, or tetrahydroquinolines have been the target of extensive attention.<sup>87–89</sup> Here we describe a recent representative heterogeneous catalytic example.

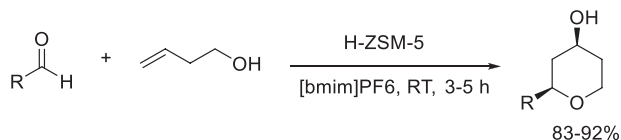
Metal-organic frameworks (MOFs) were shown to efficiently catalyze the synthesis of pyridines and achieved superior results compared to homogeneous catalytic systems.<sup>90</sup> The cyclization reaction of *N,N*-dialkylanilines with ketoxime carboxylates to produce aryl-substituted pyridines was successfully carried out by an iron-based metal-organic framework at 120°C (Scheme 4).<sup>90</sup> In addition to the better performance, the iron-MOF was recyclable in five cycles without significant loss of activity. However, it should be stressed that the reaction required the use of an oxidant in stoichiometric amount; the combination of the oxidative reagent *tert*-butylperoxide and 1,2-dichloroethane as a solvent led to the highest yields of pyridine but at the same time their presence decreases the green advantage of the reaction.



**SCHEME 4** Iron-MOF-catalyzed synthesis of pyridines via cyclization of *N,N*-dialkylanilines with ketoxime carboxylates.

## Tetrahydropyranols

The last six-membered ring cyclization of heterocycles that will be discussed in the “intermolecular cyclization” section is the Prins-cyclization to produce tetrahydropyranols, key building blocks for the synthesis of various carbohydrates, polyether antibiotics, and marine macrolides.<sup>91, 92</sup> The Prins-cyclization is commonly performed using Lewis acid catalysts that often lead to a mixture of products and make necessary multiple purification steps. Novel heterogeneous catalytic systems were developed to address this problem. Zeolites and acidic ion-exchange resins are particularly promising as they afford substantially higher yields of products and allow for milder reaction conditions (Scheme 5).<sup>91</sup> Their use in combination with recyclable ionic liquids ([bmim]PF<sub>6</sub>) proved to be a useful, eco-friendly method for the production of tetrahydropyranols.



**SCHEME 5** Heterogeneous catalytic synthesis of tetrahydropyranols in presence of ionic liquids.

### 3.8.2.1.3 Heterogeneous catalytic synthesis of five-membered rings

#### Pyrroles

The Paal-Knorr pyrrole synthesis is one of the earliest and most well-known synthetic processes in organic chemistry.<sup>1</sup> It produces pyrroles through the condensation of a 1,4-dicarbonyl compound with an excess of a primary amine or ammonia. Acidic conditions are usually employed to conduct such reactions; alternative methods based on solid acid catalysts offer major advantages over mineral acids.<sup>27, 93</sup> Representative heterogeneous catalytic examples are tabulated in Table 3.

Several studies report the use of clays as catalyst,<sup>94–97</sup> many other studies describe protocols using acids bound to a variety of support materials.<sup>98–103</sup> Banik et al. described a montmorillonite KSF-catalyzed synthesis of pyrroles performed using a minimum amount of organic solvent to ensure proper mixing

**TABLE 3** Heterogeneous catalytic Paal-Knorr pyrrole synthesis.

| Entry | Catalyst/conditions   | Yield (%) | Ref.   |
|-------|---|-----------|--------|
| 1     | Montmorillonite KSF, CH <sub>2</sub> Cl <sub>2</sub> , RT, 10–25 h  | 70–95     | 94     |
| 2     | Montmorillonite K-10, solvent-free, 3–6 min, microwave, 90°C  | 91–98     | 95, 96 |
| 3     | Fe(III)-montmorillonite, CH <sub>2</sub> Cl <sub>2</sub> , RT, 1–6 h  | 69–96     | 97     |
| 4     | Silica sulfuric acid, solvent-free, RT, 3–45 min  | 70–97     | 98     |
| 5     | Silica-supported dendritic amine, solvent-free, RT, 2 h   | 75–99     | 99     |
| 6     | Cellulose-sulfuric acid, solvent-free, RT, 4–15 min   | 83–95     | 100    |
| 7     | Fe <sub>3</sub> O <sub>4</sub> @PEG400-SO <sub>3</sub> H, solvent-free, RT, 5–120 min   | 70–96     | 101    |
| 8     | Nanomagnetically modified, heterogenized sulfuric acid, solvent-free, 60°C, 15 min–12 h   | 60–90     | 102    |
| 9     | Fe <sub>3</sub> O <sub>4</sub> /DAG-SO <sub>3</sub> H, H <sub>2</sub> O/EtOH, RT, 10–120 min  | 70–98     | 103    |
| 10    | SbCl <sub>3</sub> /SiO <sub>2</sub> , hexane, RT, 1 h   | 51–94     | 104    |
| 11    | [NaP <sub>5</sub> W <sub>30</sub> O <sub>110</sub> ] <sub>14</sub> , solvent-free, 60°C, 30–180 min   | 50–98     | 105    |
| 12    | α-Zr(O <sub>3</sub> PCH <sub>3</sub> ) <sub>1.2</sub> (O <sub>3</sub> PC <sub>6</sub> H <sub>4</sub> SO <sub>3</sub> H) <sub>0.8</sub> , solvent-free, RT, 1–24 h | 56–95     | 106    |

of the reagents, after which it was evaporated leaving the reaction mixture as a solid phase. Finally, the dry mixture was left to react at room temperature for several hours (Table 3, entry 1).<sup>94</sup> Several amines including monocyclic, bicyclic, tricyclic, tetracyclic aromatic, aliphatic, heterocyclic, and benzylic amines were used in combination with 2,5-hexanedione to afford high yields of products. A major limitation of the study is the lack of recyclability tests that could have further justified the environmental friendliness of the method. A clay of the same type, montmorillonite K-10, demonstrated high catalytic activity for the preparation of substituted pyrroles (Table 3, entry 2).<sup>95</sup> The short reaction times, solvent-free conditions and excellent yields are notable advantages of the method. Using this protocol, the same group reported the synthesis of *N*-sulfonylpyrroles by applying aryl sulfonamides as the nitrogen source.<sup>96</sup> Another study evaluated various metal-exchanged montmorillonites for the Paal-Knorr condensation.<sup>97</sup> It was found that Fe(III)-montmorillonite afforded the highest yields compared to the Zn, Co, Cu-exchanged counterparts (Table 3, entry 3). The catalyst could be easily recycled and successfully reused three consecutive times.

Several sulfonated solid-acid catalysts, namely, silica sulfuric acid,<sup>98</sup> dendritic amine grafted on mesoporous silica,<sup>99</sup> cellulose sulfuric acid,<sup>100</sup> and sulfonic acid grafted onto polyethylene glycol 400-encapsulated Fe<sub>3</sub>O<sub>4</sub> nanoparticles<sup>101</sup> catalyzed the synthesis of pyrroles employing diverse amines ranging from aromatic to aliphatic compounds, at room temperature in the absence of solvent (Table 3, entries 4–7). Additional advantages include the short reaction times, simple work-up procedure, and high yields. Other sulfonated solid-acid catalysts, such as the gamma-Fe<sub>2</sub>O<sub>3</sub>@SiO<sub>2</sub>-OSO<sub>3</sub>H<sup>102</sup> or the Fe<sub>3</sub>O<sub>4</sub>/diaminoglyoxime-SO<sub>3</sub>H<sup>103</sup> were also employed under mild reactions conditions (Table 3, entries 8 and 9). In addition, both catalysts were magnetically separable from the reaction mixture. Although these methods possess undeniable green aspects, it should be noted that the preparation of most of these solid acid catalysts employs mineral acids as a pretreatment or as a reagent. Nevertheless, they offer the possibility to recycle and reuse the catalyst, which is not feasible in single phase mineral acid-driven procedures in which the generation of waste is inevitable.

In addition to clays or sulfonated heterogeneous catalysts, silica-supported antimony(III) chloride was reported as a highly efficient heterogeneous Lewis acid catalyst for the Paal-Knorr pyrrole synthesis performed at room temperature (Table 3, entry 10).<sup>104</sup> Low catalyst loading, operational simplicity, applicability to various substrates, and recyclability of the catalyst are notable advantages of this sulfuric-acid-free method. On the contrary, the use of hexane does not work in favor of an eco-friendly label.

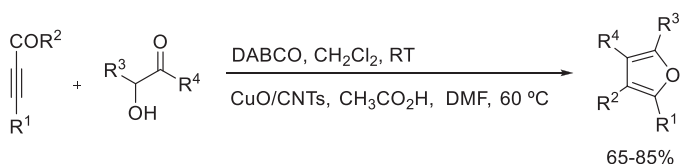
Preyssler heteropolyacids supported on mesoporous alumina, constituting a material with acid-base properties, catalyzed the synthesis of a series of pyrrole derivatives under solvent-free conditions (Table 3, entry 11).<sup>105</sup> The catalyst had a bifunctional role as it facilitated the formation of 2-amino-3-cyano-4*H*-chromenes by a multicomponent reaction and their subsequent

conversion to pyrrole via the Paal-Knorr reaction. The workup and catalyst recovery were simple, and all reactions were highly selective toward the corresponding pyrrole.

Last, potassium-exchanged layered zirconium sulfophenyl phosphonate was described to efficiently promote the Paal-Knorr condensation of several alkyl and aryl amines with 1,4-diketones under mild reaction conditions.<sup>106</sup> The basic counterpart of the catalyst ( $\text{Zr}(\text{KPO}_4)_2$ ), potassium exchanged layered zirconium phosphate, provided equivalent results although the sulfophenyl phosphonate-based catalyst exhibited superior performance when dealing with aryl amines (Table 3, entry 12).

### Furans

Although furans are not as popular building blocks as pyrroles, the development of contemporary green methods for their synthesis also attracted considerable attention. A two-step domino approach was developed for the preparation of substituted furans from electron deficient alkynes and  $\alpha$ -hydroxy ketones (Scheme 6).<sup>107</sup> After the addition of the O–H bond of the alcohol to the triple bond, the CuO/CNT (CNT = carbon nanotube) catalysts initiated the cyclization providing the products in good yields. Although the catalyst could be reused up to five times without notable loss in activity, the use of undesirable solvents ( $\text{CH}_2\text{Cl}_2$ , DMSO) in the protocol decreases the green value of the process. Electron deficient alkynes and 2-yn-1-ols can also be used in a similar synthetic method.<sup>108</sup>



**SCHEME 6** Synthesis of furans via a carbon nanotubes-supported CuO-catalyzed cyclization.

### The Huisgen 1,3-dipolar cycloaddition

The Huisgen 1,3-dipolar cycloaddition is a reaction of a dipolarophile, such as an alkene or an alkyne, with a 1,3-dipolar compound that leads to the formation of 5-membered rings.<sup>109</sup> Often the dipolar compounds involved are comprised of 3 atoms and  $4\pi$  electrons and possess formal charges. Examples of such molecules include nitrile oxides, nitrile imines, nitrile sulfides, diazo compounds, and azides. Overall, the feasibility of the cycloaddition depends critically on the nature of the central atoms involved in the bond formation process and their hybridization.<sup>109</sup> More specifically, the rate of the cycloaddition is controlled by the relative energies of the HOMO of one reactant together with the LUMO of the second reactant. The closer these molecular orbitals

are in energy the faster the rate of the reaction, however, steric factors can also interfere. Regarding the regioselectivity, it is controlled by the polarity of the reactants, complementary polarities being greatly favored.

The Huisgen cycloaddition allows for the preparation of a wide range of useful heterocycles. For instance, the reaction of azides with alkynes produces 1,2,3-triazoles that are key building blocks for the synthesis of biologically active molecules. Typically, the reaction is catalyzed by a copper salt-based catalyst with a well-established method classified as “click chemistry” that was developed by Sharpless et al.<sup>110</sup> Such reactions are reliable, and they efficiently yield functional materials. More recently, multiple methods have been developed to provide additional advantages to the Huisgen reaction most notably by using supported copper catalysts that also exhibited good recyclability, and by potentially eliminating solvents from the reaction mixture. Immobilized copper-catalysts that have been used for this purpose include zeolites,<sup>111, 112</sup> mesoporous silica,<sup>113</sup> metal oxide,<sup>114, 115</sup> ion exchange resins,<sup>116</sup> and chelate resins.<sup>116</sup> Some methods employ halides as starting materials and react them with sodium azide prior to the actual cycloaddition. In that case, the catalyst plays a dual role in catalyzing the nucleophilic substitution as well. It generates the azide in situ, and then catalyzes the Huisgen reaction successively. Several methods, their conditions and the resulting yields are presented in Table 4.

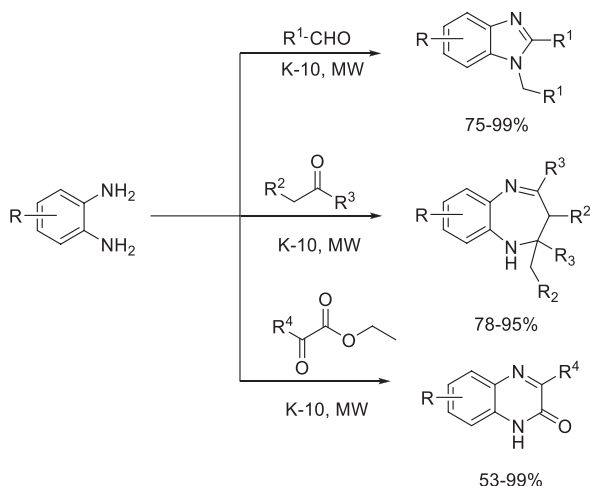
All catalysts employed demonstrated good activity, stability, and recyclability. Although the different methods yield equal performance, each of them possesses advantages and drawbacks from environmental perspectives depending on the reaction conditions used. For instance, water and solvent-free medium are more desirable than organic solvents, especially, halogenated solvents. It must be noted that the water insolubility of some substrates can limit the substrate scope of a specific reaction. In the Cu<sup>I</sup>-zeolite-catalyzed reaction, this limitation was overcome by the addition of equivalent amount of either ethanol or dioxane to the water (Table 4, entry 1).<sup>111</sup> Also, the use of neat conditions provided interesting results in combination with a chelate resin despite the need for trimethylamine as a co-catalyst. In regard to the reaction times and temperatures, most reactions were performed at mild temperatures (Table 4, entries 3–7)<sup>113–117</sup> or at moderately elevated temperatures up to 90°C (Table 4, entries 1, and 2) for several hours.<sup>111, 112</sup> The mesoporous silica-catalyzed reactions were remarkably long for some substrates although these reactions were carried out at room temperature (Table 4, entry 3).<sup>113</sup> One of the methods employing a zeolite catalyst demonstrated significantly shortened reaction times when microwave irradiation was applied at higher temperatures (up to 110°C) (Table 4, entry 2).<sup>112</sup> Finally, the environmental impact of the heterogeneous catalyst preparation also has to be taken into account. Most supported catalysts were prepared in a few steps with limited amount of supplemental reagents. Some, however, required harsh conditions; Fe<sub>3</sub>N@SiO<sub>2</sub> catalyst was prepared from two insoluble iron precursors that were incorporated into mesoporous silica microspheres after a treatment at 700°C in NH<sub>3</sub> (Table 4, entry 3).<sup>113</sup>

**TABLE 4** Heterogeneous catalytic Huisgen 1,3-dipolar cycloadditions.

| Entry | Substrate  | Catalyst/conditions  | Yield (%) | Ref. |
|-------|--|--|-----------|------|
| 1     | Sodium azide/halides, phenyl-acetylene   | Cu <sup>I</sup> -zeolite/water, 90°C, 15 h   | 58–98     | 111  |
| 2     | Sodium azide/halides, aromatic or aliphatic alkynes                                | Cu <sup>I</sup> -USY, water, 90°C, 10 h  | 72–98     | 112  |
| 3     | Aromatic or aliphatic azides, aromatic alkynes                                     | Cu <sub>3</sub> N/Fe <sub>3</sub> N@SiO <sub>2</sub> , acetonitrile, Et <sub>3</sub> N, RT, 12 h–14 days | 72–91     | 113  |
| 4     | Aliphatic or aromatic azides and alkynes   | Cu(OH) <sub>x</sub> /Al <sub>2</sub> O <sub>3</sub> , toluene, 60°C, Ar atmosphere, 1–12 h               | 81–95     | 115  |
| 5     | Aromatic azides and alkynes  | Cu(OH) <sub>x</sub> /TiO <sub>2</sub> , toluene, 60°C, Ar atmosphere, 30 min                             | 88–98     | 114  |
| 6     | Benzyl azide, propanol azide or ethyl azidoacetate, aromatic and aliphatic alkynes | Cu <sup>I</sup> -Amberlyst A-21, CH <sub>2</sub> Cl <sub>2</sub> , RT, 12 h                              | 61–99     | 117  |
| 7     | Phenylacetylene, aromatic azides   | Cu/CR11 (possessing iminodiacetic acid moieties), neat, 70°C, Et <sub>3</sub> N, 3–5 h                   | 79–98     | 116  |

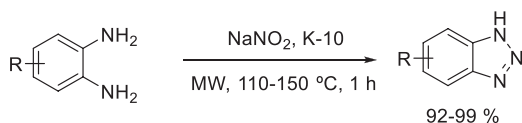
### Application of phenylenediamines and/or diazotization

Other N-containing five-membered heterocycles, playing an equally important role in pharmaceutical and medicinal chemistry, are two heteroatom-containing heterocycles such as benzimidazoles, benzodiazepines and quinoxalines and quinoxalinones.<sup>118–121</sup> Here again, solid acid catalysis has provided promising results. K-10 montmorillonite was shown to efficiently catalyze the synthesis of benzimidazoles, benzodiazepines, quinoxalinones in a solvent-free microwave-assisted method.<sup>122</sup> A variety of substituted *o*-phenylenediamines readily reacted with ketones, aldehydes, and bifunctional reagents to form the products in moderate to excellent yields in short reaction times (1–10 min) (Scheme 7).



**SCHEME 7** The microwave-assisted solvent-free synthesis of benzimidazoles, benzodiazepines, quinoxalinones catalyzed by K-10 montmorillonite.

Montmorillonite K-10 also demonstrated excellent catalytic activity in the synthesis of benzotriazoles, condensed three nitrogen-containing five-membered heterocycles relevant in the dye industry<sup>123</sup> as well as in medicinal chemistry.<sup>124, 125</sup> In a similar fashion as the previous example, the benzotriazoles were synthesized from *o*-phenylenediamines with a solvent-free approach using microwave-assisted solid phase diazotization.<sup>126</sup> The reactions were performed using  $\text{NaNO}_2$  as the nitrogen source, which does not generate any hazardous waste (Scheme 8). Substrates with electron-donating and electron-withdrawing substituents gave the corresponding products in excellent, nearly quantitative yields.



**SCHEME 8** Synthesis of benzotriazoles by the microwave-assisted, montmorillonite K-10-catalyzed solid phase diazotization of *o*-phenylenediamines.

### Oxazolidinones/oxindoles

Oxazolidinones are five-membered heterocyclic compounds that are excellent drug candidates because they possess activity against a large spectrum of Gram-positive bacteria.<sup>127</sup> Conventional synthetic routes to prepare these compounds involve the use of toxic isocyanates. As an alternative, the use of  $\text{CO}_2$  as the source of carbonyl carbon is attractive, not only because it offers a new path for preparing oxazolidinones but also because it transforms this greenhouse gas

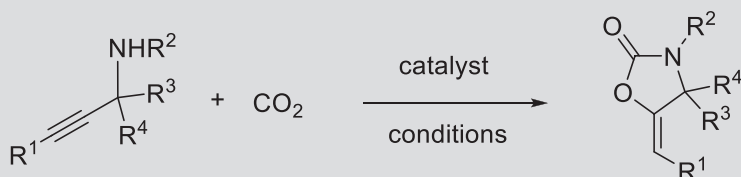
into value-added chemicals.<sup>127</sup> However, there remain limitations to this CO<sub>2</sub>-based synthesis as high pressures are usually required and complex, nonrecyclable catalysts are often employed. Several works have reported the synthesis of oxazolidinones employing porous frameworks (e.g., metal-organic frameworks, covalent organic frameworks) for all the advantages they offer, namely, their reactivity, easily tunable properties and their potential for recycling.<sup>127–130</sup> A few heterogeneous catalytic examples are collected in Table 5.

Among the methods developed, some require a co-catalyst and proceed under certain CO<sub>2</sub> pressure, while others are performed without additional activating reagents and under atmospheric pressure of CO<sub>2</sub>. For instance, no reaction was observed for the synthesis of oxazolidinones from propargylamines when the catalyst Ag-MOF, a porous Ag-Ag bond-based MOF synthesized under hydrothermal conditions, was employed alone. However, when performed with 1,8-diazabicyclo[5.4.0]-7-undecene (DBU) under the same reaction conditions, the obtained yield reached 90% or higher (Table 5, entry 1).<sup>128</sup> The combination of organic frameworks with transition metal nanoparticles appears to be a common strategy to catalyze this reaction type. A synergy can be obtained between the activity of the transition metal and the 3D hierarchical structure of the frameworks. For instance, zinc-based MOF was synthesized by confining the Ni@Pd nanoclusters together with glutamic acid within its cavities (Table 5, entry 2).<sup>129</sup> Interestingly, the catalyst was activated by visible light. Oxazolidinones were obtained in high yields at room temperature in 2 h under

**TABLE 5** Heterogeneous catalytic synthesis of oxazolidinones.

| Entry | Catalysts/conditions  | Yield (%) | Ref. |
|-------|---|-----------|------|
| 1     | Ag-MOF, DBU, 1 bar CO <sub>2</sub> , CHCl <sub>3</sub> , RT, 5 h                            | 90–98     | 128  |
| 2     | Ni@Pd/ZnGlu MNPs, 15 bar CO <sub>2</sub> , solvent-free, visible light irradiation, RT, 2 h | 88–94     | 129  |
| 3     | Ag-NPs decorated COF, 1 bar CO <sub>2</sub> , solvent-free, 40–80°C, 4–96 h                 | 29–98     | 130  |
| 4     | Cu-NPs@COF, 1,8-diazabicyclo[5.4.0]undec-7-ene, CO <sub>2</sub> 1 bar, MeCN, 50°C           | 78–96     | 127  |

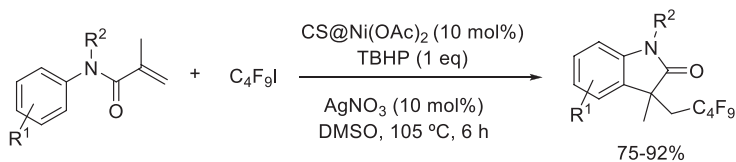
COF-covalent organic frameworks; DBU-1,8-diazabicyclo[5.4.0]-7-undecene; MOF-metal-organic framework; NP-nanoparticle.



neat conditions. However, the optimal pressure of CO<sub>2</sub> reached 15 bars. Ghosh et al. reported the same type of synthesis driven by silver nanoparticles embedded into covalent organic frameworks (COFs) (Table 5, entry 3).<sup>130</sup> The reaction proceeded under solvent-free and alkali-free conditions without the need for a co-catalyst. Moderate to high yields were obtained in different reaction times from half an hour to 96 h for the most deactivated substrates. The COFs, synthesized through a one-pot polycondensation and subsequently decorated with Ag NPs on their exterior surfaces, possess high activity mainly due to their high surface area and high CO<sub>2</sub> capturing ability. They also exhibited excellent recyclability with negligible leaching of silver from the frameworks. Another catalyst employing COF functionalized with metal nanoparticles was synthesized by a simple in situ process and catalyzed the reaction at 50°C in acetonitrile (Table 5, entry 4).<sup>127</sup> In this case, 1,8-diazabicyclo(5.4.0)undec-7-ene base was required to reach high yields.

All catalyst presented in the Table 5 were successfully recycled in several consecutive cycles.

Oxindoles are important heterocycles that can incorporate various substituents further increasing their bioactivity. Among them, the introduction of perfluoroalkyl group has the ability to notably increase lipophilicity and permeability. Most studies in the literature describing the synthesis of oxindole derivatives involve homogeneous methods employing transition-metal catalysts.<sup>131–133</sup> Recently, the first example of heterogeneous catalytic synthesis of fluorinated 3,3-disubstituted oxindoles was reported.<sup>134</sup> The catalyst, based on chitosan-supported nickel (II), showed high activity, good tolerance towards various functional groups, and good recyclability. The reaction, however, did not proceed without the presence of both the oxidant *tert*-butyl hydroperoxide (TBHP) in stoichiometric and silver nitrate in catalytic amount (Scheme 9).

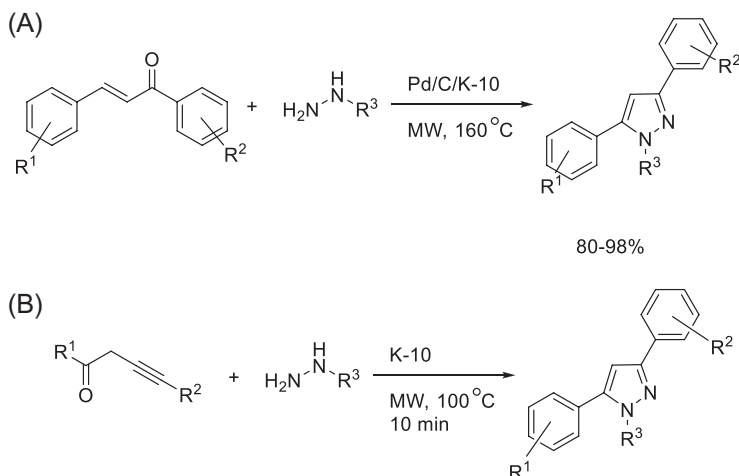


**SCHEME 9** Synthesis of perfluoroalkylated oxindoles promoted by heterogeneous chitosan@nickel(II) catalyst.

## Pyrazoles

Pyrazoles are synthesized by various methods, including the cyclization of acyclic precursors. The traditional synthesis is based on the reaction of hydrazines and 1,3-bifunctional substrates, commonly providing the two regioisomers and also requiring an aromatization step. Due to the important roles of these compounds, new environmentally benign protocols for their preparation are published frequently<sup>135–137</sup> and these developments are the topic of several review articles.<sup>138, 139</sup>

The cyclization and the subsequent aromatization of chalcones with arylhydrazones, however, can be carried out using a Pd/C-K-10 montmorillonite catalyst mixture to ensure effective cyclization and aromatization providing the expected pyrazoles in excellent yields (Scheme 10A).<sup>140</sup> A similar group of pyrazoles can also be synthesized by applying alk-3-yn-1-ones in lieu of chalcones. Interestingly, in this case there was no need for the presence of the Pd catalyst (Scheme 10B).<sup>141</sup> Both processes were activated by microwave irradiation, which ensured high yields in short reaction times. A similar cyclization of enynes was also achieved on gold nanoparticles.<sup>142</sup>



**SCHEME 10** Synthesis of pyrazoles from chalcones and arylhydrazines catalyzed by a Pd/C-K-10 montmorillonite mixture (A) and from alk-3-yn-1-ones with K-10 only (B).

### 3.8.2.2 Intramolecular cyclization reactions

#### 3.8.2.2.1 Heterogeneous catalytic synthesis of five-membered rings

##### The Nazarov cyclization

The Nazarov cyclization is employed for the synthesis of cyclopentenones from divinyl ketones. It is usually catalyzed by Lewis or Brønsted acids and requires stoichiometric amount of acids to reach high yields. Green protocols for the Nazarov reactions were designed by applying various metal-organic frameworks,<sup>143–146</sup> zeolites,<sup>147</sup> cooperation polymers,<sup>148</sup> and supported metal catalysts.<sup>149</sup> The results are shown in Table 6.

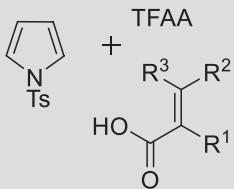
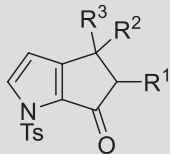
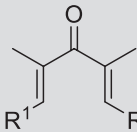
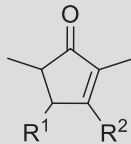
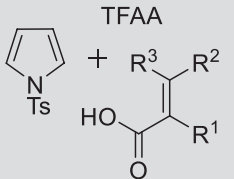
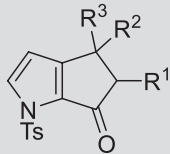
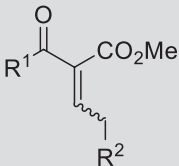
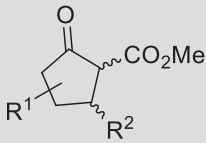
Most methods reported a tandem acylation-Nazarov cyclization sequence (Table 6, entries 1–4). In this case, the first step of the process is the reaction of trifluoroacetic acid and a cyclic compound to afford a divinyl ketone, followed by the actual Nazarov cyclization. Copper and iron-based MOFs appear to be

**TABLE 6** Heterogeneous catalytic Nazarov cyclizations.

| Entry | Starting materials | Catalyst/conditions  | Products | Yields (%) | Ref.                |
|-------|--------------------|--|----------|------------|---------------------|
|       |                    |  |          |            |                     |
| 1     |                    | Fe <sup>II</sup> -MOF, ClCH <sub>2</sub> CH <sub>2</sub> Cl, reflux, 5 h |          | 78–90      | <a href="#">143</a> |
| 2     |                    | Cu-MOF, ClCH <sub>2</sub> CH <sub>2</sub> Cl, 90°C, 3 h                  |          | 86–92      | <a href="#">144</a> |
| 3     |                    | Co-MOF, ClCH <sub>2</sub> CH <sub>2</sub> Cl, reflux, 5 h                |          | 45–79      | <a href="#">145</a> |

*Continued*

**TABLE 6** Heterogeneous catalytic Nazarov cyclizations—cont'd

| Entry | Starting materials  | Catalyst/conditions  | Products   | Yields (%) | Ref. |
|-------|---|--|--|------------|------|
| 4     |  <p>TFAA</p> | Zn-MOF, ClCH <sub>2</sub> CH <sub>2</sub> Cl, reflux, 4 h                            |  | 25–98      | 146  |
| 5     |              | H-USY-zeolite, ClCH <sub>2</sub> CH <sub>2</sub> Cl, 75°C, 2 h                       |  | 11–97      | 147  |
| 6     |  <p>TFAA</p> | Ag-cooperation polymer, ClCH <sub>2</sub> CH <sub>2</sub> Cl, reflux, 5 h            |  | 86–92      | 148  |
| 7     |              | AuCl <sub>3</sub> /AgSbF <sub>6</sub> , CH <sub>2</sub> Cl <sub>2</sub> , RT, 1–16 h |  | 64–99      | 149  |

highly active for the acylation–Nazarov cyclization given the yields obtained with similar starting materials and reaction conditions—refluxing dichloroethane for a few hours (Table 6, entries 1–3).<sup>143–145</sup> The performance provided by Zn-based MOFs were highly dependent on the structure of the MOF, which was tuned by varying the concentration of its components, the most active catalyst being  $\{[\text{Zn}_5(\text{pdpa})_2(\text{H}_2\text{O})_8]\cdot\text{H}_2\text{O}\}_n$  (Table 6, entry 4).<sup>146</sup> The general synthesis of MOF entails the mixing of the different components for several days at temperatures between 80°C and 135°C. The rather negative environmental impact of the synthesis of MOFs can be mitigated if the catalysts are recyclable in several consecutive cycles. Among the MOFs employed for Nazarov cyclization, all were recyclable in up to four cycles and one exhibited remarkable recyclability until the 10th cycle, namely the Cu-MOF (Table 6, entry 2).<sup>144</sup> However, for this example, the synthesis of the MOF required the addition of Ni foam and a surfactant to ensure a continuous and stabilized membrane without which the activity of the material was not satisfactory.<sup>144</sup> The ease of recyclability of Fe-based MOF is also noteworthy; it is due to the magnetic properties of the material. Indeed, the recovery of the catalyst from the reaction mixture aided by a magnet was rapid and efficient.<sup>143</sup>

Negatively charged zeolites can substitute acid catalysts due to the presence of external protons counterbalancing the defect of positive charges in the framework.<sup>147</sup> Thus, they have the ability to stabilize carbocations or carboxonium ions such as the intermediate generated during the Nazarov reaction when the starting material is a divinyl ketone. The commercially available H-USY zeolite efficiently catalyzed the synthesis of cyclopentenones from dienones in 2 h at 75°C (Table 6, entry 5).<sup>147</sup> Interestingly, the *cis-cis* isomers were formed as the major products; although other isomers were detected at the beginning of the reaction, they progressively disappeared to give rise to a single product. On the negative side, the substrate scope was narrow, and the yields were dependent on the substituents and their positions on the ring accounting for R<sup>1</sup>.

Coordination polymers (CPs) have emerged in the last decade as promising porous materials for the catalysis of various organic transformations.<sup>150</sup> Ag-based-CPs have shown to successfully catalyze the synthesis of cyclopentenone[*b*] pyrroles via a tandem acylation–Nazarov cyclization (Table 6, entry 6). The catalyst was prepared by mixing AgNO<sub>3</sub>, H<sub>4</sub>TTB (1,2,4,5-tetra(2*H*-tetrazole-5-yl)-benzene), and NH<sub>3</sub>·H<sub>2</sub>O with different solvents as structure-directing agents capable of influencing the structure of the catalyst depending on the size, shape, and polarity of the solvent molecules. The CP demonstrated high activity, stability, and recyclability in five catalytic cycles.<sup>148</sup>

The last example in Table 6 demonstrates the potential of supported gold catalysts in the Nazarov cyclization. Moderate to excellent cyclization yields were afforded at room temperature. The catalyst was easily prepared from a mixture of AuCl<sub>3</sub> and AgSbF<sub>6</sub>. Concerning the recyclability of the heterogeneous metal complex, it was demonstrated in only three cycles and necessitated the use of celite to separate it from the mixture.<sup>149</sup>

## Tetrahydrofurans

Tetrahydrofurans and furans are important oxygen-containing heterocycles that often exhibit interesting properties for biological applications or applications in the cosmetic industry. They can easily be synthesized by acid-promoted intramolecular cyclization of unsaturated alcohols or aryloxyacetaldehyde acetals.<sup>151,152</sup> Although traditional Brønsted acids are effective,<sup>153</sup> they are considered to have a negative impact on the environment mainly due to the waste they generate, requiring neutralization. Solid acid catalysis, and the advantages often associated with their use, have been proved equally efficient for the synthesis of tetrahydrofurans or furans. Zeolites and silica-supported-catalysts have been used for this purpose.<sup>154–156</sup> Three representative examples of such reactions are shown in Table 7.

Brønsted and Lewis acid sites-containing zeolites successfully catalyzed the conversion of diols and aryloxyacetaldehyde acetals to produce tetrahydrofurans and benzofurans, respectively in high yields. In both reactions, they exhibited good recyclability.<sup>154,155</sup> A silica-supported silver catalyst led to the formation of trisubstituted furans from diols in nearly quantitative yields; the excellent purity of the products bypassed the need for purification steps. The recyclability of the catalyst was not investigated in the study.<sup>156</sup> It must be noted that the solvents employed for all three reactions possess considerable toxicity and hazard.

### 3.8.2.2.2 Heterogeneous catalytic synthesis of six-membered rings

#### Isopulegol

Isopulegol, an intermediate of the production of menthol, and widely used for its flavoring and anesthetic properties, can easily be prepared via the ene

**TABLE 7** Heterogeneous catalytic synthesis of furans and tetrahydrofurans.

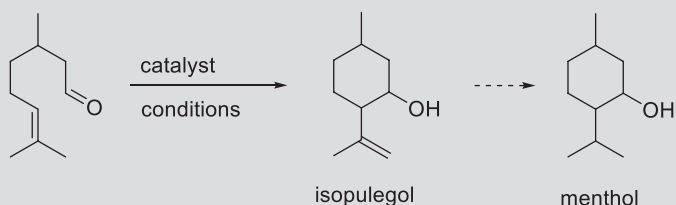
| Entry | Starting materials | Catalyst/<br>conditions   | Product | Yield<br>(%) | Ref. |
|-------|--------------------|---|---------|--------------|------|
| 1     |                    | H-BEA zeolite,<br>CH <sub>3</sub> CH <sub>2</sub> NO <sub>2</sub> ,<br>85°C, 1.5 h      |         | 95           | 154  |
| 2     |                    | H-β zeolite,<br>PhCF <sub>3</sub> reflux,<br>0.5–10 h                                   |         | 71–95        | 155  |
| 3     |                    | AgNO <sub>3</sub> -SiO <sub>2</sub> ,<br>CH <sub>2</sub> Cl <sub>2</sub> , 20°C,<br>3 h |         | 71–99        | 156  |

cyclization of citronellal.<sup>157</sup> It is commonly produced with an efficient method using a Lewis acid catalyst that unfortunately gives rise to the generation of significant amount of waste. Some methods have been reported to use potentially recyclable zeolites or silica-based catalysts, thus reducing the environmental impact of the reaction.<sup>158–160</sup> The conditions and yields of representative examples are tabulated in Table 8.

The best results were obtained with zeolites exhibiting a high concentration of acid sites and large enough pores to allow the efficient diffusion of citronellal. For example, the zeolite H-beta-11 catalyzed the reaction efficiently and selectively with 95% conversion and a diastereoselectivity of 75% in favor of (–)-isopulegol when using (+)-citronellal as the reagent (Table 8, entry 1).<sup>158</sup> The bifunctional Ir/Beta zeolite catalyst, prepared via impregnation of Beta zeolite with different concentrations of Ir, converts citronellal to menthol directly by consecutively catalyzing the cyclization and hydrogenation steps (Table 8, entry 2).<sup>159</sup> Similarly, a MOF catalyst containing palladium nanoparticles was used for the consecutive cyclization of citronellal to isopulegol and the hydrogenation to menthol resulting in 86% yield of menthol in 18 h (Table 8, entry 3).<sup>160</sup> Interestingly, higher selectivities were obtained when conducting this tandem reaction in two steps, introducing H<sub>2</sub> after the completion of the cyclization step. In fact, the desired menthol was obtained as a major product when citronellal was allowed to isomerize under a N<sub>2</sub> atmosphere until complete

**TABLE 8** Heterogeneous catalytic preparation of isopulegol from citronellal.

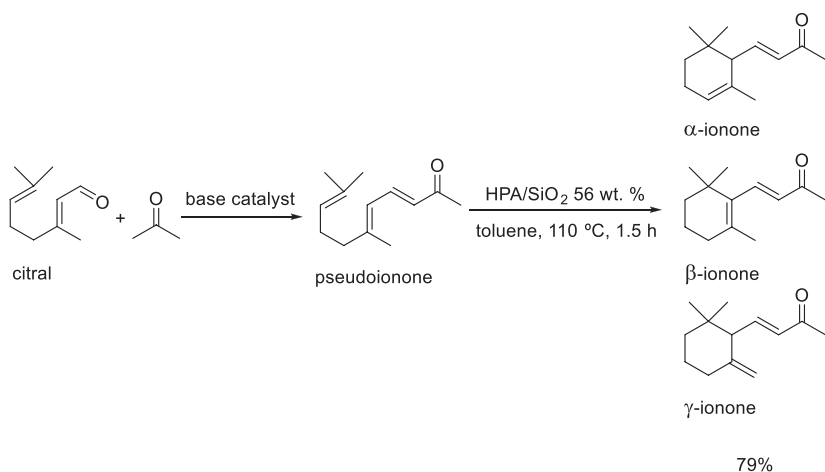
| Entry | Catalyst/conditions   | Yield (%)<br>(diastereoselectivity) | Ref. |
|-------|---|-------------------------------------|------|
| 1     | H-Beta-11/cyclohexane, 90°C, N <sub>2</sub> atmosphere, 3 h   | 95 (75 (–)-isopulegol)              | 158  |
| 2     | Ir-Beta zeolite/cyclohexane 80°C, 10 h  | 93 ((±)-menthol)                    | 159  |
| 3     | Pd-MIL-101, cyclohexane, 80°C, 18 h, 1st step in N <sub>2</sub> atm., 2nd step in H <sub>2</sub> atm. | 86 (81 (–)-menthol)                 | 160  |
| 4     | Zn/porous clay heterostructure, isopropanol, 80°C, 3 h  | 50 ((±)-isopulegol)                 | 161  |



conversion before supplying H<sub>2</sub>, which required a relatively long reaction time. Nevertheless, starting with a racemic mixture of citronellal, the catalytic method was proved to be diastereoselective. The last example offers shorter reaction times and a more environmentally friendly solvent than cyclohexane, but the yield obtained is significantly lower than that obtained with the other methods (Table 8, entry 4). The heterogeneous catalyst was prepared by immobilizing Zn on porous clay heterostructure (Zn/PCH) using several reagents including zinc acetate and saponite.<sup>161</sup>

### Ionones

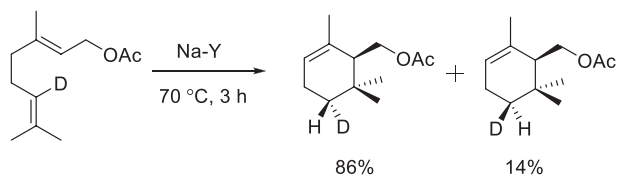
Ionones are citral-derived compounds that are widely used in the pharmaceutical and fragrance industries as well. Ionones are produced from citral in a two-step synthesis corresponding to an aldol condensation followed by a cyclization, often catalyzed by mineral acids.<sup>162</sup> Eco-friendly heterogeneous acid-based processes have been employed to promote the formation of ionones, including acidic resins<sup>163</sup> and sulfated mesoporous silica.<sup>164</sup> It was observed, however, that the yields were significantly lower than those obtained in the similar homogeneous experiments. More recently, another work reported the use of multiple solid acid catalysts for the production of ionones, notably the activities of zeolite H-BEA, Amberlyst 35W, SiO<sub>2</sub>-Al<sub>2</sub>O<sub>3</sub>, unsupported and silica-supported heteropolyacids (HPA/SiO<sub>2</sub>) were compared.<sup>165</sup> Ionone formation was greater on strong Brønsted acid sites. The best result, a yield comparable to homogeneous methods (79%), was obtained with HPA/SiO<sub>2</sub> after 1.5 h of reaction at 110°C (Scheme 11).<sup>165</sup> The high activity of the heteropolyacid catalyst was due not only to strong Brønsted acidity but also to a large surface area preventing steric hindrance and thus allowing cyclization of pseudoionone to ionone.



**SCHEME 11** Synthesis of ionones from citral using a HPA/SiO<sub>2</sub> catalyst for the cyclization step.

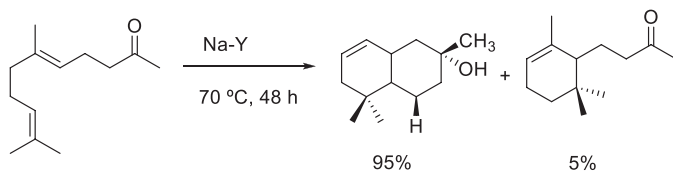
## Terpenoids

The acid-promoted cyclization of acyclic polyene terpenoids is a common pathway found in nature for the formation of cyclic or polycyclic biomolecules.<sup>166</sup> The natural pathway is governed by the enzymes called “cyclases,” the cavities of which provide a confined environment allowing for the achievement of a high degree of diastereoselectivity. Due to the difficulty to replicate the natural cyclization pathway of terpenoids because of the sensitivity of enzymes, other catalytic systems have been developed including the Lewis- and Brønsted-acid-driven reactions.<sup>167</sup> They often suffer from poor selectivities and require superstoichiometric amount of acid. More recently, methods, based on solid acids have led to interesting results on account of the specific environment that highly porous materials can provide in order to mimic the natural environment where cyclization of terpenoids usually takes place. A representative example is the cyclization of a diene terpenoid leading to  $\alpha$ -cyclogeranyl acetate catalyzed by the zeolite NaY at 70°C for 3 h (Scheme 12).<sup>168</sup> Good selectivity was achieved compared to the mineral acid-driven reaction (86:14 vs 54:46). It was proposed that the better selectivity observed originated from the predominance of the chair-like over the boat-like transition state of the terpene inside the specific environment of the zeolite while the typical mineral acid-based reaction does not favor one configuration over the other leading to nearly equal amount of the isomeric products.



**SCHEME 12** Na-Y-catalyzed synthesis of  $\alpha$ -cyclogeranyl acetate.

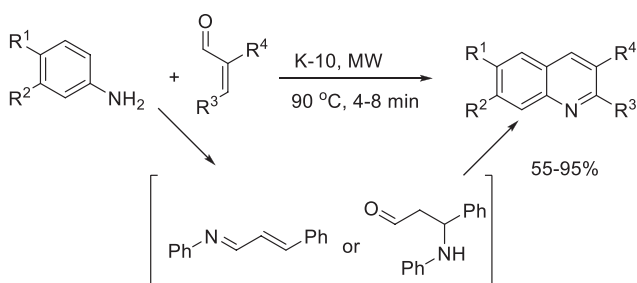
Similarly, the terpenoid geranyl acetone could be converted to  $\alpha$ -ambrinol with the same zeolite catalyst in excellent selectivity (Scheme 13).<sup>166</sup> It was demonstrated that the selectivity was proportional to the reaction time, shorter reaction times resulting in lower ratios of  $\alpha$ -ambrinol to dihydro- $\alpha$ -ionone, the byproduct. This was explained by the activation of the carbonyl group of dihydro- $\alpha$ -ionone within the zeolite leading to a second intramolecular cyclization and subsequently forming the major product. Interestingly, Brønsted or Lewis acidic conditions afforded other bicyclic products: (1*R*,2*S*,5*S*)-1,5-dimethyl-2-(prop-1-en-2-yl)-9-oxabicyclo[3.3.1]nonane or (8*aS*)-2,5,5,8*a*-tetramethyl-4*a*,5,6,7,8,8*a*-hexahydro-4*H*-chromene.



**SCHEME 13** Cyclization of geranyl acetone promoted by NaY.

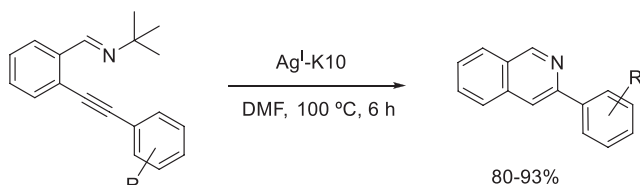
### Quinolines/isoquinolines

De Paolis et al. developed a microwave-assisted K-10 montmorillonite-catalyzed synthesis for quinolines (Scheme 14).<sup>169</sup> Although the process applies anilines and cinnamaldehydes, the two compounds form an intermediate, that undergoes an intramolecular cyclization. Although the reaction mechanism was not clear, it appears that the reaction progresses through different intermediate products when microwave or conventional heating were used. Despite potential differences in mechanism, both activation methods produced the same product. The last step of the process was an in situ aromatization providing the quinolines in good to excellent yields in very short reaction times.



**SCHEME 14** A microwave-assisted K-10 montmorillonite-catalyzed synthesis of multi-substituted quinolines.

The synthesis of substituted isoquinolines via AgI-K-10 montmorillonite-catalyzed cyclization of iminoalkynes was reported by Jeganathan et al.<sup>170</sup> Various functionalized terminal alkynes underwent cyclization to afford the desired nitrogen heterocycles in moderate to excellent yields, independently of the functional groups present (Scheme 15). The catalyst is believed to be bifunctional, acting simultaneously as an electrophile and as a base facilitating the overall cyclization process. The method possesses environmentally friendly features including the recyclability of the catalyst, the achievement of high yields, the simplicity of the procedure, and the minimization of metallic waste. To the contrary, the reaction is performed in the toxic solvent dimethylformamide and at relatively high temperature.



**SCHEME 15** Ag<sup>I</sup>-K-10 catalyzed-synthesis of isoquinolines via intramolecular cyclization of iminoalkynes.

### 3.8.3. Ring opening reactions

Ring opening reactions, although less studied than cyclizations, are extremely practical synthetic routes for the preparation of value-added chemicals of industrial importance. Different categories of ring opening reactions can be distinguished; the two main types will be reviewed in this part: ring opening of small heterocycles possibly including subsequent cycloaddition and ring opening polymerization.

#### 3.8.3.1 Ring opening of small heterocycles

Although the ring opening of cyclopropane derivatives is an important transformation that is often applied in the synthesis of biologically active compounds and natural products, it has been extensively covered in this book in the hydrogenolysis chapter. Thus, in this subchapter we only focus on heterocyclic compounds. Three-membered ring containing heterocycles such as epoxides and aziridines are versatile building blocks for the synthesis of complex molecules as they can readily undergo ring opening reactions.<sup>171–173</sup> Due to the high ring-strain, spontaneous ring opening reaction can easily occur upon a nucleophilic attack. Yet, the reaction sometimes requires a transition metal catalyst depending on the electronic configuration of the reagents.<sup>171</sup> These heterocycles are also prone to electrophilic reactions, which proceed through different mechanisms. Catalytic reactions via organometallic intermediates or via the formation of radicals are also common pathways for the ring opening of these small heterocycles. It will be demonstrated that heterogeneous catalysis is making its way into this reaction type as well. It should be noted that ring opening metathesis polymerization will not be covered in this chapter because this reaction type has already been discussed in detail in this same book in the Metathesis chapter.

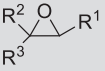
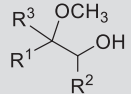
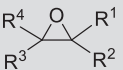
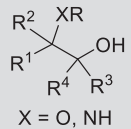
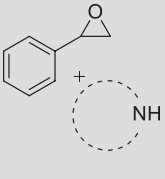
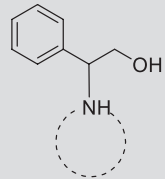
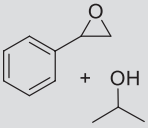
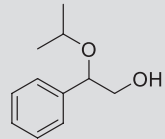
##### 3.8.3.1.1 Ring opening of epoxides

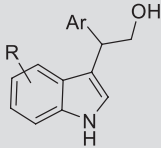
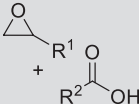
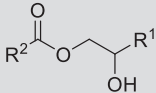
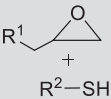
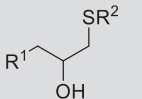
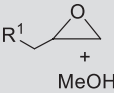
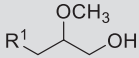
###### Synthesis of $\beta$ -substituted alcohols

Epoxides are key intermediates in organic synthesis; they can easily react with a variety of nucleophiles to afford  $\beta$ -substituted alcohols upon a ring opening reaction. This transformation is commonly performed under basic or acidic conditions,<sup>174</sup> or with the aid of metals such as lithium or metal salts such as chromium-based Lewis acid type catalysts.<sup>14</sup> In order to avoid the use of aqueous solution of harmful and corrosive mineral acids or bases or the use of stoichiometric metals and prevent the hazardous waste subsequently generated in these processes, various solid acid catalysts have been developed. A few representative examples are collected in Table 9 that shows the different methods employed for heterogeneous catalytic epoxide ring opening reactions.

Graphene oxide, originally used for its electronic, especially conductive, properties, has found applications in catalysis due to its high surface area. The most applied preparation method involving oxidation of graphite under acidic conditions, the Hummers method,<sup>184</sup> appears to provide sufficient coverage of

**TABLE 9** Ring opening of epoxides catalyzed by solid-acid catalysts.

| Entry | Reagents  | Conditions/catalyst   | Product   | Yield (%) | Ref. |
|-------|---|---|---|-----------|------|
| 1     |  | Graphene oxide, CH <sub>3</sub> OH, RT, 1–28 h                      |               | 7–99      | 175  |
| 2     |  | Graphene-SO <sub>3</sub> H, H <sub>2</sub> O, RT, 6 h               |               | 67        | 176  |
| 3     |  | [Fe(BTC)] (BTC: 1,3,5-benzenetricarboxylate), ROH, 40–90°C, 1–144 h | <br>X = O, NH | 30–93     | 177  |
| 4     |  | Fe(BTC), 60°C, 24 h   |               | 57–89     | 178  |
| 5     |  | MOF-808 (1%), 55°C, 24 h  |               | 99        | 179  |

|   |   |  |  |                                |     |
|---|---|--|--|--------------------------------|-----|
| 6 |  | Amberlyst 15/indium complex, Et <sub>2</sub> O, RT, 24 h |  | 40–62                          | 180 |
| 7 |  | Chitosan-silica sulfate nano hybrid, MeCN, reflux, 4–6 h |  | 87–96                          | 181 |
| 8 |  | Montmorillonite K-10, microwave, 60–105 s                |  | 51–92                          | 182 |
| 9 |  | FeOx-pillard bentonite, 10 min, 70°C                     |  | 45–95 (selectivity: 1.52–4.05) | 183 |

sulfate groups to make graphene oxide an excellent solid acid catalyst. For instance, it exhibited activity in the epoxide ring opening of multiple aromatic and aliphatic epoxides in the presence of methanol at room temperature (Table 9, entry 1).<sup>175</sup> Except the highly substituted substrates, that possessed significant steric hindrance, all other substrates were converted with moderate to high yields and selectivity. The products obtained were consistent with the expectations originating from the acid catalyzed S<sub>N</sub>1 ring opening mechanism. The catalyst demonstrated no significant loss of activity after recovery and reuse in three cycles. The functionalization of graphene with additional sulfate groups has also been explored to further broaden the catalytic applicability of graphene oxide. Sulfated graphene (G-SO<sub>3</sub>H), synthesized from the hydrothermal sulfonation of reduced graphene oxide with fuming sulfuric acid at 180°C, was very active for the hydration of propylene oxide (Table 9, entry 2).<sup>176</sup> In addition to being a recyclable catalyst, it was found that due to the unique structure of the solid material, mass transfer issues were minimized and did not significantly affect the yield. In fact, the static reaction led to similar results as the stirred counterpart.

Other solid-acid catalysts employed for the ring opening of epoxides include metal-organic frameworks. An iron-based metal-organic framework successfully catalyzed the ring opening of styrene oxide under mild reaction conditions with aniline in presence of alcohols serving as both the nucleophile and the solvent (Table 9, entry 3).<sup>177</sup> It was observed that the smaller the size of the alkyl chain, the more reactive the alcohol; methanol leading to faster reaction rates and better conversions than larger alcohols. The catalyst was recycled in three cycles in which consistent yields were obtained. The same type of MOF, Fe(BTC), successfully catalyzed the ring opening of styrene oxide by indole, aniline and other nitrogen-containing heterocycles (Table 9, entry 4).<sup>178</sup> In this example, control experiments performed with the homogeneous catalyst counterparts suggested that the coordinatively unsaturated sites of the MOF are responsible for the observed activity of the catalyst, namely, it acted as a Lewis acid. Interestingly, another study found evidence that there exists a correlation between the catalytic activity and the quantity of defects of the MOFs giving rise to a larger number of accessible Brønsted-acid active sites.<sup>179</sup> Thus, the inherently defect-rich UiO-type MOFs such as MOF808 or other synthetic MOFs possessing missing-linker type defects effectively and regioselectively catalyzed the styrene oxide ring opening reaction with isopropanol (Table 9, entry 5). Another Lewis acid sites-containing polymeric material based on indium effectively promoted the highly regio- and stereoselective ring opening reaction of optically active epoxides, forming new C–C as well as C–S bonds (Table 9, entry 6).<sup>180</sup> The importance of Lewis acidity was proven by using the Amberlyst-Na as a catalyst in a control reaction that did not provide any conversion. It should be noted that the supported Amberlyst 15/indium complex was easily prepared from the In(OTf)<sub>3</sub> precursor in ethanol. It was also easily recovered and recycled five times without remarkable loss in activity.

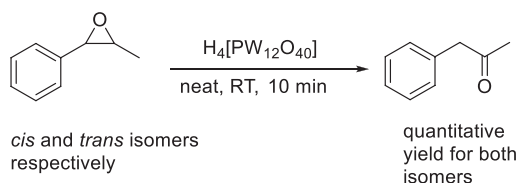
Behrouz et al. developed a chitosan-based nano-catalyst demonstrating high activity in the regioselective ring opening of epoxides with carboxylic acids

leading to 1,2-diol monoesters (Table 9, entry 7).<sup>181</sup> The method involves a synergistic acid-base activation, which allows both reactants to contribute to the initiation of the reaction. In fact, chitosan immobilized on silica constitutes an organic-inorganic hybrid material that exhibits a dual mode of activation; the silica sulfate anion acts as the base and deprotonates the carboxylic acid while the protonated chitosan acts as the acid interacting with the oxygen atom of the epoxide. As a result, the products were obtained in excellent yields under mild reaction conditions. The good recyclability of the catalyst contributes to the environmental friendliness of the method, but the solvent employed, acetonitrile, that remains undesirable in green synthesis.

Last, clays demonstrated interesting activity for the ring opening of epoxides with aromatic thiols when combined with microwave irradiation; the excellent microwave absorption properties of the clay contributed to a synergy allowing extremely short reaction times (Table 9, entry 8).<sup>182</sup> Moderate to high yields of beta-hydroxy sulfides were obtained under solvent-free conditions; cyclohexene oxide afforded the lowest yields. The styrene oxide ring opening by methanol was successfully catalyzed by iron oxide pillared clays, microporous materials consisting of swellable clays containing exchanged cations and polyoxocations in their interlayers (Table 9, entry 9).<sup>183</sup> The performance of FeOx-pillared hectorite and FeOx-pillared bentonite, synthesized by the intercalation of iron (III) chloride into clay interlayers and calcined at 300°C, was compared to that of the corresponding raw clays and to Fe<sub>2</sub>O<sub>3</sub>. Quantitative yield of 2-methoxy-2-phenylethanol was obtained using FeOx-pillared bentonite at 70°C for 10 min in excess methanol while the yields obtained with raw clay and Fe<sub>2</sub>O<sub>3</sub> did not exceed 25%. The optimum reaction conditions were applied to a wide range of epoxides.

### Synthesis of carbonyl compounds

As an interesting transformation, the ring opening isomerization of epoxides also provides a convenient route to the corresponding carbonyl compounds. In a solvent-free system stereoisomeric 1-methyl-2-phenyl-oxirans were isomerized by heteropoly acids under mild conditions (RT, 30 min). Under optimized conditions, the appropriate ketone was obtained as the major product in good to excellent yields (Scheme 16).<sup>185, 186</sup> The reaction appeared to favor the stronger acids, the weaker heteropoly acids required longer time while affording lower yields of the ketone.



**SCHEME 16** Heteropoly acid-catalyzed ring opening isomerization of 1-methyl-2-phenyl-oxirans.

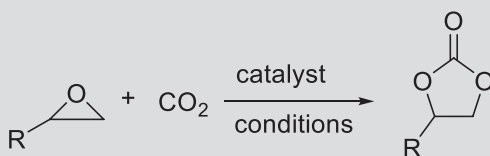
### Synthesis of cyclic carbonates

Cyclic carbonates are also commonly synthesized via a 100% atom economical reaction of an epoxide and carbon dioxide.<sup>187</sup> The purpose of the catalytic conversion of this anthropogenic gas is twofold: (1) the effective suppression of its deleterious greenhouse effect and (2) its conversion to value-added chemicals such as cyclic carbonates, that are useful intermediates in the production of pharmaceuticals, agrochemicals and fine chemicals.<sup>187</sup> The reaction entails a ring opening step and a simultaneous ring forming step with two additional atoms. In fact, this direct pathway is the most studied; it usually occurs with the aid of a homogeneous catalyst (e.g., phosphines, quaternary onium salts, transition metal complexes) or a heterogeneous catalyst (e.g., MOFs, silica-based catalysts, zeolites, carbon-based catalysts).<sup>187, 188</sup> Several examples for the application of heterogeneous catalysis in the formation of cyclic carbonates are described in Table 10.

MOFs appear to be excellent candidates for this conversion of epoxides and CO<sub>2</sub> into cyclic carbonates. Two types of binary MOFs using Cu and Zr as the metal centers were synthesized by the solvothermal method and successfully applied to the CO<sub>2</sub>-epoxide cycloaddition under solvent-free conditions (Table 10, entry 1).<sup>189</sup> In presence of the co-catalyst tetrabutylammonium bromide (TBAB), 91% yield and 99% selectivity were achieved. The excellent performance was attributed to the synergistic effect of the Cu and Zr metals

**TABLE 10** Heterogeneous catalytic synthesis of cyclic carbonates from epoxides and carbon dioxide.

| Entry | Catalysts/conditions  | Yield (%) | Ref. |
|-------|---|-----------|------|
| 1     | UiO-66/Cu-BTC, TBAB, solvent-free, 60°C, 1.2 MPa CO <sub>2</sub> , 8 h  | 91        | 189  |
| 2     | [Ni <sub>3</sub> (BTC) <sub>2</sub> (MA)(H <sub>2</sub> O)](DMF) <sub>7</sub> , TBAB, 60°C, 0.1 MPa CO <sub>2</sub> , 6 h | 88–99     | 190  |
| 3     | Co(tp)(bpy), solvent-free, 100°C, 1 MPa CO <sub>2</sub> , 7 h   | 91–94     | 191  |
| 4     | ZIF-71/TBAB, 1.2 MPa CO <sub>2</sub> , 24 h or ZIF-71, 120°C, 1.2 MPa CO <sub>2</sub> , 4 h solvent-free                  | 8–98      | 192  |
| 5     | GO, DMF, 100–140°C, 1 atm. CO <sub>2</sub> , 10–12 h  | 40–98     | 193  |



together with the Br ion of TBAB responsible for the initiation of the ring opening of the epoxide.

Li et al. described another novel MOF based on Ni metal centers and nitrogen-rich melamine which was also constructed via the solvothermal method assembling 1,3,5-benzenetricarboxylic acid (H<sub>3</sub>BTC), melamine (MA) and Ni(II) ions (Table 10, entry 2).<sup>190</sup> The highly porous material exhibited a high affinity towards binding CO<sub>2</sub> due to its Lewis-base properties, which was demonstrated by its efficiency to catalyze the CO<sub>2</sub> cycloaddition to small epoxides. Here again, the method employed TBAB as a co-catalyst and the reaction conditions were similar to the above example except that the pressure of CO<sub>2</sub> employed was more than ten times lower.

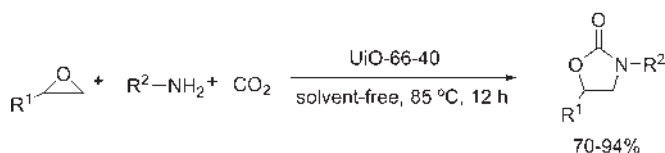
A dual-linker MOF, prepared with metal salts, terephthalic acid, and 4,4'-bipyridine as precursors, was also reported as a good catalyst for this reaction type (Table 10, entry 3).<sup>191</sup> The reaction was performed under solvent-free conditions but in this case, the catalyst showed superior activity without a co-catalyst. The MOFs afforded the cyclic carbonates in excellent yields in 7 h at 100–120°C. The co-existence of Lewis acidic sites, due to the incompletely coordinated metal cations, and basic active sites, derived from uncoordinated pyridine groups, is believed to be responsible for the high activity of the catalyst. All three types of MOFs were recyclable in five or six consecutive cycles (Table 10, entries 1–3).

A zinc-based imidazolate framework (ZIF-71), prepared from inexpensive precursors in ethanol at room temperature, was also successfully applied to the solvent-free synthesis of cyclic carbonates (Table 10, entry 4).<sup>192</sup> It was found to efficiently catalyze the cycloaddition reactions under two possible reaction conditions: high temperature and co-catalyst free or room temperature in presence of TBAB. High yields were obtained except for the sterically hindered styrene- and cyclohexene oxides. The activity of the catalyst was attributed to the presence of both acidic and basic sites at the surface of the framework, notably the co-existence of NH groups and free N-moieties enhanced the catalytic activity.

A graphene oxide-based method was described by Zhang et al. as a truly green strategy for the synthesis of cyclic carbonates from epoxides at atmospheric pressure in absence of any co-catalysts unlike most other heterogeneous methods described above (Table 10, entry 5).<sup>193</sup> High yields were, however, achieved only under harsh conditions; after over 10 h at temperatures above 100°C. Interestingly, graphene oxides (used “as-received”) possessing the highest amount of oxygen-containing groups demonstrated the highest reaction rate, which led to the hypothesis that these groups constitute the surface active sites of the catalyst responsible for the activation of the epoxide.

A similar product, a nitrogen-containing cyclic carbonate, could be synthesized with the aid of a MOF. The novel series of UiO-66 structures were successfully applied to the three-component cycloaddition of epoxides with aromatic amines and CO<sub>2</sub> (Scheme 17).<sup>194</sup> The particularity and high reactivity of the metal-organic framework lies in the presence of a linker functionalized with

free, dangling alkylamine units that replace the ordinary carboxylate coordinating groups thus creating defects responsible for driving the reaction. As a result, the reaction proceeded under solvent-free conditions at ambient pressure of CO<sub>2</sub> and 85°C. The products were isolated in high yields and high regioselectivity.

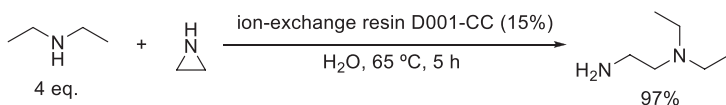


**SCHEME 17** Synthesis of oxazolidinones catalyzed by a metal-organic framework.

### 3.8.3.1.2 Ring opening of aziridines

Aziridines constitute highly reactive precursors for the synthesis of various nitrogen-containing bioactive molecules including heterocycles, alkaloids and amino acids.<sup>171, 172</sup> Their reactivity is due to the presence of an electrophilic carbon prone to nucleophilic attacks; it can easily undergo regioselective ring opening reactions.<sup>171, 172</sup>

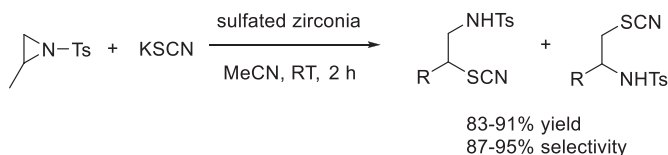
The reaction of aziridine with diethylamine is a typical nucleophilic ring opening reaction and requires a proton donor acid catalyst to activate the aziridine.<sup>195</sup> A series of ion-exchange resins was therefore investigated to select the best performing catalyst. As expected, the conversion of the aziridine depended on the number and strength of the Brønsted acid sites on the resins. The acidity also had an impact on the selectivity of the *N,N*-diethylenediamine formation. The highest yield was obtained using the catalyst D001-CC under mild conditions in water (Scheme 18). While the catalyst was recyclable five times, it should be stressed that its reuse involved mineral acid treatments as a reactivation and the catalyst loading exceeded 10%.



**SCHEME 18** Synthesis of ethylenediamine via an aziridine ring opening catalyzed by an ion-exchange resin.

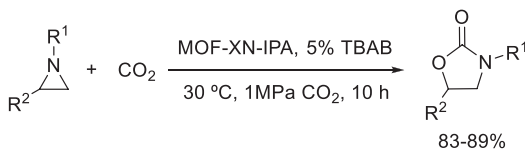
Das et al. developed a method to perform the ring opening of aziridines with potassium thiocyanate and thiols in the presence of a heterogeneous catalyst, sulfated zirconia, to give the corresponding  $\beta$ -aminothiocyanates and  $\beta$ -aminosulfides, respectively (Scheme 19).<sup>196</sup> The products were obtained in high yields and high regioselectivity under mild conditions. Interestingly, the investigation of the recyclability of the catalyst revealed that its activity gradually decreased in the ring opening with potassium thiocyanate, while no appreciable

change in activity was observed for ring opening with thiols during at least three consecutive cycles.



**SCHEME 19** Regioselective ring opening of aziridines with potassium thiocyanate and thiols using sulfated zirconia as a heterogeneous catalyst.

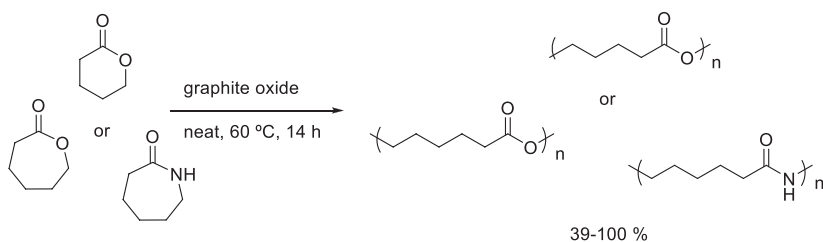
In a similar fashion as the synthesis of cyclic carbonates from epoxides and carbon dioxide, MOFs, synthesized from ligands XN (4-(4-pyridine)4,2:2,4-terpyridine) and isophthalic acid (IPA) by isothermal method, catalyzed the conversion of CO<sub>2</sub> and aziridines.<sup>197</sup> Here again, tetra-*n*-butylammonium bromide (TBAB) was used as a co-catalyst, which together with the MOF achieved high yields under mild temperature in 10 h (Scheme 20).



**SCHEME 20** Heterogeneous catalytic conversion of aziridines and CO<sub>2</sub> to oxazolidin-2-ones.

### 3.8.3.2 Ring opening polymerization

Polyesters and polyamides undeniably have numerous practical uses due to their mechanical strength, their thermal stability and their biocompatibility when prepared from lactones or lactam derivatives.<sup>198, 199</sup> These materials are prepared via two different pathways: step-growth or ring opening polymerizations.<sup>200</sup> Often, the catalysts involved in these processes are metal-based<sup>201</sup> which causes metal contamination issues and thus limits the applications of the obtained polymers in the biomedical field.<sup>202</sup> As such, the use of the nonmetallic, heterogeneous carbon catalysts is of great interests for the development of metal-free approaches.<sup>203</sup> These so-called carbocatalysts have demonstrated interesting activity as heterogeneous catalysts for the synthesis of polymeric materials. The conversion of several cyclic lactones and lactams, such as  $\epsilon$ -caprolactone,  $\epsilon$ -valerolactone, and  $\delta$ -caprolactam to their corresponding biocompatible and biodegradable polyamides and polyesters was performed using graphite oxide as the catalyst (Scheme 21).<sup>204</sup> Interestingly, the carbon catalyst was retained and evenly dispersed within the polymeric structure allowing the elimination of additional steps to introduce a carbon-filler.



**SCHEME 21** Ring opening polymerization of lactones and lactams to fullerene-reinforced polyesters and polyamides catalyzed by graphite oxide.

The ring opening polymerization of lactones has been extensively studied with heterogeneous catalytic systems.<sup>202</sup> Both nonmetal and metal-based catalysts demonstrated good performance. The results are tabulated in [Table 11](#).

Among the metal-free systems, the incorporation of organocatalysts onto the surface of insoluble supports appears to be a valuable method providing good monomer conversions while ensuring the noncontamination of the product and a simple separation of the catalyst from the reaction mixture. The dimeric 1-*tert*-butyl-2,2,4,4,4-pentakis(dimethylamino)-2Λ5, 4Λ5-catenadi-(phosphazene) supported

**TABLE 11** Ring opening polymerization of lactones by heterogeneous catalysis.

| Entry | Catalyst/conditions  | Conversion (%) | Ref. |
|-------|--|----------------|------|
| 1     | 1- <i>tert</i> -butyl-2,2,4,4,4-pentakis(dimethylamino)-2Λ5, 4Λ5-catenadi(phosphazene) supported on polystyrene, toluene, benzyl alcohol, 100°C, 12–48 h | 43–95          | 205  |
| 2     | <i>n</i> -Propylsulfonic acid-functionalized porous and nonporous silica, 27–136 h   | 38–96          | 206  |
| 3     | Polystyrene-supported Zn(acetate), Sn(ethylhexanoate), solvent-free, 1–6 h   | 90             | 207  |
| 4     | Magnetic nanoparticle supported aluminum isopropoxide, toluene, isopropanol, nitrogen atmosphere, 100°C, 10 h  | 95             | 208  |

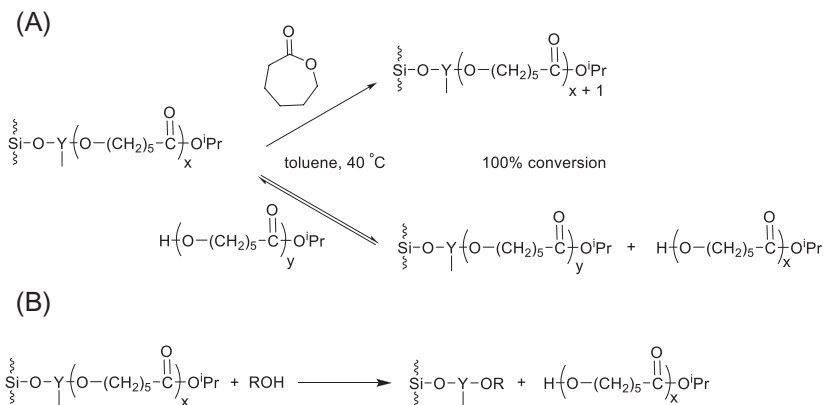
on polystyrene successfully catalyzed the ring opening polymerization (ROP) of  $\delta$ -valerolactone (Table 11, entry 1).<sup>205</sup> The use of an alcohol as an initiator provided polymers with controlled molecular weight and narrow molecular weight distributions.

*n*-Propylsulfonic acid-functionalized porous and nonporous silica materials were also evaluated for the synthesis of polycaprolactone (Table 11, entry 2).<sup>206</sup> The synthetic pathway employed progressed via three distinct steps: the functionalization of the silica surface with thiols, the capping of silanols and the oxidation of thiols groups. Although the nature of the catalyst allows for its rapid extraction from the polymerization solution and for the absence of metal residues in the polymer, the extracted solid was inefficient in recycling experiments. This drawback adds up to the nonnegligible environmental impact of its synthesis.

The metal-based catalytic systems that included Sn and Zn carboxylate were prepared by immobilizing it on polystyrene<sup>207</sup> and magnetic nanoparticle supported aluminum isopropoxide, respectively (Table 11, entries 3 and 4).<sup>208</sup> The first study reported that changing the ligand from acetate to 2-ethylhexanoate, and applying electron withdrawing groups on the catalyst greatly improved the polymerization rate. One of the advantages of the method was the low catalyst loading combined with high turnover frequency. The specificity of the second work is the ease of recovery of the catalyst due to its magnetic properties. The products obtained with either one of the methods contained only minute amounts of metal after a simple filtration or magnetic separation. Both catalysts were recovered and reused in several cycles. While the magnetic catalyst demonstrated only a slight drop in conversion, the polymer supported-catalyst exhibited a progressive loss in activity.

It is worth mentioning that most methods listed in Table 11 reported a controlled polymerization with narrow polydispersities compared to traditional homogeneous methods.

The ring opening polymerization of  $\epsilon$ -caprolactone was also performed by yttrium isopropoxide grafted onto silica surface in toluene at 40°C; another alternative to prevent heavy-metal toxicity in the synthesized polymers (Scheme 22).<sup>209</sup> The specificity of the method is the use of an alcohol in order to trigger an exchange reaction with the grafted active alkoxide groups. The role of the alcohol is dual as it controls the length of the chains and it regenerates the alkoxide at the surface of the support, which allows for the recycling of the catalyst. In addition, varying the initial monomer/(alcohol + alkoxide) molar ratio makes the degree of polymerization tunable. With regards to the catalyst preparation, it entailed a simple mixing of [tris(hexamethyldisilyl)amide]yttrium and isopropanol in toluene under mild conditions followed by the addition of a suspension of silica nanoparticles. Only the process of dehydration of silica required harsher conditions, 15 h heating at 130°C. The process can be carried out by MOF-based catalysts as well.<sup>210</sup>



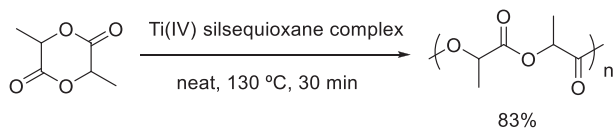
**SCHEME 22** Polymerization of  $\epsilon$ -caprolactone by yttrium isopropoxide grafted to a mineral support: competition between chain propagation and alkoxide/alcohol exchange (A); and recovery of the supported catalyst by the alcohol used as the termination agent (B).

A similar system was developed using a fixed-bed reactor for a continuous flow process. The anionic ring opening polymerization of  $\epsilon$ -caprolactone was performed with aluminum alkoxides grafted on dehydrated porous silica or alumina using alcohol molecules as a transfer agent. The fixed-bed reactor was first charged with the solid catalyst and continuously fed with a mixture of monomer and alcohol. The addition of alcohol is an essential step as it induces the transfer reaction on the solid support and consequently enables the polymer chains to move along the reactor. Conversions, as well as molecular weights were functions of the residence time of the reactants within the porous phase.<sup>211</sup>

Other heterogeneous catalytic ring opening polymerization of lactones include the polystyrene supported organotin dichloride-driven reaction.<sup>212</sup> The work reported by Deshayes et al. demonstrated that high-resolution magic-angle-spinning (MAS) NMR spectroscopy served as an invaluable technique to provide a thorough characterization of the solid catalyst as well as a powerful tool to monitor the catalytic process itself. In fact, the swelling properties of the insoluble polymeric supports allowed for sufficient molecular mobility at the interface of the catalyst so as to generate the line narrowing necessary for observation in NMR spectroscopy. In spite of the recyclability of the anchored organometallic catalyst, its laborious synthesis employs multiple reagents possessing variable toxicities.

The ring opening polymerization of polylactide, a bio-sourced thermoplastic aliphatic polyester, was successfully performed by heterogeneous catalysis. Titanium-supported silsesquioxane complexes, prepared from silica as a support and  $\text{Ti}(\text{OPr})_4$  as the metal precursor, served the purpose (Scheme 23).<sup>213</sup> The polylactide was obtained in 83% yield after only 30 min at 130°C. Interestingly, lower yields were observed when using smaller silica particles, likely a consequence of the mass transport limitation effects. When compared to the homogeneous

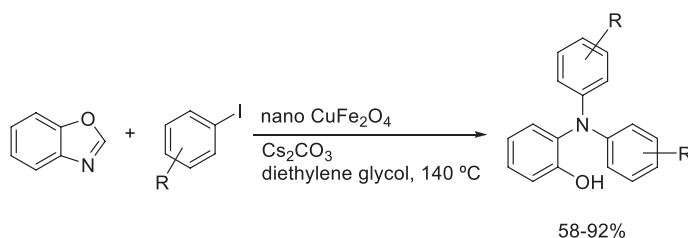
counterpart, the heterogeneous system provided narrower polydispersity index, a sign of better polymerization control. It must be noted that despite the advantages offered by the solid catalyst, its recyclability was not investigated.



**SCHEME 23** Ring opening polymerization of *rac*-lactide to polylactide catalyzed by a heterogeneous Ti(IV) silsesquioxane complex under molten conditions.

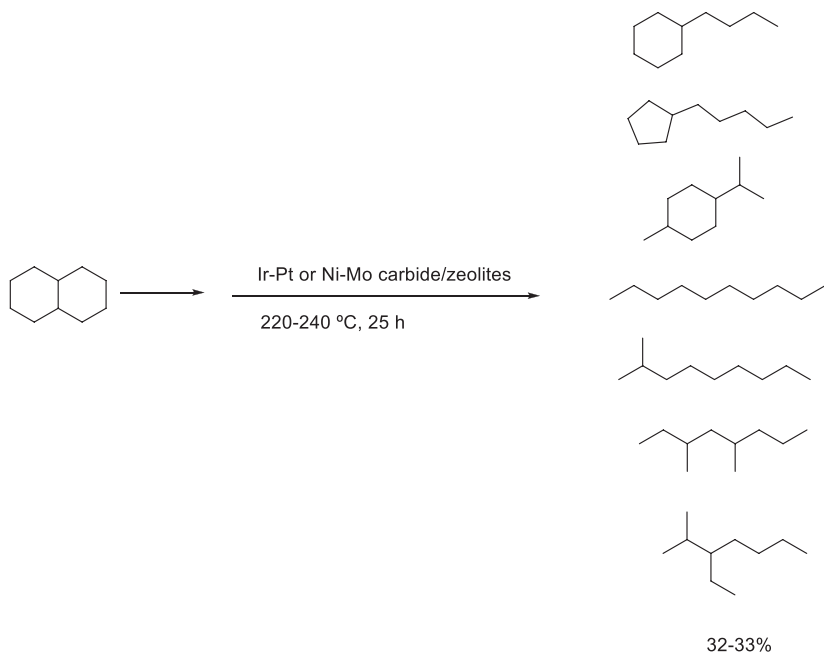
### 3.8.3.3 Other types of ring opening reactions

Nguyen et al. described a method to prepare triphenylamines via a heterogeneous catalytic ring opening-addition reaction sequence from benzoxazoles or benzothiazoles with iodoarenes. The comparative study demonstrated that  $\text{CuFe}_2\text{O}_4$  superparamagnetic nanoparticles were more active than other nickel based- or cobalt-based nano-catalyst as well as several solid catalysts such as MOF-199 or  $\text{Cu}_2(\text{BDC})_2(\text{DABCO})$  and numerous homogeneous catalysts (Scheme 24).<sup>214</sup> It was also observed that the nature of the base and the solvent played a critical role in the conversion.  $\text{Cs}_2\text{CO}_3$  as the base and diethylene glycol as the solvent provided the most effective reaction conditions. In addition to unprecedented high yields, the magnetic properties of the catalyst made it possible to separate it from the reaction mixture and reutilized it in five consecutive reactions while preserving the original catalytic activity.



**SCHEME 24** The ring opening reaction of benzoxazole with iodobenzenes to generate triphenylamines using  $\text{CuFe}_2\text{O}_4$  catalyst.

Ring opening of hydrocarbons is commonly performed by heterogeneous catalysis for diesel and aromatics production purposes.<sup>215</sup> Selective ring opening of naphthenes to paraffins is essential to upgrade the diesel oil. Catalysts supported on zeolites have the potential to increase the cetane number without losing the molecular weight of the initial aromatics.<sup>216</sup> HY- and Hbeta-supported carbide catalysts showed similar performance to that of noble metal catalysts loaded on the same supports for the ring opening of decalin. For instance, the Ni-Mo carbide supported on HY showed a ring opening yield of 33.5% at 240°C and the Pt-Ir/HY catalyst showed a 32% yield at 220°C (Scheme 25).



**SCHEME 25** Decalin ring opening reaction on Ir-Pt or Ni-Mo carbide catalysts supported on zeolites.

### 3.8.4. Conclusions and outlook

Various heterogeneous catalytic ring transformations have been reviewed with an emphasis placed on the environmentally friendliness of the methods. Representative examples of the well-established intermolecular cyclization reactions, notably the Diels-Alder and Paal-Knorr reactions, the Huisgen cycloaddition and the intramolecular cyclization reactions such as the Nazarov reaction, were described. In addition, the synthesis of multiple five and six-membered ring heterocycles of high importance were included. Regarding ring opening transformations, ring opening of small heterocycles and ring opening polymerizations were extensively reviewed as well. Among the classes of catalysts that were the most active for all reaction-type zeolites, MOFs, and clays dominated. The porosity of these heterogeneous catalysts combined with their acidic and/or basic active sites contributed to the excellent results obtained.

### References

1. Knorr, L. Synthese von Furfuranderivaten aus dem Diacetbernsteinsäureester. *Chem. Ber.* **1884**, *17*, 2863–2870.
2. Cho, H.; Madden, R.; Nisanci, B.; Török, B. The Paal-Knorr Reaction Revisited. A Catalyst and Solvent-Free Synthesis of Underivatized and N-Substituted Pyrroles. *Green Chem.* **2015**, *17*, 1088–1099.

- Zhang, L.; Wang, D.; Xing, J.; Liu, L. Facile Synthesis of (Guaiazulen-1-Yl)-1H-Pyrroles Via Paal-Knorr Reaction. *Heterocycles* **2019**, *98*, 1555–1562.
- The Nobel Prize in Chemistry. *Nobel Media AB 2020*; 1950. <https://www.nobelprize.org/prizes/chemistry/1950/summary/> (Accessed 8 November 2020).
- Dahiya, A.; Ali, W.; Patel, B. K. Catalyst and Solvent Free Domino Ring Opening Cyclization: A Greener and Atom Economic Route to 2-Iminothiazolidines. *ACS Sustain. Chem. Eng.* **2018**, *6*, 4272–4281.
- Wang, Z.; Tang, Y. Mechanistic Insights Into a Catalyst-Free Method to Construct Quinazolinones Through Multiple Oxidative Cyclization. *Tetrahedron* **2016**, *72*, 1330–1336.
- Lei, H.; Yang, Y.; Li, C.; Jia, F.; Jiang, N.; Gong, P.; Zhai, X. Catalyst-Free Cyclization- and Curtius Rearrangement-Induced Functional Group Transformation: An Improved Synthetic Strategy of First-in-Class ATX Inhibitor Ziritaxestat (GLPG-1690). *Org. Process. Res. Dev.* **2020**, *24*, 997–1005.
- Vaidya, T.; Eisenberg, R.; Frontier, A. J. Catalytic Nazarov Cyclization: The State of the Art. *ChemCatChem* **2011**, *3*, 1531–1548.
- Suzuki, I.; Hirata, A.; Takeda, K. Development of Cyclic Hydrazine and Hydrazide Type Organocatalyst-Mechanistic Aspects of Cyclic Hydrazine/hydrazide-Catalyzed Diels-Alder Reactions. *Heterocycles* **2009**, *79*, 851–863.
- Khaghaninejad, S.; Heravi, M. M. Paal-Knorr Reaction in the Synthesis of Heterocyclic Compounds. *Adv. Heterocycl. Chem.* **2014**, *111*, 95–146.
- Chassaing, S.; Beneteau, V.; Pale, P. Green Catalysts Based on Zeolites for Heterocycle Synthesis. *Curr. Opin. Green Sustain. Chem.* **2018**, *10*, 35–39.
- Dastan, A.; Kulkarni, A.; Török, B. Environmentally Benign Synthesis of Heterocyclic Compounds by Combined Microwave-Assisted Heterogeneous Catalytic Approaches. *Green Chem.* **2012**, *14*, 17–37.
- Jung, N.; Encinas, A.; Braese, S. Automated Synthesis of Heterocycles on Solid Supports. *Curr. Opin. Drug Discov. Devel.* **2006**, *9*, 713–728.
- Wang, C. Electrophilic Ring Opening of Small Heterocycles. *Synthesis* **2017**, *49*, 5307–5319.
- Danishesky, S.; Singh, R. K. Highly Activated Cyclopropane for Homoconjugate Reactions. *J. Am. Chem. Soc.* **1975**, *97*, 3239–3241.
- Török, B.; Molnár, Á.; Bartók, M. Hydrogenative Ring Opening of Propylcyclopropane Over Silica-Supported Pt and Pd Catalysts. *Catal. Lett.* **1995**, *33*, 331–339.
- Nuyken, O.; Pask, S. D. Ring-Opening Polymerization-An Introductory Review. *Polymers* **2013**, *5*, 361–403.
- Bartók, M., Ed. *Stereochemistry of Heterogeneous Metal Catalysis*; Wiley: Chichester, 1985.
- Smith, G. V.; Notheisz, F. *Heterogeneous Catalysis in Organic Chemistry*, Academic Press: San Diego, CA, 1999.
- Kokel, A.; Schäfer, C.; Török, B. Application of Microwave-Assisted Heterogeneous Catalysis in Sustainable Synthesis Design. *Green Chem.* **2017**, *19*, 3729–3751.
- Augustine, R. L. *Heterogeneous Catalysis for the Synthetic Chemist*, Marcel Dekker: New York, 1996.
- Somorjai, G. A.; Li, Y. *Introduction to Surface Chemistry and Catalysis*, 2nd ed.; Wiley: New York, 2010.
- Thomas, J. M.; Thomas, W. J. *Principles and Practice of Heterogeneous Catalysis*, Wiley-VCH: New York, Weinheim, 1996.
- Anastas, P. T.; Warner, J. C. *Green Chemistry: Theory and Applications*, Oxford University Press: Oxford, 1998.

25. Török, B.; Dransfield, T. *Green Chemistry: An Inclusive Approach*, Elsevier: Oxford, Cambridge, 2018.
26. Bag, S.; Dasgupta, S.; Török, B. Microwave-Assisted Heterogeneous Catalysis: An Environmentally Benign Tool for Contemporary Organic Synthesis. *Curr. Org. Synth.* **2011**, *8*, 237–261.
27. Kokel, A.; Schäfer, C.; Török, B. Organic Synthesis Using Environmentally Benign Acid Catalysis. *Curr. Org. Synth.* **2019**, *16*, 615–649.
28. Li, C.-J., Ed. *Green Synthesis*, Vol. 7; *Handbook of Green Chemistry-Green Processes*; Wiley-VCH: Weinheim, 2012.
29. Thebtaranonth, C.; Thebtaranonth, Y. *Cyclization Reactions*, 1st ed.; CRC Press, 1993.
30. Gilchrist, T. L. *Heterocyclic Chemistry*, 3rd ed.; Addison, Wesley, Longman: Harlow, 1997.
31. Settle, A. E.; Berstis, L.; Rorrer, N. A.; Roman-Leshkov, Y.; Beckham, G. T.; Richards, R. M.; Vardon, D. R. Heterogeneous Diels-Alder Catalysis for Biomass-Derived Aromatic Compounds. *Green Chem.* **2017**, *19*, 3468–3492.
32. News and Views. Nobel Prize for Chemistry for 1950: Prof. O. Diels and Prof. K. Alder. *Nature* **1950**, *166*, 889.
33. Oehlenschlaeger, K. K.; Guimard, N. K.; Brandt, J.; Mueller, J. O.; Lin, C. Y.; Hilf, S.; Lederer, A.; Coote, M. L.; Schmidt, F. G.; Barner-Kowollik, C. Fast and Catalyst-Free Hetero-Diels-Alder Chemistry For On Demand Cyclable Bonding/Debonding Materials. *Polym. Chem.* **2013**, *4*, 4348–4355.
34. Zhang, C.; Jiao, H.; Jia, W. Theoretical Predication of Diels-Alder Reactions of Highly Strained Dienophiles. *Comput. Theor. Chem.* **2020**, *1175*, 112734.
35. Brieger, G.; Bennett, J. The Intramolecular Diels-Alder Reaction. *Chem. Rev.* **1980**, *80*, 63–97.
36. Singleton, D.; Leung, S.; Martinez, J.; Lee, Y. Catalysis by Temporary Covalent Activation. A Novel Catalysis of Unactivated Diels-Alder Reactions. *Tetrahedron Lett.* **1997**, *38*, 3163–3166.
37. Meuzelaar, G.; Maat, L.; Sheldon, R. Diels-Alder Reactions of Carbonyl-Containing Dienophiles Catalyzed by Tungstophosphoric Acid Supported on Silica Gel. *Catal. Lett.* **1998**, *56*, 49–51.
38. Meuzelaar, G.; Maat, L.; Sheldon, R.; Kozhevnikov, I. Heteropoly Acid-Catalyzed Diels-Alder Reactions. *Catal. Lett.* **1997**, *45*, 249–251.
39. Ogasawara, Y.; Uchida, S.; Yamaguchi, K.; Mizuno, N. A Tin-Tungsten Mixed Oxide as an Efficient Heterogeneous Catalyst for C-C Bond-Forming Reactions. *Chem. Eur. J.* **2009**, *15*, 4343–4349.
40. Kiamehr, M.; Moghaddam, F. M. An Efficient ZnO-Catalyzed Synthesis of Novel Indole-Annulated Thiopyrano-Chromene Derivatives via Domino Knoevenagel-hetero-Diels-Alder Reaction. *Tetrahedron Lett.* **2009**, *50*, 6723–6727.
41. Dintzner, M.; Wucka, P.; Lyons, T. Microwave-Assisted Synthesis of a Natural Insecticide on Basic Montmorillonite K10 Clay—Green Chemistry in the Undergraduate Organic Laboratory. *J. Chem. Educ.* **2006**, *83*, 270–272.
42. Kannan, V.; Sreekumar, K. Enantioselective Aza-Diels Alder Reaction Catalyzed by Clay Supported Schiff Base Complex. *J. Heterocyclic Chem.* **2021**, *58*, 153–160.
43. Cheng, Y.; Huber, G. W. Production of Targeted Aromatics by Using Diels-Alder Classes of Reactions With Furans and Olefins Over ZSM-5. *Green Chem.* **2012**, *14*, 3114–3125.
44. Wijaya, Y. P.; Suh, D. J.; Jae, J. Production of Renewable *p*-Xylene From 2,5-Dimethylfuran via Diels-Alder Cycloaddition and Dehydrative Aromatization Reactions Over Silica-Alumina Aerogel Catalysts. *Catal. Commun.* **2015**, *70*, 12–16.

45. Gole, B.; Bar, A. K.; Mallick, A.; Banerjee, R.; Mukherjee, P. S. An Electron Rich Porous Extended Framework as a Heterogeneous Catalyst for Diels-Alder Reactions. *Chem. Commun.* **2013**, *49*, 7439–7441.
46. Ren, H.; Cheng, L.; Yang, J.; Zhao, K.; Zhai, Q.; Li, Y. Recyclable and Reusable Chiral  $\alpha$ ,  $\alpha$ -L-diaryl Prolinol Heterogeneous Catalysts Grafting to UiO-67 for Enantioselective Hydration/Aldol/Oxa-Diels Alder domino Reaction. *Catal. Commun.* **2021**, *149*, 106249.
47. Yeh, J.-Y.; Chen, S. S.; Li, S.-C.; Chen, C. H.; Shishido, T.; Tsang, D. C. W.; Yamauchi, Y.; Li, Y.-P.; Wu, K. C.-W. Diels-Alder Conversion of Acrylic Acid and 2,5-Dimethylfuran to Para-Xylene Over Heterogeneous Bi-BTC Metal-Organic Framework Catalysts Under Mild Conditions. *Angew. Chem. Int. Ed.* **2021**, *60*, 624–629.
48. Green, S. K.; Patet, R. E.; Nikbin, N.; Williams, C. L.; Chang, C.; Yu, J.; Gorte, R. J.; Caratzoulas, S.; Fan, W.; Vlachos, D. G.; Dauenhauer, P. J. Diels-Alder Cycloaddition of 2-Methylfuran and Ethylene for Renewable Toluene. *Appl. Catal. B Environ.* **2016**, *180*, 487–496.
49. Borkin, D.; Morzhina, E.; Datta, S.; Rudnitskaya, A.; Sood, A.; Török, M.; Török, B. Heteropoly Acid-Catalyzed Microwave-Assisted Three-Component Aza-Diels-Alder Cyclizations: Diastereoselective Synthesis of Potential Drug Candidates for Alzheimer's Disease. *Org. Biomol. Chem.* **2011**, *9*, 1394–1401.
50. Simon, L.; Goodman, J. M. Theoretical Study of the Mechanism of Hantzsch Ester Hydrogenation of Imines Catalyzed by Chiral BINOL-Phosphoric Acids. *J. Am. Chem. Soc.* **2008**, *130*, 8741–8747.
51. Saikia, L.; Dutta, D.; Dutta, D. K. Efficient Clay Supported Ni-0 Nanoparticles as Heterogeneous Catalyst for Solvent-Free Synthesis of Hantzsch Polyhydroquinoline. *Catal. Commun.* **2012**, *19*, 1–4.
52. de Paolis, O.; Baffoe, J.; Landge, S. M.; Török, B. Multicomponent Domino Cyclization-Oxidative Aromatization on a Bifunctional Pd/C/K-10 Catalyst: An Environmentally Benign Approach toward the Synthesis of Pyridines. *Synthesis* **2008**, 3423–3428.
53. Safaei-Ghomi, J.; Ziarati, A.; Zahedi, S. Silica (NPs) Supported Fe (III) as a Reusable Heterogeneous Catalyst for the One-Pot Synthesis of 1, 4-Dihydropyridines Under Mild Conditions. *J. Chem. Sci.* **2012**, *124*, 933–939.
54. Gupta, R.; Gupta, R.; Paul, S.; Loupy, A. Covalently Anchored Sulfonic Acid on Silica Gel as an Efficient and Reusable Heterogeneous Catalyst for the One-Pot Synthesis of Hantzsch 1,4-Dihydropyridines Under Solvent-Free Conditions. *Synthesis* **2007**, 2835–2838.
55. Mobinikhaledi, A.; Foroughifar, N.; Fard, M. A. B.; Moghanian, H.; Ebrahimi, S.; Kalhor, M. Efficient One-Pot Synthesis of Polyhydroquinoline Derivatives Using Silica Sulfuric Acid as a Heterogeneous and Reusable Catalyst Under Conventional Heating and Energy-Saving Microwave Irradiation. *Synth. Commun.* **2009**, *39*, 1166–1174.
56. Sapkal, S. B.; Shelke, K. F.; Shingate, B. B.; Shingare, M. S. Nickel Nanoparticle-Catalyzed Facile and Efficient One-Pot Synthesis of Polyhydroquinoline Derivatives Via Hantzsch Condensation Under Solvent-Free Conditions. *Tetrahedron Lett.* **2009**, *50*, 1754–1756.
57. Tamaddon, F.; Moradi, S. Controllable Selectivity in Biginelli and Hantzsch Reactions Using nanoZnO as a Structure Base Catalyst. *J. Mol. Catal. A-Chem.* **2013**, *370*, 117–122.
58. Katkar, S. S.; Mohite, P. H.; Gadekar, L. S.; Arbad, B. R.; Lande, M. K. ZnO-Beta Zeolite: As an Effective and Reusable Heterogeneous Catalyst for the One-Pot Synthesis of Polyhydroquinolines. *Green Chem. Lett. Rev.* **2010**, *3*, 287–292.
59. Rostamnia, S.; Morsali, A. Basic Isoreticular Nanoporous Metal-Organic Framework for Biginelli and Hantzsch Coupling: IRMOF-3 as a Green and Recoverable Heterogeneous Catalyst in Solvent-Free Conditions. *RSC Adv.* **2014**, *4*, 10514–10518.

60. Rao, A. V. D.; Surasani, R.; Vykunteswararao, B. P.; Bhaskarkumar, T.; Srikanth, B.; Jogdand, N. R.; Kalita, D.; Lilakar, J. K. D.; Siddaiah, V.; Sanasi, P. D.; Raghunadh, A. Sulfonic Acid-Functionalized Wang Resin (Wang-OSO<sub>3</sub>H) as Polymeric Acidic Catalyst for the Ecofriendly Multicomponent Synthesis of Polyhydroquinolines via Hantzsch Condensation. *Synth. Commun.* **2016**, *46*, 1519–1528.
61. Pagadala, R.; Maddila, S.; Dasireddy, V. D. B. C.; Jonnalagadda, S. B. Zn-VCO<sub>3</sub> Hydroxalcite: A Highly Efficient and Reusable Heterogeneous Catalyst for the Hantzsch Dihydropyridine Reaction. *Catal. Commun.* **2014**, *45*, 148–152.
62. Kidwai, M.; Chauhan, R.; Bhatnagar, D.; Singh, A. K.; Mishra, B.; Dey, S. Nafion-H-A (R)-Catalyzed Synthesis of Polyhydroquinolines via the Hantzsch Multicomponent Reaction. *Monatsh. Chem.* **2012**, *143*, 1675–1680.
63. De Souza, R. O. M. A.; da Penha, E. T.; Milagre, H. M. S.; Garden, S. J.; Esteves, P. M.; Eberlin, M. N.; Antunes, O. A. C. The Three-Component Biginelli Reaction: A Combined Experimental and Theoretical Mechanistic Investigation. *Chem. Eur. J.* **2009**, *15*, 9799–9804.
64. Heravi, M. M.; Zadsirjan, V. Recent Advances in Biginelli-Type Reactions. *Curr. Org. Chem.* **2020**, *24*, 1331–1366.
65. Rafiee, E.; Shahbazi, F. One-Pot Synthesis of Dihydropyrimidones Using Silica-Supported Heteropoly Acid as an Efficient and Reusable Catalyst: Improved Protocol Conditions for the Biginelli Reaction. *J. Mol. Catal. A-Chem.* **2006**, *250*, 57–61.
66. Shaterian, H. R.; Hosseini, A.; Ghashang, M. An Efficient Synthesis of Multi-Substituted 3,4-Dihydropyrimidin-2(1H)-ones/thiones Under Solvent-Free Microwave Irradiation Using Alumina Sulfuric Acid. *Phosphorus Sulfur Silicon Relat. Elem.* **2009**, *184*, 197–205.
67. Chanu, L. V.; Singh, T. P.; Devi, L. R.; Singh, O. M. Synthesis of Bioactive Heterocycles Using Reusable Heterogeneous Catalyst HClO<sub>4</sub>-SiO<sub>2</sub> Under Solvent-Free Conditions. *Green Chem. Lett. Rev.* **2018**, *11*, 352–360.
68. Bhuyan, D.; Saikia, M.; Saikia, L. ZnO Nanoparticles Embedded in SBA-15 as an Efficient Heterogeneous Catalyst for the Synthesis Of Dihydropyrimidinones via Biginelli Condensation Reaction. *Microporous Mesoporous Mater.* **2018**, *256*, 39–48.
69. Moghannian, H.; Fard, M. A. B.; Mobinikhaledi, A.; Ahadi, N. Bis(p-sulfoanilino)triazine-Functionalized Silica-coated Magnetite Nanoparticles as an Efficient and Magnetically Reusable Nano-Catalyst for Biginelli-type Reaction. *Res. Chem. Intermed.* **2018**, *44*, 4083–4101.
70. Gewald, K.; Schinke, E.; Böttcher, H. 2-Amino-Thiophene aus Methylenaktiven Nitrilen Carbonylverbindungen und Schwefel. *Chem. Ber.* **1966**, *99*, 94–100.
71. Rudick, J. G.; Shaabani, S.; Doemling, A. Editorial: Isocyanide-Based Multicomponent Reactions. *Front. Chem.* **2020**, *7*, 918.
72. Boltjes, A.; Dömling, A. The Groebke-Blackburn-Bienaymé Reaction. *Eur. J. Org. Chem.* **2019**, 7007–7049.
73. Ferreira, S. B.; Kaiser, C. R. Pyrazine Derivatives: A Patent Review (2008–Present). *Expert Opin. Ther. Pat.* **2012**, *22*, 1033–1051.
74. Mortzfeld, F. B.; Hashem, C.; Vrankova, K.; Winkler, M.; Rudroff, F. Pyrazines: Synthesis and Industrial Application of these Valuable Flavor and Fragrance Compounds. *Biotechnol. J.* **2020**, *15*, 2000064.
75. Jing, F.; Zhang, Y.; Luo, S.; Chu, W.; Zhang, H.; Shi, X. Catalytic Synthesis of 2-Methylpyrazine Over Cr-Promoted Copper Based Catalyst via a Cyclo-Dehydrogenation Reaction Route. *J. Chem. Sci.* **2010**, *122*, 621–630.
76. Sato, K. *Process for Preparing Pyrazines*; US Patent, US4097478A, 1977.
77. Korea Research Institute of Chemical Technology. *Japanese Patent 05, 52829*; **1993**.

78. Zhang, Y.; Jing, F.; Ma, M.; Chu, W.; Luo, S. Influences of Pore Size on Production of 2-Methylpyrazine over Bifunctional CuO/ZnO/meso-SiO<sub>2</sub> Catalysts. *Res. Chem. Intermed.* **2013**, *39*, 1301–1311.
79. Anand, R.; Hegde, S.; Rao, B.; Gopinath, C. Catalytic Synthesis of 2-Methyl Pyrazine Over Zn-Modified Zeolites. *Catal. Lett.* **2002**, *84*, 265–272.
80. Anand, R.; Jyothi, T.; Rao, B. A Comparative Study on the Catalytic Activity of ZnO Modified Zeolites in the Synthesis of Alkylpyrazines. *Appl. Catal. A-Gen.* **2001**, *208*, 203–211.
81. Narender, N.; Srinivasu, P.; Kulkarni, S.; Raghavan, K. Intermolecular Cyclization of Diethanolamine and Methylamine to N,N'-Dimethylpiperazine Over Zeolites Under High Pressure. *J. Catal.* **2001**, *202*, 430–433.
82. Allais, C.; Grassot, J.-M.; Rodriguez, J.; Constantieux, T. Metal-Free Multicomponent Syntheses of Pyridines. *Chem. Rev.* **2014**, *114*, 10829–10868.
83. Kishbaugh, T. L. S. Pyridines and Imidazopyridines with Medicinal Significance. *Curr. Top. Med. Chem.* **2016**, *16*, 3274–3302.
84. Ciufolini, M. A.; Chan, B. K. Methodology for the Synthesis of Pyridines and Pyridones: Development and Applications. *Heterocycles* **2007**, *74*, 101–124.
85. Frechet, J. Synthesis and Selected Applications of Polymers Containing Pyridine Moieties. *Heterocycles* **1983**, *20*, 387.
86. Yang, Z.; Wang, H.; Ji, G.; Yu, X.; Chen, Y.; Liu, X.; Wu, C.; Liu, Z. Pyridine-Functionalized Organic Porous Polymers: Applications in Efficient CO<sub>2</sub> Adsorption and Conversion. *New J. Chem.* **2017**, *41*, 2869–2872.
87. Cheng, C. C.; Yan, S. J. *The Friedländer Synthesis of Quinolines. Organic Reactions*, Wiley: New York, 2005.
88. Lou, S.; Zhang, J. Pyrimidines. In *Heterocyclic Chemistry in Drug Discovery*; Jie, J. L., Ed.; John Wiley & Sons: Hoboken, NJ, 2013; pp. 569–613.
89. Gore, R. P.; Rajput, A. P. A Review on Recent Progress in Multicomponent Reactions of Pyrimidine Synthesis. *Drug Invent. Today* **2013**, *5*, 148–152.
90. Ha, P. T. M.; Le, B. T. T.; To, T. C.; Doan, S. H.; Nguyen, T. T.; Phan, N. T. S. Synthesis of Aryl-Substituted Pyridines via Cyclization of N,N-Dialkylanilines With Ketoxime Carboxylates Under Metal-Organic Framework Catalysis. *J. Ind. Eng. Chem.* **2017**, *54*, 151–161.
91. Molnár, Á.; Keresszegi, C.; Beregszászi, T.; Török, B.; Bartók, M. The Prins Reaction Catalyzed by Heteropoly Acids. In *Catalysis of Organic Reactions*; Herkes, F., Ed.; Marcel Dekker: New York, 1998; pp. 507–513.
92. Yadav, J.; Reddy, B.; Reddy, M.; Niranjan, N. Eco-Friendly Heterogeneous Solid Acids as Novel and Recyclable Catalysts in Ionic Medium for Tetrahydropyrans. *J. Mol. Catal. A-Chem.* **2004**, *210*, 99–103.
93. Balakrishna, A.; Aguiar, A.; Sobral, P. J. M.; Wani, M. Y.; Almeida Silva, J.; Sobral, A. J. F. N. Paal-Knorr Synthesis of Pyrroles: From Conventional to Green Synthesis. *Catal. Rev.-Sci. Eng.* **2019**, *61*, 84–110.
94. Banik, B.; Samajdar, S.; Banik, I. Simple Synthesis of Substituted Pyrroles. *J. Organomet. Chem.* **2004**, *69*, 213–216.
95. Abid, M.; Spaeth, A.; Török, B. Solvent-Free Solid Acid-Catalyzed Electrophilic Annulations: A New Green Approach for the Synthesis of Substituted Five-Membered N-Heterocycles. *Adv. Synth. Catal.* **2006**, *348*, 2191–2196.
96. Abid, M.; Landge, S. M.; Török, B. An Efficient and Rapid Synthesis of N-substituted Pyrroles by Microwave Assisted Solid Acid Catalysis. *Org. Prep. Proced. Int.* **2006**, *35*, 495–500.

536 Heterogeneous catalysis in sustainable synthesis

97. Song, G.; Wang, B.; Wang, G.; Kang, Y.; Yang, T.; Yang, L. Fe<sup>3+</sup>-Montmorillonite as Effective, Recyclable Catalyst for Paal-Knorr Pyrrole Synthesis Under Mild Conditions. *Synth. Commun.* **2005**, *35*, 1051–1057.
98. Veisi, H. Silica Sulfuric Acid (SSA) as a Solid Acid Heterogeneous Catalyst for One-Pot Synthesis of Substituted Pyrroles Under Solvent-Free Conditions at Room Temperature. *Tetrahedron Lett.* **2010**, *51*, 2109–2114.
99. Jisha, K. A.; Sreekumar, K. Dendritic Amine on Mesoporous Silica: First Organo Base Catalyst for Paal Knorr Reaction Under Solvent Free Condition, A Green Approach. *Catal. Lett.* **2017**, *147*, 964–975.
100. Rahmatpour, A. Cellulose Sulfuric Acid as a Biodegradable and Recoverable Solid Acid Catalyst for One Pot Synthesis of Substituted Pyrroles Under Solvent-Free Conditions at Room Temperature. *React. Funct. Polym.* **2011**, *71*, 80–83.
101. Bonyasi, F.; Hekmati, M.; Veisi, H. Preparation of Core/Shell Nanostructure Fe<sub>3</sub>O<sub>4</sub>@PEG400-SO<sub>3</sub>H as Heterogeneous and Magnetically Recyclable Nanocatalyst for One-Pot Synthesis of Substituted Pyrroles by Paal-Knorr Reaction at Room Temperature. *J. Colloid Interface Sci.* **2017**, *496*, 177–187.
102. Cheraghi, S.; Saberi, D.; Heydari, A. Nanomagnetically Modified Sulfuric Acid (Gamma-Fe<sub>2</sub>O<sub>3</sub>@SiO<sub>2</sub>-OSO<sub>3</sub>H): An Efficient, Fast, and Reusable Catalyst for Greener Paal-Knorr Pyrrole Synthesis. *Catal. Lett.* **2014**, *144*, 1339–1343.
103. Veisi, H.; Mohammadi, P.; Gholami, J. Sulfamic acid Heterogenized on Functionalized Magnetic Fe<sub>3</sub>O<sub>4</sub> Nanoparticles With Diaminoglyoxime as a Green, Efficient and Reusable Catalyst for One-Pot Synthesis of Substituted Pyrroles in Aqueous Phase. *Appl. Organomet. Chem.* **2014**, *28*, 868–873.
104. Darabi, H. R.; Poorheravi, M. R.; Aghapoor, K.; Mirzaee, A.; Mohsenzadeh, F.; Asadollahnejad, N.; Taherzadeh, H.; Balavar, Y. Silica-Supported Antimony(III) Chloride as a Mild and Reusable Catalyst for the Paal-Knorr Pyrrole Synthesis. *Environ. Chem. Lett.* **2012**, *10*, 5–12.
105. Portilla-Zuniga, O.; Sathicq, A.; Martinez, J.; Rojas, H.; De Geronimo, E.; Luque, R.; Romanelli, G. P. Novel Bifunctional Mesoporous Catalysts Based on Preyssler Heteropolycacids for Green Pyrrole Derivative Synthesis. *Catalysts* **2018**, *8*, 419.
106. Curini, M.; Montanari, F.; Rosati, O.; Lioy, E.; Margarita, R. Layered Zirconium Phosphate and Phosphonate as Heterogeneous Catalyst in the Preparation of Pyrroles. *Tetrahedron Lett.* **2003**, *44*, 3923–3925.
107. Cao, H.; Jiang, H.-F.; Zhou, X.-S.; Qi, C. R.; Lin, Y.-G.; Wu, J.-Y.; Liang, Q.-M. CuO/CNTs-Catalyzed Heterogeneous Process: A Convenient Strategy to Prepare Furan Derivatives From Electron-Deficient Alkynes and [α]-Hydroxy Ketones. *Green Chem.* **2012**, *14*, 2710–2714.
108. Cao, H.; Jiang, H.; Huang, H. Transition-Metal-Catalyzed Domino Reactions: Efficient One-Pot Regiospecific Synthesis of Highly Functionalized Polysubstituted Furans from Electron-Deficient Alkynes and 2-yn-1-ols. *Synthesis* **2011**, 1019–1036.
109. Breugst, M.; Reissig, H. The Huisgen Reaction: Milestones of the 1,3-Dipolar Cycloaddition. *Angew. Chem. Int. Ed.* **2020**, *59*, 12293–12307.
110. Kolb, H. C.; Finn, M. G.; Sharpless, K. B. Click Chemistry: Diverse Chemical Function from a Few Good Reactions. *Angew. Chem. Int. Ed.* **2001**, *113*, 2056–2075.
111. Beneteau, V.; Olmos, A.; Boningari, T.; Sommer, J.; Pale, P. Zeo-Click Synthesis: Cu-I-Zeolite-Catalyzed One-Pot Two-Step Synthesis of Triazoles From Halides and Related Compounds. *Tetrahedron Lett.* **2010**, *51*, 3673–3677.
112. Chassaing, S.; Alix, A.; Boningari, T.; Sido, K. S. S.; Keller, M.; Kuhn, P.; Louis, B.; Sommer, J.; Pale, P. Copper(I)-Zeolites as New Heterogeneous and Green Catalysts for Organic Synthesis. *Synthesis* **2010**, 1557–1567.

113. Lee, B. S.; Yi, M.; Chu, S. Y.; Lee, J. Y.; Kwon, H. R.; Lee, K. R.; Kang, D.; Kim, W. S.; Bin Lim, H.; Lee, J.; Youn, H.; Chi, D. Y.; Hur, N. H. Copper Nitride Nanoparticles Supported on a Superparamagnetic Mesoporous Microsphere for Toxic-Free Click Chemistry. *Chem. Commun.* **2010**, *46*, 3935–3937.
114. Katayama, T.; Kamata, K.; Yamaguchi, K.; Mizuno, N. A Supported Copper Hydroxide as an Efficient, Ligand-free, and Heterogeneous Precatalyst for 1,3-Dipolar Cycloadditions of Organic Azides to Terminal Alkynes. *ChemSusChem* **2009**, *2*, 59–62.
115. Yamaguchi, K.; Oishi, T.; Katayama, T.; Mizuno, N. A Supported Copper Hydroxide on Titanium Oxide as an Efficient Reusable Heterogeneous Catalyst for 1,3-Dipolar Cycloaddition of Organic Azides to Terminal Alkynes. *Chem. Eur. J.* **2009**, *15*, 10464–10472.
116. Monguchi, Y.; Nozaki, K.; Maejima, T.; Shimoda, Y.; Sawama, Y.; Kitamura, Y.; Kitade, Y.; Sajiki, H. Solvent-free Huisgen cyclization using heterogeneous copper catalysts supported on chelate resins. *Green Chem.* **2013**, *15*, 490–495.
117. Girard, C.; Onen, E.; Aufort, M.; Beauviere, S.; Samson, E.; Herscovici, J. Reusable Polymer-Supported Catalyst for the [3+2] Huisgen Cycloaddition in Automation Protocols. *Org. Lett.* **2006**, *8*, 1689–1692.
118. Carta, A.; Piras, S.; Loriga, G.; Paglietti, G. Chemistry, Biological Properties and SAR Analysis of Quinoxalinones. *Mini-Rev. Med. Chem.* **2006**, *6*, 1179–1200.
119. Tahlan, S.; Kumar, S.; Narasimhan, B. Pharmacological Significance of Heterocyclic 1H-Benzimidazole Scaffolds: A Review. *BMC Chem.* **2019**, *13*. UNSP 101.
120. Ellman, J. Design, Synthesis, and Evaluation of Small-Molecule Libraries. *Acc. Chem. Res.* **1996**, *29*, 132–143.
121. Pereira, J. A.; Pessoa, A. M.; Cordeiro, M. N. D. S.; Fernandes, R.; Prudencio, C.; Noronha, J. P.; Vieira, M. Quinoxaline, Its Derivatives and Applications: A State of the Art Review. *Eur. J. Med. Chem.* **2015**, *97*, 664–672.
122. Landge, S. M.; Török, B. Synthesis of Condensed Benzo[N,N]-Heterocycles by Microwave-Assisted Solid Acid Catalysis. *Catal. Lett.* **2008**, *122*, 338–343.
123. Yen, Y.; Lee, C.; Hsu, C.; Chou, H.; Chen, Y.; Lin, J. T. Benzotriazole-Containing D- $\pi$ -A Conjugated Organic Dyes for Dye-Sensitized Solar Cells. *Chem. Asian J.* **2013**, *8*, 809–816.
124. Handratta, V.; Vasaitis, T.; Njar, V.; Gediya, L.; Kataria, R.; Chopra, P.; Newman, D.; Farquhar, R.; Guo, Z.; Qiu, Y.; Brodie, A. Novel C-17-Heteroaryl Steroidal CYP17 Inhibitors/Antiandrogens: Synthesis, In Vitro Biological Activity, Pharmacokinetics, and Antitumor Activity in the LAPC4 Human Prostate Cancer Xenograft Model. *J. Med. Chem.* **2005**, *48*, 2972–2984.
125. Fu, J.; Yang, Y.; Zhang, X.; Mao, W.; Zhang, Z.; Zhu, H. Discovery of 1H-Benzo[d][1,2,3]Triazol-1-yl 3,4,5-Trimethoxybenzoate as a Potential Antiproliferative Agent by Inhibiting Histone Deacetylase. *Bioorg. Med. Chem.* **2010**, *18*, 8457–8462.
126. Kokel, A.; Török, B. Microwave-Assisted Solid Phase Diazotation: A Method for the Environmentally Benign Synthesis of Benzotriazoles. *Green Chem.* **2017**, *19*, 2515–2519.
127. Khatun, R.; Biswas, S.; Biswas, I. H.; Riyajuddin, S.; Haque, N.; Ghosh, K.; Islam, S. M. Cu-NPs@COF: A Potential Heterogeneous Catalyst for CO<sub>2</sub> Fixation to Produce 2-Oxazolidinones as Well as Benzimidazoles Under Moderate Reaction Conditions. *J. CO<sub>2</sub> Util.* **2020**, *40*, 101180.
128. Li, S.; Tan, X.; Sun, W.; Zhang, L.; Jia, H.; Li, L.; Zhao, C.; Zhang, X. Design Catalytic Space Engineering of Ag-Ag Bond-Based Metal Organic Framework for Carbon Dioxide Fixation Reactions. *Colloids Surf. A Physicochem. Eng. Asp.* **2021**, *609*, 125529.
129. Zhi-tao, W. Cycloaddition of Propargylic Amines and CO<sub>2</sub> by Ni@Pd Nanoclusters Confined Within Metal-Organic Framework Cavities in Aqueous Solution. *Catal. Lett.* **2020**, *150*, 2352–2364.

130. Ghosh, S.; Khan, T. S.; Ghosh, A.; Chowdhury, A. H.; Haider, M. A.; Khan, A.; Islam, S. M. Utility of Silver Nanoparticles Embedded Covalent Organic Frameworks as Recyclable Catalysts for the Sustainable Synthesis of Cyclic Carbamates and 2-Oxazolidinones via Atmospheric Cyclizative CO<sub>2</sub> Capture. *ACS Sustain. Chem. Eng.* **2020**, *8*, 5495–5513.
131. Hennessy, E.; Buchwald, S. Synthesis of Substituted Oxindoles From Alpha-Chloroacetanilides via Palladium-Catalyzed C-H Functionalization. *J. Am. Chem. Soc.* **2003**, *125*, 12084–12085.
132. Wei, W.; Zhou, M.; Fan, J.; Liu, W.; Song, R.; Liu, Y.; Hu, M.; Xie, P.; Li, J. Synthesis of Oxindoles by Iron-Catalyzed Oxidative 1,2-Alkylarylation of Activated Alkenes with an Aryl C(sp<sup>2</sup>)H Bond and a C(sp<sup>3</sup>)H Bond Adjacent to a Heteroatom. *Angew. Chem. Int. Ed.* **2013**, *52*, 3638–3641.
133. Zhou, S.; Guo, L.; Wang, H.; Duan, X. Copper-Catalyzed Oxidative Benzylarylation of Acrylamides by Benzylic C-H Bond Functionalization for the Synthesis of Oxindoles. *Chem. Eur. J.* **2013**, *19*, 12970–12973.
134. Wu, H.; Zhou, M.; Li, W.; Zhang, P. Heterogeneous Chitosan@Nickel (II)-Catalyzed Tandem Radical Cyclization of N-Arylacrylamides: A General Method for Constructing Fluorinated 3,3-Disubstituted Oxindoles Using Perfluoroalkyl Iodides. *Catal. Commun.* **2020**, *133*, 105832.
135. Li, X. T.; Liu, Y. H.; Liu, X.; Zhang, Z. H. Meglumine Catalyzed One-Pot, Three-Component Combinatorial Synthesis of Pyrazoles Bearing a Coumarin Unit. *RSC Adv.* **2015**, *5*, 25625–25633.
136. Schmitt, D. C.; Taylor, A. P.; Flick, A. C.; Kyne, R. E. Synthesis of Pyrazoles From 1,3-Diols via Hydrogen Transfer Catalysis. *Org. Lett.* **2015**, *17*, 1405–1408.
137. Matcha, K.; Antonchick, A. P. Cascade Multicomponent Synthesis of Indoles, Pyrazoles and Pyridazinones by Functionalization of Alkenes. *Angew. Chem. Int. Ed.* **2014**, *53*, 11960–11964.
138. Dias, D.; Pacheco, B. S.; Cunico, W.; Pizzuti, L.; Pereira, C. M. P. Recent Advances on the Green Synthesis and Antioxidant Activities of Pyrazoles. *Mini-Rev. Med. Chem.* **2014**, *14*, 1078–1092.
139. Fustero, S.; Sanchez-Rosello, M.; Barrio, P.; Simon-Fuentes, A. From 2000 to Mid-2010: A Fruitful Decade for the Synthesis of Pyrazoles. *Chem. Rev.* **2011**, *111*, 6984–7034.
140. Landge, S. M.; Schmidt, A.; Outerbridge, V.; Török, B. Synthesis of Pyrazoles by a One-pot Tandem Cyclization-Dehydrogenation Approach on Pd/C/K-10 Catalyst. *Synlett* **2007**, 1600–1604.
141. Borkin, D. A.; Puscau, M.; Carlson, A.; Solan, A.; Wheeler, K. A.; Török, B.; Dembinski, R. Synthesis of Diversely 1,3,5-Trisubstituted Pyrazoles via 5-exo-dig Cyclization. *Org. Biomol. Chem.* **2012**, *10*, 4505–4508.
142. Nasrallah, H. O.; Min, Y.; Lerayer, E.; Nguyen, T.-A.; Poinot, D.; Roger, J.; Brandes, S.; Heintz, O.; Roblin, P.; Jolibois, F.; Poteau, R.; Coppel, Y.; Kahn, M. L.; Gerber, I. C.; Axet, M. R.; Serp, P.; Hierso, J.-C. Nanocatalysts for High Selectivity Enyne Cyclization: Oxidative Surface Reorganization of Gold Sub-2-nm Nanoparticle Networks. *JACS Au* **2021**, *1*, 187–200.
143. Shao, Z.; Liu, M.; Dang, J.; Huang, C.; Xu, W.; Wu, J.; Hou, H. Efficient Catalytic Performance for Acylation-Nazarov Cyclization Based on an Unusual Postsynthetic Oxidization Strategy in a Fe(II)-MOF. *Inorg. Chem.* **2018**, *57*, 10224–10231.
144. Huang, C.; Zhang, Y.; Yang, H.; Wang, D.; Mi, L.; Shao, Z.; Liu, M.; Hou, H. Oriented Controllable Fabrication of Metal-Organic Frameworks Membranes as Solid Catalysts for Cascade Indole Acylation-Nazarov Cyclization for Cyclopentenone[b]indoles. *Cryst. Growth Des.* **2018**, *18*, 5674–5681.

145. Liu, M.; Gao, K.; Fan, Y.; Guo, X.; Wu, J.; Meng, X.; Hou, H. Co-Cluster-Based Metal-Organic Frameworks as Selective Catalysts for Benzene Tandem Acylation-Nazarov Cyclization to Benzocyclopentanone. *Chem. Eur. J.* **2018**, *24*, 1416–1424.
146. Huang, C.; Ding, R.; Song, C.; Lu, J.; Liu, L.; Han, X.; Wu, J.; Hou, H.; Fan, Y. Template-Induced Diverse Metal-Organic Materials as Catalysts for the Tandem Acylation-Nazarov Cyclization. *Chem. Eur. J.* **2014**, *20*, 16156–16163.
147. Tejada-Serrano, M.; Sanz-Navarro, S.; Blake, F.; Leyva-Perez, A. Zeolites Catalyze the Nazarov Reaction and the Tert-Butylation of Alcohols by Stabilization of Carboxonium Intermediates. *Synthesis* **2020**, *52*, 2031–2037.
148. Huang, C.; Han, X.; Shao, Z.; Gao, K.; Liu, M.; Wang, Y.; Wu, J.; Hou, H.; Mi, L. Solvent-Induced Assembly of Silver Coordination Polymers (CPs) as Cooperative Catalysts for Synthesizing of Cyclopentenone[b]pyrroles Frameworks. *Inorg. Chem.* **2017**, *56*, 4874–4884.
149. Vaidya, T.; Cheng, R.; Carlsen, P. N.; Frontier, A. J.; Eisenberg, R. Cationic Cyclizations and Rearrangements Promoted by a Heterogeneous Gold Catalyst. *Org. Lett.* **2014**, *16*, 800–803.
150. Zhang, W.; Liao, P.; Lin, R.; Wei, Y.; Zeng, M.; Chen, X. Metal Cluster-Based Functional Porous Coordination Polymers. *Coord. Chem. Rev.* **2015**, *293*, 263–278.
151. Yada, Y.; Miyake, Y.; Nishibayashi, Y. Ruthenium-Catalyzed Intramolecular Cyclization of 3-Butyne-1,2-Diols Into Furans. *Organometallics* **2008**, *27*, 3614–3617.
152. Kraus, G.; Wang, X. An Improved Synthesis of 3-Substituted Furans From Substituted Butene-1,4-Diols. *Synth. Commun.* **1998**, *28*, 1093–1096.
153. Sanz, R.; Miguel, D.; Martinez, A.; Alvarez-Gutierrez, J. M.; Rodriguez, F. Bronsted Acid Catalyzed Propargylation of 1,3-Dicarbonyl Derivatives. Synthesis of Tetrasubstituted Furans. *Org. Lett.* **2007**, *9*, 727–730.
154. Perez-Mayoral, E.; Matos, I.; Fonseca, I.; Cejka, J. Zeolites Efficiently Promote the Cyclization of Nonactivated Unsaturated Alcohols. *Chem. Eur. J.* **2010**, *16*, 12079–12082.
155. Sun, N.; Huang, P.; Wang, Y.; Mo, W.; Hu, B.; Shen, Z.; Hu, X. Zeolite-Catalyzed Synthesis of 2,3-Unsubstituted Benzo[b]Furans via the Intramolecular Cyclization of 2-Aryloxyacetaldehyde Acetals. *Tetrahedron* **2015**, *71*, 4835–4841.
156. Hayes, S. J.; Knight, D. W.; Menzies, M. D.; O'Halloran, M.; Tan, W. An Efficient Furan Synthesis Using Heterogeneous Catalysis. *Tetrahedron Lett.* **2007**, *48*, 7709–7712.
157. Lenardao, E. J.; Botteselle, G. V.; de Azambuja, F.; Perin, G.; Jacob, R. G. Citronellal as Key Compound in Organic Synthesis. *Tetrahedron* **2007**, *63*, 6671–6712.
158. Maki-Arvela, P.; Kumar, N.; Nieminen, V.; Sjöholm, R.; Salmi, T.; Murzin, D. Cyclization of Citronellal Over Zeolites and Mesoporous Materials for Production of Isopulegol. *J. Catal.* **2004**, *225*, 155–169.
159. Neatu, F.; Coman, S.; Parvulescu, V. I.; Poncelet, G.; De Vos, D.; Jacobs, P. Heterogeneous Catalytic Transformation of Citronellal to Menthol in a Single Step on Ir-Beta Zeolite Catalysts. *Top. Catal.* **2009**, *52*, 1292–1300.
160. Cirujano, F. G.; Llabres i Xamena, F. X.; Corma, A. MOFs as Multifunctional Catalysts: One-Pot Synthesis of Menthol From Citronellal Over a Bifunctional MIL-101 Catalyst. *Dalton Trans.* **2012**, *41*, 4249–4254.
161. Rubiyanto, D.; Prakoso, N. I.; Sahroni, I.; Nurillahi, R.; Fatimah, I. ZnO-Porous Clay Heterostructure from Saponite as Green Catalyst for Citronellal Cyclization. *Bull. Chem. React. Eng. Catal.* **2020**, *15*, 137–145.
162. Brenna, E.; Fuganti, C.; Serra, S.; Kraft, P. Optically Active Ionones and Derivatives: Preparation and Olfactory Properties. *Eur. J. Org. Chem.* **2002**, *2002*, 967–978.
163. Lin, Z.; Ni, H.; Du, H.; Zhao, C. A New Type of Hybridized macroreticular Catalyst: Polystyrene With Both Perfluoroalkanesulfonic and Sulfonic Functional Groups. *Catal. Commun.* **2007**, *8*, 31–35.

540 Heterogeneous catalysis in sustainable synthesis

164. Guo, D.; Ma, Z.; Jiang, Q.; Xu, H.; Ma, Z.; Ye, W. Sulfated and Persulfated TiO<sub>2</sub>/MCM-41 Prepared by Grafting Method and Their Acid-Catalytic Activities for Cyclization Of Pseudoionone. *Catal. Lett.* **2006**, *107*, 155–159.
165. Diez, V. K.; Apesteguia, C. R.; Di Cosimo, J. I. Synthesis of Ionones by Cyclization of Pseudoionone on Solid Acid Catalysts. *Catal. Lett.* **2008**, *123*, 213–219.
166. Tsangarakis, C.; Stratakis, M. Biomimetic Cyclization of Small Terpenoids Promoted by Zeolite NaY: Tandem Formation of Alpha-Ambrinol From Geranyl Acetone. *Adv. Synth. Catal.* **2005**, *347*, 1280–1284.
167. Quilez del Moral, J. F.; Perez, A.; Barrero, A. F. Chemical Synthesis of Terpenoids With Participation of Cyclizations Plus Rearrangements of Carbocations: A Current Overview. *Phytochem. Rev.* **2020**, *19*, 559–576.
168. Raptis, C.; Lykakis, I. N.; Tsangarakis, C.; Stratakis, M. Acid-Catalyzed Cyclization of Terpenes Under Homogeneous and Heterogeneous Conditions as Probed Through Stereoisotopic Studies: A Concerted Process with Competing Preorganized Chair and Boat Transition States. *Chem. Eur. J.* **2009**, *15*, 11918–11927.
169. De Paolis, O.; Teixeira, L.; Török, B. Synthesis of Quinolines by a Solid Acid-Catalyzed Microwave-Assisted Domino Cyclization-Aromatization Approach. *Tetrahedron Lett.* **2009**, *50*, 2939–2942.
170. Jeganathan, M.; Pitchumani, K. Synthesis of Substituted Isoquinolines via Iminoalkyne Cyclization Using Ag(I) Exchanged K10-Montmorillonite Clay as a Reusable Catalyst. *RSC Adv.* **2014**, *4*, 38491–38497.
171. Padwa, A.; Murphree, S. S. Epoxides and Aziridines—A Mini Review. *ARKIVOC* **2006**, 6–33.
172. Singh, G. S.; D'hooghe, M.; De Kimpe, N. Synthesis and Reactivity of C-Heteroatom-Substituted Aziridines. *Chem. Rev.* **2007**, *107*, 2080–2135.
173. Borkin, D. A.; Carlson, A.; Török, B. K-10-Catalyzed Highly Diastereoselective Synthesis of Aziridines. *Synlett* **2010**, 745–748.
174. Parker, E.; Isaacs, N. Mechanisms of Epoxide Reactions. *Chem. Rev.* **1959**, *59*, 737–799.
175. Dhakshinamoorthy, A.; Alvaro, M.; Concepcion, P.; Fornes, V.; Garcia, H. Graphene Oxide as an Acid Catalyst for the Room Temperature Ring Opening of Epoxides. *Chem. Commun.* **2012**, *48*, 5443–5445.
176. Liu, F.; Sun, J.; Zhu, L.; Meng, X.; Qi, C.; Xiao, F. Sulfated Graphene as an Efficient Solid Catalyst for Acid-Catalyzed Liquid Reactions. *J. Mater. Chem.* **2012**, *22*, 5495–5502.
177. Dhakshinamoorthy, A.; Alvaro, M.; Garcia, H. Metal-Organic Frameworks as Efficient Heterogeneous Catalysts for the Regioselective Ring Opening of Epoxides. *Chem. Eur. J.* **2010**, *16*, 8530–8536.
178. Anbu, N.; Dhakshinamoorthy, A. Regioselective Ring Opening of Styrene Oxide by Carbon Nucleophiles Catalyzed by Metal-Organic Frameworks Under Solvent-Free Conditions. *J. Ind. Eng. Chem.* **2018**, *58*, 9–17.
179. Liu, Y.; Klet, R. C.; Hupp, J. T.; Farha, O. Probing the Correlations Between the Defects in Metal-Organic Frameworks and Their Catalytic Activity by an Epoxide Ring-Opening Reaction. *Chem. Commun.* **2016**, *52*, 7806–7809.
180. Bandini, M.; Fagioli, M.; Melloni, A.; Umani-Ronchi, A. Polymer-Supported Indium Lewis Acid: Highly Versatile Catalyst for Regio- and Stereoselective Ring-Opening of Epoxides. *Adv. Synth. Catal.* **2004**, *346*, 573–578.
181. Behrouz, S.; Rad, M. N. S.; Piltan, M. A.; Doroodmand, M. M. Chitosan-Silica Sulfate Nano Hybrid as a Novel and Highly Proficient Heterogeneous Nano Catalyst for Regioselective Ring Opening of Epoxides via Carboxylic Acids. *Helv. Chim. Acta* **2017**, *100*, e1700144.
182. Mojtahedi, M.; Ghasemi, M.; Abae, M.; Bolourchian, M. Microwave-Assisted Ring Opening of Epoxides With Thiols on Montmorillonite K-10 Solid Support. *ARKIVOC* **2005**, 68–73.

183. Trikitiwong, P.; Sukpirom, N.; Chavasiri, W. Regioselective Epoxide ring Opening Mediated by Iron Oxide-Pillared Clay. *J. Mol. Catal. A-Chem.* **2013**, *378*, 76–81.
184. Hummers, W.; Offman, R. E. Preparation of Graphitic Oxide. *J. Am. Chem. Soc.* **1958**, *80*, 1339.
185. Török, B.; Bucsi, I.; Beregszászi, T.; Molnár, Á. Rearrangements of Oxygen-Containing Compounds Induced by Heteropoly Acids. In *Catalysis of Organic Reactions*; Malz, R. E., Ed.; Marcel Dekker: New York, 1996; pp. 393–397.
186. Török, B.; Molnár, Á. Electrophilic Transformations Induced by Heteropoly Acids: Applications and Structural Studies. *C. R. Acad. Sci. Paris, Serie II c* **1998**, 381–396.
187. Marciniak, A. A.; Lamb, K. J.; Ozorio, L. P.; Mota, C. J. A.; North, M. Heterogeneous Catalysts for Cyclic Carbonate Synthesis From Carbon Dioxide and Epoxides. *Curr. Opin. Green Sustain. Chem.* **2020**, *26*, 100365.
188. Pander, M.; Janeta, M.; Bury, W. Quest for an Efficient 2-in-1 MOF-Based Catalytic System for Cycloaddition of CO<sub>2</sub> to Epoxides under Mild Conditions. *ACS Appl. Mater. Interfaces* **2021**, <https://doi.org/10.1021/acscami.0c20437>.
189. Kurisingal, J. F.; Rachuri, Y.; Gu, Y.; Kim, G.; Park, D. Binary Metal-Organic Frameworks: Catalysts for the Efficient Solvent-Free CO<sub>2</sub> Fixation Reaction via Cyclic Carbonates Synthesis. *Appl. Catal. A-Gen.* **2019**, *571*, 1–11.
190. Li, J.; Li, W.; Xu, S.; Li, B.; Tang, Y.; Lin, Z. Porous Metal-Organic Framework With Lewis Acid-Base Bifunctional Sites for High Efficient CO<sub>2</sub> Adsorption and Catalytic Conversion to Cyclic Carbonates. *Inorg. Chem. Commun.* **2019**, *106*, 70–75.
191. Song, X.; Wu, Y.; Pan, D.; Zhang, J.; Xu, S.; Gao, L.; Wei, R.; Zhang, J.; Xiao, G. Dual-Linker Metal-Organic Frameworks as Efficient Carbon Dioxide Conversion Catalysts. *Appl. Catal. A-Gen.* **2018**, *566*, 44–51.
192. Babu, R.; Kim, S.; Kurisingal, J. F.; Kim, H.; Choi, G.; Park, D. A Room Temperature Synthesizable Zeolitic Imidazolium Framework Catalyst for the Solvent-Free Synthesis of Cyclic Carbonates. *J. CO<sub>2</sub> Util.* **2018**, *25*, 6–13.
193. Zhang, S.; Zhang, H.; Cao, F.; Ma, Y.; Qu, Y. Catalytic Behavior of Graphene Oxides for Converting CO<sub>2</sub> into Cyclic Carbonates at One Atmospheric Pressure. *ACS Sustain. Chem. Eng.* **2018**, *6*, 4204–4211.
194. Helal, A.; Cordova, K. E.; Arafat, M. E.; Usman, M.; Yamani, Z. H. Defect-Engineering a Metal-Organic Framework for CO(2) Fixation in the Synthesis of Bioactive Oxazolidinones. *Inorg. Chem. Front.* **2020**, *7*, 3571–3577.
195. Wang, W.; Wei, R.; Yin, G.; Tian, J.; Duan, Y.; Chen, L.; Li, Y. The Synthesis of Asymmetric Ethylenediamine Derivatives Catalyzed by Ion-Exchange Resins. *Res. Chem. Intermed.* **2015**, *41*, 4511–4522.
196. Das, B.; Ramu, R.; Ravikanth, B.; Reddy, K. Regioselective Ring-Opening of Aziridines With Potassium Thiocyanate and Thiols Using Sulfated Zirconia as a Heterogeneous Recyclable Catalyst. *Tetrahedron Lett.* **2006**, *47*, 779–782.
197. Kang, X.; Shi, Y.; Cao, C.; Zhao, B. Stable Metal-Organic Frameworks With High Catalytic Performance in the Cycloaddition of CO<sub>2</sub> With Aziridines. *Sci. China Chem.* **2019**, *62*, 622–628.
198. Zhang, J.; Hu, C. P. Synthesis, Characterization and Mechanical Properties of Polyester-Based Aliphatic Polyurethane Elastomers Containing Hyperbranched Polyester Segments. *Eur. Polym. J.* **2008**, *44*, 3708–3714.
199. Mehdipour-Ataei, S.; Heidari, H. Synthesis and Characterization of Novel Soluble and Thermally Stable Polyamides Based on Pyridine Monomer. *Macromol. Symp.* **2003**, *193*, 159–167.
200. Ahmadnian, F.; Reichert, K. H. Kinetic Studies of Polyethylene Terephthalate Synthesis with Titanium-Based Catalyst. *Macromol. Symp.* **2007**, *259*, 188–196.

542 Heterogeneous catalysis in sustainable synthesis

201. Thomas, C. M. Stereo Controlled Ring-Opening Polymerization of Cyclic Esters: Synthesis of New Polyester Microstructures. *Chem. Soc. Rev.* **2010**, *39*, 165–173.
202. Khan, J. H.; Schue, F.; George, G. A. Heterogeneous Ring-Opening Polymerization of Lactones for Biomedical Applications. *Polym. Int.* **2009**, *58*, 296–301.
203. Dreyer, D. R.; Bielawski, C. W. Carbocatalysis: Heterogeneous Carbons Finding Utility in Synthetic Chemistry. *Chem. Sci.* **2011**, *2*, 1233–1240.
204. Dreyer, D. R.; Jarvis, K. A.; Ferreira, P. J.; Bielawski, C. W. Graphite Oxide as a Carbocatalyst for the Preparation of Fullerene-Reinforced Polyester and Polyamide Nanocomposites. *Polym. Chem.* **2012**, *3*, 757–766.
205. Ren, C.; Zhu, X.; Zhao, N.; Shen, Y.; Chen, L.; Liu, S.; Li, Z. Polystyrene Beads Supported Phosphazene Superbase as Recyclable Organocatalyst for Ring-Opening Polymerization of Delta-Valerolactone. *Eur. Polym. J.* **2019**, *119*, 130–135.
206. Wilson, B.; Jones, C. A Recoverable, Metal-Free Catalyst for the Green Polymerization of Epsilon-Caprolactone. *Macromolecules* **2004**, *37*, 9709–9714.
207. Howard, I. C.; Hammond, C.; Buchard, A. Polymer-Supported Metal Catalysts for the Heterogeneous Polymerisation of Lactones. *Polym. Chem.* **2019**, *10*, 5894–5904.
208. Long, W.; Gill, C. S.; Choi, S.; Jones, C. W. Recoverable and Recyclable Magnetic Nanoparticle supported Aluminium Isopropoxide for Ring-Opening Polymerization of Epsilon-Caprolactone. *Dalton Trans.* **2010**, *39*, 1470–1472.
209. Martin, E.; Dubois, P.; Jerome, R. Polymerization of Epsilon-Caprolactone Initiated by Y Alkoxide Grafted Onto Porous Silica. *Macromolecules* **2003**, *36*, 7094–7099.
210. Naz, F.; Ciprian, M.; Mousavi, B.; Chaemchuen, S.; Zhu, M.; Yan, S.; Verpoort, F. Solvent-Free Synthesis of Cyclic Polycaprolactone Catalysed by MOF-Derived ZnO/NCs Catalysts. *Eur. Polym. J.* **2021**, *142*, 110127.
211. Pollet, E.; Hamaide, T.; Tayakout-Fayolle, M.; Jallut, C. Heterogeneous Anionic Ring Opening Polymerization in a Fixed-Bed Reactor: Description of the Process and Modelling. *Polym. Int.* **2004**, *53*, 550–556.
212. Deshayes, G.; Poelmans, K.; Verbruggen, I.; Camacho-Camacho, C.; Degee, P.; Pinoie, V.; Martins, J.; Piotto, M.; Biesemans, M.; Willem, R.; Dubois, P. Polystyrene-Supported Organotin Dichloride as a Recyclable Catalyst in Lactone Ring-Opening Polymerization: Assessment and Catalysis Monitoring by High-Resolution Magic-Angle-Spinning NMR Spectroscopy. *Chem. Eur. J.* **2005**, *11*, 4552–4561.
213. Jones, M. D.; Davidson, M. G.; Keir, C. G.; Wooles, A. J.; Mahon, M. F.; Apperley, D. C. Heterogeneous Catalysts for the Controlled Ring-Opening Polymerisation of Rac-Lactide and Homogeneous Silsesquioxane Model Complexes. *Dalton Trans.* **2008**, 3655–3657.
214. Nguyen, O. T. K.; Nguyen, L. T.; Truong, N. K.; Nguyen, V. D.; Nguyen, A. T.; Le, N. T. H.; Le, D. T.; Phan, N. T. S. Synthesis of Triphenylamines via Ligand-Free Selective Ring-Opening of Benzoxazoles or Benzothiazoles Under Superparamagnetic Nanoparticle Catalysis. *RSC Adv.* **2017**, *7*, 40929–40939.
215. Galadima, A.; Muraza, O. Ring Opening of Hydrocarbons for Diesel and Aromatics Production: Design of Heterogeneous Catalytic Systems. *Fuel* **2016**, *181*, 618–629.
216. Mouli, K. C.; Sundaramurthy, V.; Dalai, A. K. A Comparison Between Ring-Opening of Decalin on Ir-Pt and Ni-Mo Carbide Catalysts Supported on Zeolites. *J. Mol. Catal. A-Chem.* **2009**, *304*, 77–84.

## Chapter 3.9

# Heterogeneous catalytic rearrangements and other transformations

### 3.9.1. Rearrangements

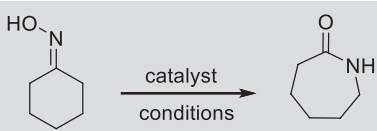
Rearrangement reactions are a special and useful group of organic transformations. Although in many cases these reactions produce undesirable by-products in various processes, there are several rearrangements that are well studied and are intentionally used to generate products from easily available starting materials. In general, during these transformations a group or an atom migrates to a different position in the carbon skeleton of the molecule, often the skeleton itself changes during the migration.<sup>1,2</sup> Rearrangements can occur via ionic or radical mechanisms.

#### 3.9.1.1 Beckmann rearrangement

The Beckmann rearrangement is a rearrangement of oximes to produce the corresponding amides induced by an electropositive nitrogen initiating an alkyl migration. This transformation is useful for the production of various key intermediates involved in the synthesis of fine chemicals, in the medical field, the agrochemical field, and the plastics sector among others.<sup>3,4</sup>

$\epsilon$ -Caprolactam probably constitutes one of the most important intermediates that can be produced via a Beckmann rearrangement; it is the precursor of the widely used nylon.<sup>4</sup> Traditionally, the industrial process for the production of caprolactam involves harmful and corrosive liquid mineral acids, such as concentrated sulfuric acid<sup>5</sup> and inevitably lead to several issues including the difficulty to separate the product, the corrosion of the reactors and the generation of a large amount of ammonium sulfate formed as by-product. Heterogeneous catalysis holds a great potential to overcome these issues. A few representative examples for solid acid-catalyzed Beckmann rearrangement of cyclohexanone oxime to  $\epsilon$ -caprolactam are collected in Table 1. In addition to its industrial importance, this particular reaction is also frequently used as a test reaction for the characterization of solid acids, such as zeolites or metal-organic frameworks.<sup>12, 13</sup> Although, Table 1 focuses on the  $\epsilon$ -caprolactam synthesis, the

**TABLE 1** Heterogeneous catalytic Beckmann rearrangement for the production of  $\epsilon$ -caprolactam.



| Entry | Catalyst/conditions   | Yield (%) | Ref. |
|-------|---|-----------|------|
| 1     | H-PDVB-SO <sub>3</sub> H, PhCN, 130°C, 1 h  | 75        | 6    |
| 2     | GO-OSO <sub>3</sub> H@SiO <sub>2</sub> , MeCN, 60°C, 2 h                                    | 98        | 7    |
| 3     | [MIMPS] <sub>3</sub> PW <sub>12</sub> O <sub>40</sub> , ZnCl <sub>2</sub> , MeCN, 90°C, 1 h | 83        | 8    |
| 4     | Ti-montmorillonite, benzonitrile, 90°C, Ar, 20 h  | 74        | 9    |
| 5     | CNTs, benzonitrile, 130°C, 6 h  | 44        | 10   |
| 6     | SBA-ar-SO <sub>3</sub> H, chlorobenzene, 130°C, 24 h  | 42        | 11   |

H-PDVB-SO<sub>3</sub>H, sulfonated poly(divinyl)benzene; GO, graphene oxide; MIMPS, sulfonated imidazolium salt; CNT, carbon nanotubes; SBA-ar-SO<sub>3</sub>H, arenesulfonic acid functionalized SBA-15; SBA, Santa Barbara Amorphous, a mesoporous silicate.

applied catalysts and conditions were found useful for generic application with broad substrate scope.

Sulfonated polymeric solid acid (H-PDVB-SO<sub>3</sub>H) was applied as a catalyst to a liquid phase Beckmann rearrangement of cyclohexanone oxime (Table 1, entry 1).<sup>6</sup> The catalyst was prepared by a copolymerization step of divinylbenzene with sodium *p*-styrene sulfonate under solvothermal condition followed by a protonation step via ion-exchange.  $\epsilon$ -Caprolactam was obtained with 75% yield in one hour at 130°C. The catalytic system could be applied to various other substrates demonstrating broad substrate scope. In addition, the catalyst showed good recyclability. Another sulfonated catalytic material, sulfonated graphene oxide coated by SiO<sub>2</sub>, demonstrated high yield and selectivity for the same reaction in 2 h at milder temperature than the sulfonated polymeric solid acid-based system (60°C vs 130°C) (Table 1, entry 2).<sup>7</sup> The mesoporous SiO<sub>2</sub> layer improved the separation of the GO-OSO<sub>3</sub>H catalyst from the reaction mixture. As a result, the catalyst could be recovered and reused with a slight decrease in yield from 98% to 90% after the sixth run.

Zhang et al. described the synthesis of amides from ketoximes catalyzed by a sulfonated imidazolium salt of phosphotungstate in the presence of zinc chloride (Table 1, entry 3).<sup>8</sup> The catalyst (10 mol%) which was combined to 30 mol% of ZnCl<sub>2</sub> converted cyclohexanone oxime to  $\epsilon$ -caprolactam and other aromatic oximes to the amide product in high yields within 1 h at 90°C in acetonitrile. Despite a successful recovery and reuse of the catalyst, the catalytic

system cannot be considered fully recyclable as the co-catalyst, zinc chloride, accounts for the waste generated.

Titanium cation-exchanged montmorillonite-catalyzed Beckmann rearrangement is a different approach offering several advantages including a wide substrate scope (aromatic, aliphatic, and alicyclic ketoximes), mild reaction conditions, good to high yields, and catalyst recyclability (Table 1, entry 4).<sup>9</sup> As an example,  $\epsilon$ -caprolactam was obtained in 74% yield in 20 h at 90°C. It should be noted that the reactions were performed under argon atmosphere and that the reaction time range was from a few hours to 20 h.

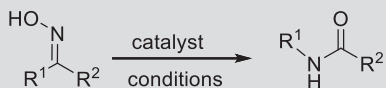
Carbon nanotubes treated with concentrated HNO<sub>3</sub> also demonstrated activity in the conversion of cyclohexanone oxime to  $\epsilon$ -caprolactam. Characterization studies revealed, as expected, that the conversion followed a linear correlation with the number of acidic sites. The maximum conversion reached was 44% after 6 h at 130°C (Table 1, entry 5).<sup>10</sup> Regarding the environmental impact, in addition to a high temperature of reaction and the use of the organic solvent benzonitrile, the recyclability of the carbon nanotubes was not studied.

Arenesulfonic acid functionalized SBA-15 (SBA-ar-SO<sub>3</sub>H) was also evaluated as a catalyst for the Beckmann rearrangement of cyclohexanone oxime (Table 1, entry 6).<sup>11</sup> The catalyst was synthesized via the co-condensation of 2-(4-chlorosulfonylphenyl)ethyltrimethoxysilane and tetraethyl orthosilicate. Different loadings of the acid were tested; both the conversion and selectivity to  $\epsilon$ -caprolactam were found to increase with the loading of arene-SO<sub>3</sub>H groups. The comparison of catalytic activity of SBA-ar-SO<sub>3</sub>H with H-ZSM-5, Al-MCM-41 and Al-SBA-15 among other mesoporous materials showed that SBA-ar-SO<sub>3</sub>H achieves superior results, although the use of chlorobenzene as a solvent, the high temperature, and the long reaction time increases the environmental impact of the protocol.

The Beckmann rearrangement of aldoximes/ketoximes has emerged as an alternative to the conventional, lower-atom economy approach employing carboxylic acids and amines to produce amides.<sup>14, 15</sup> Amides in conjugation with aromatic or heterocyclic rings are particularly relevant in the pharmaceutical industry due to the various biological activities they exhibit.<sup>3, 16, 17</sup> These applications are illustrated by several examples in Table 2.

Copper complex-functionalized magnetic core-shell nanoparticles (Fe<sub>3</sub>O<sub>4</sub>@SiO<sub>2</sub>-Lig-Cu) were developed to catalyze the Beckmann rearrangement of aldoximes to amides in an attempt to eliminate the need for catalyst filtration while taking advantage of the high-catalytic activity of metal nanoparticles (Table 2, entry 1).<sup>18</sup> The reaction was performed under mild conditions in short times using PEG as a green reaction medium. High yields of products especially for heteroaromatic amides were obtained and the compatibility of the catalyst towards a wide range of functional groups was demonstrated. The magnetic properties of the catalyst were successfully utilized to foster the recyclability of the catalyst, further improving the eco-friendly potential of the approach. KarimKoshteh and Bagheri reported a similar method employing nano Fe<sub>3</sub>O<sub>4</sub>

**TABLE 2** Heterogeneous catalytic Beckmann rearrangement of aldoximes and ketoximes.



| Entry | Substrate   | Catalyst/conditions  | Yield (%)                                      | Ref. |
|-------|---|--|--|------|
| 1     | R <sup>1</sup> , R <sup>2</sup> =CH <sub>3</sub> , aryl | Fe <sub>3</sub> O <sub>4</sub> @SiO <sub>2</sub> -Lig-Cu, PEG, 80°C, 1 h                 | 40–95  | 18   |
| 2     | R <sup>1</sup> =H, R <sup>2</sup> =aryl                 | Nano-Fe <sub>3</sub> O <sub>4</sub> , ultrasonic irradiation/H <sub>2</sub> O, 35–50 min | 95–98  | 19   |
| 3     | R <sup>1</sup> , R <sup>2</sup> =aryl                   | Ir(ppy) <sub>2</sub> (PDVB-py), DMF, MeCN, Ar, CBr <sub>4</sub> , 3W Blue LED            | 75–95  | 20   |
| 4     | 4-Hydroxyacetophenone oxime                             | Tungstated zirconia nanocatalysts, benzonitrile, 12 h, 130°C                             | 90   | 21   |
| 5     | R <sup>1</sup> =H, R <sup>2</sup> =aryl                 | GO-CoPPh, toluene, 80°C, 85–180 min  | 79–90  | 22   |
| 6     | R <sup>1</sup> =H, R <sup>2</sup> =aryl or sugar oximes | MoO <sub>3</sub> /SiO <sub>2</sub> , refluxing ethanol, 18 h                             | 70–97  | 23   |
| 7     | Benzaldoxime<br>4-Methoxybenzaldoxime                   | KFAU-Y, benzene-acetonitrile (1:1), 200°C, 2 h   | 91–99<br>98 (selectivity 36 towards the amide) | 24   |

Fe<sub>3</sub>O<sub>4</sub>@SiO<sub>2</sub>-Lig-Cu, copper complex-functionalized magnetic core-shell nanoparticles; PDVB-py, vinylpyridine-divinylbenzene copolymer; GO-CoPPh, cobalt(II) porphyrin covalently linked to graphene oxide.

under ultrasonic irradiation (Table 2, entry 2).<sup>19</sup> Advantages of the method also include easy work-up procedure, high yields of secondary amides, mild reaction conditions, and good recyclability of the magnetic nanoparticles. It should be stressed, however, that in this example, the catalyst loading was significantly higher than the one reported in the example using the above copper complex-based catalyst (0.5 equivalent cat/substrate vs 4 mol%).

Another interesting approach to produce amides employs an immobilized iridium complex photocatalyst Ir(ppy)<sub>2</sub>(PDVB-py), synthesized by immobilization of the iridium complex onto the nanoporous vinylpyridine-divinylbenzene copolymer (PDVB-py) (Table 2, entry 3).<sup>20</sup> Similarly to the above examples, high yields were obtained for a wide range of substrates (ketoximes) and the catalyst could be recycled in up to five consecutive cycles with minor loss of activity. However, unlike the first two examples employing green reaction conditions, these reactions were performed in an organic solvent, acetonitrile, in presence of an excess amount of CBr<sub>4</sub> and using a blue LED for 12 h to activate the catalyst.

An efficient heterogeneous catalytic process for the production of nonsteroidal anti inflammatory drugs was reported as an environmentally friendly alternative to the conventional homogeneous processes.<sup>25</sup> High yields of *N*-acetyl-*p*-aminophenol (paracetamol) was achieved at 130°C in 12 h in the presence of tungstated zirconia nanocatalysts (Table 2, entry 4).<sup>21</sup> The study revealed a correlation between the nanostructure and catalytic activity suggesting that the Brønsted acid sites of the catalyst are highly active even at mild temperatures.

Ghadamyari et al. reported a cobalt(II) porphyrin complex covalently linked to graphene oxide as a nano heterogeneous catalyst (GO-CoPPh) for the conversion of aldoximes to primary amides via Beckmann rearrangement (Table 2, entry 5).<sup>22</sup> The yields achieved ranged from 79% to 90% in less than 2 h in toluene. The proposed catalyst was recycled in five consecutive cycles with a slight loss of activity.

A comparative study demonstrated that silica-supported molybdenum(VI) oxide achieves similar results as beta-zeolite as a solid acid catalyst for the Beckmann rearrangement (Table 2, entry 6).<sup>23</sup> Both catalysts were found to facilitate the rearrangement of a wide range of sugar-derived ketoximes after refluxing the reaction mixture in ethanol for 18 h. A notable advantage of the method lies in the fact that commonly employed protecting groups in carbohydrate chemistry, such as isopropylidene and cyclohexylidene systems and benzyl ethers were found to be stable under the conditions employed.

Thomas et al. described that the dehydration/Beckman rearrangement reaction of benzaldoxime and 4-methoxybenzaldoxime could be catalyzed by rare earth metal ion exchanged (La<sup>3+</sup>, Ce<sup>3+</sup>, Re<sup>3+</sup>) KFAU-Y zeolites (Table 2, entry 7).<sup>24</sup> The catalyst was prepared by simple ion-exchange methods and characterized using different physico-chemical techniques revealing its acidic character, structural properties, surface area, and pore volume. The activity and selectivity of these rare-earth metal-exchanged zeolite

catalysts were compared to that of K-10 clay and silica for two substrates. Although 4-methoxybenzaldoxime was converted to the expected Beckmann rearrangement- (4-methoxyphenylformamide) and dehydration products (4-methoxybenzotrile) in high overall yields and with a selectivity that favored the nitrile formation on all catalysts, benzaldoxime was converted almost quantitatively to benzonitrile. The method is of industrial relevance because it could be performed in a continuous flow reactor at 200°C. It was however observed that the catalysts underwent rapid deactivation due to the neutralization of the acid sites with basic reactants and products.

### 3.9.1.2 Fries rearrangement

The Fries rearrangement transforms esters of aromatic hydroxyl compounds (phenols, naphthols, etc.) to aromatic ketones or other valuable intermediates for the synthesis of various specialty chemicals and pharmaceuticals.<sup>26</sup> The starting material, the ester, interacts with an acid catalyst to generate an acylium ion intermediates. Current industrial processes require a stoichiometric amount of Lewis acids (e.g.,  $\text{AlCl}_3$ ) or mineral acids as catalysts, generating significant amount of hazardous waste.<sup>27, 28</sup> Similar to typical Friedel-Crafts reactions, zeolites were among the first solid acid catalysts to be explored as an alternative to conventional homogeneous systems in an effort to reduce the environmental impact of the reaction. Mesoporous silica, heteropoly acids and acidic ion-exchange resins were also proposed as heterogenous catalysts for the Fries rearrangement.

Van Grieken et al. showed that the presence of a phenyl group close to the sulfonic acid group significantly increases the acid strength of modified mesoporous silica SBA-15 consequently enhancing the catalytic activity of the material for the Fries rearrangement (Table 3, entry 1).<sup>29</sup> As a result, the arene-sulfonic acid modified mesostructured SBA-15 successfully converted phenyl acetate to the most desired product hydroxyacetophenones (HAP). Because phenol is obtained as a by-product during the reaction, the presence of an initial amount of phenol favors the production of HAP. Interestingly, while the catalyst rapidly deactivated due to the adsorption of reaction products and/or the formation of carbonaceous deposits on the sulfonic acid sites, using dichloromethane as a solvent significantly reduced the deactivation process suggesting an easy regeneration of the catalyst, although with an undesirable solvent.

Heteropoly acids such as  $\text{H}_3\text{PW}_{12}\text{O}_{40}$  catalyzed the Fries rearrangement of aryl esters (phenyl acetate, phenyl benzoate, and *p*-tolyl acetate) to yield the acylated phenols and esters together with phenols in heterogeneous or homogeneous systems at 100–170°C (Table 3, entry 2).<sup>30, 31</sup> In the heterogeneous system, nonpolar solvents such as dodecane were employed and the heteropolyacid was preferably supported on silica allowing the recovery and reuse of the catalytic material. Although the heteropolyacid were found to be two orders of magnitude

**TABLE 3** Heterogeneous catalytic Fries rearrangements.

| Entry | Catalyst/conditions   | Yield (%)   | Ref.   |
|-------|---|---|--------|
| 1     | Arenesulfonic modified mesostructured SBA-15, dichloromethane, 100–170°C, 25 h                      | 10 (HAP)  | 29     |
| 2     | H <sub>3</sub> PW <sub>12</sub> O <sub>40</sub> , benzonitrile, 150°C, 2 h                          | 45 conversion<br>12 and 24 selectivity for 2HAP and 4HAP respectively | 30, 31 |
| 3     | Nafion-H, Nafion-H/SiO <sub>2</sub> , and Nafion-H silica nanocomposite, nitrobenzene, 220°C, 1–2 h | 45–54 conversion with up to 100 selectivity for 4HAP                  | 32     |

SBA, Santa Barbara Amorphous, a mesoporous silica.

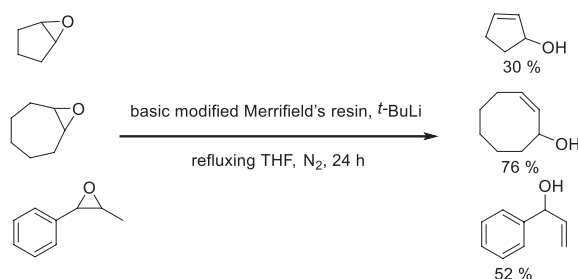
more active than H-beta zeolite, the conversion still remained under 20% and the reaction afforded four different products with rather poor selectivity.

The application of Nafion-H-based catalysts in the Fries rearrangement has been reported by Török et al. This superacidic ion exchange resin was used in its commercially available bead form and also in a simple silica-immobilized sample and as a Nafion-H silica nanocomposite. The nanocomposite showed the best performance in the reaction, resulting in significantly better conversions (up to 54%) than the catalysts in the above two examples with up to 100% selectivity for the 4HAP product.<sup>32</sup> Although the reaction is one of the best performing heterogeneous catalytic process for the Fries rearrangement, the use of the high temperature and the solvent nitrobenzene increase the environmental impact of the protocol.

### 3.9.1.3 Epoxide rearrangements

Due to the high reactivity of epoxides, they are prone to rearrangements producing various organic compounds. The production of allylic alcohols occurring

via both  $\alpha$ - or  $\beta$ -deprotonation processes is a typical example. While several homogeneous catalysts can successfully facilitate the reaction, the use of heterogeneous catalysts are preferred from an environmental point of view. Basic resins, prepared from Merrifield's resin and containing secondary amine groups were reported as efficient and selective catalysts for the synthesis of allylic alcohols (Scheme 1).<sup>33</sup> Although the resin could be regenerated and reused, the yield of reaction remained moderate and the addition of *tert*-butyllithium to the resin was required prior use.



**SCHEME 1** Synthesis of allyl alcohols via epoxide rearrangement catalyzed by a modified Merrifield's resin.

The rearrangement of  $\beta$ -pinene epoxide into myrtanal is a second example of epoxide rearrangement. Historically, myrtanal has been isolated from natural products such as the roots of Greek *Paeonia taxa* and used as antiseptic. Synthetically it can be obtained from  $\beta$ -pinene oxide in moderate yield using solid catalysts such as aluminum oxides. More recently, both grafted zeolites<sup>34</sup> and MOFs<sup>35</sup> were successfully employed as heterogeneous catalysts for the transformation. The results are presented in Table 4. Different metals

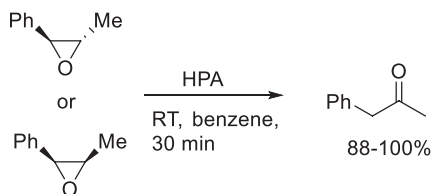
**TABLE 4** Heterogeneous catalytic rearrangement of  $\beta$ -pinene epoxide into myrtanal.

| Entry | Catalyst/conditions                    | Conversion (selectivity) (%) | Ref. |
|-------|--|------------------------------|------|
| 1     | Zr-Beta, acetonitrile, 56°C, 120 min   | 99 (83)                      | 34   |
| 2     | ZrO-MCM41, acetonitrile, 80°C, 120 min | 98 (94)                      | 35   |

were incorporated into the network of zeolite beta by isomorphous substitution (Table 4, entry 1).<sup>34</sup> After optimization of the reaction conditions, it was found that Zr-Beta in acetonitrile provided an optimum selectivity/activity balance. The zeolite was robust enough to be employed both in batch mode and in fixed-bed fashion for several times without leaching.

Corma et al. studied and compared the activity of different zirconium Lewis acid sites grafted onto a mesoporous silicate (MCM-41) and zirconium sites incorporated into inorganic-organic MOF materials for the present reaction (Table 4, entry 2).<sup>35</sup> Zirconium oxynitrate grafted onto MCM-41 was found to provide the highest catalytic activity and selectivity towards myrtanal and it was also recyclable in five consecutive cycles with minor loss of activity.

A similar epoxide rearrangement of stereoisomeric 2-methyl-3-phenyloxiranes was reported using a variety of heteropolyacids (Scheme 2).<sup>36,37</sup> Four commercially available heteropoly acids of Keggin structure were applied, and H<sub>3</sub>[PW<sub>12</sub>O<sub>40</sub>] was found to exhibit the best performance resulting in 100% yield and 100% selectivity for the formation of the appropriate methyl ketone from both the *cis* and *trans*-epoxide. Although the high yield, exclusive selectivity and mild conditions describe a green reaction, the application of benzene as a solvent should be avoided as much as possible.



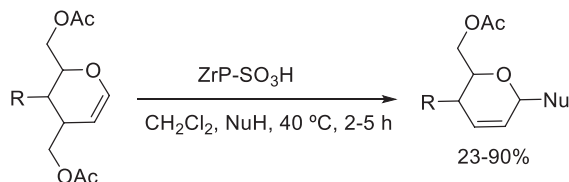
**SCHEME 2** Heteropoly acid (HPA)-catalyzed rearrangement of stereoisomeric 2-methyl-3-phenyloxiranes.

Although not strictly an epoxide rearrangement, it is worth mentioning a similar reaction of another cyclic, oxygen containing compound. The selective hydrogenation and rearrangement of a potentially biosourced and thus sustainable 5-hydroxymethylfurfural (5-HMF) to 3-hydroxymethyl-cyclopentanone (HCPN) was achieved by Zhang et al. using MOF-derived bimetallic nickel-copper catalyst in aqueous medium.<sup>38</sup> The authors reported that the combination of nickel and copper significantly enhanced the reaction providing nearly quantitative yield (>99%) for the rearrangement products.

### 3.9.1.4 Ferrier rearrangement

The transformation of glycals (1,2-unsaturated cyclic carbohydrate derivatives) into 2,3-unsaturated glycosyl derivatives, the so called “Ferrier rearrangement”, is a well-established reaction with many applications in the fields of

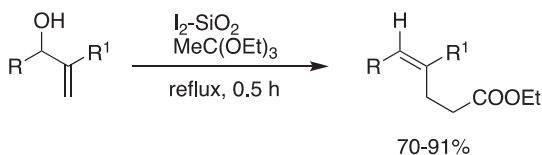
carbohydrate and organic chemistry.<sup>39</sup> Layered  $\alpha$ -zirconium sulfophenylphosphonate methanphosphonate was shown to catalyze the synthesis of Ferrier rearrangement products starting from glycols under mild reaction conditions in short time and good yields (Scheme 3).<sup>39</sup> Interestingly, it was observed that combining the heterogeneous catalyst with lithium bromide changed the regioselectivity of the process affording 2-deoxy sugars in good yields.



**SCHEME 3** Ferrier rearrangement of glycols to 2,3-unsaturated glycosyl derivatives catalyzed by layered  $\alpha$ -zirconium sulfophenylphosphonate methanphosphonate.

### 3.9.1.5 Johnson-Claisen rearrangement

The Claisen rearrangement is a carbon-carbon bond-forming intramolecular reaction occurring with an allyl vinyl ether to form a  $\gamma,\delta$ -unsaturated carbonyl compounds.  $I_2$ - $SiO_2$  was shown to efficiently catalyze the stereoselective conversions of the Baylis-Hillman adducts to ethyl alk-4-enoates via the Johnson-Claisen rearrangement by treatment with triethyl orthoacetate (Scheme 4).<sup>40</sup>

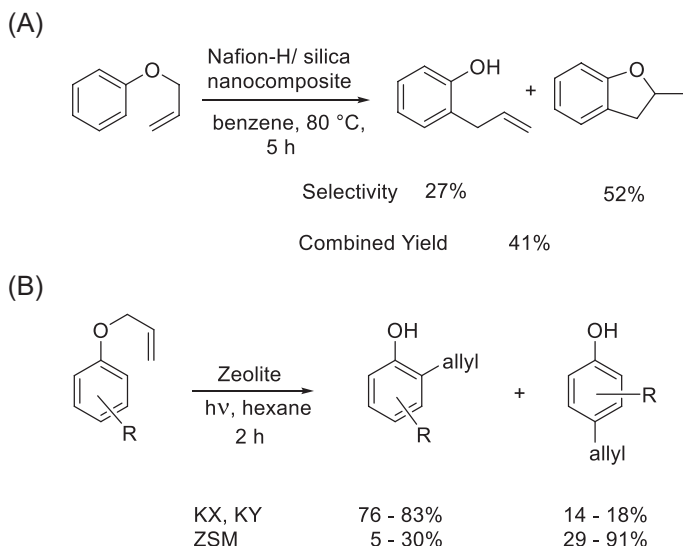


**SCHEME 4** Synthesis of ethyl alk-4-enoates from the Baylis-Hillman adducts via the Johnson-Claisen rearrangement catalyzed by  $I_2$ - $SiO_2$ .

### 3.9.1.6 The *ortho*-Claisen-rearrangement

This rearrangement is a 1,3 O  $\rightarrow$  C shift of the allyl group of phenol-allyl ethers from the phenolic O to the aromatic ring. It is an intramolecular transalkylation that can be applied for the preparation of 2-allyl-phenols.<sup>41</sup> Solid acids such as zeolites, or Nafion-H silica nanocomposite are the most common catalysts for the reaction.<sup>32,42</sup> The rearrangement favors the formation of 2-allylphenol only at low conversions; at higher conversions an intramolecular cyclization to 2-methyldihydrobenzofuran becomes the major product (Scheme 5A). In addition to this work, acidic Cs salts of phosphotungstic acid ( $H_{0.5}Cs_{2.5}[PW_{12}O_{40}]$ ) and its silica or MCM-41 supported forms were also reported to catalyze the Claisen-rearrangement.<sup>43</sup> X, Y, ZSM-5, and ZSM-11 zeolites also can initiate a photochemically activated

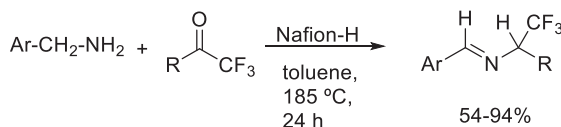
Claisen-rearrangement and result in the formation of allyl phenols (Scheme 5B). Some zeolites (KX, KY) resulted in 2-selectivity. In contrast, ZSM-5 zeolite favors the 4-isomer based on the shape selective character of ZSM-5.<sup>44</sup>



**SCHEME 5** The *ortho*-Claisen rearrangement of phenol-allyl ethers catalyzed by Nafion-H silica nanocomposite (A) and zeolites (B).

### 3.9.1.7 Benzylimine-benzaldimine rearrangement

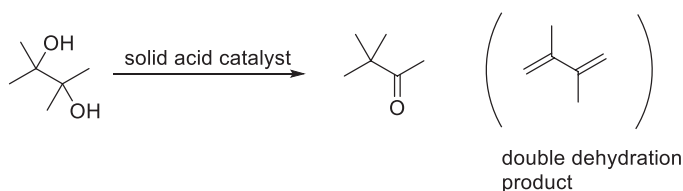
Prakash et al. reported the Nafion-H-catalyzed rearrangement of benzylimines to the corresponding benzaldimines as a convenient, simple, and effective pathway for the synthesis of fluorinated benzaldimines (Scheme 6).<sup>45</sup> The reaction conditions were extensively optimized, including the application of microwave irradiation and flow chemistry. These technologies are becoming widely applied in heterogeneous catalytic reactions.<sup>46, 47</sup> The authors described that the appropriate selection of the reaction temperature ensured that after the simple condensation the rearrangement occurred efficiently, making the aldimine the major product: at 164°C the benzylimine, and at elevated temperature (185°C) the aldimine was obtained as major product in moderate to excellent yields.



**SCHEME 6** Nafion-H-catalyzed synthesis benzaldimines from trifluoromethylketones and benzylamines.

### 3.9.1.8 Pinacol rearrangement

The pinacol rearrangement<sup>48</sup> is one of the oldest known rearrangements described first by Fittig in 1860.<sup>49</sup> The reaction has generated significant attention over time. A recent review provides an extensive summary of the developments from the early discovery to contemporary applications.<sup>50</sup> The shift in application of mineral acids toward environmentally more compatible solid acids initiated development in the heterogeneous catalytic applications of the pinacol rearrangement (Scheme 7).<sup>51,52</sup>



**SCHEME 7** A general scheme of the pinacol rearrangement.

The reaction can be catalyzed by a broad range of solid acids from heteropoly acids (HPAs),<sup>36,37,53,54</sup> pillared clays,<sup>55</sup> zeolites,<sup>56</sup> microporous polysilsesquioxanes,<sup>57</sup> silica-supported Lewis acids,<sup>58</sup> or cordierite supported Mo(VI)/ZrO<sub>2</sub>.<sup>59</sup> In general, several 1,2-diols, such as 2,3-butanediol, or hydrobenzoin undergo a pinacol style rearrangement to produce ketones or aldehydes.<sup>37</sup> Based on the reports it appears that increasing acid strength favors the pinacol rearrangement, in contrast to somewhat weaker acids that produce a product mixture with the diene as a major product.<sup>37,55</sup>

### 3.9.1.9 Baeyer-Villiger oxidation

Finally, we mention the Baeyer-Villiger oxidation that is an oxidative rearrangement of ketones or aldehydes to esters. Traditionally organic peracids were used as oxidizing agents. More contemporary applications consider other oxidizing agents that are greener and possess significantly higher atom economy, such as O<sub>2</sub>, H<sub>2</sub>O<sub>2</sub>, or organic alkyl hydroperoxides.<sup>60-62</sup> Conventionally, the process used stoichiometric reagents, and later homogeneous and heterogeneous catalytic approaches were introduced as well.<sup>63</sup> Several representative heterogeneous catalytic protocols are highlighted in Table 5.

Table 5 indicates that the Baeyer-Villiger oxidation can be catalyzed by a wide variety of catalysts. These catalysts range from complexes supported on magnetic particles (Table 5 entry 1), organic assemblies supported by sustainable materials, such as chitin (Table 5 entry 2), silica-supported, moisture stable gallium triflate (Table 5 entry 3), tin immobilized on mesoporous silica (Table 5 entry 4), a variety of zeolites doped with vanadium or tin (Table 5 entry 5), an enzyme immobilized on multiwalled carbon nanotubes (Table 5 entry 6), ion-

**TABLE 5** Heterogeneous catalytic Baeyer-Villiger oxidations.



| Entry | Substrate                                      | Catalyst/conditions  | Yield (%)                                  | Ref.      |
|-------|--|--|--|-----------|
| 1     | Substituted cycloalkyl ketones                 | CoTaPc-Fe <sub>3</sub> O <sub>4</sub> /CTO, benzaldehyde, DCE, O <sub>2</sub> , 15°C, 12 h   | 22–96 (conversion)<br>selectivity > 99     | 64        |
| 2     | Cyclic and bicyclic ketones,<br>2-adamantanone | Supramolecular flavinium assemblies immobilized on sulfated chitin, 30% H <sub>2</sub> O <sub>2</sub> , tBuOH, 25–70°C, 3–24 h                                       | 72–97                                      | 65        |
| 3     | 2-Adamantanone                                 | Ga(OTf) <sub>3</sub> -SiO <sub>2</sub> , 60% aq. H <sub>2</sub> O <sub>2</sub> , 70°C, 1 h   | 70–94 recyclable cat.                      | 66        |
| 4     | 2-Adamantanone                                 | Sn-MesoSB, 35% aq. H <sub>2</sub> O <sub>2</sub> , 3 h, 90°C   | 92–99                                      | 67        |
| 5     | Cyclopentanone, cyclohexanone                  | VO(L)H <sub>2</sub> O]-Y zeolites or FAU type stannosilicate or [Sn(salen)] <sup>2+</sup> exchanged NaY, 30% aq. H <sub>2</sub> O <sub>2</sub> or MeCN, 6–12 h, 70°C | 42–80                                      | 22, 68–72 |
| 6     | Substituted cycloalkyl ketones                 | CALB immobilized on multiwalled carbon nanotubes, 30% aq. H <sub>2</sub> O <sub>2</sub> , toluene, 30°C 1–20 h   | 91–99                                      | 73        |
| 7     | Cyclic ketones, heterocyclic methyl ketones    | Magnesium-aluminium hydroxalcite, 30% aq. H <sub>2</sub> O <sub>2</sub> , 70°C, 6 h  | 64–100 (conversion),<br>selectivity 54–100 | 74        |

CoTaPc-Fe<sub>3</sub>O<sub>4</sub>/CTO, cobalt-tetraamide-phthalocyanine (CoTaPc) immobilized onto magnetic Fe<sub>3</sub>O<sub>4</sub> chitosan microspheres (Fe<sub>3</sub>O<sub>4</sub>/CTO); DCE, dichloroethane; Sn-MesoSB, tin-containing mesoporous silica beads; VO(L)H<sub>2</sub>O]-Y zeolite, vanadium exchanged Y zeolite with Schiff base ligands; CALB, *Candida antarctica* lipase B.

exchanged hydrotalcite (Table 5 entry 7), with other materials such as multi-SO<sub>3</sub>H functionalized heteropolyanion-based ionic hybrids<sup>75</sup> or a sulfonated Schiff base-dimethyltin(IV) coordination polymer<sup>76</sup>: Except one case (Table 5 entry 1) when oxygen was used as the oxidant, hydrogen peroxide was the common oxidative reagent used. Although, oxygen from air is the greenest and most economic oxidizing agent, hydrogen peroxide also fulfills most green requirements, for example, the only byproduct is water. Although most reactions proceed with moderate to excellent yields and generally high selectivities, in most papers cycloheptanone, where it was investigated, appears to react very sluggishly, the yields for this substrate rarely reach 10%. The authors commonly note this fact, but do not comment on the reasons behind this phenomenon. In addition, most cases use truly green conditions, although occasionally some inappropriate components are also parts of the protocols. For instance, toluene, acetonitrile or dichloroethane are not green solvents and should be avoided whenever possible. It also appears that the activity of the catalysts was satisfactory and most reactions took place at ambient temperature. Even the highest reaction temperature does not exceed 90°C. Overall, the heterogeneous catalytic methods are reasonable choices to replace the traditional reagent-based protocols.

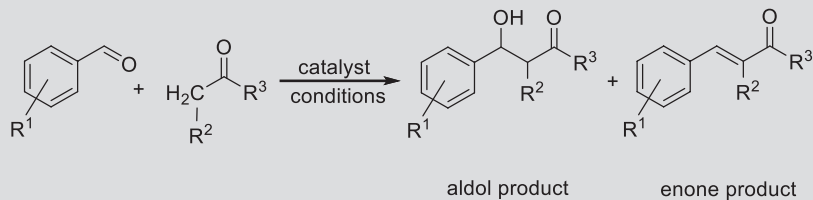
### 3.9.2. Aldol and related reactions

#### 3.9.2.1 The aldol reaction

The aldol reaction and related transformations are among the most important C–C bond forming reactions. Being a well-known reaction, many catalytic methods have been reported to carry out these reactions in nonchiral as well as in an enantioselective way.<sup>77, 78</sup> A large variety of heterogeneous catalytic systems have been used to catalyze the aldol reaction as listed below. The most common reaction is the reaction of substituted benzaldehydes with acetone or simple ketones. Representative reactions are tabulated in Table 6.

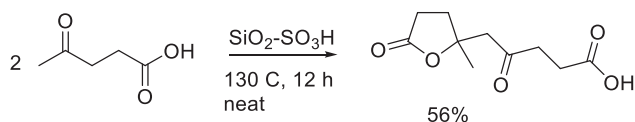
Amarasekara et al. developed the solid acid catalyzed aldol dimerization of levulinic acid for the preparation of C10 renewable fuel and chemical feedstock.<sup>83</sup> The authors investigated the solid acid-catalyzed condensation of levulinic acid applying several solid acid catalysts: Amberlyst-15, SiO<sub>2</sub>-SO<sub>3</sub>H, Dowex50WX8, Carbon-SO<sub>3</sub>H, TiO<sub>2</sub>-SO<sub>3</sub>H, Al<sub>2</sub>O<sub>3</sub>-SO<sub>3</sub>H, H<sub>3</sub>PW<sub>12</sub>O<sub>40</sub>, and Nb<sub>2</sub>O<sub>5</sub>·H<sub>2</sub>O under neat conditions at 110–130°C. Tetrahydro-2-methyl-5,γ-dioxo-2-furanpentanoic acid was reported as the major dimerization product of the reaction (Scheme 8). SiO<sub>2</sub>-SO<sub>3</sub>H provided the highest yield of the desired product. In a similar application, Ga<sub>2</sub>O<sub>3</sub>-doped sulfonated tin oxides or sulfated zirconia were applied for the aldol reaction of prenal and prenil for the synthesis of citral.<sup>84</sup>

**TABLE 6** Heterogeneous catalytic aldol reaction of benzaldehydes with simple ketones and related compounds.



| Entry | Other substrate        | Catalyst/conditions                                  | Product | Yield (%)                              | Ref. |
|-------|------------------------|--|---------|--|------|
| 1     | Acetone                | TMG/GO, 30°C, 1 h                                    |         | 27–99 high aldol selectivity           | 79   |
| 2     | Cyclohexanone          | Supramolecular hydrogel, toluene, 5–25°C, 1 h        |         | 98–99 up to 97:3 = anti:syn ratio      | 80   |
| 3     | Acetone                | MCM-41-bound secondary amines, acetone, 50°C, 6–20 h |         | 5–97                                   | 81   |
| 4     | Methyl isocyanoacetate | Cu-network catalyst, THF, Ar atmosphere, 25°C, 1–6 h |         | 95–99 (both <i>cis/trans</i> products) | 82   |

TMG/GO, 1,1,3,3-tetramethylguanidine on graphene oxide.



**SCHEME 8** Solid acid-catalyzed dimerization of levulinic acid to tetrahydro-2-methyl-5,γ-dioxo-2-furanpentanoic acid.

In addition to solid acids, solid-base catalysts are also applicable for the aldol reaction via optimizing the surface density and base strength of the amino groups immobilized on nanoporous silica.<sup>81</sup>

### 3.9.2.2 Mukaiyama reaction

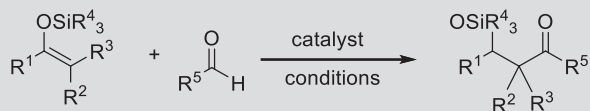
The Mukaiyama reaction, a type of aldol reaction between a silyl enol ether and an aldehyde or formate, emerged as an efficient and stereoselective strategy to produce β-hydroxyketones. In the last decades, catalytic Mukaiyama aldol reactions were developed especially with lanthanides or rare earth salts as catalysts. Heterogeneous catalysis was applied with the aim to further improve the environmental friendliness of these aldol reactions. Mesoporous materials with Lewis and Brønsted acid sites were employed for this purpose. Modified zeolites,<sup>85</sup> SBA-15,<sup>86</sup> MCM-41<sup>87, 88</sup> and sulfated zirconia<sup>89</sup> or Sn-exchanged montmorillonite<sup>90</sup> proved to be efficient heterogeneous catalysts for the synthesis of aldols via the Mukaiyama reaction (Table 7). They all exhibited the ability to convert a wide scope of substrates with good tolerance towards multiple functional groups. It should be noted that the MCM-41-catalyzed reaction did afford lower yields of aldol from acetals than from aldehydes. The recyclability of all catalysts, except the sulfated zirconia, was investigated and conclusive: they were recyclable for several cycles without loss of activity.

### 3.9.3. Condensations

#### 3.9.3.1 Schiff-base formation

Condensation reactions are common transformations for the development of C=C or C=N-bonds.<sup>91</sup> Although several types of reactions are included in this group, the most basic reaction is the formation of C=N bonds or compounds traditionally called Schiff-bases.<sup>92</sup> Schiff-bases are important compounds in many applications, from biological processes to flavoring agents.<sup>93, 94</sup> The reaction is an acid-catalyzed process, although there are reports on the reaction occurring with some substrates under catalyst-free conditions, particularly in multistep domino protocols when the Schiff-base would immediately undergo a secondary transformation.<sup>95, 96</sup> A large number of solid acids, including clays, zeolites, ion exchange resins, metal-organic frameworks,<sup>97, 98</sup> or sulfated metal oxides<sup>99</sup> have been applied in this procedure and Table 8 only includes a few representative examples.

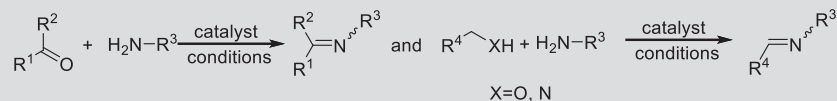
**TABLE 7** Heterogeneous catalytic Mukaiyama aldol reactions.

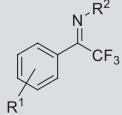
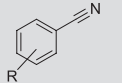
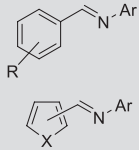
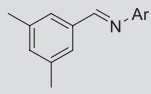
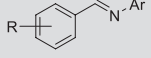


| Entry | Reactants  | Catalyst/conditions   | Yield (%) | Ref.                                    |
|-------|--|---|-----------|---|
| 1     | 1-Methoxy-2-methyl-1-trimethylsilyloxypropene with aromatic or aliphatic aldehydes | 1,5,7-Triazabicyclo[4.4.0]dec-5-ene-functionalized SBA-15, solvent-free, 12 h | 47–85     | <a href="#">86</a>                      |
| 2     | Various silyl enol ethers, benzaldehyde  | Sc <sup>III</sup> -zeolite, CH <sub>2</sub> Cl <sub>2</sub> , RT, 15 h        | 56–99     | <a href="#">85</a>                      |
| 3     | 1-Trimethylsilyloxy-1-cyclohexene with various aldehydes                           | Sulfated zirconia, CH <sub>2</sub> Cl <sub>2</sub> , RT, 36 h                 | 54–96     | <a href="#">89</a>                      |
| 4     | Various aliphatic carbonyl with silyl enolates                                     | Al-MCM-41, CH <sub>2</sub> Cl <sub>2</sub> , 0°C or 30°C, 3 h                 | 18–99     | <a href="#">87</a> , <a href="#">88</a> |
| 5     | Methyl-aryl and dialkyl ketones, silyl enolates                                    | Sn-exchanged montmorillonite, CH <sub>2</sub> Cl <sub>2</sub> , 0°C, 3 h      | 55–97     | <a href="#">90</a>                      |

SBA, Santa Barbara Amorphous, a mesoporous silica.

**TABLE 8** Heterogeneous catalytic condensation of carbonyl compounds and in situ oxidized alcohols and amines with anilines and other primary amines.



| Entry | Ketone/amine   | Catalyst/conditions   | Product   | Yield (%)                                | Ref.        |
|-------|--|---|---|--|-------------|
| 1     | Trifluoromethyl ketones/primary amines (benzyl, alkyl)       | K-10, Nafion-H, solvent-free, 175°C, 45–60 min  |  | 53–95                                    | 45, 100     |
| 2     | Substituted benzaldehydes/hydroxylamine                      | Amberlite IR 120H, solvent-free, MW-120 W, 2–3 min  |  | 75–85 (the oxim dehydrates to nitril)    | 101         |
| 3     | Heteroaromatic primary alcohols and benzyl alcohols/anilines | Cu-MOF, or Cu-MOF/Au-Pd composite, TBHP, solvent-free, 40°C, 1.45–2 h<br>γ-Al <sub>2</sub> O <sub>3</sub> -CeO <sub>2</sub> , flow reactor, 120–160°C<br>DVB-[MimLcy] <sub>n</sub> , TBHP, toluene, 120°C<br>Mesoporous Mn <sub>1</sub> Zr <sub>x</sub> O <sub>y</sub> , toluene, air, 120°C<br>CeO <sub>2</sub> , air, mesitylene, 30–100°C, 24–48 h |  | 38–98                                    | 98, 102–107 |
| 4     | Mesitylene/anilines  | (CuO <sub>x</sub> -CeO <sub>2</sub> ), air, 20°C, 24 h  |  | Low (4–10) yields but high selectivities | 108         |
| 5     | Benzyl amines  | K-10, solvent-free, or Cu-BTC (MOF-199) [copper(II)-benzene-1,3,5-tricarboxylate], Cu-chitosan beads, MW, 80–130°C, TBHP, 0.5–1.5 h   |  | 26–99                                    | 109–112     |

MOF, metal-organic framework; TBHP, *tert*butylhydroperoxide; DVB-[MimLcy]<sub>n</sub>, poly(divinyl-benzene)-based L-cysteine-paired ionic copolymer.

The K-10-catalyzed solvent-free microwave-assisted condensation of aryl trifluoromethyl ketones and different primary amines provided the corresponding trifluoromethyl imines (Table 8, entry 1) in good to excellent yields. The conditions are mostly green, except the high temperature (175°C). Even the reaction times (45–60 min), that are long by microwave standards, are a significant improvement to the traditional reaction that takes seven days at the same temperature. The catalyst could be reused without any loss of activity.<sup>100</sup> The method was successfully applied for the synthesis of chiral trifluoromethylamines via the diastereoselective hydrogenation/benzyl hydrogenolysis sequence.<sup>113</sup>

Another typical class of catalysts for the synthesis of Schiff-bases is the acidic ion exchange resins. The condensation of aryl aldehydes and hydroxylamine was successfully achieved by Varghese et al. using Amberlite IR 120H (Table 8 entry 2).<sup>101</sup> The reaction was carried out in a solvent-free manner and the products were obtained in high yields in only a few minutes reaction times. The catalyst was found recyclable four times with a negligible decrease in its activity. As another advantage, the protocol had excellent substrate tolerance. It should be noted that due to the application of hydroxyl amine in the condensation the product underwent a dehydration producing nitriles as final products.

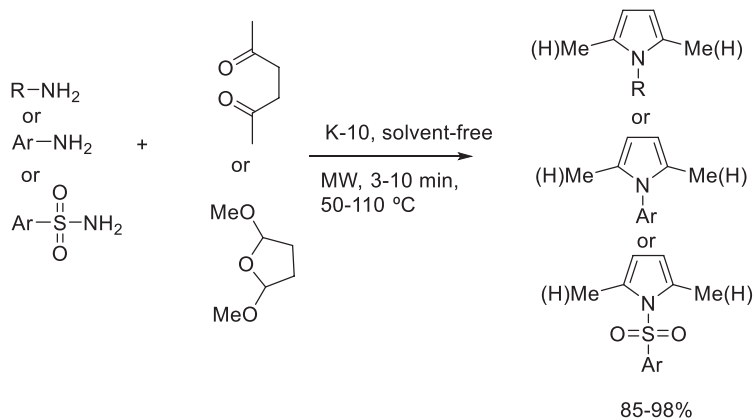
Beyond the traditional combination of carbonyl compounds with primary amines to produce imines, a contemporary trend extends the scope of substrates to alcohols, primarily to carbocyclic and heterocyclic benzyl-type alcohols (Table 8, entry 3). These alcohols first readily undergo an oxidation to the corresponding aldehyde, and then this aldehyde would react with the primary amine in a typical condensation reaction. Therefore, the catalysts that are applicable for this dual transformation must be bifunctional; they should be able to promote the oxidation as well as the condensation. A variety of catalysts were found to be excellent promoters of this two-step-one pot reaction, including metal-organic frameworks, mixed metal oxides or surface bound metal complexes. A very recent paper describes the application Au nanoparticles (NPs) dispersed on MIL-101 (Au/MIL-101) for the amine-alcohol oxidation-condensation reaction.<sup>114</sup>

In addition to the successive alcohol to aldehyde then condensation processes, the scope of the reaction has been extended to hydrocarbons as well. It is well-known, that aromatic hydrocarbons with an aryl ring-bound methylene group relatively easily undergo an oxidation on the benzylic CH positions. Tamura et al. described a similar reaction, using mesitylene in the presence of substituted anilines to generate imines (Table 8, entry 4).<sup>106</sup> The reaction was catalyzed by CuO<sub>x</sub>-CeO<sub>2</sub>, mixed oxide that was able to oxidize mesitylene to the corresponding benzaldehyde, which immediately underwent condensation with the anilines in low yields, but high selectivities.

The above idea, namely the combination of oxidation and condensation reactions could also be applied using benzylamines as well. Landge et al. successfully achieved the oxidative self-coupling of benzylamines to the corresponding

benzylidene benzylamines (Table 8, entry 5) by using a solvent-free K-10 montmorillonite-catalyzed microwave-assisted process.<sup>109</sup> It was suggested that in the first step the benzylamine underwent an oxidation to an unstable imine that immediately decomposed to benzaldehyde which reacted with the excess benzylamine in a condensation to form the imines. Based on this hypothesis the authors were able to extend the process to the oxidative coupling of benzylamines with anilines and aliphatic amines as well. Later the same group confirmed the mechanistic proposal by surface spectroscopy results.<sup>110</sup> To extend the number of suitable catalysts for this reaction, Venu et al. reported that copper-containing metal-organic frameworks were also able to catalyze this oxidation/condensation sequence of benzylamines and other amines to produce Schiff bases.<sup>111</sup>

In addition to the above processes when the imine formation results in the final product of the reaction, Török's group reported several multistep reactions, when the imine formation was only an intermediary step in the formation of several ring systems. In general, the reactions were based on the condensation of a  $\text{NH}_2$  group with a carbonyl or a carbonyl equivalent compound. Using the appropriate diketone or dimethoxy-tetrahydrofuran, the authors could achieve the synthesis of a broad variety of pyrrole derivatives, including *N*-alkyl-, *N*-aryl-, or *N*-sulfonyl pyrroles as well (Scheme 9).<sup>115-117</sup>



**SCHEME 9** Heterogeneous catalytic synthesis of pyrrole derivatives via the condensation and cyclization of amines/amides and carbonyl compounds.

The same idea and very similar protocols could enable the synthesis of several *N*-heterocyclic compounds, such as quinolines,<sup>118, 119</sup> pyrazoles,<sup>120-122</sup>  $\beta$ -carboline,<sup>123, 124</sup> benzodiazepines,<sup>125, 126</sup> and other multicyclic compounds.<sup>127</sup>

Recent examples extend the scope of the starting materials to nitrobenzenes and aldehydes under mild hydrogenative conditions. Li et al. described the multistep one-pot synthesis of imines from nitrobenzenes and biomass-derived carbonyl compounds over nitrogen-doped carbon material supported Ni

nanoparticles (Ni/CN-MgO-T). The reaction involved the reduction of the nitro group to amino and the subsequent condensation with the carbonyl.<sup>128</sup>

### 3.9.3.2 Knoevenagel condensation

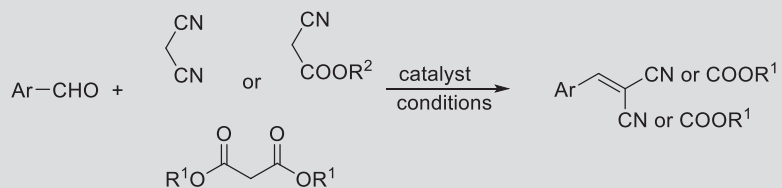
The Knoevenagel condensation is a reaction between an active methylene group containing compound, usually malononitrile, a cyanoacetate, or diethyl malonate, and a carbonyl compound, most commonly benzaldehyde and its substituted derivatives. It is a successive reaction of a nucleophilic addition of the active methylene compound to the carbonyl compound and a dehydration reaction producing an  $\alpha,\beta$ -conjugated enone or an  $\alpha,\beta$ -unsaturated nitrile. Many important molecules can be produced via this transformation. Coumarins and their derivatives are typical examples, they are important intermediates in the synthesis of cosmetics and pharmaceuticals, or other biologically active molecules such as tyroprostins.<sup>129</sup> Commonly, the Knoevenagel reaction is catalyzed by weak bases such as piperidine or ethylenediamine under homogeneous conditions.<sup>129</sup> Recently, efforts have been made to develop heterogeneous catalytic reactions providing potential recyclability in addition to improved selectivity. Some representative heterogeneous catalytic examples and the conditions under which they were used to catalyze the Knoevenagel reactions are presented in Table 9.

All solid catalysts allowed the reactions to be performed under mild conditions with the exception of the solvent-free solid base-catalyzed synthesis of cinnamic acid and coumarin derivatives (Table 9, entry 4).<sup>133</sup> This work is also the only one reporting rather low yields explained by the formation of several by-products along with the condensation process leading to the desired products. Interestingly, it should be noted that the catalyst exhibits the properties of both a base and an acid.

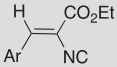
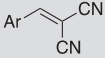
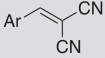
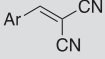
Although some reactions are performed in green solvents as water or ethanol (Table 9, entries 1, 2, and 7), some others are conducted in undesirable solvents such as toluene or benzene (Table 9, entries 3, 5, and 6). The Mn salen complex-driven reaction required toluene as the solvent in order to create heterogeneous conditions by rendering the catalyst insoluble in this specific medium (Table 9, entry 3).<sup>132</sup> The reaction, catalyzed by an amide-functionalized polymer could be performed under solvent-free conditions with excess amount of the reagent benzaldehyde producing similar results (Table 9, entry 6).

Concerning the preparation of the catalysts, the sulfonic acid-functionalized silica-coated Fe<sub>3</sub>O<sub>4</sub> nanoparticles were prepared according to a facile protocol consisting of mixing a chlorosulfonic acid to a solution of Fe<sub>3</sub>O<sub>4</sub>/SiO<sub>2</sub> (Table 9, entry 1).<sup>130</sup> The grafted silica also entailed a simple method of preparation involving diamine derivatives or polyethylenimine, (3-glycidyloxypropyl)-trimethoxysilane and activated silica (Table 9, entry 2).<sup>131</sup> The resulting material contained primary amine and other amine groups that work in cooperation to provide high activity. Similarly, the synthesis of the Hf(IV) MOF was

**TABLE 9** Heterogeneous catalytic Knoevenagel condensation reactions.



| Entry | Methylene compound                                      | Catalyst/conditions  | Product | Yield (%) | Ref. |
|-------|---|--|---------|-----------|------|
| 1     |   | Solid base derived from hydrotalcite, solvent-free, 160°C, 24 h                            |         | 30–39     | 130  |
| 2     | $\text{NC-CH}_2\text{-Y}$<br>Y = CO <sub>2</sub> Et, CN | Mn(III) salen complex, toluene, RT, 1–14 h   |         | 50–99     | 131  |
| 3     |   | Fe <sub>3</sub> O <sub>4</sub> /SiO <sub>2</sub> -SO <sub>3</sub> H, water, RT, 35–125 min |         | 87–95     | 132  |

|                               |                           |  |  |       |          |
|-------------------------------|---------------------------|--|--|-------|----------|
| 4                             | <chem>NC-CH2-CO2Et</chem> | Silica grafted polyethylenimine, EtOH, 43°C, 1–5 h   |  | 84–99 | 131, 133 |
| 5                             | <chem>NC-CH2-CN</chem>    | MOF (Hf(IV)), EtOH, RT, 4 h  |  | 56–99 | 134      |
| 6                             | <chem>NC-CH2-CN</chem>    | ZIF-9, toluene, RT, 6 h  |  | 90–99 | 135      |
| 7                             | <chem>NC-CH2-CN</chem>    | Polymer functionalized with amide groups {[Cd(4-btapa) <sub>2</sub> (NO <sub>3</sub> ) <sub>2</sub> ].6H <sub>2</sub> O.2DMF} <sub>n</sub> benzene, RT, 12 h |  | 98    | 136      |
| MOF, metal organic framework. |                           |  |  |       |          |

prepared in one step by mixing formic acid with  $\text{HfCl}_4$  and the linker  $\text{H}_2\text{BDC-N}_2\text{H}_3$  (Table 9, entry 7).<sup>136</sup> A solvothermal method was selected for the rapid preparation of zeolite ZIF-9 from cobalt nitrate hexahydrate and benzimidazole (Table 9, entry 5).<sup>134</sup> In contrast, the solid base catalyst derived from hydrocalcite as well as the amide functionalized polymer catalysts required more complex synthetic strategies (Table 9, entries 4 and 6).<sup>133, 135</sup> Both of them necessitated the preparation of catalyst precursors or ligands prior to the actual synthesis of the catalyst. The multistep preparation of precursors  $\text{Mg}/\text{Al}$ ,  $\text{Mg}-\text{Al} + \text{Ln}$  ( $\text{Ln} = \text{Dy}, \text{Gd}$ ) layered double hydroxides (LDHs) and  $\text{Li}/\text{Al}$  LDHs was necessary before reaching the final calcination step affording the mixed oxides catalyst.<sup>133</sup> Similarly, several steps led to the formation of the tridentate amide ligand (4-btapa—1,3,5-benzenetricarboxylic acid tris[*N*-(4-pyridyl)amide]) serving as the three-connector part essential for building the three dimensional highly porous coordination polymer (Table 9, entry 6).<sup>135</sup>

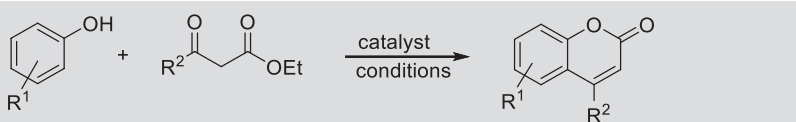
All catalysts, except the solid base and the silica-grafted polyethylenimine, exhibited good recovery and recyclability.

### 3.9.3.3 Pechmann condensation

The Pechmann condensation is a useful organic transformation producing coumarins from a phenol and a carboxylic acid or an ester containing a  $\beta$ -carbonyl group. The reaction, commonly catalyzed by an acid, involves an esterification/transesterification followed by a hydroxyalkylation of the aromatic ring by the keto group. Traditionally, the Pechmann condensation is often performed in the presence of excess amount of concentrated sulfuric acid, trifluoroacetic acid, or aluminum chloride. Heterogeneous catalysts present many advantages over these corrosive acids; they are used in catalytic amounts, notably less toxic and generate minimal amount of waste when they are successfully recycled. Representative examples for the synthesis of coumarins by heterogeneous catalytic Pechmann condensation are tabulated in Table 10.

The xanthan sulfuric acid-catalyzed Pechmann reaction is one of the simplest and most efficient methods. It produced coumarins from various substituted phenols and ethyl acetoacetates under solvent-free conditions, at room temperature and in short reaction times (Table 10, entry 1).<sup>137</sup> The catalyst was recyclable in four consecutive cycles. It was also demonstrated that tungstophosphoric acid (TPA) or molybdophosphoric acid (MPA) supported on silica are suitable catalysts for the synthesis of 4-methyl-5,7-dimethoxycoumarin (Table 10, entry 2). The use of microwave activation not only reduced the reaction times to only a few minutes, it also increased the yield to above 90%, making this solvent-free method remarkably efficient.<sup>138</sup> In fact, the results obtained were superior to the conventional sulfuric acid-based method. The Pechmann reaction of resorcinol with ethyl acetoacetate over Amberlyst-type catalysts afforded 7-hydroxy-4-methylcoumarin in high yields and reasonable reaction times (Table 10, entry 3). The temperature employed, however, was higher than

**TABLE 10** Synthesis of coumarins by heterogeneous catalytic Pechmann condensation reactions.



| Entry | Catalyst/conditions   | Yield (%) | Ref. |
|-------|---|-----------|------|
| 1     | Xanthan sulfuric acid, solvent-free, RT, 20–30 min  | 88–96     | 137  |
| 2     | H <sub>3</sub> PW <sub>12</sub> O <sub>40</sub> /silica, solvent-free, MW, 70°C, 4–10 min | 95–99     | 138  |
| 3     | Amberlyst-S, toluene, 120°C, 2 h  | 95        | 139  |
| 4     | MoO <sub>3</sub> /Al <sub>2</sub> O <sub>3</sub> , solvent-free, 150°C, 30–240 min        | 60–97     | 140  |
| 5     | Zeolites BEA or USY, PhNO <sub>2</sub> 130 °C, 23 h.                                      | 12–83     | 141  |
| 6     | CuBTC or FeBTC MOFs, PhNO <sub>2</sub> , 130°C, 23 h                                      | 2–91      | 141  |
| 7     | ZrPW, 12-TPA/ZrO <sub>2</sub> , 130°C, 30 min   | 38–66     | 142  |
| 8     | PVPP-BF <sub>3</sub> , ethanol, reflux, 2–3 h   | 76–96     | 143  |

ZrPW, zirconium(IV) phosphotungstate); 12-TPA/ZrO<sub>2</sub>, 12-tungstophosphoric acid (12-TPA) supported onto ZrO<sub>2</sub>; BTC, benzene-1,3,5-tricarboxylate; ZrPW, zirconium(IV) phosphotungstate; 12-TPA/ZrO<sub>2</sub>, tungstophosphoric acid supported on ZrO<sub>2</sub>; PVPP-BF<sub>3</sub>, polyvinylpyrrolidone-supported boron trifluoride.

that in the aforementioned methods. Nonetheless, the major advantage of these catalysts is their remarkable recyclability with a decrease in yield corresponding to 1%–2% only after each cycle upon regeneration of the resin in refluxing toluene.<sup>139</sup>

Alumina-supported MoO<sub>3</sub> is another efficient heterogeneous catalyst for the synthesis of various coumarins (Table 10, entry 4).<sup>140</sup> The reaction was performed under solvent-free conditions at 150°C. The solid catalyst was recyclable in three cycles without loss of activity. The catalytic behavior of the MOFs Cu-benzene-1,3,5-tricarboxylate (CuBTC) and Fe-benzene-1,3,5-tricarboxylate (FeBTC) and zeolites beta (BEA) and ultrastable Y (USY) was also investigated in the Pechmann condensation of various phenols with ethyl acetoacetate under identical conditions (Table 10, entries 5, 6). Significantly different behavior was observed for each catalyst type depending on the activation of the substrates. While zeolites were highly active for the transformation of the most active substrates (resorcinol and pyrogallol), they were inefficient for the conversion of naphthol. To the contrary, the MOFs converted naphthol almost quantitatively and were inactive towards resorcinol. It is believed that the presence of two active centers

in close proximity within the regular structure of the framework is of key importance for the transformation of naphthol to the Pechmann product.<sup>141</sup>

Immobilized heteropoly acid-based solid acid catalysts, ZrPW (zirconium(IV) phosphotungstate) and 12-TPA/ZrO<sub>2</sub> [12-tungstophosphoric acid (12-TPA) supported on ZrO<sub>2</sub>] have been prepared and applied in the Pechmann condensation as a test reaction converting phenols and methyl acetoacetate to coumarins under solvent-free conditions using conventional heating or microwave irradiation, which afforded similar yields in shorter reaction times (Table 10, entry 7).<sup>142</sup> Although the catalyst provided the product in moderate to good yields, the ZrPW catalyst showed outstanding recyclability with no decrease in its activity in three consecutive reactions, although a loss of activity was observed when ZrPW was not regenerated by an acid treatment after each cycle. In contrast, the other two samples exhibited gradually declining activity over three reactions.

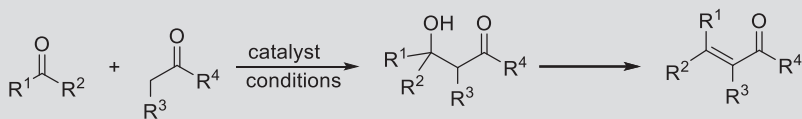
The applications of polyvinylpolypyrrolidone-supported boron trifluoride (PVPP-BF<sub>3</sub>) provided good to excellent yields in the typical Pechmann condensation of substituted phenols with ethyl acetoacetate (Table 10, entry 8).<sup>143</sup> In addition to the excellent performance, the catalyst could be regenerated easily by a simple washing, and reused. It also retained its activity after several months of storage. A similar catalyst, polyvinylpolypyrrolidone-supported copper iodide (P4VPP-CuI) was prepared by an independent group and showed nearly identical performance.<sup>144</sup>

#### 3.9.3.4 Aldol condensation

The aldol condensation is a reaction between an enol or an enolate ion with a carbonyl compound to form a  $\beta$ -hydroxyaldehyde or  $\beta$ -hydroxyketone which often lead to a conjugated enone upon dehydration. The resulting products find great applications notably as fine chemicals. Commonly, the reaction is catalyzed by strong bases such as sodium hydroxide.<sup>145</sup> Environmentally friendly solid acid catalysts are also being developed to produce a wide range of aldol condensation products while meeting the environmental standards.<sup>146</sup> The availability of a broad range of heterogeneous catalysts with unique properties make possible the adjustment of the catalyst depending on the reaction requirements. However, the design of catalyst that promotes both selectivity and reaction rate still remains a challenge. Several representative examples for heterogeneous catalytic aldol condensation are described in Table 11.

Jasminaldehyde, an  $\alpha$ -n-amylicinnamaldehyde, both widely used as a fragrance in the perfume industry, can be obtained by the aldol condensation of heptanal with benzaldehyde. The corresponding heterogeneous synthetic process has been extensively studied with various catalysts. Carboxylic acid-incorporated monodisperse microparticles, prepared by an original synthesis relying on a UV-induced photopolymerization, was applied for the synthesis of jasminaldehyde (Table 11, entry 1). Despite a good selectivity, it showed poor activity leading to only 10% yield.<sup>147</sup> Yet, it was reported that the COOH-

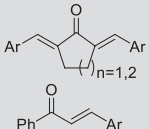
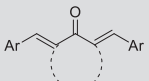
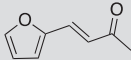
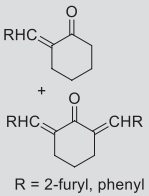
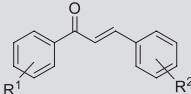
**TABLE 11** Heterogeneous catalytic aldol condensation reactions.



| Entry | Aldehyde/ketone                              | Catalyst/conditions   | Product | Yield (%) | Ref. |
|-------|--|---|---------|-----------|------|
| 1     | Benzaldehyde/heptanal                        | Carboxylic acid-incorporated monodisperse microparticles, solvent-free, 120°C |         | 10        | 147  |
| 2     | Benzaldehyde/heptanal                        | Aluminophosphate, solvent-free, 120°C, 3 h                                    |         | 83        | 148  |
| 3     | Substituted benzaldehydes/heptanal           | <i>p</i> -Toluene sulfonic acid MCM-41, solvent-free, 125°C, 13 h             |         | 60–90     | 149  |
| 4     | Benzaldehyde/heptanal                        | Chitosan, solvent-free, 160°C, 8 h  |         | 88        | 150  |
| 5     | Formaldehyde/acetic acid and methyl ester    | Zeolite H-ZSM-35, solvent-free, 350°C, 4 h                                    |         | 61        | 151  |
| 6     | Benzaldehyde/acetone                         | MgAl hydrotalcite, solvent-free, 0°C  |         | 85        | 152  |
| 7     | Substituted benzaldehydes/cycloalkyl ketones | Carbon-based solid acid, solvent-free, 70°C, 65–120 min                       |         | 85–97     | 153  |

Continued

**TABLE 11** Heterogeneous catalytic aldol condensation reactions — cont'd

| Entry | Aldehyde/ketone                              | Catalyst/conditions   | Product   | Yield (%)               | Ref.        |
|-------|--|---|---|-------------------------|-------------|
| 8     | Cyclopentanone, cyclohexanone, acetophenone  | NMSDSA, water, reflux, 14–25 min  |  | 88–95                   | 154         |
| 9     | Substituted benzaldehydes/cycloalkyl ketones | Sulfated zirconia, solvent-free, MW, 120–140°C, 20 min  |  | 79–99                   | 155         |
| 10    | Furfural/acetone                             | MgOZrO <sub>2</sub> , water, 120°C, 24 h or MgGa mixed oxides and reconstructed hydrotalcites, 50°C |  | Up to 80 (carbon yield) | 156,<br>157 |
| 11    | Furfural, benzaldehyde                       | La <sup>3+</sup> -organic zeolite, water, 25°C, 20–85 h   |  | > 95                    | 158         |
| 12    | Benzaldehydes/acetophenones                  | B(OH) <sub>3</sub> (20 mol%), solvent-free, MW, 160°C, 40 min                                       |  | 58–75                   | 159         |
|       |  | KSF montmorillonite, solvent-free, MW, 150°C, 60 min  |   | 43–97                   | 160         |

NMSDSA, nanometasilica disulfuric acid.

containing microparticles provided higher selectivity than the more conventional zeolite H-beta catalyst. An amorphous aluminophosphate catalyst exhibited both high rate and selectivity for the synthesis of jasminaldehyde (Table 11, entry 2). The catalyst is a special material of amphoteric characteristics; it contains both acid and base centers. Thus, the reaction seems to occur through a bifunctional mechanism that involves the activation of benzaldehyde, by protonation-polarization of the carbonyl group on the acid sites, and the attack of the enolate heptanal intermediate generated on the basic sites.<sup>148</sup> MCM-41 supported *p*-toluene sulfonic acid, prepared by impregnation method, was also remarkably efficient for the synthesis of jasminaldehyde and related compounds (Table 11, entry 3).<sup>149</sup> It resulted in complete conversion of the starting materials and high selectivities of the product. In addition, it was recyclable in five cycles with no appreciable loss of activity. Another original bio-sourced catalytic material, modified chitosan, afforded similar results (Table 11, entry 4); 100% conversion and 88% selectivity under solvent-free conditions at 160°C.<sup>150</sup>

Methyl acrylate and acrylic acid, widely used in the manufacturing of paints, coatings, and adhesives and currently produced by a two-step process, were prepared in a one-step aldol condensation reaction over H-ZSM-35 zeolite catalyst (Table 11, entry 5).<sup>151</sup> The optimum yield obtained was 61% with a selectivity of 88% at 350°C. Although the catalyst has potential applications at the industrial scale, it requires high temperatures to be active compared to most solid acid catalysts that are used for aldol condensation and operate below 150°C. In addition, the reactivation of the zeolite catalyst, although it may be performed, occurs at high temperature of calcination.

The condensation of benzaldehyde and acetone gives rise to  $\beta$ -aldol or benzalacetone after dehydration. The applicability of modified Mg-Al hydroxalicates were investigated for the selective synthesis of  $\beta$ -aldol (Table 11, entry 6).<sup>152</sup> The highest yield of the desired product was observed after specific activation of the solid catalyst entailing a calcination step at 450°C, followed by a rehydration step with water vapor at room temperature. The necessity of a hydration step indicates an aldolization mechanism driven by the presence of basic sites (OH<sup>-</sup>), which corroborates with the proposed mechanism for common basic catalysts.

A wide variety of  $\alpha,\beta$ -unsaturated carbonyl compounds, useful as precursors of biologically active molecules, can be synthesized from aromatic aldehydes and ketones with different sulfonated solid catalysts. A carbon-based solid acid catalyst demonstrated excellent performance under mild conditions with broad functional group tolerance (Table 11, entry 7).<sup>153</sup> Although the catalyst is highly efficient and recyclable, its synthesis has a nonnegligible impact on the environment. It is obtained by heating aromatic compounds in sulfuric acid at 390°C; the resulting sulfonated hydrocarbons are incompletely carbonized, and the final solid material consists of small polycyclic aromatic carbon sheets with attached SO<sub>3</sub>H groups.<sup>161</sup> In addition to the harsh conditions, the total yield

of the synthesis is only about 55%. Similar aldol condensation products were synthesized in the presence of nanometasilica disulfuric acid in refluxing water (Table 11, entry 8)<sup>154</sup> or sulfated zirconia in solvent-free, microwave-driven conditions at 120–140°C (Table 11, entry 9).<sup>155</sup> The same comments can be made about the excellent activity of these catalysts with significant environmental drawbacks caused by the harsh conditions employed for their synthesis.

The aldol condensation can also be applied to biomass derived compounds such as furfural and 5-hydroxymethylfurfural to produce useful intermediates easily converted to liquid alkanes (Table 11, entry 10). A bifunctional Pd/MgO-ZrO<sub>2</sub> catalyst was developed for the cross aldol-condensation of these compounds with acetone resulting in formation of water-insoluble monomer (C8–C9) and dimer (C13–C15) subsequently hydrogenated with the aid of the Pd component in the same batch reactor to form water-soluble products. The yields reported correspond to the overall carbon yield. The selectivity is highly dependent on the molar ratio of the two reactants.<sup>156</sup> It is noteworthy that the catalyst can be regenerated after a calcination step at high temperature, without which the recycling is not possible.

Dewa et al. reported a La<sup>3+</sup>-ion exchanged organic zeolite as a catalyst for aldol reactions in water. The major advantages of the catalyst are its stable behavior during hydrolysis, in addition to its microporosity allowing reversible substrate prebinding and activation in an enzyme-mimetic fashion. As a result, benzaldehyde and furfural were converted to the respective enone and diene (after aldol and concomitant dehydration reactions) in quantitative yield (Table 11, entry 11).<sup>158</sup>

Brun et al. reported the synthesis of chalcone derivatives via the aldol condensation of substituted acetophenones with benzaldehydes. The authors applied boric acid as a catalyst, which was used under microwave-assisted solvent-free conditions (Table 11, entry 12).<sup>159</sup> Due to the solvent-free nature of the reaction and the low solubility of the catalyst in the reactant mixture the transformation was heterogeneous catalytic. The chalcones were obtained in medium to good yields with nearly exclusive *E* stereoselectivity. The product isolation involved only a simple extraction step providing the product mixture in a pure form. In an alternative protocol using the same substrates, KSF montmorillonite was employed as a well-known, commercially available solid acid (Table 11, entry 12).<sup>160</sup> The chalcones were isolated in medium to good yields. The substrate tolerance is limited to electron donating substituents, the presence of electron withdrawing substituents decreased the yields.

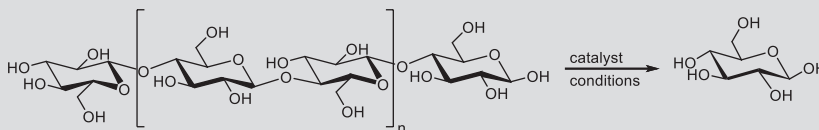
Based on the above examples, it appears that heterogeneous systems are generally applicable to synthesize various useful aldol condensation products. However, many of these catalysts promote the aldol condensation reactions at high temperatures and they sometimes suffer from selectivity issues. In addition, the deactivation of the catalyst is commonly observed, which explains the need for a reactivation step or the observed poor recyclability.

### 3.9.4. Hydrolysis

#### 3.9.4.1 Hydrolysis of cellulose

Cellulose, the most abundant component of biomass, has emerged as an alternative feedstock to petroleum-based raw materials. Significant efforts have been made to develop strategies utilizing lignocellulosic materials by accessing useful, smaller units from the long, interconnected polymeric chains.<sup>162</sup> Due to the complex structure of cellulose, composed of fibrils that are based on  $\beta$ -1,4-glycosidic bonds of D-glucose units and are connected to one another by hydrogen bonding, breaking it down still remains a challenge. Enzymatic hydrolysis, that is generally considered green, is a possible approach. In spite of the high selectivity and mild reaction conditions provided, enzymes can hardly access the core of cellulose to initiate degradation and thus, harsh pretreatments are required. The application of solid acids constitutes another environmentally friendly approach that can produce useful building blocks from cellulose without any pretreatment. Solid acids such as sulfonated carbonaceous material-based acids, polymer-based acids, and magnetic solid acids notably have been used for the production of glucose from cellulose.<sup>163–167</sup> The hydrothermal stability combined with the strong acidity of  $\text{SO}_3\text{H}$  functional groups make these sulfonated materials the catalysts of choice for the conversion of cellulose into glucose. Representative data are tabulated in [Table 12](#).

**TABLE 12** Heterogeneous catalytic conversion of cellulose to glucose over solid acid catalyst.



| Entry | Catalyst/conditions                                 | Yield (%) | Ref.                |
|-------|---|-----------|---------------------|
| 1     | Sulfonated carbon, 24 h, 150°C                      | 74        | <a href="#">163</a> |
| 2     | Sulfonated activated carbon, 24 h, 150°C            | 40        | <a href="#">164</a> |
| 3     | Carbon sulfonated, 100°C, 6 h                       | 64        | <a href="#">165</a> |
| 4     | Sulfonated silica-carbon nanocomposite, 24 h, 150°C | 50        | <a href="#">166</a> |
| 5     | Silica-magnetite mesoporous solid acid, 150°C, 3 h  | 25        | <a href="#">167</a> |

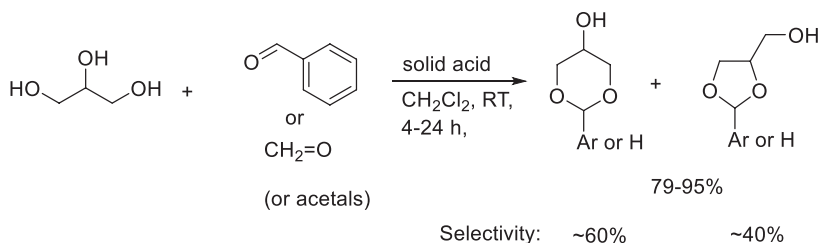
The highest yield of glucose was obtained with sulfonated carbon at 150°C in a 24 h reaction (Table 12, entry 1).<sup>163</sup> It was observed that the sulfonation protocol of the carbonated material had a significant influence on the activity and selectivity of the catalyst, the optimum conditions being 250°C for 24 h. Other factors having an effect on the catalytic activity include carbon sources and carbonization method. As an evidence, a similar but differently prepared sulfonated activated carbon catalyst employed under the same aforementioned conditions provided only moderate yield of glucose (Table 12, entry 2).<sup>164</sup> Another sulfonated carbon catalyst provided 64% of desired product, it was, however, prepared at a higher temperature of 400°C (Table 12, entry 3).<sup>165</sup> A sulfonated silica-carbon nanocomposite achieved a yield of glucose comprised in the same range as the results obtained with other carbon-based catalysts (Table 12, entry 4).<sup>166</sup> The catalyst owes its activity partially to the hybrid surface structure constituted by interpenetrated silica and carbon components. Lastly, a silica-magnetite mesoporous solid acid offered 25% of yield after 3 h of reaction time. Although the yield is significantly lower than the performance of the carbonated catalysts, the advantage of silica-magnetite-driven reaction lies in the ease of separation and subsequent reuse of the solid acid (Table 12, entry 5).<sup>167</sup> Also, the yield remains superior to the performance of most zeolites. It must be noted as a further benefit of this protocol, that the synthesis of the catalyst does not involve harsh reaction conditions and uses starting materials sourced from biomass saccharification and levulinic acid production.

### 3.9.5. Introduction and removal of protecting groups

The protection/deprotection of sensitive functional groups is a commonly applied strategy in multistep synthesis.<sup>168–171</sup> According to the Green Chemistry principles, this step should be avoided as much as possible, however, the use of protecting groups is often unavoidable when carrying out reactions on complex molecules. When the use of protecting groups cannot be eliminated from the synthesis design, the alternative is the development of green protection/deprotection methods to decrease the impact of these auxiliary steps on the environment. The application of heterogeneous catalysis in protection/deprotection chemistry is one of the current trends to address this issue.<sup>172</sup> One of the most common deprotection methods is the application of heterogeneous catalytic hydrogenolysis to remove for example benzyl, allyl, or Cbz protecting groups. The hydrogenative removal of hydrogenation sensitive groups have already been discussed in detail in this book, in Chapter 3.2 Hydrogenolysis. Thus, here we will focus on other available methods.

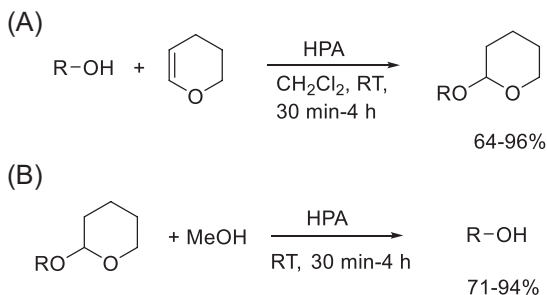
The application of heterogeneous catalysis for the protection of hydroxyl, thiol, and carboxylic acid groups is one of the most frequent approaches.<sup>173</sup> The formation of cyclic acetals is a common strategy for the protections of both hydroxyl- as well as carbonyl groups. The acid-catalyzed condensation of glycerol, a multimillion ton by-product of biodiesel formation and a renewable chemical,

with carbonyl compounds such as benzaldehyde, formaldehyde, acetone, and the transacetalization using benzaldehyde and formaldehyde acetals, respectively, was reported by Deutsch et al.<sup>174</sup> The authors applied several solid acids, such as Amberlyst-36, Nafion-NR-50, H-BEA zeolite and K-10 montmorillonite for the conversion of glycerol to novel [1,3]dioxan-5-ols and [1,3]dioxolan-4-yl-methanols that are of particular interest as precursors for 1,3-propanediol derivatives (Scheme 10). The yields were moderate to excellent for the mixture of the two products, the six membered dioxan forming in higher amount.



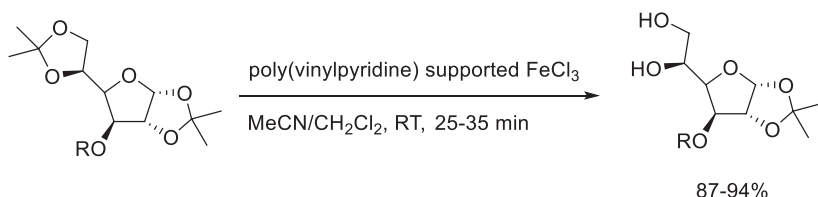
**SCHEME 10** Acetalization and transacetalization of glycerol with carbonyl compounds catalyzed by solid acids.

The acid-catalyzed tetrahydropyranation of alcohols is another commonly used method to avoid the undesired transformations of alcohols. Heteropolyacids were found to be excellent catalysts for the protection and deprotection of hydroxyl compounds with tetrahydropyran (THP).<sup>37, 175</sup> The addition of the OH group to THP occurred with excellent yields in very short times using open-chain and cyclic aliphatic alcohols and phenol (Scheme 11a). The deprotection reaction could be carried out with the same HPA catalysts under mild conditions. Although the reaction time range is the same for both reactions in the Scheme, the protection reactions occurred mostly in 30 min, only tetrahydrofurfuryl alcohol and *tert*-amylalcohol required more time (2 and 4 h). In contrast, only two substrates were deprotected in 30 min, most deprotections required 4 h to be complete (Scheme 11b).



**SCHEME 11** Heteropolyacid (HPA)-catalyzed protection (a) and deprotection (b) of alcohols via tetrahydropyranation.

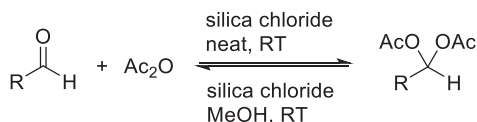
The selective protection of hydroxyl groups is particularly important in carbohydrate chemistry.<sup>176, 177</sup> The protection of diols via their reaction with acetone, namely the formation of acetonides is one of the most common reactions in the protection of carbohydrate derivatives. Thus, the selective removal of the acetonide group has been attracting extensive attention. Chari and Syamasundar reported a selective protocol for the removal of the acetonide group from the side chain of carbohydrates while the similar protective group remains in place on the ring (Scheme 12).<sup>178</sup> Other acid labile protecting groups (labeled as R in the scheme), such as *tert*-butyldimethylsilyl (TBDMS) or tetrahydropyranyl ether (THP) remained stable under the reaction conditions. Many other functionalities such as OMe, OBn, OBz, NHBoc, and OAc were also compatible with this protocol.



**SCHEME 12** Heterogeneous catalytic chemo- and regioselective deprotection of acetonides.

There are several other catalysts that were developed for a similar purpose, namely for the protection or deprotection of hydroxyl groups. These catalysts include magnetic Fe<sub>3</sub>O<sub>4</sub>-supported samples, such as sulfated zirconia (Fe<sub>3</sub>O<sub>4</sub>@ZrO<sub>2</sub>/SO<sub>4</sub><sup>2-</sup>)<sup>179</sup> or a rhodium complex (CpRu(h<sup>3</sup>-C<sub>3</sub>H<sub>5</sub>)(2-quinolinecarboxylato)]PF<sub>6</sub>@Fe<sub>3</sub>O<sub>4</sub>@SiO<sub>2</sub>).<sup>180</sup>

Hydroxyl, thiol, or amino groups are not the only functional groups that would need protection under certain reaction conditions. Ketones and aldehydes are also reactive groups and when part of a complex system, they have to be protected from undergoing undesired side reactions. The chemoselective protection/deprotection of aldehydes was reported by Datta and Pasha (Scheme 13).<sup>181</sup> The authors applied acetyl chloride as a protecting agent to prepare acylals from the aldehydes using a heterogeneous silica chloride catalyst. Both the protection and deprotection reactions occurred under mild conditions with good to excellent yields. Similar to the hydroxyl group, several other catalysts have been developed for the selective protection/deprotection of carbonyl compounds as well. For example, a ruthenium(III)-polyvinyl pyridine (RuPVP) complex was prepared and successfully applied for the chemoselective protection of aldehydes,<sup>182</sup> or a polystyrene divinyl benzene sulfonic acid (SPS) was developed for the chemospecific protection of only one of two identical carbonyls in 2,2-dialkyl-1,3-cyclohexanedione and the chemoselective protection of aliphatic or aromatic carbonyls in the presence of conjugated carbonyls.<sup>183</sup> Another example is ferric sulfate (Fe<sub>2</sub>(SO<sub>4</sub>)<sub>3</sub>×H<sub>2</sub>O) that appeared to deprotect 1,1-diacetals to aldehydes.<sup>184</sup>



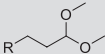
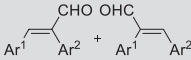
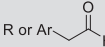
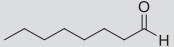
**SCHEME 13** Protection/deprotection of aldehydes with acetic anhydride catalyzed by silica chloride.

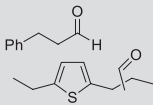
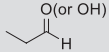
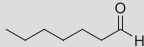
### 3.9.6. Hydroformylations

The synthesis of aldehydes via hydroformylation of alkenes with carbon monoxide and hydrogen is one of the most extensive large scale processes in the chemical industry.<sup>185, 186</sup> First described by Roelen in 1938, the transformation traditionally achieved the functionalization of C=C bonds by organometallic complex catalysis.<sup>187</sup> Despite its versatility and frequent use in the pharmaceutical and agrochemical industries, the formation of undesirable by-products by the isomerization of the olefin or the formation of hydrogenated products result in continued challenges for process chemists and engineers.<sup>188</sup> The application of stable chemo-, regio-, and stereoselective heterogeneous catalysts offer new ways to improve hydroformylation reactions. Several recent representative examples are collected in [Table 13](#).

In agreement with literature reviews, the most common catalytic metal for hydroformylation in the above applications is Rh ([Table 13](#), entries 1–7).<sup>207–211</sup> However, due to the high cost of Rh, efforts have been made to find alternative, more economic metals. The three examples that were used either individually in various forms, or as an additional metal in Rh-M bimetallic catalysts ([Table 13](#), entries 3, 6) are Fe, Ni, and Co. The Fe(III)-urea formed composite material (FeOCN, [Table 13](#), entry 4), the Co/SiO<sub>2</sub> sample ([Table 13](#), entry 7), or the Fe-Ni and the Rh-Co bimetallic catalysts ([Table 13](#), entry 6), provided reasonable yields for the products but were somewhat less effective than the other Rh catalysts. The other tendency that the analysis of recent papers reveals is the use of a variety of supports on which Rh as catalytic metal, was immobilized. In addition to the traditional support materials such as SiO<sub>2</sub> or Al<sub>2</sub>O<sub>3</sub> ([Table 13](#), entries 1,5), a broad variety of supports were applied in catalyst preparation. The most studied group is that of various polymeric materials ([Table 13](#), entries 2–4); the catalysts mostly produced excellent yields up to the quantitative formation of the aldehydes. Metal oxides, such as MgO, ZnO, CeO<sub>2</sub> are also commonly applied ([Table 13](#), entries 3,6). There are examples, using support materials that have only been recently introduced to serve in this capacity, such as reduced graphene oxide (RGO), TiO<sub>2</sub> nanotubes (TNT), sulfated carbon nitride (S-g-C<sub>3</sub>N<sub>4</sub>), or a zeolite organic framework (ZIF-8) ([Table 13](#), entries 3,4,5,7). Rh is mostly applied as traditional crystallites, nanoparticles or in the form of single atom catalysis.

**TABLE 13** Heterogeneous catalytic hydroformylation of alkenes.

| alkene or alkyne $\xrightarrow[\text{conditions}]{\text{catalyst, syngas (CO/H}_2\text{)}}$ aldehydes (or derivatives) |                                       |   |   |                      |          |
|--|---------------------------------------|---|---|----------------------|----------|
| Entry  | Alkene                                | Catalyst/conditions   | Product   | Yield (%)            | Ref.     |
| 1  | Various alkenes with alcohols         | Rh/SiO <sub>2</sub> , CO/H <sub>2</sub> (4 MPa), 120°C, 8 h   |  | 95                   | 189      |
| 2  | Symmetrical and unsymmetrical alkynes | Rh/POL-BINAP-PPh <sub>3</sub> , CO/H <sub>2</sub> (5.5 bar), toluene, 70°C, 20 h  |  | 90                   | 190      |
| 3  | Alkenes                               | Porous polymer-immobilized Rh complexes or single atom Rh, CO/H <sub>2</sub> (4.8 bar), toluene, 75°C, 30 min<br>Rh/S-g-C <sub>3</sub> N <sub>4</sub> , CO/H <sub>2</sub> (6.0 MPa), toluene, 100°C, 3 h<br>Rh-Co bimetallic catalyst, Rh/ZnO <sub>50</sub> @ZIF-8, Rh single atom catalyst on MgO and CeO <sub>2</sub> |  | 50–99                | 191–199  |
| 4  | 1-Octene                              | Rh NPs@TPBD, CO/H <sub>2</sub> (2 MPa), toluene, 60–120°C, 5 h<br>FeOCN composite, CO/H <sub>2</sub> (50 bar), toluene, 95°C,   |  | Up to 30 n/iso = 2.5 | 200, 201 |

|   |   |  |   |                        |             |
|---|---|--|---|------------------------|-------------|
| 5 | Styrene,<br>2-ethyl-5-(prop-1-enyl)<br>thiophene,<br>2-allyl-5-ethylthiophene | 0.18% Rh/Al <sub>2</sub> O <sub>3</sub> , CO/H <sub>2</sub> (4 MPa), toluene, 80°C, 20 h<br>Rh/B-TNT, CO/H <sub>2</sub> (6 MPa), toluene, 80°C, 20 h |  | 79–99 (sum of isomers) | 202,<br>203 |
| 6 | Ethane and CO <sub>2</sub>  | Dual catalyst bed: (1) Fe <sub>3</sub> Ni <sub>1</sub> /CeO <sub>2</sub> (600–800°C), (2) RhCo <sub>x</sub> /MCM-41 (200°C), flow system             |  | Up to 50               | 204         |
| 7 | 1-Hexene  | Co/SiO <sub>2</sub> , CO/H <sub>2</sub> (5 MPa), toluene, 100°C, 5 h<br>Rh/RGO, CO/H <sub>2</sub> (5 MPa), toluene, 70°C, 1 h                        |  | 30–61                  | 205,<br>206 |

Rh/POL-BINAP-PPh<sub>3</sub>, rhodium-loaded porous polymer-based organic catalyst; Rh NPs@TPBD, phosphine-contg. porous polymer (TPBD) immobilized Rh nanoparticles (NPs); Rh/S-g-C<sub>3</sub>N<sub>4</sub>, sulfated carbon nitride supported rhodium particles; Rh/ZnO<sub>50</sub>@ZIF-8-Rh-ZnO in zeolitic imidazolate framework-8 (ZIF-8); Rh/B-TNT, boron modified Rh nanoparticles immobilized on TiO<sub>2</sub> nanotubes; RGO, reduced graphene oxide.

In addition to the reaction studies, reports discussing the mechanistic aspects, such as kinetics, surface transformations, interfacial phenomena, etc. of heterogeneous catalytic hydroformylations are also available.<sup>212–214</sup>

### 3.9.7. Conclusions and outlook

In this chapter recent advances achieved in the fields of rearrangements, as well as several other reactions, that were not part of the other chapters in this book, were surveyed in the 1996–2021 period. This separate treatment was due to the often mixed nature of these transformations, for example oxidation and rearrangement (Baeyer-Villiger oxidation) or simply they did not fit into the other reaction groups. The importance of these processes is unambiguous, many of them are large scale industrial processes (hydroformylation, condensations, Beckmann rearrangement) and/or regularly applied in laboratory practice such the protection/deprotection or hydrolysis. Due to the large number of publications available in several areas, we have refrained from providing an exhaustive list of references and rather focused on mentioning representative examples for these transformations. Based on the literature data, it is reasonable to predict, that these transformations will remain important tools in the green and sustainable synthesis toolbox.

## References

1. Tabolin, A. A.; Ioffe, S. L. Rearrangement of *N*-Oxyenamines and Related Reactions. *Chem. Rev.* **2014**, *114*, 5426–5476.
2. Rojas, C. M., Ed. *Molecular Rearrangements in Organic Synthesis*; Wiley: Hoboken, NJ, 2016.
3. Dunetz, J. R.; Magano, J.; Weisenburger, G. A. Large-Scale Applications of Amide Coupling Reagents for the Synthesis of Pharmaceuticals. *Org. Process Res. Dev.* **2016**, *20*, 140–177.
4. Kristofic, M.; Marcincin, A.; Borsig, E. Preparation, Properties and Application of Modified Fibers With Piperazine Rings. *Polym. Adv. Technol.* **1999**, *10*, 179–186.
5. Wang, K.; Zhang, J.; Zheng, C.; Dong, C.; Lu, Y.; Luo, G. A Consecutive Microreactor System for the Synthesis of Caprolactam with High Selectivity. *AIChE J.* **2015**, *61*, 1959–1967.
6. Li, D.; Mao, D.; Li, J.; Zhou, Y.; Wang, J. In Situ Functionalized Sulfonic Copolymer Toward Recyclable Heterogeneous Catalyst for Efficient Beckmann Rearrangement of Cyclohexanone Oxime. *Appl. Catal. A Gen.* **2016**, *510*, 125–133.
7. Ghiaci, M.; Ghazaie, M. Modification of a Heterogeneous Catalyst: Sulfonated Graphene Oxide Coated by SiO<sub>2</sub> as an Efficient Catalyst for Beckmann Rearrangement. *Catal. Commun.* **2016**, *87*, 70–73.
8. Zhang, X.; Mao, D.; Leng, Y.; Zhou, Y.; Wang, J. Heterogeneous Beckmann Rearrangements Catalyzed by a Sulfonated Imidazolium Salt of Phosphotungstate. *Catal. Lett.* **2013**, *143*, 193–199.
9. Mitsudome, T.; Matsuno, T.; Sueoka, S.; Mizugaki, T.; Jitsukawa, K.; Kaneda, K. Titanium Cation-Exchanged Montmorillonite as an Active Heterogeneous Catalyst for the Beckmann Rearrangement Under Mild Reaction Conditions. *Tetrahedron Lett.* **2012**, *53*, 5211–5214.

10. Wen, G.; Diao, J.; Wu, S.; Yang, W.; Schoegl, R.; Su, D. S. Acid Properties of Nanocarbons and Their Application in Oxidative Dehydrogenation. *ACS Catal.* **2015**, *5*, 3600–3608.
11. Wang, X.; Chen, C.; Chen, S.; Mou, Y.; Cheng, S. Arenesulfonic Acid Functionalized Mesoporous Silica as a Novel Acid Catalyst for the Liquid Phase Beckmann Rearrangement of Cyclohexanone Oxime to  $\epsilon$ -Caprolactam. *Appl. Catal. A Gen.* **2005**, *281*, 47–54.
12. Hartmann, M.; Machokeb, A. G.; Schwieger, W. Catalytic Test Reactions for the Evaluation of Hierarchical Zeolites. *Chem. Soc. Rev.* **2016**, *45*, 3313–3330.
13. Opanasenko, M. Catalytic Behavior of Metal-Organic Frameworks and Zeolites: Rationalization and Comparative Analysis. *Catal. Today* **2015**, *243*, 2–9.
14. Tam, E. K. W.; Rita; Liu, L. Y.; Chen, A. 2-Furanylboronic Acid as an Effective Catalyst for the Direct Amidation of Carboxylic Acids at Room Temperature. *Eur. J. Org. Chem.* **2015**, *2015*, 1100–1107.
15. Wang, Z.; Bao, X.; Xu, M.; Deng, Z.; Han, Y.; Wang, N. Direct Formation of Amides from Carboxylic Acids and Amines Catalyzed by Niobium(V) Oxalate Hydrate. *ChemistrySelect* **2018**, *3*, 2599–2603.
16. Hu, L.; Chen, Z.; Xie, Y. Synthesis and Biological Activity of Amide Derivatives of Ginkgolide A. *J. Asian Nat. Prod. Res.* **2001**, *3*, 219–227.
17. Xu, J.-Y.; Dong, W.-L.; Xiong, L.-X.; Li, Z.-M. Design, Synthesis and Biological Activities of Amides(Sulfonamides) Containing N-Pyridylpyrazole. *Chem. J. Chin. Univ.* **2012**, *33*, 298–302.
18. Keyhaniyan, M.; Shiri, A.; Eshghi, H.; Khojastehnezhad, A. Novel Design of Recyclable Copper(II) Complex Supported on Magnetic Nanoparticles as Active Catalyst for Beckmann Rearrangement in Poly(Ethylene Glycol). *Appl. Organomet. Chem.* **2018**, *32*, e4344.
19. KarimKoshteh, M.; Bagheri, M. Nano  $\text{Fe}_3\text{O}_4$  as Green Catalyst for Beckmann Rearrangement under Ultrasound Irradiation. *J. Mex. Chem. Soc.* **2017**, *61*, 28–34.
20. Zhi, P.; Xi, Z.; Wang, D.; Wang, W.; Liang, X.; Tao, F.; Shen, R.; Shen, Y. Vilsmeier-Haack Reagent Mediated Synthetic Transformations With an Immobilized Iridium Complex Photoredox Catalyst. *New J. Chem.* **2019**, *43*, 709–717.
21. Yoshida, K.; Shiju, N.; Brown, R.; Wright, I.; Boyes, E.; Gai, P. Double Aberration Corrected TEM/STEM of Solid Acid Nanocatalysts in the Development of Pharmaceutical NSAIDS. *J. Phys. Conf. Ser.* **2012**, *371*, 012026.
22. Ghadamyari, Z.; Khojastehnezhad, A.; Seyedi, S. M.; Shiri, A. Co(II)-Porphyrin Immobilized on Graphene Oxide: An Efficient Catalyst for the Beckmann Rearrangement. *ChemistrySelect* **2019**, *4*, 10920–10927.
23. Dongare, M.; Bhagwat, V.; Ramana, C.; Gurjar, M. Silica Supported  $\text{MoO}_3$ : A Mild Heterogeneous Catalyst for the Beckmann Rearrangement and its Application to Some Sugar Derived Ketoximes. *Tetrahedron Lett.* **2004**, *45*, 4759–4762.
24. Thomas, B.; Prathapan, S.; Sugunan, S. Solid Acid-Catalyzed Dehydration/Beckmann Rearrangement of Aldoximes: Towards High Atom Efficiency Green Processes. *Microporous Mesoporous Mater.* **2005**, *79*, 21–27.
25. Johnston, D.; Elder, D. Synthesis of Acetaminophen-D4. *J. Label. Compd. Radiopharm.* **1988**, *25*, 1315–1318.
26. Heaney, H. In *Comprehensive Organic Synthesis*; Trost, B. M., Fleming, I., Eds.; Vol. 2: Additions to C–X  $\pi$ -Bonds, Part 2 (Heathcock, C.H. ed.); Pergamon Press: Oxford, 1991; p. 745.
27. Ollevier, T.; Desyroy, V.; Asim, M.; Brochu, M. Bismuth Triflate-Catalyzed Fries Rearrangement of Aryl Acetates. *Synlett* **2004**, 2794–2796.

28. Commariou, A.; Hoelderich, W.; Laffitte, J.; Dupont, M. Fries Rearrangement in Methane Sulfonic Acid, an Environmental Friendly Acid. *J. Mol. Catal. A Chem.* **2002**, *182*, 137–141.
29. van Grieken, R.; Melero, J.; Morales, G. Fries Rearrangement of Phenyl Acetate Over Sulfonic Modified Mesoporous SBA-15 Materials. *Appl. Catal. A Gen.* **2005**, *289*, 143–152.
30. Kozhevnikova, E.; Quartararo, J.; Kozhevnikov, I. Fries Rearrangement of Aryl Esters Catalysed by Heteropoly Acid. *Appl. Catal. A Gen.* **2003**, *245*, 69–78.
31. Kozhevnikova, E.; Derouane, E.; Kozhevnikov, I. Heteropoly Acid as a Novel Efficient Catalyst for Fries Rearrangement. *Chem. Commun.* **2002**, 1178–1179.
32. Török, B.; Kiricsi, I.; Molnár, Á.; Olah, G. A. Acidity and Catalytic Activity of a Nafion-H/Silica Nanocomposite Catalyst Compared with a Silica-Supported Nafion Sample. *J. Catal.* **2000**, *193*, 132–138.
33. Smith, K.; El-Hiti, G. A.; Matthews, I.; Al-Shamali, M.; Watson, T. Rearrangement of Epoxides to Allylic Alcohols in the Presence of Reusable Basic Resins. *Catal. Lett.* **2009**, *128*, 101–105.
34. de la Torre, O.; Renz, M.; Corma, A. Biomass to Chemicals: Rearrangement of Beta-Pinene Epoxide into Myrtanal With Well-Defined Single-Site Substituted Molecular Sieves as Reusable Solid Lewis-Acid Catalysts. *Appl. Catal. A Gen.* **2010**, *380*, 165–171.
35. Corma, A.; Orozco, L. M.; Renz, M. From MOFs to Zeolites: Zirconium Sites for Epoxide Rearrangement. *New J. Chem.* **2013**, *37*, 3496–3502.
36. Török, B.; Bucsi, I.; Beregszászi, T.; Molnár, Á. Rearrangements of Oxygen-Containing Compounds Induced by Heteropoly Acids. In *Catalysis of Organic Reactions*; Malz, R. E., Ed.; Marcel Dekker: New York, **1996**; pp. 393–396.
37. Török, B.; Molnár, Á. Electrophilic Transformations Induced by Heteropoly Acids: Applications and Structural Studies. *Compt. Rend. Acad. Sci. Paris Serie II c* **1998**, 381–396.
38. Zhang, S.; Ma, H.; Sun, Y.; Luo, Y.; Liu, X.; Zhang, M.; Gao, J.; Xu, J. Catalytic Selective Hydrogenation and Rearrangement of 5-Hydroxymethylfurfural to 3-Hydroxymethylcyclopentone Over a Bimetallic Nickel–Copper Catalyst in Water. *Green Chem.* **2019**, *21*, 1702–1709.
39. Rosati, O.; Curini, M.; Messina, F.; Marcotullio, M. C.; Cravotto, G. Ferrier Rearrangement and 2-Deoxy Sugar Synthesis from d-Glycals Mediated by Layered alpha-Zirconium Sulfophenylphosphonate-Methanphosphonate as Heterogeneous Catalyst. *Catal. Lett.* **2013**, *143*, 169–175.
40. Das, B.; Majhi, A.; Reddy, K. R.; Venkateswarlu, K. I-2-SiO<sub>2</sub>: An Efficient Heterogeneous Catalyst for the Johnson-Claisen Rearrangement of Baylis-Hillman Adducts. *J. Mol. Catal. A Chem.* **2007**, *263*, 273–275.
41. Wipf, P. In *Comprehensive Organic Synthesis*; Trost, B. M., Fleming, I., Eds.; Combining C–C  $\pi$ -Bonds, Paquette, L.A. Ed., Vol. 5; Pergamon Press: Oxford, 1991; p. 834.
42. Sheldon, R. A.; Elings, J. A.; Lee, S. K.; Lempers, H. E. B.; Downing, R. S. Zeolite-Catalysed Rearrangements in Organic Synthesis. *J. Mol. Catal. A Chem.* **1999**, *134*, 129–135.
43. Molnár, Á.; Beregszászi, T.; Fudala, A.; Lentz, P.; Nagy, J. B.; Kónya, Z.; Kiricsi, I. The Acidity and Catalytic Activity of Supported Acidic Cesium Dodecatungstophosphates Studied by MAS NMR, FTIR, and Catalytic Test Reactions. *J. Catal.* **2001**, *202*, 379–386.
44. Pitchumani, K.; Warriar, M.; Ramamurthy, V. Remarkable Product Selectivity During Photo-Fries and Photo-Claisen Rearrangements within Zeolites. *J. Am. Chem. Soc.* **1996**, *118*, 9428–9429.
45. Surya Prakash, G. K.; Glington, K. E.; Panja, C.; Gurung, L.; Battamack, P. T.; Török, B.; Mathew, T.; Olah, G. A. Thermocontrolled Benzylimine–Benzaldimine Rearrangement Over

- Nafion-H Catalysts for Efficient Entry into  $\alpha$ -Trifluoromethylbenzylamines. *Tetrahedron Lett.* **2012**, *53*, 607–611.
46. Kokel, A.; Schäfer, C.; Török, B. Application of Microwave-Assisted Heterogeneous Catalysis in Sustainable Synthesis Design. *Green Chem.* **2017**, *19*, 3729–3751.
  47. Mooney, T.; Török, B. Microwave-Assisted Flow Systems in the Green Production of Fine Chemicals. In *Nontraditional Activation Methods in Green and Sustainable Applications: Microwaves; Ultrasounds; Photo-, Electro- and Mechanochemistry and High Hydrostatic Pressure*; Török, B., Schäfer, C., Eds.; Elsevier: Oxford, Cambridge, 2021; pp. 101–136 (chapter 3).
  48. Rickborn, B. The Pinacol Rearrangement. In *Comprehensive Organic Synthesis*; Trost, B. M., Fleming, I., Eds.; Vol. 3; Pergamon: Oxford, **1991**; pp. 721–732.
  49. Fittig, R. Ueber einige Derivate des Acetons. *Justus Liebig's Ann. Chem.* **1860**, *114*, 54–63.
  50. Gao, A. X.; Thomas, S. B.; Snyder, S. A. Pinacol and Semipinacol Rearrangements in Total Synthesis. In *Molecular Rearrangements in Organic Synthesis*; Rojas, C. M., Ed.; 1st ed.; Wiley: Hoboken, NJ, 2016; pp. 3–33 (chapter 1).
  51. Molnár, Á. The Pinacol Rearrangement. In *Fine Chemicals Through Heterogeneous Catalysis*; Sheldon, R. A., Van Bekkum, H., Eds.; 2001; pp. 232–241.
  52. Courtney, T. D.; Nikolakis, V.; Mpourmpakis, G.; Chen, J. G.; Vlachos, D. G. Liquid-Phase Dehydration of Propylene Glycol Using Solid-Acid Catalysts. *Appl. Catal. A Gen.* **2012**, *449*, 59–68.
  53. Toyoshi, Y.; Nakato, T.; Okuhara, T. Solid-Solid Catalysis by Inorganic Solid Acids: Pinacol Rearrangement Over a Heteropoly Compound. *Bull. Chem. Soc. Jpn* **1998**, *71*, 2817–2824.
  54. Nakato, T.; Toyoshi, Y.; Kimura, M.; Okuhara, T. Unique Catalysis of an Acidic Salt of Heteropoly Acid, Cs<sub>2.5</sub>H<sub>0.5</sub>PW<sub>12</sub>O<sub>40</sub>, Consisting of Microcrystallites. *Catal. Today* **1999**, *52*, 23–28.
  55. Gutierrez, E.; Ruiz-Hitzky, E. In *Pillared Layered Structures: Current Trends and Applications*; Mitchell, E. V., Ed.; Elsevier: London, New York, 1990; p. 199.
  56. Toyoshi, Y.; Nakato, T.; Tamura, R.; Takahashi, H.; Tsue, H.; Hirao, K.-I.; Okuhara, T. Solid-Solid Catalysis by Ultrafine Crystallites of Heteropoly Compound for Pinacol Rearrangement. *Chem. Lett.* **1998**, 135–136.
  57. Jurado-Gonzalez, M.; Ou, D. L.; Ormsby, B.; Sullivan, A. C.; Wilson, J. R. H. A New Solid Acid Catalyst: The First Phosphonate and Phosphonic Acid Functionalized Microporous Polysilsesquioxanes. *Chem. Commun.* **2001**, 67–68.
  58. Upadhyaya, D. J.; Samant, S. D. A Facile and Efficient Pinacol-Pinacolone Rearrangement of Vicinal Diols Using ZnCl<sub>2</sub> Supported on Silica as a Recyclable Catalyst. *Appl. Catal. A Gen.* **2008**, *340*, 42–51.
  59. Saritha, S. R.; Shamshuddin, S. Z. M.; D'Souza, J. Q.; Mubark, N. M. Cordierite Honeycomb Supported Mo(VI)/ZrO<sub>2</sub> for Microwave Assisted Pinacol-Pinacolone Rearrangement. *Ind. J. Chem., Section A: Inorg., Bio-inorg., Phys., Theoret. Anal. Chem.* **2020**, *59A*, 181–188.
  60. Ten Brink, G.-J.; Arends, I. W. C. E.; Sheldon, R. A. The Baeyer–Villiger Reaction: New Developments Toward Greener Procedures. *Chem. Rev.* **2004**, *104*, 4105–4124.
  61. Miholilovic, M. D.; Rudroff, G.; Grotz, B. Enantioselective Baeyer–Villiger oxidations. *Curr. Org. Chem.* **2004**, *8*, 1057–1069.
  62. Punniyamurthy, T.; Velusamy, S.; Iqbal, J. Recent Advances in Transition Metal Catalyzed Oxidation of Organic Substrates With Molecular Oxygen. *Chem. Rev.* **2005**, *105*, 2329–2364.
  63. Jimenez-Sanchidrian, C.; Ruiz, J. R. The Baeyer–Villiger Reaction on Heterogeneous Catalysts. *Tetrahedron* **2008**, *64*, 2011–2026.

64. Tang, Z.; Xiao, J.; Li, F.; Ma, Z.; Wang, L.; Niu, F.; Sun, X. Cobalt-Tetraamide-Phthalocyanine Immobilized on Fe<sub>3</sub>O<sub>4</sub>/Chitosan Microspheres as an Efficient Catalyst for Baeyer-Villiger Oxidation. *ACS Omega* **2020**, *5*, 10451–10458.
65. Sakai, T.; Watanabe, M.; Ohkado, R.; Arakawa, Y.; Imada, Y.; Iida, H. Flavinium and Alkali-Metal Assembly on Sulfated Chitin: A Heterogeneous Supramolecular Catalyst for H<sub>2</sub>O<sub>2</sub>-Mediated Oxidation. *ChemSusChem* **2019**, *12*, 1640–1645.
66. Markiton, M.; Ciemiega, A.; Maresz, K.; Szelwicka, A.; Mrowiec-Bialon, J.; Chrobok, A. Water-Tolerant Solid Lewis-Acid Sites: Baeyer-Villiger Oxidation With Hydrogen Peroxide in the Presence of Gallium-Based Silica Catalysts. *New J. Chem.* **2018**, *42*, 13602–13611.
67. Yang, X.; Jiang, Y.; Li, Y.; Xu, X.; Li, D.; Lin, K. Mesoporous Silica Beads Containing Active and Stable Tin Species for the Baeyer-Villiger Oxidations of Cyclic Ketones. *Microporous Mesoporous Mater.* **2017**, *253*, 40–48.
68. Modi, C. K.; Solanki, N.; Vithalani, R.; Patel, D. Baeyer-Villiger Oxidation of Cyclopentanone Over Zeolite Y Entrapped Transition Metal-Schiff Base Complexes. *Appl. Organomet. Chem.* **2018**, *32*, 3910.
69. Mehta, J. P.; Parmar, D. K.; Nakum, H. D.; Godhani, D. R.; Desai, N. C. Synthesis, Characterization and Catalytic Activity of Zeolite-Y Immobilized Oxovanadium Complex on Bayer-Villiger Oxidation. *Microporous Mesoporous Mater.* **2017**, *247*, 198–207.
70. Mehta, J. P.; Parmar, D. K.; Godhani, D. R.; Nakum, H. D.; Desai, N. C. Heterogeneous Catalysts Hold the Edge Over Homogeneous Systems: Zeolite-Y Encapsulated Complexes for Baeyer-Villiger Oxidation of Cyclohexanone. *J. Mol. Catal. A Chem.* **2016**, *421*, 178–188.
71. Zhu, Z.; Xu, H.; Jiang, J.; Liu, X.; Ding, J.; Wu, P. Postsynthesis of FAU-type Stannosilicate as Efficient Heterogeneous Catalyst for Baeyer-Villiger Oxidation. *Appl. Catal. A Gen.* **2016**, *519*, 155–164.
72. Dutta, B.; Jana, S.; Bhunia, S.; Honda, H.; Koner, S. Heterogeneous Baeyer-Villiger Oxidation of Cyclic Ketones Using Tert-BuOOH as Oxidant. *Appl. Catal. A Gen.* **2010**, *382*, 90–98.
73. Markiton, M.; Boncel, S.; Janas, D.; Chrobok, A. Highly Active Nanobiocatalyst from Lipase Noncovalently Immobilized on Multiwalled Carbon Nanotubes for Baeyer-Villiger Synthesis of Lactones. *ACS Sustain. Chem. Eng.* **2017**, *5*, 1685–1691.
74. Llamas, R.; Jiménez-Sanchidrián, C.; Rafael Ruiz, J. Heterogeneous Baeyer-Villiger Oxidation of Ketones With H<sub>2</sub>O<sub>2</sub>/Nitrile, Using Mg/Al Hydrotalcite as Catalyst. *Tetrahedron* **2007**, *63*, 1435–1439.
75. Li, X.; Cao, R.; Lin, Q. Solvent-free Baeyer-Villiger Oxidation With H<sub>2</sub>O<sub>2</sub> as Oxidant Catalyzed by Multi-SO<sub>3</sub>H Functionalized Heteropolyanion-Based Ionic Hybrids. *Catal. Commun.* **2015**, *63*, 79–83.
76. Martins, L. M. D. R. S.; Hazra, S.; Guedes da Silva, M. F. C.; Pombeiro, A. J. L. A Sulfonated Schiff Base Dimethyltin(IV) Coordination Polymer: Synthesis, Characterization and Application as a Catalyst for Ultrasound- or Microwave-Assisted Baeyer-Villiger Oxidation Under Solvent-Free Conditions. *RSC Adv.* **2016**, *6*, 78225–78233.
77. Yamashita, Y.; Yasukawa, T.; Yoo, W.-J.; Kitanosono, T.; Kobayashi, S. Catalytic Enantioselective Aldol Reactions. *Chem. Soc. Rev.* **2018**, *47*, 4388–4480.
78. Mandal, S. W.; Mandiál, S. A.; Gosh, S. K.; Gosh, A.; Saha, R.; Banerjee, S.; Saha, B. Review of the Aldol reaction. *Synth. Commun.* **2016**, *46*, 1327–1342.
79. Ding, S.; Liu, X.; Xiao, W.; Li, M.; Pan, Y.; Hu, J.; Zhang, N. 1,1,3,3-Tetramethylguanidine Immobilized on Graphene Oxide: A Highly Active and Selective Heterogeneous Catalyst for Aldol Reaction. *Catal. Commun.* **2017**, *92*, 5–9.

80. Rodríguez-Llansola, F.; Miravet, J. F.; Escuder, B. A Supramolecular Hydrogel as a Reusable Heterogeneous Catalyst for the Direct Aldol Reaction. *Chem. Commun.* **2009**, 7303–7305.
81. Xie, Y.; Sharma, K. K.; Anan, A.; Wang, G.; Biradar, A. V.; Asefa, T. Efficient Solid-Base Catalysts for Aldol Reaction by Optimizing the Density and Type of Organoamine Groups on Nanoporous Silica. *J. Catal.* **2009**, *265*, 131–140.
82. Ohta, H.; Uozumi, Y.; Yamada, Y. M. A. Highly Active Copper-Network Catalyst for the Direct Aldol Reaction. *Chem. Asian J.* **2011**, *6*, 2545–2549.
83. Amarasekara, A. S.; Wiredu, B.; Grady, T. L.; Obregon, R. G.; Margetić, R. G. Solid Acid Catalyzed Aldol Dimerization of Levulinic Acid for the Preparation of C10 Renewable Fuel and Chemical Feedstocks. *Catal. Commun.* **2019**, *124*, 6–11.
84. Zhai, D.; Cao, C.; Shao, B.; Liu, D.; Song, W. Preparation of Ga<sub>2</sub>O<sub>3</sub> Doped Sulfonated Tin Oxides as a Highly Active and Recyclable Heterogeneous Solid Acid Catalyst for Aldol Reactions. *J. Nanosci. Nanotechnol.* **2019**, *19*, 3658–3662.
85. Olmos, A.; Alix, A.; Sommer, J.; Pale, P. Sc-III-Doped Zeolites as New Heterogeneous Catalysts: Mukaiyama Aldol Reaction. *Chem. Eur. J.* **2009**, *15*, 11229–11234.
86. Srivastava, R. An Efficient, Eco-Friendly Process for Aldol and Michael Reactions of Trimethylsilyl Enolate Over Organic Base-Functionalized SBA-15 Catalysts. *J. Mol. Catal. A Chem.* **2007**, *264*, 146–152.
87. Ishitani, H.; Iwamoto, M. Selective Aldol Reactions of Acetals on Mesoporous Silica Catalyst. *Tetrahedron Lett.* **2003**, *44*, 299–301.
88. Ito, S.; Yamaguchi, H.; Kubota, Y.; Asami, M. Mukaiyama Aldol Reaction Catalyzed by Mesoporous Aluminosilicate. *Chem. Lett.* **2009**, *38*, 700–701.
89. Raju, S.; Ponrathnam, S.; Rajan, C.; Srinivasan, K. Mukaiyama Aldol Reaction of a Silyl Enol Ether With Aldehydes Over Solid Sulphated Zirconia With Preferential Syn Selectivity. *Synlett* **1996**, 239–240.
90. Takehira, S.; Masui, Y.; Onaka, M. The Mukaiyama Aldol Reactions for Congested Ketones Catalyzed by Solid Acid of Tin(IV) Ion-Exchanged Montmorillonite. *Chem. Lett.* **2014**, *43*, 498–500.
91. Mackie, R. K.; Smith, D. M.; Aitken, R. A. *Guidebook to Organic Synthesis* (chapter 5); Pearson: Harlow, 1999; p. 69.
92. Qin, W.; Long, S.; Panunzio, M.; Biondi, S. Schiff Bases: A Short Survey on an Evergreen Chemistry Tool. *Molecules* **2013**, *18*, 12264–12289.
93. Uddin, M. N.; Ahmed, S. S.; Alam, M. R. REVIEW: Biomedical Applications of Schiff Base Metal Complexes. *J. Coord. Chem.* **2020**, *73*, 3109–3149.
94. Hellwig, M.; Henle, T. Baking, Ageing, Diabetes: A Short History of the Maillard Reaction. *Angew. Chem. Int. Ed.* **2014**, *53*, 10316–10329.
95. Cho, H.; Madden, R.; Nisanci, B.; Török, B. The Paal-Knorr Reaction Revisited. A Catalyst and Solvent-Free Synthesis of Underivatized and N-Substituted Pyrroles. *Green Chem.* **2015**, *17*, 1088–1099.
96. Schäfer, C.; Nisanci, B.; Bere, M. P.; Dastan, A.; Török, B. Heterogeneous Catalytic Reductive Amination of Carbonyl Compounds with Ni-Al Alloy in Water as Solvent and Hydrogen Source. *Synthesis* **2016**, *48*, 3127–3133.
97. Dhakshinamoorthy, A.; Opanasenko, M.; Cejka, J.; Garcia, H. Metal Organic Frameworks as Solid Catalysts in Condensation Reactions of Carbonyl Groups. *Adv. Synth. Catal.* **2013**, *355*, 247–268.
98. Liu, Q.; Tan, J.-Y.; Zhang, J.-Y.; Zhang, N.; Liu, Z. J. Heterometallic Metal-Organic Frameworks: Two-Step Syntheses, Structures and Catalytic for Imine Synthesis. *Microporous Mesoporous Mater.* **2021**, *310*, 110626.

99. Yang, P.; Wang, J.; Shang, Y.; Yang, J. Synthesis, Characterization and Catalytic Performance of a Novel Magnetic  $\text{SO}_4^{2-}\text{-Y}_2\text{O}_3\text{-Fe}_3\text{O}_4\text{-ZrO}_2$  Solid Acid Catalyst. *React. Kinet. Catal. Lett.* **2008**, *93*, 85–92.
100. Abid, M.; Savolainen, M.; Landge, S.; Hu, J.; Prakash, G. K. S.; Olah, G. A.; Török, B. Synthesis of Trifluoromethyl-Imines by Solid Acid/Superacid Catalyzed Microwave Assisted Approach. *J. Fluor. Chem.* **2007**, *128*, 587–594.
101. Varghese, A.; Nizam, A.; Kulkarni, R.; George, L. Amberlite IR-120H: An Improved Reusable Solid Phase Catalyst for the Synthesis of Nitriles Under Solvent Free Microwave Irradiation. *Eur. J. Chem.* **2012**, *3*, 247–251.
102. Kargar, P. G.; Aryanejad, S.; Bagherzade, G. Simple Synthesis of the Novel Cu-MOF Catalysts for the Selective Alcohol Oxidation and the Oxidative Cross-Coupling of Amines and Alcohols. *Appl. Organomet. Chem.* **2020**, *34*, 5965.
103. Cao, X.; Qin, J.; Gou, G.; Li, J.; Wu, W.; Luo, S.; Luo, Y.; Dong, Z.; Ma, J.; Long, Y. Continuous Solvent-Free Synthesis of Imines Over  $\text{uip-}\gamma\text{-Al}_2\text{O}_3\text{-CeO}_2$  Catalyst in a Fixed Bed Reactor. *Appl. Catal. B Environ.* **2020**, *272*, 118958.
104. Du, S.; Zhang, C.; Jiang, Y.; Jiang, P.; Leng, Y. Au Nanoparticle-Immobilized L-Cysteine-Paired Porous Ionic Copolymer as an Efficient Catalyst for Additive-Free Oxidative Coupling of Alcohols and Amines. *Catal. Commun.* **2019**, *129*, 105746.
105. Wu, S.; Zhang, H.; Cao, Q.; Zhao, Q.; Fang, W. Efficient Imine Synthesis Via Oxidative Coupling of Alcohols With Amines in an Air Atmosphere Using a Mesoporous Manganese-Zirconium Solid Solution Catalyst. *Catal. Sci. Technol.* **2021**, *11*, 810–822.
106. Tamura, M.; Tomishige, K. Scope and Reaction Mechanism of  $\text{CeO}_2$ -Catalyzed One-Pot Imine Synthesis From Alcohols and Amines. *J. Catal.* **2020**, *389*, 285–296.
107. Zhong, M.; Zhang, S.; Dong, A.; Sui, Z.; Feng, L.; Chen, Q. Cu-MOF/Au–Pd Composite Catalyst: Preparation and Catalytic Performance Evaluation. *J. Mater. Sci.* **2020**, *55*, 10388–10398.
108. Tamura, M.; Li, Y.; Tomishige, K. One-Pot Imine Synthesis From Methylarenes and Anilines Under Air Over Heterogeneous Cu-Oxide-Modified  $\text{CeO}_2$  Catalyst. *Chem. Commun.* **2020**, *56*, 7337–7340.
109. Landge, S. M.; Atanassova, V.; Thimmaiah, M.; Török, B. Microwave-Assisted Oxidative Coupling of Amines to Imines on Solid Acid Catalysts. *Tetrahedron Lett.* **2007**, *48*, 5161–5164.
110. Atanassova, V.; Ganno, K.; Kulkarni, A.; Landge, S. M.; Curtis, S.; Foster, M.; Török, B. Oxidative Coupling of Amines to Imines on K-10 Montmorillonite: A Mechanistic Study. *Appl. Clay Sci.* **2011**, *53*, 220–226.
111. Venu, B.; Shirisha, V.; Vishali, B.; Naresh, G.; Kishore, R.; Sreedhar, I.; Venugopal, A. A Cu-BTC Metal–Organic Framework (MOF) as an Efficient Heterogeneous Catalyst for the Aerobic Oxidative Synthesis of Imines From Primary Amines Under Solvent Free Conditions. *New J. Chem.* **2020**, *44*, 5972–5979.
112. Chutimasakul, T.; Nakhonpanom, P. N.; Tirdtrakool, W.; Intanin, A.; Bunchuay, T.; Chantivas, R.; Tantirungrotechai, J. Uniform Cu/Chitosan Beads as a Green and Reusable Catalyst for Facile Synthesis of Imines Via Oxidative Coupling Reaction. *RSC Adv.* **2020**, *10*, 21009–21018.
113. Dasgupta, S.; Morzhina, E.; Schäfer, C.; Mhadgut, S. C.; Prakash, G. K. S.; Török, B. Synthesis of Chiral Trifluoromethyl Benzylamines by Heterogeneous Catalytic Reductive Amination. *Top. Catal.* **2016**, *59*, 1207–1213.
114. Gumus, I.; Ruzgar, A.; Karatas, Y.; Gülcan, M. Highly Efficient and Selective One-Pot Tandem Imine Synthesis Via Amine-Alcohol Cross-Coupling Reaction Catalysed by Chromium-Based MIL-101 Supported Au Nanoparticles. *Mol. Catal.* **2021**, *501*, 111363.

115. Abid, M.; Spaeth, A.; Török, B. Solvent-Free Solid Acid Catalyzed Electrophilic Annulations: A New Green Approach for the Synthesis of Substituted Five-Membered N-Heterocycles. *Adv. Synth. Catal.* **2006**, *348*, 2191–2196.
116. Abid, M.; Teixeira, L.; Török, B. Triflic Acid Controlled Successive Annellation of Aromatic Sulfonamides: An Efficient One-Pot Synthesis of N-sulfonyl Pyrroles, Indoles and Carbazoles. *Tetrahedron Lett.* **2007**, *48*, 4047–4050.
117. Abid, M.; DePaolis, O.; Török, B. A Novel One-Pot Synthesis of N-Acylindoles from Primary Aromatic Amides. *Synlett* **2008**, 410–413.
118. Kulkarni, A.; Török, B. Microwave-Assisted Multicomponent Domino Cyclization-Aromatization: An Efficient Approach for the Synthesis of Substituted Quinolines. *Green Chem.* **2010**, *12*, 875–878.
119. De Paolis, O.; Teixeira, L.; Török, B. Synthesis of Quinolines by a Solid Acid-Catalyzed Microwave-Assisted Domino Cyclization-Aromatization Approach. *Tetrahedron Lett.* **2009**, *50*, 2939–2942.
120. Borkin, D. A.; Puscau, M.; Carlson, A.; Wheeler, A. K.; Török, B.; Dembinski, R. Synthesis of Diversely 1,3,5-Substituted Pyrazoles Via 5-Exo-Dig Cyclization. *Org. Biomol. Chem.* **2012**, *10*, 4505–4508.
121. Rudnitskaya, A.; Borkin, D. A.; Huynh, K.; Török, B.; Stieglitz, K. Rational Design, Synthesis and Potency of N-Substituted-Indoles, Pyrroles and Triaryl-Pyrazoles as Potential Fructose 1,6-Bisphosphatase Inhibitors. *ChemMedChem* **2010**, *5*, 384–389.
122. Landge, S. M.; Török, B. Synthesis of 1,3,5-Triphenylpyrazole by a Heterogeneous Catalytic Domino Reaction. In *Experiments in Green and Sustainable Chemistry*; Roesky, H. W., Kennepohl, D., Eds.; Wiley-VCH: New York-Weinheim, **2009**; pp. 45–49.
123. Cho, H.; Török, F.; Török, B. Energy Efficiency of Heterogeneous Catalytic Microwave-assisted Organic Reactions. *Green Chem.* **2014**, *16*, 3623–3634.
124. Kulkarni, A.; Abid, M.; Török, B.; Huang, X. A Direct Synthesis of  $\beta$ -Carbolines Via a Three-Step One-Pot Domino Approach With Bifunctional Pd/C/K-10 Catalyst. *Tetrahedron Lett.* **2009**, *50*, 1791–1794.
125. Young, J.; Schäfer, C.; Solan, A.; Baldrice, A.; Belcher, M.; Nişancı, B.; Wheeler, K. A.; Trivedi, E.; Török, B.; Dembinski, R. Regio- and Stereoselective Hydroamination of alk-3-Ynones With *o*-Phenylenediamines. Synthesis of Diversely Substituted 3*H*-1,5-Benzodiazepines Via 3-Amino-2-Alkenones. *RSC Adv.* **2016**, *6*, 107081–107093.
126. Landge, S. M.; Török, B. Synthesis of Condensed Benzo[*N,N'*]-Heterocycles by Microwave-Assisted Solid Acid Catalysis. *Catal. Lett.* **2008**, *122*, 338–343.
127. Borkin, D. A.; Morzhina, E.; Datta, S.; Rudnitskaya, A.; Sood, A.; Török, M.; Török, B. Heteropoly Acid-Catalyzed Microwave-Assisted Three-Component Aza-Diels-Alder Cyclizations: Diastereoselective Synthesis of Potential Drug Candidates for Alzheimer's Disease. *Org. Biomol. Chem.* **2011**, *9*, 1394–1401.
128. Li, B.; Wang, Y.; Chi, Q.; Yuan, Z.; Liu, B.; Zhang, Z. Direct Synthesis of Imines From Nitro Compounds and Biomass-Derived Carbonyl Compounds Over Nitrogen-Doped Carbon Material Supported Ni Nanoparticles. *New J. Chem.* **2021**, *45*, 4464–4471.
129. Yadav, J.; Reddy, B.; Basak, A.; Visali, B.; Narsaiah, A.; Nagaiah, K. Phosphane-Catalyzed Knoevenagel Condensation: A Facile Synthesis of Alpha-Cyanoacrylates and Alpha-Cyanoacrylonitriles. *Eur. J. Org. Chem.* **2004**, 546–551.
130. Nemati, F.; Heravi, M. M.; Rad, R. S. Nano-Fe<sub>3</sub>O<sub>4</sub> Encapsulated-Silica Particles Bearing Sulfonic Acid Groups as a Magnetically Separable Catalyst for Highly Efficient Knoevenagel Condensation and Michael Addition Reactions of Aromatic Aldehydes with 1,3-Cyclic Diketones. *Chin. J. Catal.* **2012**, *33*, 1825–1831.

131. Ribeiro, S. M.; Serra, A. C.; Rocha Gonsalves, A. M. D. Silica Grafted Polyethylenimine as Heterogeneous Catalyst for Condensation Reactions. *Appl. Catal. A Gen.* **2011**, *399*, 126–133.
132. Kantam, M.; Bharathi, B. Mn(III) Salen Catalyst for Knoevenagel Condensation—A Novel Heterogeneous System. *Catal. Lett.* **1998**, *55*, 235–237.
133. Angelescu, E.; Pavel, O.; Birjega, R.; Zavoianu, R.; Costentin, G.; Che, M. Solid Base Catalysts Obtained From Hydrotalcite Precursors, for Knoevenagel Synthesis of Cinamic Acid and Coumarin Derivatives. *Appl. Catal. A Gen.* **2006**, *308*, 13–18.
134. Nguyen, L. T. L.; Le, K. K. A.; Truong, H. X.; Phan, N. T. S. Metal-Organic Frameworks for Catalysis: The Knoevenagel Reaction Using Zeolite Imidazolate Framework ZIF-9 as an Efficient Heterogeneous Catalyst. *Catal. Sci. Technol.* **2012**, *2*, 521–528.
135. Hasegawa, S.; Horike, S.; Matsuda, R.; Furukawa, S.; Mochizuki, K.; Kinoshita, Y.; Kitagawa, S. Three-Dimensional Porous Coordination Polymer Functionalized With Amide Groups Based on Tridentate Ligand: Selective Sorption and Catalysis. *J. Am. Chem. Soc.* **2007**, *129*, 2607–2614.
136. Das, A.; Anbu, N.; Dhakshinamoorthy, A.; Biswas, S. A Highly Catalytically Active Hf(IV) Metal-Organic Framework for Knoevenagel Condensation. *Microporous Mesoporous Mater.* **2019**, *284*, 459–467.
137. Kuarm, B. S.; Madhav, J. V.; Rajitha, B. Xanthan Sulfuric Acid: An Efficient and Recyclable Solid Acid Catalyst for Pechmann Condensation. *Synth. Commun.* **2012**, *42*, 1770–1777.
138. Torviso, R.; Mansilla, D.; Belizan, A.; Alesso, E.; Moltrasio, G.; Vazquez, P.; Pizzio, L.; Blanco, M.; Caceres, C. Catalytic Activity of Keggin Heteropolycompounds in the Pechmann Reaction. *Appl. Catal. A Gen.* **2008**, *339*, 53–60.
139. Sabou, R.; Hoelderich, W.; Ramprasad, D.; Weinand, R. Synthesis of 7-Hydroxy-4-Methyleoumarin Via the Pechmann Reaction with Amberlyst Ion-Exchange Resins as Catalysts. *J. Catal.* **2005**, *232*, 34–37.
140. Singhal, S.; Jain, S. L.; Sain, B. MoO<sub>3</sub>/Al<sub>2</sub>O<sub>3</sub>: An Efficient and Reusable Heterogeneous Catalyst for Solvent-Free Synthesis of Coumarins Via Pechmann Condensation. *Heterocycles* **2008**, *75*, 1205–1211.
141. Opanasenko, M.; Shamzhy, M.; Cejka, J. Solid Acid Catalysts for Coumarin Synthesis by the Pechmann Reaction: MOFs Versus Zeolites. *ChemCatChem* **2013**, *5*, 1024–1031.
142. Ghodke, S.; Chudasama, U. Solvent Free Synthesis of Coumarins Using Environment Friendly Solid Acid Catalysts. *Appl. Catal. A Gen.* **2013**, *453*, 219–226.
143. Mokhtary, M.; Najafizadeh, F. Polyvinylpyrrolidone-Bound Boron Trifluoride (PVPP-BF<sub>3</sub>); a Mild and Efficient Catalyst for Synthesis of 4-Metyl Coumarins Via the Pechmann Reaction. *C. R. Chim.* **2012**, *15*, 530–532.
144. Albadi, J.; Shirini, F.; Abasi, J.; Armand, N.; Motaharizadeh, T. A Green, Efficient and Recyclable Poly(4-Vinylpyridine)-Supported Copper Iodide Catalyst for the Synthesis of Coumarin Derivatives Under Solvent-Free Conditions. *C. R. Chim.* **2013**, *16*, 407–411.
145. Paul, S.; Gupta, M. A Simple and Efficient Method for Selective Single Aldol Condensation Between Arylaldehydes and Acetone. *Synth. Commun.* **2005**, *35*, 213–222.
146. Zeidan, R. K.; Davis, M. E. The Effect of Acid-Base Pairing on Catalysis: An Efficient Acid-Base Functionalized Catalyst for Aldol Condensation. *J. Catal.* **2007**, *247*, 379–382.
147. Kim, J.; Jin, S. H.; Kang, K.; Chung, Y.; Lee, C. Preparation of Chemically Uniform and Monodisperse Microparticles as Highly Efficient Solid Acid Catalysts for Aldol Condensation. *Chem. Eng. Sci.* **2018**, *175*, 168–174.
148. Climent, M.; Corma, A.; Fornes, V.; Guil-Lopez, R.; Iborra, S. Aldol Condensations on Solid Catalysts: A Cooperative Effect Between Weak Acid and Base Sites. *Adv. Synth. Catal.* **2002**, *344*, 1090–1096.

149. Ganga, V. S. R.; Abdi, S. H. R.; Kureshy, R. I.; Khan, N. H.; Bajaj, H. C. *p*-Toluene Sulfonic Acid (PTSA)-MCM-41 as a Green, Efficient and Reusable Heterogeneous Catalyst for the Synthesis of Jasminaldehyde Under Solvent-Free Condition. *J. Mol. Catal. A. Chem.* **2016**, *420*, 264–271.
150. Sudheesh, N.; Sharma, S. K.; Shukla, R. S. Chitosan as An Eco-Friendly Solid Base Catalyst for the Solvent-Free Synthesis of Jasminaldehyde. *J. Mol. Catal. A Chem.* **2010**, *321*, 77–82.
151. Komatsu, T.; Mitsuhashi, M.; Yashima, T. Aldol Condensation Catalyzed by Acidic Zeolites. Impact of Zeolites and Other Porous Materials on the New Technologies at the Beginning of the New Millennium, Pts A and B, *Stud. Surf. Sci. Catal.* **2002**, *142*, 667–674.
152. Rao, K.; Gravelle, M.; Valente, J.; Figueras, F. Activation of Mg-Al Hydrotalcite Catalysts for Aldol Condensation Reactions. *J. Catal.* **1998**, *173*, 115–121.
153. Zali, A.; Ghani, K.; Shokrolahi, A.; Keshavarz, M. H. Carbon-Based Solid Acid as an Efficient and Reusable Catalyst for Cross-Aldol Condensation of Ketones With Aromatic Aldehydes Under Solvent-Free Conditions. *Chin. J. Catal.* **2008**, *29*, 602–606.
154. Nakhaei, A.; Morsali, A.; Davoodnia, A. An Efficient Green Approach to Aldol and Cross-Aldol Condensations of Ketones with Aromatic Aldehydes Catalyzed by Nanometasilica Disulfuric Acid in Water. *Russ. J. Gen. Chem.* **2017**, *87*, 1073–1078.
155. Rawal, K.; Mishra, M. K.; Dixit, M.; Srinivasarao, M. Microwave Assisted Solvent Free Synthesis Of Alpha,Alpha'-Bis (Arylidene) Cycloalkanones by Sulfated Zirconia Catalyzed Cross Aldol Condensation of Aromatic Aldehydes and Cycloalkanones. *J. Ind. Eng. Chem.* **2012**, *18*, 1474–1481.
156. Barrett, C. J.; Chheda, J. N.; Huber, G. W.; Dumesic, J. A. Single-Reactor Process for Sequential Aldol-Condensation and Hydrogenation of Biomass-Derived Compounds in Water. *Appl. Catal. B Environ.* **2006**, *66*, 111–118.
157. Kikhtyanin, O.; Čapek, L.; Tišler, Z.; Velvarská, R.; Panasewicz, A.; Diblíková, P.; Kubička, D. Physico-Chemical Properties of MgGa Mixed Oxides and Reconstructed Layered Double Hydroxides and Their Performance in Aldol Condensation of Furfural and Acetone. *Front. Chem.* **2018**, *6*, 176.
158. Dewa, T.; Saiki, T.; Aoyama, Y. Enolization and Aldol Reactions of Ketone with a La<sup>3+</sup>-Immobilized Organic Solid in Water. A Microporous Enolase Mimic. *J. Am. Chem. Soc.* **2001**, *123*, 502–503.
159. Brun, E.; Safer, A.; Carreaux, F.; Bourahla, K.; L'helgoua'ch, J. M.; Bazureau, J. P.; Villalgorido, J. M. Microwave-Assisted Condensation Reactions of Acetophenone Derivatives and Activated Methylene Compounds with Aldehydes Catalyzed by Boric Acid Under Solvent-Free Conditions. *Molecules* **2015**, *20*, 11617–11631.
160. Rocchi, D.; González, J. F.; Menéndez, J. C. Montmorillonite Clay-Promoted, Solvent-Free Cross-Aldol Condensations under Focused Microwave Irradiation. *Molecules* **2014**, *19*, 7317–7326.
161. Hara, M.; Yoshida, T.; Takagaki, A.; Takata, T.; Kondo, J.; Hayashi, S.; Domen, K. A Carbon Material as a Strong Protonic Acid. *Angew. Chem. Int. Edit.* **2004**, *43*, 2955–2958.
162. Huang, Y.; Fu, Y. Hydrolysis of Cellulose to Glucose by Solid Acid Catalysts. *Green Chem.* **2013**, *15*, 1095–1111.
163. Pang, J.; Wang, A.; Zheng, M.; Zhang, T. Hydrolysis of Cellulose Into Glucose Over Carbons Sulfonated at Elevated Temperatures. *Chem. Commun.* **2010**, *46*, 6935–6937.
164. Onda, A.; Ochi, T.; Yanagisawa, K. Selective Hydrolysis of Cellulose Into Glucose Over Solid Acid Catalysts. *Green Chem.* **2008**, *10*, 1033–1037.
165. Suganuma, S.; Nakajima, K.; Kitano, M.; Yamaguchi, D.; Kato, H.; Hayashi, S.; Hara, M. Hydrolysis of Cellulose by Amorphous Carbon Bearing SO<sub>3</sub>H, COOH, and OH groups. *J. Am. Chem. Soc.* **2008**, *130*, 12787–12793.

590 Heterogeneous catalysis in sustainable synthesis

166. Van de Vyver, S.; Peng, L.; Geboers, J.; Schepers, H.; de Clippel, F.; Gommès, C. J.; Goderis, B.; Jacobs, P. A.; Sels, B. F. Sulfonated Silica/Carbon Nanocomposites as Novel Catalysts for Hydrolysis of Cellulose to Glucose. *Green Chem.* **2010**, *12*, 1560–1563.
167. Lai, D.; Deng, L.; Guo, Q.; Fu, Y. Hydrolysis of Biomass by Magnetic Solid Acid. *Energy Environ. Sci.* **2011**, *4*, 3552–3557.
168. Green, T. W.; Wuts, P. G. M. *Protective Groups in Organic Synthesis*, 2nd ed.; Wiley: New York, 1991.
169. Kocienski, P. J. *Protective Groups*; Thieme: Stuttgart, New York, 1994.
170. Smith, M.; March, J. *March's Advanced Organic Chemistry*, 6th ed.; Wiley: Hoboken, NJ, 2007.
171. Wuts, P. *Greene's Protective Groups in Organic Synthesis*, 5th ed.; Wiley & Sons, 2014.
172. Sartori, G.; Ballini, R.; Bigi, F.; Bosica, G.; Maggi, R.; Righi, P. Protection (and Deprotection) of Functional Groups in Organic Synthesis by Heterogeneous Catalysis. *Chem. Rev.* **2004**, *104*, 199–250.
173. Changmaia, B.; Rokhum, L. Nanostructured Catalysts in the Protection and Deprotection of Hydroxyl and Thiol Groups. In *Advanced Heterogeneous Catalysts, Volume 1: Applications at the Nano-Scale*; ACS Symposium Series, Vol. 1359; 2020; pp. 129–150.
174. Deutsch, J.; Martin, A.; Lieske, H. Investigations on Heterogeneously Catalysed Condensations of Glycerol to Cyclic Acetals. *J. Catal.* **2007**, *245*, 428–435.
175. Molnár, Á.; Beregszászi, T. Mild and Efficient Tetrahydropyranlation and Deprotection of Alcohols Catalyzed by Heteropoly Acids. *Tetrahedron Lett.* **1996**, *37*, 8597–8600.
176. Xavier, N. M.; Lucas, S. D.; Rauter, A. P. Zeolites as Efficient Catalysts for Key Transformations in Carbohydrate Chemistry. *J. Mol. Catal. A Chem.* **2009**, *305*, 84–89.
177. Rauter, A. P.; Xavier, N. M.; Lucas, S. D.; Santos, M. Zeolites and Other Silicon-Based Promoters in Carbohydrate Chemistry. *Adv. Carbohydr. Chem. Biochem.* **2010**, *63*, 29–99.
178. Chari, M. A.; Syamasundar, K. Polymer-Supported Ferric Chloride as a Heterogeneous Catalyst for Chemoselective Deprotection of Acetonides. *Synthesis* **2005**, 708–710.
179. Ghafari, H.; Paravand, F.; Rashidizadeh, A. Nano Fe<sub>3</sub>O<sub>4</sub>@ZrO<sub>2</sub>/SO<sub>4</sub><sup>2-</sup>: A Highly Efficient Catalyst for the Protection and Deprotection of Hydroxyl Groups Using HMDS Under Solvent-Free Condition. *Phosphorus Sulfur Silicon Rel. Elements* **2017**, *192*, 129–135.
180. Tanaka, S.; Seki, T.; Minematsu, Y.; Kitamura, M. [CpRu(η<sup>3</sup>-C<sub>3</sub>H<sub>5</sub>)(2-Pyridinecarboxylato)] PF<sub>6</sub> Complex Supported on a Ferromagnetic Microsize Particle Fe<sub>3</sub>O<sub>4</sub>@SiO<sub>2</sub>. In *Pacificchem 2010, International Chemical Congress of Pacific Basin Societies, Honolulu, HI, United States, December 15-20, 2010, ORGN-110*; 2010.
181. Datta, B.; Pasha, M. A. Chemoselective Protection and Deprotection of Aldehydes Using Solid-Supported Reagent (Silica Chloride) Under Solvent-Free Conditions. *Synth. Commun.* **2011**, *41*, 1160–1166.
182. Kshirsagar, S. W.; Patil, N. R.; Samant, S. D. Chemoselective Protection of Aldehydes in the Presence of Ketones Using RuPVP Complex as a Heterogeneous Catalyst. *Synth. Commun.* **2010**, *40*, 407–413.
183. Verma, S. K.; Sathe, M.; Kaushik, M. P. Chemoselective and Chemospecific Protection and Deprotection of a Carbonyl Group Using Polystyrene Divinylbenzene Sulfonic Acid. *Synth. Commun.* **2010**, *40*, 1701–1707.
184. Li, L.; Zhang, X.; Zhang, G.; Qu, G. Efficient and chemoselective deprotection of 1,1-diacetates using Fe<sub>2</sub>(SO<sub>4</sub>)<sub>3</sub>·x H<sub>2</sub>O as a heterogeneous catalyst. *J. Chem. Res.* **2004**, 39–40.
185. Franke, R.; Selent, D.; Börner, A. Applied Hydroformylation. *Chem. Rev.* **2012**, *112*, 5675–5732.

186. Zhuchkov, D. P.; Nenasheva, M. V.; Terenina, M. V.; Kardasheva, Y. S.; Gorbunov, D. N.; Karakhanov, E. A. Polymeric Heterogeneous Catalysts in the Hydroformylation of Unsaturated Compounds. *Petrol. Chem.* **2021**, *61*, 1–14.
187. Cornils, B.; Herrmann, W. A.; Rasch, M. Otto Roelen, Pioneer in Industrial Homogeneous Catalysis. *Angew. Chem. Int. Ed. Eng.* **1994**, *33*, 2144–2163.
188. Ana, R. A.; Peixoto, A. F.; Calvete, M. J. F.; Gois, P. M. P.; Pereira, M. M. Rhodium (I) N-Heterocyclic Carbene Complexes as Catalysts for Hydroformylation of Olefins: An Overview. *Curr. Org. Synth.* **2011**, *8*, 764–775.
189. Li, X.; Qin, T.; Li, L.; Wu, B.; Lin, T.; Zhong, L. One-Pot Synthesis of Acetals by Tandem Hydroformylation-Acetalization of Olefins Using Heterogeneous Supported Catalysts. *Catal. Lett.* **2021**, *151*, 2638–2646.
190. Zuyu, L.; Chen, J.; Chen, X.; Zhang, K.; Lv, Zhao, H.; Zhang, G.; Xie, C.; Zong, L.; Jia, X. Porous Organic Polymer Supported Rhodium as a Heterogeneous Catalyst for Hydroformylation of Alkynes to  $\alpha$ ,  $\beta$ -Unsaturated Aldehydes. *Chem. Commun.* **2019**, *55*, 13721–13724.
191. Verheyen, T.; Santillo, N.; Marinelli, D.; Petricci, E.; De Borggraeve, W. M.; Vaccaro, L.; Smet, M. An Effective and Reusable Hyperbranched Polymer Immobilized Rhodium-Catalyst for the Hydroformylation of Olefins. *ACS Appl. Polym. Mater.* **2019**, *1*, 1496–1504.
192. Jia, X.; Liang, Z.; Chen, J.; Lv, J.; Zhang, K.; Gao, M.; Zong, L.; Xie, C. Porous Organic Polymer Supported Rhodium as a Reusable Heterogeneous Catalyst for Hydroformylation of Olefins. *Org. Lett.* **2019**, *21*, 2147–2150.
193. Wang, Y.; Yan, L.; Li, C.; Jiang, M.; Wang, W.; Ding, Y. Highly Efficient Porous Organic Copolymer Supported Rh Catalysts for Heterogeneous Hydroformylation of Butenes. *Appl. Catal. A Gen.* **2018**, *551*, 98–105.
194. Li, C.; Yan, L.; Lu, L.; Xiong, K.; Wang, W.; Jiang, M.; Liu, J.; Song, X.; Zhan, Z.; Jiang, Z. D. Y. Single Atom Dispersed Rh-Biphephos & PPh<sub>3</sub>@Porous Organic Copolymers: Highly Efficient Catalysts for Continuous Fixed-Bed Hydroformylation of Propene. *Green Chem.* **2016**, *18*, 2995–3005.
195. Shi, Y.; Lu, Y.; Ren, T.; Li, J.; Hu, Q.; Hu, X.; Zhu, B.; Huang, W. Rh Particles Supported on Sulfated g-C<sub>3</sub>N<sub>4</sub>: A Highly Efficient and Recyclable Heterogeneous Catalyst for Alkene Hydroformylation. *Catalysts* **2020**, *10*, 1359.
196. Huang, N.; Liu, B.; Lan, X.; Wang, T. Insights into the Bimetallic Effects of a RhCo Catalyst for Ethene Hydroformylation: Experimental and DFT Investigations. *Ind. Eng. Chem. Res.* **2020**, *59*, 18771–18780.
197. Chen, L.; Tian, J.; Song, H.; Gao, Z.; Wei, H.; Wang, W.; Ren, W. Enhancing the Stability of the Rh/ZnO Catalyst by the Growth of ZIF-8 for the Hydroformylation of Higher Olefins. *RSC Adv.* **2020**, *10*, 34381–34386.
198. Amsler, J.; Sarma, B. B.; Agostini, G.; Prieto, G.; Plessow, P. N.; Studt, F. Prospects of Heterogeneous Hydroformylation with Supported Single Atom Catalysts. *J. Am. Chem. Soc.* **2020**, *142*, 5087–5096.
199. Shi, Y.; Ji, G.; Hu, Q.; Lu, Y.; Hu, X.; Zhu, B.; Huang, W. Highly Uniform Rh Nanoparticles Supported on Boron Doped g-C<sub>3</sub>N<sub>4</sub> as a Highly Efficient and recyclable catalyst for Heterogeneous Hydroformylation of Alkenes. *New J. Chem.* **2020**, *44*, 20–23.
200. Gorbunov, D. N.; Nenasheva, M. V.; Matsukevich, R. P.; Terenina, M. V.; Kardasheva, Y. S.; Karakhanov, E. A. Heterogeneous Catalyst Based on Phosphine-Containing Organic Polymer for Hydroformylation of Octene-1. *Petrol. Chem.* **2021**, *61*, 688–696.

592 Heterogeneous catalysis in sustainable synthesis

201. Srivastava, A. K.; Ali, M.; Siangwata, S.; Satrawala, N.; Smith, G. S.; Joshi, R. K. Multitasking FeOCN Composite as an Economic, Heterogeneous Catalyst for 1-Octene Hydroformylation and Hydration Reactions. *Asian J. Org. Chem.* **2020**, *9*, 377–384.
202. Paganelli, S.; Tassini, R.; Rathod, V. D.; Onida, B.; Fiorilli, S.; Piccolo, O. A Low Rhodium Content Smart Catalyst for Hydrogenation and Hydroformylation Reactions. *Catal. Lett.* **2021**, *151*, 1508–1521.
203. Shi, Y.; Hu, X.; Chen, L.; Lu, Y.; Zhu, B.; Zhang, S.; Huang, W. Boron Modified TiO<sub>2</sub> Nanotubes Supported Rh-Nanoparticle Catalysts for Highly Efficient Hydroformylation of Styrene. *New J. Chem.* **2017**, *41*, 6120–6126.
204. Xie, Z.; Xu, Y.; Xie, M.; Chen, X.; Lee, J. H.; Stavitski, E.; Kattel, S.; Chen, J. G. Reactions of CO<sub>2</sub> and Ethane Enable CO Bond Insertion for Production of C<sub>3</sub> Oxygenates. *Nat. Commun.* **2020**, *11*, 1887.
205. Zhao, J.; He, Y.; Wang, F.; Zheng, W.; Huo, C.; Liu, X.; Jiao, H.; Yang, Y.; Li, Y.; Wen, X. Suppressing Metal Leaching in a Supported Co/SiO<sub>2</sub> Catalyst With Effective Protectants in the Hydroformylation Reaction. *ACS Catal.* **2020**, *10*, 914–920.
206. Tan, M.; Yang, G.; Wang, T.; Vitidsant, T.; Li, J.; Wei, Q.; Ai, P.; Wu, M.; Zheng, J.; Tsubaki, N. Active and Regioselective Rhodium Catalyst Supported on Reduced Graphene Oxide for 1-Hexene Hydroformylation. *Catal. Sci. Technol.* **2016**, *6*, 1162–1172.
207. Vasylyev, M.; Alper, H. Conventional and Tandem Hydroformylation. *Synthesis* **2010**, 2893–2900.
208. Neves, A. C. B.; Calvete, M. J. F.; Pinho-Melo, T. M. V. D.; Pereira, M. M. Immobilized Catalysts for Hydroformylation Reactions. A Versatile Tool for Aldehyde Synthesis. *Eur. J. Org. Chem.* **2012**, *2012*, 6309–6320.
209. Gonsalvi, L.; Guerriero, A.; Monflier, E.; Hapiot, F.; Peruzzini, M. The Role of Metals and Ligands in Organic Hydroformylation. *Top. Curr. Chem.* **2013**, *342*, 1–47 (Hydroformylation for Organic Synthesis).
210. Hanf, S.; Rupflin, L. A.; Glaeser, R.; Schunk, S. A. Current State of the Art of the Solid Rh-Based Catalyzed Hydroformylation of Short-Chain Olefins. *Catalysts* **2020**, *10*, 510.
211. Liu, L.; Corma, A. Metal Catalysts for Heterogeneous Catalysis: From Single Atoms to Nanoclusters and Nanoparticles. *Chem. Rev.* **2018**, *118*, 4981–5079.
212. Sneed, B. T.; Kuo, C.-H.; Brodsky, C. N.; Tsung, C.-K. Iodide-Mediated Control of Rhodium Epitaxial Growth on Well-Defined Noble Metal Nanocrystals: Synthesis, Characterization, and Structure-Dependent Catalytic Properties. *J. Am. Chem. Soc.* **2012**, *134*, 18417–18426.
213. Su, J.; Xie, C.; Chen, C.; Yu, Y.; Kennedy, G.; Somorjai, G. A.; Yang, P. Insights into the Mechanism of Tandem Alkene Hydroformylation over a Nanostructured Catalyst with Multiple Interfaces. *J. Am. Chem. Soc.* **2016**, *138*, 11568–11574.
214. Wang, L.; Zhang, W.; Wang, S.; Gao, Z.; Luo, Z.; Wang, X.; Zeng, R.; Li, A.; Li, H.; Wang, M.; Zheng, X.; Zhu, J.; Zhang, W.; Ma, C.; Si, R.; Zeng, J. Atomic-Level Insights in Optimizing Reaction Paths for Hydroformylation Reaction over Rh/CoO Single-Atom Catalyst. *Nat. Commun.* **2016**, *7*, 14036.

## Chapter 3.10

# Asymmetric synthesis by solid catalysts

### 3.10.1 Introduction

Although the phenomenon of chirality has been observed in the early 1800s by Malus and Biot, the first chiral compound, isomers of sodium ammonium tartrate, was isolated by Louis Pasteur in 1848.<sup>1</sup> Pasteur's discovery opened a new and important field in chemistry and medicine, and working with chiral compounds, whether it is their synthesis or application, is one of the leading research areas today. When considering the synthesis of an organic molecule, both in industrial and academic settings, several important issues arise. Among these, the preparation of the correct enantiomer, in high chemical and optical purity became an increasingly important aspect. This is especially true when the synthesized molecule is intended for use in biological systems (i.e., as pharmaceuticals, agrochemicals).<sup>2, 3</sup> It is worth noting that 56% of the drugs currently on the market are chiral compounds and an overwhelming majority of these molecules (88%) are sold in the form of racemic mixtures.<sup>4</sup> A multitude of methods have been developed to achieve the goal of enantioselective synthesis.<sup>5, 6</sup> Early examples include the use of chiral starting materials derived from nature (chiral pool)<sup>7, 8</sup> or the use of chiral auxiliaries.<sup>9, 10</sup> While these concepts have been proven to be very successful, the application of catalytic methods has a great appeal to the synthetic chemist, allowing to generate a large amount of chiral material using only a small amount of chiral catalyst. The catalytic methods are also more efficient in using the resources. In addition to the economic factor, catalysis is one of the basic principles of green chemistry and the development of environmentally benign and sustainable synthetic processes is a major goal of research and development in the 21st century.<sup>11, 12</sup> Although the majority of the work in enantioselective catalysis currently lies within the field of homogeneous catalysis, the application of heterogeneous systems has been of increasing interest in the recent years. Heterogeneous catalysis has several distinct advantages compared to homogeneous systems.<sup>13</sup> Due to the heterogeneous nature of the system, catalyst recovery and recycling is usually easily achieved, and catalyst stability and decomposition is often less problematic compared to homogeneous systems. In contrast, the introduction of chirality

into a heterogeneous system is often more challenging. A major issues are the insufficient interaction with the substrate and the leaching of the chiral modifier from the catalyst. One of the first heterogeneous enantioselective catalysts that could provide a meaningful enantiomeric excess was based on a natural protein (silk fibers)-supported palladium catalyst, that was used to synthesize amino acids.<sup>14</sup> Consequently, much of the research in the field of heterogeneous enantioselective catalysis in the recent years has focused on the development of catalytic systems that combine the advantages of homogeneous and heterogeneous catalysts.<sup>15–20</sup> Following this approach, chiral homogeneous catalysts are modified and connected to a heterogeneous support, often by forming a covalent bond between the surface of the support and the ligand or by incorporating the ligand in the support, for example by means of copolymerization. While these zwitter-systems address some issues (i.e., catalyst recovery problems of homogeneous and low tunability of heterogeneous systems) other problems such as metal leaching are not yet solved.

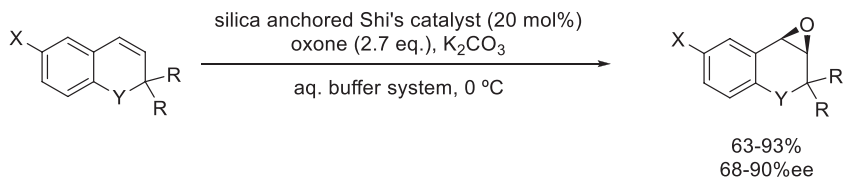
In order to fully investigate the environmental impact of a catalytic system many factors such as leaching, and the fate of the catalyst should be considered. Unfortunately, this information is not always available in the literature. In this chapter, the application of heterogeneous catalytic systems in enantioselective transformations will be reviewed, with a focus on environmentally benign systems. A selection of examples from various different transformations is presented, with a focus on examples from the recent literature.

### 3.10.2 Oxidation reactions

Oxidation reactions are an important group of synthetic processes and as such they have been covered in detail in the appropriate chapter on Oxidation in this book. Therefore, in the current subchapter, the focus will be on asymmetric catalytic oxidations only without discussing the fundamentals of the included reactions.

#### 3.10.2.1 Epoxidation

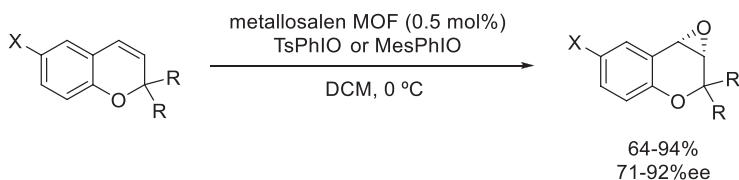
The group of Brown developed a heterogeneous variation of Shi's catalyst for the epoxidation of benzylic double bonds.<sup>21</sup> The catalyst was prepared by anchoring a variation of Shi's catalyst to the surface of a mesoporous silica via a thiol linker. The catalyst was able to perform the epoxidation of several different substituted substrates using oxone as oxidizing agent in an aqueous solvent system (Scheme 1). The products are mostly obtained in high yields and enantioselectivities. The reaction required a relatively high catalyst loading of 20 mol% to prevent the direct racemic oxidation to take place. Catalyst recycling experiments showed that the product selectivity dropped significantly after the second run, most likely due to the degradation of the catalyst by Bayer-Villiger reaction.



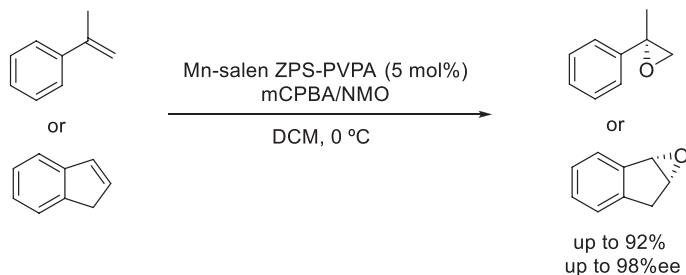
**SCHEME 1** Enantioselective epoxidation of alkenes using a heterogenized Shi-type catalyst.

Xia et al. achieved the epoxidation of similar chromene substrates using a metal-organic framework (MOF)-based catalyst containing a metallosalen linker unit.<sup>22</sup> Salen linker units containing a mixture of Cu and Fe as well as Cu and Mn ions were effective catalysts for the reaction using a hypervalent iodine species as the oxidant (Scheme 2). The MOF-catalyst was shown to be recyclable up to five times without loss of activity. A downside from the environmental point of view is the need for a chlorinated solvent in the reaction.

A chiral Jacobsen catalyst grafted onto a zirconium poly(styrene-phenylvinylphosphonate)-phosphate (ZPS-PVPA) support was used for the asymmetric epoxidation of  $\alpha$ -methylstyrene and indene (Scheme 3).<sup>23</sup> The catalytic system applied mCPBA and NMO as oxidizing agents and achieved yields up to 92% and enantioselectivities up to 98% depending on the linker used to bind the catalytically active Mn-salen unit to the polymer. The disadvantage of the process is the need for dichloromethane as a solvent, however, it is compensated by the reusability of the catalyst and the scalability of the catalytic system.



**SCHEME 2** Epoxidation of chromenes using metallosalen MOF catalysts.



**SCHEME 3** Polymer supported Mn-salen-catalyzed epoxidation of  $\alpha$ -methylstyrene and indene.

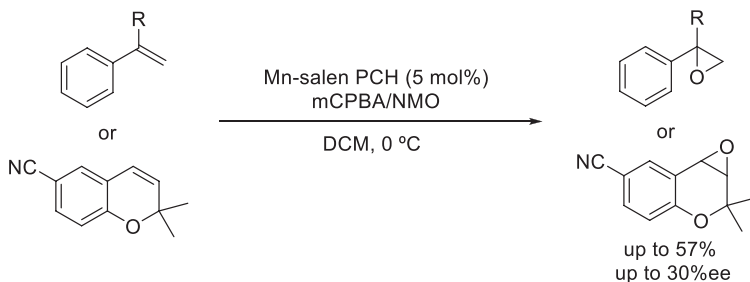
The catalyst can be recycled up to seven times without losing its activity and selectivity and the reaction was easily scaled up by a factor of 200 showing that the system might be used for industrial applications.

In a similar approach the groups of Pires and Freire used organo-functionalized porous clay hetero-structures to bind a Mn-salen complex and used it for the epoxidation of styrenes and chromenes (Scheme 4).<sup>24</sup> Only low conversion and enantioselectivity was obtained under the conditions tested, even though the results were better than compared to the nonheterogenized version of the catalyst.

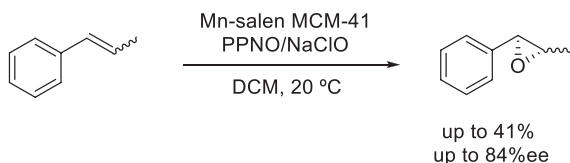
Zhang et al. used a Mn-salen complex immobilized on MCM-41 for epoxidation of  $\beta$ -methylstyrenes (Scheme 5).<sup>25</sup> Both the *cis* and the *trans* isomer could be transformed using the catalyst that was prepared by linking the salen unit to the MCM-41 framework. The researchers could show that incorporating rigid structures into the linker yielded higher conversions and selectivities than using flexible linker units. In a similar application, clay supported Mn-salen complexes were also found effective for alkene epoxidation.<sup>26</sup>

### 3.10.2.2 Dihydroxylation

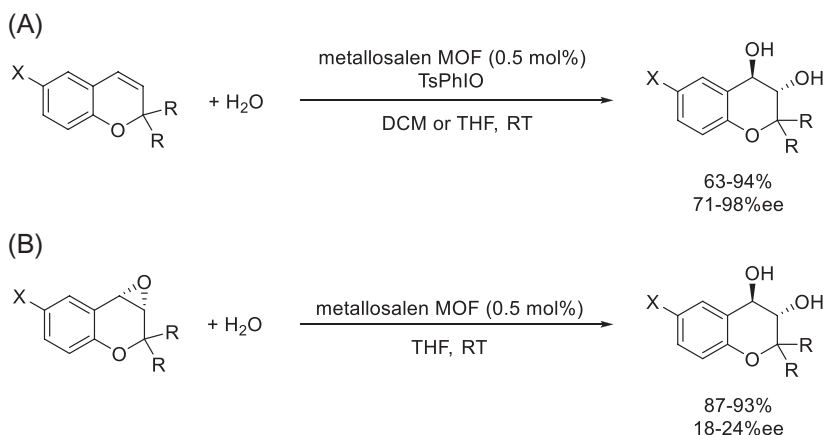
Xia et al. reported that the metallosalen MOF catalyst they developed can not only be used for epoxidation but also for the further functionalization of the products. Performing the reaction in the presence of water resulted in the formation of the diol in high yields and enantioselectivities (Scheme 6A).<sup>22, 27</sup>



**SCHEME 4** Epoxidation of styrenes and chromenes catalyzed by an organo-functionalized porous clay hetero-structure bound Mn-salen complex.



**SCHEME 5** An MCM-41 immobilized Mn-salen complex-catalyzed epoxidation of *cis* and *trans*  $\beta$ -methylstyrenes.

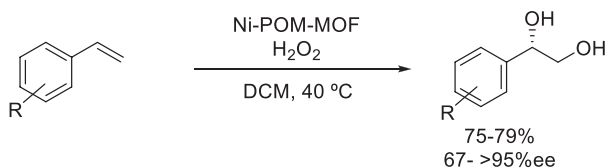


**SCHEME 6** One-pot (A) and sequential (B) epoxidation-hydrolysis of chromenes catalyzed by a metallosalen containing metal-organic framework.

Interestingly, the enantioselectivity is nearly completely lost when the reaction is performed in two steps rather than in a one-pot procedure (Scheme 6B).

As described in the same work, performing the epoxidation reaction in the presence of other nucleophiles allowed for the introduction of nitrogen and sulfur containing functional groups in the product. A less environmentally friendly chromium containing MOF had to be used for these transformations.

The asymmetric dihydroxylation of styrenes was achieved by the group of Duan using a chiral heterogeneous polyoxometalate metal-organic framework.<sup>28</sup> By incorporating a polyoxometalate cluster, nickel-ions and a proline-derived organocatalyst the authors achieved the dihydroxylation of different substituted styrenes in high yields and enantioselectivities (Scheme 7). Although a green oxidizing agent, hydrogen peroxide, could be applied, the reaction required the use of dichloromethane as a solvent, increasing the environmental impact of the system. The authors of the study could show that the configuration of the product depended on the chiral amine used as modifier; switching to the opposite enantiomer yielded the opposite configuration of the chiral center in the product.



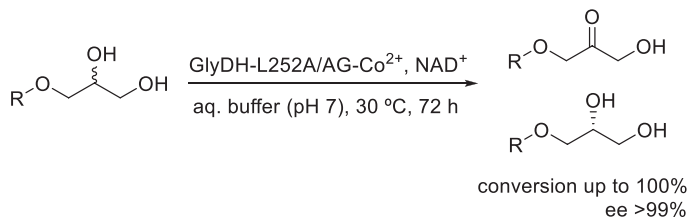
**SCHEME 7** Asymmetric dihydroxylation of styrenes catalyzed by a chiral heterogeneous polyoxometalate metal-organic framework.

### 3.10.2.3 Other oxidations

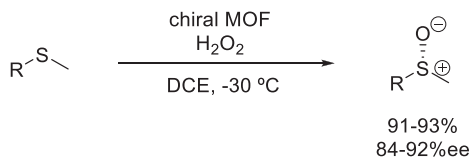
The enantioselective oxidation of alkyl and aryl glyceryl monoethers was carried out by an immobilized biocatalyst. Velasco-Lozano et al. designed a catalyst in which glycerol dehydrogenase, that was obtained from *Bacillus stearothermophilus* (BsGlyDH) was immobilized on cobalt-activated agarose microbeads 4BCL (AG-Co<sup>2+</sup>). The authors used this catalyst in the oxidation of alkyl/aryl glyceryl monoethers to corresponding 3-alkoxy/aryloxy-1-hydroxyacetones. The enzyme showed excellent enantioselectivity in oxidizing the (*S*)-isomer of the alcohol in >99% ee leaving the (*R*)-3-ethoxypropan-1,2-diol behind (Scheme 8).<sup>29</sup> The catalyst was found to be highly stable under the experimental conditions, in the recycling studies it did not show any decrease in activity or selectivity even after six consecutive reactions.

The enantioselective oxidation of sulfides to sulfoxides was achieved using a chiral phosphonate MOF.<sup>30</sup> Chiral BINOL units were used to build the metal-organic framework thus allowing for the reaction to be performed enantioselectively (Scheme 9). While hydrogen peroxide was used as the oxidant, the reaction was performed in dichloroethane, a nongreen solvent. No overoxidation of the product was observed under the conditions applied. In a similar application, a Ti(IV)- or V(V)-exchanged K-10 montmorillonite, respectively, doped with various chiral modifiers were also investigated in the enantioselective oxidation of sulfides, however, even the best enantiomeric excess, obtained using (*R*)-BINOL as the chiral modifier, did not exceed 18%.<sup>31, 32</sup>

The  $\beta$ -hydroxylation of unsaturated trifluoromethyl ketones was achieved by Li et al. using a cinchona-functionalized mesostructured silica.<sup>33</sup> The modified cinchona alkaloid was bound to the mesostructured silica using thiol-ene



**SCHEME 8** Heterogeneous catalytic oxidative kinetic resolution of alkyl and aryl glyceryl monoethers catalyzed by an agarose gel-immobilized enzyme (GlyDH-L252A/AG-Co<sup>2+</sup>).



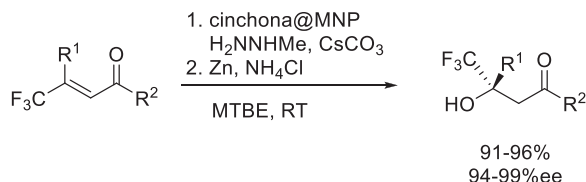
**SCHEME 9** Enantioselective oxidation of sulfides to sulfoxides by a chiral phosphonate MOF-based catalyst.

click chemistry. The thus prepared catalyst allowed for the sequential one-pot epoxidation-relay reduction reaction to take place and the products were formed in excellent yields and selectivities (Scheme 10). The catalytic system could be reused up to eight times without significant loss of its catalytic activity. The drawback of the reaction is the use of a hydrazine in the oxidation step and methyl-*tert*-butyl ether as the solvent.

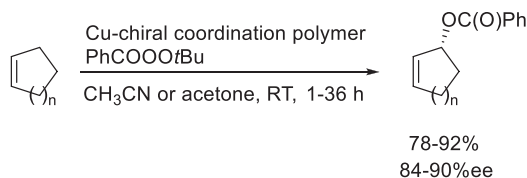
The Kharasch-Sosnovsky allylic oxidation of alkenes is an interesting process to produce allylic ethers.<sup>34, 35</sup> The reaction is commonly catalyzed by Cu-complexes in the homogeneous phase. The enantioselective version of the reaction has also been attracted considerable attention.<sup>36</sup> Aldea et al. described an enantioselective oxidation of cycloalkenes by using a chiral coordination polymer-based catalyst (Scheme 11).<sup>37</sup> The reusable catalyst acts via an interesting mechanism. The coordination polymer disassembles, and the reaction occurs in the solution and after the reaction is complete the catalyst re-assembles and can be recycled seven times without a meaningful drop in yield or enantioselectivity.

### 3.10.3 Hydrogenation

The enantioselective hydrogenation of C=C and C=X double bonds is of immense importance in synthetic organic chemistry yielding a large array of valuable products. Therefore, research in this field has been manifold and the progress has been continuously reviewed.<sup>38-40</sup> As such only a selection of recently published work with a focus on the environmental impact of the method is presented here.



**SCHEME 10** Enantioselective  $\beta$ -hydroxylation of unsaturated trifluoromethyl ketones catalyzed by a cinchona-functionalized mesostructured silica.



**SCHEME 11** The enantioselective Kharasch-Sosnovsky allylic oxidation of cycloalkenes catalyzed by a recyclable coordination polymer.

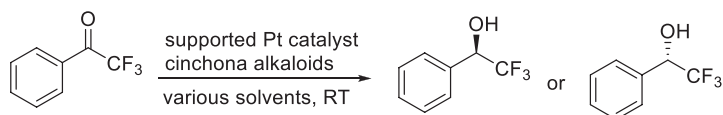
### 3.10.3.1 Reduction of carbonyl compounds

#### 3.10.3.1.1 Reduction of mono-carbonyl compounds

The application of cinchona modified noble metal catalysts for the hydrogenation of carbonyl compounds is one of the most commonly applied enantioselective catalytic processes for the reduction of the C=O group, although it is best applicable for the hydrogenation of  $\alpha$ -dicarbonyl compounds. The alkaloid that is added to the metal catalyst adsorbs on the metal surface thus creating a chiral environment and ensuring the enantiodifferentiation in the reaction.<sup>41,42</sup> Several attempts were made to use this catalytic system for the reduction of ketones to their corresponding secondary alcohols with moderate success. Substituted acetophenones readily underwent reduction, however, with low (<20%ee) enantioselectivity. The highest enantiomeric excesses were obtained with activated carbonyls such as 2,2,2-trifluoroacetophenone (Scheme 12). In one example a Pt/Al<sub>2</sub>O<sub>3</sub> catalyst was applied with natural and modified cinchona alkaloids in a continuous-flow fixed-bed reactor yielding the product in 30%ee.<sup>43</sup> Using a similar catalyst with natural cinchonas under sonochemical activation improved the enantioselectivity up to 49%ee.<sup>44</sup> Finally, the application of a magnetically recoverable Pd/SiO<sub>2</sub>/Fe<sub>3</sub>O<sub>4</sub> catalyst, resulted in the alcohol in up to 80%ee.<sup>45</sup>

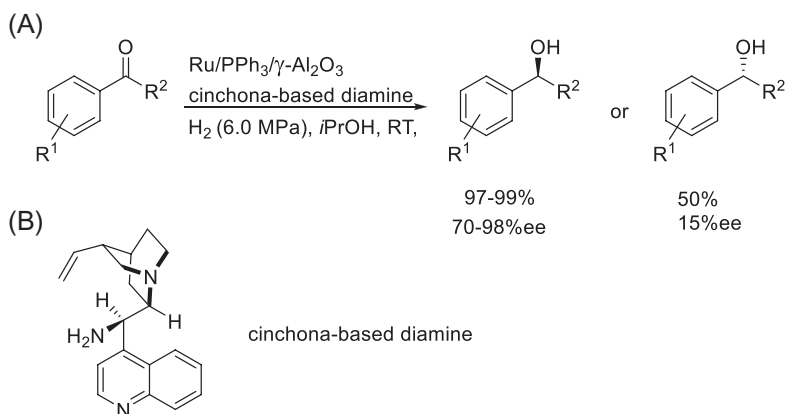
Nonactivated aromatic ketones were also hydrogenated using a Ru- $\gamma$ -Al<sub>2</sub>O<sub>3</sub> catalyst which was stabilized by PPh<sub>3</sub> (Scheme 13A). As a chiral modifier a cinchona alkaloid-based diamine (Scheme 13B) was used. High, nearly quantitative yields were obtained accompanied by excellent enantioselectivities for *ortho*-substituted aromatic ketones producing the (*S*)-enantiomer. In one case the (*R*)-enantiomer was obtained, however, both the yield and the optical purity was quite low (Scheme 13).<sup>46</sup> The authors also applied the same diamine modifier with an Ir/PPh<sub>3</sub>/SiO<sub>2</sub> catalysts and achieved up to 96%ee, especially for *ortho*-substituted aryl ketones.<sup>47</sup>

The same group applied the above cinchona-based diamino chiral auxiliary (Scheme 13B) for the enantioselective hydrogenation of heterocyclic aryl methyl ketones, this time using a triphenylphosphine-stabilized SiO<sub>2</sub>-supported iridium as a catalyst.<sup>48</sup> Out of different chiral amine modifiers,



|   |             |
|---|-------------|
| Pt/Al <sub>2</sub> O <sub>3</sub> flow system       | up to 30%ee |
| Pt/Al <sub>2</sub> O <sub>3</sub> ultrasound        | up to 49%ee |
| Pt/SiO <sub>2</sub> /Fe <sub>3</sub> O <sub>4</sub> | up to 80%ee |

**SCHEME 12** The heterogeneous enantioselective hydrogenation of 2,2,2-trifluoroacetophenone on cinchona-modified Pt catalysts.



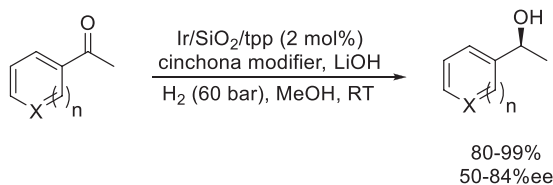
**SCHEME 13** The heterogeneous enantioselective hydrogenation of aryl alkyl ketones on cinchona-based diamine modified triphenylphosphine-stabilized Ru/γ-alumina catalyst.

9-amino(9-deoxy)epicinchonine proved to be the most effective allowing for the reaction to be performed at room temperature and 60 bar hydrogen pressure. A variety of heteroaromatic methyl ketones could be reduced with good yields and moderate enantioselectivity (Scheme 14). Methanol was used as the solvent for the reaction. The authors did not perform any recyclability study for the catalyst.

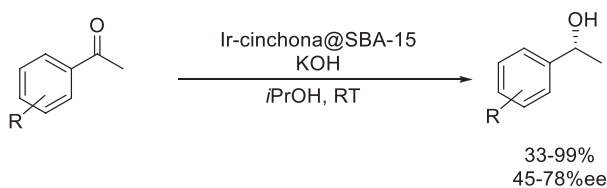
In a follow-up study, the authors showed that an increased amount of surface silanol groups on the surface of the support material resulted in a higher activity of the catalytic system.<sup>49</sup>

The concept of transfer hydrogenation was also applied by Shen et al. in the iridium-catalyzed reduction of substituted acetophenones.<sup>50</sup> The iridium was complexed to 9-amino *epi*-cinchonine bound to SBA-15 with a sulfide tether. The reduced acetophenones were obtained in mostly good yields and moderate enantioselectivities (Scheme 15). While recycling studies with the catalyst showed that the performance of the system declined after the third run, extensive washing of the catalyst was able to restore its initial activity.

In addition to the widespread use of cinchona-modified solid catalysts, the application of successful homogeneous metal complex-based catalysts in their immobilized form is also a general trend in asymmetric hydrogenations.



**SCHEME 14** The heterogeneous enantioselective hydrogenation of heteroaryl methyl ketones on cinchona-based diamine-modified Ir/SiO<sub>2</sub>/tpp catalyst.



**SCHEME 15** The heterogeneous catalytic enantioselective transfer hydrogenation of substituted acetophenones on cinchona-based Ir/SBA catalyst.

The immobilization can be achieved by many means, for example, anchoring the active component onto a support material via physisorption or covalent bonding.<sup>51</sup> These immobilized metal complexes were found to be highly active and selective, up to 98%ee, in the enantioselective hydrogenation of ketones. A few representative examples are tabulated in [Table 1](#).

More recent applications also take advantage of the proven efficacy of surface-bound metal complexes in preparing new heterogeneous hydrogenation catalysts. The group of Lin used an anchored ruthenium-BINAP catalyst for the reduction of various aryl ketones.<sup>59</sup> The reaction can be performed under moderate hydrogen pressure in isopropanol as the solvent to obtain the desired alcohol in excellent yields and selectivities ([Scheme 16](#)). Two different methods were explored for the attachment of the catalytically active ruthenium center, both yielding the product in equally high yields. The use of magnetic (magnetite) nanoparticles (MNPs) allowed for the easy recovery of the catalyst after the reaction. The recovered catalyst could be reused up to nine times before a decrease in activity was observed.

The asymmetric transfer hydrogenation using an immobilized rhodium complex was investigated by Barrón-Jaime et al. ([Scheme 17](#)).<sup>60</sup> The catalyst was prepared by anchoring a chiral amine to different supports followed by complexation with a rhodium salt. Even though the yields of the alcohol obtained by the reduction of acetophenone were good, the enantioselectivity was only moderate in the case of some support materials. Although the polymer-bound version of the catalyst showed higher activity and selectivity in the initial run, the silica-bound version gave more consistent results in catalyst recycling experiments. All heterogenized catalysts tested were inferior in their catalytic performance as compared to the homogeneous version of the Rh-complex.

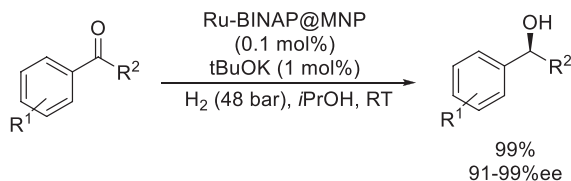
The group of Liu performed several studies on the use of chiral rhodium and ruthenium catalysts bound to mesoporous silica matrixes for the enantioselective transfer hydrogenation of aryl methyl ketones.<sup>61-63</sup> In all studies a linker with a diamine unit is fixed to the silica and then coordinated with the catalytically active metal center. The reaction was performed in water as a solvent and used sodium formate as the hydrogen transfer agent providing the desired alcohols in high yields and enantiomeric excess ([Scheme 18](#)). Interestingly the enantioselectivity changes from (*R*) to (*S*) when Rh is switched to Ru. Recycling

**TABLE 1** Asymmetric hydrogenation of ketones catalyzed by immobilized chiral organometallic complexes.

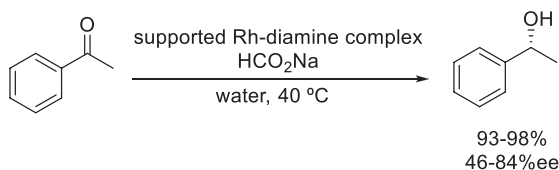
| Entry | Substrate   | Catalyst   | Conditions  | ee (%)   | Comments  | Ref. |
|-------|---|--|---|----------|---|------|
| 1     | Aromatic ketones  | [RuCl <sub>2</sub> ( <i>p</i> -cymene)] <sub>2</sub> with polymer supported chiral sulfonamides                        | Transfer hydrogenation<br>5 eq HCOONa, H <sub>2</sub> O<br>(2 mL) | Up to 98 | Recyclable catalyst (no loss of activity and selectivity)                       | 52   |
|       |   | Chiral cyclohexyldiamine based Ru—PPh <sub>3</sub> stabilized complex on mesoporous silica                             | <i>i</i> PrOH, H <sub>2</sub> (27 atm.), 70°C                     | Up to 76 | Similar activity as the homogeneous analog, recycled four times                 | 53   |
|       |   | Ru(II)-(1 <i>R</i> ,2 <i>S</i> )-(+)- <i>cis</i> -1-amino-2-indanol/SBA-15   | <i>i</i> PrOH, KOH, 60°C, 1 h                                     | Up to 77 | Moderate to good ee's, conversions  | 54   |
|       |   | C <sub>2</sub> -symmetric bis(sulfonamide)-cyclohexane-1,2-diamine-Rh <sup>III</sup> Cp* on silica gel and polystyrene | Transfer hydrogenation<br>HCOONa, H <sub>2</sub> O, 40°C          | Up to 92 | Excellent yields, selectivities, recyclable catalyst                            | 55   |
| 2     | Acetophenone  | RuCl <sub>2</sub> (PPh <sub>3</sub> ) <sub>2</sub> S-1,2-diphenylethylenediamine/mesoporous SiO <sub>2</sub>           | <i>i</i> PrOH, 10 h, RT, H <sub>2</sub> (3 MPa)                   | Up to 78 | Recyclable catalyst (negligible loss of activity/selectivity in four reactions) | 56   |
|       |   | 1 <i>S</i> ,2 <i>S</i> -DPEN-Ru(II)Cl <sub>2</sub> (TPP) <sub>2</sub> encapsulated in SBA-16 <sup>a,b</sup>            | <i>i</i> PrOH, H <sub>2</sub> (3.0 MPa), 25°C, base               | Up to 75 | Excellent conversions, recyclable catalyst (seven times)                        | 57   |
|       | <i>p</i> -CF <sub>3</sub> -, <i>p</i> -NH <sub>2</sub> -acetophenones | Rh complex immobilized on Al <sub>2</sub> O <sub>3</sub>   | EtOH, Et <sub>3</sub> N, H <sub>2</sub> (2.5 MPa), 50°C, 6 h      | Up to 80 | Lower activity than homogeneous analog, moderate yield                          | 58   |

<sup>a</sup> TPP, triphenylphosphine.

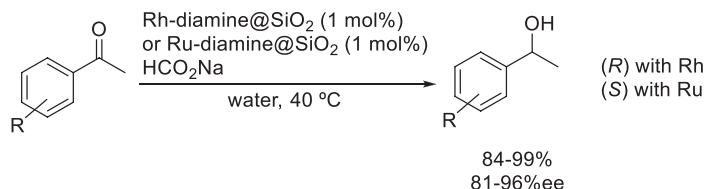
<sup>b</sup> DPEN, 1,2-diphenylethylenediamine; SBA, Santa Barbara Amorphous, a mesoporous material.



**SCHEME 16** The heterogeneous enantioselective hydrogenation of aryl alkyl ketones catalyzed by a magnetic nanoparticle (MNP)-supported Ru-BINAP complex.



**SCHEME 17** The heterogeneous enantioselective hydrogenation of acetophenone catalyzed by a Rh-chiral diamine complex immobilized on various supports.



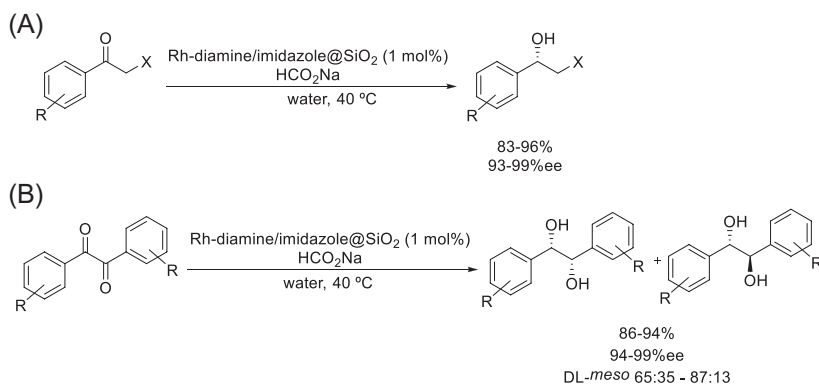
**SCHEME 18** Enantioselective hydrogenation of substituted acetophenones catalyzed by silica-bound Rh- and Ru-chiral diamine complexes.

experiments showed that both catalysts could be reused up to ten times without loss in activity and enantioselectivity.

The same reactivity was observed when the active rhodium catalyst was bound to a polyhedral oligomeric silsesquioxane. Similar results with regard to yield, enantioselectivity and recyclability were obtained compared to the silica bound version of the catalyst.<sup>64</sup>

The same group showed that an imidazole modified version of the Ru-chiral diamine complex immobilized on mesoporous organosilica could be used for the asymmetric transfer hydrogenation of different substituted  $\alpha$ -halo ketones (Scheme 19A) and benzils (Scheme 19B).<sup>65</sup> All reactions gave the desired products in high yields and enantioselectivities. Both chlorine and bromine remained intact in the  $\alpha$ -position and the catalyst could be recycled up to eight times before a decrease in activity was noted. The results obtained were similar to what was reported for the homogeneous version of the catalyst.

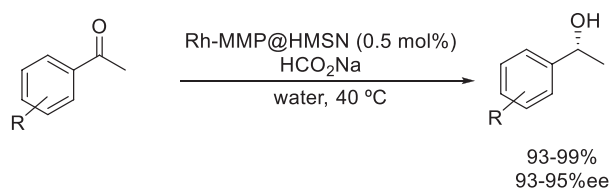
Hollow structured mesoporous silica nanospheres (HMSN) were used by Jing et al. as nanoreactors for the transfer hydrogenation of aromatic ketones.<sup>66</sup>



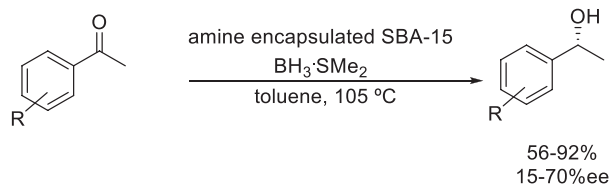
**SCHEME 19** Enantioselective hydrogenation of substituted  $\alpha$ -haloacetophenones (A) and benzils (B) catalyzed by silica-bound Rh- and Ru-chiral diamine complexes.

The active catalyst was prepared by the polymerization of a chiral Rh-amine complex within the nanosphere. A variety of substituted acetophenones was reduced to the corresponding benzyl alcohols with high yields and enantioselectivities (Scheme 20). Although the catalyst was shown to be recyclable up to four times, it should be noted that increased reaction times were needed to ensure high conversion of the substrate.

Balakrishnan and Velmathi developed a metal-free heterogeneous reduction of acetophenones using a chiral amine anchored to SBA-15.<sup>67</sup> BH<sub>3</sub> was used as the reducing agent to form the secondary alcohols in good yields and enantioselectivities (Scheme 21). Recycling studies of the catalyst showed that there is a slight loss in activity after each run. Even though toluene had to be used as



**SCHEME 20** Enantioselective hydrogenation of substituted acetophenones catalyzed by a hollow-structured mesoporous silica nanospheres (HMSN)-immobilized Rh-amine complex.



**SCHEME 21** Asymmetric catalytic hydrogenation of substituted acetophenones catalyzed by a SBA-encapsulated chiral amine.

the solvent, the fact that the reaction is metal-free is appealing from the green chemistry point of view.

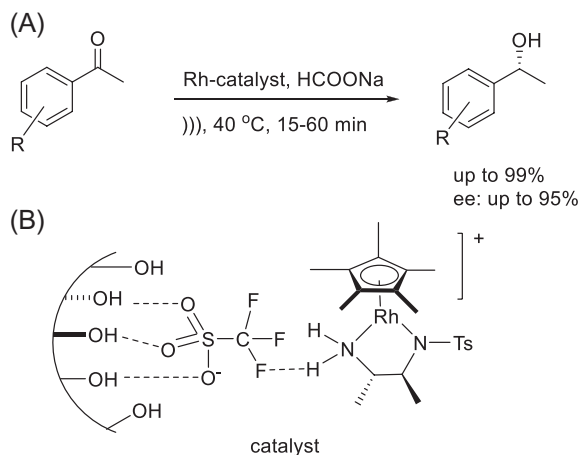
Similar SBA immobilized chiral catalysts were prepared by Li et al. The authors developed a chiral transfer hydrogenation process for the reduction of aryl ketones in a sonochemically activated protocol (Scheme 22A).<sup>68</sup> The novel catalyst used in this process was a cationic rhodium complex  $(\text{Cp}^*\text{RhTsDPEN})^+(\text{CF}_3\text{SO}_3)^-$  entrapped within Me-SBA-15 and Me-SBA-16 (Scheme 22B) using an ion-pair immobilization method. This strategy appears to work well as a generic method for the anchoring of various metal complexes to catalyst supports easing the recovery of these chiral catalysts. The above immobilized cationic rhodium catalyst could be applied in an aqueous medium under ultrasonic irradiation. The reaction provided the products in excellent yields and enantioselectivities.

### 3.10.3.1.2 Reduction of 1,2-dicarbonyl compounds

With the principles and tendencies in heterogeneous catalytic enantioselective hydrogenations of ketones outlined above, here we will survey the similar hydrogenations of 1,2-dicarbonyl compounds. This group of substrates include 1,2-diketones and other  $\alpha$ -activated dicarbonyls (ketoesters, ketoacetals, etc.) as the most popular substrates.

As a general tendency, the activated carbonyl compounds are more likely to participate in effective heterogeneous catalytic enantioselective hydrogenations, and thus, the second group of substrates overwhelmingly dominate this field. However, there are a few examples available for the hydrogenation of 1,2-diketones as well.<sup>42, 69-71</sup>

As mentioned previously the group of Cheng and Liu showed that an imidazole-stabilized Rh-chiral diamine complex anchored on mesoporous

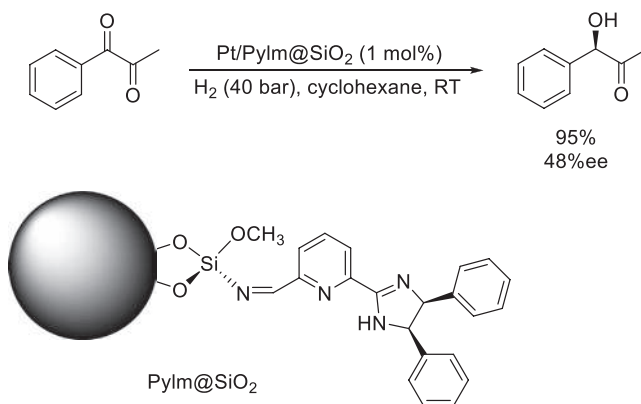


**SCHEME 22** Reduction of acetophenone derivatives by a transfer hydrogenation process (A) catalyzed by an immobilized cationic rhodium complex (B).

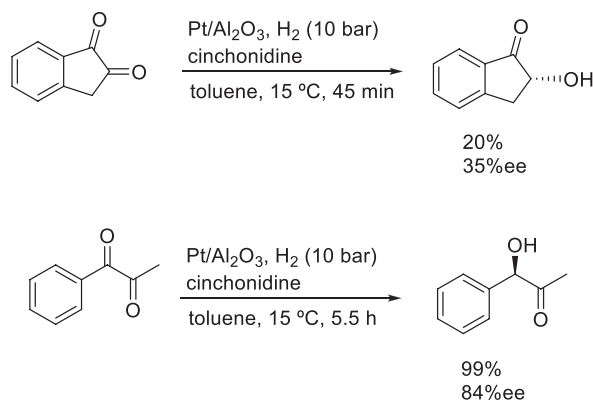
organosilica can be used for the asymmetric transfer hydrogenation of benzils (Scheme 19B).<sup>65</sup> The reduction of benzils provided the corresponding diols in high yields and enantioselectivities using sodium formate as hydrogen donor. Good DL to *meso* ratios were obtained and the reusability of the catalyst was shown in nine consecutive runs.

Campos and his group developed a new chiral modifier (Pylm) for the enantioselective reduction of 1-phenyl-1,2-propanedione (PPD).<sup>72</sup> The modifier was bound to a SiO<sub>2</sub> surface followed by the deposition of Pt-nanoparticles. While high conversions could be obtained with only 1% Pt loading, the enantioselectivities obtained were only moderate (Scheme 23). During their recycling experiments the authors found that the activity of the catalyst increased with each additional run while enantioselectivity decreased. This was caused by the leaching of the chiral modifier from the catalyst. It should be noted that the use of cyclohexane as a solvent is undesirable from an environmental point of view. In a similar work, a cinchonidine modified Ir/SiO<sub>2</sub> catalyst was applied in the hydrogenation of PPD producing good enantiodifferentiation (up to 80%ee).<sup>73</sup>

Busygin et al. described the hydrogenation of 1,2-indanedione and phenyl-1,2-propanedione on a cinchonidine-modified Pt/Al<sub>2</sub>O<sub>3</sub> catalyst (Scheme 24).<sup>74</sup> The reaction could provide the product in nearly quantitative yields; however, the conversion significantly affected the optical purity of the products. Interestingly, the two substrates behaved differently from this point of view. The enantiomeric excess of the product gradually decreased with increasing conversion in the case of indanedione; the best enantioselectivity was obtained at relatively low conversion. In contrast, the phenylpropanedione reduction resulted in higher enantioselectivities with increasing yields. Overall, the enantioselectivity was moderate to good in the reactions. The complete hydrogenation of the diketones, the diol, was the major byproduct in both cases.



**SCHEME 23** Heterogeneous catalytic enantioselective hydrogenation of 1-phenyl-1,2-propanedione by a transfer hydrogenation process catalyzed by an immobilized cationic rhodium complex.

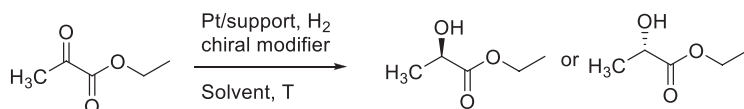


**SCHEME 24** Heterogeneous catalytic enantioselective hydrogenation of 1,2-indanedione and 1-phenyl-1,2-propanedione catalyzed by a cinchonidine-modified Pt/Al<sub>2</sub>O<sub>3</sub>.

In the asymmetric hydrogenation of other activated 1,2-dicarbonyl compounds the hydrogenation of  $\alpha$ -ketoesters, particularly ethyl pyruvate, plays a major role. The ethyl pyruvate hydrogenation, also known as Orito's reaction, is a commonly applied test reaction during the development of new enantioselective heterogeneous hydrogenation catalysts (Scheme 25).

The reaction has generated significant interest since its discovery. Some representative examples are summarized in Table 2.

Table 2 shows the applications of the ethyl pyruvate hydrogenation as a broadly accepted test reaction for evaluating the activity and selectivity of chirally-modified solid metal catalysts. There are two major directions that have been pursued, one is the preparation of new metal catalysts, such as the K-10 montmorillonite-supported Pt that contained the cinchona alkaloid immobilized by ionic interactions between the basic modifier and the acidic surface (Table 2, entry 2). The other major direction is the development of new chiral modifiers and their testing with often well-known catalysts (Table 2 entries 3–6, 9). Despite the significant efforts not many of these new directions resulted in a catalytic system that is comparable in efficacy and selectivity to the originally optimized Pt/Al<sub>2</sub>O<sub>3</sub> catalyst. In a few reports  $\alpha$ - and  $\beta$ -isochinonines were used as modifiers (Table 2 entries 3, 11). These investigations helped to clarify the major role that the anti-open conformation of the alkaloid plays in the enantiodifferentiation during these reactions.



**SCHEME 25** Heterogeneous catalytic enantioselective hydrogenation of ethyl pyruvate on a chirally modified supported Pt catalyst.

**TABLE 2** Enantioselective heterogeneous catalytic hydrogenation of ethyl pyruvate using chirally modified metal catalysts.

| Entry | Catalyst                                     | Modifier   | ee (%)  | Comments  | Ref.   |
|-------|--|--|---|---|--------|
| 1     | Pt/Al <sub>2</sub> O <sub>3</sub>            | Cinchonidine, cinchonine   | Up to 98  | The catalyst was pretreated with the modifier under ultrasonic irradiation                                    | 75–77  |
| 2     | Pt/K-10                                      | Cinchonidine   | Up to 75  | The modifier was anchored to the surface by ionic interactions  | 78, 79 |
| 3     | Pt/Al <sub>2</sub> O <sub>3</sub>            | $\alpha$ - and $\beta$ -isocinchonines   | 20–35   | Lack of acceleration in presence of the rigid modifiers   | 80     |
| 4     | Pt/Al <sub>2</sub> O <sub>3</sub>            | Aryl-[1,2,5,6-tetrahydro-pyridinyl] methanols  | Up to 75  |   | 81     |
| 5     | Pt/Al <sub>2</sub> O <sub>3</sub>            | (9-Anthryl)-(2-piperidyl)- and (9-anthryl) (2-pyridyl)-methanols   | N/A   | Revision on the role of the <i>erythro</i> isomer   | 82     |
| 6     | Pt/ $\gamma$ -Al <sub>2</sub> O <sub>3</sub> | Various chiral modifiers, best performance: cinchonidine   | Up to 63 (both enantiomers, with different modifiers) | Continuous micro-structured flow reactor  | 83     |
| 7     | Pt/Al <sub>2</sub> O <sub>3</sub>            | Cinchonidine   | N/A   | Effect of additives on the enantioselection studied, preadsorbed quinoline and acridine enhance rate and ee's | 84     |
| 8     | Pt/Al <sub>2</sub> O <sub>3</sub>            | Quinine, cinchonine  | N/A   | Nonlinear phenomenon  | 85     |
| 9     | Pt/SiO <sub>2</sub>                          | ( <i>S</i> )-(+)-1-aminoindan, ( <i>S</i> )-(+)-1-indanol, and (1 <i>R</i> , 2 <i>S</i> )-(+)- <i>cis</i> -1-amino-2-indanol | Up to 63  | Most effective modifier ( <i>S</i> )-(+)-1-aminoindan   | 86     |
| 10    | Pt/HPS <sup>a</sup>                          | Cinchonidine   | Up to 73  | –   | 87     |
| 11    | Pt/Al <sub>2</sub> O <sub>3</sub>            | Cinchonine, $\alpha$ -isocinchonine  | Up to 89  | Mechanistic proof for <i>antiopen</i> conformation of the alkaloid  | 88, 89 |

HPS, hypercrosslinked polystyrene, N/A- non applicable, the goal of the study was not to optimize for high ee.

Although the ethyl pyruvate related papers dominate the literature in the field of  $\alpha$ -ketoester hydrogenation, there are several other derivatives that have been enantioselectively hydrogenated on heterogeneous metal catalysts, often providing excellent enantioselectivities. Many of them are valuable synthetic building blocks for the preparation of complex chiral compounds. A few representative examples are collected in [Table 3](#).

More recent applications appear to focus on the preparation of new heterogeneous hydrogenation catalysts by applying support materials that were unconventional earlier in these hydrogenations. These supports include carbon nanotubes, polymer-capped materials or chiral polymers.<sup>102</sup>

Sharma and Sharma used Pt-functionalized multiwalled carbon nanotubes (MWNT) as heterogeneous catalyst for the reduction of methyl pyruvate.<sup>103</sup> The authors applied cinchonidine as chiral modifier and the reaction proceeded with excellent enantioselectivities and yields ([Scheme 26](#)). The authors showed that the catalyst could be recycled up to 10 times with only a slight loss in catalytic activity. Unfortunately, new chiral modifier had to be used for each run, reducing the benefit gained through the recycling.

In a subsequent study the same authors reported that a Pt-functionalized chiral polyamide can be efficiently used as a catalyst for the reduction of ethyl 2-oxo-4-phenylbutanoate.<sup>104</sup> The chiral polymer is assumed to adopt a helical conformation thus generating a chiral environment for the platinum nanoparticles allowing for the asymmetric reduction ([Scheme 27](#)). The reaction could be performed without the use of any solvent at room temperature, yielding the enantiomerically pure  $\alpha$ -hydroxy ester in excellent yields.

### 3.10.3.1.3 Reduction of 1,3-dicarbonyl compounds

In addition to the highly effective applications for the reduction of 1,2-dicarbonyl compounds, the enantioselective heterogeneous catalytic hydrogenation of 1,3-dicarbonyl compounds also attracted significant attention.

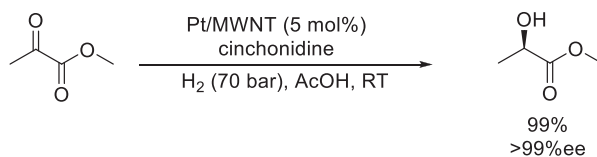
One of the most explored areas is the hydrogenation of  $\beta$ -ketoesters and  $\beta$ -diketones catalyzed by tartaric acid-modified Raney Ni catalysts.<sup>105</sup> The catalyst was prepared from commercially available NiAl alloy in the presence of tartaric acid enantiomers, respectively, using ultrasonic irradiation. The freshly prepared chirally-modified Raney Ni was applied in the hydrogenation of 1,3-dicarbonyl compounds,<sup>106</sup> including methyl 3-cyclopropyl-3-oxopropanoate, providing the hydroxyketone in nearly quantitative yields and 98% ee ([Scheme 28](#)).<sup>107, 108</sup> The reaction is a very sensitive catalytic system, with many parameters, such as the added base, playing an important role.<sup>109</sup>

The enantioselective hydrogenation of 1,1,1-trifluoro-2,4-diketones has been achieved by Baiker's group ([Scheme 29](#)).<sup>69, 110</sup> The authors used a Pt/Al<sub>2</sub>O<sub>3</sub> catalyst and a series of chiral modifiers were tested, such as cinchonidine, O-Me-cinchonidine, or (*R,R*)-pantoyl-naphthylethylamine. The reactions occurred with relatively low to moderate yields, however, 100% chemoselectivity, and moderate to high enantioselectivities. The relatively good performance

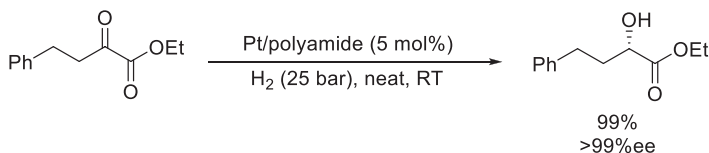
**TABLE 3** Enantioselective heterogeneous catalytic hydrogenation of  $\alpha$ -ketoesters and related compounds using chirally modified metal catalysts.

| Entry | Substrate   | Catalyst  | Modifier  | ee (%)   | Remarks   | Ref.   |
|-------|---|---|---|----------|---|--------|
| 1     | Dialkyl-2-oxoglutarates   | Pt/Al <sub>2</sub> O <sub>3</sub>                   | Cinchonidine, cinchonine  | Up to 96 | ( <i>R</i> ) products form with higher ee-s, and 76% for ( <i>S</i> )-products  | 90     |
| 2     | Phenylglyoxylic acid  | Pt/Al <sub>2</sub> O <sub>3</sub>                   | $\beta$ -/socinchonine  | Up to 94 | Conformation of adsorbed modifier, substrate and solvent affect the ee  | 91     |
| 3     | Substituted $\alpha$ -ketoesters                                      | Pt/Al <sub>2</sub> O <sub>3</sub>                   | Cinchonidine, cinchonine  | Up to 98 | The catalyst-modifier system was enhanced with ultrasonic irradiation   | 92–94  |
| 4     | Ketopantolactone  | Pt/Al <sub>2</sub> O <sub>3</sub>                   | <i>O</i> -(2-Pyridyl)-cinchonidine, <i>O</i> -phenylcinchonidine and cinchonidine | Up to 80 | Substrate-modifier interaction for <i>O</i> -(2-pyridyl)-cinchonidine and inversion of ee was observed                | 42     |
| 5     | Methyl benzoylformate, ketopantolactone, pyruvaldehyde dimethylacetal | Pt/Al <sub>2</sub> O <sub>3</sub>                   | $\alpha$ -Isoquinine, quinine, quinidine, cinchonine, cinchonidine                | Up to 96 | % ee affected by orientation of the quinuclidine <i>N</i> -lone pair relative to quinoline                            | 70     |
|       |   |   |   |          | Flow system   | 95     |
|       |   |   |   |          | Nonlinear phenomenon  | 96     |
| 6     | Methylglyoxal 1,1-dimethyl acetal and its derivatives                 | Pt/Al <sub>2</sub> O <sub>3</sub>                   | Quinine, quinidine, cinchonine, cinchonidine                                      | Up to 97 | Cinchonidine provided the best selectivity for the ( <i>R</i> ), and cinchonine for the ( <i>S</i> )-enantiomer (88%) | 97, 98 |
| 12    | Methyl benzoylformate, ketopantolactone                               | Pt/SiO <sub>2</sub> /Fe <sub>3</sub> O <sub>4</sub> | Cinchona alkaloids  | Up to 80 | Magnetically recoverable catalyst   | 45     |
|       |   | Pt/Al <sub>2</sub> O <sub>3</sub>                   |   |          | Mechanistic details   | 99     |
| 14    | Ethyl 3-methyl-2-oxobutyrate  | Rh/Al <sub>2</sub> O <sub>3</sub>                   | Cinchona alkaloids  | up to 74 | ee depends on Rh content, nanoparticles offer no improvement  | 100    |
| 15    | Ketopantolactone  | Pt/Al <sub>2</sub> O <sub>3</sub> <sup>c</sup>      | Cinchona alkaloids  | Up to 92 | 4–15 times rate enhancement increasing Pt(111)/Pt(100) ratio improved rate/ee   | 101    |

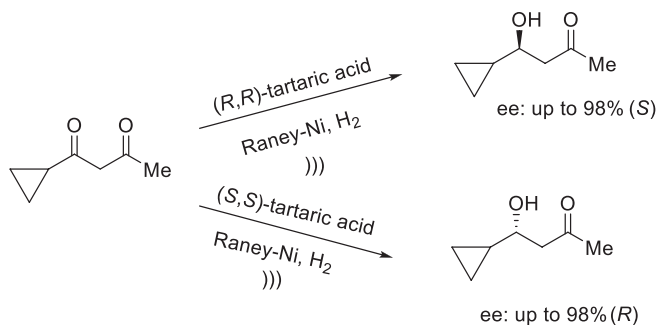
612 Heterogeneous catalysis in sustainable synthesis



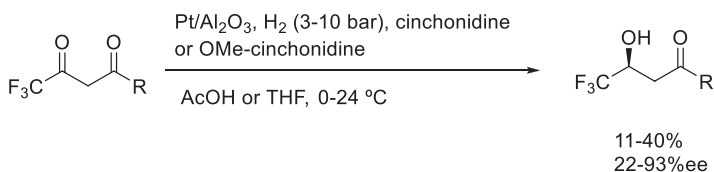
**SCHEME 26** Heterogeneous catalytic enantioselective hydrogenation of methyl pyruvate on a cinchonidine-modified functionalized multiwall carbon nanotubes-supported Pt catalyst.



**SCHEME 27** Heterogeneous catalytic enantioselective hydrogenation of ethyl 2-oxo-4-phenylbutanoate on a cinchonidine-modified polyamide-supported Pt catalyst.



**SCHEME 28** Enantioselective heterogeneous catalytic hydrogenation of methyl 3-cyclopropyl-3-oxopropanoate on tartaric acid-modified Raney Ni catalyst.



**SCHEME 29** Enantioselective heterogeneous catalytic hydrogenation of 1,1,1-trifluoro-2,4-diketones on cinchona alkaloid-modified Pt catalysts.

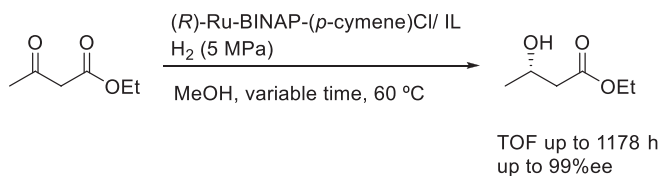
of the system was attributed to the effective interaction between chiral modifier and the enolate ion pair. In a similar process ethyl 2-fluoroacetoacetate was hydrogenated on a cinchonidine-modified Pt/Al<sub>2</sub>O<sub>3</sub> catalyst.<sup>111</sup> A dynamic kinetic resolution of unreacted enantiomer was described as the mechanism of the enantiodifferentiation (82%ee).

Similar to several examples discussed above, immobilized chiral complexes were also applied in the hydrogenation of  $\beta$ -ketoesters. Floris et al. immobilized a (*R*)-[RuCl(binap)(*p*-cymene)]Cl complex in ionic liquids (IL) and used this catalyst for the hydrogenation of methyl acetoacetate to methyl-3-hydroxybutyrate with high enantioselectivity (up to 97%) in a mixed methanol/IL phase (Scheme 30).<sup>112</sup> The ionic liquids were based on quaternary ammonium salts, specifically, *n*-alkyl-triethylammonium bis(trifluoro-methane sulfonyl) imides. In addition to the excellent ee values, the authors proved that the immobilized catalytic complex could be reused.

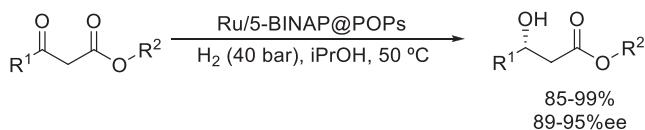
Wang et al. synthesized a porous polymer (POPs) including chiral BINAP units for the reduction of  $\beta$ -ketoesters.<sup>113</sup> The BINAP functionality was then used to coordinate a Ru-ion as active hydrogenation catalyst. A variety of substrates was reduced in isopropanol as a green solvent with high selectivity and yield (Scheme 31). The catalyst could be recycled up to six times without decrease in yield or enantioselectivity.

The group of Kunz developed a method for the enantioselective reduction of  $\beta$ -ketoesters with proline-functionalized Pt-nanoparticles using chiral amines as modifiers. Out of several chiral amines tested, proline proved to give the best results using the Al<sub>2</sub>O<sub>3</sub>-supported Pt-nanoparticles (Pt@Al<sub>2</sub>O<sub>3</sub>).<sup>114</sup> Using substrates with different steric demand, the authors could show that increasing size on the keto-side of the molecule increases enantioselectivity while bulky ester functionalities have the opposite effect. All reactions were run to full conversion yielding the products in moderate to good enantiomeric excess (Scheme 32).

The transfer hydrogenation of  $\beta$ -ketophosphonates was achieved by Han et al. using a Ru catalyst immobilized on mesostructured silica.<sup>115</sup> A variety of substrates with different aromatic groups was reduced in excellent yields and enantioselectivities (Scheme 33). The reactions were performed under mild conditions using formic acid as a hydrogen donor. It should be noted that under

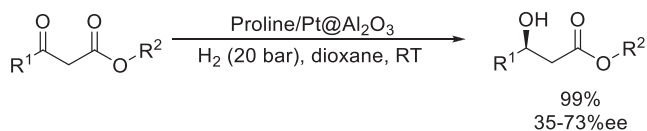


**SCHEME 30** Enantioselective heterogeneous catalytic hydrogenation of ethyl acetoacetate by an ionic liquid-immobilized (*R*)-[RuCl(binap)(*p*-cymene)]Cl complex.

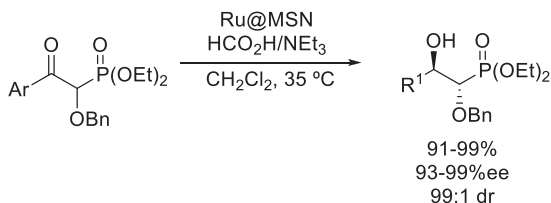


**SCHEME 31** Enantioselective heterogeneous catalytic hydrogenation of  $\beta$ -ketoesters by a porous polymer (POP)-immobilized Ru-BINAP complex.

614 Heterogeneous catalysis in sustainable synthesis



**SCHEME 32** Enantioselective heterogeneous catalytic hydrogenation of  $\beta$ -ketoesters by proline-modified alumina-supported Pt nanoparticles.



**SCHEME 33** Enantioselective heterogeneous catalytic hydrogenation of  $\beta$ -ketophosphonates by a mesostructured silica-supported Ru.

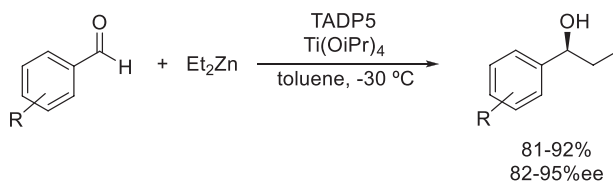
the conditions applied the benzyl protecting group was not removed. Only the use of dichloromethane as solvent for the reaction tarnishes the benefit of the reaction with regard to green chemistry principles.

### 3.10.3.1.4 Reductive alkylation

Zhu et al. designed a heterogeneous catalyst (TADP5) for the asymmetric addition of  $\text{ZnEt}_2$  to benzaldehydes (Scheme 34).<sup>116</sup> Pillar[5]arene units were linked by chiral TADDOL units that then coordinated the titanium species to generate the catalytic center. The thus prepared catalyst allowed the addition reaction to take place with high yields and enantioselectivities. While the catalyst could be recycled up to six times without significant loss in activity; unfortunately, the reaction required toluene as solvent and a reaction temperature of  $-30^\circ\text{C}$ . The same reaction was also carried out using a silica-immobilized chiral amino alcohol with good yields but only moderate enantioselectivities.<sup>117</sup>

### 3.10.3.2 Reduction of C=C double bonds

Although the enantioselective heterogeneous catalytic hydrogenation of carbonyl compounds dominated this field, significant efforts have been made to extend the application of the systems used above to the enantioselective



**SCHEME 34** Enantioselective heterogeneous catalytic addition of  $\text{Et}_2\text{Zn}$  to benzaldehydes.

hydrogenation of C=C bonds.<sup>38, 118, 119</sup> The most successful examples belong to the hydrogenation of activated alkenes, focusing on  $\alpha,\beta$ -unsaturated carbonyl compounds, such as carboxylic acids or ketones.

The above detailed cinchona alkaloid-modified noble metal catalytic approach has been extended to the enantioselective C=C bond hydrogenation of  $\alpha,\beta$ -unsaturated carboxylic acids as well, however, in this case mostly using Pd-based catalysts.

Several reports attest that the Pd surface can also be efficiently modified by one of these chiral modifiers and result in reductions with high enantioselectivities. Representative examples are tabulated in Table 4.

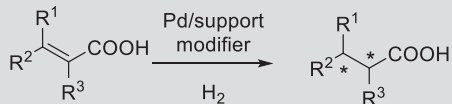
Most investigations use Pd/Al<sub>2</sub>O<sub>3</sub> catalyst, however, TiO<sub>2</sub>, SiO<sub>2</sub> or C are also commonly applied supports. One example used a less traditional support, multiwall carbon nanotubes (MWCNT). Several of these studies involve addition of an achiral primary amine (often benzylamine) additive in addition to the chiral modifier in order to enhance the enantiodifferentiation. The effect of the structure of the primary amine additive, however, has also been thoroughly investigated. The common conclusion was that benzyl amine decreases the initial rate of reaction as it interacts with the carboxylic acid and at the same time increases the enantioselectivity. This suggests that the nature of the enantiodifferentiation is quite different from the kinetic type that occurred in the C=O hydrogenation reactions.

Similar to the contemporary examples in the C=O hydrogenation, efforts have been made to apply immobilized metal complexes for the hydrogenation of unsaturated acids. The group of Bakos used phosphotungstic acid (PTA) to anchor a chiral Rh-complex on Al<sub>2</sub>O<sub>3</sub> for the asymmetric hydrogenation of (*Z*)- $\alpha$ -acetamidocinnamic acid.<sup>135</sup> The reduced compound was obtained in high yield and excellent enantioselectivity (Scheme 35). Compared to the homogeneous variation of the catalyst (which uses the green solvent ethylene carbonate) the environmentally harmful solvent CH<sub>2</sub>Cl<sub>2</sub> had to be used for the heterogeneous reaction. Recycling studies showed that while the activity of the catalyst dropped significantly after the second run, the enantioselectivity was barely affected. When the same catalyst was used in a continuous flow system the catalytic activity remained high for a prolonged amount of time.

Yu et al. described a self-supported Rh-coordination polymer for the reduction of several different unsaturated carboxylic acid derivatives (Scheme 36).<sup>136</sup> Chiral BINAP ligands in the linker unit of the polymer generated the chiral environment for the Rh catalyst and allowed the reduction to take place with almost quantitative yields and excellent enantioselectivities for different enamides and  $\alpha,\beta$ -unsaturated esters.

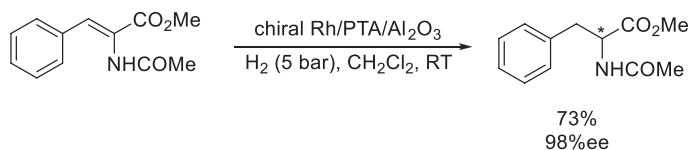
In addition to carboxylic acid derivatives the enantioselective C=C hydrogenation of unsaturated ketones also attracted significant attention. The proline-modified palladium catalyst for the asymmetric hydrogenation of isophorone (3,3,5-trimethyl-2-cyclohexenone, Scheme 37) was first introduced by Tungler's group in the late 1980s.<sup>119, 137</sup>

**TABLE 4** Heterogeneous catalytic hydrogenations of various unsaturated carboxylic acid derivatives on cinchona-modified Pd catalysts.

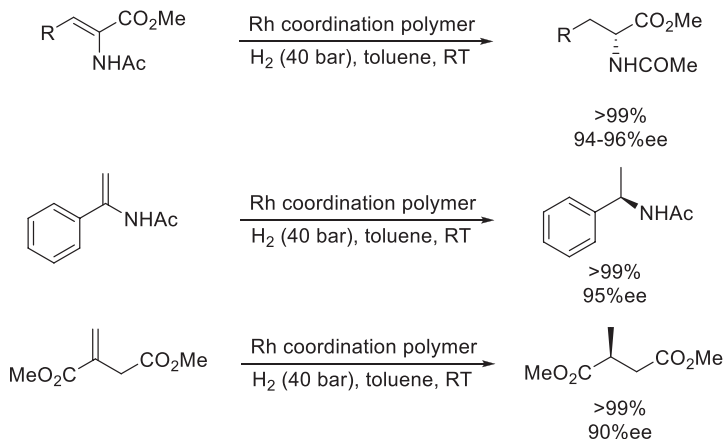


| Entry | Substrate  | Catalyst  | Modifier                                   | ee (%)   | Comments   | Ref.     |
|-------|--|---|--|----------|--|----------|
| 1     | 2-Methyl-2-pentenoic acid                            | Pd/Al <sub>2</sub> O <sub>3</sub>                       | Natural and derivatized cinchona alkaloids | Up to 66 | Ultrasonic pretreatment improved the ee values. toluene/MeOH solvent | 120–122  |
| 2     | Pentenoic- and cinnamic acid derivatives             | Pd/Al <sub>2</sub> O <sub>3</sub>                       | Cinchona alkaloids                         | Up to 70 | MeOH solvent   | 123      |
| 3     | <i>N</i> -acetyldehydroamino acids                   | Pd/Al <sub>2</sub> O <sub>3</sub>                       | Cinchona alkaloids                         | up to 60 | MeOH solvent   | 124      |
| 4     | Fluorinated ( <i>E</i> )-2,3-diphenylpropenoic acids | Pd/Al <sub>2</sub> O <sub>3</sub>                       | Cinchonidine                               | Up to 96 | Aq. DMF as solvent   | 125      |
| 5     | Methoxy-substituted 2,3-diphenylpropenoic acids      | Pd/Al <sub>2</sub> O <sub>3</sub>                       | Cinchonidine                               | Up to 90 | Aq. DMF as solvent   | 126      |
| 6     | ( <i>E</i> )-2-methyl-2-butenic acid                 | Pd/SiO <sub>2</sub> , Pd/Al <sub>2</sub> O <sub>3</sub> | Cinchonidine                               | Up to 99 | Hexane or toluene as solvent   | 127, 128 |
| 7     | Fluorinated unsaturated carboxylic acids             | Pd/Al <sub>2</sub> O <sub>3</sub>                       | Cinchona alkaloids                         | Up to 43 | Benzylamine as additive, toluene/MeOH as solvent                     | 129      |
| 8     | Cinnamic acid derivatives                            | Pd/C  | Cinchonidine                               | Up to 92 | Aq. dioxane as solvent   | 130      |
| 9     | Heteroaromatics substituted propenoic acids          | Pd/Al <sub>2</sub> O <sub>3</sub>                       | Cinchonidine                               | Up to 80 | Aq. DMF as solvent   | 131      |
| 10    | ( <i>E</i> )- $\alpha$ -phenylcinnamic acid          | Pd/TiO <sub>2</sub>                                     | Cinchonidine                               | Up to 91 | Aq. dioxane as solvent   | 132      |
| 11    | $\alpha,\beta$ -unsaturated carboxylic acids         | TiO <sub>2</sub> -MWCNT                                 | Cinchonidine                               | Up to 52 | Toluene/MeOH/aq. DMF   | 133      |
| 12    | Substituted unsaturated carboxylic acids             | Pd/C  | Cinchonidine                               | Up to 92 | Aq. dioxane as solvent   | 134      |

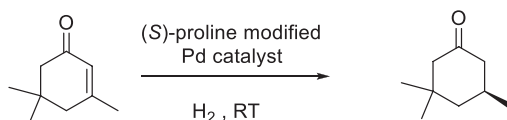
MWCNT, multiwalled carbon nanotubes.



**SCHEME 35** Enantioselective heterogeneous catalytic hydrogenation of (Z)- $\alpha$ -acetamidocinnamic acid on a phosphotungstic acid (PTA) anchored alumina-supported chiral Rh-complex.



**SCHEME 36** Enantioselective heterogeneous catalytic hydrogenation of unsaturated carboxylic acid derivatives on a self-supported Rh coordination polymer.



**SCHEME 37** Asymmetric hydrogenation of C=C bond of isophorone on Pd catalysts using (S)-proline as a chiral modifier.

This field has been reinvigorated starting in the early 2000s and new findings have been published ever since. The ultrasonic pretreatment that has been proven to be effective in the sonochemical asymmetric hydrogenation ketosteroids, found extended use in the hydrogenation of isophorone using proline-modified Pd/Al<sub>2</sub>O<sub>3</sub> catalyst as well. Mhadgut et al. reported that ultrasonic pretreatment of a commercially available Pd/Al<sub>2</sub>O<sub>3</sub> catalyst in the presence of the chiral modifier proline resulted in a reasonable enhancement in the enantioselectivity of the hydrogenation reaction of isophorone (up to 85%ee).<sup>138</sup> Later, several reports have been published describing the effect of solvent, catalyst support, reaction time, modifier structure and hydrogen pressure. The reaction

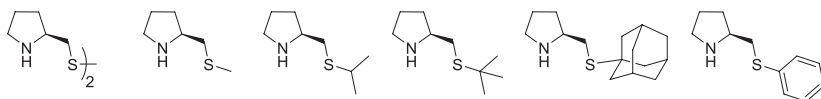
mechanism involves the racemic or near-racemic hydrogenation of isophorone to ( $\pm$ ) 3,3,5-trimethylcyclohexanone (TMCH) and it has been confirmed that the enantiodifferentiation is mainly based on a secondary kinetic resolution of the hydrogenation products. It was reported that the use of supports with high basicity ( $\text{SrCO}_3$ ,  $\text{CaCO}_3$ ,  $\text{BaCO}_3$ ) further enhanced the ee values up to 99%, albeit the system was limited to low yields (<50%) as a result of secondary kinetic resolution.<sup>139</sup> Later a homogeneous version of the kinetic resolution was proposed.<sup>140, 141</sup> Other studies also confirmed that basic supports such as MgO gave moderate yields (43%) but excellent ee values, up to 95%.<sup>142, 143</sup> It was also reported that structural changes implemented to the proline structure usually resulted in a decrease in enantioselectivity and at the same time this study provided experimental evidence for the role of the catalyst in the enantioselection.<sup>144</sup> These observations were confirmed by another report.<sup>137</sup>

In contrast to the above studies that used proline in stoichiometric amount, Watson et al. carried out this hydrogenation using catalytic amount of proline-based surface-tethered chiral modifiers (Scheme 38) although the reaction resulted in rather low ee values.<sup>145</sup>

As an extension of the proline-based studies, several other catalysts have been prepared and applied in the reaction, including a chirally imprinted metallo-organic hybrid Pd catalyst (up to 16%ee),<sup>41</sup> Ni-Al-Cr alloy (racemic),<sup>146</sup> or polymer-supported Pd (up to 40%ee, polymer: poly(vinyl-pyridine) (PVP), aminomethylated polystyrene (AMPS), Amberlyst-OH (AOH)).<sup>147</sup> A recent study investigated a broad range of noble metal (Pd/C, Pt/C, Ir/C, Ru/C, Pd/SiO<sub>2</sub>, Pt/SiO<sub>2</sub>, Ir/SiO<sub>2</sub>, Ru/SiO<sub>2</sub>), and nonnoble metal catalysts (Raney Ni, Raney Co, Raney Cu, Raney Fe, Ni/SiO<sub>2</sub>, Co/SiO<sub>2</sub>, Cu/SiO<sub>2</sub>, Fe/SiO<sub>2</sub>).<sup>148</sup> Other investigations focused on the clarification of the mechanistic details using in situ spectroscopic and catalytic tools. The data provided strong evidence for the existence of two competing enantioselective processes leading to opposing enantioselection.<sup>149</sup>

### 3.10.4 Aldol-reaction and related chemistry

The aldol reaction and its related transformations have been established as a major tool for the formation of carbon-carbon bonds. A variety of methods have been developed to perform these reactions in an enantioselective fashion. Most of the reactions rely on the use of a homogeneous catalyst and the field has been reviewed regularly.<sup>150, 151</sup> The reactions below use a heterogeneous catalyst, a system much less frequently investigated compared to the homogeneous variant.



**SCHEME 38** Proline-based surface-tethered chiral modifiers for the Pd-catalyzed asymmetric hydrogenation of isophorone.

### 3.10.4.1 Aldol reactions

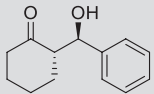
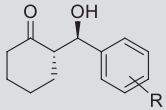
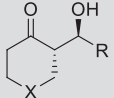
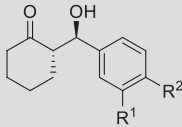
The enantioselective aldol addition of cyclohexanone to substituted benzaldehydes has been used in several studies as test reaction for the performance of a variety of heterogeneous catalysts in aldol chemistry. The results of these studies are summarized in Table 5.

As can be seen in Table 5 most catalysts (entries 1–5) used for aldol reactions are amines typically used in homogeneous catalytic systems that were heterogenized by binding them to polymer or inorganic support materials, respectively. Exceptions are the chiral covalent organic frameworks (CCOF, Table 5 entry 6) and lipidic cubic phases (LCP, Table 5 entry 8). While the chitosan aerogel (AG) used in Table 5 entry 7 is made from a naturally occurring resource, chitosan is usually applied as support material only, its direct use as a catalyst is yet to be explored in detail.

Ma et al. used a cinchona derivative as an organocatalyst tethered to aluminum phosphate (AIP@QNPC) as a heterogeneous system for the asymmetric aldol addition of cyclohexanone and different benzaldehydes (Table 5 entry 1). The products were obtained in high yields in most cases and with high enantiomeric excesses and syn/anti ratios.<sup>152</sup> The catalytic system could be reused 10 times without losing its activity and selectivity. The same reaction was performed by the group of Cui using a proline functionalized polystyrene as catalyst (Table 5 entry 2). The reaction was best performed in a water/petroleum ether mixture providing medium to good yields and selectivities.<sup>153</sup> Catalyst recycling was possible in three subsequent reactions. The application of proline bound to a helically chiral polyacetylene for the aldol addition of *p*-nitrobenzaldehyde and cyclohexanone in water as solvent was described by Deng and coworkers (Table 5 entry 3).<sup>154</sup> Unfortunately only one reaction was described with this interesting approach and the recyclability was not tested. A broader substrate scope was obtained by the group of Ma using a co-polymer of cinchonine and acrylonitrile in water (Table 5 entry 4).<sup>155</sup> Mostly good yields with excellent selectivities were obtained and catalyst recycling was tested in seven consecutive runs without loss of activity. Sadiq and his coworkers were able to prepare a heterogeneous catalyst for the aldol reaction of cyclohexanone and benzaldehyde by grafting different amino acids onto graphene (Table 5 entry 5).<sup>156</sup> The reaction was best performed using alanine as the amino acid and water as the solvent. Up to five runs with the same catalyst were possible without a significant drop in catalytic activity. Cui and Liu and their groups developed a chiral covalent organic framework (CCOF) which is effective as catalyst for the aldol reaction between different nitrobenzaldehydes and cyclohexanone (Table 5 entry 6).<sup>157</sup> Although the obtained yields are good in general, the enantioselectivities were low for certain examples. DMF was used as a co-solvent together with water and the catalyst was recycled five times with only a small loss in activity. A variety of aldehydes and cyclohexanone derivatives were coupled using chitosan aerogel beads in water as catalytic system (Table 5 entry 7).<sup>158</sup>

**TABLE 5** Heterogeneous catalytic enantioselective aldol reaction of cyclohexanone with substituted benzaldehydes.

| Entry | Catalyst                                  | Conditions              | Product | Yield (%) | Anti/syn   | %ee   | Recycl.  | Ref.                |
|-------|---|-------------------------|---------|-----------|------------|-------|----------|---------------------|
|       |   |                         |         |           |            |       |          |                     |
| 1     | AIP@QNPC (5 mol%)                         | H <sub>2</sub> O, RT    |         | 12–98     | 82:18–95:5 | 87–98 | 10 times | <a href="#">152</a> |
| 2     | L-Pro@PS                                  | PE/H <sub>2</sub> O, RT |         | 45–92     | 57:43–92:8 | 64–94 | 3 times  | <a href="#">153</a> |
| 3     | L-Pro@chiral polyacetylene (5 mol%)       | H <sub>2</sub> O, RT    |         | 76        | 78:22      | 80    | n/a      | <a href="#">154</a> |
| 4     | CN-derivate@poly acrylonitrile (7.5 mol%) | H <sub>2</sub> O, RT    |         | 18–98     | 39:61–98:2 | 61–99 | 7 times  | <a href="#">155</a> |

|   |                |                             |   |        |             |       |         |                          |
|---|----------------|-----------------------------|---|--------|-------------|-------|---------|--------------------------|
| 5 | L-Ala@graphene | H <sub>2</sub> O, 40°C      |  | 85     | 87:13       | 94    | 5 times | <a href="#">156</a>      |
| 6 | CCOF           | DMF/H <sub>2</sub> O,<br>RT |  | 77–97  | 50:50–90:10 | 14–96 | 5 times | <a href="#">157</a>      |
| 7 | Chitosan AG    | H <sub>2</sub> O, RT        |  | 10–95  | 53:47–87:13 | 15–85 | 4 times | <a href="#">158, 159</a> |
| 8 | LCP            | H <sub>2</sub> O, RT        |  | 35–100 | 66:34–90:10 | 67–93 | 5 times | <a href="#">160</a>      |

AIP@QNPC-cinchona derivative as organocatalyst tethered to an aluminiumphosphate; PS, polystyrene; CCOF, chiral covalent organic framework; AG, aerogel; LCP, lipidic cubic phases.

A broad range of yield and selectivity was observed and was dependent on the substrates used. The authors could prove the recyclability of the catalyst in four reactions without change in activity and selectivity. The group of Landau developed lipidic mesophases (LCP) as reactors for the asymmetric aldol reaction of cyclohexanone with benzaldehydes in water (Table 5 entry 8).<sup>160</sup> The catalyst could be reused five times giving the desired product in medium to excellent yield as well as enantioselectivity and *syn/anti* ratios.

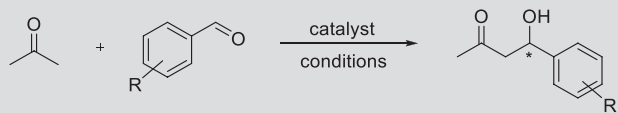
Another test reaction used to characterize solid catalysts for the aldol-reaction is between benzaldehydes and acetone as reaction partners (see Table 6). As in the previous examples the catalysts used are made by immobilizing a usually homogeneous organocatalyst to a heterogeneous support material thus creating the desired catalytic system.

The group of Yin was able to fix L-Proline on to a graphene oxide support (L-Pro@GO) for the aldol reaction of acetone with a selection of benzaldehydes bearing an electron-withdrawing group (Table 6 entry 1).<sup>161</sup> The reactions were performed using acetone as the reactant and solvent in-one thus eliminating the need for an additional solvent. Medium to good enantioselectivities were obtained and the catalytic system was reused seven times without a drop in yield and selectivity being observed. A very similar substrate scope was investigated by Liu et al. using a catalyst consisting of a cinchonine-proline adduct immobilized on a polyoxometalate (D-P-cinchonine@POM).<sup>162</sup> Although the yields and selectivities that were obtained are comparable to the L-Pro@GO system, the catalyst could only be recycled twice before a notable loss in yield and an increase in reaction time was observed. The group of Fülöp developed a heterogeneous catalyst based on a peptide covalently bound to polystyrene resin.<sup>163</sup> The catalyst was successfully applied in the aldol reaction of acetone with different benzaldehydes in a flow reactor (Table 6 entry 3). The yields obtained were good for most substrates and the catalyst performed better in a flow system compared to the traditional batch approach. Twenty reaction cycles were performed with the flow system without a drop in yield and selectivity.

Pericas and his co-workers developed a heterogeneous catalyst for the Robinson annulation of cyclic 1,3-diketones with vinyl ketones also under continuous flow conditions.<sup>164</sup> The catalyst consisting of a polymer-bound amine was able to produce the desired cyclized products in high yields and excellent enantioselectivities (Scheme 39). The researchers showed that the catalyst could be recycled 10 times without a change in its activity. The environmentally benign solvent 2-methyltetrahydrofuran (2-MeTHF) was used for the transformation further decreasing the environmental impact of the reaction.

Pothanagandhi and Vijayakrishna synthesized several chiral poly(ionic liquids) (PIL-resins) and used them as catalyst for the Baylis-Hillman reaction between methyl-vinyl ketones and *p*-nitrobenzaldehyde (Scheme 40).<sup>165</sup> The reaction was best performed under solvent-free conditions giving yields of up to 94%. Unfortunately, the obtained enantiomeric excess was low. The catalyst could be recycled up to four times while maintaining its catalytic activity.

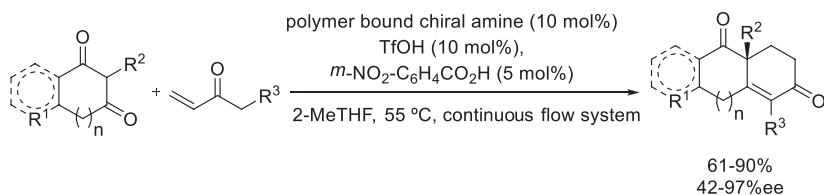
**TABLE 6** Heterogeneous catalytic enantioselective aldol reaction of acetone with substituted benzaldehydes.



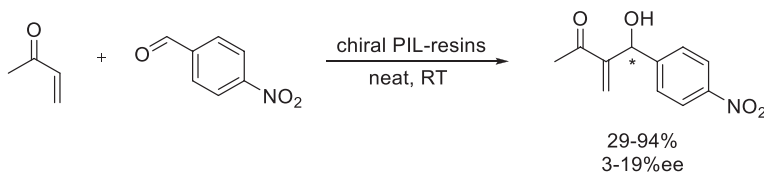
| Entry | Catalyst             | Conditions  | Product | Yield (%) | %ee   | Recycl.  | Ref.                |
|-------|----------------------|---|---------|-----------|-------|----------|---------------------|
| 1     | L-Pro@GO             | Acetone, 30°C                                     |         | 43–96     | 55–79 | 7 times  | <a href="#">161</a> |
| 2     | D-P-cinchonine@POM   | Acetone, RT                                       |         | 67–90     | 57–80 | 2 times  | <a href="#">162</a> |
| 3     | Pro-Pro-Asp-NH-resin | Acetone, RT, continuous flow (0.1 mL/min, 60 bar) |         | 27–99     | 70–80 | 20 times | <a href="#">163</a> |

EWG, electron withdrawing group; GO, graphene oxide; POM, polyoxometalate.

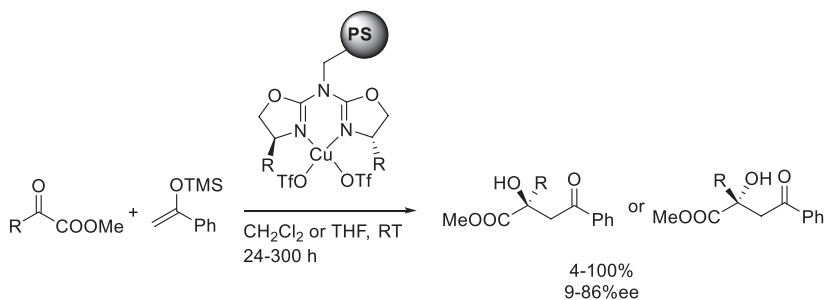
624 Heterogeneous catalysis in sustainable synthesis



**SCHEME 39** Robinson annulation of cyclic 1,3-diketones with vinyl ketones under continuous flow conditions catalyzed by a polymer-bound amine.



**SCHEME 40** Baylis-Hillman reaction between methyl-vinyl ketones and *p*-nitrobenzaldehyde catalyzed by chiral poly(ionic liquids) (PIL-resins).



**SCHEME 41** The Mukaiyama aldol reaction of  $\alpha$ -ketoesters and 1-phenyl-(trimethylsilyloxy)ethene catalyzed by Box and azaBox-Cu(II) complexes immobilized on polystyrene.

Multipurpose Box and aza-Box-based complexes have been reported as effective immobilized asymmetric catalysts.<sup>166</sup> Box and azaBox-Cu(II) complexes immobilized on polystyrene have been found as highly active and selective catalysts for the Mukaiyama aldol reaction (Scheme 41).<sup>167</sup> The reaction provided widely varied yields and selectivities depending on the experimental conditions. The catalyst showed stable activity and selectivity in two consecutive reactions, further recycling was not studied.

### 3.10.4.2 Michael additions

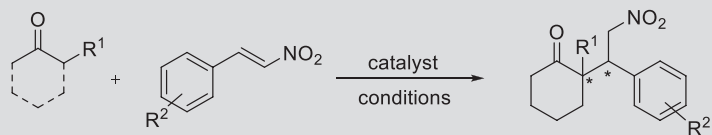
Michael reactions represent another important transformation to form C–C bonds. The results of enantioselective Michael addition using nitrostyrene and various carbonyl compounds are summarized in Table 7.

**TABLE 7** Heterogeneous catalytic enantioselective Michael reactions of nitrostyrene with carbonyl compounds.

| Entry | Catalyst                                     | Conditions                        | Product | Yield (%) | Syn/anti   | %ee   | Recycl. | Ref.                |
|-------|--|-----------------------------------|---------|-----------|------------|-------|---------|---------------------|
|       |  |                                   |         |           |            |       |         |                     |
| 1     | DUT-67-proline<br>(5 mol%)                   | iPrOH/EtOH, 50°C                  |         | 93        | 96:4       | 38    | 5 times | <a href="#">168</a> |
| 2     | L-Pro-Lap RD                                 | CHCl <sub>3</sub> /EtOH (9:1), RT |         | 86–99     | 91:9–97:3  | 25–92 | 3 times | <a href="#">169</a> |
| 3     | Poly(St-co-ProTMS-co-AA) HBs(a)<br>(15 mol%) | CHCl <sub>3</sub> , RT            |         | 86–98     | 81:19–93:7 | 93–99 | 4 times | <a href="#">170</a> |

*Continued*

**TABLE 7** Heterogeneous catalytic enantioselective Michael reactions of nitrostyrene with carbonyl compounds—cont'd

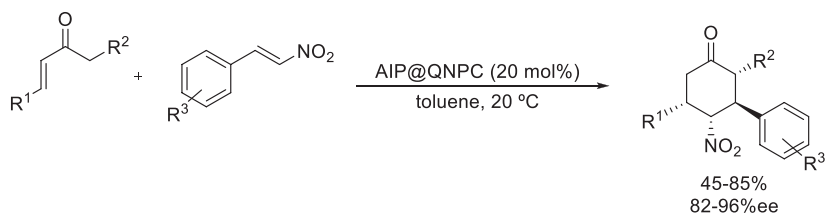


| Entry | Catalyst                    | Conditions                      | Product | Yield (%) | Syn/anti   | %ee   | Recycl. | Ref.                |
|-------|-----------------------------|---------------------------------|---------|-----------|------------|-------|---------|---------------------|
| 4     | Tfp2-COF (10 mol%)          | EtOH/H <sub>2</sub> O, RT       |         | 92–95     | 94:6       | 85–86 | 5 times | <a href="#">171</a> |
| 5     | SQ-supp. chiral pyrrolidine | Neat, RT                        |         | 85–91     | 97:3–99:1  | 95–98 | 4 times | <a href="#">172</a> |
| 6     | JH-CPP                      | EtOH/H <sub>2</sub> O (1:1), RT |         | 67–99     | 74:26–97:3 | 93–99 | 2 times | <a href="#">173</a> |

DUT, a proline-modified zirconium-based metal organic framework; L-Pro-Lap, L-proline absorbed on laponite; Poly(St-co-ProTMS-co-AA) HBs, hollow nanospheres made of a copolymer containing a proline derivative; COF, covalent organic framework; SQ, supp. chiral pyrrolidine; JH-CPP, Jørgensen-Hayashi catalyst embedded in porous polymer.

Senkovska, Kaskel and their co-workers developed a proline-modified zirconium-based metal organic framework (Zr-MOF) for the Michael reaction of cyclohexanone with nitrostyrene (Table 7 entry 1).<sup>168</sup> The reaction could be performed in the environmentally benign solvent EtOH/*i*PrOH and the catalyst could be recycled five times. Even though the system gave high yield and diastereoselectivity (*syn* vs. *anti*), its application is limited by the fact that only one substrate was tested and the enantioselectivity obtained was rather low. Szöllösi et al. described the use of proline absorbed on laponite for the Michael addition of different aldehydes and ketones to nitrostyrene (Table 7 entry 2).<sup>169</sup> Although the yield and diastereoselectivity was high for all substrates tested, several reactions resulted in only low enantioselectivity. Reusability tests showed that the catalyst loses its activity after three runs although the stereoselectivity is maintained. When additional proline was added, the activity of the catalyst was restored leading to the assumption that leaching of the proline is the major cause of the activity loss. Another drawback of the reaction system is the use of chloroform as part of the solvent system. Chloroform was also used by the group of Ma for the Michael addition of propanal with different substituted nitrostyrenes (Table 7 entry 3).<sup>170</sup> The catalytic system used consisted of hollow nanospheres made of a copolymer containing a proline derivative (Poly(St-co-ProTMS-co-AA) HBs(a)). The system performed well with respect to yield and stereoselectivity of the transformation and was recyclable four times before a drop in diastereoselectivity was observed. A chiral covalent organic framework containing pyrrolidine units (Tfp<sub>2</sub>-COF) was used for the Michael addition of cyclohexanone with some substituted nitrostyrenes (Table 7 entry 4).<sup>171</sup> The reaction could be performed in water/ethanol mixture and the products were obtained in high yields and stereoselectivities. Recycling of the catalyst was possible five times without loss of activity. A chiral pyrrolidine bridged polyhedral oligomeric silsesquioxane (SQ-supp. chiral pyrrolidine) was developed for the same reaction (Table 7 entry 5).<sup>172</sup> With a similar substrate scope as described earlier, the authors obtained high yields with excellent stereoselectivities. No solvent was used, and the catalyst could be recycled four times with just a slight decrease in activity. The group of Wang developed a porous polymer with an embedded Jørgensen-Hayashi catalyst (JH-CPP) for the enantioselective Michael-addition of different aldehydes and several nitrostyrenes (Table 7 entry 6).<sup>173</sup> The system works well with ethanol/water mixture as solvent producing good to excellent yields and stereoselectivities. Recycling experiments showed that while the stereoselectivity was maintained for four runs, the yield of the reaction dropped significantly after the second use.

The group of Ma showed that their cinchona-derived catalyst (AIP@QNPC) is not only able to perform the aldol-addition but can also be used for a cascade Michael reaction of unsaturated ketones with nitrostyrenes.<sup>152</sup> The reaction yielded the desired cyclic products in good yields and high enantio- and diastereoselectivities (Scheme 42). Unfortunately, toluene had to be used as solvent in order to perform this interesting tandem reaction.

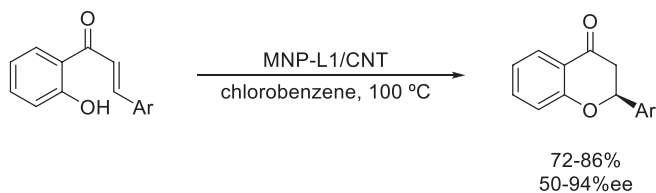


**SCHEME 42** An enantioselective cascade Michael reaction of unsaturated ketones with nitrostyrenes catalyzed by a cinchona-derived catalyst.

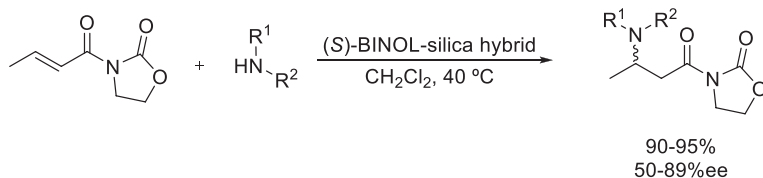
Shaikh et al. used chiral ferrites in carbon nanotubes as nanoscale reaction vessels (MNP-L1/CNT) as catalyst in the intramolecular oxa-Michael addition of chalcones.<sup>174</sup> The catalyst was prepared by treating the ferrite material with a chiral phosphoric acid to obtain the cyclic products in high yields and enantioselectivities (Scheme 43). The catalyst could be easily recycled due to its magnetic properties and reused without loss of activity. The fact that chlorobenzene had to be used at 100°C increases the environmental impact of the reaction.

The aza-Michael addition of amines to an unsaturated amide was carried out using a chiral silica hybrid catalyst containing (*S*)-BINOL units (Scheme 44).<sup>175</sup> While the yield obtained for the reaction was high in all cases the reaction suffers from a low enantioselectivity in some cases and the required use of dichloromethane as solvent. Unfortunately, the absolute configuration of the product was not determined and no information about the recycling of the catalyst is given.

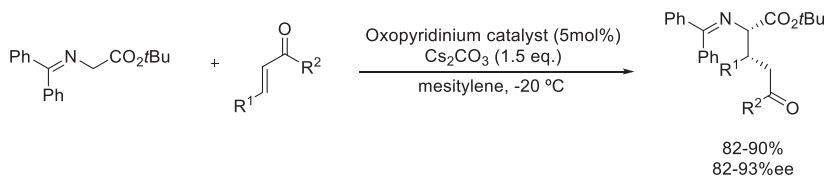
Kobayashi et al. developed a polystyrene-supported chiral oxopyridinium phase transfer catalyst for the Michael addition of imines to unsaturated ketones



**SCHEME 43** An enantioselective intramolecular oxa-Michael addition of chalcones catalyzed by chiral ferrites in carbon nanotubes as nanoscale reaction vessels (MNP-L1/CNT).



**SCHEME 44** The enantioselective aza-Michael addition of amines to an unsaturated amide catalyzed by a chiral silica hybrid catalyst containing (*S*)-BINOL.



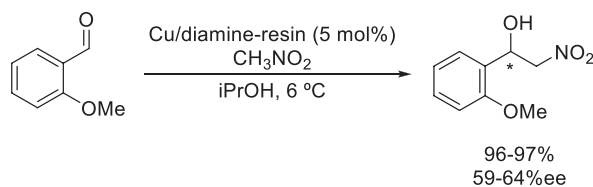
**SCHEME 45** A polystyrene-supported chiral oxopyridinium phase transfer catalyst-promoted Michael addition of imines to unsaturated ketones.

(Scheme 45).<sup>176</sup> While the reaction performed well, using a rather unusual imine substrate that gave the products in high yields and enantioselectivities, the environmental impact of the solvent mesitylene should not be neglected. The catalyst can be easily recovered and recycled five times without losing its activity and enantioselectivity.

### 3.10.4.3 Henry reactions

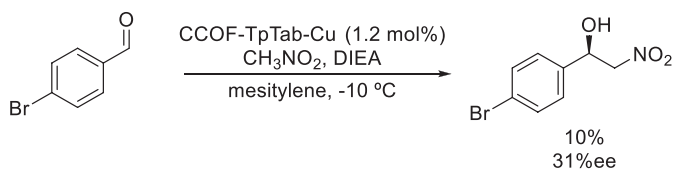
Novakova et al. synthesized a supported diamine-copper complex for the asymmetric Henry reaction between nitromethane and 2-methoxybenzaldehyde.<sup>177</sup> The reaction proceeds with good yield and moderate enantioselectivity. While the authors tested a variety of benzaldehydes for a homogeneous version of the catalyst, the heterogeneous version was only investigated for this one substrate (Scheme 46). The catalyst was shown to be recyclable four times before a decrease in activity was observed. The reaction was performed in isopropanol as green solvent. Depending on the configuration of the diamine used, both enantiomers of the product can be synthesized.

The group of Cui synthesized a chiral covalent organic framework containing amine binding sites able to coordinate a copper atom (CCOF-TpTab-Cu). The material could not only be used for enantioselective sensing of saccharides but was also shown to be useful as catalyst for the Henry reaction of *p*-bromobenzaldehyde and nitromethane.<sup>178</sup> Although the catalyst was able to perform the addition reaction with yields up to 90%, the best enantiomeric excess (31%ee) was obtained at low conversions (Scheme 47). Mesitylene was used as the solvent leaving room for improvement with regard to the greenness of the reaction. A related, pyridine-based chiral ionic covalent organic framework has also been applied in the Henry reaction with similar success.<sup>179</sup>



**SCHEME 46** A resin-supported chiral diamine-copper complex for the asymmetric Henry reaction between nitromethane and 2-methoxybenzaldehyde.

630 Heterogeneous catalysis in sustainable synthesis



**SCHEME 47** A chiral covalent organic frameworks (CCOF-TpTab-Cu)-catalyzed enantioselective Henry reaction of *p*-bromobenzaldehyde and nitromethane.

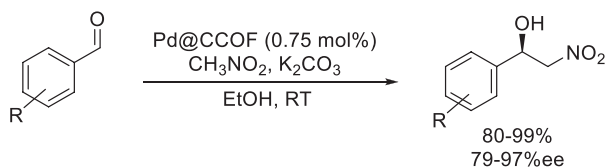
A chiral covalent organic framework containing palladium nanoparticles was used as a catalyst for the Henry reaction of benzaldehydes by Ma et al.<sup>180</sup> The reaction yielded a broad variety of the desired products, with several different substituents on the aromatic ring, in excellent yields and enantioselectivities (Scheme 48). The reaction was performed in ethanol as a green solvent at ambient temperature and the catalyst could be recycled up to five times with only minimal loss of activity.

### 3.10.5 Multicomponent and various other reactions

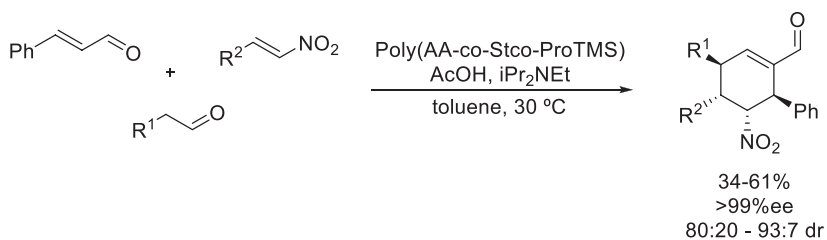
#### 3.10.5.1 Multicomponent reactions

The group of Ma developed a heterogeneous catalyst consisting of a Jørgensen-type catalyst anchored on hollow polyacrylamide spheres.<sup>181</sup> The catalyst proved to be effective for the three-component coupling of cinnamaldehyde, nitrostyrenes, and aliphatic aldehydes by an organocascade reaction. The desired cyclohexene derivatives were obtained in moderate yields with excellent enantioselectivities and good diastereomeric ratios (Scheme 49). The catalyst could be reused in five consecutive cycles without losing its catalytic activity or selectivity.

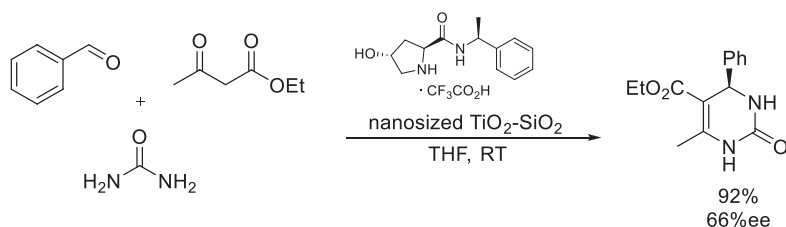
Fedorova et al. showed that the asymmetric Biginelli reaction can be catalyzed by nanosized metal oxide particles and a proline-derived chiral modifier.<sup>182</sup> The desired product was obtained in good yield and moderate enantioselectivity (Scheme 50). The authors showed that several factors such as particle size of the catalyst, water content of the solvent or the order of addition played a critical role for the performance of the reaction. While the catalyst could be recycled multiple times, the yield dropped significantly after the third run.



**SCHEME 48** The enantioselective Henry reaction of benzaldehydes with nitromethane catalyzed by a chiral covalent organic framework containing palladium nanoparticles.

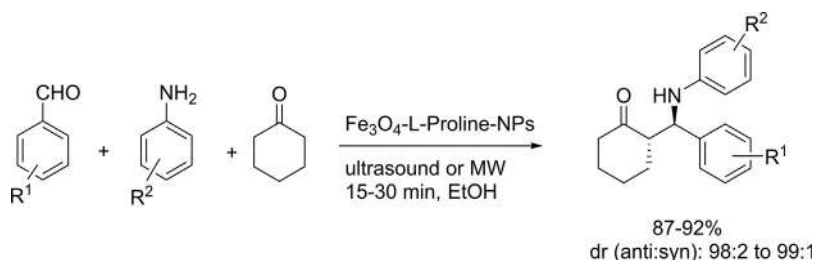


**SCHEME 49** The enantioselective three-component coupling of cinnamaldehyde, nitrostyrenes, and aliphatic aldehydes catalyzed by a Jørgensen-type catalyst anchored on hollow polyacrylamide spheres.



**SCHEME 50** An asymmetric Biginelli reaction catalyzed by nanosized metal oxide particles and a proline-derived chiral modifier.

Ghomia and Zahedi developed an enantioselective Mannich reaction of cyclohexanone, various substituted aromatic amines, and aromatic aldehydes.<sup>183</sup> The authors applied ultrasounds or microwave irradiation, respectively, to enhance the reaction rate as well as the selectivity. Fe<sub>3</sub>O<sub>4</sub>-L-proline nanoparticles were applied as the chiral catalyst in EtOH as a green solvent (Scheme 51). The inexpensive, magnetic catalyst was easily recyclable with a simple external magnet. Reusability, eco-friendly solvent, short reaction times, high yields, and easy workup make this protocol an environmentally benign alternative to traditional methods.



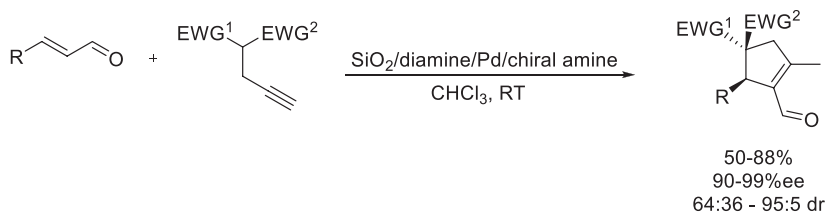
**SCHEME 51** Application of a magnetic Fe<sub>3</sub>O<sub>4</sub>-L-proline nanoparticles (NPs) as chiral catalyst for the enantioselective Mannich reaction of cyclohexanone, aromatic amines, and aromatic aldehydes.

### 3.10.5.2 Cascade and tandem reactions

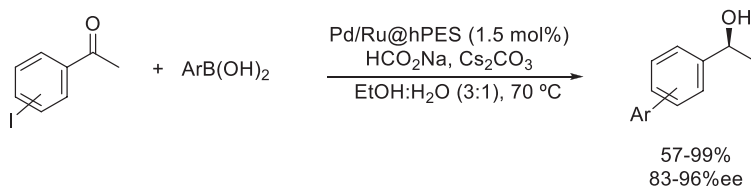
The group of Córdova developed a bifunctional SiO<sub>2</sub>-supported catalyst for a conjugate addition, ring closing cascade reaction of cinnamaldehydes and alkynes.<sup>184</sup> In order to obtain the desired products the researchers modified the SiO<sub>2</sub> surface with a Jørgensen-type organocatalyst to promote the Michael addition and a Pd-center allowing for the ring closing reaction to take place. The reaction afforded tetrasubstituted cyclopentenones in moderate yields and high enantio- and diastereoselectivities (Scheme 52). Unfortunately, the reaction had to be performed in chloroform in order to obtain reasonable yields, thus increasing the environmental impact of the procedure. Recycling studies showed limited recyclability due to the leaching of the chiral amine from the catalyst.

The one-pot tandem Suzuki coupling/ketone reduction reaction of arylboronic acids with iodoacetophenones was achieved by using a bimetallic (Pd/Ru) hyperbranched polyethoxysiloxane (Pd/Ru@hPES) catalyst.<sup>185</sup> The reaction gave mostly excellent yields and enantioselectivities with sodium formate as hydrogen transfer agent and water/ethanol mixture as a solvent (Scheme 53). No decrease in yield was observed in the first four reuses of the catalyst, after that a slight decline in performance was detected. The decreased yield was attributed to the leaching of Ru from the system as the keto-compound was obtained instead of the alcohol.

A bifunctional heterogeneous catalyst containing basic sites as well as Rh centers on mesostructured silica nanoparticles (DABCO/Rh@MSNs) was used by Liao et al. to catalyze the tandem ketone reduction followed by cyclization or substitution.<sup>186</sup> The reaction starts with the asymmetric transfer hydrogenation



**SCHEME 52** The enantioselective conjugate addition-ring closing cascade reaction of cinnamaldehydes and alkynes catalyzed by bifunctional SiO<sub>2</sub>-supported Jørgensen-type organocatalyst.

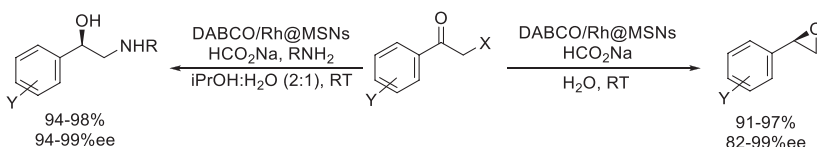


**SCHEME 53** The one-pot tandem Suzuki coupling/ketone reduction of arylboronic acids with iodoacetophenones catalyzed by a bimetallic (Pd/Ru)-doped hyperbranched polyethoxysiloxane (Pd/Ru@hPES).

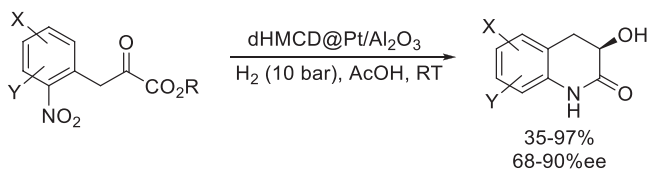
to reduce the ketone followed by the cyclization to form the epoxide in the absence of an additional nucleophile. If a nucleophile is present, substitution takes place instead (Scheme 54). The cyclization pathway can be shut down when the catalyst is prepared without the basic sites.<sup>187</sup>

Szöllösi et al. described the enantioselective reduction/cyclization cascade reaction to form 3-hydroxy-3,4-dihydroquinolin-2(1H)-ones using a Pt/Al<sub>2</sub>O<sub>3</sub> catalyst modified with a cinchonidine derivative (dHMCD@Pt/Al<sub>2</sub>O<sub>3</sub>).<sup>188</sup> Starting from 2-nitro-phenylpyruvates the desired products were obtained in good yields and high enantioselectivities after two reduction and one cyclization steps (Scheme 55).

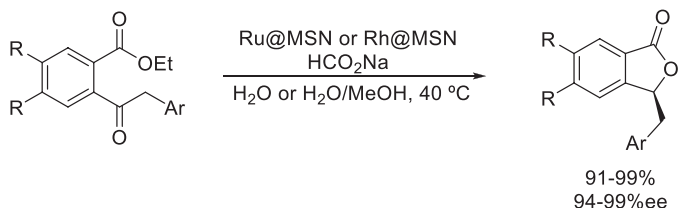
The group of Liu performed several studies regarding the tandem reduction-lactonization of ethyl 2-acylarylcarboxylates to generate phthalides. The authors described the use of both nanospheres functionalized with Rh<sup>189, 190</sup> as well as Ru<sup>115</sup> (Rh@MSN or Ru@MSN) to perform the desired reaction. The products were obtained in high yields and enantioselectivities using aqueous solvent systems (Scheme 56).



**SCHEME 54** Basic sites and Rh centers-containing mesostructured silica nanoparticles (DABCO/Rh@MSNs)-catalyzed enantioselective tandem ketone reduction followed by cyclization or substitution.



**SCHEME 55** An enantioselective reduction/cyclization cascade of 2-nitro-phenylpyruvates to form 3-hydroxy-3,4-dihydroquinolin-2(1H)-ones catalyzed by a Pt/Al<sub>2</sub>O<sub>3</sub> modified with a cinchonidine derivative (dHMCD@Pt/Al<sub>2</sub>O<sub>3</sub>).



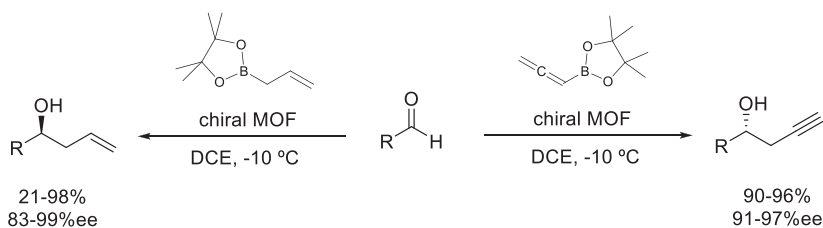
**SCHEME 56** The enantioselective tandem reduction-lactonization of ethyl 2-acylarylcarboxylates to phthalides catalyzed by nanospheres functionalized with Rh or Ru (Rh@MSN or Ru@MSN).

### 3.10.5.3 Other reactions

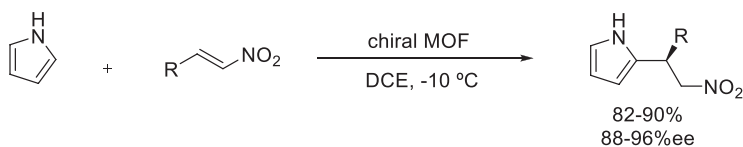
The chiral phosphonate MOF developed by Chen et al. for the oxidation of sulfides also proved to be effective for the allylboration and propargylation of aldehydes (Scheme 57), as well as the Friedel-Craft alkylation of pyrrole with nitrostyrenes (Scheme 58).<sup>30</sup> Recycling studies were performed for the catalyst and indicated that no catalyst degradation took place even after 10 runs.

Ansari et al. developed an enantioselective heterogeneous catalytic Strecker reaction using quinine thiourea catalyst bound to SBA-15 support (SBA-Qnthio).<sup>191</sup> A variety of isatin N-Boc ketimines were submitted to the reaction and yielded the desired products in high yields and enantioselectivities (Scheme 59). However the reaction uses TMSCN, a nongreen reagent, and CH<sub>2</sub>Cl<sub>2</sub> as a solvent that should be avoided, if possible. The catalyst was found to be recyclable five times without losing its activity or selectivity.

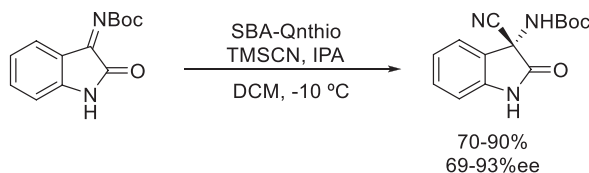
The group of Wang described the heterogeneous Diels-Alder reaction of cinnamaldehydes with cyclopentadiene using a MacMillan-type catalyst-containing chiral nanoporous organic polymer (Mac-CPOP).<sup>192</sup> The reaction performed well using a water-methanol mixture as solvent yielding the de-



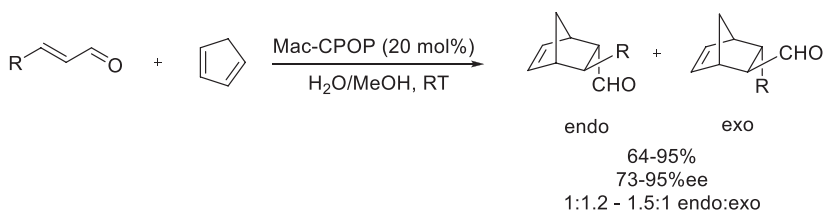
**SCHEME 57** The enantioselective allylboration and propargylation of aldehydes catalyzed by a chiral phosphonate MOF.



**SCHEME 58** Enantioselective Friedel-Craft alkylation of pyrrole with nitrostyrenes catalyzed by a chiral phosphonate MOF.



**SCHEME 59** An enantioselective heterogeneous catalytic Strecker reaction of isatin N-Boc ketimines and TMSCN catalyzed by a quinine thiourea catalyst bound to SBA-15 support (SBA-Qnthio).



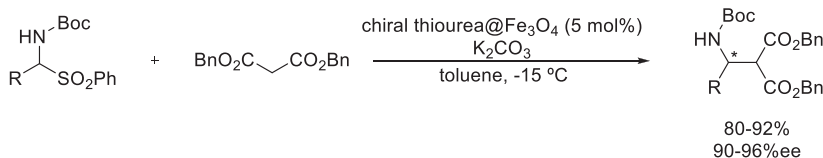
**SCHEME 60** An enantioselective heterogeneous catalytic Diels-Alder reaction of cinnamaldehydes with cyclopentadiene using a MacMillan-type catalyst-containing chiral nanoporous organic polymer (Mac-CPOP).

sired bicyclic compounds in high yields and enantioselectivities (Scheme 60). Unfortunately, the *exo* and *endo* products were obtained in equal ratios for most products described. The catalyst could be recycled and only showed a slight decrease in activity over the course of six runs.

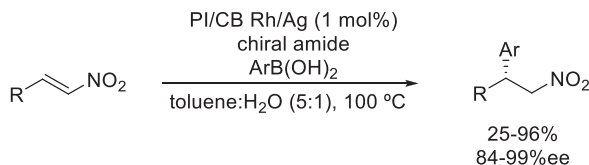
Zhu et al. developed a chiral thiourea-based catalyst for the Mannich-type reaction of  $\alpha$ -amid sulfones with dibenzyl malonate.<sup>193</sup> The thiourea catalyst was grafted onto magnetic nanoparticles allowing for the easy separation of the catalyst after the reaction. The Mannich product was obtained in high yields and enantioselectivities after initial formation of an imine by loss of the sulfone moiety (Scheme 61). Depending on the configuration of the stereogenic centers in the catalyst both enantiomers of the product could be obtained selectively. Recycling experiments showed that both yield and enantioselectivity remained stable in 15 consecutive runs.

The group of Kobayashi investigated the coupling reaction of aryl boronic acids with nitrostyrenes using polymer-incarcerated Rh nanoparticles in a cross-linked polystyrene (PI/CB Rh/Ag) and a chiral amide ligand.<sup>194</sup> The products were obtained in mostly high yields and excellent enantioselectivities using a toluene-water mixture as solvent (Scheme 62). Only a low catalyst loading of 1 mol% was needed and the catalyst could be recycled up to five times, albeit with gradually decreasing yield.

Dong, Liu and Cui synthesized chiral porous organic framework (cPOF)-containing coordinated Rh units and showed that it can be used as heterogeneous catalyst for the coupling of arylboronic acids to 2-cyclohexenone.<sup>195</sup> Although the desired products were obtained mostly in high yields and enantioselectivities, the reaction had to be performed in a dioxane-water mixture



**SCHEME 61** A heterogeneous catalytic enantioselective Mannich-type reaction of  $\alpha$ -amid sulfones with dibenzyl malonate catalyzed by a magnetic nanoparticles-supported chiral thiourea.

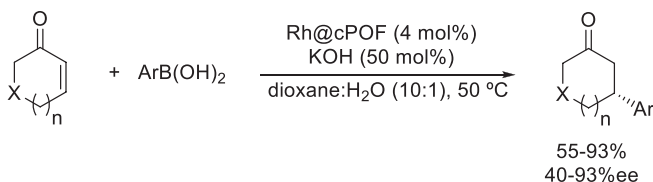


**SCHEME 62** An enantioselective heterogeneous catalytic coupling reaction of aryl boronic acids with nitrostyrenes catalyzed by cross-linked polystyrene-incarcerated Rh/Ag nanoparticles (PI/CB Rh/Ag) and a chiral amide ligand.

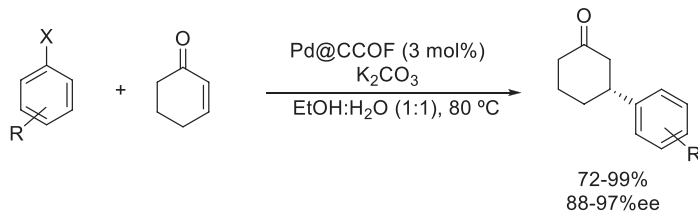
containing 50 mol% KOH, increasing the environmental impact of the system (Scheme 63). The recycling experiments showed that while it was possible to reuse the catalyst, in order to preserve its activity, additional Rh-salt had to be added in each subsequent run.

The group of Dong reported that their Pd-loaded homochiral covalent organic framework (Pd@CCOF) can not only be used for the asymmetric Henry reaction but also for the reductive Heck reaction of 2-cyclohexenones with aromatic halides.<sup>180</sup> The reaction gave high yields and enantioselectivities for a variety of aromatic substrates in a green, ethanol-water mixture as the solvent (Scheme 64). Recycling experiments showed that the catalyst could be recycled up to five times with only a minimal loss in activity and selectivity.

Chiral imines are important compounds, particularly in medicinal chemistry applications, and their environmentally benign synthesis attracted significant attention. Ellman et al. described the synthesis of chiral *tert*-butylsulfinylamines, commonly used as chiral auxiliaries for the synthesis of chiral amines.<sup>196</sup> The authors described their method to be as effective as other similar protocols to



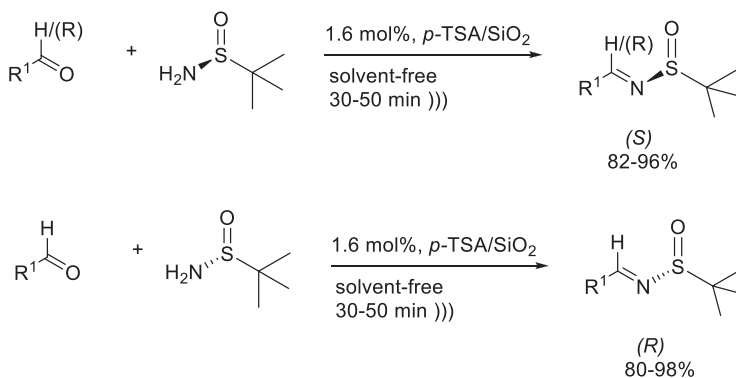
**SCHEME 63** A chiral porous organic framework (cPOF) containing coordinated Rh units-promoted heterogeneous catalytic enantioselective coupling of arylboronic acids to 2-cyclohexenone derivatives.



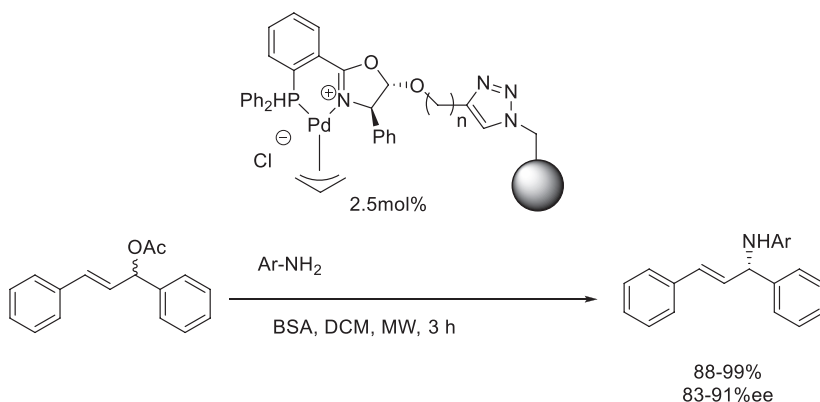
**SCHEME 64** A Pd-loaded homochiral covalent organic framework (Pd@CCOF)-catalyzed asymmetric reductive Heck reaction of 2-cyclohexenones with aromatic halides.

produce chiral amine-containing precursors and more complex products.<sup>197-199</sup> A heterogeneous catalytic alternative by a simple sonochemical protocol was reported by Appa et al. for the synthesis of *tert*-butylsulfinylimines from various aldehydes under solvent-free conditions.<sup>200</sup> The authors prepared a silica-supported *p*-toluenesulfonic acid (*p*-TSA/SiO<sub>2</sub>) as an efficient, safe, and inexpensive catalyst for the reaction (Scheme 65). The process took place with the complete retention of the original stereochemistry in the case of both enantiomers.

Popa et al. reported a continuous-flow protocol for the asymmetric allylic amination of racemic enolic acetates using a phosphinoxazoline-Pd catalyst immobilized on a resin support (Scheme 66).<sup>201</sup> The resin-immobilized complex was prepared using click chemistry and was efficiently applied in the allylic amination. The microwave-assisted version of the reaction was particularly efficient.



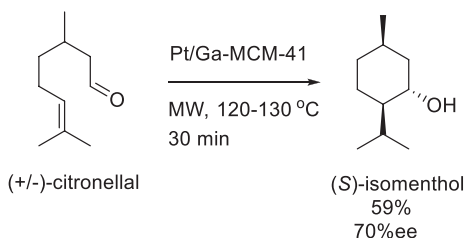
**SCHEME 65** A silica-supported *p*-toluenesulfonic acid (*p*-TSA/SiO<sub>2</sub>)-catalyzed synthesis of chiral sulfinylimines.



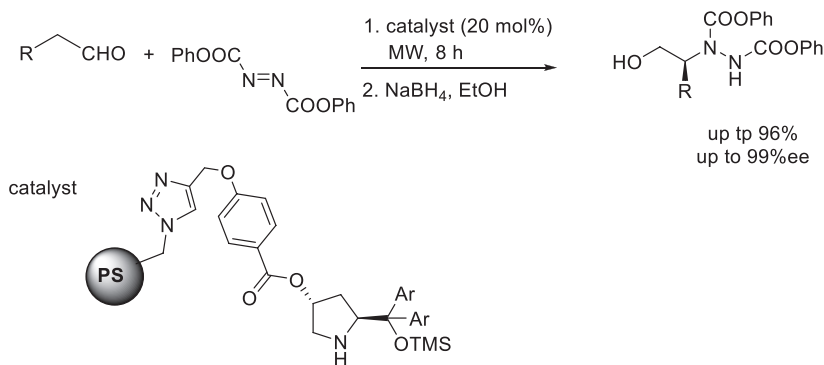
**SCHEME 66** Asymmetric allylic amination of racemic enol acetates by a resin-supported phosphinoxazoline-Pd catalyst.

Balu et al. reported a microwave-assisted one-step cyclization/hydrogenation process for the synthesis of menthols via the transformation of citronellal to the target compounds (Scheme 67).<sup>202</sup> The reaction was carried out in a one-pot manner using microwave irradiation to activate the system. The authors used Pt nanoparticles supported on Ga-doped MCM-41, a mesoporous material, as a catalyst. Using (+)-citronellal as the substrate, the protocol provided (–)-menthol with high diastereoselectivities. The catalyst preparation was optimized as well and the 2% Pt/Ga-MCM-41 was found to exhibit the best performance. The reaction was also carried out with enantiomerically pure (+)-citronellal leading to a 55% maximum selectivity to (–)-menthol. The enantioselectivity was enhanced by the addition of cinchonidine; in this case (–)-menthol was obtained with up to a 75% ee. The catalyst was highly stable under the reaction conditions and was found to be reusable.

Beletskaya et al. prepared a new proline-based heterogeneous catalyst for the addition of aliphatic aldehydes to azodicarboxylates (Scheme 68).<sup>203</sup> The catalyst was synthesized by anchoring  $\alpha,\alpha$ -bis[bis-3,5-(trifluoromethyl)phenyl]prolinol silyl ether onto polystyrene. It was found to be ideal for this transformation providing the products in high yields (up to 96%) and nearly exclusive



**SCHEME 67** Application of Pt supported on Ga-doped MCM-41 in an asymmetric hydrogen transfer/cyclization of (+/–)-citronellal to (S)-isomenthol.



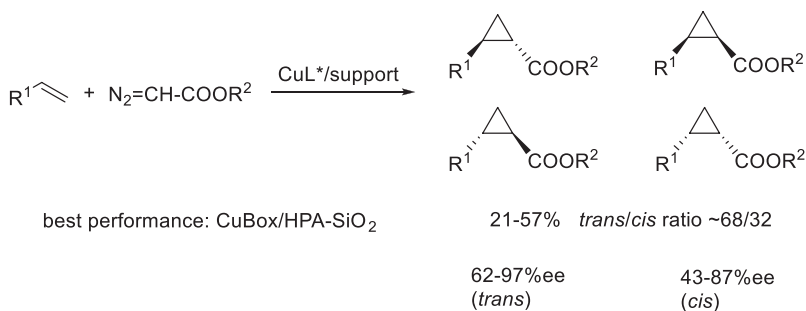
**SCHEME 68** A microwave-assisted enantioselective heterogeneous catalytic addition of aliphatic aldehydes to azodicarboxylates promoted by a polystyrene-anchored proline-based chiral organo-catalyst (PS, polystyrene).

enantioselectivity (up to 99%). In addition, the catalyst could be recycled in three subsequent runs without any loss of its performance.

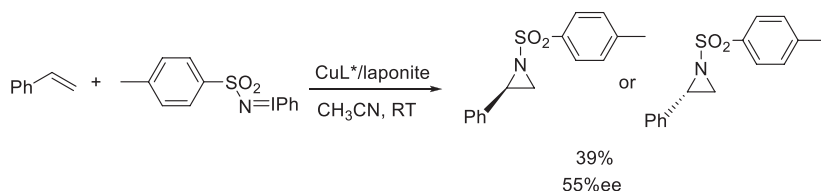
The enantioselective addition of carbene equivalents to alkenes readily yields chiral cyclopropanes<sup>204–206</sup> while the similar reactions with nitrene precursors result in the formation of aziridines,<sup>207, 208</sup> both are important building blocks.

Although most cyclopropanation reactions are catalyzed by homogeneous catalysts, extensive studies have been carried out over the years to develop heterogeneous catalytic alternatives for these reactions.<sup>209, 210</sup> The most common modifier in heterogeneous applications is the immobilized bis(oxazoline) (Box)-based ligands in the form of Cu-complexes.<sup>211</sup> The reaction is usually carried out with alkenes and diazo compounds (ethyl diazoacetate is the most common) (Scheme 69). These complexes have been immobilized on a large variety of supports, such as mesoporous silica,<sup>212</sup> laponite clay,<sup>213–216</sup> HPA-silica,<sup>217</sup> silica,<sup>218</sup> or polymers.<sup>219, 220</sup> In fact, this cyclopropanation is a commonly applied test reaction for these immobilized complex-containing catalysts. Interestingly, some derivatives (e.g., copper-pyridineoxazoline, Cu-pyox) are poor catalysts in homogeneous cyclopropanations, however, the immobilization of the complex significantly improves the enantioselectivity, up to sevenfold compared to that of the homogeneous Cu-pyox catalysts.<sup>221</sup> The solid cyclopropanation catalysts were found generally recyclable, in many cases they remained catalytically stable in 14 reaction cycles maintaining their activity and selectivity.<sup>205</sup>

The above described immobilized CuBox-complexes have been applied in a similar reaction of alkenes using a nitrene analog, such as TosN=IPh, to produce aziridines (Scheme 70).<sup>222</sup> The complex was anchored to an anionic support using a laponite clay. Although the reaction is important and the catalyst was found to be recyclable, the moderate enantioselectivities render the process as impractical at this point. Another clay, K-10 montmorillonite was reported to efficiently catalyze the aziridation of alkenes with ethyl diazoacetate and produce the *cis* products in high yields (up to 95%) and exclusive diastereoselectivity.<sup>223</sup>



**SCHEME 69** Enantioselective heterogeneous catalytic cyclopropanation of alkenes with ethyl diazoacetate promoted by a silica-supported heteropoly acid anchored copper-bis(oxazoline) complex.



**SCHEME 70** Enantioselective heterogeneous catalytic aziridination of alkenes with  $\text{TosN=IPh}$ , promoted by laponite-supported copper-bis(oxazolidine) complexes.

### 3.10.6 Conclusions and outlook

In light of the above-mentioned works, the field of heterogeneous asymmetric catalysis has enjoyed extensive attention in the past two decades. It does not only apply to fields that are traditionally strong within heterogeneous catalysis (i.e., catalytic hydrogenation) but also to important areas of organic synthesis that used to be rooted in homogeneous catalysis (i.e., aldol reaction, Michael addition, aziridination, etc.). This represents a desirable tendency in the development of protocols that consider the environmental impact of these transformations. Due to the lack of inherently chiral heterogeneous materials most approaches currently under investigation involve the incorporation or fixation of a small chiral molecule to a heterogeneous support. Future development in the field is likely to involve inherently chiral materials; the first promising results have been recently obtained using helically chiral polymers or chiral metal-organic frameworks and related materials.

## References

1. Drayer, D. E. The Early History of Stereochemistry. In *Drug Stereochemistry. Analytical Methods and Pharmacology*; Wainer, I. W., Ed.; 2nd ed.; Marcel Dekker Publisher: New York, 1993; pp. 1–24.
2. Blaser, H.-U.; Pfaltz, A.; Wennemers, H. Chiral Compounds. In *Ullmann's Encyclopedia of Industrial Chemistry*; 7th ed.; 2012. a18\_177.pub2.
3. Fraile, J. M.; Garcia, J. I.; Mayoral, J. A. Noncovalent Immobilization of Enantioselective Catalysts. *Chem. Rev.* **2009**, *109*, 360–417.
4. Katzung, B. G. The Nature of Drugs. In *Basic and Clinical Pharmacology*; 9th ed.; Lange Medical Books/McGraw Hill: New York, 2004; pp. 3–5.
5. Corey, E. J.; Kürti, L. *Enantioselective Chemical Synthesis: Methods, Logic, and Practice*; Direct Book Publishing LLC: Dallas, TX, 2010.
6. David Krupadanam, G. L. *Fundamentals of Asymmetric Synthesis*; CRC Press: Oakville, 2014.
7. Brill, Z. G.; Condakes, M. L.; Ting, C. P.; Maimone, T. J. Navigating the Chiral Pool in the Total Synthesis of Complex Terpene Natural Products. *Chem. Rev.* **2017**, *117*, 11753–11795.
8. Blaser, H. U. The Chiral Pool as a Source of Enantioselective Catalysts and Auxiliaries. *Chem. Rev.* **1992**, *92*, 935–952.

- Gnas, Y.; Glorius, F. Chiral Auxiliaries—Principles and Recent Applications. *Synthesis* **2006**, *12*, 1899–1930.
- Diaz-Muñoz, G.; Miranda, I. L.; Sartori, S. K.; de Rezende, D. C.; Alves Nogueira Diaz, M. Use of Chiral Auxiliaries in the Asymmetric Synthesis of Biologically Active Compounds: A Review. *Chirality* **2019**, *31*, 776–812.
- Anastas, P. T.; Warner, J. C. *Green Chemistry: Theory and Practice*; Oxford University Press: New York, 1998.
- Török, B.; Dransfield, T. *Green Chemistry: An Inclusive Approach*; Elsevier: Oxford, Cambridge, 2018.
- Bartók, M.; Wittman, G. In *Stereochemistry of Heterogeneous Metal Catalysis*; Bartók, M., Ed.; Wiley: Chichester, 1985 (chapter 11).
- Akabori, S.; Sakurai, S.; Izumi, Y.; Fujii, Y. An Asymmetric Catalyst. *Nature* **1956**, *178*, 323–324.
- Gheorghie, A.; Strudwick, B.; Dawson, D. M.; Ashbrook, S. E.; Woutersen, S.; Dubbeldam, D.; Tanase, S. Synthesis of Chiral MOF-74 Frameworks by Post-Synthetic Modification by Using an Amino Acid. *Chem. Eur. J.* **2020**, *26*, 13957–13965.
- Yasukawa, T.; Miyamura, H.; Kobayashi, S. Chiral Rhodium Nanoparticle-Catalyzed Asymmetric Arylation Reactions. *Acc. Chem. Res.* **2020**, *53*, 2950–2963.
- Rufete-Beneite, M.; Roman-Martinez, M. C. Heterogenization of a Chiral Molecular Catalyst on a Carbon Support Using Tryptophan as Anchor Molecule. *Eur. J. Inorg. Chem.* **2021**, 223–225.
- Shukla, M.; Barick, K. C.; Salunke, H. G.; Chandra, S. Chiral salen—Ni (II) Based Spherical Porous Silica as Platform for Asymmetric Transfer Hydrogenation Reaction and Synthesis of Potent Drug Intermediate Montekulast. *Mol. Catal.* **2021**, *502*, 111367.
- Ren, H.; Cheng, L.; Yang, J.; Zhao, K.; Zhai, Q.; Li, Y. Recyclable and Reusable Chiral  $\alpha$ ,  $\alpha$ -L-Diaryl Prolinol Heterogeneous Catalyst Grafting to UiO-67 for Enantioselective Hydration/aldol/oxa-Diels Alder Domino Reaction. *Catal. Commun.* **2021**, *149*, 106249.
- Gok, Y.; Gok, H. Z. Synthesis, Characterization and Catalytic Performance in Enantioselective Reactions by Mesoporous Silica Materials Functionalized With Chiral Thiourea-Amine Ligand. *Res. Chem. Intermed.* **2021**, *47*, 853–874.
- Brown, L. J.; Brown, R. J. D.; Raja, R. Heterogenisation of Ketone Catalysts Within Mesoporous Supports for Asymmetric Epoxidation. *RSC Adv.* **2013**, *3*, 843–850.
- Xia, Q.; Li, Z.; Tan, C.; Liu, Y.; Gong, W.; Cui, Y. Multivariate Metal–Organic Frameworks as Multifunctional Heterogeneous Asymmetric Catalysts for Sequential Reactions. *J. Am. Chem. Soc.* **2017**, *139*, 8259–8266.
- Huang, J.; Ding, W.; Cai, J. Heterogeneous Jacobsen's Catalyst on Alkoxy-Modified Zirconium Poly (Styrene-Phenylvinylphosphonate)-Phosphate (ZPS-PVPA) for Asymmetric Epoxidation. *Appl. Organomet. Chem.* **2017**, *31*, e3861.
- Kuźniarska-Biernacka, I.; Pereira, C.; Carvalho, A. P.; Pires, J.; Freire, C. Epoxidation of Olefins Catalyzed by Manganese(III) Salen Complexes Grafted to Porous Heterostructured Clays. *Appl. Clay Sci.* **2011**, *53*, 195–203.
- Zhang, H.; Zou, Y.; Wang, Y.-M.; Shen, Y.; Zheng, X. Asymmetric Epoxidation of *cis/trans*- $\beta$ -Methylstyrene Catalysed by Immobilised Mn(Salen) with Different Linkages: Heterogenisation of Homogeneous Asymmetric Catalysis. *Chem. Eur. J.* **2014**, *20*, 7830–7841.
- Fraile, J. M.; Garcia, J. I.; Massam, J.; Mayoral, J. A. Clay-Supported Non-Chiral and Chiral Mn(salen) Complexes As Catalysts for Olefin Epoxidation. *J. Mol. Catal. A Chem.* **1998**, *136*, 47–57.

27. Li, Z.; Liu, Y.; Xia, Q.; Cui, Y. Chiral Binary Metal–Organic Frameworks for Asymmetric Sequential Reactions. *Chem. Commun.* **2017**, *53*, 12313–12316.
28. Han, Q.; He, C.; Zhao, M.; Qi, B.; Niu, J.; Duan, C. Engineering Chiral Polyoxometalate Hybrid Metal–Organic Frameworks for Asymmetric Dihydroxylation of Olefins. *J. Am. Chem. Soc.* **2013**, *135*, 10186–10189.
29. Velasco-Lozano, S.; Roca, M.; Leal-Duaso, A.; Mayoral, J. A.; Pires, E.; Moliner, V.; López-Gallego, F. Selective Oxidation of Alkyl and Aryl Glyceryl Monoethers Catalysed by an Engineered and Immobilised Glycerol Dehydrogenase. *Chem. Sci.* **2020**, *11*, 12009–12020.
30. Chen, X.; Peng, Y.; Han, X.; Liu, Y.; Lin, X.; Cui, Y. Sixteen Isostructural Phosphonate Metal–Organic Frameworks With Controlled Lewis Acidity and Chemical Stability for Asymmetric Catalysis. *Nat. Commun.* **2017**, *8*, 2171.
31. Khedher, I.; Ghorbel, A.; Fraile, J. M.; Mayoral, J. A. Ti<sup>IV</sup> Exchanged K10-Montmorillonite: Characterization and Catalytic Properties in Liquid-Phase Sulfide Oxidation. *J. Chem. Res.* **2008**, 604–608.
32. Khedher, I.; Ghorbel, A.; Fraile, J. M.; Mayoral, J. A. Vanadium Sites in V-K10: Characterization and Catalytic Properties in Liquid-Phase Sulfide Oxidation. *J. Mol. Catal. A Chem.* **2006**, *255*, 92–96.
33. Li, C.; Shu, X.; Li, L.; Zhang, G.; Jin, R.; Cheng, T.; Liu, G. A Cinchona Alkaloid-Functionalized Mesoporous Silica for Construction of Enriched Chiral  $\beta$ -Trifluoromethyl- $\beta$ -Hydroxy Ketones over An Epoxidation-Relay Reduction Process. *Chem. Asian J.* **2016**, *11*, 2072–2077.
34. Andrus, M. B. Stereoselective Synthesis Allylic and Benzylic Oxidation. In *Science of Synthesis*; Vol. 3; Georg Thieme Verlag: Stuttgart, Germany, 2011; pp. 469–482.
35. Marín-Barrios, R.; Guerra, F. M.; García-Cabeza, A. L.; Moreno-Dorado, F. J.; Massanet, G. M. Multivariate Optimization of the Kharasch-Sosnovsky Allylic Oxidation of Olefins. *Tetrahedron* **2012**, *68*, 1105–1108.
36. Mayoral, J. A.; Rodríguez-Rodríguez, S.; Salvatella, L. Theoretical Insights into Enantioselective Catalysis: The Mechanism of the Kharasch-Sosnovsky Reaction. *Chem.-Eur. J.* **2008**, *14*, 9274–9285.
37. Aldea, L.; Delso, I.; Hager, M.; Glos, M.; Garcia, J. I.; Mayoral, J. A.; Reiser, O. A Reusable Enantioselective Catalytic System for the Kharasch-Sosnovsky Allylic Oxidation Of Alkenes Based on a Ditopic Azabis(Oxazoline) Ligand. *Tetrahedron* **2012**, *68*, 3417–3422.
38. Meemken, F.; Baiker, A. Recent Progress in Heterogeneous Asymmetric Hydrogenation of C=O and C=C Bonds on Supported Noble Metal Catalysts. *Chem. Rev.* **2017**, *117*, 11522–11569.
39. Cheng, T.; Zhao, Q.; Zhang, D.; Liu, G. Silica-Supported Chiral Catalysts for Asymmetric Transfer Hydrogenation. *Curr. Org. Chem.* **2015**, *19*, 667–680.
40. Li, X.; Wu, P. Enantioselective Hydrogenation Catalyzed by Chiral Nanoporous Materials. *Curr. Org. Chem.* **2014**, *18*, 1242–1261.
41. Durán Pachón, L.; Yosef, I.; Markus, T. Z.; Naaman, R.; Avnir, D.; Rothenberg, G. Chiral Imprinting Of Palladium With Cinchona Alkaloids. *Nat. Chem.* **2009**, *1*, 160–164.
42. Hoxha, F.; Königsmann, L.; Vargas, A.; Ferri, D.; Baiker, A. Role of Guiding Groups in Cinchona-Modified Platinum for Controlling the Sense of Enantiodifferentiation in the Hydrogenation of Ketones. *J. Am. Chem. Soc.* **2007**, *129*, 10582–10590.
43. Szöri, K.; Balázsik, K.; Cserényi, S.; Szöllösi, G.; Bartók, M. Inversion of Enantioselectivity in the 2,2,2-Trifluoroacetophenone Hydrogenation Over Pt-Alumina Catalyst Modified by Cinchona Alkaloids. *Appl. Catal. A* **2009**, *362*, 178–184.
44. Balázsik, K.; Török, B.; Felföldi, K.; Bartók, M. Sonochemical Enantioselective Hydrogenation of Trifluoromethyl Ketones over Platinum Catalysts. *Ultrason. Sonochem.* **1999**, *5*, 149–155.

45. Panella, B.; Vargas, A.; Baiker, A. Magnetically Separable Pt Catalyst for Asymmetric Hydrogenation. *J. Catal.* **2009**, *261*, 88–93.
46. Jiang, H.; Chen, H.; Li, R. Cinchona-Modified Ru Catalysts for Enantioselective Heterogeneous Hydrogenation of Aromatic Ketones. *Catal. Commun.* **2010**, *11*, 584–587.
47. Jiang, H.; Yang, C.; Li, C.; Fu, H.; Chen, H.; Li, R.; Li, X. Heterogeneous Enantioselective Hydrogenation of Aromatic Ketones Catalyzed by Cinchona- and Phosphine-Modified Iridium Catalysts. *Angew. Chem. Int. Ed.* **2008**, *47*, 9240–9244.
48. Li, C.; Zhang, L.; Zheng, C.; Zheng, X.; Fu, H.; Chen, H.; Li, R. Heterogeneous Asymmetric Hydrogenation of Heteroaromatic Methyl Ketones Catalyzed by Cinchona-Modified Iridium Catalysts. *Tetrahedron Asymmetry* **2014**, *25*, 821–824.
49. Li, C.; Zhang, L.; Liu, H.; Zheng, X.; Fu, H.; Chen, H.; Li, R. Heterogeneous Asymmetric Hydrogenation of Aromatic Ketones Enhanced by Silanols on Highly Monodispersed Silica Spheres. *Catal. Commun.* **2014**, *54*, 27–30.
50. Shen, Y.; Chen, Q.; Lou, L.-L.; Yu, K.; Ding, F.; Liu, S. Asymmetric Transfer Hydrogenation of Aromatic Ketones Catalyzed by SBA-15 Supported Ir(I) Complex Under Mild Conditions. *Catal. Lett.* **2010**, *137*, 104–109.
51. Corma, A.; Garcia, H. Silica-Bound Homogenous Catalysts as Recoverable and Reusable Catalysts in Organic Synthesis. *Adv. Synth. Catal.* **2006**, *348*, 1391–1412.
52. Arakawa, Y.; Haraguchi, N.; Itsuno, S. Design of Novel Polymer-Supported Chiral Catalyst for Asymmetric Transfer Hydrogenation in Water. *Tetrahedron Lett.* **2006**, *47*, 3239–3243.
53. Sahoo, S.; Kumar, P.; Lefebvre, F.; Halligudi, S. B. Immobilized Chiral Diamino Ru Complex as Catalyst for Chemo- and Enantioselective Hydrogenation. *J. Mol. Catal. A Chem.* **2007**, *273*, 102–108.
54. Parambadath, S.; Singh, A. P. Ru(II)-Chiral (1*R*,2*S*)-(+)-*cis*-1-Amino-2-Indanol Immobilized Over SBA-15 for Asymmetric Transfer Hydrogenation Reaction of Prochiral Ketones. *Catal. Today* **2009**, *141*, 161–167.
55. Cortez, N. A.; Aguirre, G.; Parra-Hake, M.; Somanathan, R. New Heterogenized C<sub>2</sub>-Symmetric bis(Sulfonamide)-Cyclohexane-1,2-Diamine-Rh<sup>III</sup>Cp\* Complexes and Their Application in the Asymmetric Transfer Hydrogenation (ATH) of Ketones in Water. *Tetrahedron Lett.* **2009**, *50*, 2228–2231.
56. Lou, L.; Peng, X.; Yu, K.; Liu, S. Asymmetric Hydrogenation of Acetophenone Catalyzed by Chiral Ru Complex in Mesoporous Material Supported Ionic Liquid. *Catal. Commun.* **2008**, *9*, 1891–1893.
57. Liu, J.; Fan, B.; Liang, D.; Shi, X.; Li, R.; Chen, H. Asymmetric Hydrogenation of Aromatic Ketones by Chiral (1*S*,2*S*)-DPEN-Ru(II)Cl<sub>2</sub>(TPP)<sub>2</sub> Encapsulated in SBA-16. *Catal. Commun.* **2010**, *11*, 373–377.
58. Zsigmond, Á.; Undrala, S.; Notheisz, F.; Szöllösy, Á.; Bakos, J. The Effect of Substituents of Immobilized Rh Complexes on the Asymmetric Hydrogenation of Acetophenone Derivatives. *Cent. Eur. J. Chem.* **2008**, *6*, 549–554.
59. Hu, A.; Liu, S.; Lin, W. Immobilization of Chiral Catalysts on Magnetite Nanoparticles for Highly Enantioselective Asymmetric Hydrogenation of Aromatic Ketones. *RSC Adv.* **2012**, *2*, 2576–2580.
60. Barrón-Jaime, A.; Narvaez-Garayzar, O. F.; González, J.; Ibarra-Galván, V.; Aguirre, G.; Parra-Hake, M.; Chavéz, D.; Somanathan, R. Asymmetric Transfer Hydrogenation of Prochiral Ketones in Aqueous Media with Chiral Water-Soluble and Heterogenized Bifunctional Catalysts of the RhCp\*-Type Ligand. *Chirality* **2011**, *23*, 178–184.
61. Liu, R.; Cheng, T.; Kong, L.; Chen, C.; Liu, G.; Li, H. Highly Recoverable Organoruthenium-Functionalized Mesoporous Silica Boosts Aqueous Asymmetric Transfer Hydrogenation Reaction. *J. Catal.* **2013**, *307*, 55–61.

62. Cheng, T.; Long, J.; Liang, X.; Liu, R.; Liu, G. Exploiting Mesoporous Silica Matrixes for Aqueous Asymmetric Transfer Hydrogenation: Morphology and Surface Chemistry Dominate Catalytic Performance. *Mater. Res. Bull.* **2014**, *53*, 1–6.
63. Gao, F.; Jin, R.; Zhang, D.; Liang, Q.; Ye, Q.; Liu, G. Flower-Like Mesoporous Silica: A Bifunctionalized Catalyst for Rhodium-Catalyzed Asymmetric Transfer Hydrogenation of Aromatic Ketones in Aqueous Medium. *Green Chem.* **2013**, *15*, 2208–2214.
64. Tang, S.; Jin, R.; Zhang, H.; Yao, H.; Zhuang, J.; Liu, G.; Li, H. Recoverable Organorhodium-Functionalized Polyhedral Oligomeric Silsesquioxane: A Bifunctional Heterogeneous Catalyst for Asymmetric Transfer Hydrogenation of Aromatic Ketones in Aqueous Medium. *Chem. Commun.* **2012**, *48*, 6286–6288.
65. Zhou, F.; Hu, X.; Gao, M.; Cheng, T.; Liu, G. An Imidazolium-Modified Chiral Rhodium/Diamine-Functionalized Periodic Mesoporous Organosilica for Asymmetric Transfer Hydrogenation of  $\alpha$ -Haloketones and Benzils in Aqueous Medium. *Green Chem.* **2016**, *18*, 5651–5657.
66. Jing, L.; Zhang, X.; Guan, R.; Yang, H. Construction of a Chiral Macromolecular Catalyst in Hollow Silica Nanoreactors for Efficient and Recyclable Asymmetric Catalysis. *Catal. Sci. Technol.* **2018**, *8*, 2304–2311.
67. Balakrishnan, U.; Velmathi, S. Chirally Functionalized SBA-15 as Efficient Heterogeneous Catalyst for Asymmetric Ketone Reduction. *J. Nanosci. Nanotechnol.* **2013**, *13*, 1–8.
68. Xu, Y.; Cheng, T.; Long, J.; Liu, K.; Qian, Q.; Gao, F.; Liu, G.; Lia, H. An Ion-Pair Immobilization Strategy in Rhodium-Catalyzed Asymmetric Transfer Hydrogenation Of Aromatic Ketones. *Adv. Synth. Catal.* **2012**, *354*, 3250–3258.
69. Diezi, S.; Ferri, D.; Vargas, A.; Mallat, T.; Baiker, A. The Origin of Chemo- and Enantioselectivity in the Hydrogenation of Diketones on Platinum. *J. Am. Chem. Soc.* **2006**, *128*, 4048–4057.
70. Balázsik, K.; Martinek, T. A.; Bucsi, I.; Szöllösi, G.; Fogassy, G.; Bartók, M.; Olah, G. A. A New Rigid Cinchona Modified ( $\alpha$ -IQ) Platinum Catalyst for the Enantioselective Hydrogenation of Activated Ketones: Data to the Origin of Enantioselection. *J. Mol. Catal. A Chem.* **2007**, *272*, 265–274.
71. Studer, M.; Blaser, H.-U.; Okafor, V. Hydrogenation of Butane-2,3-dione With Heterogeneous Cinchona Modified Platinum Catalysts: A Combination of an Enantioselective Reaction and Kinetic Resolution. *Chem. Commun.* **1998**, 1053–1054.
72. Campos, C. H.; Torres, C. C.; Leyton, A.; Belmar, J.; Mella, C.; Osorio-Vargas, P.; Ruiz, D.; Fierro, J. L. G.; Reyes, P. A New Non-Cinchona Chiral Modifier Immobilized on Pt/SiO<sub>2</sub> Catalysts for Enantioselective Heterogeneous Hydrogenation. *Appl. Catal. A Gen.* **2015**, *498*, 76–87.
73. Marzioletti, T.; Oportus, M.; Ruiz, D.; Fierro, J.; Reyes, P. Enantioselective Hydrogenation of 1-Phenyl-1,2-Propanedione, Ethyl Pyruvate and Acetophenone on Ir/SiO<sub>2</sub> Catalysts. Effect of Iridium Loading. *Catal. Today* **2008**, *133*, 711–719.
74. Busygin, I.; Rosenholm, M.; Toukoniitty, E.; Murzin, D. Y.; Leino, R. Hydrogenation of 1,2-Indanedione Over Heterogeneous Cinchonidine-Modified Platinum Catalysts. *Catal. Lett.* **2007**, *117*, 91–98.
75. Török, B.; Balázsik, K.; Szakonyi, G.; Felföldi, K.; Bartók, M. Enantiodifferentiation in Asymmetric Sonochemical Hydrogenations. *Catal. Lett.* **1998**, *52*, 81–84.
76. Török, B.; Balázsik, K.; Szöllösi, G.; Felföldi, K.; Kun, I.; Bartók, M. Ultrasonics in Heterogeneous Metal Catalysis. Sonochemical Chemo- and Enantioselective Hydrogenations over Supported Platinum Catalysts. *Ultrason. Sonochem.* **1999**, *6*, 97–103.

77. Szőri, K.; Török, B.; Felföldi, K.; Bartók, M. Enantioselective Hydrogenation of  $\alpha$ -Ketoesters over a Pt/Al<sub>2</sub>O<sub>3</sub> Catalyst. Effect of Steric Constraints on the Enantioselection. In *Catalysis of Organic Reactions*; Ford, M., Ed.; Marcel Dekker: New York, 2000 (chapter 44, 489).
78. Balázsik, K.; Török, B.; Szakonyi, G.; Bartók, M. Enantioselective Hydrogenations over K-10 Montmorillonite-Supported Noble Metal Catalysts with Anchored Modifier. *Appl. Catal. A Gen.* **1999**, *182*, 53–63.
79. Török, B.; Balázsik, K.; Kun, I.; Szöllösi, G.; Szakonyi, G.; Bartók, M. Clay-Supported Noble Metal Catalysts in Enantioselective Hydrogenations. *Stud. Surf. Sci. Catal.* **1999**, *125*, 555–563.
80. Margitfalvi, J.; Tálas, E. Anomalous Behavior of Rigid Cinchona Alkaloids in the Enantioselective Hydrogenation of Ethyl Pyruvate in an Aprotic Solvent. *Appl. Catal. A Gen.* **2006**, *301*, 187–195.
81. Azyat, K.; Solladié-Cavallo, A.; Klein, A.; Welter, R. Enantiopure aryl-[1,2,5,6-Tetrahydro-Pyridinyl] Methanols and Their use for Heterogeneous Hydrogenation of Ethyl Pyruvate. *C. R. Chim.* **2007**, *10*, 1180–1186.
82. Solladié-Cavallo, A.; Marsol, C.; Azyat, K.; Roje, M.; Welch, C.; Chilenski, J.; Taillason, P.; D'Orchymont, H. Enantiopure (9-Anthryl)(2-piperidyl)- and (9-Anthryl)(2-pyridyl)Methanols—Their Use as Chiral Modifiers for Heterogeneous Hydrogenation of Keto Esters over Pt/Al<sub>2</sub>O<sub>3</sub>. *Eur. J. Org. Chem.* **2007**, 826–830.
83. Abdallah, R.; Fumey, B.; Meille, V.; de Bellefon, C. Micro-Structured Reactors as a Tool for Chiral Modifier Screening in Gas–Liquid–Solid Asymmetric Hydrogenations. *Catal. Today* **2007**, *125*, 34–39.
84. Tálas, E.; Margitfalvi, J. L. Effect of Achiral Condensed Aromatic Additives on the Enantioselective Hydrogenation of Ethyl Pyruvate Over Cinchonidine-Platinum Catalysts. *Catal. Commun.* **2008**, *9*, 984–989.
85. Balázsik, K.; Cserényi, S.; Szöllösi, G.; Fülöp, F.; Bartók, M. New Data on the Orito Reaction: Effect of Substrate Structure on Nonlinear Phenomenon. *Catal. Lett.* **2008**, *125*, 401–407.
86. Merlo, A. B.; Ruggera, J. F.; Santori, G. F.; Moglioni, A.; Moltrasio Iglesias, G. Y.; Casella, M. L.; Ferretti, O. A. Use of (*S*)-(+)-1-Aminoindan, (*S*)-(+)-1-Indanol and (*1R*, *2S*)-(+)-cis-1-Amino-2-Indanol as Chiral Modifiers in the Enantioselective Hydrogenation of Ethyl Pyruvate With Pt/SiO<sub>2</sub> Catalysts. *Catal. Today* **2008**, *133–135*, 654–660.
87. Bykov, A.; Matveeva, V.; Sulman, M.; Valetskiy, P.; Tkachenko, O.; Kustov, L.; Bronstein, L.; Sulman, E. Enantioselective catalytic hydrogenation of activated ketones using polymer-containing nanocomposites. *Catal. Today* **2009**, *140*, 64–69.
88. Bartók, M.; Török, B.; Balázsik, K.; Bartók, T. Enantioselective Hydrogenation of Ethyl Pyruvate over Cinchonine and  $\alpha$ -Isocinchonine Modified Platinum Catalysts. *Catal. Lett.* **2001**, *73*, 127–131.
89. Bartók, M.; Felföldi, K.; Török, B.; Bartók, T. A New Cinchona-Modified Platinum Catalyst for the Enantioselective Hydrogenation of Pyruvate: The Structure of the 1:1 Alkaloid-Reactant Complex. *Chem. Commun.* **1998**, 2605–2606.
90. Balázsik, K.; Szőri, K.; Felföldi, K.; Török, B.; Bartók, M. Asymmetric Synthesis of Alkyl 5-oxo-Tetrahydrofuran-2-Carboxylates by Enantioselective Hydrogenation of Dialkyl 2-Oxoglutarates over Cinchona Modified Pt/Al<sub>2</sub>O<sub>3</sub> Catalysts. *Chem. Commun.* **2000**, 555–556.
91. Szőri, K.; Balázsik, K.; Felföldi, K.; Bartók, M. Study of Enantioselective Hydrogenation of Bulky Esters of Phenylglyoxylic Acid on Pt-CD and Pt- $\beta$ -ICN Chiral Catalysts: Steric Effect of Ester Groups and Inversion of Enantioselectivity. *J. Catal.* **2006**, *241*, 149–154.

92. Török, B.; Balázsik, K.; Török, M.; Szöllösi, G.; Bartók, M. Asymmetric Sonochemical Hydrogenation of  $\alpha$ -Ketoesters over Cinchona-Modified Platinum Catalysts. *Ultrason. Sonochem.* **2000**, *7*, 151–158.
93. Török, B.; Balázsik, K.; Szöllösi, G.; Felföldi, K.; Bartók, M. Ultrasonics in Asymmetric Syntheses. Sonochemical Enantioselective Hydrogenation of Prochiral C=O Groups over Platinum Catalysts. *Chirality* **1999**, *11*, 470–474.
94. Török, B.; Balázsik, K.; Török, M.; Felföldi, K.; Bartók, M. Enantiodifferentiation in Cinchona-Modified Platinum-Catalyzed Sonochemical Hydrogenations. *Catal. Lett.* **2002**, *81*, 55–62.
95. Szöllösi, G.; Cserényi, S.; Fülöp, F.; Bartók, M. New Data to the Origin of Rate Enhancement on the Pt-Cinchona Catalyzed Enantioselective Hydrogenation of Activated Ketones Using Continuous-Flow Fixed-Bed Reactor System. *J. Catal.* **2008**, *260*, 245–253.
96. Balázsik, K.; Szöllösi, G.; Bartók, M. New Data of Nonlinear Phenomenon in the Heterogeneous Enantioselective Hydrogenation of Activated Ketones. *Catal. Lett.* **2008**, *124*, 46.
97. Török, B.; Felföldi, K.; Balázsik, K.; Bartók, M. New Synthesis of a Useful C3 Chiral Building Block by Heterogeneous Method: Enantioselective Hydrogenation of Methylglyoxal 1,1-Dimethyl Acetal over Cinchona Modified Pt/Al<sub>2</sub>O<sub>3</sub> Catalysts. *Chem. Commun.* **1999**, 1725–1726.
98. Studer, M.; Burkhardt, S.; Blaser, H.-U. Enantioselective Hydrogenation of  $\alpha$ -Keto Acetals with Cinchona Modified Pt Catalyst. *Chem. Commun.* **1999**, 1727–1728.
99. Tálas, E.; Margitfalvi, J. L.; Egyed, O. Additional Data to the Origin of Rate Enhancement in the Enantioselective Hydrogenation of Activated Ketones Over Cinchonidine Modified Platinum Catalyst. *J. Catal.* **2009**, *266*, 191–198.
100. Hoxha, F.; van Vegten, N.; Urakawa, A.; Krumeich, F.; Mallat, T.; Baiker, A. Remarkable Particle Size Effect in Rh-Catalyzed Enantioselective Hydrogenations. *J. Catal.* **2009**, *261*, 224–231.
101. Schmidt, E.; Vargas, A.; Mallat, T.; Baiker, A. Shape-Selective Enantioselective Hydrogenation on Pt Nanoparticles. *J. Am. Chem. Soc.* **2009**, *131*, 12358–12367.
102. Chung, I.; Song, B.; Kim, J.; Yun, Y. Enhancing Effect of Residual Capping Agents in Heterogeneous Enantioselective Hydrogenation of  $\alpha$ -keto Esters over Polymer-Capped Pt/Al<sub>2</sub>O<sub>3</sub>. *ACS Catal.* **2021**, *11*, 31–42.
103. Sharma, P.; Sharma, R. K. Platinum Functionalized Multiwall Carbon Nanotube Composites as Recyclable Catalyst for Highly Efficient Asymmetric Hydrogenation of Methyl Pyruvate. *RSC Adv.* **2015**, *5*, 102481–102487.
104. Sharma, P.; Sharma, R. K. Platinum Functionalized Chiral Polyamides: Efficient Heterogeneous Catalyst for Solvent Free Asymmetric Hydrogenation of Ethyl 2-oxo-4-Phenylbutanoate. *ChemistrySelect* **2017**, *2*, 513–520.
105. Izumi, A. Modified Raney Nickel (MRNi) Catalyst: Heterogeneous Enantiodifferentiating (Asymmetric) Catalyst. *Adv. Catal.* **1983**, *32*, 215–271.
106. Choliq, A. A.; Nakae, R.; Watanabe, M.; Misaki, T.; Fujita, M.; Okamoto, Y.; Sugimura, T. Enhanced Enantioselectivity Achieved at Low Hydrogen Pressure for the Asymmetric Hydrogenation of Methyl Acetoacetate over a Tartaric Acid NaBr-Modified Raney Nickel Catalyst: A Kinetic Study. *Bull. Chem. Soc. Jpn.* **2019**, *92*, 1175–1180.
107. Nakagawa, S.; Sugimura, T.; Tai, A. Almost Perfect Enantio-Differentiating Hydrogenation of Methyl 3-Cyclopropyl-3-Oxopropanoate Over Tartaric Acid Modified Raney Nickel Catalyst. *Chem. Lett.* **1997**, *9*, 859–860.
108. Sugimura, T. Recent Progress in Tartaric Acid-Modified Raney Nickel System for Enantio-Differentiating Hydrogenation. *Catal. Surv. Jpn.* **1999**, *3*, 37–42.

109. Cai, S.; Ma, K.; Chen, H.; Zheng, Y.; Jiang, J.; Li, R. Effects of Sodium Acetate and Residual Aluminum on the Hydrogenation Rate, Optical Yield and Catalyst Durability for the Enantio-Differentiating Hydrogenation of Methyl Acetoacetate Over Tartaric Acid-Modified Raney Nickel Catalysts. *Catal. Lett.* **2009**, *128*, 227–234.
110. Hess, R.; Diezi, S.; Mallat, T.; Baiker, A. Chemo- and Enantioselective Hydrogenation of the Activated Keto Group Of Fluorinated  $\beta$ -Diketones. *Tetrahedron-Asymmetry* **2004**, *15*, 251–257.
111. Szőri, K.; Szöllösi, G.; Bartók, M. Dynamic Kinetic Resolution over Cinchona-Modified Platinum Catalyst: Hydrogenation of Racemic Ethyl 2-Fluoroacetoacetate. *Adv. Synth. Catal.* **2006**, *348*, 515–522.
112. Floris, T.; Kluson, P.; Bartek, L.; Pelantova, H. Quaternary Ammonium Salts Ionic Liquids for Immobilization of Chiral Ru-BINAP Complexes in Asymmetric Hydrogenation of  $\beta$ -Ketoesters. *Appl. Catal. A Gen.* **2009**, *366*, 160–165.
113. Wang, T.; Lyu, Y.; Xiong, K.; Wang, W.; Zhang, H.; Zhan, Z.; Jiang, Z.; Ding, Y. Chiral BINAP-Based Hierarchical Porous Polymers as Platforms for Efficient Heterogeneous Asymmetric Catalysis. *Chin. J. Catal.* **2017**, *38*, 890–898.
114. Schrader, I.; Neumann, S.; Šulce, A.; Schmidt, F.; Azov, V.; Kunz, S. Asymmetric Heterogeneous Catalysis: Transfer of Molecular Principles to Nanoparticles by Ligand Functionalization. *ACS Catal.* **2017**, *7*, 3979–3987.
115. Han, B.; Zhao, L.; Song, Y.; Zhao, Z.; Yang, D.; Liu, R.; Liu, G. A Superhydrophobic Mesoporous Silica as a Chiral Organometallic Immobilization Platform for Heterogeneous Asymmetric Catalysis. *Catal. Sci. Technol.* **2018**, *8*, 2920–2927.
116. Zhu, H.; Shi, B.; Gao, L.; Liu, Y.; Liu, P.-R.; Shanguan, L.; Mao, Z.; Huang, F. Pillar[5]arene-Based Chiral 3D Polymer Network for Heterogeneous Asymmetric Catalysis. *Polym. Chem.* **2017**, *8*, 7108–7112.
117. Fraile, J. M.; Mayoral, J. A.; Serrano, J.; Pericas, M. A.; Sola, L.; Castellnou, D. New Silica-Immobilized Chiral Amino Alcohol for the Enantioselective Addition of Diethylzinc to Benzaldehyde. *Org. Lett.* **2003**, *5*, 4333–4335.
118. Blaser, H. U.; Malan, C.; Pugin, B.; Spindler, F.; Steiner, H.; Studer, M. Selective Hydrogenation for Fine Chemicals: Recent Trends and New Developments. *Adv. Synth. Catal.* **2003**, *345*, 103–151.
119. Tugler, A.; Sipos, E.; Háda, V. Heterogeneous Catalytic asymmetric Hydrogenation of the C=C Bond. *Curr. Org. Chem.* **2006**, *10*, 1569–1583.
120. Borszky, K.; Mallat, T.; Baiker, A. Enantioselective Hydrogenation of 2-Methyl-2-Pentenoic Acid Over Cinchonidine-Modified Pd/Alumina. *Catal. Lett.* **1996**, *41*, 199–202.
121. Kun, I.; Török, B.; Felföldi, K.; Bartók, M. Asymmetric Hydrogenation of 2-Methyl-2-Pentenoic Acid Over Cinchona Modified Pd/Al<sub>2</sub>O<sub>3</sub> Catalysts. *Appl. Catal. A Gen.* **2000**, *203*, 71–79.
122. Török, B.; Balázsik, K.; Felföldi, K.; Bartók, M. Asymmetric Reactions in Sonochemistry. *Ultrasonics Sonochem.* **2001**, *8*, 191–200.
123. Hermán, B.; Szöllösi, G.; Fülöp, F.; Bartók, M. Enantioselective Hydrogenation of  $\alpha,\beta$ -Unsaturated Carboxylic acids in Fixed-Bed Reactor. *Appl. Catal. A Gen.* **2007**, *331*, 39–43.
124. Szöllösi, G.; Szabó, E.; Bartók, M. Enantioselective Hydrogenation of N-Acetyldehydroamino Acids Over Supported Palladium Catalysts. *Adv. Synth. Catal.* **2007**, *349*, 405–410.
125. Szöllösi, G.; Hermán, B.; Felföldi, K.; Fülöp, F.; Bartók, M. Up to 96% Enantioselectivities in the Hydrogenation of Fluorine Substituted (*E*)-2,3-Diphenylpropenoic Acids over Cinchonidine-Modified Palladium Catalyst. *Adv. Synth. Catal.* **2008**, *350*, 2804–2814.

126. Szöllösi, G.; Hermán, B.; Felföldi, K.; Fülöp, F.; Bartók, M. Effect of the Substituent Position on the Enantioselective Hydrogenation of Methoxy-Substituted 2,3-Diphenylpropenoic Acids Over Palladium Catalyst. *J. Mol. Catal. A Chem.* **2008**, *290*, 54–59.
127. Impalá, D.; Franceschini, S.; Piccolo, O.; Vaccari, A. Pd-based Sol–Gel Catalysts for the Enantioselective Hydrogenation of (*E*)-2-Methyl-2-Butenoic Acid. *Catal. Lett.* **2008**, *125*, 243–249.
128. Szöllösi, G.; Makra, Z.; Bartók, M. Enantioselective Hydrogenation of (*E*)-2-Methyl-2-Butenoic Acid Over Cinchonidine Modified pd Catalyst. Effect of the Structure of Achiral Amine Additives. *React. Kinet. Catal. Lett.* **2009**, *96*, 319–325.
129. Szöllösi, G.; Varga, T.; Felföldi, K.; Cserényi, S.; Bartók, M. Enantioselective Hydrogenation of Fluorinated Unsaturated Carboxylic Acids Over Cinchona Alkaloid Modified Palladium Catalysts. *Catal. Commun.* **2008**, *9*, 421–424.
130. Misaki, T.; Otsuka, H.; Uchida, T.; Kubota, T.; Okamoto, Y.; Sugimura, T. Substrate Adsorption on the Cinchonidine-Modified Pd/C During the Enantio-Differentiating Hydrogenation as a Vital Stereocontrol Factor. *J. Mol. Catal. A Chem.* **2009**, *312*, 48–52.
131. Hermán, B.; Szöllösi, G.; Felföldi, K.; Fülöp, F.; Bartók, M. Enantioselective Hydrogenation of Propenoic Acids Bearing Heteroaromatic Substituents Over Cinchonidine Modified Pd/Alumina. *Catal. Commun.* **2009**, *10*, 1107–1110.
132. Kubota, T.; Kubota, H.; Kubota, T.; Moriyasu, E.; Uchida, T.; Nitta, Y.; Sugimura, T.; Okamoto, Y. Enantioselective Hydrogenation of (*E*)- $\alpha$ -phenylcinnamic Acid over Cinchonidine-modified Pd Catalysts Supported on TiO<sub>2</sub> and CeO<sub>2</sub>. *Catal. Lett.* **2009**, *129*, 387–393.
133. Szöllösi, G.; Németh, Z.; Hernádi, K.; Bartók, M. Preparation and Characterization of TiO<sub>2</sub> Coated Multi-walled Carbon Nanotube-supported Pd and its Catalytic Performance in the Asymmetric Hydrogenation of  $\alpha,\beta$ -Unsaturated Carboxylic Acids. *Catal. Lett.* **2009**, *132*, 370.
134. Sugimura, T.; Uchida, T.; Watanabe, J.; Kubota, T.; Okamoto, Y.; Misaki, T.; Okuyama, T. Structural Requirements for Substrate in Highly Enantioselective Hydrogenation Over the Cinchonidine-Modified Pd/C. *J. Catal.* **2009**, *262*, 57–64.
135. Balogh, S.; Farkas, G.; Madarász, J.; Szöllösi, A.; Kovács, J.; Darvas, F.; Üрге, L.; Bakos, J. Asymmetric Hydrogenation of CvC Double Bonds Using Rh-Complex Under Homogeneous, Heterogeneous and Continuous Mode Conditions. *Green Chem.* **2012**, *14*, 1146–1151.
136. Yu, L.; Wang, Z.; Wu, J.; Tu, S.; Ding, K. Directed Orthogonal Self-Assembly of Homochiral Coordination Polymers for Heterogeneous Enantioselective Hydrogenation. *Angew. Chem. Int. Ed.* **2010**, *49*, 3627–3630.
137. Fodor, M.; Tungler, A.; Vida, L. Asymmetric Hydrogenation of Isophorone in the Presence of (*S*)-Proline: Revival of a 20 Years Old Reaction. *Catal. Today* **2009**, *140*, 58–63.
138. Mhadgut, S. C.; Bucsi, I.; Török, M.; Török, B. Sonochemical Asymmetric Hydrogenation of Isophorone on Proline Modified Pd/Al<sub>2</sub>O<sub>3</sub> Catalysts. *Chem. Commun.* **2004**, *9*, 84–985.
139. Mhadgut, S. C.; Török, M.; Esquibel, J.; Török, B. Highly Asymmetric Heterogeneous Catalytic Hydrogenation of Isophorone on Proline Modified Base-Supported Palladium Catalysts. *J. Catal.* **2006**, *238*, 441–448.
140. McIntosh, A. I.; Watson, D. J.; Burton, J. W.; Lambert, R. M. Heterogeneously Catalyzed Asymmetric CdC Hydrogenation: Origin of Enantioselectivity in the Proline-Directed Pd/Isophorone System. *J. Am. Chem. Soc.* **2006**, *128*, 7329–7334.
141. McIntosh, A. I.; Watson, D. J.; Lambert, R. M. Mechanistic Insights into the Proline-Directed Enantioselective Heterogeneous Hydrogenation of Isophorone. *Langmuir* **2007**, *23*, 6113–6118.

142. Zhan, E.; Li, S.; Xu, Y.; Shen, W. Heterogeneous Enantioselective Hydrogenation of Isophorone Over Proline Modified Pd Catalysts. *Catal. Commun.* **2007**, *8*, 1239–1243.
143. Li, S.; Zhan, E.; Li, Y.; Xu, Y.; Shen, W. Enantioselective Hydrogenation of Isophorone and Kinetic Resolution of 3,3,5-Trimethylcyclohexanone Over Pd Catalysts in the Presence of (S)-Proline. *Catal. Today* **2008**, *131*, 347–352.
144. Mhadgut, S. C.; Török, M.; Dasgupta, S.; Török, B. Nature of Proline-Induced Enantiodifferentiation in Asymmetric Pd Catalyzed Hydrogenations: Is the Catalyst Really Indifferent? *Catal. Lett.* **2008**, *123*, 156–163.
145. Watson, D. J.; Jesudason, R. J. B.; Beaumont, S. K.; Kyriakou, G.; Burton, J. W.; Lambert, R. M. Heterogeneously Catalyzed Asymmetric Hydrogenation of C=C Bonds Directed by Surface-Tethered Chiral Modifiers. *J. Am. Chem. Soc.* **2009**, *131*, 14584–14589.
146. Pisarek, M.; Łukaszewski, M.; Winiarek, P.; Kedzierzawski, P.; Janik-Czachor, M. Influence of Cr Addition to Raney Ni Catalyst on Hydrogenation of Isophorone. *Catal. Commun.* **2008**, *10*, 213–216.
147. Schäfer, C.; Mhadgut, S. C.; Kugyela, N.; Török, M.; Török, B. Proline-Induced Enantioselective Heterogeneous Catalytic Hydrogenation of Isophorone on Basic Polymer-Supported Pd Catalysts. *Catal. Sci. Technol.* **2015**, *5*, 716–723.
148. Xu, L.; Sun, S.; Zhang, X.; Gao, H.; Wang, W. Study on the Selective Hydrogenation of Isophorone. *RSC Adv.* **2021**, *11*, 4465–4471.
149. Rodríguez-García, L.; Hungerbühler, K.; Baiker, A.; Meemken, F. Enantioselection on Heterogeneous Noble Metal Catalyst: Proline-Induced Asymmetry in the Hydrogenation of Isophorone on Pd Catalyst. *J. Am. Chem. Soc.* **2015**, *137*, 12121–12130.
150. Yamashita, Y.; Yasukawa, T.; Yoo, W.-J.; Kitano, T.; Kobayashi, S. Catalytic Enantioselective Aldol Reactions. *Chem. Soc. Rev.* **2018**, *47*, 4388–4480.
151. Mandal, S. W.; Mandal, S. A.; Gosh, S. K.; Gosh, A.; Saha, R.; Banerjee, S.; Saha, B. Review of the Aldol Reaction. *Synth. Commun.* **2016**, *46*, 1327–1342.
152. Xie, G.; Feng, D.; Ma, X. 9-Amino(9-deoxy)epi-Cinchona Alkaloid-Tethered Aluminium Phosphonate Architectures for Heterogeneous Cooperative Catalysis: Asymmetric Aldol And Double-Michael Cascade Reaction. *Mol. Catal.* **2017**, *434*, 86–95.
153. Guo, G.; Wu, Y.; Zhao, X.; Wang, J.; Zhang, L.; Cui, Y. Polymerization of L-Proline Functionalized Styrene and Its Catalytic Performance as a Supported Organocatalyst for Direct Enantioselective Aldol Reaction. *Tetrahedron Asymmetry* **2016**, *27*, 740–746.
154. Zhang, D.; Zhang, H.; Song, C.; Yang, W.; Deng, J. Chiral Microspheres Constructed by Helical Substituted Polyacetylene: A New Class of Organocatalyst Toward Asymmetric Catalysis. *Synth. Met.* **2012**, *162*, 1858–1863.
155. Zhou, J.; Wan, J.; Ma, X.; Wang, W. Copolymer-Supported Heterogeneous Organocatalyst for Asymmetric Aldol Addition in Aqueous Medium. *Org. Biomol. Chem.* **2012**, *10*, 4179–4185.
156. Sadiq, M.; Aman, R.; Saeed, K.; Ahmad, M. S.; Zia, M. A. Green and Sustainable Heterogeneous Organo-Catalyst for Asymmetric Aldol Reactions. *Mod. Res. Catal.* **2015**, *4*, 43–49.
157. Zhang, J.; Han, X.; Wu, X.; Liu, Y.; Cui, Y. Multivariate Chiral Covalent Organic Frameworks with Controlled Crystallinity and Stability for Asymmetric Catalysis. *J. Am. Chem. Soc.* **2017**, *39*, 8277–8285.
158. Gioia, C.; Ricci, A.; Bernardi, L.; Bourahla, K.; Tanchoux, N.; Robitzer, M.; Quignard, F. Chitosan Aerogel Beads as a Heterogeneous Organocatalyst for the Asymmetric Aldol Reaction in the Presence of Water: An Assessment of the Effect of Additives. *Eur. J. Org. Chem.* **2013**, 588–594.

**650** Heterogeneous catalysis in sustainable synthesis

159. Ricci, A.; Bernadi, L.; Gioia, C.; Vierucci, S.; Robitzer, M.; Quignard, F. Chitosan Aerogel: A Recyclable, Heterogeneous Organocatalyst for the Asymmetric Direct Aldol Reaction in Water. *Chem. Commun.* **2010**, *46*, 6288–6290.
160. Duss, M.; Salvati Manni, L.; Moser, L.; Handschin, S.; Mezzenga, R.; Jessen, H. J.; Landau, E. M. Lipidic Mesophases as Novel Nanoreactor Scaffolds for Organocatalysts: Heterogeneously Catalyzed Asymmetric Aldol Reactions in Confined Water. *ACS Appl. Mater. Interfaces* **2018**, *10*, 5114–5124.
161. Tan, R.; Li, C.; Luo, J.; Kong, Y.; Zheng, W.; Yin, D. An Effective Heterogeneous L-Proline Catalyst for the Direct Asymmetric Aldol Reaction Using Graphene Oxide as Support. *J. Catal.* **2013**, *298*, 138–147.
162. Chen, Q.; Xin, C.; Lou, L.-L.; Yu, K.; Ding, F.; Liu, S. Polyoxometalate Supported Cinchona-Derived Chiral Amine for Asymmetric Organocatalysed Aldol Reaction. *J. Inorg. Organomet. Polym.* **2013**, *23*, 467–471.
163. Ötvös, S. B.; Mándity, I. M.; Fülöp, F. Asymmetric Aldol Reaction in a Continuous-Flow Reactor Catalyzed by a Highly Reusable Heterogeneous Peptide. *J. Catal.* **2012**, *295*, 179–185.
164. Cañellas, S.; Ayats, C.; Henseler, A. H.; Pericàs, M. A. A Highly Active Polymer-Supported Catalyst for Asymmetric Robinson Annulations in Continuous Flow. *ACS Catal.* **2017**, *7*, 1383–1391.
165. Pothanagandhi, N.; Vijayakrishna, K. RAFT Derived Chiral and Achiral Poly(Ionic Liquids) Resins: Synthesis and Application in Organocatalysis. *Eur. Polym. J.* **2017**, *95*, 785–794.
166. Fraile, J. M.; Perez, I.; Mayoral, J. A.; Reiser, O. Multipurpose Box- and Azabox-Based Immobilized Chiral Catalysts. *Adv. Synth. Catal.* **2006**, *348*, 1680–1688.
167. Fraile, J. M.; Perez, I.; Mayoral, J. A. Comparison of Immobilized Box and azaBox-Cu(II) Complexes as Catalysts for Enantioselective Mukaiyama Aldol Reactions. *J. Catal.* **2007**, *252*, 303–311.
168. Nguyen, K. D.; Kutzscher, C.; Drache, F.; Senkovska, I.; Kaskel, S. Chiral Functionalization of a Zirconium Metal–Organic Framework (DUT-67) as a Heterogeneous Catalyst in Asymmetric Michael Addition Reaction. *Inorg. Chem.* **2018**, *57*, 1483–1489.
169. Szöllösi, G.; Gombkötő, D.; Mogyorós, A. Z.; Fülöp, F. Surface-Improved Asymmetric Michael Addition Catalyzed by Amino Acids Adsorbed on Laponite. *Adv. Synth. Catal.* **2018**, *360*, 1992–2004.
170. Zhao, Z.; Feng, D.; Xie, G.; Ma, X. Functionalized Hollow Double-Shelled Polymeric Nano-Bowls as Effective Heterogeneous Organocatalysts for Enhanced Catalytic Activity in Asymmetric Michael Addition. *J. Catal.* **2018**, *359*, 36–45.
171. Zhang, J.; Han, X.; Wu, X.; Liu, Y.; Cui, Y. Chiral DHIP- and Pyrrolidine-Based Covalent Organic Frameworks for Asymmetric Catalysis. *ACS Sustain. Chem. Eng.* **2019**, *7*, 5065–5071.
172. Luanphaisarnnont, T.; Hanprasit, S.; Somjit, V.; Ervithayasuporn, V. Chiral Pyrrolidine Bridged Polyhedral Oligomeric Silsesquioxanes as Heterogeneous Catalysts for Asymmetric Michael Additions. *Catal. Lett.* **2018**, *148*, 779–786.
173. Wang, C. A.; Zhang, Z. K.; Yue, T.; Sun, Y. L.; Wang, L.; Wang, W. D.; Zhang, Y.; Liu, C.; Wang, W. “Bottom-Up” Embedding of the Jørgensen–Hayashi Catalyst into a Chiral Porous Polymer for Highly Efficient Heterogeneous Asymmetric Organocatalysis. *Chem. Eur. J.* **2012**, *18*, 6718–6723.
174. Shaikh, M.; Atyam, K. K.; Sahu, M.; Ranganath, K. V. S. Enhanced Reactivity and Selectivity of Asymmetric oxa-Michael Addition of 2'-Hydroxychalcones in Carbon Confined Spaces. *Chem. Commun.* **2017**, *53*, 6029–6032.

175. Saeidian, H.; Paghbandeh, H.; Parvin, Z.; Mirjafary, Z.; Ghaffarzadeh, M. Facile Synthesis of a New Chiral BINOL–Silica Hybrid Catalyst for Asymmetric Diels–Alder and Aza Michael Reactions. *Catal. Lett.* **2018**, *148*, 1366–1374.
176. Miguélez, J.; Miyamura, H.; Kobayashi, S. A Polystyrene-Supported Phase-Transfer Catalyst for Asymmetric Michael Addition of Glycine-Derived Imines to  $\alpha,\beta$ -Unsaturated Ketones. *Adv. Synth. Catal.* **2017**, *359*, 2897–2900.
177. Nováková, G.; Drabina, P.; Svoboda, J.; Sedlák, M. Copper(II) Complexes of 2-(Pyridine-2-yl)Imidazolidine-4-Thione Derivatives for Asymmetric Henry Reactions. *Tetrahedron Asymmetry* **2017**, *28*, 791–796.
178. Han, X.; Zhang, J.; Huang, J.; Wu, X.; Yuan, D.; Liu, Y.; Cui, Y. Chiral Induction in Covalent Organic Frameworks. *Nat. Commun.* **2018**, *9*, 1294.
179. Chen, M.; Zhang, J.; Liu, C.; Li, H.; Yang, H.; Feng, Y.; Zhang, B. Construction of Pyridine-Based Chiral Ionic Covalent Organic Frameworks as a Heterogeneous Catalyst for Promoting Asymmetric Henry Reactions. *Org. Lett.* **2021**, *23*, 1748–1752.
180. Ma, H.-C.; Kan, J.-L.; Chen, G.-J.; Chen, C.-X.; Dong, Y.-B. Pd NPs-Loaded Homochiral Covalent Organic Framework for Heterogeneous Asymmetric Catalysis. *Chem. Mater.* **2017**, *29*, 6518–6524.
181. Dai, F.; Zhao, Z.; Xie, G.; Feng, D.; Ma, X. Novel Functional Hollow and Multihollow Organic Microspheres: Enhanced Efficiency in a Complex, Heterogeneous, Asymmetric, Three-Component/Triple Organocascade Reaction. *ChemCatChem* **2017**, *9*, 89–93.
182. Fedorova, O. V.; Titova, Y. A.; Vigorov, A. Y.; Toporova, M. S.; Alisienok, O. A.; Murashkevich, A. N.; Krasnov, V. P.; Rusinov, G. L.; Charushin, V. N. Asymmetric Biginelli Reaction Catalyzed by Silicon, Titanium and Aluminum Oxides. *Catal. Lett.* **2016**, *146*, 493–498.
183. Ghomia, J. S.; Zahedi, S. Power Ultrasound, Microwaves, and Nanomagnetite Organocatalyst: A Comparison Protocol in Anti-Selective Aldol and Mannich Reaction. *Polycycl. Aromat. Compd* **2016**, *38*, 338–345.
184. Deiana, L.; Ghisu, L.; Afewerki, S.; Verho, O.; Johnston, E. V.; Hedin, N.; Bacsik, Z.; Córdova, A. Enantioselective Heterogeneous Synergistic Catalysis for Asymmetric Cascade Transformations. *Adv. Synth. Catal.* **2014**, *356*, 2485–2492.
185. Zhang, G.; Liu, R.; Chou, Y.; Wang, Y.; Cheng, T.; Liu, G. Multiple Functionalized Hyperbranched Polyethoxysiloxane Promotes Suzuki Coupling Asymmetric Transfer Hydrogenation One-Pot Enantioselective Organic Transformations. *ChemCatChem* **2018**, *10*, 1882–1888.
186. Liao, H.; Chou, Y.; Wang, Y.; Zhang, H.; Cheng, T.; Liu, G. Multistep Organic Transformations over Base-Rhodium/Diamine-Bifunctionalized Mesoporous Silica Nanoparticles. *ChemCatChem* **2017**, *9*, 3197–3202.
187. Wang, J.; Wu, L.; Hu, X.; Liu, R.; Jin, R.; Liu, G. One-Pot Synthesis of Optically Pure  $\beta$ -Hydroxy Sulfones via a Heterogeneous Ruthenium/Diamine-Promoted Nucleophilic Substitution-Asymmetric Transfer Hydrogenation Tandem Process. *Catal. Sci. Technol.* **2017**, *7*, 4444–4450.
188. Szöllösi, G.; Makra, Z.; Kovács, L.; Fülöp, F.; Bartók, M. Preparation of Optically Enriched 3-Hydroxy-3,4-dihydroquinolin-2(1H)-ones by Heterogeneous Catalytic Cascade Reaction over Supported Platinum Catalyst. *Adv. Synth. Catal.* **2013**, *355*, 1623–1629.
189. Liu, R.; Jin, R.; An, J.; Zhao, Q.; Cheng, T.; Liu, G. Hollow-Shell-Structured Nanospheres: A Recoverable Heterogeneous Catalyst for Rhodium-Catalyzed Tandem Reduction/Lactonization of Ethyl 2-Acylarylcarboxylates to Chiral Phthalides. *Chem. Asian J.* **2014**, *9*, 1388–1394.

652 Heterogeneous catalysis in sustainable synthesis

190. Kong, L.; Zhao, J.; Cheng, T.; Lin, J.; Liu, G. A Polymer-Coated Rhodium/Diamine-Functionalized Silica for Controllable Reaction Switching in Enantioselective Tandem Reduction–Lactonization of Ethyl 2-Acylarylcarboxylates. *ACS Catal.* **2016**, *6*, 2244–2249.
191. Ansari, A.; Gupta, N.; Jakhar, A.; Khan, N. H.; Kureshy, R. I. Quinine Thiourea Immobilized on SBA-15 as an Efficient Recyclable Catalyst for Asymmetric Strecker Reaction of Isatin N-protected Ketimines. *ChemistrySelect* **2017**, *2*, 11912–11917.
192. Wang, C.-A.; Li, Y.-W.; Han, Y.-F.; Zhang, J.-P.; Wu, R.-T.; He, G.-F. The “Bottom-Up” Construction of Chiral Porous Organic Polymers for Heterogeneous Asymmetric Organocatalysis: MacMillan Catalyst Built-in Nanoporous Organic Frameworks. *Polym. Chem.* **2017**, *8*, 5561–5569.
193. Zhu, H.; Jiang, X.; Li, X.; Hou, C.; Jiang, Y.; Hou, K.; Wang, R.; Li, Y. Highly Enantioselective Synthesis of N-Protected  $\beta$ -Amino Malonates Catalyzed by Magnetically Separable Heterogeneous Rosin-Derived Amino Thiourea Catalysts: A Stereocontrolled Approach to  $\beta$ -Amino Acids. *ChemCatChem* **2013**, *5*, 2187–2190.
194. Miyamura, H.; Nishino, K.; Yasukawa, T.; Kobayashi, S. Rhodium-Catalyzed Asymmetric 1,4-Addition Reactions of Aryl Boronic Acids With Nitroalkenes: Reaction Mechanism and Development of Homogeneous and Heterogeneous Catalysts. *Chem. Sci.* **2017**, *8*, 8362–8372.
195. Dong, J.; Liu, Y.; Cui, Y. Chiral Porous Organic Frameworks for Asymmetric Heterogeneous Catalysis and Gas Chromatographic Separation. *Chem. Commun.* **2014**, *50*, 14949–14952.
196. Xu, H.-C.; Chowdhury, S.; Ellman, J. A. Asymmetric Synthesis of Amines Using *tert*-Butanesulfinamide. *Nat. Protoc.* **2013**, *8*, 2271–2280.
197. Zhou, W.; Nie, X.-D.; Zhang, Y.; Si, C.-M.; Zhou, Z.; Sun, X.; Wei, B.-G. A practical Approach to Asymmetric Synthesis of Dolastatin 10. *Org. Biomol. Chem.* **2017**, *15*, 6119–6131.
198. Liu, X.; Hu, Y.-J.; Fan, J.-H.; Zhao, J.; Li, S.; Li, C.-C. Recent Synthetic Studies Towards Natural Products via [5 + 2] Cycloaddition Reactions. *Org. Chem. Front.* **2018**, *5*, 1217–1228.
199. Nugent, T. C.; El-Shazly, M. Chiral Amine Synthesis. Recent Developments and Trends for Enamide Reduction, Reductive Amination, and Imine Reduction. *Adv. Synth. Catal.* **2010**, *352*, 753–819.
200. Appa, R. M.; Lakshmidhevi, J.; Prasad, S. S.; Muralidhar, B.; Naidu, B. R.; Narasimhulu, M.; Venkateswarlu, K. First Sonochemical, Simple and Solvent-Free Synthesis of Chiral *tert*-Butanesulfinimines Using Silica Supported *p*-Toluenesulfonic Acid. *Synth. Commun.* **2019**, *49*, 56–64.
201. Popa, D.; Marcos, R.; Sayalero, S.; Vidal-Ferran, A.; Pericos, M. A. Towards Continuous Flow, Highly Enantioselective Allylic Amination: Ligand Design, Optimization and Supporting. *Adv. Synth. Catal.* **2009**, *351*, 1539–1556.
202. Balu, A. M.; Campelo, J. M.; Luque, R.; Romero, A. A. One-Step Microwave-Assisted Asymmetric Cyclisation/Hydrogenation of Citronellal to Menthols Using Supported Nanoparticles on Mesoporous Materials. *Org. Biomol. Chem.* **2010**, *8*, 2845–2849.
203. Guryev, A. A.; Anokhin, M. V.; Averin, A. D.; Beletskaya, I. P. Polymer-Immobilized  $\alpha,\alpha$ -bis[bis-3,5-(Trifluoromethyl)Phenyl]Prolinol Silylether: Synthesis and Application in the Asymmetric  $\alpha$ -Amination of Aldehydes. *Mendeleev Commun.* **2015**, *25*, 410–411.
204. Fraile, J. M.; Lopez-Ram-de-Viu, P.; Mayoral, J. A.; Roldan, M.; Santafe-Valero, J. Enantioselective C-H Carbene Insertions With Homogeneous and Immobilized Copper Complexes. *Org. Biomol. Chem.* **2011**, *9*, 6075–6081.

205. Garcia, J. I.; Herrerias, C. I.; Lopez-Sanchez, B.; Mayoral, J. A.; Reiser, O. Polytopic Oxazoline-Based Chiral Ligands for Cyclopropanation Reactions: A New Strategy to Prepare Highly Recyclable Catalysts. *Adv. Synth. Catal.* **2011**, *353*, 2691–2700.
206. Fraile, J. M.; Garcia, J. I.; Herrerias, C. I.; Mayoral, J. A.; Pires, E. Enantioselective Catalysis With Chiral Complexes Immobilized on Nanostructured Supports. *Chem. Soc. Rev.* **2009**, *38*, 695–706.
207. Sweeney, J. B. Aziridines: Epoxides' Ugly Cousins? *Chem. Soc. Rev.* **2002**, *31*, 247–258.
208. Müller, P.; Fruit, C. Enantioselective Catalytic Aziridinations and Asymmetric Nitrene Insertions into CH Bonds. *Chem. Rev.* **2003**, *103*, 2905–2920.
209. Torviso, M. R.; Mansilla, D. S.; Fraile, J. M.; Mayoral, J. A. The Importance of Copper Placement in Chiral Catalysts Supported on Heteropolyanions: Lacunary vs External Exchanged. *Mol. Catal.* **2020**, *489*, 110935.
210. Jimenez-Oses, G.; Vispe, E.; Roldan, M.; Rodriguez-Rodriguez, S.; Lopez-Ram-de-Viu, P.; Salvatella, L.; Mayoral, J. A.; Fraile, J. M. Stereochemical Outcome of Copper-Catalyzed C-H Insertion Reactions. An Experimental and Theoretical Study. *J. Org. Chem.* **2013**, *78*, 5851–5857.
211. Fraile, J. M.; Garcia, J. I.; Mayoral, J. A. Recent Advances in the Immobilization of Chiral Catalysts Containing bis(Oxazolines) and Related Ligands. *Coord. Chem. Rev.* **2008**, *252*, 624–646.
212. Fakhfakh, F.; Baraket, L.; Ghorbel, A.; Fraile, J. M.; Mayoral, J. A. Catalytic Activity of Copper-bis(Oxazoline) Grafted on Mesoporous Silica in Enantioselective Cyclopropanation. *React. Kinet. Mech. Catal.* **2015**, *116*, 119–130.
213. Aldea, L.; Fraile, J. M.; Garcia-Marin, H.; Garcia, J. I.; Herrerias, C. I.; Mayoral, J. A.; Perez, I. Study of the Recycling Possibilities for Azabis(Oxazoline)-Cobalt Complexes as Catalysts for Enantioselective Conjugate Reduction. *Green Chem.* **2010**, *12*, 435–440.
214. Fraile, J. M.; Mayoral, J. A.; Munoz, A.; Santafe-Valero, J. Carbenoid Insertions into Benzylic C-H Bonds With Heterogeneous Copper Catalysts. *Tetrahedron* **2013**, *69*, 7360–7364.
215. Garcia, J. I.; Lopez-Sanchez, B.; Mayoral, J. A.; Pires, E.; Villalba, I. Surface Confinement Effects in Enantioselective Catalysis: Design of New Heterogeneous Chiral Catalysts Based on C1-Symmetric Bisoxazolines and Their Application in Cyclopropanation Reactions. *J. Catal.* **2008**, *258*, 378–385.
216. Fraile, J. M.; Garcia, J. I.; Mayoral, J. A.; Roldan, M. Simple and Efficient Heterogeneous Copper Catalysts for Enantioselective C-H Carbene Insertion. *Org. Lett.* **2007**, *9*, 731–733.
217. Rosario, T. M.; Blanco, M. N.; Caceres, C. V.; Fraile, J. M.; Mayoral, J. A. Supported Heteropolyanions as Solid Counterions for the Electrostatic Immobilization of Chiral Copper Complexes. *J. Catal.* **2010**, *275*, 70–77.
218. Fakhfakh, F.; Baraket, L.; Ghorbel, A.; Fraile, J. M.; Herrerias, C. I.; Mayoral, J. A. Effect of Support Properties on the Performance of Silica-Supported bis(Oxazoline)-Copper Chiral Complexes. *J. Mol. Catal. A Chem.* **2010**, *329*, 21–26.
219. Burguete, M. I.; Cornejo, A.; Garcia-Verdugo, E.; Garcia, J.; Jose, G. M.; Luis, S. V.; Martinez-Merino, V.; Mayoral, J. A.; Sokolova, M. Bisoxazoline-Functionalized Enantioselective Monolithic Mini-Flow-Reactors: Development of Efficient Processes From Batch to Flow Conditions. *Green Chem.* **2007**, *9*, 1091–1096.
220. Castellnou, D.; Sola, L.; Jimeno, C.; Fraile, J. M.; Mayoral, J. A.; Riera, A.; Pericas, M. A. Polystyrene-Supported (*R*)-2-Piperazino-1,1,2-triPhenylethanol: A Readily Available Supported Ligand With Unparalleled Catalytic Activity and Enantioselectivity. *J. Org. Chem.* **2005**, *70*, 433–438.

654 Heterogeneous catalysis in sustainable synthesis

221. Aranda, C.; Cornejo, A.; Fraile, J. M.; Garcia-Verdugo, E.; Gil, M. J.; Luis, S. V.; Mayoral, J. A.; Martinez-Merino, V.; Ochoa, Z. Efficient Enhancement of Copper-Pyridineoxazoline Catalysts Through Immobilization and Process Design. *Green Chem.* **2011**, *13*, 983–990.
222. Fraile, J. M.; Garcia, J. I.; Lafuente, G.; Mayoral, J. A.; Salvatella, L. Bis(oxazoline)-Copper Complexes, Immobilized by Electrostatic Interactions, as Catalysts for Enantioselective Aziridination. *ARKIVOC* **2004**, 67–73.
223. Borkin, A.; Carlson, A.; Török, B. K-10-Catalyzed Highly Diastereoselective Synthesis of Aziridines. *Synlett* **2010**, 745–748.

# Index

Note: Page numbers followed by *f* indicate figures, *t* indicate tables, and *s* indicate schemes.

## A

Acetophenone, 243, 243s  
  derivatives, 606, 606s  
Activated carbon materials, 37  
Activation energy, 4–5  
Acylation, 344–355  
  with activated carboxylic acid derivatives, 348–355  
  with carboxylic acids, 345–347  
Adamantyl bromide, 341  
Additives, 7  
Adipic acid, 248, 248s  
Adsorption, 10–11  
Agitation, 14  
 $\alpha$ -ketoester hydrogenation, 610, 611t  
Aldol condensation, 568–572, 569–570t  
Aldol reaction, 556–558, 557t  
Aldoximes, 544t, 545, 546t  
Aliphatic bond formation, 459–464, 475–479  
Alkyl and aryl glyceryl monoethers, 598, 598s  
Alkylation, 318–344  
  with alcohols and ethers, 326–338  
  with aldehydes and ketones, 326–338  
  with alkyl halides, 338–341  
  with hydrocarbons, 318–325  
Alkylcycloalkane ring opening hydrogenolysis, 158, 161f  
Alkyl halides, 186, 189t  
Alkyne metathesis, 302–303  
Allyl alcohols, 549–550, 550s  
Allylic alcohols, 176, 176s  
Allylic amination, 637, 637s  
Aluminosilicates, 45–49  
Aluminum oxide, 33–34  
Amberlyst, 51–52, 319, 341  
 $\alpha$ -amino-amides, 479, 479s  
2'-Aminobenzothiazolomethylnaphthol derivatives, 338, 339s  
3-Aminocarbazoles, 111, 111s  
2-Amino-3-cyanopyridine derivatives, 474, 474s  
2-Amino-4*H*-pyran derivatives, 471, 471s

3-Aminoimidazo[1,2-*a*]pyridines, 468, 468t  
Amorphous metal alloys, 30  
Aniline, 250–251, 251s  
Anthraquinone, 354–355, 354s  
Arenesulfonic acid functionalized SBA-15, 545  
Aromatic alkenes, cross metathesis of, 283, 283s  
Aromatic electrophilic alkylation, 318  
Arylated benzimidazoles, 405, 405s  
Arylated fluorenones, 404, 404s  
Aryl-halides, hydrogenolysis of, 186, 187–188t  
Aryl-thioethers, 431, 431s  
Asymmetric synthesis, solid catalysts, 593–594  
  aldol reactions, cyclohexanone, 619–624, 620–621t  
  cascade and tandem reactions, 632–633  
  Henry reactions, 629–630  
  hydrogenation  
    asymmetric hydrogenation of ketones, immobilized chiral organometallic complexes, 601–602, 603t  
    mono-carbonyl compounds, reduction of, 600–614  
  Michael additions, 624–629, 625–626t  
  multicomponent reactions, 630–631  
  oxidation reactions  
    dihydroxylation, 596–597  
    epoxidation, 594–596  
Azamacrocyclic, 190–193, 193s  
Azides, 117–118  
Aziridines, 639, 640s

## B

Batch reactors, 14  
Bayer-Villiger reaction, 554–556, 555t, 594  
Baylis-Hillman reaction, 622, 624s  
Beckmann rearrangement reactions, 543–548, 546t  
Benzils, 604, 605s  
Benzothiazoles, 250, 250s  
Benzyl ethers, 169, 172–173t

- Benzylimine-benzaldimine rearrangement reactions, 553
- Biaryl ethers, 429–430, 429–430s
- Biginelli reaction, 443, 450–452, 450–451*t*, 497
- Bioderived alkenes, 305–309
- Biomass-based materials, 37
- Biomass-sourced manganese, 233, 233s
- Bipyridine-5-carbonitriles, 449, 449s
- Bis(pyrazolyl)methanes, 457, 457s
- $\beta$ -ketoesters, 613, 613–614s
- $\beta$ -ketophosphonates, 613–614, 614s
- Brønsted acid sites, 493–496, 508, 512, 520, 524
- Buchwald-Hartwig coupling reaction, 429, 429s
- Bulk metals, 28
- Butyl butyrate, 176–177, 177s
- C**
- Camphor derivative, 164–165, 165s
- $\epsilon$ -Caprolactam, 543–544, 544*t*
- Carbamatoalkyl naphthols, 478–479, 479s
- Carbocatalysis, 57
- Carbon-based supports, 35–36
- Carbon-carbon multiple bond hydrogenations, 86–96
- Carbon composites, 56
- Carbonyl-based multicomponent reactions
- aliphatic bonds, formation of, 459–464
  - 5-membered rings, 453–458
  - 6-membered rings, 444–453
- Carbonyl compounds, hydrogenations of, 103–107
- Catalysis
- green chemistry principles, 2–3
  - types, 9
- Catalyst poisons, 6
- Catalysts
- definition, 3–4
  - recycling, 7
  - regeneration, 7
  - reuse, 7
  - types, 9
- Catalyst supports, 31–37
- Catalytic cycle, 3–4, 4*f*
- Catalytic hydrogenation, 85
- Catalytic reactors, 14–15
- Catellani reaction, 389, 389s
- C–Br bond, 186
- C–C bond-forming reactions
- Heck coupling reactions
  - solvent-free reactions, 389–391
  - in solvents, 380–389, 381–383*t*
  - without palladium, 392–393
- Hiyama coupling reactions, 407–411
- Kumada coupling reactions, 414–415
- Negishi coupling reactions, 411–413
- Sonogashira coupling reactions, 415–424
- Suzuki coupling reactions
- palladium-containing reactions, 393–405, 395–399*t*
  - without palladium, 405–407
- Tsuji-Trost allylation reactions, 424–425
- C–C bond hydrogenolysis, 158–167
- C–Cl bond, 186
- Cellulose, hydrolysis reactions of, 573–574
- C–F bond, 186
- C-halogen bonds, 186–190, 187–189*t*, 191–192*t*
- Chan-Lam coupling reaction, 428, 428s
- Chauvin mechanism, 279
- Chemical adsorption, 10–11
- Chemical promoters, 7
- Chemoselectivity, 7–9
- Chiral covalent organic framework (CCOF), 619–622
- Chiral heterogeneous polyoxometalate metal-organic framework, 597, 597s
- Chiral imines, 636–637, 637s
- Chiral porous organic framework (cPOF), 635–636, 636s
- Chitosan, 37
- Chitosan-supported CuO catalyst, 426, 427s
- Chitosan-supported Ni catalyst, 406–407, 407s
- Chromenopyridines, 323–324, 324s
- Cinchona-modified Pd catalysts, 615, 616*t*
- cis*-alkenes, epoxidation of, 233, 234s
- Claisen rearrangement, 552
- Clay catalysts, 45–48
- Click chemistry, 503, 637
- C–N bond-forming reactions, 426–429
- C–N bond hydrogenolysis, 177–186
- C–O bond-forming reactions, 429–430
- C–O bond hydrogenolysis, 167
- allylic alcohols, photocatalytic transfer
  - hydrogenolysis of, 176, 176s
  - benzyl ethers, 169, 172–173*t*
  - butyl butyrate, 176–177, 177s
  - cyclic ethers, 167, 168*t*, 169
  - cyclohexene epoxide, 169–174, 174s
  - 1,3-dioxane, partial hydrogenolysis of, 174, 174s
  - epoxide, 175, 175–176s

- 3-hydroxy-4-phenylbutan-2-one,
    - enantioselective synthesis of, 174, 174s
    - protected diol, debenzoylation of, 175, 175s
    - simple ethers and alcohols, 169, 170–171t
  - Combined heterogeneous-homogeneous
    - solvent-free Heck reaction, 391, 391s
  - Composite materials, 56–57
  - Coordination polymers (CPs), 511
  - Copper-based metal-organic framework,
    - 427–428, 428s
  - Copper complex-functionalized magnetic core-shell nanoparticles, 545–547
  - Copper-free Sonogashira reactions, 416,
    - 417–420t
  - Coumarin-based 1,4-dihydropyridines, 447, 448s
  - Covalent organic frameworks (COFs), 506–507
  - Cross-coupling reactions
    - C–N bond-forming reactions, 426–429
    - C–O bond-forming reactions, 429–430
    - C–S bond-forming reactions, 430–431
      - green chemistry applications, 379
  - Cross-linked chitosan-cellulose beads
    - supported Pd(II) ions, 403, 403s
  - Cross-linked polymer-supported ionic liquid
    - immobilized palladium, 424, 424s
  - Cross metathesis (CM), 280–287
  - C–S bond-forming reactions, 430–431
  - C–S bond hydrogenolysis
    - organosulfur compounds, 195, 196t, 197
    - Raney Ni catalyst
      - cispentacin precursor, 197, 197s
      - cysteine-perfluoroaryl thioethers, 198, 198s
      - methylthioxy group, 197, 197s
      - thiocarbonyl group, 197, 198s
  - Cycliacylation reactions, 356–357
  - Cyclic ethers, 167, 168t
  - Cyclization
    - C–C bonds, 492
    - C–X bonds (X being a heteroatom), 492
    - intermolecular cyclization reactions
      - Diels-Alder and hetero-Diels-Alder reactions, 492–496, 494–495t
      - five-membered rings, heterogeneous catalytic synthesis of, 500–508
      - six-membered rings, heterogeneous catalytic synthesis of, 497–499
    - intramolecular cyclization reactions, 508–516
    - ring opening reactions, 517–529
  - Cycloalkane hydrogenolysis, 158, 159–160t
  - Cyclodextrins, 38–39
  - Cyclohexane ring opening hydrogenolysis, 158
  - Cyclohexanone oxime, 111, 111s
  - Cyclohexene epoxide, 169–174, 174s
  - Cyclohexyl amine, 111–112, 112s
  - Cyclooctene
    - epoxidation of, 231, 231s
    - ring opening/ring closing metathesis of, 298, 298s
  - Cyclopentane ring opening hydrogenolysis, 158
  - Cyclopropanation reactions, 639, 639s
  - Cyclopropane hydrogenolysis, 158, 161
    - and acceptor, 162, 162s
    - with donor, 162, 162s
    - gem*-dimethyl norbornyl carboxylic acids, 164, 164s
    - nonpeptidic cathepsin S inhibitors, synthesis of, 163, 163s
    - parallel ring opening of, 167, 167s, 174, 174s
    - Pd/C catalyst, 162, 162s
    - tetrasubstituted cyclopropanes, 161, 161s
  - Cyclopropyl hydrogenolysis, 162–163, 163s, 166–167, 166s
    - bicyclic cyclopropyl lactones, 161, 161s
    - of dual metalloprotease inhibitor
      - intermediate, 163, 163s
      - during (–)-hamigeran B synthesis, 164, 164s
      - reactivity under various experimental conditions, 166–167, 166s
      - spirocyclopropyloxindoles, 167, 167s
      - during (+)-sulcatine G synthesis, 164, 164s
  - Cysteine-perfluoroaryl thioethers, 198, 198s
- ## D
- Decahydroacridinediones, 90, 90s
  - 1-Decene, 306, 307s
  - Dehalogenation, 186–190
  - Dehydrogenation reactions, 263–268
  - Dehydrohalogenation, 190
    - alkyl halides, 186, 189t
    - aryl-halides, 186, 187–188t
    - halogenated aromatics, 190, 191–192t
  - Desorption, 10–11
  - Desoxyhypnophilin, 166, 166s
  - Diastereoselectivity, 7–9
  - Diels-Alder cyclization, 491
  - 5,6-Dihydroneucleosides, 90–91, 91s
  - 1,4-Dihydropyran[2,3-*c*]pyrazoles, 471, 472t
  - Dihydroxylation reactions, 235–241
  - Domino C–C-coupling/oxidation reaction, 243, 243s

## E

- Electrochemical oxidative cleavage, 250, 250s
- Enantioselective dihydroxylation, 240–241, 241s
- Enantioselective heterogeneous catalytic epoxidation, 234, 234s
- Enantioselectivity, 7–9
- Epoxidation reactions, 228–235
- Epoxide
  - hydrogenolysis, 175, 175–176s
- Epoxide rearrangement reactions, 549–551
- Epoxides, ring opening reactions
  - $\beta$ -substituted alcohols, synthesis of, 517–521
  - carbonyl compounds, synthesis of, 521, 522t
  - cyclic carbonates, synthesis of, 522–524
- Ethyl 2-acylarylcarboxylates, 633, 633s
- Ethyl alk-4-enoates, 552, 552s
- Ethyl pyruvate hydrogenation, 608, 608s, 609t

## F

- Fe<sub>3</sub>O<sub>4</sub>@SiO<sub>2</sub>-EP-NH-HPA (IV) nanocatalyst, 472–473, 473s
- Ferrier rearrangement reactions, 551–552
- 5-membered heterocycles, 466–469
- Five-membered rings, heterogeneous catalytic synthesis of
  - Huisgen 1,3-dipolar cycloaddition, 502–503, 504t
  - oxazolidinones/oxindoles, 505–507, 506t, 524s
  - phenylenediamines/diazotization, application of, 504–505
  - pyrazoles, 507–508
  - pyrroles, 500–502
- Flow reactors, 15
- (*R*)-Fridamycin E, 93, 96s
- Friedel-Crafts reactions
  - acylation, 344–355
  - alkylation, 318–344, 634
- Fries rearrangement reactions, 548–549
- Furo[3,4-*b*]chromene derivatives, 452, 452s

## G

- Gewald reactions, 453–454, 454t, 497
- Glycols
  - epoxidation-methanolysis of, 233, 233s
  - transformation of (*see* Ferrier rearrangement)
- Gold, 26
- Graphene oxide, 517–520
- Graphene oxide-chitosan immobilized Pd nanoparticles, 429, 429s

- Graphene oxide nanosheet immobilized Pd nanoparticles, 408, 408s
- Graphene oxide-supported Ni catalyst, 415, 415s
- Graphene-supported Co nanoparticle catalyst, 407, 407s
- Groebke-Blackburn-Bienaymé reaction, 468, 468t, 497
- Grubbs-Herrmann catalyst, 299, 300s

## H

- $\alpha$ -Haloacetophenones, 604, 605s
- Halogenation reactions, 357–360
- Hamigeran B, 90–91, 91s
- Hantzsch synthesis, 497
- Hantzsch-type multicomponent reaction, 444, 445–446t, 453, 453s
- Heck coupling reactions
  - solvent-free reactions, 389–391
  - in solvents, 380–389, 381–383t
  - without palladium, 392–393
- Heteroaromatic methyl ketones, 600–601, 601s
- Hetero-Diels-Alder reactions, 492–496, 494–495t
- Heterogeneous catalysis
  - active site, of solid catalysts, 11
  - advantages, 9
  - anchoring effects, 11–12
  - catalytic reactors, 14–15
  - catalytic surfaces, 10
  - chemical adsorption, 10–11
  - cross-coupling reactions
    - C–C bond-formation (*see* C–C bond-forming reactions)
    - C–N bond-forming reactions, 426–429
    - C–O bond-forming reactions, 429–430
    - C–S bond-forming reactions, 430–431
    - green chemistry applications, 379
  - drawbacks, 9–10
  - experimental variables, 12–14
  - green chemistry principles, 3
  - hydrogenations
    - aldehydes and ketones, 103, 104–105t
    - alkenes and cycloalkenes, 87, 88–89t
    - alkynes and dienes, 91, 92t
    - benefits, 85
    - carbocyclic aromatic compounds, 96, 97–98t
    - drawbacks, 85–86
    - imines, 114, 115t
    - nitriles, 112, 113t
    - nitrobenzenes, 108, 109–110t

- nonconventional activation methods, 123–130
  - laboratory applications, 9
  - metathesis (*see* Metathesis reactions)
  - oxidations
    - C–C bonds, 263–268
    - cleavage reactions, 243–251
    - C–N bonds, 260–263
    - C–O bonds, 251–260
    - C–X bonds, 263–268
    - dihydroxylation reactions, 235–241
    - epoxidation reactions, 228–235
    - Wacker-type reactions, 241–243
  - physical adsorption, 10–11
  - rearrangement (*see* Rearrangement reactions)
  - Heterogeneous Catalysis for the Synthetic Chemist* (Augustine), 81
  - Heterogeneous catalytic asymmetric metathesis, 303–305
  - Heterogeneous catalytic hydrogenolysis. *See* Hydrogenolysis
  - Heterogenized metal complexes, 37–38
  - Heteropoly acid-catalyzed alkylation, 331, 332s
  - Heteropoly acids (HPAs), 44–45, 548–549, 551, 554
  - Hiyama coupling reactions, 407–411, 408s
  - Hollow structured mesoporous silica nanospheres (HMSN), 604–605, 605s
  - Hoveyda-Grubbs catalysts, 280–282, 288–299, 289–295t, 301, 305–306, 309
  - Huisgen reaction, 503
  - Hummers method, 517–520
  - Hydrodesulfurization. *See* C–S bond hydrogenolysis
  - Hydroformylations, 577–580, 578–579t
  - Hydrogenation reactions
    - aromatic and heteroaromatic compounds, 96–102
    - $\alpha,\beta$ -unsaturated carbonyl compounds, 118–119
    - carbon-carbon multiple bond, 86–96
    - carbonyl compounds, 103–107
    - C=C double bonds, reduction of, 614–618
    - mono-carbonyl compounds, reduction of
      - 1,2-dicarbonyl compounds, 606–610
      - 1,3-dicarbonyl compounds, 610–614
    - reductive alkylation, 614
    - multiple functional groups, 123
    - nitrogen-containing groups, 108–118
    - nonconventional activation methods, 123–130
  - Hydrogenolysis, 157, 157s, 201
    - of azido group in diazido pyrazolonones, 195, 195s
    - of azido-sugars, 195, 195s
    - of biomass-related compounds
      - biomass-derived oxygen-containing aliphatic compounds, 199–201, 202–203t
      - biomass-derived oxygen-containing heterocycles, 199, 200t
    - bond polarization, 157
    - C–C bond, 158–167
    - C–halogen bonds, 186–190
    - C–N bond, 177–186
    - C–O bond, 167
      - allylic alcohols, photocatalytic transfer hydrogenolysis of, 176, 176s
      - benzyl ethers, 169, 172–173t
      - butyl butyrate, 176–177, 177s
      - cyclic ethers, 167, 168t, 169
      - cyclohexene epoxide, 169–174, 174s
      - 1,3-dioxane, partial hydrogenolysis of, 174, 174s
      - epoxide, 175, 175–176s
      - 3-hydroxy-4-phenylbutan-2-one, enantioselective synthesis of, 174, 174s
      - protected diol, debenzoylation of, 175, 175s
      - simple ethers and alcohols, 169, 170–171t
    - C–Sn organometallic compounds, 198
  - definition, 157
  - hydrodesulfurization (*see* C–S bond hydrogenolysis)
  - N–N bond, 190
    - azamacrocyclic, 190–193, 193s
    - azido group, 194, 194s
    - azo and azoxy compounds, 193–194, 193–194s
    - pyrazolidines, 190, 190s
  - N–O bond, 194, 194s
  - Si–Si bond, 198
  - Sn–C bond, 198
  - Hydrolysis reactions, 573–574
  - Hydroxyacetophenones (HAP), 548
  - Hydroxyalkylation reactions, 318–344
  - 3-Hydroxy-3,4-dihydroquinolin-2(1H)-ones, 633, 633s
  - 3-Hydroxy-4-phenylbutan-2-one, 174, 174s
- I**
- Imidazo[1, 2-*a*]pyridines, 469, 469s
  - Imidazo-fused polyheterocycles, 466, 468s

- Imine metathesis, 285, 286s  
Imines, 114–116  
Imino-pyrrolidinethiones, 466, 467s  
Immobilized metal complex, 288–297  
Indoles, 102, 102s  
  alkaloids, 324, 324s  
  N-arylation of, 426, 426s  
(3'-Indolyl)pyrazolo[3,4-*b*] pyridines, 473, 474s  
Intramolecular cyclization reactions  
  5-membered-rings  
    Nazarov cyclization, 508–511, 509–510r  
    tetrahydrofurans, 512, 512r  
  6-membered-rings  
    ionones, 514, 514s  
    isopulegol, 512–514, 513r  
    quinolines/isoquinolines, 516  
    terpenoids, 515  
Intramolecular transacylations, 355  
Intramolecular transalkylations, 343–344  
Iodine, 186  
Ion exchange resins, 51–53  
Ionic liquid-based composites, 56  
Ionic liquid immobilized Pd catalyst, 425, 425s  
Ionic liquid immobilized (*R*)-[RuCl  
  (binap)(*p*-cymene)] Cl complex,  
  613, 613s  
Ion-pair immobilization method, 606  
Ipatieff's experiments, 1–2  
Iridium, 26  
Isocyanide-based multicomponent reactions  
  aliphatic bond formation, 475–479  
  5-membered rings, 466–469  
  6-membered rings, 469–475  
Isonitrile-based multicomponent reactions.  
  See Isocyanide-based multicomponent  
  reactions
- J**  
Jasminaldehyde, 568–571  
Johnson-Claisen rearrangement reactions, 552
- K**  
K-10-catalyzed intramolecular cyclialkylation,  
  324, 324s, 333–336, 336s  
K-10-catalyzed solvent-free microwave-  
  assisted condensation, 561  
Keggin-type heteropolyacids, 472–473  
Ketoximes, 545, 546r  
Kharasch-Sosnovsky allylic oxidation, 599, 599s  
K-10 montmorillonite catalysis, 323–325,  
  323–324s, 330–331  
Knoevenagel condensation, 563–566, 564–565r  
Kumada coupling reactions, 414–415
- L**  
Layered double hydroxide (LDH)-based Pd-  
  Os-oxide-W-oxide catalyst, 391, 391s  
Lewis acid catalysts, 499, 508, 512–513, 517,  
  520  
Lewis acid sites, 493–496  
Lifetime, catalyst's, 6  
Linalool, 93, 96s  
Lindlar catalyst, 6, 6f  
Lipidic cubic phases (LCP), 619  
Long chain alkenes, cross metathesis of, 282,  
  282s  
L-Proline on a graphene oxide support  
  (L-Pro@GO), 622
- M**  
MacMillan-type catalyst, 634–635, 635s  
Magnetically recoverable immobilized Pd  
  nanoparticles, 430, 430s  
Magnetically recyclable Pd catalyst, 400, 409,  
  409s  
Magnetic catalyst supports, 34–35  
Magnetite nanoparticles (MnPs), 602  
Mannich reaction, 443, 460, 461–462r  
Massive metals, 28  
MCM-41-supported Grubbs-type catalyst, 299,  
  299s  
MCM-supported Pd catalyst, 410, 410s, 416,  
  416s  
MCRs. See Multicomponent reactions (MCRs)  
Mesoporous solids, 55–56  
Metal blacks, 28–29  
Metal carbonates, 34  
Metal catalysts, 23–39  
Metal nanoparticle-based catalysts, 38–39  
Metal-organic frameworks (MOFs), 53–55,  
  496, 508–511, 520, 522–523, 595  
Metal oxides, 41–44  
Metathesis reactions  
  advantages, 280  
  alkyne metathesis, 302–303  
  asymmetric catalysis, 303–305  
  bioderived alkenes, 305–309  
  CM (see Cross metathesis (CM))  
  RCM (see Ring closing metathesis (RCM))  
  ROM (see Ring opening metathesis (ROM))  
4-Methoxy-styrene, cross metathesis of,  
  281–282, 282s  
Methylbenzyl-indoles, 330, 330s

- Methyl cinnamate, epoxidation of, 234, 234s  
Methylcyclobutane, 158, 161f  
Methylcyclopentane ring opening  
  hydrogenolysis, 158, 161, 161f  
Methyl 3-cyclopropyl-3-oxopropanoate, 610, 612s  
Methyl 9-decenoate, 306, 307s  
Methyl oleate  
  cross metathesis, 306, 307s  
  self-metathesis, 307–309, 308t  
Methyltrioxorhenium (MTO) catalysts, 306  
Microwave-assisted Cu/C-catalyzed Ullmann coupling, 429, 429s  
Microwave-assisted hydrogenations, 123–126, 127t  
Microwave-assisted Negishi coupling reaction, 413, 413–414s  
Microwave-assisted Ni/C-catalyzed Suzuki coupling reaction, 405, 405s  
Microwave-assisted organic synthesis (MAOS), 123–126  
Mizoroki-Heck coupling reactions, 380–393  
Molecular sieves, 55–56  
Monolithic disk-supported Mo complex, 300, 300s  
Mukaiyama reaction, 558, 559t  
Multicomponent reactions (MCRs), 496  
  carbonyl-based, 444–464  
  isocyanides, 464–479  
Multisubstituted pyridines, 474–475, 475s  
Multisubstituted pyrroles, 454–455, 455s  
Multiwall carbon nanotubes (MWCNT), 615  
Multiwall carbon nanotubes supported  
  Pd-salen complex catalyzed Hiyama coupling, 408–409, 409s  
Myrtanal, 550–551, 550t
- N**  
Nafion-H particles, 51–53  
Nafion-H silica nanocomposite, 549, 552–553  
Nafion-H/silica nanocomposite-catalyzed Claisen rearrangement, 343–344, 344s  
Nafion-H/silica nanocomposite-catalyzed Fries rearrangement, 355, 355s  
Nanoacids, 56–57  
Nanosized MCM-41-supported Pd catalyst, 411–412, 412s  
N-aryl-tetrazoles, 458, 458s  
N-cyclohexyl-3-aryl-quinoxaline-2-amines, 469–470, 470s  
Negishi coupling reactions, 411–413
- Ni/C-catalyzed reactions  
  Kumada coupling reactions, 414, 414s  
  Negishi reaction, 413, 413s  
Nickel, 25  
Ni-ferrite-based magnetic nanoparticle catalyzed synthesis, 406, 406s  
Nitration reactions, 360–364  
Nitriles, 112–114  
N–N bond hydrogenolysis, 190  
  azamacrocyclic, 190–193, 193s  
  azido group, 194, 194s  
  azo and azoxy compounds  
    Ni-Al alloy in water, 193, 193s  
    Pd/MCM-41 catalysts, 194, 194s  
    Zn catalyst, 193, 193s  
  pyrazolidines, 190, 190s  
Noble metal oxides, 29–30  
N–O bond hydrogenolysis, 194, 194s  
Nonmetallic catalysts, 39–57
- O**  
Olefin cross metathesis, 280  
Olefin metathesis, 286–287, 286f, 305  
Organocatalysts, 37–38  
Organosilane nanoparticle-supported Pd catalyst, 424–425, 425s  
Orito's reaction, 608  
*Ortho*-Claisen rearrangement reactions, 552–553  
Osmium-catalyzed dihydroxylations, 235–240, 236–237t  
Oxidative cleavage reactions, 243–251  
Oximes, oxidative aromatization of, 268, 268s  
Oxindoles, 507  
Oxiranes, 167, 168t, 169
- P**  
Paal-Knorr pyrrole synthesis, 491, 500–502, 500t  
Palladium, 25  
Palladium-catalyzed coupling reactions. *See* Heck coupling reactions; Suzuki coupling reactions; Tsuji-Trost allylation reactions  
Palladium proline complex, 430, 431s  
Paracetamol, 547  
Partial hydrogenation, 93, 94–95t, 96s  
Passerini reaction, 475, 476–477t, 478  
Pd-loaded homochiral covalent organic framework (Pd@CCOF), 636, 636s  
Pd/PS-NHC-catalyzed Heck reaction, 388, 388s

Pd/ZnO-catalyzed Hiyama coupling reaction, 410, 410s  
Pechmann condensation, 337–338, 338s, 566–568  
Phase transfer catalysts, 9  
1-Phenyl-1,2-propanedione (PPD), 607, 607s  
Phillips triolefin process, 280  
Phosphotungstic acid (PTA), 615  
Photocatalytic transfer hydrogenation method, 176, 176s  
Phthalazine-trione derivatives, 456–457, 457s  
Physical adsorption, 10–11  
Pillared clays (PILCs), 55–56  
Pillared layer solids, 55–56  
Pinacol rearrangement reactions, 554, 554s  
Platinum, 26  
Poly(ionic liquids) (PIL-resins), 622, 624s  
Polyimide covalent organic framework immobilized Cu (Cu@PI-COF), 428, 428s  
Polyionic gel-supported bimetallic Rh/Pd-catalyzed one-pot hydrosilylation-Hiyama coupling reaction, 411, 411s  
Polymer-bound molybdenum-catalyzed epoxidation, 229, 229s  
Polymeric materials, 36–37  
Polystyrene-bound diamine (PSAP)-immobilized copper-catalyzed reactions, 427, 427s  
Poly-substituted 3-pyrrolin-2-ones, 455, 456s  
Polyvinylpyrrolidone-supported boron trifluoride, 568  
Preyssler heteropolyacids, 501–502  
Preyssler nanoparticle-catalyzed synthesis, 478–479, 479s  
Prins cyclization, 499  
Proline modified palladium catalyst, 615, 617–618, 617s  
Propane metathesis, 285, 285s  
Propargylamines, 464, 465t  
Propene, synthesis of, 287, 287t  
Propylcyclobutane, 158  
Propylcyclopropane, 158  
Protection/deprotection reactions, 574–576  
Pyrazine derivatives, 470–471, 470s  
Pyrazolidines, 190, 190s  
Pyrazolidinones, 90, 90s  
Pyrimido[1,6-*a*]quinolones, 448, 448s  
Pyrrole derivatives, 562, 562s

## Q

Quinolines, 102, 102s  
Quinoxaline derivatives, 470–471, 470s

## R

Raney Ni-catalyzed hydrogenolysis  
cispentacin precursor, 197, 197s  
cysteine-perfluoroaryl thioethers, 198, 198s  
enantiomeric cyclopropanes, ring opening of, 162, 162s  
methylthioxy group, 197, 197s  
spiro[cyclopropyl-1,3'-oxindoles], 167, 167s  
thiocarbonyl group, 197, 198s  
Reaction rate, 5  
Rearrangement reactions  
aldol condensation, 568–572  
aldol reaction, 556–558  
Baeyer-Villiger oxidation, 554–556  
Beckmann, 543–548  
benzylimine-benzaldimine, 553  
epoxide, 549–551  
Ferrier, 551–552  
Fries, 548–549  
hydrolysis, 573–574  
Johnson-Claisen, 552  
Knoevenagel condensation, 563–566  
Mukaiyama reaction, 558  
*ortho*-Claisen, 552–553  
Pechmann condensation, 566–568  
pinacol, 554  
Schiff-base formation, 558–563  
Reduction, 85  
Regioselective hydrogenation, 118–123  
Regioselectivity, 7–9  
Rh-chiral diamine complex, 602–604, 604s  
Rhodium, 26  
Ring closing metathesis (RCM), 288–300, 289–295t  
Ring opening metathesis (ROM), 301–302  
Ring opening reactions  
benzoxazoles/benzothiazoles, 529  
ring opening of hydrocarbons, 529  
ring opening polymerization (ROP), 525–529, 526s, 526t  
selective ring opening of naphthenes, 529  
of small heterocycles  
aziridines, 524–525, 525s  
epoxides, 517–524  
Ring transformations, heterogeneous catalysis  
C–C bonds, 492  
C–X bonds (X being a heteroatom), 492  
intermolecular cyclization reactions  
Diels-Alder and hetero-Diels-Alder reactions, 492–496, 494–495t  
five-membered rings, heterogeneous catalytic synthesis of, 500–508  
six-membered rings, heterogeneous catalytic synthesis of, 497–499

- intramolecular cyclization reactions, 508–516
  - ring opening reactions, 517–529
  - Ru-chiral diamine complex, 602–604, 604s
  - Ru encapsulated yolk shell structure silica catalyst, 283, 283s
  - Ruthenium, 26
  - Rylander's seminal monograph, 86
- S**
- Sabatier's experiments, 1
  - Santa Barbara Amorphous-15 (SBA-15), 55
  - Sativene, 90–91, 91s
  - SBA-15 grafted copper catalyst, 431, 431s
  - SBA-15 immobilized Pd catalyst, 426, 426s
  - SBA-supported Ni complex, 414–415, 415s
  - SBA-supported Pd-catalyzed Suzuki coupling reaction, 404, 404s
  - Scandium triflate-catalyzed alkylation, 331–332, 332s
  - Schiff-base formation, 558–563
  - Schrock molybdenum-based carbene complex, 284, 300
  - Selectivity, 7
  - Self-supported catalysts, 37
  - 2-Semidines, 111
  - Shell higher olefin process, 280
  - Shi's catalyst, 594, 595s
  - Silica-immobilized Ni-DABCO complex, 392, 392s
  - Silica-supported catalysts, 281
  - Silica-supported heteropoly acid catalysis, 325, 325s
  - Silica-supported heteropoly acid-catalyzed cyclialkylations, 356, 356s
  - Silica supported Hoveyda-Grubbs catalyst, 305–306, 306s
  - Silica-supported Pd catalyst, 425, 425s
  - Silica-supported Pd-catalyzed Negishi coupling reaction, 412, 413s
  - Silica-supported Preyssler nanoparticle-catalyzed synthesis, 478–479, 479s
  - Silica support materials, 31–33
  - Si–Si bond, 198
  - 6-membered heterocycles, 469–475
  - Six-membered rings, heterogeneous catalytic synthesis of
    - pyrazines and piperazines, 497–498
    - pyridines, 499
    - tetrahydropyrans, 499
  - Skeletal metals, 29
  - Sn–C bond, 198
  - Sol-gel condensation-polymerization method, 42, 43s
  - Solid acid catalysis, 512, 517, 518–519r, 520
  - Solid catalysts, 550–551, 563, 571–572
    - schematic classification, 23, 24f
  - Solvent-free Heck reactions, 389–391
  - Sonochemical hydrogenations, 126, 128–129r
  - Sonogashira coupling reactions, 415–424
  - Spent catalysts, 7
  - Spirocyclopropyl
    - camphor derivative, 164–165, 165s
    - spirocyclopropylcyclooctane, 165, 165s
    - spirocyclopropyl-cyclopentane, 165, 165s
    - spirocyclopropyl-cyclopropane, 165, 166s
    - spirocyclopropyloxindoles, 167, 167s
  - Sporopollenin, 387
  - Sterically crowded aryl tosylate, 413, 414s
  - Strecker synthesis, 443, 459, 459r
  - Structural promoters, 7
  - Structure-insensitive reactions, 11
  - Structure-sensitive reactions, 11
  - Sulfonated carbon-silica composites, 56
  - Sulfonated polymeric solid acid, 544
  - Sulfonation reactions, 364–365
  - Sulfonyl 9-fluorenylidene, 338, 338s
  - Supercritical fluids, 13
  - Supported metal catalyst, 30–37
  - Supported metal oxide catalysts, 44
  - Suzuki coupling reactions
    - palladium-containing reactions, 393–405, 395–399r
    - without palladium, 405–407
  - Suzuki-Miyaura coupling reactions, 393–407
  - Synthetic zeolites, 51
- T**
- Tandem hydroxylacetylation-acetylation reaction, 241, 241s
  - Tartaric acid-modified Raney Ni catalysts, 610
  - Terminal alkenes, cross metathesis of, 284, 284s
  - Tetrabutylammonium bromide (TBAB), 522–523
  - Tetrahydrodipyrzoloxyridines, 447, 447s
  - Tetrahydro-2-methyl-5,γ-dioxo-2-furanpentanoic acid, 556, 558s
  - Thiazolidin-2-imines, 458, 458s
  - Three-component coupling reactions, 431, 431s
  - Titanium cation-exchanged montmorillonite-catalyzed Beckmann rearrangement, 545
  - Transfer hydrogenation, 601
  - Trans-stilbene, dihydroxylations of, 235, 238s
  - 2,2,2-Trifluoroacetophenone, 600, 600s
  - Tsuji-Trost allylation reactions, 424–425

Tungstophosphoric acid ( $\text{H}_3\text{PW}_{12}\text{O}_{40}$ ), 493  
Turnover frequency (TOF), 5

## U

Ugi condensation, 443, 475, 476–477*t*, 479  
UiO-66 nanocatalyst, 469, 469*s*  
Ullmann coupling reaction, 426–427, 427*s*,  
429, 429*s*  
Ultrasound-assisted hydrogenations, 126–130  
Unsupported metals, 28–30

## V

Volatile organic compound (VOCs), 186

## W

Wacker-type oxidation reactions, 241–243

## X

Xanthan sulfuric acid-catalyzed Pechmann  
reaction, 566–567

## Z

Zafirlukast, 332, 333*s*  
Zeolite-catalyzed photochemical reactions  
  Claisen rearrangement, 344, 344*s*  
  Fries rearrangement, 355, 356*s*  
Zeolites, 48–51, 493–496  
Ziegler catalyst, 279  
Zinc-based imidazolate framework (ZIF-71), 523  
Zirconium metal-organic framework, 469  
Zirconium poly(styrene-phenylvinylphosphonate)-  
  phosphate (ZPS-PVPA), 595–596  
ZnO nanoparticle-immobilized Pd catalyst,  
  429–430, 430*s*

## Heterogeneous Catalysis in Sustainable Synthesis

Béla Török, Christian Schäfer and Anne Kokel

*A practical guide to using solid catalysts in synthesis for increased sustainability and novel applications*

**Heterogeneous Catalysis in Sustainable Synthesis** is a practical guide to the use of solid catalysts in synthetic chemistry that focuses on environmentally benign applications. Collating essential information on solid catalysts into a single volume, the book reveals how the efficient use of heterogeneous catalysts in synthetic chemistry can support sustainable applications. Beginning with a review of the fundamentals of heterogeneous catalytic synthesis and solid catalysts, the book then explores a broad variety of heterogeneous catalytic applications in sustainable synthesis, including hydrogenation, hydrogenolysis, oxidation, metathesis, Friedel–Crafts and related reactions, multicomponent reactions, cross-couplings, cyclizations–ring openings, and rearrangements. A chapter is also dedicated to the application of heterogeneous catalysis in the production of chiral compounds.

Based on the extensive experience of its expert authors, the book aims to encourage and support synthetic chemists in using solid catalysts in their own work, while also highlighting the important link between heterogeneous catalysis and sustainability to all those interested.

### Key Features

- Combines foundational knowledge with a focus on practical applications
- Organizes information by reaction type, allowing readers to easily find examples of how to carry out specific reaction types with solid catalysts
- Highlights emerging areas such as nanoparticle catalysis and metal-organic framework (MOF)-based catalysts

**Béla Török** is Professor of Chemistry, Department of Chemistry, University of Massachusetts, Boston, United States.

**Christian Schäfer** is Lecturer and Research Scientist, Department of Chemistry, University of Massachusetts, Boston, United States.

**Anne Kokel** is Researcher in Green Chemistry, Department of Chemistry, University of Massachusetts, Boston, United States.



ELSEVIER

[elsevier.com/books-and-journals](http://elsevier.com/books-and-journals)

ISBN 978-0-12-817825-6



9 780128 178256